

UNIVERSIDADE DE SÃO PAULO
MUSEU DE ZOOLOGIA

Veronica Slobodian

Taxonomic revision of *Pimelodella* Eigenmann &
Eigenmann, 1888 (Siluriformes: Heptapteridae): an
integrative proposal to delimit species using a
multidisciplinary strategy

São Paulo
2017

Veronica Slobodian

Taxonomic revision of *Pimelodella* Eigenmann & Eigenmann, 1888 (Siluriformes: Heptapteridae): an integrative proposal to delimit species using a multidisciplinary strategy

Revisão taxonômica de *Pimelodella* Eigenmann & Eigenmann, 1888 (Siluriformes: Heptapteridae): uma proposta integrativa para a delimitação de espécies com estratégias multidisciplinares

v.1

Original version

Thesis Presented to the Post-Graduate Program of the Museu de Zoologia da Universidade de São Paulo to obtain the degree of Doctor of Science in Systematics, Animal Taxonomy and Biodiversity

Advisor: Mário César Cardoso de Pinna, PhD.

São Paulo
2017

“I do not authorize the reproduction and dissemination of this work in part or entirely by any electronic or conventional means.”

Serviço de Biblioteca e Documentação
Museu de Zoologia da Universidade de São Paulo

Cataloging in Publication

Slobodian, Veronica

Taxonomic revision of *Pimelodella* Eigenmann & Eigenmann, 1888 (Siluriformes: Heptapteridae) : an integrative proposal to delimit species using a multidisciplinary strategy / Veronica Slobodian ; orientador Mário César Cardoso de Pinna. São Paulo, 2017.

2 v. (811 f.)

Tese de Doutorado – Programa de Pós-Graduação em Sistemática, Taxonomia e Biodiversidade, Museu de Zoologia, Universidade de São Paulo, 2017.

Nome: SLOBODIAN, Veronica

Título: Taxonomic revision of *Pimelodella* Eigenmann & Eigenmann, 1888 (Siluriformes: Heptapteridae): an integrative proposal to delimit species using a multidisciplinary strategy

Thesis Presented to the Post-Graduate Program of the Museu de Zoologia da Universidade de São Paulo to obtain the degree of Doctor of Science in Systematics, Animal Taxonomy and Biodiversity.

Aprovado: ___ / ___ / _____

Comissão Julgadora

Prof. Dr. _____ Instituição: _____

Julgamento: _____ Assinatura: _____

Prof. Dr. _____ Instituição: _____

Julgamento: _____ Assinatura: _____

Prof. Dr. _____ Instituição: _____

Julgamento: _____ Assinatura: _____

Prof. Dr. _____ Instituição: _____

Julgamento: _____ Assinatura: _____

Prof. Dr. _____ Instituição: _____

Julgamento: _____ Assinatura: _____

*To all my female role models, who taught me that a woman's place
is wherever she wants to be.*

Acknowledgements

A work of this magnitude could not be single driven. I might be the main conductor, but several people and institution were crucial to the execution of this thesis, and to those I am extremely grateful. Obviously, the human memory is not flawless and, unintentionally, several people might unfortunately have been left behind in order to complete this summary of everyone I am grateful. For those I apologize, and believe me, I expressed all my gratitude to you in several moments (at least in my head).

First of all, I would like to thank my advisor, Mário de Pinna, for the opportunity, for embracing this project and even pushing it to its limits. It was more difficult to execute than I have foreseen, but most of the path was also fun and intriguing.

I also would like to thank Flávio Bockmann, my former (and eternal) advisor. The first person who insist I should work with *Pimelodella*, the first to believe in my potential. He was the person who brought me back from the abyss of disbelief and desperation so many times, and always saw the best side of everything. If I am an ichthyologist right now, most of my qualities I am in debt to him for.

I also counted with the guidance of several other senior researchers, which contributed in so many ways to my formation. I thank John Lundberg for trying to dissuade me of this crazy project, and when I would not abandon it, would give me a “plan B”, all the recommendations needed, access to material, radiographs, photos, financial aid from the Academy, and several hours of inspiring conversation. Without those, this thesis would not be a fraction of what it is. I thank also Lynne Parenti, who accepted to be my advisor during the period I spent in the National Museum of Natural History, never measuring efforts to provide me with everything I needed in order to make the most of my time there. In Smithsonian, I also counted with the support and enthusiasm of Dave Johnson, who helped in my confidence, and pushed me to my best, always believing in me and my work (even when I was not comfortable enough to talk about it), and to him I am also grateful in an indescribable manner. And I could not forget about Richard Vari, who was my first contact in Smithsonian, accepted my request to spend one year there, and got me in contact with Lynne. Richard was one of the most amazing people I ever knew, and I hope he had a grasp of the impact he had on the life of so many young ichthyologists, offering us the advisement and infrastructure we need in order to expand our horizon.

Several other professors and staff were crucial in some point of my work. That is why I also thank the professors from Ichthyology division at Museu de Zoologia, for all the talk, support, and suggestions along my thesis execution. To Naércio Menezes, Aléssio Datovo, Heraldo Britski and José de Lima Figueiredo I thank for being such amazing teachers, always providing me some guidance even I was not their official student. I also thank Osvaldo Oyakawa, Michel Gianeti, Thiago Loboda and Natália Luchetti for the aid so many times with collection matters, company, suggestions and everything; and Jaqueline Battiliana for the guidance in the MZ molecular laboratory. I thank Bruce Collette, Carole Baldwin, Victor Springer, Stanley Weitzman, Thomas Munroe, Ai Nonaka, Roy McDiarmid, Rayna Bell and Kevin de Queiroz for all the conversation, work related or not, during the time in Smithsonian. I thank all NMNH fish staff, Jeff Williams, Kris Murphy, Sandra Raredon, and I especially thank to Jeff Clayton, for the incommensurable help with absolutely everything I needed. I also thank my former professors at FFCLRP, especially Eduardo Almeida, whose company at the Systematics' discussion group, discussions at the Biological Taxonomy discipline, and suggestion to work on Species Trees were crucial to this work.

And several other people shared with me the perks and despair of a PhD. My laboratory colleagues accompanied me during this entire journey, and supported me during times most needed (this support being coffee, conversation, beer, the traditional academic support, or everything together). I thank Murilo Pastana for all the company, support, help with photographs, and endless discussions on several topics, from the reality of species to methodology on systematics. To Priscila Camelier I thank especially for the help (and patience) with issues related to molecular analysis, and for answering my messages even when at the bar (poetic license). To Luiz Peixoto I thank for listening all the times I could not think straight and had to talk out loud to make sense. To Marina Loeb I thank for all the lunch times together and help with maps. To Vinícius Espíndola I thank the teas and help with figures references. To Vitor Abrahão I thank for the help extracting and sequencing several specimens. To Caio Neto, Fernando Dagosta, Gustavo Ballen, Henrique Varella, Igor Mourão, Ilana Fichberg, João Gabriel Gênova, Manoela Marinho, Paulo Presti, Tulio Teixeira, Vinícius Reis and William Ohara I thank for the company, discussion, and help in so many times. I also thank my laboratory colleagues at Smithsonian, Casey Dillman and David de Santana, for all the help provided, especially David who helped me with all the molecular procedures at LAB facility, always available to solve any doubts and without who the molecular part of this work would not be possible. I also thank Ana Cristina Fazza for teaching me everything I needed to know from extraction to sequencing molecular data, even

explaining the reasons for each solution and step. And I cannot thank enough to Gabriela Camacho, who helped me with the Species Tree analysis while just finishing her PhD, and saved my life (and sanity) doing it.

This work was only possible with the help of so many curators, collection managers, students and other collection staff around the world, who received me in their collections, took photographs, sent me information when I could not visit in person, and never denied me information needed. To Mariangeles Arce, Mark Sabaj and Kyle Luckenbill I am thankful for the help and for making me feel like home so many times, during my visits to ANSP, and Mariangeles and Brian for always receiving me in their home. To Susan Mochel, Kevin Swagel and Caleb McMahan for the great time I had in Chicago and FMNH. Furthermore, I thank all the curators, students and staff from the following collections: Melanie Stiassny Barbara Brown and Radford Arrindell (AMNH); Jonathan Armbruster and David Werneke (AUM); Ralf Britz, James Maclaine and Oliver Crimmen (BMNH); Luiz Rocha and Dave Catania (CAS); Francisco Langeani (DZSJRJ); Ivan Mojica and Henry Agudelo Zamora (ICN-MHN); Jansen Zuanon, Lucia Rapp Py-Daniel and Efrem Ferreira (INPA); Cláudio Oliveira, Viviani França de Sene, Luz Ochoa, Bruno Melo, Camila Souza and Eric Ywamoto (LBP); Maria Elina Bichuette (LESCI); Flávio Bockmann, Ricardo Castro, Hertz Figueiredo, André Esguícero and Malu Araújo (LIRP); Carlos Lucena, Margarete Lucena, Roberto Reis, Bárbara Calegari, Maria Laura Delapieve (MCP-PUCRS); Karsten Hartel and Andrew Williston (MCZ); Oscar Lasso Alcalá (MHNLS); Gabsi Zora (MNHN); Marcelo Britto, Paulo Buckup and Cristiano Moreira (MNRJ); Wolmar Wosiacki, Izaura Maschio, Guilherme Dutra and Marina Mendonça (MPEG); Giuliano Doria (MSNG); Lenice Souza-Shibatta (MZUEL); Urs Wüest (NMBA); Anja Palandacic and Alexander Naseka (NMW); Carla Pavanelli (NUP); Ronald de Rooter (RMNH); Telton Ramos (UFPB); Caroline Ramos (UFRO); Monique Fasel (ZMA); Peter Bartsch and Johanna Kapp (ZMB); and Dirk Neumann (ZSM).

Furthermore, several people contributed in some way or another during the last four years. The company of these people could not be strictly work related, but was essential. To my family I thank for all the support in so many ways I cannot describe. To my mother, father and brother I thank for believing in me and being my safe place. To Igor I thank for the patience (especially in the last months), for being an amazing partner and stimulating me to be my best. For accompany me a year abroad while I was pursuing my dreams and never hesitating, not even in sight of hindrance, always by my side and walking along with me. Without your encouragement and companionship this journey would be much more difficult.

Also, thanks for helping me with the Examined Material list, that I know was a huge amount of work to organize.

And I am a fortunate person, by having so many incredible, supporting friends, who housed me, cheered me up, listen to me complaining, made company and helped me during this years in a way that listing all the names would be unfair and extremely extensive, but some I cannot leave without notice. To Gabriela Coutinho, Helena Spiritus, Gabriel Kiipper, Rafael Kanamaru, Ariane Sasso, Paula Ruocco, Douglas Onodera, Livia Ciabatti, Bárbara Paes, Gabriel Pato, Raíssa Rosa, Flávia Sant'Anna, Diogo Couto, Bárbara Zaidan, Maile Vidigal, Rafael Polidoro and Fernanda Vidal I thank for countless conversation hours, discussions, programing, housing, cheering, and everything else that contributed, directly or indirectly, to this thesis.

Lastly, a taxonomic revision of this amplitude counted with the structure and financial support of several projects, institutions and funding agencies. FAPESP funded this Ph.D. project (#2013/18623-4), and the fellowship I had at the one-year term in NMNH (#2016/01073-0). The molecular taxonomy received aid of FAPESP (#2015/26804-4) and NMNH Laboratories of Analytical Biology (LAB). Museu de Zoologia da Universidade de São Paulo and National Museum of Natural History gave the infrastructure for this research, and molecular analyses were conducted at MZUSP Molecular Laboratory and NMNH LAB. All Catfish Species Inventory (NSF DEB-0315963) provided several photographs and x-rayed images of type materials. All specimens' radiographs taken in Brazil used LIRP x-ray facility. I also thank Alexandra Elbakyan and Sci-hub for demolishing pay-walls and making scientific publications available to everyone in need.

“It is an important and popular fact that things are not always what they seem. For instance, on the planet Earth, man had always assumed that he was more intelligent than dolphins because he had achieved so much — the wheel, New York, wars and so on — while all the dolphins had ever done was muck about in the water having a good time. But conversely, the dolphins had always believed that they were far more intelligent than man—for precisely the same reasons.

Curiously enough, the dolphins had long known of the impending destruction of the planet earth and had made many attempts to alert mankind to the danger; but most of their communications were misinterpreted as amusing attempts to punch footballs or whistle for tidbits, so they eventually gave up and left the Earth by their own means shortly before the Vogons arrived.

The last ever dolphin message was misinterpreted as a surprisingly sophisticated attempt to do a double backward somersault through a hoop while whistling the “Star Spangled Banner,” but in fact the message was this:

So long and thanks for all the fish.”

The Hitchhiker’s Guide to the Galaxy, Chapter 23, Douglas Adams

Abstract

Primary taxonomic research in neotropical ichthyology still suffers from limited integration between morphological and molecular tools, despite major recent advancements in both fields. Such tools, if used in an integrative manner, could help in solving long-standing taxonomic problems. The genus *Pimelodella* Eigenmann & Eigenmann, 1888 is a perfect case for an integrative and multidisciplinary approach in taxonomy. *Pimelodella* is a genus of the Heptapteridae broadly distributed throughout trans- and cis-Andean South America, and one of the main components of Neotropical Ichthyofauna. Nowadays is the most species-rich genus of the family, with 79 valid species. However, the validity and delimitation of those species is extremely problematic, due their broad geographic distribution, conserved morphology, and ancient and imprecise descriptions. *Pimelodella* is undoubtedly one of the most severe taxonomic bottlenecks in neotropical ichthyology. This project presents a taxonomic revision of *Pimelodella* using an integrative morphological-molecular approach. The traditional taxonomic revision covers the genus in its entirety, with all the components of this kind of study. All types were examined, and the number of valid species herein recognized was reduced to 55 species, for which full descriptions are presented. The molecular taxonomy was done for a circumscribed subset of the genus, with representation enough to understand the molecular divergences and compare them with the traditional taxonomy results, allowing an evaluation of the results of the revision.

Keywords: Integrative taxonomy. Neotropical Ichthyofauna. Comparative Anatomy. Species Trees.

Resumo

A pesquisa taxonômica primária ainda apresenta pouca integração entre as ferramentas morfológicas e moleculares para o estudo de peixes neotropicais, apesar de grandes avanços recentes em ambos os campos. Tais ferramentas, se usadas de maneira integrativa, poderiam solucionar grupos reconhecidos por representarem problemas taxonômicos renitentes. O gênero *Pimelodella* Eigenmann & Eigenmann, 1888 se enquadra como um ótimo caso para a aplicação de uma estratégia integrativa e multidisciplinar. *Pimelodella* é um gênero da família Heptapteridae, distribuído amplamente por drenagens sul-americanas trans- e cis-andinas e compreende um dos principais componentes da ictiofauna neotropical. Atualmente é reconhecido como o maior gênero da família, com 79 espécies válidas descritas. Entretanto, a validade e delimitação dessas espécies é problemática, devido à elevada diversidade do gênero, aliada à ampla distribuição, morfologia conservada e descrições antigas e imprecisas. Trata-se de um dos grandes gargalos taxonômicos na sistemática e taxonomia de peixes neotropicais. Este projeto apresenta uma revisão taxonômica de *Pimelodella* utilizando uma abordagem integrativa morfológica-molecular. A revisão taxonômica clássica cobre a integridade da diversidade do gênero, com todos os componentes deste tipo de estudo. Todos os tipos foram examinados, e o número de espécies válidas é aqui reduzido para 55 espécies, para as quais descrições completas são apresentadas. A parte molecular foi realizada em um subgrupo delimitado, com diversidade suficiente para que as estimativas de divergência molecular pudessem ser comparadas aos resultados da revisão morfológica, fornecendo um modelo de avaliação para o restante da revisão.

Palavras-chave: Taxonomia integrativa. Ictiofauna Neotropical. Anatomia Comparada. Árvores de espécies.

Tables list

Table 1. Nominal species available for *Pimelodella* genus.

Table 2. Species analyzed in PCAs.

Table 3. Species currently placed in *Pimelodella* and their status as proposed by this work.

Table 4. Morphometric data of *Pimelodella australis* based on type and comparative materials.

Table 5. Morphometric data of *Pimelodella avanhandavae* based on type and comparative materials.

Table 6. Morphometric data of *Pimelodella boliviana* based on type and comparative materials.

Table 7. Morphometric data of *Pimelodella insignis*, junior-synonym of *P. boschmai*, based on type material.

Table 8. Morphometric data of *Pimelodella brasiliensis* and its junior-synonyms, *P. eigenmanni* and *P. rendahli*, based on type materials.

Table 9. Morphometric data of *Pimelodella brasiliensis* and its junior-synonyms, *P. eigenmanni* and *P. rendahli*, based on type materials, discriminated by original species name.

Table 10. Morphometric data of *Pimelodella buckleyi* based on type and comparative materials.

Table 11. Morphometric data of *Pimelodella chagresi* based on type and comparative materials.

Table 12. Morphometric data of *Pimelodella conquetaensis* based on type material.

Table 13. Morphometric data of *Pimelodella cristata* and its junior-synonyms, *P. cristata*, *P. breviceps*, *P. dorseyi*, *P. hartwelli*, *P. ophthalmica*, *P. parnahybae*, *P. steindachneri*, *P. wessellii*, *P. witmeri*, based on type and comparative materials.

Table 14. Morphometric data of *Pimelodella cristata* and its junior-synonyms, *P. cristata*, *P. breviceps*, *P. dorseyi*, *P. hartwelli*, *P. ophthalmica*, *P. parnahybae*, *P. steindachneri*, *P. wessellii*, *P. witmeri*, based on type and comparative materials, discriminated by original species name.

Table 15. Meristic data of *P. cristata* and its junior-synonyms, *P. cristata*, *P. breviceps*, *P. cyanostygma*, *P. dorseyi*, *P. hartwelli*, *P. ophthalmica*, *P. parnahybae*, *P. steindachneri*, *P. wessellii*, *P. witmeri*, discriminated by the original species name and region.

Table 16. Morphometric data of *Pimelodella cruxenti* based on type (as presented in original description) and comparative materials.

Table 17. Morphometric data of *Pimelodella elongata* based on type and comparative material.

Table 18. Morphometric data of *Pimelodella enochi* and *P. papariae*, its junior-synonym, based on type material and discriminated by original species name.

Table 19. Morphometric data of *Pimelodella eutaenia* based on type and comparative material.

Table 20. Morphometric data of *Pimelodella figueroai* based on type material.

Table 21. Morphometric data of *Pimelodella geryi* and *P. procera*, its junior-synonym, based on type and comparative materials.

Table 22. Morphometric data of *Pimelodella geryi* and *P. procera*, its junior-synonym, based on type and comparative materials, discriminated by original species name.

Table 23. Morphometric data of *Pimelodella gracilis* and *P. taenioptera*, its junior-synonym, based on type and comparative materials.

Table 24. Morphometric data of *Pimelodella gracilis* and *P. taenioptera*, its junior-synonym, based on type and comparative materials, discriminated by original species name.

Table 25. Morphometric data of *Pimelodella griffini* based on type material.

Table 26. Morphometric data of *Pimelodella grisea* based on type material.

Table 27. Morphometric data of *Pimelodella harttii* based on type material.

Table 28. Morphometric data of *Pimelodella hasemani* based on type and comparative materials.

Table 29. Morphometric data of *Pimelodella howesi* based on type and comparative materials.

Table 30. Morphometric data of *Pimelodella humeralis* based on type material.

Table 31. Morphometric data of *Pimelodella ignobilis* and *P. pappenheimi*, its junior-synonym, based on type and comparative materials.

Table 32. Morphometric data of *Pimelodella ignobilis* and *P. pappenheimi*, its junior-synonym, based on type and comparative materials, discriminated by original species name.

Table 33. Morphometric data of *Pimelodella itapicuruenensis* based on type material.

Table 34. Morphometric data of *Pimelodella kronei* and *P. transitoria*, its junior-synonym, based on type and comparative materials.

Table 35. Morphometric data of *Pimelodella kronei* and *P. transitoria*, its junior-synonym, based on type and comparative materials, discriminated by original species name.

Table 36. Morphometric data of *Pimelodella lateristriga* and *P. bahiana*, its junior-synonym, based on type and comparative materials.

Table 37. Morphometric data of *Pimelodella lateristriga* and *P. bahiana*, its junior-synonym, based on type and comparative materials, discriminated by original species name.

Table 38. Morphometric data of *Pimelodella laticeps* based on type material.

Table 39. Morphometric data of *Pimelodella laurenti* based on type and comparative materials.

Table 40. Morphometric data of *Pimelodella leptosoma* based on type and comparative materials.

Table 41. Morphometric data of *Pimelodella linami* based on type material.

Table 42. Morphometric data of *Pimelodella longipinnis* based on type material.

Table 43. Morphometric data of *Pimelodella macturki* based on type material.

Table 44. Morphometric data of *Pimelodella meeki* and *P. rudolphi*, its junior-synonym, based on type and comparative materials.

Table 45. Morphometric data of *Pimelodella meeki* and *P. rudolphi*, its junior-synonym, based on type and comparative materials, discriminated by original species name.

Table 46. Morphometric data of *Pimelodella megalops* based on type and comparative materials.

Table 47. Morphometric data of *Pimelodella megalura* based on type material.

Table 48. Morphometric data of *Pimelodella metae* based on type material.

Table 49. Morphometric data of *Pimelodella modesta* based on type and comparative materials.

Table 50. Morphometric data of *Pimelodella montana* based on type and comparative materials.

Table 51. Morphometric data of *Pimelodella mucosa* based on type and comparative materials.

Table 52. Morphometric data of *Pimelodella notomelas* based on type and comparative materials.

Table 53. Morphometric data of *Pimelodella odynea* based on type material.

Table 54. Morphometric data of *Pimelodella pectinifera* based on type material.

Table 55. Morphometric data of *Pimelodella peruana* based on type and comparative materials.

Table 56. Morphometric data of *Pimelodella reyesi* based on type and comparative materials.

Table 57. Morphometric data of *Pimelodella robinsoni* and *P. wolfi*, its junior-synonym, based on type material.

Table 58. Morphometric data of *Pimelodella robinsoni* and *P. wolfi*, its junior-synonym, based on type material, discriminated by original species name.

Table 59. Morphometric data of *Pimelodella roccae* based on type and comparative materials.

Table 60. Morphometric data of *Pimelodella serrata* and *P. chaparae*, its junior-synonym, based on type and comparative materials.

Table 61. Morphometric data of *Pimelodella serrata* and *P. chaparae*, its junior-synonym, based on type and comparative materials, discriminated by original species name.

Table 62. Morphometric data of *Pimelodella spelaea* based on type material.

Table 63. Morphometric data of *Pimelodella straminea* based on type material.

Table 64. Morphometric data of *Pimelodella taeniophora* based on type and comparative materials.

Table 65. Morphometric data of *Pimelodella tapatapae* based on type material.

Table 66. Morphometric data of *Pimelodella vittata* based on type and comparative materials.

Table 67. Morphometric data of *Pimelodella yuncensis* and *P. peruensis*, its junior-synonym, based on type and comparative materials.

Table 68. Morphometric data of *Pimelodella yuncensis* and *P. peruensis*, its junior-synonym, based on type and comparative materials, discriminated by original species name.

Table 69. Identification Key for the valid *Pimelodella* species diagnosable in this work.

Table 70. Complete material list analyzed for molecular taxonomy.

Table 71. Successfully sequenced specimens per gene.

Table 72. Fragment length, number of parsimony informative sites, GC content and mean bootstrap values per gene.

Figures list

Figure 1: Schematic for particular measurements taken point-to-point in a generalized *Pimelodella* specimen

Figure 2: Schematic for head laterosensory canals, dorsal view, in a generalized *Pimelodella* specimen. Scale bar 2mm.

Figure 3: Schematic for head laterosensory canals, lateral view, in a generalized *Pimelodella* specimen. Scale bar 2mm.

Figure 4: Schematic for head laterosensory canals, ventral view, in a generalized *Pimelodella* specimen. Scale bar 2mm.

Figure 5: *Pimelodella australis*, holotype, FMNH 57962, 61.0 mm SL. Left lateral (A), and dorsal (B) views. Photo taken by M. W. Littmann.

Figure 6: Ventral view of left pectoral-fin spine of *Pimelodella australis*, holotype, 61.0mm SL, total length of spine 12.6 mm.

Figure 7: Schematic left lateral view of *Pimelodella australis*.

Figure 8: *Pimelodella avanhandavae*, holotype, FMNH 57981, 69.0 mm SL. Left lateral (A), and dorsal (B) views. Photo taken by M. W. Littmann.

Figure 9: Ventral view of left pectoral-fin spine of *Pimelodella avanhandavae* FMNH 57982, paratype, 78.8 mm SL, total length of spine 13.4 mm.

Figure 10: Schematic left lateral view of *Pimelodella avanhandavae*.

Figure 11: *Pimelodella boliviana*, holotype, FMNH 57976, 68.9 mm SL. Left lateral (A), and dorsal (B) views. Photo taken by M. W. Littmann.

Figure 12: Ventral view of left pectoral-fin spine of *Pimelodella boliviana* A) FMNH 57977, paratype, 66.9 mm SL, total length of spine 11.5 mm; B) MZUSP 26015, 71.3 mm SL, total length of spine 11.7 mm.

Figure 13: Schematic left lateral view of *Pimelodella boliviana*.

Figure 14: *Pimelodella boschmai*, holotype, RMNH 23248, 73.0 mm SL. Left lateral (A), and dorsal (B) views. Photo taken by Ronald de Ruiter.

Figure 15: Ventral view of left pectoral-fin spine of A) *Pimelodella boschmai*, RMNH 23248, holotype, 73.0 mm SL; B) *Pimelodella insignis*, MZUSP 22317, syntype 66.4 mm SL, total length of spine 12.8 mm.

Figure 16: Schematic left lateral view of *Pimelodella boschmai*

Figure 17: *Pimelodella brasiliensis*, holotype, NMW 45612, 140.6 mm SL. Left lateral (A), and dorsal (B) views. Photos taken by Mark Sabaj. *Pimelodella eigenmanni*, junior-

synonym of *P. brasiliensis*, paralectotype, MCZ 7438, 130.7 mm SL, left lateral (C), and dorsal (D) views. *Pimelodella rendahli*, junior-synonym of *P. brasiliensis*, holotype, ZMB 32031, 80.7 mm SL, left lateral (E), and dorsal (F) views, photo taken by ZMB staff.

Figure 18: Ventral view of left pectoral-fin spine of *Pimelodella brasiliensis*, NMW 45612, holotype, 140.6 mm SL, total length of spine 26.6 mm.

Figure 19: Schematic left lateral view of *Pimelodella brasiliensis*

Figure 20: *Pimelodella buckleyi*, lectotype, BMNH 1880.12.8.98, 109.6 mm SL. Left lateral (A), and dorsal (B) views. Photo taken by Mark Allen.

Figure 21: Ventral view of left pectoral-fin spine of *Pimelodella buckleyi*, BMNH 1880.12.8.98, lectotype, 109.6 mm SL, total length of spine 15.3 mm.

Figure 22. Schematic left lateral view of *Pimelodella buckleyi*

Figure 23. *Pimelodella chagresi*, lectotype, MCZ 4947, 111.8 mm SL. Left lateral (A), and dorsal (B) views.

Figure 24. Ventral view of left pectoral-fin spine of *Pimelodella chagresi*, CAS 57903, 83.5 mm SL, total length of spine 15.1 mm.

Figure 25. Schematic left lateral view of *Pimelodella chagresi*

Figure 26. *Pimelodella conquetaensis*, holotype, ZMB 32032, 93.2 mm SL. Left lateral (A), and dorsal (B) views. Photo taken by Mark Allen.

Figure 27. Ventral view of left pectoral-fin spine of *Pimelodella conquetaensis*, ZMB 32032, holotype, 93.2 mm SL, total length of spine 16.5 mm.

Figure 28. Schematic left lateral view of *Pimelodella conquetaensis*

Figure 29. *Pimelodella cristata*, lectotype, ZMB 3053, 202.5 mm SL. Left lateral (A), and dorsal (B) views.

Figure 30. Ventral view of left pectoral-fin spine of *Pimelodella cristata*, ZMB 3052, paralectotype, 177.5 mm SL, total length of spine 27.8 mm.

Figure 31. Schematic left lateral view of *Pimelodella cristata*.

Figure 32. Framed graphic of PC1 against PC2 of a Principal Component Analysis using all morphometric data scaled to SL or HL (except caudal-fin lobes, due to usual incompleteness of those in the material), based on type and comparative materials of *P. cristata*, *P. cruxenti*, *P. breviceps*, *P. dorseyi*, *P. gracilis*, *P. hartwelli*, *P. humeralis*, *P. ophthalmica*, *P. parnahybae*, *P. steindachneri*, *P. taenioptera*, *P. wessellii*, *P. witmeri*. Cumulative proportion of importance of components: 39.4%; proportion of Variance: PC1—20.3%; PC2—19.1%; standard deviation: PC1—2.01; PC2—2.0.

Figure 33. Framed graphic of PC1 against PC2 of a Principal Component Analysis using all morphometric data scaled to SL or HL (except caudal-fin lobes, due to usual incompleteness of those in the material), based on type and comparative materials, separated by drainages as follows: Amazon— Amazon rivers' specimens of *P. cristata*, *P. breviceps*, *P. hartwelli*, *P. ophthalmica* and Amazon rivers' specimens of *P. steindachneri*; Guiana Shield— Guiana Shield rivers' specimens of *P. cristata* and *P. wessellii*; Northeastern Brazil— *P. dorseyi*, *P. parnahybae*, Parnaíba drainage type-specimen of *P. steindachneri* and *P. witmeri*; Paraná— *P. gracilis* and *P. taenioptera*; *P. humeralis*. Cumulative proportion of importance of components: 37.8%; proportion of Variance: PC1— 21.5%; PC2— 16.3%; standard deviation: PC1— 2.07; PC2— 1.8.

Figure 34. *Pimelodella breviceps*, holotype, NMW 45615, 326.2 mm SL. Left lateral (A), and dorsal (B) views.

Figure 35. *Pimelodella cyanostigma*, lectotype, ANSP 8382, 59.8 mm SL. Left lateral (A), and dorsal (B) views. Photo taken by Mark Sabaj.

Figure 36. *Pimelodella dorseyi*, holotype, ANSP 69375, 95.8 mm SL. Left lateral (A), and dorsal (B) views. Photo taken by Murilo Pastana.

Figure 37. *Pimelodella hartwelli*, holotype, ANSP 68644, 103.2 mm SL. Left lateral (A), and dorsal (B) views.

Figure 38. *Pimelodella ophthalmica*, holotype, ANSP 21102, 109.9 mm SL. Left lateral (A), and dorsal (B) views.

Figure 39. *Pimelodella parnahybae*, holotype, ANSP 69337, 84.0 mm SL. Left lateral (A), and dorsal (B) views. Photo taken by Kyle Luckenbill.

Figure 40. *Pimelodella steindachneri*, lectotype, MCZ 7487, 150.4 mm SL. Left lateral (A), and dorsal (B) views. Photo taken by MCZ staff.

Figure 41. *Pimelodella wessellii*, holotype, NMW 79188, 157.9 mm SL. Left lateral (A), and dorsal (B) views. Photo taken by Mark Sabaj and Kyle Luckenbill.

Figure 42. *Pimelodella witmeri*, holotype, ANSP 69383, 137.5 mm SL. Left lateral (A), and dorsal (B) views. Photo taken by Kyle Luckenbill.

Figure 43. *Pimelodella cruxenti*, lectotype, MHNLS 95.8 mm SL. Left lateral (A), and dorsal (B) views. Photo taken by Oscar Lasso-Alcalá.

Figure 44. Ventral view of left pectoral-fin spine of *Pimelodella cruxenti*, ANSP 160647, 75.2 mm SL.

Figure 45. Schematic left lateral view of *Pimelodella cruxenti*.

Figure 46. Left lateral view (A) and dorsal view of head (B) of *Pimelodella cruxenti*, ANSP 160673, 127.7 mm SL. Photo taken by Mark Sabaj.

Figure 47. *Pimelodella elongata*, lectotype, BMNH 1860.6.16.182, 136.8 mm SL. Left lateral (A), and dorsal (B) views. Photo taken by Mark Allen.

Figure 48. Ventral view of left pectoral-fin spine of *Pimelodella elongata*, BMNH 1860.6.16.186, paralectotype, 96.1 mm SL, total length of spine 12.1 mm.

Figure 49. Schematic left lateral view of *Pimelodella elongata*

Figure 50. *Pimelodella enochi*, holotype, ANSP 69378, 44.9 mm SL. Left lateral (A), and dorsal (B) views. Photo taken by Murilo Pastana.

Figure 51. Ventral view of left pectoral-fin spine of *Pimelodella enochi*, ANSP 69378, 44.9 mm SL, total length of spine 6.8 mm.

Figure 52. Schematic left lateral view of *Pimelodella enochi*.

Figure 53. *Pimelodella papariae*, junior synonym of *P. enochi*, holotype, ANSP 69387, 109.6 mm SL. Left lateral (A), and dorsal (B) views. Photo taken by Murilo Pastana.

Figure 54. Ventral view of left pectoral-fin spine of *Pimelodella papariae*, ANSP 69387, 109.6 mm SL, total length of spine (approximate) 18.5 mm (tip of spine was broken, and figure correspond to the complete aspect).

Figure 55. *Pimelodella eutaenia*, lectotype, BMNH 1913.10.1.37, 126.3 mm SL. Left lateral (A), and dorsal (B) views. Photo taken by Mark Allen.

Figure 56. Ventral view of left pectoral-fin spine of *Pimelodella eutaenia*, BMNH 1913.10.1.37, 126.3 mm SL, total length of spine 20.2 mm (A); BMNH 1913.10.1.38, 65.5 mm SL, total length of spine 12 mm (B).

Figure 57. Schematic left lateral view of *Pimelodella eutaenia*

Figure 58. *Pimelodella floridablancaensis*, junior-synonym of *P. eutaenia*, paratype, CAR 695, 85.8 mm SL. Figure obtained from Ardila Rodriguez (2017).

Figure 59. Ventral view of left pectoral-fin spine of *Pimelodella floridablancaensis*, CAR 07, obtained from Ardila Rodriguez (2017). Sizes of specimen or structure were not indicated, but paratype list cited c&s specimens between 74.9–93.2 mm SL.

Figure 60. *Pimelodella figueroai*, ICN-MHN 2900, 71.8 mm SL. Left lateral view. Photo taken by Mauricio Leiva.

Figure 61. *Pimelodella geryi*, holotype, ZMA 102235, 58 mm SL. Left lateral (A), and dorsal (B) views. Photo taken by Ronald De Ruiter.

Figure 62. Ventral view of left pectoral-fin spine of *Pimelodella geryi*, holotype, ZMA 102235, 58 mm SL, total length of spine 10.0 mm (approximately).

Figure 63. Schematic left lateral view of *Pimelodella geryi*

Figure 64. *Pimelodella procera*, junior-synonym of *P. geryi*, paratype, 61.5 mm SL. Left lateral view. Photo taken by Mário de Pinna.

Figure 65. *Pimelodella gracilis*, holotype, MHNH 9284-A, 170.1 mm SL. Left lateral (A), and dorsal (B) views. Photo taken by Mélyne Hautecoeur.

Figure 66. Ventral view of left pectoral-fin spine of *Pimelodella gracilis*, holotype, MHNH 9284-A, 170.1 mm SL, total length of spine 28.5 mm.

Figure 67. Schematic left lateral view of *Pimelodella gracilis*.

Figure 68. *Pimelodella taenioptera*, junior-synonym of *P. gracilis*, lectotype, MNRJ 691A, 157.8 mm SL. Left lateral (A), and dorsal (B) views.

Figure 69. Material identified as *Pimelodella taenioptera* from Souza-Shibatta *et al.* (2013), showing color pattern and dorsal-fin filament. MZUEL 6456, 124.6 mm SL, photo extracted from Souza-Shibatta *et al.* (2013).

Figure 70. Framed graphic of PC1 against PC2 of a Principal Component Analysis using all morphometric data scaled to SL or HL (except caudal-fin lobes, due to usual incompleteness of those in the material), based on type and comparative materials of *Pimelodella* species with 46 or more total vertebrae (except *P. cruxenti*), discriminated by the names considered as valid in this work, being *P. cristata*, *P. gracilis* and *P. humeralis*. Cumulative proportion of importance of components: 37.8%; proportion of Variance: PC1— 21.4%; PC2— 16.5%; standard deviation: PC1— 2.07; PC2— 1.8.

Figure 71. *Pimelodella griffini*, holotype, FMNH 57974, 67.2 mm SL. Left lateral (A), and dorsal (B) views. Photo taken by M. W. Littmann.

Figure 72. Ventral view of left pectoral-fin spine of *Pimelodella griffini*, holotype, FMNH 57974, 67.2 mm SL, total length of spine 11.3 mm.

Figure 73. Schematic left lateral view of *Pimelodella griffini*.

Figure 74. *Pimelodella grisea*, lectotype, BMNH 1902.5.27.36, 119.7 mm SL. Left lateral (A), and dorsal (B) views. Photo taken by Mark Allen.

Figure 75. Ventral view of left pectoral-fin spine of *Pimelodella grisea*, lectotype, BMNH 1902.5.27.36, 119.7 mm SL, total length of spine 22.4 mm.

Figure 76. Schematic left lateral view of *Pimelodella grisea*.

Figure 77. *Pimelodella harttii*, holotype, NMW 45784, 150.2 mm SL. Left lateral (A), and dorsal (B) views.

Figure 78. Ventral view of left pectoral-fin spine of *Pimelodella harttii*, holotype, NMW 45784, 150.2 mm SL, total length of spine 25.6 mm.

Figure 79. Schematic left lateral view of *Pimelodella harttii*.

Figure 80. *Pimelodella hasemani*, holotype, FMNH 57980, 60.6 mm SL. Left lateral (A), and dorsal (B) views. Photo taken by M. W. Littmann.

Figure 81. Ventral view of left pectoral-fin spine of *Pimelodella hasemani*, FMNH 57980, 60.6 mm SL, total length of spine 10.6 mm.

Figure 82. Schematic left lateral view of *Pimelodella hasemani*.

Figure 83. *Pimelodella hasemani*, UFRO-I 9741, 56.5 mm SL. Left lateral (A), and dorsal (B) views.

Figure 84. *Pimelodella howesi*, ANSP 69036, 79.3 mm SL. Left lateral (A), and dorsal (B) views.

Figure 85. Ventral view of left pectoral-fin spine of *Pimelodella howesi*, ANSP 69036, 79.3 mm SL, total length of spine 14.1 mm.

Figure 86. Schematic left lateral view of *Pimelodella howesi*.

Figure 87. *Pimelodella humeralis*, holotype, MPEG 34994, 77.4 mm SL. Left lateral (A) and dorsal (B) views.

Figure 88. Ventral view of left pectoral-fin spine of *Pimelodella humeralis*, holotype, MPEG 34994, 77.4 mm SL, total length of spine 12.0 mm.

Figure 89. Schematic left lateral view of *Pimelodella humeralis*.

Figure 90. *Pimelodella ignobilis*, lectotype, NMW 44479, 91.1 mm SL. Left lateral (A) and dorsal (B) views.

Figure 91. Ventral view of left pectoral-fin spine of *Pimelodella ignobilis*, paralectotype, NMW 44479, 98.9 mm SL, total length of spine 19.0 mm.

Figure 92. Schematic left lateral view of *Pimelodella ignobilis*.

Figure 93. *Pimelodella pappenheimi*, junior-synonym of *P. ignobilis*, lectotype, ZMB 31951, 103.1 mm SL. Left lateral (A) and dorsal (B) views.

Figure 94. *Pimelodella itapicuruensis*, FMNH 57986, 60.2 mm SL. Left lateral (A) and dorsal (B) views.

Figure 95. Ventral view of left pectoral-fin spine of *Pimelodella itapicuruensis*, FMNH 57986, 60.2 mm SL, total length of spine 11.2 mm.

Figure 96. Schematic left lateral view of *Pimelodella itapicuruensis*.

Figure 97. *Pimelodella kronei*, holotype, MNRJ 836, 120.1 mm SL. Left lateral (A) and dorsal (B) views.

Figure 98. Ventral view of left pectoral-fin spine of *Pimelodella kronei*, LESCOI 170, 93.4 mm SL, total length of spine 12.5 mm.

Figure 99. Schematic left lateral view of *Pimelodella kronei*.

Figure 100. Map of stream routs and flux of Areias system, obtained from Genthner *et al.* (2006: fig. 6). Arrows: Areias (1) and Bombas (2) resurgences.

Figure 101. Right lateral view of head of *P. kronei*. Infraorbital series and nasal removed. (A) MZUSP 38725, Bombas resurgence, Iporanga; (B) MZUSP 27168, Areias system, Iporanga.

Figure 102. Right lateral view of head of *P. transitoria*. Infraorbital series and nasal removed. MZUSP 63365, Ribeirão Furnas, Areias system, Iporanga.

Figure 103. Right lateral view of *P. lateristriga*. Infraorbital series and nasal removed. USNM 301676, Rio Mucuri, Northeastern Mata Atlântica region.

Figure 104. (A) Dorsal view; (B) Ventral view; and (C) Left lateral view of head of a *Pimelodella*, showing the overall arrangement of cephalic laterosensorial system. Grey legends are for a simple pore for both *P. kronei* and *P. transitoria*. Purple legends are for different conditions (loss or duplication) of a pore in individuals of both species. Red legends are for loss or duplication of a pore exclusively for *P. kronei* specimens. Scale bar: 2mm.

Figure 105. Ventral view of left pectoral-fin spine of *Pimelodella kronei*, LESCI uncat. 113.2 mm SL, length of spine 12.5 mm, Areias system (A); LESCI 167 144.4 mm SL, length of spine 20.4 mm, Areias system (B); LESCI 169 110.7 mm SL, length of spine 13.4 mm, Bombas resurgence (C); and *P. transitoria*, LESCI uncat. 101.8 mm SL, length of spine 16.7 mm, Rio Betari, alojamento ouro grosso (D); LESCI 95 85.5 mm SL, length of spine 14.0 mm, Rio Betari (E); LESCI 168 98.1 mm SL, length of spine 15.9 mm, Gruta da Casa de Pedra (F).

Figure 106. Left lateral view of *Pimelodella transitoria*, LESCI 168, 98.1 mm SL.

Figure 107. Neotype of *Pimelodella transitoria*, a junior-synonym of *P. kronei*, MZUSP 403, 107.4 mm SL. Photo taken by Murilo Pastana.

Figure 108. *Pimelodella lateristriga*, holotype, ZMB 3038, 95,9 mm SL. Left lateral (A) and dorsal (B) views. Photo taken by Johanna Kapp.

Figure 109. Ventral view of left pectoral-fin spine of: (A) *Pimelodella lateristriga*, holotype, ZMB 3038, 95,9 mm SL, total length of spine 18.0 mm (approximated); (B) *Pimelodella lateristriga*, MZUSP 114867, 84 mm SL, total length of spine 14.5 mm; (C) *Pimelodella lateristriga*, MZUSP 93863, 99.5 mm SL, total length of spine 15.7 mm; (D) *Pimelodella bahiana*, lectotype, MNHN B612, 93.4 mm SL, total length of spine 16.1 mm.

Figure 110. Schematic left lateral view of *Pimelodella lateristriga*.

Figure 111. *Pimelodella lateristriga*, MZUSP 121461, 112.7 mm SL. Left lateral (A) and dorsal (B) views. Photo taken by Murilo Pastana.

Figure 112. *Pimelodella bahiana*, lectotype, MNHN B612, 93.4 mm SL. Left lateral (A) and dorsal (B) views. Photo taken by MNHN staff.

Figure 113. *Pimelodella laticeps*, holotype, FMNH 57969, 49.0 mm SL. Left lateral (A) and dorsal (B) views. Photo taken by M. W. Littmann.

Figure 114. Ventral view of left pectoral-fin spine of *Pimelodella laticeps*, holotype, FMNH 57969, 49.0 mm SL, total length of spine 9.6 mm.

Figure 115. Schematic left lateral view of *Pimelodella laticeps*.

Figure 116. *Pimelodella laurenti*, holotype, ANSP 69380, 66.5 mm SL. Left lateral (A) and dorsal (B) views. Photo taken by Murilo Pastana.

Figure 117. Ventral view of left pectoral-fin spine of *Pimelodella laurenti*, holotype, ANSP 69380, 66.5 mm SL, total length of spine 12.7 mm.

Figure 118. Schematic left lateral view of *Pimelodella laurenti*.

Figure 119. Left lateral view of *Pimelodella laurenti*, MZUSP 39441, 62.8 mm SL.

Figure 120. *Pimelodella leptosoma*, holotype, ANSP 39340, 59.6 mm SL. Left lateral (A) and dorsal (B) views. Photo taken by Mark Sabaj.

Figure 121. Ventral view of left pectoral-fin spine of *Pimelodella leptosoma*, holotype, ANSP 39340, 59.6 mm SL, total length of spine 8.5 mm.

Figure 122. Schematic left lateral view of *Pimelodella leptosoma*.

Figure 123. *Pimelodella leptosoma*, ANSP 179754. Left lateral (A) and dorsal (B) views. Photo taken by Mark Sabaj.

Figure 124. *Pimelodella linami*, USNM 121132, holotype, 74.7 mm SL. Left lateral (A) and dorsal (B) views. Photo taken by Sandra Raredon.

Figure 125. Ventral view of left pectoral-fin spine of *Pimelodella linami*, USNM 121132, holotype, 74.7 mm SL, total length of spine 10.7 mm.

Figure 126. Schematic left lateral view of *Pimelodella linami*.

Figure 127. *Pimelodella longipinnis*, AMNH 8642, holotype, 84.6 mm SL. Left lateral (A) and dorsal (B) views. Photo taken by Melanie Stiassny.

Figure 128. Ventral view of left pectoral-fin spine of *Pimelodella longipinnis*, AMNH 8642, holotype, 84.6 mm SL, total length of spine 11.7 mm.

Figure 129. Schematic left lateral view of *Pimelodella longipinnis*.

Figure 130. Radiograph of *Pimelodella longipinnis*, AMNH 8642, holotype, 84.6 mm SL. Left lateral view.

Figure 131. *Pimelodella macturki*, holotype, FMNH 53234, 53.5 mm SL. Left lateral (A) and dorsal (B) views. Photo taken by M. W. Littmann.

Figure 132. Ventral view of left pectoral-fin spine of *Pimelodella macturki*, paratype, BMNH 1911.10.31.54, 52.9 mm SL, total length of spine 9.8 mm.

Figure 133. Schematic left lateral view of *Pimelodella macturki*.

Figure 134. *Pimelodella martinezi*, holotype, 68 mm SL, image from Fernández-Yépez (1970), unnum. page, pl. 35. Left lateral (A) and dorsal view of head (B).

Figure 135. Schematic left lateral view of *Pimelodella martinezi*.

Figure 136. *Pimelodella meeki*, holotype, FMNH 3400, 100.2 mm SL. Left lateral (A) and dorsal (B) views. Photo taken by M. W. Littmann.

Figure 137. Ventral view of left pectoral-fin spine of *Pimelodella meeki*, FMNH 57993, 97.1 mm SL, total length of spine 12 mm.

Figure 138. Schematic left lateral view of *Pimelodella meeki*.

Figure 139. *Pimelodella meeki*, MZUSP 51651, 112.2 mm SL. Left lateral (A) and dorsal (B) views. Photo taken by Murilo Pastana.

Figure 140. *Pimelodella rudolphi*, lectotype, MNRJ 857A, 73.9 mm SL. . Left lateral (A) and dorsal (B) views.

Figure 141. *Pimelodella megalops*, FMNH 53231, holotype, 74.7 mm SL. Left lateral (A) and dorsal (B) views. Photo taken by M. W. Littmann.

Figure 142. Ventral view of left pectoral-fin spine of *Pimelodella megalops*, BMNH 1911.10.31.51, paratype, 67.5 mm SL, total length of spine 13.1 mm.

Figure 143. Schematic left lateral view of *Pimelodella megalops*.

Figure 144. *Pimelodella megalura*, MNRJ 865A, lectotype, 128.6 mm SL. Left lateral (A) and dorsal (B) views.

Figure 145. Ventral view of left pectoral-fin spine of *Pimelodella megalura*, MNRJ 865A, lectotype, 128.6 mm SL, total length of spine 15.2 mm.

Figure 146. Schematic left lateral view of *Pimelodella megalura*.

Figure 147. *Pimelodella metae*, FMNH 58441, holotype, 58.0 mm SL. Left lateral (A) and dorsal (B) views. Photo taken by M. W. Littmann.

Figure 148. Ventral view of left pectoral-fin spine of *Pimelodella metae*, FMNH 58441, holotype, 58.0 mm SL, total length of spine 9.1 mm.

Figure 149. Schematic left lateral view of *Pimelodella metae*.

Figure 150. *Pimelodella modesta*, BMNH 1860.6.16.190, lectotype, 100.4 mm SL. Left lateral (A) and dorsal (B) views. Photo taken by Mark Allen.

Figure 151. Ventral view of left pectoral-fin spine of *Pimelodella modesta*, BMNH 1860.6.16.190, lectotype, 100.4 mm SL, total length of spine 14.8 mm.

Figure 152. Schematic left lateral view of *Pimelodella modesta*.

Figure 153. *Pimelodella montana*, CAS 63719, lectotype, 87.4 mm SL. Left lateral (A) and dorsal (B) views. Photo taken by CAS staff.

Figure 154. Ventral view of left pectoral-fin spine of *Pimelodella montana*, CAS 63719, paralectotype, 85 mm SL, total length of spine 11 mm.

Figure 155. Schematic left lateral view of *Pimelodella montana*.

Figure 156. *Pimelodella mucosa*, CAS 63720, holotype, 97.4 mm SL. Left lateral (A) and dorsal (B) views. Photo taken by CAS staff.

Figure 157. Ventral view of left pectoral-fin spine of *Pimelodella mucosa*, CAS 63720, holotype, 97.4 mm SL, total length of spine 22.8 mm.

Figure 158. Schematic left lateral view of *Pimelodella mucosa*.

Figure 159. *Pimelodella notomelas*, FMNH 57967, holotype, 38.9 mm SL. Left lateral (A) and dorsal (B) views. Photo taken by M. W. Littmann.

Figure 160. Ventral view of left pectoral-fin spine of *Pimelodella notomelas*, FMNH 57967, holotype, 38.9 mm SL, total length of spine 7.4 mm.

Figure 161. Schematic left lateral view of *Pimelodella notomelas*.

Figure 162. *Pimelodella odynea*, USNM 121133, holotype, 88.3 mm SL. Left lateral (A) and dorsal (B) views. Photo taken by Sandra Raredon.

Figure 163. Ventral view of left pectoral-fin spine of *Pimelodella odynea*, USNM 121133, holotype, 88.3 mm SL, total length of spine 12.9 mm.

Figure 164. Schematic left lateral view of *Pimelodella odynea*.

Figure 165. *Pimelodella pectinifera*, holotype, MCZ 7508, 150.9 mm SL. Left lateral (A) and dorsal (B) views. Photo taken by MCZ staff.

Figure 166. Ventral view of left pectoral-fin spine of *Pimelodella pectinifera*, holotype, MCZ 7508, 150.9 mm SL, total length of spine 31.4 mm.

Figure 167. Schematic left lateral view of *Pimelodella pectinifera*.

Figure 168. *Pimelodella peruana*, holotype, CAS 63721, 40.3 mm SL. Left lateral (A) and dorsal (B) views. Photo taken by CAS staff.

Figure 169. Ventral view of left pectoral-fin spine of *Pimelodella peruana*: (A) holotype, CAS 63721, 40.3 mm SL, total length of spine 6.3 mm; (B) FMNH 102541, 69.9 mm SL, total length of spine 11.2 mm.

Figure 170. Schematic left lateral view of *Pimelodella peruana*.

Figure 171. *Pimelodella reyesi*, ICN-MHN 1331, 98.1 mm SL. Left lateral (A) and dorsal (B) views. Photo taken by Henry Zamora.

Figure 172. Ventral view of left pectoral-fin spine of *Pimelodella reyesi*, ICN-MHN 1331, 98.1 mm SL, total length of spine 18.6 mm.

Figure 173. Schematic left lateral view of *Pimelodella reyesi*.

Figure 174. *Pimelodella robinsoni*, holotype, ANSP 69386, 73 mm SL. Left lateral (A) and dorsal (B) views. Photo taken by Murilo Pastana.

Figure 175. Ventral view of left pectoral-fin spine of *Pimelodella wolfi*, junior-synonym of *P. robinsoni*, holotype, ANSP 69388, 88.9 mm SL, total length of spine 11.3 mm SL.

Figure 176. Schematic left lateral view of *Pimelodella robinsoni*.

Figure 177. *Pimelodella wolfi*, junior-synonym of *P. robinsoni*, holotype, ANSP 69388, 88.9 mm SL. Left lateral (A) and dorsal (B) views. Photo taken by Murilo Pastana.

Figure 178. *Pimelodella roccae*, holotype, MCZ 30975, 139.8 mm SL. Left lateral (A) and dorsal (B) views. Photo taken by MCZ staff.

Figure 179. Ventral view of left pectoral-fin spine of *Pimelodella roccae*, holotype, MCZ 30975, 139.8 mm SL, total length of spine 23.8 mm.

Figure 180. Schematic left lateral view of *Pimelodella roccae*.

Figure 181. *Pimelodella serrata*, holotype, FMNH 57979, 55.7 mm SL. Left lateral (A) and dorsal (B) views. Photo taken by M. W. Littmann.

Figure 182. Left lateral detail of dorsal fin of *Pimelodella serrata*, UFRO-I 9739, 77.1 mm SL, to show dorsal-fin spine morphology.

Figure 183. Ventral view of left pectoral-fin spine of *Pimelodella serrata*, holotype, FMNH 57979, 55.7 mm SL, total length of spine 7.7 mm.

Figure 184. Schematic left lateral view of *Pimelodella serrata*.

Figure 185. *Pimelodella serrata*, UFRO 9745, 83.4 mm SL. Left lateral (A) and dorsal (B) views. Photo extracted from Bockmann & Slobodian (2013).

Figure 186. *Pimelodella chaparae*, junior-synonym of *P. serrata*, holotype, ANSP 69021, 48.1 mm SL. Left lateral (A) and dorsal (B) views. Photo taken by Kyle Luckenbill.

Figure 187. *Pimelodella spelaea*, holotype, MZUSP 81726, 78.9 mm SL. Left lateral (A) and dorsal (B) views. Photo taken by Eduardo Baena.

Figure 188. Ventral view of left pectoral-fin spine of *Pimelodella spelaea*, holotype, MZUSP 81726, 78.9 mm SL, total length of spine 11.0 mm.

Figure 189. Schematic left lateral view of *Pimelodella spelaea*.

Figure 190. *Pimelodella straminea*, lectotype, ANSP 21581, 41.2 mm SL. Left lateral (A) and dorsal (B) views. Photo taken by Kyle Luckenbill.

Figure 191. Ventral view of left pectoral-fin spine of *Pimelodella straminea*, lectotype, ANSP 21581, 41.2 mm SL, total length of spine 7.6 mm.

Figure 192. Schematic left lateral view of *Pimelodella straminea*.

Figure 193. *Pimelodella taeniophora*, lectotype, BMNH 1895.5.17.27, 76.6 mm SL. Left lateral (A) and dorsal (B) views. Photo taken by Mark Allen.

Figure 194. Ventral view of left pectoral-fin spine of *Pimelodella taeniophora*, lectotype, BMNH 1895.5.17.27, 76.6 mm SL, total length of spine 13.6 mm.

Figure 195. Schematic left lateral view of *Pimelodella taeniophora*.

Figure 196. *Pimelodella taeniophora*, MZUEL 6460, 93.2 mm SL, female, extracted from Souza-Shibatta *et al.* (2013).

Figure 197. *Pimelodella tapatapae*, holotype, CAS 57469, 121.6 mm SL. Left lateral (A) and dorsal (B) views.

Figure 198. Ventral view of left pectoral-fin spine of *Pimelodella tapatapae*, holotype, CAS 57469, 121.6 mm SL, total length of spine 18.1 mm.

Figure 199. Schematic left lateral view of *Pimelodella tapatapae*.

Figure 200. *Pimelodella vittata*, lectotype, ZMB 9175, 61.8 mm SL. Left lateral (A) and dorsal (B) views. Photo taken by ZMB staff.

Figure 201. Ventral view of left pectoral-fin spine of *Pimelodella vittata*, paralectotype, ZMB 9175, 53.2 mm SL, total length of spine 9.0 mm.

Figure 202. Schematic left lateral view of *Pimelodella vittata*.

Figure 203. *Pimelodella vittata*, paralectotype, NMW 44442, 57.5 mm SL. Left lateral (A) and dorsal (B) views. Photo taken by Mark Sabaj.

Figure 204. *Pimelodella yuncensis*, lectotype, ZMS 7870, 37.8 mm SL. Left lateral (A) and dorsal (B) views. Photo taken by Natasha Khardina.

Figure 205. Ventral view of left pectoral-fin spine of *Pimelodella yuncensis*, lectotype, ZMS 7870, 37.8 mm SL, total length of spine 5.3 mm.

Figure 206. Schematic left lateral view of *Pimelodella yuncensis*.

Figure 207. Left lateral view of *Pimelodella yuncensis*, CAS 75890, 61.0 mm SL.

Figure 208. Holotype of *Rhamdia gilli*, USNM 53472, 138 mm SL.

Figure 209. *Pimelodella peruensis*, junior-synonym of *P. yuncensis*, holotype, ANSP 21932, 48.2 mm SL. Left lateral (A) and dorsal (B) views.

Figure 210. *Rhamdia altipinnis*, holotype, NMW 45601, 61.2 mm SL. Left lateral (A) and dorsal (B) views.

Figure 211. *Imparfinis macrocephalus*, paratype, MCZ 35879, 23.7 mm SL. Left lateral (A) and dorsal (B) views.

Figure 212. CT scan of *Imparfinis macrocephalus*, paratype, MCZ 35879, 23.7 mm SL. Left lateral (A) and dorsal (B) views. Scans obtained by Andrew Williston.

Figure 213. *Pimelodus parvus* Güntert, 1942, holotype, NMBA 5302, 19.4 mm SL. Left lateral (A) and dorsal (B) views. Photo taken by Natasha Khardina.

Figure 214. Simplified version of the species tree reconstructed through ASTRAL-III, based on COI, CytB, 36268e1 and 4174e20 genes, for a total of 90 specimens (80 *Pimelodella*).

Figure 215. Clade A relative to Figure 214. Branch values correspond to bootstrap (%).

Figure 216. Clade B relative to Figure 214. Branch values correspond to bootstrap (%).

Figure 217. Clade C relative to Figure 214. Branch values correspond to bootstrap (%).

Figure 218. Clade D relative to Figure 214. Branch values correspond to bootstrap (%).

Figure 219. Clade E relative to Figure 214. Branch values correspond to bootstrap (%).

Figure 220. Simplified version of the species tree reconstructed through ASTRAL-III, based on COI, CytB, 36268e1 and 4174e20 genes. Nodes with bootstrap value inferior to 50% were collapsed. Dotted boxes present the delimitation for taxa illustrated in Figures 221–226.

Figure 221. Clade A relative to Figure 220. Branch values correspond to bootstrap (%).

Figure 222. Clades B1, B2 and other taxa according to delimitation box in Figure 220. Branch values correspond to bootstrap (%).

Figure 223. Clade B3, according to delimitation box in Figure 220. Branch values correspond to bootstrap (%).

Figure 224. Clade C', according to delimitation box in Figure 220. Branch values correspond to bootstrap (%).

Figure 225. Clade D' and other taxa according to delimitation box in Figure 220. Branch values correspond to bootstrap (%).

Figure 226. Clade E', according to delimitation box in Figure 220. Branch values correspond to bootstrap (%).

Figure 227. Best tree obtained by a Maximum Likelihood analysis on concatenate matrix of COI, CytB, 36268e1 and 4174e20 genes. Node values correspond to bootstrap (%). Nodes with “–” were not recovered in bootstrap tree. Dotted boxes present the delimitation for taxa illustrated in Figures 228–233.

Figure 228. Clade A, according to delimitation box in Figure 227. Branch values correspond to bootstrap (%).

Figure 229. Clade B2”, according to delimitation box in Figure 227. Branch values correspond to bootstrap (%).

Figure 230. Clade B3”, according to delimitation box in Figure 227. Branch values correspond to bootstrap (%), clades not recovered in bootstrap tree are indicate by –.

Figure 231. Specimens of orange delimitation box of Figure 227, corresponding to clade C” and other taxa. Branch values correspond to bootstrap (%), clades not recovered in bootstrap tree are indicate by –.

Figure 232. Specimens of green delimitation box of Figure 227, corresponding to clade D” and other taxa. Branch values correspond to bootstrap (%).

Figure 233. Clade E”, according to delimitation box in Figure 227. Branch values correspond to bootstrap (%), clades not recovered in bootstrap tree are indicate by –.

Figure 234. Distribution map of the following *Pimelodella*: *P. australis*.— red star: holotype and paratypes; *P. boschmai*.— purple star: holotype, purple circle: other material; *P. brasiliensis*.— yellow star: holotype, yellow circle: other material, yellow triangle: lectotype of *P. eigenmanni*, junior-synonym of *P. brasiliensis*; *P. harttii*.— dark blue star: holotype, dark blue circle: other material; *P. ignobilis*.— green star: holotype; green circle: other material; *P. kronei*.— light blue star: holotype, light blue circle: other material; light blue triangle: neotype of *P. transitoria*, junior-synonym of *P. kronei*; *P. lateristriga*.— pink star: holotype, pink circle: other material, pink triangle: lectotype of *P. bahiana*, junior-synonym of *P. lateristriga*.

Figure 235. Distribution map of the following *Pimelodella*: *P. avanhandavae*.— red star: holotype, red circle: other material; *P. gracilis*.— purple star: lectotype, purple circle: other material, purple triangle: lectotype of *P. taenioptera*, junior-synonym of *P. gracilis*; *P. griffini*.— yellow star (same place as blue star): holotype, yellow circle: other material; *P.*

laticeps.— dark blue star: holotype; dark blue circle: other material; *P. longipinnis*.— light green star: holotype; *P. meeki*.— dark green star: holotype, dark green circle: other material, dark green triangle: lectotype of *P. rudolphi*, junior-synonym of *P. meeki*; *P. pectinifera*.— light blue star: holotype; *P. straminea*.— pink star: holotype, pink circle: other material; *P. taeniophora*. — orange star: lectotype, orange circle: other material.

Figure 236. Distribution map of the following *Pimelodella*: *P. enochi*.— red star: holotype, red circle: other material, red triangle: holotype of *P. papariae*, junior-synonym of *P. enochi*; *P. itapicuruensis*.— purple star: holotype, purple circle: other material; *P. laurenti*.— yellow star: holotype, yellow circle: other material; *P. mucosa*.— dark blue star: holotype; dark blue circle: other material; *P. notomelas*.— light green star: holotype, light green circle: other material; *P. robinsoni*.— dark green star: holotype, dark green circle: other material, dark green triangle: holotype of *P. wolffi*, junior-synonym of *P. robinsoni*; *P. spelaea*.— light blue star: holotype, light blue circle: other material; *P. vittata*.— pink star: holotype, pink circle: other material.

Figure 237. Distribution map of the following *Pimelodella*: *P. boliviana*.— red star: holotype, red circle: other material; *P. hasemani*.— purple star: holotype, purple circle: other material; *P. howesi*.— yellow star: holotype, yellow circle: other material; *P. megalura*.— dark blue star: holotype; dark blue circle: other material; *P. montana*.— light green star: holotype, light green circle: other material; *P. modesta*.— dark green star: holotype, dark green circle: other material; *P. peruana*.— pink star: holotype, pink circle: other material; *P. roccae*.— orange star: holotype, orange circle: other material.

Figure 238. Distribution map of the following *Pimelodella*: *P. buckleyi*.— red star: lectotype, red circle: other material, red triangle: paralectotype of *P. cyanostigma*, junior-synonym of *P. buckleyi*, red diamond: holotype of *P. copei*, junior-synonym of *P. buckleyi*; *P. conquetaensis*.— purple star: holotype; *P. cruxenti*.— yellow star: lectotype, yellow circle: other material; *P. elongata*.— dark blue star: lectotype; dark blue circle: other material; *P. eutaenia*.— light green star: lectotype, light green circle: other material; *P. figueroai*.— dark green star: paratype; *P. grisea*.— pink star: holotype, pink circle: other material.

Figure 239. Distribution map of the following *Pimelodella*: *P. chagresi*.— red star: lectotype, red circle: other material; *P. linami*.— purple star: holotype; *P. metae*.— yellow star: holotype, yellow circle: other material; *P. odynea*.— dark blue star: holotype; dark blue circle: other material; *P. reyesi*.— light green circle: other material; *P. serrata*.— dark green star: holotype, dark green circle: other material, dark green triangle: holotype of *P. chaparae*, junior-synonym of *P. serrata*; *P. yuncensis*.— pink star: lectotype, pink circle: other material.

Figure 240. Distribution map of the following *Pimelodella*: *P. cristata*.— red star: lectotype, red circle: other material, red triangle: holotype of *P. breviceps*, junior-synonym of *P. cristata*, red diamond: lectotype of *P. cyanostygma*, junior-synonym of *P. cristata*, red arrow: holotype of *P. dorseyi*, junior-synonym of *P. cristata*, red half diamond: holotype of *P. hartwelli*, junior-synonym of *P. cristata*, red pentagon: holotype of *P. parnahybae*, junior-synonym of *P. cristata*, red square: lectotype of *P. steindachneri*, junior-synonym of *P. cristata*, red ellipse: holotype of *P. wessellii*, junior-synonym of *P. cristata*, red airplane: holotype of *P. witmeri*, junior-synonym of *P. cristata*; *P. geryi*.— purple star: holotype, purple circle: other material, purple triangle: holotype of *P. procera*, junior-synonym of *P. geryi*; *P. humeralis*.— yellow star: holotype, yellow circle: other material; *P. leptosoma*.— dark blue star: holotype; dark blue circle: other material; *P. macturki*.— light green star: holotype, light green circle: other material; *P. megalops*.— dark green star: holotype, dark green circle: other material.

Attachments list

Attachment 1. Original description of *Pimelodella humeralis*, in the article “A new species of *Pimelodella* (Siluriformes: Heptapteridae) from the Guiana Shield, Brazil” of Slobodian *et al.* (2017).

Attachment 2. R script to calculate ML trees and other results, to be used by ASTRAL in order to calculate the Species Tree.

Summary

Volume 1

Introduction	1
The <i>Pimelodella</i> genus Eigenmann & Eigenmann, 1888.....	1
General objectives and thesis approach.....	3
Chapter 1: Taxonomic revision of <i>Pimelodella</i> Eigenmann & Eigenmann, 1888	4
Introduction	5
Taxonomic history of the genus <i>Pimelodella</i>	5
Objectives	10
Material and Methods	11
Methods to gather common taxonomic data.....	11
Anatomic illustration, nomenclature and institutional codes.....	12
Maps and assessment of geographic distribution.....	12
Principal Component Analysis (PCA).....	12
Material examined.....	14
Results	15
<i>Pimelodella</i> Eigenmann & Eigenmann, 1888.....	15
<i>Pimelodella australis</i> Eigenmann, 1917.....	23
<i>Pimelodella avanhandavae</i> Eigenmann, 1917.....	29
<i>Pimelodella boliviana</i> Eigenmann, 1917.....	33
<i>Pimelodella boschmai</i> Van der Stigchel, 1964.....	36
<i>Pimelodella brasiliensis</i> (Steindachner, 1877).....	41
<i>Pimelodella buckleyi</i> (Boulenger, 1887).....	49
<i>Pimelodella chagresi</i> (Steindachner, 1876a).....	55
<i>Pimelodella conquetaensis</i> Ahl, 1925.....	61
<i>Pimelodella cristata</i> (Müller & Troschel, 1849).....	64
<i>Pimelodella cruxenti</i> Fernandez-Yépez, 1950.....	79
<i>Pimelodella elongata</i> (Günther, 1860).....	83
<i>Pimelodella enochi</i> Fowler, 1941a.....	87
<i>Pimelodella eutaenia</i> Regan, 1913.....	92
<i>Pimelodella figueroai</i> Dahl, 1961.....	97
<i>Pimelodella geryi</i> Hoedeman, 1961.....	100
<i>Pimelodella gracilis</i> (Valenciennes, 1835).....	104
<i>Pimelodella griffini</i> Eigenmann, 1917.....	113
<i>Pimelodella grisea</i> (Regan, 1903).....	117
<i>Pimelodella harttii</i> (Steindachner, 1877).....	120
<i>Pimelodella hasemani</i> Eigenmann, 1917.....	124
<i>Pimelodella howesi</i> Fowler, 1940b.....	129
<i>Pimelodella humeralis</i> Slobodian, Akama & Dutra, 2017.....	134
<i>Pimelodella ignobilis</i> (Steindachner, 1907).....	135
<i>Pimelodella itapicuruensis</i> Eigenmann, 1917.....	140
<i>Pimelodella kronei</i> (Miranda Ribeiro, 1907a).....	144

<i>Pimelodella lateristriga</i> (Lichtenstein, 1823)	152
<i>Pimelodella laticeps</i> Eigenmann, 1917	159
<i>Pimelodella laurenti</i> Fowler, 1941a	163
<i>Pimelodella leptosoma</i> (Fowler, 1914)	167
<i>Pimelodella linami</i> Schultz, 1944	170
<i>Pimelodella longipinnis</i> (Borodin, 1927b)	174
<i>Pimelodella macturki</i> Eigenmann, 1912	177
<i>Pimelodella martinezi</i> Fernández-Yépez, 1970	181
<i>Pimelodella meeki</i> Eigenmann, 1910	184
<i>Pimelodella megalops</i> Eigenmann, 1912	189
<i>Pimelodella megalura</i> Miranda Ribeiro, 1918	194
<i>Pimelodella metae</i> Eigenmann, 1917	198
<i>Pimelodella modesta</i> (Günther, 1860)	201
<i>Pimelodella montana</i> Allen in Eigenmann & Allen, 1942	205
<i>Pimelodella mucosa</i> Eigenmann & Ward in Eigenmann, McAtee & Ward, 1907	208
<i>Pimelodella nigrofasciata</i> (Perugia, 1897)	212
<i>Pimelodella notomelas</i> Eigenmann, 1917	212
<i>Pimelodella odynea</i> Schultz, 1944	215
<i>Pimelodella pectinifera</i> Eigenmann & Eigenmann, 1888	219
<i>Pimelodella peruana</i> Eigenmann & Myers in Eigenmann & Allen, 1942	223
<i>Pimelodella reyesi</i> Dahl in Dahl & Medem, 1964	226
<i>Pimelodella robinsoni</i> (Fowler, 1941)	229
<i>Pimelodella roccae</i> Eigenmann 1917	232
<i>Pimelodella serrata</i> Eigenmann, 1917	237
<i>Pimelodella spelaea</i> Trajano, Reis & Bichuette, 2004	241
<i>Pimelodella straminea</i> (Cope, 1894)	244
<i>Pimelodella taeniophora</i> (Regan, 1903)	249
<i>Pimelodella tapatapae</i> Eigenmann, 1920	254
<i>Pimelodella vittata</i> (Lütken, 1874)	257
<i>Pimelodella yuncensis</i> Steindachner, 1902	261
Other species formerly treated in <i>Pimelodella</i>	266

Chapter 2: Molecular taxonomy of *Pimelodella* Eigenmann & Eigenmann, 1888.269

Introduction	270
Integrative taxonomic methods for species delimitation	270
Material and Methods	272
Taxon sampling	272
Molecular data collection	272
Processing, alignment of sequenced data and obtaining models	275
Phylogenetic inferences	275
Results	276
Species tree analysis	276
Concatenate matrix analysis	279
Material examined	282

Final conclusions: Integrative taxonomy delimitation	286
Final conclusions.....	287
Bibliographic References.....	291

Volume 2

Tables, figures and attachments	318
--	------------

Introduction

The *Pimelodella* genus Eigenmann & Eigenmann, 1888

Pimelodella Eigenmann & Eigenmann 1888 is an important component of the freshwater fish fauna of the Neotropics. With 79 species currently considered as valid, *Pimelodella* is the most species-rich genus of Heptapteridae, a family comprising 211 species in 24 genera (Eschmeyer, Fricke & van der Laan, 2017). *Pimelodella* is distributed throughout cis- and trans-andean Neotropical drainages, from Panamá to Argentina (Eschmeyer, Fricke & van der Laan, 2017). Due to unsettled taxonomic and systematic problems, the genus represents one of the most difficult bottlenecks for understanding the diversity of Neotropical freshwater fishes.

Pimelodella was described in 1888 by Eigenmann & Eigenmann, to include *Pimelodus cristatus* Müller & Troschel, 1849 as type-species, *P. pectinifer* as a new species, plus several additional species previously included in *Pimelodus* (*P. brasiliensis* Steindachner, 1877, *P. buckleyi* Boulenger, 1887, *P. chagresi* Steindachner, 1876, *P. cristatus*, *P. elongatus* Günther, 1860, *P. gracilis* Valenciennes, 1835, *P. harttii* Steindachner, 1877, *P. lateristrigus* Lichtenstein, 1823, *P. modestus* Günther, 1860, *P. vittata* Lütken, 1874 and *P. wesseli* Steindachner, 1877) The genus was diagnosed by: “head entirely covered in skin; occipital process narrow, of the same width throughout, meeting the dorsal plate; fontanel prolonged backward to the occipital process with a bridge across it behind the eye” (Eigenmann & Eigenmann, 1888: 131).

Carl Eigenmann (1917) revised *Pimelodella* and *Typhlobagrus*, the latter a monotypic genus proposed by Miranda Ribeiro (1907) for his new troglobitic species *T. kronei*. Eigenmann (1917) recognized 35 taxa in *Pimelodella* (34 species plus one subspecies) including 12 taxa (11 species plus one subspecies) then described as new. Eigenmann (1917) also provided a diagnosis of the genus based on several non-unique features: “nares remote; teeth villiform, in bands; gill-membranes free from the isthmus; dorsal short, with a feeble, pungent spine; anal short, with 11–15 rays; pectoral with a strong pungent spine variously armed with thorn-like teeth on its posterior (inner) edge; a long, adnate, adipose fin; caudal fin deeply forked, one or the other lobe frequently wider, or longer; well-developed maxillary barbels reaching to end of pectoral, or beyond the caudal; two pairs of mental barbels, sometimes in a; nearly straight line; a frontal and a parietal fontanel, the latter reaching to the base of the occipital process, which is narrow and reaches, or nearly reaches, the plate in front

of the dorsal; humeral process spine-like; roof of mouth without teeth; head covered with thin skin” (Eigenmann, 1917: p. 229).

Since Eigenmann’s (1917), *Typhlobagrus* has been synonymized with *Pimelodella*, and several other species have been newly described, removed from or transferred to *Pimelodella* (Ferraris, 2007), reaching a present total of 92 available names (Eschmeyer, Fricke & van der Laan, 2017) (Table 1). Several authors made substantial contributions to the taxonomy of the genus, e.g. Regan (1903, 1913), Miranda-Ribeiro (1907, 1911, 1914, 1918), Fowler (1914, 1915, 1940a, b, c, 1941a, b), Ahl (1925) and Dahl (1961, 1964). Revisionary work on other heptapterid genera resulted in the transfer, by default, of some species to *Pimelodella* without detailed studies on the systematics of the genus (Silfvergrip, 1996; Bockmann & Miquelarena, 2008), thus increasing its taxonomic complexity.

The diagnosis proposed by Eigenmann (1917) is insufficient to properly delimit *Pimelodella*, so that the genus has been redefined in subsequent contributions (Bockmann & Miquelarena, 2008; Slobodian, 2013; Slobodian & Bockmann, 2013). However, *Pimelodella* remains without a phylogenetic diagnosis, and its diversity remains poorly understood.

Despite a plethora of publications on *Pimelodella*, only few works after Eigenmann (1917) had an actual comparative scope: Mees’ (1974, 1986) focused on *Pimelodella* species in Surinam and French Guiana; Guazzelli’s (1997) investigated the taxonomy of eight *Pimelodella* species from Brazilian southern and southeastern coastal drainages; and Souza-Shibatta *et al.* (2013) measured the cytogenetic, morphologic and morphometric differences among *Pimelodella* in the Brazilian Pantanal (Mato Grosso do Sul and Mato Grosso States).

Today, *Pimelodella* is a genus rife with taxonomic problems of various sorts, large documented diversity, broadly distributed species, and outdated or inadequate descriptions. Taxonomic problems also stem from a highly conservative morphology and a lack of comprehensive studies on the numerous specimens vouchered in natural history collections. Many species of *Pimelodella* lack rigorous taxonomic study and, to some degree, those considered valid merely correspond to a list of unchallenged available names (Slobodian *et al.*, 2017). Identification of *Pimelodella* species is expectedly troublesome, a fact blatantly demonstrated in collection material: the majority of material representing *Pimelodella* is undetermined, or wrongly identified at species level. In addition, phylogenetic work on the genus invariably stumble upon resilient taxonomic problems mentioned above, and therefore have limited applicability.

General objectives and thesis approach

The main purpose of this work is to mitigate the lack of knowledge on the taxonomy of *Pimelodella*. To that end, I present a thorough taxonomic revision encompassing all available names in *Pimelodella*, having as primary source of information external anatomy, morphometric, meristic and osteological data. Concomitantly, a molecular study was conducted for a sample of *Pimelodella* species, in order to discuss the molecular diversity and the explanatory power of molecular taxonomy in delimiting species of the genus, as seen through the results of the classical taxonomic results. With both morphological and molecular data, an integrative approach was conducted to characterize *Pimelodella* species on a biologically-broad basis, including also distributional and ecological data whenever available.

The work is divided in two chapters: The first reviews the taxonomy of *Pimelodella* with traditional morphological data, following a classical approach with descriptions and diagnoses of valid species, synonymies and a discussion on taxonomically-significant morphological characters.

The second chapter includes an essay on the molecular diversity of *Pimelodella* and the explanatory power of molecular characters to unravel the taxonomy of the genus using species trees methodology. This strategy is based on gathering information from several gene trees and then analyzing the divergence pattern of loci, time of divergence and probable events of coalescence (*cf.* Edwards *et al.*, 2007; Liu & Pearl, 2007; Carstens & Knowles, 2007; Liu *et al.*, 2008; Kubatko *et al.*, 2009). The results were compared with the obtained through a traditional concatenate analysis.

A final discussion offers an integrative approach to the taxonomy of *Pimelodella* using multidisciplinary strategies and data from both morphological and molecular results.

Chapter 1
Taxonomic revision of *Pimelodella*
Eigenmann & Eigenmann, 1888

Introduction

Taxonomic history of the genus *Pimelodella*

Pimelodella was described in 1888 by Eigenmann & Eigenmann to include 11 species previously allocated in *Pimelodus* or *Pseudorhamdia* (*P. brasiliensis*, *P. buckleyi*, *P. chagresi*, *P. cristatus*, *P. elongatus*, *P. gracilis*, *P. harttii*, *P. lateristriga*, *P. modestus*, *P. vittata*, *P. wessellii*) plus a newly-described *P. pectinifer*. At the time of description, Eigenmann & Eigenmann (1888) also synonymized part of described *Pseudorhamdia* to *Pimelodella* (*Pseudorhamdia* original type is *P. maculatus*, not included among the *Pimelodella*, so *Pseudorhamdia* genus do not have priority over *Pimelodella*). The genus was proposed to accommodate *Pimelodus* species with a narrow supraoccipital process, reaching the anterior nuchal plate, and a completely opened posterior fontanel (Eigenmann & Eigenmann, 1888: 131). Eigenmann & Eigenmann (1888) implicitly arranged genera due to some sort of perceived similarity (Bockmann, 1998), and *Pimelodella* was listed immediately after the genus *Rhamdia* Bleeker (1858) (and *Rhamdella*, a subgenus), and in an appendix Eigenmann & Eigenmann (1888: 172) placed *Heptapterus* Bleeker (1858) and *Nannoglanis* Boulenger (1887) after *Rhamdella*.

In 1890, Eigenmann & Eigenmann redescribed species of *Pimelodella* in detail, also offering an identification key. In 1891, Eigenmann & Eigenmann produced a catalog, in which then 12 known species were listed. Between 1891 and 1910, the species *Pimelodus eigenmanni* Boulenger 1891, *Pimelodella yuncensis* Steindachner, 1902, *Pimelodus (Pimelodella) griseus* Regan, 1903, *Pimelodus (Pimelodella) taeniophorus* Regan, 1903 and *Pimelodella mucosa* Eigenmann & Ward, 1907 were described.

Another catalog was produced by Eigenmann (1910), where the new species cited above were indicated under or transferred to *Pimelodella*, along with *P. meeki* as a *nomen novum* for the unavailable *P. eigenmanni* Meek (1905), and the citation of the names *P. macturkii* (*sic*) and *P. megalops* as manuscripts in preparation, which were later formally described by Eigenmann (1912). Between 1912 and 1917, *Pimelodella eutaenia* Regan, 1913, *Pimelodella taenioptera* Miranda Ribeiro, 1913, *Pimelodella copei* Fowler, 1915 and *Pimelodella peruensis* Fowler, 1915 were described.

The last taxonomic revision of *Pimelodella* was then made by Eigenmann (1917) in which 12 new taxa were described (11 new species and 1 new subspecies), and *P. wessellii* was synonymized to *P. cristata*. In that work, a new diagnosis was proposed for the genus.

Eigenmann's revision (1917) delimited the geographic distribution of *Pimelodella* to rivers from Panamá to Argentina, a range which remains correct today. Most of the species were described (or redescribed) and illustrated, and all known species had their pectoral-fin spines illustrated. A key is presented for the 35 taxa of *Pimelodella* and 1 *Typhlobagrus* (interpreted as an offshoot of *Pimelodella* at that time, later into *Pimelodella*). This is the most comprehensive work on *Pimelodella* taxonomy to date, and after that *Pimelodella* was treated just in part, either subsets of species or isolated descriptions.

Fowler (1940a, b, 1941a) described several *Pimelodella* species in many works on the fauna of specific regions or rivers. However, his works include little discussion on the differences among the species, but solely descriptions and, at most, comparisons with a few species from nearby localities. After Eigenmann, Fowler was the author who described most species of *Pimelodella*: *P. copei* and *P. peruense* (Fowler, 1915); *P. hartwelli* (Fowler, 1940a); *P. chaparae*, *P. cochabambae* (transferred to *Imparfinis* by Mees & Cala, 1989) and *P. howesi* (Fowler, 1940b); *P. dorseyi*, *P. enochi*, *P. laurenti*, *P. paharybae* and *P. witmeri* (Fowler, 1941a); and also *Rhamdella leptosoma* (Fowler, 1914), *R. papariae*, *R. robinsoni* and *R. wolffi* (Fowler, 1941a), now in *Pimelodella*.

Eigenmann & Allen (1942) presented the distribution of the *Pimelodella* species, their diagnosis and referred material; plus descriptions of *P. montana* Allen, 1942 in Eigenmann & Allen, 1942, and *P. peruana* Eigenmann & Myers in Eigenmann & Allen, 1942. Catalogs such as Gosline (1945) and Fowler (1951) included all species of *Pimelodella* described to the respective dates (Fowler, 1951 includes only Brazilian species). Also, *Caecorhamdella brasiliensis* Borodin (1927a) and *Typhlobagrus kronei* Miranda Ribeiro, 1907 were maintained under those genera (Gosline, 1945: 34; 43; Fowler, 1951: 518–519; 578–579).

Schultz (1944) was the first to synonymize *Brachyrhamdia* in *Pimelodella*, but without discussion. In the same work, *P. linami* and *P. chagresi odynea* were described from the Maracaibo, but without much resort to comparative material. Innes & Myers (1950) also suggested *Brachyrhamdia* as a junior-synonym of *Pimelodella*. Two other genera synonymized with *Pimelodella* were *Typhlobagrus* Miranda Ribeiro, 1907a (Pavan, 1946: 359) and *Caecorhamdella* Borodin, 1927a (Trajano & Britski, 1992: 83).

Dahl (1961) published the first comparison of *Pimelodella* species bearing filaments on dorsal fin, *P. griffini*, *P. linami* and *P. figueiroi*. Dahl (1961) proposes that the filamentous prolongation of the dorsal fin as absent in an adult females and immature specimens of *P. figueiroi*, suggesting the filament as a secondary sexual character of the adult male. He further suggested that the same might apply to other *Pimelodella* species. *Pimelodella boschmai* was

described by van der Stigchel (1964), but the only comparison made with other filamentous *Pimelodella* was with *P. griffini*.

Another important author in understanding the diversity of *Pimelodella*, Mees (1974, 1983, 1986), who offered general comparisons for *Pimelodella* identification. He objected to Fowler's descriptions (1940b, 1941a), in which different species were described on the basis of differences on eye size. Mees' own findings showed that character as related to sexual dimorphism in *P. cristata*. Mees (1974) also suggested that *Pimelodus altipinnis* was in fact a *Pimelodella*, following an earlier suggestion of Van der Stigchel, 1946; that *P. altipinnis* (Steindachner, 1874), *P. geryi* Hoedeman (1961) and *P. wessellii* (Steindachner, 1876) were junior-synonyms of *P. cristata*, and that *P. insignis* was a junior-synonym of *P. boschmai*. Mees (1974) also proposed *P. gracilis* (Valenciennes, 1835) as senior-synonym of *P. cristata* or, alternatively, that *P. gracilis* was confined to the Uruguay-Paraná-La Plata basins. Similar forms from Guianas, Orinoco and Suriman were, in that case, *P. cristata*, and similar forms from Amazon would be *P. steindachneri*. Discussions on the value of coloration patterns in species identification were made, with the observation that single species of *Pimelodella* from different rivers may differ to a limited degree (Mees, 1974).

In a work about the naked catfishes from French Guiana, Mees (1983) narrowed the type-locality of *P. lateristriga*, to the vicinity of the city of Rio de Janeiro, based on data about the travels of the collector, von Olfers. He also highlighted differences in vertebral counts and color pattern for material identified as *P. cristata*. Despite the recognized need for further study, he did not think those characteristics were sufficient to discriminate species (Mees, 1983).

The first time *Pimelodella* was studied under a cladistic perspective was in Howes (1983), in which it grouped the genus with *Rhamdia* and *Heptapterus* inside the Pimelodidae. However, the family Heptapteridae as currently composed, was first diagnosed (as a unnamed group) in Lundberg & McDade (1986). Therein, *Pimelodella* was also attributed to a monophyletic subgroup including also *Brachyrhamdia*, *Cetopsorhamdia*, *Goeldiella*, *Pimelodella*, *Pimelodus heteropleura*, *Rhamdella*, *Rhamdia*, *Typhlobagrus* and an unidentified *Nannorhamdia*, based on the synapomorphy "fifth transverse process smaller than fourth, but similarly expanded and notched" (Lundberg & McDade, 1986: 6).

Axelrod & Burgess in Axelrod (1987) expressed doubt whether *Brachyrhamdia* was be distinguishable from *Pimelodella*. Later, Burgess (1989) transferred *B. imitator*, *B. marthae* and *B. meesi* into *Pimelodella*, without further explanation about the move.

Silfvergrip (1996) provisionally transferred *Pimelodus bahianus* to *Pimelodella*, and made some comparisons of anatomic features of *Pimelodella* and *Rhamdia*, especially in characters of dorsal, pectoral and adipose fins, and on sexual dimorphism. Silfvergrip also suggested *Pimelodus breviceps* might be a *Pimelodella*

Guazzelli (1997), in her unpublished dissertation, made a taxonomic review of *Pimelodella* species from South and Southeastern coastal drainages of Brazil. In that work, seven described species were proposed as valid (*P. australis*, *P. brasiliensis*, *P. ignobilis*, *P. kronei*, *P. lateristriga*, *P. pappenheimi*, and *P. transitoria*), a new species was proposed for the rio Paraíba do Sul, and *P. harttii* and *P. pectinifera* were included as junior synonyms of *P. lateristriga*.

Bockmann (1998), in his unpublished thesis, made the most comprehensive study yet on generic relationships in Heptapteridae. *Brachyrhamdia*, *Caecorhamdella* and *Typhlobagrus* were included as junior-synonyms of *Pimelodella*. Bockmann (1998) included only 8 *Pimelodella* species in his analysis, 5 of which belonging to *Brachyrhamdia*.

Guazzelli (2003), in her unpublished thesis, proposed a phylogenetic hypothesis for species of *Pimelodella*, including 18 described and 17 undetermined or new species. Guazzelli (2003) maintained *Brachyrhamdia* as a junior-synonym of *Pimelodella*. The clade including *Pimelodella*+*Brachyrhamdia* in her analysis is corroborated by 7 synapomorphies, all of which homoplastic (Guazzelli, 2003).

Relationships among *Pimelodella* species in Guazzelli (2003) are massively unresolved, the only exception being a group formed by *P. cristata*, *P. witmeri* and 7 new species (clade 58, diagnosed by 4 homoplastic synapomorphies). Guazzelli (2003) also highlights the need of extensive revisionary work on *Pimelodella*, before its biodiversity is realistically known.

Bockmann & Guazzelli (2003) presented a checklist of Heptapteridae species, in which they transferred to *Pimelodella* the species *Nannorhamdia macrocephala*, *Pimelodus breviceps*, *Rhamdia eigenmanniorum*, *Pimelodus ophthalmicus*, *Pimelodus taeniophorus* and *Pimelodus wessellii*, erected *Pimelodella chagresi odynea* to full species and synonymized *P. insignis* to *P. boschmai*. However, no explicit reasons were presented for implementing those taxonomic changes. That work treated *Brachyrhamdia* as a valid genus, and *Typhlobagrus* and *Caecorhamdella* as junior-synonyms of *Pimelodella* (Bockmann & Guazzelli, 2003).

Leiva (2005), in his unpublished dissertation, made a taxonomic review of *Pimelodella* species from trans-Andean Colombian rivers. In that work, he indicated *P. chagresi*, *P. eutaenia*, *P. grisea*, *P. modestus*, *P. odynea* and *P. reyesi* as valid species, describing three additional new species (Leiva, 2005).

Ferraris (2007) proposed *P. bahianus* and *P. rendahli* as *species inquirenda* in *Pimelodella*. That work also treated *Brachyrhamdia* as a valid genus, and *Typhlobagrus* and *Caecorhamdella* as junior-synonyms of *Pimelodella* (Ferraris, 2007).

Bockmann & Miquelarena (2008) suggested *Nannorhamdia macrocephala*, *Rhamdella leptosoma*, *R. papariae*, *R. robinsoni* and *R. wolfi* as probably members of *Pimelodella*, transferred *Rhamdella ignobilis* and *R. longipinnis* to *Pimelodella*, and suggested *Pimelodus exsudans*, *P. jenynsii* and *Rhamdella straminea* as members of *Pimelodella* or *Rhamdia*. That work suggested *Brachyrhamdia* as a valid genus, recovered as sister-group of *Pimelodella*, but did not proposed apomorphies for the latter clade.

Nannorhamdia macrocephala was suggested as a *Pimelodella* due to the presence of long maxillary barbers, inner caudal-fin rays that do not articulate directly on the hypural plates and with interradiial membranes only along their basal halves, all synapomorphies of *Pimelodella* according to Bockmann (1998), and despite the supraoccipital process short, not reaching the prenuchal plate (Bockmann & Miquelarena, 2008).

Rhamdella leptosoma was suggested (Bockmann & Miquelarena, 2008) as a possible *Pimelodella* due to overall appearance and geographical distribution (since the *Rhamdella*, as defined in that work, was limited to southern South America), and despite the short supraoccipital process. *Rhamdella papariae*, *R. robinsoni* and *R. wolfi* were suggested as belonging to *Pimelodella* on the basis of information in original descriptions and associated illustrations (e.g. slender body, large eyes, well-developed supraoccipital process, long maxillary barbel, reaching anal-fin base, robust pectoral spine, dark stripe along lateral surface of the body, etc.) (Bockmann & Miquelarena, 2008). Type material of *Rhamdella ignobilis* and *R. longipinnis* was examined and supported their transfer to *Pimelodella* on the basis of long maxillary barbels and a sharp long supraoccipital process that contacts the predorsal plate (Bockmann & Miquelarena, 2008).

Bockmann & Miquelarena (2008) also suggested *Pimelodus exsudans* Jenyns, 1842 and *Pimelodus jenynsii* Günther, 1864 as *Pimelodella* or *Rhamdia* based on the descriptions of both species, and arguing that the characters suggested by Eigenmann & Eigenmann (1888, 1890) to place both in *Rhamdella* are not accurate enough to justify this transfer. Also, Bockmann & Guazzelli (2008) argued *Rhamdella* genus does not occur in Rio de Janeiro vicinities, the collection locality of *Pimelodus exsudans* and *P. jenynsii*. *Rhamdella straminea* was also suggested as a *Pimelodella* or *Rhamdia* due to the presence of long maxillary barbels reaching the middle of ventral fins, despite the long cranial fontanel (Bockmann & Miquelarena, 2008).

Slobodian (2013), in an unpublished dissertation, produced a phylogenetic analysis of *Brachyrhamdia*, including all its species plus 12 of *Pimelodella*. That work recovered *Brachyrhamdia* as an apical lineage inside a widely unresolved *Pimelodella*, with 14 apomorphic characters, 6 of which exclusive and unreversed (clade 19). The clade encompassing *Pimelodella+Brachyrhamdia* (clade 7) is diagnosed by numerous synapomorphies and can be considered as well-corroborated (Slobodian, 2013).

Despite recovering *Brachyrhamdia* as an apical lineage inside *Pimelodella*, Slobodian (2013) suggested *Brachyrhamdia* should remain valid, because is an easily recognizable and diagnosable clade, while *Pimelodella* is probably a paraphyletic group, whose species' relationships can only be resolved in the scope of a more inclusive work.

Pimelodella remains without any published phylogenetic diagnosis and its monophyly is uncertain, but an assemblage composed of its species can be distinguished from other heptapterids, including *Brachyrhamdia*, by a unique character combination (Slobodian *et al.* 2017). *Pimelodella* nowadays includes 79 valid species, from a total of 92 available names, and is the most species-rich genus of Heptapteridae, a family composed of 211 species in 24 genera (Eschmeyer, Fricke & van der Laan, 2017). *Pimelodella* is distributed throughout cis- and trans-Andean Neotropical drainages from Panamá to Argentina (Eschmeyer, Fricke & van der Laan, 2017). The majority of species in the genus have never been subject to rigorous taxonomic study and those considered as valid often merely correspond to a selected list of available names (Slobodian *et al.*, 2017).

Objectives

The aim of this work is to present a thorough taxonomic revision of *Pimelodella*, encompassing all available names and using data from external anatomy, morphometrics, meristics, pigmentation and osteology data. It is subdivided into the following stages:

- Datasheet for all valid species, with individual diagnosis, description, morphometric and meristic data, synonymies and geographic distribution;
- Analysis of anatomical features, especially osteological, whenever significant for species delimitation;
- Discussion on anatomical characters and morphometric data relevant for species diagnosis and delimitation, and their distribution within the genus, based on Principal Component Analysis results and direct observation;
- Comments on the species proposed as junior-synonyms;
- Schematic illustrations of diagnostic characters, in order to facilitate the species' identification;
- Identification key for all valid species of *Pimelodella*.

Material and Methods

Methods to gather common taxonomic data

Measurements are point-to-point distances taken with digital calipers under a dissecting scope, following Slobodian *et al.* (2017). Figure 1 shows schematic representation for the following: Head length (from tip of snout to distal point of supraoccipital process;) head depth (measured at supraoccipital process anterior limit); eye diameter (longitudinal diameter of eye globe); mouth gape (including lips, measured at external limit); barbels lengths (with barbel straightened along lateral or ventral surface of body); predorsal length (from tip of snout to anterior tip of spinelet); peduncle length (posterior to adipose, measured from posterior to adipose-fin base terminus until caudal-fin insertion), and peduncle depth (measured just posterior to adipose-fin base terminus).

Measurements of head parts are presented as proportions of head length (HL), except for measurements of barbels which are proportions of standard length (SL); head length and measurements of body parts are given as proportions of standard length. Meristics and description of fin position follow Bockmann & Castro (2010). Vertebral counts include those elements involved in the Weberian complex counted as five, plus all free vertebrae, plus the compound caudal centrum (PU1+U1) counted as one (Lundberg & Baskin, 1969). Number of specimens with each meristic value are presented in parenthesis, and an asterisk indicates values for holotypes.

Clearing and staining procedures follow Taylor and Van Dyke (1985); osteological data on remaining specimens was obtained with the aid of X-ray images.

Synonym includes main works on taxonomy, systematics and distribution. Revisionary works, phylogenies and taxonomic lists are indicated as such. Works with mention to species features and authorship, isolated or in comparison with other species, are generally indicated as “taxonomic treatment”. Other works on particular features (such as cytogenetics, ecology and behavior) are indicated explicitly.

Anatomic illustration, nomenclature and institutional codes.

Photographs were taken by the author except when stated otherwise. Internal morphology photos were taken with a microscope attached with a digital camera. Photos were treated in Adobe Photoshop CS6, and illustrations were made in Adobe Illustrator CS6 with Wacom graphic tablet.

Osteological terminology and laterosensory-canal nomenclature follow Bockmann & Miquelarena (2008), and are summarized in Figures 2–4. Nomenclature of pectoral-fin and dorsal-fin spines ornamentations follow Vanscoy *et al.* (2015). Dentations are considered retrorse if pointed towards base of the spine; antrorse if pointed toward the apex of the spine; and straight if neither. The distal tip of pectoral-fin spine may bear 1–2 incipient, incompletely ossified dentations, such incipient dentations are not included in dentation counts.

Institutional codes follow Sabaj (2016). Abbreviations: Min—minimum; Max—maximum; n—number of specimens; x—average; SD—standard deviation

Maps and assessment of geographic distribution

Maps were produced with the aid of Google Earth Pro 7.3 and Quantum GIS 2.18, following instructions of Calegari *et al.* (2016). Geographic coordinates for type material are exactly as provided in original description, or approximated when not presented in description, with corrections or more accurate information on localities presented between brackets. Geographic coordinates of comparative material were gathered from collection information associated with respective lot, whenever available, or approximate when derived from locality name. Only materials with reliable locality information and identification were included in maps. Comments on species distribution, when necessary, are made in respective species’ datasheet. Freshwater ecoregions recognized in Abell *et al.* (2008) are used to express distribution.

Principal Component Analysis (PCA)

Multivariate analysis has lately been replacing univariate analysis in a broad spectrum of biological applications, as a means to explain data in complex patterns (James &

McCulloch, 1990). Principal Component Analysis (PCA) is an ordination procedure in which the matrix of distances or similarities among the objects is reduced to few dimensions, and displayed in a graphic space in which the axes are gradients of combinations of the attributes (James & McCulloch, 1990). PCA reorganizes information in a dataset of samples, discriminating variables (Principal Components, or “PCs”) that account for the majority of the variability in the dataset (Davies & Fearn, 2004), and then identifying possible patterns (Smith, 2002).

Therefore, PCA is an Exploratory Data Analysis which allows assessing in simple manner the characteristics most significant in explaining the variability of a given dataset. It reduces the dimensionality of data from a large number of variables to a few PCs which retain a very high percentage of information content (Davies & Fearn, 2004; Swarbrick, 2012), thus highlighting similarities and differences (Smith, 2002). The PCA defines which variables most contribute to the greatest sources of variability and shows which variables are related to each other, discriminating important information from noise (Swarbrick, 2012).

The information is usually presented in two-dimension plots, with two PCs against each other, and is applied to visualize clusters in the data that relate samples and variables (James & McCulloch, 1990). PCA can be used as an Unsupervised Classification Method (Swarbrick, 2012), to test whether a priori delimitation is explained by a dataset (James & McCulloch, 1990). If distinct groups (clusters) recovered are according to the prior knowledge of discrimination, it can be concluded that the measured properties are capable of classifying the samples (Swarbrick, 2012) (*e.g.* if morphometric data for two species analyzed in PCA results in distinct clusters in the plot, the morphometric data used is sufficient to discriminate them properly). To calculate PCs, each variable has its value normalized to scale the data, and then reorganized in a two-dimension plot representing the growth of the data most reflective of the variability of the dataset, in covariance (Schlegel, 2017). The results are usually presented scaled, as a scatterplot, with variance values informed.

In taxonomy, the use of PCA has recently increased in order to assess the principal elements in diagnosing species, and also helping in discriminating variability in populations (*e.g.* Retzer & Page, 1996; Cox-Fernandes *et al.*, 2009, Claverie & Wainwright, 2014). Because PCA is an exploratory analysis, it must not be used to describe species *per se*, but rather to test if a priori identification of species can be explained by a certain dataset. Because it is based on either variances and covariances or correlations, PCA is sensitive to outliers, and the coefficients of individual components are highly subject to sampling variability (James & McCulloch, 1990).

The application of PCA on *Pimelodella* morphometrics can bring a robust basis to discuss delimitation of species based on this kind of data, and even allow an identification of those measurements most significant in taxonomic delimitations. However, distinctiveness of a particular taxon is inversely proportional to the number of specimens examined (Sabaj & Arce, 2017), and this is particularly relevant in species of *Pimelodella*, which are represented by abundant study material.

Principal Component Analyses were performed on all species with available morphometric data (Table 2). Follow-up analyses for certain groups of species were subsequently produced, and are discussed in the respective species' section. In PCAs, all measures were included *a priori*, with exception of Total Length. In order not to exclude many specimens from the analysis, when a measure was not measured in a particular specimen, the mean of this measure for all specimens (normalized) was used instead.

The Principal Components of the datasets were obtained from the correlation matrix, since components may be more interpretable if the original values have wide variances, as the presented case (Schlegel, 2017). The correlation matrix results in a scaled and more balanced representation of the components (Schlegel, 2017). The alternative covariance matrix was not used because variables with larger variances might dominate and distort the principal components of that matrix.

The scaled PCA was performed in RStudio 1.0.143, using the libraries “FactoMineR”, “ggfortify” and “cluster”, with the function “prcomp”. The outputs generated by this function expressed as a matrix of variable loadings (*i.e.* a matrix whose columns contain the eigenvectors for each PC), the standard deviation for each PC, and a matrix with standard deviation, proportion of variance and cumulative proportion for each component. With these results, the role of each measure in the PCs can be assessed, thus permitting a better understanding of the function of the morphometric data in explaining the morphological variation.

Scatterplots produced by “autoplot” function, regarding the first two PCs (the ones embracing most of the morphological variation) per individual of each species, are also presented. Data regarding individual species PCA, or analysis with groups of species are presented and discussed in relevant sections.

Material examined

Material examined is presented as follows. Specimens are preserved in ethanol 70%, unless indicated otherwise: cleared and stained materials (c&s) are preserved in glycerol, and

skeleton preparations (sk) are preserved in dry. X-rayed specimens are indicated by “xr”. The list is organized first by species, then by alphabetical order of institutional code, and finally by catalog number. Nominal species that were synonymized are referred in the section correspondent to valid species material examined, under original species name.

Results

***Pimelodella* Eigenmann & Eigenmann, 1888**

Pseudorhamdia Steindachner, 1876b: 191 [synonym of *Pimelodus*, based on *Pseudorhamdia maculatus* (Lacepede, 1803), invalid].

Pimelodella Eigenmann & Eigenmann, 1888: 131–133 [type species *Pimelodus cristatus* Müller & Troschel, 1849; by original designation; list of species belonging to genus]. — Eigenmann & Eigenmann, 1890: 147–162 [identification key, taxonomic treatment]. — Eigenmann & Eigenmann, 1891: 29 [taxonomic list]. — Eigenmann, 1905: 19 [list]. — Eigenmann, McAtee & Ward, 1907: 148 [list]. — Eigenmann, 1910: 388–389 [list]. — Regan 1911: 571–573 [taxonomic treatment, identification key for Pimelodidae genera]. — Eigenmann, 1912: 167–171 [taxonomic treatment, identification key]. — Fowler, 1915: 214–218 [taxonomic treatment]. — Eigenmann, 1917: 229–258, plates XXIX–XXXV [taxonomic revision, geographic distribution, identification key, illustrations]. — Eigenmann, 1921a: 4 [geographic distribution]. — Eigenmann, 1921b: 510 [list]. — Eigenmann, 1922: 41–44 [geographic distribution; identification key]. — Eigenmann, 1923: 209 [geographic distribution]. — Pearson, 1924: 18–19 [identification key]. — Myers, 1927: 123 [relationship with *Brachyrhamdia*]. — Behre, 1928: 421–423 [geographic distribution]. — Fowler, 1939: 222–224 [taxonomic treatment]. — Fowler, 1940b: 64 [taxonomic treatment]. — Fowler, 1941a: 127–135 [taxonomic treatment]. — Eigenmann & Allen, 1942: 43, 47, 98–102 [geographic distribution, list, taxonomic treatment]. — Schultz, 1944: 185–189, 209–214 [identification key for Pimelodidae genera, taxonomic treatment, identification key]. — Gosline, 1945: 43–47 [taxonomic treatment]. — Van der Stigchel, 1946: 53–54 [taxonomic treatment]. — Fowler, 1951: 534–551 [taxonomic treatment]. — Dahl, 1961: 496–502 [taxonomic treatment]. — Gery, 1969: 841; fig 4:35 [list, illustration]. — Mees, 1974: 142–152 [taxonomic treatment]. — Howes, 1983: 37–38 [phylogenetic analysis of Pimelodidae]. — Santos, *et al.*, 1984: 60–61

[identification key of Pimelodidae genera]. — Lundberg & McDade, 1986: 4–8 [phylogenetic relationships of Pimelodidae]. — Lundberg *et al.*, 1988: 136 [phylogenetic relationships of Pimelodidae]. — Burgess, 1989: 272–274; 280–281 [biology; taxonomic treatment]. — Malabarba 1989: 141 [taxonomic treatment]. — Ferraris, 1991: 27; 48 [aquarium care]. — Lundberg, Bornbusch & Mago-Leccia, 1991a: 198–204 [composition of Rhamdiinae, diagnosis, phylogenetic relationships]. — Lundberg *et al.*, 1991b: 860 [composition of Rhamdiinae]. — de Pinna, 1993: 61 [composition of Rhamdiinae II]. — Silfvergrip, 1996: 45–75 [morphological comparison with *Rhamdia*]. — Guazzelli, 1997: 1–150 [taxonomic review of coastal south and southeastern Brazilian species]. — Bockmann, 1998: 1–599 [Heptapteridae phylogenetic analysis]. — de Pinna, 1998: 59; 315–316 [fossil record; Heptapterinae composition]. — Britski, Silimon & Lopes, 1999: 96; 97 [key for genus; taxonomic treatment]. — Le Bail *et al.*, 2000: 74; 130–144 [Pimelodidae genera list; taxonomic list]. — Bizerril & Primo, 2001: 60 [taxonomic treatment]. — Perdices *et al.*, 2002: 176 [relationship with *Rhamdia*]. — Bockmann & Guazzelli, 2003: 406–407; 409–410; 417–421 [historical review; biology; taxonomic treatment]. — Godinho & Godinho, 2003: 121 [egg structure]. — Guazzelli, 2003: 1–232 [phylogenetic relationships]. — Chernoff *et al.*, 2003: 67 [biological importance]. — Lopez *et al.*, 2003: 62 [list]. — Rosa *et al.*, 2003: 177 [list, geographic distribution]. — Lasso *et al.*, 2004: 171 [list]. — Mojica *et al.*, 2004: 743 [list]. — Trajano *et al.*, 2004: 316 [genus validity]. — Leiva, 2005: 1–74 [taxonomic review of trans-andean Colombian species]. — Maldonado-Ocampo *et al.*, 2006: 27–28; 30; 164–167 [identification key of Siluriformes families; identification key of Heptapteridae genera; taxonomic treatment of Colombian species]. — Nelson, 2006: 174 [taxonomic treatment of Heptapteridae genera]. — Proudlove, 2006: 131 [validity]. — Ferraris, 2007: 189–195 [taxonomic treatment]. — Lucinda *et al.*, 2007: 79 [list]. — Bockmann & Miquelarena, 2008: 31–47 [phylogenetic analysis of Heptapteridae]. — Maldonado-Ocampo *et al.*, 2008: 201–202 [list]. — Vari *et al.*, 2009: 43 [list, geographic distribution]. — Sullivan *et al.*, 2013: 105 [phylogenetic relationships of Heptapteridae]. — Bockmann & Slobodian, 2013: 15–19; 58–65; 66–69 [historical treatment; taxonomic treatment; geographic distribution; identification key].

Rhamdia [non Bleeker, 1858]. — Miranda Ribeiro, 1911: 263–282 [taxonomic treatment].

Typhlobagrus Miranda Ribeiro, 1907: 1 [type species *Typhlobagrus kronei* Miranda Ribeiro, 1907, by original designation]. — Eigenmann, 1910: 387 [taxonomic treatment]. —

Haseman, 1911: 323–326 [taxonomic treatment]. — Miranda Ribeiro, 1911: 250 [taxonomic treatment]. — Eigenmann, 1917: 230, 255, plate XXXIV–XXXV [geographic distribution, taxonomic revision, illustrations]. — Gosline, 1945: 43 [taxonomic treatment]. — Pavan, 1946: 359 [junior synonym of *Pimelodella*]. — Fowler, 1951: 578–579 [taxonomic treatment]. — de Pinna 1998: 316: [synonym of *Pimelodella*]. — Bockmann & Guazzelli, 2003: 406–408; 417 [historical treatment; synonym of *Pimelodella*]. — Nelson, 2006: 174 [synonym of *Pimelodella*]. — Ferraris, 2007: 189 [synonym of *Pimelodella*].

Pimelodus [non Lacepède 1803]. — Eigenmann & Norris, 1900: 354 [taxonomic list]. — Miranda Ribeiro, 1911: 293 [taxonomic treatment]. — Eigenmann, 1912: 171–172; 177 [identification key, taxonomic treatment].

Caecorhamdella Borodin, 1927: 1–6 [type species *Caecorhamdella brasiliensis* Borodin, 1927, by original designation]. — Gosline, 1945: 34 [taxonomic treatment]. — Fowler, 1951: 518–519 [taxonomic treatment] — Trajano & Britski, 1992: 83 [synonymy of *Caecorhamdella brasiliensis* to *Pimelodella kronei* (Miranda Ribeiro, 1907)]. — de Pinna 1998: 316 [synonym of *Pimelodella*]. — Bockmann & Guazzelli, 2003: 407; 417 [historical treatment; synonym of *Pimelodella*]. — Nelson, 2006: 174 [synonym of *Pimelodella*]. — Ferraris, 2007: 189 [synonym of *Pimelodella*].

Pimelodella [non Eigenmann & Eigenmann, 1888]. — Axelrod, 1987: 22–25 [taxonomic treatment]. — Bockmann & Guazzelli, 2003: 411 [synonym of *Brachyrhamdia*].

Diagnosis

Distinguished from all Heptapteridae genera, except *Brachyrhamdia*, *Goeldiella*, *Rhamdella* and *Rhamdia* by limits of eye well defined by free orbital rim, especially pronounced anteriorly and dorsally. *Pimelodella* distinguishes from *Brachyrhamdia* by the body elongated, posterior fontanel opened in a long slit, and 37–52 total vertebrae (*vs.* body deep and compact, posterior fontanel as a small orifice at the base of supraoccipital; 33–36, rarely 37 total vertebrae in *Brachyrhamdia*). It distinguishes from *Goeldiella* by the supraoccipital process narrow; and cephalic laterosensory canals opening in skin into single pores (*vs.* supraoccipital process triangular, with broad base; and cephalic laterosensory canals opening in skin into multiple pores in *Goeldiella*). It differs from *Rhamdella* by the presence of a high dorsal lamina of Weberian complex vertebrae; hypural 5 free, separated from the plate formed by hypurals 3 and 4; and median caudal-fin rays not directly attached to hypural plates (*vs.* dorsal lamina of Weberian complex vertebrae low and curved; hypurals 3,

4 and 5 completely co-ossified into dorsal caudal plate; median caudal-fin rays directly attached to hypural plates in *Rhamdella*). It distinguishes from *Rhamdia* by the posterior fontanel opened in a long slit (*vs.* posterior fontanel completely closed, or as a small orifice at the base of supraoccipital in *Rhamdia*).

Furthermore, the species of *Pimelodella* genus can be readily distinguished from other genera of Heptapteridae by the following unique character combination: body moderately elongated, usually between 12–30 cm standard length; supraoccipital process long, usually reaching the anterior nuchal plate; anterior and posterior fontanels open, long, separated by epiphyseal bar; limits of eye well defined by free orbital rim, especially pronounced anteriorly and dorsally; pectoral fin with strong and pungent spine, bearing anterior and posterior dentations, and 7–10 (usually 8) branched rays; branchiostegal rays 6–7 (usually 6); caudal fin deeply forked; median caudal-fin rays not articulated to hypural plate; hypural 5 as a single structure and not fused to hypurals 3+4; body usually with dark midlateral stripe extending from the snout or posterior to the head until the insertion of or onto the centralmost caudal-fin rays (Slobodian *et al.*, 2017).

Common features to Pimelodella species

The following features are general to all species of *Pimelodella*, and some are not repeated in individual species accounts.

Body elongated, compressed, elliptical in cross-section. Greatest body depth at dorsal-fin origin, greatest body width at cleithrum. Dorsal profile straight to convex from snout to dorsal-fin origin, usually slightly concave from that point to adipose-fin origin. Profile straight to convex along adipose fin base, and concave along caudal peduncle. Ventral profile of body convex from snout to posterior limit of branchiostegal membrane, convex to concave between branchiostegal membrane and pelvic-fin origin, usually concave from the latter to anal-fin origin, and broadly concave from that point to caudal insertion.

Pseudotympanum large, oval, dorsal to posterior process of cleithrum and reaching between 6th to 10th vertebrae. Posterior process of cleithrum triangular, its dorsal border straight to concave. Axillary pore present at pectoral-fin base. Anus and urogenital papilla adjacent.

Head deep, mouth subterminal. Teeth small and villiform, absent in the palate. Premaxilla with 8–11 teeth rows, each row with 14–21 teeth; dentary with 7–9 rows, each row with 20–28 teeth. Eye slightly elliptical, its greatest depth along horizontal axis, placed dorsolaterally. Limits of eye well defined by a free orbital rim; margin distinctly invaginated, especially along anterior and dorsal portions. Anterior naris tubular; posterior naris enclosed

anteromedially by shallow flap. Anterior nares near to upper lip, posterior nares approximately through half of preorbital length. Barbels thin, and slightly depressed, elliptical in cross-section. Base of maxillary barbels above upper lip, lateral to anterior naris. Maxillary barbels usually reaching at least vertical through pelvic-fin insertion when lying stretched parallel to main body axis. Base of outer mental barbels medial to mouth extremity, through vertical of posterior naris or posteriorly. Outer mental barbels reaching at least terminus of branchiostegal membrane when lying stretched along body ventral region. Base of inner mental barbels mesial and anterior to outer, reaching at least middle of branchiostegal membrane when lying stretched along body ventral region. Branchiostegal membranes almost entirely free, united to isthmus only at medial apex and not joined to each other anteriorly. Anterior and posterior fontanels long, narrow, separated by the epiphyseal bar, anterior fontanel the longest. Supraoccipital process long, usually reaching anterior nuchal plate.

Dorsal fin triangular, distal margin convex, dorsal-fin rays usually I,6 plus anteriormost spinelet. Distal extremity of first pterygiophore expanded, forming typical median, anteriormost nuchal plate 1. Distal extremity of second pterygiophore expanded laterally, forming typically paired second nuchal plates. Spinelet large with wide base and rounded distal tip. Unbranched dorsal-fin ray mostly rigid, ossified to a spine, might present dentations on posterior margin, and serrae on anterior margin.

Pectoral fin triangular with concave distal border, pectoral-fin rays I,7–I,10. First pectoral-fin ray with proximal portion rigid, forming a spine, and short distal tip flexible and distinctly segmented. Might present serrae and dentations on anterior margin. Posterior margin of pectoral-fin spine with straight or retrorse dentations, of variable size and morphology.

Extended pelvic fin triangular with straight distal border, pelvic-fin rays usually i,5. First unbranched ray distinctly shorter than first and second branched rays.

Distal border of extended anal fin convex. Unbranched anal-fin rays ii–vi, branched anal-fin rays 7–12. Two or three anteriormost anal-fin rays vestigial, unsegmented, embedded in thick skin fold.

Adipose fin round to long, less than two to more than four times in standard length, emerging gradually, its posterior limit as a rounded, free lobe.

Caudal fin deeply forked, dorsal lobe usually I,7, ventral lobe usually I,8. Parhypural not fused to Hypural 1. Hypurals 1 and 2 completely co-ossified into single ventral caudal plate. Hypurals 3 and 4 completely fused to each other. Hypural 5 usually not fused to hypural 3+4. Single rod-like autogenous epural. Hypurapophysis and secondary hypurapophysis

fused, forming a horizontal shelf (hypurapophysis type C of Lundberg & Baskin, 1969). Median caudal-fin rays not articulated directly to caudal plate. Six to eight, usually seven rays articulated to dorsal caudal-fin plate (4–6 on hypurals 3+4 and 2 on hypural 5) and 7–9, usually eight rays articulated to ventral caudal-fin plate (5–7 on hypurals 1+2 and 2 on parhypural).

Total vertebrae 37–52, being five of the Weberian complex vertebra, and one of the caudal complex vertebrae. Centrum 1 autogenous disk-like element attached to complex vertebra via sutures and connective tissue. Complex vertebra centra 2–4 and vertebra 5 centrum sutured to each other. Transverse process of vertebrae 4 divided by a deep notch in an anterior branch, simple, and a posterior branch, expanded, laminar, branched at least one time in two main arms. Transverse process of vertebrae 5 expanded, laminar, usually branched. Transurator of tripus curved medially. Eight to 10 pleural ribs associated to parapophyses from vertebra 6 on, distal extremities of ribs tapered. Neural and hemal spines of caudal vertebrae mostly straight sloped at approximately 60° relative to vertebral column in anterior caudal vertebrae, progressively inclining to 45° in the posterior caudal vertebrae.

Head laterosensory canals with simple (unbranched) tubes usually ending in single pore. Supraorbital canal continuous and connected to infraorbital branch anteriorly (forming complex s2+i2 pore), and posteriorly to the otic branch. Supraorbital laterosensory canal with at least five branches: s1, s2, s3, s6 (epiphyseal branch), and s8 (parietal branch). Contralateral epiphyseal branches may be fused to each other medially, with single opening, or not fused, and opening in separated pores. Contralateral parietal branches usually opening in pores notably posterior to suture between frontal and supraoccipital bones. Postotic (or temporal) sensory canal extends from posterior limit of otic sensory canal to anterior limit of lateral line, with three branches (po1, po2, and po3). First postotic branch (po1) usually fused to posteriormost branch preoperculomandibular sensory (pm11), forming po1+pm11 complex pore. Infraorbital sensory canal with six branches, connecting posteriorly to the otic branch. Preoperculomandibular sensory canal with 11 branches and pores; anteriormost preoperculomandibular sensory branch (pm1) not fused to its antimeric branch. Lateral-line sensory canal complete, continuous with postotic sensory canal anteriorly and extending to base of caudal-fin rays. First lateral-line pore below level of adjacent pores of lateral line.

Most species present a dark midlateral stripe extending from the snout or posterior to the head until the insertion of or onto the median caudal-fin rays.

Distribution

Pimelodella can be found in both Atlantic and Pacific drainages, in all major basins. The northernmost occurrence is in Panamá (there is an uncertified occurrence in Costa Rica), and the southernmost are from south of Peru and central Argentina (Bockmann & Guazzelli, 2003; Eschmeyer, Fricke & van der Laan, 2017; Bockmann & Slobodian, *in press*).

Habitat

Pimelodella species are common component of Neotropical freshwater bodies, from streams to average-sized rivers, with part of its species somewhat broadly distributed, and others endemic to some basin (Bockmann & Guazzelli, 2003; Eschmeyer, Fricke & van der Laan, 2017; Bockmann & Slobodian, *in press*; pers. obs.).

Pimelodella species usually swim in the water column, close to the substrate and with some tendency for cryptic behavior, sheltering in rock crevices and vegetation during daylight, and more active at twilight (Aranha *et al.*, 1998; Bockmann & Guazzelli, 2003; Ruíz Diaz *et al.*, 2008; pers. obs.). *Pimelodella* species often congregate in small shoals up to ten individuals, and their greatest abundance is in streams with dense vegetation coverage and clear or black waters, usually associated with marginal lakes, rocky bottom or sandy beaches (Bockmann & Guazzelli, 2003; Arrington & Winemiller, 2006; Slobodian *et al.*, 2017; pers. obs.).

Trophic ecology

Pimelodella species feed mainly on aquatic and/or terrestrial arthropods (Mazzoni *et al.*, 2010; Moraes *et al.*, 2013), with occasional plant items (Soares-Porto, 1994). Opportunistic lepidophagy has been reported in some species of *Pimelodella* (Costa, 1987; Saul, 1975; Soares-Porto, 1994). Opportunistic behaviour, picking up items from the substrate, was described for *P. pappenheimi* (Aranha *et al.*, 1998). Moraes *et al.* (2013) reported ontogenetic changes in the diet of *P. lateristriga*, with juveniles consuming mostly animal items whereas adults consumed relatively larger amounts of vegetable matter, although in small net quantities.

Also for *P. lateristriga*, the preference for autochthonous or allochthonous arthropods changes during the life cycle, with juveniles showing a higher intake of autochthonous/aquatic items and adults eating a larger proportion of allochthonous/terrestrial items (Mazzoni & Costa, 2007; Moraes *et al.*, 2013). Because aquatic arthropods are found on the bottom of streams, while allochthonous fall on the surface and float or drift in mid-water, adults and juveniles of *Pimelodella* may feed on different strata of the water column (Moraes *et al.*, 2013).

Reproduction

Pimelodella boschmai, *P. insignis*, *P. figueroai*, *P. griffini*, *P. linami*, *P. megalura* and *P. taenioptera* were described on the basis of the presence of a filament on the unbranched dorsal-fin ray, a trait now known to be sexually dimorphic, present only in adult males. Additional sexually dimorphic traits include an enlarged urogenital papilla and prolongation of first to third branched dorsal-fin rays (Dahl, 1961; Van der Stigchel, 1964; Mees, 1974, Souza-Shibatta *et al.*, 2013; Bockmann & Slobodian, 2013; Lundberg & Rapp Py-Daniel, unpublished; pers. obs.). An extreme condition of sexual dimorphism is found in *P. cristata*, where the male is melanic, has a large body size, and an extremely prolonged dorsal fin (Lundberg & Rapp Py-Daniel, unpublished; pers. obs.).

Trajano & Britski (1992) also suggested the dorsal fin-spine length as sexually dimorphic for *P. kronei*, and Mees (1974) reported sexual differences in eye size in *P. cristata*.

A study on *P. lateristriga* (Moraes *et al.*, 2013) determined that sexual maturity is reached at 44.5 mm SL in the species, and that reproduction happens throughout the year, with a small peak of gonadal maturation frequency during spring and summer, and larger sizes among females. *Pimelodella cristata* matures at 116 mm SL (Mees, 1986). *Pimelodella pappenheimi*, on the other hand, reaches sexual maturity at 63 mm SL, has two spawning periods during summer, no size differences between sexes, and its females displays burrowing behavior during the reproductive period, presumably for protection of the brood (Amaral *et al.*, 1998).

Pimelodella species have XX/XY sex chromosome system (Dias & Foresti, 1993; Garcia & Almeida-Toledo, 2010; Condé-Saldaña *et al.*, 2017). There is relatively high levels of karyotype variation among species of the genus, with diploid numbers spanning $2n=46$ (more common) (*P. avanhandavae*, *P. boschmai*, *P. gracilis*, *P. griffini*, *P. laurenti*, *P. meeki*, *P. spelaea*, *P. vittata* and *Pimelodella* sp.), $2n=50$ (*Pimelodella* cf. *chagresi*), $2n=52$ (*Pimelodella* aff. *avanhandavae*, *P. taenioptera*), and $2n=58$ (*P. lateristriga*, *P. kronei*, *P. transitoria*) (Garcia & Almeida-Toledo, 2010; Dazzani *et al.*, 2012; De Borba *et al.*, 2012; Fernandes *et al.*, 2013; Gouveia *et al.*, 2013; Souza-Shibatta *et al.*, 2013; Conde-Saldaña *et al.*, 2017).

Specific composition

There are currently 92 specific names available in *Pimelodella*, 79 of which have been considered as valid (Eschmeyer, Fricke & van der Laan, 2017). The next section presents the species herein recognized as valid (summarized in Table 3). Species moved from *Pimelodella*

into other genera will be discussed at the end of this chapter. The genus *Brachyrhamdia* is considered distinct from *Pimelodella*, and thus is not included below.

***Pimelodella australis* Eigenmann, 1917**

Pimelodella laticeps australis Eigenmann, 1917: 231, 233, 243–244 [original description; “Uruguayana”, State of Rio Grande de Sul, Brazil; holotype: FMNH 57962 (formerly CM 6950)]. — Henn, 1928: 77 [type catalog]. — Gosline, 1945: 44 [taxonomic treatment, distribution]. — Fowler, 1951: 544–545 [taxonomic treatment]. — Ibarra & Stewart, 1987: 66 [type catalog]. — Malabarba, 1989: 141–142 [taxonomic list]. — Burgess, 1989: 280 [taxonomic treatment].

Pimelodella australis. — Guazzelli, 1997: 14–31 [taxonomic review of coastal south and southeastern Brazilian species]. — Bockmann, 1998: 114, 370–372 [systematic treatment]. — Bockmann & Guazzelli, 2003: 417 [taxonomic treatment]. — Guazzelli, 2003: 14–16, 240 [phylogenetic relationships]. — Ferraris, 2007: 189 [taxonomic treatment]. — Volcan *et al.*, 2012: 81 [taxonomic list]. — Litz & Koerber, 2014: 20 [taxonomic list]. — Bertaco *et al.*, 2016: 417 [taxonomic list]. — Nión *et al.*, 2016: 33 [taxonomic list].

Pimelodella garbei Miranda Ribeiro, 1918: 639–640 [original description; “Itaqui– Rio Grande do Sul”, Brazil; lectotype: MNRJ 923A, designated by Miranda Ribeiro (1953: 403); name a misspelling of genus name].

Pimelodella garbei. — Gosline, 1945: 45 [emendation of originally-assigned genus name; taxonomic treatment]. — Miranda Ribeiro 1953: 403 [lectotype designation]. — Britski 1969: 205 [type catalog]. — Burgess, 1989: 280 [taxonomic treatment]. — Guazzelli, 1997: 14, 136 [suggested synonym of *P. australis*]. — Bockmann & Guazzelli, 2003: 418 [synonym of *P. australis*]. — Litz & Koerber, 2014: 20 [synonym of *P. australis*]. — Ferraris 2007: 189 [synonym of *P. australis*].

Pimelodella portalegrensis. — Silfvergrip & Paepke, 1997: 172 [*nomen nudum*, not published; name in label by E. Ahl; formerly *Pimelodella lateristriga* ZMB 7437 and ZMB 25128 (last one reassigned to ZMB 32030, but latter number the same for the holotype of *P. conquetanesis*)].

Diagnosis

Pimelodella australis differs from all *Pimelodella* species but *P. laticeps* by the presence of a dark brown coloration region between dorsal and adipose fins (Figs. 7, 9). It differs from *P. laticeps* by the presence of paired dark fields along supraoccipital process (*vs.*

absence); a hyaline stripe in the dorsal fin not extending over unbranched fin ray (*vs.* extending); and the presence of paired dorsolateral dark stripes along the first half of the adipose-fin base present (*vs.* absent). *Pimelodella australis* can be further diagnosed by the combination of the following traits: maxillary barbel reaching between verticals through anterior tip of pelvic-fins base and first third of anal fin adpressed; supraoccipital process narrow, roughly triangular; dorsal-fin spine roughly three-fourths of first dorsal-fin ray total length; pectoral fin spine curved, with retrorse dentations along basal two thirds of spine, distalmost dentations straighter; adipose fin four times in SL; 39–41 total vertebrae; S6 contralateral canals emerging in two distantly-positioned pores, far apart; dark brown, wide, poorly-defined midlateral stripe, extending between orbit and caudal peduncle; paired dark brown dorsal stripes present alongside supraoccipital process; and dark brown mark present between dorsal and adipose fins.

Description

Measurements in Table 4. Body of moderately deep, depth at dorsal-fin origin five times in standard length, and compressed, body width at dorsal-fin origin six to eight times in SL (Fig. 5). Greatest body depth at dorsal-fin origin. Dorsal profile convex from snout to dorsal fin, slightly concave from dorsal to adipose fin, slightly convex along adipose fin, and concave along caudal peduncle. Ventral profile of body slightly convex from snout to branchiostegal membrane, also convex between branchiostegal membrane and pectoral-fins, and between pectoral end pelvic fins, slightly concave from pelvic to anal fin, and also concave from that point to caudal peduncle.

Pseudotympanum large, oval, dorsal to posterior process of cleithrum and reaching 6th (3)–7^{th*} (1) vertebrae. Posterior process of cleithrum triangular, narrow, its dorsal margin slightly concave. Anus and urogenital papilla adjacent. Urogenital papilla tubular, triangular, short. Anus between verticals through last fifth and end of adpressed dorsal fin; urogenital papilla between verticals through last third to fifth of adpressed pelvic-fins.

Head deep, depth at base of supraoccipital-process half of head length. Mouth sub terminal. Eye slightly elliptical, four to five times in head. Bony interorbital distance roughly equal to eye diameter. Barbels thin, slightly depressed and elliptical in cross-section. Maxillary barbel reaching between verticals through pelvic-fin base and first third of adpressed anal fin. Outer mental barbel, when stretched parallel to main body axis, finishing between half pectoral-fin base and pectoral-fin first third adpressed. Inner mental barbel, when stretched parallel to main body axis, finishing between verticals of posterior ventral limit of branchiostegal membrane and half the way between this membrane and vertical

through pectoral-fins insertions. Supraoccipital process narrow, roughly triangular. Dorsal lamina of Weberian complex vertebrae reaching the supraoccipital process only at its anteriormost part. Branchiostegal rays 7* (1).

Dorsal fin triangular, distal margin convex, overall short (longest dorsal-fin ray length five times in SL), depressed tip reaching between verticals through last third or fifth of adpressed pelvic-fins. Dorsal fin I,6 (31) plus anteriormost spinelet. Distance between terminus of dorsal-fin base and adipose-fin origin roughly equal to dorsal-fin base. Anteriormost dorsal-fin pterygiophore inserted posterior to neural spine of vertebrae 4 (6); posteriormost dorsal-fin pterygiophore located anterior to neural (or pseudoneural) spine of vertebrae 11 (6). Unbranched dorsal-fin ray mostly ossified as a spine, rigid part relatively long (ca. 75% or more of first dorsal-fin ray total length), distal third of anterior margin with smooth serrae.

Pectoral-fin rays I,7 (14)– I,8* (15), pectoral fin triangular with concave distal border, First pectoral-fin ray curved with proximal part rigid, forming a spine (Fig. 6), and short distal tip flexible and distinctly segmented. Anterior margin of pectoral-fin spine with smooth serrae along its distal third, and minute, straight dentations along its basal half or two-thirds; posterior margin with 8–11 straight to retrorse dentations along its basal half to two-thirds. Dentations triangular, 2–3 distalmost less curved than ones along most of margin, with 2–3 nearest base of ray again less curved. Also 2–3 unossified distal dentations (not counted). Smaller specimens (less than 50 mm SL) with dentations relatively larger than in specimens over 60 mm SL.

Pelvic-fin rays i,5 (30), extended pelvic fin triangular with straight distal border. Pelvic-fin origin at vertical through terminus of dorsal-fin base. Tip of adpressed pelvic fin between verticals through anterior tip of adipose fin and its first tenth. First unbranched and flexible ray distinctly shorter than second and third rays, second ray the longest, but barely longer than third ray; remaining rays progressively shorter.

Anal-fin rays v,7 (2); iv,8 (1); v,8 (7); vi,8* (3); iv,9 (5); v,9 (5) or vi,9 (1); distal margin of extended anal fin convex. Two or three anteriormost anal-fin rays vestigial, unsegmented, embedded in thick skin fold. Anal fin origin between verticals through end of first third to almost half of adipose-fin base; adpressed anal-fin terminus between verticals through distal point of adipose-fin base or a point slightly anterior to that. Anterior anal-fin pterygiophore inserted posterior to hemal spine of vertebrae 20* (3), 21 (2) or 23 (1). Posterior anal-fin pterygiophore inserted anteriorly to hemal spine of vertebrae 28 (1), 29* (4) or 30 (1).

Adipose fin short, four times or more in SL, forming ascending elevated curve in lateral profile, with deepest point approximately at midlength. Adipose fin emerging gradually, its posterior limit as a rounded, free lobe. Adipose-fin origin at vertical through vertebral centra 18 (1) or 21* (3); adipose-fin terminus at vertical through vertebral centra 31 (1) to 35* (1).

Caudal fin deeply forked, dorsal lobe usually slightly longer than ventral lobe. Caudal peduncle length posterior to adipose-fin roughly a third longer than its depth. Dorsal lobe with 7 (23) branched, 1 (23) unbranched principal and 11 (1)–16 (3) (holotype 13) procurrent fin-rays. Ventral lobe with 8 (23) branched, 1 (23) unbranched principal and 11 (2)–18 (1) (holotype 16) procurrent fin-rays. Hypural 5 free. Median caudal-fin rays not articulated directly to hypural plate. Seven (6) rays articulating with dorsal caudal-fin plate (5 on hypurals 3+4 and 2 on hypural 5) and 8 (6) rays articulating with ventral caudal-fin plate (6 on hypurals 1+2 and 2 on parhypural).

Total vertebrae 39*(4)–41(1). Ribs 8*(4)–10 (1).

Epiphyseal branch of cephalic laterosensory canal (S6) emerging as two widely-distanced pores in all 44 examined specimens.

Coloration in alcohol

Background body coloration yellowish. Ventral region of head and body lighter than dorsal regions. Dark brown midlateral stripe (Fig. 7), poorly-defined, wide, extending from orbit to caudal peduncle, near where it widens slightly. Paired dark brown dorsal stripes along margins of supraoccipital process, to terminus of prenuchal plate, and lighter stripes along anterior half of adipose fin. Dark brown mark present between dorsal and adipose fins, conjoined with paired stripes along adipose fin. Dark grayish region as large as the pseudotympanum, located dorsal to it, almost reaching dorsal stripe near supraoccipital process. Dorsal fin overall dark brown, with hyaline stripe near base, which does not cover the unbranched dorsal-ray and membrane between it and the first branched-ray, which are overall dark.

Geographic distribution

Pimelodella australis was described from “Uruguayana”, the city of Uruguaiana, Rio Grande do Sul state, within the range of the rio Uruguay system, with additional specimens from coastal South Atlantic basins in Rio Grande do Sul State. This corresponds to its currently known range, from regions 332 (Lower Uruguay) and 334 (Laguna dos Patos),

mainly in coastal rivers from Rio Grande do Sul State, in Lagoa dos Patos and rio Uruguay systems.

Comments

Pimelodella garbei was described by Miranda Ribeiro (1918) for Itaqui, Rio Grande do Sul state, Brazil. In 1997, Guazzelli suggested that it was indistinguishable from *P. australis*, and the species was formerly synonymized with the latter in by Bockmann & Guazzelli (2003).

Examination of relevant type material corroborates the synonym of the two species. Despite the advanced loss of dark pigmentation in the type-material of both species, part of the conspicuous coloration marks diagnostic of *P. australis* is still visible in the type specimens of *P. garbei*. Measurements and counts also match, so that little room remains for considering *P. garbei* as separate from *P. australis*. Further comments on these taxa are presented below in this Chapter.

Pimelodella laticeps australis mentioned by Pearson (1924) for Rio Beni basin is probably not assignable to *P. australis*. However, Pearson's specimens were not examined for this study and their taxonomic status cannot be precisely determined at this time.

Material examined

Pimelodella australis. — FMNH 57962, 1, xr, 61.0 mm SL, holotype, Brazil, Rio Grande do Sul, Uruguayana, Rio Uruguay, 29°45'03"S, 5°05'44"W; FMNH 57963, 21, xr, 40.5–70.8 mm SL, paratypes, Brazil, Rio Grande do Sul, Uruguayana, Rio Uruguay, 29°45'03"S, 5°05'44"W; FMNH 57964, 16, xr, 39.9–63.1 mm SL, paratypes, Brazil, Rio Grande do Sul, Cacequy, Rio Ibicuhy, into the Rio Uruguay, 29°51'23"S, 54°49'55"W; FMNH 57965, 2, xr, 43.6–44.5 mm SL, paratype, Brazil, Rio Grande do Sul, Cachoeira, Rio Jacuhy, into Lago de Patos, 29°58'29"S, 51°14'41"W; FMNH 57966, 4, xr, 43.2–48.9 mm SL, paratypes, Brazil, Rio Grande do Sul, Porto Alegre, Rio Guahyba in front of town, 30°02'27"S, 51°14'34"W; MZUSP 9620, 1, Brazil, Rio Grande do Sul, Pelotas; MZUSP 25030, 2, 34.6–46.3 mm SL, Brazil, Rio Grande do Sul, Porto Alegre, stream at Belém-Novo County, near Porto Alegre, 30°12'0.0"S, 51°12'0.0"W; MZUSP 25206, 32, Brazil, Rio Grande do Sul, Rio Grande-Cassino road, Senandes Stream, 32°3'0.0"S, 52°5'0.0"W; MZUSP 25210, 1, 45.0 mm SL, Brazil, Rio Grande, Saco do Justino, south from Mangueira Lake, 32°3'0.0"S, 52°5'0.0"W; MZUSP 25216, 1, 36.8 mm SL, Brazil, Rio Grande do Sul, stream in the way to Fazenda Caçapava (Est. No. 3), 32°29'0.0"S, 52°35'0.0"W; MZUSP 28249, 5, Brazil, Rio Grande do Sul, Cruzeiro Do Sul, Sampaio stream, 29°29'0.0"S, 52°8'0.0"W; MZUSP 40976,

5, Brazil, Rio Grande do Sul, Palmitinho, Lageado União stream, Linha dos Lima, 30°21'0.0"S, 53°34'0.0"W; MZUSP 63926, 3, 57.0–72.4 mm SL, Brazil, São Sepé River, in a bridge sideways to BR-153, ca. 3km south from São Sepé, Rio Jacuí basin, 30°11'8.0"S, 53°33'35.0"W; MZUSP 63935, 3, Brazil, Rio Grande do Sul, São Francisco de Assis, Inhacundá River at São Francisco de Assis, ca. 500m above Olaria, Uruguay River basin, 29°32'27.0"S, 55°7'45.0"W; MZUSP 63943, 1, Brazil, Rio Grande do Sul, Francisco de Assis, Sanga Funda stream ca. 15 km southeast from São Francisco de Assis, 29°39'2.0"S, 55°0'6.0"W; MZUSP 74146, 1, 28.7 mm SL, Brazil, Rio Grande do Sul, São Leopoldo, Rio dos Sinos, Banhado do Schreck, 29°45'0.0"S, 51°10'0.0"W; USNM 235077, 1, 44.2 mm SL, Brazil, Rio Grande Do Sul, Arroio Bolacha About 1/2 km Southwest From Where Road Between Rio Grande and Cassino Crosses Arroio Bolacha, 32°10'12.0"S, 52°10'12.0"W; USNM 285628, 2, 36.2–52.9 mm SL, Brazil, Rio Grande Do Sul, Itaqui, Ibicui River next to mouth (Affluent to Uruguay River), 29°25'04.5"S, 56°45'55.7"W; USNM 285872, 4, 47.6–79.8 mm SL, Brazil, Rio Grande Do Sul, Palmitinho, Arroio Lageado Uniao, at Linha dos Lima (Affluent to Pardo River, Uruguay River), 27°21'07.1"S, 53°33'28.1"W; USNM 320368, 6, 79.5–107.7 mm SL, Brazil, Santa Catarina, Garuva, Rio Garuva, under the bridge at BR-101, 26°01'34.5"S, 48°51'35.0"W.

Pimelodella garbei. — MNRJ 923A, 1, xr, 62.6 mm SL, lectotype, Brazil, Rio Grande do Sul, Itaqui, Rio Uruguay, 29°06'58.6"S, 56°33'28.7"W; MNRJ 923, 10, 47.0–59.3 mm SL, paralectotype, Brazil, Rio Grande do Sul, Itaqui, Rio Uruguay, 29°06'58.6"S, 56°33'28.7"W; MZUSP 1057, 1, 52.4 mm SL, paralectotype, Brazil, Rio Grande do Sul, Itaqui, Rio Uruguai, 29°8'0.0"S, 56°36'0.0"W; MZUSP 5280, 1, 43.1 mm SL, paralectotype, Brazil, Rio Grande do Sul, Itaqui, Rio Uruguai, 29°8'0.0"S, 56°36'0.0"W; MZUSP 5281, 1, 44.6 mm SL, paralectotype, Brazil, Rio Grande do Sul, Itaqui, Rio Uruguai, 29°8'0.0"S, 56°36'0.0"W; MZUSP 5282, 1, 44.9 mm SL, paralectotype, Brazil, Rio Grande do Sul, Itaqui, Rio Uruguai, 29°8'0.0"S, 56°36'0.0"W; MZUSP 5283, 1, 47.8 mm SL, paralectotype, Brazil, Rio Grande do Sul, Itaqui, Rio Uruguai, 29°8'0.0"S, 56°36'0.0"W; MZUSP 5284, 1, 49.5 mm SL, paralectotype, Brazil, Rio Grande do Sul, Itaqui, Rio Uruguai, 29°8'0.0"S, 56°36'0.0"W; MZUSP 5285, 1, 49.3 mm SL, paralectotype, Brazil, Rio Grande do Sul, Itaqui, Rio Uruguai, 29°8'0.0"S, 56°36'0.0"W; MZUSP 5286, 1, xr, 50.3 mm SL, paralectotype, Brazil, Rio Grande do Sul, Itaqui, Rio Uruguai, 29°8'0.0"S, 56°36'0.0"W; MZUSP 5287, 1, 47.2 mm SL, paralectotype, Brazil, Rio Grande do Sul, Itaqui, Rio Uruguai, 29°8'0.0"S, 56°36'0.0"W; MZUSP 5288, 1, 48.9 mm SL, paralectotype, Brazil, Rio Grande do Sul, Itaqui, Rio Uruguai, 29°8'0.0"S, 56°36'0.0"W; MZUSP 5289, 1, 51.6 mm SL, paralectotype, Brazil, Rio Grande

do Sul, Itaqui, Rio Uruguai, 29°8'0.0"S, 56°36'0.0"W; MZUSP 5290, 1, 50.8 mm SL, paralectotype, Brazil, Rio Grande do Sul, Itaqui, Rio Uruguai, 29°8'0.0"S, 56°36'0.0"W; MZUSP 5291, 1, 49.8 mm SL, paralectotype, Brazil, Rio Grande do Sul, Itaqui, Rio Uruguai, 29°8'0.0"S, 56°36'0.0"W; MZUSP 5292, 1, xr, 54.3 mm SL, paralectotype, Brazil, Rio Grande do Sul, Itaqui, Rio Uruguai, 29°8'0.0"S, 56°36'0.0"W; MZUSP 5293, 1, 57.3 mm SL, paralectotype, Brazil, Rio Grande do Sul, Itaqui, Rio Uruguai, 29°8'0.0"S, 56°36'0.0"W; MZUSP 5494, 1, 56.8 mm SL, paralectotype, Brazil, Rio Grande do Sul, Itaqui, Rio Uruguai, 29°8'0.0"S, 56°36'0.0"W; MZUSP 5296, 1, 56.5 mm SL, paralectotype, Brazil, Rio Grande do Sul, Itaqui, Rio Uruguai, 29°8'0.0"S, 56°36'0.0"W; MZUSP 5298, 1, 56.7 mm SL, paralectotype, Brazil, Rio Grande do Sul, Itaqui, Rio Uruguai, 29°8'0.0"S, 56°36'0.0"W.

***Pimelodella avanhandavae* Eigenmann, 1917**

Pimelodella avanhandavae Eigenmann, 1917: 230, 232, 240, pl. XXIX, fig. 3, pl. XXXV, fig. 8 [original description; “Rio Tieté at Salto Avanhandava, above the fall”, State of São Paulo, Brazil; holotype: FMNH 57981 [formerly CM 6969a]. — Henn, 1928: 77 [type catalog]. — Gosline, 1945: 43 [taxonomic treatment, distribution]. — Fowler, 1951: 534, fig. 548 [taxonomic treatment]. — Ibarra & Stewart, 1987: 65 [type catalog]. — Burgess, 1989: 280 [taxonomic treatment]. — Bockmann & Guazzelli, 2003: 417 [taxonomic treatment]. — Shibatta & Cheida, 2003: 470 [taxonomic list]. — Trajano *et al.*, 2004: 317 [taxonomic review]. — Ferraris, 2007: 189 [taxonomic treatment]. — Graça & Pavanelli, 2007: 146 [taxonomic list]. — Langeani *et al.* 2007: 187 [taxonomic list]. — Pavanelli *et al.* 2007: 62 [taxonomic list]. — Cunico *et al.*, 2009: 278 [taxonomic list]. — Teresa & Casatti, 2010: 448 [taxonomic list].

Diagnosis

Pimelodella avanhandavae differs from all *Pimelodella* species but *P. chagresi*, *P. eutaenia*, *P. gracilis*, *P. griffini*, *P. montana*, *P. odynea*, *P. peruana*, *P. reyesi* and *P. roccae* by having a paired dorsolateral brown stripe along body (Figs. 8, 10). It differs from *P. eutaenia*, *P. griffini*, *P. peruana*, *P. reyesi* and *P. roccae* by this stripe extending from supraoccipital process until half to last third of adipose-fin base (*vs.* extending to adipose fin origin in *P. eutaenia* and *P. peruana*; adipose-fin terminus in *P. griffini*, *P. reyesi*, and *P. roccae*). It differs from *P. chagresi*, *P. montana* and *P. gracilis* by having 41–45 total vertebrae (39–41 total vertebrae in *P. chagresi*, *P. montana*; and 46, rarely 45 total vertebrae in *P. gracilis*). It differs from *P. odynea* by having maxillary barbels reaching up to vertical through first fifth of adpressed anal fin (*vs.* maxillary barbels surpassing adpressed anal fin);

and dorsal fin with a hyaline stripe near base (*vs.* dorsal fin completely pigmented). *Pimelodella avanhandavae* can be further diagnosed by the combination of the following traits: maxillary barbel reaching between verticals through anterior tip of anal and its last fifth adpressed; dorsal-fin spine ca. of 75% of first dorsal-fin total length; posterior margin of pectoral-fin spine bearing 8–12 retrorse dentations along its basal two-thirds; adipose fin long, less than three times in SL; 41–45 total vertebrae; dark brown midlateral stripe wide, well-delimited, extending between snout and centralmost caudal-fin rays; and darker brown coloration dorsally, as a poorly-defined stripe along dorsolateral region of body, alongside supraoccipital process to approximately first third to half of adipose-fin base.

Description

Measurements in Table 5. Body of moderately deep, depth at dorsal-fin insertion five times or more in SL, and compressed, body width at dorsal-fin insertion six times or more in SL (Fig. 8). Greatest body depth at dorsal-fin origin. Dorsal profile convex from snout to dorsal-fin origin, slightly concave from dorsal to adipose fin, slightly convex along adipose fin, and concave along the caudal peduncle. Ventral profile of body slightly convex from snout to branchiostegal membrane, also convex between branchiostegal membrane and pectoral-fins, and between pectoral end pelvic fins, slightly concave from pelvic to anal fin, and also concave from that point along the caudal peduncle.

Pseudotympanum large, oval, dorsal to posterior process of cleithrum and reaching 6th* (3) or 7th (1) vertebrae. Posterior process of cleithrum triangular, narrow, its dorsal margin slightly concave. Anus and urogenital papilla adjacent. Urogenital papilla tubular, triangular, short. Anus between verticals through last fourth and terminus of adpressed dorsal fin; urogenital papilla between verticals through last third to fourth of adpressed pelvic fin.

Head deep, depth at base of supraoccipital-process half of head length. Mouth sub terminal. Eyes slightly elliptical, four to five times in head. Bony interorbital distance equal to or slightly smaller than eye diameter. Barbels thin, slightly depressed and elliptical in cross-section. Maxillary barbel reaching between verticals through anal-fin origin and its adpressed last fifth. Outer mental barbel, when stretched parallel to main body axis, finishing between half and last fifth of adpressed pectoral-fin. Inner mental barbel, when stretched parallel to main body axis, finishing between verticals of pectoral-fin insertion and terminus. Supraoccipital process narrow, rectangular, with a constant width long its length and narrowing at its distal point. Dorsal lamina of Weberian complex vertebrae reaching the supraoccipital process only at anteriormost part, or along the anterior half, but never along its entire length. Branchiostegal rays 6 (1).

Dorsal fin triangular, distal margin convex, short (second branched dorsal-fin ray a fifth or less in SL), depressed tip finishing between verticals through half and last fifth of adpressed pelvic-fins. Dorsal fin I,6 (13) plus anteriormost spinelet. Distance between terminus of dorsal-fin base and adipose-fin origin roughly half of dorsal-fin base. Anteriormost dorsal-fin pterygiophore inserted posterior to neural spine of vertebrae 4 (6); posteriormost dorsal-fin pterygiophore located anterior to neural (or pseudoneural) spine of vertebrae 11 (6). Unbranched dorsal-fin ray mostly ossified as a spine, rigid part relatively long (ca. 75% of first dorsal-fin ray total length), distal third of anterior margin with smooth serrae, and distal third of posterior margin with smooth straight dentations.

Pectoral-fin rays I,7 (1)– I,9 (2), usually I,8* (8), pectoral fin triangular with concave distal border. First pectoral-fin ray curved with proximal part rigid, forming a spine (Fig. 9), and short distal tip flexible and distinctly segmented. Moderate length spine, five and half times or less in SL. Anterior margin of pectoral-fin spine with serrae along its distal third, and small straight dentations along its basal half. Posterior margin of pectoral-fin spine bearing 8–12 retrorse dentations along its basal two-thirds. Dentations large and curved, smaller near base of spine. Also 1–3 unossified distal dentations, not counted.

Pelvic-fin rays i,5 (12), extended pelvic fin triangular with straight distal border. Anterior portion of pelvic-fin base at vertical through end of dorsal-fin base. Tip of adpressed pelvic fin between verticals through first third to first fifth of adipose fin. First unbranched and flexible ray distinctly shorter than second and third rays, which are roughly the same size; remaining rays progressively shorter.

Anal-fin rays v,6 (1); iv,7 (1) ;v,7 (2); iv,8 (2) or v,8* (3); distal margin of extended anal fin convex. Two or three anteriormost anal-fin rays vestigial, unsegmented, embedded in thick skin fold. Anal fin origin between verticals through terminus of first third to almost half of adipose-fin base; anal-fin adpressed terminus always slightly anterior to vertical through adipose-fin terminus. Tip of anteriormost anal-fin pterygiophore inserted posterior to hemal spine of vertebrae 21 (1) or 23* (5). Tip of posteriormost anal-fin pterygiophore inserted anteriorly to hemal spine of vertebrae 29 (1) or 31* (5).

Adipose fin less than three times in SL, forming ascending elevated curve in lateral profile, with deepest point approximately at midlength. Adipose fin emerging gradually, its posterior limit as a rounded, free lobe. Adipose-fin origin at vertical through vertebral centra 17 (1)– 21 (2) (holotype 18); adipose-fin terminus at vertical through vertebral centra 35 (1*)– 41 (1) (holotype 39).

Caudal fin deeply forked, its dorsal lobe usually slightly longer than ventral lobe. Caudal peduncle length posterior to adipose-fin roughly the same as its depth or slightly longer. Dorsal lobe with 7 (7) branched, 1 (7) unbranched principal, and 8 (1)–15* (2) procurrent fin-rays. Ventral lobe with 8 (7) branched, 1 (7) unbranched principal, and 10 (1)–18 (1) (holotype 17) procurrent fin-rays. Hypural 5 free. Median caudal-fin rays not articulated directly to hypural plate. Seven (6) rays articulated to dorsal caudal-fin plate (5 on hypurals 3+4 and 2 on hypural 5) and 8 (6) rays articulated to ventral caudal-fin plate (6 on hypurals 1+2 and 2 on parhypural).

Total vertebrae 41 (1)–45 (1) (holotype 44). Ribs 9 (1)–10* (4).

Epiphyseal branch of cephalic laterosensory canal (S6) emerging as two narrowly-distanced pores, after a small canal towards head midline (17*), or one unique pore, as soon as those two canals intersect (12). One specimen with just one opening, at top of head, after a small canal connecting both S6 canals.

Coloration in alcohol

Background body coloration yellowish. Ventral region of head and body lighter than dorsal regions. Dark brown midlateral stripe (Fig. 10), well-delimited, wide, extending from snout to centralmost caudal-fin rays. Paired dark brown dorsolateral, poorly-defined stripes along margins of supraoccipital process to approximately first third to half of adipose-fin base, getting lighter and poorly-defined posteriorly. Dorsal fin with dark brown stripe near its base, followed by a hyaline stripe, and distal half dark brown. Cephalic pigmentation as a slightly darker brown region at posterior fontanel.

Geographic distribution

Pimelodella avanhandavae was described from Rio Tiete at Salto Avanhandava. This corresponds to its currently known range, from region 344 (Upper Paraná), mainly Upper Paraná river system in São Paulo State.

Material examined

Pimelodella avanhandavae. — FMNH 57981, 1, xr, 69.0 mm SL, holotype, Brazil, São Paulo, Rio Tieté at Salto Avanhandava, above the fall, 21°14'12"S, 49°55'48"W; FMNH 58982, 23, xr, 46.5–80.2 mm SL, paratypes, Brazil, São Paulo, Rio Tieté at Salto Avanhandava, above the fall, 21°14'12"S, 49°55'48"W; FMNH 58068, 7, xr, 43.8–60.2 mm SL, paratypes, Brazil, São Paulo, Rio Tieté at Salto Avanhandava, above the fall, 21°14'12"S, 49°55'48"W; MZUSP 22829, 14, 42.5–75.7 mm SL, Brazil, Paraná River, in front of Jupia, 20°15'0.0"S, 51°7'0.0"W.

***Pimelodella boliviana* Eigenmann, 1917**

Pimelodella boliviana Eigenmann, 1917: 230–231, 233, 245, pl. XXXI, fig. 2, pl. XXXV, fig. 30 [original description; “Santa Cruz de la Sierra, Bolivia”; holotype: FMNH 57976 (formerly CM 6964a)]. — Henn, 1928: 77 [type catalog]. — Fowler, 1940b: 78, 80 [comparison with *P. howesi*]. — Eigenmann & Allen, 1942: 100 [taxonomic treatment]. — Fowler, 1945b: 46 [taxonomic list]. — Gosline, 1945: 44 [taxonomic treatment, distribution]. — Fowler, 1948: 535, fig. 549 [taxonomic treatment]. — Fowler, 1951: 535. — Ortega & Vari, 1986: 14 [taxonomic list]. — Ibarra & Stewart, 1987: 65 [type catalog]. — Burgess, 1989: 280 [taxonomic treatment]. — Bockmann & Guazzelli, 2003: 417 [taxonomic treatment]. — Ferraris, 2007: 189 [taxonomic treatment]. — Bockmann & Slobodian, 2013: 59, 69, fig. 36.1A–B [taxonomic review, key]. — Sarmiento *et al.*, 2014: 158, 191 [taxonomic list].

Pimelodella cf. boliviana — Chernoff *et al.*, 2000: 282 [taxonomic list]

Diagnosis

Pimelodella boliviana differs from all *Pimelodella* species with exception of *P. avanhandavae*, *P. buckleyi*, *P. eutaenia*, *P. figueroai*, *P. howesi*, *P. itapicuruensis*, *P. leptosoma*, *P. martinezi*, *P. megalura* and *P. serrata* by 44 total vertebrae (information unknown in *P. figueroai* and *P. martinezi*). It differs from all above, except *P. howesi* and *P. serrata* by the maxillary barbel reaching the caudal-fin origin (Figs. 11, 13). It differs from *P. howesi* and *P. serrata* by the posterior margin of pectoral-fin spine bearing 8–9 minute and smooth retrorse dentations along its basal two-thirds (Fig. 12) (*vs.* posterior margin of pectoral-fin spine bearing 10–14 retrorse dentations along its basal two thirds, these dentations large, with curved apex, and smaller near base of spine in *P. howesi*; posterior margin of pectoral-fin spine bearing 16–21 large, retrorse dentations along roughly all margin, these dentations are acute, hook-like in *P. serrata*). *Pimelodella boliviana* can be further diagnosed by the combination of the following traits: maxillary barbel very long, almost reaching or surpassing caudal-fin insertion; dorsal lamina of Weberian complex vertebrae usually deep, reaching the supraoccipital process along all its length; posterior margin of pectoral-fin spine bearing 8–9 minute and smooth retrorse dentations along its basal two-thirds; adipose fin long, three times in SL; 44 total vertebrae; epiphyseal branch of cephalic laterosensory canal opening in two distantly-positioned pores; dark brown midlateral stripe poorly-defined, of moderate width, extending from snout to caudal peduncle, and lighter along median caudal-fin rays.

Description

Measurements in Table 6. Body depressed, depth at dorsal-fin insertion more than six times in standard length, and compressed, body width at dorsal-fin origin more than seven and half times in SL (Fig. 11). Greatest body depth at dorsal-fin origin. Dorsal profile convex from snout to dorsal fin, slightly concave from dorsal to adipose fin, slightly convex along adipose fin, and concave along caudal peduncle. Ventral profile of body slightly convex from snout to branchiostegal membrane, also convex between branchiostegal membrane and pectoral-fins, and between pectoral end pelvic fins, slightly concave from pelvic to anal fin, and also concave from that point to caudal peduncle.

Pseudotympanum large, oval, dorsal to posterior process of cleithrum and reaching the straight line of 7th (2) vertebrae. Posterior process of cleithrum triangular, narrow, its dorsal margin straight. Anus and urogenital papilla adjacent. Urogenital papilla tubular, triangular, short. Anus between verticals through last fourth or third of adpressed dorsal fin; urogenital papilla between verticals through half and last third of adpressed pelvic fin.

Head moderated depth, depth at base of supraoccipital-process always smaller than half of head length. Mouth sub terminal. Eye slightly elliptical, four to four and half times in head. Bony interorbital a quarter smaller than diameter. Barbels thin, slightly depressed and elliptical in cross-section. Maxillary barbel almost reaching or surpassing caudal-fin insertion. Outer mental barbel, when stretched parallel to main body axis, finishing between last fifth and terminus of adpressed pectoral-fin. Inner mental barbel, when stretched parallel to main body axis, finishing between verticals through half pectoral-fin base and pectoral fin terminus. Supraoccipital process narrow, rectangular, with a constant width long its length and narrowing at its distal point. Dorsal lamina of Weberian complex vertebrae usually deep, reaching the supraoccipital process along its entire length. Branchiostegal rays 6 (1).

Dorsal fin triangular, distal margin convex, short (second branched dorsal-fin ray five times or more in SL), depressed tip reaching verticals between last fifth and terminus of adpressed pelvic fins. Dorsal fin I,6 (3) plus anteriormost spinelet. Distance between dorsal and adipose fins half to two-thirds of dorsal-fin base. Anteriormost dorsal-fin pterygiophore inserted posterior to neural spine of vertebrae 4 (2); posteriormost dorsal-fin pterygiophore located anterior to neural (or pseudoneural) spine of vertebrae 11 (2). Unbranched dorsal-fin ray mostly ossified as a spine, rigid part short (ca. 66% of first dorsal-fin ray total length) and delicate.

Pectoral-fin rays I,8 (3), pectoral fin triangular with concave distal border. First pectoral fin ray long, roughly straight, with proximal part rigid, forming a spine (Fig. 12A),

and short distal tip flexible and distinctly segmented. Pectoral fin spine roughly six times in SL. Anterior margin of pectoral-fin spine with smooth serrae along its distal two-thirds to half. Posterior margin of pectoral-fin spine bearing 8–9 minute and smooth retrorse dentations along its basal two-thirds. Also 1–2 unossified distal dentations (not counted).

Pelvic-fin rays $i,5$ (3), extended pelvic fin triangular with straight distal margin. Pelvic-fin origin between verticals through last fourth and sixth of dorsal-fin base. Tip of adpressed pelvic fin slightly after vertical through anterior tip of adipose fin. First unbranched and flexible ray distinctly shorter than second and third rays, being the third ray the longest, but barely longer than second; remaining rays progressively shorter.

Anal-fin rays $vi,7^*$ (1) or $v,8$ (2); distal margin of extended anal fin convex. Two or three anteriormost anal-fin rays vestigial, unsegmented, embedded in thick skin fold. Anal fin origin between verticals through terminus of first fourth to first third of adipose-fin base; anal-fin adpressed terminus slightly anterior to vertical through adipose-fin terminus. Tip of anteriormost anal-fin pterygiophore inserted posterior to hemal spine of vertebrae 22 (1) or 24* (1). Tip of posteriormost anal-fin pterygiophore inserted anterior to hemal spine of vertebrae 31 (1) or 32* (1).

Adipose fin long, three times in SL, forming ascending elevated curve in lateral profile, with highest point approximately at midlength. Adipose fin emerging gradually, its posterior limit as a rounded, free lobe. Adipose-fin origin at vertical through vertebral centra 17* (1)–18 (1); adipose-fin terminus at vertical through vertebral centra 38 (1)–39* (1).

Caudal fin deeply forked, its dorsal lobe slightly longer than ventral lobe. Caudal peduncle length posterior to adipose-fin roughly a third longer than its depth. Dorsal lobe with 7 (3) branched, 1 (3) unbranched principal and 13* (1)–14 (1) procurrent fin-rays. Ventral lobe with 8 (3) branched, 1 (3) unbranched principal and 11* (1)–15 (1) procurrent fin-rays. Hypural 5 free. Median caudal-fin rays not directly articulated to hypural plates. Six* (1)–7 (1) rays articulated directly to dorsal caudal-fin plate (5 on hypurals 3+4 and 1 or 2 on hypural 5) and 7* (1)–8 (1) rays articulated directly to ventral caudal-fin plate (5 or 6 on hypurals 1+2 and 2 on parhypural).

Total vertebrae 44 (2). Ribs 8 (2).

Epiphyseal branch of cephalic laterosensory canal (S6) opening in two widely-distanced pores, opening after a small canal towards head midline.

Coloration in alcohol

Background body coloration yellowish. Ventral region of head and body lighter than dorsal. Dark brown midlateral stripe (Fig. 13), poorly-defined, of moderate width, extending

from snout to caudal peduncle, and lighter along median caudal-fin rays. Dorsal fin distal half dark brown. Paired dark brown dorsal stripes along margins of supraoccipital process. Dark brown cephalic pigment at posterior fontanel region.

Geographic distribution

Pimelodella boliviana was described from “Santa Cruz de la Sierra”, a city in Bolivia, where there occur rivers from Mamoré River basin. The currently known range is from regions 316 (Amazonas Lowlands), 318 (Mamore-Madre de Dios Piedmont), 319 (Guaporé-Itenez), mainly in Madeira-Mamoré-Madre de Dios system, in Bolívia, Brazil and Peru.

Comments

Specimens of *P. boliviana* may have slightly variation on colour pattern and pectoral-fin spine morphology. Some material may present the dark midlateral stripe slightly wider than the described here, and the pectoral-fin spine dentations on lateral margin can be more inconspicuous (as illustrated in fig. 12A), or retrorse and notably inclined (Fig. 12B). However, overall, both pectoral and dorsal-fin spines of *P. boliviana* are more delicate than the ones from *P. howesi*, *P. hasemani* and *P. serrata*, from the same basin.

Material examined

Pimelodella boliviana. — FMNH 57976, 1, xr, 68.9 mm SL, holotype, Bolivia, Santa Cruz de La Sierra, 17°55'34"S, 62°48'20"W; FMNH 57977, 1, xr, 66.9 mm SL, paratype, Bolivia, Prov. del Sara Buenavista, 17°29'08"S, 63°40'32"W, MZUSP 26015, 1, 71.3 mm SL, Peru, Depto. Ucayali, Prov. Coronel Portillo, Masisea, Lobococha, 8°23'30.1"S, 74°31'31.5"W.

***Pimelodella boschmai* Van der Stigchel, 1964**

Pimelodella boschmai Van der Stigchel, 1964: 327–330, fig. 1 [original description; “Mogi-Guassu (river) below the Emas falls”, Pirassununga, State of São Paulo, Brazil; holotype: RMNH 23248, male]. — Mees, 1974: 152 [synonym of *P. insignis* to *P. boschmai*]. — Burgess, 1989: 280 [taxonomic treatment]. — Bockmann & Guazzelli, 2003: 417 [taxonomic treatment]. — Guazzelli, 2003: 16, 214 [phylogenetic relationships]. — Trajano *et al.*, 2004: 317 [taxonomic review]. — Ferraris, 2007: 190 [taxonomic treatment]. — Langeani *et al.* 2007: 187 [taxonomic list].

Pimelodella insignis Schubart, 1964: 6–9, fig. 1 [original description; “Rio Mogi Guaçu, abaixo do pesqueiro da EEBP; Cochoeira [sic] de Emas, na topava; Rio Mogi Guaçu, abaixo do pesqueiro; Rio Mogi Guaçu, abaixo da cachoeira; Rio Mogi Guaçu; Rio Mogi Guaçu, pesqueiro da EEBP”; syntypes: EEBP 497, 497 [bis], 498, 499, 620,

620a, 647]. — Mees, 1974: 152 [junior-synonym of *P. boschmai*]. — Bockmann, 1994: 764 [morphology]. — Bockmann & Guazzelli, 2003: 417 [junior-synonym of *P. boschmai*]. — Ferraris, 2007: 190 [junior-synonym of *P. boschmai*].

Diagnosis

Pimelodella boschmai can be diagnosed from all *Pimelodella* species by having a dark midlateral stripe extending from snout to orbit, and then posterior to opercle until caudal-fin origin (Figs. 14, 16). *Pimelodella boschmai* can be further diagnosed by the combination of the following traits: maxillary barbel reaching approximately the first third of anal fin base; unbranched dorsal-fin ray might present a filamentous prolongation; posterior margin of pectoral-fin spine with usually 8–12 retrorse dentations at proximal half to two-thirds of spine, these dentations are triangular, broad-based, getting smaller and straighter towards both apex and base of spine; adipose fin relatively long, three times or less in SL; 40–42 total vertebrae; epiphyseal branch of cephalic laterosensory connecting at midline, proceeding posteriorly as a single canal and opening in a single pore; dark brown midlateral stripe narrow to moderated width and poorly-defined, extending posterior to pseudotympanum to caudal-fin origin; also a brown stripe from snout to orbit.

Description

Measurements in Table 7, based on syntypes of *P. insignis*, a junior-synonym of *P. boschmai*. Description based on types of both *P. boschmai* and *P. insignis*, and comparative material. Body moderately deep, depth at dorsal-fin origin five times or more in standard length, and compressed, body width at dorsal-fin origin six and half to seven times in SL (Fig. 14). Dorsal profile convex from snout to eyes, straight from eyes to dorsal fin, slightly concave from dorsal to adipose fin, slightly convex along adipose fin, and concave along caudal peduncle. Ventral profile of body slightly convex from snout to branchiostegal membrane, and between pectoral and pelvic fins, and convex from pelvic to caudal peduncle.

Pseudotympanum large, oval, dorsal to posterior process of cleithrum and reaching 6th (4) vertebrae. Posterior process of cleithrum triangular, dorsal margin slightly concave. Anus and urogenital papilla adjacent. Urogenital papilla tubular, triangular, long in specimens with dorsal-fin filament, being the distance between anus and urogenital papilla ten times in SL). Anus through the vertical of last fifth of adpressed dorsal fin; urogenital papilla between verticals through terminus of adpressed dorsal fin and first third of adipose-fin base.

Head deep, depth at base of supraoccipital-process half of head length. Mouth sub terminal. Eye slightly elliptical, five to six times in head. Bony interorbital distance roughly

equal to eye diameter. Barbels thin, and slightly depressed and elliptical in cross-section. Maxillary barbel reaching approximately the first third of anal fin base. Outer mental barbel, when stretched parallel to main body axis, finishing slightly posterior to first third of pectoral-fin base. Inner mental barbel, when stretched parallel to main body axis, finishing midway between branchiostegal membrane ventral limit and pectoral-fin insertion. Supraoccipital process subrectangular, narrowing at its distal tip, when reaches the nuchal plate. Head roof lightly ornamented. Branchiostegal rays 6 (4).

Dorsal fin triangular, distal margin concave, overall short (second branched dorsal-fin ray length five times in SL), reaching the vertical through last third of adpressed pelvic fin, except by a filamentous first-ray extension which, when present, can reach up to adipose fin midlength. Dorsal fin I,6 (4) plus anteriormost spinelet. Distance between terminus of dorsal-fin base and adipose-fin origin between half and two-thirds of dorsal-fin base length. Anteriormost dorsal-fin pterygiophore inserted posterior to neural spine of vertebrae 4 (4); posteriormost dorsal-fin pterygiophore located anterior to neural (or pseudoneural) spine of vertebrae 11 (4). Unbranched dorsal-fin ray mostly ossified as a spine, anterior margin bearing smooth serrae along roughly its distal fourth and posterior margin with minute smooth straight dentations along its distal fourth.

Pectoral-fin rays I,7* (3) or I,8 (1), pectoral fin triangular with concave distal border. First pectoral-fin ray curved, with proximal part rigid, forming a spine (Fig. 15), and short distal tip flexible and distinctly segmented. Pectoral fin spine five to five and half times in SL. Anterior margin of pectoral-fin spine with straight dentations along its basal half, and smooth serrae along its distal half. Posterior margin of pectoral-fin spine with usually 8–12 retrorse dentations at proximal half to two-thirds of spine, plus sometimes 1–3 unossified distalmost dentations. Dentations triangular, broad-based, near apex and base of spine dentations smaller and straighter.

Pelvic-fin rays i,5 (4), extended pelvic fin triangular with straight distal border. Pelvic-fin origin at vertical through dorsal-fin terminus. Tip of adpressed pelvic fin through vertical of adipose-fin first fifth. First unbranched and flexible ray distinctly shorter than second and third rays, which are roughly the same size; remaining rays progressively shorter.

Anal-fin rays v,8 (2) or iv,9* (2); distal border of extended anal fin convex. Two or three anteriormost anal-fin rays vestigial, unsegmented, embedded in thick skin fold. Anal fin origin slightly posterior to vertical through end of first third or half of adipose-fin base; anal-fin adpressed terminus slightly posterior to vertical through the last third of adipose-fin base. Tip of anteriormost anal-fin pterygiophore inserted posterior to hemal spine of vertebrae 20*

(2), 21 (1) or 22 (1). Tip of posteriormost anal-fin pterygiophore inserted anterior to hemal spine of vertebrae 27 (1), 28* (1) or 29 (2).

Adipose fin three times or less in SL, forming ascending elevated curve in lateral profile, deepest point approximately at midlength. Adipose fin emerging gradually, and posterior limit as rounded, free lobe. Adipose-fin origin at vertical through vertebral centra 17–19 (holotype 18); adipose-fin terminus at vertical through vertebral centra 34–36*.

Caudal fin deeply forked, dorsal lobe slightly longer than ventral lobe. Caudal peduncle length posterior to adipose-fin approximately a third longer than its depth. Dorsal lobe with 7 (4) branched, 1 (4) unbranched principal and 12*–20 procurrent fin-rays. Ventral lobe with 8 (4*) branched, 1 (4) unbranched principal and 16–21 (holotype 18) procurrent fin-rays. Hypural 5 free. Medial caudal-fin rays not articulated directly to hypural plate. Seven (4) rays articulated to dorsal caudal-fin plate (5 on hypurals 3+4 and 2 on Hypural 5) and 8 (4) rays articulated to ventral caudal-fin plate (6 on hypurals 1+2 and 2 on parhypural).

Total vertebrae 40* (2)–42 (2). Ribs 8* (2)–9 (2).

Epiphyseal branch of cephalic laterosensory canal (S6) connecting at midline, proceeding posteriorly as a single canal and opening in a single pore.

Coloration in alcohol

Background body coloration yellowish. Ventral region of head and body lighter than dorsal regions. Dark brown midlateral stripe (Fig. 16), narrow to moderated width, poorly-delimited, extending posterior to pseudotympanum to caudal-fin insertion. Also another paired brown stripe from snout to orbit. Regions at pseudotympanum and distal half of dorsal-fin rays slightly darker, brown to grayish pigmented; cephalic brown pigment at posterior fontanel.

Geographic distribution

Both *Pimelodella boschmai* and its junior-synonym, *P. insignis*, were described from Mogi-Guaçu River at Cachoeira de Emas region, Pirassununga municipality, São Paulo state, Brazil. This corresponds to its currently known range, from region 344 (Upper Parana), mainly Mogi-Guaçu river, Upper Paraná river system, in São Paulo State.

Comments

Despite Van der Stigchel (1964) comment that the filament is in the first branched dorsal-fin ray, meanwhile Schubart (1964) described as a filamentous prolongation of the dorsal-fin spine, Mees (1974) argued *P. boschmai* and *P. insignis* would be, in fact, one species. Also, Van der Stigchel (1964) mentioned have received his specimens from Schubart,

in a way that both materials are probably belonging to the same samples. Since *P. boschmai* was published months before *P. insignis*, the first has the priority, as pointed out by Mees (1974) when synonymizing both, a taxonomic decision I agree with.

I also observed a material collected for cytogenetic studies (UFSCar uncat, in examined material), from Mogi-Guaçu region near Cachoeira de Emas, with sexes determined by gonadal analysis. None of those specimens had dorsal-fin filaments, but all the other characteristics are congruent with the description of *P. boschmai*. Also, none of those specimens had mature gonads (O. M. Filho, pers. comm.), in a manner that maybe the filament is present only during sexual maturity in males. This is congruent with Van der Sitgchel (1964) reports that the two specimens from type-series without filament had also smaller urogenital papilla and, upon dissection, proved to be females.

Material examined

Pimelodella boschmai. — RMNH 23248, 1, xr, holotype, Brazil, São Paulo, Pirassununga, Mogi-guassu river below Ema falls, 21°55'35"S, 47°21'58"W, observed photos and x-rays; Lab. de Citogenética da UFSCar 3331, 1, Brazil, São Paulo, Pirassununga, Cachoeira de Emas, +ou- 100 metros abaixo da escada da represa, 21°55'33.9"S, 47°22'03.8"W; Lab. de Citogenética da UFSCar 3332, 1, Brazil, São Paulo, Pirassununga, Cachoeira de Emas, +ou- 100 metros abaixo da escada da represa, 21°55'33.9"S, 47°22'03.8"W; Lab. de Citogenética da UFSCar 3470, 1, Brazil, São Paulo, Pirassununga, Cachoeira de Emas, +ou- 100 metros abaixo da escada da represa, 21°55'33.9"S, 47°22'03.8"W; Lab. de Citogenética da UFSCar 3478, 1, Brazil, São Paulo, Pirassununga, Cachoeira de Emas, +ou- 100 metros abaixo da escada da represa, 21°55'33.9"S, 47°22'03.8"W; Lab. de Citogenética da UFSCar 3480, 1, Brazil, São Paulo, Pirassununga, Cachoeira de Emas, +ou- 100 metros abaixo da escada da represa, 21°55'33.9"S, 47°22'03.8"W; Lab. de Citogenética da UFSCar 3486, 1, Brazil, São Paulo, Pirassununga, Cachoeira de Emas, +ou- 100 metros abaixo da escada da represa, 21°55'33.9"S, 47°22'03.8"W; Lab. de Citogenética da UFSCar 3610, 1, Brazil, São Paulo, Pirassununga, Cachoeira de Emas, +ou- 100 metros abaixo da escada da represa, 21°55'33.9"S, 47°22'03.8"W; Lab. de Citogenética da UFSCar 3611, 1, Brazil, São Paulo, Pirassununga, Cachoeira de Emas, +ou- 100 metros abaixo da escada da represa, 21°55'33.9"S, 47°22'03.8"W; Lab. de Citogenética da UFSCar 3619, 1, Brazil, São Paulo, Pirassununga, Cachoeira de Emas, +ou- 100 metros abaixo da escada da represa, 21°55'33.9"S, 47°22'03.8"W; Lab. de Citogenética da UFSCar 3623, 1, Brazil, São Paulo, Pirassununga, Cachoeira de Emas, +ou- 100 metros abaixo da escada da represa, 21°55'33.9"S,

47°22'03.8"W; Lab. de Citogenética da UFSCar 3662, 1, Brazil, São Paulo, Pirassununga, Cachoeira de Emas, +ou- 100 metros abaixo da escada da represa, 21°55'33.9"S, 47°22'03.8"W; MZUSP 22543, 1, 69.3 mm SL, Brazil, São Paulo, Pirassununga, Cachoeira de Emas, 21°55'0.0"S, 47°23'0.0"W.

***Pimelodella brasiliensis* (Steindachner, 1877)**

Pimelodus (*Pseudorhamdia*) *brasiliensis* Steindachner, 1877: 608–611, pl. 7 [original description; “Rio Parahyba”, Paraíba do Sul river, Brazil; holotype: NMW 45612].

Pimelodella brasiliensis. — Eigenmann & Eigenmann, 1888: 133 [taxonomic treatment]. — Eigenmann & Eigenmann, 1890: 149, 162 [key to *Pimelodella* species; taxonomic revision]. — Eigenmann & Eigenmann, 1891: 29 [taxonomic treatment]. — Eigenmann, 1910: 389 [taxonomic treatment]. — Eigenmann, 1917: 242 [taxonomic revision]. — Gosline, 1945: 44 [taxonomic treatment]. — Fowler, 1951: 535–536 [taxonomic treatment]. — Burgess, 1989: 280 [taxonomic treatment]. — Guazzelli, 1997: 123–128 [taxonomic review of coastal south and southeastern Brazilian species]. — Bizerril & Primo, 2001: 28 [taxonomic list]. — Bockmann & Guazzelli, 2003: 417 [taxonomic treatment]. — Ferraris, 2007: 190 [taxonomic treatment].

Rhamdia brasiliensis. — Miranda Ribeiro, 1911: 275 [taxonomic treatment].

Pimelodella buckleyi [non Boulenger, 1887]. — Eigenmann & Eigenmann, 1888: 133 [taxonomic treatment]. — Eigenmann & Eigenmann, 1890: 149, 158–159 [key to *Pimelodella* species; taxonomic revision]. — Eigenmann & Eigenmann, 1891: 29 (*in partim*) [taxonomic treatment]. — Eigenmann, 1910: 389 [taxonomic treatment; junior-synonym of *P. eigenmanni*].

Pimelodella eigenmanni Boulenger, 1891: 232 [original description; “Macacos”, probably “Macacos Valley”, actual Paracambi, Rio de Janeiro State, Southeastern Brazil; and not Ribeirão dos Macacos, Rio das Velhas basin, as usually presented (see discussion); syntypes: BMNH 1889.11.14.6 MCZ 7438 and 7510 (see discussion)]. — Eigenmann, 1910: 389 [taxonomic treatment]. — Eigenmann, 1917: 232, 248, pl. XXXV, fig. 15 [taxonomic revision] — Gosline, 1945: 44 [taxonomic treatment]. — Fowler, 1951: 359 [taxonomic treatment]. — Ibarra & Stewart, 1987: 66 [type catalog]. — Burgess, 1989: 280 [taxonomic treatment]. — Bockmann & Guazzelli, 2003: 418 [taxonomic treatment]. — Ferraris, 2007: 191 [taxonomic treatment].

Rhamdia eigenmanniorum Miranda Ribeiro, 1911: 273–274 [*nomen novum*, translation of Eigenmann & Eigenmann (1890: 158–159) description of *P. buckleyi*; “Rio

Parahyba”]. — Eigenmann, 1917: 248 [synonym of *P. eigenmanni*] — Fowler, 1951: 359 [synonym of *P. eigenmanni*].

Pimelodella eigenmanniorum. — Bockmann & Guazzelli, 2003: 418 [taxonomic treatment]. — Ferraris, 2007: 191 [taxonomic treatment].

Pimelodella rendahli Ahl, 1925: 106–107 [original description; “ohne genauen Fundort” (without exact location), South America; holotype: ZMB 32031]. — Gosline, 1945: 44 [taxonomic treatment]. — Fowler, 1951: 549 [taxonomic treatment]. — Silfvergrip & Paepke, 1997: 167, fig. 4 [type catalog]. — Bockmann & Guazzelli, 2003: 421 [taxonomic treatment]. — Ferraris, 2007: 196 [taxonomic treatment].

Diagnosis

Pimelodella brasiliensis can be diagnosed from all *Pimelodella* species except *P. avanhandavae*, *P. boschmai*, *P. buckleyi*, *P. elongata*, *P. eutaenia*, *P. figueroai*, *P. geryi*, *P. griffini*, *P. harttii*, *P. hasemani*, *P. howesi*, *P. ignobilis*, *P. itapicuruensis*, *P. kroni*, *P. lateristriga*, *P. leptosoma*, *P. longipinnis*, *P. martinezi*, *P. megalops*, *P. megalura*, *P. metae*, *P. odynea*, *P. pectinifera*, *P. peruana*, *P. reyesi*, *P. robinsoni*, *P. roccae*, *P. serrata*, *P. taeniophora* and *P. vittata* by having 42–43 total vertebrae (unknown in *P. figueroai* and *P. martinezi*). From the above mentioned, it differs from *P. itapicuruensis*, *P. leptosoma*, *P. longipinnis*, *P. megalura*, *P. metae* and *P. robinsoni* by having the supraoccipital process reaching the anterior prenuchal plate (*vs.* supraoccipital process not reaching the anterior prenuchal plate in *P. itapicuruensis*, *P. leptosoma*, *P. longipinnis*, *P. megalura*, *P. metae* and *P. robinsoni*; unknown in *P. reyesi*). It differs from *P. avanhandavae*, *P. eutaenia*, *P. griffini*, *P. harttii*, *P. kroni*, *P. odynea*, *P. peruana*, *P. reyesi*, *P. roccae*, *P. taeniophora* and *P. vittata* by the absence of a dorsolateral paired stripe on body (*vs.* presence of a dorsolateral paired stripe on body in *P. avanhandavae*, *P. eutaenia*, *P. griffini*, *P. harttii*, *P. kroni*, *P. odynea*, *P. peruana*, *P. reyesi*, *P. roccae*, *P. taeniophora* and *P. vittata*). It differs from *P. boschmai*, *P. buckleyi*, *P. elongata*, *P. hasemani*, *P. howesi* and *P. megalops* by having the epiphyseal branch of laterosensory canal emerging as two pores near each other, or one pore, just as the contralateral canals connect (*vs.* epiphyseal branch of laterosensory canal with contralateral canals connecting, processing posteriorly as a single canal, and opening in a single pore at top of head in *P. boschmai*, *P. buckleyi*, *P. elongata* and *P. howesi*; contralateral canals emerging in two separate pores, far from each other, in *P. hasemani* and *P. megalops*). It differs from *P. figueroai*, *P. geryi*, *P. ignobilis*, *P. lateristriga*, *P. martinezi*, *P. pectinifera* and *P. serrata* by having the midlateral stripe of moderate width, not well delimited, and head overall darker

(vs. head not darker in all but *P. lateristriga*; midlateral stripe wide in *P. geryi*, *P. ignobilis*, *P. lateristriga*; midlateral stripe narrow in *P. figueroai* and *P. martinezi*; midlateral stripe narrow to moderate width but head not darker in *P. serrata*).

Pimelodella brasiliensis can be further diagnosed by the combination of the following traits: maxillary barbel reaching between half and terminus of anal fin; dorsal-fin spine three fourths or more of first dorsal-fin total length; posterior margin of pectoral-fin spine with 10–18 minute, retrorse to straight dentations, from region just beyond base of spine to slightly short of the last fourth of spine; adipose fin moderated length, four times in SL; 42–43 total vertebrae; epiphyseal branch of laterosensory canal emerging as a single pore immediately after canals connect, or not connecting, and emerging as two pores near each other; dark brown midlateral stripe moderated width, not well-delimited, extending from orbit to caudal-fin insertion; head overall darker, brownish, and dorsal-fin with hyaline base and distal half dark brown pigmented.

Description

Measurements in Table 8. Body moderately deep, depth at dorsal-fin origin five to five and half times in standard length, and compressed, body width at dorsal-fin origin seven times in SL (Fig. 17). Dorsal profile convex from snout to dorsal fin, slightly concave from dorsal to adipose fin, slightly convex along adipose fin, and concave along caudal peduncle. Ventral profile of body slightly convex from snout to branchiostegal membrane, slightly concave between pectoral end pelvic fins, and convex from pelvic to caudal peduncle.

Pseudotympanum large, oval, dorsal to posterior process of cleithrum and reaching 7th (1) vertebrae. Posterior process of cleithrum triangular, dorsal margin concave. Axillary pore small, immediately above the posterior portion of pectoral-fin base, at crest of posterior cleithral process (the difficulty in finding it may be the reason Steindachner described it as absent). Anus and urogenital papilla adjacent. Urogenital papilla tubular, triangular, short. Anus between verticals through first third and half adpressed pelvic fin; urogenital papilla between verticals through second third and almost terminus of adpressed pelvic fin.

Head deep, depth at supraoccipital-process base roughly half of head length. Mouth sub terminal. Eye slightly elliptical, four to five times in head. Bony interorbital distance narrow, slightly greater than half eye diameter. Barbels thin, slightly depressed and elliptical in cross-section. Maxillary barbel reaching between half and terminus of anal fin. Outer mental barbel, when stretched parallel to main body axis, finishing between first third and half of adpressed pectoral fin. Inner mental barbel, when stretched parallel to main body axis, finishing slightly posterior to branchiostegal membrane ventral limit. Supraoccipital process

subrectangular, but with a narrow constriction at its base, and tapered at its distal tip, when reaches anterior preopercular plate. Head roof ornamented. Dorsal lamina of Weberian complex vertebrae of medium depth, reaching the supraoccipital process only at anteriormost part. Branchiostegal rays 6 (3).

Dorsal fin triangular, distal margin concave, of moderated length (second branched dorsal-fin ray four and half to five times in SL), depressed tip reaching between the verticals through last fourth and short of terminus of adpressed pelvic fins. Dorsal fin with I,6 (5) or I,7* (1) plus anteriormost spinelet. Distance between terminus of dorsal-fin base and adipose-fin origin slightly greater than dorsal-fin base. Anteriormost dorsal-fin pterygiophore inserted posterior to neural spine of vertebrae 4 (2); posteriormost dorsal-fin pterygiophore located anterior to neural (or pseudoneural) spine of vertebrae 11 (2). Unbranched dorsal-fin ray mostly ossified as a spine, rigid part relatively long (ca. 75% of first dorsal-fin ray total length), delicate. Distal third of dorsal-fin spine anterior margin with smooth serrae, and basal two-thirds bearing smooth straight dentations.

Pectoral-fin rays I,8* (5) or I,9 (1), pectoral fin triangular with concave distal margin. First pectoral-fin ray curved, with proximal part rigid (Fig. 18), forming a spine, and short distal tip flexible and distinctly segmented. Pectoral fin spine five times or slightly more in SL. Anterior margin of pectoral-fin spine with smooth straight dentations along its basal two-thirds, and smooth serrae along its distal third. Posterior margin of pectoral-fin spine with 10–18 minute, retrorse to straight dentations, from region just beyond base of spine to slightly short of the last fourth of spine, plus 3–5 unossified distalmost dentations. When retrorse, those dentations are inclined and acute, but straight dentations (near distal half of spine) are small.

Pelvic-fin rays i,5 (6), extended pelvic fin triangular with straight distal border. Pelvic-fin origin at vertical through terminus of dorsal-fin base or a point slightly posterior to that. Tip of adpressed pelvic fin between verticals through origin and first fourth of adipose-fin base. First unbranched and flexible ray distinctly shorter than second and third rays, third ray the longest; remaining rays progressively shorter.

Anal-fin rays iv,8* (1); iv,9 (2); v,9 (2); or iv,10 (1), distal margin of extended anal fin convex. Two anteriormost anal-fin rays vestigial, unsegmented, embedded in thick skin fold. Anal fin origin between verticals through first fourth or third of adipose-fin base. Anal-fin adpressed terminus slightly posterior to vertical through adipose-fin terminus. Tip of anteriormost anal-fin pterygiophore inserted posterior to hemal spine of vertebrae 21* (1) or

22 (1). Tip of posteriormost anal-fin pterygiophore inserted anterior to hemal spine of vertebrae 29* (1) or 30 (1).

Adipose fin four times in SL, forming ascending elevated curve in lateral profile, with deepest point approximately at midlength. Adipose fin emerging gradually, posterior limit as rounded, free lobe. Adipose-fin origin at vertical through vertebral centrum 23 (2); adipose-fin terminus at vertical through vertebral centra 35 (1) or 37* (1).

Caudal fin deeply forked, its dorsal lobe slightly longer than ventral lobe. Caudal peduncle very long, its length posterior to adipose-fin almost twice longer than its depth. Dorsal lobe with 7 (2) branched, 1 (2) unbranched principal and 13 (1)– 18 (1) procurrent fin-rays. Ventral lobe with 8 (2) branched, 1 (2) unbranched principal and 18* (1)– 24 (1) procurrent fin-rays. Hypural 5 free. Median caudal-fin rays not directly attached to caudal plate. Seven (2) rays articulated to dorsal caudal-fin plate (5 on hypurals 3+4 and 2 on Hypural 5) and 7 (1) or 8* (1) rays articulated to ventral caudal-fin plate (5 or 6 on hypurals 1+2 and 2 on parhypural).

Total vertebrae 42 (1)–43* (1). Ribs 9* (1)– 10 (1).

Epiphyseal branch of cephalic laterosensory canal (S6) with contralateral canals connected, emerging as a single pore immediately after canals connect, or not connecting, and emerging as two pores narrowly-distanced.

Coloration in alcohol

Background body coloration yellowish. Ventral region of head and body lighter than dorsal regions. Dark brown midlateral stripe moderated width (Fig. 19), poorly-defined, extending from orbit to caudal-fin origin. Head overall darker, brownish. Dorsal fin with hyaline base and distal half dark brown pigmented.

Geographic distribution

Pimelodella brasiliensis was described from Rio Paraíba do Sul, and its junior-synonym, *P. eigenmanni*, from Rio Paraíba do Sul and probably Rio Guandu (see comments), from Southeastern Atlantic basin. *Pimelodella rendahli*, another junior-synonym of *P. brasiliensis*, has no exact collecting location. Its currently known range is from region 329 (Paraíba do Sul) streams of Southeastern Atlantic basin, in São Paulo and Minas Gerais States, Brazil.

Comments

Upon the examination of *P. brasiliensis* and *P. eigenmanni* type materials I can suggest the synonym of both species. *Pimelodella eigenmanni* has the same characteristic

diagnostics as *P. brasiliensis*, being: maxillary barbel reaching at least the vertical through adipose-fin origin; head roof ornamented; distance between terminus of dorsal-fin base and adipose-fin origin slightly greater than dorsal-fin base; dorsal-fin spine relatively long (approximately less than a fourth shorter than the first dorsal-fin ray total length), delicate; anterior margin of pectoral-fin spine bearing smooth serrae along its distal half; posterior margin of pectoral-fin spine bearing smooth dentations along its basal two thirds, the dentations near the base are more acute and retrorse; progressively being smoother, with larger bases, and straight-oriented near the tip, the distal ones smallest; adipose fin three and half times in SL, total vertebrae 42–43. Comparative measurements of *P. brasiliensis* and *P. eigenmanni* types are shown in Table 9.

Boulenger (1891) described *P. eigenmanni* regarding one specimen from “Macacos” received from C. Eigenmann, from MCZ, comparing with his *P. buckleyi* and a *P. vittata* (Lütken, 1874). In this description, Boulenger says that Eigenmann & Eigenmann’s *P. buckleyi* are undoubtedly different from his types, proposing so a new species, *P. eigenmanni*, based on Eigenmann & Eigenmann (1990) description. Since Boulenger (1891) explicitly states he “propose for the species described by Dr. and Mrs. Eigenmann as *P. buckleyi* the name of *Pimelodus (Pimelodella) eigenmanni*”, the type series of this new species “consists of or includes the specimen or specimens which had been misidentified, whether the later author refers to them directly or through an illustration or a description” (ICZN, Art. 72.4.2), and therefore includes BMNH 1889.11.14.6, MCZ 7438 and 7510 as syntypes.

Miranda Ribeiro (1911) makes a thoroughly historic compendium of Brazilian fishes described by other researchers. In this work he declares a *nomen novum* for the *Rhamdia buckleyi* (*Pimelodus buckeyi* Boulenger, 1887) described by Eigenmann & Eigenmann, 1890, calling it *Rhamdia eigenmanniorum* (pages 19 and 273–274.) The description provided by Miranda Ribeiro is a translation of Eigenmann & Eigenmann (1890) description for *P. buckleyi* from Rio Parahyba (Paraíba do Sul) and “Macacos”.

Miranda Ribeiro (1911) perhaps missed the description of *Pimelodella eigenmanni* by Boulenger (1891) in a footnote, despite having consulted this work, as shown by the other species described by Boulenger between 1891 and 1898 that were cited (Miranda Ribeiro, 1911: 18). Therefore, I suggest that *P. eigenmanniorum* described by Miranda Ribeiro (1911) is, actually, a junior-synonym of *P. eigenmanni* (Boulenger, 1891), as was also formerly suggested by Eigenmann (1917) and Fowler (1951).

Other issues regarding *P. eigenmanni* are related with the type series. The type presented in BMNH collection has a label showing only “*Pimelodella. Pimelodus*

eigenmanni. Macacos. Mus. Comp. Zool.”, what agrees with the statement that Boulenger examined one specimen from Macacos received from MCZ. Although, despite not examining all material described by Eigenmann & Eigenmann (1890), Boulenger proposes for the species described by Eigenmann & Eigenmann (1890) the name *P. eigenmanni*. Eigenmann & Eigenmann (1890) analyzed specimens from Macacos and from Paraíba do Sul Rivers, and the only specimens from MCZ likely to be the ones identified as *P. buckleyi* are from lots MCZ 7438 (5 specimens, has identification as *P. buckleyi* inside jar) and MCZ 7510 (1 specimen, also has identification as *P. buckleyi* inside jar). Given the above mentioned, and according to ICZN, Article 72.4.2, I designate the inclusion of MCZ 7438 and MCZ 7510, together with BMNH 1889.11.14.6, as the type-series for *P. eigenmanni*, being BMNH specimen the lectotype (Fig. 17 C, D), and the remaining as paralectotypes (ICZN, Recommendation 73B; Art. 74).

The locality of “Macacos” of both BMNH 1889.11.14.6 and MCZ 7438 is commonly referred as “Ribeirão dos Macacos”, a Rio das Velhas tributary in Minas Gerais State. This is probably related to the use of “Macacos” as the aforementioned locality in the Thayer Expedition (Higuchi, 1996), which material is deposited at MCZ, and was collected between 1865 and 1866.

However, Eigenmann & Eigenmann (1890: 490) used for “Macacos” a locality on Amazon delta, where Rio Pará connects with Amazon River, what gave rise to several species with uncommon distributions. Miranda Ribeiro (1911: 350), however, stated “Macacos” locality as pertaining to Rio de Janeiro State, without further comments about this decision, and was followed by Mees (1974). Eigenmann & Eigenmann (1890) listed for “Macacos” *Rhamdia quelen*, *Rhamdella minuta*, *Pimelodella buckleyi* (?), *Centromochlus albescens*, *Pygidium maculatum* (?), *Loricaria lima*, *Plecostomus commersonii*, *Plecostomus vermicularis*, *Callichthys callichthys*. From those, *Centromochlus albescens*, *Loricaria lima*, *Plecostomus commersonii*, *Plecostomus vermicularis* are well-known to occur in Southeastern Brazil, as recognized by Mees (1974), what further supports Miranda Ribeiro’s statement.

Other three lots are catalogued in MCZ under the same collector as *P. eigenmanni* MCZ 7438: MCZ 7857 *Plecostomus vermicularis* (syntype) (now in *Hypostomus*); MCZ 7819 *Plecostomus punctatus* (now in *Hypostomus*); and MCZ 15153 *Geophagus brasiliensis*.

Geophagus brasiliensis has a more widespread area of occurrence, in coastal drainages of Brazil, Argentina and Uruguay (e.g. Eschmeyer, Fricke & van der Laan, 2017). *Hypostomus punctatus* is known from Southeastern Brazilian coastal drainages (e.g. Weber, 2003; Ferraris, 2017) and possibly de La Plata river drainage, in Brazil and Uruguay.

Hypostomus vermicularis is currently a junior-synonym of *H.luetkeni*, and was described by Eigenmann & Eigenmann (1888) based on 37 specimens from “Rio Parahyba; Rio de Janeiro; Mendez; Macacos; Goyaz”. All localities, except “Goyaz” and “Macacos” are in the State of Rio de Janeiro following Mazzoni *et al.* (1994), and for those authors the locality “ ‘Macacos’ showed to be very inaccurate and currently not recognizable” (Mazzoni *et al.*, 1994: 10). *Hypostomusluetkeni*, senior-synonym of *H. vermicularis*, occurs in Rio Paraíba do Sul basin (Mazzoni *et al.*, 1994).

Therefore, as above explained, the other three specimens from the same collecting event as MCZ 7438 *P. eigenmanni* are species known to occur only in coastal drainages, and not in Rio das Velhas basin, or even Amazon basin. Furthermore, the collector of “Macacos” syntypes was W. M. Roberts (K. Hartel, *pers. comm.*), an engineer that supervised the construction of “Dom Pedro (II) Railroad” between the years 1857 and 1865 (Roberts, 1828–1959). This railroad was supposed to connect several cities in Minas Gerais, São Paulo and Rio de Janeiro States, arriving in the Baía de Guanabara (Giesbrecht, 2017). In 1860 a branch between “Belém” (now Japeri, Rio de Janeiro State) and “Macacos” (Vale dos Macacos, now Paracambi, Rio de Janeiro State) was finished (Giesbrecht, 2017). The Rio Guandu is a Southeastern Coastal River that crosses Paracambi, and probably the locality referred as “Macacos” by W.M. Roberts. The same railroad continues towards Monte Azul, a city 58km north of Ribeirão dos Macacos, Rio das Velhas basin. However, at the time the construction of this railroad arrived that region (after 1883) (Giesbrecht, 2017), and W.M. Roberts have already left Brazil, in 1881 (Roberts, 1828–1959). So, the here designated lectotype and paralectotype MCZ 7438 of *P. eigenmanni* probably were collected at Rio Guandu, Vale dos Macacos (now Paracambi), in Southeastern Coastal drainages of Brazil.

Pimelodella rendahli is another junior-synonym of *P. brasiliensis*, only known from type material, which has no exact locality information. However, upon type examination, I believe this species is indistinguishable from *P. brasiliensis*. The measurements (presented comparatively in Table 9), color pattern and pectoral-fin morphology of *P. rendahli* are extremely similar to *P. brasiliensis*, what allow me this synonym. Furthermore, *P. rendahli* type is also presented in Figure 17.

Material examined

Pimelodella brasiliensis — NMW 45612, 1, xr, 140.6 mm SL, holotype, Brazil, "Rio Parahyba" (probably Paraíba do Sul), 22°31'06"S, 44°41'49"W; MZUSP 108488, 2, Brazil, Minas Gerais, Teófilo Otoni, Rio Todos os Santos, affluent of Rio Mucuri, 17°51'7.0"S,

41°34'37.0"W; MZUSP 108512, 1, Brazil, Minas Gerais, Teofilo Otoni, Rio Todos os Santos, affluent of Rio Mucuri, 17°51'49.0"S, 41°33'44.0"W.

Pimelodella eigenmanni. — BMNH 1889.11.14.6, 1, xr, 105.4 mm SL, lectotype, Brazil, Minas Gerais, "Macacos" (probably Ribeirao dos Macacos, trib. of Rio das Velhas), 20°2'S, 43°50'W; MCZ 7438, 5, xr, 94.8–130.7 mm SL, paralectotypes, Brazil, Minas Gerais, "Macacos" (probably Ribeirao dos Macacos, trib. of Rio das Velhas), 20°2'S, 43°50'W; MCZ 7510, 1, xr, 135.6 mm SL, paralectotype, Brazil, Rio de Janeiro, "Rio Parahyba" (Rio Paraiba do Sul, between Barra do Pirai and Tres Rios, D. Pedro II Railroad), 22°16'S, 42°45'W.

Pimelodella rendahli. — ZMB 32031, 1, xr, 80.7 mm SL, holotype, Aquarium import.

***Pimelodella buckleyi* (Boulenger, 1887)**

Rhamdia cyanostigma (*in partim*) Cope, 1870: 569 [original description; "Pebas, Equador", Peru; syntypes ANSP 8381 71.7 mm SL]. — Eigenmann & Eigenmann, 1890: 164 [doubtful species of *Pimelodus*]. — Fowler, 1915: 218 [transfer to *Pimelodella*].

Pimelodus cyanostigma (*in partim*). — Cope, 1878: 675 [taxonomic treatment]. — Eigenmann & Norris, 1900: 353 [taxonomic treatment].

Pimelodella cyanostigma (*in partim*). — Fowler, 1915: 218 [transfer to *Pimelodella*]. — Eigenmann, 1917: 230, 232, 242 (*in partim*) [taxonomic revision]. — Eigenmann & Allen, 1942: 23, 101–102 [taxonomic list, taxonomic treatment]. — Gosline, 1945: 43 [taxonomic list]. — Fowler, 1951: 538 [taxonomic list]. — Burgess, 1989: 280 [taxonomic list]. — Ortega & Vari, 1986: 14 [taxonomic list]. — Bockmann & Guazzelli, 2003: 418 [taxonomic treatment]. — Ferraris, 2007: 190 [taxonomic treatment].

Pimelodus lateristriga [non Lichtenstein]. — Cope, 1872: 270 [taxonomic treatment]. — Fowler, 1915: 216 [synonym of *P. copei*].

Pimelodus buckleyi Boulenger, 1887: 275, pl. XX, fig. 1 [original description; "Canelos", Ecuador; syntypes: BMNH 1880.12.8.98–99].

Pimelodella buckleyi. — Eigenmann & Eigenmann, 1891: 29 (*in partim*) [taxonomic treatment]. — Boulenger, 1891: 232 [description of *P. eigenmanni*]. — Eigenmann, 1910: 389 [taxonomic treatment]. — Eigenmann, 1917: 230, 232, 240–241, fig. 1 [taxonomic revision]. — Pearson, 1924: 13–14 [taxonomic treatment]. — Eigenmann & Allen, 1942: 43, 48, 50, 53, 99 [taxonomic list; taxonomic treatment]. — Gosline, 1945: 44 [taxonomic treatment]. — Fowler, 1951: 536 [taxonomic treatment]. — Ortega & Vari, 1986: 14 [taxonomic treatment]. — Burgess, 1989: 280 [taxonomic

treatment]. — Bockmann & Guazzelli, 2003: 417 [taxonomic treatment]. — Ferraris, 2007: 190 [taxonomic treatment]. — Sarmiento *et al.*, 2014: 191 [taxonomic list]

Pimelodella copei Fowler, 1915: 216, fig. 5 [original description, based on Cope's specimen of *P. lateristriga*]. — Fowler, 1951: 536 [taxonomic treatment]. — Böhlke, 1984: 141 [type catalog]. — Bockmann & Guazzelli, 2003: 417 [synonym of *P. buckleyi*]. — Ferraris, 2007: 190 [synonym of *P. buckleyi*].

Diagnosis

Pimelodella buckleyi can be distinguished from all *Pimelodella* species except *P. geryi*, *P. grisea*, *P. leptosoma*, *P. metae* and *P. notomelas*, by the presence of dorsal fin distal third extremely dark brown to black (Figs. 20, 22). *Pimelodella buckleyi* distinguishes from *P. metae* by this dark distal portion of dorsal fin reaches the entire distal third extension (*vs.* nor reaching the tip of dorsal fin). It distinguishes from *P. grisea* and *P. metae* by the presence of 43–44 total vertebrae (*vs.* 39–41 in *P. grisea*, 40 in *P. metae*). It distinguishes from *P. geryi* by having a dark brown midlateral stripe wide and sparse, from snout to caudal-fin insertion (*vs.* dark black midlateral stripe wide, well delimited, from snout until distal portion of median caudal-fin rays in *P. geryi*). It distinguishes from *P. leptosoma* by having the supraoccipital process reaching the anterior prenuchal plate (*vs.* almost reaching in *P. leptosoma*). It distinguishes from *P. notomelas* by having maxillary barbel reaching between verticals through anal-fin origin and half its base (*vs.* maxillary barbel always surpassing caudal fin origin in *P. notomelas*). *Pimelodella buckleyi* can be further diagnosed by the combination of the following traits: maxillary barbel reaching between verticals through anal-fin origin and half its base; dorsal-fin spine two thirds of first dorsal-fin total length, distal third of anterior margin with smooth serrae; posterior margin of pectoral-fin spine bearing very smooth and sparse dentations, or no dentations at all; 43 or 44 total vertebrae; body with midlateral dark brown stripe large and sparse; from snout to caudal-fin insertion; distal third of dorsal-fin rays extremely dark brown, mark present even at uncolored specimens; dark brown oval mark may be present at anterior limit of lateral line, above pseudotympanum anteriorly.

Description

Measurements in Table 10. Body moderately deep, depth at dorsal-fin origin five to six times in standard length, and compressed, body width at dorsal-fin origin six to almost eight times in SL (Fig. 20). Greatest body depth at dorsal-fin origin. Dorsal profile convex from snout to dorsal fin, slightly concave from dorsal to adipose fin, slightly convex along

adipose fin, and concave along caudal peduncle. Ventral profile of body slightly convex from snout to branquiostegal membrane, concave between pectoral end pelvic fins, and convex from pelvic to caudal peduncle.

Pseudotympanum large, oval, dorsal to posterior process of cleithrum and reaching 6th*(3)–7th (2) vertebrae. Posterior process of cleithrum triangular, its dorsal margin straight. Anus and urogenital papilla adjacent. Urogenital papilla tubular, triangular, short. Anus at vertical through first third of adpressed pelvic fin; urogenital papilla finishing between verticals through three-fifths and two-thirds of adpressed pelvic fin.

Head depressed to moderately deep, depth at base of supraoccipital-process two to three times in head length. Mouth sub terminal. Eye slightly elliptical, four to five times in head length. Bony interorbital distance a fourth smaller than eye diameter. Barbels thin, slightly depressed and elliptical in cross-section. Maxillary barbel reaching between verticals through anal-fin origin and half its base. Outer mental barbel, when stretched parallel to main body axis, finishing at or short of adpressed pectoral fin terminus. Inner mental barbel, when stretched parallel to main body axis, finishing between verticals through half and terminus of pectoral fin. Supraoccipital process subrectangular, narrow, and narrowing at its distal point. Dorsal lamina of Weberian complex vertebrae, despite notably deep, reaching supraoccipital process just at its anteriormost part or until half its extension, but never along its entire length. Branchiostegal rays 6* (2) or 7 (1).

Dorsal fin triangular, distal margin concave, overall short (second branched dorsal-fin ray five times in SL), depressed tip finishing at vertical through adpressed pelvic fin terminus. Dorsal fin with I,6 (5) plus anteriormost spinelet. Distance between terminus of dorsal-fin base and adipose-fin origin half to two-thirds of dorsal-fin base. Anteriormost dorsal-fin pterygiophore inserted posterior to neural spine of vertebrae 4 (1), or 5* (4); posteriormost dorsal-fin pterygiophore located anterior to neural (or pseudoneural) spine of vertebrae 11 (1) or 12* (4). Unbranched dorsal-fin ray mostly ossified as a spine, rigid part relatively short (ca. 66% of first dorsal-fin total length), distal third of anterior margin with smooth serrae.

Pectoral-fin rays I,7 (1)–I,8* (2), pectoral fin triangular with concave distal margin. First pectoral fin ray roughly straight, with proximal part rigid, forming a spine (Fig. 21), and short distal tip flexible and distinctly segmented. Pectoral fin spine six to seven times in SL. Anterior margin of pectoral-fin spine with smooth straight dentations along its basal half, and serrae (6–8) along its distal half. Posterior margin of pectoral-fin spine bearing very smooth and sparse dentations, or no dentations at all.

Pelvic-fin rays i,5 (5), extended pelvic fin triangular with straight distal margin. Pelvic-fin origin between verticals through last third and last fourth of dorsal-fin base. Tip of adpressed pelvic fin through vertical of dorsal fin adpressed terminus or slightly posterior. First unbranched and flexible ray distinctly shorter than second and third rays, which are the longest and roughly the same size; remaining rays progressively shorter.

Anal-fin rays iv,8 (1), v,8 (2), vi,8 (1) or v,9* (1); distal margin of extended anal fin convex. Two or three anteriormost anal-fin rays vestigial, unsegmented, embedded in thick skin fold. Anal fin origin at vertical through the first third or fourth of adipose-fin base; anal-fin adpressed terminus at vertical through adipose-fin terminus or slightly anterior. Tip of anteriormost anal-fin pterygiophore inserted posterior to hemal spine of vertebrae 23* (4) or 24 (1). Tip of posteriormost anal-fin pterygiophore inserted anterior to hemal spine of vertebrae 30 (2) or 31* (3).

Adipose fin long, two and half to three times in SL, forming ascending elevated curve in lateral profile, deepest point approximately at midlength. Adipose fin emerging gradually, posterior limit as rounded, free lobe. Adipose-fin origin at vertical through vertebral centra 20 (1)–23 (1) (lectotype 21); adipose-fin terminus at vertical through vertebral centra 38 (2) to 40* (2).

Caudal fin deeply forked, its lobes subequal. Caudal peduncle length posterior to adipose fin almost equal to its depth. Dorsal lobe with 7 (5) branched, 1 (5) unbranched principal and 15* (1)–18 (1), usually 17 (3), procurrent fin-rays. Ventral lobe with 8 (5) branched, 1 (5) unbranched principal and 17 (2)–20 (1) (lectotype 18) procurrent fin-rays. Hypural 5 free. Median caudal-fin rays not articulated directly to hypural plate. Seven (5) rays articulated to dorsal caudal-fin plate (5 on hypurals 3+4 and 2 on hypural 5) and 7* (4)–8 (1) rays articulated to ventral caudal-fin plate (5 or 6 on hypurals 1+2 and 2 on parahypural).

Total vertebrae 43(2)–44* (3). Ribs 7* (1)–10 (1).

Epiphyseal branch of cephalic laterosensory canal on head (S6) with contralateral canals connecting midline, following posteriorly as a small canal and opening in a single pore.

Coloration in alcohol

Background body coloration yellowish. Ventral region of head and body lighter than dorsal regions. Dark brown midlateral stripe wide, poorly-delimited (Fig. 22), extending from snout to caudal-fin insertion. Dorsal fin dusky, with an hyaline stripe at its second fourth, and distal third of dorsal-fin rays extremely dark brown, mark present even at uncolored specimens. A dark brown oval mark may be present at anterior limit of lateral line, above pseudotympanum anteriorly. Cephalic dark brown pigment at posterior fontanel region.

Geographic distribution

Pimelodella buckleyi was described from “Canelos”, Ecuador, probably Bobonaza River, part of Pastaza River basin, Marañon system. *Pimelodella copei*, its junior-synonym, was described from Ampyiacu River, a small tributary of Amazon River in Peru. *Pimelodella cyanostigma* has one syntype indistinguishable from *P. buckleyi*, and was collected in Pebas, probably a location near the one from *P. copei*. *Pimelodella buckleyi* currently known range is from regions 313 and 316 (Western Amazon Piedmont and Amazonas Lowlands), in Ecuador and Peru. Other locations reported for *Pimelodella buckleyi* in Ucayali, Huallaga, Purus and Beni basins (*e.g.* Eigenmann & Allen, 1942) should be analyzed further.

Comments

Pimelodella buckleyi was described by Boulenger (1887) based on two syntypes. However, during the description he cited the total length of the biggest one, 150 mm (in contrast to the 133.2 mm I measured, but the specimen has only the lower caudal lobe, in a manner my measurement can be slightly different from his). Based on this and the conservation status of the specimens, I hereby designate BMNH 1880.12.8.98 as the Lectotype and BMNH 1880.12.8.99 as Paralectotype.

Pimelodella copei was described by Fowler (1915) based on two specimens from Ambyiacu river, also Ecuador (now Peru). *Pimelodella copei* was synonymized with *P. buckleyi* by Eigenmann (1917), arguing the description was based on Cope’s (1872) specimens of *P. lateristriga*, like the ones Boulenger used to describe *P. buckleyi*. Analyzing the type material and literature of both species I ratify the decision of Eigenmann (1917) to synonymize this species with *P. buckleyi*.

Both *P. buckleyi* and *P. copei* descriptions cite Cope (1872): “*Pimelodus lateristriga* (*non* Muller and Troschel) Cope, Proc. Acad. Nat. Sci. Phila., 1871 (1872), p. 270”. In turn, Cope’s work is about fishes from the Ampyiacu river (1872), in which he compares some specimens identified as *P. lateristriga* with a *P. lateristriga* from Günther’s Catalog of the British Museum (1864), citing some differences in the length of barbels and number of dorsal and anal-fin rays.

Pimelodella buckleyi (Boulenger, 1887) was described from specimens from Canelos, Ecuador, probably Bobonaza river, which is part of Pastaza river basin, a large tributary of the Marañon river. *Pimelodella copei* Fowler (1915) was described from Ambyiacu river, near Pebas (Ecuador, now Peru), a small tributary of the Amazon river. The Bobonaza River is part of Western Amazon Piedmont; whereas Ambyiacu is part of Amazonas Lowlands (313 and 316 regions, respectively, following Abell *et al.*, 2008).

Both localities are part of Amazon-Orinoco-Guiana core, being Amazon-Orinoco-La Plata lowlands (Albert, Petri & Reis, 2011), a region known by its high diversity (e.g. Kullander, 1986; Albert *et al.*, 2011). Also, both localities are closely related to each other in BPA analysis (Albert & Carvalho, 2011).

Observing *P. buckleyi* and *P. copei* types, both are indistinguishable, corresponding to the same species. Therefore, here I report that *P. copei* has a similar combination of diagnostic characteristics of *P. buckleyi*, being: head shallow to moderated deep, depth at supraoccipital-process base two to three times in head length; comparatively shorter than mental barbel, reaching between verticals through anal-fin origin and half its base; outer mental barbel, when stretched parallel to main body axis, finishing at or short of terminus of adpressed pectoral fins; inner mental barbel, when stretched parallel to main body axis, finishing between verticals through half and terminus of pectoral fin; dorsal lamina of Weberian complex vertebrae reaching the supraoccipital process just at its anteriormost part or until half its extension, but never along its entire length; unbranched dorsal-fin ray mostly ossified as a spine, rigid part relatively short (slightly more than a third shorter than the first dorsal-fin total length), distal third of anterior margin with smooth serrae; anterior margin of pectoral-fin spine with smooth straight dentations along its basal half, and serrae (6–8) along its distal half; posterior margin of pectoral-fin spine bearing very smooth and sparse dentations, or no dentations at all; 43 or 44 total vertebrae. Despite *P. copei* types being extremely uncolored compared to *P. buckleyi*, both the dark blotch at anterior part of pseudotympanum and the darker region distally on dorsal-fin rays could be observed, both diagnostic characteristics of *P. buckleyi*.

Pimelodella cyanostigma was described by Cope (1870) as *Rhamdia cyanostigma*, and transferred to *Pimelodus* by Cope (1878), when said as allied to *Pimelodus ophthalmicus* Cope 1878, now in *Pimelodella*. This was considered a doubtful species in *Pimelodus* by Eigenmann & Eigenmann (1890: 164), and transferred to *Pimelodella* by Fowler (1915).

Despite its poor preservation, I conclude that one of the syntypes belongs to a different species than the other two. The larger specimen, of 71.7 mm SL, apparently is indistinguishable from *P. buckleyi*, having also the reference to a dark mark at the dorsolateral region, near the limit of head (although, the placement of this spot is slightly different in *P. cyanostigma* description, described as “above the posterior margin of the orbit”). Other morphometric and meristic characteristics support this identification, being: maxillary barbel reaching half of adipose fin; long outer mental barbels, reaching four-fifths of pectoral-fins adpressed; short dorsal fin, second branched ray five times in SL; distance between terminus

of dorsal-fin base and adipose-fin origin half to two-thirds of dorsal-fin base; adipose fin three times in SL; 44 total vertebrae; dorsal lamina of Weberian complex vertebrae reaching the supraoccipital process just at its anteriormost part; anterior margin of spiny portion of first pectoral-fin ray with smooth straight dentations along its basal half, and *serrae* (6–8) along its distal half; posterior margin of spiny portion of first pectoral-fin ray bearing very smooth and sparse dentations.

The other two specimens (59.8 and 50.6 mm SL) are related to *P. cristata*, and will be discussed under this species' comment section. In order to facilitate the synonym, I hereby designate the *P. cyanostigma* 59.8 mm SL specimen the lectotype, and the 71.7 mm SL and 50.6 mm SL the paralectotypes.

Material examined

Pimelodella buckleyi. — BMNH 1880.12.8.98-99, 2, xr, 89.7–109.5 mm SL, syntypes, Ecuador, Canelos, 1°35'19"S, 77°45'45"W; ANSP 146005, 1, 139.1 mm SL, Ecuador, Napo, Feeder stream on Rio Napo Ca. 15 mi. downstream from Missahualli, 0°56'0.0"N, 77°30'0.0"W; FMNH 95324, 3, xr, 88.9–117.8 mm SL, Ecuador, Napo, Quebrada Yaucanayacu, trib. of Rio Payamino downstream from Rio Tiquino, 0°25'36.1"S, 77°19'23.9"W; USNM 163904, 2, 110.1–120.9 mm SL, Ecuador, Rio Pucuno, Trib. of Suno; Alt. 350-400 m, 0°46'48.0"S, 77°16'12.0"W; USNM 163905, 3, 69.3–118.5 mm SL, Ecuador, Pacayacu, Trib. of Bobonaza; Alt. 350-480 m, 2°03'00.0"S, 76°58'48.0"W.

Pimelodella cope. — ANSP 8362, 1, xr, 115.1 mm SL, holotype, Ecuador, Ambyiacu River, near Pebas, 3°19'26"S, 71°51'38"W; ANSP 8363, 1, xr, 115.6 mm SL, paratype, Ecuador, Ambyiacu River, near Pebas, 3°19'26"S, 71°51'38"W.

Pimelodella cyanostigma. — ANSP 8381, 1, xr, 71.7 mm SL, syntype, Ecuador, Pebas, 3°19'26"S, 71°51'38"W.

***Pimelodella chagresi* (Steindachner, 1876a)**

Pimelodus (*Pseudorhamdia*) *chagresi* Steindachner, 1876a: 584–586 [original description; “Rio Chagres und dessen Nebenflüsse bei Obispo”, San Juan del Obispo, Guatemala; types unknown, probably NMW (Bockmann & Guazzelli, 2003; Ferraris, 2007)].

Pimelodella chagresi. — Eigenmann & Eigenmann, 1888: 133 [taxonomic treatment]. — Eigenmann & Eigenmann, 1890: 149, 160–162 [key to *Pimelodella* species; taxonomic revision]. — Eigenmann & Eigenmann, 1891: 29 [taxonomic treatment]. — Eigenmann, 1905: 19 [taxonomic list]. — Eigenmann, 1910: 389 [taxonomic treatment]. — Eigenmann, 1917: 252, 253–254, pl. XXXIII, fig. 3, pl. XXXV, figs.

24–25 [taxonomic revision]. — Eigenmann, 1922a: 43,222 [taxonomic treatment]. — Schultz, 1944: 210, 214 [taxonomic treatment]. — Fowler, 1945a: 108 [taxonomic treatment]. — Cala, 1977: 11 [taxonomic list]. — Burgess, 1989: 280 [taxonomic treatment]. — Galvis *et al.*, 1997: 64 [taxonomic list]. — Bussing 1998: 145 [taxonomic list]. — Bockmann & Guazzelli, 2003: 417 [taxonomic treatment]. — Leiva, 2005: 15–16, 44–45 [taxonomic review; redescription]. — Ferraris, 2007: 190 [taxonomic treatment]. — Angulo *et al.*, 2013: 993 [taxonomic list]. — Ardila Rodriguez, 2017: 7–8 [taxonomic treatment].

Pimelodella chagrensis. — Eigenmann, 1924: 238 [ecology].

Diagnosis

Pimelodella chagresi differs from all *Pimelodella* species but *P. avanhandavae*, *P. eutaenia*, *P. gracilis*, *P. griffini*, *P. montana*, *P. odynea*, *P. peruana*, *P. reyesi* and *P. roccae* by having a dorsolateral brown stripe along body (Figs. 23, 25). It differs from *P. eutaenia*, *P. griffini*, *P. peruana*, *P. reyesi* and *P. roccae* by this stripe extending from supraoccipital process until half to last third of adipose-fin base (*vs.* adipose fin origin in *P. eutaenia* and *P. peruana*; adipose-fin terminus in *P. griffini*, *P. reyesi*, and *P. roccae*). It differs from *P. avanhandavae* and *P. gracilis* by having 39–41 total vertebrae (41–45 in *P. avanhandavae*; and 46, rarely 45 total vertebrae in *P. gracilis*). It differs from *P. montana* by having a totally dark pigmented dorsal fin (*vs.* dorsal fin with basal dark, followed by a hyaline stripe, then distal half dark in *P. montana*). *Pimelodella chagresi* can be further diagnosed by the combination of the following traits: maxillary barbel reaching between verticals through pelvic-fin adpressed terminus and last fifth of adpressed anal-fin; dorsal lamina of Weberian complex vertebrae deep, reaching the supraoccipital process along its entire length; dorsal-fin spine three fourths of first dorsal-fin ray total length; posterior margin of pectoral-fin spine with edentulous shaft at first fourth, followed by 9–13 retrorse dentations along the entire margin, except its last fifth, these dentations are long, acute, inclined, except the distalmost 2–3, that are shorter and straighter; adipose fin of moderated length, three and half times in SL; epiphyseal branch of cephalic laterosensory canal opening as a single pore; dark brown midlateral stripe wide, well-defined, from snout until end of median caudal-fin rays; dorsal fin completely dusky, without any hyaline stripes; dorsal body region diffusely brown, as a paired dorsolateral stripe along supraoccipital process until two thirds of adipose fin.

Description

Measurements in Table 11. Body moderately deep, depth at dorsal-fin origin five to five and half times in standard length, and compressed, body width at dorsal-fin origin six to eight times in SL (Fig. 23). Dorsal profile straight to slightly convex from snout to dorsal fin, slightly concave from dorsal to adipose fin, slightly convex along adipose fin, and concave along caudal peduncle. Ventral profile of body slightly convex from snout to branchiostegal membrane, and between pectoral and pelvic fins, slightly concave from pelvic to anal fin, and also concave from there to caudal peduncle.

Pseudotympanum large, oval, dorsal to posterior process of cleithrum and reaching 6th* (1) or 7th (1) vertebrae. Posterior process of cleithrum long, narrow, its margin slightly concave. Anus and urogenital papilla adjacent. Urogenital papilla tubular, triangular, small. Anus between verticals through second-fifth and half of adpressed pectoral-fin; urogenital papilla reaching between verticals through second-third and fifth-seventh of adpressed pelvic fin.

Head deep, depth at base of supraoccipital process half of head length. Mouth sub terminal. Eye slightly elliptical, four and half to five times in head length. Bony interorbital distance slightly smaller than eye diameter. Barbels thin, slightly depressed and elliptical in cross-section. Maxillary barbel reaching between verticals through adpressed pelvic-fin terminus and last fifth of adpressed anal-fin. Outer mental barbel, when stretched parallel to main body axis, finishing at half of adpressed pectoral fin. Inner mental barbel, when stretched parallel to main body axis, finishing between vertical through origin and terminus of pectoral fin. Supraoccipital process subrectangular, large, and narrowing at its distal point. Dorsal lamina of Weberian complex vertebrae deep, reaching the supraoccipital process along its entire length. Branchiostegal rays 6 (9).

Dorsal fin triangular, distal margin convex, short (second branched dorsal-fin ray slightly more than five times in SL), depressed tip finishing between verticals through half and second-third of adpressed pelvic fin. Dorsal fin with I,6 (12) plus anteriormost spinelet. Distance between terminus of dorsal-fin base and adipose-fin origin slightly larger than dorsal-fin base. Anteriormost dorsal-fin pterygiophore inserted posterior to neural spine of vertebrae 4 (9); posteriormost dorsal-fin pterygiophore located anterior to neural (or pseudoneural) spine of vertebrae 11* (7) or 12 (2). Unbranched dorsal-fin ray mostly ossified as a spine, rigid part ca. 75% of first dorsal-fin ray total length, distal third of anterior margin with serrae, and minute and smooth, straight dentations along posterior margin.

Pectoral-fin rays I,8 (8)–I,9* (1), pectoral fin triangular with convex distal margin. First pectoral-fin ray curved, with proximal part rigid, forming a spine (Fig. 24), and short distal tip flexible and distinctly segmented. Pectoral-fin spine five to six times in SL. Anterior margin of pectoral-fin spine with serrae along its distal fifth to third, followed by small straight dentations covering two-thirds of margin, and a shaft at basal third. Posterior margin of pectoral-fin spine with edentulous shaft at first fourth, followed by 9–13 retrorse dentations along the entire margin, except its last fifth. Dentations long, acute, inclined, except the distalmost 2–3, that are shorter and straighter.

Pelvic-fin rays i,5 (9), extended pelvic fin triangular with convex distal margin. Pelvic-fin origin between verticals through sixth branched dorsal ray and a point slightly posterior to dorsal-fin terminus. Pelvic-fin adpressed terminus slightly posterior to vertical through adipose-fin origin. First unbranched and flexible ray distinctly shorter than second and third rays, which are roughly the same size; remaining rays progressively shorter.

Anal-fin rays iv,8 (2), v,8 (3), iv,9* (3) or v,9 (2); distal margin of extended anal fin convex. Two or three anteriormost anal-fin rays vestigial, unsegmented, embedded in thick anterior skin fold. Anal fin origin between verticals through first fourth and second-fifth of adipose-fin base; anal-fin adpressed terminus at vertical through adipose-fin terminus or a point slightly anterior to that. Tip of anteriormost anal-fin pterygiophore inserted posterior to hemal spine of vertebrae 20* (3) or 21 (6). Tip of posteriormost anal-fin pterygiophore inserted anterior to hemal spine of vertebrae 27 (3), 28* (5), or 30 (1).

Adipose fin three and half times in SL, forming ascending elevated curve in lateral profile, deepest point approximately at midlength. Adipose fin emerging gradually, posterior limit as rounded, free lobe. Adipose-fin origin at vertical through vertebral centra 19* (2)–23 (1), usually 21 (4); adipose-fin terminus at vertical through vertebral centra 34 (4) to 36 (3) (lectotype 35).

Caudal fin deeply forked, its dorsal lobe usually slightly longer than ventral lobe. Caudal peduncle length posterior to adipose-fin a third longer than its depth. Dorsal lobe with 7 (8) branched, 1 unbranched principal and 4(1)–20 (1) (lectotype 16) procurrent fin-rays. Ventral lobe with 8 (8) branched, 1 unbranched principal and 13 (1)–19 (1) (lectotype 15) procurrent fin-rays. Hypural 5 free. Median caudal-fin rays not articulated directly to hypural plate. Seven (8) rays articulated to dorsal caudal-fin plate (5 on hypurals 3+4 and 2 on hypural 5) and 8 (8) rays articulated to ventral caudal-fin plate (6 on hypurals 1+2 and 2 on parahypural).

Total vertebrae 39 (4)–41 (1) (lectotype 40). Ribs 8* (5)–9 (4).

Epiphyseal branch of cephalic laterosensory canal opening as a single pore, at top of head, right after the connection of both canals, or present two pores narrow-distanced.

Coloration in alcohol

Background body coloration yellowish. Ventral region of head and body lighter than dorsal regions. Dark brown midlateral stripe wide, well-defined, from snout until end of median caudal-fin rays (Fig. 25). Dorsal fin completely dusky, without any hyaline stripes. Dorsal body region diffusely brown, as a paired dorsolateral stripe extending along supraoccipital process to two thirds of adipose fin. Cephalic dark brown pigment at posterior fontanel region.

Geographic distribution

Pimelodella chagresi was described from Rio Chagres and its tributaries in Panamá. Its currently known range is from regions 206 (Chiriqui), 207 (Panama Isthmus), 208 (Santa Maria), 209 (Chagres), 210 (Tuira), in several streams in Panamá and Guatemala.

Comments

What is usually referred as *P. chagresi* from Chocó department, in Colombia, has some morphological differences from the types of *P. chagresi* and comparative material of Panamá and Guatemala. I suggest that material identified as *P. chagresi* from Colombian Chocó is probably *P. eutaenia*, and will be further discussed in this species section. Also, some morphological differences have been pointed out between *Pimelodella chagresi* from Chagres and Magdalena (e.g. Leiva, 2005). Therefore, there is a need of further investigation into the different morphotypes of *P. chagresi*, in order to better delimit its distribution.

Specimens identified as *Pimelodella* cf. *chagresi* from Upper Rio Magdalena had their karyotype characterized, as diploid number $2n=50$, a diploid number only found for this species among the *Pimelodella*, and sex chromosome system XX/XY (Conde-Saldaña *et al.*, 2017)

There is also some uncertainty in literature about *P. chagresi* types, if they were in NMW or MCZ (e.g. Bockmann & Guazzelli, 2003; Ferraris, 2007; Eschmeyer, Fricke & van der Laan, 2017). Although, the MCZ website has a thoroughly explanation about Hassler Expedition, the second of Agassiz expeditions, from 1871 to 1872 (http://www.mcz.harvard.edu/Departments/Ichthyology/expeditions_thayer_hassler.html). It is said that Franz Steindachner worked on Hassler fish collections while at MCZ for eight months after the expedition, despite thousands of specimens being said to have been taken to Vienna by Steindachner in 1873.

There are specimens of *P. chagresi* registered under MCZ Catalogue as pertained to Hassler Expedition, locality of Obispo River, Panama, 1872, being thus probably part of the type material. The total length of the bigger specimens is also roughly similar to the described, of 5"10 inches, approximately 127.25 mm (our measure of 111.61 mm for the smallest and 142.47 mm for the largest). Although, only two specimens of the supposedly four syntypes were found. These two are probably the ones examined by Eigenmann & Eigenmann, 1890, who say "We have examined two specimens from the Obispo River, Panama, .146 m. and .12 m. They were collected by Dr. Steindachner, Hassler Expedition, in 1872, and are probably two of the four type specimens." (Eigenmann & Eigenmann, 1890: 161).

In Vienna, NMW 45798 (120.8 mm) and NMW 45799 (119.2 mm) are probably the other two type-specimens, since the characteristics are undoubtedly from *P. chagresi*. Between all those syntypes, I choose one specimen that was thoroughly examined, is in good condition, and agrees with the original description as a lectotype. So, I hereby designate MCZ 4947, 111.8 mm SL as lectotype of *P. chagresi*, and therefore the other specimens as paralectotypes (MCZ 4947 91.4 mm SL, NMW 45798, NMW 45799).

Material examined

Pimelodella chagresi. — MCZ 4947, 2, xr, 91.4–111.8 mm SL, lectotype and paralectotype, Panamá, Río Obispo, Río Chagres drainage, 9°06'47"N, 79°41'17"W; NMW 45798, 1, 120.8 mm SL, paralectotype, Panamá, Río Obispo, Río Chagres drainage, 9°06'47"N, 79°41'17"W; NMW 45799, 1, 119.2 mm SL, paralectotype, Panamá, Río Obispo, Río Chagres drainage, 9°06'47"N, 79°41'17"W; AMNH 11408, 15, Panama, Rio Chucunaque, 1 mile below Yonisa; CAS 57903, 1, 83.5 mm SL, Panama, Darien, Chucunaque River, 8°09'22.7"N, 77°41'23.8"W; CAS 75793, 3, 57.6 mm SL, Panama, Canal Zone, Frijoles, Rio Frijoles, a tributary of the middle fork of Rio Chagres, 9°09'40.8"N, 79°43'42.9"W; CAS 75796, 2, Panama, Canal Zone, Rio Gatun & creek at Monte Liria, 9°14'01.5"N, 79°50'37.7"W; USNM 78258, 5, 45.1–76.2 mm SL, Panama, Reservoir Creek, Gorgona, Canal Zone, 9°06'43.5"N, 79°41'48.4"W; USNM 78260, 26, 29.7–84.9 mm SL, Panama, Rio Gatunocello, Alhajuella, 9°12'54.8"N, 79°39'22.9"W; USNM 78266, 6, 32.2–80.6 mm SL, Panama, Rio Indio, 8°46'38.1"N, 80°08'48.8"W; USNM 78268, 1, 53.4 mm SL, Panama, Rio Indio, Gatun, Canal Zone, 8°58'12.9"N, 80°10'16.0"W; USNM 78276, 2, 30.9–74.7 mm SL, Panama, Rio Chorrera, 8°22'15.0"N, 80°20'01.7"W; USNM 79160, 17, 50.5–82.1 mm SL, Panama, Gatun River, Monte Lirio, Canal Zone, 9°15'40.1"N, 79°47'39.9"W; USNM 207953, 32, Panama, Veraguas, Creek 1 mi S. of Santa Fe., 8°29'02.6"N, 81°03'30.2"W; USNM

293591, 3, 39.4–78.9 mm SL, Panama, Comarca Kuna Yala, Rio Madinga Between Rio Pingandi + Pueblo Madinga (Atlantic), 9°28'12.0"N, 79°06'00.0"W; USNM 320088, 33, 32.7–77.8 mm SL, Panama, Chiriqui, Rio Caimito - Same As HI-73, 8°29'06.1"N, 82°33'19.1"W.

***Pimelodella conquetaensis* Ahl, 1925**

Pimelodella conquetaensis Ahl, 1925: 106 [original description; “Rio Coquetá, S. O. Columbien”, Caquetá River, Colombia; holotype: ZMB 32030]. — Gosline, 1945: 44 [taxonomic treatment]. — Fowler, 1951: 537 [taxonomic treatment]. — Burgess, 1989: 280 [taxonomic treatment]. — Silfvergrip & Paepke, 1997: 166–167, fig. 3 [type catalog]. — Paepke, 1998: 92 [type list, but wrong type number assigned in text]. — Bockmann & Guazzelli, 2003: 417 [taxonomic treatment]. — Ferraris, 2007: 190 [taxonomic treatment]. — Maldonado-Ocampo *et al.*, 2008: 202 [taxonomic list]

Pimelodella coguetaensis. — Burgess, 1989: 280 [taxonomic treatment, misspelling].

Pimelodella caquetaensis. — Silfvergrip & Paepke, 1997: 166–167, fig. 3 [name correction for specific epithet following the river name, Caquetá]. — Paepke, 1998: 92 [type list, but wrong type number assigned in text, as ZMB 32298].

Diagnosis

Pimelodella conquetaensis can be distinguished from all *Pimelodella* species except *P. australis*, *P. boschmai*, *P. chagresi*, *P. enochi*, *P. grisea*, *P. ignobilis*, *P. laticeps*, *P. laurenti*, *P. macturki*, *P. meeki*, *P. notomelas*, *P. spelaea*, *P. straminea*, *P. taeniophora* and *P. yuncensis* by having 40 total vertebrae. It differs from *P. australis*, *P. chagresi*, *P. laurenti*, *P. meeki*, *P. notomelas*, *P. spelaea* and *P. taeniophora* by the absence of a dorsolateral paired stripe on body (*vs.* presence of a dorsolateral paired stripe on body in from *P. australis*, *P. chagresi*, *P. laurenti*, *P. meeki*, *P. notomelas*, *P. spelaea* and *P. taeniophora*). It differs from *P. ignobilis*, *P. laticeps*, *P. straminea* and *P. yuncensis* by the maxillary barbel reaching half anal fin base (*vs.* maxillary barbel reaching at best anal-fin origin in *P. ignobilis*, *P. laticeps*, *P. straminea* and *P. yuncensis*). It differs from *P. boschmai*, *P. enochi*, *P. grisea* and *P. macturki* by having the supraoccipital process narrow (*vs.* supraoccipital process of moderate width in *P. boschmai*, *P. enochi*, *P. grisea* and *P. macturki*).

Furthermore, *P. conquetaensis* can be diagnosed by maxillary barbel reaching at least half of anal-fin base; posterior margin of pectoral-fin spine bearing 12 retrorse dentations along its basal two-thirds, these dentations being triangular and inclined; adipose fin of

moderated length, three and half times in SL; midlateral dark brown stripe wide and not well delimited, at least after orbit until caudal-fin insertion.

Description

Measurements in Table 12. Body of moderated height, depth at dorsal-fin origin almost six times in standard length, and of moderated width, body width at dorsal-fin origin six and half times in SL (Fig. 26). Greatest body depth at dorsal-fin origin. Dorsal profile convex from snout to dorsal fin, concave from the latter to adipose fin, slightly convex along adipose fin, and concave along the caudal peduncle. Ventral profile of body slightly convex from snout to branquiostegal membrane, concave between pectoral end pelvic fins, slightly convex from pelvic to anal fin, and concave from there to caudal peduncle.

Pseudotympanum large, oval, dorsal to posterior process of cleithrum and reaching 6th (1) vertebrae. Posterior process of cleithrum triangular, its dorsal border concave. Anus and urogenital papilla adjacent. Urogenital papilla tubular, triangular, small. Anus at vertical through last third of adpressed dorsal fin; urogenital papilla almost reaching vertical through terminus of adpressed dorsal fin.

Head deep, depth at supraoccipital-rocess base more than half of head length. Mouth sub terminal. Eye slightly elliptical, four and half times in head. Bony interorbital distance short, slightly more than half eye diameter. Barbels thin, slightly depressed and elliptical in cross-section. Maxillary barbel severed, reaching at least half of anal-fin base. Outer mental barbel, when stretched parallel to main body axis, finishing at terminus of adpressed pectoral fin. Inner mental barbel severed, but when stretched parallel to main body axis, reaching at least pectoral-fin origin. Supraoccipital process long, shape subrectangular, narrow, distal third slightly tapered. Dorsal lamina of Weberian complex vertebrae reaching the supraoccipital process just near its anteriormost part. Branchiostegal rays 6 (1).

Dorsal fin triangular, distal margin concave, short (second branched dorsal-fin ray five times in SL), depressed tip reaching vertical through last fifth of adpressed pelvic fins. Dorsal fin with I,6 (1) plus anteriormost spinelet. Distance between terminus of dorsal-fin base and adipose-fin origin slightly smaller than dorsal-fin base. Anteriormost dorsal-fin pterygiophore inserted posterior to neural spine of vertebrae 4 (1); posteriormost dorsal-fin pterygiophore located ahead of neural (or pseudoneural) spine of vertebrae 11 (1). Unbranched dorsal-fin ray mostly ossified as a spine, distally broken.

Pectoral-fin rays I,9 (1), pectoral fin triangular with concave distal border. First pectoral-fin ray curved with proximal part rigid (Fig. 27), forming a spine (spine length five and half times in SL), and short distal tip flexible and distinctly segmented. Anterior margin

pectoral-fin spine with smooth serrae along its distal half and small straight dentations along its basal half. Posterior margin of pectoral-fin spine bearing 12 retrorse dentations along its basal two-thirds, these dentations being triangular and inclined.

Pelvic-fin rays I,5 (1), extended pelvic fin triangular with straight distal border. Pelvic-fin origin at vertical through terminus of dorsal-fin base. Tip of adpressed pelvic fin barely surpassing vertical through anterior adipose fin origin. First unbranched and flexible ray almost the same size as second and third rays; remaining rays progressively shorter.

Anal-fin rays iii,8 (1); distal border of extended anal fin convex. Two anteriormost anal-fin rays vestigial, unsegmented, embedded in thick skin fold. Anal fin origin at vertical through first third of adipose-fin base; anal-fin adpressed terminus at vertical through adipose-fin terminus. Tip of anteriormost anal-fin pterygiophore inserted posterior to hemal spine of vertebrae 22 (1). Tip of posteriormost anal-fin pterygiophore inserted ahead of hemal spine of vertebrae 29 (1).

Adipose fin three and half times in SL, forming ascending elevated curve in lateral profile, with deepest point approximately midlength. Adipose fin emerging gradually, its posterior limit as a rounded, free lobe. . Adipose-fin origin at vertical through vertebral centra 20 (1); adipose-fin terminus at vertical through vertebral centra 35 (1).

Caudal fin severed. Caudal peduncle posterior to adipose fin slightly shorter than its depth. Dorsal lobe probably with 7 (1) branched, 1 unbranched principal and 12 (1) unbranched fin-rays. Ventral lobe probably with 8 (1) branched, 1 unbranched principal and 10 (1) unbranched fin-rays. Hypural 5 completely free, not fused to hypural 4. Median caudal-fin rays not articulated directly to caudal plate. Seven (1) rays articulated to dorsal caudal-fin plate (5 on hypurals 3+4 and 2 on hypural 5) and 7 (1) rays articulated to ventral caudal-fin plate (5 on hypurals 1+2 and 2 on parahypural).

Total vertebrae 40 (1). Ribs 9 (1).

Due to preservation status, it was impossible to delimit number and position of laterosensory canal pores.

Coloration in alcohol

Background body coloration yellowish. Ventral region of head and body lighter. Extremely unpigmented type specimen. The midlateral dark brown stripe appears to be wide and not well delimited, at least after orbit until caudal-fin insertion. Original description points to a midlateral dark stripe barely visible, and dark colored dorsal fin.

Geographic distribution

Pimelodella conquetaensis was described from Rio Caquetá, Colombia, from upper Japurá River basin. It is known from regions 313 (Western Amazon Piedmont) and maybe 314 (Rio Negro), in upper Amazon system.

Comments

The type material is in poor preservation status, and no other more recent material from Rio Caquetá was found, but similar material from Rio Negro maybe pertains to this species. Therefore, the distribution of *Pimelodella conquetaensis* is Upper Japurá and Negro rivers. Due to preservation of taxonomic stability, the name correction proposed by Silfvergrip & Paepke (1997) to *Pimelodella caquetaensis* is not incorporated in this work.

Also, there is some confusion about the catalog number of *P. conquetaensis* type. Paepke (1998: 92) indicates ZMB 32298 as the type of *P. conquetaensis* and ZMB 32030 as the type for *Pimelodella portoalegrensis* (*nomen nudum*). Meanwhile, Bockmann & Guazzelli (2003), Ferraris (2007) and Eschmeyer, Fricke & van der Laan (2017) indicate ZMB 32030 as *P. conquetaensis* holotype. I was able to examine the material and *P. conquetaensis* holotype is, in fact, ZMB 32030. One of the types for *P. portoalegrensis* (never formally described and, therefore, a *nomen nudum*) is ZMB 25128, which was posteriorly reassigned to ZMB 32030, a flagrantly confusion, since the catalog number was taken, in a manner the lot of *P. portoalegrensis* still have its former catalog number, and a label inside with the new (and previously occupied) number.

Material examined

Pimelodella conquetaensis. — ZMB 32030, 1, xr, 93.2 mm SL, holotype, Colômbia, "vom Rio Coqueta, S. O. Columbien" (probably Rio Caquetá, Colômbia), 1°09'39"S, 69°24'55"W.

***Pimelodella cristata* (Müller & Troschel, 1849)**

Pimelodus cristatus Müller & Troschel, 1849a: 628 [original description; "Takutu und Mahu", Tacutu and Mahu rivers, Upper Rio Branco basin, Guyana; syntypes: ZMB 3052–3053]. — Müller & Troschel, 1849b: 4 [detailed description]. — Günther, 1864: 117 [taxonomic treatment]. — Cope, 1878: 675 [taxonomic treatment]. — Steindachner, 1882: 4 [taxonomic list].

Pimelodella cristatus. — Eigenmann & Eigenmann, 1888: 132 [taxonomic treatment]. — Eigenmann & Eigenmann, 1890: 147; 150–151 [key to *Pimelodella* species; taxonomic revision]. — Eigenmann & Eigenmann, 1891: 29 [taxonomic list].

- Pimelodella cristata*. — Eigenmann, 1910: 388 [taxonomic treatment]. — Eigenmann, 1912: 168–169 [taxonomic review]. — Fowler, 1914: 263 [taxonomic list]. — Fowler, 1915: 214 [taxonomic list]. — Eigenmann, 1917: 230; 231–232; 236–237; pl. XXIX, fig. 2, pl. XXXV, fig. 38–40 [taxonomic revision]. — Fowler, 1939: 285 [taxonomic list]. — Eigenmann & Allen, 1942: 43; 48; 100 [taxonomic list; taxonomic treatment]. — Gosline, 1945: 43 [taxonomic list]. — Van der Stigchel, 1946: 54–55 [taxonomic treatment]. — Fowler, 1951: 537–538 [taxonomic treatment]. — Boeseman, 1953: 2, 6–7 [taxonomic list]. — Mees, 1974: 144–150, fig. 33 (top left) [taxonomic treatment]. — Mees, 1983: 48–49 [taxonomic treatment]. — Mees, 1985: 244–245 [taxonomic treatment]. — Ortega & Vari, 1986: 14 [taxonomic list]. — Burgess 1989: 280 [taxonomic list]. — Silfvergrip & Paepke 1997: 168–169 [type catalog]. — Le Bail *et al.*, 2000: 132 [taxonomic list]. — Bockmann & Guazzelli, 2003: 417 [taxonomic treatment]. — Guazzelli, 2003: 16, 214 [phylogenetic relationships]. — Lasso *et al.*, 2004: 171 [taxonomic list]. — Lasso *et al.*, 2006: 210 [taxonomic list]. — Chernoff *et al.*, 2005: 282 [taxonomic list]. — Ferraris, 2007: 190 [taxonomic treatment]. — Maldonado-Ocampo *et al.*, 2008: 202 [taxonomic list]. — Vari *et al.*, 2009: 43 [taxonomic list]. — Le Bail *et al.*, 2012: 304 [taxonomic list]. — Mol *et al.*, 2012 [taxonomic list]. — De Souza *et al.*, 2012: 37 [taxonomic list].
- Pimelodus breviceps* Kner, 1858: 418–420 [original description; “Marabitanos”, Marabitanas, Amazonas State, Brazil; holotype: NMW 45615]. — Günther, 1864: 122 [taxonomic treatment].
- Pseudopimelodus breviceps*. — Gill, 1858 [taxonomic treatment, transfer to *Pseudopimelodus* (*apud* Silfvergrip & Paepke, 1997, not observed)].
- Rhamdia breviceps*. — Eigenmann & Eigenmann, 1888: 124 [taxonomic treatment, doubtful species in *Rhamdia*]. — Eigenmann & Eigenmann, 1890: 121 [taxonomic treatment]. — Eigenmann & Eigenmann, 1891: 28 [taxonomic list]. — Eigenmann 1910: 385 [taxonomic list]. — Gosline, 1945: 36 [taxonomic list]. — Burgess, 1989: 278 [taxonomic list].
- Pimelodella breviceps*. — Silfvergrip, 1996: 16 [taxonomic treatment, transference to *Pimelodella*]. — Bockmann & Guazzelli, 2003: 417 [taxonomic treatment]. — Ferraris, 2007: 190 [taxonomic treatment].
- Rhamdia cyanostigma (in partim)* Cope, 1870: 569 [original description; “Pebas, Equador”, Peru; syntypes ANSP 8382 59.8 mm SL, ANSP 8383 50.6 mm SL]. — Eigenmann &

- Eigenmann, 1890: 164 [doubtful species of *Pimelodus*]. — Fowler, 1915: 218 [transfer to *Pimelodella*]. — Böhlke, 1984: 141 [type catalog].
- Pimelodus cyanostigma* (*in partim*). — Cope, 1878: 675 [taxonomic treatment]. — Eigenmann & Norris, 1900: 353 [taxonomic treatment].
- Pimelodella cyanostigma* (*in partim*). — Fowler, 1915: 218 [transfer to *Pimelodella*]. — Eigenmann, 1917: 230, 232, 242 (*in partim*) [taxonomic revision]. — Eigenmann & Allen, 1942: 23, 101–102 [taxonomic list, taxonomic treatment]. — Gosline, 1945: 43 [taxonomic list]. — Fowler, 1951: 538 [taxonomic list]. — Burgess, 1989: 280 [taxonomic list]. — Ortega & Vari, 1986: 14 [taxonomic list]. — Bockmann & Guazzelli, 2003: 418 [taxonomic treatment]. — Ferraris, 2007: 190 [taxonomic treatment].
- Pimelodus* (*Pseudorhamdia*) *wessellii* Steindachner, 1876c: 56 (footnote) [original description]. — Cope, 1878: 675 [taxonomic treatment]. — Eigenmann, 1912: 168 [synonym of *P. cristata*]. — Gosline, 1945: 43 [synonym of *P. cristata*]. — Van der Stigchel, 1946: 54 [synonym of *P. cristata*].
- Pimelodella wessellii*. — Eigenmann & Eigenmann, 1888: 132 [taxonomic treatment]. — Eigenmann & Eigenmann, 1890: 148. — Eigenmann & Eigenmann, 1891: 29 [taxonomic treatment]. — Eigenmann, 1910: 389 [taxonomic treatment]. — Vari *et al.*, 2009: 43 [taxonomic list]. — Van der Stigchel, 1946: 54 [synonym of *P. cristata*]. — Bockmann & Guazzelli, 2003: 421 [taxonomic treatment]. — Ferraris, 2007: 195 [taxonomic treatment].
- Rhamdia wessellii*. — Miranda Ribeiro, 1911: 268–269 [taxonomic treatment]. — Van der Stigchel, 1946: 55 [synonym of *P. cristata*].
- ?*Pimelodella wessellii*. — Eigenmann, 1912: 168 [synonym of *P. cristata*].
- Pimelodus ophthalmicus* Cope, 1878: 675 [original description; “Peruvian Amazon”, Peru; holotype: ANSP 21102]. — Eigenmann & Eigenmann, 1888: 132 [synonym of *P. cristata*]. — Eigenmann & Eigenmann, 1890: 150 [synonym of *P. cristata*]. — Eigenmann & Eigenmann, 1891: 29 [synonym of *P. cristatus*]. — Eigenmann, 1910: 388 [synonym of *P. cristata*]. — Eigenmann, 1912: 168 [synonym of *P. cristata*]. — Fowler, 1915: 214 [synonym of *P. cristata*]. — Gosline, 1945: 43 [synonym of *P. cristata*]. — Van der Stigchel, 1946: 54 [synonym of *P. cristata*]. — Fowler, 1951: 538 [synonym of *P. cristata*]. — Böhlke, 1984: 142 [type catalog].
- Pimelodella ophthalmica*. — Bockmann & Guazzelli, 2003: 420 [taxonomic treatment, transference to *Pimelodella*]. — Ferraris, 2007: 193–194 [taxonomic treatment].

- Pimelodus insignis* [non Schomburgk, 1841]. — Eigenmann & Eigenmann, 1888: 132 [synonym of *P. cristatus*].
- ?*Pimelodus insignis* [non Schomburgk, 1841]. — Eigenmann & Eigenmann, 1890: 150 [synonym of *P. cristatus*]. — Eigenmann, 1912: 162 [synonym of *P. cristata*].
- Rhamdia insignis* [non Schomburgk, 1841]. — Miranda Ribeiro, 1911: 267–268, fig. 2 [taxonomic treatment]. — Van der Stigchel, 1946: 54 [synonym of *P. cristata*].
- Pimelodus agassizii* [non Steindachner, 1876c]. — Cope, 1878: 675 [taxonomic treatment]. — Eigenmann & Eigenmann, 1890: 150. — Eigenmann & Eigenmann, 1891: 29 [taxonomic list]. — Eigenmann, 1910: 388 [synonym of *P. cristata*]. — Eigenmann, 1912: 168 [synonym of *P. cristata*]. — Gosline, 1945: 43 [synonym of *P. cristata*]. — Van der Stigchel, 1946: 54 [synonym of *P. cristata*]. — Fowler, 1951: 538 [synonym of *P. cristata*].
- Pimelodus agasizii* [non Steindachner, 1876c]. — Eigenmann & Eigenmann, 1888: 132 [synonym of *P. cristatus*, misspelling].
- Pimelodus (Pseudorhamdia) gracilis* [non Valenciennes, 1835]. — Steindachner, 1879: 9 [taxonomic list].
- Pimelodella gracilis* [non Valenciennes, 1835]. — Eigenmann, 1910: 389 (*in partim*) [taxonomic list]. — Fowler, 1940: 64 [taxonomic treatment]. — Fowler, 1941: 127 [taxonomic treatment]. — Eigenmann & Allen, 1942: 50, 102 (*in partim*) [taxonomic list, taxonomic treatment]. — Schultz, 1944: 211–212 (*in partim*) [taxonomic treatment]. — Gosline, 1945: 43 (*in partim*) [taxonomic list]. — Fowler, 1951: 540 (*in partim*) [taxonomic list]. — Ortega & Vari, 1986: 14 [taxonomic list]. — Chernoff *et al.*, 2000: 282 [taxonomic list]. — Bockmann & Guazzelli, 2003: 418 (*in partim*) [taxonomic treatment]. — Rosa *et al.*, 2003: 177 [taxonomic list]. — Lasso *et al.*, 2004: 171 [taxonomic list]. — Maldonado-Ocampo *et al.*, 2008: 202 [taxonomic list]. — Ferraris, 2007: 191 (*in partim*) [taxonomic treatment].
- Rhamdia gracilis* [non Valenciennes, 1835]. — Miranda Ribeiro, 1911: 269–270 (*in partim*) [taxonomic treatment]. — Eigenmann, 1917: 230 (*in partim*) [taxonomic revision]. — Rosa *et al.*, 2003: 177 [taxonomic list].
- Pimelodella gracile* [non Valenciennes, 1835]. — Fowler, 1914: 263, fig. 13 [taxonomic list, misspelling].
- Pimelodella cf. gracilis*. — Cabrera & Vaca, 2006: 27 [taxonomic list].
- Rhamdia lateristriga* [non Lichtenstein, 1823]. — Miranda Ribeiro, 1911: 271–272 (*in partim*) [taxonomic treatment].

- Pimelodella lateristriga* (*in partim*) [non Lichtenstein, 1823]. — Eigenmann & Allen, 1942: 99 [taxonomic treatment].
- Pimelodella steindachneri* Eigenmann, 1917: 230, 232, 237–238, pl. XXXV figs. 42–44 [original description: “Maues, Rio Madeira”, “Para”, “Cujadas”, “Santarem”, “Puty”, “Manacapuru”; syntypes: MCZ 7566, 7487, 7472, 7567, 7588, 7542, respectively]. — Gosline, 1945: 43 [taxonomic list]. — Fowler, 1951: 550 [taxonomic list]. — Burgess, 1989: 281 [taxonomic list]. — Bockmann & Guazzelli, 2003: 421 [taxonomic treatment]. — Ferraris, 2007: 195 [taxonomic treatment]. — Bockmann & Slobodian, 2013: 16–17, 69 [taxonomic treatment, key].
- Pimelodella hartwelli* Fowler, 1939: 222–223, figs. 4–7 [original description; “Ucayali River, Contamana, Peru”; holotype: ANSP 68644]. — Eigenmann & Allen, 1942: 47, 99 [taxonomic list, taxonomic treatment]. — Gosline, 1945: 45 [taxonomic list]. — Fowler, 1951: 542, fig. 556 [taxonomic list]. — Böhlke, 1984: 141 [type catalog]. — Ortega & Vari, 1986: 14 [taxonomic list]. — Burgess, 1989: 280 [taxonomic list]. — Bockmann & Guazzelli, 2003: 419 [taxonomic treatment]. — Ferraris, 2007: 192 [taxonomic treatment].
- Pimelodella dorseyi* Fowler, 1941a: 127–129, figs. 4–7 [original description; “Rio Salgade, Icó, Ceará”, Brazil; holotype: ANSP 69375]. — Gosline, 1945: 46 [taxonomic list]. — Fowler, 1951: 538, fig. 552 [taxonomic list]. — Böhlke, 1984: 141 [type catalog]. — Burgess, 1989: 280 [taxonomic list]. — Bockmann & Guazzelli, 2003: 418 [taxonomic treatment]. — Rosa *et al.*, 2003: 177 [taxonomic list]. — Ferraris, 2007: 190 [taxonomic treatment].
- Pimelodella parnahybae* Fowler, 1941a: 129–130, figs. 8–11 [original description; “Rio Parnahyba, Therezina, Piahy”, Brazil; holotype: ANSP 69377]. — Gosline, 1945: 46 [taxonomic list]. — Fowler, 1951: 547–548, fig. 563 [taxonomic list]. — Böhlke, 1984: 141 [type catalog]. — Burgess, 1989: 281 [taxonomic list]. — Bockmann & Guazzelli, 2003: 420 [taxonomic treatment]. — Rosa *et al.*, 2003: 177 [taxonomic list]. — Ferraris, 2007: 194 [taxonomic treatment]. — Reis *et al.*, 2016: 28 [taxonomic list, endemism].
- Pimelodella witmeri* Fowler, 1941a: 133–135, figs. 20–22 [original description; “Rio Jaguaribe, Orós, Ceará”, Brazil; holotype: ANSP 69383]. — Gosline, 1945: 47 [taxonomic list]. — Fowler, 1945: 551, fig. 567 [taxonomic list]. — Böhlke, 1984: 141 [type catalog]. — Burgess, 1989: 281 [taxonomic list]. — Bockmann &

Guazzelli, 2003: 421 [taxonomic treatment]. — Rosa *et al.*, 2003: 177 [taxonomic list]. — Ferraris, 2007: 195 [taxonomic treatment].

Diagnosis

Pimelodella cristata can be distinguished from most of its congeners, with exception of *P. cruxenti*, *P. gracilis* and *P. humeralis*, by having more than 46 total vertebrae (*vs.* 37 to 44 total vertebrae, rarely 45). Moreover, it differs from *P. cruxenti* by having a light colored body (*vs.* body overall brownish) (Figs. 29, 31). Differs from *P. gracilis* by the presence of a narrow midlateral stripe, from opercle to caudal-fin insertion (*vs.* wide midlateral dark brown or gray stripe, from opercle to caudal-fin insertion, and another paired, diffuse, dark stripe in dorsal region of body, from lateral extension of supraoccipital process, and along dorsal region of body until adipose-fin insertion to terminus). It differs from *P. humeralis* by the absence of a dark anteriorly oblique blotch in the humeral region, and by the pectoral-fin spine bearing smooth serrae along its anterior margin distal half, and posterior margin bearing 22–27 retrorse dentations along almost all the margin (*vs.* anterior margin of pectoral-fin spine with minute, smooth-sided, straight dentations along its basal half, and serrae along its distal half; posterior margin with 8–11 retrorse dentations along its basal three-quarters). *Pimelodella cristata* can be further signosed by the combination of the following traits: head lateral profile straight from snout to dorsal-fin insertion; maxillary barbel long, usually reaching at least the vertical through adipose-fin terminus; outer mental barbel reaching between the verticals through first third and terminus of adressed pectoral-fin; dorsal-fin spine long, roughly a fourth or less shorter than first dorsal-fin total length; pectoral-fin spine bearing smooth serrae along its anterior margin distal half, and posterior margin bearing 22–27 retrorse dentations along almost all the margin, the dentations being triangular and inclined; adipose fin very long, between 36.7–45.2% SL, but usually above 40% SL; total vertebrae 46–52; one single opening of epiphyseal branch of cephalic laterosensory canal on head, after a small tube that connects both contralateral S6 branches; midlateral stripe dark brown, very narrow, posterior to opercle to caudal-fin insertion (maybe absent in preserved material); and dorsal-fin hyaline near the base, followed by a dark brown stripe, then a hyaline stripe, and distal half dusky.

Description

Measurements in Table 13. Body of moderately deep, depth at dorsal-fin origin five to seven times in standard length, and compressed, body width at dorsal-fin origin six times or more in SL (Fig. 29). Greatest body depth at dorsal-fin origin. Dorsal profile convex from

snout to dorsal-fin origin, slightly concave from dorsal to adipose fin, slightly convex along adipose fin, and concave at the caudal peduncle. Ventral profile of body slightly convex from snout to branchiostegal membrane, between pectoral end pelvic fins, and from pelvic to anal fin, and concave from that point along the caudal peduncle.

Pseudotympanum large, oval, above posterior process of cleithrum and reaching 6th (10) to 8th (1) vertebrae. Posterior process of cleithrum triangular, its dorsal margin straight or slightly concave. Anus and urogenital papilla adjacent. Urogenital papilla tubular, triangular, average sized. Anus between verticals through first third and half of adpressed pelvic fins; urogenital papilla reaching between verticals through second and last fifth of adpressed pelvic fins.

Head of average depth, depth at base of supraoccipital process a third to half of head length. Mouth sub terminal. Eye slightly elliptical, four to five times in head. Bony interorbital distance almost equal to eye diameter. Barbels thin, slightly depressed and elliptical in cross-section. Maxillary barbel reaching between verticals through half adpressed anal-fin and surpassing caudal-fin insertion. Outer mental barbel, when stretched parallel to main body axis, finishing between first fourth of adpressed pectoral-fin and pelvic-fin origin. Inner mental barbel, when stretched parallel to main body axis, finishing between branchiostegal membrane ventral limit and half adpressed pectoral-fin. Supraoccipital process subrectangular, comparatively wide, with a constant width long its length and distal third slightly tapered, sometimes with a discrete constriction near base. Dorsal lamina of Weberian complex vertebrae reaching the supraoccipital process at its anteriormost part, or along its entire extension. Branchiostegal rays 6* (16), rarely 7 (1).

Dorsal fin triangular, distal margin concave, average sized (second branched dorsal-fin ray four to five times in SL), depressed tip finishing between verticals through first third and terminus of adpressed pelvic fin. Dorsal fin with I,6 (45) plus anteriormost spinelet. Distance between terminus of dorsal-fin base and adipose-fin origin smaller than half dorsal-fin base. Anteriormost dorsal-fin pterygiophore inserted posterior to neural spine of vertebrae 4 (39); posteriormost dorsal-fin pterygiophore located anterior to neural (or pseudoneural) spine of vertebrae 11* (33), rarely 12 (4). Unbranched dorsal-fin ray mostly ossified as a spine, rigid part usually long (ca. 75% of first dorsal-fin total length), distal half on anterior side with really smooth serrae, and distal half of posterior side with small straight to retrorse dentations.

Pectoral-fin rays I,7 (1)– I,10 (1), usually I,9* (15), pectoral fin triangular with concave distal border. First pectoral-fin ray curved with proximal part rigid, forming a spine (Fig. 30), and short distal tip flexible and distinctly segmented. Comparatively moderated

length spine, five times or less in SL. Anterior margin of pectoral-fin spine with smooth serrae along its distal half. Posterior margin of pectoral-fin spine bearing 20–27 retrorse dentations along almost all the margin. These dentations are triangular and inclined. Also 1–2 unossified distal dentations, not counted.

Pelvic-fin rays i,5 (36), extended pelvic fin triangular with straight distal border. Anterior portion of pelvic-fin base between verticals through sixth branched dorsal-fin ray and half adpressed dorsal-fin. Tip of adpressed pelvic fin between verticals through first fifth or third of adipose fin. First unbranched and flexible ray distinctly shorter than second and third rays, which are roughly the same size; remaining rays progressively shorter.

Anal-fin rays iv,7 (1); v,7 (1); iv,8 (2); v,8 (4), iv,9 (5); v,9 (6); vi,9 (1); iv,10 (4); v,10 (8); vi,10* (4); iv,11 (2); v,11 (3) or vi,11 (2); distal margin of extended anal fin convex. Two to four anteriormost anal-fin rays vestigial, unsegmented, embedded in thick skin fold. Anal fin origin between verticals through first third and half of adipose-fin base; anal-fin adpressed terminus always slightly anterior to vertical through adipose-fin terminus. Tip of anteriormost anal-fin pterygiophore inserted posterior to hemal spine of vertebrae 21 (5), 23 (7), 24 (13), 25* (12) or 26 (1). Tip of posteriormost anal-fin pterygiophore inserted ahead of hemal spine of vertebrae 28 (1), 30 (1), 31 (4), 32 (2), 33 (7), 35* (9) or 36 (3).

Adipose fin two to less than three times in SL, forming ascending elevated curve in lateral profile, with deepest point approximately at last third. Adipose fin emerging gradually, its posterior limit as a rounded, free lobe. Adipose-fin origin at vertical through vertebral centra 15 (2)–21 (2) (lectotype 16); adipose-fin terminus at vertical through vertebral centra 37 (1) to 47 (1) (lectotype 43).

Caudal fin deeply forked, its lobes may be subequal (10*), dorsal lobe longer (7), or ventral lobe longer (7). Caudal peduncle length posterior to adipose-fin slightly longer than its depth. Dorsal lobe with 7 (40) branched, 1 (40) unbranched principal, and 9 (1)–20 (2) (lectotype 14) procurrent fin-rays. Ventral lobe with 8* (36), rarely 9 (2) branched, 1 (38) unbranched principal, and 13 (1)–24 (2) (lectotype 20) procurrent fin-rays. Hypural 5 free. Median caudal-fin rays not articulated directly to hypural plate. Seven* (26), rarely 8 (3) or 9 (1) rays articulated to dorsal caudal-fin plate (5, 6 or 7 on hypurals 3+4 and 2 on hypural 5) and 8 (16), rarely 7* (6), 9 (5) or 10 (3) rays articulated to ventral caudal-fin plate (5, 6, 7 or 8 on hypurals 1+2 and 2 on parhypural).

Total vertebrae 46 (3)–52 (1), usually 50* (13). Ribs 8 (4)–10 (19) (lectotype 9).

One single opening of epipheseal branch of cephalic laterosensory canal on head, on S6 pore, after a small canal that connects both contralateral S6 branches.

Coloration in alcohol

Background body coloration yellowish. Ventral region of head and body lighter than dorsal regions. Dark brown midlateral stripe (Fig. 31), narrow, usually poorly-defined, extending from a region posterior to opercle or pseudotympanum until caudal-fin origin. Dorsal fin with a hyaline stripe near the base, followed by a narrow dark brown stripe, then a hyaline stripe, and distal half dusky. Some variation may exist, from totally unpigmented specimens to others with scattered dark melanophores distributed evenly on dorsal region of head.

Geographic distribution

Pimelodella cristata was described from rio Takutu and rio Mahu, tributaries of Upper Rio Branco, in Guyana. Its junior-synonyms were described from various different localities, as follows: *P. breviceps* (Marabitanas, Upper Rio Negro basin, Brazil); *P. cyanostigma* (Pebas, Ampyiacu River basin, Peru); *P. dorseyi* (Rio Salgado, Jaguaribe River basin, Brazil); *P. hartwelli* (Ucayali River, Peru); *P. ophthalmica* (Peruvian Amazon), *P. parnahybae* (Rio Parnaíba, Brazil), *P. steindachneri* (several rivers in Amazon basin and Northeastern Brazil—see comments); *P. wessellii* (Essequibo River, Guyana); *P. witmeri* (Jaguaribe River, Ceará, Brazil). *Pimelodella cristata* is known from regions 308, 310, 311, 314, 315, 316, 318, 325 and 326, and probably 319, 320, 321, 322, 323 and 324, comprising several drainages in Amazon, Guianas, Orinoco, Northeastern Coastal drainages and Parnaíba (see comments below).

Comments

Müller & Troschel (1949a) succinctly described *P. cristata*, later expanded in Müller & Troschel (1849b) as “Nob. Nov. Spec”, indicating a specimen of 9 ½ inches (approximately 241 mm). Specimen ZMB 3053 is 242 mm in total length (present-day measurement) fitting closely the size reported in the paper and is hereby designated as lectotype, with and ZMB 3052 (213 mm TL) as paralectotype of *P. cristata*.

As mentioned in the Diagnosis, *Pimelodella cristata* can be distinguished from all congeners by a set of characteristics. Those characteristics do not differ significantly in the type-materials of its numerous synonyms, namely *P. cristata*, *P. breviceps*, *P. dorseyi*, *P. hartwelli*, *P. ophthalmica*, *P. parnahybae*, *P. steindachneri*, *P. wessellii*, *P. witmeri* (cf. Table 14).

All specimens of *Pimelodella cristata* from Guiana Shield rivers with radiographs examined (regions 308, 310, 311 and 315 of Abell *et al.*, 2008; in a total of 15 radiographed specimens, from 9 different localities) fit the relevant diagnostic characters, with the addition

of 49–52 total vertebrae, mode 50 (an exception being ANSP 177229, with 46 total vertebrae), and the first pterygiophore of the anal-fin inserted posterior to the haemal spine of vertebrae 24 or 25 (Table 15). Those characteristics are also found in *P. wessellii*, described from Essequibo drainage. In sum, from the 16 Guiana Shield specimens, only 4 (25%) have less than 50 total vertebrae (Table 15).

Morphotypes similar to *P. cristata* from the Amazon basin (regions 314, 316 and 318 of Abell *et al.*, 2008), including the types of *P. breviceps*, *P. cyanostigma*, *P. hartwelli*, *P. ophthalmica*, *P. steindachneri* and comparative material (17 radiographed specimens, 14 different localities), have 47–51 total vertebrae, mode 49 or 50, and 11 of them have less than 50 total vertebrae (65%) (Table 15). The first pterygiophore of the anal-fin in those specimens is inserted posterior to haemal spine of vertebrae 21 to 25 (Table 15). All other characteristics are congruent with those for Guiana Shield *P. cristata*. *Pimelodella steindachneri* was described with some hesitation by Eigenmann (1917), with specimens similar to *P. cristata* from Amazon basin and northeastern Brazil, but Eigenmann only indicated its distribution as restricted to the Amazon basin.

Morphotypes similar to that of *P. cristata* from Northeastern drainages of Brazil (regions 325 and 326 of Abell *et al.*, 2008), include one syntype of *P. steindachneri* (MCZ 7588), while Fowler (1941a) described *Pimelodella dorseyi*, *P. parhanybae* and *P. witmeri*. The latter author indicated as diagnostic features of *P. dorseyi* the “uniform coloration and with only a very narrow dark axial lateral band” and “long maxillary barbels, armature of the dorsal and pectoral spines” (Fowler, 1941a: 129). In the description of *P. parnahybae*, the indicated diagnostic features were a conic and compressed head and body, and large eye, features known to vary even inside a single population (Borodin, 1924 for body shape; Mees, 1974 for eye size as sexually dimorphic). Also in the description of *P. parnahybae*, Fowler (1941a: 130) proposed that the long barbels approach this species to *P. hartwelli* and *P. dorseyi*. Diagnostic features mentioned for *P. witmeri* were the long adipose fin, absence of midlateral dark stripe, small caudal fin and large eye (Fowler, 1941a: 135). Eye size in *P. witmeri* is quite similar to that of *P. parnahybae*, while its coloration pattern is similar to *P. dorseyi*, and adipose fin size to both species.

Examination of radiographs of type specimens of all three species, plus the syntype of *P. steindachneri* from Rio Parnaíba basin, and additional comparative material shows no differences indicative of taxonomic differentiation. All specimens have 46–48 total vertebrae, and the first pterygiophore of the anal-fin inserted posterior to haemal spine of vertebrae 21 to

24 (Table 15). All other characteristics are congruent with those found in Guiana Shield *P. cristata* (the pectoral-fin spine of *P. witmeri* types is severed and could not be verified).

A small difference in the number of vertebrae and insertion of anal fin can be observed among specimens from Guiana Shield, Amazon and Northeastern Brazil rivers, with those from Guiana Shield with a tendency towards higher number of vertebrae (Table 15). However, there is overlap in those figures and this character is insufficient to separate the groups into separate species. All other characteristics are congruent with those found in Guiana Shield *P. cristata*. The exception is the holotype of *P. breviceps*, which is the most aberrant of the mentioned specimens, but mainly due to secondary sexual characteristics (dorsal fin and urogenital papilla longer, see more in Sexual Dimorphism section), and which is probably a male specimen of *P. cristata* in full reproductive morphology.

The morphological variation in all species mentioned above, as in other *Pimelodella* species with 46 or more total vertebrae, is very incipient, and separation in different species is unwarranted under examination of wide-ranging comparative material. Of those characteristics commonly used in diagnosis of other *Pimelodella* species, those related to morphometrics are highly overlapping (Table 14). A Principal Component Analysis was performed for all *Pimelodella* species with 46 or more total vertebrae (except *P. cyanostigma*, due to poor preservation of material), and the graphic of PC1 against PC2 shows an overall overlap of almost all populations, with exception those referable to *P. cruxenti* and *P. humeralis* (Fig. 32). Figure 33 presents a similar PCA with all *Pimelodella* species with 46 or more total vertebrae, excluding *P. cruxenti* (which is notably different from the remaining species), however, in this figure all specimens from the same basin are grouped, instead of discriminated by species name. This Figure 33 shows that even material from different basins almost completely overlap in PCA, showing the insufficiency of morphometric data in discriminating even *P. cristata* from *P. gracilis*, a species with other diagnostic characters than morphometric data. More about the differences between *P. cristata* and *P. gracilis* are presented in the later species' section.

In sum, despite a small variation found in the number of vertebrae of Guiana Shield *P. cristata* when compared with similar morphotypes from the Amazon and Northeastern Brazil basins, this and other morphological characters found are not sufficient to justify the separation of these forms into more than one species. Therefore, *P. breviceps*, *P. cyanostigma*, *P. dorseyi*, *P. hartwelli*, *P. ophthalmica*, *P. parnahybae*, *P. steindachneri*, *P. wessellii* and *P. witmeri* are all considered as junior-synonyms of *P. cristata*. The geographic distribution of the latter is expanded to drainages in Amazon, Guianas, Orinoco, Northeastern

Coastal drainages and Parnaíba (specifically regions 308, 310, 311, 314, 315, 316, 318, 325 and 326). Material examined by Guazzelli (2003) from specimens similar to *P. cristata* belong to regions 319, 320, 321, 322, 323 and 324, but were not radiographed, and their inclusion under *P. cristata* comparative material and distribution is still uncertain. However, this species needs further study, and the inclusion of more material, or data, can bring light to the obviously difficult morphological delimitation of this species.

Designation of lectotypes and paralectotypes of *Pimelodella* species included in *P. cristata* synonym are as follow:

Pimelodella cyanostigma (Cope, 1878). — Lectotype: ANSP 8382, 59.8 mm SL; Paralectotypes: ANSP 8381 71.7 mm SL (synonym of *P. buckleyi*) and ANSP 8383 50.6 mm SL.

Pimelodella steindachneri Eigenmann, 1917. — Lectotype: MCZ 7487 (“Pará”, Rio Amazonas at Pará, Brazil); Paralectotypes: MCZ 7472, 7542, 7566, 7567, 7588.

Some synonyms of *P. cristata* previously proposed in the literature have been found to be erroneous or unjustified, and they are discussed in the next paragraphs, in the same order presented in the synonym section.

Pimelodus insignis

The synonym of *Pimelodus insignis* Schomburgk to *P. cristata* (Eigenmann & Eigenmann 1888: 132; Eigenmann & Eigenmann, 1890: 150) was not confirmed.. Eigenmann & Eigenmann (1890) synonymized *P. insignis* to *P. cristata* based on the name the Wapisiana people gave to the fish (Konnairu) and on the lengths (eighteen inches) of cited specimens in both Schomburgk (1841), for *P. insignis*, and Müller & Troschel (1849a), for *P. cristata*. However, the remaining of the description of *P. insignis* does not match a *Pimelodella* species. *Pimelodella insignis* is currently believed to be a junior-synonym of *Pinirampus pirinampu* (Spix & Agassiz, 1829) (e.g. Lundberg & Littmann, 2003). Eigenmann (1917) later recognized his earlier mistake.

Probably following Eigenmann & Eigenmann (1888, 1890), Miranda Ribeiro (1911) reassigned *Pimelodus insignis* to *Rhamdia*, as he had also done to all other *Pimelodella* species described so far. The specimens described by Miranda Ribeiro (1911) and illustrated in fig. 2, however, are unlike those of Schomburgk (1841) and probably indeed belong to *Pimelodella*. The occurrence of *Rhamdia insignis* was designated as “S. Gonçalo, Avary, Villa Bella, Jutahy, Tapajoz, Mucury, Tabatinga, Javary, Coary, Capim, Takutu, Mahu” and shares much resemblance with that reported for *Pimelodella cristata* in Eigenmann &

Eigenmann (1890), namely “San Gonçallo; Avary; Villa Bella; Jutahy; Tapajos; Rio Mucuri; Tabatinga; Hyavary; Coary”. Fowler (1954) included the aforementioned citation of *Rhamdia insignis* to the synonym of *Calophysus macropterus* (Lichtenstein, 1819), which is also mistaken.

Pimelodus agassizii

Pimelodus agassizii Steindachner (1876c) was included as *P. cristata* junior-synonym by Eigenmann & Eigenmann (1888: 132) and Eigenmann & Eigenmann (1890: 150). However, other authors have already excluded this species from *P. cristata* synonym, and included as a junior-synonym of *P. pirinampu* (e.g. Burgess, 1989: 275; Eschmeyer, Fricke & van der Laan, 2017). I agree with the latter, and therefore exclude *P. agassizii* from *P. cristata* synonym.

Pimelodus altipinnis

The synonym of *P. altipinnis* (Steindachner, 1864) under *P. cristata* made by Mees (1974) is also mistaken. *Pimelodus altipinnis* was described succinctly in an abstract by Steindachner (1864a), based in one small specimen (NMW 45601), and later described in more detail in Steindachner (1864b, pl. II, figs. 3 and 4). Subsequently, Steindachner (1876a) redescribed *Pimelodus altipinnis* based on numerous material from “Para, Santarem und Cameta” (Steindachner, 1876a: 605–607). I analyzed all the material from NMW that Steindachner received between 1864 and 1876 belonging to *P. altipinnis* from the above-mentioned localities (corresponding to NMW 45582, 45585, 45591, 45597, 45602, 45603), and all of those belong to *Pimelodus*, while his *P. altipinnis* is a *Rhamdia*, as explained as follows.

Eigenmann (1912), based on Steindachner (1864b), suggested that *P. altipinnis* perhaps belonged to *Pimelodella*: “The species has the general characters of a *Pimelodella*, and it would not be surprising if the small type in the Vienna Museum should prove to be a *Pimelodella* and distinct from the specimens subsequently referred to the same name” (Eigenmann, 1912: 177). This suggestion was followed by Van der Stigchel (1946), also without consulting the type-material. Mees (1974), examined the type and identified it as a typical *Pimelodella*, “with a narrow occipital process meeting the equally narrow dorsal plate”, and proposed it as a female of *P. cristata* (Mees, 1974: 148). Examination of type material material (NMW 45601) and its radiographs shows that the type of *P. altipinnis* is actually a *Rhamdia* due its closed posterior fontanel (with just a small residual opening) and supraoccipital process not reaching the anterior prenuchal plate.

Mees' (1974) synonym of *P. geryi* to *P. cristata*, is also not corroborated, and *P. geryi* is actually a very distinctive species (see discussion later in this species section).

Further comments

Former records of *P. gracilis* from Amazon, Guianas and Orinoco were treated as part of *P. cristata* because the two species, though similar, are distinguishable. *Pimelodella gracilis* is known only from the Uruguay-Paraná-La Plata basins. Therefore, Mees (1974) is correct that *P. gracilis* from British Guiana (e.g. Fowler, 1914) and Orinoco (e.g. Steindachner, 1879; Schultz, 1944) are in fact *P. cristata*. Part of *P. lateristriga* records for Amazon and Orinoco are also included under *P. cristata* synonym.

Photographs of the types of *P. breviceps*, *P. cyanostigma*, *P. dorseyi*, *P. hartwelli*, *P. ophthalmica*, *P. parnahybae*, *P. steindachneri*, *P. wessellii* and *P. witmeri* are presented in figures 34–42.

Material examined

Pimelodella breviceps. — NMW 45615, 1, xr, 326.2 mm SL, holotype, Brazil, Amazonas, "Marabitanos" (probably Marabitanas), 0°26'04"N, 68°48'51"W.

Pimelodella cristata. — ZMB 3052, 1, xr, 177.4 mm SL, syntype, Guyana, "Takutu und Mahu" (probably Tacutu and Mahu rivers, Guyana), 3°33'46"N, 59°52'08"W; ZMB 3053, 1, xr, 202.5 mm SL, syntype, Guyana, "Takutu und Mahu" (probably Tacutu and Mahu rivers, Guyana), 3°33'46"N, 59°52'08"W; AMNH 54945, 11, 117.9 mm SL, Surinam, Nickerie District, Corintijn river, camp hydro, ca. kilometer 370, ca. 30 kilometers north of tiger falls large pool at foot of path from camp, 5°50'44.9"N, 57°06'02.9"W; ANSP 8362, 1, xr, Holotype, Peru, Ambyiacu River near Pebas, 3°19'35.5"S, 71°52'47.9"W; ANSP 69021, 1, xr, 48.7 mm SL, Holotype, Bolivia, Boca Chapare, Rio Chimore, 17°13'38.3"S, 65°03'58.1"W; ANSP 144003, 17, xr, Peru, Madre de Dios, Near Boca Manu, mouth of Pinquen River (tributary Rio Manu), 12°10'0.0"S, 71°1'0.0"W; ANSP 165356, 15, 34.64–109.35 mm SL, Venezuela, Rio Cunaviche, ca. 20km SW of Cunaviche on S, Francisco Apure-Puerto Paes Hwy, 7°20'0"N, 67°35'0"W; ANSP 167907, 7, xr, Venezuela, Bolívar, Morichal (San Antonio area) on El Manteco-El Yagual road, Rio Supamo/Cuyuni Drainage, 7°10'0"N, 62°30'0"W; ANSP 175789, 1, xr, Guyana, Essequibo River, sand bar some 50 minutes upstream from Kurupukari field station, 4°42'47"N, 58°42'40"W; ANSP 175790, 3, xr, Guyana, Flooded roadside pool/creek along Kurupukari-Surama River road, 4°15'25"N, 58°54'7"W; ANSP 175791, 1, xr, Guyana, Small creeks crossing Kurupukari-Surama River road ca. 3.0 miles from Kurupukari field station, 4°22'29"N, 58°50'30"W; ANSP 177229, 8, 70.2–129.3 mm SL, 1 c&s, Guyana, Essequibo, Burro Burro River, Water Dog Falls (camp), Station 4A,

4°40'48"N, 58°50'46"W; ANSP 198174, 14, 64.4–132.9 mm SL, 2 c&s, Venezuela, Amazonas, Rio Orinoco (Atlantic Dr.), beach and bedrock outcrop, 50 km east of San Fernando de Atabapo, 3°58'13"N, 67°15'18"W; INPA 2589, 2, xr, Brazil, Amazonas, Presidente Figueiredo, 2°02'04.0"S, 60°01'30.0"W; INPA 7154, 2, Brazil, Pará, Aveiro, 3°36'20.0"S, 55°19'54.1"W; INPA 11149, 6, xr, Brazil, Pará, Oriximiná, 1°45'56.0"S, 55°51'58.0"W; INPA 12522, 6, xr, Brazil, Rondônia, Ariquemes, 9°54'48.0"S, 63°02'26.9"W; INPA 14952, 1, xr, Brazil, Amazonas, Presidente Figueiredo, 2°02'04.0"S, 60°01'30.0"W; INPA 14955, 2, xr, Brazil, Amazonas, Presidente Figueiredo, 2°02'04.0"S, 60°01'30.0"W; INPA 22346, 1, Brazil, Rondônia, Porto Velho, 8°45'43.0"S, 63°54'14.0"W; INPA 22984, Brazil, Rondônia, Costa Marques, 12°26'42.0"S, 64°13'37.9"W; INPA 22985, Brazil, Rondônia, Costa Marques, 12°26'42.0"S, 64°13'37.9"W; INPA 24471, Brazil, Rondônia, Costa Marques, 12°26'42.0"S, 64°13'37.9"W; MZUSP 23030, 1, xr, Brazil, Pará, Boa Vista, Castanhal Igarapé Apeu, 1°17'0.0"S, 47°55'0.0" W; MZUSP 23588, 1, 82.6 mm SL, Brazil, Amazonas, Tefe, Rio Uraricoera, Igarapé na fazenda Canadá, 3°28'0.0"N, 60°58'0.0"W; MZUSP 23609, 3, 110.6–138.9 mm SL, Brazil, Roraima, Corredeiras do Rio Uraricoera, Ilha Maracá, 3°28'0.0"N, 60°58'0.0"W; MZUSP 27485, 1, 57.3 mm SL, Brazil, Amazonas, Tefe, Costa Japão, Baixo Rio Japurá, 3°22'0.0"S, 64°43'0.0"W; MZUSP 27918, 1, 117.1 mm SL, Brazil, Amazonas, Humaitá, Igarapé Joari, 7°31'0.0"S, 63°2'0.0"W; MZUSP 50519, 1, xr, 118.1 mm SL, Brazil, Acre, Rio Tejo, Foz do Bajé, 8°56'0.0"S, 72°34'0.0"W; MZUSP 57188, 1, 83.8 mm SL, Brazil, Amazonas, Rio Purus, próximo à foz, 3°59'46.0"S, 61°29'28.0"W; MZUSP 81528, 1, 165.4 mm SL, Brazil, Amazonas, Rio Tiquié, comunidade de Boca do Sal, 0°16'22.0"N, 69°54'3.0"W; ZSM 6070.

Pimelodella cyanostigma. — ANSP 8382, 1, xr, 59.8 mm SL, syntype, Ecuador, Pebas, 3°19'26"S, 71°51'38"W; ANSP 8383, 1, xr, 50.6 mm SL, syntype, Ecuador, Pebas, 3°19'26"S, 71°51'38"W.

Pimelodella dorseyi. — ANSP 69375, 1, xr, 95.8 mm SL holotype, Brazil, Ceará, Rio Salgado, Icó, 6°23'59"S, 38°52'04"W; ANSP 69376, 1, xr, 95.8 mm SL, paratype, Brazil, Ceará, Rio Salgado, Icó, 6°23'59"S, 38°52'04"W.

Pimelodella hartwelli. — ANSP 68644, 1, xr, 103.2 mm SL, holotype, Peru, Contamana; Ucayali River, 7°21'23.1"S, 75°00'36.3"W.

Pimelodella ophthalmica. — ANSP 21102, 1, xr, 109.4 mm SL, holotype, Peru, Peruvian Amazon.

Pimelodella parnahybae. — ANSP 69377, 1, xr, 84.0 mm SL, holotype, Brazil, Rio Parnahyba, Therezina, Piahy, 5°03'38"S, 42°50'25"W; MZUSP 5066, 19, 49.1–87.2 mm SL,

Brazil, Maranhão, Grajau, Rio Grajaú, 5°49'0.0"S, 46°9'0.0"W; MZUSP 5076, 1, 54.1 mm SL, Brazil, Maranhão, Barra Do Corda Rio Corda, 5°30'0.0"S, 45°14'0.0"W; MZUSP 22255, 5, 69.6–135.9 mm SL, Brazil, Maranhão, Rio Corda, 5°30'47.3"S, 45°14'34.5"W; MZUSP 38886, 3, 81.4–101 mm SL, Brazil, Minas Gerais, Rio Paranaíba, project UHE Bocaina, 18°13'0.0"S, 47°35'0.0"W; MZUSP 43592, 1, 145 mm SL, Brazil, Maranhão, Lago dos Viana, Pindaré-Mearim system, 3°13'0.0"S, 45°10'0.0"W; MZUSP 97955, 1, 114.4 mm SL, Brazil, Piauí, Parnagua, island at Parnaguá Lake, Parnaguá county, 10°14'41.0"S, 44°38'50.0"W; MZUSP 98633, 6, 73.8–107.2 mm SL, Brazil, Piauí, Parnagua, Praia dos Crioulinhos, Lagoa de Parnaguá, Parnaguá county, 10°14'41.0"S, 44°38'50.0"W; MZUSP 104556, 3, 128.5–152.2 mm SL, Brazil, Maranhão, Itapecuru-Mirim, Rio Itapecuru, 3°31'39.0"S, 44°24'19.0"W.

Pimelodella steindachneri. — MCZ 7487, 1, xr, 150.4 mm SL, lectotype, Brazil, Pará, ("Pará and Marajo" [Belem, Rio do Para, Ilha de Marajo, Baia de Marajo], 1°27'S, 48°29'W; MCZ 7472, 1, xr, 135.5 mm SL, paralectotype, Brazil, Amazonas, Lago Cudajas (Lago Badajos), 3°24'S, 62°38'W; MCZ 7542, 1, xr, 165.4 mm SL, paralectotype, Brazil, Amazonas, ("Lago Manacapuru; Manacapouru" [Lago Grande de Manacapuru]), 3°6'S, 61°30'W; MCZ 7566, 2, xr, 96.8–123.6 mm SL, syntype, Brazil, Amazonas, Maues ("Mahues" [Rio Maues at Maues]), 3°22'S, 57°38'W; MCZ 7567, 1, xr, 106.4 mm SL, paralectotype, Brazil, Pará, Santarém, (Rio Amazonas at Santarém), 2°26'S, 54°41'W; MCZ 7588, 1, xr, 120.2 mm SL, paralectotype, Brazil, Piauí, Teresina, Rio Poti (tributary of Rio Parnaíba), 5°5'S, 42°49'W.

Pimelodella wessellii. — NMW 79188, 1, xr, 157.9 mm SL, holotype, Guyana, Essequibo river, 4°18'07"N, 58°28'57"W.

Pimelodella witmeri. — ANSP 69383, 1, xr, 137.5 mm SL, holotype, Brazil, Ceará, Oros, Rio Jaguaribe, 6°14'23"S, 38°54'43"W; ANSP 69384, 3, xr, 75.8–132.3 mm SL, paratype, Brazil, Ceará, Oros, Rio Jaguaribe, 6°14'23"S, 38°54'43"W.

Rhamdia altipinnis: NMW 45601, 1, xr, 61.2 mm SL, holotype, Guyana, Demerara, 5°47'57"N, 58°21'34"W.

***Pimelodella cruxenti* Fernandez-Yépez, 1950**

Pimelodella cruxenti Fernandez-Yépez, 1950: 5–7 [original description; "Rio Autana, Hoya del Orinoco, Venezuela"; holotype: AFY 48161 (probably lost)]. Burgess, 1989: 280 [taxonomic list]— Lasso *et al.*, 1997: 11 [type catalog]. — Bockmann & Guazzelli, 2003: 417–418 [taxonomic treatment]. — Ferraris, 2007: 190 [taxonomic treatment].

Rhamdella cruxenti. — Lasso *et al.*, 2004: 127 [taxonomic list, transference to *Rhamdella*].

Diagnosis

Pimelodella cruxenti can be diagnosed from all *Pimelodella* with exception of *P. modesta*, *P. montana*, *P. laticeps*, *P. pectinifera* and *P. yuncensis* by having an overall dark brown body. It differs from those by having a long adipose fin, two times or less in SL (*vs.* adipose fin roughly three times in SL in *P. modesta*, *P. montana*; four times in SL in *P. laticeps*, *P. pectinifera*; two and half to four times in SL in *P. yuncensis*). Furthermore, *P. cruxenti* can be diagnosed by maxillary barbel usually surpassing caudal-fin origin; posterior margin of pectoral-fin spine bearing 7–8 smooth retrorse dentations along basal three fourths; adipose fin very long, two times or less in SL; 47 total vertebrae; background body coloration brownish, with a dark brown midlateral stripe narrow, not well delimited, extending from a region posterior to opercle until caudal-fin insertion; and dorsal fin overall brown, except by a hyaline stripe near its base, which does not encompass the unbranched dorsal-ray and membrane between it and the first branched-ray.

Description

Measurements in Table 16. Body of moderated depth, depth at dorsal-fin insertion five to seven times in SL and compressed, more than seven times in SL (Fig. 43). Greatest body depth at dorsal-fin origin. Dorsal profile convex from snout to dorsal fin, slightly concave from dorsal to adipose fin, slightly convex along adipose fin, and concave at the caudal peduncle. Ventral profile of body slightly convex from snout to branquiostegal membrane, also convex between pectoral end pelvic fins, slightly convex from pelvic to anal fin, and concave from this point along the caudal peduncle.

Pseudotympanum large, oval, above posterior process of cleithrum and reaching 6th vertebrae. Posterior process of cleithrum triangular, short, its dorsal border straight. Anus and urogenital papilla adjacent. Urogenital papilla tubular, triangular, average sized. Anus at vertical through first third of adpressed pelvic fins; urogenital papilla reaching vertical through second fifth of adpressed pelvic fins.

Head deep, depth at supraoccipital-process base more than half of head length. Mouth sub terminal. Eye slightly elliptical, four to five times in head. Bony interorbital distance a fourth or a fifth smaller than eye diameter. Barbels thin, slightly depressed and elliptical in cross-section. Maxillary barbel usually surpassing caudal-fin insertion. Outer mental barbel, when stretched parallel to main body axis, finishing at vertical through half adpressed pelvic fin. Inner mental barbel, when stretched parallel to main body axis, finishing at pectoral-fin origin. Supraoccipital process roughly triangular, narrow, almost reaching anterior prenuchal

plate. Dorsal lamina of Weberian complex vertebrae reaching the supraoccipital process just at its anteriormost part. Branchiostegal rays 6 (2).

Dorsal fin triangular, distal margin convex, long (second branched dorsal-fin ray four times in SL), depressed tip finishing at vertical through last fourth of adpressed pelvic fin. Dorsal fin with I,6 (5) plus anteriormost spinelet. Distance between terminus of dorsal-fin base and adipose-fin origin very narrow, a tenth of dorsal-fin base. Anteriormost dorsal-fin pterygiophore inserted posterior to neural spine of vertebrae 4 (1) or 5 (1); posteriormost dorsal-fin pterygiophore located ahead of neural (or pseudoneural) spine of vertebrae 11 (1) or 12 (1). Unbranched dorsal-fin ray mostly ossified as a spine, rigid relatively short (a third shorter than the first dorsal-fin total length).

Pectoral-fin rays I,7 (1) or I,8 (1), pectoral fin triangular with convex distal border. First pectoral-fin ray roughly straight with proximal part rigid, forming a spine (Fig. 44), and short distal tip flexible and distinctly segmented. Comparatively short spine, seven to ten times in SL. Anterior margin of pectoral-fin spine with smooth serrae along its distal half. Posterior margin of pectoral-fin spine bearing 7–8 smooth retrorse dentations along basal three quarters. These dentations are small, extremely inclined and spaced one from the following.

Pelvic-fin rays i,5 (2), extended pelvic fin triangular with straight distal border. Anterior portion of pelvic-fin base at vertical through dorsal-fin terminus. Tip of adpressed pelvic fin at vertical through first third of adipose fin. First unbranched and flexible ray distinctly shorter than second and third rays, which are roughly the same size; remaining rays progressively shorter.

Anal-fin rays v,7 (1) or iv,8 (1), distal border of extended anal fin convex. Two anteriormost anal-fin rays vestigial, unsegmented, embedded in thick skin fold. Anal fin origin at verticals through second fifth of adipose-fin base; anal-fin adpressed terminus slightly anterior to vertical through adipose-fin terminus. Tip of anteriormost anal-fin pterygiophore inserted posterior to hemal spine of vertebrae 23 (1) or 24 (1). Tip of posteriormost anal-fin pterygiophore inserted ahead of hemal spine of vertebrae 31 (2).

Adipose fin very long, two times or less in SL, forming ascending elevated curve in lateral profile, with deepest point at half. Adipose fin emerging gradually, its posterior limit as a rounded, free lobe. Adipose-fin origin at vertical through vertebral centrum 17 (2); adipose-fin terminus at vertical through vertebral centra 35 (1) or 46 (1).

Caudal fin deeply forked, ventral lobe longer. Caudal peduncle length posterior to adipose-fin half its depth. Dorsal lobe with 7 (2) branched, 1 (2) unbranched principal, and 13

(1) procurent fin-rays. Ventral lobe with 8 (2), 1 (2) unbranched principal, and 17 (1) procurent fin-rays. Hypural 5 completely free, not fused to hypural 3+4. Median caudal-fin rays not articulated directly to caudal plate. Seven* (2) rays articulated to dorsal caudal-fin plate (5 on hypurals 3+4 and 2 on hypural 5) and 8 (2) rays articulated to ventral caudal-fin plate (6 on hypurals 1+2 and 2 on parhypural).

Total vertebrae 47 (2). Ribs 9 (1) or 10 (1).

One single opening of epipheseal branch of lateral sensory canal on head, on S6 pore, after a small tube that connects both contralateral S6 branches.

Coloration in alcohol

Background body coloration brownish. Ventral region of head and body lighter. Dark brown midlateral stripe (Fig. 45) narrow, not well delimited, extending from a region posterior to opercle until caudal-fin insertion. Dorsal fin overall brown, except by a hyaline stripe near its base, which does not encompass the unbranched dorsal-ray and membrane between it and the first branched-ray, which are overall dark.

Geographic distribution

Pimelodella cruxenti was described from “Rio Autana”, in Orinoco basin, Venezuela. It is known from area 308 (Orinoco Guiana Shield), in Rio Autana and Rio Sipapo, from Orinoco basin in Venezuela.

Comments

Pimelodella cruxenti was described based in one holotype and three paratypes. The holotype has 110.6 mm SL, under AFY 48161, and the paratypes 85.8, 96.9 and 102.8 mm SL, under AFY 48232, posteriorly transferred to MHNLS 1766. Whereabouts of holotype are unknown. Lasso *et al.* (1997) comment MHNLS 1766 has only two specimens (85.8 and 96.8 mm SL), and the whereabouts of 102.8 mm SL specimen are unknown. However, Lasso-Alcalá (*pers. comm.*) is producing a new type catalog of MHNLS, and found out MHNLS 1766 was catalogued in August 23, 1991, and the former curator, C. Lasso, separated two specimens from this lot in a new number (MHNLS 8878), which the identified as *Rhamdia* sp (Lasso-Alcalá, *pers. comm.*).

In fact, those two specimens of MHNLS 8878 are from *Rhamdia* (probably *R. mulleri*), and distinct from the ones of MHNLS 1766, which are undoubtedly *Pimelodella*. The two *Rhamdia mulleri* have 184.82 and 85.95 mm SL, in a manner the larger one never belonged to the type-series, however the size of the smaller one is congruent with one of the original paratypes (85.8 mm SL), and I have no other information that can securely connect

this specimen to the type-series other than it was found by C. Lasso in the same lot as the other paratypes. Among the specimens of 1766, they have 95.76 and 84.3 mm SL, and are also somewhat similar with two paratype's SL from the original description (96.9 and 85.8 mm SL, respectively). So, probably the MHNLS 1766 are in fact part of Fernandez-Yépez original assigned type-series.

I could observe a comparative *Pimelodella* material from Autana congruent with *P. cruxenti* description (ANSP 160647 and 160673, figure 46), and of *Rhamdia mulleri* identified as those by Silfvergrip (1996) (MZUSP 7355 and 23034), and they are notably different, having *R. mulleri* the posterior fontanel closed and, at least among the material I observed, a blotched color pattern (but Silfvergrip commented some material can have a midlateral stripe). Therefore, in Rio Autana there are both a *Pimelodella* and a *Rhamdia* species that, despite superficial similarities, pertain to those different genera and, in sum, I indicate *P. cruxenti* is a valid species.

Since the whereabouts of AFY 48161, holotype of *P. cruxenti*, are unknown, I designate MHNLS 1766 95.76 mm SL as the lectotype and MHNLS 1766 84.3 mm SL the paralectotype of *P. cruxenti*.

Material examined

Pimelodella cruxenti. — MHNLS 1766, 1, lectotype, 95.8 mm SL, Venezuela, Rio Autana, Hoya del Orinoco; MHNLS 1766, 1, paralectotype, 84.3 mm SL, Venezuela, Rio Autana, Hoya del Orinoco; ANSP 160647, 1, 75.2 mm SL, Venezuela, Rio Sipapo, backwater channel behind sandbar 6-7 km above Pendare, 4°51'0.0"N, 67°43'0.0"W; ANSP 160673, 2, xr, 88.1–127.7 mm SL, Venezuela, Amazonas, Small caño ca 5 km below Raudal Peresa, Rio Autana, 4°46'0.0"N, 67°19'0.0"W.

***Pimelodella elongata* (Günther, 1860)**

Pimelodus elongatus Günther, 1860: 238, pl. X, fig. B [original description; “Fresh waters of Esmeraldas”, Rio Esmeralda basin, Ecuador; syntypes: BMNH 1860.6.16.182-185 (4), 1860.6.16.186-189 (4), BMNH 1860.6.16.191 and 194 (2)]. — Günther, 1864: 118 [type catalog, taxonomic treatment].

Pimelodella elongatus. — Eigenmann & Eigenmann, 1888: 133 [taxonomic treatment]. — Eigenmann & Eigenmann, 1890: 149, 155 [key to *Pimelodella* species; taxonomic revision]. — Eigenmann & Eigenmann, 1891: 29 [taxonomic treatment].

Pimelodella elongata. — Eigenmann, 1910: 389 [taxonomic treatment]. — Eigenmann, 1917: 254 [taxonomic revision]. — Eigenmann, 1921b: 518 [taxonomic list]. — Eigenmann,

1922a: 42 [taxonomic treatment]. — Eigenmann, 1922c: 209 [taxonomic treatment]. — Gosline, 1945: 46 [taxonomic treatment]. — Chirichigno, 1963: 28 [taxonomic list]. — Ortega & Vari, 1986: 14 [taxonomic list]. — Burgess, 1989: 280 [taxonomic treatment]. — Bockmann & Guazzelli, 2003: 418 [taxonomic treatment]. — Ferraris, 2007: 189 [taxonomic treatment].

Diagnosis

Pimelodella elongata differs from all *Pimelodella* species with exception of *P. boliviana*, *P. boschmai*, *P. brasiliensis*, *P. coquetanesis*, *P. enochi*, *P. eutaenia*, *P. geryi*, *P. grisea*, *P. hasemani*, *P. howesi*, *P. ignobilis*, *P. megalops*, *P. modesta*, *P. montana*, *P. robinsoni* and *P. tapatapae* by having the basal part of dorsal fin hyaline, and distal part darkly pigmented. It differs from *P. boliviana* and *P. coquetanesis* by having 41–43 total vertebrae (vs. 44 total vertebrae in *P. boliviana*; 40 total vertebrae in *P. coquetaensis*). It differs from *P. montana*, *P. robinsoni* and *P. yuncensis* by having the supraoccipital process reaching the anterior prenuchal plate (vs. supraoccipital process not reaching the anterior prenuchal plate in *P. montana*, *P. robinsoni* and *P. yuncensis*). It differs from *P. boschmai*, *P. brasiliensis*, *P. enochi*, *P. eutaenia*, *P. geryi*, *P. hasemani*, *P. howesi*, *P. ignobilis*, *P. megalops* and *P. modesta* by having the maxillary barbel reaching between half adressed pectoral fin to first fourth of adressed pelvic fin (vs. maxillary barbell at least surpassing the adressed pelvic fin terminus in *P. boschmai*, *P. brasiliensis*, *P. enochi*, *P. eutaenia*, *P. geryi*, *P. hasemani*, *P. howesi*, *P. ignobilis*, *P. megalops* and *P. modesta*). It differs from *P. grisea* by having the dorsal lamina of Weberian complex vertebrae reaching the supraoccipital process just anteriormost (vs. dorsal lamina of Weberian complex vertebrae reaching the supraoccipital process along its entire extension in *P. grisea*).

Furthermore, *P. elongata* can be diagnosed by the dorsal profile straight from snout to dorsal fin; maxillary barbel usually reaching between middle and adressed terminus of pectoral fin; posterior margin of pectoral-fin spine with 8–12 retrorse dentations along its basal two thirds, these dentations being long, curved; adipose fin moderated length, three to three and half times in SL; 41–43 total vertebrae; medium brown midlateral stripe, wide, not well delimited, extending from snout to caudal-fin insertion.

Description

Measurements in Table 17. Body depressed, depth at dorsal-fin origin six to seven and half times in standard length, and compressed, body width at dorsal-fin origin seven and half to nine times in SL (Fig. 47). Dorsal profile straight from snout to dorsal fin, concave from

dorsal to adipose fin, slightly convex along adipose fin, and concave along the caudal peduncle. Ventral profile of body slightly convex from snout to branchiostegal membrane, concave between pectoral and pelvic fins, slightly concave from pelvic to anal fin, and also concave from there along the caudal peduncle.

Pseudotympanum large, oval, above posterior process of cleithrum and reaching the straight line of 6th (3) vertebrae. Posterior process of cleithrum triangular, its dorsal border straight. Axillary pore small, as a slit ventral to posterior process of cleithrum, near the base of pectoral fin. Anus and urogenital papilla adjacent. Urogenital papilla tubular, triangular, short. Anus between verticals through first third and half adpressed pelvic fin; urogenital papilla between verticals through terminus of adpressed dorsal fin and a point slightly anterior to that.

Head depressed to average deep, depth at supraoccipital-process base two and half to slightly more than two times in head length. Mouth sub terminal. Eye slightly elliptical, four to five times in head. Bony interorbital distance usually smaller than eye diameter. Barbel thin, depressed and elliptical in cross-section. Maxillary barbel usually reaching between middle and adpressed terminus of pectoral fin, but some specimens might have it slightly longer, reaching at best the first fourth of adpressed pelvic fin. Outer mental barbel, when stretched parallel to main body axis, finishing slightly anterior to half of pectoral-fins base. Inner mental barbels, when stretched parallel to main body axis, finishing between branchiostegal membrane ventral limit and origin of pectoral fin. Supraoccipital process roughly rectangular, but with a narrow constriction at its base, and tapered at its distal tip, when reaches the nuchal plate. Dorsal lamina of Weberian complex vertebrae of medium height, reaching the supraoccipital process just at its anteriormost part. Branchiostegal rays 6 (8)–7* (2)

Dorsal fin triangular, distal margin convex, short (second branched dorsal-fin five or more times in SL) reaching the vertical through distal third of adpressed pelvic fins. Dorsal fin with I,6 (10) plus anteriormost spinelet. Distance between terminus of dorsal-fin base and adipose-fin origin slightly smaller than dorsal-fin base. Anteriormost dorsal-fin pterygiophore inserted posterior to neural spine of vertebrae 4 (10); posteriormost dorsal-fin pterygiophore located ahead of neural (or pseudoneural) spine of vertebrae 11 (10). Unbranched dorsal-fin ray mostly ossified as a spine, rigid part relatively short (approximately a third shorter than first dorsal-fin total length).

Pectoral-fin rays I,8* (9) or I,9 (1), pectoral fin triangular with concave distal border. First pectoral-fin ray roughly straight, with proximal part rigid (Fig. 48), forming a short spine

(six to seven times in SL), and short distal tip flexible and distinctly segmented. Anterior margin pectoral-fin spine with small straight dentations along its basal two thirds and smooth serrae along its distal third. Posterior margin of pectoral-fin spine with 8–12 retrorse dentations along its basal two thirds, plus 2–3 unossified distalmost dentations. Those dentations are long, curved.

Pelvic-fin rays i,5 (10), extended pelvic fin triangular with straight distal border. Pelvic-fin origin slightly posterior to vertical through dorsal-fin terminus. Tip of adpressed pelvic fin through vertical of first fifth of adipose-fin base. First unbranched and flexible ray distinctly shorter than second and third rays, which are subequal; remaining rays progressively shorter.

Anal-fin rays v,7 (1); vi,7 (1); v,8* (4), v,9 (3) or vi,9 (1), distal border of extended anal fin convex. Two or three anteriormost anal-fin rays vestigial, unsegmented, embedded in thick skin fold. Anal-fin origin at vertical through first third of adipose-fin base. Anal-fin adpressed terminus slightly anterior to vertical through adipose-fin terminus. Tip of anteriormost anal-fin pterygiophore inserted posterior to hemal spine of vertebrae 20 (1), 21 (2) or 22* (7). Tip of posteriormost anal-fin pterygiophore inserted ahead of hemal spine of vertebrae 28 (1), 29* (5) or 30 (4).

Adipose fin three to three and half times in SL, forming ascending elevated curve in lateral profile, with deepest point approximately at last third. Adipose fin emerging gradually, its posterior limit as a rounded, free lobe. Adipose-fin origin at vertical through vertebral centra 20 (3) to 23 (1) (lectotype 22); adipose-fin terminus at vertical through vertebral centra 36 (2) to 38 (2) (lectotype 37).

Caudal fin deeply forked, lobes subequal to dorsal lobe slightly longer. Caudal peduncle medium, its length posterior to adipose-fin shorter or just slightly longer than its depth. Dorsal lobe with 7 (9) branched, 1 (9) unbranched principal and 8 (1)–18 (1) (lectotype 18) procurrent fin-rays. Ventral lobe with 8 (9), 1 (9) unbranched principal branched and 16* (1)–20 (1) procurrent fin-rays. Hypural 5 completely free, not fused to hypural 3+4 (8). Median caudal-fin rays not directly articulated to caudal plate. Seven (9) rays articulated to dorsal caudal-fin plate (5 on hypurals 3+4 and 2 on hypural 5) and 7* (4) or 8 (5) rays articulated to ventral caudal-fin plate (5 or 6 on hypurals 1+2 and 2 on parahypural).

Total vertebrae 41 (2)–43* (6). Ribs 6 (1)–9 (5) (lectotype 7).

Epypheseal branch of cephalic laterosensory canal (S6) connecting the contralateral canals at midline, emerging as a single pore, after a small canal towards posterior region of head.

Coloration in alcohol

Background body coloration yellowish. Ventral region of head and body lighter. Medium brown midlateral stripe, wide (Fig. 49), not well delimited, extending from snout to caudal-fin insertion. Dorsal medium brown pigmented, except by a lighter stripe near the base.

Geographic distribution

Pimelodella elongata was described from Rio Esmeraldas, in Pacific slope of Ecuador. Its known from region 301 (North Andean Pacific Slopes), in Ecuador and northern Peru.

Comments

Despite BMNH 1860.6.16.182-185 (4), 1860.6.16.186-189 (4), BMNH 1860.6.16.191 and 194 being all stated as syntypes, Günther (1890) published a table with one specimen only, with 6 inches, 8 lines of total length, approximately 169.3 mm. From the syntypes, only BMNH 1860.6.16.182 has a length similar to that (165.7 mm TL). Therefore, I hereby designate BMNH 1860.6.16.182 as the lectotype of *P. elongata* and all other syntypes as paralectotypes.

Material examined

Pimelodella elongata. — BMNH 1860.6.16.182, 1, xr, 136.8 mm SL, lectotype, Ecuador, Esmeraldas, "Freshwaters of Esmeraldas", 0°56'20"N, 79°38'52"W; BMNH 1860.6.16.183–185, 3, xr, 54.6–92.0 mm SL, syntypes, Ecuador, Esmeraldas, "Freshwaters of Esmeraldas", 0°56'20"N, 79°38'52"W; BMNH 1860.6.16.186-189, 4, xr, 71.3–96.1 mm SL, syntypes, Ecuador, Esmeraldas, "Freshwaters of Esmeraldas", 0°56'20"N, 79°38'52"W; BMNH 1860.6.16.191 and 194, 2, xr, 84.5–93.8 mm SL, syntypes, Ecuador, Esmeraldas, "Freshwaters of Esmeraldas", 0°56'20"N, 79°38'52"W; USNM 177241, 4, 59.9–92 mm SL, Ecuador, Prov. Guayas, Rio Chimbo, Near Bucay, W. Foot Andes, 2°07'12.0"S, 79°41'24.1"W.

***Pimelodella enochi* Fowler, 1941a**

Pimelodella enochi Fowler, 1941a: 130–132, figs. 12–15 [original description; "Açude Piloos, Parahyba, Brazil"]; holotype: ANSP 69378]. — Gosline, 1945: 46 [taxonomic treatment]. — Fowler, 1951: 539, fig 533 [taxonomic treatment]. — Böhlke, 1984: 141 [type catalog]. — Burgess, 1989: 280 [taxonomic treatment]. — Bockmann & Guazzelli, 2003: 418 [taxonomic treatment]. — Rosa *et al.*, 2003: 177 [taxonomic list]. — Ferraris, 2007: 191 [taxonomic treatment].

Rhamdella papariae Fowler, 1941a: 135–136, figs. 27–30 [original description; “Lago Papary, Rio Grande do Norte, Brazil”; holotype: ANSP 69387]. — Gosline, 1945: 35 [taxonomic treatment]. — Fowler, 1951: 566–567, fig 573 [taxonomic treatment]. — Böhlke, 1984: 142 [type catalog]. — Burgess, 1989: 278 [taxonomic treatment]. — Bockmann & Guazzelli, 2003: 422 [taxonomic treatment]. — Rosa *et al.*, 2003: 177 [taxonomic list]. — Ferraris, 2007: 195 [taxonomic treatment].

Pimelodella papariae. — Bockmann & Miquelarena, 2008: 45–46 [taxonomic revision of *Rhamdella*, transfer to *Pimelodella*]

Diagnosis

Pimelodella enochi differs from all *Pimelodella* species with exception of *P. boliviana*, *P. boschmai*, *P. brasiliensis*, *P. coquetanesis*, *P. elongata*, *P. eutaenia*, *P. geryi*, *P. grisea*, *P. hasemani*, *P. howesi*, *P. ignobilis*, *P. megalops*, *P. modesta*, *P. montana*, *P. robinsoni* and *P. tapatapae* by having the basal part of dorsal fin hyaline, and distal part darkly pigmented. It differs from *P. montana*, *P. robinsoni* and *P. yuncensis* by having the supraoccipital process reaching the anterior prenuchal plate (*vs.* supraoccipital process not reaching the anterior prenuchal plate in *P. montana*, *P. robinsoni* and *P. yuncensis*). It differs from *P. boliviana*, *P. brasiliensis*, *P. eutaenia*, *P. geryi*, *P. hasemani* and *P. howesi* by having 40–41 total vertebrae (*vs.* 42 or more total vertebrae *P. boliviana*, *P. brasiliensis*, *P. eutaenia*, *P. geryi*, *P. hasemani* and *P. howesi*). It differs from *P. boschmai*, *P. elongata* and *P. megalops* by having the epiphyseal branch of laterosensory canal on head emerging as two separate pores, near each other (*vs.* contralateral canals connecting in midline, proceeding posteriorly as a single canal and emerging in a single pore in *P. boschmai* and *P. elongata*; two pores emerging far a part from each other in *P. megalops*). It differs from *P. grisea* and *P. ignobilis* by having the supraoccipital process rectangular (*vs.* triangular in *P. grisea* and *P. ignobilis*). It differs from *P. coquetaensis* and *P. modesta* by having the pectoral-fin spine roughly straight, with small, smooth dentations on posterior margin (*vs.* pectoral-fin spine curved, with triangular, inclined dentations on posterior margin in *P. coquetaensis*; pectoral-fin spine curved, with moderate dentations on posterior margin in *P. modesta*).

Furthermore, *P. enochi* can be diagnosed by maxillary barbel reaching between half and terminus of anal-fin base; posterior margin of pectoral-fin spine bearing 8–12 retrorse dentations along its basal half to two thirds, those dentations being shallow, smooth, relatively far from each other; adipose fin moderated to long, three times in SL; 40–41 total vertebrae; dark brown midlateral stripe of moderated width, not well-delimited, from snout until caudal-fin insertion.

Description

Measurements in Table 18. Body depressed, depth at dorsal-fin origin six to seven and half times in standard length, and compressed, roughly seven and half times in SL (Fig. 50). Dorsal profile convex from snout to supraoccipital process, straight from this point to dorsal fin origin, slightly concave from dorsal fin to adipose, and also slightly concave along adipose and caudal peduncle. Ventral profile of body slightly convex from snout to branquiostegal membrane, convex between pectoral and pelvic fins, and straight from pelvic along caudal peduncle.

Pseudotympanum large, oval, dorsal to posterior process of cleithrum and reaching 6th (2) or 7^{th*} (1) vertebrae. Posterior process of cleithrum triangular, its dorsal border straight or slightly concave. Axillary pore small, as a slit ventral to posterior process of cleithrum, near the base of pectoral fin. Anus and urogenital papilla adjacent. Urogenital papilla tubular, triangular, short. Anus between verticals through first third and half adpressed pelvic fin; urogenital papilla between verticals through last third and almost end of adpressed pelvic fin.

Head depressed, depth at supraoccipital process two and half times in head length. Mouth sub terminal. Eyes slightly elliptical, four to five and half times in head. Bony interorbital distance narrow, approximately two-thirds of eye diameter. Barbels thin, slightly depressed and elliptical in cross-section. Maxillary barbel reaching between half and terminus of anal-fin base. Outer mental barbel, when stretched parallel to main body axis, finishing between first third and half of adpressed pectoral fin. Inner mental barbel, when stretched parallel to main body axis, finishing between posterior limit of branchiostegal membrane and pectoral-fin origin. Supraoccipital process roughly rectangular, moderate width, tapered at its distal point. Dorsal lamina of Weberian complex vertebrae reaching the supraoccipital process just at its anteriormost part, or along part of the anteriormost region, but never along its entire extension. Branchiostegal rays 6 (3).

Dorsal fin triangular, distal margin convex, relatively short (second branched dorsal-fin ray five times or more in SL), depressed tip reaching between the verticals through half and last fourth of adpressed pelvic fin. Dorsal fin with I,6 (3) plus anteriormost spinelet. Distance between terminus of dorsal-fin base and adipose-fin origin roughly two thirds of dorsal-fin base. Anteriormost dorsal-fin pterygiophore inserted posterior to neural spine of vertebrae 4 (3); posteriormost dorsal-fin pterygiophore located ahead of neural (or pseudoneural) spine of vertebrae 11* (2) or 12 (1). Unbranched dorsal-fin ray mostly ossified as a spine, rigid part relatively short (approximately a third shorter than dorsal-fin first ray total length), bearing smooth serrae at its anterior margin distal third.

Pectoral-fin rays I,7* (1)– I,8 (2), pectoral fin triangular with concave distal border. First pectoral-fin ray almost straight, with proximal part rigid (Fig. 51), forming a spine of moderated length (more than five times in SL) and short distal tip flexible and distinctly segmented. Anterior margin of pectoral-fin spine with small straight dentations along its basal half and serrae along its distal half. Posterior margin of pectoral-fin spine bearing 8–12 retrorse dentations along its basal half to two thirds. Those dentations are shallow, smooth, relatively far from each other. In the smaller specimens (less than 50 mm SL) they are relatively bigger.

Pelvic-fin rays i,5 (3), extended pelvic fin triangular with convex distal border. Pelvic-fin origin between verticals through dorsal-fin terminus and half dorsal-fin adpressed. Tip of adpressed pelvic fin between verticals through dorsal-fin adpressed terminus and first fourth of adipose-fin base. First unbranched and flexible ray distinctly shorter than second and third rays, which are subequal; remaining rays progressively shorter.

Anal-fin rays v,6 (1); iv, 7 (1) or iv,8* (1), distal border of extended anal fin convex. Two or three anteriormost anal-fin rays vestigial, unsegmented, embedded in thick skin fold. Anal-fin origin between verticals through first fourth and second fifth of adipose-fin base. Anal-fin adpressed terminus slightly anterior to adipose fin terminus. Tip of anteriormost anal-fin pterygiophore inserted posterior to hemal spine of vertebrae 21 (1) 22* (1) or 23 (1). Tip of posteriormost anal-fin pterygiophore inserted ahead of hemal spine of vertebrae 27 (1) or 28* (2).

Adipose fin three times in SL, forming ascending elevated curve in lateral profile, with deepest point approximately at midlength. Adipose fin emerging gradually, its posterior limit as a rounded, free lobe. Adipose-fin origin at vertical through vertebral centra 18* (2) or 20 (1); adipose-fin terminus at vertical through vertebral centra 34* (1) or 35 (2).

Caudal fin deeply forked, lobes subequal. Caudal peduncle long, its length posterior to adipose fin slightly longer than its depth. Dorsal lobe with 7 (3) branched, 1 (3) unbranched principal and 8 (1) –15* (2) procurrent fin-rays. Ventral lobe with 8 (3) branched, 1 (3) unbranched principal and 10 (1) –15* (1) procurrent fin-rays. Hypural 5 separated from hypurals 3+4. Median caudal-fin rays not directly articulated to caudal plate. Seven (3) rays articulated to dorsal caudal-fin plate (5 on hypurals 3+4 and 2 on hypural 5) and 8 (3) rays articulated to ventral caudal-fin plate (6 on hypurals 1+2 and 2 on parahypural).

Total vertebrae 40* (1)–41 (2). Ribs 9 (3).

Epiphyseal branch of laterosensory canal (S6) with contralateral canals emerging as two separated pores near to each other.

Coloration in alcohol

Background body coloration yellowish. Ventral region of head and body lighter. Dark brown midlateral stripe of moderated width (Fig. 52), not well-delimited, from snout until caudal-fin insertion. Dorsal region of head along posterior fontanel with dark brown cephalic pigment. Basal half of dorsal fin hyaline, distal half dusky.

Geographic distribution

Pimelodella enochi was described from “Açude Piloes”, Rio Paraíba basin, Paraíba State, and its junior-synonym, *P. papariae*, was described from “Lago Papary” (Lagoa Papari), Rio Grande do Norte State, both in drainages from Northeastern Brazil. It is known, therefore, from region 326 (Northeastern Caatinga and Coastal Drainages), in Paraíba and Rio Grande do Norte States, Brazil.

Comments

Upon the examination of *P. enochi* and *P. papariae* type materials, I can suggest the synonym of both species. *Pimelodella enochi* seems to be correspondent to smaller, possibly juvenile, specimens of *P. papariae*. Because of this, *P. papariae* has comparatively slightly smaller eyes, shorter dorsal fin, slightly shorter maxillary barbel and smoother pectoral-fin spine dentations. The Table 18 has the comparison between the morphometric data of both species. The Figures 53 and 54 are related to the holotype of *P. papariae* and its pectoral-fin spine, respectively, which can serve as a approximation of an adult of *P. enochi*.

Furthermore, a personal communication of prof. Telton Ramos, who collected intensively in Rio Trairi, the river that forms Lago Papari, said they did not collect *Hypostomus papariae*, *Pimelodella papariae* or *Pseudancistrus papariae*, the three species described by Fowler (1941a) for this locality. However, in a nearby basin (Rio Piranhas) his team collected both *Pimelodella* sp. and *Pseudancistrus* sp., which is the same basin that forms Açude Pilões, the type-locality of *P. enochi*. Therefore, this indicates that maybe the locality of “Lago Papari” is inaccurate, and points toward the synonym of *P. papariae* to *P. enochi*.

Material examined

Pimelodella enochi. — ANSP 69378, 1, xr, 44.9 mm SL, holotype, Brazil, Paraíba, Açude Piloes, 6°41'19"S, 38°31'18"W; ANSP 69379, 1, xr, 45.3 mm SL, paratype, Brazil, Paraíba, Açude Piloes, 6°41'19"S, 38°31'18"W.

Pimelodella papariae. — ANSP 69387, 1, xr, 107.6 mm SL, holotype, Brazil, Rio Grande do Norte, Lago Papary, 6°03'18"S, 35°12'10"W.

***Pimelodella eutaenia* Regan, 1913**

Pimelodella eutaenia Regan, 1913: 466–476 [original description; “Rio Condoto and the Rio Sipi”, Colombian Pacific drainages; syntypes (supposedly five, but only four found): BMNH 1913.10.1.37–40]. — Eigenmann, 1917: 254–255, pl. XXXIV, fig. 7, pl. XXXV, figs. 35–36 [taxonomic revision]. — Eigenmann, 1922a: 43–44 [taxonomic treatment]. — Gosline, 1945: 46 [taxonomic treatment]. — Burgess, 1989: 280 [taxonomic treatment]. — Bockmann & Guazzelli, 2003: 418 [taxonomic treatment]. — Leiva, 2005: 51–52, fig. 14i [taxonomic review, redescription]. — Mojica *et al.*, 2004: 743 [taxonomic list]. — Maldonado-Ocampo *et al.*, 2006: 165 [taxonomic treatment]. — Ferraris, 2007: 191 [taxonomic treatment]. — Maldonado-Ocampo *et al.*, 2008: 202 [taxonomic list].

Pimelodella sp. 1 Leiva, 2005: 51–52, fig. 14j [taxonomic review].

Pimelodella floridablancaensis Ardila Rodriguez 2017: 2–8 [original description; “quebrada Aranzoque, en la baja del Puente del Limoncito, parte alta del río Lebrija”, Magdalena River basin, Floridablanca municipality, Colombia; holotype: CAR 800].

Diagnosis

Pimelodella eutaenia differs from all *Pimelodella* species but *P. avanhandavae*, *P. chagresi*, *P. gracilis*, *P. griffini*, *P. montana*, *P. odynea*, *P. peruana*, *P. reyesi* and *P. roccae* by having a dorsolateral brown stripe along body. It differs from *P. avanhandavae*, *P. chagresi*, *P. gracilis*, *P. griffini*, *P. montana*, *P. odynea*, *P. reyesi* and *P. roccae* by this stripe extending from supraoccipital process until adipose-fin origin or, at best, first third of adipose-fin base (*vs.* reaching posterior to first third of adipose-fin base in *P. avanhandavae*, *P. chagresi*, *P. gracilis*, *P. griffini*, *P. montana*, *P. odynea*, *P. reyesi* and *P. roccae*). It differs from *P. peruana* by having distal two thirds of dorsal-fin brown, and caudal fin lobes hyaline (*vs.* dorsal-fin hyaline and ventral lobe of caudal fin brown). Furthermore, *P. eutaenia* can be diagnosed by maxillary barbel reaching between verticals through half and adpressed terminus of anal fin; dorsal lamina of Weber complex vertebrae high, reaching the supraoccipital process along all its extension; dorsal-fin spine three fourths of first dorsal-fin ray total length; posterior margin of pectoral-fin spine bearing 7–9 retrorse dentations along its basal half to two-thirds; adipose fin short to moderated length, three to four times in SL; total vertebrae 42–44; dark brown midlateral stripe of moderated length to wide, from snout to caudal-fin insertion; paired diffuse dark brown stripes along supraoccipital process until first third of adipose-fin base, more diffuse posteriorly.

Description

Measurements in Table 19. Body of moderated height, depth at dorsal-fin insertion five times or slightly more in standard length, and moderated compressed, body width at dorsal-fin insertion six to seven times in SL (Fig. 55). Dorsal profile straight from snout to dorsal fin, concave from dorsal to adipose fin, slightly convex along adipose fin, and concave along the caudal peduncle. Ventral profile of body slightly convex from snout to branquiostegal membrane, convex between pectoral end pelvic fins, slightly concave from pelvic to anal fin, and also concave from there along the caudal peduncle.

Pseudotympanum large, oval, dorsal to posterior process of cleithrum and reaching the straight line of 6th (2) or 7th (1) vertebrae. Posterior process of cleithrum triangular, its dorsal border slightly concave. Anus and urogenital papilla adjacent. Urogenital papilla tubular, triangular, short. Anus between verticals through first third and half adpressed pelvic fin; urogenital papilla between verticals through second third and last fourth of adpressed pelvic fin.

Head of moderated depth, depth at supraoccipital-process base less than half head length. Mouth sub terminal. Eye slightly elliptical, four and half to five and half times in head length. Bony interorbital distance slightly more than half eye diameter. Barbels thin, slightly depressed and elliptical in cross-section. Maxillary barbel reaching between verticals through half and adpressed terminus of anal fin. Outer mental barbel, when stretched parallel to main body axis, reaching between verticals through half and adpressed pectoral-fin terminus. Inner mental barbel, when stretched parallel to main body axis, finishing between ventral posterior limit of branchiostegal membrane and pectoral-fin terminus. Supraoccipital process slightly triangular, narrow, tapered at its distal point. Dorsal lamina of Weber complex vertebrae high, reaching the supraoccipital process along all its extension. Branchiostegal rays 6 (4).

Dorsal fin triangular, distal margin concave, moderated length (second branched dorsal-fin ray four to six times in SL), depressed tip finishing between verticals through second third and last fourth of adpressed pelvic fin. Dorsal fin with I,6 (15) plus anteriormost spinelet. Distance between terminus of dorsal-fin base and adipose-fin origin slightly smaller than dorsal-fin base. Anteriormost dorsal-fin pterygiophore inserted posterior to neural spine of vertebrae 4 (15); posteriormost dorsal-fin pterygiophore located ahead of neural (or pseudoneural) spine of vertebrae 11* (8) or 12 (7). Unbranched dorsal-fin ray mostly ossified as a spine, rigid part relatively long (less than one-fourth shorter than first dorsal-fin ray total length), distal third of anterior margin bearing smooth serrae.

Pectoral-fin rays I,7 (3)– I,9* (3), usually I,8 (5), pectoral fin triangular with concave distal border. First pectoral-fin ray roughly straight (Fig. 56), with proximal part rigid, forming a spine of medium length (five and half to eight times in SL), and short distal tip flexible and distinctly segmented. Anterior margin of pectoral-fin spine with small, straight dentations along its basal half and serrae along its distal half. Posterior margin of pectoral-fin spine bearing 7–9 retrorse dentations along its basal half to two-thirds. In smaller specimens the dentations are comparatively bigger, with broad base and retrorse, occupying half the spine. In bigger specimens the dentations are comparatively smaller, triangular and not so retrorse, occupying up to two thirds of spine. Also 2–3 unossified distal dentations.

Pelvic-fin rays i,5 (11), extended pelvic fin triangular with straight distal border. Pelvic-fin origin at vertical through dorsal-fin terminus. Pelvic fin adpressed terminus at vertical through adipose-fin origin. First unbranched and flexible ray distinctly shorter than second and third rays, which are roughly the same size; remaining rays progressively shorter.

Anal-fin rays v,7 (4); iv,8 (1); v,8 (5); vi,8 (2) or v,9* (2); distal border of extended anal fin convex. Two or three anteriormost anal-fin rays vestigial, unsegmented, embedded in thick skin fold. Anal-fin origin between verticals through end of first fifth or fourth of adipose-fin base; anal-fin adpressed terminus slightly anterior or at vertical through adipose-fin terminus. Tip of anteriormost anal-fin pterygiophore inserted posterior to hemal spine of vertebrae 22* (6) or 23 (8), rarely 24 (1). Tip of posteriormost anal-fin pterygiophore inserted ahead of hemal spine of vertebrae 29 (1), 30* (10) or 31 (4).

Adipose fin three to four times in SL, forming ascending elevated curve in lateral profile, with deepest point approximately at last third. Adipose fin emerging gradually, its posterior limit as a rounded, free lobe. Adipose-fin origin at vertical through vertebral centra 21 (1)– 23* (5); adipose-fin terminus at vertical through vertebral centra 37 (1)– 39 (3) (lectotype 38).

Caudal fin deeply forked, ventral lobe almost always broken in examined specimens. Caudal peduncle length posterior to adipose fin slightly longer than its depth. Dorsal lobe with 7* (11), rarely 6 (1) or 8 (1) branched, 1 unbranched principal and 12 (1)–18* (2) procurrent fin-rays. Ventral lobe with 8 (13) branched, 1 unbranched principal and 15 (1)–22 (1) (lectotype 21) procurrent fin-rays. Hypural 5 completely free, not fused to hypural 3+4. Median caudal-fin rays not articulated directly to caudal plate. Seven* (12), rarely 6 (1) rays articulated to dorsal caudal-fin plate (4 or 5 on hypurals 3+4 and 2 on hypural 5) and 7* (4) or 8 (9) rays articulated to ventral caudal-fin plate (5 or 6 on hypurals 1+2 and 2 on parahypural).

Total vertebrae 42* (1)–44 (5). Ribs 9* (10)–10 (5).

S6 canals usually connecting in head midline, and opening in a single pore right after the connection of both canals. One specimen with two pores close to each other.

Coloration in alcohol

Background body coloration yellowish. Ventral region of head and body lighter. Dark brown midlateral stripe of moderated length to wide, from snout to caudal-fin insertion (Fig. 57). Region along posterior fontanel with dark brown cephalic pigment. Paired diffuse dark brown stripes along supraoccipital process until first third of adipose-fin base, more diffuse posteriorly. Dorsal fin dusky, except by a hyaline stripe near the fin base.

Geographic distribution

Pimelodella eutaenia was described from Rio Condoto and Rio Sipi, from San Juan River basin in Colombia. *Pimelodella floridablancaensis*, its junior-synonym, was described from Rio Magdalena basin. Therefore, *P. eutaenia* is known from regions 301 (North Andean Pacific Slopes) and 302 (Magdalena-Sinu), in Colombia.

Comments

Despite a superficial external similarity, *Pimelodella eutaenia* differs from *P. chagresi* by having. 42–44 total vertebrae (vs. 39–41 in *P. chagresi*); 9–10 ribs (vs. 8–9 in *P. chagresi*); tip of anteriormost anal-fin pterygiophore inserted posterior to hemal spine of vertebrae 22–24 (vs. 20–21 in *P. chagresi*); tip of posteriormost anal-fin pterygiophore inserted ahead of hemal spine of vertebrae 29–31 (vs. 27, 28 or 30 in *P. chagresi*); maxillary barbel always surpassing half anal-fin base (vs. rarely surpassing anal-fin origin in *P. chagresi*); posterior margin of pectoral-fin spine bearing 7–9 triangular, slightly retrorse dentations along its basal half to two-thirds (vs. posterior margin of pectoral-fin spine with edentulous shaft at first fourth, followed by 9–13 retrorse dentations along the entire margin, except its last fifth; these dentations are long, acute, inclined in *P. chagresi*); paired stripes on dorsal region of body diffuse (vs. well-delimited in *P. chagresi*); dorsal fin dusky, except by a hyaline stripe near its base (vs. dorsal fin completely dusky in *P. chagresi*). Thus, I believe both *P. eutaenia* and *P. chagresi* are distinct species, and the material usually referred as *P. chagresi* from Magdalena and rivers in Colombian Chocó might be, in fact, *P. eutaenia*. I also hereby designate BMNH 1913.10.1.37 as the lectotype, and remaining syntypes as paralectotypes.

Ardila Rodriguez (2017) described *Pimelodella floridablancaensis* based on specimens of Magdalena River basin, and compared this species with non-type material of *P. chagresi*, *P. reyesi* and *P. odynea*. However, Ardila Rodriguez (2017) does not indicate any *P.*

chagresi material in his comparative material list, which additionally presents specimens of *P. eutaenia* and *P. modesta*, not compared in description with his *P. floridablancaensis*, despite the specimen indicated for *P. eutaenia* being presented in Figure 15 of his work.

Unfortunately, I had no access to *P. floridablancaensis* type material, but could compare Ardila Rodrigues (2017) description with other material I examined, and came to the conclusion that *P. floridablancaensis* is a junior-synonym of *P. eutaenia*.

The presented diagnosis of *P. floridablancaensis* consists almost only on color pattern data, which is a dark midlateral stripe from snout to caudal-fin insertion; dorsal region of body darker; dorsal fin without any coloration marks; and dorsal caudal-fin lobe longer than ventral. All those characteristics are congruent with both *P. chagresi* and *P. eutaenia*, except the dorsal-fin coloration, which is present in these last two. Although, observing Ardila Rodrigues (2017) photos of *P. floridablancaensis* I could observe the same color pattern of *P. eutaenia* dorsal fin, being a dorsal fin dusky, except by a hyaline stripe near its base (Fig. 58).

Ardila Rodrigues (2017) comparisons of *P. floridablancaensis* with *P. chagresi* relies on characters that do not occur in the last as described on type-material, like the maxillary barbel reaching the vertical through dorsal-fin adpressed terminus (when it reaches anal-fin insertion); dorsal fin four times in SL (three and half times in SL in my data); 7 branchiostegal rays (6 branchiostegal rays in my data). Moreover, despite having *P. eutaenia* in his comparative material, Ardila Rodrigues made no attempt of comparing *P. floridablancaensis* with that species.

Pimelodella floridablancaensis has 35–37 free vertebrae, what must be the equivalent of 41–43 total vertebrae, and falls into *P. eutaenia* interval. Also, *P. floridablancaensis* has 9–10 ribs and anteriormost pterygiophore of anal fin inserted posterior to haemal spine of vertebrae 23 or 24 (18 or 19th free vertebrae), also congruent with the found for *P. eutaenia*. All other described characteristics, including pectoral-fin spine morphology (presented here in Figure 59) do not diverge substantially from *P. eutaenia* specimens. Thus, I indicate *P. floridablancaensis* is a junior-synonym of *P. eutaenia*, and the distribution of the last comprehends rivers in Magdalena basin and North Andean Pacific Slope drainages.

Material examined

Pimelodella eutaenia. — BMNH 1913.10.1.37, 1, xr, 126.3 mm SL, lectotype, Colômbia, "Rio Condoto (Spurrell) and the Rio Sipi (Palmer)", 5°05'44"N, 76°39'27"W; BMNH 1913.10.1.38–40, 3, xr, 51.0–65.5 mm SL, paralectotypes, Colômbia, "Rio Condoto (Spurrell) and the Rio Sipi (Palmer)", 5°05'44"N, 76°39'27"W; CAS 75787, 2, Colombia, Choco, Quibdo, at junction of Rios Quito and Atrato, 5°41'03.8"N, 76°40'01.3"W; CAS

75788, 1, 80.4 mm SL, Colombia, Meta, Cumaral, on llanos NE of Villavicencio, 4°16'03.3"N, 73°28'46.9"W; CAS 75806, 20, xr, Colombia, Choco, upper Rio San Juan at Istmina, 5°09'09.9"N, 76°41'09.5"W; USNM 76926, 6, xr, 63.28–134.2 mm SL, Colombia, Rio Telembi, Barbacoas, 1°30'29.3"N, 77°57'26.4"W; USNM 320089, 1, 110.5 mm SL, Colombia, Choco, Rio Salado, C. 1/4 mi. Upstream Fr. Junct. With Rio Truando, 7°06'01.2"N, 77°23'42.5"W; USNM 320090, 3, 60.8–90.3 mm SL, Colombia, Choco, Creek of Upper Rio Nercua, Large Trib. of Rio Truando, 7°03'54.7"N, 7°27'03.5"W; USNM 320091, 4, 128.6 mm SL, Colombia, Choco, Rio Salado Near Teresita, 7°06'29.9"N, 77°26'06.3"W; USNM 320092, 3, 69.2–113.1 mm SL, Colombia, Choco, Rio Ucati(?) at Acandi, 8°29'33.8"N, 77°16'58.2"W; USNM 320093, 1, Colombia, Rio Pavarando, Trib. of Rio Salaqui, 7°14'21.0"N, 77°29'27.9"W.

***Pimelodella figueroai* Dahl, 1961**

Pimelodella figueroai Dahl, 1961: 498–500, unnumbered figure [original description; “Caño Lozada”, Guayabero River basin, Upper Orinoco drainage, Colombia; holotype lost (Cala, 1981), paratypes ICN-MHN 2900]. — Cala, 1977: 11 [taxonomic list]. — Bockmann, 1994: 768 [taxonomic treatment, *Pimelodella* species with filament]. — Bockmann & Guazzelli, 2003: 418 [taxonomic treatment]. — Ferraris, 2007: 191 [taxonomic treatment]. — Maldonado-Ocampo *et al.*, 2008: 202 [taxonomic list].

Diagnosis

Pimelodella figueroai differs from all *Pimelodella* species except *P. longipinnis*, *P. martinezi*, *P. pectinifera*, *P. peruana*, *P. reyesi* and *P. spelaea* by having the dorsal fin completely hyaline. It differs from *P. pectinifera* and *P. peruana* by having the adipose fin three and half times in SL (*vs.* adipose fin four times or more in SL in *P. pectinifera* and *P. peruana*). It differs from *P. longipinnis* by having the supraoccipital process reaching the anterior prenuchal plate (*vs.* supraoccipital process not reaching the anterior prenuchal plate in *P. longipinnis*). It differs from *P. reyesi* and *P. spelaea* by having dentations on basal three fourths of posterior margin of pectoral fin (*vs.* dentations on basal two thirds of posterior margin of pectoral fin in *P. reyesi* and *P. spelaea*). It differs from *P. martinezi* by having caudal fin lobes subequal (*vs.* the dorsal caudal fin lobe slightly longer than the ventral lobe in *P. martinezi*).

Furthermore, *P. figueroai* can be diagnosed by maxillary barbel reaching half of adipose fin; might present a filamentous prolongation on dorsal-fin unbranched ray; posterior

margin of pectoral-fin spine bearing about 15 retrorse dentations along its basal three fourths; adipose fin of moderated length, three and half times in SL.

Description

Measurements in Table 20. Body depressed, depth at dorsal-fin origin almost seven times in standard length, and compressed, body width at dorsal-fin origin eight times in SL (Fig. 60). Dorsal profile straight from snout to dorsal fin, slightly concave from dorsal to adipose fin, slightly convex along adipose fin, and concave along the caudal peduncle. Ventral profile of body slightly convex from snout to branquiostegal membrane, convex between pectoral end pelvic fins, slightly concave from pelvic to anal fin, and also concave from there along the caudal peduncle. Posterior process of cleithrum triangular, its dorsal border straight.

Head deep, depth at supraoccipital-process base half of head length. Mouth sub terminal. Eye slightly elliptical, slightly more than four times in head length. Barbels thin, and elliptical in cross-section. Maxillary barbel reaching half of adipose fin. Outer mental barbel, when stretched parallel to main body axis, finishing at adpressed pectoral fin. Inner mental barbels, when stretched parallel to main body axis, finishing at a point slightly posterior to pectoral-fin origin.

Dorsal fin triangular, distal margin convex, short (second branched dorsal-fin ray almost four and half times in SL), depressed tip finishing at half of adpressed pelvic fin. Dorsal fin with I,6 plus anteriormost spinelet. Distance between terminus of dorsal-fin base and adipose-fin origin roughly equal to dorsal-fin base. Unbranched dorsal-fin ray with proximal part ossified as a spine, adult males present a soft filamentous prolongation of the dorsal-fin first ray. This filament is long, considerably longer than the rigid part of first dorsal-fin ray, being equivalent to more than one-fourth of standard length in the holotype.

Pectoral-fin rays I,8 or I,9, pectoral fin triangular with concave distal border. First pectoral-fin ray with proximal part rigid (almost seven times in SL), forming a spine, and short distal tip flexible and distinctly segmented. Anterior margin of pectoral-fin spine “finely serrated for about half its length, about the middle of spine in males, and smooth in females” (Dahl, 1961). Posterior margin of pectoral-fin spine bearing about 15 retrorse dentations along its basal three fourths.

Pelvic-fin rays i,5. Pelvic-fin origin at vertical through dorsal-fin terminus. Pelvic-fin adpressed terminus at vertical through first fifth of adipose fin.

Anal-fin rays iii,8; v,8 (1); distal border of extended anal fin convex. Anal-fin origin at vertical through first third of adipose-fin base; anal-fin adpressed terminus slightly anterior to vertical through adipose-fin terminus.

Adipose fin of moderated length, three and half times in SL, forming ascending elevated curve in lateral profile, with deepest point approximately at midlength. Adipose fin emerging gradually, its posterior limit as a rounded, free lobe.

Caudal fin deeply forked, lobes subequal. Caudal peduncle length posterior to adipose-fin slightly longer than its depth. Dorsal lobe with 7 or 8* branched and 1 unbranched principal rays. Ventral lobe with 8 branched and 1 unbranched principal rays.

Coloration in alcohol

Background body coloration yellowish. Ventral region of head and body lighter. Dark brown midlateral stripe apparently narrow, not well delimited, at least from opercle to caudal-fin insertion.

Geographic distribution

Pimelodella figueroai was described from “Caño Lozada, approximately 17. Kilometers above its junction with Guayabero River”, in Guaviare River basin, Upper Orinoco drainage. It is known from region 306 (Orinoco Piedmont).

Comments

Pimelodella figueroai was described based in one holotype and 12 paratypes but, unfortunately, the holotype is probably lost (Cala, 1981). Measurements in Table 20 correspond to one paratype ICN-MHN 2900, and counts and description are based in the aforementioned paratype and information of the original description. To better establish the identity of this species is needed observation of more material from Upper Orinoco drainage. Among the material from Upper Orinoco, I found only material from Rio Meta, and none comparable with *P. figueroai* description.

More investigation is needed also in the comparison of *P. figueroai* and *P. linami*, from Rio Torbes, lower Orinoco. Both were described with special focus to the presence of the dorsal-fin filamentous prolongation and, despite Dahl (1961) statement that *P. linami* differs from *P. figueroai* in several characteristics, none of those were commented along the text, and both species morphometric data are somewhat similar. However, *P. figueroai* paratype is extremely unpigmented, in a manner that *P. linami* coloration marks could not be observed, and I maintain both species as valid a priori, since more material is needed before taking any taxonomic decisions in this case.

Material examined

Pimelodella figueroai. — ICN-MNH 2900, 1, paratype, 71.8 mm SL, Colombia, La Macarena. Río Guayabero, Caño Losada.

***Pimelodella geryi* Hoedeman, 1961**

Pimelodella geryi Hoedeman, 1961: 134 [original description; “Litany river, village Aloiké”, Alowike, Surinam (Mees, 1974: 144); holotype: ZMA 102235]. — Mees, 1974: 144, 148 [junior synonym of *P. cristata*]. — Burgess, 1989: 280 [taxonomic treatment]. — Nijssen *et al.*, 1982: 60 [type catalog]. — Nijssen *et al.*, 1993: 224 [type catalog]. — Le Bail *et al.*, 2000: 134–135, unnum. fig. [taxonomic treatment]. — Bockmann & Guazzelli, 2003: 418 [taxonomic treatment]. — Ferraris, 2007: 191 [taxonomic treatment]. — Vari *et al.*, 2009: 43, 80 [taxonomic list]. — Le Bail *et al.*, 2012: 304 [taxonomic list]. — Slobodian *et al.*, 2017: 93–94 [comparison with *P. humeralis*].

Pimelodella procera Mees 1983: 49–54, fig. 3, 4 (upper) [original description; “Crique Balaté”, Maroni-Marowijne River basin, French Guyana; RMNH 28588]. — Burgess, 1989: 281 [taxonomic treatment]. — Le Bail *et al.*, 2000: 140–141, unnum. fig. [taxonomic treatment]. — Bockmann & Guazzelli, 2003: 420 [taxonomic treatment]. — Ferraris, 2007: 194 [taxonomic treatment]. — Vari *et al.*, 2009: 43 [taxonomic list]. — Le Bail *et al.*, 2012: 304 [taxonomic list].

Diagnosis

Pimelodella geryi can be distinguished from all *Pimelodella* species except *P. buckleyi*, *P. grisea*, *P. leptosoma*, *P. metae* and *P. notomelas*, by the presence of dorsal fin distal third extremely dark brown to black. It differs from *P. buckleyi* dark black midlateral stripe wide, well delimited, from snout until distal portion of median caudal-fin rays (*vs.* dark brown midlateral stripe wide and sparse, from snout to caudal-fin insertion). It distinguishes from *P. grisea* and *P. metae* by the presence of 42–43 total vertebrae (*vs.* 39–41 in *P. grisea*, 40 in *P. metae*). It distinguishes from *P. leptosoma* by having the supraoccipital process reaching the anterior prenuchal plate (*vs.* almost reaching in *P. leptosoma*). It differs from *P. notomelas* by the midlateral stripe notably dark, extending from snout to middle caudal-fin rays (*vs.* midlateral stripe lighter, extending posterior to opercle to caudal-fin origin). Furthermore, *P. geryi* can be diagnosed by maxillary barbel reaching between verticals through half adipose fin and surpassing caudal-fin insertion; posterior margin of pectoral-fin spine bearing 6 retrorse dentations along its basal half, notably inclined and pointy; adipose fin of moderated length, three to four times in SL; 42–43 total vertebrae; dark black midlateral

stripe wide, well delimited, from snout until distal portion of median caudal-fin rays; and distal third to half of dorsal fin with black pigmentation, as a conspicuous dark mark.

Description

Measurements in Table 21. Body depressed, depth at dorsal-fin insertion five to six times in standard length, and compressed, body width at dorsal-fin insertion seven to eight times in SL (Fig. 61). Dorsal profile slightly convex from snout to dorsal fin, concave from dorsal to adipose fin, straight along adipose fin, and concave along the caudal peduncle. Ventral profile of body slightly concave from snout to branchiostegal membrane, convex between pectoral end pelvic fins, slightly convex from pelvic to anal fin, and concave from there along the caudal peduncle.

Pseudotympanum large, oval, above posterior process of cleithrum and reaching the straight line of 7th (1) vertebrae. Posterior process of cleithrum triangular, its dorsal border slightly concave. Anus and urogenital papilla adjacent. Urogenital papilla tubular, triangular, short. Anus between verticals through first fourth or third of adpressed pelvic fin; urogenital papilla between verticals through last third or fourth of adpressed pelvic fin.

Head depressed, depth at supraoccipital-process base almost two and half times in head length. Mouth sub terminal. Eye slightly elliptical, four times in head. Bony interorbital distance slightly more than half eye diameter. Barbels thin, slightly depressed and elliptical in cross-section. Maxillary barbel reaching between verticals through half adipose fin and surpassing caudal-fin insertion. Outer mental barbel, when stretched parallel to main body axis, finishing between first third and terminus of adpressed pectoral fin. Inner mental barbel, when stretched parallel to main body axis, finishing between branchiostegal membrane posterior limit and pectoral-fin origin. Supraoccipital process subrectangular, narrow, and tapered at its distal point. Branchiostegal rays 6 (3).

Dorsal fin triangular, distal margin concave, average sized (second branched dorsal-fin ray four to five times in SL), depressed tip finishing between the verticals through half and last third of adpressed pelvic fin. Dorsal fin with I,6 (5) plus anteriormost spinelet. Distance between terminus of dorsal-fin base and adipose-fin origin equal or slightly larger than dorsal-fin base. Anteriormost dorsal-fin pterygiophore inserted posterior to neural spine of vertebrae 4 (1); posteriormost dorsal-fin pterygiophore located ahead of neural (or pseudoneural) spine of vertebrae 11 (1). Unbranched dorsal-fin ray mostly ossified as a spine, rigid part of moderated length (approximately a fourth shorter than the first dorsal-fin ray total length), distal fourth of anterior margin with smooth serrae (despite its original description saying it does not have serrae on it).

Pectoral-fin rays I,8* (4) or I,9 (1), pectoral fin triangular with concave distal border. First pectoral-fin ray roughly straight, with proximal part rigid, forming a spine (Fig. 62), and short distal tip flexible and distinctly segmented. Pectoral-fin spine five times in SL. Anterior margin of pectoral-fin spine with serrae along its distal half. Posterior margin of pectoral-fin spine bearing 6 retrorse dentations along its basal half, notably inclined and pointy.

Pelvic-fin rays i,5 (4) or i,6 (1), extended pelvic fin triangular with straight distal border. Anterior portion of pelvic-fin base between verticals through dorsal-fin terminus and last third of adpressed dorsal fin. Tip of adpressed pelvic fin between verticals through adipose-fin origin and its first seventh. First unbranched and flexible ray distinctly shorter than second and third rays, which are roughly the same size; remaining rays progressively shorter.

Anal-fin rays iii,8 (1); iv,8 (1), iv,9 (1) or iv,10 (1); distal border of extended anal fin convex. Two anteriormost anal-fin rays vestigial, unsegmented, embedded in thick skin fold. Anal fin origin at vertical through first third of adipose-fin base; anal-fin terminus at vertical through adipose-fin terminus. Tip of anteriormost anal-fin pterygiophore inserted posterior to hemal spine of vertebrae 22 (1). Tip of posteriormost anal-fin pterygiophore inserted ahead of hemal spine of vertebrae 30 (1).

Adipose fin three to four times in SL, forming ascending elevated curve in lateral profile, with deepest point approximately at last third. Adipose fin emerging gradually, its posterior limit as a rounded, free lobe.

Caudal fin deeply forked, dorsal lobe usually slightly longer than ventral. Caudal peduncle length posterior to adipose-fin a third to half longer than its depth. Dorsal lobe with 7 (5) branched, 1 (5) unbranched principal, and 13 (1)–15 (1) procurrent fin-rays. Ventral lobe with 8 (5) branched, 1 (5) unbranched principal, and 20 (1)–21 (1) procurrent fin-rays. Hypural 5 completely free, not fused to hypural 3+4. Median caudal-fin rays not articulated directly to caudal plate. Seven* (26), rarely 8 (3) or 9 (1) rays articulated to dorsal caudal-fin plate (5, 6 or 7 on hypurals 3+4 and 2 on hypural 5) and 8 (16), rarely 7* (6), 9 (5) or 10 (3) rays articulated to ventral caudal-fin plate (5, 6, 7 or 8 on hypurals 1+2 and 2 on parhypural).

Total vertebrae 42*(1)– 43 (1). Ribs 8 (2).

Epiphyseal branch of laterosensory canal on head (S6) with contralateral canals connecting at midline, and opening as a single pore right after the connection.

Coloration in alcohol

Background body coloration yellowish. Ventral region of head and body lighter. Dark black midlateral stripe (Fig. 63) wide, well delimited, from snout until distal portion of

median caudal-fin rays. Distal third to half of dorsal fin with black pigmentation, as a conspicuous dark mark.

Geographic distribution

Pimelodella geryi was described from Litany River at Village Aloiké, French Guiana, information that was posteriorly corrected to Alowike, Surinam (Mees, 1974:144), from Maroni/Marowijne basin. *Pimelodella procera*, its junior-synonym, was described from “Crique Balaté”, a location on French Guiana, also from Maroni/Marowijne basin. Therefore, *P. geryi* is known from regions 311 (Guianas) and 315 (Amazonas Guiana Shield), in rivers in French Guyana, Surinam and Brazil.

Comments

In his list of Auchenipteridae and Pimelodidae from Surinam, Mees (1974) suggests *P. geryi* is a junior-synonym of *P. cristata*, based on the adipose-fin length (Mees, 1974: 148). The material Mees (1974) examined and classified under the name of *P. cristata* is vast, of over a thousand specimens, of several different localities in Surinam, and must be thoroughly examined before accepting the identification of all those material as *P. cristata*.

Pimelodella cristata have always a higher number of vertebrae (more than 46 total vertebrae), a very long adipose fin, a particular morphology of the pectoral-fin spine (vide *P. cristata* section), and lateral dark stripe narrow or almost absent. On the other hand, *P. geryi* presents a lower count on vertebrae (42–43 total vertebrae), smaller adipose fin, pectoral-fin spine with fewer dentations along its posterior margin, a remarkably dark lateral stripe, wide, from snout to centralmost caudal-fin rays and also a conspicuous dark tip of the dorsal fin (not reported on original description). Therefore, both species are notably different.

However, here I propose *P. procera* Mees 1983 is in fact a junior-synonym of *P. geryi*. Upon examining *P. procera* type-specimens, they have the same conspicuous characteristics above described, including the dorsal-fin tip remarkably darker. No attempt was made by Mees (1983) in comparing *P. procera* with *P. geryi*, since it was formerly synonymized to *P. cristata*. In Table 22 the morphometric data of both *P. geryi* and *P. procera* material is presented comparatively. *Pimelodella procera* paratype is presented in Figure 64.

Identification of material as *P. geryi* for Colombia (e.g. Mojica *et al.* 2005, Bogota-Gregory & Maldonado-Ocampo 2006, Maldonado-Ocampo *et al.*, 2006) is probably wrong, and based only in the presence of the black distal half of dorsal fin on some fishes of that region, like *P. buckleyi*.

Material examined

Pimelodella geryi. — ZMA 102235, 1, xr, 58.0 mm SL, holotype, French Guyana, mainland, Litany River, village Aloiké, 3°19'41.81"N, 54°3'14.65" W; AMNH 55012, 29, Surinam, Nickerie District, Small stream on lucie river camp to paramaribo road, ca. 25 kilometers north of sisa creek crossing, at kilometer 212, 3°35'00.0"N, 57°40'00.0"W; ANSP 177230, 2, 67.8–77.52 mm SL, Guyana, Essequibo, Siparuni river, Tumble Down Creek, 4°48'39"N, 58°51'11"W; MZUSP 108940, 2, xr, 84.6–113.1 mm SL, Guyana, Potaro-Siparuni, Rio Kuribrong, Pouis Landing (15-19.iv e 1.v.2010), 5°33'36.0"N, 59°17'36.0"W.

Pimelodella procera. — RMNH 28588, 1, xr, holotype, French Guyana, "Crique Balaté", Maroni-Marowine basin, 5°28'53"N, 54°02'46"W; MBNH 1983-5, 3, xr, 61.5–91.2 mm SL, paratypes, French Guyana, "Crique Balaté", Maroni-Marowine basin, 5°28'53"N, 54°02'46"W.

***Pimelodella gracilis* (Valenciennes, 1835)**

Pimelodus gracilis Valenciennes, 1835: pl. 2, fig. 5 [original pictorial description; name available from plate, description was published in Valenciennes, 1847]. — Cuvier & Valenciennes, 1840: 181–183 [append description; "Corrientes dans le Parana et les autres rivières au-dessus de 28 de latitude sud", Corrientes, Argentina; holotype: MNHN A-9284]. — Valenciennes, 1847: 7 [append description related to original plate; indicated number of plate and figure are not as presented in original plate]. — Kner, 1858: 418 (*in partim*) [taxonomic treatment]. — Günther, 1864: 121 [taxonomic treatment].

Pimelodella gracilis. — Eigenmann & Eigenmann, 1888: 132 [taxonomic treatment (see comments)]. — Eigenmann & Eigenmann, 1890: 148, 153–154 [key to *Pimelodella* species; taxonomic revision (see comments)]. — Eigenmann & Eigenmann, 1891: 29 [taxonomic list]. — Eigenmann, McAtee & Ward, 1907: 114 [taxonomic list]. — Bertoni, 1914: 6 [taxonomic list]. — Miranda Ribeiro, 1914: 5 [taxonomic list]. — Eigenmann, 1917: 238–239, pl. XXXV, fig. 37 [taxonomic revision]. — Pearson, 1924: 14 [taxonomic treatment]. — Bertoni, 1939: 52 [taxonomic list]. — Eigenmann & Allen, 1942: 53, 102 (*in partim*) [taxonomic list, taxonomic treatment]. — Schultz, 1944: 211–212 (*in partim*) [taxonomic treatment]. — Gosline, 1945: 43 (*in partim*) [taxonomic list]. — Van der Stigchel, 1946: 55–56 [taxonomic treatment]. — Fowler, 1951: 540, fig. 554 (*in partim*) [taxonomic treatment]. — Mees, 1974: 149–150 [comparison with *P. cristata*, clarification on type-locality]. — Lopez *et al.*, 1981: unnum. pages. [taxonomic list]. — Lopez *et al.*, 1982: 9 [taxonomic list]. — Burgess,

1989: 280 [taxonomic treatment]. — Britski *et al.*, 1999: 98 [taxonomic treatment]. — Bockmann & Guazzelli, 2003: 418 (*in partim*) [taxonomic treatment]. — Lopez *et al.*, 2003: 62 [taxonomic list]. — Litz & Koerber, 2014: 20–21 [taxonomic list]. — Ferraris, 2007: 191 (*in partim*) [taxonomic treatment]. — Graça & Pavanelli, 2007: 147 [taxonomic treatment]. — Langeani *et al.*, 2007: 187 [taxonomic list]. — Ruiz Diaz *et al.*, 2008: 1–4 [taxonomic treatment]. — Mirande & Koerber, 2015: 34 [taxonomic list]. — Koerber *et al.*, 2017: 51 [taxonomic list].

Rhamdia gracilis. — Miranda Ribeiro, 1911: 269–270 (*in partim*) [taxonomic treatment].

Pimelodella taenioptera Miranda Ribeiro, 1914: 5–6, unnum. fig. [original description; “Tapyrapoan, Rio Sepotuba”, Mato Grosso State, Brazil; lectotype: MNRJ 691A (designated by Miranda Ribeiro, 1953: 404)]. — Pearson, 1924: 14 [taxonomic treatment]. — Fowler, 1951: 550, fig. 566 [taxonomic treatment]. — Burgess, 1989: 280 [taxonomic treatment]. — Bockmann, 1994: 768 [taxonomic treatment, presence of filament]. — Britski *et al.*, 1999: 98 [taxonomic treatment]. — Bockmann & Guazzelli, 2003: 421 [taxonomic treatment]. — Graça & Pavanelli, 2007: 148 [taxonomic treatment]. — Ferraris, 2007: 195 [taxonomic treatment]. — Ruiz Diaz *et al.*, 2008: 1–4 [taxonomic treatment].

Pimelodella griffini [non Eigenmann, 1917]. — Pearson, 1924: 15 [taxonomic treatment]. — Castello, 1969: 407–415 [taxonomic treatment].

Pimelodella cristata [non Müller & Troschel, 1849]. — Lopez *et al.*, 2003: 62 [taxonomic list].

Pimelodella sp. N. — Bockmann & Slobodian, 2013: 65, fig. 36.1G [taxonomic treatment].

Diagnosis

Pimelodella gracilis differs from all *Pimelodella* species, with exception of *P. avanhandavae*, *P. chagresi*, *P. eutaenia*, *P. griffini*, *P. montana*, *P. odynea*, *P. peruana*, *P. reyesi* and *P. roccae* by having a dorsolateral brown stripe along body. It differs from *P. avanhandavae*, *P. chagresi*, *P. eutaenia*, *P. griffini*, *P. montana*, *P. odynea*, *P. peruana* and *P. roccae* by having 46, rarely 45 total vertebrae (*vs.* 41–45 in *P. avanhandavae*, *P. eutaenia*, *P. odynea* and *P. peruana*; 39–42 in *P. chagresi*, *P. griffini*, *P. montana* and *P. roccae*). It differs from *P. reyesi* by having maxillary barbel reaching between verticals through half anal-fin base and surpassing caudal-fin origin (*vs.* maxillary barbel reaching anal fin origin in *P. reyesi*). Furthermore, *P. gracilis* can be diagnosed by maxillary barbel reaching between verticals through half anal-fin base and surpassing caudal-fin origin; dorsal lamina of Weberian complex vertebrae reaching the supraoccipital process along its entire extension;

posterior margin of pectoral-fin spine bearing 16–24 retrorse dentations along its basal three fourths, these dentations larger and more inclined near distal tip, and smaller nearer pectoral-fin base; adipose fin very long, slightly more than two to two and half times in SL; one single opening of epiphyseal branch of lateral sensory canal on head, on S6 pore, after a small tube that connects both contralateral S6 branches; dark brown midlateral stripe wide, not well delimited, extending from snout to distal end of median caudal-fin rays; paired wide dark brown dorsal stripe, not well delimited, along supraoccipital process until first third of adipose-fin base, getting fainter posteriorly.

Description

Measurements in Table 23. Body depressed, depth at dorsal-fin origin five and half to eight and half times in standard length, and compressed, body width at dorsal-fin origin six and half to ten times in SL (Fig. 65). Greatest body depth at dorsal-fin origin. Dorsal profile roughly straight from snout to dorsal fin, concave from dorsal to adipose fin, slightly convex along adipose fin, and concave along the caudal peduncle. Ventral profile of body slightly convex from snout to pectoral fins, concave between pectoral and pelvic fins, slightly convex from pelvic to anal fin, and concave from this point along the caudal peduncle.

Pseudotympanum large, oval, above posterior process of cleithrum and reaching the straight line of 6th (2) or 7th (1) vertebrae. Posterior process of cleithrum triangular, long, its dorsal border straight. Anus and urogenital papilla adjacent. Urogenital papilla tubular, triangular, short. Anus between verticals through second fifth and first third of adpressed pelvic fin; urogenital papilla between verticals through last fourth and terminus of adpressed pelvic fin.

Head of moderated depth, depth at supraoccipital-process base two to slightly less than two and half times in head length. Mouth sub terminal. Eye slightly elliptical, four and half to six times in head. Bony interorbital distance roughly equal to eye diameter. Barbels thin, slightly depressed and elliptical in cross-section. Maxillary barbel reaching between verticals through half anal-fin base and surpassing caudal-fin origin. Outer mental barbel, when stretched parallel to main body axis, finishing between half adpressed pectoral-fin and pelvic-fin origin. Inner mental barbel, when stretched parallel to main body axis, finishing between pectoral-fin origin and its half adpressed. Supraoccipital process subrectangular, comparatively large, with a constant width long its length and distal third slightly tapered, sometimes with a discrete constriction near base. Dorsal lamina of Weberian complex vertebrae reaching the supraoccipital process along its entire extension. Branchiostegal rays 5* (1) or 6 (1).

Dorsal fin triangular, distal margin concave, moderate length (second branched dorsal-fin ray four to six times in SL), depressed tip finishing between verticals through two fifths and last fourth of adpressed pelvic fin. Dorsal fin with I,6 (9) plus anteriormost spinelet. Distance between terminus of dorsal-fin base and adipose-fin origin a third to half dorsal-fin base. Anteriormost dorsal-fin pterygiophore inserted posterior to neural spine of vertebrae 4 (6); posteriormost dorsal-fin pterygiophore located ahead of neural (or pseudoneural) spine of vertebrae 11 (6). Unbranched dorsal-fin ray mostly ossified as a spine (spine a third shorter than the first dorsal-fin total length), and may present a filamentous prolongation. Posterior distal half of dorsal-fin spine with smooth retrorse dentations.

Pectoral-fin rays I,8* (5) or I,9(3), pectoral fin triangular with concave distal border. First pectoral-fin ray curved with proximal part rigid, forming a spine (Fig. 66), and short distal tip flexible and distinctly segmented. Pectoral-fin spine five to six times in SL. Anterior margin of pectoral-fin spine with small, straight dentations along the basal three fourths, and serrae along its distal fourth. Posterior margin of pectoral-fin spine bearing 16–24 retrorse dentations along its basal three fourths. These dentations are larger and more inclined near distal tip, and smaller nearer pectoral-fin base. Also 1–3 unossified distal dentations, not counted.

Pelvic-fin rays i,5 (8), extended pelvic fin triangular with straight distal border. Anterior portion of pelvic-fin base between verticals through sixth branched ray and terminus of dorsal fin. Tip of adpressed pelvic fin between verticals through first sixth or fourth of adipose. First unbranched and flexible ray distinctly shorter than second and third rays (first and second branched rays, respectively), which are roughly the same size; remaining rays progressively shorter.

Anal-fin rays iv,7 (2); v,7 (1); v,8 (1) or iv,9* (3); distal border of extended anal fin convex. Two or three anteriormost anal-fin rays vestigial, unsegmented, embedded in thick skin fold. Anal fin origin at vertical through second fifth of adipose-fin base; anal-fin adpressed terminus always slightly anterior to vertical through adipose-fin terminus. Tip of anteriormost anal-fin pterygiophore inserted posterior to hemal spine of vertebrae 23* (3) or 24 (3). Tip of posteriormost anal-fin pterygiophore inserted ahead of hemal spine of vertebrae 31* (5) or 32 (1).

Adipose fin slightly more than two to two and half times in SL, forming ascending elevated curve in lateral profile, with deepest point approximately at its half. Adipose fin emerging gradually, its posterior limit as a rounded, free lobe. Adipose-fin origin at vertical

through vertebral centra 16 (1)– 19 (1) (holotype 18); adipose-fin terminus at vertical through vertebral centra 40 (1)– 42* (2).

Caudal fin deeply forked, lobes may be subequal (2), dorsal lobe longer* (3), or ventral lobe longer (4). Caudal peduncle length posterior to adipose-fin slightly longer to two times its depth. Dorsal lobe with 7 (8) branched, 1 (8) unbranched principal, and 14 (1)–18 (1) (holotype 16) procurrent fin-rays. Ventral lobe with 8 (8), 1 (8) unbranched principal, and 9 (1)– 24 (1) (holotype 13) procurrent fin-rays. Hypural 5 completely free, not fused to hypural 3+4. Median caudal-fin rays not articulated directly to caudal plate. 7 (5) rays articulated to dorsal caudal-fin plate (5 on hypurals 3+4 and 2 on hypural 5) and 8 (5) rays articulated to ventral caudal-fin plate (6 on hypurals 1+2 and 2 on parahypural).

Total vertebrae 46* (4), rarely 45 (1). Ribs 9 (1)– 10* (3).

One single opening of epiphyseal branch of lateral sensory canal on head, on S6 pore, after a small tube that connects both contralateral S6 branches.

Coloration in alcohol

Background body coloration yellowish. Ventral region of head and body lighter. Dark brown midlateral stripe (Fig. 67) wide, not well delimited, extending from snout to distal end of median caudal-fin rays. Paired wide dark brown dorsal stripe, not well delimited, along supraoccipital process until first third of adipose-fin base, getting fainter posteriorly. Cephalic dark brown pigment along posterior fontanel region. Dorsal fin with dark brown pigment near base, followed by a hyaline stripe, and distal two thirds dusky.

Geographic distribution

Pimelodella gracilis was described from Rio Paraná in Argentina. *Pimelodella taenioptera*, its junior-synonym, was described from Rio Sepotuba, Upper Paraguay River basin. Therefore, *P. gracilis* is known from regions 318 (Mamore-Madre de Dios Piedmont), 343 (Paraguay) and 344 (Upper Paraná), possibly 345 (Lower Paraná) in Argentina, Brazil and Paraguay (see comments).

Comments

There has been some doubt about the type of *P. gracilis*, if MNHN 9284-A or MNHN 9285 (*e.g.* Bertin & Estève, 1950; Ferraris, 2007; Eschmeyer, Fong & van der Laan, 2017). Bockmann & Guazzelli (2003) suggested MNHN 9284-A was the holotype, but without justifying the statement. Upon examination, MNHN 9285 is undoubtedly a *Rhamdia*, whilst Valenciennes (1835) plate corresponds to a *Pimelodella* (due to, for example, the

supraoccipital process reaching the supraoccipital plate), thus, the holotype must be MNHN 9284-A.

When describing *P. taenioptera*, Miranda Ribeiro (1914) comments this species is very similar to *P. gracilis*, but differs both in terms of absence of coloration and presence of a dorsal-fin filament in *P. taenioptera*. The absence of coloration in the type material might be due to preservation process, and neither a collector nor a collection date was presented for this material. No other material observed from Paraguay or Paraná basins with the other diagnostic characteristics had coloration marks absent, but the same pattern as presented for *P. cristata*. Regarding the filamentous prolongation of first dorsal-fin rays, they are a secondary sexually dimorphic character, presented in mature males (Mees, 1974, Souza-Shibatta *et al.*, 2013; Bockmann & Slobodian, 2013), and Souza-Shibatta *et al.* (2013) found it in two species occurring in Paraguay River basin, *P. taenioptera* and *P. griffini*.

In this work I found no evidence *P. taenioptera* (Fig. 68, 69) is distinguishable from *P. gracilis*, and suggest, thus, the first is a junior-synonym of the last. Morphometric data for *P. gracilis* discriminated by original species name is presented in Table 22. *Pimelodella gracilis* can be identified by the following: head lateral profile straight from snout to dorsal-fin insertion; maxillary barbel reaching between verticals through half anal-fin base and surpassing caudal-fin origin; outer mental barbel, when stretched parallel to main body axis, finishing between half adpressed pectoral-fin and pelvic-fin origin; anterior margin of pectoral-fin spine with small, straight dentations along the basal three fourths, and serrae along its distal fourth; posterior margin of pectoral-fin spine bearing 16–24 retrorse dentations along its basal three fourths, the dentations are larger and more inclined near distal tip, and smaller nearer pectoral-fin base; adipose-fin very long, between 38.7–44.5% SL; total vertebrae 45–46; one single opening of epiphyseal branch of lateral sensory canal on head, after a small tube that connects both contralateral S6 branches, all the former overlapping with the present in *P. cristata*. It differs from *P. cristata* by having a conspicuous coloration pattern, with a dark brown midlateral stripe wide, not well delimited, extending from snout to distal end of median caudal-fin rays; paired wide dark brown dorsal stripe, not well delimited, along supraoccipital process until first third of adipose-fin base, getting fainter posteriorly; cephalic dark brown pigment along posterior fontanel region; and dorsal fin with dark brown pigment near base, followed by a hyaline stripe, and distal two thirds dusky.

When comparing *P. cristata* and *P. gracilis*, the last has its vertebrae count and anal-fin insertion more alike the *P. cristata* from Northeastern Brazil, where I found a tendency to a lower number of vertebrae (Table 15). However, the coloration pattern can be used to

promptly distinguish both, and is consistent in all material observed. As formerly commented in *P. cristata* section, the morphological variation among *Pimelodella* species with more than 46 total vertebrae is very incipient (except for *P. cruxenti*), and characteristics relative to morphometrics are highly overlapping (Figs. 32–33), in a manner they are usually insufficient to discriminate species from this group. Figure 70 presents the graphic of PC1 against PC2 of a Principal Component Analysis performed for all *Pimelodella* species with 46 or more total vertebrae (except *P. cruxenti*), discriminated by the species I consider valid in this work.

In sum, this work suggests *P. gracilis* is a valid species, having *P. taenioptera* as its junior-synonym, and can be diagnosed from all other *Pimelodella* species, with exception of *P. cristata* and *P. humeralis*, by having 46 total vertebrae. Furthermore, *P. gracilis* differs from *P. cristata* and *P. humeralis* in the coloration pattern (presence of a wide, not well delimited, midlateral dark brown stripe, from snout to distal end of median caudal-fin rays; and paired, not well delimited, dark brown stripe along dorsal region of body, from supraoccipital process to first third of adipose-fin base vs. narrow, well delimited midlateral dark brown stripe, from region posterior to head to caudal-fin origin in *P. cristata* and *P. humeralis*; and presence of a humeral dark brown mark in *P. humeralis*); and from *P. humeralis* by having posterior margin of pectoral-fin spine bearing 16–24 retrorse dentations along its basal three fourths (vs. posterior margin of pectoral-fin spine with 8–11 retrorse dentations along its basal three-quarters).

Souza-Shibatta *et al.* (2013) made a karyotype analysis of *Pimelodella* from Miranda River, Paraguay basin, and found two species regarding the number of chromosomes. To the one with $2n = 52$ chromosomes they gave the name of *P. taenioptera*, and *P. griffini* to the one of $2n = 46$. Between those two groups, they found an overlapping in the morphometric characteristics, and argue they were cryptic species whose identification was only possible with the use of various analysis techniques.

I could examine part of the specimens used in Souza-Shibatta *et al.* (2013) work, and have the opinion that, despite the overlap in morphometric, both species are readily recognizable as distinct, the most striking characters being the number of vertebrae (45–46 for their *P. taenioptera* and 41–42 for their *P. griffini*) and adipose-fin length (38.7–44.5% SL for *P. taenioptera* and 35.0–38.4% SL for their *P. griffini*). Therefore, I can argue that Souza-Shibatta *et al.* (2013) *P. taenioptera* is distinguishable from their *P. griffini* not only by the number of chromosomes, but also morphological and morphometric characteristics. Since *P. taenioptera* is undistinguishable from *P. gracilis* unless by the possible presence of filaments in dorsal-fin in mature males, what Souza-Shibatta *et al.* (2013) refer as *P. taenioptera* is, in

fact, *P. gracilis*, and this last species has chromosomes $2n = 52$. Furthermore, what Souza-Shibatta *et al.* (2013) treats as *P. griffini* I believe is, in fact, *P. taenioptera*, and will discuss in the scope of this last species.

Castello (1969) reported *P. griffini* for Argentina, however, based on the description of the specimens observed in that work, I believe they pertain to *P. gracilis* species.

Regarding doubtful specimens in *P. gracilis* synonym, Eigenmann & Eigenmann (1888, 1890) assigned to this species specimens of “Goyaz” (Goiás State, Brazil). Based on description, those specimens looked alike *P. laurenti* Fowler, 1941a, and Eigenmann himself have posteriorly raised doubt if those specimens were, in fact, *P. gracilis* (Eigenmann, 1917: 238–239). Eigenmann (1917) also indicates *P. gracilis* occurs in Uruguay basin, however, despite this occurrence being possible, and even assigned in other works (*e.g.* Litz & Koerber, 2014), no material from that basin was observed in this work for *P. gracilis*. I also disagree with Eigenmann inclusion of *P. taenioptera* (Regan, 1903) in the synonym if *P. gracilis*, and the first is going to be treated as a valid species in this work and distinguishable from the last.

As previously commented, in this thesis, mentions to *P. gracilis* from most of Amazon, the Guianas and Orinoco were treated as part of *P. cristata* synonym, since both species, despite similar, are distinguishable, but *P. gracilis* is known from mainly Uruguay and Paraná basins. In the same manner, *P. cristata* from Uruguay and Paraná basins are treated under *P. gracilis* synonym.

Is noteworthy Pearson (1924) reports a *P. gracilis* for Beni river basin, stating “(IU) 17085 probably represent the true *P. gracilis*. (IU) 17092, 17093 and 17084 have a longer and weaker dorsal spine, which is prolonged in a filament in some specimens. It is irregular and much weaker than that of *P. griffini* and seems close to Ribeiro's *P. taenioptera*. 17084 have the upper caudal lobe only slightly prolonged”. I could examine specimens from Rio Madeira basin that are indistinguishable from *P. gracilis*, reported as *Pimelodella* sp. N in Bockmann & Slobodian (2013: 65). Pearson (1924) *P. griffini* is possibly the same as *P. gracilis*, with the filament in dorsal fin reported as presented only in males.

Material examined

Pimelodella gracilis. — MNHN A-9284, 1, xr, 170.1 mm SL, syntype, Argentina, “Corrientes dans le Parana et les autres rivières au-dessus de 28° de latitud sud”, 28°00'47"S, 58°49'52"W; ANSP 182412, 2, 75.12–77.17 mm SL, Argentina, Corrientes, Various sites including main & braided side channels and backwaters of R. Parana & lower Guayquiraro, ca. 25 km S of Esquina; ANSP 182415, 3, 115.12–139.8 mm SL, Argentina, Corrientes, Rio Parana (left bank) at private park (Club San Martin) near town of Perichon, N of rt. 12, NE of

Corrientes; ANSP 203154, 15, 60.65–109.71 mm SL, Uruguay, Nuevo Berlin, Rio Uruguay, Rio de La Plata drainage, 32°58'33.3"S, 58°04'00.8"W; ANSP 203155, 1, 72.87 mm SL, Uruguay, Rio Uruguay, Rio de La Plata drainage, 34°47'35.5"S, 56°26'56.6"W; ANSP 203156, 1, 57.31 mm SL, Uruguay, Rio Uruguay, Rio de La Plata drainage, 34°47'35.5"S, 56°26'56.6"W; CAS 6667, 3, xr, Brazil, Goias, R. Tocantins at Peixe, 12°01'57.5"S, 48°31'34.6"W; CAS 75812, 1, xr, 119.9 mm SL, Argentina, Entre Rios, Parana River, 32°48'11.3"S, 60°41'15.2"W; FMNH 57948, 8, xr, 111.9 mm SL, 1 c&s, Brazil, Uruguayana, 29°44'56.8"S, 57°05'45.6"W; LIRP 10014, 1, xr, 67.1 mm SL, Brazil, Rondonia, Porto Velho, Foz do Igarapé Belmont, Rio Madeira, 8°38'36"S, 63°51'16"W; LIRP 10023, 3, xr, 80.5–90.4 mm SL, Brazil, Rondonia, Costa Marques, Rio Guaporé, next to Baía das Onças, 12°07'30"S, 64°44'08"W; MZUSP 337, 5, 99.2–119.0 mm SL, Argentina, Paraná, Entre Rios, 31°42'26.8"S, 60°30'57.9"W; MZUSP 2250, 1, 108.3 mm SL, Brazil, São Paulo, Piracicaba, Rio Piracicaba, 22°41'21.6"S, 47°41'12.6"W; MZUSP 22153, 1, 121.7 mm SL, Brazil, São Paulo, Piracicaba, 22°41'0.0"S, 47°51'0.0"W; MZUSP 23195, 1, 189.7 mm SL, Brazil, Mato Grosso, Rio Taquari, about 150 km from Coxim county, 18°13'0.0"S, 55°10'0.0"W; MZUSP 24856, 2, 106.1–115.7 mm SL, Brazil, Mato Grosso, Cuiabá, Rio Cuiabá, a ca. 500m abaixo da ponte nova, 15°37'0.0"S, 56°6'0.0"W; MZUSP 27728, 3, 135.1–202.7 mm SL, Brazil, Mato Grosso do Sul, Coxim, Rio Taquari, 18°30'0.0"S, 54°45'0.0"W; MZUSP 28571, 2, 78.1–86.3 mm SL, Brazil, Mato Grosso do Sul, Coxim, Rio Taquari, near Coxim county, 18°30'0.0"S, 54°45'0.0"W; MZUSP 38033, 7, 59.9–71.1 mm SL, Brazil, Mato Grosso do Sul, Corumba, Rio Paraguai, Morrinhos, 19°0'0.0"S, 57°39'0.0"W; MZUSP 82381, 1, 117.2 mm SL, Brazil, São Paulo, Porto Cabral, Rio Paraná, 22°15'0.0"S, 52°30'0.0"W; MZUSP 87788, 1, 148 mm SL, Brazil, Mato Grosso, Rio Sepotuba, Salto Maciel Tangará da Serra, 15°55'59.0"S, 57°39'0.0"W; USNM 232282, xr, 64.4–76.4 mm SL, Paraguay, Cordillera Dept., Lago Ypacarai, 63 km W of Military Base At San Bernardino, 25°21'00.9"S, 57°17'06.8"W; USNM 232283, xr, 91.2 mm SL, Paraguay, Alto Parana Dept., Puerto Bemone On Rio Parana, 24°52'32.9"S, 54°25'34.4"W.

Pimelodella taenioptera. — MNRJ 691A, 1, xr, 123.4 mm SL, lectotype, Brazil, Mato Grosso, rio Sepotuba, Tapirapuã, Com. Rondon, 14°50'56"S, 57°45'24"W; MNRJ 691, 2, xr, 119.7–125.0 mm SL, paralectotypes, Brazil, Mato Grosso, rio Sepotuba, Tapirapuã, Com. Rondon, 14°50'56"S, 57°45'24"W; MZUEL 6456, 1, xr, 124.6 mm SL, Brazil, Mato Grosso do Sul, Rio Miranda, 19°34'36"S, 57°1'5"W; MZUEL 6458, 6, xr, 60.5–105.9 mm SL, Brazil, Mato Grosso do Sul, Rio Miranda, 19°34'36"S, 57°1'5"W; USNM 194293, 3, xr, 75.6–79.6 mm SL, Brazil, Mato Grosso, Upper Juruena, Tapajos-Amazon Dr., 8°04'18.9"S,

58°17'11.5"W; USNM 199186, 2, xi, 75.5–97.6 mm SL, Brazil, Mato Grosso, Upper Yuruena, 8°04'18.9"S, 58°17'11.5"W.

***Pimelodella griffini* Eigenmann, 1917**

Pimelodella griffini Eigenmann, 1917: 250, pl. XXXII, fig. 3, pl. XXXV, fig. 31 [original description; “mountain rills near Sapucay, Paraguay”; holotype: FMNH 57974]. — Gosline, 1945: 45 [taxonomic list]. — Fowler, 1951: 541–542, fig. 555 (*in partim*) [taxonomic list]. — Schubart, 1964: 8–9 [comparison with *P. insignis*]. — Mees, 1974: 152 [comparison with *P. boschmai*]. — Henn, 1977: 67 [type catalog]. — Ibarra & Stewart, 1987: 66 [type catalog]. — Burgess, 1989: 280 [taxonomic list]. — Bockmann, 1994: 768 [*Pimelodella* species with filament]. — Bockmann & Guazzelli, 2003: 418 [taxonomic treatment]. — Ferraris, 2007: 191 [taxonomic treatment]. — Koerber *et al.*, 2017: 51 [taxonomic list].

Diagnosis

Pimelodella griffini differs from all *Pimelodella* species, with exception of *P. avanhandavae*, *P. chagresi*, *P. eutaenia*, *P. gracilis*, *P. montana*, *P. odynea*, *P. peruana*, *P. reyesi* and *P. rocae* by having a dorsolateral brown stripe along body. It differs from *P. avanhandavae*, *P. eutaenia*, *P. gracilis*, *P. odynea* and *P. peruana* by having 41–42 total vertebrae (*vs.* 41–45 in *P. avanhandavae*, *P. eutaenia*, *P. odynea* and *P. peruana*; 46 total vertebrae in *P. gracilis*). It differs from *P. chagresi*, *P. montana*, *P. reyesi* and *P. rocae* by having maxillary barbel reaching between verticals through half and terminus of adpressed pelvic fin (*vs.* reaching posterior to adpressed pelvic fin terminus in *P. chagresi*, *P. montana*, *P. reyesi* and *P. rocae*). Furthermore, *P. griffini* can be diagnosed by maxillary barbel reaching between verticals through half and terminus of adpressed pelvic fin; unbranched dorsal-fin ray mostly ossified as a spine, rigid part curved and may present a filamentous prolongation; adipose fin more than three and half times in SL; 41–42 total vertebrae; dark brown midlateral stripe wide, extending from snout to caudal-fin origin; paired dark brown stripes, not well-delimited, along supraoccipital process running dorsal region of body until posterior region of adipose-fin base.

Description

Measurements in Table 25. Body of moderate depth, depth at dorsal-fin insertion five to six times in standard length, and compressed, body width at dorsal-fin origin six and half to seven times in SL (Fig. 71). Greatest body depth at dorsal-fin origin. Dorsal profile convex from snout to dorsal fin, slightly concave from dorsal to adipose fin, slightly convex along

adipose fin, and concave along the caudal peduncle. Ventral profile of body slightly convex from snout to branchiostegal membrane, also convex between branchiostegal membrane and pectoral-fins, and between pectoral and pelvic fins, slightly concave from pelvic to anal fin, and also concave from there along the caudal peduncle.

Pseudotympanum large, oval, above posterior process of cleithrum and reaching the straight line of 7th (1) or 8^{th*} (1) vertebrae. Posterior process of cleithrum triangular, narrow, its dorsal border straight. Anus and urogenital papilla adjacent. Urogenital papilla tubular, triangular, shorter in specimens without filament, a little longer in specimens with filament. Anus between verticals through half of pelvic-fins adpressed and a point slightly anterior to that; urogenital papilla between verticals through last third to terminus of adpressed pelvic fin.

Head of moderated depth, depth at supraoccipital-process base always more than two times in head length. Mouth sub terminal. Eye slightly elliptical, four to five times in head. Bony interorbital distance almost equal to eye diameter. Barbels thin, depressed and elliptical in cross-section. Maxillary barbel reaching between verticals through half and terminus of adpressed pelvic fin. Outer mental barbel, when stretched parallel to main body axis, finishing between verticals through half and terminus of adpressed pectoral fin. Inner mental barbel, when stretched parallel to main body axis, finishing between verticals through posterior limit of branquiostegal membrane distal limit and a point slightly posterior to that. Supraoccipital process narrow, subrectangular, tapered at its distal point. Dorsal lamina of Weber complex vertebrae of medium height, reaching the supraoccipital process just at its anteriormost part. Branchiostegal rays 8 (1).

Dorsal fin triangular, distal margin convex, short (second branched dorsal-fin ray five times in SL). Without the filament, dorsal fin reaches between half to terminus of adpressed pelvic fin. When present, filament can reach between last fourth of adpressed pelvic fin to first fourth of adpressed anal fin. Dorsal fin with I,6 (4) plus anteriormost spinelet. Distance between terminus of dorsal-fin base and adipose-fin origin roughly the same as dorsal-fin base. Anteriormost dorsal-fin pterygiophore inserted posterior to neural spine of vertebrae 4 (3); posteriormost dorsal-fin pterygiophore located ahead of neural (or pseudoneural) spine of vertebrae 11* (2) or 12 (1). Unbranched dorsal-fin ray mostly ossified as a spine, rigid part curved and may present a filamentous prolongation. When filament is absent, dorsal-fin spine relatively short (a third shorter than first dorsal-fin total length); when filament is present, it is at least two times the spine. Dorsal-fin spine bears smooth serrae at its anterior distal half.

Pectoral-fin rays I,8 (4), pectoral fin triangular with concave distal border. First pectoral-fin ray curved, with proximal part rigid, forming a spine (Fig. 72) and short distal tip

flexible and distinctly segmented. Pectoral-fin spine six to seven and half times in SL. Anterior margin of pectoral-fin spine with small straight dentations along its basal half and serrae along its distal third. Posterior margin of pectoral-fin spine bearing 9–12 straight to retrorse dentations along its basal half to two-thirds. These dentations are triangular, the 2–3 distalmost have a broader base, are smaller and straighter. Also sometimes 2–3 unossified distal dentations, not counted.

Pelvic-fin rays I,5 (4), extended pelvic fin triangular with straight distal border. Anterior portion of pelvic-fin base between verticals through dorsal-fin terminus and last fourth of adpressed dorsal fin. Tip of adpressed pelvic fin between verticals through adipose fin origin and its first tenth. First unbranched and flexible ray distinctly shorter than second and third rays, second branched ray the longest; remaining rays progressively shorter.

Anal-fin rays v,7 (1); vi,7 (1); v,8 (1) or iv,11* (1); distal border of extended anal fin convex. Two or three anteriormost anal-fin rays vestigial, unsegmented, embedded in thick skin fold. Anal fin origin between verticals through first fifth to third of adipose-fin base; anal-fin adpressed terminus at adipose fin terminus. Tip of anteriormost anal-fin pterygiophore inserted posterior to hemal spine of vertebrae 22 (3*). Tip of posteriormost anal-fin pterygiophore inserted ahead of hemal spine of vertebrae 29 (2) or 30* (1).

Adipose fin more than three and half times in SL, forming ascending elevated curve in lateral profile, with deepest point approximately at its half. Adipose fin emerging gradually, its posterior limit as a rounded, free lobe. Adipose-fin origin at vertical through vertebral centra 20 (1)–22* (1); adipose-fin terminus at vertical through vertebral centra 35* (2)– 36 (1).

Caudal fin deeply forked, lobes damaged. Caudal peduncle length posterior to adipose-fin slightly longer than its depth. Dorsal lobe with 7 (4) branched, 1 (4) unbranched principal and 9 (1)–16* (1) procurrent fin-rays. Ventral lobe with 8 (4) branched, 1 (4) unbranched principal and 16 (1)–21 (1) (holotype 17) procurrent fin-rays. Hypural 5 completely free, not fused to hypural 3+4. Median caudal-fin rays not articulated directly to caudal plate. Seven (3) rays articulated to dorsal caudal-fin plate (5 on hypurals 3+4 and 2 on hypural 5) and 8 (3) rays articulated to ventral caudal-fin plate (6 on hypurals 1+2 and 2 on parahypural).

Total vertebrae 41 (1)– 42* (2). Ribs 9* (1)– 10 (2).

One single opening of epiphyseal branch of lateral sensory canal on head, on S6 pore, after a small tube that connects both contralateral S6 branches.

Coloration in alcohol

Background body coloration yellowish to light brown. Ventral region of head and body lighter. Dark brown midlateral stripe (Fig. 73), wide, extending from snout to caudal-fin origin. Paired dark brown stripes, not well-delimited, along supraoccipital process running dorsal region of body until posterior region of adipose-fin base. Cephalic dark brown pigment along posterior fontanel region. Dorsal fin overall dark brown, except by a hyaline stripe near its base.

Geographic distribution

Pimelodella griffini was described from mountain rills near Sapucay, Paraguay, in Lower Paraguay basin. It is known from region 343 (Paraguay).

Comments

Pearson (1924) and Fowler (1940b) suggested *P. griffini* occurs in Beni basin, what is probably wrong. I observed material of Madeira-Mamoré-Madre de Dios basin, which has a paired brown stripe, along dorsal region of body (Bockmann & Slobodian, 2013: 65), and could have been confused with *P. griffini*. However, what we called *Pimelodella* sp. N has longer adipose fin, longer maxillary barbel, and different ornamentation on pectoral-fin spine, and probably is *P. gracilis*.

Castello (1969) suggested *P. griffini* occurs in Argentina, as also part of Paraguay basin, in Rio Bermejo. However, his description of the specimens observed include a long adipose fin, and longer barbels than the ones of *P. griffini*. Therefore, I suggest Castello (1969) specimens were, probably, *P. gracilis*, and subsequent articles following him for the occurrence of *P. griffini* in Argentina (*e.g.* Lopez *et al.*, 2003; Mirande & Koerber, 2015) are incorrect.

What Souza-Shibatta *et al.* (2013) identified as *P. griffini* I believe is, in fact, *P. taeniophora*, and will be treated in this species section. *Pimelodella griffini* differs from *P. taeniophora* by a smaller adipose fin (23.3–23.6% SL *vs.* 34.4–40.8% SL in *P. taeniophora*), shorter maxillary barbel (54.9–61% SL *vs.* 73.9–115.5% SL in *P. taeniophora*), and pectoral-fin spine morphology (anterior margin of pectoral-fin spine bearing 9–12 straight to retrorse dentations along its basal half to two-thirds, these dentations are triangular, the 2–3 distalmost have a broader base, are smaller and straighter *vs.* posterior margin of pectoral-fin spine bearing 10–13 retrorse dentations along its basal two-thirds, these dentations are triangular, inclined, the ones nearer base more inclined in *P. taeniophora*).

Material examined

Pimelodella griffini. — FMNH 57974, 1, xr, 67.2 mm SL, holotype, Paraguay, Sapucaí, (Mountain rills near Sapucay), 25°39'25"S, 56°57'18"W; FMNH 57975, 7, xr, 43.8–69.9 mm SL, paratypes, Paraguay, Sapucaí, (Mountain rills near Sapucay), 25°39'25"S, 56°57'18"W; MZUSP 90671, 34, 41.3–50.1 mm SL, Brazil, Mato Grosso, Cáceres, Rio Sepotuba (trecho médio), 15°16'35.0"S, 57°42'50.0"W.

***Pimelodella grisea* (Regan, 1903)**

Pimelodus (*Pimelodella*) *griseus* Regan, 1903: 625–626 [original description; “Durango, Sapayo and Vaqueria Rivers, N.W. Ecuador”]; syntypes: BMNH 1902.5.27.36, 1902.7.29.47, 1902.7.29.58].

Pimelodella grisea. — Eigenmann, 1910: 389 [taxonomic treatment]. — Regan, 1913: 467 [taxonomic treatment]. — Eigenmann, 1917: 252, pl. XXXIII, fig. 2, pl. XXXV, fig. 32–33 [taxonomic revision]. — Eigenmann, 1921b: 514 [taxonomic list]. — Eigenmann, 1922a: 42 [taxonomic treatment]. — Gosline, 1945: 46 [taxonomic treatment]. — Burgess, 1989: 280 [taxonomic treatment]. — Bockmann & Guazzelli, 2003: 418 [taxonomic treatment]. — Mojica *et al.*, 2004: 743 [taxonomic list]. — Leiva, 2005: 49 [taxonomic review]. — Ferraris, 2007: 191 [taxonomic treatment]. — Maldonado-Ocampo *et al.*, 2008: 202 [taxonomic list].

Diagnosis

Pimelodella grisea can be distinguished from all *Pimelodella* species except *P. buckleyi*, *P. geryi*, *P. leptosoma*, *P. metae* and *P. notomelas*, by the presence of dorsal fin distal third extremely dark brown. It differs from *P. buckleyi*, *P. geryi*, *P. leptosoma* and *P. metae* by having 39–41 total vertebrae (*vs.* 41–43 total vertebrae in *P. buckleyi*, *P. geryi* and *P. metae*; 41–44 in *P. leptosoma*). It differs from *P. notomelas* by having maxillary barbel reaching between half of adpressed pelvic fin and anal fin adpressed terminus (*vs.* maxillary barbels always surpassing caudal-fin origin in *P. notomelas*). Furthermore, *P. grisea* can be diagnosed by maxillary barbel reaching between half of adpressed pelvic fin and anal fin adpressed terminus; dorsal lamina of Weberian complex vertebrae high, reaching the supraoccipital process along all its length; posterior margin of pectoral-fin spine bearing 12–15 retrorse dentations along all margin but distal fourth, these dentations are large, pointed, hook-like; adipose fin short, three to almost four times in SL; 39–41 total vertebrae; dark brown midlateral stripe, average width, extending from snout to caudal-fin origin; distal half of dorsal fin dark brown.

Description

Measurements in Table 26. Body deep, depth at dorsal-fin origin five times in standard length, and wide, body width at dorsal-fin origin four to six times in SL (Fig. 74). Dorsal profile straight to slightly convex from snout to dorsal fin, concave from dorsal to adipose fin, slightly convex along adipose fin, and concave along the caudal peduncle. Ventral profile of body slightly convex from snout to branchiostegal membrane, convex between pectoral end pelvic fins, slightly concave from pelvic to anal fin, and also concave from there along the caudal peduncle.

Pseudotympanum large, oval, above posterior process of cleithrum and reaching the straight line of 6th (3). Posterior process of cleithrum triangular, its dorsal border slightly concave. Axillary pore conspicuous, ventral to posterior process of cleithrum, near the base of pectoral fins. Anus and urogenital papilla adjacent. Urogenital papilla tubular, triangular, short. Anus at vertical through half adpressed pelvic fin; urogenital papilla between verticals through last fifth or fourth of adpressed pelvic fin.

Head deep, depth at supraoccipital-process base two times in head length. Mouth sub terminal. Eye slightly elliptical, four and half to five times in head length. Bony interorbital distance large larger than eye diameter. Barbels thin, depressed, and elliptical in cross-section. Maxillary barbel reaching between half of adpressed pelvic fin and end anal fin adpressed terminus. Outer mental barbel, when stretched parallel to main body axis, finishing between half and last third of adpressed pectoral fin. Inner mental barbel, when stretched parallel to main body axis, finishing at pectoral-fin origin. Supraoccipital process slightly triangular, and tapered at its distal point. Dorsal lamina of Weberian complex vertebrae high, reaching the supraoccipital process along all its length. Branchiostegal rays 6* (2)–7 (1).

Dorsal fin triangular, distal margin concave, short (second branched dorsal-fin ray five or more times in SL) reaching between the verticals through half and last third of adpressed pelvic fin. Dorsal fin with I,6 (3) plus anteriormost spinelet. Distance between terminus of dorsal-fin base and adipose-fin origin larger than dorsal-fin base. Anteriormost dorsal-fin pterygiophore inserted posterior to neural spine of vertebrae 4 (3); posteriormost dorsal-fin pterygiophore located ahead of neural (or pseudoneural) spine of vertebrae 11* (1) or 12 (2). Unbranched dorsal-fin ray mostly ossified as a spine, rigid part of relatively medium length (approximately a fourth shorter than the first dorsal-fin ray total length) with smooth serrae at its anterior distal third.

Pectoral-fin rays I,8 (3), pectoral fin triangular with concave distal border. First pectoral-fin ray curved, with proximal part rigid (Fig. 75), forming a spine and short distal tip

flexible and distinctly segmented. Pectoral-fin spine five to six times in SL. Anterior margin of pectoral-fin spine with straight to antrorse dentations along the basal three fourths of margin, and distal fourth with serrae (usually the distalmost ones more antrorse, and the ones from basal half straighter). Posterior margin of pectoral-fin spine bearing 12–15 retrorse dentations along all margin but distal fourth. These dentations are large, pointed, hook-like. Also, 2–3 unossified distal dentations, not counted.

Pelvic-fin rays i,5 (3), extended pelvic fin triangular with straight distal border. Pelvic-fin origin at vertical through last fourth of dorsal-fin base. Tip of adpressed pelvic fin between verticals through adipose fin origin or slightly posterior to that. First unbranched and flexible ray distinctly shorter than second and third rays, which are subequal; remaining rays progressively shorter.

Anal-fin rays v,9* (2) or iv,10 (1); distal border of extended anal fin convex. Two or three anteriormost anal-fin rays vestigial, unsegmented, embedded in thick skin fold. Anal fin origin between verticals through first fifth to third of adipose-fin base; anal-fin adpressed terminus slightly anterior to vertical adipose-fin terminus. Tip of anteriormost anal-fin pterygiophore inserted posterior to hemal spine of vertebrae 19* (2) or 21 (1). Tip of posteriormost anal-fin pterygiophore inserted ahead of hemal spine of vertebrae 27* (1) or 29 (2).

Adipose fin three to almost four times in SL, forming ascending elevated curve in lateral profile, with deepest point approximately at last third. Adipose fin emerging gradually, its posterior limit as a rounded, free lobe. Adipose-fin origin at vertical through vertebral centra 21* (2) to 24 (1); adipose-fin terminus at vertical through vertebral centra 33* (1) to 35 (1).

Caudal fin deeply forked, lobes subequal or dorsal lobe slightly longer. Caudal peduncle length posterior to adipose-fin slightly longer than its depth. Dorsal lobe with 7 (3) branched, 1 (9) unbranched principal and 16 (1)–21* (2) procurrent fin-rays. Ventral lobe with 8 (3) branched, 1 (9) unbranched principal and 16 (1)–23* (2) procurrent fin-rays. Hypural 5 completely free, not fused to hypural 3+4. Median caudal-fin rays not articulated directly to caudal plate. Six* (1) or 7 (2) rays articulated to dorsal caudal-fin plate (4–5 on hypurals 3+4 and 2 on hypural 5) and 7* (1) or 8 (2) rays articulated to ventral caudal-fin plate (5–6 on hypurals 1+2 and 2 on parahypural).

Total vertebrae 39* (1)–41 (1). Ribs 9 (3).

Epiphyseal branch of laterosensory canal on head (S6) with contralateral canals connected, emerging as a single pore, right after the connection of both canals, or two pores close to each other.

Coloration in alcohol

Background body coloration yellowish. Ventral region of head and body lighter. Dark brown midlateral stripe (Fig. 76), average width, extending from snout to caudal-fin origin. Distal half of dorsal fin dark brown.

Geographic distribution

Pimelodella grisea was described based on three syntypes, from rivers Durango, Sapayo and Vaqueria, in coastal drainages on Northwestern Ecuador. It is known from region 301 (North Andean Pacific Slopes), in Ecuador and Colombia.

Comments

Regan (1903) *Pimelodella grisea* original description is based in a single specimen, of 140 mm TL. From the syntypes, the one nearest to this total length is BMNH 1902.7.29.47, which, however, is the one in worst preservation condition. Therefore, I hereby designate BMNH 1902.5.27.36 as the lectotype, and remaining specimens as paralectotype. In this manner, the type-locality is going to be “Rio Durango, N.W. Ecuador, in conformation with BMNH 1902.5.27.36 label.

Pimelodella grisea is syntopic with *P. eutaenia*, found both species in USNM 76926.

Material examined

Pimelodella grisea. — BMNH 1902.5.27.36, 1, xr, 119.7 mm SL, lectotype, Ecuador, Rio Durango, 1°05'09"N, 78°41'44"W; BMNH 1902.7.29.47, 1, xr, 116.8 mm SL, paralectotype, Ecuador, Rio Vaqueria, 1°12'22"N, 79°02'41"W; BMNH 1902.7.29.58, 1,xr, 99.7 mm SL, paralectotype, Ecuador, Rio Sapayo, 0°46'58"N, 78°58'46"W; USNM 177241, 1, 59.9 mm SL, Ecuador, Rio Chimbo, Near Bucay, Prov. Guayas, W. Foot Andes, 2°07'12.0"S 79°41'24.1"W.

***Pimelodella harttii* (Steindachner, 1877)**

Pimelodus (Pseudorhamdia) harttii Steindachner, 1877: 611–614 [original description; “Rio Parahyba”, Paraíba do Sul river, Brazil; holotype: NMW 45784].

Pimelodella harttii. — Eigenmann & Eigenmann, 1888: 133 [taxonomic treatment]. — Eigenmann & Eigenmann, 1890: 158 [key to *Pimelodella* species; taxonomic revision]. — Eigenmann & Eigenmann, 1891: 29 [taxonomic treatment]. — Fowler, 1951: 542 [taxonomic treatment].

Pimelodella hartii. — Eigenmann, 1910: 389 [taxonomic treatment, misspelling]. — Bockmann & Guazzelli, 2003: 418 [taxonomic treatment, misspelling]. — Ferraris, 2007: 191 [taxonomic treatment, misspelling].

Rhamdia harttii. — Miranda Ribeiro, 1911: 270–271 [taxonomic treatment].

Pimelodella hartti. — Eigenmann, 1917: 248–249 [taxonomic treatment, misspelling]. — Gosline, 1945: 45 [taxonomic treatment, misspelling]. — Burgess, 1989: 280 [taxonomic treatment, misspelling].

Diagnosis

Pimelodella harttii can be diagnosed from all *Pimelodella* species with exception of *P. australis*, *P. avanhandavae*, *P. chagresi*, *P. elongata*, *P. griffini*, *P. grisea*, *P. ignobilis*, *P. kronei*, *P. laticeps*, *P. linami*, *P. meeki*, *P. modesta*, *P. pectinifera*, *P. spelaea* and *P. straminea* by having the maxillary barbel reaching between half and terminus of adpressed pelvic fin (*vs.* surpassing anal fin origin in all other species). It differs from *P. chagresi*, *P. elongata*, *P. grisea*, *P. ignobilis*, *P. modesta*, *P. pectinifera* and *P. spelaea* by having the dorsal fin basal portion dark pigmented, followed by a hyaline stripe, and distal part dark colored (*vs.* completely dark pigmented in *P. chagresi*; basal portion of dorsal fin base hyaline, and distal dark pigmented in *P. elongata*, *P. grisea*, *P. ignobilis* and *P. modesta*; dorsal fin completely hyaline in *P. pectinifera* and *P. spelaea*). It differs from *P. australis*, *P. laticeps*, *P. linami*, *P. meeki* and *P. straminea* by having 42 total vertebrae (41 or less total vertebrae in *P. australis*, *P. laticeps*, *P. linami*, *P. meeki* and *P. straminea*). It differs from *P. avanhandavae*, *P. griffini* and *P. kronei* by having the supraoccipital process of moderate width and triangular (*vs.* supraoccipital process narrow and subrectangular in *P. avanhandavae* and *P. griffini*; supraoccipital process narrow and triangular in *P. kronei*).

Furthermore, *P. harttii* can be diagnosed by maxillary barbels reaching between half and terminus of adpressed pelvic fin; posterior margin of pectoral-fin spine with 10–12 retrorse dentations, from region just beyond base of spine to or slightly short of the last third of spine, these dentations are subtriangular, the ones near the base of spine more hook-like, progressively triangular and with broader bases towards distal of spine; adipose fin short, more than three and half times in SL; dark brown midlateral stripe with moderated width, well-delimited, extending from snout or posterior to orbit until caudal-fin origin; paired dark brown area along supraoccipital process.

Description

Measurements in Table 27. Body of moderate depth, depth at dorsal-fin origin five times in standard length; and average width, body width at dorsal-fin origin five and half times in SL (Fig. 77). Dorsal profile slightly concave from snout to dorsal fin, straight from dorsal to adipose fin and along adipose extension, and concave along the caudal peduncle. Ventral profile of body straight from snout to branchiostegal membrane, slightly concave from this point to pelvic fin, and roughly straight from pelvic along the caudal peduncle.

Pseudotympanum large, oval, dorsal to posterior process of cleithrum and reaching the straight line of 6th (1) vertebrae. Posterior process of cleithrum triangular, concave. Anus and urogenital papilla adjacent. Urogenital papilla tubular, triangular, short. Anus vertical through second fifth of adpressed pelvic fin; urogenital papilla at the vertical through the last fourth of adpressed pelvic fin.

Head depressed, depth at supraoccipital-process base more than two and half times in head length. Mouth sub terminal. Eye slightly elliptical, five times in head. Bony interorbital distance roughly equal to eye diameter. Barbels thin, slightly depressed and elliptical in cross-section. Maxillary barbels reaching between half and terminus of adpressed pelvic fin. Outer mental barbel, when stretched parallel to main body axis, finishing between pectoral-fin terminus and half adpressed pectoral fin. Inner mental barbel, when stretched parallel to main body axis, finishing slightly ventral limit of branchiostegal membrane. Supraoccipital process triangular. Dorsal lamina of Weber complex vertebrae of medium height, reaching the supraoccipital process just at its anteriormost part. Branchiostegal rays 7 (1).

Dorsal fin triangular, distal margin concave, short (first dorsal-fin ray five times in SL), reaching the vertical through last third of adpressed pelvic fin. Dorsal fin with I,6 (1) plus anteriormost spinelet. Distance between terminus of dorsal-fin base and adipose-fin origin larger than dorsal-fin base. Anteriormost dorsal-fin pterygiophore inserted posterior to neural spine of vertebrae 4 (1); posteriormost dorsal-fin pterygiophore located ahead of neural (or pseudoneural) spine of vertebrae 11 (1). Unbranched dorsal-fin ray mostly ossified as a spine, rigid part of relatively medium length (approximately a fourth shorter than the first dorsal-fin ray total length). Distal third of dorsal-fin spine anterior margin with smooth serrae.

Pectoral-fin rays I,7 (1), pectoral fin triangular with concave distal border. First pectoral-fin ray curved, with proximal part rigid (Fig. 78), forming a spine and short distal tip flexible and distinctly segmented. Pectoral-fin spine five and half times in SL. Anterior margin of pectoral-fin spine with smooth straight to antrorse dentations along its basal half, and smooth serrae along its distal third. Posterior margin of pectoral-fin spine with 10–12

retorse dentations, from region just beyond base of spine to or slightly short of the last third of spine, plus sometimes 1–2 unossified distalmost dentations, not counted. Those dentations are subtriangular, the ones near the base of spine more hook-like, progressively triangular and with broader bases towards distal of spine.

Pelvic-fin rays i,5 (1), extended pelvic fin triangular with straight distal border. Pelvic-fin origin at vertical through last third of adpressed dorsal fin. Tip of adpressed pelvic fin at vertical through the anterior limit of adipose fin. First unbranched and flexible ray distinctly shorter than second and third rays, third ray the longest; remaining rays progressively shorter.

Anal-fin rays v,9 (1); distal border of extended anal fin convex. Three anteriormost anal-fin rays vestigial, unsegmented, embedded in thick skin fold. Anal fin origin at vertical through first fourth of adipose-fin base. Anal-fin adpressed terminus anterior to vertical through adipose-fin terminus. Tip of anteriormost anal-fin pterygiophore inserted posterior to hemal spine of vertebrae 21 (1). Tip of posteriormost anal-fin pterygiophore inserted ahead of hemal spine of vertebrae 30 (1).

Adipose fin short, more than three and half times in SL, forming ascending elevated curve in lateral profile, with deepest point approximately midlength. Adipose fin emerging gradually, its posterior limit as a rounded, free lobe. Adipose-fin origin at vertical through vertebral centrum 22 (1); adipose-fin terminus at vertical through vertebral centrum 36 (1).

Caudal fin deeply forked, with upper lobe slightly deteriorated, but possibly longer than ventral lobe. Caudal peduncle length posterior to adipose fin longer than its depth. Dorsal lobe with 7 (1) branched, 1 (1) unbranched principal and 19 (1) procurrent fin-rays. Ventral lobe with 8 (1) branched, 1 (1) unbranched principal and 21 (1) procurrent fin-rays. Hypural 5 completely free, not fused to hypurals 3+4. Median caudal-fin rays not attached directly to caudal plate. Seven (1) rays articulated to dorsal caudal-fin plate (5 on hypurals 3+4 and 2 on hypural 5) and 8 (1) rays articulated to ventral caudal-fin plate (6 on hypurals 1+2 and 2 on parahypural).

Total vertebrae 42 (1). Ribs 8 (1).

Epiphyseal branch of laterosensory canal in head (S6) with contralateral canals connected, emerging as a single pore right after the connection of the two contralateral canals.

Coloration in alcohol

Background body coloration yellowish. Ventral region of head and body lighter. Dark brown midlateral stripe with moderated width (Fig. 79), well-delimited, extending from snout or posterior to orbit until caudal-fin origin. Paired dark brown area along supraoccipital

process. Cephalic dark brown pigment along posterior fontanel. Dorsal-fin with dark brown pigment near base, followed by hyaline stripe, and distal half of dorsal fin dark brown.

Geographic distribution

Pimelodella harttii was described from Rio Paraíba do Sul, in Southeastern Atlantic basin. It is known from regions 328 (Northeastern Mata Atlântica) and 329 (Paraíba do Sul).

Comments

Pimelodella harttii was described based on one specimen in the same article Steindachner (1877) described *P. brasiliensis*, also from Paraíba do Sul River. Both species share similarities in morphometrics and body shape, with exception of barbels length (longer in *P. brasiliensis*) and the pectoral-fin spine (posterior margin of pectoral-fin spine with 10–18 minute, retrorse to straight dentations, from region just beyond base of spine to slightly short of the last fourth of spine in *P. brasiliensis*; and spine with 10–12 retrorse, triangular dentations, from region just beyond base of spine to or slightly short of the last third of spine). It is possible that *P. harttii* is a junior-synonym of *P. brasiliensis*, but both species were maintained as valid before the observation of more comparative material.

Material examined

Pimelodella harttii. — NMW 45784, 1, xr, 150.2 mm SL, holotype, Brazil, "Rio Parahyba" (probably Paraíba do Sul), 22°31'06"S, 44°41'49"W; MZUSP 108489, 3, 65.3–87.9 mm SL, Brazil, Minas Gerais, Teófilo Otoni, Rio Todos os Santos, affluent to Rio Mucuri, next to COPASA water capture, 17°52'11.0"S, 41°32'5.0"W.

***Pimelodella hasemani* Eigenmann, 1917**

Pimelodella lateristriga [non Lichtenstein, 1823]. — Eigenmann & Eigenmann, 1888: 133 (*in partim*) [taxonomic treatment]. — Eigenmann & Eigenmann, 1890: 156 (*in partim*) [taxonomic treatment].

Pimelodella hasemani Eigenmann, 1917: 241–242, pl. XXX, fig. 7, pl. XXXV, fig. 2–3 [original description; “San Antonio de Rio Madeira”, Brazil; holotype: FMNH 57980 (formerly CM 6968a)]. — Fowler, 1940: 77 [taxonomic treatment, comparison with *P. chaparae*]. — Eigenmann & Allen, 1942: 43, 48, 53, 100 [taxonomic list, taxonomic treatment]. — Gosline, 1945: 44 [taxonomic treatment]. — Fowler, 1951: 542–543 [taxonomic treatment]. — Saul, 1975: 116 [ecology]. — Henn, 1977: 67 [type catalog]. — Ortega & Vari, 1986: 14 [taxonomic list]. — Ibarra & Stewart, 1987: 66 [type catalog]. — Burgess, 1989: 280 [taxonomic treatment]. — Bockmann &

Guazzelli, 2003: 419 [taxonomic treatment]. — Ferraris, 2007: 192 [taxonomic treatment]. — Maldonado-Ocampo *et al*, 2008: 202 [taxonomic list].

Pimelodella howesi [non Fowler, 1940]. — Bockmann & Slobodian, 2013: 61 (*in partim*), unnum. fig., fig. 36.1D [taxonomic treatment].

Diagnosis

Pimelodella hasemani differs from all *Pimelodella* except *P. australis*, *P. boliviana*, *P. coquetaensis*, *P. figueroai*, *P. laticeps*, *P. martinexi*, *P. megalops*, *P. notomelas*, *P. reyesi*, *P. straminea* and *P. tapatapae* by having the epiphyseal branch of laterosensory canal on head emerging as two separate pores, far apart (state unknown in *P. coquetaensis*, *P. figueroai*, *P. martinexi*, *P. reyesi* and *P. tapatapae*). It differs from *P. australis*, *P. figueroai*, *P. laticeps*, *P. notomelas*, *P. reyesi* and *P. straminea* by having the dorsal fin basal portion hyaline, and distal portion darkly pigmented (*vs.* dorsal fin completely hyaline in *P. figueroai* and *P. reyesi*; dorsal fin with basal portion dark pigmented, followed by a hyaline stripe, and distal portion hyaline in *P. australis*, *P. laticeps*, *P. notomelas* and *P. straminea*). It differs from *P. boliviana*, *P. coquetaensis* and *P. tapatapae* by having 42–43 total vertebrae (*vs.* 41 or less vertebrae in *P. coquetaensis* and *P. tapatapae*; 44 total vertebrae in *P. boliviana*). It differs from *P. martinexi* and *P. megalops* by the supraoccipital process of moderate width and triangular (*vs.* narrow and rectangular in *P. martinexi* and *P. megalops*).

Furthermore, *P. hasemani* can be diagnosed by maxillary barbel reaching between verticals through first fourth and anal-fin terminus; dorsal lamina of Weberian complex vertebrae high, reaching the supraoccipital process along all its extension; posterior margin of pectoral-fin spine bearing 10–17 retrorse dentations along its basal half to four fifths; these dentations are triangular, large, hook-like; adipose fin short, three to four times in SL; caudal fin deeply forked, ventral lobe longer; 42–43 total vertebrae; epiphyseal branch of laterosensory canal emerging as two separate pores, far apart; dark brown midlateral stripe, narrow to average width not well-delimited, posterior to head or pseudotympanum to caudal-fin origin.

Description

Measurements in Table 28. Body of moderate depth, depth at dorsal-fin origin five and half to six times in standard length, and compressed, body width at dorsal-fin origin six to nine times in SL (Fig. 80). Greatest body depth at dorsal-fin origin. Dorsal profile convex from snout to dorsal fin, slightly concave from dorsal to adipose fin, slightly convex along adipose fin, and concave along caudal peduncle. Ventral profile of body slightly convex from

snout to branquiostegal membrane, and from there to pectoral fin, slightly concave between pectoral end pelvic fin, and concave from pelvic along the caudal peduncle.

Pseudotympanum large, oval, dorsal to posterior process of cleithrum and reaching 6th*(3)–7th (5) vertebrae. Posterior process of cleithrum triangular, its dorsal border slightly concave. Anus and urogenital papilla adjacent. Urogenital papilla tubular, triangular, short. Anus between verticals through first fourth and third of adpressed pelvic fin; urogenital papilla finishing at vertical through last third of adpressed pelvic fin.

Head depressed, depth at supraoccipital-process base two to three times in head length. Mouth sub terminal. Eye slightly elliptical, slightly more than three to four times in head length. Bony interorbital distance half eye diameter. Posterior nare nearer eyes than snout. Barbels thin, slightly depressed and elliptical in cross-section. Maxillary barbel reaching between verticals through first fourth and anal-fin terminus. Outer mental barbel, when stretched parallel to main body axis, finishing between verticals through half adpressed pectoral fin and slightly posterior to its adpressed terminus. Inner mental barbel, when stretched parallel to main body axis, finishing between verticals through branchiostegal membrane ventral limit and pectoral-fin terminus. Supraoccipital process triangular to subrectangular, distally tapered. Dorsal lamina of Weberian complex vertebrae high, reaching the supraoccipital process along all its extension. Branchiostegal rays 7 (1).

Dorsal fin triangular, distal margin convex, moderated length (second branched dorsal-fin ray five to six times in SL), depressed tip finishing between verticals through last fourth and adpressed pelvic-fins terminus. Dorsal fin with I,6 (10) plus anteriormost spinelet. Distance between terminus of dorsal-fin base and adipose-fin origin the same or slightly larger than dorsal-fin base. Anteriormost dorsal-fin pterygiophore inserted posterior to neural spine of vertebrae 4 (9); posteriormost dorsal-fin pterygiophore located ahead of neural (or pseudoneural) spine of vertebrae 11 (9). Unbranched dorsal-fin ray mostly ossified as a spine, rigid part relatively long (usually less than a fourth shorter than the first dorsal-fin total length), straight, with smooth serrae at its anterior distal fourth and small, straight to retrorse dentations along almost all posterior margin.

Pectoral-fin rays I,7 (3)–I,8* (4), pectoral fin triangular with concave distal border. First pectoral-fin ray curved, with proximal part rigid, forming a spine (Fig. 81), and short distal tip flexible and distinctly segmented. Pectoral-fin spine long, four and half to six times in SL. Anterior margin of pectoral-fin spine with small, well delimited, straight dentations along almost all margin, except by distal fourth, which was serrae. Posterior margin of pectoral-fin spine bearing 10–17 retrorse dentations along its basal half to four fifths. These

dentations are triangular, large, hook-like. Also, sometimes 1–3 distalmost unossified dentations, not counted.

Pelvic-fin rays i,5 (7), extended pelvic fin triangular with straight distal border. Pelvic-fin origin between verticals through last sixth and terminus of dorsal-fin base. Tip of adpressed pelvic fin through vertical of adipose fin origin or slightly posterior. First unbranched and flexible ray distinctly shorter than second and third rays, which are the longest and roughly the same size; remaining rays progressively shorter.

Anal-fin rays iv,7 (3); v,7 (1); iv,8* (4); v,8 (1) or v,10 (1); distal border of extended anal fin convex. Two or three anteriormost anal-fin rays vestigial, unsegmented, embedded in thick skin fold. Anal fin origin at vertical through first fourth to third of adipose fin; anal-fin adpressed terminus at vertical through adipose-fin terminus or slightly posterior. Tip of anteriormost anal-fin pterygiophore inserted posterior to hemal spine of vertebrae 21 (1), 22 (2) or 23* (6). Tip of posteriormost anal-fin pterygiophore inserted ahead of hemal spine of vertebrae 28 (1), 29 (2), 30* (5) or 31 (1).

Adipose fin three to four times in SL, forming ascending elevated curve in lateral profile, with deepest point approximately midlength. Adipose fin emerging gradually, its posterior limit as a rounded, free lobe. Adipose-fin origin at vertical through vertebral centra 17 (1)– 22 (1) (holotype 20); adipose-fin terminus at vertical through vertebral centra 35 (4)– 37 (1) (holotype 36).

Caudal fin deeply forked, ventral lobe longer. Caudal peduncle length posterior to adipose fin almost twice to its depth. Dorsal lobe with 7 (10) branched, 1 (10) unbranched principal and 13 (1)–19* (1) procurrent fin-rays. Ventral lobe with 8 (10) branched, 1 (10) unbranched principal and 12 (1)– 18 (1) (holotype 14) procurrent fin-rays. Hypural 5 completely free, not fused to hypural 3+4. Median caudal-fin rays not articulated directly to caudal plate. Seven (8) rays articulated to dorsal caudal-fin plate (5 on hypurals 3+4 and 2 on hypural 5) and 8* (7), rarely 9 (1) rays articulated to ventral caudal-fin plate (6 or 7 on hypurals 1+2 and 2 on parahypural).

Total vertebrae 42* (4)– 43 (5). Ribs 8 (6).

Epiphyseal branch of laterosensory canal (S6) with contralateral canals emerging separately, as two pores, far apart.

Coloration in alcohol

Background body coloration yellowish. Ventral region of head and body lighter. Dark brown midlateral stripe, narrow to average width (Fig. 28), not well-delimited, posterior to head or pseudotympanum to caudal-fin origin. Dorsal region of head and body with scattered

brown melanophores, especially between dorsal and adipose fins. Cephalic dark brown pigment along posterior fontanel. Distal half of dorsal-fin dark brown.

Geographic distribution

Pimelodella hasemani was described based on materials from Rio Madeira, Rio Iça and Rio Jutai (tributaries of Rio Solimões), and a Rio Amazonas tributary at Obidos, Pará State, Brazil. It is known from regions 316 (Amazonas Lowlands), 318 (Mamoré-Madre de Díos) and 319 (Guaporé-Itenez).

Comments

In MCZ 7502, the specimen with 33.1 mm SL is a *Pimelodus* sp.

The type series of *P. hasemani* is somewhat broadly distributed in Madeira and Amazon basin. Observing the specimens, they are much alike, including the osteological features observed in radiographs. However, I have not found comparative material of *P. hasemani* from regions other than Madeira-Mamoré-Guaporé basins, and believe its distribution into further east of Amazon basin, as assigned by the locality of Óbidos, Pará, is at least suspicious.

Part of the material identified as *P. howesi* by Bockmann & Slobodian (2013) is, in fact, *P. hasemani* (Fig. 83). The authors suggest specimens with less than 55.0 mm SL of *P. howesi* have a different aspect, with narrower dark midlateral stripe and larger dentations on pectoral-fin (Bockmann & Slobodian, 2013: 61). I observed again this material and part of it is *P. howesi* (e.g. UFRO-I 9745), meanwhile part is *P. hasemani* (UFRO-I 9741).

Saul (1975) studied ecological aspects of some siluriforms, and reported *P. hasemani* swims in moderated-flowing streams, particularly common over sand and mud bottoms free of vegetation, but also present over rock and gravel bottoms, feeding on small invertebrates and plants. Despite there is not a secure way to identify if what Saul (1975) studied was *P. hasemani*, other studies on *Pimelodella* species found similar results (e.g. Soares-Porto, 1994; Mazzoni *et al.*, 2010; Moraes *et al.*, 2013).

Material examined

Pimelodella hasemani. — FMNH 57980, 1, xr, 60.6 mm SL, holotype, Brazil, Rondônia, Porto Velho, "San Antonio de Rio Madeira", 8°46'08"S, 63°54'25"W; CAS 75823, 3, paratypes, Brazil, Amazonas, Rio Iça; Rio Putomajo, Rio Içá (tributary of Rio Solimoes near the Brazilian-Colombian border. In Colombian territory, Rio Içá is called Rio Putomayo), 3°7'S, 67°58'W; MCZ 7502, 3, 35.6–40.2 mm SL, paratypes, Brazil, Pará, Óbidos (Rio Amazonas at Obidos), 1°52'S, 55°30'W; MCZ 7572, 1, xr, 50.9 mm SL,

paratype, Brazil, Amazonas, Rio Hyutahy (Rio Jutai, tributary of Rio Solimoes), 2°43'S, 66°57'W; MCZ 7577, 49, 35.1–50.1 mm SL, paratypes, Brazil, Amazonas, Rio Ica; Rio Putomajo, Rio Içá (tributary of Rio Solimoes near the Brazilian-Colombian border. In Colombian territory, Rio Içá is called Rio Putomayo), 3°7'S, 67°58'W; MCZ 7579, 2, 50.1–55.5 mm SL, Brazil, Pará, Óbidos (Rio Amazonas at Obidos), 1°52'S, 55°30'W; MCZ 7580, 9, xr, 37.0–54.2 mm SL, paratypes, Brazil, Pará, Óbidos (Rio Amazonas at Obidos), 1°52'S, 55°30'W; MCZ 7581, 1, xr, 39.1 mm SL, paratype, Brazil, Pará, Óbidos (Rio Amazonas at Obidos), 1°52'S, 55°30'W; MZUSP 26186, 6, 33.5–39.1 mm SL, Peru, Ucayali, Prov. Cel. Portillo, Rio Ucayali, Bagazan, 8°24'16.3"S, 74°28'35.1"W; AMNH 230942, 6, Venezuela, Territorio Federal Amazonas, Rio Cuao, beach downstream of raudal del danto, 5°02'37.5"N, 67°33'27.7"W; MZUSP 48977, 1, 53.0 mm SL, Brazil, Rondônia, Rio Machado, Jamarizinho, 8°45'07.8"S, 63°26'57.7"W; UFRO-I 9741, 1, 56.47, Brazil, Amazonas, Nova Olinda Do Norte, Rio Madeira, à montante de Nova Olinda do Norte, 3°56'04"S, 59°12'19"W; USNM 326339, 1, 37.3–54.1 mm SL, Brazil, Mato Grosso, Rio Guapore At Pontes E Lacerda, BR-174, 15°12'00.0"S, 59°21'00.0"W.

***Pimelodella howesi* Fowler, 1940b**

Pimelodella howesi Fowler, 1940b: 77–80, figs. 32–34 [original description; “Boca Chapare, Chimore River, Bolivia”]; holotype: ANSP 69036]. — Gosline, 1945: 46 [taxonomic treatment]. — Fowler, 1951: 543, fig. 557 [taxonomic treatment]. — Böhlke, 1984: 141 [type catalog]. — Burgess, 1989: 280 [taxonomic treatment]. — Bockmann & Guazzelli, 2003: 419 [taxonomic treatment]. — Ferraris, 2007: 192 [taxonomic treatment]. — Bockmann & Slobodian, 2013: 61 (*in partim*), fig. 36.1C [taxonomic treatment].

Diagnosis

Pimelodella howesi differs from all *Pimelodella* species except *P. boliviana*, *P. boschmai*, *P. chagresi*, *P. cristata*, *P. eutaenia*, *P. figueroai*, *P. geryi*, *P. gracilis*, *P. grisea*, *P. hasemani*, *P. laurenti*, *P. macturki*, *P. martinezi*, *P. megalops*, *P. mucosa*, *P. odynea*, *P. peruana*, *P. reyesi*, *P. serrata*, *P. straminea* and *P. taeniophora* by having the dorsal lamina of Weberian complex vertebrae reaching the supraoccipital process along all its extension (state unknown in *P. boschmai*, *P. figueroai*, *P. geryi*, *P. martinezi* and *P. reyesi*). It differs from *P. boschmai*, *P. chagresi*, *P. cristata*, *P. gracilis*, *P. grisea*, *P. laurenti*, *P. macturki*, *P. megalops*, *P. mucosa*, *P. reyesi*, *P. straminea* and *P. taeniophora* by having 43–44 total vertebrae (vs. 42 or less total vertebrae in *P. boschmai*, *P. chagresi*, *P. grisea*, *P. laurenti*, *P.*

macturki, *P. megalops*, *P. mucosa*, *P. reyesi*, *P. straminea*; 46 or more total vertebrae in *P. cristata* and *P. gracilis*). It differs from *P. boliviana*, *P. eutaenia*, *P. geryi*, *P. hasemani* and *P. serrata* by having the epiphyseal branch of laterosensory canal on head with contralateral canals connecting at midline, proceeding posteriorly as a single canal, and opening in a single pore (*vs.* epiphyseal branch of laterosensory canal on head with contralateral canals emerging in two pores far apart in *P. boliviana* and *P. hasemani*; epiphyseal branch of laterosensory canal on head with contralateral canals connecting at midline and immediately emerging as a single pore, or with two pores near each other in *P. eutaenia*, *P. geryi* and *P. serrata*). It differs from *P. figueroai*, *P. odynea* and *P. peruana* by the posterior margin of pectoral fin bearing large, curved dentations along basal two thirds (*vs.* moderate dentations on pectoral fin posterior margin basal three fourths in *P. figueroai*; moderate to large, not notably curved dentations along basal two thirds in *P. odynea*; triangular, broad based dentations along posterior margin three fourths in *P. peruana*). It differs from *P. martinezi* by having a moderate to large midlateral stripe (*vs.* narrow midlateral stripe in *P. martinezi*).

Furthermore, *P. howesi* can be diagnosed by maxillary barbel reaching between last fifth of adipose-fin and surpassing caudal fin origin; dorsal lamina of Weber complex vertebrae high, reaching the supraoccipital process along almost all its extension; dorsal-fin spine with serrae along distal half of its anterior margin, and small, retrorse dentations along distal two thirds of posterior margin; posterior margin of pectoral-fin spine bearing 10–14 retrorse dentations along its basal two thirds, these dentations large, with curved apex, and smaller near base of spine; adipose fin long, two and half to three in SL; 43–44 total vertebrae; dark brown midlateral stripe average width to wide, not well delimited, extending from snout until median caudal-fin rays; ventral lobe of caudal fin might be slightly darker.

Description

Measurements in Table 29. Body of moderated depth, depth at dorsal-fin insertion six to seven times in SL and compressed, more than eighth times in SL (Fig. 84). Greatest body depth at dorsal-fin origin. Dorsal profile convex to straight from snout to dorsal fin, concave from dorsal to adipose fin, slightly convex along adipose fin, and concave along the caudal peduncle. Ventral profile of body slightly convex from snout to branquiostegal membrane, concave between branquiostegal membrane and pectoral-fins, and between pectoral end pelvic fins, slightly concave from pelvic to anal fin, and also concave from there along the caudal peduncle.

Pseudotympanum large, oval, above posterior process of cleithrum and reaching the straight line of 7th (3) vertebrae. Posterior process of cleithrum triangular, broad, its dorsal

border straight. Anus and urogenital papilla adjacent. Urogenital papilla tubular, triangular, short. Anus between verticals through first third and half adpressed pelvic fin; urogenital papilla reaching between verticals through second third and last sixth of adpressed pelvic fins.

Head of average depth, depth at supraoccipital-process base slightly more than two times in head length. Mouth sub terminal. Eye slightly elliptical, five to six times in head length. Bony interorbital distance equal to eye diameter. Barbels thin, slightly depressed and elliptical in cross-section. Maxillary barbel reaching between last fifth of adipose-fin and surpassing caudal fin origin. Outer mental barbel, when stretched parallel to main body axis, finishing between verticals through last fourth of adpressed pectoral fin pelvic fin terminus. Inner mental barbel, when stretched parallel to main body axis, finishing between verticals through half pectoral fin base and half adpressed pectoral fin. Supraoccipital process wide, subrectangular, tapered distally. Dorsal lamina of Weber complex vertebrae high, reaching the supraoccipital process along almost all its extension. Branchiostegal rays 6 (4).

Dorsal fin triangular, distal margin convex, moderated length (second branched dorsal-fin ray five times in SL), depressed tip finishing between last third and adpressed pelvic fin terminus. Dorsal fin with I,6 (6) plus anteriormost spinelet. Distance between terminus of dorsal-fin base and adipose-fin origin narrow, half dorsal fin base. Anteriormost dorsal-fin pterygiophore inserted posterior to neural spine of vertebrae 4 (5); posteriormost dorsal-fin pterygiophore located ahead of neural (or pseudoneural) spine of vertebrae 11 (1) or 12* (4). Unbranched dorsal-fin ray mostly ossified as a spine, approximately a fourth shorter than the first dorsal-fin total length, its tip slightly curved. Dorsal-fin spine with serrae along distal half of its anterior margin, and small, retrorse dentations along distal two thirds of posterior margin.

Pectoral-fin rays I,8 (1) or I,8* (3), pectoral fin triangular with convex distal border. First pectoral-fin ray curved, with proximal part rigid, forming a spine (Fig. 85), and short distal tip flexible and distinctly segmented. Comparatively long spine, four to five times in SL. Anterior margin of pectoral-fin spine with small, straight dentations along its basal half, and serrae along its distal half. Posterior margin of pectoral-fin spine bearing 10–14 retrorse dentations along its basal two thirds, these dentations large, with curved apex, and smaller near base of spine. In smaller specimens the dentations are comparatively bigger, with broader bases and distinctly retrorse, occupying basal half of spine. Also 2–3 unossified distal dentations, not counted.

Pelvic-fin rays i,5 (6), extended pelvic fin triangular with straight distal border. Anterior portion of pelvic-fin base between vertical through last dorsal-fin branched ray and a

point slightly posterior to dorsal fin terminus. Tip of adpressed pelvic fin between verticals through first sixth or fifth of adipose fin. First unbranched and flexible ray distinctly shorter than second and third rays, which are roughly the same size; remaining rays progressively shorter.

Anal-fin rays iv,7 (1); iii,9* (1) or iv,9 (4), distal border of extended anal fin convex. Two anteriormost anal-fin rays vestigial, unsegmented, embedded in thick skin fold. Anal fin origin at vertical through second fifth of adipose fin base; anal-fin adpressed terminus slightly anterior to vertical through adipose-fin terminus. Tip of anteriormost anal-fin pterygiophore inserted posterior to hemal spine of vertebrae 23 (3) or 24* (3). Tip of posteriormost anal-fin pterygiophore inserted ahead of hemal spine of vertebrae 29 (1), 30 (2) or 31* (3).

Adipose fin two and half to three in SL, forming ascending elevated curve in lateral profile, with deepest point at half. Adipose fin emerging gradually, its posterior limit as a rounded, free lobe. Adipose-fin origin at vertical through vertebral centrum 17 (2); adipose-fin terminus at vertical through vertebral centra 35 (1) or 46 (1), forming ascending elevated curve in lateral profile, with deepest point at half. Adipose fin emerging gradually, its posterior limit as a rounded, free lobe. Adipose-fin origin at vertical through vertebral centra 17 (2)– 18* (2).

Caudal fin deeply forked, dorsal lobe longer. Caudal peduncle length posterior to adipose-fin two times its depth. Dorsal lobe with 7 (4) branched, 1 (4) unbranched principal, and 13 (1)– 16* (1) procurrent fin-rays. Ventral lobe with 8 (4), 1 (4) unbranched principal, and 14* (1)– 17 (1) procurrent fin-rays. Hypural 5 completely free, not fused to hypural 3+4. Median caudal-fin rays not articulated directly to caudal plate. Seven* (5) rays articulated to dorsal caudal-fin plate (5 on hypurals 3+4 and 2 on hypural 5) and 8 (4), rarely 9 (1) rays articulated to ventral caudal-fin plate (6 or 7 on hypurals 1+2 and 2 on parhypural).

Total vertebrae 43 (2)– 44* (5). Ribs 8 (1)– 9 (3).

One single opening of epipheseal branch of lateral sensory canal on head, on S6 pore, after a small tube that connects both contralateral S6 branches

Coloration in alcohol

Background body coloration brownish. Ventral region of head and body lighter. Dark brown midlateral stripe (Fig. 86) average width to wide, not well delimited, extending from snout until median caudal-fin rays. Ventral lobe of caudal fin may be slightly darker. Dorsal fin hyaline near base, and light brown along the remaining length of rays.

Geographic distribution

Pimelodella howesi was described from Boca Chapare and Todos Santos, in Chimore and Chapare Rivers, from Upper Mamoré River basin. It is known from areas 313 (Western Amazon Piedmont), 317 (Ucayali-Urubamba Piedmont), 318 (Mamoré- Madre de Dios) and 319 (Guaporé-Itenez) (see comments).

Comments

Part of what Bockmann & Slobodian (2013) identified as *P. howesi* are, in fact, *P. hasemani* (see *P. hasemani* section for more details), what is understandable, since smaller specimens of *P. howesi* have larger eyes, relatively larger dentation on pectoral-fin spine and shorter adipose fin, variation common along the ontogenetical development of a particular species. However, upon examination of the entire type-series of *P. howesi*, which have specimens from 30.7 to 79.3 mm SL, I could observe that even smaller specimens of *P. howesi* have smaller eyes, compared to same-size specimens of *P. hasemani* (Tables 28 and 29). Besides, all *P. howesi* have a more robust dorsal-fin spine, with distal point slightly curved anteriorly (Fig. 84), if compared with the more delicate dorsal-fin spine of *P. hasemani* (Figs. 80, 83).

Specimens with morphology similar to *P. howesi* were found in Upper Rio Meta (area 313), and tentatively identified as pertaining to this species. This includes Western Amazon Piedmont in the geographical distribution of *P. howesi*, which majority of the material belongs to Madeira, Mamoré, Guaporé and Madre de Dios basins. Nevertheless, more investigation about this material from Upper Rio Meta is needed, in order to confirm or refute the distribution here suggested.

Pimelodella howesi occurs syntopically with *P. serrata* in Rio Meta, Rio Ucayali and Rio Madre de Dios basins, with *P. roccae* in Rio Ucayali basin and with *P. metae* in Rio Meta basin.

Material examined

Pimelodella howesi. — ANSP 69036, 1, xr, 79.3 mm SL, holotype, Bolívia, Boca chaparae, Rio Chimore, 15°56'42"S, 64°45'27"W; ANSP 69037-69056, 25, xr, 30.7–73.8 mm SL, paratypes, Bolívia, Boca chaparae, Rio Chimore, 15°56'42"S, 64°45'27"W; ANSP 69057-69064, 8, xr, 51.2–60.6 mm SL, paratypes, Bolívia, Todos os Santos, Rio Chapare, Cochabamba, 16°59'11"S, 65°07'50"W; ANSP 138091, 4, 60.8–103.0 mm SL, Colombia, Meta, Rio Negro, downstream from main Villavicencio-Puerto Lopez highway at La Balsa, W side of river, Negro-Humea-Meta Dr., 4°4'0.0"N, 73°4'0.0"W; ANSP 138828, 10, 64.7–137.7 mm SL, Colombia, Meta, Rio Negrito midway between La Argelia and La

Balsa (Plancha 267 - Rio Guayuriba), 4°4'0.0"N, 73°4'0.0"W; ANSP 139199, 22, 69.2–119.7, Rio Negro, just downstream from main Villavicencio-Puerto Lopez highway at La Balsa, E side of river, Humea-Meta drainage, 4°4'0.0"N, 73°4'0.0"W; ANSP 144003, 17, 76.3–121.6 mm SL, 2 c&s, Peru, Madre de Dios, Near Boca Manu, mouth of Pinquen River (tributary Rio Manu), 12°10'0.0"S, 71°1'0.0"W; ANSP 149938, 1, 68.0 mm SL, Peru, Cunaviche, Rio Cunaviche, ca. 20km SW of Cunaviche on S, Francisco Apure-Puerto Paes Hwy, 3°42'46.9"S, 73°13'39.6"W; MZUSP 115626, 1, 58.2, Brazil, Mato Grosso, Pontes e Lacerda, Rio Guaporé, under the bridge in the road between Pontes e Lacerda and Vila Bela da Santíssima Trindade, sideways to Clube e Rest. Beira Rio, 15°12'57.0"S, 59°21'18.6"W; MZUSP 26063, 2, 67.4 mm SL, Peru, Depto. Huánuco, Tournavista, Rio Pachitea, 8°56'05.9"S, 74°42'26.7"W; MZUSP 25977, 18, 46.8–75.2 mm SL, Peru, Depto Ucayali, Prov. Coronel Portillo, Masisea, Rio Ucayali, 8°34'08.9"S, 74°21'24.2"W; MZUSP 38705, 5, 50.9–60.4 mm SL, Ecuador, Napo, Rio Aguarico, 1 km above mouth of Rio Lagartococha, Rio Napo basin, 0°38'0.0"S, 75°18'0.0"W; MZUSP 26319, 6, 58.4–80.7 mm SL, Peru, Depto. Ucayali, Prov. Cel. Portillo, Pucallpa, Cashibococha, 8°20'10.1"S, 74°39'14.0"W; MZUSP 42210, 4, 47.3–71.1 mm SL, Peru, Depto. Ucayali, Prov. Cel. Portillo, afluyente to Rio Ucayali, in Pucallpa region, 8°23'41.9"S, 74°31'21.0"W; UFRO-I 9745, 1, 84.0 mm SL, Brazil, Rondonia, Costa Marques, Rio Guaporé, next to mouth of Rio Cautário, 12°13'36.60"S, 64°31'29.60"W.

***Pimelodella humeralis* Slobodian, Akama & Dutra, 2017**

Pimelodella sp.—Aleixo *et al.*, 2011: 20 [in list of species].

Pimelodella humeralis Slobodian, Akama & Dutra, 2017: 85–100, figs. 1–3 [original description; “Brazil, Pará, Almeirim, Rio Ipitinga, Rio Jari basin, left bank tributary of the Rio Amazonas”; holotype: MPEG 34994].

Diagnosis

Pimelodella humeralis differs from all congeners by having a dark anteriorly oblique blotch in the humeral region, its anterior limit slightly ahead of vertical through the spinelet, and its posterior limit at vertical through the base of second branched dorsal-fin ray. Moreover, *P. humeralis* differs from most congeners (except *P. cristata*, *P. cruxenti* and *P. gracilis*) by having 47 to 49 total vertebrae (vs. 37 to 44 total vertebrae). *Pimelodella humeralis* differs from *P. cristata* by having 8–11 retrorse triangular, broad-based and strongly inclined dentations confined to basal three-fourths of pectoral-fin spine posterior margin (vs. pectoral-fin spine posterior margin bearing 22–27 retrorse dentations along almost all the margin, the dentations being triangular and inclined). It differs from *P. cruxenti* by

having an overall light colored body (*vs.* overall brownish body in *P. cruxenti*). It differs from *P. gracilis* by having dark midlateral stripe from pseudotympanum to the caudal-fin insertion narrow (*vs.* wide), and dorsal region of body lacking dark stripes (*vs.* paired diffuse dark stripes evident from posterior region of head to at least adipose-fin insertion).

Description

This species was described in Slobodian *et al.* (2017), and the full description is presented in Attachment 1. For comparison purposes, *P. humeralis* measurements are presented in Table 30, and images in Figures 87–89.

Comments

There are several *Pimelodella* species with 46 or more total vertebrae this work synonymizes to *P. cristata* and *P. gracilis*. Therefore, comparisons of *P. humeralis* with those species synonymized to the before mentioned fall into *P. cristata* or *P. gracilis* morphological variation, and need no further discussion.

***Pimelodella ignobilis* (Steindachner, 1907)**

Rhamdella ignobilis Steindachner, 1907: 484–486 [original description, “Flusse Cubataõ um Staate Santa Catharina bei Theresopolis (Brasilien)”, Brazil; syntypes: NMW 44479]. — Fowler, 1914: 263 [taxonomic treatment, comparison with *Rhamdella eriarcha*]. — Gosline, 1945: 35 [taxonomic treatment]. — Fowler, 1951: 564 [taxonomic treatment]. — Burgess, 1989: 278 [taxonomic treatment]. — Lucena & Lucena, 1990: 100 [locality]. — Bockmann & Guazzelli, 2003: 422 [taxonomic treatment]. — Ferraris, 2007: 196 [taxonomic treatment].

Rhamdia ignobilis. — Eigenmann, 1910: 387 [taxonomic treatment, used the genus *Rhamdia*, but treated under *Rhamdella*]. — Miranda Ribeiro, 1911: 263 [taxonomic treatment].

Pimelodella ignobilis. — Guazzelli, 1997: 32–46 [taxonomic review of Southeastern Brazil *Pimelodella* species, transfer to *Pimelodella*]. — Bockmann & Miquelarena, 2008: 45–47 [taxonomic treatment].

Pimelodella pappenheimi Ahl, 1925: 107–108 [original description; “Rio Pedro bei Humboldt, Sta Catharina, Brasilien”, Brazil; syntypes: ZMB 31951]. — Gosline, 1945: 45 [taxonomic treatment]. — Fowler, 1951: 547 [taxonomic treatment]. — Burgess, 1989: 281 [taxonomic treatment]. — Paepke, 1995: 92 [taxonomic list]. — Guazzelli, 1997: 47–62 [taxonomic review of Southeastern Brazil *Pimelodella* species]. — Silfvergrip & Paepke, 1997: 167 [type catalog]. — Amaral *et al.*, 1998:

106–110 [reproduction]. — Bockmann & Guazzelli, 2003: 420 [taxonomic treatment].
— Ferraris, 2007: 194 [taxonomic treatment].

Diagnosis

Pimelodella ignobilis can be diagnosed from all *Pimelodella* species except *P. australis*, *P. avanhandavae*, *P. buckleyi*, *P. cruxenti*, *P. gracilis*, *P. griffini*, *P. harttii*, *P. itapicuruensis*, *P. kronei*, *P. lateristriga*, *P. laticeps*, *P. laurenti*, *P. leptosoma*, *P. linami*, *P. macturki*, *P. martinezi*, *P. meeki*, *P. megalura*, *P. metae*, *P. mucosa*, *P. notomelas*, *P. roccae*, *P. straminea*, *P. taeniophora* and *P. vittata* by having the dorsal fin darkly pigmented near base, followed by an hyaline stripe, and distal portion dark pigmented (unknown in *P. martinezi*). It differs from all above mentioned except *P. australis*, *P. cruxenti*, *P. meeki*, *P. straminea* and *P. vittata* by the dorsal fin hyaline stripe does not encompass the unbranched fin ray. It differs from *P. cruxenti* by having 40–43 total vertebrae (*vs.* 47 total vertebrae in *P. cruxenti*). It differs from *P. australis* by not having a dark mark between dorsal and adipose fins (*vs.* dark mark dorsal on body, between dorsal and adipose fins in *P. australis*). It differs from *P. meeki* by not having a paired stripe along supraoccipital process, and supraoccipital process triangular, with moderate width (*vs.* having a a paired stripe along supraoccipital process, and supraoccipital process rectangular, narrow in *P. meeki*). It differs from *P. straminea* by having maxillary barbel reaching between half adpressed pelvic fin and anal fin origin and dorsal region of head and body slightly, but notably darker (*vs.* maxillary barbel reaching between second third and terminus of adpressed pelvic fin, and dorsal region of head not notably darker in *P. straminea*). It differs from *P. vittata* by the dorsal fin three and half to four times in SL and curved pectoral-fin spine, posterior margin of spine with usually 10–17 retrorse dentations, from region just beyond base of spine to or slightly short of the last third of spine, the distalmost smaller (*vs.* adipose fin two and half to three times in SL, and pectoral fin spine roughly straight, posterior margin of spine bearing 4–9 retorse, small, triangular dentations along basal half to two thirds of margin in *P. vittata*).

Furthermore, *P. ignobilis* can be diagnosed by maxillary barbel reaching between half adpressed pelvic fin and anal fin origin; posterior margin of pectoral-fin spine with usually 10–17 retrorse dentations, from region just beyond base of spine to or slightly short of the last third of spine, the distalmost smaller; adipose fin three and half to four times in SL; 40–43 total vertebrae; dark brown midlateral stripe wide, not well delimited, extending from snout to caudal-fin origin, dorsal region of head and body slightly darker, dorsal fin overall dark brown, except by a hyaline stripe near its base, which does not encompass the dorsal-fin spine.

Description

Measurements in Table 31. Body of moderated height, depth at dorsal-fin origin five to seven times in standard length, and compressed, body width at dorsal-fin origin six to eight times in SL (Fig. 90). Dorsal profile convex from snout to dorsal fin, slightly concave from dorsal to adipose fin, slightly convex along adipose fin, and concave along caudal peduncle. Ventral profile of body slightly convex from snout to branchiostegal membrane, convex between pectoral end pelvic fins, and convex from pelvic to caudal peduncle.

Pseudotympanum large, oval, dorsal to posterior process of cleithrum and reaching 6th* (2)–8th (8) vertebrae. Posterior process of cleithrum triangular, concave. Anus and urogenital papilla adjacent. Urogenital papilla tubular, triangular, short. Anus between verticals through first third and half adpressed pelvic fin; urogenital papilla between verticals through half and terminus of adpressed pelvic fin.

Head deep, depth at supraoccipital-process base roughly two times or less in head length. Mouth sub terminal. Eye slightly elliptical, four to five and half times in head. Bony interorbital distance slightly smaller than eye diameter. Barbels thin, and slightly depressed and elliptical in cross-section. Maxillary barbel reaching between half adpressed pelvic fin and anal fin origin. Outer mental barbel, when stretched parallel to main body axis, finishing between first third and half adpressed pectoral fin. Inner mental barbel, when stretched parallel to main body axis, finishing between branchiostegal membrane ventral limit and pectoral fin origin. Supraoccipital process roughly triangular. Dorsal lamina of Weberian complex vertebrae of moderated height, reaching the supraoccipital process just at its anteriormost part. Branchiostegal rays 5 (1) 6* (10).

Dorsal fin triangular, distal margin concave, of moderated length (second branched dorsal-fin ray four to five and half times in SL), depressed tip reaching between the verticals through half and terminus of adpressed pelvic fin. Dorsal fin with I,6* (16), rarely 7 (1), plus anteriormost spinelet. Distance between terminus of dorsal-fin base and adipose-fin origin roughly equal to dorsal-fin base. Anteriormost dorsal-fin pterygiophore inserted posterior to neural spine of vertebrae 4 (14); posteriormost dorsal-fin pterygiophore located ahead of neural (or pseudoneural) spine of vertebrae 11 (14). Unbranched dorsal-fin ray mostly ossified as a spine, rigid part relatively long (approximately a fourth shorter than the first dorsal-fin ray total length).

Pectoral-fin rays I,7* (3)– I,9 (4), usually I,8 (10), pectoral fin triangular with concave distal border. First pectoral-fin ray curved, with proximal part rigid (Fig. 91), and short distal tip flexible and distinctly segmented. Pectoral fin spine five to almost six times in SL.

Anterior margin of pectoral-fin spine with smooth, straight dentations along its basal two thirds, and smooth serrae along its distal third. Posterior margin of pectoral-fin spine with usually 10–17 retrorse dentations, from region just beyond base of spine to or slightly short of the last third of spine, the distalmost smaller, plus sometimes 2–3 unossified distalmost dentations, not counted.

Pelvic-fin rays i,5 (16), extended pelvic fin triangular with straight distal border. Pelvic-fin origin at vertical through dorsal fin terminus. Tip of adpressed pelvic fin between verticals through origin and first third of adipose-fin base. First unbranched and flexible ray distinctly shorter than second and third rays, which are subequal; remaining rays progressively shorter.

Anal-fin rays v,7 (1); vii,7 (1); iv,8* (4); v,8 (3); vi,8 (1); v,9 (5); vi,9 (1); or v,10 (1), distal border of extended anal fin convex. Two to three anteriormost anal-fin rays vestigial, unsegmented, embedded in thick skin fold. Anal fin origin between verticals through first fourth and half adipose fin. Anal-fin adpressed terminus at vertical through adipose-fin terminus. Tip of anteriormost anal-fin pterygiophore inserted posterior to hemal spine of vertebrae 19 (1), 20 (2), 21 (3), 22* (6), or 23 (2). Tip of posteriormost anal-fin pterygiophore inserted ahead of hemal spine of vertebrae 28 (1), 29* (7), 30 (4), or 31 (2).

Adipose fin three and half to four times in SL, forming ascending elevated curve in lateral profile, with deepest point approximately midlength. Adipose fin emerging gradually, its posterior limit as a rounded, free lobe. Adipose-fin origin at vertical through vertebral centra 20 (3)– 24 (2) (lectotype 21); adipose-fin terminus at vertical through vertebral centra 34* (2)– 36 (2).

Caudal fin deeply forked, dorsal lobe slightly longer than ventral lobe. Caudal peduncle posterior to adipose-fin base almost twice longer than its depth. Dorsal lobe with 7 (17) branched, 1 (17) unbranched principal and 11 (1)– 12 (1) procurrent fin-rays (lectotype 16). Ventral lobe with 8 (17) branched, 1 (17) unbranched principal and 11 (1)– 21 (1) procurrent fin-rays (lectotype 16). Hypural 5 separated from hypurals 3+4. Median caudal-fin rays not directly attached to caudal plate. Seven (14) rays articulated to dorsal caudal-fin plate (5 on hypurals 3+4 and 2 on Hypural 5) and 7 (3), 8 (10) or 9* (1) rays articulated to ventral caudal-fin plate (5, 6 or 7 on hypurals 1+2 and 2 on parhypural).

Total vertebrae 40 (1)–43 (2), usually 42* (6). Ribs 8 (7)– 9 (4).

Epihyseal branch of laterosensory canal on head (S6) with contralateral canals emerging separately, as two pores near each other.

Coloration in alcohol

Background body coloration brownish. Ventral region of head and body lighter. Dark brown midlateral stripe wide (Fig. 92), not well delimited, extending from snout to caudal-fin origin. Dorsal region of head and body slightly darker. Dorsal fin overall dark brown, except by a hyaline stripe near its base, which does not encompass the dorsal-fin spine.

Geographic distribution

Pimelodella ignobilis was described from Rio Cubatão, in Santa Catarina State, Brazil. *Pimelodella pappenheimi*, its junior-synonym, was described from Humboldt, nowadays Corupá municipality, Santa Catarina State. Both localities are in region 331 (Southeastern Mata Atlantica). Therefore, *P. ignobilis* is known from several streams of Southeastern Mata Atlântica, in Paraná and Santa Catarina States, Brazil.

Comments

Rhamdella ignobilis was transferred to *Rhamdia* by Eigenmann (1910) without any explicit reasons to that. Guazzelli (1997) points out *Rhamdella ignobilis* is, in fact, a *Pimelodella*. However, the first publication to state *R. ignobilis* as a *Pimelodella* was Bockmann & Miquelarena (2008).

Pimelodella ignobilis was described based on three syntypes. Analyzing them, the specimen with 91.1 mm SL is the one presenting the better preservation state and in which the characteristics described are better observed. Therefore, I hereby designate this specimen as the lectotype, and the other two will remain as paralectotypes.

Pimelodella pappenheimi was described by Ahl (1925) based on two specimens. Since the syntype with 103.1 mm SL is in better preservation condition and according to the original description, I hereby designate this specimen as the lectotype, meanwhile the 111.2 mm SL specimen remains as paralectotype.

The locality of “Therezopolis”, type-locality of *P. ignobilis* correspond to a german colony of same name, now part of Águas Mornas municipality, Santa Catarina State (*e.g.* Lucena & Lucena, 1990). In similar manner, the locality of Humboldt, type-locality of *P. pappenheimi*, is now part of Corupá municipality, in Santa Catarina State; and “Rio Pedro” probably corresponds to Rio Itapocu, since “itapocu”, in tupi dialect (spoke by the native-americans of this region) means “Pedra Comprida” or “Pedra Estourada”. MNRJ 831 if from same locality, collector and date as the type-material, and probably topotypes collected at the same occasion.

Observing the types of *P. ignobilis* and *P. pappenheimi* I can argue they are indistinguishable. Table 32 has the comparison between the morphometric data of both species, and figure 93 is related to the lectotype of *P. pappenheimi*.

Material examined

Pimelodella ignobilis. — NMW 44479, 1, xr, 91.1 mm SL, lectotype, Brazil, Santa Catarina, Águas Mornas (“Flusse Cubatão um Staate Santa Catharina bei Theresopolis, Brazilien”), 27°42'24"S, 48°48'22"W; NMW 44479, 2, xr, 109.9–129.25 mm SL, paralectotypes, Brazil, Santa Catarina, Águas Mornas (“Flusse Cubatão um Staate Santa Catharina bei Theresopolis, Brazilien”), 27°42'24"S, 48°48'22"W; USNM 320368, 6, 79.5–107.7, Brazil, Santa Catarina, Rio Garuva, Sob a Ponte Na Br 101, Garuva.

Pimelodella pappenheimi. — ZMB 31951, 1, xr, 103.1 mm SL, lectotype, Brazil, Santa Catarina, Corupá (“Rio Pedro bei Humboldt, Sta Catharina, Brazilien”), 26°25'53"S, 49°14'09"W; ZMB 31951, 1, xr, 111.2 mm SL, paralectotype, Brazil, Santa Catarina, Corupá (“Rio Pedro bei Humboldt, Sta Catharina, Brazilien”), 26°25'53"S, 49°14'09"W; MZUSP 24584, 4, 92.7–100 mm SL, Brazil, Santa Catarina, Joinville, Rio Cubatão, near Joinville, 26°10'0.0"S, 48°54'0.0"W; MZUSP 28991, 5, 71.4–88 mm SL, Brazil, Santa Catarina, Rio Viralata, affluent of Prata, 26°48'0.0"S, 49°51'0.0"W; MZUSP 41787, 5, 77.4–101 mm SL, 1 c&s, Brazil, Santa Catarina, Guaruva, Rio Guaruva, under the bridge at BR-101, 26°02'18.5"S, 48°51'36.0"W; USNM 064895, 1, 98.5 mm SL, Brazil, Santa Catarina, Joinville, Rio Humboldt, near Joinville, 26°18'39.6"S, 48°48'51.6"W; USNM 279540, 4, 51.5–94.4 mm SL, Brazil, Santa Catarina, Corupá, stream affluent of Rio Itapocu, 26°25'45.7"S, 49°14'13.2"W.

***Pimelodella itapicuruensis* Eigenmann, 1917**

Pimelodella itapicuruensis Eigenmann, 1917: 247–248, pl. XXXI, fig. 3, pl. XXXV, fig. 12 [original description; “Queimadas, Rio Itapicurú”, Northeastern Brazil; holotype: FMNH 57986 (formerly CM 6974)]. — Henn, 1928: 77 [type catalog]. — Gosline, 1945: 45 [taxonomic treatment]. — Fowler, 1951: 543, fig. 558 [taxonomic treatment]. — Ibarra & Stewart, 1987: 66 [type catalog]. — Burgess, 1989: 280 [taxonomic treatment]. — Bockmann & Guazzelli, 2003: 419 [taxonomic treatment]. — Rosa *et al.*, 2003: 177 [taxonomic list]. — Ferraris, 2007: 192 [taxonomic treatment]. — Slobodian *et al.*, 2017: 93–94, fig. 6B [comparison with *P. humeralis*, drawing of pectoral-fin spine].

Diagnosis

Pimelodella itapicuruensis differs from all *Pimelodella* species except *P. leptosoma*, *P. longipinnis*, *P. megalura*, *P. metae*, *P. montana*, *P. reyesi*, *P. robinsoni*, *P. tapatapae* and *P. yuncensis* by having the supraoccipital process not reaching the anterior preopercular plate (unknown in *P. reyesi*). It differs from *P. tapatapae* and *P. yuncensis* by having the maxillary barbel reaching between verticals through anal fin origin and terminus (*vs.* maxillary barbel reaching caudal fin origin in *P. tapatapae*; maxillary barbel reaching between half adpressed pectoral and terminus of adpressed pelvic fin in *P. yuncensis*). It differs from *P. leptosoma*, *P. longipinnis*, *P. megalura*, *P. metae*, *P. reyesi* and *P. robinsoni* by having a dark paired dorsolateral stripe extending along supraoccipital process (*vs.* dark paired dorsolateral stripe absent in *P. leptosoma*, *P. metae* and *P. robinsoni*; dark diffuse region from supraoccipital process to adipose fin in *P. megalura*; dark paired dorsolateral stripe extending up to first third of adipose fin or posteriorly in *P. montana* and *P. reyesi*).

Furthermore, *P. itapicuruensis* can be diagnosed by maxillary barbel reaching between verticals through anal fin origin and terminus; supraoccipital process almost reaches the anterior preopercular plate; unbranched dorsal-fin ray mostly ossified as a spine, rigid part relatively short, approximately half first dorsal fin total length, delicate and straight; posterior margin of pectoral-fin spine bearing 5–7 small, retrorse dentations along roughly basal half, these dentations are triangular, with broad bases, shallow; adipose fin two and half to three times in SL; 41–44 total vertebrae; dark brown midlateral stripe narrow to moderate width, not well-delimited, from snout to median caudal-fin rays; paired diffuse dark brown stripes along supraoccipital process until dorsal-fin terminus.

Description

Measurements in Table 33. Body of moderate depth, depth at dorsal-fin insertion five to seven times in standard length, and compressed, body width at dorsal-fin insertion five and half to nine times in SL (Fig. 94). Dorsal profile convex from snout to dorsal fin, slightly concave from dorsal to adipose fin, convex along adipose fin, and concave along the caudal peduncle. Ventral profile of body slightly convex from snout to branquiostegal membrane, convex between pectoral end pelvic fins, slightly concave from pelvic to anal fin, and also concave from there along the caudal peduncle.

Pseudotympanum large, oval, dorsal to posterior process of cleithrum and reaching the straight line of 6th* (3) or 7th (2) vertebrae. Posterior process of cleithrum triangular, short, its dorsal border slightly concave. Anus and urogenital papilla adjacent. Urogenital papilla tubular, triangular, short. Anus between verticals through first third and half adpressed pelvic

fin; urogenital papilla between verticals through last fourth and terminus of adpressed pelvic fin.

Head of moderated depth, depth at supraoccipital-process base slightly less to slightly more than half head length. Mouth sub terminal. Eye slightly elliptical, four to five times in head length. Bony interorbital distance slightly smaller than eye diameter. Barbels thin, slightly depressed and elliptical in cross-section. Maxillary barbel reaching between verticals through anal fin origin and terminus. Outer mental barbel, when stretched parallel to main body axis, reaching between verticals through pectoral fin terminus and adpressed terminus. Inner mental barbel, when stretched parallel to main body axis, finishing between ventral posterior limit of branchiostegal membrane and pectoral-fin terminus. Supraoccipital process slightly triangular, narrow, tapered at its distal point. Supraoccipital process almost reaches the anterior prenuchal plate. Dorsal lamina of Weber complex vertebrae of moderated height, reaching the supraoccipital process just at its anteriormost part. Branchiostegal rays 6 (2) or 7* (3).

Dorsal fin triangular, distal margin concave, moderated length, (second branched dorsal-fin ray four to five and half times in SL), depressed tip finishing between verticals through first and last fourth of adpressed pelvic fin. Dorsal fin with I,6 (14) plus anteriormost spinelet. Distance between terminus of dorsal-fin base and adipose-fin origin slightly smaller than dorsal-fin base. Anteriormost dorsal-fin pterygiophore inserted posterior to neural spine of vertebrae 5 (6); posteriormost dorsal-fin pterygiophore located ahead of neural (or pseudoneural) spine of vertebrae 11* (3) or 12 (3). Unbranched dorsal-fin ray mostly ossified as a spine, rigid part relatively short (approximately half first dorsal fin total length), delicate and straight.

Pectoral-fin rays I,8* (8)– I,9 (6), pectoral fin triangular with concave distal border. First pectoral-fin ray roughly straight (Fig. 95), with proximal part rigid, forming a spine and short distal tip flexible and distinctly segmented. Pectoral-fin spine five and half to seven times in SL. Anterior margin of pectoral-fin spine with serrae along its distal two fifths. Posterior margin of pectoral-fin spine bearing 5–7 small, retrorse dentations along roughly basal half. These dentations are triangular, with broad bases, shallow.

Pelvic-fin rays i,5 (11), extended pelvic fin triangular with straight distal border. Pelvic-fin origin at vertical through dorsal-fin terminus. Pelvic fin adpressed terminus between verticals through origin and first fifth of adipose fin base. First unbranched and flexible ray distinctly shorter than second and third rays, third ray the longest; remaining rays progressively shorter.

Anal-fin rays v,7 (2); vi,7 (1); iii,8* (1); v,8 (4); vi,8 (1); iv,9 (1) or vi,9 (1); distal border of extended anal fin convex. One to three anteriormost anal-fin rays vestigial, unsegmented, embedded in thick skin fold. Anal-fin origin between verticals through first fourth or third of adipose fin; anal-fin adpressed terminus slightly anterior or at vertical through adipose-fin terminus. Tip of anteriormost anal-fin pterygiophore inserted posterior to hemal spine of vertebrae 21* (3), 22 (1) or 23 (2). Tip of posteriormost anal-fin pterygiophore inserted ahead of hemal spine of vertebrae 28* (2), 29 (3) or 30 (1).

Adipose fin two and half to three times in SL, forming ascending elevated curve in lateral profile, with deepest point approximately midlength. Adipose fin emerging gradually, its posterior limit as a rounded, free lobe. Adipose-fin origin at vertical through vertebral centra 18 (2)– 22* (1); adipose-fin terminus at vertical through vertebral centra 35* (3)– 39 (2).

Caudal fin deeply forked, dorsal lobe slightly longer. Caudal peduncle length posterior to adipose fin slightly longer than its depth. Dorsal lobe with 7* (8), rarely 6 (1), 1 unbranched principal (9) and 10 (2)–14 (1) (holotype 13) procurrent fin-rays. Ventral lobe with 8 (8), rarely 7 (1) branched, 1 unbranched principal (9) and 10 (1)–13 (1) (holotype 11) procurrent fin-rays. Hypural 5 completely free, not fused to hypural 3+4. Median caudal-fin rays not articulated directly to caudal plate. Seven (6) rays articulated to dorsal caudal-fin plate (5 on hypurals 3+4 and 2 on hypural 5) and 8 (5) rays articulated to ventral caudal-fin plate (6 on hypurals 1+2 and 2 on parahypural).

Total vertebrae 41* (3)–44 (1). Ribs 8 (5)–10 (1) (holotype 9).

Epiphyseal branch of laterosensory canal on head (S6) with contralateral canals usually connecting in head midline, and opening in a single pore right after the connection of both canals. One specimen with two pores close to each other.

Coloration in alcohol

Background body coloration yellowish. Ventral region of head and body lighter. Dark brown midlateral stripe narrow to moderated width (Fig. 96), not well-delimited, from snout to median caudal-fin rays. Dorsal fin overall dark brown, with a hyaline stripe near its base. Dark brown cephalic pigment at posterior fontanel region. Paired diffuse dark brown stripes along supraoccipital process until dorsal-fin terminus.

Geographic distribution

Pimelodella itapicuruensis was described from Rio Itapicuru and its tributaries, in Bahia, Brazil. It is known from region 328 (Northeastern Mata Atlântica).

Material examined

Pimelodella itapicuruisis. — FMNH 57986, 1, xr, 60.2 mm SL, holotype, Brazil, Bahia, Queimadas, Rio Itapicurú, 10°58'14"S, 39°37'34"W; FMNH 57987, 13, xr, 56.1–79.3 mm SL, paratypes, Brazil, Bahia, Queimadas, Rio Itapicurú, 10°58'14"S, 39°37'34"W; FMNH 57951, 1, xr, 57.5 mm SL, paratype, Brazil, Bahia, Jacobina (Rio de Jacobina into Rio Itapicurú, 11°11'09"S, 40°30'36"W; FMNH 57953, 5, xr, 45.2–56.0 mm SL, paratypes, Brazil, Bahia, Bom Fim (Bom Fin, Rio Itapicurú, 6 miles north of Fazenda Amaratu), 10°24'48"S, 40°10'51"W; FMNH 57988, 2, 62.4–67.6 mm SL, paratypes, Brazil, Bahia, Jacobina, Rio Agua Branca, into Itapicurú, Swift rocky stream from Serra de Jacobina, 12°03'40"S, 40°34'55"W; MZUSP 88169, 4, 39.3–50.1 mm SL, Brazil, stream between BR-324 and Itaitu, afl. of Rio Itapicurú-Mirim, 11°19'41.0"S, 40°28'11.0"W.

***Pimelodella kronei* (Miranda Ribeiro, 1907a)**

Typhlobagrus kronei Miranda Ribeiro, 1907a: 3 unnum. pages, 1 unnum. fig. [original description, “águas das cavernas do Iporanga”, Ribeira de Iguape basin, São Paulo State, Brazil; holotype: MNRJ 836]. — Miranda Ribeiro, 1907b: 186 [taxonomic treatment]. — Eigenmann, 1910: 387 [taxonomic treatment]. — Miranda Ribeiro, 1911: 250–252, fig. 2, 2A–B [taxonomic treatment]. — Haseman, 1911: 323–326 [taxonomic treatment, synonym to *Pimelodella lateristriga* var. *kroneri*]. — Eigenmann, 1917: 255–256, pl. XXXIV, fig. 2, pl. XXXV, fig. 18–19 [taxonomic revision]. — Miranda Ribeiro, 1918b: 728 [taxonomic list]. — Norman, 1926: 326, 329 [taxonomic treatment, taxonomic list]. — Borodin, 1927a: 2 [genus *Typhlobagrus* synonym of *Pimelodella*, comparison with *Caecorhamdella brasiliensis*]. — Gosline, 1945: 43 [taxonomic treatment]. — Pavan, 1946: 359 [synonym of *Typhlobagrus* to *Pimelodella*]. — Fowler, 1951: 578–579, fig. 581 [taxonomic treatment]. — Burgess, 1989: 270, 280 [taxonomic treatment]. — Trajano & Britski, 1992: 53–89 [taxonomic treatment]. — Felice, 2006: 21–23 [historical treatment].

Pimelodella lateristriga var. *kroneri*. — Haseman, 1911: 323–326 [taxonomic treatment].

Typhlobagrus kronei. — Haseman, 1911: 324 [taxonomic treatment, misspelling].

Pimelodella kronei. — Pavan, 1946: 343–361 [taxonomic treatment, ecology, transfer to *Pimelodella*]. — Trajano, 1987: 1–136 [taxonomic treatment, biology]. — Almeida-Toledo, 1992: 255–262 [cytogenetic]. — Trajano & Britski, 1992: 53–89 [taxonomic treatment]. — Trajano, 1997: 121 [taxonomic treatment]. — Trajano & Bockmann, 1999: 124–129 [taxonomic treatment; systematic treatment; ecology]. — Romero & Paulson, 2001: 26 [taxonomic treatment]. — Bockmann & Guazzelli, 2003: 419

[taxonomic treatment]. — Trajano *et al.*, 2004: 316–323 [comparison with *P. spelaea*]. — Trajano, 2006a: 47 [taxonomic list]. — Trajano, 2006b: 24–26 [historical treatment]. — Trajano *et al.*, 2006: 53–66 [taxonomic treatment, ecology, biology]. — Ferraris, 2007: 192 [taxonomic treatment]. — Bockmann & Castro, 2010: 698–699 [comparison with *Rhamdiopsis krugi*].

Caecorhamdella brasiliensis Borodin, 1927a: 1–6 [original description, “Province of São Paulo”; holotype: AMNH 8604]. — Gosline, 1945: 34 [taxonomic treatment]. — Miranda Ribeiro, 1951: 518–519, fig. 537 [taxonomic treatment]. — Burgess, 1989: 253–254, 278 [taxonomic treatment]. — Trajano & Britski, 1992: 53–89 [taxonomic treatment, synonym to *P. kronei*]. — Romero & Paulson, 2001: 26 [synonym of *P. kronei*].

Pimelodella transitoria Miranda Ribeiro, 1907b: 186 [original description; “Ribeirão do Alambary— Iporanga; neotype (hereby designated) MZUSP 403]. — Gosline, 1945: 45 [taxonomic treatment]. — Pavan, 1946: 343–361 [taxonomic treatment, ecology]. — Trajano, 1987: 1–136 [taxonomic treatment, biology]. — Burgess, 1989: 281 [taxonomic treatment]. — Almeida-Toledo, 1992: 255–262 [cytogenetic]. — Trajano & Britski, 1992: 53–89 [taxonomic treatment]. — Trajano & Bockmann, 1999: 124–129 [taxonomic treatment; systematic treatment; ecology]. — Bockmann & Guazzelli, 2003: 421 [taxonomic treatment]. — Trajano, 2006a: 47 [taxonomic list]. — Trajano *et al.*, 2006: 53–66 [taxonomic treatment, ecology, biology]. — Ferraris, 2007: 195 [taxonomic treatment]. — Bockmann & Castro, 2010: 699 [taxonomic treatment].

Rhamdia transitoria. — Miranda Ribeiro, 1911: 274 [taxonomic treatment].

Pimelodella transitoria = *lateristriga*?. — Eigenmann, 1917: 249 (*in partim*)

Diagnosis

Pimelodella kronei differs from all *Pimelodella* species except *P. australis*, *P. avanhandavae*, *P. buckleyi*, *P. cruxenti*, *P. gracilis*, *P. griffini*, *P. harttii*, *P. ignobilis*, *P. itapicuruensis*, *P. lateristriga*, *P. laticeps*, *P. laurenti*, *P. leptosoma*, *P. linami*, *P. macturki*, *P. martinezi*, *P. meeki*, *P. megalura*, *P. metae*, *P. montana*, *P. mucosa*, *P. notomelas*, *P. roccae*, *P. straminea*, *P. taeniophora* and *P. vittatta* by having the dorsal fin with a darker region near the base, followed by a hyaline stripe, and distally darker (unknown in *P. martinezi*). It differs from *P. itapicuruensis*, *P. leptosoma*, *P. megalura*, *P. metae* and *P. montana* by having the supraoccipital process reaching the anterior prenuchal plate (*vs.* supraoccipital process not reaching the anterior prenuchal plate in *P. itapicuruensis*, *P. leptosoma*, *P. megalura*, *P. metae* and *P. montana*). It differs from *P. avanhandavae*, *P. buckleyi*, *P. cruxenti*, *P. gracilis*, *P.*

laurenti, *P. roccae*, *P. taeniophora* and *P. vittata* by having the adipose fin three to four and half times in SL (*vs.* adipose fin up to three times in SL in *P. avanhandavae*, *P. buckleyi*, *P. cruxenti*, *P. gracilis*, *P. laurenti*, *P. roccae*, *P. taeniophora* and *P. vittata*). It differs from by having maxillary barbels reaching between vertical through dorsal-fin spine and anal-fin origin (*vs.* maxillary barbels reaching posteriorly than anal-fin origin in *P. lateristriga*, *P. macturki*, *P. martinezi*, *P. mucosa* and *P. notomelas*). It differs from *P. griffini*, *P. ignobilis*, *P. laticeps*, *P. linami* and *P. straminea* by having a paired dorsolateral dark stripe along supraoccipital process (*vs.* paired dorsolateral dark stripe absent in *P. ignobilis*, *P. laticeps*, *P. linami* and *P. straminea*; paired dorsolateral dark stripe reaching up to adipose fin terminus in *P. griffini*). It differs from *P. australis* and *P. meeki* by the hyaline stripe on dorsal fin encompass the unbranched fin ray (*vs.* hyaline stripe on dorsal fin does not encompass the unbranched fin ray in *P. australis* and *P. meeki*). It differs from *P. harttii* by having the posterior margin of pectoral-fin spine with usually 5–9 straight to slightly retrorse dentations, from region just beyond base of spine to approximately half of spine (*vs.* posterior margin of pectoral-fin spine with 10–12 retrorse dentations, from region just beyond base of spine to or slightly short of the last third of spine, those dentations are subtriangular, the ones near the base of spine more hook-like, progressively triangular and with broader bases towards distal of spine in *P. harttii*).

Pimelodella kronei can be further diagnosed by the combination of the following traits: maxillary barbels reaching between vertical through dorsal-fin spine and anal-fin origin; eyes might be absent; posterior margin of pectoral-fin spine with usually 5–9 straight to slightly retrorse dentations, from region just beyond base of spine to approximately half of spine; adipose fin short, three to four and half times in SL; from totally unpigmented to specimens with a medium brown midlateral stripe with moderated width, not well-delimited, from region posterior to opercle to caudal-fin origin. Dorsal fin can have light brown pigmentation along entire fin, except by a hyaline stripe near base; dorsal region of head darker than body.

Description

Measurements in Table 34. Body of moderately deep, depth at dorsal-fin origin five to six times in standard length; and average width, body width at dorsal-fin origin five and half to eight and half times in SL (Fig. 97). Dorsal profile convex from snout to dorsal fin, concave from dorsal to adipose fin, convex along adipose extension, and concave along the caudal peduncle. Ventral profile of body slightly convex from snout to branchiostegal

membrane, convex from this point to pelvic fin, and also convex from pelvic along the caudal peduncle.

Pseudotympanum large, oval, dorsal to posterior process of cleithrum and reaching the straight line of 6th* (1) or 7th vertebrae. Posterior process of cleithrum triangular, concave. Anus and urogenital papilla adjacent. Urogenital papilla tubular, triangular, short. Anus between verticals through first third and half adressed pelvic fin; urogenital papilla between verticals through second third and last fourth od adressed pelvic fin.

Head moderately depressed, depth at supraoccipital-process base slightly less than two to two and half times in head length. Mouth sub terminal. Eye might be absent, extremely reduced or present. When present, eye slightly elliptical, five to six times in head. Bony interorbital distance three to four times in head. When eyes absent, frontal bone between orbits present a secondary bony extension, covering part of orbit. Barbels thin, slightly depressed and elliptical in cross-section. Frequently barbels are damaged or severed. Maxillary barbels reaching between vertical through dorsal-fin spine and anal-fin origin. Outer mental barbel, when stretched parallel to main body axis, finishing between pectoral-fin origin and its first fourth adressed. Inner mental barbel, when stretched parallel to main body axis, finishing between ventral limit of branchiostegal membrane and a point slightly posterior to that. Supraoccipital process roughly triangular, narrow. Dorsal lamina of Weber complex vertebrae of medium height, reaching the supraoccipital process just at its anteriormost part. Branchiostegal rays 7 (1).

Dorsal fin triangular, distal margin convex, short (second dorsal-fin ray five to eight times in SL), reaching the vertical through last third or fourth of adressed pelvic fin. Dorsal fin with I,6 (25) plus anteriormost spinelet. Distance between terminus of dorsal-fin base and adipose-fin origin roughly the same as dorsal-fin base. Anteriormost dorsal-fin pterygiophore inserted posterior to neural spine of vertebrae 4 (1); posteriormost dorsal-fin pterygiophore located ahead of neural (or pseudoneural) spine of vertebrae 11 (1). Unbranched dorsal-fin ray mostly ossified as a spine, rigid part ca. 75% of first dorsal-fin ray total length.

Pectoral-fin rays I,7 (2)– I,10 (1), usually I,9 (15) (holotype I,8), pectoral fin triangular with convex distal border. First pectoral-fin ray curved, with proximal part rigid (Fig. 98), forming a spine and short distal tip flexible and distinctly segmented. Pectoral-fin spine five to almost eight times in SL. Anterior margin of pectoral-fin spine with smooth, straight dentations along its basal half, and smooth serrae along its distal half. Posterior margin of pectoral-fin spine with usually 5–9 straight to slightly retrorse dentations, from region just

beyond base of spine to approximately half of spine, plus sometimes 1–2 unossified distalmost dentations, not counted.

Pelvic-fin rays i,5 (25), extended pelvic fin triangular with convex distal border. Pelvic-fin origin between verticals through dorsal fin terminus and its second third adpressed. Tip of adpressed pelvic fin at vertical through adipose-fin origin or a point slightly posterior to that. First unbranched and flexible ray distinctly shorter than second and third rays, third ray usually the longest; remaining rays progressively shorter.

Anal-fin rays iv,8 (2); v,8 (3); iii,9 (1); iv,9 (4); v,9 (6); vii,9 (1); iii,10* (1); iv,10 (2); or v,10 (2); distal border of extended anal fin convex. One to four anteriormost anal-fin rays vestigial, unsegmented, embedded in thick skin fold. Anal fin origin between verticals through first seventh and first third of adipose-fin base. Anal-fin adpressed terminus at vertical through adipose-fin terminus. Tip of anteriormost anal-fin pterygiophore inserted posterior to hemal spine of vertebrae 20 (1). Tip of posteriormost anal-fin pterygiophore inserted anterior to hemal spine of vertebrae 28 (1).

Adipose fin three to four and half times in SL, forming ascending elevated curve in lateral profile, with deepest point approximately midlength. Adipose fin emerging gradually, its posterior limit as a rounded, free lobe. Adipose-fin origin at vertical through vertebral centrum 24 (1); adipose-fin terminus at vertical through vertebral centrum 34 (1).

Caudal fin deeply forked, upper lobe slightly longer than ventral lobe. Caudal peduncle length posterior to adipose fin half longer than its depth. Dorsal lobe with 7 (19), rarely 8 (1) branched, 1 (20) unbranched principal and 5 (1)–18* (1) procurrent fin-rays. Ventral lobe with 8 (18), rarely 9 (2) branched, 1 (20) unbranched principal and 6 (1)–18* (1) procurrent fin-rays. Hypural 5 completely free, not fused to hypurals 3+4. Median caudal-fin rays not attached directly to caudal plate. Seven (1) rays articulated to dorsal caudal-fin plate (5 on hypurals 3+4 and 2 on hypural 5) and 7 (1) rays articulated to ventral caudal-fin plate (5 on hypurals 1+2 and 2 on parahypural).

Total vertebrae 42 (1). Ribs 8 (1).

Ephiphyseal branch of cephalic laterosensory canal on head (S6) usually emerging as two widely-distanced pores (but see comments about variation).

Coloration in alcohol

Background body coloration yellowish. Ventral region of head and body lighter than dorsal regions. From totally unpigmented to specimens with a medium brown midlateral stripe with moderated width (Fig. 99), not well-delimited, from region posterior to opercle to caudal-fin origin. Dorsal fin can have light brown pigmentation along entire fin, except by an

hyaline stripe near base. Dorsal region of head darker than body. Might present medium brown cephalic pigment along posterior fontanel region, and diffuse paired dark stripe along supraoccipital process.

Geographic distribution

Pimelodella kronei and its junior-synonym, *P. transitoria*, were described from rivers that permeate the karstic area, especially Rio Iporanga, in Ribeira de Iguape Basin. This corresponds to its known distribution, from region 330 (Ribeira de Iguape).

Comments

Several authors made comparative studies between *P. kronei* and *P. transitoria* (e.g. Pavan, 1946; Trajano, 1987; Trajano & Britski, 1992; Almeida-Toledo *et al.*, 1992), under the assumption the latter is a putative ancestor of the first. At the same time, those same authors point to extreme morphological similarities between both species. They assume that *P. kronei* is isolated from *P. transitoria* and, therefore, a different species. This isolation was argued mainly on the basis of behavioral characters (Pavan, 1946; Trajano, 1987). Traditional external morphological characters used to distinguish the species, e.g. coloration and eyes, showed partial overlap between the two species, and only the length of dorsal-fin spine was regarded as a morphological characteristic feature that unambiguously distinguish them (Trajano & Britski, 1992).

Pavan (1946) was the first author to hypothesize the close relationship between *P. kronei* from the Areias cave system and *P. transitoria* from the region just outside that cave, when compared with *P. kronei* from the Bombas cave system. Trajano & Britski (1992) and Almeida-Toledo *et al.* (1992) argue that there were not enough data to support or contradict Pavan (1946) hypothesis, and that more studies were needed. Guil (2011) discusses morphological differences between *P. kronei* from Areias and Bombas cave systems, but also stress the need for more studies. Almeida-Toledo *et al.* (1992) characterized both species with $2n = 58$ chromosomes.

I examined populations of *P. kronei* of distinct areas from the same karstic area (Iporanga, Upper Ribeira de Iguape basin, Southeast Atlantic basin): 1) Areias system and Córrego Seco (right margin affluent of Betari River); 2) Bombas cave system (also with a right margin affluent of Betari River, but isolated from Areias, e.g. Fig. 100); and 3) Alambari de Cima and Abismo Gurutuva (left margin tributaries of Betari River).

Those populations of *P. kronei* bear no significant morphological differences. Populations of *P. transitoria* near those localities also bear no consistent morphological

differences among themselves, but their amount of morphological variation is somewhat broader than in other species of *Pimelodella*.

Compared to *P. transitoria*, specimens of *Pimelodella kronei* bear a secondary bone expansion above the orbit, involving especially the sphenotic, frontal and lateral ethmoid bones; the infraorbital bone series delimit a smaller orbital cavity; the eyes absent or extremely reduced; the orbit filled with fatty tissue and extreme reduction of pigmentation. All such traits are traditional troglomorphic characteristics common in cave fishes (eg. Romero & Paulson, 2001; Bichuette & Trajano, 2005). The hypertrophy of *adductor mandibulae (segmenta facialis, pars rictalis)*, *adductor arcus palatini* and *levator arcus palatini* are evident, occupying part of orbital cavity (Fig 101). There is also a relatively high variability in the number of pores from cephalic laterosensorial canal (Fig. 104), already reported for other troglomorphic fishes (Rizzato & Bichuette, 2014).

Pimelodella transitoria specimens bear almost no osteological differences with *P. kronei* which are not related to the loss of eyes. The conditions of their superficial cephalic musculature (Fig. 102) lies intermediate between those of *Pimelodella lateristriga* (Fig. 103) and *P. kronei*. Other differences reported between *P. kronei* and *P. transitoria* reside mainly in the color pattern (Fig. 97, 106) and slightly reduced serrae on anterior margin of pectoral-fin spine, which is extremely variable among examined specimens referable to the two forms (Fig. 98, 105). Material identified as *P. transitoria* from other coastal basins besides Ribeira de Iguape and even from localities in the Ribeira basin distant from the karstic area of Areias system are probably misidentifications. All those materials misidentified as *P. transitoria* usually belong to *P. lateristriga* (the species commonly found in coastal rivers, from Southeast Atlantic basin of Brazil) *P. brasiliensis* or *P. harttii* (described from Paraíba do Sul basin).

Differences and similarities among *P. kronei* and *P. transitoria* are thoroughly discussed in the literature (e.g. Pavan, 1946; Trajano, 1989; Trajano, 1991; Trajano, 1994; Trajano & Britski 1992). Those studies, as the respective species description, rely almost exclusively on troglomorphic characteristics for *P. kronei*. This category of characters can be used in species' delimitation if there is indication of population segregation sufficient to indicate separate different evolutionary lineages. My results support that specimens of *P. transitoria* are impossible to separate from *P. kronei*. when samples across their ranges and variation are considered.

Unpublished data (P. Figueiredo & J. Muriel-Cunha, pers. comm.) on the phylogeography of *P. kronei* and *P. transitoria*, from the same karstic area, reported networks

of seven haplotypes for CytB and eight for COI, with genetic divergence between 0–1.13%, and 0–1.43%, respectively. A phylogeographic analysis of *Pimelodella kronei* indicates patterns of gene flow and panmixia in Areias, Córrego Seco and Gurutuva localities (the areas 1 and 3 I explicit above), meanwhile the Bombas (area 2) population appears to be relatively divergent, and may represent a new lineage inside *Pimelodella kronei*, closer to Areias than to Gurutuva. The authors concluded the populations traditionally assigned to *P. kronei* and *P. transitoria* from different caves in the same karstic area cannot be discriminated into more than one species based on genetic data, a conclusion congruent with my results. There is enough evidence to support *P. transitoria* as part of the same lineage as *P. kronei*, and indistinguishable from the latter except by troglomorphic characteristics. Additionally, genetic difference found between *P. kronei* from different cave systems seems to be greater than those between *P. kronei* and *P. transitoria* from the same cave system, which also supports the synonymy of *P. transitoria* to *P. kronei*. Measurements discriminated by the two species' original names are presented in Table 35.

The holotype of *P. transitoria* is lost, and MZUSP 403 is herein designated as the neotype of *P. transitoria* (Fig. 107). This specimen, like the one used by Miranda Ribeiro (1907b) to describe the species, was collected by Ricardo Krone in 1909, in a locality named “Rio Lambari, Iporanga”, which might be the same as “Ribeirão do Alambary, Iporanga” reported as the type-locality of *P. transitoria*. That specimen matches all characteristics reported by Miranda Ribeiro (1907b) for the species.

Material examined

Pimelodella kronei. — LESCI 167, 1, 144.4 mm SL, Brazil, 24°35'0.0"S, 48°36'0.0"W; LESCI 169, 1, 110.7 mm SL, Brazil, 24°35'0.0"S, 48°36'0.0"W; LESCI 170, 2, 84.1–114.4 mm SL, Brazil, 24°35'0.0"S, 48°36'0.0"W; LESCI uncat, 1, 164.7 mm SL, Brazil, 24°35'0.0"S, 48°36'0.0"W; LESCI uncat, 6, 75.9–123.9 mm SL, Brazil, Abyss of Gurutuva, 24°35'0.0"S, 48°36'0.0"W; LESCI uncat, 1, 113.2 mm SL, Brazil, Areias, 24°35'0.0"S, 48°36'0.0"W; LESCI uncat, 1, 72.9 mm SL, Brazil, Areias, 24°35'0.0"S, 48°36'0.0"W; LESCI uncat, 2, 76.2–81.0 mm SL, Brazil, Areias/córrego seco, 24°35'0.0"S, 48°36'0.0"W; MNRJ 836, 1, xr, 120.1 mm SL, holotype, Brazil, São Paulo, Iporanga, “Iguape, em aguas das cavernas do Iporanga, também no estado de S. Paulo”, 24°29'29"S, 48°36'18"W; MZUSP 297, 3, Brazil, São Paulo, probably Iporanga, 24°35'0.0"S, 48°36'0.0"W; MZUSP 3661, 4, Brazil, São Paulo, Gruta das Areias, 24°35'0.0"S, 48°36'0.0"W; MZUSP 22196, 2, Brazil, São Paulo, Gruta das Areias, 24°35'0.0"S, 48°36'0.0"W; MZUSP 22581, 6, Brazil, São Paulo, Iporanga, near to gruta da Areia, 24°35'0.0"S, 48°36'0.0"W; MZUSP 24383, Brazil, São

Paulo, Gruta das Areias, 24°35'0.0"S, 48°36'0.0"W; MZUSP 27163, 11, Brazil, São Paulo, Iporanga, Bombas, 24°35'0.0"S, 48°36'0.0"W; MZUSP 27166, 3, Brazil, São Paulo, Iporanga, Bombas, 24°35'0.0"S, 48°36'0.0"W; MZUSP 27167, 4, Brazil, São Paulo, Iporanga, Bombas, 24°35'0.0"S, 48°36'0.0"W; MZUSP 27168, 5, Brazil, São Paulo, Iporanga, Areias, 24°35'0.0"S, 48°36'0.0"W; MZUSP 27169, 4, Brazil, São Paulo, Iporanga, Areias, 24°35'0.0"S, 48°36'0.0"W; MZUSP 27170, 7, Brazil, São Paulo, Iporanga, Areias de Cima, 24°35'0.0"S, 48°36'0.0"W; MZUSP 36499, 11, Brazil, São Paulo, Iporanga, Areias, 24°35'0.0"S, 48°36'0.0"W; MZUSP 36507, 28, Brazil, São Paulo, Vale do Ribeira, 24°35'0.0"S, 48°36'0.0"W; MZUSP 36508, 4, Brazil, São Paulo, Iporanga, Bombas, 24°35'0.0"S, 48°36'0.0"W; MZUSP 36509, 5, Brazil, São Paulo, Iporanga, Bombas, 24°35'0.0"S, 48°36'0.0"W; MZUSP 36510, 3, Brazil, São Paulo, Iporanga, Bombas, 24°35'0.0"S, 48°36'0.0"W; MZUSP 38725, 12, Brazil, São Paulo, Iporanga, Ressurgência das Bombas, 24°35'0.0"S, 48°36'0.0"W; MZUSP 38726, 15, Brazil, São Paulo, Iporanga, Caverna Areia de Cima, 24°35'0.0"S, 48°36'0.0"W; MZUSP 42591, 1, Brazil, São Paulo, Iporanga, Caverna das areias de cima, 24°35'0.0"S, 48°36'0.0"W.

Pimelodella transitoria. — MZUSP 403, 1, 109.5 mm SL, neotype, Brazil, São Paulo, Iporanga, Rio Lambari, 24°34'51.7"S, 48°35'44.8"W; LESCI 95, 1, 85.5 mm SL, Brazil, São Paulo, Iporanga, Rio Betari, Alto Ribeira, 24°35'S, 48°36'W (aprox.); LESCI 168, 1, 98.1 mm SL, Brazil, São Paulo, Iporanga, Gruta da Casa de Pedra; LESCI uncat, 1, 101.8 mm SL, separated from the lot, LESCI uncat, 1, 137.9 mm SL, Caverna Casa de Pedra, 24°35'S, 48°36'W (aprox.); LESCI uncat, 1, 142.0, Areias, 24/11/85, 24°35'S, 48°36'W (aprox.); LESCI uncat, 1, 121.7 mm SL, Casa de Pedra, ind IV, 24°35'S, 48°36'W (aprox.); LESCI uncat, 1, 143.6 mm SL, Casa de Pedra, ind V, 24°35'S, 48°36'W (aprox.); LESCI uncat, 1, 125.3 mm SL, Casa de Pedra, T9, 24°35'S, 48°36'W (aprox.); MNRJ 403, 1, 105.4 mm SL;; MZUSP 63365, 7, 63.9–83.8 mm SL, Brazil, São Paulo, Iporanga, Ribeirão Furnas, Núcleo Santana, PETAR, 24°32'8.0"S, 48°42'10.0"W; MZUSP 38605, 15, 46.5–97.0 mm SL, Brazil, São Paulo, Juquiá, Ribeirão Poço Grande, affluent of Rio Juquiá, road SP-79, 8 km from Juquiá, 24°20'0.0"S, 47°38'0.0"W; MZUSP 50732, 4, 78.9, Brazil, São Paulo, Iporanga, Rio Betari, abaixo da casa do Valente, 24°34'0.0"S, 48°40'0.0"W.

***Pimelodella lateristriga* (Lichtenstein, 1823)**

Pimelodes lateristrigus Lichtenstein, 1823: 112 [original description; “Brasil”; holotype: ZMB 3038]. — Lundberg & Littmann, 2003: 440 [taxonomic treatment, *species inquirendae* in *Pimelodus*].

- Pimelodus lateristrigus* Müller & Troschel, 1849b: 3–4 [original description; “Brasilien, durch v. Olfers”]; holotype: ZMB 3038]. — Silfvergrip & Paepke, 1997: 170, fig. 6 [type catalog; correction on priority to Lichtenstein, 1823].
- Pimelodus lateristriga*. — Günther, 1864: 118–119 [taxonomic treatment].
- Pimelodus (Pseudorhamdia) lateristriga*. — Steindachner, 1877: 603–608 (*in partim*) [taxonomic treatment]
- Pimelodella lateristriga*. — Eigenmann & Eigenmann, 1888: 133 (*in partim*) [taxonomic treatment]. — Eigenmann & Eigenmann, 1890: 149; 156–158 (*in partim*) [key to *Pimelodella* species; taxonomic revision]. — Eigenmann & Eigenmann, 1891: 29 [taxonomic list]. — Eigenmann, 1910: 389 (*in partim*) [taxonomic list]. — Haseman, 1911: 323, 325 [taxonomic treatment, comparison with *T. kronei*]. — Eigenmann, 1917: 245–247, pl. XXXV, fig. 11 (*in partim*) [taxonomic revision]. — Miranda Ribeiro, 1918: 731–732 [taxonomic treatment]. — Borodin, 1927a: 3–4 [comparison with *Typhlobagrus kronei*]. — Eigenmann & Allen, 1942: 99 (*in partim*) [taxonomic treatment]. — Gosline, 1945: 45 (*in partim*) [taxonomic treatment]. — Van der Sitgchel, 1946: 58–59 [taxonomic treatment]. — Fowler, 1951: 544 (*in partim*) [taxonomic treatment]. — Schubart, 1964: 6–9, fig. 2 [taxonomic treatment, comparison with *P. insignis*]. — Mees, 1983: 53–54, fig. 4 [taxonomic treatment; restriction of type-locality to Rio de Janeiro vicinities]. — Burgess, 1989: 280 [taxonomic treatment]. — Guazzelli, 1997: 89–109 [taxonomic review of *Pimelodella* from southeastern and southern Brazilian drainages]. — Bockmann & Guazzelli, 2003: 419 [taxonomic treatment]. — Rosa *et al*, 2003: 177 [taxonomic list]. — Ferraris, 2007: 192 [taxonomic treatment].
- Rhamdia lateristriga*. — Miranda Ribeiro, 1911: 271–272 (*in partim*) [taxonomic treatment].
- Pimelodus bahianus* Castelnau, 1855: 35, p. XVI, fig. 2 [original description; “eaux douces des environs de Bahia”, freshwaters from Bahia, State of Bahia, Brazil; syntypes: MNHN B-0612]. — Günther, 1864: 114 [taxonomic list]. — Miranda Ribeiro, 1911: 452 [synonym of *Rhamdia quelen*]. — Bertin & Estève, 1950: 57 [type catalog]. — Silfvergrip, 1996: 16 [taxonomic treatment; associated with *Pimelodella*]. — Ferraris, 2007: 195 [taxonomic treatment, *species inquirenda* in *Pimelodella*].
- ?*Pimelodus bahianus*. — Eigenmann & Eigenmann, 1890: [synonym of *Rhamdia quelen*]. — Gosline, 1945: 36 [synonym of *Rhamdia quelen*]. — Fowler, 1951: 575 [synonym of *Rhamdia quelen*].

Pimelodella transitoria = *lateristriga*? — Eigenmann, 1917: 249, pl. XXXV, fig. 10 (*in partim*) [taxonomic treatment].

Diagnosis

Pimelodella lateristriga differs from all *Pimelodella* species except *P. australis*, *P. avanhandavae*, *P. buckleyi*, *P. cruxenti*, *P. gracilis*, *P. griffini*, *P. harttii*, *P. ignobilis*, *P. itapicuruensis*, *P. kronei*, *P. laticeps*, *P. laurenti*, *P. leptosoma*, *P. linami*, *P. macturki*, *P. martinezi*, *P. meeki*, *P. megalura*, *P. metae*, *P. montana*, *P. mucosa*, *P. notomelas*, *P. roccae*, *P. straminea*, *P. taeniophora* and *P. vittata* by having the dorsal fin with a darker region near the base, followed by a hyaline stripe, and distally darker (unknown in *P. martinezi*). It differs from *P. itapicuruensis*, *P. leptosoma*, *P. megalura*, *P. metae* and *P. montana* by having the supraoccipital process reaching the anterior preopercular plate (*vs.* supraoccipital process not reaching the anterior preopercular plate in *P. itapicuruensis*, *P. leptosoma*, *P. megalura*, *P. metae* and *P. montana*). It differs from by maxillary barbel reaching between verticals through anal-fin origin and its adpressed terminus (*vs.* maxillary barbel reaching up to anal-fin origin in *P. australis*, *P. griffini*, *P. harttii*, *P. ignobilis*, *P. kronei*, *P. laticeps*, *P. linami*, *P. meeki* and *P. straminea*; maxillary barbel surpassing caudal fin origin in *P. cruxenti*, *P. mucosa* and *P. notomelas*). It differs from *P. buckleyi*, *P. gracilis*, *P. laurenti* and *P. macturki* by having 42 total vertebrae (*vs.* 43–44 total vertebrae in *P. buckleyi*; 46 total vertebrae in *P. gracilis*; 39–41 total vertebrae in *P. laurenti* and *P. macturki*). It differs from *P. martinezi* by having a wide, well delimited midlateral dark stripe (*vs.* narrow, not well delimited midlateral dark stripe). It differs from *P. buckleyi*, *P. roccae* and *P. vittata* by having large, hook-like dentations along pectoral fin spine posterior margin basal half to three fourths (*vs.* posterior margin of pectoral-fin spine with small, smooth dentations in *P. buckleyi* and *P. roccae*; small triangular dentations in *P. vittata*). It differs from *P. avanhandavae* and *P. taeniophora* by the absence of a paired dorsolateral stripe along body (*vs.* presence of a paired dorsolateral stripe along dorsak region until half of adipose-fin base in *P. avanhandavae*; presence of a paired dorsolateral stripe along supraoccipital process in *P. taeniophora*).

Furthermore, *P. lateristriga* can be diagnosed by the presence of maxillary barbel reaching between verticals through anal-fin origin and its adpressed terminus; posterior margin of pectoral-fin spine bearing 7–13 retrorse dentations along its basal half to three fourths, these dentations are large, hook-like; adipose fin three to three and half times in SL; dark brown midlateral stripe wide, well delimited, from snout to caudal-fin origin or along median caudal-fin rays; head overall darker.

Description

Measurements in Table 36. Body of moderate depth, depth at dorsal-fin origin five to seven and half times in standard length, and compressed, body width at dorsal-fin origin seven and half to nine times in SL (Fig. 108). Greatest body depth at dorsal-fin origin. Dorsal profile convex from snout to dorsal-fin origin, concave from dorsal to adipose fin, slightly convex along adipose fin, and concave at the caudal peduncle. Ventral profile of body slightly convex from snout to branchiostegal membrane, concave between pectoral end pelvic fins, slightly convex from pelvic to anal fin, and concave from this point along the caudal peduncle.

Pseudotympanum large, oval, above posterior process of cleithrum and reaching 6th (1) vertebrae. Posterior process of cleithrum triangular, its dorsal border concave. Anus and urogenital papilla adjacent. Urogenital papilla tubular, triangular, average sized. Anus between verticals through first third and second fifth of adpressed pelvic fin; urogenital papilla reaching between verticals through last third and last sixth of adpressed pelvic fin.

Head moderate depressed, depth at supraoccipital-process base slightly less than two to two and half times in head length. Mouth sub terminal. Eye slightly elliptical, four and half to five and half times in head. Bony interorbital distance a third smaller than eye diameter. Barbels thin, slightly depressed and elliptical in cross-section. Maxillary barbel reaching between verticals through anal-fin origin and its adpressed terminus. Outer mental barbel, when stretched parallel to main body axis, finishing between first third and almost terminus of adpressed pectoral fin. Inner mental barbel, when stretched parallel to main body axis, finishing between branchiostegal membrane ventral limit and pectoral fin terminus. Supraoccipital process subrectangular, narrow, and distal third slightly tapered. Dorsal lamina of Weberian complex vertebrae reaching the supraoccipital process at its anteriormost part. Branchiostegal rays 6 (1).

Dorsal fin triangular, distal margin concave, short (second branched dorsal-fin ray five to nine times in SL), depressed tip finishing between verticals through half and last third of adpressed pelvic fin. Dorsal fin with I,6 (45) plus anteriormost spinelet. Distance between terminus of dorsal-fin base and adipose-fin origin a third shorter than dorsal-fin base. Anteriormost dorsal-fin pterygiophore inserted posterior to neural spine of vertebrae 4 (1); posteriormost dorsal-fin pterygiophore located ahead of neural (or pseudoneural) spine of vertebrae 11 (1). Unbranched dorsal-fin ray mostly ossified as a spine, rigid part usually long (less than a quarter shorter than the first dorsal-fin total length), distal half on anterior side with smooth serrae.

Pectoral-fin rays I,7 (1)– I,9 (3), usually I,8* (5), pectoral fin triangular with concave distal border. First pectoral-fin ray curved with proximal part rigid, forming a spine (Fig. 109A), and short distal tip flexible and distinctly segmented. Pectoral-fin spine four to six times in SL. Anterior margin of pectoral-fin spine with smooth, straight dentations along its basal half. Posterior margin of pectoral-fin spine bearing 7–13 retrorse dentations along its basal half to three fourths. These dentations are large, hook-like, comparatively larger in some specimens (Fig. 109C, D). Also 1–2 unossified distal dentations, not counted.

Pelvic-fin rays i,5 (10), extended pelvic fin triangular with straight distal border. Anterior portion of pelvic-fin base between verticals through dorsal fin terminus or a point slightly posterior to that. Tip of adpressed pelvic fin between verticals through adipose fin origin and its first eight. First unbranched and flexible ray distinctly shorter than second and third rays, which are roughly the same size; remaining rays progressively shorter.

Anal-fin rays v,7* (1); iii,8 (1); v,8 (1); iii,9 (1); iv,9 (1); v,9 (2); or iv,10 (2); distal border of extended anal fin convex. Two to four anteriormost anal-fin rays vestigial, unsegmented, embedded in thick skin fold. Anal fin origin between verticals through first sixth and second fifth of adipose-fin base; anal-fin adpressed terminus at vertical through adipose-fin terminus. Tip of anteriormost anal-fin pterygiophore inserted posterior to hemal spine of vertebrae 21 (1). Tip of posteriormost anal-fin pterygiophore inserted ahead of hemal spine of vertebrae 29 (1).

Adipose fin three to three and half times in SL, forming ascending elevated curve in lateral profile, with deepest point approximately at last third. Adipose fin emerging gradually, its posterior limit as a rounded, free lobe. Adipose-fin origin at vertical through vertebral centrum 19 (1); adipose-fin terminus at vertical through vertebral centrum 35 (1).

Caudal fin deeply forked, dorsal lobe slightly longer. Caudal peduncle length posterior to adipose-fin two times its depth. Dorsal lobe with 7 (9) branched, 1 (9) unbranched principal, and 8*(1)–16 (2) procurrent fin-rays. Ventral lobe with 8 (9) branched, 1 (9) unbranched principal, and 13* (1)–28 (2) procurrent fin-rays. Hypural 5 completely free, not fused to hypural 3+4. Median caudal-fin rays not articulated directly to caudal plate. Seven (1) rays articulated to dorsal caudal-fin plate (5 on hypurals 3+4 and 2 on hypural 5) and 8 (1) rays articulated to ventral caudal-fin plate (6 on hypurals 1+2 and 2 on parhypural).

Total vertebrae 42 (1). Ribs 8 (1).

Epiphyseal branch of lateral sensory canal on head (S6) opening in two separated pores.

Coloration in alcohol

Background body coloration yellowish. Ventral region of head and body lighter. Dark brown midlateral stripe (Fig. 110, 111) wide, well delimited, from snout to caudal-fin origin or along median caudal-fin rays. Cephalic dark brown pigment along posterior fontanel region. Head overall darker. Dorsal fin overall dark, except by a hyaline stripe near its base. Some small variation on coloration can be found, from specimens with an overall darker body, and wider, well-delimited, midlateral stripe (*e.g.* from Cachoeira de Macacu and Macaé, Rio de Janeiro State); to lighter specimens, with narrower and lighter midlateral stripe (*e.g.* Espírito Santo State).

Geographic distribution

Pimelodella lateristriga was described for “Brazil”, and its locality was narrowed to Rio de Janeiro and vicinities by Mees (1983), in the basis of collector data. *Pimelodella bahiana*, its junior-synonym, was described from fresh water bodies in Bahia State, Brazil. Therefore, *Pimelodella lateristriga* is known from regions 329 (Paraíba do Sul), 330 (Ribeira de Iguape) and 328 (Northeastern Mata Atlântica), in São Paulo, Minas Gerais, Rio de Janeiro, Espírito Santo and Bahia States, Brazil.

Comments

Eigenmann (1910) suggested that the report of *P. lateristriga* from the Paraguay basin made by Boulenger (1896) actually refers to *P. taeniophora*, a decision corroborated here. However, Eigenmann & Eigenmann (1888, 1890) and Eigenmann (1910, 1917) report *Pimelodella lateristriga* for several rivers in the Amazon and Paraguay basins, decisions followed by other authors (see synonym). Mees (1974, 1983) proposes that records of *P. lateristriga* from Surinam and Guianas are misidentifications of *P. cristata*, and suggests its distribution as restricted to the region of Rio de Janeiro region, based on data on the collector (von Olfers). However, part of Mees’ specimens of *P. lateristriga* (RMNH 17301) is probably *P. brasiliensis* or *P. harttii*, since the dentations on posterior margin of pectoral-fin spine are small.

Mention of *P. lateristriga* from locations outside coastal Southeastern basins of Brazil were all referable to other species (when unambiguous identification was possible)

Eigenmann’s (1917) suggestion that *P. transitoria* is indistinguishable from *P. lateristriga* is probably due the fact that his material of *P. transitoria* was, in fact, *P. lateristriga*. The pectoral-fin spine illustrated for *P. transitoria* (Eigenmann, 1917: pl. XXXV, fig. 10) is much more similar to those of *P. lateristriga* than to material identified as *P.*

transitoria by Miranda Ribeiro. As discussed under the entry for *P. kronei*, *P. transitoria* is a junior-synonym of *P. kronei*, but *P. lateristriga* is distinguishable from it.

Pimelodus bahianus remained a long time as junior-synonym of *Rhamdia quelen* following Eigenmann & Eigenmann (1890), who have not justified that decision but which nonetheless was followed by several authors (see synonymy). Silfvergrip (1997) transferred *Pimelodus bahianus* provisionally to *Pimelodella*, but that species remains as *species inquirenda* in *Pimelodella* to this date. Examination of the type-material of *Pimelodus bahianus* shows that it belongs to *Pimelodella* and that it is indistinguishable from *P. lateristriga*. Additional comparative material from Bahia state is also consistent with *P. lateristriga*. Type-specimens of *Pimelodella bahiana* have dentations on the pectoral-fin spine (Fig. 109D) larger than those of *P. lateristriga* (Fig. 109A). However, there is overlapping variation in size and shape of pectoral-fin spine dentation in specimens from other localities (e.g. Fig 109B, C), which supports synonymization of the two taxa. However, *P. lateristriga* from Espírito Santo and Bahia States tend to be lighter colored when compared with specimens from Minas Gerais, Rio de Janeiro, and São Paulo States, though to a degree not sufficient to indicate specific differentiation.

Specimen MNHN B612 93.4 mm SL is designated here as the lectotype (Fig. 112), with remaining specimen (101.0 mm SL) as paralectotypes. The comparative measurements for *P. lateristriga* and specimens previously assignable to *P. bahiana* are presented in Table 37.

Material examined

Pimelodella lateristriga. — ZMB 3038, 1, xr, 95.9 mm SL, holotype, Brazil, Rio de Janeiro, [Mees (1983) limits to near Rio de Janeiro based on collector and year described for Müller & Troschel, 1849], 22°52'55"S, 43°14'39"W; ANSP 174039, 1, 86.43 mm SL, Brazil, Rio de Janeiro, Arroio at Fazenda Conceição on highway BR 101 approx. 5 km S of the border between Rio de Janeiro/Espírito Santo, 21°19'14"S, 41°19'42"W; ANSP 174041, 2, 88.71–86.43 mm SL, Brazil, Espírito Santo, Rio Novo do Sul (Rio Noa) on highway BR-101 just to S of Rio Novo do Sul, 20°52'33"S, 40°57'50"W; LIRP 7847, 2, 94.2 mm SL, Brazil, Espírito Santo, Sao Jose do Calçado, Rio Itabapoana, almost 300 m downstream from UHE Rosal's Power Station, 20°57'19.0"S, 41°43'01.0"W; MZUSP 41859, 1, 70.7 mm SL, Brazil, São Paulo, Registro, Rio Quilombo, in Fazenda Dalila, 24°22'0.0"S, 47°51'0.0"W; MZUSP 58724, 2, 112–117.1 mm SL, Brazil, São Paulo, Peruipe, Rio Itinguçu, affluent of Rio Una do Prelado - E.E.J.I., 24°23'59.0"S, 47°7'25.0"W; MZUSP 90744, 11, 38.1–59.0 mm SL, Brazil, Espírito Santo, Iconha, Rio Iconha, 20°49'13.0"S, 40°47'46.0"W; MZUSP 93863, 1, 99.5 mm

SL, Brazil, Espírito Santo, Pedro Canario, Rio Dourado, afl. Rio Itaúnas, under the bridge at BR-101, 18°15'9.0"S, 39°57'13.0"W; MZUSP 93864, 1, 61.2 mm SL, Brazil, Minas Gerais, Nanuque, Córrego do Ene, afl. Rio Mucuri, at BR-478, in the way to Teófilo Otoni, 17°48'30.0"S, 40°24'13.0"W; MZUSP 114867, 1, 84 mm SL, Brazil, São Paulo, Itanhaém, Rio Branco, in Sítio do Sr. Luís, 6,4 km after the dam, dirt road left of the main entrance, 24°01'44.0"S, 46°43'19.6"W; MZUSP 121279, 2, 93.3–96.2 mm SL, Brazil, Rio de Janeiro, Itaguaí, Rio Mazomba, vicinity of Mazomba, 22°51'37.0"S, 43°52'34.0"W; MZUSP 121310, 1, 94.7 mm SL, Brazil, Rio de Janeiro, Macaé, Rio Aduelas, afluyente do rio São Pedro, under the bridge at km 157 of BR-101, Rio Macaé basin, 22°15'59.9"S, 41°51'31.0"W; MZUSP 121461, 9, 54.4–112.7 mm SL, Brazil, Rio de Janeiro, Conceição De Macabu, Rio Aduelas, affluent of Rio São Pedro, in Fazenda Sossego, Rio Macaé basin, 22°11'56.0"S, 41°50'23.0"W; USNM 100917, 1, 64.9 mm SL, Brazil, Rio de Janeiro, Therezopolis, Guapi, 22°25'14.7"S, 42°58'20.9"W; USNM 129923, 3, 40.0–46.3 mm SL, Brazil, Rio de Janeiro, Vicinity Rio De Janeiro, 22°49'43.5"S, 43°37'34.3"W; USNM 129925, 4, 51.5–62.0 mm SL, Brazil, Rio de Janeiro, Vicinity Rio De Janeiro, 22°49'43.5"S, 43°37'34.3"W; USNM 301676, 1 musc., Brazil, Minas Gerais, Rio Mucuri drainage, Rio Mucuri, approx. 26 km SE of town of Nanuque on Fazenda Santa Clara, approx. 1 km downstream from camp site, side channel of main river, 17°53'47.3"S, 40°12'22.9"W; USNM 320324, 1, 76.3 mm SL, Brazil, Minas Gerais, Ipatinga, Rio Taquarucu, at road BR-381, 19°28'57.0"S, 42°32'53.3"W.

Pimelodella bahiana. — MNHN B 612, 1, xr, 93.4 mm SL, lectotype, Brazil, Bahia, Freshwaters of Bahia, 12°54'47"S, 38°24'37"W; MNHN B 612, 1, xr, 100.1 mm SL, syntypes, Brazil, Bahia, Freshwaters of Bahia, 12°54'47"S, 38°24'37"W; MZUSP 39102, 2, 51.7–61.8 mm SL, Brazil, Rio do Caí at Limoeiro farm, 17°5'0.0"S, 39°13'0.0"W; MZUSP 39104, 3, 29.3–58.6 mm SL, Brazil, Bahia, Rio do Sul, at Cumuruxatiba-Itamaraju road, before Fazenda Limoeiro, 17°3'0.0"S, 39°29'0.0"W; MZUSP 63459, 2, 81–91.5 mm SL, Brazil, Bahia, Prado, pier at Jucuruçú River bank, 17°20'26.0"S, 39°13'43.0"W.

***Pimelodella laticeps* Eigenmann, 1917**

Pimelodella laticeps Eigenmann, 1917: 243, fig. 2, pl. XXX, fig. 2, pl. XXXV, fig. 9 [original description; "Sapucay, Paraguay"; holotype: FMNH 57969 (formerly CM 6957a)]. — Henn, 1928: 77 [type catalog]. — Gosline, 1945: 44 [taxonomic treatment]. — Fowler, 1951: 545, fig. 559 (*in partim*) [taxonomic treatment]. — López *et al.*, 1981: unnum. pages [taxonomic list]. — López *et al.*, 1982: 7–9 [taxonomic list]. — Ibarra & Stewart, 1987: 66 [type catalog]. — Burgess, 1989: 280 [taxonomic treatment]. —

Bockmann & Guazzelli, 2003: 419 [taxonomic treatment]. — López *et al.*, 2003: 62 [taxonomic list]. — Ferraris, 2007: 192 [taxonomic treatment]. — Litz & Koerber, 2014: 21 [taxonomic list]. — Mirande & Koerber, 2015: 34 [taxonomic list]. — Koerber *et al.*, 2017: 51 [taxonomic list].

Diagnosis

Pimelodella laticeps can be diagnosed from all *Pimelodella* with exception of *P. cruxenti*, *P. modesta*, *P. montana*, *P. pectinifera* and *P. yuncensis* by having an overall dark brown body. It differs from *P. cruxenti*, *P. modesta*, *P. montana* and *P. yuncensis* by having the adipose fin four times in SL (*vs.* adipose fin roughly two times or less in SL in *P. cruxenti*; adipose fin roughly three times in SL in *P. modesta* and *P. montana*; two and half to four times in SL in *P. yuncensis*). It differs from *P. pectinifera* by having a dark mark between dorsal and adipose fins (*vs.* mark absent in *P. pectinifera*). Furthermore, *P. laticeps* can be diagnosed by maxillary barbel reaching between pelvic fin origin and its first third adpressed; posterior margin of pectoral-fin spine with 10–12 slightly retrorse dentations along its basal two thirds, these dentations are not notably retrorse, the ones nearer base and apex are smaller and straighter; adipose fin short, four times in SL; epiphyseal branch of cephalic laterosensory canal (S6) emerging as two separate pores, apart from each other; dark brown midlateral stripe wide, not well delimited, posterior to head until caudal-fin insertion; region above pseudotympanum region and dorsal to it with slightly darker pigmentation; dark brown region between dorsal and adipose fins.

Description

Measurements in Table 38. Body moderated depth, depth at dorsal-fin origin slightly more than five times in standard length, and moderated compressed, body width at dorsal-fin origin six to seven times in SL (Fig. 113). Dorsal profile convex from snout to dorsal fin, slightly concave from dorsal to adipose fin, slightly convex along adipose fin, and concave along the caudal peduncle. Ventral profile of body slightly convex from snout to branchiostegal membrane, also convex between pectoral and pelvic fins, slightly concave from pelvic to anal fin, and also concave from there along the caudal peduncle.

Pseudotympanum large, oval, above posterior process of cleithrum and reaching the straight line of 7th* (3) or 8th (1) vertebrae. Posterior process of cleithrum triangular, narrow, its dorsal border slightly concave. Anus and urogenital papilla adjacent. Urogenital papilla tubular, triangular, short. Anus at vertical through first third of adpressed pelvic fin; urogenital papilla at vertical through last sixth of adpressed pelvic fin.

Head deep, depth at supraoccipital-process base two times or less in head length. Mouth sub terminal. Eye slightly elliptical, five and half to six and half times in head. Bony interorbital distance larger than eye diameter. Barbel thin, depressed and elliptical in cross-section. Maxillary barbel reaching between pelvic fin origin and its first third adpressed. Outer mental barbel, when stretched parallel to main body axis, finishing between verticals through first and second fifth of adpressed pelvic fin. Inner mental barbels, when stretched parallel to main body axis, finishing between branchiostegal membrane ventral limit and pectoral-fin origin. Supraoccipital process narrow, triangular. Dorsal lamina of Weberian complex vertebrae of medium height, reaching the supraoccipital process just at its anteriormost part. Branchiostegal rays 6 (4).

Dorsal fin triangular, distal margin convex, short (second branched dorsal-fin five to six and half times in SL) reaching between verticals through half and distal third of adpressed pelvic fin. Dorsal fin with I,6 (2) or I,7* (1) plus anteriormost spinelet. Distance between terminus of dorsal-fin base and adipose-fin origin the same or slightly larger than dorsal-fin base. Anteriormost dorsal-fin pterygiophore inserted posterior to neural spine of vertebrae 4 (4); posteriormost dorsal-fin pterygiophore located ahead of neural (or pseudoneural) spine of vertebrae 10* (2) or 11 (2).

Pectoral-fin rays I,8* (3) or I,9 (1), pectoral fin triangular with concave distal border. First pectoral-fin ray roughly straight, with proximal part rigid, forming a spine (Fig. 114), and short distal tip flexible and distinctly segmented. Pectoral-fin spine four to five and half times in SL. Anterior margin pectoral-fin spine with small, straight dentations along basal half, and smooth serrae along distal half of anterior margin. Posterior margin of pectoral-fin spine with 10–12 slightly retrorse dentations along its basal two thirds. These dentations are not notably retrorse, the ones nearer base and apex are smaller and straighter. Also, 1–3 unossified distalmost dentations.

Pelvic-fin rays i,5 (3), extended pelvic fin triangular with straight distal border. Pelvic-fin origin between verticals through dorsal-fin terminus and half adpressed dorsal fin. Tip of adpressed pelvic fin between verticals through adipose fin origin and its first sixth. First unbranched and flexible ray distinctly shorter than second and third rays, third ray the longest; remaining rays progressively shorter.

Anal-fin rays v,8 (1); vi,8 (1); vi,9 (1); or iii,10* (1), distal border of extended anal fin convex. Two or three anteriormost anal-fin rays vestigial, unsegmented, embedded in thick skin fold. Anal-fin origin between verticals through first fourth or third of adipose-fin base. Anal-fin adpressed terminus slightly posterior to vertical through adipose-fin terminus. Tip of

anteriormost anal-fin pterygiophore inserted posterior to hemal spine of vertebrae 21* (3) or 22 (1). Tip of posteriormost anal-fin pterygiophore inserted ahead of hemal spine of vertebrae 29* (3) or 30 (1).

Adipose fin four times in SL, forming ascending elevated curve in lateral profile, with deepest point approximately at midlength. Adipose fin emerging gradually, its posterior limit as a rounded, free lobe. Adipose-fin origin at vertical through vertebral centra 20 (2)– 22* (1); adipose-fin terminus at vertical through vertebral centra 32* (1)–35 (1).

Caudal fin deeply forked, lobes subequal. Caudal peduncle length posterior to adipose-fin slightly longer than its depth. Dorsal lobe with 7 (3) branched, 1 (3) unbranched principal and 9 (1)–14* (1) procurrent fin-rays. Ventral lobe with 8 (3), 1 (3) unbranched principal branched and 11 (1)–15* (1) procurrent fin-rays. Hypural 5 completely free, not fused to hypural 3+4. Median caudal-fin rays not directly articulated to caudal plate. Seven (3) rays articulated to dorsal caudal-fin plate (5 on hypurals 3+4 and 2 on hypural 5) and 8 (3) rays articulated to ventral caudal-fin plate (6 on hypurals 1+2 and 2 on parahypural).

Total vertebrae 39 (2)–40* (2). Ribs 8 (2)– 9* (2).

Epypheseal branch of cephalic laterosensory canal (S6) emerging as two separate pores, apart from each other.

Coloration in alcohol

Background body coloration yellowish. Ventral region of head and body lighter. Dark brown midlateral stripe wide (Fig. 115), not well delimited, posterior to head until caudal-fin insertion. Region above pseudotympanum region and dorsal to it with slightly darker pigmentation. Dark brown region between dorsal and adipose fins. Dorsal region of head and body slightly darker. Dorsal fin overall dark, except by a hyaline stripe near its base.

Geographic distribution

Pimelodella laticeps was described from Sapucay, Rio Paraguay basin, in Paraguay. It is known from regions 342 (Chaco), 343 (Paraguay) and 345 (Lower Paraná), in Paraguay, Argentina and Uruguay (see comments).

Comments

Several works report *P. laticeps* to Paraguay, Argentina and Uruguay (see synonym). Despite those material have not been checked, since the coloration pattern of *P. laticeps* is very conspicuous when compared with other *Pimelodella*, I maintained those literature in the synonym a priori. However, material of Argentina and Uruguay should be examined in order to securely delimit *P. laticeps* distribution.

Furthermore, fossils of Heptapteridae were found in the Cenozoic of Buenos Aires province, Argentina, and one of them identified as pertaining to *Pimelodella* cf. *P. laticeps* (Arratia & Cione, 1996 *apud* Bockmann & Guazzelli, 2003). Those materials, however, deserve further studies to verify the identifications (Bockmann & Guazzelli, 2003).

Material examined

Pimelodella laticeps. — FMNH 57969, 1, xr, 49.0 mm SL, holotype, Paraguay, Sapucaí, 25°39'25"S, 56°57'18"W; FMNH 57970, 3, xr, 61.5–72.7 mm SL, paratypes, Paraguay, Sapucaí, 25°39'25"S, 56°57'18"W; USNM 101283, 1, 80.2 mm SL, Argentina, San Pedro, 220 K. North of Buenos Aires, 33°39'14.5"S, 59°39'18.0"W.

***Pimelodella laurenti* Fowler, 1941a**

Pimelodella laurenti Fowler, 1941a: 132–133, figs. 16–19 [original description; “Jatobá, Rio São Francisco, Pernambuco”]; holotype: ANSP 69380 (incorrectly published as 19380). — Gosline, 1945: 47 [taxonomic treatment]. — Fowler, 1951: 545–546, fig 560 [taxonomic treatment]. — Böhlke, 1984: 141 [type catalog]. — Burgess, 1989: 280 [taxonomic treatment]. — Bockmann & Guazzelli, 2003: 419 [taxonomic treatment]. — Rosa *et al.*, 2003: 177 [taxonomic list]. — Trajano *et al.*, 2004: 318 [taxonomic treatment, comparison with *P. spelaea*]. — Ferraris, 2007: 192 [taxonomic treatment].

Pseudorhamdia lateristriga. — Lütken, 1875: 171 [taxonomic treatment].

Diagnosis

Pimelodella laurenti differs from all *Pimelodella* species except *P. australis*, *P. avanhandavae*, *P. buckleyi*, *P. cruxenti*, *P. gracilis*, *P. griffini*, *P. harttii*, *P. ignobilis*, *P. itapicuruensis*, *P. kronei*, *P. lateristriga*, *P. laticeps*, *P. leptosoma*, *P. linami*, *P. macturki*, *P. martinezi*, *P. meeki*, *P. megalura*, *P. metae*, *P. montana*, *P. mucosa*, *P. notomelas*, *P. roccae*, *P. straminea*, *P. taeniophora* and *P. vittata* by having the dorsal fin with a darker region near the base, followed by a hyaline stripe, and distally darker (unknown in *P. martinezi*). It differs from *P. itapicuruensis*, *P. leptosoma*, *P. megalura*, *P. metae* and *P. montana* by having the supraoccipital process reaching the anterior prenuchal plate (vs. supraoccipital process not reaching the anterior prenuchal plate in *P. itapicuruensis*, *P. leptosoma*, *P. megalura*, *P. metae* and *P. montana*). It differs from *P. cruxenti*, *P. gracilis*, *P. harttii*, *P. kronei*, *P. lateristriga* and *P. vittata* by having 39–41 total vertebrae (vs. 42 or more vertebrae in *P. cruxenti*, *P. gracilis*, *P. harttii*, *P. kronei*, *P. lateristriga* and *P. vittata*). It differs from *P. australis*, *P. griffini*, *P. ignobilis*, *P. laticeps*, *P. linami*, *P. meeki* and *P. straminea* by maxillary barbel

reaching between adpressed anal fin and surpassing caudal-fin origin (*vs.* maxillary barbel reaching at best anal-fin origin in *P. australis*, *P. griffini*, *P. ignobilis*, *P. laticeps*, *P. linami*, *P. meeki* and *P. straminea*). It differs from *P. martinezi* and *P. notomelas* by having a moderate to large dark midlateral stripe (*vs.* narrow midlateral stripe in *P. martinezi* and *P. notomelas*). It differs from *P. mucosa* and *P. roccae* by having posterior margin of pectoral-fin spine bearing 11–13 retrorse, large, inclined dentations along its basal two thirds (*vs.* small, smooth dentations on posterior margin of pectoral-fin spine in *P. mucosa* and *P. roccae*). It differs from *P. avanhandavae* and *P. macturki* by having a paired dorsolateral stripe along supraoccipital process (*vs.* paired dorsolateral stripe reaching up to half adipose-fin base in *P. avanhandavae*; paired dorsolateral absent in *P. macturki*). It differs from *P. taeniophora* by having the supraoccipital process narrow, dorsal lamina of Weberian complex vertebrae reaching the supraoccipital process along its entire extension, and epiphyseal branch of laterosensory canal on head opening in a single pore, at the contralateral canals connection (*vs.* supraoccipital process of moderate width, dorsal lamina of Weberian complex vertebrae reaching the supraoccipital process just at its anteriormost part, and epiphyseal branch of laterosensory canal on head with contralateral canals connecting at midline, proceeding posteriorly as a single canal, and opening in a single pore).

Furthermore, *P. laurenti* can be diagnosed by maxillary barbel reaching between adpressed anal fin and surpassing caudal-fin origin; dorsal lamina of Weberian complex vertebrae reaching the supraoccipital process along its entire extension; posterior margin of pectoral-fin spine bearing 11–13 retrorse dentations along its basal two thirds, these dentations are large, inclined and sharply pointed; adipose fin two to three times in SL; caudal fin deeply forked, dorsal lobe notably longer; 39–41 total vertebrae; dark brown midlateral stripe of moderated width to large, not well delimited, from snout along median caudal-fin rays; paired dorsal dark stripes along supraoccipital process, and dark region at dorsal-fin rays base.

Description

Measurements in Table 39. Body of moderated depth, depth at dorsal-fin origin four and half to five and half times in standard length, and moderated compressed, five to eight times in SL (Fig. 116). Dorsal profile convex from snout to supraoccipital process, convex from dorsal fin to adipose, and concave along caudal peduncle. Ventral profile of body slightly convex from snout to branchiostegal membrane, concave between pectoral and pelvic fins, slightly concave from pelvic to anal fin, and straight from this point along caudal peduncle.

Pseudotympanum large, oval, dorsal to posterior process of cleithrum and reaching 6th* (1) or 7th (1) vertebrae. Posterior process of cleithrum triangular, its dorsal border concave. Anus and urogenital papilla adjacent. Urogenital papilla tubular, triangular, short. Anus at vertical through second fifth of adpressed pelvic fin; urogenital papilla between verticals through last third and terminus of adpressed pelvic fin.

Head deep, depth at supraoccipital process less than two times in head length. Mouth sub terminal. Eyes slightly elliptical, four to five times in head. Bony interorbital distance roughly a fourth smaller than eye diameter. Barbels thin, slightly depressed and elliptical in cross-section. Maxillary barbel reaching between adpressed anal fin and surpassing caudal-fin origin. Outer mental barbel, when stretched parallel to main body axis, finishing between last fourth and terminus of adpressed pectoral fin. Inner mental barbel, when stretched parallel to main body axis, finishing at pectoral fin terminus. Supraoccipital process subrectangular, narrow, tapered at its distal point. Dorsal lamina of Weberian complex vertebrae reaching the supraoccipital process along its entire extension. Branchiostegal rays 6 (1).

Dorsal fin triangular, distal margin concave, of moderated length (second branched dorsal-fin ray four and half to five and half times or more in SL), depressed tip reaching the vertical through second fifth of adpressed pelvic fin. Dorsal fin with I,6 (5) plus anteriormost spinelet. Distance between terminus of dorsal-fin base and adipose-fin origin roughly two thirds of dorsal-fin base. Anteriormost dorsal-fin pterygiophore inserted posterior to neural spine of vertebrae 4 (2); posteriormost dorsal-fin pterygiophore located ahead of neural (or pseudoneural) spine of vertebrae 11 (2). Unbranched dorsal-fin ray mostly ossified as a spine, rigid part relatively long (a fourth shorter than dorsal-fin first ray total length), bearing serrae at anterior margin distal third, and smooth retrorse dentations at its posterior margin distal two thirds.

Pectoral-fin rays I,8 (3)– I,9* (2), pectoral fin triangular with concave distal border. First pectoral-fin ray almost straight, with proximal part rigid (Fig. 117), forming a spine, and short distal tip flexible and distinctly segmented. Pectoral-fin spine roughly five and half times in SL. Anterior margin of pectoral-fin spine with smooth, straight dentations along its basal three fourths and smooth serrations at its distal fourth. Posterior margin of pectoral-fin spine bearing 11–13 retrorse dentations along its basal two thirds. These dentations are large, inclined and sharply pointed. Also, 1–2 distalmost unossified dentations, not counted.

Pelvic-fin rays i,5 (5), extended pelvic fin triangular with convex distal border. Pelvic-fin origin between verticals through dorsal fin terminus and a point slightly posterior to that. Tip of adpressed pelvic fin at vertical through first fifth of adipose-fin base. First unbranched

and flexible ray distinctly shorter than second and third rays, which are subequal; remaining rays progressively shorter.

Anal-fin rays iv,6 (1); iv,7 (1); v,8 (2); or v,9* (1); distal border of extended anal fin convex. Two anteriormost anal-fin rays vestigial, unsegmented, embedded in thick skin fold. Anal-fin origin between verticals through first fourth or third of adipose fin base. Anal-fin adpressed terminus at vertical through adipose fin terminus. Tip of anteriormost anal-fin pterygiophore inserted posterior to hemal spine of vertebrae 21* (1) or 22 (1). Tip of posteriormost anal-fin pterygiophore inserted ahead of hemal spine of vertebrae 26* (1) or 28 (1).

Adipose fin two to three times in SL, forming ascending elevated curve in lateral profile, with deepest point approximately at midlength. Adipose fin emerging gradually, its posterior limit as a rounded, free lobe. Adipose-fin origin at vertical through vertebral centra 16* (1)– 19 (1); adipose-fin terminus at vertical through vertebral centra 35* (1)– 36 (1).

Caudal fin deeply forked, dorsal lobe notably longer. Caudal peduncle length posterior to adipose fin slightly longer than its depth. Dorsal lobe with 7 (3) branched, 1 (3) unbranched principal and 15* (1) –17 (1) procurrent fin-rays. Ventral lobe with 8 (3), rarely 9* (1) branched, 1 (4) unbranched principal and 11 (1) –19* (1) procurrent fin-rays. Hypural 5 separated from hypurals 3+4. Median caudal-fin rays not directly articulated to caudal plate. Seven (2) rays articulated to dorsal caudal-fin plate (5 on hypurals 3+4 and 2 on hypural 5) and 8 (2) rays articulated to ventral caudal-fin plate (6 on hypurals 1+2 and 2 on parahypural).

Total vertebrae 39* (1)–41 (1). Ribs 8 (2).

Contralateral epiphyseal branch of cephalic laterosensory canal (S6) unite in midline, and open in dorsal region of head as a single pore.

Coloration in alcohol

Background body coloration yellowish. Ventral region of head and body lighter. Dark brown midlateral stripe of moderated width to large (Fig. 118, 119), not well delimited, from snout along median caudal-fin rays. Dorsal fin mostly light colored, except by a dusky region at its distal third and at dorsal-fin base. Paired dorsal dark stripes along supraoccipital process, and dark region at dorsal-fin rays base. Cephalic dark brown pigment along posterior fontanel region.

Geographic distribution

Pimelodella laurenti was described from Rio São Francisco basin. It is known from region 327 (S. Francisco).

Comments

Holotype was incorrectly published as ANSP 19380, and paratypes as 19381 and 19382; correct numbers are ANSP 69380, 69381 and 69382, respectively (Böhlke, 1984).

Register of *P. lateristriga* from Rio das Velhas basin was treated here under *P. laurenti* synonym, due to general similarity in pectoral-fin spine and body shape between both species.

Material examined

Pimelodella laurenti. — ANSP 69380, 1, xr, 66.5 mm SL, holotype, Brazil, Pernambuco, Jatoba, Rio San Francisco, 9°11'42"S, 38°16'43"W; ANSP 69381, 2, xr, 59.5–67.2 mm SL, paratypes, Brazil, Pernambuco, Jatoba, Rio San Francisco, 9°11'42"S, 38°16'43"W; MZUSP 39441, 2, 62.8 mm SL, Brazil, Minas Gerais, Rio Formoso, affluent of rio São Francisco, 17°26'0.0"S, 44°57'0.0"W; MZUSP 47310, 14, 32.2–92.7 mm SL, Brazil, Minas Gerais, stream affluent to rio Jequitai, at BR-135, between Buenopolis and Engenheiro Dolabela, 17°45'0.0"S, 44°6'0.0"W.

***Pimelodella leptosoma* (Fowler, 1914)**

Rhamdella leptosoma Fowler, 1914: 260–263, fig. 12 [original description; “Rupununi River, British Guiana”; holotype: ANSP 39340]. — Gosline, 1945: 34 [taxonomic treatment]. — Böhlke, 1984: 141–142 [type catalog]. — Burgess, 1989: 278 [taxonomic treatment]. — Bockmann & Guazzelli, 2003: 422 [taxonomic treatment]. — Ferraris, 2007: 196 [taxonomic treatment]. — Bockmann & Miquelarena, 2008: 45–47 [taxonomic treatment, *Rhamdella* revision, possibly in *Pimelodella*]. — Le Bail, 2012: 304 [taxonomic list].

Rhamdella cf. *leptosoma*. — Le Bail *et al.*, 2000: 142–143, unnum. fig. [taxonomic treatment].

Pimelodella leptosoma. — Slobodian *et al.*, 2017: 93–94, fig. 6C [taxonomic treatment, comparison with *P. humeralis*].

Diagnosis

Pimelodella leptosoma can be distinguished from all *Pimelodella* species except *P. buckleyi*, *P. grisea*, *P. geryi*, *P. metae* and *P. notomelas*, by the presence of dorsal fin distal third extremely dark brown to black. It differs from all above, except *P. metae* by having the supraoccipital process not reaching the anterior prenuchal plate. It differs from *P. metae* by the posterior margin of pectoral-fin spine bearing 8–9 broad-based, triangular, strongly inclined, blade-like retrorse dentations along basal two thirds (*vs.* posterior margin of

pectoral-fin spine bearing 4–5 smooth, retrorse to straight dentations along its basal half in *P. metae*). Furthermore, *P. leptosoma* can be diagnosed by maxillary barbel reaching between half adpressed anal fin and its terminus; supraoccipital process narrow, subrectangular, not reaching anterior preopercular plate; posterior margin of pectoral-fin spine bearing 8–9 broad-based, triangular, strongly inclined, blade-like retrorse dentations along basal two thirds; adipose fin slightly more than two and half times in SL; total vertebrae 41–44; dark black midlateral stripe moderately large, not well delimited, from snout to caudal-fin origin; dorsal fin with a medium brown stripe at base, followed a hyaline stripe occupying almost basal half of spine, and distal third dark brown to black.

Description

Measurements in Table 40. Body extremely depressed, depth at dorsal-fin origin six to eight times in standard length, and compressed, body width at dorsal-fin origin seven to ten times in SL (Fig. 120). Dorsal profile convex from snout to dorsal fin, slightly concave from dorsal to adipose fin, slightly convex along adipose fin, and concave along the caudal peduncle. Ventral profile of body slightly convex from snout to branchiostegal membrane, concave between pectoral and pelvic fins, slightly concave from pelvic to anal fin, and also concave from there along the caudal peduncle. Posterior process of cleithrum triangular, broad, its dorsal border straight.

Head depressed, depth at supraoccipital-process base two and half to slightly more than two times in head length. Mouth sub terminal. Eye slightly elliptical, slightly more than three to four and half times in head length. Barbels thin, and elliptical in cross-section. Maxillary barbel reaching between half adpressed anal fin and its terminus. Outer mental barbel, when stretched parallel to main body axis, finishing between verticals through half adpressed pectoral fin and dorsal fin terminus. Inner mental barbels, when stretched parallel to main body axis, finishing between verticals through pectoral fin origin and terminus. Supraoccipital process narrow, subrectangular, not reaching anterior preopercular plate. Dorsal lamina of Weberian complex vertebrae reaching supraoccipital process just at its anteriormost part.

Dorsal fin triangular, distal margin convex, short (second branched dorsal-fin ray five to five and half times in SL), depressed tip finishing between verticals through last third and last fourth of adpressed pelvic fin. Dorsal fin with I,6 (8) plus anteriormost spinelet. Distance between terminus of dorsal-fin base and adipose-fin origin half to two thirds of dorsal-fin base. Anteriormost dorsal-fin pterygiophore inserted posterior to neural spine of vertebrae 5 (8); posteriormost dorsal-fin pterygiophore located ahead of neural (or pseudoneural) spine of

vertebrae 12 (8). Unbranched dorsal-fin ray with proximal part ossified as a spine, spinous part short (approximately two thirds or less of first dorsal-fin total length).

Pectoral-fin rays I,8 (2)– I,10 (1) (holotype I,9), pectoral fin triangular with convex distal border. First pectoral-fin ray with proximal part rigid, roughly straight forming a spine (Fig. 121), and short distal tip flexible and distinctly segmented. Pectoral-fin spine short, six to seven times in SL. Anterior margin of pectoral-fin spine with smooth serrae along its distal half. Posterior margin of pectoral-fin spine bearing 8–9 broad-based, triangular, strongly inclined, blade-like retrorse dentations along basal two thirds. Also 1–3 distalmost unossified dentations, not counted.

Pelvic-fin rays i,5 (9). Pelvic-fin origin between verticals through fifth dorsal-fin ray and dorsal-fin terminus. Pelvic-fin adpressed terminus between verticals through adipose-fin origin and first fifth of adipose-fin base.

Anal-fin rays iv,7 (2); iv,8 (1); v,8 (3); or v.9* (2); distal border of extended anal fin convex. Anal-fin origin between verticals through first fourth and first third of adipose-fin base; anal fin adpressed terminus slightly anterior to vertical through adipose-fin terminus. Tip of anteriormost anal-fin pterygiophore inserted posterior to hemal spine of vertebrae 22 (4), 23* (2) or 24 (2). Tip of posteriormost anal-fin pterygiophore inserted ahead of hemal spine of vertebrae 29 (1), 30 (3), 31* (2) or 32 (1).

Adipose fin slightly more than two and half times in SL, forming ascending elevated curve in lateral profile, with deepest point approximately at last third. Adipose fin emerging gradually, its posterior limit as a rounded, free lobe. Adipose-fin origin at vertical through vertebral centra 17 (1)– 21 (2) (holotype 19); adipose fin terminus at vertical through vertebral centra 37 (1)– 39*(4).

Caudal fin deeply forked, dorsal lobe usually longer than ventral. Caudal peduncle length posterior to adipose-fin a fourth longer than its depth. Dorsal lobe with 7 (7) branched, 1 (7) unbranched principal, and 10 (1)–17 (1) (holotype 12) procurrent fin-rays. Ventral lobe with 8* (5), rarely 7 (1) or 9 (1) branched, 1 (7) unbranched principal, and 10 (1)–18 (1) (holotype 11) procurrent fin-rays. Hypural 5 completely free, not fused to hypural 3+4. Median caudal-fin rays not articulated directly to caudal plate. Seven (6) rays articulated to dorsal caudal-fin plate (5 on hypurals 3+4 and 2 on hypural 5) and 8 (4), rarely 7* (1) or 9 (1) rays articulated to ventral caudal-fin plate (5, 6, or 7 on hypurals 1+2 and 2 on parhypural).

Total vertebrae 41(1)– 44* (3). Ribs 8* (3)– 9 (5).

Epiphyseal branch of laterosensory canal in the head (S6) emerging as two separated pores.

Coloration in alcohol

Background body coloration yellowish. Ventral region of head and body lighter. Dark black midlateral stripe (Fig. 122, 123) moderated large, not well delimited, from snout to caudal-fin origin. Dorsal fin with a medium brown stripe at base, followed a hyaline stripe occupying almost basal half of spine, and distal third dark brown to black.

Geographic distribution

Pimelodella leptosoma was described from Rupununi River, in Guyana. It is known from regions 311 (Guianas) and 315 (Amazonas Guiana Shield), in Guyana, French Guyana, Surinam and Brazil.

Comments

Rhamdella leptosoma was suggested as a possible *Pimelodella* by Bockmann & Miquelarena (2008) due to overall appearance, and geographical distribution (since the *Rhamdella*, as defined in this work, would be limited to southern South America), despite the shorter supraoccipital process.

Material examined

Pimelodella leptosoma. — ANSP 39340, 1, xr, 59.6 mm SL, holotype, Guyana, "Rupununi river, British Guyana", 3°55'01"N, 59°16'27"W; ANSP 39341, 1, xr, 57.9 mm SL, paratype, Guyana, "Rupununi river, British Guyana", 3°55'01"N, 59°16'27"W; AMNH 54942, 31, 92.7 mm SL, Surinam, Nickerie District, Corintijn river, camp hydro, ca. kilometer 370, ca. 30 kilometers north of tiger falls large pool at foot of path from camp, 5°50'44.9"N, 57°06'02.9"W; ANSP 180825, 46, Guyana, Rupununi (Region 9), Kumu Creek (Takutu R.-R. Branco Dr.), 15.2 km SE of Lethem, 3°15'34"N, 59°43'25"W; MPEG 15743, 9, Brazil, Pará, Almerim, rio Ipitinga 0°49'38.3"N, 53°55'29.6"W; MZUSP 30779, 33, xr, 63.7–75.5 mm SL, Brazil, Roraima, Rio Branco, Cachoeira do Bem Querer, Igarapé, 1°56'0.0"N, 61°0'0.0"W; USNM 225733, 17, xr, 72.8 mm SL, Surinam, Nickerie District, Interconnected Rock Pools Near Camp Hydro, 3°42'00.0"N, 57°58'12.0"W; USNM 225733, 17, xr, 1 c&s (72.9 mm SL), Surinam, Nickerie District, pool in front of Camp Hydro, 3°42'00.0"N, 57°58'12.0"W.

***Pimelodella linami* Schultz, 1944**

Pimelodella linami Schultz, 1944: 210–211, pl. I, fig. D [original description; "Rio Torbes, 1 km. above Tariba, Venezuela, Orinoco system"; holotype: USNM 121132]. — Gosline, 1945: 45 [taxonomic treatment]. — Burgess, 1989: 280 [taxonomic treatment]. — Ferraris & Vari, 1992: 35 [type catalog]. — Bockmann, 1994: 768 [taxonomic treatment, *Pimelodella* species with filament]. — Bockmann & Guazzelli,

2003: 419 [taxonomic treatment]. — Lasso *et al.*, 2004: 171 [taxonomic list]. — Ferraris, 2007: 192 [taxonomic treatment].

Diagnosis

Pimelodella linami differs from all *Pimelodella* species except *P. australis*, *P. avanhandavae*, *P. buckleyi*, *P. cruxenti*, *P. gracilis*, *P. griffini*, *P. harttii*, *P. ignobilis*, *P. itapicuruensis*, *P. kronei*, *P. lateristriga*, *P. laticeps*, *P. laurenti*, *P. leptosoma*, *P. macturki*, *P. martinezi*, *P. meeki*, *P. megalura*, *P. metae*, *P. montana*, *P. mucosa*, *P. notomelas*, *P. roccae*, *P. straminea*, *P. taeniophora* and *P. vittata* by having the dorsal fin with a darker region near the base, followed by a hyaline stripe, and distally darker (unknown in *P. martinezi*). It differs from *P. itapicuruensis*, *P. leptosoma*, *P. megalura*, *P. metae* and *P. montana* by having the supraoccipital process reaching the anterior prenuchal plate (*vs.* supraoccipital process not reaching the anterior prenuchal plate in *P. itapicuruensis*, *P. leptosoma*, *P. megalura*, *P. metae* and *P. montana*). It differs from *P. avanhandavae*, *P. buckleyi*, *P. cruxenti*, *P. gracilis*, *P. lateristriga*, *P. laurenti*, *P. macturki*, *P. martinezi*, *P. mucosa*, *P. notomelas*, *P. roccae*, *P. taeniophora* and *P. vittata* by having the maxillary barbel reaching adpressed pelvic fin terminus (*vs.* maxillary barbel reaching at least anal-fin origin in *P. avanhandavae*, *P. buckleyi*, *P. cruxenti*, *P. gracilis*, *P. lateristriga*, *P. laurenti*, *P. macturki*, *P. martinezi*, *P. mucosa*, *P. notomelas*, *P. roccae*, *P. taeniophora* and *P. vittata*). It differs from *P. australis*, *P. harttii*, *P. ignobilis*, *P. laticeps*, *P. kronei*, *P. meeki* and *P. straminea* by epiphyseal branch of laterosensory canal on head with contralateral canals connecting at midline, proceeding posteriorly as a single canal, and opening in a single pore (*vs.* epiphyseal branch of laterosensory canal on head with contralateral canals opening in two, far apart pores in *P. australis*, *P. laticeps*, and *P. straminea*; epiphyseal branch of laterosensory canal on head with contralateral canals connecting in midline and immediately opening in a single pore, or not connecting, and opening in two pores near each other in *P. harttii*, *P. ignobilis*, *P. kronei* and *P. meeki*). It differs from *P. griffini* by the absence of a paired dorsolateral dark stripe on body (*vs.* presence of a paired dorsolateral dark stripe on body extending up to terminus of adipose-fin base).

Furthermore, *P. linami* can be diagnosed by the presence of maxillary barbel reaching adpressed pelvic fin terminus; unbranched dorsal-fin ray might present a filamentous prolongation; posterior margin of pectoral-fin spine bearing 10–12 retrorse, triangular, inclined, dentations along its basal two-thirds; adipose fin three and half times in SL; 41 total vertebrae; dark brown midlateral stripe wide, not well delimited, from snout to caudal-fin origin.

Description

Measurements in Table 41. Body average depressed, depth at dorsal-fin origin almost six times in standard length, and compressed, body width at dorsal-fin origin eight times in SL (Fig. 124). Dorsal profile convex from snout to dorsal fin, concave from dorsal to adipose fin, convex along adipose fin, and concave along the caudal peduncle. Ventral profile of body slightly convex from snout to branquiostegal membrane, convex between pectoral and pelvic fins, slightly concave from pelvic to anal fin, and also concave from there along the caudal peduncle.

Pseudotympanum large, oval, dorsal to posterior process of cleithrum and reaching the straight line of 6th (1) vertebrae. Posterior process of cleithrum triangular, short, its dorsal border distinctly concave. Anus and urogenital papilla adjacent. Urogenital papilla tubular, triangular, long. Anus at vertical through second fifth of adipose fin; urogenital papilla at vertical through first seventh of adipose fin.

Head deep, depth at supraoccipital-process base more than half head length. Mouth sub terminal. Eye slightly elliptical, five and half times in head. Bony interorbital distance slightly less than eye diameter. Barbels thin, slightly depressed and elliptical in cross-section. Maxillary barbel reaching adipose fin terminus. Outer mental barbel, when stretched parallel to main body axis, reaching half adipose fin. Inner mental barbel, when stretched parallel to main body axis, almost reaching pectoral-fin origin. Supraoccipital process roughly triangular, narrow. Dorsal lamina of Weber complex vertebrae of moderated height, reaching the supraoccipital process along just at its anteriormost region. Branchiostegal rays 6 (1).

Dorsal fin triangular, distal margin convex, moderated length (second branched dorsal-fin ray almost five and half times in SL), depressed tip finishing at vertical through half of adipose fin. Dorsal fin with I,6 (1) plus anteriormost spinelet. Distance between terminus of dorsal-fin base and adipose-fin origin slightly more than dorsal-fin base. Anteriormost dorsal-fin pterygiophore inserted posterior to neural spine of vertebrae 4 (1); posteriormost dorsal-fin pterygiophore located ahead of neural (or pseudoneural) spine of vertebrae 12 (1). Unbranched dorsal-fin ray with proximal part ossified as a spine, holotype present a soft filamentous prolongation of the dorsal-fin first ray. This filament is long, considerably longer than the rigid part of first dorsal-fin ray, being equivalent to almost a third of standard length in the holotype.

Pectoral-fin rays I,7 (1), pectoral fin triangular with concave distal border. First pectoral fin ray roughly straight, with proximal part rigid, forming a spine (Fig. 125), and

short distal tip flexible and distinctly segmented. Pectoral-fin spine seven times in SL. Anterior margin of pectoral-fin spine with small, straight dentations along its basal half and serrae along its distal half. Posterior margin of pectoral-fin spine bearing 10–12 retrorse dentations along its basal two-thirds. These dentations are inclined, similar in size. Also, 1–2 distalmost unossified dentations.

Pelvic-fin rays $i,5$ (1), extended pelvic fin triangular with straight distal border. Pelvic-fin origin at vertical through dorsal-fin terminus. Pelvic fin adpressed terminus at vertical through a point slightly posterior to adipose-fin origin. First unbranched and flexible ray distinctly shorter than second and third rays, which are roughly the same size; remaining rays progressively shorter.

Anal-fin rays $v,8$ (1); distal border of extended anal fin convex. Three anteriormost anal-fin rays vestigial, unsegmented, embedded in thick skin fold. Anal-fin origin at vertical through second seventh of adipose-fin base; anal-fin adpressed terminus slightly anterior or at vertical through adipose-fin terminus. Tip of anteriormost anal-fin pterygiophore inserted posterior to hemal spine of vertebrae 23 (1). Tip of posteriormost anal-fin pterygiophore inserted ahead of hemal spine of vertebrae 29 (1).

Adipose fin three and half times in SL, forming ascending elevated curve in lateral profile, with deepest point approximately at midlength. Adipose fin emerging gradually, its posterior limit as a rounded, free lobe. Adipose-fin origin at vertical through vertebral centrum 22 (1); adipose-fin terminus at vertical through vertebral centrum 36 (1).

Caudal fin deeply forked, dorsal lobe slightly longer. Caudal peduncle length posterior to adipose fin roughly the same as its depth. Dorsal lobe with 7 (1), rarely 6 (1) or 8 (1) branched, 1 unbranched principal and 16 (1) procurrent fin-rays. Ventral lobe with 8 (1) branched, 1 unbranched principal and 17 (1) procurrent fin-rays. Hypural 5 completely free, not fused to hypural 3+4. Median caudal-fin rays not articulated directly to caudal plate. Seven (1) rays articulated to dorsal caudal-fin plate (5 on hypurals 3+4 and 2 on hypural 5) and 8 (1) rays articulated to ventral caudal-fin plate (6 on hypurals 1+2 and 2 on parahypural).

Total vertebrae 41 (1). Ribs 9 (1).

Epiphyseal branch of laterosensory canal on head (S6) connecting contralateral branches in head midline, proceeding posteriorly as an unified canal, and opening in a single pore.

Coloration in alcohol

Background body coloration yellowish. Ventral region of head and body lighter. Dark brown midlateral stripe wide (Fig. 126), not well delimited, from snout to caudal-fin origin.

Cephalic dark brown pigment along posterior fontanel. Dorsal fin overall dark brown, except by a hyaline stripe near its base, which does not encompass unbranched dorsal-fin ray.

Geographic distribution

Pimelodella linami was described from Rio Torbes, in Orinoco system, Venezuela, and its only known from the holotype. Therefore, it occurs in region 305 (Orinoco high Andes).

Comments

Pimelodella linami was described based in one specimen. More investigation is needed also in the comparison of *P. linami* and *P. figueroai*, from Guaviare River, Orinoco Piedmont. Both were described with special focus to the presence of the dorsal-fin filamentous prolongation and, despite Dahl (1961) statement that *P. linami* differs from *P. figueroai* in several characteristics, none of those were commented along the text, and both species morphometric data are somewhat similar. However, *P. figueroai* paratype is extremely unpigmented, in a manner that *P. linami* coloration marks could not be observed, and I maintain both species as valid a priori, since more material is needed before taking any taxonomic decisions in this case.

Material examined

Pimelodella linami. — USNM 121132, 1, xr, 74.7 mm SL, holotype, Venezuela, Táriba, "Rio Torbes, 1km above Táriba, Orinoco system", 7°50'04"N, 72°12'30"W.

***Pimelodella longipinnis* (Borodin, 1927b)**

Rhamdella longipinnis Borodin, 1927b: 6–7 [original description; “Prov. St. Paulo, ?, Brazil”]; holotype: AMNH 8642]. — Gosline, 1945: 35 [taxonomic treatment]. — Fowler, 1951: 565 [taxonomic treatment]. — Burgess, 1989: 278 [taxonomic treatment]. — Bockmann & Guazzelli, 2003: 422 [taxonomic treatment]. — Ferraris, 2007: 196 [taxonomic treatment]. — Bockmann & Miquelarena, 2008: 45–47 [taxonomic treatment, *Rhamdella* revision, transfer to *Pimelodella*].

Diagnosis

Pimelodella longipinnis differs from all *Pimelodella* species except *P. cristata*, *P. hasemani*, *P. humeralis*, *P. martinezi*, *P. megalops*, *P. modesta*, *P. notomelas*, *P. peruana*, *P. robinsoni*, *P. serrata*, *P. spelaea*, *P. tapatapae* and *P. yuncensis* by having a narrow midlateral stripe, posterior to opercle to caudal-fin origin. It differs from all above mentioned by having the supraoccipital process not reaching the anterior preopercular plate. Furthermore, *P. longipinnis* can be diagnosed by the presence of maxillary barbel reaching vertical through

anal fin terminus; dorsal-fin spine approximately half first dorsal-fin ray total length; posterior margin of pectoral-fin spine bearing 8–9 retrorse dentations along its basal two-thirds, the distalmost dentations broader and the proximal more acute; adipose fin almost three times in SL; hypural 5 fused to plate formed by hypurals 3+4; 42 total vertebrae; dark brown midlateral stripe narrow, posterior to orbit until caudal-fin origin.

Description

Measurements in Table 42. Body depressed, depth at dorsal-fin insertion slightly more than seven times in standard length, and compressed, body width at dorsal-fin insertion slightly less than ten times in SL (Fig. 127). Dorsal profile slightly convex from snout to dorsal fin, concave from dorsal to adipose fin, convex along adipose fin, and concave along the caudal peduncle. Ventral profile of body slightly convex from snout to branchiostegal membrane, concave between pectoral and pelvic fins, concave from pelvic to anal fin, and straight from there along the caudal peduncle.

Pseudotympanum large, oval, above posterior process of cleithrum and reaching the straight line of 7th (1) vertebrae. Posterior process of cleithrum triangular, broad, its dorsal border straight. Anus and urogenital papilla adjacent. Urogenital papilla tubular, triangular, short. Anus at vertical through first third of adpressed pelvic fin; urogenital papilla at vertical through last third of adpressed pelvic fin.

Head deep, depth at supraoccipital-process base slightly less than two times in head length. Mouth sub terminal. Eye slightly elliptical, five times in head. Bony interorbital distance slightly less than eye diameter. Barbels thin, slightly depressed and elliptical in cross-section. Maxillary barbel reaching vertical through anal fin terminus. Outer mental barbel, when stretched parallel to main body axis, finishing at half pectoral fin adpressed. Inner mental barbel, when stretched parallel to main body axis, finishing at pectoral-fin origin. Supraoccipital process narrow, subrectangular, almost reaching anterior prenuchal plate. Dorsal lamina of Weberian complex vertebrae reaching supraoccipital process just at its anteriormost part.

Dorsal fin triangular, distal margin concave, average sized (first branched dorsal-fin ray four and half times in SL), depressed tip finishing at last fourth of adpressed pelvic fin. Dorsal fin with I,6 (1) plus anteriormost spinelet. Distance between terminus of dorsal-fin base and adipose-fin origin slightly less than dorsal-fin base. Anteriormost dorsal-fin pterygiophore inserted posterior to neural spine of vertebrae 4 (1); posteriormost dorsal-fin pterygiophore located ahead of neural (or pseudoneural) spine of vertebrae 12 (1).

Unbranched dorsal-fin ray mostly ossified as a spine, rigid part short (approximately half first dorsal-fin ray total length).

Pectoral-fin rays I,8 (1), pectoral fin triangular with concave distal border. First pectoral-fin ray roughly straight, with proximal part rigid, forming a spine (Fig. 128), and short distal tip flexible and distinctly segmented. Pectoral-fin spine slightly more than seven times in SL. Anterior margin of pectoral-fin spine with smooth, straight dentations along basal two thirds, and serrae along its distal half. Posterior margin of pectoral-fin spine bearing 8–9 retrorse dentations along its basal two-thirds, the distalmost dentations broader and the proximal more acute. Also, 1–2 distalmost unossified dentations, not counted.

Pelvic-fin rays i,5 (1), extended pelvic fin triangular with straight distal border. Anterior portion of pelvic-fin base at vertical through sixth branched dorsal-fin ray. Tip of adpressed pelvic fin slightly posterior to vertical through adipose-fin origin. First unbranched and flexible ray distinctly shorter than second and third rays, which are roughly the same size; remaining rays progressively shorter.

Anal-fin rays vi,9 (1); distal border of extended anal fin convex. Three anteriormost anal-fin rays vestigial, unsegmented, embedded in thick skin fold. Anal fin origin between at vertical through first third of adipose-fin base; anal-fin terminus at vertical through adipose-fin terminus. Tip of anteriormost anal-fin pterygiophore inserted posterior to hemal spine of vertebrae 22 (1). Tip of posteriormost anal-fin pterygiophore inserted ahead of hemal spine of vertebrae 31 (1).

Adipose fin almost three times in SL, forming ascending elevated curve in lateral profile, with deepest point approximately at midlength. Adipose fin emerging gradually, its posterior limit as a rounded, free lobe. Adipose fin origin at vertical through vertebral centrum 20 (1). Adipose fin terminus at vertical through vertebral centrum 37 (1).

Caudal fin deeply forked, lobes damaged. Caudal peduncle length posterior to adipose-fin a third to half longer than its depth. Dorsal lobe with 7 (1) branched, 1 (1) unbranched principal, and 13 (1) procurrent fin-rays. Ventral lobe with 8 (1) branched, 1 (1) unbranched principal, and 14 (1) procurrent fin-rays. Hypural 5 fused to plate formed by hypurals 3+4. Median caudal-fin rays not articulated directly to caudal plate. Seven (1) rays articulated to dorsal caudal-fin plate and 8 (1) rays articulated to ventral caudal-fin plate (6 on hypurals 1+2 and 2 on parhypural).

Total vertebrae 42 (1). Ribs 8 (1).

Epiphyseal branch of laterosensory canal in the head (S6) emerging as two separated pores.

Coloration in alcohol

Background body coloration yellowish. Ventral region of head and body lighter. Despite original description does not indicates any marks, has a dark brown midlateral stripe (Fig. 129), narrow, not well-delimited, posterior to orbit until caudal-fin origin. Cephalic dark brown pigment along posterior fontanel. Dark brown region at dorsal-fin base.

Geographic distribution

Pimelodella longipinnis was described from São Paulo State, Brazil, and it is known only from the type material, being found in probably region 330 (Ribeira de Iguape) or 344 (Upper Paraná) (see comments).

Comments

Rhamdella longipinnis was described based on material received from Museu Paulista by the American Museum of Natural History. However, the location is not accurate, being referred only as “São Paulo prov.”, and with a “?” by Borodin (1927b), but without any explanation on the doubt.

Rhamdella longipinnis was transferred to *Pimelodella* by Bockmann & Miquelarena (2008) due the presence of long maxillary barbels and a sharp long supraoccipital process that contacts the prenuchal plate. However, the supraoccipital process does not contact the anterior prenuchal plate, as can be observed at the species radiograph (Fig. 130). This is an intriguing species, since has the hypural 5 not fused to the dorsal hypural plate, and supraoccipital process as before mentioned, both characters found in *Rhamdella* species; however, the overall body shape is similar to *Pimelodella*, as also the dorsal lamina of Weberian complex vertebrae, which is present and high (meanwhile extremely low in *Rhamdella*). This species deserves a more detailed study, and inclusion of comparative material, in order to try to solve its taxonomic status. Despite large sampling in São Paulo rivers, I have not found any comparative material similar to *P. longipinnis*.

Material examined

Pimelodella longipinnis. — AMNH 8642, 1, xr, 84.6 mm SL, holotype, Brazil, São Paulo, (Alto Paraná or Coastal basins in São Paulo), 23°50'49"S, 46°29'03"W.

***Pimelodella macturki* Eigenmann, 1912**

Pimelodella macturkii. — Eigenmann, 1910: 389 [*nomen nudum*].

Pimelodella macturki Eigenmann, 1912: 170–171, pl. XVI, fig. 1 [original description; “Creek in Mora Passage”, Guyana; holotype: FMNH 53234 (formerly CM 1695)]. — Eigenmann, 1917: 248, pl. XXXV, fig. 27 [taxonomic revision]. — Gosline, 1945: 45

[taxonomic treatment]. — Böhlke, 1953: 44 [type catalog]. — Mees, 1974: 151–153 [taxonomic treatment]. — Njissen *et al.*, 1982: 60 [type catalog] — Mees, 1983: 51–52, fig. 4 [taxonomic treatment, comparison with *P. procera*]. — Mees, 1985: 239, 245, fig. 1 [taxonomic treatment]. — Mees, 1986: 316 [taxonomic treatment]. — Ibarra & Stewart, 1987: 66 [type catalog]. — Burgess, 1989: 281 [taxonomic treatment]. — Njissen *et al.*, 1993: 224 [type catalog]. — Le Bail *et al.*, 2000: 136–137, unnum. fig. [taxonomic treatment]. — Bockmann & Guazzelli, 2003: 419 [taxonomic treatment]. — Ferraris, 2007: 192–193 [taxonomic treatment]. — Vari *et al.*, 2009: 43 [taxonomic list]— Le Bail *et al.*, 2012: 304 [taxonomic treatment].

Pimelodella macturkii. — Henn, 1928: 77 [type catalog, misspelling]. — Van der Stigchel, 1946: 57–58 [taxonomic treatment, misspelling].

C. macturki. — Mees, 1974: 142, 152 [taxonomic treatment, misspelling].

Diagnosis

Pimelodella macturki differs from all *Pimelodella* species by having the distal third of dorsal-fin dark brown or black, mainly in anteriormost rays. Furthermore, it can be diagnosed by the presence of maxillary barbel reaching between verticals through anal-fin origin and its last third; dorsal lamina of Weberian complex vertebrae reaching the supraoccipital process along its entire extension; anterior distal half of dorsal-fin spine with smooth serrae; posterior distal half of dorsal-fin spine with smooth, straight to retrorse dentations; posterior margin of pectoral-fin spine bearing 7–10 retrorse dentations along its basal two thirds, these dentations are large, acute, hook-like; adipose fin short, three to four and half times in SL; 39–41 total vertebrae; medium brown midlateral stripe of moderate width, well delimited, possibly posterior to orbit to caudal-fin origin; anterodorsal region of pseudotympanum with higher concentration of brown melanophores, but not delimiting a mark.

Description

Measurements in Table 43. Body average depressed, depth at dorsal-fin origin four and half to five and half times in standard length, and average compressed, body width at dorsal-fin origin six and half to eight and half times in SL (Fig. 131). Greatest body depth at dorsal-fin origin. Dorsal profile convex from snout to dorsal fin, concave from dorsal to adipose fin, convex along adipose fin, and concave along the caudal peduncle. Ventral profile of body convex from snout to pectoral fins, convex between pectoral and pelvic fins, concave from pelvic to anal fin, and concave from this point along the caudal peduncle.

Pseudotympanum large, oval, above posterior process of cleithrum and reaching the straight line of 6th (3) or 7^{th*} (1) vertebrae. Posterior process of cleithrum triangular, short, its dorsal border slightly concave to straight. Anus and urogenital papilla adjacent. Urogenital papilla tubular, triangular, short. Anus between verticals through first third and half adpressed pelvic fin; urogenital papilla between verticals through half and last third of adpressed pelvic fin.

Head of moderated depth, depth at supraoccipital-process base two to slightly more than two and half times in head length. Mouth sub terminal. Eye slightly elliptical, four to five times in head. Bony interorbital distance five and half to six and half times in head. Barbels thin, slightly depressed and elliptical in cross-section. Maxillary barbel reaching between verticals through anal-fin origin and its last third. Outer mental barbel, when stretched parallel to main body axis, finishing between half and last third of adpressed pectoral-fin. Inner mental barbel, when stretched parallel to main body axis, finishing between half and terminus of pectoral fin. Supraoccipital process subrectangular, tapered distally. Dorsal lamina of Weberian complex vertebrae reaching the supraoccipital process along its entire extension. Branchiostegal rays 6 (3)–7* (2).

Dorsal fin triangular, distal margin concave, moderate length (second branched dorsal-fin ray five to six and half times in SL), depressed tip finishing between half and last sixth of adpressed pelvic fin. Dorsal fin with I,6 (9) plus anteriormost spinelet. Distance between terminus of dorsal-fin base and adipose-fin origin roughly equal to dorsal-fin base. Anteriormost dorsal-fin pterygiophore inserted posterior to neural spine of vertebrae 4 (10); posteriormost dorsal-fin pterygiophore located ahead of neural (or pseudoneural) spine of vertebrae 11 (10). Unbranched dorsal-fin ray mostly ossified as a spine, moderate length (spine between a third and a fourth shorter than the first dorsal-fin total length). Anterior distal half of dorsal-fin spine with smooth serrae; posterior distal half of dorsal-fin spine with smooth, straight to retrorse dentations.

Pectoral-fin rays I,7 (6)–I,9 (1) (holotype I,8), pectoral fin triangular with concave distal border. First pectoral-fin ray curved with proximal part rigid, forming a spine (Fig. 132), and short distal tip flexible and distinctly segmented. Pectoral-fin spine five to five and half times in SL. Anterior margin of pectoral-fin spine with straight dentations along all margin, except the distalmost third, which has serrae. Posterior margin of pectoral-fin spine bearing 7–10 retrorse dentations along its basal two thirds. These dentations are large, acute, hook-like. Also 1–3 unossified distal dentations, not counted.

Pelvic-fin rays i,5 (15), extended pelvic fin triangular with straight distal border. Anterior portion of pelvic-fin base between verticals through sixth dorsal-fin branched ray and half adpressed dorsal fin. Tip of adpressed pelvic fin between verticals through adipose-fin origin and its first seventh. First unbranched and flexible ray distinctly shorter than second and third rays, which are roughly the same size; remaining rays progressively shorter.

Anal-fin rays v,7 (1); vi,7 (1); iv,8* (7); v,8 (4); vi,8 (3); iv,9 (2); or v,9 (1); distal border of extended anal fin convex. Two or three anteriormost anal-fin rays vestigial, unsegmented, embedded in thick skin fold. Anal fin origin between verticals through first tenth and first third of adipose-fin base; anal-fin adpressed terminus at or slightly posterior to vertical through adipose-fin terminus. Tip of anteriormost anal-fin pterygiophore inserted posterior to hemal spine of vertebrae 20* (4) or 21 (5). Tip of posteriormost anal-fin pterygiophore inserted ahead of hemal spine of vertebrae 27* (5), 28 (4) or 29 (1).

Adipose fin short, three to four and half times in SL, forming ascending elevated curve in lateral profile, with deepest point approximately at its half. Adipose fin emerging gradually, its posterior limit as a rounded, free lobe. Adipose-fin origin at vertical through vertebral centra 15 (1)–21 (3) (holotype 18); adipose-fin terminus at vertical through vertebral centra 30 (1)–35 (1) (holotype 32).

Caudal fin deeply forked, dorsal lobe might be longer or shorter than ventral. Caudal peduncle length posterior to adipose-fin almost twice its depth. Dorsal lobe with 7 (15) branched, 1 (15) unbranched principal, and 12 (1)–17* (3) (holotype 16) procurrent fin-rays. Ventral lobe with 8 (15), 1 (15) unbranched principal, and 9 (1)–21 (1) (holotype 18) procurrent fin-rays. Hypural 5 completely free, not fused to hypural 3+4. Median caudal-fin rays not articulated directly to caudal plate. Seven (4) rays articulated to dorsal caudal-fin plate (5 on hypurals 3+4 and 2 on hypural 5) and 8 (4) rays articulated to ventral caudal-fin plate (6 on hypurals 1+2 and 2 on parahypural).

Total vertebrae 39 (3)–41 (3) (holotype 41). Ribs 8 (7).

Epiphyseal branch of laterosensory canal on head (s6) usually emerging as two separate pores, near each other.

Coloration in alcohol

Background body coloration yellowish. Ventral region of head and body lighter. Medium brown midlateral stripe (Fig. 133) of moderate width, well delimited, possibly posterior to orbit to caudal-fin origin. Anterodorsal region of pseudotympanum with higher concentration of brown melanophores, but not delimiting a mark. Cephalic dark brown

pigment at posterior fontanel region. Dorsal fin with a medium brown stripe near base, followed by a hyaline stripe, and distal third dark brown or black, mainly in anteriormost rays.

Geographic distribution

Pimelodella macturki was described from costal drainages of Guyana. It is known from areas 310 (Essequibo) and 311 (Guianas), mainly in Approuague, Coratjin and Nickerie rivers basins, in Surinam and Guyana.

Material examined

Pimelodella macturki. — FMNH 53234, 1, xr, 53.5 mm SL, holotype, Guyana, Creek into Mora Passage, 8°21'N, 59°46'W; BMNH 1911.10.31.54, 1, xr, 51.4, paratype, Guyana, Creek into Mora Passage, 8°21'N, 59°46'W; BMNH 1911.10.31.55, 1, xr, 39.7 mm SL, paratype, Guyana, Trenches at Morawhanna, 8°16'N, 59°45'W; CAS 63691, 3, xr, paratype, Guyana, Georgetown trenches, 6°47'02"N, 58°10'28"W; CAS 63692, 1, xr, 51.4 mm SL, paratype, Guyana, Georgetown trenches, 6°47'02"N, 58°10'28"W; CAS 63693, 4, xr, paratypes, Guyana, Choca trenches at Morowhanna, 8°16'N, 59°45'W; FMNH 7388, 1, 36.4 mm SL, paratype, Guyana, Mora Passage, 8°21'N, 59°46'W; FMNH 53235, 4, 43.5–55.0 mm SL, paratypes, Guyana, Trenches at Morawhanna, 8°16'N, 59°45'W; FMNH 53573, 44.3–60.4 mm SL, paratypes, Guyana, Trenches at Morawhanna, 8°16'N, 59°45'W; FMNH 53574, 1, xr, 52.0 mm SL, paratype, Guyana, Georgetown trenches, 6°47'02"N, 58°10'28"W; MCZ 30073, 1, xr, 48.1 mm SL, paratype, Guyana, Creek into Mora Passage, 8°21'N, 59°46'W; MCZ 30074, 1, 43.8 mm SL, paratype, Guyana, Trenches at Morawhanna, 8°16'N, 59°45'W; USNM 66263, 1, xr, 37.6 mm SL, paratype, Guyana, Trenches at Morawhanna, 8°16'N, 59°45'W.

***Pimelodella martinezi* Fernández-Yépez, 1970**

Pimelodella martinezi Fernández-Yépez, 1970: unnum. page, pl. 35, 2 figures [original description; “bajo Unare”; holotype: AFY 70–403, 68 mm SL (number for holotype not mentioned, types probably lost)]. — Burgess, 1989: 281 [taxonomic treatment]. — Bockmann, 1994: 768 [taxonomic treatment, species with filament]. — Bockmann & Guazzelli, 2003: 419 [taxonomic treatment]. — Lasso *et al.*, 2004: 171 [taxonomic list]. — Ferraris, 2007: 193 [taxonomic treatment].

Diagnosis

Pimelodella martinezi differs from all *Pimelodella* species except *P. cristata*, *P. hasemani*, *P. humeralis*, *P. longipinnis*, *P. megalops*, *P. modesta*, *P. notomelas*, *P. peruana*, *P. robinsoni*, *P. serrata*, *P. spelaea*, *P. tapatapae* and *P. yuncensis* by having a narrow

midlateral stripe. It differs from *P. cristata*, *P. hasemani*, *P. humeralis*, *P. longipinnis* and *P. notomelas* by also having dark lateral stripes, of moderate width, from snout to opercle (*vs.* stripes absent on head in *P. cristata*, *P. hasemani*, *P. humeralis*, *P. longipinnis* and *P. notomelas*). It differs from *P. megalops*, *P. modesta*, *P. notomelas*, *P. robinsoni*, *P. serrata*, *P. tapatapae* and *P. yuncensis* by having a dorsal fin completely hyaline (*vs.* with some pigmentation in *P. megalops*, *P. modesta*, *P. notomelas*, *P. robinsoni*, *P. serrata*, *P. tapatapae* and *P. yuncensis*). It differs from *P. peruana* by having the ventral lobe of caudal fin hyaline (*vs.* dark pigmented in *P. peruana*). It differs from *P. spelaea* by having maxillary barbel reaching terminus of adpressed anal fin (*vs.* maxillary barbel reaching between half adpressed pelvic fin and half adpressed anal fin in *P. spelaea*) and absence of coloration along supraoccipital process until dorsal fin terminus (*vs.* presence in *P. spelaea*). Furthermore, *P. martinezi* can be diagnosed by the presence of maxillary barbel reaching terminus of adpressed anal fin; unbranched dorsal-fin ray might present a filamentous prolongation; adipose fin slightly more than three times in SL; medium brown midlateral stripe narrow, not well delimited, posterior to pseudotympanum to caudal-fin origin; medium brown stripe from snout to orbit, and from orbit to opercle.

Description

Dorsal profile convex from snout to dorsal fin, slightly concave from dorsal to adipose fin, slightly convex along adipose fin, and concave along caudal peduncle (Fig. 134). Ventral profile of body slightly convex from snout to branchiostegal membrane, convex between pectoral end pelvic fins, and concave from pelvic to caudal peduncle.

Pseudotympanum large, oval, dorsal to posterior process of cleithrum and reaching straight line of unbranched dorsal-fin ray. Posterior process of cleithrum triangular.

Head length two times in SL. Mouth sub terminal. Eye slightly elliptical. Bony interorbital distance roughly eye diameter. Barbels thin, and slightly depressed and elliptical in cross-section. Maxillary barbel reaching terminus of adpressed anal fin. Outer mental barbel, when stretched parallel to main body axis, finishing almost at pectoral fin adpressed terminus. Inner mental barbel, when stretched parallel to main body axis, finishing at half adressed pectoral fin. Supraoccipital process subrectangular, narrow, distally tapered.

Dorsal fin triangular, distal margin convex, depressed tip reaching vertical through last fourth of adpressed pelvic fin. Dorsal fin with I,6 (1), plus anteriormost spinelet. Distance between terminus of dorsal-fin base and adipose-fin origin shorter than dorsal-fin base. Unbranched dorsal-fin ray mostly ossified as a spine, with a long filamentous prolongation that surpasses the vertical through anal-fin origin.

Pectoral-fin rays I,8 (1), pectoral fin triangular with concave distal border. First pectoral-fin ray curved, with proximal part rigid and short distal tip flexible and distinctly segmented.

Pelvic-fin rays i,5 (1), extended pelvic fin triangular with straight distal border. Pelvic-fin origin at vertical through sixth branched dorsal fin ray. Tip of adpressed pelvic fin at vertical through first fifth of adipose-fin base.

Anal-fin rays iii,8 (1); distal border of extended anal fin convex. Anal fin origin at vertical through first fifth of adipose-fin base; anal-fin adpressed terminus slightly anterior to vertical though adipose fin terminus.

Adipose fin slightly more than three times in SL, forming ascending elevated curve in lateral profile, with deepest point approximately midlength. Adipose fin emerging gradually, its posterior limit as a rounded, free lobe.

Caudal fin deeply forked, dorsal lobe slightly longer than ventral lobe. Caudal peduncle posterior to adipose-fin base slightly shorter than its depth.

Coloration in alcohol

Original description does not emphasize any coloration marks. However, photos suggest background body coloration yellowish, medium brown midlateral stripe narrow (Fig. 135), not well delimited, posterior to pseudotympanum to caudal-fin origin. Also, a medium brown stripe from snout to orbit, and from orbit to opercle. Cephalic dark brown pigment along posterior fontanel. Dark brown region at dorsal portion of pseudotympanum.

Geographic distribution

Pimelodella martinezi was described from Rio Unare, and it is known only from its description, therefore, from region 304 (South American Caribbean drainages– Trinidad).

Comments

Pimelodella martinezi is known only from its description, since the whereabouts of Fernández-Yépez collection is still unknown (Lasso-Alcalá, pers. comm.). The before mentioned description, coloration and geographic distribution are based on original description information and photos. It shares some resemblance with *P. figueroai*, from region 306 (Orinoco piedmont), and has the same dorsal-fin filamentous prolongation described for *P. linami*, from region 305 (Orinoco high Andes). To solve the taxonomic status of these three species, there is necessity of consulting more material of those regions and, therefore, I maintain *P. martinezi* as valid a priori.

***Pimelodella meeki* Eigenmann, 1910**

Pimelodella eigenmanni Meek, 1905: 241 [original description; “São Paulo, Brazil”; holotype: FMNH 3400 (not 4000, as in description); unavailable name, preoccupied by *Pimelodus* (*Pimelodella*) *eigenmannii* Boulenger, 1891].

Pimelodella meeki Eigenmann, 1910: 389 [*nomen novum* for *P. eigenmannii* Meek, 1905]. — Eigenmann, 1917: 249–250, pl. XXXII, fig. 1–2, pl. XXXV, fig. 13–14 [taxonomic revision]. — Ahl, 1925: 106 [taxonomic treatment, comparison with *P. pappenheimi*]. — Gosline, 1945: 45 [taxonomic treatment]. — Fowler, 1951: 546, fig. 561 [taxonomic treatment]. — Ibarra & Stewart, 1987: 66 [type catalog]. — Burgess, 1989: 281 [taxonomic treatment]. — Bockmann & Guazzelli, 2003: 419 [taxonomic treatment]. — Ferraris, 2007: 193 [taxonomic treatment]. — Langeani *et al.*, 2007: 187 [taxonomic treatment].

Pimelodella rudolphi Miranda Ribeiro, 1918: 637–638 [original description; several localities, lectotype from “Mercado de São Paulo”; lectotype: MNRJ 875A (designated by Miranda Ribeiro, 1953)]. — Gosline, 1945: 45 [taxonomic treatment]. — Fowler, 1951: 550 [taxonomic treatment]. — Burgess, 1989: 281 [taxonomic treatment]. — Bockmann & Guazzelli, 2003: 421 [taxonomic treatment]. — Ferraris, 2007: 194 [taxonomic treatment].

Diagnosis

Pimelodella meeki differs from all *Pimelodella* species except *P. australis*, *P. avanhandavae*, *P. buckleyi*, *P. cruxenti*, *P. gracilis*, *P. griffini*, *P. harttii*, *P. ignobilis*, *P. itapicuruensis*, *P. kronei*, *P. lateristriga*, *P. laticeps*, *P. laurenti*, *P. leptosoma*, *P. linami*, *P. macturki*, *P. martinezi*, *P. megalura*, *P. metae*, *P. montana*, *P. mucosa*, *P. notomelas*, *P. roccae*, *P. straminea*, *P. taeniophora* and *P. vittata* by having the dorsal fin with a darker region near the base, followed by a hyaline stripe, and distally darker (unknown in *P. martinezi*). It differs from *P. itapicuruensis*, *P. leptosoma*, *P. megalura*, *P. metae* and *P. montana* by having the supraoccipital process reaching the anterior prenuchal plate (*vs.* supraoccipital process not reaching the anterior prenuchal plate in *P. itapicuruensis*, *P. leptosoma*, *P. megalura*, *P. metae* and *P. montana*). It differs from *P. buckleyi*, *P. cruxenti*, *P. gracilis*, *P. harttii*, *P. kronei*, *P. lateristriga*, and *P. vittata* by having 40–41 total vertebrae (*vs.* 42 or more vertebrae in *P. buckleyi*, *P. cruxenti*, *P. gracilis*, *P. harttii*, *P. kronei*, *P. lateristriga*, and *P. vittata*). It differs from by having a paired dorsolateral stripe along supraoccipital process (*vs.* paired dorsolateral stripe absent in *P. ignobilis*, *P. laticeps*, *P. linami*, *P. macturki* and *P. straminea*; paired dorsolateral stripe extending at least to half

adipose fin in *P. avanhandavae*, *P. griffini* and *P. roccae*; paired dorsolateral stripe extending until half dorsal-fin base in *P. mucosa*). It differs from *P. laurenti*, *P. martinezi*, *P. notomelas* and *P. taeniophora* by maxillary barbel reaching between verticals through pelvic fin origin and anal fin origin (*vs.* maxillary barbel surpassing anal fin origin in *P. laurenti*, *P. martinezi*, *P. notomelas* and *P. taeniophora*). It differs from *P. australis* by the absence of a dark region between dorsal and adipose fins (*vs.* presence of a dark region between dorsal and adipose fins in *P. australis*).

Furthermore, *P. meeki* can be diagnosed by the presence of maxillary barbel reaching between verticals through pelvic fin origin and anal fin origin; dorsal-fin spine approximately three fourths of first dorsal-fin ray total length, curved, distal third of anterior margin with smooth serrae; posterior margin of pectoral-fin spine bearing 5–10 straight to retrorse dentations along its basal half to two thirds, these dentations are triangular, the 2–3 distalmost are straighter, shorter and with larger bases; adipose fin short, three to four times in SL; medium brown midlateral stripe average width to wide, not well delimited, from snout to anterior of median caudal fin rays; paired brown stripes along supraoccipital process; dorsal fin overall brown, except by a hyaline stripe near its base which does not encompass the unbranched dorsal-fin ray and region between this and first branched ray.

Description

Measurements in Table 44. Body moderate depressed, depth at dorsal-fin insertion four to five and half times in standard length, and moderate compressed, body width at dorsal-fin insertion five to seven times in SL (Fig.136). Dorsal profile slightly convex from snout to dorsal fin, slightly concave from dorsal to adipose fin, slightly convex along adipose fin, and concave along the caudal peduncle. Ventral profile of body slightly convex from snout to branchiostegal membrane, convex between pectoral end pelvic fins, slightly convex from pelvic to anal fin, and concave from there along the caudal peduncle.

Pseudotympanum large, oval, above posterior process of cleithrum and reaching the straight line of 6th* (5) to 8th (2) vertebrae. Posterior process of cleithrum triangular, long, its dorsal border slightly concave. Anus and urogenital papilla adjacent. Urogenital papilla tubular, triangular, short. Anus between verticals through second fifth and second third of adpressed pelvic fin; urogenital papilla between verticals through second third and terminus of adpressed pelvic fin.

Head of moderate depth, depth at supraoccipital-process base slightly less to slightly more than two times in head length. Mouth sub terminal. Eye slightly elliptical, four and half to five and half times in head. Bony interorbital slightly shorter than eye diameter. Barbels

thin, slightly depressed and elliptical in cross-section. Maxillary barbel reaching between verticals through pelvic fin origin and anal fin origin. Outer mental barbel, when stretched parallel to main body axis, finishing between pectoral fin terminus and half pectoral fin adpressed. Inner mental barbel, when stretched parallel to main body axis, finishing between branchiostegal membrane ventral limit and halfway between this point and pectoral-fin origin. Supraoccipital process subrectangular, narrow, and tapered at its distal point. Dorsal lamina of Weberian complex vertebrae reaching the supraoccipital process just at its anteriormost part. Branchiostegal rays 6 (3).

Dorsal fin triangular, distal margin convex, average sized (second branched dorsal-fin ray four to five and half times in SL), depressed tip finishing between the verticals through first third and last fourth of adpressed pelvic fin. Dorsal fin with I,6 (18) plus anteriormost spinelet. Distance between terminus of dorsal-fin base and adipose-fin origin slightly shorter to slightly larger than dorsal-fin base. Anteriormost dorsal-fin pterygiophore inserted posterior to neural spine of vertebrae 4 (10); posteriormost dorsal-fin pterygiophore located ahead of neural (or pseudoneural) spine of vertebrae 11 (10). Unbranched dorsal-fin ray mostly ossified as a spine, rigid part of moderated length (approximately a fourth shorter than the first dorsal-fin ray total length), curved, distal third of anterior margin with smooth serrae.

Pectoral-fin rays I,7* (14), rarely I,8 (1), pectoral fin triangular with concave distal border. First pectoral-fin ray curved, with proximal part rigid, forming a spine (Fig. 137), and short distal tip flexible and distinctly segmented. Pectoral-fin spine five and half to six and half times in SL. Anterior margin of pectoral-fin spine with smooth, straight dentations along its basal half, and smooth serrae along its distal third. Posterior margin of pectoral-fin spine bearing 5–10 straight to retrorse dentations along its basal half to two thirds. These dentations are triangular, the 2–3 distalmost are straighter, shorter and with larger bases. Also, 1–3 distalmost unossified dentations.

Pelvic-fin rays i.5 (17), extended pelvic fin triangular with straight distal border. Anterior portion of pelvic-fin base between verticals through dorsal fin terminus and last third of adpressed dorsal fin. Tip of adpressed pelvic fin between verticals through adipose-fin origin and its first seventh. First unbranched and flexible ray distinctly shorter than second and third rays, which are roughly the same size; remaining rays progressively shorter.

Anal-fin rays iv,6 (2); ii,7 (1); iv,7 (3); v,7* (2); ii,8 (1); iii,8 (2); iv,8 (2); v,8 (1); iii,9 (1); or v,9 (1); distal border of extended anal fin convex. Two anteriormost anal-fin rays vestigial, unsegmented, embedded in thick skin fold. Anal fin origin between verticals through first fourth and half of adipose-fin base; anal-fin terminus at vertical through adipose-

fin terminus or a point slightly posterior to that. Tip of anteriormost anal-fin pterygiophore inserted posterior to hemal spine of vertebrae 20* (4), 21 (5) or 22 (1). Tip of posteriormost anal-fin pterygiophore inserted ahead of hemal spine of vertebrae 27* (4) or 28 (6).

Adipose fin three to four times in SL, forming ascending elevated curve in lateral profile, with deepest point approximately at last third. Adipose fin emerging gradually, its posterior limit as a rounded, free lobe. Adipose fin origin at vertical through vertebral centra 18 (2)–22 (1) (holotype 19); adipose fin terminus at vertical through vertebral centra 33 (1)–35 (2) (holotype 34).

Caudal fin deeply forked, dorsal lobe usually slightly longer than ventral. Caudal peduncle length posterior to adipose-fin roughly the same as its depth. Dorsal lobe with 7 (9) branched, 1 (9) unbranched principal, and 12 (1)–19* (1) procurrent fin-rays. Ventral lobe with 8 (9) branched, 1 (9) unbranched principal, and 11 (1)–21 (1) (holotype 20) procurrent fin-rays. Hypural 5 completely free, not fused to hypural 3+4. Median caudal-fin rays not articulated directly to caudal plate. Seven (9) rays articulated to dorsal caudal-fin plate (5 on hypurals 3+4 and 2 on hypural 5) and 8* (7), rarely 7 (2) rays articulated to ventral caudal-fin plate (5 or 6 on hypurals 1+2 and 2 on parhypural).

Total vertebrae 40(6)–41* (4). Ribs 8 (2)–10 (2) (holotype 9).

Epiphyseal branch of laterosensory canal on head with contralateral branches connecting at midline and emerging on a single pore, just after the connection in specimens with more than 60 mm SL; and emerging as two separate pores, near each other, in specimens with 45 mm SL or less.

Coloration in alcohol

Background body coloration yellowish. Ventral region of head and body lighter. Medium brown midlateral stripe (Fig. 138, 139) average width to wide, not well-delimited, from snout to anterior of median caudal fin rays. Paired brown stripes along supraoccipital process. Brown cephalic pigment along posterior fontanel region. Dorsal fin overall brown, except by a hyaline stripe near its base which does not encompass the unbranched dorsal-fin ray and region between this and first branched ray.

Geographic distribution

Pimelodella meeki was described based on a specimen from “São Paulo, Brazil”. *Pimelodella rudolphi*, its junior-synonym, was described from several localities in São Paulo State, Brazil. Therefore, *P. meeki* is known from streams in region 344 (Upper Paraná).

Comments

Meek (1905) described *P. eigenmanni* based on a Field Columbian Museum (now Field Museum of Natural History) lot number 4,000. Although, the catalogue number published record is from a completely different species, *Enoplosus armatus* (Shawn, 1790), collected in Melbourn, Australia. This points toward a mistake in the lot number at the moment of publication. Inside FMNH 3400 jar, although, there was a paper designating this specimen as the type of *P. eigenmanni*, and with a location congruent to the one published. The specimen length is somewhat different from the published one (101,5 mm), what may be some error on the length record. Ibarra & Stewart (1987) type catalog indicate FMNH 3400 as the type of *P. eigenmanni*.

Eigenmann (1910: 389) implicitly designated a *nomen novum* for *P. eigenmanni* as *P. meeki* (due to preoccupation in *Pimelodella* by *Pimelodus eigenmanni* Boulenger, 1891). Despite Eigenmann (1910) have not explicitly proposed the replacement (*nomen novum*), in the first page of the article he defines “under each species are given its synonyms” (Eigenmann, 1910: 375), and *P. eigenmanni* is presented in such matter, as *P. meeki* synonym.

Eigenmann (1917) redescribed *P. meeki* and added other specimens to the comparative series (FMNH 57991 and 57993, formerly CM 6078 and CM 6080, respectively). FMNH 57993 has a label written “type” is tied to one specimen, what must be ignored, since FMNH 3400 is actually the holotype of *P. meeki*. Also, FMNH 57991 and 57993 have labels written “*P. griffini*, types”, meanwhile, those lots were never cited for *P. griffini*, described from Sapucay, Paraguay.

Furthermore, Ibarra & Stewart (1987) indicate five paratypes of *P. eigenmanni* Meek, what probably corresponds to FMNH 3401. However, no indication of other material was made in the original description. In sum, the only type material of *P. meeki* is FMNH 3400, the holotype, and other referred material should remain without any type status.

Pimelodella rudolphi (Fig. 140) was described by Miranda Ribeiro (1918) based on specimens from Rio Sorocaba, Rio Tietê, Rio Tamanduateí, Rio Feio and Mercado de São Paulo. Miranda Ribeiro (1953) assigned the lectotype as one of the specimens from Mercado de São Paulo, the lot with less locality accuracy (since probably this was the locality of bought, not collection). Upon examination of all type series, despite small variation, all seems to belong to the same species, and are indistinguishable from *P. meeki*. *Pimelodella rudolphi* has similar measurements, color pattern and pectoral-fin morphology, and was also described from specimens from the same basin as *P. meeki*, justifying the synonym. In any way,

measurements of *P. rudolphi* and *P. meeki* are presented in Table 45, discriminated by original species name.

Material examined

Pimelodella meeki. — FMNH 3400, 1, xr, 100.2 mm SL, holotype, Brazil, São Paulo, 23°30'39"S, 46°50'33"W; FMNH 57991, 24, 30.2–42.3 mm SL, 3 xr, Brazil, Mogy das Cruzes; FMNH 57993, 3, 65.7–97.6 mm SL, 1xr, Brazil, São Paulo, Sapina; MZUSP 51651, 1, 112.23 mm SL, Brasil, São Paulo, Paraibuna Rio Pardo, Bairro do Carvoeiro, right entrance before Posto do Espigao, SP-199, 23°23'0.0"S, 45°40'0.0"W.

Pimelodella rudolphi. — MNRJ 857, 1, xr, 73.9 mm SL, lectotype, Brazil, São Paulo, Mercado de São Paulo; MZUSP 1061, 1, xr, 66.2 mm SL, paralectotype, Brazil, São Paulo, Rio Tamanduateí, Rio Tietê basin, 23°32'14"S, 46°37'35"W; MZUSP 2259, 1, xr, 41.4 mm SL, paralectotype, Brazil, São Paulo, Sorocaba, Rio Tietê drainage, 23°27'05"S, 47°27'40"W; MZUSP 2260, 1, xr, 87.3 mm SL, paralectotype, Brazil, São Paulo, Rio Tietê, 23°30'50"S, 46°49'24"W; MZUSP 2261, 1, xr, 101.2 mm SL, paralectotype, Brazil, São Paulo, Rio Tietê, 23°30'50"S, 46°49'24"W; MZUSP 5260, 1, xr, paralectotype, Brazil, São Paulo, Sorocaba, Rio Tietê drainage, 23°27'05"S, 47°27'40"W; MZUSP 5261, 1, xr, 42.6 mm SL, Brazil, São Paulo, Sorocaba, Rio Tietê drainage, 23°27'05"S, 47°27'40"W; MZUSP 5262, 1, xr, 90.5 mm SL, paralectotype, Brazil, São Paulo, Rio Tietê, 23°30'50"S, 46°49'24"W; MZUSP 5263, 1, xr, 99.5 mm SL paralectotype, Brazil, São Paulo, Rio Tietê, 23°30'50"S, 46°49'24"W; MZUSP 5264, 1, xr, 86.4 mm SL, paralectotype, Brazil, São Paulo, Rio Tietê, 23°30'50"S, 46°49'24"W.

***Pimelodella megalops* Eigenmann, 1912**

Pimelodella megalops Eigenmann, 1910: 389 [*nomen nudum*].

Pimelodella megalops Eigenmann, 1912: 169–170, pl. XV, fig. 2 [original description; “Tumatumari”, Guyana; holotype: FMNH 53231 (formerly CM 1692)]. — Eigenmann, 1917: 242, pl. XXXV, fig. 28 [taxonomic revision] — Ahl, 1925: 106 [taxonomic treatment, comparison with *P. conquetaensis*]. — Henn, 1928: 77 [type catalog]. — Gosline, 1945: 44 [taxonomic treatment]. — Van der Stigchel, 1946: 56–57 [taxonomic treatment]. — Böhlke, 1953: 44 [type catalog]. — Hoedeman, 1961: 134 [comparison with *P. geryi*]. — Mees, 1983: 52 [comparison with *P. procera*]. — Mees, 1986: 316–317 [taxonomic treatment]. — Ibarra & Stewart, 1987: 66 [type catalog]. — Burgess, 1989: 281 [taxonomic treatment]. — Nijssen *et al.*, 1982: 60

[type catalog]. — Njissen *et al.*, 1993: 224 [type catalog]. — Le Bail *et al.*, 2000: 138–139, unnum. fig. [taxonomic treatment]. — Bockmann & Guazzelli, 2003: 419 [taxonomic treatment]. — Lasso *et al.*, 2004: 171 [taxonomic list]. — Ferraris, 2007: 193 [taxonomic treatment]. — Vari *et al.*, 2009: 43 [taxonomic list]. — Le Bail *et al.*, 2012: 304 [taxonomic list].

Diagnosis

Pimelodella megalops differs from all differs from all *Pimelodella* species except *P. cristata*, *P. hasemani*, *P. humeralis*, *P. longipinnis*, *P. martinezi*, *P. modesta*, *P. notomelas*, *P. peruana*, *P. robinsoni*, *P. serrata*, *P. spelaea*, *P. tapatapae* and *P. yuncensis* by having a narrow midlateral stripe. It differs from *P. cristata*, *P. hasemani*, *P. humeralis*, *P. longipinnis* and *P. notomelas* by also having dark lateral stripes, from snout to opercle (*vs.* stripes absent on head in *P. cristata*, *P. hasemani*, *P. humeralis*, *P. longipinnis* and *P. notomelas*). It differs from *P. peruana* and *P. spelaea* by having pigmentation on dorsal fin (*vs.* dorsal-fin completely hyaline). It differs from *P. martinezi*, *P. modesta*, *P. robinsoni* and *P. yuncensis* by having maxillary barbel reaching between verticals through anal fin adpressed terminus and caudal-fin origin (*vs.* maxillary barbels reaching, at best, anal fin terminus in *P. martinezi*, *P. modesta*, *P. robinsoni* and *P. yuncensis*). It differs from *P. serrata* by having basal half of dorsal fin hyaline (*vs.* dorsal fin completely pigmented in *P. serrata*). It differs from *P. tapatapae* by having large dentations on pectoral-fin spine (*vs.* small dentations in pectoral-fin spine in *P. tapatapae*). Furthermore, *P. megalops* can be diagnosed by maxillary barbel reaching between verticals through anal fin adpressed terminus and caudal-fin origin; eye three to four times in head; bony interorbital distance a third of eye diameter; dorsal lamina of Weber complex vertebrae reaching the supraoccipital process along its entire length; dorsal-fin spine three fourths of first dorsal-fin total length, with small, retrorse dentations along posterior margin distal half; posterior margin of pectoral-fin spine bearing 12–16 retrorse dentations along all its margin but the distal fourth, these dentations are big, distinctly retrorse and acute; adipose fin short, three to five times in SL; caudal fin deeply forked, ventral lobe usually slightly longer; epiphyseal branch of laterosensory canal on head (S6) with contralateral canals opening in two separate pores; medium brown midlateral stripe narrow and well delimited, from snout to caudal-fin origin.

Description

Measurements in Table 46. Body compressed, depth at dorsal-fin insertion five and half to eight times in standard length, and compressed, body width at dorsal-fin origin eight to

ten times in SL (Fig. 141). Greatest body depth at dorsal-fin origin. Dorsal profile convex from snout to dorsal fin, concave from dorsal to adipose fin, slightly convex along adipose fin, and concave along the caudal peduncle. Ventral profile of body slightly convex from snout to branchiostegal membrane, concave between branchiostegal membrane and pectoral-fins, slightly concave between pectoral and pelvic fins, and also concave from there along the caudal peduncle.

Pseudotympanum large, oval, above posterior process of cleithrum and reaching the straight line of 6th (1) or 8^{th*} (3) vertebrae (holotype 7th). Posterior process of cleithrum triangular, long, its dorsal border slightly concave. Anus and urogenital papilla adjacent. Urogenital papilla tubular, triangular, medium to great (distance between anus and urogenital papilla terminus eleven to twenty five times in SL). Anus between verticals through last third or fourth of adpressed pelvic fin; urogenital papilla between verticals through second third to terminus of adpressed pelvic fin.

Head depressed, depth at supraoccipital-process base two to two and half times in head length. Mouth sub terminal. Eye slightly elliptical, three to four times in head. Bony interorbital distance a third of eye diameter. Barbels thin, depressed and elliptical in cross-section. Maxillary barbel reaching between verticals through anal fin adpressed terminus and caudal-fin origin. Outer mental barbel, when stretched parallel to main body axis, finishing between verticals through last fourth of adpressed pectoral fin and pelvic fin origin. Inner mental barbel, when stretched parallel to main body axis, finishing between verticals through origin and terminus of pectoral fin. Supraoccipital process narrow, subrectangular, tapered at its distal point. Dorsal lamina of Weber complex vertebrae reaching the supraoccipital process along its entire length. Branchiostegal rays 6 (5)– 7* (2).

Dorsal fin triangular, distal margin convex, short (second branched dorsal-fin ray five to five and half times in SL), adpressed terminus reaching between verticals through second third and terminus of pelvic fin. Dorsal fin with I,6 (21) plus anteriormost spinelet. Distance between terminus of dorsal-fin base and adipose-fin origin usually slightly smaller than dorsal-fin base. Anteriormost dorsal-fin pterygiophore inserted posterior to neural spine of vertebrae 4 (13); posteriormost dorsal-fin pterygiophore located ahead of neural (or pseudoneural) spine of vertebrae 11* (7) or 12 (6). Unbranched dorsal-fin ray mostly ossified as a spine, medium to long (a fourth or less shorter than first dorsal-fin total length), with small, retrorse dentations along posterior margin distal half.

Pectoral-fin rays I,7 (8)– I,9* (1), pectoral fin triangular with concave distal border. First pectoral-fin ray curved, with proximal part rigid, forming a spine (Fig. 142) and short

distal tip flexible and distinctly segmented. Pectoral-fin spine five to five and half times in SL. Anterior margin of pectoral-fin spine with small, straight dentations along its basal third and serrae along its distal third. Posterior margin of pectoral-fin spine bearing 12–16 retrorse dentations along all its margin but the distal fourth. These dentations are big, distinctly retrorse and acute. Also sometimes 1–3 unossified distal dentations, not counted.

Pelvic-fin rays I,5 (19), extended pelvic fin triangular with straight distal border. Anterior portion of pelvic-fin base between verticals through dorsal fin terminus and half dorsal fin adpressed. Tip of adpressed pelvic fin between verticals through adipose-fin origin and a point slightly posterior to that. First unbranched and flexible ray distinctly shorter than second and third rays, which are roughly the same size; remaining rays progressively shorter.

Anal-fin rays iii,7 (1); vi,7 (2); v,7 (2); vi,7 (1); v,8 (4*); iv,9 (4); or v,9 (3); distal border of extended anal fin convex. One to three anteriormost anal-fin rays vestigial, unsegmented, embedded in thick skin fold. Anal fin origin between verticals through first fourth or third of adipose fin base; anal-fin adpressed terminus at adipose fin terminus or slightly posterior. Tip of anteriormost anal-fin pterygiophore inserted posterior to hemal spine of vertebrae 21 (2) or 22* (11). Tip of posteriormost anal-fin pterygiophore inserted ahead of hemal spine of vertebrae 27 (1), 28 (2), 29 (3) or 30* (7).

Adipose fin three to five times in SL, forming ascending elevated curve in lateral profile, with deepest point approximately at midlength. Adipose fin emerging gradually, its posterior limit as a rounded, free lobe. Adipose-fin origin at vertical through vertebral centra 20* (6)– 22 (1); adipose-fin terminus at vertical through vertebral centra 33 (1)–36 (4) (holotype 35).

Caudal fin deeply forked, ventral lobe usually slightly longer. Caudal peduncle length posterior to adipose-fin almost twice its depth. Dorsal lobe with 7 (21) branched, 1 (21) unbranched principal and 10 (1)–19* (1) procurrent fin-rays. Ventral lobe with 8 (22) branched, 1 (22) unbranched principal and 9 (1)–22* (1). Hypural 5 completely free, not fused to hypural 3+4. Median caudal-fin rays not articulated directly to caudal plate. Seven* (12), rarely 6 (1) rays articulated to dorsal caudal-fin plate (4 or 5 on hypurals 3+4 and 2 on hypural 5) and 8* (12), rarely 9 (1) rays articulated to ventral caudal-fin plate (6 or 7 on hypurals 1+2 and 2 on parhypural).

Total vertebrae 39 (1)– 42* (10). Ribs 7 (2)– 9* (2).

Epiphyseal branch of laterosensory canal on head (S6) with contralateral canals opening in two separate pores.

Coloration in alcohol

Background body coloration yellowish to light brown. Ventral region of head and body lighter. Medium brown midlateral stripe (Fig. 143) narrow and well delimited, from snout to caudal-fin origin. Dark brown cephalic pigment along posterior fontanel region. Dorsal fin basal half hyaline, distal half light brown.

Geographic distribution

Pimelodella megalops was described from “Tumatumari”, in Essequibo River drainage, Guyana. It is known from regions 307 (Orinoco llanos), 310 (Essequibo), 311 (Guianas), 314 (Rio Negro), 315 (Amazonas Guiana Shield), 316 (Amazonas lowlands) and 322 (Xingu) (see comments), in Guyana, Surinam, Brazil and Venezuela.

Comments

Pimelodella megalops was described from region 310 (Essequibo), and material from region 311 (Guianas) could be securely identified as belonging to this species. However, a similar morphotype was found in several other basins, and even reported in the literature (*e.g.* Lasso *et al.*, 2004). This material identified as *P. megalops* from Orinoco, Amazonas lowlands, Rio Negro and Xingu deserves more investigation, in order to certainly delimit this species distribution.

Material examined

Pimelodella megalops. — FMNH 53231, 1, xr, 74.7 mm SL, holotype, Guyana, Tumatumari, 5°22'N, 59°0'W; BMNH 1911.10.31.52, 4, xr, 61.3–69.4 mm SL, paratypes, , Guyana, Tumatumari, 5°22'N, 59°0'W; CAS 63717, 5, xr, 58.4–70.4 mm SL, paratypes, Guyana, Potaro river at Tumatumari, Essequibo river drainage, 5°22'N, 59°0'W; CAS 63718, 1, 68.8 mm SL, Guyana, Essequibo River at Crab Falls, 5°24'00.0"N, 58°51'00.0"W; FMNH 7387, 2, 59.6–65.1 mm SL, paratypes, Guyana, Mazaruni-Potaro, Lower Potaro River at Tumatumari, 5°22'N, 59°0'W; FMNH 53232, 32, 42.1–72.5 mm SL, paratypes, Guyana, Mazaruni-Potaro, Lower Potaro River at Tumatumari, 5°22'N, 59°0'W; FMNH 53233, 1, xr, 44.0 mm SL, paratype, Guyana, Crab Falls, 5°24'19"N, 58°51'7.2"W; MCZ 30075, 2, xr, 52.8–61.2 mm SL, paratype, Guyana, Mazaruni-Potaro, Lower Potaro River at Tumatumari, 5°22'N, 59°0'W; ANSP 189112, 1, 66.2 mm SL, Suriname, Sipalawini, Litanie River at mouth and confluence with Marowini River, just upstream from settlement of Konya Kondre, 3°17'24"N, 54°4'38"W; MZUSP 30629, 3, 37.8–41.3 mm SL, Brazil, Roraima, Rio Branco, Marará, 1°30'0.0"N, 61°16'0.0"W; MZUSP 92812, 6, 60.4–71.1 mm SL, Brazil, Pará, Itaituba, Rio Tapajós, left bank, 4°16'14.0"S, 55°58'34.0"W; MZUSP 97341, 28, 45.2–55.5 mm SL, Brazil, Pará, Novo Progresso, Rio Jamanxim, next to vila Mil, 7°43'51.0"S,

55°16'36.0"W; MZUSP 116975, 1, 49.4 mm SL, Brazil, Roraima, Boa Vista, Rio Uraricoera, in Alagadiço, Rio Branco basin, 3°22'31.0"N, 60°35'44.0"W; USNM 36856, 12, 51–58.4 mm SL, Brazil, Pará, Altamira, Cachoeira do Espelho, Rio Xingu, 3°48'0.0"S, 52°32'0.0"W; USNM 53399, 2, 44.7–49 mm SL; USNM 66262, 2, xr, 6.1–67.9 mm SL, Paratype, Guyana, Tumatumari, British Guyana, 5°15'44.5"N, 59°08'47.0"W; USNM 89836, 4, 59.6–65.9 mm SL, Brazil, Mato Grosso, Paranatinga, Rio Maria, in its mouth on Rio Culuene, 14°0'32.0"S, 53°20'46.0"W; USNM 91990, 11, 43.3–68.0 mm SL, Brazil, Mato Grosso, Paranatinga, Rio Culuene, in the area reserved for the PCH Paranatinga II, 13°49'0.0"S, 53°15'0.0"W; USNM 92164, 4, 48.6–63.7 mm SL, Brazil, Amazonas, Igarapé Castanha (afl. rio Tiquié), beaches in Santa Rosa community (3-4.ix.2006), 0°4'41.0"N, 69°41'26.0"W; USNM 92215, 5, 33.6–69.7 mm SL, Brazil, Amazonas, Rio Tiquié, Pirarara Poço community's harbor (6-9.ix.2006), 0°8'40.0"N, 69°12'48.0"W; USNM 109614, 6, 44.9–46.4 mm SL, Brazil, Amazonas, Santa Isabel Do Rio Negro, stone slab in the left bank of Rio Neuixi, next to junction with Rio Negro, 0°21'45.0"S, 65°4'13.0"W; USNM 109690, 7, 40.1–53.2 mm SL, Brazil, Amazonas, Santa Isabel Do Rio Negro, Rio Negro, right bank downstream of Rio Jurubaxi, 0°30'6.0"S, 64°49'11.0"W; USNM 111593, 6, 42.0–51.5 mm SL, Brazil, Pará, Altamira, Rio Iriri, island beach just bellow the camp, 3°49'09.0"S, 52°38'11.0"W; USNM 111813, 1, 58.6, Brazil, Pará, Altamira, Rio Iriri, next to mouth of Rio Xingú and next to camp, 3°49'40.0"S, 52°41'31.0"W; USNM 406472, 4, 57.6–68.1 mm SL, Guyana, Cuyuni-Mazaruni, Braided channel about 15km upstream from Devil's Hole on Cuyuni River, Habitats include sandbars, beaches, banks with overhanging vegetation, and fast rapids over bedrock and loose stone, 6°47'49.6"N, 59°59'34.1"W; USNM 409800, 1, 64.4 mm SL, Surinam, Upper Paloemeu River, ~500 km downstream of basecamp, Collected in the main channel of the river in shallow areas, mostly inner bends of the stream, 2°29'22.1"N, 55°36'38.5"W.

***Pimelodella megalura* Miranda Ribeiro, 1918**

Pimelodella megalura Miranda Ribeiro, 1918: 638–639 [original description; “S. Luiz de Caceres: Matto-Grosso”, Brazil; lectotype: MNRJ 865A (designated by Miranda Ribeiro, 1953)]. — Gosline, 1945: 45 [taxonomic treatment]. — Fowler, 1951: 546 [taxonomic treatment]. — Miranda Ribeiro, 1953: 403 [type catalog, lectotype designation]. — Burgess, 1989: 281 [taxonomic treatment]. — Britski *et al.*, 1999: 98 [taxonomic treatment]. — Bockmann & Guazzelli, 2003: 419–420 [taxonomic treatment]. — Ferraris, 2007: 193 [taxonomic treatment].

Diagnosis

Pimelodella megalura differs from all *Pimelodella* species except *P. itapicuruensis*, *P. leptosoma*, *P. longipinnis*, *P. metae*, *P. montana*, *P. reyesi*, *P. robinsoni*, *P. tapatapae* and *P. yuncensis* by the supraoccipital process not reaching the anterior prenuchal plate (unknown in *P. reyesi*). It differs from *P. longipinnis*, *P. metae*, *P. montana*, *P. reyesi*, *P. tapatapae* and *P. yuncensis* by having 43–46 total vertebrae (vs. 42 or less total vertebrae in *P. longipinnis*, *P. metae*, *P. montana*, *P. reyesi*, *P. tapatapae* and *P. yuncensis*). It differs from *P. itapicuruensis*, *P. leptosoma* and *P. robinsoni* by having dorsal region body from supraoccipital process to adipose slightly darker, and dorsal caudal fin lobe notably longer than ventral lobe (vs. body without the dorsal region body darker, and dorsal caudal fin lobe subequal or slightly longer than ventral lobe in *P. leptosoma* and *P. robinsoni*; paired dorsolateral dark stripe until dorsal-fin terminus, and dorsal lobe slightly longer than ventral in *P. itapicuruensis*).

Furthermore, *P. megalura* can be diagnosed by the presence of maxillary barbel reaching between verticals through anal-fin origin and terminus; supraoccipital process not reaching the anterior prenuchal plate; dorsal-fin spine half of first dorsal-fin ray total length; posterior margin of pectoral-fin spine bearing 8–10 small, retrorse dentations along its basal two thirds; adipose fin long, roughly two and half times in SL; dorsal lobe or caudal fin slightly to notably longer than ventral; hypural 5 may be completely free or fused to hypural 3+4; 43–46 total vertebrae; medium brown midlateral stripe wide, not well delimited, from snout to distal portion of median caudal-fin rays; dorsal region body from supraoccipital process to adipose slightly darker.

Description

Measurements in Table 47. Body depressed, depth at dorsal-fin insertion six to eight times in standard length, and compressed, body width at dorsal-fin insertion seven to eight times in SL (Fig. 144). Dorsal profile slightly convex from snout to dorsal fin, concave from dorsal to adipose fin, slightly convex along adipose fin, and concave along the caudal peduncle. Ventral profile of body slightly convex from snout to branchiostegal membrane, concave between pectoral end pelvic fins, slightly concave from pelvic to anal fin, and straight from there along the caudal peduncle.

Pseudotympanum large, oval, above posterior process of cleithrum and reaching the straight line of 6th* (3) or 7th (2) vertebrae. Posterior process of cleithrum triangular, its dorsal border slightly concave. Anus and urogenital papilla adjacent. Urogenital papilla tubular, triangular, short. Anus between verticals through first third and second fifth of adpressed

pelvic fin; urogenital papilla between verticals through second fifth and last fourth of adpressed pelvic fin.

Head average depressed, depth at supraoccipital-process base slightly less or slightly more than two times in head length. Mouth sub terminal. Eye slightly elliptical, four and half to almost six times in head. Bony interorbital distance slightly less than eye diameter. Barbels thin, slightly depressed and elliptical in cross-section. Maxillary barbel reaching between verticals through anal-fin origin and terminus. Outer mental barbel, when stretched parallel to main body axis, finishing between first third and last fourth of adpressed pectoral fin. Inner mental barbel, when stretched parallel to main body axis, finishing between pectoral-fin origin and terminus. Supraoccipital process roughly triangular, narrow, almost reaching anterior prenuchal plate. Dorsal lamina of Weberian complex vertebrae reaching the supraoccipital process at its anteriormost region. Branchiostegal rays 6 (1).

Dorsal fin triangular, distal margin concave, average sized (second branched dorsal-fin ray five to five and half times in SL), depressed tip finishing between the verticals through second third and terminus of adpressed pelvic fin. Dorsal fin with I,6 (6) plus anteriormost spinelet. Distance between terminus of dorsal-fin base and adipose-fin origin half to two thirds of dorsal-fin base. Anteriormost dorsal-fin pterygiophore inserted posterior to neural spine of vertebrae 5 (1); posteriormost dorsal-fin pterygiophore located ahead of neural (or pseudoneural) spine of vertebrae 11 (1) or 12* (4). Unbranched dorsal-fin ray mostly ossified as a spine, rigid part short (approximately a third to half of first dorsal-fin ray total length).

Pectoral-fin rays I,7* (2) or I,8 (4), pectoral fin triangular with convex distal border. First pectoral-fin ray curved, with proximal part rigid, forming a spine (Fig. 145), and short distal tip flexible and distinctly segmented. Pectoral-fin spine six to nine times in SL. Anterior margin of pectoral-fin spine with smooth serrae at its distal half. Posterior margin of pectoral-fin spine bearing 8–10 small, retrorse dentations along its basal two thirds.

Pelvic-fin rays i,5 (6), extended pelvic fin triangular with straight distal border. Anterior portion of pelvic-fin base between verticals through fifth branched dorsal-fin ray and dorsal fin terminus. Tip of adpressed pelvic fin between verticals through a point slightly anterior to adipose-fin origin and first tenth of adipose-fin base. First unbranched and flexible ray distinctly shorter than second and third rays, third ray the longest; remaining rays progressively shorter.

Anal-fin rays iv,7 (1); vi,8 (1); ii,9 (1), iv,9*(1); v,9 (1); or vi,9 (1); distal border of extended anal fin convex. Two or three anteriormost anal-fin rays vestigial, unsegmented, embedded in thick skin fold. Anal fin origin between verticals through first fourth and almost

half of adipose-fin base; anal-fin terminus between verticals through last seventh and almost terminus of adipose fin. Tip of anteriormost anal-fin pterygiophore inserted posterior to hemal spine of vertebrae 21 (2), 22* (1) or 23 (2). Tip of posteriormost anal-fin pterygiophore inserted ahead of hemal spine of vertebrae 30 (1), 31 (2) or 32* (2).

Adipose fin roughly two and half times in SL, forming ascending elevated curve in lateral profile, with deepest point approximately midlength. Adipose fin emerging gradually, its posterior limit as a rounded, free lobe. Adipose fin origin at vertical through vertebral centra 18 (1)– 21* (2). Adipose fin terminus at vertical through vertebral centra 38* (1)– 41 (1).

Caudal fin deeply forked, dorsal lobe slightly to notably longer than ventral. Caudal peduncle length posterior to adipose-fin a fourth longer than its depth. Dorsal lobe with 7 (5) branched, 1 (5) unbranched principal, and 11 (1)–16 (1) (lectotype 13) procurrent fin-rays. Ventral lobe with 8 (5) branched, 1 (5) unbranched principal, and 15* (1)–20 (1) procurrent fin-rays. Hypural 5 may be completely free (3) or fused* (2) to hypural 3+4. Seven* (5) rays articulated to dorsal caudal-fin plate (5 on hypurals 3+4 and 2 on hypural 5, when this last is free) and 8 (5) rays articulated to ventral caudal-fin plate (6 on hypurals 1+2 and 2 on parhypural).

Total vertebrae 43* (1)– 46 (1). Ribs 8* (4)– 9(1).

Epiphyseal branch of laterosensory canal on head (S6) with contralateral canals emerging as two separate pores.

Coloration in alcohol

Background body coloration yellowish. Ventral region of head and body lighter. Medium brown midlateral stripe (Fig. 146) wide, not well delimited, from snout to distal portion of median caudal-fin rays. Dorsal region body from supraoccipital process to adipose slightly darker. Dorsal fin brown near base, followed by a hyaline stripe, and distal half brown.

Geographic distribution

Pimelodella megalura was described from Cáceres, Mato Grosso State, Brazil. It is known from region 343 (Paraguay), in streams of Upper Paraguay in Brazil.

Comments

This is an intriguing species, since part of its specimens has the hypural 5 fused to the dorsal hypural plate, and supraoccipital process not reaching the anterior prenuchal plate, both characters found in *Rhamdella* species; however, the overall body shape is similar to

Pimelodella, as also the dorsal lamina of Weberian complex vertebrae, which is present and high (meanwhile extremely low in *Rhamdella*). This species deserves a more detailed study, and inclusion of comparative material, in order to try to solve its taxonomic status.

Material examined

Pimelodella megalura. — MNRJ 865A, lectotype, xr, 128.6 mm SL, Brazil, Mato Grosso, São Luiz de Cáceres, 16°04'01"S, 57°41'44"W; MNRJ 865, 3, xr, 85.1–131.6 mm SL, lectótipos, Brazil, Mato Grosso, São Luiz de Cáceres, 16°04'01"S, 57°41'44"W; MZUSP 1986, 1, paralectótipo, Brazil, Mato Grosso, São Luiz de Cáceres, 16°04'01"S, 57°41'44"W; MZUSP 5265 a 5279, 12, xr, 70.0–143.6 mm SL, paralectótipos, Brazil, Mato Grosso, São Luiz de Cáceres, 16°04'01"S, 57°41'44"W.

***Pimelodella metae* Eigenmann, 1917**

Pimelodella metae Eigenmann, 1917: 244–245 pl. XXXI, fig. 1, pl. XXXV, fig. 21–22 [original description; “Rio Negro, Villavicencio”, Colombia; holotype: FMNH 58441 (formerly CM 7441)]. — Eigenmann, 1920: 4–5 [taxonomic list, taxonomic treatment]. — Eigenmann, 1922a: 222 [taxonomic treatment]. — Henn, 1928: 77 [type catalog]. — Fowler, 1943: 244 [taxonomic treatment]. — Schultz, 1944: 212 [taxonomic treatment]. — Gosline, 1945: 44 [taxonomic treatment]. — Cala, 1977: 11 [taxonomic list]. — Ibarra & Stewart, 1987: 66 [type catalog]. — Burgess, 1989: 281 [taxonomic treatment]. — Bockmann & Guazzelli, 2003: 420 [taxonomic treatment]. — Lasso *et al.*, 2004: 171 [taxonomic list]. — Ferraris, 2007: 193 [taxonomic treatment]. — Maldonado-Ocampo *et al.*, 2008: 202 [taxonomic list].

Diagnosis

Pimelodella metae can be distinguished from all *Pimelodella* species except *P. buckleyi*, *P. grisea*, *P. geryi*, *P. leptosoma* and *P. notomelas*, by the presence of dorsal fin distal third extremely dark brown to black. It differs from all above mentioned, except *P. leptosoma*, by having the supraoccipital process not reaching the anterior prenuchal plate. It differs from *P. leptosoma* by the posterior margin of pectoral-fin spine bearing 4–5 smooth, retrorse to straight dentations along its basal half (*vs.* posterior margin of pectoral-fin spine bearing 8–9 broad-based, triangular, strongly inclined, blade-like retrorse dentations along basal two thirds). Furthermore, *P. metae* can be diagnosed by the presence of maxillary barbel reaching between anal fin origin and terminus; supraoccipital process almost reaching the anterior prenuchal plate; posterior margin of pectoral-fin spine bearing 8–9 broad-based, triangular, strongly inclined, blade-like retrorse dentations along basal two thirds; adipose fin

more than two and half to three times in SL; dark brown midlateral stripe of moderated width, not well delimited, from snout until caudal fin origin, maybe median caudal-fin rays; dorsal fin medium brown near base, followed by a hyaline stripe, then a dark brown to black stripe, and distal portion of rays clear.

Description

Measurements in Table 48. Body moderated depth, depth at dorsal-fin origin five and half to six times in standard length, and compressed, body width at dorsal-fin origin four to six to eight times in SL (Fig. 147). Dorsal profile convex from snout to dorsal fin, slightly concave from dorsal to adipose fin, slightly convex along adipose fin, and concave along the caudal peduncle. Ventral profile of body convex from snout to branchiostegal membrane, convex between pectoral and pelvic fins, also convex from pelvic to anal fin, and concave from there along the caudal peduncle.

Pseudotympanum large, oval, above posterior process of cleithrum and reaching the straight line of 6th (1) or 7^{th*} (3) vertebrae. Posterior process of cleithrum triangular, narrow, its dorsal border slightly concave to straight. Anus and urogenital papilla adjacent. Urogenital papilla tubular, triangular, short. Anus at vertical through first third of adpressed pelvic fin; urogenital papilla between verticals through last third and last fifth of adpressed pelvic fin.

Head depressed, depth at supraoccipital-process base usually less than two times in head length. Mouth sub terminal. Eye slightly elliptical, five times in head. Bony interorbital distance slightly less than eye diameter. Barbels thin, depressed, and elliptical in cross-section. Maxillary barbel reaching between anal fin origin and terminus. Outer mental barbel, when stretched parallel to main body axis, finishing between half and last third of adpressed pectoral fin. Inner mental barbel, when stretched parallel to main body axis, finishing between pectoral fin origin and terminus. Supraoccipital process roughly triangular, narrow, almost reaches the anterior prenuchal plate. Dorsal lamina of Weberian complex vertebrae reaching the supraoccipital process just at its anteriormost part. Branchiostegal rays 6 (2).

Dorsal fin triangular, distal margin convex, moderate length (second branched dorsal-fin ray four and half to five times in SL), reaching between the verticals through last fourth and almost terminus of adpressed pelvic fin. Dorsal fin with I,6* (3), rarely I,7 (1), plus anteriormost spinelet. Distance between terminus of dorsal-fin base and adipose-fin origin slightly smaller than dorsal-fin base. Anteriormost dorsal-fin pterygiophore inserted posterior to neural spine of vertebrae 5 (5); posteriormost dorsal-fin pterygiophore located ahead of neural (or pseudoneural) spine of vertebrae 11* (3) or 12 (1). Unbranched dorsal-fin ray

mostly ossified as a spine, rigid part relatively short (two thirds or less of first dorsal-fin ray total length), with smooth serrae at its anterior distal third.

Pectoral-fin rays I,7 (1)– I,9* (1), pectoral fin triangular with concave distal border. First pectoral-fin ray roughly straight, with proximal part rigid (Fig. 148), forming a spine and short distal tip flexible and distinctly segmented. Pectoral-fin spine five and half to slightly less than six times in SL. Anterior margin of pectoral-fin spine with smooth serrae along its distal third. Posterior margin of pectoral-fin spine bearing 4–5 smooth, retrorse to straight dentations along its basal half.

Pelvic-fin rays i,5 (4), extended pelvic fin triangular with straight distal border. Pelvic-fin origin between verticals through last fifth of dorsal-fin base and its terminus. Tip of adpressed pelvic fin between verticals through adipose-fin origin and a point slightly anterior to that. First unbranched and flexible ray distinctly shorter than second and third rays, which are subequal; remaining rays progressively shorter.

Anal-fin rays iv,7 (2); v,7 (1); or vi,8* (1); distal border of extended anal fin convex. Two or three anteriormost anal-fin rays vestigial, unsegmented, embedded in thick skin fold. Anal fin origin between verticals through first fourth and almost half adipose fin; anal-fin adpressed terminus at or slightly anterior to vertical through adipose-fin terminus. Tip of anteriormost anal-fin pterygiophore inserted posterior to hemal spine of vertebrae 22* (3) or 23 (1). Tip of posteriormost anal-fin pterygiophore inserted ahead of hemal spine of vertebrae 29* (3) or 30 (1).

Adipose fin more than two and half to three times in SL, forming ascending elevated curve in lateral profile, with deepest point approximately at midlength. Adipose fin emerging gradually, its posterior limit as a rounded, free lobe. Adipose-fin origin at vertical through vertebral centra 17 (1) to 21 (2) (holotype 20); adipose-fin terminus at vertical through vertebral centra 35* (2) to 36 (1).

Caudal fin deeply forked, dorsal lobe slightly longer. Caudal peduncle length posterior to adipose-fin a third longer than its depth. Dorsal lobe with 7 (4) branched, 1 (4) unbranched principal and 8 (1)–10* (1) procurrent fin-rays. Ventral lobe with 8 (4) branched, 1 (4) unbranched principal and 9* (1)–16 (1) procurrent fin-rays. Hypural 5 completely free, not fused to hypural 3+4. Median caudal-fin rays not articulated directly to caudal plate. Seven* (2), rarely 6 (1) rays articulated to dorsal caudal-fin plate (4–5 on hypurals 3+4 and 2 on hypural 5) and 8* (3), rarely 7 (1) rays articulated to ventral caudal-fin plate (5–6 on hypurals 1+2 and 2 on parahypural).

Total vertebrae 41* (3)– 42 (1). Ribs 8* (3)–9 (1).

Epiphyseal branch of laterosensory canal on head (S6) with contralateral canals emerging as two separate pores, near each other.

Coloration in alcohol

Background body coloration yellowish. Ventral region of head and body lighter. Dark brown midlateral stripe (Fig. 149) of moderated width, not well delimited, from snout until caudal fin origin, maybe median caudal-fin rays. Dorsal fin medium brown near base, followed by a hyaline stripe, then a dark brown to black stripe, and distal portion of rays clear.

Geographic distribution

Pimelodella metae was described from Rio Meta basin, in Orinoco system. It is known from regions 305 (Orinoco High Andes) and 306 (Orinoco piedmont), in several streams of Orinoco system and Lake Valencia, in Colombia and Venezuela.

Material examined

Pimelodella metae. — FMNH 58441, 1, xr, 58.0 mm SL, holotype, Colômbia, Meta, Villavicencio, Rio Negro, 4°02'59"N, 73°16'53"W; CAS 75835, 1, xr, 34.9 mm SL, paratype, Colômbia, Meta, Quebrada Cramalote at municipio Villavicencio, Boro Heste, Rio Orinoco basin. Another label reads "Rio Negro, Villavicencio", 4°02'59"N, 73°16'53"W; FMNH 58442, 2, xr, 64.3–74.0 mm SL, paratypes, Colômbia, Meta, Cabuyaro, Barrigona, Rio Meta (possibly Puerto Barrigon, Meta dept.), 4°09'51"N, 73°00'50"W; ANSP 138091, 3, 54.1–55.9 mm SL, Colombia, Meta, Rio Negro, downstream from main Villavicencio-Puerto Lopez highway at La Balsa, W side of river, Negro-Humea-Meta Dr., 4°4'0.0"N, 73°4'0.0"W; ANSP 138828, 1, 58.14 mm SL, 2 c&s, Colombia, Meta, Rio Negrito midway between La Argelia and La Balsa (Plancha 267 - Rio Guayuriba) , 4°4'0.0"N, 73°4'0.0"W.

***Pimelodella modesta* (Günther, 1860)**

Pimelodus modestus Günther, 1860: 239, pl. X, fig. C [original description; “Fresh waters of Esmeraldas”; syntypes: BMNH 1860.6.16.190–191]. — Günther, 1864: 177–178 [taxonomic treatment].

Pimelodella modestus. — Eigenmann & Eigenmann, 1888: 133 [taxonomic revision, transfer to *Pimelodella*]. — Eigenmann & Eigenmann, 1890: 155 [key to *Pimelodella* species; taxonomic revision]. — Eigenmann & Eigenmann, 1891: 29 [taxonomic treatment]. — Eigenmann, 1905: 19 [taxonomic list]. — Eigenmann, 1910: 389 [taxonomic treatment]. — Bockmann & Guazzelli, 2003: 420 [taxonomic treatment]. — Lasso *et al.*, 2004: 127, 171 [taxonomic treatment, taxonomic list]. — Mojica *et al.*, 2004: 743

[taxonomic list]. — Maldonado-Ocampo *et al.*, 2006: 167 [taxonomic treatment]. — Maldonado-Ocampo *et al.*, 2008: 202 [taxonomic list].

Rhamdia modesta. — Miranda Ribeiro, 1911: 272–273, fig. 110 (*in partim*) [taxonomic treatment].

Pimelodella modesta. — Eigenmann, 1917: 252–253, pl. XXXV, fig. 34 [taxonomic revision]. — Eigenmann, 1921b: 514 [taxonomic list]. — Eigenmann, 1922: 42 [taxonomic treatment]. — Gosline, 1945: 46 [taxonomic treatment]. — Leiva, 2005: 50 [taxonomic treatment]. — Ferraris, 2007: 193 [taxonomic treatment].

Diagnosis

Pimelodella modesta can be diagnosed from all *Pimelodella* with exception of *P. cruxenti*, *P. laticeps*, *P. montana*, *P. pectinifera* and *P. yuncensis* by having an overall dark brown body. It differs from *P. cruxenti* by having maxillary barbels reaching between adpressed pelvic fin and anal fin origin (*vs.* surpassing anal fin origin in *P. cruxenti*). It differs from *P. montana* by not having a paired dorsolateral stripe along body (*vs.* having a paired dorsolateral stripe, from supraoccipital process to first third of adipose-fin base). It differs from *P. pectinifera* and *P. yuncensis* by the narrow, hyaline stripe near dorsal-fin base, remaining dorsal fin dark brown to black (dorsal-fin hyaline in *P. pectinifera*; dorsal-fin completely pigmented in *P. yuncensis*). Furthermore, *P. modesta* can be diagnosed by the presence of maxillary barbels reaching between adpressed pelvic fin and anal fin origin; posterior margin of pectoral-fin spine with 10–12 retrorse dentations along its basal two thirds; adipose fin roughly three times in SL; 41 total vertebrae; body overall yellowish to grayish, dark brown midlateral stripe narrow, well delimited, from snout to caudal-fin origin; dorsal region of body overall darker; ventral caudal lobe darker.

Description

Measurements in Table 49. Body of moderated depth to deep, depth at dorsal-fin origin four and half to six and half times in standard length; and moderated width, body width at dorsal-fin origin five and half to nine times in SL (Fig. 150). Dorsal profile convex from snout to dorsal fin, concave from dorsal to adipose fin, convex along adipose extension, and concave along the caudal peduncle. Ventral profile of body slightly convex from snout to branchiostegal membrane, concave from branchiostegal membrane to pectoral fin, slightly concave from this point to pelvic fin, and concave straight from pelvic along the caudal peduncle.

Pseudotympanum large, oval, dorsal to posterior process of cleithrum and reaching the straight line of 7th (2) vertebrae. Posterior process of cleithrum triangular, dorsal border slightly concave. Anus and urogenital papilla adjacent. Urogenital papilla tubular, triangular, short. Anus at vertical through half adpressed pelvic fin; urogenital papilla at the vertical through the last fourth of adpressed pelvic fin.

Head usually deep, depth at supraoccipital-process base from slightly more than two to slightly more than one and half times in head length. Mouth sub terminal. Eye slightly elliptical, five to five and half times in head. Bony interorbital distance roughly equal to eye diameter. Barbels thin, slightly depressed and elliptical in cross-section. Maxillary barbels reaching between adpressed pelvic fin and anal fin origin. Outer mental barbel, when stretched parallel to main body axis, finishing between first third and last fourth of adpressed pectoral fin. Inner mental barbel, when stretched parallel to main body axis, finishing between branchiostegal membrane ventral limit and pectoral fin terminus. Supraoccipital process subrectangular, tapered at distal point. Dorsal lamina of Weber complex vertebrae of medium height, reaching the supraoccipital process just at its anteriormost part. Branchiostegal rays 6 (2).

Dorsal fin triangular, distal margin concave, short (second branched dorsal-fin ray four and half to five and half times in SL), reaching between verticals through last third and fourth of adpressed pelvic fin. Dorsal fin with I,6 (1) plus anteriormost spinelet. Distance between terminus of dorsal-fin base and adipose-fin origin slightly smaller than dorsal-fin base. Anteriormost dorsal-fin pterygiophore inserted posterior to neural spine of vertebrae 4 (2); posteriormost dorsal-fin pterygiophore located ahead of neural (or pseudoneural) spine of vertebrae 11 (2). Unbranched dorsal-fin ray mostly ossified as a spine, rigid part relatively short (approximately two thirds of first dorsal-fin ray total length).

Pectoral-fin rays I,7* (1)– I,8 (3), pectoral fin triangular with concave distal border. First pectoral-fin ray curved, with proximal part rigid (Fig. 151), forming a spine and short distal tip flexible and distinctly segmented. Pectoral-fin spine six to almost seven times in SL. Anterior margin of pectoral-fin spine with small, straight dentations along all margin, except distal third, which has smooth serrae. Posterior margin of pectoral-fin spine with 10–12 retrorse dentations along its basal two thirds, plus sometimes 1–2 unossified distalmost dentations, not counted.

Pelvic-fin rays i,5 (4), extended pelvic fin triangular with straight distal border. Pelvic-fin origin at vertical through dorsal fin terminus. Tip of adpressed pelvic fin between verticals

through adipose-fin origin and its first fifth. First unbranched and flexible ray distinctly shorter than second and third rays, which are subequal; remaining rays progressively shorter.

Anal-fin rays v,8* (4); distal border of extended anal fin convex. Three anteriormost anal-fin rays vestigial, unsegmented, embedded in thick skin fold. Anal fin origin between verticals through first fourth or third of adipose-fin base. Anal-fin adpressed terminus slightly anterior to vertical through adipose-fin terminus. Tip of anteriormost anal-fin pterygiophore inserted posterior to hemal spine of vertebrae 21 (2). Tip of posteriormost anal-fin pterygiophore inserted ahead of hemal spine of vertebrae 28 (2).

Adipose fin roughly three times in SL, forming ascending elevated curve in lateral profile, with deepest point approximately midlength. Adipose fin emerging gradually, its posterior limit as a rounded, free lobe. Adipose-fin origin at vertical through vertebral centrum 20 (2); adipose-fin terminus at vertical through vertebral centra 35* (1) or 36 (1).

Caudal fin deeply forked, upper lobe longer than ventral lobe. Caudal peduncle length posterior to adipose fin roughly equal to its depth. Dorsal lobe with 7 (3) branched, 1 (3) unbranched principal and 16 (1)– 17* (1) procurrent fin-rays. Ventral lobe with 8 (3) branched, 1 (3) unbranched principal and 15 (1)– 19* (1) procurrent fin-rays. Hypural 5 completely free, not fused to hypurals 3+4. Median caudal-fin rays not attached directly to caudal plate. Seven (2) rays articulated to dorsal caudal-fin plate (5 on hypurals 3+4 and 2 on hypural 5) and 8 (2) rays articulated to ventral caudal-fin plate (6 on hypurals 1+2 and 2 on parahypural).

Total vertebrae 41 (2). Ribs 9 (2).

Epiphyseal branch of laterosensory canal in head (S6) with contralateral canals connected, emerging as a single pore right after the connection of the two contralateral canals.

Coloration in alcohol

Background body coloration yellowish to grayish. Ventral region of head and body lighter. Dark brown midlateral stripe narrow (Fig. 152), well delimited, from snout to caudal-fin origin. Dorsal region of body overall darker. Cephalic dark brown pigment along posterior fontanel region. A narrow, hyaline stripe near dorsal-fin base, remaining dorsal fin dark brown to black. Ventral caudal lobe darker.

Geographic distribution

Pimelodella modesta was described from Esmeralda River basin, in Northwestern Ecuador. It is known from regions 209 (Chagres) and 301 (North Andean Pacific slopes), in several streams in Eastern Panamá, Southern Colombia and Ecuador.

Comments

When describing *P. modesta*, Günther (1860) presents the measurements of only one specimen, of 113.6 mm TL, which is nearer to the syntype BMNH 1860.6.16.190 (121.1 mm TL, my measurement). Therefore, I hereby designate this specimen as the lectotype and BMNH 1860.6.16.191 as paralectotype of *P. modesta*.

Miranda Ribeiro (1911) reference to *P. modesta* in Juruá River, Amazonas State (region 316- Amazonas lowlands) is probably equivocated.

Material examined

Pimelodella modesta. — BMNH 1860.6.190, 1, xr, 113.6 mm SL, lectotype, Ecuador, "Fresh waters of Esmeralda", 0°56'31"N, 79°38'47"W; BMNH 1860.6.191, 1, xr, 77.5 mm SL, paralectotype, Ecuador, "Fresh waters of Esmeralda", 0°56'31"N, 79°38'47"W; MZUSP uncat., Ecuador, 4, 135.05–175.66 mm SL, Ecuador; USNM 076928, 8, 55.8–91.9 mm SL, Colombia, Rio Telembi, San Loranzo (or Coranzo?), 1°33'31.4"N, 77°51'31.5"W.

***Pimelodella montana* Allen in Eigenmann & Allen, 1942**

Pimelodella montana Allen in Eigenmann & Allen, 1942: 100–101, pl. XIII, fig. 2 [original description; "Rio Huallaga, Huánuco", Peru; syntypes: CAS 63719 (formerly IU 17830)]. — Gosline, 1945: 46 [taxonomic treatment]. — Fowler, 1951: 546 [taxonomic treatment]. — Ortega & Vari, 1986: 14 [taxonomic list]. — Bockmann & Guazzelli, 2003: 420 [taxonomic treatment]. — Ferraris, 2007: 193 [taxonomic treatment].

Diagnosis

Pimelodella montana can be diagnosed from all *Pimelodella* with exception of *P. cruxenti*, *P. laticeps*, *P. modesta*, *P. pectinifera* and *P. yuncensis* by having an overall dark brown body. It differs from all above by also having a paired dorsolateral stripe, from supraoccipital process to first third of adipose-fin base. Furthermore, *P. montana* can be diagnosed by the presence of maxillary barbel reaching between anal fin origin and short of adpressed anal fin terminus; supraoccipital process almost reaching anterior prenuchal plate; posterior margin of pectoral-fin spine with 8–9 small, retrorse dentations along its basal half; dark brown midlateral stripe wide, well delimited, from snout to distal of median caudal-fin rays; paired dorsal dark brown stripe, along supraoccipital process to first third of adipose-fin base, not well delimited.

Description

Measurements in Table 50. Body deep, depth at dorsal-fin origin four and half to five and half times in standard length, and wide, body width at dorsal-fin origin five to seven times in SL (Fig. 153). Dorsal profile convex from snout to dorsal fin, concave from dorsal to adipose fin, slightly convex along adipose fin, and concave along caudal peduncle. Ventral profile of body slightly concave from snout to branchiostegal membrane, convex between pectoral end pelvic fins, slightly concave from pelvic to anal fin, and concave from there to caudal peduncle.

Pseudotympanum large, oval, dorsal to posterior process of cleithrum and reaching 6th* (1) vertebrae. Posterior process of cleithrum triangular, dorsal border slightly concave. Anus and urogenital papilla adjacent. Urogenital papilla tubular, triangular, short. Anus between verticals through second fifth and half adpressed pelvic fin; urogenital papilla between verticals through last fourth and last fifth of adpressed pelvic fin.

Head deep, depth at supraoccipital-process base less than two times in head length. Mouth sub terminal. Eye slightly elliptical, five to six times in head. Bony interorbital distance notably larger than eye diameter. Barbels thin, and slightly depressed and elliptical in cross-section. Maxillary barbel reaching between anal fin origin and short of adpressed anal fin terminus. Outer mental barbel, when stretched parallel to main body axis, finishing between second third and almost terminus of adpressed pectoral fin. Inner mental barbel, when stretched parallel to main body axis, finishing between branchiostegal membrane ventral limit and first third of adpressed pectoral fin. Supraoccipital process roughly triangular, almost reaching anterior prenuchal plate. Dorsal lamina of Weberian complex vertebrae of moderated height, reaching the supraoccipital process just at its anteriormost part. Branchiostegal rays 7 (1).

Dorsal fin triangular, distal margin concave, of short length (second branched dorsal-fin ray five to six and half times in SL), depressed tip reaching between verticals through half and last third of adpressed pelvic fin. Dorsal fin with I,6 (4), plus anteriormost spinelet. Distance between terminus of dorsal-fin base and adipose-fin origin equal or slightly shorter than dorsal-fin base. Anteriormost dorsal-fin pterygiophore inserted posterior to neural spine of vertebrae 5 (1); posteriormost dorsal-fin pterygiophore located ahead of neural (or pseudoneural) spine of vertebrae 11 (1). Unbranched dorsal-fin ray mostly ossified as a spine, rigid part of moderated length (two thirds of first dorsal-fin ray total length).

Pectoral-fin rays I,7* (1)– I,8 (3), pectoral fin triangular with concave distal border. First pectoral-fin ray roughly straight, with proximal part rigid (Fig. 154), and short distal tip

flexible and distinctly segmented. Pectoral fin spine six to eight times in SL. Anterior margin of pectoral-fin spine with small, smooth dentations along basal half and smooth serrae along distal half. Posterior margin of pectoral-fin spine with 8–9 small, retrorse dentations along its basal half.

Pelvic-fin rays i,5 (4), extended pelvic fin triangular with straight distal border. Pelvic-fin origin at vertical through dorsal fin terminus. Tip of adpressed pelvic fin between verticals through first fifth and first third of adipose-fin base. First unbranched and flexible ray distinctly shorter than second and third rays, which are subequal; remaining rays progressively shorter.

Anal-fin rays iv,8 (3) or iv,9* (1); distal border of extended anal fin convex. Two anteriormost anal-fin rays vestigial, unsegmented, embedded in thick skin fold. Anal fin origin between verticals through first and second third of adipose-fin base. Anal-fin adpressed terminus at vertical through adipose-fin terminus. Tip of anteriormost anal-fin pterygiophore inserted posterior to hemal spine of vertebrae 21 (1). Tip of posteriormost anal-fin pterygiophore inserted ahead of hemal spine of vertebrae 29 (1).

Adipose fin two and half to slightly more than three times in SL, forming ascending elevated curve in lateral profile, with deepest point approximately midlength. Adipose fin emerging gradually, its posterior limit as a rounded, free lobe. Adipose-fin origin at vertical through vertebral centrum 18 (1); adipose-fin terminus at vertical through vertebral centrum 34 (1).

Caudal fin deeply forked, dorsal lobe subequal to slightly longer than ventral lobe. Caudal peduncle posterior to adipose-fin base slightly larger than its depth. Dorsal lobe with 7 (3) branched, 1 (3) unbranched principal and 15 (1) procurrent fin-rays. Ventral lobe with 8 (3) branched, 1 (3) unbranched principal and 14 procurrent fin-rays. Hypural 5 separated from hypurals 3+4. Median caudal-fin rays not directly attached to caudal plate. Seven (1) rays articulated to dorsal caudal-fin plate (5 on hypurals 3+4 and 2 on Hypural 5) and 8 (1) rays articulated to ventral caudal-fin plate (6 on hypurals 1+2 and 2 on parhypural).

Total vertebrae 41 (1). Ribs 9 (1).

Epihyseal branch of laterosensory canal on head (S6) with contralateral canals connecting at midline, following posteriorly as a single canal and opening in a single pore.

Coloration in alcohol

Background body coloration brownish. Ventral region of head and body lighter. Dark brown midlateral stripe wide (Fig. 155), well delimited, from snout to distal of median caudal-fin rays. Paired dorsal dark brown stripe, along supraoccipital process to first third of

adipose-fin base, not well delimited. Dark brown cephalic pigment along posterior fontanel. Dorsal fin overall dark brown to black, except by a hyaline stripe near its basal half.

Geographic distribution

Pimelodella montana was described from Huallaga River, in Huánuco, Peru. It is known from region 312 (Amazon high Andes) in Peru.

Comments

Pimelodella montana was described based on five syntypes, from 86 to 91 mm SL (Allen in Eigenmann & Allen, 1942: 100). However, on plate XII, fig. 2 is presented one specimen, whose legend is “*Pimelodella montana* Allen, sp. nov., type. 17830, 93 mm., Rio Huallaga, Huánuco”. Since the specimen whose size is most similar to the illustrated is the largest one (87.4 mm SL, my measure), I hereby designate this as the lectotype, and remaining specimens as paralectotypes.

Material examined

Pimelodella montana. — CAS 63719, 1, xr, 87.4 mm SL, lectotype, Peru, Rio Huallaga at Huanuco, 8°36'31"S, 76°16'04"W; MZUSP 110466, 1, 110 mm SL, Peru, Huánuco, Tingo Maria, Quebrada Sta. Rosa de Chaparilla, 9°13'31.0"S, 75°59'17.0"W; MZUSP 110494, 3, 103.3–155.6 mm SL, Peru, Huánuco, Tingo Maria, left bank of Rio Huallaga downstream from mouth of Quebrada Acerradero, next to Balneário, 9°15'13.0"S, 76°0'33.0"W.

***Pimelodella mucosa* Eigenmann & Ward in Eigenmann, McAtee & Ward, 1907**

Pimelodella mucosa Eigenmann & Ward in Eigenmann, McAtee & Ward, 1907: 114–114, pl.

XXXII, fig. 1 [original description; “Bahia Negra”, Paraguay; holotype: CAS 63720 (formerly 10125)]. — Eigenmann, 1910: 389 [taxonomic treatment]. — Bertoni, 1913: 7 [taxonomic list]. — Eigenmann, 1917: 250–251, pl. XXXIII, fig. 1, pl. XXXV, fig. 4–6 [taxonomic revision]. Bertoni, 1939: 52 [taxonomic list]. — Fowler, 1940: 95 [taxonomic treatment]. — Gosline, 1945: 45 [taxonomic treatment]. — Fowler, 1951: 546–547 [taxonomic treatment]. — Burgess, 1989: 281 [taxonomic treatment]. — Lundberg *et al.*, 1991a: 192 [taxonomic treatment, enlarged cephalic laterosensory canals]. — Britski *et al.*, 1999: 98 [taxonomic treatment]. — Bockmann & Guazzelli, 2003: 420 [taxonomic treatment]. — Ferraris, 2007: 193 [taxonomic treatment]. — Aguilera & Azpelicueta, 2015: 1–3 [taxonomic treatment, geographic distribution]. — Koerber *et al.*, 2017: 52 [taxonomic list].

Diagnosis

Pimelodella mucosa differs from all *Pimelodella* species except *P. serrata* by the presence of openings of laterosensory canal at dentary and hyomandibula large and conspicuous. It differs from *P. serrata* by posterior margin of pectoral-fin spine bearing 14–18 small, retrorse dentations along its basal two thirds (vs. posterior margin of pectoral-fin spine bearing 16–21 large, retrorse dentations along roughly all margin). Furthermore, *P. mucosa* can be diagnosed by maxillary barbel surpassing caudal-fin origin; dorsal lamina of Weber complex vertebrae of high, reaching the supraoccipital process along its entire length; head roof heavily ornamented; posterior margin of pectoral-fin spine bearing 14–18 small, retrorse dentations along its basal two thirds; adipose fin short, roughly three and half times in SL; 41 total vertebrae; dark brown midlateral stripe wide, not well delimited, extending from snout to caudal-fin origin; paired dorsal brown stripes along supraoccipital process until half dorsal-fin base.

Description

Measurements in Table 51. Body deep, depth at dorsal-fin insertion four or less times in standard length, and wide, body width at dorsal-fin insertion five and half to six times in SL (Fig. 156). Dorsal profile convex from snout to dorsal fin, straight from dorsal to adipose fin, slightly convex along adipose fin, and concave along the caudal peduncle. Ventral profile of body concave from snout to branquiostegal membrane, convex between pectoral end pelvic fins, slightly concave from pelvic to anal fin, and also concave from there along the caudal peduncle.

Pseudotympanum large, oval, dorsal to posterior process of cleithrum and reaching the straight line of 8th (1) vertebrae. Posterior process of cleithrum triangular, its dorsal border straight. Anus and urogenital papilla adjacent. Urogenital papilla tubular, triangular, short. Anus at vertical through second fifth of adpressed pelvic fin; urogenital papilla between verticals through last third or fourth of adpressed pelvic fin.

Head deep, depth at supraoccipital-process base equal or more than half head length. Mouth sub terminal. Eye slightly elliptical, less than five times in head length. Bony interorbital distance notably larger than eye diameter. Barbels thin, slightly depressed and elliptical in cross-section. Maxillary barbel surpassing caudal-fin origin. Outer mental barbel, when stretched parallel to main body axis, reaching between verticals through first and last third of adpressed pectoral fin. Inner mental barbel, when stretched parallel to main body axis, finishing between ventral posterior limit of branchiostegal membrane and pectoral-fin terminus. Supraoccipital process broad, subrectangular, tapered at its distal point, and with a

constriction near its base. Dorsal lamina of Weber complex vertebrae of high, reaching the supraoccipital process along its entire length. Branchiostegal rays 6 (1). Head roof heavily ornamented.

Dorsal fin triangular, distal margin concave, moderated length, (second branched dorsal-fin ray five times in SL), depressed tip finishing between verticals through pelvic fin adpressed terminus or a point slightly anterior to that. Dorsal fin with I,6 (2) plus anteriormost spinelet. Distance between terminus of dorsal-fin base and adipose-fin origin slightly smaller than dorsal-fin base. Anteriormost dorsal-fin pterygiophore inserted posterior to neural spine of vertebrae 4 (1); posteriormost dorsal-fin pterygiophore located ahead of neural (or pseudoneural) spine of vertebrae 11 (1). Unbranched dorsal-fin ray mostly ossified as a spine, rigid part relatively long (three fourths or more of first dorsal fin total length).

Pectoral-fin rays I,8 (2), pectoral fin triangular with concave distal border. First pectoral-fin ray curved (Fig. 157), with proximal part rigid, forming a spine and short distal tip flexible and distinctly segmented. Pectoral-fin spine four to four and half times in SL. Anterior margin of pectoral-fin spine with small, smooth, straight to antrorse dentations along its basal half and serrae along distal half. Posterior margin of pectoral-fin spine bearing 14–18 retrorse dentations along its basal two thirds. These dentations are, despite conspicuous, relatively small and numerous. Also 1–2 distalmost unossified dentations, not counted.

Pelvic-fin rays i,5 (2), extended pelvic fin triangular with straight distal border. Pelvic-fin origin at vertical through dorsal-fin terminus. Pelvic fin adpressed terminus between verticals through adipose fin origin or a point slightly posterior. First unbranched and flexible ray distinctly shorter than second and third rays, which are subequal; remaining rays progressively shorter.

Anal-fin rays iv,8 (1), or v,9* (1); distal border of extended anal fin convex. One to three anteriormost anal-fin rays vestigial, unsegmented, embedded in thick skin fold. Anal-fin origin between verticals through first fourth or third of adipose-fin base; anal-fin adpressed terminus slightly anterior or at vertical through adipose-fin terminus. Tip of anteriormost anal-fin pterygiophore inserted posterior to hemal spine of vertebrae 20 (1). Tip of posteriormost anal-fin pterygiophore inserted ahead of hemal spine of vertebrae 28 (1).

Adipose fin roughly three and half times in SL, forming ascending elevated curve in lateral profile, with deepest point approximately midlength. Adipose fin emerging gradually, its posterior limit as a rounded, free lobe. Adipose-fin origin at vertical through vertebral centrum 20 (1); adipose-fin terminus at vertical through vertebral centrum 33 (1).

Caudal fin deeply forked, ventral lobe slightly longer. Caudal peduncle length posterior to adipose fin a third or less longer than its depth. Dorsal lobe with 7 (2), 1 unbranched principal (2) and 16 (1) procurrent fin-rays. Ventral lobe with 8 (2), 1 unbranched principal (2) and 16 (1) procurrent fin-rays. Hypural 5 completely free, not fused to hypural 3+4. Median caudal-fin rays not articulated directly to caudal plate. Seven (1) rays articulated to dorsal caudal-fin plate (5 on hypurals 3+4 and 2 on hypural 5) and 8 (1) rays articulated to ventral caudal-fin plate (6 on hypurals 1+2 and 2 on parahypural).

Total vertebrae 41 (1). Ribs 8 (1)

Epiphyseal branch of laterosensory canal on head (S6) with contralateral canals emerging as two separated pores. Openings of laterosensory canal at dentary and hyomandibula large and conspicuous.

Coloration in alcohol

Background body coloration yellowish. Ventral region of head and body lighter. Dark brown midlateral stripe wide (Fig. 158), not well delimited, extending from snout to caudal-fin origin. Paired dorsal brown stripes along supraoccipital process until half dorsal-fin base. Dorsal fin with a brown stripe near its base, followed by a hyaline stripe, and distal half brown. Cephalic brown pigment along posterior fontanel region.

Geographic distribution

Pimelodella mucosa was described from Rio Paraguay basin, in Bahia Negra, Paraguay. It is known from region 343 (Paraguay), in Paraguay, Brazil and Argentina (see comments).

Comments

Eigenmann (1917) refers to a *P. mucosa* material from Mamoré River, which is included here a priori, despite the disjunctive suspicious distribution for this species. Chernoff *et al.* (2000: 282) also refer to this species in Bolivian Amazon. I observed several materials from Madeira-Mamoré-Madre de Dios and Bolivian Amazon basin, and found nothing alike *P. mucosa* in those basins. However, *P. serrata*, a species that occurs in those locations, has a deep body and enlarged cephalic laterosensory canals, especially on dentary, alike *P. mucosa*.

Material examined

Pimelodella mucosa. — CAS 63720, 1, xr, 97.4 mm SL, holotype, Paraguay, Rio Paraguay; Bahia Negra on west bank, 20°13'47"S, 58°09'54"W; MZUSP 25091, 2, 85.7–95.9 mm SL, Brazil, Mato Grosso, Corumba, fifth bridge after Rio Miranda (south), 19°41'0.0"S, 56°58'0.0"W.

***Pimelodella nigrofasciata* (Perugia, 1897)**

Pimelodus nigrofasciatus Perugia, 1897: 18–19 [original description; “Rio Beni. Missioni Mosenetes”]; holotype: MSGN 8039 (lost)].

Pimelodella nigrofasciata — Burgess, 1989: 281 [taxonomic treatment, uncertain status in *Pimelodella*]. — Bockmann & Guazzelli, 2003: 420 [taxonomic treatment]. — Ferraris, 2007: 193 [taxonomic treatment]. — Bockmann & Slobodian, 2013: 16, 65 [taxonomic treatment].

Comments

The type of *Pimelodella nigrofasciata* is lost, probably since the flood in the Museo Civico di Storia Naturale “Giacomo Doria” (Giuliano Doria, pers. comm.). In Perugia (1897) description we can surely assess the information this species is a *Pimelodella*, due to the supraoccipital process reaching the anterior prenuchal plate, and long posterior fontanel. However, other information provided in the original description does not permit a better assessment of this species taxonomic identity, since does not inform any characteristics that could be related to comparative material collected in th region. Is possible this species is a synonym of other species that occur in the Beni River (e.g. *Pimelodella boliviana*, *P. hasemani*, *P. howesi*, *P. serrata*), but unfortunately I could not better define its status.

***Pimelodella notomelas* Eigenmann, 1917**

Pimelodella notomelas Eigenmann, 1917: 244, pl. XXX, fig. 3, pl. XXXV, fig. 41 [original description; “San Luiz de Caceres”, Brazil; holotype FMNH 57967 (formerly CM 6955)]. — Henn, 1928: 77 [type catalog]. — Gosline, 1945: 44 [taxonomic treatment]. — Fowler, 1951: 547, fig. 562 [taxonomic treatment]. — Ibarra & Stewart, 1987: 66 [type catalog]. — Burgess, 1989: 281 [taxonomic treatment]. — Britski *et al.*, 1999: 99 [taxonomic treatment]. — Bockmann & Guazzelli, 2003: 420 [taxonomic treatment]. — Ferraris, 2007: 193 [taxonomic treatment].

Diagnosis

Pimelodella notomelas can be distinguished from all *Pimelodella* species except *P. buckleyi*, *P. grisea*, *P. geryi*, *P. leptosoma* and *P. metae*, by the presence of dorsal fin distal third extremely dark brown to black. It differs from *P. leptosoma* and *P. metae* by having the supraoccipital process reaching the anterior prenuchal plate (vs. supraoccipital process not reaching the anterior prenuchal plate in *P. leptosoma* and *P. metae*). It differs from *P. buckleyi*, *P. grisea* and *P. geryi* by having the maxillary barbell always surpassing caudal-fin origin (vs. reaching between origin and half of anal-fin base in *P. buckleyi*; reaching between

half adpressed pelvic and anal fin terminus in *P. grisea*; reaching between half adipose-fin base and caudal-fin origin in *P. geryi*). Furthermore, *P. notomelas* can be diagnosed by maxillary barbell always surpassing caudal-fin origin; posterior margin of pectoral-fin spine with 4–6 notably triangular, short and straight dentations along its basal two thirds; adipose fin short, three to three and half times in SL; 40 total vertebrae; light brown midlateral stripe narrow, not well delimited, posterior to pseudotympanum until caudal-fin origin; head dorsally darker; dorsal fin with a medium brown stripe near base, followed by a hyaline stripe, and distal half dark brown to black.

Description

Measurements in Table 52. Body of moderated depth, depth at dorsal-fin origin five and half to six times in standard length; and compressed, body width at dorsal-fin origin roughly eight times in SL (Fig 159). Dorsal profile convex from snout to dorsal fin, slightly concave from dorsal to adipose fin, slightly convex along adipose extension, and concave along the caudal peduncle. Ventral profile of body slightly convex from snout to branchiostegal membrane, convex from this point to pelvic fin, and concave from pelvic along the caudal peduncle.

Pseudotympanum large, oval, dorsal to posterior process of cleithrum and reaching the straight line of 6th (2) vertebrae. Posterior process of cleithrum triangular, dorsal border straight. Anus and urogenital papilla adjacent. Urogenital papilla tubular, triangular, short. Anus between verticals through first fourth and third of adpressed pelvic fin; urogenital papilla between verticals through half and last third of adpressed pelvic fin.

Head moderate depressed, depth at supraoccipital-process base roughly two times in head length. Mouth sub terminal. Eye slightly elliptical, four to five times in head. Bony interorbital distance smaller than eye diameter. Barbels thin, slightly depressed and elliptical in cross-section. Maxillary barbels always surpassing caudal-fin origin. Outer mental barbel, when stretched parallel to main body axis, finishing at adpressed pectoral fin or slightly anterior to that. Inner mental barbel, when stretched parallel to main body axis, finishing between half and pectoral fin terminus. Supraoccipital process roughly triangular, narrow. Dorsal lamina of Weber complex vertebrae of medium height, reaching the supraoccipital process just at its anteriormost part. Branchiostegal rays 6 (2).

Dorsal fin triangular, distal margin convex, of moderated length (second dorsal-fin ray four and half to six times in SL), reaching the vertical through adpressed pelvic fin or a point slightly anterior to that. Dorsal fin with I,6 (9) plus anteriormost spinelet. Distance between terminus of dorsal-fin base and adipose-fin origin roughly the same or slightly smaller than

dorsal fin base. Anteriormost dorsal-fin pterygiophore inserted posterior to neural spine of vertebrae 4 (2); posteriormost dorsal-fin pterygiophore located ahead of neural (or pseudoneural) spine of vertebrae 11 (2). Unbranched dorsal-fin ray mostly ossified as a spine, rigid part three fourths or more of first dorsal-fin ray total length.

Pectoral-fin rays I,7* (6)– I,9 (3), pectoral fin triangular with concave distal border. First pectoral-fin ray roughly straight, with proximal part rigid, forming a spine (Fig. 160), and short distal tip flexible and distinctly segmented. Pectoral-fin spine four and half to five times in SL. Anterior margin of pectoral-fin spine with small, straight dentations along all margin, except distal third, which has serrae. Posterior margin of pectoral-fin spine with 4–6 notably triangular, short and straight dentations along its basal two thirds. Sometimes 1–2 unossified distalmost dentations, not counted.

Pelvic-fin rays i,5 (9), extended pelvic fin triangular with convex distal border. Pelvic-fin origin at vertical through half adpressed dorsal fin. Tip of adpressed pelvic fin at vertical through a point slightly posterior to adipose fin origin. First unbranched and flexible ray distinctly shorter than second and third rays, which are subequal; remaining rays progressively shorter.

Anal-fin rays iv,7 (1); v,7* (4); or v,8 (1); distal border of extended anal fin convex. Two anteriormost anal-fin rays vestigial, unsegmented, embedded in thick skin fold. Anal fin origin between verticals through first third and second fifth of adipose-fin base. Anal-fin adpressed terminus always posterior to vertical through adipose-fin terminus. Tip of anteriormost anal-fin pterygiophore inserted posterior to hemal spine of vertebrae 21 (2). Tip of posteriormost anal-fin pterygiophore inserted ahead of hemal spine of vertebrae 28 (2).

Adipose fin three to three and half times in SL, forming ascending elevated curve in lateral profile, with deepest point approximately midlength. Adipose fin emerging gradually, its posterior limit as a rounded, free lobe. Adipose-fin origin at vertical through vertebral centrum 24 (2); adipose-fin terminus at vertical through vertebral centra 34* (1)– 35 (1).

Caudal fin deeply forked, lobes subequal. Caudal peduncle length posterior to adipose fin a fourth longer than its depth. Dorsal lobe with 7 (5) branched, 1 (5) unbranched principal and 11 (1)–14* (1) procurrent fin-rays. Ventral lobe with 8 (5) branched, 1 (5) unbranched principal and 9* (1)– 11 (1) procurrent fin-rays. Hypural 5 completely free, not fused to hypurals 3+4. Median caudal-fin rays not attached directly to caudal plate. Seven (2) rays articulated to dorsal caudal-fin plate (5 on hypurals 3+4 and 2 on hypural 5) and 8 (2) rays articulated to ventral caudal-fin plate (6 on hypurals 1+2 and 2 on parahypural).

Total vertebrae 40 (2). Ribs 8 (2).

Ephiphyseal branch of laterosensory canal on head (S6) emerging as two pores, far apart from each other.

Coloration in alcohol

Background body coloration yellowish. Ventral region of head and body lighter. Light brown midlateral stripe narrow (Fig. 161), not well delimited, posterior to pseudotympanum until caudal-fin origin. Head dorsally darker. Paired dark stripe along supraoccipital process. Dark brown region between dorsal and adipose fins. Dorsal fin with a medium brown stripe near base, followed by a hyaline stripe, and distal half dark brown to black.

Geographic distribution

Pimelodella notomelas was described from Cáceres, Mato Grosso State, Brazil. It is known from region 343 (Paraguay), in Upper Paraguay basin in Brazil.

Material examined

Pimelodella notomelas. — FMNH 57967, 1, xr, 38.9 mm SL, holotype, Brazil, Mato Grosso, Cáceres (“San Luiz de Caceres. Old cut-off of Rio Paraguay and Rio Paraguay”), 16°04'01"S, 57°41'44"W; FMNH 57968, 5, 27.6–39.5 mm SL, paratypes Brazil, Mato Grosso, Cáceres (“San Luiz de Caceres. Old cut-off of Rio Paraguay and Rio Paraguay”), 16°04'01"S, 57°41'44"W; FMNH 57983, 2, xr, 42.0–42.3 mm SL, paratypes, Brazil, Mato Grosso, Campo Alegre, Rio Jauru (“Campos Alegre, Rio Jauru, into Rio Paraguay. Twenty-eight miles above mouth of Rio Jauru and about thirty southwest of São Luiz de Careers”), 16°12'53"S, 57°57'51"W; MZUSP 45875, 1, 30.1 mm SL, Uruguay, Depto. Soriano, Villa Soriano, Rio Negro, 33°22'58.8"S, 58°19'13.3"W.

***Pimelodella odynea* Schultz, 1944**

Pimelodella chagresi odynea Schultz, 1944: 213–214, pl. 2, fig. A [original description; “Rio San Juan at the bridge south of Mene Grande, Motatán system, Maracaibo basin]. — Gosline, 1945: 46 [taxonomic treatment]. — Burgess, 1989: 280 [taxonomic treatment]. — Ferraris & Vari, 1992: 35 [type catalog]. — Provenzano *et al.*, 1998: 22 [type catalog].

Pimelodella odynea. — Bockmann & Guazzelli, 2003: 420 [taxonomic treatment]. — Lasso *et al.*, 2004: 171 [taxonomic treatment]. — Leiva, 2005: 48 [taxonomic review of trans-Andean *Pimelodella*]. — Ferraris, 2007: 193 [taxonomic treatment]. — Ardila Rodriguez, 2017: 5–7 [taxonomic treatment, comparison with *P. floridablancaensis*].

Pimelodella doyneia. — Ardila Rodriguez, 2017: 7 [taxonomic treatment, comparison with *P. floridablancaensis*, misspelling].

Diagnosis

Pimelodella odynea differs from all *Pimelodella* species, with exception of *P. avanhandavae*, *P. chagresi*, *P. eutaenia*, *P. gracilis*, *P. griffini*, *P. montana*, *P. peruana*, *P. reyesi* and *P. roccae* by having a dorsolateral brown stripe along body. It differs from *P. chagresi* and *P. gracilis* and by having 41–43 total vertebrae (vs. 39–41 total vertebrae in *P. chagresi*; 46 total vertebrae in *P. gracilis*). It differs from by having the dorsal fin completely pigmented, without a hyaline stripe (vs. dorsal fin having a hyaline stripe in *P. avanhandavae*, *P. eutaenia*, *P. griffini*, *P. montana* and *P. roccae*; dorsal fin completely hyaline in *P. peruana* and *P. reyesi*). Furthermore, *P. odynea* can be diagnosed by maxillary barbel reaching between verticals through anal fin terminus and caudal fin origin; posterior margin of pectoral-fin spine bearing 7–12 retrorse, moderate to large dentations along basal two thirds; adipose fin almost three to three and half times in SL; dorsal caudal fin lobe usually distinctly longer; dark brown midlateral stripe wide, well delimited, extending from snout to distal portion of median caudal fin rays; paired dark brown dorsal stripe, not well delimited, along supraoccipital process to approximately the first third to terminus of adipose-fin base, getting lighter and weaker posteriorly; dorsal fin brown, with no hyaline stripe.

Description

Measurements in Table 53. Body of moderated depth, depth at dorsal-fin origin four and half to seven times in standard length, and moderated compressed, body width at dorsal-fin origin five and half to eight times in SL (Fig. 162). Greatest body depth at dorsal-fin origin. Dorsal profile convex from snout to dorsal-fin origin, concave from dorsal to adipose fin, slightly convex along adipose fin, and concave at the caudal peduncle. Ventral profile of body slightly convex from snout to branchiostegal membrane, concave between pectoral end pelvic fins, convex from pelvic to anal fin, and concave from this point along the caudal peduncle.

Pseudotympanum large, oval, above posterior process of cleithrum and reaching 7th (2) vertebrae. Posterior process of cleithrum triangular, narrow, its dorsal border slightly concave. Anus and urogenital papilla adjacent. Urogenital papilla tubular, triangular, shorter in part of specimens (possibly females), and longer in other. Anus between verticals through first third and half adpressed pelvic fin; urogenital papilla reaching between verticals through last fourth of adpressed pelvic fin and adipose-fin origin.

Head moderated depressed, depth at supraoccipital-process base slightly less to slightly more than two times in head length. Mouth sub terminal. Eye slightly elliptical, five to six and half times in head. Bony interorbital distance a slightly smaller than eye diameter.

Barbels thin, slightly depressed and elliptical in cross-section. Maxillary barbel reaching between verticals through anal fin terminus and caudal fin origin. Outer mental barbel, when stretched parallel to main body axis, finishing between half adpressed pectoral fin and midway between dorsal fin terminus and adipose fin origin. Inner mental barbel, when stretched parallel to main body axis, finishing between origin and terminus of pectoral fin. Supraoccipital process subrectangular, distal third slightly tapered. Dorsal lamina of Weberian complex vertebrae reaching the supraoccipital process until its midlength or entire extension. Branchiostegal rays 6 (11).

Dorsal fin triangular, distal margin concave, of moderate length (second branched dorsal-fin ray four to five and half times in SL), depressed tip almost reaching adipose fin origin. Dorsal fin with I,6 (40) plus anteriormost spinelet. Distance between terminus of dorsal-fin base and adipose-fin origin slightly smaller than dorsal-fin base. Anteriormost dorsal-fin pterygiophore inserted posterior to neural spine of vertebrae 4 (36); posteriormost dorsal-fin pterygiophore located ahead of neural (or pseudoneural) spine of vertebrae 11 (11) or 12* (25). Unbranched dorsal-fin ray mostly ossified as a spine, rigid part relatively short (two thirds of first dorsal-fin total length), distal third on anterior side with smooth serrae.

Pectoral-fin rays I,7 (1)–I,10 (1), usually I,9 (16) (holotype I,8), pectoral fin triangular with concave distal border. First pectoral-fin ray roughly straight to slightly curved, with proximal part rigid, forming a spine (Fig. 163), and short distal tip flexible and distinctly segmented. Pectoral-fin spine five to eight times in SL. Anterior margin of pectoral-fin spine with small, straight dentations along its basal half and serrae along distal half. Posterior margin of pectoral-fin spine bearing 7–12 retrorse dentations along basal two thirds. These dentations are notably retrorse, however, in smaller specimens (less than 50 mm SL) they are comparatively larger, with broader bases, meanwhile in larger specimens they are comparatively smaller, and with narrower bases. Also 1–2 unossified distal dentations, not counted.

Pelvic-fin rays i,5 (24), extended pelvic fin triangular with straight distal border. Anterior portion of pelvic-fin base between verticals through dorsal fin terminus and half dorsal fin adpressed. Tip of adpressed pelvic fin between verticals through adipose fin origin and its first tenth. First unbranched and flexible ray distinctly shorter than second and third rays, third ray the longest; remaining rays progressively shorter.

Anal-fin rays iii,7 (1); iv,7 (6); v,7 (4); vi,7 (2); iv,8 (4); v,8* (11); vi,8 (1); iv,9 (1); v,9 (2); vi,9 (1); or v,10 (2); distal border of extended anal fin convex. Two to four anteriormost anal-fin rays vestigial, unsegmented, embedded in thick skin fold. Anal fin

origin between verticals through first fourth or third of adipose fin base; anal-fin adressed terminus slightly anterior to or at vertical through adipose-fin terminus. Tip of anteriormost anal-fin pterygiophore inserted posterior to hemal spine of vertebrae 21 (10), 22* (22) or 23 (6). Tip of posteriormost anal-fin pterygiophore inserted ahead of hemal spine of vertebrae 28 (9), 29* (15), 30 (11) or 31 (1).

Adipose fin almost three to three and half times in SL, forming ascending elevated curve in lateral profile, with deepest point approximately at midlength. Adipose fin emerging gradually, its posterior limit as a rounded, free lobe. Adipose-fin origin at vertical through vertebral centra 19 (2)– 23 (1), usually 21 (16) (holotype 20); adipose-fin terminus at vertical through vertebral centra 35 (4)– 38 (1), usually 36* (23).

Caudal fin deeply forked, dorsal lobe usually distinctly longer, especially in specimens with more than 50 mm SL. Caudal peduncle length posterior to adipose-fin slightly longer than its depth. Dorsal lobe with 7* (35), rarely 6 (4) branched, 1 (39) unbranched principal, and 9 (1)–19 (2) (holotype 17) procurrent fin-rays. Ventral lobe with 8* (33), rarely 7 (4) or 9 (2) branched, 1 (39) unbranched principal, and 7 (1)–20 (2) (holotype 18) procurrent fin-rays. Seven* (32), rarely 6 (2) rays articulated to dorsal caudal-fin plate (4 or 5 on hypurals 3+4 and 2 on hypural 5) and 8* (28), rarely 7 (2) or 9 (3) rays articulated to ventral caudal-fin plate (5, 6 or 7 on hypurals 1+2 and 2 on parhypural).

Total vertebrae 41* (19)– 43 (2). Ribs 8 (5)– 10 (6), usually 9* (17).

Epiphyseal branch of laterosensory canal on head (S6) connecting both contralateral canals at midline, following as a single canal posteriorly and opening in a single pore. Smaller specimens might have the contralateral canals not connecting, opening in two pores nearby.

Coloration in alcohol

Background body coloration yellowish. Ventral region of head and body lighter. Dark brown midlateral stripe wide (Fig. 164), well delimited, extending from snout to distal portion of median caudal fin rays. Paired dark brown dorsal stripe, not well delimited, along supraoccipital process to approximately the first third to terminus of adipose-fin base, getting lighter and weaker posteriorly. Dorsal fin brown, with no hyaline stripe. Cephalic brown pigment along posterior fontanel region.

Geographic distribution

Pimelodella odynea was described from Rio Motatán, Maracaibo system. It is known from area 303 (Maracaibo), in Venezuela.

Comments

Among *Pimelodella odynea* type series, there were three specimens of *Imparfinis* sp. (two in USNM 121113 and one in USNM 121134).

Material examined

Pimelodella odynea. — USNM 121133, 1, xr, 88.3 mm SL, holotype, Venezuela, Rio San Juan Above Bridge South of Mene Grande, 9°48'34"N, 70°55'48"W; USNM 82618, 1, xr, paratype, Venezuela, Sierra de Perija, 9°23'28"N, 72°59'30"W; USNM 101610, 1, xr, paratype, Colômbia, Rio Pamplonita, Near Cucuta, Santander Del Norte, 7°49'53"N, 72°31'16"W; USNM 121134, 47, xr, 44.7–81.5, paratypes, Venezuela, Rio Motatan At Bridge 22 km, North of Motatan, Maracaibo Basin, 9°34'40"N, 70°34'48"W; USNM 121135, 2, xr, 52.2–60.8 mm SL, paratypes, Venezuela, Rio Apon About 35 km So. of Rosario Maracaibo Basin, 10°04'20"N, 72°31'34"W; USNM 121136, 103, xr, 23.4–78.8 mm SL; paratypes, Venezuela, Rio Motatan 8 km. Below Motatan, 9°19'04"N, 70°35'46"W; USNM 121137, 3, xr, 68.7–75.5 mm SL, paratypes, Venezuela, Rio San Pedro At Bridge S. of Mene Grande, Motatan System, Maracaibo Basin, 9°48'34"N, 70°55'48"W; USNM 121138, 3, xr, 49.3–80.1 mm SL, paratypes, Venezuela, Rio Machango at Bridge So. of Lagunillas, Maracaibo Basin, 8°28'31"N, 71°23'19"W; USNM 121139, 1, xr, 74.0 mm SL, paratype, Venezuela, Rio Tachira, 7 km. N. of San Antonio, Catatumbo System, Maracaibo Basin, 7°52'37"N, 72°27'08"W; USNM 121140, 86, xr, 25.4–85.67 mm SL, paratypes, Venezuela, Rio Motatan 4 km. Above Motatan, Maracaibo Basin, 9°25'19"N, 70°34'59"W; USNM 121141, 24, xr, 53.1–82.3 mm SL, paratypes, Venezuela, Rio San Juan at Bridge Trib of Rio Motatan, Maracaibo Basin, 9°39'41"N, 70°31'32"W; USNM 121142, 18, xr, 31.4–89.4 mm SL, paratypes, Venezuela, Zulia, Rio Socuy 3 km. Above Mouth; Maracaibo Basin, 10°43'39"N, 72°28'48"W; USNM 121143, 8, xr, paratypes, Venezuela, Rio Jimelles 12 km E. of Motatan, Trib. Of Rio Motatan, Maracaibo basin, 9°24'45"N, 70°29'25"W; USNM 121144, 2, xr, 66.4–77.1 mm SL, paratypes, Venezuela, Rio Machango 20km above bridge, south of Lagunillas, Maracaibo Basin, 8°28'31"N, 71°23'19"W; USNM 121213, 17, xr, 39.4–68.1 mm SL, paratypes, Venezuela, Rio Negro Below Mouth of Rio Yasa, Maracaibo Basin, 9°45'N, 72°25'W; USNM 121252, 1, xr, 99.6 mm SL, paratype, Colômbia, Cucuto, 8°06'44"N, 72°24'59"W.

***Pimelodella pectinifera* Eigenmann & Eigenmann, 1888**

Pimelodella pectinifer Eigenmann & Eigenmann, 1888: 132–133 [original description; “Campos”, Rio Paraíba do Sul basin, Rio de Janeiro State, Brazil; holotype: MCZ 7508]. — Eigenmann & Eigenmann, 1890: 154–155 [taxonomic revision]. —

Eigenmann & Eigenmann, 1891: 29 [taxonomic treatment]. — Eigenmann, 1910: 389 [taxonomic treatment]. — Bockmann & Guazzelli, 2003: 420 [taxonomic treatment]. — Ferraris, 2007: 194 [taxonomic treatment].

Rhamdia pectinifer. — Miranda Ribeiro, 1911: 270 [taxonomic treatment].

Pimelodella pectinifera. — Eigenmann, 1917: 241, pl. XXXV, fig. 26 [taxonomic revision]. — Gosline, 1945: 44 [taxonomic treatment]. — Fowler, 1951: 548 [taxonomic treatment]. — Burgess, 1989: 281 [taxonomic treatment]. — Guazzelli, 1997: 89 [taxonomic review of *Pimelodella* from Southeastern Brazil; junior-synonym of *P. lateristriga*].

Diagnosis

Pimelodella pectinifera can be distinguished from all *Pimelodella* with exception of *P. cruxenti*, *P. laticeps*, *P. montana*, *P. modesta* and *P. yuncensis* by having an overall dark brown body. It differs from *P. cruxenti* and *P. montana* by the maxillary barbel reaching second third of adpressed pelvic fin (*vs.* maxillary barbel surpassing caudal-fin origin in *P. cruxenti*; reaching between anal-fin origin and terminus in *P. montana*). It differs from *P. laticeps* and *P. yuncensis* by having a complete hyaline dorsal fin (*vs.* dorsal fin with pigmentation in *P. laticeps* and *P. yuncensis*). Furthermore, *P. pectinifera* can be diagnosed by maxillary barbel reaching second third of adpressed pelvic fin; dorsal fin spine bearing serrae at anterior margin distal two fifths; posterior margin of pectoral-fin spine bearing 21–22 dentations along almost entire margin, these dentations are usually curved, retrorse, with narrow bases, but distalmost are straighter, with broader bases; adipose fin short, four times in SL; caudal fin dorsal lobe notably longer; 42 total vertebrae; uniform brownish coloration.

Description

Measurements in Table 54. Body of moderated depth, depth at dorsal-fin origin five times in standard length, and moderated compressed, almost seven times in SL (Fig. 165). Dorsal profile convex from snout to supraoccipital process, concave from dorsal fin to adipose, slightly convex along adipose fin, and concave along caudal peduncle. Ventral profile of body slightly convex from snout to branquiostegal membrane, convex between pectoral and pelvic fins, slightly concave from pelvic to anal fin, and concave from this point along caudal peduncle.

Pseudotympanum large, oval, dorsal to posterior process of cleithrum and reaching 7th (1) vertebrae. Posterior process of cleithrum triangular, long, its dorsal border concave. Anus and urogenital papilla adjacent. Urogenital papilla tubular, triangular, short. Anus at vertical

through first third of adpressed pelvic fin; urogenital papilla at vertical through second third of adpressed pelvic fin.

Head deep, depth at supraoccipital process less than than two times in head length. Mouth sub terminal. Eyes slightly elliptical, slightly more than five times in head. Bony interorbital distance slightly smaller than eye diameter. Barbels thin, slightly depressed and elliptical in cross-section. Maxillary barbel reaching second third of adpressed pelvic fin. Outer mental barbel, when stretched parallel to main body axis, finishing at vertical through third fifth of adpressed pectoral fin. Inner mental barbel, when stretched parallel to main body axis, finishing at pectoral fin origin. Supraoccipital process subrectangular, narrow, tapered at its distal point. Dorsal lamina of Weberian complex vertebrae reaching the supraoccipital process just at its anteriormost part. Branchiostegal rays 6 (1).

Dorsal fin triangular, distal margin concave, of moderated length (second branched dorsal-fin ray five times in SL), depressed tip reaching the vertical through second third of adpressed pelvic fin. Dorsal fin with I,6 (1) plus anteriormost spinelet. Distance between terminus of dorsal-fin base and adipose-fin origin slightly smaller than dorsal fin base. Anteriormost dorsal-fin pterygiophore inserted posterior to neural spine of vertebrae 4 (1); posteriormost dorsal-fin pterygiophore located ahead of neural (or pseudoneural) spine of vertebrae 11 (1). Unbranched dorsal-fin ray mostly ossified as a spine, rigid part curved, bearing serrae at anterior margin distal two fifths.

Pectoral-fin rays I,9 (21), pectoral fin triangular with concave distal border. First pectoral-fin curved, with proximal part rigid, forming a spine (Fig. 166), and short distal tip flexible and distinctly segmented. Pectoral-fin spine five times in SL. Anterior margin of pectoral-fin spine with small dentations along basal two thirds, distalmost antrorse, and the remaining straight, and serrae at distal seventh. Posterior margin of pectoral-fin spine bearing 21–22 dentations along almost entire margin. These dentations are usually curved, retrorse, with narrow bases, but distalmost are straighter, with broader bases.

Pelvic-fin rays i,5 (1), extended pelvic fin triangular with convex distal border. Pelvic-fin origin slightly posterior to dorsal fin terminus. Tip of adpressed pelvic fin at vertical through adipose fin origin. First unbranched and flexible ray distinctly shorter than second and third rays, which are subequal; remaining rays progressively shorter.

Anal-fin rays vi,10 (1), distal border of extended anal fin convex. Two anteriormost anal-fin rays vestigial, unsegmented, embedded in thick skin fold. Anal-fin origin at vertical through first sixth of adipose-fin base. Anal-fin adpressed terminus at vertical through adipose fin terminus. Tip of anteriormost anal-fin pterygiophore inserted posterior to hemal spine of

vertebrae 21 (1). Tip of posteriormost anal-fin pterygiophore inserted ahead of hemal spine of vertebrae 28 (1).

Adipose fin four times in SL, forming ascending elevated curve in lateral profile, with deepest point approximately at midlength. Adipose fin emerging gradually, its posterior limit as a rounded, free lobe. Adipose-fin origin at vertical through vertebral centrum 22 (1); adipose-fin terminus at vertical through vertebral centrum 36 (1).

Caudal fin deeply forked, dorsal lobe notably longer. Caudal peduncle length posterior to adipose fin a third longer than its depth. Dorsal lobe with 7 (1) branched, 1 (1) unbranched principal and 19 (1) procurrent fin-rays. Ventral lobe with 8 (1) branched, 1 (1) unbranched principal and 19 (1) procurrent fin-rays. Hypural 5 separated from hypurals 3+4. Median caudal-fin rays not directly articulated to caudal plate. Seven (1) rays articulated to dorsal caudal-fin plate (5 on hypurals 3+4 and 2 on hypural 5) and 8 (1) rays articulated to ventral caudal-fin plate (6 on hypurals 1+2 and 2 on parahypural).

Total vertebrae 42 (1). Ribs 9 (1).

Contralateral epiphyseal branch of cephalic laterosensory canal (S6) unite in midline, and open in dorsal region of head as a single pore.

Coloration in alcohol

Known only from extremely unpigmented type. Original description reports uniform light brownish color (Fig. 167).

Geographic distribution

Pimelodella pectinifera was described from Campos, Rio Muriaé basin, Paraíba do Sul drainage. It is only known from its type material, and therefore, from region 329 (Paraíba do Sul).

Comments

Guazzelli (1997) suggested *P. pectinifera* would be a junior-synonym of *P. lateristriga* based on proportions and pectoral-fin spine morphology. Although the proportions are similar, the pectoral-fin spine is very different between those two species, as also the reported coloration pattern (*P. lateristriga* always presents a distinguishable dark midlateral stripe, meanwhile coloration of *P. pectinifera* is uniformly brown). Therefore, I maintain this species as valid despite no comparative material have been found in accordance with the description.

Furthermore, the species was described with specific epithet “pectinifer”, and treated in the literature sometimes with agreement in gender (“pectinifera”), sometimes not. Since

Eigenmann himself (1917) changed the epithet to agree in gender, and the ICZN does not oppose explicitly to this, here I propose the spelling “pectinifera” is to be preferred.

Material examined

Pimelodella pectinifera. — MCZ 7508, 1, xr, 150.9 mm SL, holotype, Brazil, Rio de Janeiro, Campos, Rio Muriaé (“at Campos, 3 mi. from town”), 21°45'S, 41°21'W.

***Pimelodella peruana* Eigenmann & Myers in Eigenmann & Allen, 1942**

Pimelodella peruana Eigenmann & Myers in Eigenmann & Allen, 1942: 101, pl. III, fig. 5 [original description; “Inahuaya, Rio Ucayali”, Peru; holotype: CAS 63721 (formerly IU 15868, number previously assigned to other species)]. — Gosline, 1945: 46 [taxonomic treatment]. — Fowler, 1951: 548 [taxonomic treatment]. — Ortega & Vari, 1986: 14 [taxonomic treatment]. — Burgess, 1989: 281 [taxonomic treatment]. — Bockmann & Guazzelli, 2003: 420 [taxonomic treatment]. — Ferraris, 2007: 194 [taxonomic treatment].

Diagnosis

Pimelodella peruana differs from all *Pimelodella* species, with exception of *P. avanhandavae*, *P. chagresi*, *P. eutaenia*, *P. gracilis*, *P. griffini*, *P. montana*, *P. odynea*, *P. reyesi* and *P. roccae* by having a dorsolateral brown stripe along body. It differs from all above mentioned by also having the ventral lobe of caudal fin heavily pigmented. Furthermore, *P. peruana* can be diagnosed by the maxillary barbel reaching between adipose fin origin and adpressed anal fin; dorsal lamina of Weberian complex vertebrae reaching the supraoccipital process at its anteriormost part or along its entire extension; dorsal-fin spine bearing smooth serrae at distal half of posterior margin; posterior margin of pectoral-fin spine bearing 10–16 large, retrorse dentations along its basal three fourths to almost entire margin, these dentations are triangular, inclined and with broad bases; adipose fin short, less than four to four and half times in SL; dark brown midlateral stripe narrow, well delimited, extending from snout to caudal-fin origin; paired dorsal dark brown stripes along supraoccipital process until adipose fin origin; lower caudal-fin lobe notably darker; region over pseudotympanum with dark brown melanophores, from region just dorsal to posterior process of cleithrum to midlateral stripe.

Description

Measurements in Table 55. Body depresses, depth at dorsal-fin origin six to seven and half times in standard length, and compressed, body width at dorsal-fin origin six and half to nine times in SL (Fig. 168). Dorsal profile convex from snout to dorsal fin, slightly concave

from dorsal to adipose fin, straight along adipose fin, and concave along the caudal peduncle. Ventral profile of body slightly convex from snout to branchiostegal membrane, convex between pectoral end pelvic fins, slightly concave from pelvic to anal fin, and straight from there along the caudal peduncle.

Pseudotympanum large, oval, dorsal to posterior process of cleithrum and reaching 6th (2) vertebrae. Posterior process of cleithrum triangular, its dorsal border slightly concave. Anus and urogenital papilla adjacent. Urogenital papilla tubular, triangular, short. Anus between verticals through first third and second fifth of adpressed pelvic fin; urogenital papilla between verticals through last third and last sixth of adpressed pelvic fin.

Head depressed, depth at supraoccipital process usually more than two times in head length. Mouth sub terminal. Eyes slightly elliptical, four to four and half times in head. Bony interorbital distance half eye diameter. Barbels thin, slightly depressed and elliptical in cross-section. Maxillary barbel reaching between adipose fin origin and adpressed anal fin. Outer mental barbel, when stretched parallel to main body axis, finishing between pectoral fin terminus and pelvic fin terminus. Inner mental barbel, when stretched parallel to main body axis, finishing between ventral limit of branchiostegal membrane and second third of adpressed pectoral fin. Supraoccipital process subrectangular, narrow, tapered at its distal point. Dorsal lamina of Weberian complex vertebrae reaching the supraoccipital process at its anteriormost part or along its entire extension. Branchiostegal rays 6 (2)– 7* (1).

Dorsal fin triangular, distal margin convex, short (second branched dorsal-fin ray almost five to five and half times in SL), depressed tip reaching between verticals through half and last third of adpressed pelvic fin. Dorsal fin with I,6 (4) plus anteriormost spinelet. Distance between terminus of dorsal-fin base and adipose-fin origin larger than dorsal fin base. Anteriormost dorsal-fin pterygiophore inserted posterior to neural spine of vertebrae 4 (4); posteriormost dorsal-fin pterygiophore located ahead of neural (or pseudoneural) spine of vertebrae 11* (1) or 12 (3). Unbranched dorsal-fin ray mostly ossified as a spine, rigid part relatively long (three fourths or more of dorsal-fin first ray total length), bearing smooth serrae at distal half of posterior margin.

Pectoral-fin rays I,7* (1)– I,8 (3), pectoral fin triangular with concave distal border. First pectoral-fin ray curved, with proximal part rigid, forming a spine (Fig. 169A), and short distal tip flexible and distinctly segmented. Pectoral-fin spine five and half to six and half times in SL. Anterior margin of pectoral-fin spine with smooth, straight dentations along its basal half and smooth serrae along distal half. Posterior margin of pectoral-fin spine bearing 10–16 large, retrorse dentations along its basal three fourths to almost entire margin. These

dentations are triangular, inclined and with broad bases. Also, 1–2 distalmost unossified dentations, not counted.

Pelvic-fin rays i,5 (4), extended pelvic fin triangular with straight distal border. Pelvic-fin origin between verticals through dorsal fin terminus and a point slightly posterior to that. Tip of adpressed pelvic fin at vertical through adipose fin origin. First unbranched and flexible ray distinctly shorter than second and third rays, which are subequal; remaining rays progressively shorter.

Anal-fin rays iv,8* (2); vi,8 (1) or v,9 (1); distal border of extended anal fin convex. Two or three anteriormost anal-fin rays vestigial, unsegmented, embedded in thick skin fold. Anal-fin origin between verticals through first tenth and first fourth of adipose fin base. Anal-fin adpressed terminus at vertical through adipose fin terminus. Tip of anteriormost anal-fin pterygiophore inserted posterior to hemal spine of vertebrae 22* (1) or 23 (3). Tip of posteriormost anal-fin pterygiophore inserted ahead of hemal spine of vertebrae 29* (1), 30 (1) or 31 (2).

Adipose fin less than four to four and half times in SL, forming ascending elevated curve in lateral profile, with deepest point approximately at midlength. Adipose fin emerging gradually, its posterior limit as a rounded, free lobe. Adipose-fin origin at vertical through vertebral centra 23 (2)– 24* (2); adipose-fin terminus at vertical through vertebral centra 33* (1)– 36 (2).

Caudal fin deeply forked, lobes subequal. Caudal peduncle length posterior to adipose fin almost twice its depth. Dorsal lobe with 7 (4) branched, 1 (4) unbranched principal and 14 (1) –20 (1) (holotype 16) procurrent fin-rays. Ventral lobe with 8 (4) branched, 1 (4) unbranched principal and 15* (2) –21 (1) procurrent fin-rays. Hypural 5 separated from hypurals 3+4. Median caudal-fin rays not directly articulated to caudal plate. Seven (4) rays articulated to dorsal caudal-fin plate (5 on hypurals 3+4 and 2 on hypural 5) and 8 (1) rays articulated to ventral caudal-fin plate (6 on hypurals 1+2 and 2 on parahypural).

Total vertebrae 42* (1)–43 (3). Ribs 8* (1)– 9 (3).

Contralateral epiphyseal branch of cephalic laterosensory canal (S6) unite in midline, following posteriorly as an unique canal, and open in dorsal region of head as a single pore.

Coloration in alcohol

Background body coloration yellowish. Ventral region of head and body lighter. Dark brown midlateral stripe narrow (Fig. 170), well delimited, extending from snout to caudal-fin origin. Paired dorsal dark brown stripes along supraoccipital process until adipose fin origin. Lower caudal-fin lobe notably darker. Region over pseudotympanum with dark brown

melanophores, from region just dorsal to posterior process of cleithrum to midlateral stripe. Cephalic brown pigment along posterior fontanel region.

Geographic distribution

Pimelodella peruana was described from Ucayali River, in Peru. It is known from regions 313 (Western Amazon Piedmont) and 317 (Ucayali- Urubamba piedmont), in Peru and Ecuador (see comments).

Comments

Material similar to *P. peruana* was found in Rio Napo basin, Ecuador. The slightly larger specimens (more than 60 mm SL) from this region have small differences in the pectoral-fin morphology (Fig. 169B), and slightly longer barbels, what can be due to larger size, or maybe belong to a different species. They were considered here as belonging to *P. peruana* a priori, and incorporated here as comparative material.

Material examined

Pimelodella peruana: CAS 63721, 1, xr, 40.3 mm SL, holotype, Peru, Rio Ucayali at Inahuaya, 7°07'09"S, 75°15'24"W; ANSP 149939, 1, 72.8 mm SL, Peru, Loreto, Vicinity Iquitos, left bank Rio Amazonas (Maranon) due S of Isla Iquitos, Sta, 3°42'32.0"S, 73°13'55.8"W; FMNH 94972, 6, 2 c&s, Ecuador, Rio Payamino, first beach on the left, 1km upstream from mouth of Napo (at bend in the river), 0°28'00.1"S, 76°59'53.9"W; FMNH 102541, 63, Ecuador, Rio Payamino, first beach on the left, 1km upstream from mouth of Napo (at bend in the river), 0°28'00.1"S, 76°59'53.9"W.

***Pimelodella reyesi* Dahl in Dahl & Medem, 1964**

Pimelodella reyesi Dahl in Dahl & Medem, 1964: 37–39, unnum. fig. [original description; “Rio Manso del Sinú”, Colombia; holotype: probably lost]. — Bockmann & Guazzelli, 2003: 421 [taxonomic treatment]. — Leiva, 2005: 52 [taxonomic review of trans-Andean *Pimelodella*]. — Ferraris, 2007: 194 [taxonomic treatment]. — Maldonado-Ocampo *et al.*, 2008: 202 [taxonomic list]. — Ardila Rodriguez, 2017: 7, fig. 4 [taxonomic treatment, comparison with *P. floridablancaensis*].

Pimelodella reyesis. — Ardila Rodriguez, 2017: table 1 [topotypes measurements, misspelling].

Dignosis

Pimelodella reyesi differs from all *Pimelodella* species, with exception of *P. avanhandavae*, *P. chagresi*, *P. eutaenia*, *P. gracilis*, *P. griffini*, *P. montana*, *P. odynea*, *P. peruana* and *P. roccae* by having a dorsolateral brown stripe along body. It differs from *P.*

avanhandavae, *P. chagresi*, *P. eutaenia*, *P. gracilis*, *P. griffini*, *P. montana*, *P. odynea* and *P. roccae* by having a completely hyaline dorsal fin (*vs.* dorsal fin pigmented in *P. avanhandavae*, *P. chagresi*, *P. eutaenia*, *P. gracilis*, *P. griffini*, *P. montana*, *P. odynea* and *P. roccae*). It differs from *P. peruana* by not having the ventral lobe of caudal fin heavily pigmented (*vs.* ventral lobe of caudal fin heavily pigmented in *P. peruana*) and adipose fin three and half times in SL (*vs.* adipose fin four times or more in SL in *P. peruana*). Furthermore, *P. reyesi* can be diagnosed by the maxillary barbel reaching anal fin origin; posterior margin of pectoral-fin spine bearing large, retrorse dentations along its basal two thirds; adipose fin three and half times in SL; dark brown midlateral stripe wide, well delimited, extending from snout until caudal-fin origin; paired dark brown dorsal stripe, not well delimited, from supraoccipital process to adipose fin terminus.

Description

Measurements in Table 56. Body moderate depressed, depth at dorsal-fin origin almost four and half times in standard length, and moderate compressed, body width at dorsal-fin origin five and half times in SL (Fig. 171). Dorsal profile convex from snout to dorsal fin, slightly concave from dorsal to adipose fin, slightly convex along adipose fin, and concave along the caudal peduncle. Ventral profile of body slightly convex from snout to branchiostegal membrane, convex between pectoral end pelvic fins, slightly concave from pelvic to anal fin, and also concave from there along the caudal peduncle. Posterior process of cleithrum triangular, broad, its dorsal border roughly straight.

Head depressed, depth at supraoccipital-process base less than half head length. Mouth sub terminal. Eye slightly elliptical, five and half to six times in head length. Bony interorbital distance equal to or slightly larger than eye diameter. Barbels thin, slightly depressed and elliptical in cross-section. Maxillary barbel reaching anal fin origin. Outer mental barbel, when stretched parallel to main body axis, reaching last fourth of adpressed pectoral fin. Inner mental barbel, when stretched parallel to main body axis, almost reaching half pectoral fin base.

Dorsal fin triangular, distal margin convex, moderated length (second branched dorsal-fin ray almost four times in SL), depressed tip finishing at vertical through last fourth of adpressed pelvic fin. Dorsal fin with I,6 (7) plus anteriormost spinelet. Distance between terminus of dorsal-fin base and adipose-fin origin slightly smaller than dorsal-fin base. Unbranched dorsal-fin ray with proximal part ossified as a spine, rigid part relatively long (three fourths or more of first dorsal fin total length).

Pectoral-fin rays I,7* (5)– I.8 (2), pectoral fin triangular with concave distal border. First pectoral fin ray roughly straight, with proximal part rigid, forming a spine (Fig. 172), and short distal tip flexible and distinctly segmented. Pectoral-fin spine five to six times in SL. Anterior margin of pectoral-fin spine with serrae along its distal half. Posterior margin of pectoral-fin spine bearing large, retrorse dentations along its basal two thirds.

Pelvic-fin rays i,5 (7), extended pelvic fin triangular with straight distal border. Pelvic-fin origin slightly posterior to a vertical through dorsal fin terminus. Pelvic fin adpressed terminus at vertical through first fourth of adipose fin base. First unbranched and flexible ray distinctly shorter than second and third rays, which are roughly the same size; remaining rays progressively shorter.

Anal-fin rays v,8* (7); or v,9 (1); distal border of extended anal fin convex. Two anteriormost anal-fin rays vestigial, unsegmented, embedded in thick skin fold. Anal-fin origin at vertical through first third of adipose fin base; anal fin adpressed terminus at vertical through adipose fin terminus.

Adipose fin three and half times in SL, forming ascending elevated curve in lateral profile, with deepest point approximately at midlength. Adipose fin emerging gradually, its posterior limit as a rounded, free lobe.

Caudal fin deeply forked, lobes subequal. Dorsal lobe with 7 (2) branched and 1 (2) unbranched principal rays. Ventral lobe with 8 (2) branched, 1 (2) unbranched principal rays.

Coloration in alcohol

Background body coloration yellowish. Ventral region of head and body lighter. Dark brown midlateral stripe wide (Fig. 173), well delimited, extending from snout until caudal-fin origin. Paired dark brown dorsal stripe, not well delimited, from supraoccipital process to adipose fin terminus. Cephalic dark brown pigment along posterior fontanel region.

Geographic distribution

Pimelodella reyesi was described from Rio Manso, affluent of Rio Sinu, Magdalena drainage. It is known from region 302 (Magdalena-Sinu).

Comments

Measurements for holotype were extracted from original description, since Dahl's types are probably lost (*e.g.* Cala, 1981). The examined material is from ICN-MHN collection, and according with original description and locality. Leiva (2005) reports 41–42 total vertebrae for *P. reyesi*, however, examination of more material related to this species is necessary, to properly assess its taxonomic identity and fully describe it.

Material examined

Pimelodella reyesi. — ICN-MHN 1331, 1, 98.1 mm SL, Colombia, Quibdó, Rio Atrato.

***Pimelodella robinsoni* (Fowler, 1941)**

Rhamdella robinsoni Fowler, 1941: 135, figs. 23–26 [original description; “São José do Egito, Pernambuco”, Brazil; holotype: 69386]. — Gosline, 1945: 35 [taxonomic treatment]. — Fowler, 1951: 567, fig. 574 [taxonomic treatment]. — Böhlke, 1984: 142 [type catalog]. — Burgess, 1989: 278 [taxonomic treatment]. — Bockmann & Guazzelli, 2003: 422 [taxonomic treatment]. — Rosa *et al.*, 2003: 177 [taxonomic list]. — Ferraris, 2007: 197 [taxonomic treatment]. — Bockmann & Miquelarena, 2008: 46–47 [taxonomic treatment, transfer to *Pimelodella*].

Rhamdella wolffi Fowler, 1941: 136–138, fig. 31–34 [taxonomic treatment]. — Gosline, 1945: 35 [taxonomic treatment]. — Fowler, 1951: 567, fig. 575 [taxonomic treatment]. — Böhlke, 1984: 142 [type catalog]. — Burgess, 1989: 278 [taxonomic treatment]. — Bockmann & Guazzelli, 2003: 422 [taxonomic treatment]. — Ferraris, 2007: 197 [taxonomic treatment]. — Bockmann & Miquelarena, 2008: 46–47 [taxonomic treatment, transfer to *Pimelodella*].

Rhamdia wolffi. — Burgess, 1989: 279 [taxonomic treatment; treatment under *Rhamdia* without any justification]. — Rosa *et al.*, 2003: 177 [taxonomic list].

Diagnosis

Pimelodella robinsoni differs from all *Pimelodella* species except *P. itapicuruiensis*, *P. leptosoma*, *P. longipinnis*, *P. megalura*, *P. metae*, *P. montana*, *P. reyesi*, *P. tapatapae* and *P. yuncensis* by having the supraoccipital process not reaching the anterior preopercular plate (unknown in *P. reyesi*). It differs from by having the maxillary barbel reaching between first third and terminus of anal fin (*vs.* maxillary barbel reaching caudal-fin origin in *P. tapatapae*; maxillary barbel reaching between half pectoral fin adpressed and terminus of adpressed pelvic in *P. yuncensis*). It differs from by the absence of dorsolateral dark coloration on body (*vs.* presence of a paired dorsolateral dark stripe on body in *P. itapicuruiensis*, *P. montana* and *P. reyesi*; dorsal region of body from supraoccipital process to adipose fin darker in *P. megalura*). It differs from *P. leptosoma*, *P. longipinnis* and *P. metae* by having the basal portion of dorsal fin hyaline, and distal two thirds dusky (*vs.* dorsal fin darker near base, followed by a hyaline stripe and distal third extremely dark in *P. leptosoma*; dorsal fin completely hyaline in *P. longipinnis*; dorsal fin medium brown near base, followed by an hyaline stripe, then a dark brown to black stripe, and distal portion of rays clear in *P. metae*).

Furthermore, *P. robinsoni* can be diagnosed by the maxillary barbel reaching between first third and terminus of anal fin; supraoccipital process not reaching the anterior prenuchal plate; posterior margin of pectoral-fin spine bearing 8–10 retrorse dentations along basal two thirds, these dentations are triangular, with broad bases; adipose fin two and half to slightly more than three times in SL; 41–43 total vertebrae; dark brown midlateral stripe of moderated width, not well delimited, from snout to caudal fin origin; distal two thirds of dorsal fin dusky.

Description

Measurements in Table 57. Body average depressed, depth at dorsal-fin origin five to six times in standard length, and moderate compressed, body width at dorsal-fin origin six to eight and half times in SL (Fig. 174). Dorsal profile convex from snout to dorsal fin, slightly concave from dorsal to adipose fin, slightly convex along adipose fin, and concave along the caudal peduncle. Ventral profile of body slightly convex from snout to branchiostegal membrane, convex between pectoral end pelvic fins, slightly concave from pelvic to anal fin, and also concave from there along the caudal peduncle. Posterior process of cleithrum triangular, broad, its dorsal border concave. Pseudotympanum large, reaching the vertical through 6th (1) to 8^{th*} (1) vertebrae.

Head deep, depth at supraoccipital-process base less than two times in head length. Mouth sub terminal. Eye slightly elliptical, four to five and half times in head. Bony interorbital distance slightly less than eye diameter. Barbels thin, and elliptical in cross-section. Maxillary barbel reaching between first third and terminus of anal fin. Outer mental barbel, when stretched parallel to main body axis, finishing between verticals through pectoral fin terminus and first third of adpressed pectoral fin. Inner mental barbels, when stretched parallel to main body axis, finishing between verticals through branchiostegal membrane ventral limit and pectoral fin origin. Supraoccipital process roughly triangular, narrow, almost reaching anterior prenuchal plate. Dorsal lamina of Weber complex vertebrae of moderated height, reaching the supraoccipital process along just at its anteriormost region or part of its extension, but never along its entire length. Branchiostegal rays 6 (4).

Dorsal fin triangular, distal margin convex, short (second branched dorsal-fin ray five to slightly more than six times in SL), depressed tip finishing between verticals through second fifth and second third of adpressed pelvic fin. Dorsal fin with I,6 (8) plus anteriormost spinelet. Distance between terminus of dorsal-fin base and adipose-fin origin a third less than dorsal-fin base. Anteriormost dorsal-fin pterygiophore inserted posterior to neural spine of vertebrae 4 (4); posteriormost dorsal-fin pterygiophore located ahead of neural (or

pseudoneural) spine of vertebrae 11 (4). Unbranched dorsal-fin ray with proximal part ossified as a spine.

Pectoral-fin rays I,7* (1)– I,9 (2), pectoral fin triangular with convex distal border. First pectoral-fin ray with proximal part rigid, forming a roughly straight spine (Fig. 175), and short distal tip flexible and distinctly segmented. Pectoral-fin spine slightly more than six to seven and half times in SL. Anterior margin of pectoral-fin spine with smooth serrae along distal third. Posterior margin of pectoral-fin spine bearing 8–10 retrorse dentations along basal two thirds. These dentations are triangular, with broad bases.

Pelvic-fin rays i,5 (4). Pelvic-fin origin between verticals through fifth branched dorsal fin ray and dorsal fin terminus. Pelvic-fin adpressed terminus between verticals through first seventh and first fourth of adipose-fin base. First unbranched and flexible ray distinctly shorter than second and third rays, which are roughly the same size or third ray the longest; remaining rays progressively shorter.

Anal-fin rays v,7 (1); vi,7 (1); or v,8* (2); distal border of extended anal fin convex. Two or three anteriormost anal-fin rays vestigial, unsegmented, embedded in thick skin fold. Anal-fin origin at vertical through a point slightly anterior to adipose fin origin and first third of adipose-fin base; anal-fin adpressed terminus slightly anterior or at vertical through adipose-fin terminus. Tip of anteriormost anal-fin pterygiophore inserted posterior to hemal spine of vertebrae 20 (1), 21 (1) or 22* (2). Tip of posteriormost anal-fin pterygiophore inserted ahead of hemal spine of vertebrae 28 (2), 29 (1) or 30* (1).

Adipose fin two and half to slightly more than three times in SL, forming ascending elevated curve in lateral profile, with deepest point approximately at midlength. Adipose fin emerging gradually, its posterior limit as a rounded, free lobe. Adipose-fin origin at vertical through vertebral centra 19 (3)– 23* (1); adipose-fin terminus at vertical through vertebral centra 35 (2)– 38 (1) (holotype 36).

Caudal fin deeply forked, lobes subequal. Caudal peduncle length posterior to adipose fin slightly longer than its depth. Dorsal lobe with 7 (4) branched, 1 (4) unbranched principal and 16* (2)– 17 (2) procurrent fin-rays. Ventral lobe with 8 (4) branched, 1 (4) unbranched principal and 15 (1)–17* (3) procurrent fin-rays. Hypural 5 completely free, not fused to hypural 3+4. Median caudal-fin rays not articulated directly to caudal plate. Seven (4) rays articulated to dorsal caudal-fin plate (5 on hypurals 3+4 and 2 on hypural 5) and 7 (1), 8 (2) or 9 (1) rays articulated to ventral caudal-fin plate (5, 6 or 7 on hypurals 1+2 and 2 on parahypural).

Total vertebrae 41 (3)– 43* (1). Ribs 7* (1)– 10 (1).

Epiphyseal branch of laterosensory canal on head (S6) connecting contralateral branches in head midline, and opening in a single pore; or not connecting, and opening in two pores nearby.

Coloration in alcohol

Background body coloration yellowish. Ventral region of head and body lighter. Dark brown midlateral stripe of moderated width (Fig. 176), not well delimited, from snout to caudal fin origin. Distal two thirds of dorsal fin dusky.

Geographic distribution

Pimelodella robinsoni was described from São José do Egito, Pernambuco State, São Francisco River Basin. *Pimelodella robinsoni*, its junior-synonym, was described from Rio Choró, Ceará. Therefore, *P. robinsoni* is known from regions 326 (Northeastern Caatinga and Coastal drainages) and 327 (S. Francisco).

Comments

Both *Rhamdella robinsoni* and *R. wolfi* were transferred to *Pimelodella* by Bockmann & Miquelarena (2008), with the justification that information in original descriptions and associated illustrations (*e.g.* slender body, large eyes, well-developed supraoccipital process, long maxillary barbel, reaching anal-fin base, robust pectoral spine, dark stripe along lateral surface of the body, etc.) were congruent with *Pimelodella* genus.

Observing *P. wolfi* types (Fig. 177) I have no reason to believe they are distinguishable from *P. robinsoni*. The features traditionally used as diagnostic for *Pimelodella* species, like barbels and adipose-fin length, pectoral-fin morphology, and coloration pattern, are very similar between both (despite the pectoral-fin spine being partially broken in both species, characteristics could be inferred). Therefore, I hereby synonymize *P. wolfi* to *P. robinsoni*, described one page before the first. In anyway, Table 58 presents the measurements of both species, discriminated by original species name.

Material examined

Pimelodella robinsoni. — ANSP 69386, 1, xr, 73.0 mm SL, holotype, Brazil, Pernambuco, São Jose do Egito, 7°31'05"S, 37°14'56"W.

Pimelodella wolfi. — ANSP 69388, 1, xr, 88.9 mm SL, holotype, Brazil, Ceará, Rio Choro, 4°12'35"S, 38°14'59"W; ANSP 69389–91, 3, xr, 67.1–71,0 mm SL, paratype, Brazil, Ceará, Rio Choro, 4°12'35"S, 38°14'59"W.

***Pimelodella roccae* Eigenmann 1917**

P. gracilis [non Valenciennes, 1935]. — Pearson, 1924: 14 [taxonomic treatment].

Pimelodella roccae Eigenmann, 1917: 240, pl. XXXV, fig. 7 [Urubamba Valley, no type assigned]. — Pearson, 1924: 54 [distribution]. — Fowler, 1939: 287 [taxonomic list]. — Fowler, 1940: 94 [taxonomic list]. — Eigenmann *in* Eigenmann & Allen, 1942: 98–99, pl. X, fig. 4, 4a [detailed description; “Rio Comerciato, 1800 feet elevation, Middle Urubamba and Beni basin of Bolivia”; holotype MCZ 30975]. — Gosline, 1945: 43 [taxonomic treatment]. — Fowler, 1951: 549 [taxonomic treatment]. — Ortega & Vari, 1986: 15 [taxonomic list]. — Burgess, 1989: 281 [taxonomic treatment]. — Chernoff *et al.*, 2000: 282 [taxonomic list]. — Bockmann & Guazzelli, 2003: 420 [taxonomic treatment]. — Ferraris, 2007: 194 [taxonomic treatment].

Diagnosis

Pimelodella roccae differs from all *Pimelodella* species, with exception of *P. avanhandavae*, *P. chagresi*, *P. eutaenia*, *P. gracilis*, *P. griffini*, *P. montana*, *P. odynea*, *P. peruana* and *P. reyesi* by having a dorsolateral brown stripe along body. It differs from *P. peruana* and *P. reyesi* by having the dorsal fin pigmented (*vs.* dorsal fin hyaline in *P. peruana* and *P. reyesi*). It differs from *P. gracilis* by having 41–42 total vertebrae (*vs.* 46 total vertebrae in *P. gracilis*). It differs from *P. chagresi*, *P. eutaenia*, *P. griffini* and *P. odynea* by having dorsal fin with a dark brown stripe near its base, followed by a hyaline stripe, and distal third dark again (*vs.* dorsal fin completely pigmented in *P. chagresi* and *P. odynea*; dorsal fin with hyaline stripe near base, and distal part of rays pigmented in *P. eutaenia* and *P. griffini*). It differs from *P. avanhandavae* by having posterior margin of pectoral-fin spine bearing 16–20 retrorse, small, triangular dentations along basal three fourths (*vs.* posterior margin of pectoral-fin spine bearing 8–12 retrorse, large, curved, dentations along its basal two thirds in *P. avanhandavae*). It differs from *P. montana* by having the supraoccipital process reaching the anterior preopercular plate (*vs.* supraoccipital process not reaching the anterior preopercular plate in *P. montana*). Furthermore, *P. roccae* can be diagnosed by maxillary barbel reaching between verticals through first fourth of adpressed anal fin and caudal-fin origin; adipose fin two and half to almost three times in SL; dark brown midlateral stripe of moderate width, not well-delimited extending from snout to caudal-fin origin; paired dorsal brown stripe, not well delimited, from supraoccipital process until adipose fin terminus, getting lighter posteriorly.

Description

Measurements in Table 59. Body moderate depressed, depth at dorsal-fin insertion slightly more than seven times in standard length, and moderate compressed, body width at

dorsal-fin insertion six to seven and half times in SL (Fig. 178). Dorsal profile convex from snout to dorsal fin, concave from dorsal to adipose fin, convex along adipose fin, and concave along the caudal peduncle. Ventral profile of body slightly convex from snout to branchiostegal membrane, convex between pectoral end pelvic fins, slightly concave from pelvic to anal fin, and concave from there along the caudal peduncle.

Pseudotympanum large, oval, above posterior process of cleithrum and reaching the straight line of 7th (2) vertebrae. Posterior process of cleithrum triangular, broad, its dorsal border straight to notably concave. Anus and urogenital papilla adjacent. Urogenital papilla tubular, triangular, short. Anus between verticals through first third to half adpressed pelvic fin; urogenital papilla between verticals through second third to last fourth of adpressed pelvic fin.

Head depth at supraoccipital-process base slightly less to slightly more than two times in head length. Mouth sub terminal. Eye slightly elliptical, five and half to six and half times in head. Bony interorbital distance slightly more than eye diameter. Barbels thin, slightly depressed and elliptical in cross-section. Maxillary barbel reaching between verticals through first fourth of adpressed anal fin and caudal-fin origin. Outer mental barbel, when stretched parallel to main body axis, finishing between last fourth and terminus of adpressed pectoral fin. Inner mental barbel, when stretched parallel to main body axis, finishing between half and terminus of pectoral fin. Supraoccipital process roughly triangular. Dorsal lamina of Weberian complex vertebrae reaching the supraoccipital process just at its anteriormost part.

Dorsal fin triangular, distal margin concave, average sized (second branched dorsal-fin ray five to five and half times in SL), depressed tip finishing between half and last sixth of adpressed pelvic fin. Dorsal fin with I,6 (1) plus anteriormost spinelet. Distance between terminus of dorsal-fin base and adipose-fin origin slightly shorter than dorsal-fin base. Anteriormost dorsal-fin pterygiophore inserted posterior to neural spine of vertebrae 4 (4); posteriormost dorsal-fin pterygiophore located ahead of neural (or pseudoneural) spine of vertebrae 11* (3) or 12 (1). Unbranched dorsal-fin ray mostly ossified as a spine, rigid part of moderate length (approximately two thirds of first dorsal-fin ray total length).

Pectoral-fin rays I,7 (1)– I,8* (3), pectoral fin triangular with concave distal border. First pectoral-fin ray curved, with proximal part rigid, forming a spine (Fig. 179), and short distal tip flexible and distinctly segmented. Pectoral-fin spine five and half to six and half times in SL. Anterior margin of pectoral-fin spine with small, straight dentations along basal two thirds, and serrae along distal third. Posterior margin of pectoral-fin spine bearing 16–20

retrorse dentations along basal three fourths. These dentations are relatively small, triangular, distalmost smoother. Also, 1–2 distalmost unossified dentations, not counted.

Pelvic-fin rays i,5 (4), extended pelvic fin triangular with straight distal border. Anterior portion of pelvic-fin base at vertical through dorsal fin terminus. Tip of adpressed pelvic fin between verticals through first sixth and first fifth of adipose-fin base. First unbranched and flexible ray distinctly shorter than second and third rays, which are roughly the same size; remaining rays progressively shorter.

Anal-fin rays vi,7* (1); vi,8 (1); or iv,10 (1); distal border of extended anal fin convex. Two or three anteriormost anal-fin rays vestigial, unsegmented, embedded in thick skin fold. Anal fin origin between verticals through slightly posterior to adipose fin origin and first third of adipose fin base. Tip of anteriormost anal-fin pterygiophore inserted posterior to hemal spine of vertebrae 21* (2) or 22 (2). Tip of posteriormost anal-fin pterygiophore inserted ahead of hemal spine of vertebrae 28 (2) or 29* (2).

Adipose fin two and half to almost three times in SL, forming ascending elevated curve in lateral profile, with deepest point approximately at midlength. Adipose fin emerging gradually, its posterior limit as a rounded, free lobe. Adipose fin origin at vertical through vertebral centra 16 (1)– 19* (2). Adipose fin terminus at vertical through vertebral centra 36 (1)– 39 (2) (holotype 37).

Caudal fin deeply forked, dorsal lobe slightly longer. Caudal peduncle length posterior to adipose-fin roughly the same as its depth. Dorsal lobe with 7 (4) branched, 1 (4) unbranched principal, and 7 (1)– 14* (1) procurrent fin-rays. Ventral lobe with 8 (4) branched, 1 (4) unbranched principal, and 10 (1)– 18* (1) procurrent fin-rays. Hypural 5 free, not fused to plate formed by hypurals 3+4. Median caudal-fin rays not articulated directly to caudal plate. Seven (2) rays articulated to dorsal caudal-fin plate and 7 (1) or 8* (1) rays articulated to ventral caudal-fin plate (5 or 6 on hypurals 1+2 and 2 on parhypural).

Total vertebrae 41 (1)– 42* (3). Ribs 9* (2)– 10 (2).

Epiphyseal branch of laterosensory canal in the head (S6) connecting contralateral canals, and proceeding posteriorly as a single canal, opening as a single pore.

Coloration in alcohol

Background body coloration yellowish, dorsally brownish. Ventral region of head and body lighter. Dark brown midlateral stripe of moderate width (Fig. 180), not well delimited, extending from snout to caudal-fin origin. Paired dorsal brown stripe, not well delimited, from supraoccipital process until adipose fin terminus, getting lighter posteriorly. Dorsal fin with a

dark brown stripe near its base, followed by a hyaline stripe, and distal third dark again. Cephalic brown pigment along posterior fontanel.

Geographic distribution

Pimelodella roccae was described from Rio Comerciato, Middle Urubamba and Beni basin. It is known of regions 312 (Amazonas High Andes) and 317 (Ucayali-Urubamba Piedmont), in streams of Urubamba, Beni and Huallaga drainages in Bolivia and Peru.

Comments

Eigenmann (1917) first mentioned his *Pimelodella roccae*, but only giving its full description in Eigenmann *in* Eigenmann & Allen (1942), assigning a holotype and specifying its type-locality, also referring to previous mentions of the name as *nomen nudum*. However, according with ICZN, a name published before 1931 is available if accompanied by an indication, which can be an illustration, and Eigenmann (1917) illustrated in plate XXXV, fig. 7 *P. roccae* pectoral-fin spine, making therefore the name available. Thus, *Pimelodella roccae* should be referred as authored by Eigenmann (1917), and not Eigenmann *in* Eigenmann & Allen, 1942.

Pearson (1924) reference to *P. gracilis* from Beni River is probably a *P. roccae*, due to similar coloration pattern between those two species.

Material examined

Pimelodella roccae. — MCZ 30975, 1, xr, 139.9 mm SL, holotype, Peru, Cusco, Río Comerciato [Río Compursiato] (altitude 1800 ft), 12°28'S, 73°7'W; CAS 63722, 1, xr, 91.4 mm SL, paratype, Bolivia, Rio Comerciato, 12°28'S, 73°7'W; MZUSP 25977, 1, 74.3 mm SL, Peru, Depto. Ucayali, Prov. Cel. Portillo, Masisea, Rio Ucayali, 8°34'23.6"S, 74°21'05.9"W; MZUSP 26319, 1, 80.7 mm SL, Peru, Depto. Ucayali, Prov. Cel. Portillo, Pucallpa, Cashibococha, 8°20'19.0"S, 74°39'12.5"W; MZUSP 26383, 1, 97.0 mm SL, Peru, Depto. Ucayali, Pucallpa, Estrada Pucallpa-Huánuco, Nuevo Requena, Rio Aguaytia, 9°02'23.8"S, 75°30'16.2"W; MZUSP 100564, 12, 64.1–92.1 mm SL, Brazil, Mato Grosso, Aripuanã, Rio Aripuanã, porto dos pescadores, abaixo do salto de Dardanelos/Andorinhas, 10°10'6.0"S, 59°26'50.0"W; MZUSP 110454, 1, 133.6 mm SL, Peru, Depto. Huánuco, Huánuco, Tingo Maria, Rio Thullumayo or Chancadora, junction with Rio Azul, 9°10'35.0"S, 75°57'46.0"W; MZUSP 110494, 3, xr, 103.5–154.5 mm SL, Peru, Huánuco, Tingo, Maria left bank of Rio Huallaga downstream from mouth of Quebrada Acerradero, near Balneário, 9°15'13.0"S, 76°0'33.0"W.

***Pimelodella serrata* Eigenmann, 1917**

Pimelodella serrata Eigenmann, 1917: 235–236, pl. XXIV, fig. 1; pl. XXXV, fig. 1 [original description; “San Joaquin, Bolivia”; holotype: FMNH 57979 (formerly CM 6967)]. — Henn, 1928: 78 [type catalog]. — Fowler, 1939: 224 [taxonomic treatment, comparison with *P. hartwelli*] — Gosline, 1945: 43 [taxonomic treatment]. — Fowler, 1951: 549–550, fig. 565 [taxonomic treatment]. — Ortega & Vari, 1986: 15 [taxonomic list]. — Ibarra & Stewart, 1987: 66 [type catalog]. — Burgess, 1989: 281 [taxonomic treatment]. — Chernoff *et al.*, 2000: 282 [taxonomic list]. — Bockmann & Guazzelli, 2003: 421 [taxonomic treatment]. — Ferraris, 2007: 194–195 [taxonomic treatment]. — Bockmann & Slobodian, 2013: 18; 61–63, unnum. fig. page 62, fig. 36.1E [taxonomic treatment; sympatrid with *P. howesi*; similarities with *P. chaparae*].

Pimelodella chaparae Fowler, 1940b: 75–77, fig. 29–31 [original description; “Boca Chapare, Cochabamba, Bolivia”; holotype: ANSP 69021]. — Gosline, 1945: 46 [taxonomic treatment]. — Fowler, 1951: 536, fig. 551 [taxonomic treatment]. — Böhlke, 1984: 141 [type catalog]. — Burgess, 1989: 280 [taxonomic treatment]. — Bockmann & Guazzelli, 2003: 417 [taxonomic treatment]. — Ferraris, 2007: 190 [taxonomic treatment]. — Bockmann & Slobodian, 2013: 18; 63 [taxonomic treatment; similarities with *P. serrata*].

Diagnosis

Pimelodella serrata differs from all *Pimelodella* species except *P. mucosa* by the presence of openings of laterosensory canal at dentary and hyomandibula large and conspicuous. It differs from *P. mucosa* by having posterior margin of pectoral-fin spine bearing 16–21 large, retrorse dentations along roughly all margin (*vs.* posterior margin of pectoral-fin spine bearing 14–18 small, retrorse dentations along its basal two thirds). Furthermore, *P. serrata* can be diagnosed by dorsal profile straight from snout to dorsal fin; maxillary barbel reaching between verticals through anal fin terminus and surpassing caudal fin origin; dorsal lamina of Weberian complex vertebrae reaching the supraoccipital process along its entire extension; dorsal fin spine robust, bearing small, straight dentations along almost entire posterior margin; posterior margin of pectoral-fin spine bearing 16–21 large, retrorse dentations along roughly all margin, these dentations are acute, hook-like; adipose fin two and half to three and half times in SL; 41–44 total vertebrae; brown midlateral stripe of narrow to moderate width, not well delimited, extending from snout to caudal-fin origin.

Description

Measurements in Table 60. Body average depressed, depth at dorsal-fin origin five to almost seven times in standard length, and compressed, body width at dorsal-fin origin six and half to almost eleven times in SL (Fig. 181). Greatest body depth at dorsal-fin origin. Dorsal profile straight from snout to dorsal fin, slightly concave from dorsal to adipose fin, slightly convex along adipose fin, and concave along the caudal peduncle. Ventral profile of body slightly convex from snout to pectoral fins, convex between pectoral and pelvic fins, slightly concave from pelvic to anal fin, and concave from this point along the caudal peduncle.

Pseudotympanum large, oval, above posterior process of cleithrum and reaching the straight line of 6th (1) to 8th (1) (holotype 7th) vertebrae. Posterior process of cleithrum triangular, long, its dorsal border straight to slightly concave. Anus and urogenital papilla adjacent. Urogenital papilla tubular, triangular, short in some specimens, medium in others. Anus between verticals through first third and second fifth of adpressed pelvic fin; urogenital papilla between verticals through last third and surpassing terminus of adpressed pelvic fin.

Head depressed, depth at supraoccipital-process base more than two to two and half times in head length. Mouth sub terminal. Eye slightly elliptical, four to five times in head. Bony interorbital distance a third less than eye diameter. Barbels thin, slightly depressed and elliptical in cross-section. Maxillary barbel reaching between verticals through anal fin terminus and surpassing caudal fin origin. Outer mental barbel, when stretched parallel to main body axis, finishing between second third of adpressed pectoral fin and half adpressed pelvic fin. Inner mental barbel, when stretched parallel to main body axis, finishing between pectoral fin origin and first fourth of adpressed pectoral fin. Supraoccipital process subrectangular to triangular, wide. Dorsal lamina of Weberian complex vertebrae reaching the supraoccipital process along its entire extension. Branchiostegal rays 6* (2)–7 (3).

Dorsal fin triangular, distal margin concave, moderate length (second branched dorsal-fin ray four and half to six times in SL), depressed tip finishing between second and last fifth of adpressed pelvic fin. Dorsal fin with I,6 (10) plus anteriormost spinelet. Distance between terminus of dorsal-fin base and adipose-fin origin notably shorter than dorsal-fin base. Anteriormost dorsal-fin pterygiophore inserted posterior to neural spine of vertebrae 4 (7); posteriormost dorsal-fin pterygiophore located ahead of neural (or pseudoneural) spine of vertebrae 11* (5) or 12 (2). Unbranched dorsal-fin ray mostly ossified as a spine, long (spine three fourths of first dorsal-fin total length). Dorsal fin spine robust, bearing small, straight dentations along almost entire posterior margin (Fig. 182).

Pectoral-fin rays I,7 (4)–I,9* (3), pectoral fin triangular with concave distal border. First pectoral-fin ray curved with proximal part rigid, forming a spine (Fig. 183), and short distal tip flexible and distinctly segmented. Pectoral-fin spine large, three and half to five and half times in SL. Anterior margin of pectoral-fin spine with small, but definite, antrorse dentations along roughly all margin. Posterior margin of pectoral-fin spine bearing 16–21 large, retrorse dentations along roughly all margin. These dentations are acute, hook-like.

Pelvic-fin rays i,5 (9), extended pelvic fin triangular with straight distal border. Anterior portion of pelvic-fin base between verticals through dorsal fin terminus and a point slightly posterior to that. Tip of adpressed pelvic fin between verticals through first eighth and first third of adipose fin. First unbranched and flexible ray distinctly shorter than second and third rays, third ray the longest; remaining rays progressively shorter.

Anal-fin rays iv,7 (2); iv,8* (2); v,8 (3); or v,9 (2); distal border of extended anal fin convex. Two or three anteriormost anal-fin rays vestigial, unsegmented, embedded in thick skin fold. Anal fin origin between verticals through first third and half adipose-fin base; anal-fin adpressed terminus at vertical through adipose-fin terminus. Tip of anteriormost anal-fin pterygiophore inserted posterior to hemal spine of vertebrae 21* (2), 22 (2) or 23 (4). Tip of posteriormost anal-fin pterygiophore inserted ahead of hemal spine of vertebrae 29* (2) or 30 (5).

Adipose fin two and half to three and half times in SL, forming ascending elevated curve in lateral profile, with deepest point approximately at its half. Adipose fin emerging gradually, its posterior limit as a rounded, free lobe. Adipose-fin origin at vertical through vertebral centra 16* (3)– 20 (1); adipose-fin terminus at vertical through vertebral centra 35 (1)– 38 (1) (holotype 37).

Caudal fin deeply forked, lobes subequal or ventral lobe slightly longer than dorsal. Caudal peduncle length posterior to adipose-fin roughly the same as to slightly larger than its depth. Dorsal lobe with 7 (9) branched, 1 (9) unbranched principal, and 12 (1)–21 (1) (holotype 18) procurrent fin-rays. Ventral lobe with 8 (9), 1 (9) unbranched principal, and 14* (1)– 25 (1) procurrent fin-rays. Hypural 5 completely free, not fused to hypural 3+4. Median caudal-fin rays not articulated directly to caudal plate. Seven (5) rays articulated to dorsal caudal-fin plate (5 on hypurals 3+4 and 2 on hypural 5) and 8* (4), rarely 9 (1) rays articulated to ventral caudal-fin plate (6 or 7 on hypurals 1+2 and 2 on parahypural).

Total vertebrae 41 (2)– 44 (2) (holotype 42). Ribs 7 (1)– 8 (5).

Epiphyseal branch of laterosensory canal on head (s6) usually uniting at midline and emerging as an unique pore; or not united, but two pores near each other. Openings of laterosensory canal at dentary and hyomandibula large and conspicuous.

Coloration in alcohol

Background body coloration yellowish. Ventral region of head and body lighter. Brown midlateral stripe of narrow to moderate width (Fig. 184, 185), not well delimited, extending from snout to caudal-fin origin. Cephalic brown pigment at posterior fontanel region. Dorsal fin light brown.

Geographic distribution

Pimelodella serrata was described from San Joaquin, Bolivia, and Bockmann & Guazzelli (2003) suggest from the Machupo River basin, Upper Guaporé. *Pimelodella chaparae*, its junior synonym, was described from Boca Chapare, also in Bolivia. Therefore, *P. serrata* is known from regions 313 (Western Amazon Piedmont), 317 (Ucayali-Urubamba Piedmont), 318 (Mamore-Madre de Dios Piedmont) and 319 (Guapore-Itenez).

Comments

When describing *P. chaparae* (Fig. 186) Fowler (1940b), the author diagnosed the species based on “its distinctive pectoral armature” and compared it with *P. hasemani*, but made no effort of comparing it with *P. serrata*. The pectoral-fin spine morphology of *P. serrata* is notably different from that of all other *Pimelodella* species, with exception of *P. chaparae*, which I designate here as a junior-synonym of the first. Other diagnostic characteristics, like the long barbels, head lateral profile notably straight, robust dorsal-fin spine and color pattern also allow me to support this synonym. The measurements of *P. serrata* and *P. chaparae*, separated by original species name, can be found in Table 61.

Pimelodella serrata occurs syntopically with *P. howesi* in Rio Meta, Rio Ucayali and Rio Madre de Dios basins.

Material examined

Pimelodella serrata. — FMNH 57978, 1, xr, 55.7 mm SL, holotype, Bolivia, San Joaquin, Rio Machupo, 13°02'24"S, 64°38'51"W; FMNH 57979, 1, xr, 86.0 mm SL, paratype, Bolivia, San Joaquin, Rio Machupo, 13°02'24"S, 64°38'51"W; ANSP 131360, 1, 74.5 mm SL, Colombia, Meta, Rio Negro, downstream from main Villavicencio-Puerto Lopez highway at La Balsa, W side of river, Negro-Humea-Meta Dr. 4°4'0.0"N, 73°4'0.0"W; ANSP 131361, 2, 69.9–78.2 mm SL, Colombia, Meta, Rio Negro, just downstream from main Villavicencio-Puerto Lopez highway at La Balsa, E side of river, Humea-Meta drainage, 4°4'0.0"N,

73°4'0.0"W; ANSP 138828, 5, 66.3–84.3 mm SL, 2 c&s, Colombia, Meta, Rio Negrito midway between La Argelia and La Balsa (Plancha 267 - Rio Guayuriba), 4°4'0.0"N, 73°4'0.0"W; LIRP 10029, 15, 73.8–83.4 mm SL, Brazil, Rondônia, Guajara-Mirim, Rio Mamoré, 11°30'08.6"S, 65°11'17.5"W; MZUSP 26063, 1, 56.8 mm SL, Peru, Depto. Huánuco, Huánuco, Tournavista, Rio Pachitea, 8°56'12.9"S, 74°42'23.4"W; MZUSP 82383, 1, 71.3 mm SL, Brazil, Amazonas, Rio Juruá, 10.2 km below Lago Pauapixuna, 2°41'7.0"S, 65°48'27.0"W; MZUSP 93078, 3, 80.0–99.4 mm SL, Brazil, Amazonas, Igarapé Castanha (affluent of Rio Tiquié), vicinity of Sítio São Pedro, 0°11'0.0"N, 69°35'0.0"W; MZUSP 92549, 8, 41.6–102.5 mm SL, Brazil, Amazonas, Igarapé Castanha (affluent of Rio Tiquié), near mouth, 0°12'0.0"N, 69°35'0.0"W; MZUSP 92169, 25, 48.4–78.0 mm SL, Brazil, Amazonas, Igarapé Castanha (affluent of Rio Tiquié), beaches in Santa Rosa community (3-4.ix.2006), 0°4'41.0"N, 69°41'26.0"W.

Pimelodella chaparae. — ANSP 69021, 1, xr, 48.1 mm SL, holotype, Bolívia, Boca Chaparae, Cochabamba, 15°56'04"S, 64°45'11"W; ANSP 69022-69035, 14, xr, 32.6–51.2 mm SL, paratypes, Bolívia, Boca Chaparae, Cochabamba, 15°56'04"S, 64°45'11"W.

***Pimelodella spelaea* Trajano, Reis & Bichuette, 2004**

Pimelodella spelaea Trajano, Reis & Bichuette, 315–325, fig. 1 [original description; “State of Goiás, São Domingos, upper Tocantins River basin, subterranean stream tributary to São Bernardo River inside São Bernardo Cave”; holotype: MZUSP 81726]. — Proudlove, 2006: 143 [taxonomic treatment]. — Ferraris, 2007: 195 [taxonomic treatment]. — Bockmann & Castro, 2010: 674, 697 [taxonomic treatment].

Diagnosis

Pimelodella spelaea differs from all *Pimelodella* species except *P. cristata*, *P. hasemani*, *P. humeralis*, *P. longipinnis*, *P. megalops*, *P. modesta*, *P. notomelas*, *P. peruana*, *P. robinsoni*, *P. martinezi*, *P. serrata*, *P. tapatapae* and *P. yuncensis* by having a narrow midlateral stripe. It differs from all above mentioned by having a slightly darker pigmented region between dorsal and adipose fins. Furthermore, *P. spelaea* can be diagnosed by maxillary barbel reaching between half adpressed pelvic fin and half adpressed anal fin; posterior margin of pectoral-fin spine bearing 8–10 retrorse dentations along its basal two thirds, these dentations are triangular, with broad bases, shorter near base of spine; adipose fin slightly more than three to more than three and half times in SL; 40–41 total vertebrae; light brown midlateral stripe narrow, not well delimited, extending from snout to a point anterior to caudal-fin origin, lighter at head, from snout to opercle, and posterior to line through half

adipose fin; paired light brown dorsolateral stripe along supraoccipital process until dorsal fin terminus; also a light brown region between dorsal and adipose fins, sometimes reaching along anterior sixth of adipose fin base.

Description

Measurements in Table 62. Body of moderate height, depth at dorsal-fin origin five and half to almost seven times in standard length, and compressed, body width at dorsal-fin origin seven to almost ten times in SL (Fig. 187). Dorsal profile convex from snout to dorsal fin, slightly concave from dorsal to adipose fin, slightly convex along adipose fin, and concave along caudal peduncle. Ventral profile of body slightly convex from snout to branchiostegal membrane, convex between pectoral end pelvic fins, and slightly concave from pelvic to anal fin, and concave along caudal peduncle.

Pseudotympanum large, oval, dorsal to posterior process of cleithrum and reaching 7th (1)–8th (2) vertebrae. Posterior process of cleithrum triangular, short, slightly concave. Anus and urogenital papilla adjacent. Urogenital papilla tubular, triangular, short. Anus between verticals through half and second third of adpressed pelvic fin; urogenital papilla between verticals through last fourth and terminus of adpressed pelvic fin.

Head moderate depressed, depth at supraoccipital-process base from slightly more to slightly less than two times in head length. Mouth sub terminal. Eye slightly elliptical, almost six to six and half times in head. Bony interorbital distance a third larger than eye diameter. Barbels thin, and slightly depressed and elliptical in cross-section. Maxillary barbel reaching between half adpressed pelvic fin and half adpressed anal fin. Outer mental barbel, when stretched parallel to main body axis, finishing between half and last third of adpressed pectoral fin. Inner mental barbel, when stretched parallel to main body axis, finishing between midway between ventral limit of branchiostegal membrane and pectoral fin, and half pectoral-fin base. Supraoccipital process subrectangular, narrow, tapered at distal third. Dorsal lamina of Weberian complex vertebrae of moderate height, reaching the supraoccipital process just at its anteriormost part. Branchiostegal rays 6 (2).

Dorsal fin triangular, distal margin concave, of moderate length (second branched dorsal-fin ray five to six and half times in SL), depressed tip reaching between the verticals through second fifth and last third of adpressed pelvic fin. Dorsal fin with I,6 (7), plus anteriormost spinelet. Distance between terminus of dorsal-fin base and adipose-fin origin slightly shorter than dorsal-fin base. Anteriormost dorsal-fin pterygiophore inserted posterior to neural spine of vertebrae 4 (3); posteriormost dorsal-fin pterygiophore located ahead of neural (or pseudoneural) spine of vertebrae 11 (2) or 12 (1). Unbranched dorsal-fin ray mostly

ossified as a spine, rigid part relatively long (three fourths or more of first dorsal-fin ray total length).

Pectoral-fin rays I,8 (1)– I,9* (6), pectoral fin triangular with concave distal border. First pectoral-fin ray curved, with proximal part rigid (Fig. 188), and short distal tip flexible and distinctly segmented. Pectoral fin spine five and half to seven times in SL. Anterior margin of pectoral-fin spine with small, smooth dentations along its basal half, and smooth serrae along distal third. Posterior margin of pectoral-fin spine bearing 8–10 retrorse dentations along its basal two thirds. These dentations are triangular, with broad bases, shorter near base of spine, plus sometimes 1–2 unossified distalmost dentations, not counted.

Pelvic-fin rays i,5 (7), extended pelvic fin triangular with straight distal border. Pelvic-fin origin between verticals through dorsal fin terminus and second third of adpressed dorsal fin. Tip of adpressed pelvic fin between verticals through adipose-fin origin and first fifth of adipose-fin base. First unbranched and flexible ray distinctly shorter than second and third rays, which are subequal; remaining rays progressively shorter.

Anal-fin rays v,7 (1); ii,8 (1); iii,8* (1); v,8 (1); iii,9 (1); or v,9 (2); distal border of extended anal fin convex. Two to three anteriormost anal-fin rays vestigial, unsegmented, embedded in thick skin fold. Anal fin origin between verticals through first fourth and first third of adipose-fin base. Anal-fin adpressed terminus at vertical through adipose-fin terminus. Tip of anteriormost anal-fin pterygiophore inserted posterior to hemal spine of vertebrae 21 (2) or 22 (1). Tip of posteriormost anal-fin pterygiophore inserted ahead of hemal spine of vertebrae 28 (1) or 29 (2).

Adipose fin slightly more than three to more than three and half times in SL, forming ascending elevated curve in lateral profile, with deepest point approximately midlength. Adipose fin emerging gradually, its posterior limit as a rounded, free lobe. Adipose-fin origin at vertical through vertebral centra 19 (1)– 21 (1); adipose-fin terminus at vertical through vertebral centra 34 (1)– 35 (2).

Caudal fin deeply forked, dorsal lobe slightly longer than ventral lobe. Caudal peduncle posterior to adipose-fin base more than twice its depth. Dorsal lobe with 7 (7) branched, 1 (7) unbranched principal and 11* (1)– 15 (1) procurrent fin-rays. Ventral lobe with 8 (6), rarely 9 (1) branched, 1 (7) unbranched principal and 7 (1)– 16 (1) procurrent fin-rays (holotype 9). Hypural 5 fused to plate formed by hypurals 3+4. Median caudal-fin rays not directly attached to caudal plate. Seven (3) rays articulated to dorsal caudal-fin plate and 7 (1) or 8 (2) rays articulated to ventral caudal-fin plate (5 or 6 on hypurals 1+2 and 2 on parhypural).

Total vertebrae 40 (1)–41 (2). Ribs 10 (3).

Epihyseal branch of laterosensory canal on head (S6) with contralateral canals connecting at midline, and opening in a single pore just after the canals connection.

Coloration in alcohol

Background body coloration yellowish. Ventral region of head and body lighter. Light brown midlateral stripe narrow (Fig. 189), not well delimited, extending from snout to a point anterior to caudal-fin origin, lighter at head, from snout to opercle, and posterior to line through half adipose fin. Paired light brown dorsolateral stripe along supraoccipital process until dorsal fin terminus. Also a light brown region between dorsal and adipose fins, sometimes reaching along anterior sixth of adipose fin base. Cephalic brown pigment at posterior fontanel region. Trajano *et al.* (2004) report concentrated chromatophores on pseudotympanum.

Geographic distribution

Pimelodella spelaea was described from a small upper tributary of the São Bernardo River inside the São Bernardo Cave, upper Tocantins River. It is known only from its type-locality, in region 324 (Tocantins-Araguaia).

Material examined

Pimelodella spelaea. — MZUSP 81726, 1, xr, 78.9 mm SL, holotype, Brazil, Goiás, São Domingos, subterranean stream affluent of São Bernardo river, inside São Bernardo cave, Upper Tocantins, 13°49'S, 46°21'W; MZUSP 81727, 1, xr, 42.4 mm SL, paratype, Brazil, Goiás, São Domingos, subterranean stream affluente of São Bernardo river, inside São Bernardo cave, Upper Tocantins, 13°49'S, 46°21'W; MZUSP 81728, 1, xr, 47.1 mm SL, paratype, Brazil, Goiás, São Domingos, subterranean stream affluente of São Bernardo river, inside São Bernardo cave, Upper Tocantins, 13°49'S, 46°21'W; MZUSP 81729, 4, xr, 69.0–76.6 mm SL, paratypes, Brazil, Goiás, São Domingos, subterranean stream affluente of São Bernardo river, inside São Bernardo cave, Upper Tocantins, 13°49'S, 46°21'W.

***Pimelodella straminea* (Cope, 1894)**

Rhamdella straminea Cope, 1894: 93–94 [original description; “Rio Grande do Sul”]; syntypes: ANSP 21581–84; ANSP 21604]. — Fowler, 1915: 213 [taxonomic treatment; specifying the locality; inclusion of ANSP 23216 in type series] — Böhkle, 1984: 142 [type catalog]. — Malabarba, 1989: 143 [taxonomic treatment, junior-synonym of *R. eriarcha*]. — Bockmann & Guazzelli, 2003: 422 [taxonomic treatment, junior-synonym of *R. eriarcha*]. — Ferraris, 2007: 196 [taxonomic treatment, junior-

synonym of *R. eriarcha*]. — Bockmann & Miquelarena, 2008: 45–47 [taxonomic treatment, in *Rhamdia* or *Pimelodella*, but not *Rhamdella*].

Rhamdia straminea. — Eigenmann, 1910: 387 [taxonomic treatment, used the genus *Rhamdia*, but treated under *Rhamdella*]. — Gosline, 1945: 38 [taxonomic treatment]. — Fowler, 1951: 578 [taxonomic treatment]. — Burgess, 1989: 279 [taxonomic treatment]. — Lucena & Silva, 1991: 38 [taxonomic treatment].

Diagnosis

Pimelodella straminea differs from all *Pimelodella* species except *P. australis*, *P. avanhandavae*, *P. buckleyi*, *P. cruxenti*, *P. gracilis*, *P. griffini*, *P. harttii*, *P. ignobilis*, *P. itapicuruensis*, *P. kronei*, *P. lateristriga*, *P. laticeps*, *P. laurenti*, *P. leptosoma*, *P. linami*, *P. macturki*, *P. martinezi*, *P. meeki*, *P. megalura*, *P. metae*, *P. montana*, *P. mucosa*, *P. notomelas*, *P. roccae*, *P. taeniophora* and *P. vittata* by having the dorsal fin with a darker region near the base, followed by a hyaline stripe, and distally darker (unknown in *P. martinezi*). It differs from *P. itapicuruensis*, *P. leptosoma*, *P. megalura*, *P. metae* and *P. montana* by having the supraoccipital process reaching the anterior prenuchal plate (vs. supraoccipital process not reaching the anterior prenuchal plate in *P. itapicuruensis*, *P. leptosoma*, *P. megalura*, *P. metae* and *P. montana*). It differs from *P. avanhandavae*, *P. buckleyi*, *P. cruxenti*, *P. gracilis*, *P. lateristriga*, *P. laurenti*, *P. macturki*, *P. martinezi*, *P. mucosa*, *P. notomelas*, *P. roccae*, *P. taeniophora* and *P. vittata* by having the maxillary barbel reaching between verticals through second third and terminus of adpressed pelvic fin (vs. maxillary barbel reaching at least anal-fin origin in *P. avanhandavae*, *P. buckleyi*, *P. cruxenti*, *P. gracilis*, *P. lateristriga*, *P. laurenti*, *P. macturki*, *P. martinezi*, *P. mucosa*, *P. notomelas*, *P. roccae*, *P. taeniophora* and *P. vittata*). It differs from *P. australis*, *P. griffini*, *P. harttii*, *P. kronei* and *P. meeki* by the absence of a paired dorsolateral stripe on body (vs. presence of a paired dorsolateral stripe on supraoccipital process in *P. australis*, *P. harttii*, *P. kronei* and *P. meeki*; presence of a paired dorsolateral stripe reaching adipose fin terminus in *P. griffini*). It differs from *P. laticeps* and *P. linami* by the hyaline stripe in dorsal fin not encompassing the unbranched fin ray (vs. hyaline stripe in dorsal fin encompass the unbranched fin ray in *P. laticeps* and *P. linami*). It differs from *P. ignobilis* by the maxillary barbel reaching between second third and terminus of adpressed pelvic fin, and dorsal region of head not notably darker (vs. maxillary barbel reaching between half adpressed pelvic fin and anal fin origin and dorsal region of head and body slightly, but notably darker in *P. ignobilis*).

Furthermore, *P. straminea* can be diagnosed by maxillary barbel reaching between verticals through second third and terminus of adpressed pelvic fin; dorsal lamina of Weber

complex vertebrae reaching the supraoccipital process along its entire length; posterior margin of pectoral-fin spine bearing 7–10 retrorse dentations along basal two thirds; these dentations are moderate to large; adipose fin slightly more than three and half to four times in SL; ventral caudal fin lobe usually slightly longer; 40–41 total vertebrae; medium brown midlateral stripe wide, not well delimited, extending from snout to caudal fin origin; dorsal fin brown, except by a hyaline stripe near its base, which does not encompass the unbranched ray.

Description

Measurements in Table 63. Body compressed, depth at dorsal-fin insertion five and half to seven times in standard length, and compressed, body width at dorsal-fin origin eight to ten times in SL (Fig. 190). Greatest body depth at dorsal-fin origin. Dorsal profile convex from snout to dorsal fin, concave from dorsal to adipose fin, slightly convex along adipose fin, and concave along the caudal peduncle. Ventral profile of body slightly convex from snout to branchiostegal membrane, also convex between branchiostegal membrane and pectoral-fins, slightly concave between pectoral and pelvic fins, and also concave from there along the caudal peduncle.

Pseudotympanum large, oval, above posterior process of cleithrum and reaching the straight line of 7th (1) vertebrae. Posterior process of cleithrum triangular, short, its dorsal border slightly concave. Anus and urogenital papilla adjacent. Urogenital papilla tubular, triangular, short to medium. Anus at vertical through half adpressed pelvic fin; urogenital papilla between verticals through second third and terminus of adpressed pelvic fin.

Head moderate depressed, depth at supraoccipital-process base slightly less to slightly more than two times in head length. Mouth sub terminal. Eye slightly elliptical, four to four and half times in head. Bony interorbital distance a fourth smaller than eye diameter. Barbels thin, depressed and elliptical in cross-section. Maxillary barbel reaching between verticals through second third and terminus of adpressed pelvic fin. Outer mental barbel, when stretched parallel to main body axis, finishing between verticals through pectoral fin origin and its first third adpressed. Inner mental barbel, when stretched parallel to main body axis, finishing at vertical through ventral limit of branchiostegal membrane. Supraoccipital process triangular, narrow. Dorsal lamina of Weber complex vertebrae reaching the supraoccipital process along its entire length. Branchiostegal rays 6 (2).

Dorsal fin triangular, distal margin convex, short (first branched dorsal-fin ray four and half to five and half in SL), adpressed terminus reaching between verticals through first sixth and last fourth of adpressed pelvic fin. Dorsal fin with I,6 (4) plus anteriormost spinelet.

Distance between terminus of dorsal-fin base and adipose-fin origin usually slightly less than dorsal-fin base. Antermost dorsal-fin pterygiophore inserted posterior to neural spine of vertebrae 4 (3); posteriormost dorsal-fin pterygiophore located ahead of neural (or pseudoneural) spine of vertebrae 11 (3). Unbranched dorsal-fin ray mostly ossified as a spine, long (three fourths or more of first dorsal-fin total length).

Pectoral-fin rays I,7 (1)– I,8 (1), pectoral fin triangular with concave distal border. First pectoral-fin ray curved, with proximal part rigid, forming a spine (Fig. 191) and short distal tip flexible and distinctly segmented. Pectoral-fin spine four and half to five times in SL. Anterior margin of pectoral-fin spine with small, smooth, straight dentations along its two thirds and smooth serrae along its distal third. Posterior margin of pectoral-fin spine bearing 7–10 retrorse dentations along basal two thirds. These dentations are moderate to large. Also sometimes 1–3 unossified distal dentations, not counted.

Pelvic-fin rays I,5 (19), extended pelvic fin triangular with straight distal border. Anterior portion of pelvic-fin base between verticals through dorsal fin terminus and a point slightly posterior to that. Tip of adpressed pelvic fin between verticals through adipose-fin origin and a point slightly posterior to that. First unbranched and flexible ray.

Anal-fin rays iv,8 (1); or v,9 (2); distal border of extended anal fin convex. One or two anteriormost anal-fin rays vestigial, unsegmented, embedded in thick skin fold. Anal fin origin between verticals through first fourth and second fifth of adipose-fin base; anal-fin adpressed terminus at adipose fin terminus or slightly posterior. Tip of anteriormost anal-fin pterygiophore inserted posterior to hemal spine of vertebrae 21 (1), 22 (1) or 23 (1). Tip of posteriormost anal-fin pterygiophore inserted ahead of hemal spine of vertebrae 30 (3).

Adipose fin slightly more than three and half to four times in SL, forming ascending elevated curve in lateral profile, with deepest point approximately at midlength. Adipose fin emerging gradually, its posterior limit as a rounded, free lobe. Adipose-fin origin at vertical through vertebral centra 19 (1)– 22 (2); adipose-fin terminus at vertical through vertebral centra 33 (1)– 36 (1).

Caudal fin deeply forked, ventral lobe usually slightly longer. Caudal peduncle length posterior to adipose-fin a fourth longer than its depth. Dorsal lobe with 6* (1) or 7 (3) branched and 1 (4) unbranched rays. Ventral lobe with 6* (1) or 8 (3) branched and 1 (4) unbranched rays. Hypural 5 completely free, not fused to hypural 3+4. Median caudal-fin rays not articulated directly to caudal plate. Seven* (3) rays articulated to dorsal caudal-fin plate (5 on hypurals 3+4 and 2 on hypural 5) and 8 (2), or 9 (1) rays articulated to ventral caudal-fin plate (6 or 7 on hypurals 1+2 and 2 on parahypural).

Total vertebrae 40* (3)– 41 (1). Ribs 8* (3)– 9 (1).

Epiphyseal branch of laterosensory canal on head (S6) with contralateral canals opening in two separate pores.

Coloration in alcohol

Background body coloration yellowish. Ventral region of head and body lighter. Medium brown midlateral stripe wide (Fig. 192), not well delimited, extending from snout to caudal fin origin. Brown cephalic pigment along posterior fontanel region. Dorsal fin brown, except by a hyaline stripe near its base, which does not encompass the unbranched ray.

Geographic distribution

Pimelodella straminea was described from Rio Grande do Sul, probably Rio Jucaí, in Lagoa dos Patos system. It is known from region 334 (Laguna dos Patos).

Comments

This species have a conturbated taxonomic history. Eigenmann (1910) transferred *Rhamdella straminea* to *Rhamdia* genus, without giving justification to this decision, and was followed by Gosline (1945), Fowler (1951) and Burgess (1989). Fowler (1915: 213) specifies the collecting locality of *Rhamdella straminea* to “Rio Jacuhy”, in Rio Grande do Sul State, and adds ANSP 23216 as identical to the remaining material examined by Cope. Böhlke (1984: 142) included this last in the types of *R. straminea*.

Malabarba (1989: 143) included *Rhamdella straminea* in *R. eriarcha* synonym, arguing the species from Lagoa dos Patos system are probably synonyms, as apparently just one species of this genus occurs in that locality, and this decision was followed by Bockmann & Guazzelli (2003). Lucena & Silva (1991) followed Fowler (1951) and included *Rhamdella straminea* under *Rhamdia* again. Silfvergrip (1996) did not include *R. straminea* in his *Rhamdia* revision.

Bockmann & Miquelarena (2008) argue that, due the presence of long maxillary barbels and difficult in delimiting the limit of the posterior fontanel, *Rhamdella straminea* should be placed in *Pimelodella* or *Rhamdia*, but not *Rhamdella*, and this question should be treated in Bockmann & Sabaj (in prep).

My opinion is that *Rhamdella straminea* is, in fact, a *Pimelodella*, due the presence of the genus diagnostic characteristics (like posterior fontanel long, and supraoccipital process reaching the preopercular plate), with exception of ANSP 23216, which is a *Rhamdia*. Also, *P. straminea* is probably a senior-synonym of *P. australis*. However, since the type-material is extremely degraded, it is maintained as valid a priori, meanwhile more comparative material

of Lagoa dos Patos system is examined. I also hereby designate ANSP 21581 as the lectotype of *P. straminea*, and ANSP 21582–84 and 21604 as paralectotypes. ANSP 23216 should not be included on the type-material list, since apparently was not examined by Cope (1894), who explicit cites five specimens.

Material examined

Pimelodella straminea: ANSP 21581, 1, xr, 41.2 mm SL, lectotype, Brazil, Rio Grande do Sul, countryside, near the mountains, 27°21'13"S, 54°01'27"W; ANSP 21583, 1, xr, 44.0 mm SL, paralectotype, Brazil, Rio Grande do Sul, countryside, near the mountains, 27°21'13"S, 54°01'27"W; ANSP 21584, 1, xr, 44.9 mm SL, paralectotype, Brazil, Rio Grande do Sul, countryside, near the mountains, 27°21'13"S, 54°01'27"W; ANSP 21604, 1, xr, 54.7 mm SL, paralectotype, Brazil, Rio Grande do Sul, countryside, near the mountains, 27°21'13"S, 54°01'27"W.

***Pimelodella taeniophora* (Regan, 1903)**

Pimelodus lateristrigus [non Müller & Troschel, 1849]. — Boulenger, 1896: 27 (*in partim*, Descalvados) [taxonomic list].

Pimelodella lateristriga. — Eigenmann, McAtee & Ward, 1907: 148 (*in partim*) [taxonomic list]. — Eigenmann, 1910: 389 (*in partim*) [taxonomic list].

Pimelodus (Pimelodella) taeniophorus Regan, 1903: 625 [original description; “Descalvados, Matto Grosso”, Brazil; syntypes: BMNH 1895.5.17.27–28]. — Eigenmann, 1917: 238 [taxonomic treatment, junior-synonym of *P. gracilis*]. — Gosline, 1945: 43 [taxonomic treatment, junior synonym of *P. gracilis*]. — Fowler, 1951: 541 [taxonomic treatment, junior-synonym of *P. gracilis*].

Pimelodella taeniophorus. — Eigenmann, McAtee & Ward, 1907: 148 [taxonomic list].

Pimelodella taeniophora. — Eigenmann, 1910: 389 [taxonomic treatment]. — Bertoni, 1913: 7 [taxonomic list]. — Bertoni, 1939: 52 [taxonomic list]. — Bockmann & Guazzelli, 2003: 421 [taxonomic treatment]. — Ferraris, 2007: 195 [taxonomic treatment].

Pimelodella griffini [non Eigenmann, 1917]. — Souza-Shibatta *et al.*, 2013: 101–109 [taxonomic treatment, cytogenetic].

Diagnosis

Pimelodella taeniophora differs from all *Pimelodella* species except *P. australis*, *P. avanhandavae*, *P. buckleyi*, *P. cruxenti*, *P. gracilis*, *P. griffini*, *P. harttii*, *P. ignobilis*, *P. itapicuruiensis*, *P. kronei*, *P. lateristriga*, *P. laticeps*, *P. laurenti*, *P. leptosoma*, *P. linami*, *P. macturki*, *P. martinezi*, *P. meeki*, *P. megalura*, *P. metae*, *P. montana*, *P. mucosa*, *P.*

notomelas, *P. roccae*, *P. straminea* and *P. vittata* by having the dorsal fin with a darker region near the base, followed by a hyaline stripe, and distally darker (unknown in *P. martinezi*). It differs from *P. itapicuruensis*, *P. leptosoma*, *P. megalura*, *P. metae* and *P. montana* by having the supraoccipital process reaching the anterior prenuchal plate (vs. supraoccipital process not reaching the anterior prenuchal plate in *P. itapicuruensis*, *P. leptosoma*, *P. megalura*, *P. metae* and *P. montana*). It differs from *P. australis*, *P. buckleyi*, *P. griffini*, *P. harttii*, *P. ignobilis*, *P. kronei*, *P. laticeps*, *P. linami*, *P. meeki* and *P. straminea* by the maxillary barbel reaching between verticals through anal fin terminus and surpassing caudal fin origin (vs. maxillary barbel reaching at best half adpressed anal fin in *P. australis*, *P. buckleyi*, *P. griffini*, *P. harttii*, *P. ignobilis*, *P. kronei*, *P. laticeps*, *P. linami*, *P. meeki* and *P. straminea*). It differs from *P. cruxenti*, *P. gracilis*, *P. laurenti*, *P. macturki*, *P. mucosa* and *P. notomelas* by having 42 total vertebrae (vs. 41 or less total vertebrae in *P. laurenti*, *P. macturki*, *P. mucosa* and *P. notomelas*; 46 or more total vertebrae in *P. cruxenti* and *P. gracilis*). It differs from *P. avanhandavae*, *P. lateristriga*, *P. martinezi*, *P. roccae* and *P. vittata* by having the caudal lobes subequal (vs. dorsal lobe of caudal fin slightly longer than ventral lobe in *P. avanhandavae*, *P. lateristriga*, *P. martinezi*, *P. roccae* and *P. vittata*).

Furthermore, *P. taeniophora* can be diagnosed by maxillary barbel reaching between verticals through anal fin terminus and surpassing caudal fin origin; unbranched dorsal-fin ray might present a filamentous prolongation; dorsal-fin spine bearing smooth serrae at its anterior distal third; posterior margin of pectoral-fin spine bearing 10–13 retrorse dentations along basal two thirds, these dentations are large, triangular, inclined, the basal ones more inclined; adipose fin two and half to almost three times in SL; 40–42 total vertebrae; dark brown midlateral stripe wide, not well delimited, extending from snout until median caudal-fin rays; paired dorsolateral brown stripe not well delimited along supraoccipital process.

Description

Measurements in Table 64. Body moderate depressed, depth at dorsal-fin insertion five to more than six and half times in standard length, and compressed, body width at dorsal-fin insertion six and half to eight and half times in SL (Fig. 193). Dorsal profile convex from snout to dorsal fin, concave from dorsal to adipose fin, slightly convex along adipose fin, and concave along the caudal peduncle. Ventral profile of body slightly convex from snout to branchiostegal membrane, concave between pectoral end pelvic fins, slightly convex from pelvic to anal fin, and concave from there along the caudal peduncle.

Pseudotympanum large, oval, above posterior process of cleithrum and reaching the straight line of 7th* (2) or 8th (5) vertebrae. Posterior process of cleithrum triangular, its dorsal

border straight to slightly concave. Anus and urogenital papilla adjacent. Urogenital papilla tubular, triangular, short. Anus between verticals through second fifth and last third of adpressed pelvic fin; urogenital papilla between verticals through first third and terminus of adpressed pelvic fin.

Head average depressed, depth at supraoccipital-process base slightly less or slightly more than two times in head length. Mouth sub terminal. Eye slightly elliptical, four to five times in head. A fourth shorter than eye diameter. Barbels thin, slightly depressed and elliptical in cross-section. Maxillary barbel reaching between verticals through anal fin terminus and surpassing caudal fin origin. Outer mental barbel, when stretched parallel to main body axis, finishing between half and adpressed terminus of pectoral fin. Inner mental barbel, when stretched parallel to main body axis, finishing between pectoral fin terminus and its first third adpressed. Supraoccipital process subrectangular, tapered at distal third. Dorsal lamina of Weberian complex vertebrae reaching the supraoccipital process at anterior part or its entire extension. Branchiostegal rays 6 (3).

Dorsal fin triangular, distal margin concave, average sized (second branched dorsal-fin ray four and half to five and half times in SL), depressed tip finishing between the verticals through half and last fourth of adpressed pelvic fin. Dorsal fin with I,6 (9) plus anteriormost spinelet. Distance between terminus of dorsal-fin base and adipose-fin origin roughly half dorsal-fin base. Anteriormost dorsal-fin pterygiophore inserted posterior to neural spine of vertebrae 4 (7); posteriormost dorsal-fin pterygiophore located ahead of neural (or pseudoneural) spine of vertebrae 11 (7). Unbranched dorsal-fin ray mostly ossified as a spine, usually a fourth shorter than first dorsal-fin ray total length, but some specimens may present a filamentous prolongation. Dorsal-fin spine bearing smooth serrae at its anterior distal third.

Pectoral-fin rays I,7 (1)–I,9 (2) (lectotype I,8), pectoral fin triangular with convex distal border. First pectoral-fin ray curved, with proximal part rigid, forming a spine (Fig. 194), and short distal tip flexible and distinctly segmented. Pectoral-fin spine five to almost six times in SL. Anterior margin of pectoral-fin spine with small, smooth, straight dentations along basal half and serrae along distal half. Posterior margin of pectoral-fin spine bearing 10–13 retrorse dentations along basal two thirds. These dentations are large, triangular, inclined, the basal ones more inclined. Also sometimes 1–3 distalmost unossified dentations, not counted.

Pelvic-fin rays i,5 (6), extended pelvic fin triangular with straight distal border. Anterior portion of pelvic-fin base between verticals through fifth branched dorsal fin ray and dorsal fin terminus. Tip of adpressed pelvic fin between verticals through first seventh and

first third of adipose fin base. First unbranched and flexible ray distinctly shorter than second and third rays, which are subequal; remaining rays progressively shorter.

Anal-fin rays iv,6 (1); iv,7* (5); or iv,8 (3); distal border of extended anal fin convex. Two or three anteriormost anal-fin rays vestigial, unsegmented, embedded in thick skin fold. Anal fin origin between verticals through second fifth and half adipose-fin base; anal-fin terminus between verticals through last eighth and terminus of adipose fin. Tip of anteriormost anal-fin pterygiophore inserted posterior to hemal spine of vertebrae 20* (1), 21 (3) or 22 (3). Tip of posteriormost anal-fin pterygiophore inserted ahead of hemal spine of vertebrae 27* (2) or 28 (5).

Adipose fin two and half to almost three times in SL, forming ascending elevated curve in lateral profile, with deepest point approximately midlength. Adipose fin emerging gradually, its posterior limit as a rounded, free lobe. Adipose fin origin at vertical through vertebral centra 17 (1)– 19 (2) (lectotype 18). Adipose fin terminus at vertical through vertebral centra 35 (1)– 38 (1) (lectotype 36).

Caudal fin deeply forked, lobes subequal. Caudal peduncle length posterior to adipose-fin slightly larger than its depth. Dorsal lobe with 7 (9) branched, 1 (9) unbranched principal, and 13 (1)–20 (1) (lectotype 15) procurrent fin-rays. Ventral lobe with 8 (9) branched, 1 (9) unbranched principal, and 16* (1)–21 (1) procurrent fin-rays. Hypural 5 completely free, not fused to hypural 3+4. Seven (6), rarely 6* (1) rays articulated to dorsal caudal-fin plate (4 or 5 on hypurals 3+4 and 2 on hypural 5) and 8 (7) rays articulated to ventral caudal-fin plate (6 on hypurals 1+2 and 2 on parhypural).

Total vertebrae 40* (1)– 42 (5). Ribs 8* (6)– 9(1).

Epiphyseal branch of laterosensory canal on head (S6) with contralateral canals connecting at midline, proceeding posteriorly as a single canal and opening in a single pore.

Coloration in alcohol

Background body coloration yellowish. Ventral region of head and body lighter. Dark brown midlateral stripe wide (Fig. 195), not well delimited, extending from snout until median caudal-fin rays. Paired dorsolateral brown stripe not well delimited along supraoccipital process. Cephalic dark brown pigment along posterior fontanel region. Dorsal fin overall dark brown, except by a hyaline stripe near its base.

Geographic distribution

Pimelodella taeniophora was described from Descalvados, Mato Grosso State, Brazil, Paraguay River basin. It is known from region 343 (Paraguay).

Comments

Pimelodella taeniophora was described based on two syntypes, however, just one of them was effectively described in Regan (1903) description, with 85 mm TL. The specimen nearest to this measure is BMNH 1895.5.17.27, with 96.5 mm TL, 76.6 mm SL, which I hereby designate the lectotype, and BMNH 1895.5.17.28 remains as paralectotype.

What Souza-Shibatta *et al.* (2013) identified as *P. griffini* (Fig. 196) I believe is, in fact, *P. taeniophora*. *Pimelodella griffini* differs from *P. taeniophora* by a smaller adipose fin (23.3–23.6% SL vs. 34.4–40.8% SL in *P. taeniophora*), shorter maxillary barbel (54.9–61% SL vs. 73.9–115.5% SL in *P. taeniophora*), and pectoral-fin spine morphology (posterior margin of pectoral-fin spine bearing 9–12 straight to retrorse dentations along its basal half to two-thirds, these dentations are triangular, the 2–3 distalmost have a broader base, are smaller and straighter vs. posterior margin of pectoral-fin spine bearing 10–13 retrorse dentations along its basal two-thirds, these dentations are triangular, inclined, the ones nearer base more inclined in *P. taeniophora*). Therefore, *P. taeniophora* has chromosomes $2n = 46$, and might present sexual dimorphism in terms of a filamentous prolongation on dorsal-fin unbranched ray.

Material examined

Pimelodella taeniophora. — BMNH 1895.5.27, 1, 76.6 mm SL, lectotype, Brazil, Mato Grosso, Descalvados, 16°44'03"S, 57°44'49"W; BMNH 1895.5.28, 1, xr, 59.6 mm SL, syntypes, Brazil, Mato Grosso, Descalvados, 16°44'03"S, 57°44'49"W; USNM 1698, 3, xr, 61.1–62.9 mm SL, Paraguay?; MZUEL 6457, 1, xr, 78.7, mm SL, Brazil, Mato Grosso do Sul, Corumba, Rio Miranda, 19°34'36"S, 57°1'5"W; MZUEL 6460, 6, xr, 66,7–97.1 mm SL, Brazil, Mato Grosso do Sul, Rio Miranda, 19°34'36"S, 57°1'5"W; MZUSP 25128, 1, 65.5 mm SL, Brazil, Mato Grosso, Cáceres, Rio Paraguai, Cáceres harbor, 16°4'0.0"S, 57°41'0.0"W; MZUSP 42451, 16, 53.1–62.5 mm SL, Brazil, Mato Grosso, Pontes e Lacerda, Rio Guaporé, 15°14'0.0"S, 59°20'0.0"W; MZUSP 44487, 64, 34.4–51.8 mm SL, Brazil, Mato Grosso, Pontes e Lacerda, Rio Guaporé and attached flooded area in Pontes e Lacerda (affluent of Rio Madeira), 15°14'0.0"S, 59°20'0.0"W; MZUSP 44289, 1, 42.1 mm SL, Brazil, Mato Grosso, Jangada Ribeirao, Chiqueirao, ca. 21 km west from Jangada (affluent of Rio Jangada, Rio Cuiabá), 15°7'0.0"S, 56°38'0.0"W; MZUSP 59991, 14, 40.8–64.2 mm SL, Brazil, Mato Grosso do Sul, Bodoquena, Rio Salobra, under the bridge, about 18 km coming from road between Bonito to Bodoquena, 20°40'14.0"S, 56°45'35.0"W; USNM 199172, 5, 72.1–94.1 mm SL, Brazil, Mato Grosso, Upper Yuruena, 9°25'09.6"S, 58°28'40.9"W; USNM 326327, 4, 46.5–50.5 mm SL, Brazil, Mato Grosso, Rio Jauquara in Jauquara (afluente of Rio Dos

Passaros, Rio Paraguai), Barra Do Bugres, 15°09'37.2"S, 57°04'55.8"W; USNM 326339, 64, 37.3–54.1 mm SL, Brazil, Mato Grosso, Rio Guapore at Pontes e Lacerda, BR-174, 15°12'00.0"S, 59°21'00.0"W; USNM 326724, 19, 45.9–78.6 mm SL, Brazil, Mato Grosso, Riacho Monjolinho (Riacho 2) affluente of Rio Preto, at road to Sao Francisco, Diamantino county, 14°24'19.7"S 56°26'14.4"W.

***Pimelodella tapatapae* Eigenmann, 1920**

Pimelodella tapatapae Eigenmann, 1920: 5–6 [original description; “Mouth of Rio Tapa Tapa”, Venezuela; holotype: CAS 57469 (formerly IU 15094)]. — Schultz, 1944: 210 [taxonomic treatment]. — Burgess, 1989: 281 [taxonomic treatment]. — Bockmann & Guazzelli, 2003: 421 [taxonomic treatment]. — Lasso *et al.*, 2004: 171 [taxonomic list]. — Ferraris, 2007: 195 [taxonomic treatment].

Pimelodella tapatae. — Gosline, 1945: 44 [taxonomic treatment, misspelling].

Diagnosis

Pimelodella tapatapae differs from all *Pimelodella* species except *P. itapicuruiensis*, *P. leptosoma*, *P. longipinnis*, *P. megalura*, *P. metae*, *P. montana*, *P. reyesi*, *P. robinsoni* and *P. yuncensis* by having the supraoccipital process not reaching the anterior preopercular plate (unknown in *P. reyesi*). It differs from all above mentioned by having the maxillary barbel reaching caudal-fin origin (*vs.* maxillary barbel reaching at best the adpressed anal fin in *P. itapicuruiensis*, *P. leptosoma*, *P. longipinnis*, *P. megalura*, *P. metae*, *P. montana*, *P. reyesi*, *P. robinsoni* and *P. yuncensis*).

Furthermore, *P. tapatapae* can be diagnosed by maxillary barbel almost reaching caudal-fin origin; supraoccipital process almost reaches the anterior preopercular plate; dorsal lamina of Weberian complex vertebrae concave; unbranched dorsal-fin ray mostly flexible, just basal half partially ossified, delicate; posterior margin of pectoral-fin spine bearing 25–30 small, retrorse dentations along its basal three fourths, these dentations are delicate, numerous; adipose fin slightly more than three times in SL; ventral caudal fin lobe slightly longer; 41 total vertebrae; dark brown midlateral stripe of moderate width, not well delimited, extending from snout to caudal-fin origin.

Description

Measurements in Table 65. Body moderate depth, depth at dorsal-fin origin less than five times in standard length, and moderate compressed, body width at dorsal-fin origin six and half times in SL (Fig. 197). Dorsal profile convex from snout to dorsal fin, slightly concave from dorsal to adipose fin, slightly convex along adipose fin, and concave along the

caudal peduncle. Ventral profile of body convex from snout to branchiostegal membrane, convex between pectoral end pelvic fins, also convex from pelvic to anal fin, and concave from there along the caudal peduncle.

Pseudotympanum large, oval, above posterior process of cleithrum and reaching the straight line of 7th (1) vertebrae. Posterior process of cleithrum triangular, short, its dorsal border slightly concave. Anus and urogenital papilla adjacent. Urogenital papilla tubular, triangular, short. Anus at vertical through second fifth of adpressed pelvic fin; urogenital papilla at verticals through last fourth of adpressed pelvic fin.

Head moderate depressed, depth at supraoccipital-process base slightly less than two times in head length. Mouth sub terminal. Eye slightly elliptical, slightly more than five times in head. Bony interorbital distance a fourth larger than eye diameter. Barbels thin, depressed, and elliptical in cross-section. Maxillary barbel almost reaching caudal-fin origin. Outer mental barbel, when stretched parallel to main body axis, finishing almost at adpressed pectoral fin terminus. Inner mental barbel, when stretched parallel to main body axis, finishing at half pectoral-fin base. Supraoccipital process slightly triangular, narrow, almost reaches the anterior prenuchal plate. Dorsal lamina of Weberian complex vertebrae concave, reaching the supraoccipital process just at its anteriormost part. Branchiostegal rays 6 (1).

Dorsal fin triangular, distal margin convex, moderate length (second branched dorsal-fin ray slightly more than five times in SL) reaching the vertical through third fifth of adpressed pelvic fin. Dorsal fin with I,6 (1), plus anteriormost spinelet. Distance between terminus of dorsal-fin base and adipose-fin origin a third of dorsal-fin base. Anteriormost dorsal-fin pterygiophore inserted posterior to neural spine of vertebrae 4 (1); posteriormost dorsal-fin pterygiophore located ahead of neural (or pseudoneural) spine of vertebrae 9. Unbranched dorsal-fin ray mostly flexible, just basal half partially ossified, delicate.

Pectoral-fin rays I,8 (1), pectoral fin triangular with concave distal border. First pectoral-fin ray roughly straight, with proximal part rigid (Fig. 198), forming a spine and short distal tip flexible and distinctly segmented. Pectoral-fin spine almost seven times in SL. Anterior margin of pectoral-fin spine with smooth serrae along almost all margin. Posterior margin of pectoral-fin spine bearing 25–30 small, retrorse dentations along its basal three fourths. These dentations are delicate, numerous. Also 3 distalmost unossified dentations, not counted.

Pelvic-fin rays i,5 (1), extended pelvic fin triangular with straight distal border. Pelvic-fin origin at vertical through fifth branched dorsal fin ray. Tip of adpressed pelvic fin at

vertical through first fifth of adipose-fin base. First unbranched and flexible ray distinctly shorter than second and third rays, which are subequal; remaining rays progressively shorter.

Anal-fin ray iv,7; distal border of extended anal fin convex. Two anteriormost anal-fin rays vestigial, unsegmented, embedded in thick skin fold. Anal fin origin at vertical through second fifth of adipose-fin base; anal-fin adpressed terminus at vertical through adipose-fin terminus. Tip of anteriormost anal-fin pterygiophore inserted posterior to hemal spine of vertebrae 19 (1). Tip of posteriormost anal-fin pterygiophore inserted ahead of hemal spine of vertebrae 26.

Adipose fin slightly more than three times in SL, forming ascending elevated curve in lateral profile, with deepest point approximately at midlength. Adipose fin emerging gradually, its posterior limit as a rounded, free lobe. Adipose-fin origin at vertical through vertebral centrum 18 (1); adipose-fin terminus at vertical through vertebral centrum 36 (1).

Caudal fin deeply forked, ventral lobe slightly longer. Caudal peduncle length posterior to adipose-fin roughly equal to its depth. Dorsal lobe with 7 (1) branched, 1 (1) unbranched principal and 14 (1) procurrent fin-rays. Ventral lobe with 8 (1) branched, 1 (1) unbranched principal and 15 (1) procurrent fin-rays. Hypural 5 completely free, not fused to hypural 3+4. Median caudal-fin rays not articulated directly to caudal plate. Seven (1) rays articulated to dorsal caudal-fin plate (5 on hypurals 3+4 and 2 on hypural 5) and 8 (1) rays articulated to ventral caudal-fin plate (6 on hypurals 1+2 and 2 on parahypural).

Total vertebrae 41 (1). Ribs 10 (1).

Coloration in alcohol

Background body coloration yellowish. Ventral region of head and body lighter. Dark brown midlateral stripe of moderate width (Fig. 199), not well delimited, extending from snout to caudal-fin origin. Dorsal fin hyaline at base, dusky above hyaline.

Geographic distribution

Pimelodella tapatapae was described from Rio Tapatapa, Lake Valencia basin. It is known from region 304 (South American Caribbean drainages- Trinidad) in Venezuela.

Comments

Pimelodella tapatapae was originally identified as *Rhamdia tofatoa* sp. n. (CAS staff, pers. comm.), a species never described. It has a supraoccipital process not reaching the anterior prenuchal plate, like the *Rhamdia* and *Rhamdella*, and delicate dorsal-fin spine, like *Rhamdella*. However, it also has the hypural 5 completely free, dorsal lamina of Weberian complex vertebrae high, and long barbels, like *Pimelodella*. The posterior fontanel is narrow,

not alike the found in any of the three before mentioned genera. It is surely a intriguing species, and maybe belongs to a new genus, but is here treated provisionally as a *Pimelodella*, as so far is only known from its holotype.

Material examined

Pimelodella tapatapae. — CAS 57469, 1, xr, 121.6 mm SL, holotype, Venezuela, Mouth of Río Tapatapa (into lake Valencia), 10°13'56"N, 67°39'12"W.

***Pimelodella vittata* (Lütken, 1874)**

Pseudorhamdia vittatus Lütken, 1874: 34 [original description; “in flumine Rio das Velhas”]; syntypes: ZMB 9175, ZMUC 271, 274, 275, 283–285, NMW 44442]. — Lütken, 1875: 173–174, unnum. fig. page 173 [detailed description]. — Nielsen, 1974: 50 [type catalog]. — Fricke, 1997: 17 [type catalog]. — Silfvergrip & Paepke, 1997: 171 [type catalog]. — Britski *in* Alves & Pompeu, 2001: 22 [taxonomic treatment]. — Lütken, Alves & Pompeu, 2001: 71–72, unnum. fig. [translation of original description to Portuguese]. — Fricke, 2005: 43 [type catalog].

Pimelodella vittata. — Eigenmann & Eigenmann, 1888: 133 [taxonomic revision, transfer to *Pimelodella*]. — Eigenmann & Eigenmann, 1890: 159–160 [key to *Pimelodella* species; taxonomic revision]. — Eigenmann & Eigenmann, 1891: 29 [taxonomic treatment]. — Eigenmann, 1910: 389 [taxonomic treatment]. — Eigenmann, 1917: 274, pl. XXXV, fig. 16–17 [taxonomic revision]. — Gosline, 1945: 45 [taxonomic treatment]. — Fowler, 1951: 551 [taxonomic treatment]. — Burgess, 1989: 281 [taxonomic treatment]. — Britski *in* Alves & Pompeu, 2001: 22 [taxonomic treatment]. — Bockmann & Guazzelli, 2003: 421 [taxonomic treatment]. — Rosa *et al.*, 2003: 177 [taxonomic list]. — Alves & Pompeu, 2005: 593 [taxonomic list, ecology]. — Ferraris, 2007: 195 [taxonomic treatment].

Rhamdia vittata. — Miranda Ribeiro, 1911: 272 [taxonomic treatment].

Diagnosis

Pimelodella vittata differs from all *Pimelodella* species except *P. australis*, *P. avanhandavae*, *P. buckleyi*, *P. cruxenti*, *P. gracilis*, *P. griffini*, *P. harttii*, *P. ignobilis*, *P. itapicuruensis*, *P. kronei*, *P. lateristriga*, *P. laticeps*, *P. laurenti*, *P. leptosoma*, *P. linami*, *P. macturki*, *P. martinezi*, *P. meeki*, *P. megalura*, *P. metae*, *P. montana*, *P. mucosa*, *P. notomelas*, *P. roccae*, *P. straminea* and *P. taeniophora* by having the dorsal fin with a darker region near the base, followed by a hyaline stripe, and distally darker (unknown in *P. martinezi*). It differs from *P. itapicuruensis*, *P. leptosoma*, *P. megalura*, *P. metae* and *P.*

montana by having the supraoccipital process reaching the anterior prenuchal plate (vs. supraoccipital process not reaching the anterior prenuchal plate in *P. itapicuruensis*, *P. leptosoma*, *P. megalura*, *P. metae* and *P. montana*). It differs from *P. australis*, *P. buckleyi*, *P. cruxenti*, *P. gracilis*, *P. laticeps*, *P. laurenti*, *P. linami*, *P. macturki*, *P. meeki*, *P. mucosa*, *P. notomelas* by having 42 total vertebrae (vs. 41 or less total vertebrae in *P. australis*, *P. laticeps*, *P. laurenti*, *P. linami*, *P. macturki*, *P. meeki*, *P. mucosa*, *P. notomelas* and *P. straminea*; 43 or more total vertebrae in *P. buckleyi*, *P. cruxenti* and *P. gracilis*). It differs from *P. avanhandavae*, *P. harttii*, *P. ignobilis*, *P. kronei* and *P. lateristriga* by the epiphyseal branch of laterosensory canal on head with contralateral canals connecting at midline, proceeding posteriorly as a single canal, and opening in a single pore (vs. epiphyseal branch of laterosensory canal on head with contralateral canals not connecting at midline and opening in two pores, near each other, or connecting and immediately opening in a single pore in *P. avanhandavae*, *P. harttii*, *P. ignobilis*, *P. kronei* and *P. lateristriga*). It differs from *P. griffini*, *P. roccae* and *P. taeniophora* by the hyaline stripe on dorsal fin does not encompass the unbranched fin ray (vs. hyaline stripe on dorsal fin encompass the unbranched fin ray in *P. griffini*, *P. roccae* and *P. taeniophora*). It differs from *P. martinezi* by the supraoccipital process triangular, and maxillary barbel reaching between anal fin origin and first third of adpressed anal fin (vs. supraoccipital process subrectangular, and maxillary barbel reaching anal fin terminus).

Furthermore, *P. vittata* can be diagnosed by maxillary barbel reaching between anal fin origin and first third of adpressed anal fin; posterior margin of pectoral-fin spine bearing 4–9 retorse dentations along basal half to two thirds of margin, these dentations are triangular, small; adipose fin two and half to slightly more than three times in SL; 42 total vertebrae; dark brown midlateral stripe wide, not well delimited, extending from snout to caudal fin origin; paired dorsolateral brown stripe along posterior fontanel and dorsal-fin base; dorsal fin dark at base, followed by a hyaline stripe only in interradiial membrane, and distal half brown.

Description

Measurements in Table 66. Body moderate depth, depth at dorsal-fin origin five to almost six times in standard length, and compressed, body width at dorsal-fin origin slightly more than six to slightly more than seven times in SL (Fig. 200). Dorsal profile convex from snout to dorsal fin, concave from dorsal to adipose fin, slightly convex along adipose fin, and concave along the caudal peduncle. Ventral profile of body slightly convex from snout to branchiostegal membrane, convex between pectoral end pelvic fins, concave from pelvic to anal fin, and also concave from there along the caudal peduncle.

Pseudotympanum large, oval, above posterior process of cleithrum and reaching the straight line of 7th (2) vertebrae. Posterior process of cleithrum triangular, its dorsal border straight. Anus and urogenital papilla adjacent. Urogenital papilla tubular, triangular, short. Anus at vertical through half adpressed pelvic fin; urogenital papilla between verticals through last third and terminus of adpressed pelvic fin.

Head moderate depressed, depth at supraoccipital-process base slightly less to slightly more than two times in head length. Mouth sub terminal. Eye slightly elliptical, four and half to six and half times in head. Bony interorbital distance slightly less than eye diameter. Barbels thin, depressed, and elliptical in cross-section. Maxillary barbel reaching between anal fin origin and first third of adpressed anal fin. Outer mental barbel, when stretched parallel to main body axis, finishing between pectoral fin terminus and last third of adpressed pectoral fin. Inner mental barbel, when stretched parallel to main body axis, finishing between pectoral fin origin and a point slightly posterior to that. Supraoccipital process roughly triangular, narrow. Dorsal lamina of Weberian complex vertebrae reaching the supraoccipital process just at its anteriormost part. Branchiostegal rays 6 (2).

Dorsal fin triangular, distal margin convex, moderate length (second branched dorsal-fin ray slightly more than four to five and half times in SL), reaching between the verticals through last third and terminus of adpressed pelvic fin. Dorsal fin with I,6 (11), plus anteriormost spinelet. Distance between terminus of dorsal-fin base and adipose-fin origin slightly less than dorsal-fin base. Anteriormost dorsal-fin pterygiophore inserted posterior to neural spine of vertebrae 4 (3); posteriormost dorsal-fin pterygiophore located ahead of neural (or pseudoneural) spine of vertebrae 11 (3). Unbranched dorsal-fin ray mostly ossified as a spine, rigid part of moderate length to long (almost or three fourths of first dorsal-fin ray total length), with smooth serrae at its anterior distal third, and small, smooth dentations on posterior distal half.

Pectoral-fin rays I,7 (2)– I,9 (1) (holotype I,8), pectoral fin triangular with concave distal border. First pectoral-fin ray roughly straight, with proximal part rigid (Fig. 201), forming a spine and short distal tip flexible and distinctly segmented. Pectoral-fin spine five to seven and half times in SL. Anterior margin of pectoral-fin spine with small, straight dentations along basal half and smooth serrae along distal half. Posterior margin of pectoral-fin spine bearing 4–9 retorse dentations along basal half to two thirds of margin. These dentations are triangular, small. Also sometimes 1–2 distalmost unossified dentations.

Pelvic-fin rays i,5 (11), extended pelvic fin triangular with straight distal border. Pelvic-fin origin at vertical through dorsal fin terminus. Tip of adpressed pelvic fin between

verticals through first tenth and seventh of adipose fin base. First unbranched and flexible ray distinctly shorter than second and third rays, which are subequal; remaining rays progressively shorter.

Anal-fin rays iii,7 (1); iv,8* (1); v,8 (1); or v,9 (1); distal border of extended anal fin convex. One to three anteriormost anal-fin rays vestigial, unsegmented, embedded in thick skin fold. Anal fin origin between verticals through first fourth of adipose fin base or a point slightly anterior to that; anal-fin adpressed terminus at vertical through adipose-fin terminus. Tip of anteriormost anal-fin pterygiophore inserted posterior to hemal spine of vertebrae 21 (2). Tip of posteriormost anal-fin pterygiophore inserted ahead of hemal spine of vertebrae 29 (2).

Adipose fin two and half to slightly more than three times in SL, forming ascending elevated curve in lateral profile, with deepest point approximately at midlength. Adipose fin emerging gradually, its posterior limit as a rounded, free lobe. Adipose-fin origin at vertical through vertebral centrum 18 (2);); adipose-fin terminus at vertical through vertebral centra 36 (1) or 37* (1).

Caudal fin deeply forked, dorsal lobe slightly longer. Caudal peduncle length posterior to adipose-fin slightly larger than its depth. Dorsal lobe with 7 (10) branched, 1 (10) unbranched principal and 8* (1)–16 (1) procurrent fin-rays. Ventral lobe with 8 (10) branched, 1 (10) unbranched principal and 7* (1)–20 (1) procurrent fin-rays. Hypural 5 completely free, not fused to hypural 3+4. Median caudal-fin rays not articulated directly to caudal plate. Seven* (2) rays articulated to dorsal caudal-fin plate (5 on hypurals 3+4 and 2 on hypural 5) and 8* (1) or 9 (1) rays articulated to ventral caudal-fin plate (6 or 7 on hypurals 1+2 and 2 on parahypural).

Total vertebrae 42 (3). Ribs 8* (2)–9 (1).

Epiphyseal branch of laterosensory canal on head (S6) with contralateral canals connecting at midhead, proceeding posteriorly as a single canal and opening in a single pore.

Coloration in alcohol

Background body coloration yellowish. Ventral region of head and body lighter. Dark brown midlateral stripe wide (Fig. 202), not well delimited, extending from snout to caudal fin origin. Paired dorsolateral brown stripe along posterior fontanel and dorsal-fin base. Cephalic dark brown pigment at posterior fontanel region. Dorsal fin dark at base, followed by a hyaline stripe only in interradiial membrane, and distal half brown.

Geographic distribution

Pimelodella vittata was described from Rio das Velhas basin, from São Francisco drainage. It is known from regions 327 (S. Francisco) and 328 (Northeastern Mata Atlantica), in Brazil.

Comments

From the type series, I was able to examine SMNS 2025, ZMB 9175 and NMW 44442. Among them, I hereby designate the specimen of ZMB 9175 with 61.8 mm SL as lectotype, and remain specimens as paralectotypes. The aforementioned specimen is extremely unpigmented, but otherwise is a good representative of this species. Among the paralectotypes, the color pattern is better preserved on NMW 44442 specimens (Fig. 203).

Alves & Pompeu (2005) reported *Pimelodella vittata* diet as based mainly in insects, and extinct in Rio das Velhas basin.

Material examined

Pimelodella vittata. — ZMB 9175, 1, xr, 61.8 mm SL, lectotype, Brazil, Minas Gerais, small lakes and streams into Rio das Velhas, 19°32'25"S, 43°56'34"W; ZMB 9175, 1, xr, 53.2 mm SL, syntypes, Brazil, Minas Gerais, small lakes and streams into Rio das Velhas, 19°32'25"S, 43°56'34"W; MZUSP 88162, 5, 46.2–54.8 mm SL, Brazil, Bahia, Iaçu, Rio Paraguassú, at Fazenda Os Touros, 18Km from Iaçu, 12°41'11.0"S, 40°7'5.0"W; USNM 44979, 1, 68.3 mm SL, Brazil, Lagos Santa (Lagoa Santa?), 19°38'19.0"S 43°53'32.9"W.

***Pimelodella yuncensis* Steindachner, 1902**

Pimelodella yuncensis Steindachner, 1902: 135–136 [original description; “Bache in Pacasmayo, Nordperu” (Stream in Pacasmayo, Northern Peru); syntype: ZMS 7870]. — Eigenmann, 1910: 389 [taxonomic treatment]. — Eigenmann, 1917: 253, pl. XXXV, fig. 23 [taxonomic revision]. — Eigenmann, 1921b: 514 [taxonomic list]. — Eigenmann, 1922b: 41–42 [key to *Pimelodella* species; taxonomic treatment]. — Eigenmann, 1922c: 208 [taxonomic treatment]. — Eigenmann, 1924: 238 [taxonomic treatment]. — Gosline, 1945: 46 [taxonomic treatment]. — Silfvergrip, 1996: 99 [taxonomic treatment, comparison with *Rhamdia xetequepeque*]. — Ortega & Vari, 1986: 15 [taxonomic list]. — Burgess, 1989: 281 [taxonomic treatment]. — Bockmann & Guazzelli, 2003: 421 [taxonomic treatment]. — Ferraris, 2007: 195 [taxonomic treatment].

Rhamdia gilli Starks, 1906: 769–770, pl. LXV, fig. 1 [original description; “Eten, Peru, Rio Eten”; holotype: USNM 53472]. — Eigenmann, 1910: 387 [taxonomic treatment, used

the genus *Rhamdia*, but treated under *Rhamdella*]. — Eigenmann, 1917: 253 [taxonomic treatment, junior synonym of *Pimelodella yuncensis*]. — Gosline, 1945: 46 [taxonomic treatment, junior-synonym of *P. yuncensis*]. — Burgess, 1989: 278 [taxonomic treatment]. — Ferraris & Vari, 1992: 38 [type catalog]. — Bockmann & Miquelarena, 2008: 45, 47 [taxonomic treatment, junior-synonym of *R. quelen*].

Rhamdella gilli Gosline, 1945: 35 [taxonomic treatment]. — Bockmann & Guazzelli, 2003: 422 [taxonomic treatment]. — Ferraris, 2007: 196 [taxonomic treatment].

Pimelodella peruense Fowler, 1915: 214–2016, fig. 4 [original description; “Peruvian Amazon”; holotype: ANSP 21932]. — Fowler, 1939: 287 [taxonomic list]. — Böhlke, 1984: 142 [type catalog].

Pimelodella puruensis. — Eigenmann, 1917: 240 [taxonomic treatment, misspelling]. — Eigenmann & Allen, 1942: 43, 98 [taxonomic list, taxonomic treatment, misspelling]. — Gosline, 1945: 44 [taxonomic treatment, misspelling].

Pimelodella peruensis. — Fowler, 1951: 548, fig. 564 [taxonomic treatment, name correction]. — Ortega & Vari, 1986: 14 [taxonomic list]. — Burgess, 1989: 281 [taxonomic treatment]. — Bockmann & Guazzelli, 2003: 420 [taxonomic treatment]. — Ferraris, 2007: 194 [taxonomic treatment].

Diagnosis

Pimelodella yuncensis can be diagnosed from all *Pimelodella* with exception of *P. cruxenti*, *P. laticeps*, *P. modesta*, *P. montana* and *P. pectinifera* by having an overall dark brown body. It differs from all above mentioned by having the supraoccipital process not reaching the anterior preopercular plate. Furthermore, *P. yuncensis* can be diagnosed by maxillary barbels reaching between half adpressed pectoral fin and terminus of adpressed pelvic fin; supraoccipital process not reaching the anterior preopercular plate; posterior margin of pectoral-fin spine with 5–7 retrorse dentations along basal two thirds, these dentations are triangular, relatively short; adipose fin two and half to four times in SL; 37–41 total vertebrae; dark brown midlateral stripe narrow, not well delimited, extending from snout to caudal fin origin; region adjacent to this stripe lighter; dorsal fin completely brown, without hyaline stripe.

Description

Measurements in Table 67. Body deep, depth at dorsal-fin origin four and half to almost six times in standard length; and compressed, body width at dorsal-fin origin six to ten times in SL (Fig. 204). Dorsal profile convex from snout to dorsal fin, concave from dorsal to

adipose fin, slightly concave along adipose extension, and concave along the caudal peduncle. Ventral profile of body slightly convex from snout to branchiostegal membrane, concave from branchiostegal membrane to pectoral fin, slightly concave from this point to pelvic fin, and concave straight from pelvic along the caudal peduncle.

Pseudotympanum large, oval, dorsal to posterior process of cleithrum and reaching the straight line of 7th (4) or 8th (2) vertebrae. Posterior process of cleithrum triangular, short, its dorsal border slightly concave. Anus and urogenital papilla adjacent. Urogenital papilla tubular, triangular, short. Anus between verticals through second fifth and half adressed pelvic fin; urogenital papilla between verticals through third fifth and a point slightly posterior to pelvic fin adressed terminus.

Head usually deep, depth at supraoccipital-process base usually less than two times in head length. Mouth sub terminal. Eye slightly elliptical, four and half to five and half times in head. Bony interorbital distance roughly equal to eye diameter. Barbels thin, slightly depressed and elliptical in cross-section. Maxillary barbels reaching between half adressed pectoral fin and terminus of adressed pelvic fin. Outer mental barbel, when stretched parallel to main body axis, finishing between pectoral fin origin and first fourth of adressed pectoral fin. Inner mental barbel, when stretched parallel to main body axis, almost reaching branchiostegal membrane ventral limit or slightly surpassing this point. Supraoccipital process narrow, triangular, not reaching the anterior prenuchal plate. Dorsal lamina of Weber complex vertebrae of medium height, reaching the supraoccipital process just at its anteriormost part. Branchiostegal rays 6* (10)– 7 (1).

Dorsal fin triangular, distal margin concave, of moderate length (second branched dorsal-fin ray five to six and half times in SL), reaching between verticals through half and last third of adressed pelvic fin. Dorsal fin with I,6 (12) plus anteriormost spinelet. Distance between terminus of dorsal-fin base and adipose-fin origin roughly the same as dorsal-fin base. Anteriormost dorsal-fin pterygiophore inserted posterior to neural spine of vertebrae 4 (17); posteriormost dorsal-fin pterygiophore located ahead of neural (or pseudoneural) spine of vertebrae 10 (1), 11* (14) or 12 (2). Unbranched dorsal-fin ray mostly ossified as a spine, rigid part relatively short (approximately two thirds of first dorsal-fin ray total length).

Pectoral-fin rays I,7 (1)– I,9 (3) (lectotype I,8), pectoral fin triangular with concave distal border. First pectoral-fin ray curved, with proximal part rigid (Fig. 205), forming a spine and short distal tip flexible and distinctly segmented. Pectoral-fin spine almost six to seven times in SL. Anterior margin of pectoral-fin spine with small, sparse, smooth, straight dentations along basal two thirds, and serrae along distal third. Posterior margin of pectoral-

fin spine with 5–7 retrorse dentations along basal two thirds. These dentations are triangular, relatively short. Plus sometimes 1–2 unossified distalmost dentations, not counted.

Pelvic-fin rays i,5 (12), extended pelvic fin triangular with straight distal border. Pelvic-fin origin at vertical through dorsal fin terminus. Tip of adpressed pelvic fin between verticals through adipose fin origin and its first tenth. First unbranched and flexible ray distinctly shorter than second and third rays, which are subequal; remaining rays progressively shorter.

Anal-fin rays iii,7* (1); iv,7 (1); v,7 (1); iv,8 (1); v,8 (1); iv,9 (2); or v,9 (3); distal border of extended anal fin convex. One to three anteriormost anal-fin rays vestigial, unsegmented, embedded in thick skin fold. Anal fin origin between verticals through first fifth and first third of adipose-fin base. Anal-fin adpressed terminus at vertical through adipose-fin terminus. Tip of anteriormost anal-fin pterygiophore inserted posterior to hemal spine of vertebrae 19 (4), 20 (8), 21* (5) or 22 (2). Tip of posteriormost anal-fin pterygiophore inserted ahead of hemal spine of vertebrae 27 (11), 28* (4), 29 (2), or 30 (1).

Adipose fin two and half to four times in SL, forming ascending elevated curve in lateral profile, with deepest point approximately midlength. Adipose fin emerging gradually, its posterior limit as a rounded, free lobe. Adipose-fin origin at vertical through vertebral centra 16 (1)– 21 (2) (lectotype 18); adipose-fin terminus at vertical through vertebral centra 33 (3)– 37 (2) (lectotype 34).

Caudal fin deeply forked, lobes subequal. Caudal peduncle length posterior to adipose fin roughly equal to its depth. Dorsal lobe with 7 (11), rarely 5 (1) branched, 1 (12) unbranched principal and 10* (1)– 17 (2) procurrent fin-rays. Ventral lobe with 8 (11), rarely 6 (1) branched, 1 (12) unbranched principal and 8* (1)– 30 (1) procurrent fin-rays. Hypural 5 completely free, not fused to hypurals 3+4. Median caudal-fin rays not attached directly to caudal plate. Seven (9), rarely 6 (1) or 8* (1) rays articulated to dorsal caudal-fin plate (4, 5 or 6 on hypurals 3+4 and 2 on hypural 5) and 8* (9), rarely 7 (1) rays articulated to ventral caudal-fin plate (5 or 6 on hypurals 1+2 and 2 on parahypural).

Total vertebrae 37 (2)– 41 (2) (lectotype 39). Ribs 8 (5)– 10 (2) (lectotype 9).

Epiphyseal branch of laterosensory canal in head (S6) with contralateral canals connected, emerging as a single pore right after the connection of the two contralateral canals.

Coloration in alcohol

Background body coloration yellowish to brownish. Ventral region of head and body lighter. Dark brown midlateral stripe narrow (Fig. 206, 207), not well delimited, extending

from snout to caudal fin origin. Region adjacent to this stripe lighter. Cephalic dark brown pigment along posterior fontanel region. Dorsal fin completely brown, without hyaline stripe.

Geographic distribution

Pimelodella yuncensis was described from Rio Jequetepeque basin, Northwestern Peru. *Pimelodella peruensis*, its junior-synonym, was described from Peruvian Amazon. *Rhamdia gilli*, another junior-synonym, was described from Eten River, also Northwestern Peru. Therefore, *Pimelodella yuncensis* is known from region 336 (Central Andean Pacific slopes).

Comments

Rhamdia gilli (Fig. 208) Starks (1906) was included in *P. yuncensis* synonym by Eigenmann (1917). Gosline (1945) treated this species both as *Rhamdella gilli* and *Rhamdia gilli*, the last under *P. yuncensis* synonym. Silfvergrip (1996:31) transferred it tentatively to *Rhamdella*, due the presence of an opened posterior fontanel, but also treated it in the synonym of *Rhamdia quelen* (Silfvergrip, 1996: 96). Bockmann & Guazzelli (2003) tentatively treated this species as *Rhamdella gilli*, following Eigenmann (1910) and Gosline (1945). Bockmann & Miquelarena (2008) argued that, despite the opened posterior fontanel, *R. gilli* is very similar to *R. quelen* in overall appearance, and tentatively treated it as a junior-synonym of *R. quelen*.

I agree with Eigenmann (1917) that *R. gilli* is a junior-synonym of *P. yuncensis*. The body shape, pectoral-fin spine morphology and coloration are very similar of the one found in *P. yuncensis*, and additionally to the opened posterior fontanel, I would add that also the transverse processes of Weberian complex vertebrae are more alike the ones from *Pimelodella* species than *Rhamdia*.

Pimelodella peruensis (Fig. 209) was described by Fowler (1915) from a small specimen from "Peruvian Amazon". Eigenmann (1917) and Eigenmann & Allen (1942) misspelled this species as *P. puruensis*, including it in the revised material, but suggesting it might be a younger form of other species, since it was only known from the small holotype. I believe this species is indistinguishable from *P. yuncensis*, with which shares the overall body shape, proportions, and particular coloration pattern, very different from other *Pimelodella*. The comparative measurements of *P. yuncensis* and *P. peruensis* are presented in Table 68.

Pimelodella yuncensis was described from two syntypes, but apparently the one in NMW is lost, and the other from ZSM is poorly preserved. However, there is plenty

comparative material from the region, including topotypes (*e.g.* CAS 75890, 75896), which could be compared. I hereby designate ZSM 7870 as the lectotype, and suggest CAS 75890 and CAS 75896 as securely identified material, better preserved.

Material examined

Pimelodella yuncensis. — ZSM 7870, 1, xr, lectotype, Peru, Pacasmayo (Río Jequetepeque basin), 7°19'22"S, 79°31'34"W; CAS 75890, 15, xr, Peru, Cajamarca, Upper Río Jequetepeque at Llallan, inland from Pacasmayo at 2,437 ft. elev., 7°12'37.0"S, 78°55'21.8"W; CAS 75896, 25, xr, Peru, La Libertad, near railway bridge at Cultambo, a station near Pacasmayo on Río Jequetepeque; water clear; river alternating between swift stretches & quiet pools, 7°19'26.8"S, 79°26'09.9"W; USNM 167856, 3, 66.9–67.4 mm SL, Peru, Creek From Laguna Near Pacasmayo, 7°15'50.5"S, 79°15'16.0"W; USNM 177198, 4, 61.1–95.7 mm SL, Ecuador, San Miguel De Los Colorados, Pichincha Prov, 0°19'48.0"S, 79°19'12.0"W; USNM 441704, 1, 65.4 mm SL, Peru, Creek From Laguna Near Pacasmayo, 7°15'50.5"S, 79°15'16.0"W.

Pimelodella peruensis. — ANSP 21932, 1, xr, 48.2 mm SL, holotype, Peru, Peruvian Amazon, 3°30'22"S, 72°11'26"W.

Other species formerly treated in *Pimelodella*

There are several species formerly treated in *Pimelodella* genus that were excluded in the context of this work. Since I believe they do not belong to *Pimelodella*, they will not be treated thoroughly in the revision. However, here follows my reasons to exclude them from the genus.

***Brachyrhamdia* species**

The catfish genus *Brachyrhamdia* was described by Myers (1927) by original designation as allied to *Pimelodella*, and nowadays is nested within the Heptapteridae family (Bockmann & Guazzelli, 2003; Ferraris, 2007, Eschmeyer, Fricke & van der Laan, 2017) The genus had its validity questioned several times in the literature, due to its uncertain phylogenetic placement among other basal genera of Heptapteridae (Bockmann, 1998; Guazzelli, 2003; Bockmann & Miquelarena, 2008) and resemblance with other heptapterids, being considered indistinguishable from *Pimelodella* (Schultz, 1944; Innes & Myers, 1950; Sands, 1985; Lundberg & McDade, 1986; Axelrod & Burgess *in* Axelrod, 1987; Bockmann, 1998) or even *Rhamdia* Bleeker (1858) (Zarske, 2003). Despite any detailed systematic work on the genus, it has been maintained as valid by default (Bockmann & Guazzelli, 2003;

Ferraris, 2007; Bockmann & Miquelarena, 2008), with six valid species occurring through Amazon and Orinoco basins: *B. imitator* Myers (1927); *B. heteropleura* (Eigenmann, 1912); *B. marthae* Sands & Black (1985); *B. meesi* Sands & Black (1985); *B. rambarrani* (Axelrod & Burgess in Axelrod, 1987); and *B. thayeria* Slobodian & Bockmann (2013).

Slobodian (2013) recovered *Brachyrhamdia* as an apical group inside a broadly unresolved *Pimelodella*, supported by 14 synapomorphies, 6 of them exclusive. Also, an ongoing work (Slobodian & Bockmann, in prep.) recovered *Pimelodella* as paraphyletic, with part of *Pimelodella* species as a monophyletic group more closely related to *Brachyrhamdia*, and those *Pimelodella*+*Brachyrhamdia* sister-group to a clade formed by the rest of *Pimelodella* (proposed as a new genus). Meanwhile all nominal *Pimelodella* were treated in this work, including the ones pertaining to the putative new genus, I consider *Brachyrhamdia* as a valid genus, easily recognizable from *Pimelodella* (e.g. Slobodian & Bockmann, 2013), and its species were not included here.

***Pimelodus altipinnis* Steindachner, 1864**

Pimelodus altipinnis Steindachner, 1864 (Fig. 210), as explained under *P. cristata* section, was suggested as a *Pimelodella* by Eigenmann (1912), based on Steindachner (1864b) description, saying “The species has the general characters of a *Pimelodella*, and it would not be surprising if the small type in the Vienna Museum should prove to be a *Pimelodella* and distinct from the specimens subsequently referred to the same name” (Eigenmann, 1912: 177). This suggestion was followed by Van der Stigchel (1946) and Mees (1974), the last one consulting the type-material and assigning it as a female of *P. cristata*. I also consulted this material (NMW 45601), and radiographs of the specimen, but disagree with Mees (1974) conclusion. The type of *P. altipinnis* is, in fact, a *Rhamdia* due its closed posterior fontanel (remaining just a small residual opening) and supraoccipital process not reaching the anterior prenuchal plate.

***Pimelodella cochabambae* Fowler, 1940b**

Mees & Cala (1989) provided evidence that *Pimelodella cochabambae* is, in fact, an *Imparfinis*, and suggest it probably is a junior-synonym of *Imparfinis minutus*. Despite the transference to *Imparfinis* being well accepted, this species have not been synonymized to *I. minutus* so far (Bockmann & Guazzelli, 2003; Ferraris, 2007), and *I. cochabambae* is currently considered a valid species.

***Nannorhamdia macrocephala* Miles, 1943**

Miles (1945) transferred *N. macrocephala* to *Rhamdella* genus. Since Mees (1974) and Mees & Cala (1989) considered *Nannorhamdia* as a junior-synonym of *Imparfinis*, *Nannorhamdia macrocephala* Miles, 1943 was treated as *Imparfinis macrocephalus* in Mees & Cala (1989) review (followed by Burgess, 1989). Bockmann (1998) transferred this to *Pimelodella* genus, and argued USNM 120157 lot of *N. macrocephala* paratypes is the only lot with type status known for this species. Posterior works (e.g. Bockmann & Guazzelli, 2003; Ferraris, 2007) treated this species as a *Pimelodella*.

However, despite the holotype of this species being probably lost (Cala, 1981), MCZ 35876 is another lot of paratypes of *N. macrocephala*, from which I was able to observe CT scans. The paratypes of *N. macrocephala* are small, and their radiographs do not recover enough information to better conclude to which genus it belongs, but probably specimens from USNM 120157 correspond to more than one species (as also reported by Bockmann, 1998). In the CT scans of MCZ 35876 (Fig. 211) we can observe the very wide posterior fontanel, short supraoccipital process, and transverse process of fourth vertebrae only once branched, nothing alike what is found in *Pimelodella*. I believe this species shares resemblance with what Bockmann (1998) treated as the undescribed genus *Maculirhamdia*, composed by *Imparfinis pseudonemacheir* and *I. stictonotus*. For this reason, I believe is better to transfer *N. macrocephala* to *Imparfinis* genus, and the investigation of *Imparfinis* should solve the correct placement of this species.

***Pimelodella parva* Güntert, 1942**

Pimelodella parva (Fig. 212) was described for Paraguay River basin, and upon examination of the holotype I could infer this species is a juvenile of *Pimelodus*. The name *Pimelodus parvus* is previously occupied by *Pimelodus (Rhamdia) parvus* Boulenger (1898), and the problems related to this species are already being tackled in an ongoing work (Rocha & Slobodian, in prep.).

Chapter 2
Molecular taxonomy of *Pimelodella*
Eigenmann & Eigenmann, 1888

Introduction

Integrative taxonomic methods for species delimitation

Taxonomy is the science that pioneers the exploration of life on the planet, providing information subsidiary to ecology, conservation, and virtually all other studies related to living beings. However, taxonomy is not only a tool of technical support for the rest of biology, but a scientific field with its own struggles and objectives.

Although taxonomic studies have existed long before the advent of phylogenetic systematics, this paradigm provided a conceptual and philosophical framework that greatly benefited taxonomy: it brought testability to taxonomic delimitations, with the use of tools for the organization of organisms subjects according to their evolutionary relationships, and helped minimize authority influence in taxonomic decisions (Godfray & Knapp, 2004).

Besides phylogenetic systematics, advancement of several other methods and techniques in the past few decades allowed progress on species recognition and delimitation (Sites & Marshall, 2003; Camargo & Sites, 2013). Such advancements were particularly visible computational time and laboratory techniques (mainly molecular and cytogenetic data). However, such advances have normally been circumscribed to their particular area of expertise, with only partial incorporation into mainstream taxonomic research.

Integrative taxonomy brings an embracing approach, proposing that species delimitation should consider several sources of data (Padial *et al.*, 2010), and that congruence and incongruence among results can be understood in light of each method's characteristics. Sources of data comprehend morphology, molecular, cytogenetic, ecology, reproduction, behavior, geographical distribution, among others (Knowles & Carstens, 2007), and can increase the explanatory power of species hypotheses.

However, it is not uncommon that different sources diverge in their results about species boundaries. Such cases must be analyzed case by case (Schlick-Steiner *et al.*, 2010). When different data disagree, reasons for such discordance should be analyzed (Schlick-Steiner *et al.*, 2010; Carstens *et al.*, 2013) according to possible evolutionary explanations.

Advances in methodologies and techniques for molecular data now allow faster extraction, sequencing and interpretation of results, resulting in substantial increase in their use in taxonomy and systematics (Camargo & Sites, 2013). The pursuit for a single genetic marker for exclusive species delimitation culminated in the initial success of the Barcode of Life project. Hebert *et al.* (2003a) proposed a portion of Cytochrome C Oxidase I (COI) as a global maker for biological identification, with initial success rates between 96–100% (Hebert

et al., 2003a; Barrett & Hebert, 2005). However, several well-established population genetics theories raised doubts about the limitations of such genetic data in delimiting species (Moritz & Cicero, 2004).

The limiting factors for DNA Barcode are several: species delimitation based on exclusivity criteria are usually incongruent with the delimitation through other sources of data (Sites & Marshall, 2004); DNA Barcode is usually not very effective for species recently diverged, without well-established geographical delimitation, and when dealing with a great amount of specimens per species. Posterior studies reported success rates have dropped to less than 70% of accuracy in species delimitation (Meyer & Paulay, 2005; Meier *et al.*, 2008; Elias *et al.*, 2007; Knowles & Carstens, 2007; Whitworth *et al.*, 2007; Wiemans & Fiedler, 2007; Hollingsworth *et al.*, 2009).

In the light of single loci limitations, the best approach to study molecular data in taxonomy includes the use of multiple loci, in order to avoid the “local optimum” given by a single gene tree (Edwards, 2009). Several studies argue that the increase in the number of loci analyzed results in increased accuracy in species delimitation (*e.g.* Dupuis *et al.*, 2012), above all if the species have recently diverged (Knowles & Carstens, 2007).

When using molecular data for taxonomy, different loci often results in different gene trees, and the incongruences among those must be dealt in order to reconstruct a single species tree topology. Myriad processes can lead to incongruences between different gene trees, or even between a particular gene tree and the final species tree: horizontal transfer (including hybridization); gene duplication and extinction; and deep coalescence (Maddison, 1997). Among these, deep coalescence explanation argues ancestral polymorphisms can persist through speciation events, being most likely in large populations with short divergence periods, so that a particular gene tree may not be congruent with the species divergence sequence (Maddison, 1997; Knowles & Carstens, 2007).

Several programs and methods intend to deal with deep coalescence problems, using Maximum Likelihood and Bayesian premises, like STEM (Kubatko *et al.*, 2009), BEST (Liu & Pearl, 2007; Liu, 2008), BUCKy (Ané *et al.*, 2007), and ASTRAL (Mirarab *et al.*, 2014). The efficiency of those methods is estimated mainly by simulations and computational models, which estimate relative performances in finding the “true” species tree for a specific database (*e.g.* Degnan & Rosenberg, 2006; Knowles & Carstens, 2007; Heled & Drummond, 2010). Works on real groups are getting more common, and demonstrated to recover probable and well-supported species trees (*e.g.* Belfiore *et al.*, 2008; Brumfield *et al.*, 2008; Andrade *et al.*, 2015; Streicher, *et al.*, 2015).

In this chapter, the molecular taxonomy of *Pimelodella* species is studied by species tree and concatenated matrix methods. Results are interpreted against results from morphological delimitation and geographic distribution.

Material and Methods

Taxon sampling

Several species of *Pimelodella*, from most of its geographic range, were included, along with outgroup Heptapteridae taxa. The initial dataset comprises a total of 93 specimens belonging to *Pimelodella*, seven Heptapteridae genera, and one Pimelodidae (*Pimelodus*). Among Heptapteridae, representatives of *Brachyglanis*, *Imparfinis*, *Phenacorhamdia*, *Rhamdia* and *Rhamdioglanis* were included (10 specimens), besides several *Pimelodella*, that comprehends 83 specimens total. Samples of *Pimelodella* were initially identified to species level following results of Chapter 1, and found to represent 26 *Pimelodella* species, 18 already described and and 8 possibly new. The complete list of material examined is presented in Table 70.

The trees were rooted in *Pimelodus* sp.

Molecular data collection

Two mitochondrial (Cytochrome Oxidase C, subunit I and Cytochrome B) and two nuclear (exon-primed intron-crossing (EPIC) markers 39298e1 and 4274e20) were used as sources of data. Cytochrome Oxidase C, subunit I (COI) is one of the most used mitochondrial genes for phylogenetic analysis, as well as for species identification with DNA Barcoding (Hebert *et al.*, 2003a). Despite its limitations (*e.g.* Moritz & Cicero, 2004), COI is a broadly used gene, with a differentiation rate sufficient to detect species differentiation (Hebert *et al.*, 2003a).

Cytochrome B (CytB) is another mitochondrial gene that has been well studied (*e.g.* Irwin *et al.*, 1991). Although more conservative than COI, CytB appears to evolve at approximately three times the rate found in 12S and 16S at lower genetic distances, and closer to twice the rate of these genes at higher genetic distances in some fishes (Sullivan *et al.*, 2000).

The two nuclear genes are exon-primed intron-crossing (EPIC) markers, 39298e1 and 4274e20 (from Li *et al.*, 2010). Introns have been successfully used in species-level studies (*e.g.* Li *et al.*, 2010), and to sequence introns, the primers are designed on adjacent exon regions, and amplify across the intron (therefore, exon-primed intron-crossing). Because

exons are usually more conserved than introns, the EPIC markers can generally be applied across a wider taxonomic range of organisms. Thus, those markers were chosen also because of their amplification and sequencing rates between 44–100% in different species and because they are easily amplified across a broad taxonomic range of teleosts. Their ability to reconstruct species phylogenies has been demonstrated, and they are useful for examining genetic variation at intraspecific and interspecific level simultaneously (Li *et al.*, 2010; Thompson *et al.*, 2014).

Total genomic DNA was extracted from muscle tissues preserved in 96% ethanol using Invitrogen PureLink Genomic DNA kit (Thermo Fisher), according to manufacturer's instructions. Quantification used Qubit 2.0 fluorometer Invitrogen (Thermo Fisher). Partial sequences of the genes were amplified by polymerase chain reaction (PCR) as follows:

Cytochrome C Oxidase subunit I

Mitochondrial gene. Primers used were COI FishF1 (5' TCAACCAACCACAAAGACATTGGCAC 3') and FishR1 (5' TAGACTTCTGGGTGGCCAAAGAATCA 3') described by Ward *et al.* (2005). Amplifications were performed in a total volume of 10 μ L, with 1 μ L of 10x buffer (10 mM Tris-HCl+1.5 mM MgCl₂), 0.5 μ L dNTPs (2.0mM each), 0.4 μ L MgCl₂ (50nM), 0.1 μ L Platinum *Taq* Polymerase (Invitrogen), 0.3 μ L of each primer (0.01mM), 6.4 μ L of distilled water and 1 μ L of template DNA. The thermo-cycler profile consisted of an initial denaturation step at 95°C for 5 minutes, followed by 35 cycles of chain denaturation (95°C for 30s), annealing (56°C for 30s) and nucleotide extension (72°C 45s) each, plus a final extension step at 72°C for 5 minutes (modification of Ward *et al.*, 2005).

Cytochrome B

Mitochondrial gene. Primers used were CytB GLUDG-L (5' TGA CTTGAARAACCA YCGTTG 3') and CytB CB3-H (5' GGCAAATAGGAARTATCATTC 3') described by Palumbi *et al.* (1991). Amplifications were performed in a total volume of 10 μ L, with same proportions as for COI. The thermo-cycler profile consisted of an initial denaturation step at 95°C for 30s, followed by 35 cycles of chain denaturation (94°C for 30s), annealing (48°C for 60s) and nucleotide extension (72°C 1min30s) each, plus a final extension step at 72°C for 5 minutes (modification of Palumbi *et al.*, 1991).

36298e1

Nuclear gene. Primers used were 36298e1F (5'GATCCTGAGGGAYTCCCA YGGTGT 3') and 36298e1R (5'GGGCCAGGACTCTCYTGGTCTTG TAGT 3') described by Li *et al.* (2010). Amplifications were performed in a total volume of 10 μ L, with same proportions as for COI. The thermo-cycler profile consisted of an initial denaturation step at 95°C for 5 minutes, followed by 35 cycles of chain denaturation (95°C for 30s), annealing (60°C for 30s) and nucleotide extension (72°C 45s) each, plus a final extension step at 72°C for 5 minutes.

4174e20

Nuclear gene. Primers used were 4174e20F (5'CTYTCGCTGGCTTTGTCTCAAATCA 3') and 4174e20R (5'CTTTACCATCKCCACTRAAATCCAC 3') described by Li *et al.* (2010). Amplifications were performed in a total volume of 10 μ L, with same proportions as for COI. The thermo-cycler profile consisted of an initial denaturation step at 95°C for 5 minutes, followed by 35 cycles of chain denaturation (95°C for 30s), annealing (60°C for 30s) and nucleotide extension (72°C 45s) each, plus a final extension step at 72°C for 5 minutes.

PCR products were visually identified on an 1.5% Agarose SB gel (2 μ L Gel Red per plate, 2 μ L loading dye and 2 μ L PCR product per sample), running at 100V, 100mA for 8 minutes in an electrophoresis chamber, and revealed in a transilluminator station.

Successfully amplified samples were purified to remove unincorporated primers and dNTPs with ExoSapIT Enzyme Mix (Affymetrix). A 2 μ L total volume solution was prepared (0.8 μ L ExoSap enzyme, 1.2 μ L distilled water) and added to the 8 μ L PCR product for each sample. The thermo-cycler profile consists of 36°C for 30 minutes, and 80°C for 20 minutes.

The purified PCR products were then sequenced using BigDye v2.1 cycle sequencing agent, in a total volume of 10 μ L, with 1.75 μ L of 5x BigDye buffer, 0.5 μ L of BigDye, 0.5 μ L of 1.0 μ M primer per direction, 6.25 μ L of nuclease-free water and 1 μ L of PCR product. The thermo-cycler profile consisted of 35 cycles of denaturation (95°C 30s), annealing (50°C 30s), and extension (60°C 4 min). The BigDye products were purified with Sephadex G-50 (Sigma-Aldrich) for exceeding fluorescent ddNTPs, and dried at 95°C for 30 minutes. The purified products were then loaded on an automatic sequencer ABI 3730XL in Laboratories of Analytical Biology at National Museum of Natural History, Smithsonian Institution. All

sequences were read for forward and reverse. The successfully sequenced specimens for each gene are presented in Table 71.

Processing, alignment of sequenced data and obtaining models

The obtained electropherograms were individually inspected and assembled in contigs of forward and reverse strands using Geneious v. 10.0.9 (Kearse *et al.*, 2012). All sequences of each gene were independently aligned using the MUSCLE alignment algorithm (Edgar, 2004) in Geneious with 10 iterations. Aligned sequences were re-checked individually for obvious misalignments in Geneious.

The aligned sequences were saved in nexus format, and The Akaike information criteria (AIC) was employed to evaluate the best fitting nucleotide substitution models independently for each matrix using MrModelTest v.2.2 (Nylander, 2004) in PAUP* (Swofford, 1998).

Phylogenetic inferences

Two analyses were performed with the obtained gene matrices, in order to compare the explanatory power of each one separately for the taxonomy of *Pimelodella*: a Species Tree was inferred by Maximum Likelihood method based on separate gene trees; and a Maximum Likelihood best tree was searched in a concatenated matrix of all genes. Both methods are explained as follows.

Species Tree inference

In order to accommodate possible inconsistencies among the different gene trees, a Maximum likelihood species tree was inferred. Unrooted gene trees were estimated with Maximum Likelihood using RAxML v. 8.2.7 (Stamatakis, 2014) in RStudio v. 1.0.143 (RStudio team, 2016), for best tree and bootstrap, under GTRGAMMAI model with 200 rapid bootstrap replicates, on individual loci. Number of informative parsimony sites, percentage of GC content, length of alignment and average bootstrap values were also calculated with a customized R script, using packages ips 0.0-7 and ape, for each gene. Full script is presented in Attachment 2. Subsequently, Species Tree analyses were then performed in ASTRAL-III (Sayyari & Mirarab, 2016) using gene trees and bootstrap trees as input, with the tree rooted at *Pimelodus*. All above analysis were performed on a MacBook computer. Obtained trees were visualized in MEGA v.5.0 (Tamura *et al.* 2011) and treated in Adobe Photoshop and Illustrator. Nodes below 50% of bootstrap values were collapsed and the collapsed tree is presented comparatively.

Concatenated matrix tree inference

Aligned genes were concatenated into a single matrix and phylogenetic relationships inferred by Maximum Likelihood method, performed at CIPRES Science Gateway portal (Miller *et al.*, 2010), using RAxML v. 8.2.10 (Stamatakis, 2014), random starting trees, GTRGAMMA model and 1000 bootstrap iterations. *Pimelodus* was used to root the tree. Obtained best tree and bootstrap tree were compared, but best tree kept. Trees were visualized in MEGA v.5.0, and treated in Adobe Photoshop and Illustrator.

Results

Genes amplified and sequenced per specimen are presented in Table 71. All data obtained was included in analyses, despite the fact that missing data might have topological and branch length consequences for phylogenetic reconstruction under maximum likelihood method (Naylor *et al.*, 2012). Also, some variation observed among closely related taxa might be the consequence of minor differences induced by small sections of missing data. Eighty *Pimelodella* sequences were included, representing to 26 species (18 valid and 8 possibly new), plus 10 specimens of five other Heptapteridae genera and one *Pimelodus* (Pimelodidae).

Species tree analysis

For each gene matrix, the fragment length, number of parsimony informative sites, GC content and mean bootstrap values are presented in Table 72. A summarized version of the species tree generated through ASTRAL-III is presented in Figure 214. That tree version is merely illustrative, to show the overall arrangement taxa, but most of the deeper nodes recovered have low bootstrap value. The full tree was divided in particular clades, with bootstrap values, is presented in Figures 215–219.

The collapsed version of the species tree, with nodes with bootstrap values below 50% collapsed, is presented (summarized) in Figure 220. With the exception of Clade A, none of the clades in Figures 215–219 were fully recovered, and most *Pimelodella* species are in a basal polytomy with other Heptapteridae genera analyzed. Figure 220 clades are presented in Figures 221–226 .

Most uses of mitochondrial data employ sequence variation as a measure of rate variation in a lineage. Measurements of “species distinctness”, however, can be misleading, and inside one particular group some species might show little mitochondrial DNA divergence, while being diagnosable by independent criteria such as morphometrics and color

pattern (Naylor *et al.*, 2012). On the other hand, inside the same particular group, populations of a species might show sequence divergence greater than what is seen in other species. Below, each case is discussed separately, with an interpretation of molecular taxonomy results in light of morphological delimitation presented in Chapter 1.

The first dichotomy separates a group formed by all the material identified as belonging to *Pimelodella cristata* and one *Pimelodella* sp. *cristata* group (Figs. 214, 220: Clade A, 99% bootstrap value) from the remaining taxa analyzed (which include other *Pimelodella* species and representatives of other five Heptapteridae genera) (97% bootstrap value). This clade A (Fig. 215, 221) is composed of *Pimelodella cristata* from several drainages, and a putatively new species similar to *Pimelodella cristata*, however with a very different color pattern, here designated *Pimelodella* sp. *cristata* group. *Pimelodella cristata* from Tapajós (region 320) and Amazonas Guiana Shield (region 315) were recovered as monophyletic groups. However, one *P. cristata* from Madeira-Mamoré basin (region 318) was recovered more closely related to *P. cristata* from other basin than to *P. cristata* from Madeira-Mamoré.

In this case, molecular data was mostly congruent with morphological identification, but failed to recover a putatively new species as different from other *Pimelodella cristata*. The latter is a broadly distributed species, with little morphological variation, and promptly distinguishable from most of its congeners by the more numerous vertebrae (46–52) and lighter coloration (see Chapter 1 for more information). The molecular data, as the morphological, grouped all *Pimelodella cristata* together, and did not bring a much better resolution to this problem.

The dichotomy that recovered clade B (Fig. 216) as sister to the remaining species has a very low bootstrap value (9%), and the relationships among all the species but the ones pertaining to clade A must be treated as unresolved at this point. Therefore, I will only discuss the relationships with higher support values, not collapsed in Figure 220 large polytomy.

All *Rhamdia* specimens analyzed were recovered as a monophyletic group (Fig. 216; 222: B1), but their relationships with other Heptapteridae are not well-supported. *Pimelodella mucosa* was recovered in B2 clade (Fig. 222) as more closely related to other Heptapteridae than to other *Pimelodella* species. This may be due an artifact related to missing data, since only mitochondrial genes were successfully sequenced for that species. However, it is important to notice that *Pimelodella mucosa* is notably different from other *Pimelodella* species regarding the morphology.

A large section of *Pimelodella* species was recovered in clade B3 (Fig. 223). Specimens of *Pimelodella gracilis* were placed in a large polytomy, some of them more closely related to *Pimelodella taeniophora* than to other *Pimelodella gracilis* specimens. As aforementioned, some variation observed among closely related taxa might be consequence of minor differences induced by small sections of missing data. But even disregarding that, molecular data disagree with the recognition of *Pimelodella gracilis* and *P. taeniophora* as different species. This topic deserves further study, because not all specimens included in this analysis were radiographed, and both species are distinguished on the basis of vertebral counts. Also, some individuals of *Pimelodella avanhandavae* were recovered in this clade, meanwhile other were recovered in clade C (Fig. 217, 224).

Several specimens of *Pimelodella meeki* from different localities were placed in a single clade (Figs. 216, 223), with 97% bootstrap value, in agreement with their morphological delimitation. However, in the collapsed tree, specimens of both *Pimelodella howesi* and *P. brasiliensis* appear in a polytomy. There was a difference in the number of genes successfully sequenced for specimens of each species, and this may account for the failure in recovering the species.

The Clade C was recovered with 70% of bootstrap value (Figs. 217, 224), composed of another part of the specimens identified as *Pimelodella gracilis*, *Pimelodella* aff. *gracilis*, *Pimelodella* sp. *cristata* group and *Pimelodella avanhandavae*. All of those have 46 or more total vertebrae, except *P. avanhandavae* (which has 41–45 total vertebrae). Although molecular data recovers *Pimelodella* sp. *cristata* group from Guianas as a monophyletic group, they did not recover *Pimelodella gracilis*, or even the *P. gracilis* from the Paraguay basin, as monophyletic. Once again, missing data imbalances might explain this result. The separation of all *Pimelodella avanhandavae* and *P. gracilis* specimens in two somewhat distantly-related groups deserves further investigation.

Clade D (Fig. 218) is not strongly supported, and some of its species are scattered in a large polytomy (as presented in Fig. 225). Among those, *Pimelodella modesta* specimens were placed in a well-supported clade (100% bootstrap value). Also recovered was a clade formed by species of *Pimelodella* from coastal drainages in Southern and Southeastern Brazil: *Pimelodella australis*, *P. ignobilis*, *P. lateristriga* and *P. kronei*. Meanwhile specimens of *P. australis* were recovered as a monophyletic group (despite incomplete gene sampling for one specimen), *Pimelodella ignobilis*, *P. lateristriga* and *P. kronei* were placed in a polytomy. *Pimelodella ignobilis* is easily diagnosable from *P. lateristriga* and *P. kronei* (see Chapter 1), especially by features of coloration pattern and pectoral-fin spine morphology. Specimens of

Pimelodella lateristriga and *P. kronei* included in this work, however, are all from the same basin (Ribeira de Iguape), and the inclusion of *P. lateristriga* from other localities is necessary to properly tackle this problem. Some authors in the past have already suggested *P. transitoria* (here synonymized under *P. kronei*) as indistinguishable from *P. lateristriga* (Haseman, 1911; Eigenmann, 1917), and the molecular results here corroborate that conclusion.

Clade E (Figure 219) differs from E' (Figure 226) by the exclusion, in the latter, of *Pimelodella serrata*, which falls into the large basal polytomy (and both specimens of *P. serrata* were not recovered as a monophyletic group). Among species common to clade E and E', all but one *Pimelodella boliviana* are successfully recovered as a monophyletic group, with two of them having complete gene data, and two with three genes sequenced (one of these falling outside the *P. boliviana* clade). Specimens of *P. leptosoma* and *Pimelodella* aff. *boliviana* were successfully recovered as monophyletic clades, despite different gene sampling for individual specimens.

In sum, the species tree methodology somewhat agreed with morphological delimitation, recovering part of *Pimelodella* species as well-supported monophyletic groups. However, the blatant exceptions are *Pimelodella avanhandavae* and *P. gracilis*, which were recovered as paraphyletic groups, and even specimens from the same basin placed far apart. Those species deserve further investigation, since in Chapter 1 I propose *P. gracilis* is easily diagnosable by the higher total vertebrae count (46 or more). However, I could not radiograph all specimens used in the molecular analyses to confirm this character, and some specimens included here are probably juveniles (less than 60 mm SL). After radiographing all specimens, I can proceed in re-investigating the morphological data used to delimit the species, and see if my initial identification survives this reciprocal illumination of morphological and molecular data.

Pimelodella lateristriga+*P. kronei* came out as a monophyletic group in this analysis, and some authors (Haseman, 1911; Eigenmann, 1917) have suggested that non-troglobitic *P. kronei* was indistinguishable from *P. lateristriga*. Since this work only included non-troglobitic *P. kronei*, and *P. lateristriga* only from Ribeira de Iguape, synonymy between the two species cannot yet be formally proposed.

Concatenate matrix analysis

A concatenated matrix of all gene matrices was assembled, and the best tree obtained from Maximum Likelihood (ML) analysis is presented in Figure 227. Node labels include

bootstrap values of 50% or more, except when the node was not recovered in the bootstrap tree (presented a “–” instead). In order to better illustrate and compare with the Species Tree results, Figures 228–233 shows sections of the tree in Figure 227, delimited by dotted boxes. The color code is that presented in Figures 214–226.

Clade A recovered by the ML analysis (Fig. 228) is consistent with the clade A recovered by the Species Tree (ST) analysis, also with similar internal relationships. As explained for ST, this clade A is composed of *Pimelodella cristata* from several drainages, and a putatively new species similar to *Pimelodella cristata*. Once again, one specimen of *Pimelodella cristata* from Madeira-Mamoré basin (region 318) was recovered as more closely related to *Pimelodella cristata* from other basins than to those from its own basin. All molecular taxonomy results thus point to *Pimelodella* sp. cristata group belonging in fact to *Pimelodella cristata*, and *Pimelodella cristata* being a monophyletic group recognizable by both morphological and molecular data.

The clade B2” (Figure 229) corresponds to clades B1+B2 of Figure 220, and reunite all other analyzed Heptapteridae genera and *Pimelodella mucosa*, with 79% bootstrap value. Once again, *Pimelodella mucosa* was recovered as more closely related to other Heptapteridae than to other *Pimelodella* species. The long length of the branch of this clade uniting *Pimelodella mucosa*+other Heptapteridae genera (except *Rhamdia*) must be taken in consideration before dismiss the result completely in the light of morphological delimitation. The long branch might indicate several synapomorphies uniting *Pimelodella mucosa*+other Heptapteridae genera, but as well might an artifact of long-branch attraction to the outgroups (Bergsten, 2005).

Clade B3” (Figure 230) in the ML analysis corresponds to clade B3 of ST analysis (Figure 223), however, its internal relationships were recovered somewhat differently. As obtained in the ST analysis, in the ML some specimens of *Pimelodella gracilis* were recovered as more closely related to *Pimelodella taeniophora* than to other individuals of *Pimelodella gracilis*, and one *P. gracilis* was recovered as closely related to some *P. avanhandavae*. The group formed by some *Pimelodella gracilis* and all *Pimelodella taeniophora* was recovered with 99% of bootstrap. Therefore, both analyses of molecular data disagree with the recognition of *Pimelodella avanhandavae*, *P. gracilis* and *P. taeniophora* as different species.

Furthermore, in the B3” clade, specimens of *Pimelodella meeki* from different localities were not recovered as a single clade in the ML analysis (Fig. 230). The clade formed by part of *Pimelodella meeki*, *P. brasiliensis*, *Pimelodella* sp. and *P. gracilis*+ *P.*

taeniophora+ *P. avanhandavae* was not recovered in the bootstrap tree, so that relationships of part of *P. meeki* with the remaining *P. meeki* are somewhat indecisive. For this portion of the ML tree, *Pimelodella brasiliensis*, *P. howesi* and *Pimelodella* sp. were recovered as monophyletic, while only *Pimelodella* sp. was recognized as diagnosable by both ST and ML analyses. Morphological and molecular delimitations of *P. avanhandavae*, *P. meeki*, *P. gracilis* and *P. taeniophora* disagree, and those species deserve further study.

Another part of *P. gracilis* specimens were recovered in clade C'' (Fig. 231, orange), as more closely related to part of *Pimelodella avanhandavae* than to other *P. gracilis*. *Pimelodella* sp. cristata group from Guianas was recovered as a monophyletic group, which is congruent with morphological delimitation. The relationship of that clade with other *Pimelodella* has low bootstrap support (Fig. 227), as also seen in the ST analysis (Fig. 220). Once again, *P. serrata* specimens were not recovered as monophyletic, despite belonging to a species easily recognizable by morphological data (see Chapter 1). *Pimelodella megalops* specimens were recovered as a monophyletic group in the ML analysis, differently from the ST.

Clade D'' (Fig. 232, green) from ML analysis was recovered with the same composition as clade D from ST analysis (Fig. 225, green). Both molecular analyses recovered *Pimelodella australis* as a monophyletic group, congruent with morphological delimitation, but recovered *P. ignobilis*, *P. kronei* and *P. lateristriga* as indistinguishable from each other, part of a large clade with 100% of bootstrap value. Inclusion of *P. lateristriga* from other localities is necessary before any further discussions about *P. kronei* and *P. ignobilis* validity.

Clade E'' (Fig. 233) has the same composition as clade E' (Fig. 226). All *Pimelodella leptosoma* specimens were recovered as a monophyletic group, with high bootstrap value (90%), as well as *Pimelodella* aff. *boliviana* (99% bootstrap value). However, despite all specimens of the latter being recovered as monophyletic, that whole clade was not recovered in the bootstrap tree.

In sum, a maximum likelihood analysis on a concatenated matrix mostly agreed with the apical monophyletic groups in a species tree analysis, with exception of small differences regarding *Pimelodella boliviana*, *P. brasiliensis*, *P. howesi* and *P. meeki*. The former three species were not recovered in the ST analysis, but were recovered in the ML analysis, and the last was not recovered in ML, but recovered in the ST analysis. In both molecular analyses, *Pimelodella gracilis* was recovered as paraphyletic, with part of its specimens more closely

related to *P. avanhandavae* and another part to *P. taeniophora*. *Pimelodella avanhandavae* was also recovered as paraphyletic in both analyses.

Material examined

Pimelodella material

Pimelodella australis.— LBP 3332, 2,(20457), Brazil, Rio Grande do Sul, Rio Grande, Atlântico, nameless little stream, 32°09'06.9"S, 52°06'24.2"W; LBP 4782, 1, (25614), Brazil, Rio Grande do Sul, Barra do Ribeiro, Atlântico, Rio Guahyba, 30°18'03.9"S, 51°20'40.8"W; LBP 18896, (54987).

Pimelodella avanhandavae.— LBP 6634, 4, (31967, 31970), Brazil, Paraná, Marilena, Rio Paraná/Bacia do Prata, Rio Água da Marilena, 22°38'52.4"S, 53°04'43.0"W.

Pimelodella boliviana.— LBP 4082, 7, (23503), Brazil, Acre, Mâncio Lima, Rio Moa/Rio Juruá, Rio Japiim, 07°34'28.8S, 72°55'24.9"W; LBP 11002, 3, (50527, 50528, 50529), Brazil, Rondônia, Guarajá Mirim, Amazonas/Madeira, Rio Lajeado, 10°26'23.5"S, 65°20'34.1"W.

Pimelodella aff. boliviana.— LBP 12044, (51805, 51805), Brazil.

Pimelodella brasiliensis.— LBP 8302, 4, (40012, 40014), Brazil, São Paulo, Araras, Rio Paraná/La Plata Basin, Rio Araras, 22°22'42.4"S, 47°25'37.9"W.

Pimelodella cristata.— LBP 4092, 1, (23530), Brazil, Acre, Mâncio Lima, Rio Moa/Rio Juruá/ Rio Japiim, 07°34'28.8"S, 72°55'24.9"W; LBP 5286, 3, (26772, 26773), Brazil, Amapá, Laranjal do Jari, Rio Jari/Rio Amazonas, Igarapé Uiratapurú, 00°34'03"S, 52°34'41"W; LBP 12874, (53498); LBP 13766, (57080, 57081, 57082, 57083); UFRO 7502, 1, (5920), Brazil, Rondônia, Porto Velho, mouth of Rio Machado, Rio Madeira, 08°04'12,80"S, 62°53'36,70"W; UFRO 17668, 1, (8030), Brazil, Rondônia, Costa Marques, Rio Guaporé, 12°05'29.20"S, 64°42'11.60"W.

Pimelodella gracilis.— LBP 9, 22, (3548, 3549, 3588, 3589, 3598, 3599), Brazil, Mato Grosso do Sul, Corumbá, Rio Paraguai, Rio Miranda, 19°34,630"S, 57°01,123"W; LBP 8075, 1, (37213), Brazil, Paraná, Foz do Iguaçu, La Plata Basin, Rio Paraná, 25°25'11.4"S, 54°32'08.2"W; LBP 9240, 2, (44455, 44456), Brazil, Mato Grosso, Cáceres, La Plata Basin, Rio Paraguai, 16°05'14.8"S, 57°42'17.8"W; UFRO 14300, 1, (2303), Brazil, Rondônia, Porto Velho, Rio Guaporé, upstream from Baía das Onças, 12°05'31,1"S, 15°05'10"W; ANSP 182412, 27, (A5063, A5066), Argentina, Corrientes, Various sites including main & braided side channels and backwaters of R. Parana & lower Guayquiraró, ca. 25 km S of Esquina, 30°15'0.0"S, 59°36'30"W; ANSP 182415, 3, (A5205, A5209), Argentina, Corrientes, Rio

Parana (left bank) at private park (Club San Martin) near town of Perichon, N of rt. 12, NE of Corrientes.

Pimelodella aff. gracilis.— LBP 15863, (64153).

Pimelodella howesi.— UFRO 13484, 7, (6674), Brazil, Rondônia, Porto Velho, Ensecadeira da Cachoeira de Santo Antônio, Rio Madeira, 08°48'30"S, 63°36'53"W; UFRO 23913, 1, (7304), Brazil, Rondônia, Guarajá Mirim, Pacaás, Rio Mamoré, 10°51'11,8"S, 65°17'43,4"W.

Pimelodella ignobilis.— LBP 3628, 2, (21648), Brazil, Santa Catarina, Jaraguá do Sul, Atlântico, Rio Itapucu, 25°26'49.3"S, 49°09'37.6"W.

Pimelodella kronei.— LBP 7488, 3, (35557, 35590), Brazil, São Paulo, Registro, Atlântico, Rio Ribeira de Iguape, 24°23'29.8"S, 47°50'06.6"W; LBP 7889, 1, (37053), Brazil, São Paulo, Ubatuba, Atlântico, Rio Indaiá, 23°24'15.3"S, 45°03'50.6"W; LESCO uncat, 3, (not individually numbered), Brazil, Areias/córrego seco, 24°35'0.0"S, 48°36'0.0"W.

Pimelodella lateristriga.— LBP 6835, 8, (33100, 33104), Brazil, São Paulo, Miracatu, Ribeira de Iguape/Atlântico, Rio Fau, 24°12,441'S, 47°28,616'W; LBP 7899, 1, (37071), Brazil, São Paulo, Ubatuba, Atlântico, mouth of Rio Indaiá, 23°23'59.0"S, 45°04'07.2"W.

Pimelodella leptosoma.— LBP 9134, 11, (42728, 43042, 43043), Brazil, Pará, Capitão Poço, Rio Guamá/Amazonas, Igarapé Açu, 01°34'28.3"S, 47°02'03.5"W.

Pimelodella aff. leptosoma.— LBP 5286, 3, (26771), Brazil, Amapá, Laranjal do Jari, Rio Jari/Rio Amazonas, Igarapé Uirapuru, 00°34'03" S, 52°34'41"W.

Pimelodella meeki.— LBP 821, 10, (8610, 8621, 8623, 8645), Brazil, São Paulo, Penápolis; LBP 3667, 3, (21748), Brazil, São Paulo, Botucatu, Rio Tietê/Rio Paraná, Rio Alambari, 22°45'48.2"S, 48°15'41.8"W; LBP 14600, (61044, 61045).

Pimelodella megalops.— ANSP 189112, 5, (6998, 7001), Suriname, Sipalawini, Litanie River at mouth and confluence with Marowini River, just upstream from settlement of Konya Kondre, 3°17'24"N, 54°4'38"W.

Pimelodella aff. megalops.— ANSP 185051, 2, (P4042), Venezuela, Amazonas, Rio Orinoco at Puerto Venado, 4.3 km S of Samariapo, 56.4 km SW of Puerto Ayacucho, 5°12'38"N, 67°48'18"W.

Pimelodella modesta.— LBP 9345, 1, (43902), Peru, Pampa de Hospital/Tumbes, Rio Tumbes/Pacífico, Quebrada Cabuyal, 03°43'07.9"S, 80°25'34.5"W; LBP 9362, 2, (43950, 43951), Peru, Matapalo/Tumbes, Rio Zarumilla/Pacífico, Quebrada Faical, 03°41'24.6"S, 80°13'00.9"W.

Pimelodella mucosa.— LBP 9, 22, (3587), Brazil, Mato Grosso do Sul, Corumbá, Rio Paraguai, Rio Miranda, 19°34,630'S, 57°01,123'W.

Pimelodella serrata.— LBP 4082, 7, (23504), Brazil, Acre, Mâncio Lima, Rio Moa/Rio Jaruá, Rio Japiim, 07°34'28.8"S, 72°55'24.9"W; UFRO 14298, 1, (2304), Brazil, Rondônia, Porto Velho, Rio Guaporé, upstream from Baía das Onças, 12°05'31,1"S, 15°05'10"W.

Pimelodella taeniophora.— LBP 8476, 2, (42467, 42468), Brazil, Mato Grosso, Cáceres, Rio Paraguai/La Plata Basin, Rio Paraguai, 16°03'50.7"S, 57°42'29.8"W.

Pimelodella vittata.— LBP 10477, 1, (49157), Brazil, Minas Gerais, Paracatu, Rio São Francisco, Lagoa Marginal, 17°15'00.2"S, 46°25'21.8"W.

Pimelodella sp..— ANSP 179752, 9, (2089), Guyana, Up. Demerara-Barbice, Essequibo River (east bank) at Kurukupari, 4°39'41"N, 58°40'31"W; LBP 9496, 4, (44621, 44623, 44624), Brazil, Distrito Federal, Brasília, Rio São Francisco, Ribeirão Santa Rita, 15°34'53.7"S, 47°20'34.6"W.

Pimelodella sp. cristata group.— ANSP 189109, 18, (6922, 6923, 6950), Suriname, Sipalawini, Lawa River (Marowijne Dr.), base camp ca. 8 km south-southwest of Anapaike/Kawemhakan (airstrip), 3°19'31"N, 54°3'48"W; LBP 2189, 1, (15549), Venezuela, Caicara del Orinoco/Bolivar, Rio Orinoco, Laguna de Castilleros, 07°30'50,9"N, 66°09'19,8"W.

Other Heptapteridae

Brachyglanis sp..— LBP 1737, 8, (12883), Brazil, Amazonas, Rio Urubu/Rio Amazonas, Corredeira da Pantera, 02°02'32.7"S, 59°50'57.0"W.

Imparfinis sp..— LBP 3667, 3, (21749), Brazil, São Paulo, Botucatu, Rio Tietê/ Rio Paraná, Rio Alambari, 22°45'48.2"S, 48°15'41.8"W; LBP 5027, 1, (25969), Brazil, São Paulo, Rio Claro, Rio Tietê, Rio Passa-Cinco, 22°21'51"S, 47°30'49"W.

Imparfinis stictonotus.— LBP 9942, 1, (46681), Venezuela, Guárico, Cabruta, Orinoco, Rio Manapire, 7°52'04.1"N, 66°12'40.1"W.

Phenacorhamdia sp..— LBP 2468, 1, (16321), Brazil, Mato Grosso, Barra do Garça, Rio Araguaia, Córrego Fundo, 15°52'40.4" S, 52°18'15.5" W.

Rhamdia quelen.— LBP 7395, 7, (35394, 35395), Brazil, São Paulo, Itapeúna, Rio Ribeira de Iguape/Atlântico, Rio Jaguar, 24°35'41.1"S, 48°12'53.3"W.

Rhamdia sp..— LBP 3628, 2, (21649), Brazil, Santa Catarina, Jaraguá do Sul, Atlântico, Rio Itapucu, 25°26'49.3"S, 49°09'37.6"W; LBP 9496, 4, (44622), Brazil, Distrito Federal, Brasília, Rio São Francisco, Ribeirão Santa Rita, 15°34'53.7"S, 47°20'34.6"W.

Rhamdioglanis frenatus.— LBP 8176, 3, (38152), Brazil, São Paulo, Mongagua, Atlântico, Rio Mongagua, 24°05'21.8"S, 46°39'22.4"W.

Tauayia bifasciata.— LBP 826, 3, (8720), Brazil, São Paulo, Pindamonhangaba, 23°02.585'S, 45°23.362'W.

Pimelodidae

Pimelodus sp..— UFRO 17108, 1, (7982), Brazil, Rondônia, Porto Velho, mouth of Rio Cautário, 12°10'58,10"S, 64°34'59,80"W.

Final conclusions

Integrative taxonomy delimitation

Final conclusions

Revisionary taxonomy is frequently dismissed as merely descriptive, which belies its strong intellectual content and hypothesis-driven nature (Wheeler, 2004). And even descriptive taxonomy is not just a tool to be used by the rest of biological studies, but the pioneering exploration of life on Earth, having several derivative functions as it lays the foundation for phylogenetic, ecology and conservational studies (Wilson, 2004), among several others. Without a previous well-done taxonomical study, the unfolding conclusions of other disciplines are weak, unstable and unreliable, at least, and might have cascade-like processes affecting hypotheses and ideas (Bortolus, 2008).

Taxonomic assessment of complex and hyperdiverse groups is not a trivial task for several reasons. The issues of species delimitation and even species conceptualization are long treated in the literature (*e.g.* Baum & Shaw, 1995; Mayden, 1997; de Pinna, 1999; Wheeler & Meier, 2000; de Queiroz, 2007; Camargo & Sites, 2013; Carstens *et al.*, 2013), and are topics still far from being extinguished. Furthermore, working hypothesis on species limits become mired in light of the morphological variation distributed across many specimens and localities (Sabaj & Arce, 2017).

In order to work with practical taxonomy, one has to forego on an unified species concept which embraces both species conceptualization and delimitation at the same time (de Queiroz, 2007), since the practical mishaps are somewhat dependent on the specificities of the biological group in question. The species conceptualization used here in this thesis refer to species necessarily as separately evolving metapopulation lineages, view shared by all contemporary species concepts (de Queiroz, 2007). However, despite fulfilling the necessary properties for species conceptualization, the hypothesis of species as separately evolving metapopulation lineages is not sufficient to species delimitation.

The sufficient assumptions for species delimitation rely on operational criteria, and an unification of those throughout all biological studies is on the verge of impossible. Given species are natural kinds, they can be recognized by homeostatic property clusters (*e.g.* Boyd, 1999), and not by an immutable set of necessary and sufficient conditions. This view is adequate to the Realism accommodation thesis, which claims that the accommodation of inferential practices to relevant causal structures establishes the reliability and inducibility of the system in question (Boyd, 1999; 2002).

The before mentioned operational criteria is adequate to the taxonomic study here conducted, since in the light of more characters and evidence, the boundaries of a given

species can slightly change, but be recognizable nevertheless. The species here recognized have fuzzy boundaries (Kosco, 1993), and the epistemic access condition is based on what is predicated by the type under given conceptual resources. Therefore, in light of the morphological characters (measurements, counts, coloration pattern, etc.) presented by the type, other specimens are accommodated to the conceptual matrix outlined. Likewise, in the light of molecular data, the morphological characters used to delimit a particular species are revisited and questioned about their sufficiency.

The here presented species delimitations are the result of accommodation of morphological variation into a particular species conceptual description, in a manner the species can be recognized, despite the variation found. Most of the time, the morphological and molecular delimitations were congruent. When congruence was not achieved, initial identification was revisited in light of the new evidence.

So far, most of species recovered by molecular taxonomy were also recognized by the used morphological criteria. Some notable exceptions will be discussed furthermore.

Pimelodella avanhandavae, *P. gracilis* and *P. taeniophora* were not recognized as monophyletic entities (and, therefore, separately evolving metapopulation lineages) in molecular analyses. This topic deserves further investigation, since *Pimelodella avanhandavae* can be distinguished from the other two by 42–44 (rarely 41 or 45) total vertebrae, maxillary barbel reaching between origin and adressed last fifth of anal fin, and pectoral fin spine morphology (Fig. 9). *Pimelodella gracilis* have 46 or more total vertebrae, maxillary barbel reaching between half anal-fin base and surpassing caudal-fin origin, and different pectoral fin spine morphology (Fig. 66). *Pimelodella taeniophora* have 40–42 total vertebrae, maxillary barbels as long as the ones of *P. gracilis*, but different pectoral-fin spine morphology (Fig. 194). It is noteworthy these three species have somewhat similar coloration patterns and, in the absence of x-rays, the identification of juvenile specimens (like were part of the specimens used in the molecular analyses) can be troublesome. Furthermore, pectoral-fin spine morphology can vary slightly ontogenetically (e.g. figures 56; 169), what makes the identification of juveniles of *Pimelodella* even more difficult. In the light of molecular results, x-rays of all *P. avanhandavae*, *P. gracilis* and *P. taeniophora* specimens must be taken, in order to re-investigate their identification.

Based on morphological characters, I proposed the synonym of *P. transitoria* to *P. kronei*, both described from Ribeira de Iguape basin. Other authors in the past have already suggested also that *P. transitoria* would be indistinguishable from *P. lateristriga* (Haseman, 1911; Eigenmann, 1917), and the molecular results here corroborate that conclusion.

However, the specimens of *P. lateristriga* included in the molecular analyses belong only to Ribeira de Iguape basin, meanwhile this species have a more broad distribution along several coastal basins in Southeastern and Northeastern Brazil. I believe the inclusion of *P. lateristriga* molecular material from other localities is necessary to properly tackle this problem, and I decide to maintain *P. kronei* as valid until then.

Pimelodella mucosa was recovered in molecular analyses as more closely related to other Heptapteridae genera than to other *Pimelodella*. Despite being recognizable as a *Pimelodella*, *P. mucosa* is notably different from other *Pimelodella* species. The inclusion of more *P. mucosa* molecular material is necessary, in order to investigate if this peculiar outcome is an artifact related to missing data, or if *P. mucosa* is indeed a extremely modified species, even belonging to a new genus. But in any way, this is an interesting outcome.

Considering all morphological diversity, I could observe some characters are more useful to species delimitation, and those were particularly treated under each species diagnosis. Despite small geographic variation in more broadly-distributed species, most *Pimelodella* have somewhat constant coloration patterns, what may serve as a first approach in order to identify those species with notable marks (like paired dorsal stripes, and dark marks on dorsal fin and body). The length of barbels is also useful to species delimitation, especially to those species that have notably short or notably long barbels. The length of adipose fin is also useful to species delimitation. Most of other measurements are somewhat constant among all *Pimelodella* species, but slightly differences and tendencies can give a grasp onto species identification, especially in the context of geographically restricted species. On the other hand, the absence of significant differences on morphometric, meristic and coloration data lead me to synonymize several species to a broadly-distributed *P. cristata*.

The number of total vertebrae and pectoral-fin spine morphology were also very useful characters used to species delimitation. However, acquisition of x-rays might be a hindrance to species identification using number of vertebrae as a character; and several *Pimelodella* species present severed pectoral spines (commonly entangled in fishing nets), what also makes the identification of collection material sometimes troublesome.

Regarding the geographic distribution, most of *Pimelodella* species are restricted to one or few hydrographic ecoregions, as can be observed on the maps presented in Figures 234–240, and detailed in each species' section. Species with broader distributions usually do not have blatant diagnostic features (such as coloration marks, or particularly different pectoral-fin spine morphology), what makes their delimitation and identification even more

troublesome. Particularly for the case of broadly-distributed species, the inclusion of molecular data can bring light to recognition of separately evolving metapopulation lineages.

In sum, this thesis intended to discuss an integrative approach to species delimitation in *Pimelodella*, and so far the delimitations are mostly congruent across methods. The inferences drawn from species delimitation are, however, conservative, in order not to falsely delimit entities that do not represent actual evolutionary lineages (*vide* Carstens *et al.*, 2013). Also, species delimitation might change in the light of new evidence (both increase in sampling as well as different data sources), but this thesis can be considered a first approach in helping to solve the intricacies of species delimitation of a morphologically and species diverse group as *Pimelodella*. Based on the results and problems here presented, specific issues can be approached in the future, with a more intensive sampling of geographical restricted species, and inclusion of molecular data for a more inclusive dataset.

Bibliographic References

- Abell, R., Thieme, M. L., Revenga, C., Bryer, M., Kottelat, M., Bogutskaya, N., Coad, B., Mandrak, N., Balderas, S.C., Bussing, W. & M.L. Stiassny. 2008. Freshwater ecoregions of the world: a new map of biogeographic units for freshwater biodiversity conservation. **BioScience**, **58** (5): 403–414.
- Ahl, E. 1925. Neue südamerikanische Fische aus dem Zool. Museum Berlin. **Sitzungsberichte der Gesellschaft Naturforschender Freunde zu Berlin**: 106–109.
- Albert J. S., Bart Jr. H. L. & R. E. Reis. 2011. Species richness and cladal diversity. *In*: Albert, J. S. & Reis, R. E. (Eds.). **Historical biogeography of Neotropical freshwater fishes**. Berkeley, University of California Press, pp. 89–104.
- Albert, J. S. & T. P. Carvalho. 2011. Neogene assembly of modern faunas *In*: Albert, J. S. & Reis, R. E. (Eds.). **Historical biogeography of Neotropical freshwater fishes**. Berkeley, University of California Press, pp. 119–136.
- Albert, J. S., P. Petri & R. E. Reis. 2011. Major biogeographic and phylogenetic patterns. *In*: Albert, J. S. & Reis, R. E. (Eds.). **Historical biogeography of Neotropical freshwater fishes**. Berkeley, University of California Press, pp. 21–57.
- Aleixo, A., Montag, L.F.A., Wosiacki, W.B., Silva, F.R., Freitas, T.M.S., Peixoto, L.A.W., Araújo, A.B., Avila-Pires, T.C., Hoogmoed, M.S., Rocha, W.A., Poletto, F., Lima, M.F.C., Silva, M.C., Rossi, R.V., Miranda, C.L., Fonseca, R.T.D., Silva, M.R.P., Souza, M.G.C., Coelho, R.F.R. & Carmo, A. 2011 Diagnóstico da Biodiversidade das Unidades de Conservação Estaduais do Mosaico Calha Norte, estado do Pará – Reserva Biológica Maicuru. *In*: **Secretaria de Estado de Meio Ambiente, Plano de manejo da Reserva Biológica Maicuru**: Anexos, Secretaria de Estado de Meio Ambiente, Belém, pp. 5–71.
- de Almeida-Toledo, L. F., Foresti, F., Trajano, E. & S. De Almeida Toledo Filho. 1992. Cytogenetic analysis of the Brazilian blind catfish *Pimelodella kronei* and its presumed ancestor, *P. transitoria*. **Caryologia** **45**: 255–262.
- Alves, C.B.M. & Pompeu, P.S. 2005. Historical changes in the Rio das Velhas fish fauna-Brazil. **American Fisheries Society Symposium** **45**: 587–602.
- Amaral M. F., Aranha, J. M. R. & M. S. Menezes. 1998. Reproduction of the Freshwater Catfish *Pimelodella pappenheimi* in Southern Brazil. **Studies on Neotropical Fauna and Environment** **33** (2): 106–110.

- Andrade, S.C.S., Novo, M., Kawauchi, G.Y., Worsaae, K., Pleijel, F., Giribet, G. & Rouse G.W. 2015. Articulating archiannelids: phylogenomics and annelid relationships, with emphasis on meiofaunal taxa. **Molecular biology and Evolution** **32**(11): 2860–2875.
- Ané, C., Larget, B., Baum, D. A., Smith, S. D., & Rokas, A. 2007. Bayesian estimation of concordance among gene trees. **Molecular Biology and Evolution** **24**(2): 412–426.
- Angulo, A., C. A. Garita-Alvarado, W. A. Bussing & M. I. López. 2013. Annotated checklist of the freshwater fishes of continental and insular Costa Rica: additions and nomenclatural revisions. **Check List** **9** (5): 987–1019.
- Aranha, J. M. R.; Takeuti, D. F. & T. M. Yoshimura. 1998. Habitat use and food partitioning of the fishes in a coastal stream of Atlantic Forest, Brazil. **Revista de Biología Tropical** **46** (4): 951–959.
- Ardila Rodríguez, C. A. 2017. *Pimelodella floridablancaensis* sp. nov. una nueva especie de pez (Siluriformes: Heptapteridae) del Municipio de Floridablanca, Cuenca del Río Magdalena, Departamento de Santander - Colombia. **Peces del Departamento de Santander - Colombia** **9**: 1–20.
- Arratia, G. & A. Cione. 1996. The record of fossil fishes of southern South America. **Münchener Geowissenschaftliche Abhandlungen, Reihe A - Geologie und Paläontologie** **30**: 9–72.
- Arrington, D. A. & K. O. Winemiller. 2006. Habitat affinity, the seasonal flood pulse, and community assembly in the littoral zone of a Neotropical floodplain river. **Journal of the North American Benthological Society** **25** (1): 126–141.
- Axelrod, H. R. 1987. Two new species of catfishes (Siluriformes, Callichthyidae and Pimelodidae) from the Rio Unini, Amazonas, Brazil. **Tropical Fish Hobbyist** **35** (12): 22–25.
- Barrett, R. D., & Hebert, P. D. 2005. Identifying spiders through DNA barcodes. **Canadian Journal of Zoology** **83**(3): 481–491.
- Baum, D.A. & Shaw, K.L. 1995. Genealogical perspectives on the species problem. **Experimental and molecular approaches to plant biosystematics** **53**(289-303): 123–124.
- Behre, E. H. 1928. A list of the fresh water fishes of western Panama between 81°45' and 83°15'W. **Annals of the Carnegie Museum** **18** (2–4): 305–328, Pl. 1
- Belfiore, N. M., Liu, L., & Moritz, C. 2008. Multilocus phylogenetics of a rapid radiation in the genus *Thomomys* (Rodentia: Geomyidae). **Systematic Biology** **57**(2): 294–310.
- Bergsten, J. 2005. A review of long- branch attraction. **Cladistics** **21**(2): 163–193.

- Bertaco, V. A., Ferrer, J.; Carvalho, F. R. & L. R. Malabarba. 2016. Inventory of the freshwater fishes from a densely collected area in South America – a case study of the current knowledge of Neotropical fish diversity. **Zootaxa** **4138** (3): 401–440.
- Bertoni, A. W. 1914. Fauna Paraguaya. **Catálogos sistemáticos de los vertebrados del Paraguay. Peces, batracios, reptiles, aves y mamíferos conocidos hasta 1913.** Asunción. 83p.
- Bertoni, A. W. 1939. Catálogos sistemáticos de los Vertebrados del Paraguay. **Revista de la Sociedad Científica del Paraguay** **4**(4): 1–60.
- Bichuette, M.E. & Trajano, E. 2005. A new cave species of *Rhamdia* (Siluriformes: Heptapteridae) from Serra do Ramalho, northeastern Brazil, with notes on ecology and behavior. **Neotropical Ichthyology** **3**(4): 587–595.
- Bizerril, C. R. S. F. & P. B. S. Primo. 2001. Peixes de Águas Interiores do Estado do Rio de Janeiro. **Rio de Janeiro: Femar**: 95–96/162–164.
- Bockmann, F.A., 1994. Description of *Mastiglanis-asopos*, a new pimelodid catfish from northern Brazil, with comments on phylogenetic-relationships inside the subfamily Rhamdiinae (Siluriformes, Pimelodidae). **Proceedings of the Biological Society of Washington** **107**(4): 760–777.
- Bockmann, F. A. 1998. **Análise filogenética da família Heptapteridae (Teleostei, Ostariophysi, Siluriformes) e redefinição de seus gêneros.** Universidade de São Paulo, São Paulo. Unpublished PhD thesis. 599p.
- Bockmann, F. A. & G. M. Guazzelli. 2003. Family Heptapteridae (Heptapterids). *In*: Roberto Esser dos Reis; Sven O. Kullander; Carl J. Ferraris Jr.. (Org.). **Check List of the Freshwater Fishes of South and Central America.** Porto Alegre: EDIPUCRS. v. 1, p. 406–431.
- Bockmann, F. A. & A. M. Miquelarena. 2008. Anatomy and phylogenetic relationships of a new catfish species from northeastern Argentina with comments on the phylogenetic relationships of the genus *Rhamdella* Eigenmann & Eigenmann 1888 (Siluriformes, Heptapteridae). **Zootaxa**, **1780**: 1-54.
- Bockmann, F. A. & V. Slobodian. 2013. Heptapteridae. *In*: Queiroz, L. J; Torrente-Vilara. G.; Ohara, W. M.; Silva, T. H. P; Zuanon, J & C. R. C. Doria. (Eds.) **Peixes do Rio Madeira.** São Paulo: Diaeto, v. 3, pp. 12–71.
- Bockmann, F.A. & R. M. C. Castro. 2010. The blind catfish from the caves of Chapada Diamantina, Bahia, Brazil (Siluriformes: Heptapteridae): description, anatomy,

- phylogenetic relationships, natural history, and biogeography. **Neotropical Ichthyology**, **8**(4): 673–706.
- Bockmann, F. A. & V. Slobodian. *In press*. Family Heptapteridae- Three-barbeled catfishes. *In*: van der Sleen, P. & J. S. Alberts (Eds.). **Field Guide to the Fishes of the Amazon, Orinoco, and Guianas**. Princeton University Press. Princeton. Pp 233–252.
- Boeseman, M. 1953. Scientific results of the Surinam Expedition 1948–1949. Part II. Zoology No. 2. The Fishes (I). **Zoologische Mededelingen (Leiden)** **32** (1): 1–24.
- Bogota-Gregory J. D. & J. A. Maldonado-Ocampo. 2006. Peces de la zona hidrogeografica de la Amazonia. Colombia. **Biota Colombiana** **7**(1): 55–94
- Böhlke, E. B. 1984. Catalog of type specimens in the ichthyological collection of the Academy of Natural Sciences of Philadelphia. **Special Publication, Academy of Natural Sciences of Philadelphia** **14**: i–viii + 1–216.
- Böhlke, J. E. 1953. A catalogue of the type specimens of Recent fishes in the Natural History Museum of Stanford University. **Stanford Ichthyological Bulletin** **5**(1): 1–168.
- de Borba, R. S., da Silva, E. L., Pacheco, A. C. S., Parise-Maltempi, P. P. & A. L. Alves. 2012. Trends in the karyotypic evolution of the Neotropical catfish family Heptapteridae Bockmann 1998 (Teleostei: Siluriformes). **Reviews in Fish Biology and Fisheries** **22**: 509–518.
- Borodin, N. A. 1927a. A new blind catfish from Brazil. **American Museum Novitates** **263**: 1–5.
- Borodin, N. A. 1927b. Some new catfishes from Brazil. **American Museum Novitates** **266**: 1–7.
- Bortolus, A. 2008. Error cascades in the biological sciences: the unwanted consequences of using bad taxonomy in ecology. **AMBIO: A Journal of the Human Environment** **37**(2): 114–118.
- Boulenger, G. A. 1887. An account of the fishes collected by Mr. C. Buckley in eastern Ecuador. **Proceedings of the Zoological Society of London, 1887** (2): 274–283, Pls. 20–24.
- Boulenger, G. A. 1891. An account of the siluroid fishes obtained by Dr. H. von Ihering and Herr Sebastian Wolff in the Province Rio Grande do Sul, Brazil. **Proceedings of the Zoological Society of London 1891**(2): 231–235.
- Boulenger, G. A. 1896. On a Collection of Fishes from the Rio Paraguay. **Transactions of the Zoological Society of London** **14**: 25–39, pl. III–VIII.

- Boyd R. 1999. Homeostasis, species, and higher taxa. In: Wilson, R. (ed.) **Species: New Interdisciplinary Studies**. Cambridge, MA. MIT Press. pp. 141–185.
- Boyd, R. 2002. Scientific realism. *Stanford Encyclopedia of Philosophy*. Accessed at 14 December, 2017 (<https://stanford.library.sydney.edu.au/archives/spr2009/entries/scientific-realism/>).
- Britski, H. A. 1969. Lista dos tipos de peixes das coleções do Departamento de Zoologia da Secretaria da Agricultura de São Paulo. **Papéis Avulsos do Departamento de Zoologia, Secretaria da Agricultura, São Paulo** 22 (19): 197–215.
- Britski, H.A.. 2001. Sobre a obra Velhas-Flodens Fiske [Peixes do Rio das Velhas]. In Alves, C.B.M. & Pompeu, P.S., (eds). **Peixes do Rio das Velhas: passado e presente**. SEGRAC, Belo Horizonte. pp.15–22.
- Britski, H.A., de Silimon, K.Z.D.S. & Lopes, B.S. 1999. **Peixes do Pantanal: manual de identificação**. Brasília: Embrapa-SPI. 184p.
- Britski, H. A., Silimon, K. Z. de S. & B. S. Lopes. 1999. **Peixes do Pantanal. Manual de identificação**. Brasília: Embrapa-SPI; Corumbá: Embrapa-CPAP, 184p.
- Brumfield, R. T., Liu, L., Lum, D. E., & Edwards, S. V. 2008. Comparison of species tree methods for reconstructing the phylogeny of bearded manakins (Aves: Pipridae, Manacus) from multilocus sequence data. **Systematic Biology** 57(5): 719–731.
- Burgess, W. E. 1989. **An atlas of freshwater and marine catfishes. A preliminary survey of the Siluriformes**. Tropical Fish Hobbyist Publications, Neptune. 783p.
- Bussing, W. A. 1998. Peces de las aguas continentales de Costa Rica. [Freshwater Fishes of Costa Rica]. **Revista de Biología Tropical** 46 (Suppl. 2): 1–468.
- Cabrera, V.H.G. & C. H. Vaca. 2006. **Peces de pando, Bolivia: especies de importancia comercial en mercados de la ciudad de Cobija: especímenes capturados en ríos Tahuamanu-Manuripi-Orthon**. Volume 1. Environmental & Conservation Programs y Dpto. de Ictiología The Field Museum. (<http://fm2.fieldmuseum.org/animalguides/guideimages.asp?ID=18>) Accessed at 03 November 2017.
- Cala, P. 1977. Los peces de la orinoquía colombiana: lista preliminar anotada. **Lozania (Acta Zoologica Colombiana)** 24: 1–21.
- Cala, P. 1981. Catalogo de los ejemplares tipo en la coleccion de peces del Instituto de Ciencias Naturales, Museo de Historia de la Universidad Nacional de Colombia. **Lozania (Acta Zoologica Colombiana)** 34: 1–5.

- Calegari, B. B., Delapieve, M. L. S. & L. Souza. 2016. Tutorial para preparação de mapas de distribuição geográfica. **Boletim da Sociedade Brasileira de Ictiologia** **118**: 15–30.
- Camargo, A., & Jack Jr. Sites. (2013). **Species delimitation: a decade after the renaissance**. INTECH Open Access Publisher.
- Carstens, B. C., Pelletier, T. A., Reid, N. M., & Satler, J. D. 2013. How to fail at species delimitation. **Molecular ecology**, **22**(17): 4369–4383.
- Castello, H.P. 1969. *Pimelodella griffini* (Pisces, Pimelodidae) nueva cita para la fauna argentina. Consideraciones acerca de la alimentación, del sistema reproductor y de una papila urogenital en tres especies del género *Pimelodella*. **Physis**, **28**(77): 407–415.
- Carstens, B. C. & L. L. Knowles. 2007. Estimating species phylogeny from gene-tree probabilities despite incomplete lineage sorting: an example from *melanoplus* grasshoppers. **Systematic Biology** **56**: 400–411.
- Castelnau, F. L. 1855. Poissons. *In*: **Animaux nouveaux or rares recueillis pendant l'expédition dans les parties centrales de l'Amérique du Sud, de Rio de Janeiro a Lima, et de Lima au Para; exécutée par ordre du gouvernement Français pendant les années 1843 a 1847 ...** Part 7, Zoologie. Paris (P. Bertrand). v. 2, i–xii + 1–112, Pls. 1–50.
- Chirichigno, N. 1963. Estudio de la Fauna Ictiologica de los Esteros y parte baja de los Rios del Departamento de Tumbes (Peru). **Serie de Divulgation Cientifica, Servicio de Pesqueria, Peru** **22**:1–87.
- Chernoff, B., Machado Allison, A., Willink, P., Sarmiento, J., Barrera, S., Menezes, N. & H. Ortega. 2000. Fishes of three Bolivian rivers: Diversity, distribution and conservation. **Interciencia** **25** (6): 273–283.
- Chernoff, B., Machado-Allison, A., Riseng, K. & J. R. Montambault. 2005. **A Biological Assessment of the Aquatic Ecosystems of the Caura River Basin, Bolívar State, Venezuela**. RAP Bulletin of Biological Assessment 28. Conservation International, Washington, DC. 284 p.
- Claverie, T. & P. Wainwright. 2014. A Morphospace for Reef Fishes: Elongation Is the Dominant Axis of Body Shape Evolution. **PloS one**. **9**. e112732. 10.1371/journal.pone.0112732.
- Conde-Saldaña C.C., Barreto, C. A. V., Villa-Navarro, F. A. & J. A. Dergam. 2017. **Zebrafish** **1**: 1–8. ahead of print. <https://doi.org/10.1089/zeb.2017.1469>
- Cope, E. D. 1870. Contribution to the ichthyology of the Marañon. **Proceedings of the American Philosophical Society** **11**: 559–570.

- Cope, E. D. 1878. Synopsis of the fishes of the Peruvian Amazon, obtained by Professor Orton during his expeditions of 1873 and 1877. **Proceedings of the American Philosophical Society** **17** (101): 673–701.
- Cope, E. D. 1894. On the fishes obtained by the Naturalist Expedition in Rio Grande do Sul. **Proceedings of the American Philosophical Society** **33**: 84–108, Pls. 4–9.
- Costa, W. J. E. M. 1987. Feeding habits of a fish community in a tropical coastal stream, rio Mato Grosso, Brazil. **Studies on Neotropical Fauna Environment** **22** (3): 145–153.
- Cox-Fernandes, C., Lundberg, J. G. & J. P. Sullivan. 2009. *Oedemognathus exodon* and *Sternarchogiton nattereri* (Apteronotidae, Gymnotiformes): the case for sexual dimorphism and conspecificity. **Proceedings of the Academy of Natural Sciences of Philadelphia**, **158**(1), 193–207.
- Cunico, A. M., da Graça, W. J., Agostinho, A. A., Domingues, W. M. & J. D. Latini. 2009. Fish, Maringá urban streams, Pirapó river drainage, upper Paraná river basin, Paraná State, Brazil. **Check List**, **5** (2): 273–280.
- Cuvier, G. & A. Valenciennes. 1840. **Histoire naturelle des poissons**. Tome quinzième. Suite du livre dix-septième. Siluroïdes. v. 15: i–xxxix + 1–540, Pls. 421–455.
- Dahl, G. 1961. Nematognathous fishes collected during the Macarena Expedition 1959. Dedicated to the memory of the Colombian ichthyologist, Doctor Ricardo Lozano. Decd May 23rd, 1959. Part II: Pimelodidae, Callophysidae. **Novedades Colombianas** **1**(6): 483–514.
- Dahl, G. & F. Medem. 1964. Informe sobre la fauna acuatica del Rio Sinu. I Parte. Los Peces y la Pesca del Rio Sinu. Corporacion Autonoma Regional de los Valles del Magdalena y del Sinu -CVM-. **Departamento de Investigaciones Ictiologicas y Faunisticas**: 1–109.
- Davies, T. & T. Fearn. 2004. Back to basics: the principles of principal component analysis. **Spectroscopy Europe**, **16**(6), 20–23.
- Dazzani, B., Garcia, C., Peixoto, M., Trajano, E. & L.F. de Almeida-Toledo. 2012. Cytogenetic and molecular analyses in troglobitic and epigeic species of Pimelodella (Siluriformes: Heptapteridae) from Brazil. **Neotropical Ichthyology** **10**: 623–6.
- Degnan, J. H., & Rosenberg, N. A. 2006. Discordance of species trees with their most likely gene trees. **PLoS Genet** **2**(5): e68.

- Dupuis, J. R., Roe, A. D., & Sperling, F. A. 2012. Multi- locus species delimitation in closely related animals and fungi: one marker is not enough. **Molecular ecology** **21**(18): 4422–4436.
- Edgar, R.C. 2004. MUSCLE: multiple sequence alignment with high accuracy and high throughput. **Nucleic acids research** **32**(5): 1792–1797
- Edwards, S. V. 2009. Is a new and general theory of molecular systematics emerging? **Evolution** **63**(1): 1–19.
- Eigenmann, C. H. 1905. The Fishes of Panamá. **Science, New Series**, 22 (549): 18–20.
- Eigenmann, C. H. 1910. Catalogue of the fresh-water fishes of tropical and south temperate America. **Reports of the Princeton University expeditions to Patagonia 1896-1899. Zoology**. **3** (4): 375–511.
- Eigenmann, C. H. 1912. Some results from an ichthyological reconnaissance of Colombia, South America. Part I. **Indiana University Studies** **16**: 1–27.
- Eigenmann, C.H., 1917. *Pimelodella and Typhlobagrus*. **Memoirs of the Carnegie Museum**, **7**, 229–258, pls. 29–35.
- Eigenmann, C. H. 1920. The fishes of Lake Valencia, Caracas, and of the Rio Tuy at El Concejo, Venezuela. **Indiana University Studies** **7** (44): 1–13, Pls. 1–3.
- Eigenmann, C. H. 1921a. The Origin and Distribution of the Genera of the Fishes of South America West of the Maracaibo, Orinoco, Amazon, and Titicaca Basins **Proceedings of the American Philosophical Society** **60** (1): 1–6.
- Eigenmann, C. H. 1921b The Nature and Origin of the Fishes of the Pacific Slope of Ecuador, Peru and Chili. **Proceedings of the American Philosophical Society**, **60** (4): 503–523.
- Eigenmann, C. H. 1922a. The fishes of western South America, Part I. The fresh-water fishes of northwestern South America, including Colombia, Panama, and the Pacific slopes of Ecuador and Peru, together with an appendix upon the fishes of the Rio Meta in Colombia. **Memoirs of the Carnegie Museum** **9** (1): 1–346, Pls. 1–38
- Eigenmann, C. H. 1922b. The Fishes of the Pacific Slope of South America and the Bearing of Their Distribution on the History of the Development of the Topography of Peru, Ecuador and Western Colombia. **The American Naturalist** **57** (650): 193–210.
- Eigenmann, C. H. 1922c. Yellow Fever and Fishes. **Proceedings of the American Philosophical Society** **61**(3) 204–211.
- Eigenmann, C. H. 1924. Yellow Fever and Fishes in Colombia. **Proceedings of the American Philosophical Society** **63** (3): 236–238.

- Eigenmann, C. H., & Allen, W. R. 1942. **Fishes of Western South America: 1. The Intercordilleran and Amazonian Lowlands of Peru. 2. The High Pampas of Peru, Bolivia and Northern Chile; With a Revision of the Peruvian Gymnotidae and of the Genus Orestias.** University of Kentucky. 524p.
- Eigenmann, C.H. & B.A Bean. 1907. An account of Amazon River fishes collected by JB Steere; with a note on *Pimelodus clarias*. **Proceedings of the United States National Museum** **31**: 659–668.
- Eigenmann, C. H. & R. S. Eigenmann. 1888. Preliminary notes on South American Nematognathi. I. **Proceedings of the California Academy of Sciences (Series 2)** **1** (2): 119–172.
- Eigenmann, C. H. & R. S. Eigenmann. 1890. A revision of the South American Nematognathi or cat-fishes. **Occasional Papers California Academy of Sciences** **1**: 1–508.
- Eigenmann, C. H. & R. S. Eigenmann. 1891. A catalogue of the fresh-water fishes of South America. **Proceedings of the United States National Museum** **14** (842): 1–81.
- Eigenmann, C. H., W. L. McAtee and D. P. Ward. 1907. On further collections of fishes from Paraguay. **Annals of the Carnegie Museum** **4** (2): 110–157, Pls. 31–45.
- Eigenmann, C. H. & A. A. Norris. 1900. Sobre alguns peixes de S. Paulo, Brazil. **Contribuições do laboratório ictiológico da Universidade de Indiana** **33**(4): 349–362
- Elias, M., Hill, R. I., Willmott, K. R., Dasmahapatra, K. K., Brower, A. V., Mallet, J., & Jiggins, C. D. 2007. Limited performance of DNA barcoding in a diverse community of tropical butterflies. **Proceedings of the Royal Society of London B: Biological Sciences** **274**(1627): 2881–2889.
- Eschmeyer, W. N. and R. Fricke, and R. van der Laan (eds). 2017. CATALOG OF FISHES: GENERA, SPECIES, REFERENCES. (<http://researcharchive.calacademy.org/research/ichthyology/catalog/fishcatmain.asp>). Electronic version accessed 01 August 2017.
- Edwards, S. V., Liu, L., & Pearl, D. K. 2007. High-resolution species trees without concatenation. **Proceedings of the National Academy of Sciences**, **104**(14), 5936–5941
- Felice, V. 2006. Ricardo Krone e o bagre cego de Iporanga: o início de tudo. *In*: Trajano, E. (org.) **Sistema Areias. 100 anos de estudos**. São Paulo: Redespeleo Brasil. 21–23 pp

- Fernandes, C. A., Damásio, J. F., Guterres, Z. R. & M. C. F. Abelha. 2013. Cytogenetic studies in two species of genus *Pimelodella* (Teleostei, Siluriformes, Heptapteridae) from Iguatemi River Basin, Brazil. **Cytologia** **78**: 91–95.
- Fernández-Yépez, A. 1950. Algunos peces del Rio Autana. Novedades Cientificas, **Contribuciones Ocasionales del Museo de Historia Natural La Salle, Serie Zoológica 2**: 1–18, Pls. 1–3.
- Fernández-Yépez, A. 1970. Analisis ictiológico del Complejo Hidrográfico (07) "Rio Unare." **Dirección de Obras Hidráulicas, Ministerio de Obras Publicas, Republica de Venezuela**: 1–20, 41 pls.
- Ferraris, C. J., Jr. 1991. **Catfish in the aquarium**. Tetra Press, Morris Plains, 199p.
- Ferraris, C. J., Jr. 2007. Checklist of catfishes, recent and fossil (Osteichthyes: Siluriformes), and catalogue of siluriform primary types. **Zootaxa**, **1418**: 1-628.
- Ferraris, C. J., Jr. & R. P. Vari. 1992. Catalog of type specimens of Recent fishes in the National Museum of Natural History, Smithsonian Institution, 4: Gonorynchiformes, Gymnotiformes, and Siluriformes (Teleostei: Ostariophysi). **Smithsonian Contributions to Zoology** **535**: 1–52.
- FEOW. 2015. Freshwater regions of the world. (<http://www.feow.org/globalmap>). Electronic version accessed 01 August 2017.
- Fowler, H. W. 1914. Fishes from the Rupununi River, British Guiana. **Proceedings of the Academy of Natural Sciences of Philadelphia** **66**: 229–284.
- Fowler, H. W. 1915. Notes on nematognathous fishes. **Proceedings of the Academy of Natural Sciences of Philadelphia** **67**: 203–243.
- Fowler, H. W. 1939. A Collection of Fishes Obtained by Mr. William C. Morrow in the Ucayali River Basin, Peru. **Proceedings of the Academy of Natural Sciences of Philadelphia** **91**: 219–289
- Fowler, H. W. 1940a. A collection of fishes obtained by Mr. William C. Morrow in the Ucayali River Basin, Peru. **Proceedings of the Academy of Natural Sciences of Philadelphia** **91** (for 1939): 219–289.
- Fowler, H. W. 1940b. Zoological results of the second Bolivian expedition for the Academy of Natural Sciences of Philadelphia, 1936-1937. Part I.--The fishes. **Proceedings of the Academy of Natural Sciences of Philadelphia** **92**: 43–103.
- Fowler, H. W. 1941a. A collection of fresh-water fishes obtained in eastern Brazil by Dr. Rodolpho von Ihering. **Proceedings of the Academy of Natural Sciences of Philadelphia** **93**: 123–199.

- Fowler, H. W. 1943. A collection of fresh-water fishes from Colombia, obtained chiefly by Brother Nicéforo Maria. **Proceedings of the Academy of Natural Sciences of Philadelphia** **95**: 223–266.
- Fowler, H. W. 1945a. Colombian zoological survey. Pt. I.--The freshwater fishes obtained in 1945. **Proceedings of the Academy of Natural Sciences of Philadelphia** **97**: 93–135.
- Fowler, H. W. 1945 b. **Los Peces del Peru. Catálogo sistemático de los peces que habitan en aguas peruanas**. Lima, Peru. Museo de Historia Natural "Javier Prado" Universidad Nacional Mayor de San Marcos. 298p.
- Fowler, H. W. 1948. Os peixes de água doce do Brasil. Volume 1. 1a entrega. **Arquivos de Zoologia do Estado de São Paulo** **6**: 1–204.
- Fowler, H. W. 1951. Os peixes de água doce do Brasil. Volume 1. 3a entrega. **Arquivos de Zoologia do Estado de São Paulo** **6**: 405–628.
- Fricke, R. 1995. Types in the fish collection of the Staatliches Museum für Naturkunde in Stuttgart. Part 3. Types of fishes described in 1850-1994. **Stuttgarter Beiträge zur Naturkunde. Serie A (Biologie)** **524**: 1–30.
- Fricke, R. 2005. Types in the fish collection of the Staatliches Museum für Naturkunde in Stuttgart, described in 1845-2004. **Stuttgarter Beiträge zur Naturkunde. Serie A (Biologie)** **684**: 1–95.
- Galvis, G., J. I. Mojica & M. Camargo. 1997. **Peces del Catatumbo**. Asociación Cravo Norte, Colombia. 118p.
- Garcia C & L. F. Almeida-Toledo. 2010. Comparative chromosomal analyses in species of the genus *Pimelodella* (Siluriformes, Heptapteridae): occurrence of structural and numerical polymorphisms. **Caryologia** **63**:3 2–40.
- Genthner, C., Ferrari, J. A. & L. F. S. Da Rocha. 2006. Geologia. In: Trajano, E. (org.) **Sistema Areias. 100 anos de estudos**. São Paulo: Redespeleo Brasil. 35–42 pp.
- Gery, J. 1969. The fresh-water fishes of South America. **Biogeography and ecology in South America** **2**: 828–848
- Giesbrecht, R. M. 2017. Estações Ferroviárias do Brasil— EFCB: Linha do Centro. <http://www.estacoesferroviarias.com.br> Accessed at 08 November 2017.
- Graça, W. J. & C. S. Pavanelli. 2007. **Peixes da planície de inundação do alto rio Paraná e áreas adjacentes**. EDUEM, Maringá, 2007. 241 p.
- Godfray H. C. J. & S. Knapp. 2004. Introduction. **Philosophical Transactions of the Royal Society of London, series B** **359**: 559–569

- Godinho, A.L. & H. P. Godinho. 2003. **Águas, peixes e pescadores do São Francisco das Minas Gerais**. Belo Horizonte: PUC Minas, 468p.
- Gosline, W. A. 1945. Catálogo dos nematognatos de água-doce da América do sul e central. **Boletim do Museu Nacional Rio de Janeiro Zoologia 33**: 1–138.
- Gouveia, J. G., de Moraes, V. P. O., Sampaio, T. R., da Rosa, R. & A.L. Dias. 2013. Considerations on karyotype evolution in the genera *Imparfinis* Eigenmann and Norris 1900 and *Pimelodella* Eigenmann and Eigenmann 1888 (Siluriformes: Heptapteridae). **Reviews in Fish Biology and Fisheries 23**: 215–227.
- Guazzelli, G. M. 1997. **Revisão das espécies de *Pimelodella* Eigenmann & Eigenmann 1888 (Teleostei: Siluriformes: Pimelodidae) dos sistemas costeiros do Sul e Sudeste do Brasil**. Pontifícia Universidade Católica do Rio Grande do Sul. Unpublished Msc. dissertation. 150p.
- Guazzelli, G. M. 2003. **Relações filogenéticas do gênero *Pimelodella* Eigenmann & Eigenmann 1888 (Siluriformes, Pimelodidae)**. Universidade de São Paulo, São Paulo. Unpublished PhD. thesis. 232p.
- Guil, A. L. F. 2011. **Ecologia populacional do bagre cego de Iporanga, *Pimelodella kronei* (Siluriformes: Heptapteridae), do Vale do Alto Ribeira, Iporanga - SP: uma comparação com Trajano, 1987**. Universidade de São Paulo, São Paulo. Unpublished Master's dissertation. 117p.
- Güntert, H. 1942. Beschreibung einiger zum Teil noch unbekannter südamerikanischer Siluriden aus dem Naturhistorischen Museum in Basel. **Zoologischer Anzeiger 138** (1/2): 27–40.
- Günther, A. 1860. Third list of cold-blooded vertebrata collected by Mr. Fraser in Ecuador. **Proceedings of the Zoological Society of London 1860** (2): 233–240, Pisces Pl. 10.
- Günther, A. 1864. **Catalogue of the Fishes in the British Museum, vol. 5**.—Catalogue of the Physostomi, Containing the Families Siluridae, Characinidae, Haplochitonidae, Sternoptychidae, Scopelidae, Stomiatidae in the Collection of the British Museum, Trustees, London, xxii + 455 p.
- Haseman, J. D. 1911. Descriptions of some new species of fishes and miscellaneous notes on others obtained during the expedition of the Carnegie Museum to central South America. **Annals of the Carnegie Museum 7**(3–4): 315_328, Pls. 46–52.
- Hebert, P. D., Cywinska, A., & Ball, S. L. 2003a. Biological identifications through DNA barcodes. **Proceedings of the Royal Society of London B: Biological Sciences, 270**(1512),:313–321.

- Heled, J., & Drummond, A. J. 2010. Bayesian inference of species trees from multilocus data. **Molecular biology and evolution** **27**(3): 570–580.
- Henn, A. W. 1928. List of types of fishes in the collection of the Carnegie Museum on September 1, 1928. *Annals of the Carnegie Museum* **19** (4): 51–99.
- Hoedeman, J. J. 1961. Notes on the ichthyology of Surinam and other Guianas. 8. Additional records of siluriform fishes (2). **Bulletin of Aquatic Biology** **2** (23): 129–139.
- Hollingsworth, P. M., Forrest, L. L., Spouge, J. L., Hajibabaei, M., Ratnasingham, S., van der Bank, M., & Wilkinson, M. J. 2009. A DNA barcode for land plants. **Proceedings of the National Academy of Sciences** **106**(31): 12794–12797.
- Howes, G. J. 1983. Problems in catfish anatomy and phylogeny exemplified by the Neotropical Hypophthalmidae (Teleostei: Siluroidei). **Bulletin of the British Museum (Natural History), Zoology series**, **45** (1): 1-39.
- Ibarra, M. & D. J. Stewart. 1987. Catalogue of type specimens of Recent fishes in Field Museum of Natural History. **Fieldiana Zoology (New Series)** **35**: 1–112.
- Innes, W.T. & G. S. Myers. 1950. The “Imitator catfish,” which mimics a *Corydoras*. **The Aquarium**, **19** (9): 222-223.
- Irwin, D.M., Kocher, T.D. & Wilson, A.C. 1991. Evolution of the cytochrome b gene of mammals. **Journal of molecular evolution** **32**(2): 128–144.
- James, F. C. & C. E. McCulloch. 1990. Multivariate analysis in ecology and systematics: panacea or Pandora's box? **Annual review of Ecology and Systematics** **21**(1): 129–166.
- Kearse, M., Moir, R., Wilson, A., Stones-Havas, S., Cheung, M., Sturrock, S., Buxton, S., Cooper, A., Markowitz, S., Duran, C. & Thierer, T. 2012. Geneious Basic: an integrated and extendable desktop software platform for the organization and analysis of sequence data. **Bioinformatics** **28**(12): 1647–1649.
- Kner, R. 1858. Ichthyologische Beiträge. II. Abtheilung. **Sitzungsberichte der Kaiserlichen Akademie der Wissenschaften. Mathematisch-Naturwissenschaftliche Classe** **26** (373): 373–448, Pls. 1–9.
- Knowles, L. L., & Carstens, B. C. 2007. Delimiting species without monophyletic gene trees. **Systematic biology** **56**(6): 887–895.
- Koerber, S., Vera-Alcaraz, H.S. & Reis, R.E. 2017. Checklist of the Fishes of Paraguay (CLOFPY). **Ichthyological Contributions of PecesCriollos** **53**: 1–99
- Kosco B. 1993. **Fuzzy thinking – the new science of fuzzy logic**. London: Harper Collins. 336p.

- Kubatko, L.; Carstens, B. & L. Knowles. 2009. STEM: species tree estimation using maximum likelihood for gene trees under coalescence. **Bioinformatics** **25**(7): 971-973.
- Kullander, S. O. 1986. **Cichlid fishes of the Amazon River drainage of Peru**. Swedish Museum of Natural History, Stockholm, 431 pp.
- Langeani, F., Castro, R. M. C., Oyakawa, O. T.; Shibatta, O. A.; Pavanelli, C. S. & L. Casatti. 2007. Diversidade da ictiofauna do Alto Rio Paraná: composição atual e perspectivas futuras. **Biota Neotropica** **7** (3): 181–197.
- Lasso, C. A., Ponte, V. & Lasso-Alcalá, O. M. 1997. Catálogo de la colección de tipos de peces de la Fundación La Salle de Ciencias naturales. Parte I: Museo de Historia Natural la Salle (MHNLS). **Memoria de la Sociedad de Ciencias Naturales La Salle** **57**(147): 37–52.
- Lasso, C. A., Lew, D., Taphorn, D., DoNascimento, C., Lasso-Alcalá, O., Provenzano, F. & A. Machado-Allison. 2004. Biodiversidad ictiológica continental de Venezuela. Parte I. Lista de especies y distribución por cuencas. **Memoria de la Fundación La Salle de Ciencias Naturales**, **159** (160): 105–195.
- Lasso, C., Giraldo, A., Lasso-Alcalá, O., León-Mata, O., DoNascimento, C., Milani, N., Rodríguez-Olarte, D., Senaris, J. & D. Taphorn. 2006. Peces de los ecosistemas acuáticos de la confluencia de los ríos Orinoco y Ventuari, Estado Amazonas, Venezuela: resultados del AquaRAP 2003. **Evaluación Rápida de la Biodiversidad de los Ecosistemas Acuáticos de la Confluencia de los Ríos Orinoco y Ventuari, Estado Amazonas, Venezuela**: 114–122.
- Le Bail, P.-Y., P. Keith & P. Planquette. 2000. **Atlas des poissons d'eau douce de Guyane**. Tome 2 - fascicule II. Siluriformes. Publications scientifiques du MNHN, Paris. 307p.
- Le Bail, P. Y., Covain, R., Jégu, M., Fisch-Muller, S., Vigouroux, R. & P. Keith. 2012. Updated checklist of the freshwater and estuarine fishes of French Guiana. **Cybium**, **36** (1); 293–319.
- Leiva C., M. 2005. **Revisión Taxonómica del género *Pimelodella*, Eigenmann & Eigenmann, 1888 (*Pisces, Siluriformes: Heptapteridae*) de la región transandina de Colombia**. Universidad Tradicional de Colombia, Bogotá. Unpublished Msc. Dissertation. 70p.
- Li, C., Riethoven, J.J.M. and Ma, L., 2010. Exon-primed intron-crossing (EPIC) markers for non-model teleost fishes. **BMC Evolutionary Biology** **10**(1): 90 (12p)
- Lichtenstein, M. H. C. 1819. Ueber einige neue Arten von Fischen aus der Gattung *Silurus*. **Zoologisches Magazin (Wiedemann)** **1819** **1**(3): 57–63.

- Lichtenstein, M. H. C. 1823. **Verzeichniss der Doubletten des zoologischen Museums der Königl.** Universität zu Berlin, nebst Beschreibung vieler bisher unbekannter Arten von Säugethieren, Vögeln, Amphibian und Fishen. T. Trautwein, Berlin. I–x + 1–118, 1 pl.
- Litz, T. O. & S. Koerber. 2014. Check list of the freshwater fishes of Uruguay (CLOFF-UY). **Ichthyological Contributions of PecesCriollos 28**: 1–40.
- Liu, L. 2008. BEST: Bayesian estimation of species trees under the coalescent model. **Bioinformatics 24**(21): 2542–2543.
- Liu, L. & D. K Pearl. 2007. Species trees from gene trees: reconstructing Bayesian posterior distributions of a species phylogeny using estimated gene tree distributions. **Systematic Biology 56**: 504–514.
- Liu L.; Pearl, D. K.; Brumfield, R. T. & S. V. Edwards .2008. Estimating species trees using multiple-allele DNA sequence data. **Evolution 62**(8): 2080-91.
- López, H. L., Menni, R. C. & R. A. Ringuelet. 1981. Bibliografía de los peces de agua Dulce de Argentina y Uruguay 1967–1981. **Biología Acuática 1**: 1–81.
- López, H. L., Menni, R. C. & R. A. Ringuelet. 1982. Bibliografía de los peces de agua Dulce de Argentina y Uruguay Suplemento 1982. **Biología Acuática 3**: 1–23.
- López, H. L., Miquelarena, A. M. & R. C. Menni. 2003. **Lista comentada de los peces continentales de la Argentina**. ProBiota: Serie Técnica y Didáctica 5. 85p.
- Lucena, Z.D. & Lucena, C.D. 1990. Sobre a localidade-tipo das espécies de peixes descritas por Steindachner (1907). **Comunicações do Museu de Ciências e Tecnologia, Pontifícia Universidade Católica do Rio Grande do Sul, Série Zoologia. Porto Alegre 3**(1): 99–102.
- Lucena, C. A. S. de & J. F. P. da Silva. 1991. Descrição de uma nova espécie do gênero *Rhamdella* Eigenmann & Eigenmann, 1888 (Siluriformes: Pimelodidae) para o médio rio Uruguai, sul do Brasil. **Comunicações do Museu de Ciências de PUCRS 4**(3): 28–47.
- Lucinda, P. H., Freitas, I. S., Soares, A. B., Marques, E. E., Agostinho, C .S. & R. J. de Oliveira. 2007. Fish, Lajeado reservoir, rio Tocantins drainage, state of Tocantins, Brazil. **Check List, 3** (2): 70–83.
- Lundberg, J.G. & J. N. Baskin. 1969. The caudal skeleton of the catfishes, order Siluriformes. **American Museum Novitates, 2398**: 1–49.
- Lundberg, J.G., Linares, O.J., Antonio, M.E. & P. Nass. 1988. *Phractocephalus hemiliopterus* (Pimelodidae, Siluriformes) from the upper Miocene Urumaco Formation, Venezuela: a

- further case of evolutionary stasis and local extinction among South American fishes. **Journal of Vertebrate Paleontology** **8** (2): 131–138.
- Lundberg, J. G. & L. A. McDade 1986. On the South American catfish *Brachyramdia imitator* Myers (Siluriformes, Pimelodidae), with a phylogenetic evidence for a large intrafamilial lineage. **Notulae Naturae (Philadelphia)** **463**: 1-24.
- Lundberg, J. G., A. H. Bornbusch & Mago-Leccia, F. 1991a. *Gladioglanis conquistador* N. Sp. from Ecuador with diagnosis of the subfamilies Rhamdiinae Blekker and Pseudopmelodinae N. Subf. (Siluriformes, Pimelodidae). **Copeia**, **1991** (1): 190-209.
- Lundberg, J. G., F. Mago-Leccia & P. Nass. 1991b. *Exallodontus aguanai*, a new genus and species of Pimelodidae (Pisces: Siluriformes) from deep river channels of South America, and delimitation of the subfamily Pimelodinae. **Proceedings of the Biological Society of Washington** **104** (4): 840–869
- Lundberg, J.G. & M. W. Littmann. 2003. Family Pimelodidae (Long-whiskered catfishes). *In*: Roberto Esser dos Reis; Sven O. Kullander; Carl J. Ferraris Jr.. (Org.). **Check List of the Freshwater Fishes of South and Central America**. Porto Alegre: EDIPUCRS. v. 1. 432–446 pp.
- Lütken, C. F. 1874. Siluridae novae Brasiliae centralis a clarissimo J. Reinhardt in provincia Minas-geraës circa oppidulum Lagoa Santa, praecipue in flumine Rio das Velhas et affluentibus collectae, secundum characteres essentialia breviter descriptae. **Oversigt over det Kongelige Danske Videnskabernes Selskabs Forhandling og dets Medlemmers Arbejder (Kjøbenhavn)** **1874** (1): 29–36.
- Lütken, C. F. 1875. Velhas-Flodens Fiske. Et Bidrag til Brasiliens Ichthyologi; efter Professor J. Reinhardts Indsamlinger og Optegnelser. Det. Kongelige Danske visenskabernes selskabs skrifter. **Naturvidenskabelig og matematisk afdeling. 5te Raekk [Ser. 5]** **12**(2): 121–253 + 2 unnum. + I–XXI, Pls. 1–5.
- Lütken, C.F., Alves, C.B.M. & Pompeu, P.S. 2001. Peixes do rio das Velhas: uma contribuição para a ictiologia do Brasil. *In* Alves, C.B.M. & Pompeu, P.S., (eds). **Peixes do Rio das Velhas: passado e presente**. SEGRAC, Belo Horizonte. pp.23–164.
- Maddison, W. P. 1997. Gene trees in species trees. **Systematic biology** **46**(3): 523–536.
- Malabarba, L. R. 1989. Histórico sistemático e lista comentada das espécies de peixes de água doce do sistema da Laguna dos Patos, Rio Grande do Sul, Brasil. **Comunicações do Museu de Ciências de PUCRS** **2** (8): 107–179.
- Maldonado-Ocampo, J. A., Ortega-Lara, A., Usma, J.S., Galvis, G., Villa-Navarro, F.A., Vásquez, L., Prada-Pedrerros, S. & C. Ardila. 2006. **Peces de los Andes de Colombia**.

- Instituto de Investigación de Recursos Biológicos Alexander von Humboldt, Bogotá, DC. 346p.
- Maldonado-Ocampo, J. A., Vari, R. P. & J. Saulo Usma. 2008. Checklist of the freshwater fishes of Colombia. **Biota Colombiana**, **9** (2): 143–237.
- Mayden, R.L., 1997. A hierarchy of species concepts: the denouement in the saga of the species problem. *In* M. F. Claridge, H. A. Dawah & M. R. Wilson (eds.). **Species: The units of diversity**. Chapman & Hall. pp. 381–423.
- Mazzoni, R. & L. D. S. Costa. 2007. Feeding ecology of streamdwelling fishes from a coastal stream in the Southeast of Brazil. **Brazilian Archives of Biology and Technology** **50** (4): 627–635.
- Meek, S. E. 1905. Two new species of fishes from Brazil. **Proceedings of the Biological Society of Washington** **18**: 241–242.
- Mees, G. F. 1974. The Auchenipteridae and Pimelodidae of Suriname (Pisces, Nematognathi). **Zoologische Verhandelingen (Leiden)** **132**: 1–256, Pls. 1–15.
- Mees, G. F. 1983. Naked catfishes from French Guiana (Pisces, Nematognathi). **Zoologische Mededelingen (Leiden)** **57**(5): 43–58.
- Mees, G. F. 1985. Further records of Auchenipteridae and Pimelodidae from Suriname (Pisces: Nematognathi). **Zoologische Mededelingen (Leiden)** **59** (21): 239–249.
- Mees, G. F. 1986. Records of Auchenipteridae and Pimelodidae from French Guiana (Pisces, Nematognathi). **Proceedings of the Koninklijke Nederlandse Akademie van Wetenschappen (Series C, Biological and Medical Sciences)** **89** (3): 311–325.
- Mees, G. F. & P. Cala. 1989. Two new species of *Imparfinis* from northern South America (Pisces, Nematognathi, Pimelodidae). **Proceedings of the Koninklijke Nederlandse Akademie van Wetenschappen (Series C, Biological and Medical Sciences)** **92** (3): 379–394.
- Meier, R., Zhang, G., & Ali, F. 2008. The use of mean instead of smallest interspecific distances exaggerates the size of the “barcoding gap” and leads to misidentification. **Systematic Biology** **57**(5): 809–813.
- Meyer, C. P., & Paulay, G. 2005. DNA barcoding: error rates based on comprehensive sampling. **PLoS biology** **3**(12): 2229.
- Miles, C. W. 1943. Estudio economico y ecologico de los peces de agua dulce del valle de Cauca. **Publicaciones de Secretaria Agricultura y Fomento del Departamento**: 1–99.

- Miles, C. 1945. Some newly recorded fishes from the Magdalena River system. **Caldasia** **3** (15): 453–464.
- Miller, M.A., Pfeiffer, W. & Schwartz, T. 2010. Creating the CIPRES Science Gateway for inference of large phylogenetic trees. **Proceedings of the Gateway Computing Environments Workshop (GCE)**: 1–8.
- Mirarab, S., Reaz, R., Bayzid, M.S., Zimmermann, T., Swenson, M.S. & T. Warnow. 2014. ASTRAL: genome-scale coalescent-based species tree estimation. **Bioinformatics** **30**(17): i541–i548.
- Miranda Ribeiro, A. de. 1907a. Uma novidade ichthyologica. Kosmos, Rio de Janeiro **Rev. Art. Sci. Litt.** **4** (1): 3 unnum. pp.
- Miranda Ribeiro, A. de. 1907b. Peixes do Iporanga – S. Paulo. Resultados de excursões do Sr. Ricardo Krone, membro correspondente do Museu Nacional do Rio de Janeiro. **Boletim Sociedade Nacional Agricultura, Rio de Janeiro [Lavoura]** **11** (5): 185–190.
- Miranda Ribeiro, A. de. 1911. Fauna brasiliense. Peixes. Tomo IV (A) [Eleutherobranchios Aspirophoros]. **Arquivos do Museu Nacional de Rio de Janeiro** **16**: 1–504, Pls. 22–54.
- Miranda Ribeiro, A. de. 1914. Pimelodidae, Trachycorystidae, Cetopsidae, Bunocephalidae, Auchenipteridae, e Hypophthalmidae. In: **Comissão de Linhas Telegraphicas Estrategicas de Matto-Grosso ao Amazonas. Anexo 5**: 1–13, Pls. 1–2.
- Miranda Ribeiro, A. de. 1918. Tres generos e dezeseite especies novas de peixes Brasileiros. **Revista do Museu Paulista** **10**: 631–646, 1 pl.
- Miranda Ribeiro, A. de. 1918b. Lista dos peixes Brasileiros do Museu Paulista. Primeira parte. **Revista do Museu Paulista** **10**: 705–736.
- Miranda Ribeiro, P. de. 1953. Tipos das espécies e subespécies do Prof. Alipio de Miranda Ribeiro depositados no Museu Nacional. **Arquivos do Museu Nacional de Rio de Janeiro** **42**: 389–417.
- Mirande, J.M. & Koerber, S. 2015. Checklist of the freshwater fishes of Argentina (CLOFFAR). **Ichthyological Contributions of Peces Criollos** **36**: 1–68.
- Mojica, J., Usma, J. & G. Galvis. 2004. Peces dulceacuícolas en el Chocó biogeográfico. In: Rangel, J.O. (ed.). **Diversidad Biótica IV, El Chocó Biogeográfico/Costa Pacífica**. Universidad Nacional de Colombia, Instituto de Ciencias Naturales, Conservación Internacional, Bogotá. 725–744p.
- Mojica J. I., G. Galvis, F. Arbelaez, M. Santos, S. Vejarano, E. Prieto-Piraquive, M. Arce, P. Sanchez- Duarte, C. Castellanos, A. Gutierrez, S. R. Duque, J. Lobon-Cervia & C.

- Granado-Lorencio. 2005. Peces de la cuenca del río Amazonas en Colombia: Región de Leticia. **Biota Colombiana** 6(2): 191–210.
- Mol, J. H., Vari, R. P., Covain, R., Willink, P. W. & S. Fisch-Muller. 2012. Annotated checklist of the freshwater fishes of Suriname. **Cybium**, 36(1): 263–292.
- Moraes, M.; Silva Filho, J. J. D.; Costa, R.; Miranda, J. C.; Rezende, C. F. & R. Mazzoni. 2013. Life history and ontogenetic diet shifts of *Pimelodella lateristriga* (Lichtenstein 1823) (Osteichthyes, Siluriformes) from a coastal stream of Southeastern Brazil. **North-Western Journal of Zoology** 9 (2): 300–309.
- Moritz, C., & Cicero, C. 2004. DNA barcoding: promise and pitfalls. **PLoS biology** 2: 1529–1531.
- Müller, J. & F. H. Troschel. 1849a. Fische. *In*: **Reisen in Britisch-Guiana in den Jahren 1840-44. Im Auftrag Sr. Majestät des Königs von Preussen ausgeführt von Richard Schomburgk. [Versuch einer Fauna und Flora von Britisch-Guiana.]** v. 3. Berlin. pp. 618–644.
- Müller, J. & F. H. Troschel. 1849b. Horae Ichthyologicae. **Beschreibung und Abbildung neuer Fische. Berlin.** v 3: 1–27 + additional p. 24, Pls. 1–5.
- Myers, G. S. 1927. Descriptions of new South American fresh-water fishes collected by Dr. Carl Ternetz. **Bulletin of the Museum of Comparative Zoology** 68 (3): 107–135.
- Nelson, J. S. 2006. **Fishes of the World**. 4th edition. John Wiley & Sons, Hoboken, N. J. I–xix + 1–601.
- Nielsen, J. G. 1974. Fish types in the Zoological Museum of Copenhagen. **Zoological Museum, University of Copenhagen, Denmark**: 1–115.
- Nijssen, H., Tuijl, van L. & Isbrücker, I.J.H. 1982. A Catalogue of the type-specimens of Recent fishes in the Institute of Taxonomic Zoology (Zoölogisch Museum), University of Amsterdam, The Netherlands. **Verslagen en Technische Gegevens** 33(1): 1–173
- Nijssen, H., van Tuijl, L. & Isbrücker, J.H. 1993. Revised catalogue of the type specimens of recent fishes in the Institute of Taxonomic Zoology (Zoölogisch Museum), University of Amsterdam, the Netherlands. **Bulletin Zoologisch Museum** 13(18): 211–260.
- Ni3n, H., Rios, C. & P. Meneses. 2016. **Peces del Uruguay: Lista sistemática y nombres comunes**. Segunda edición corregida y ampliada. i-xi + 174p.
- Norman, J.R. 1926. XLI.—A new blind catfish from Trinidad, with a list of the blind cave-fishes. **Journal of Natural History** 18(106): 324–331.
- Nylander, J.A.A. 2004. **Mr Model test v2**. Program distributed by the author. Evolutionary Biology Centre, Uppsala University.

- Ortega, H. & R. P. Vari. 1986. Annotated checklist of the freshwater fishes of Peru. **Smithsonian Contributions to Zoology** **437**: iii + 1–25.
- Padial, J. M., Miralles, A., De la Riva, I., & Vences, M. 2010. Review: The integrative future of taxonomy. **Frontiers in Zoology** **7**: 1–14.
- Paepke, H.-J. 1995. Über das Leben und Werk von Ernst Ahl. **Mitteilungen aus dem Zoologischen Museum in Berlin** **71** (1): 79–101.
- Palumbi, S. R., Martin, A., Romano, S., McMillan, W.O., Stice, L. & Grabowski, G.. 1991 The simple fool's guide to PCR. Version 2.0, October, 2002. Department of Zoology, University of Hawaii, Honolulu. 46p.
- Pavan, C. 1946. Observations and experiments on the cave fish *Pimelodella kronei* and its relatives. **American Naturalist**, **80** (792): 343-361.
- Pavanelli, C. S., da Graça, W. J., Zawadzki, C. H., Britski, H. A., Vidotti, A. P., Avelino, G. S. & S. Veríssimo. 2007. Fishes from the Corumbá Reservoir, Paranaíba River drainage, upper Paraná River basin, State of Goiás, Brazil. **Check List**, **3** (1): 58–64.
- Pearson, N. E. 1924. The fishes of the eastern slope of the Andes. I. The fishes of the Rio Beni basin, Bolivia, collected by the Mulford expedition. **Indiana University Studies** **11** (64): 1–83, Pls. 1–12.
- Perdices, A., Bermingham, E., Montilla, A. & I. Doadrio. 2002. Evolutionary history of the genus *Rhamdia* (Teleostei: Pimelodidae) in central America. **Molecular Phylogenetics and Evolution**, **25** (1): 172–189.
- Perugia, A. 1897. Di alcuni pesci raccolti in Bolivia dal Prof. Luigi Balzan. **Annali del Museo Civico di Storia Naturale di Genova (Serie 2)** **18**: 16–27.
- Pinna, M. C. C. 1993 Higher-level phylogeny of Siluriformes, with a new classification of the order (Teleostei, Ostariophysi). Unpublished PhD Thesis, The City University of New York, New York. 482p.
- Pinna, M. C. C. 1998 Phylogenetic relationships of neotropical siluriformes (Teleostei:Ostariophysi): Historical overview and synthesis of hypotheses. *In*: Malabarba, L. R., Reis, R. E., Vari, R. P., Lucena, Z. M. S. & C. A. S. Lucena (eds). *Phylogeny and Classification of Neotropical Fishes*. EDIPUCRS, Porto Alegre, pp 279–330.
- Pinna, M. C. C. 1999. Species concepts and phylogenetics. **Reviews in Fish biology and Fisheries** **9**(4): 353–373.

- Proudlove, G. S. 2006. Subterranean fishes of the World. An account of the subterranean (hypogean) fishes described up to 2003 with a bibliography 1541–2004. International Society for Subterranean Biology, Moulis. 300p.
- Provenzano, F., Marcano, A. & Mondaca, P. 1998. Catálogo de ejemplares tipos en la colección de peces del Museo de Biología de la Universidad Central de Venezuela.(MBUCV-V). **Acta Biologica Venezuelica** **18**(1): 1–24.
- de Queiroz, K. 2007. Species concepts and species delimitation. **Systematic biology** **56**(6): 879–886.
- Regan, C. T. 1903. Descriptions of new South-American fishes in the collection of the British Museum. **Annals and Magazine of Natural History (Series 7)** **12** (72) (art. 64): 621–630
- Regan, C. T. 1911. The classification of the Teleostean fishes of the order Ostariophysi. - 2. Siluroidea. **Annals and Magazine of Natural History (Series 8)** **8** (47): 553–577.
- Regan, C. T. 1913. Fishes from Peru, collected by Dr. H. O. Forbes. **Annals and Magazine of Natural History (Series 8)** **12** (69): 278–280.
- Reis, R. E., Albert, J. S., Di Dario, F., Mincarone, M. M., Petry, P. & L. A. Rocha. 2016. Fish biodiversity and conservation in South America. **Journal of Fish Biology**, **89**(1): 12–47.
- Retzer, M. E., & L. M. Page. 1997. Systematic of the Stick Catfishes, *Farlowella* Eigenmann & Eigenmann (Pisces, Loricariidae). **Proceedings of the Academy of Natural Sciences of Philadelphia**, **147**: 33–88.
- Rizzato, P.P. & Bichuette, M.E. 2014. *Ituglanis boticario*, a new troglomorphic catfish (Teleostei: Siluriformes: Trichomycteridae) from Mambai karst area, central Brazil. **Zoologia (Curitiba)** **31**(6): 577–598.
- Roberts, W. M. 1828–1959. William Milnor Roberts Papers. Collection 783, Montana State University Library. (<http://archiveswest.orbiscascade.org/ark:/80444/xv01281>) Accessed at 08 November 2017.
- Romero, A. & Paulson, K.M. 2001. It's a wonderful hypogean life: a guide to the troglomorphic fishes of the world. **Environmental Biology of Fishes** **62**(1–3): 13–41.
- Rosa, R. S., Menezes, N. A., Britski, H. A., Costa, W. J. E. M. & F. Groth. 2003. Diversidade, padrões de distribuição e conservação dos peixes da Caatinga. *In*: Leal, I. R. (ed). **Ecologia e conservação da Caatinga**, Editora universitária UFPE, Pernambuco. 135–180 p.

- RStudio Team. 2016. **RStudio: Integrated Development for R**. RStudio, Inc., Boston, MA. <http://www.rstudio.com/>
- Ruiz Diaz, F.; Soneira, P.; Almirón, A.; Casciotta, J.; Gonzalez, A. & S. Sánchez. 2008. First record of *Pimelodella taenioptera* Miranda Ribeiro, 1914 (Siluriformes, Heptapteridae) from the río Paraná above río Paraguay confluence, Argentina. **Ichthyological Contributions of PecesCriollos 10**: 1–4.
- Sabaj, M. H. 2016. Standard symbolic codes for institutional resource collections in herpetology and ichthyology: an online reference (v6. 5). **American Society of Ichthyologists and Herpetologists**, USA.
- Sabaj, M. H. & Arce, M. 2017. Taxonomic assessment of the Hard-Nosed Thornycats (Siluriformes: Doradidae: *Trachydoras* Eigenmann 1925) with description of *Trachydoras gepharti*, n. sp. **Proceedings of the Academy of Natural Sciences of Philadelphia, 166** (1): 1–53.
- Sands, D. D. 1985. *Brachyrhamdia*, cryptic or mimetic catfishes from South America. Zoomimesis, Camouflage or Mimicry. 58(9)–58(11) pp. *In*: D. Sands, **Catfishes of the World. Volume three: Supplements (First Set)**. Dunure Enterprises, Dunure.
- Sands, D. D. & B. K. Black. 1985. Two new species of *Brachyrhamdia*, Myers, 1927, from Brazil and Peru, together with a redefinition of the genus. *In*: D. Sands, **Catfishes of the World. Volume three: Supplements (First Set)**: 58(1)–58(8).
- Santos, G. M., Jegu, M. & B. Merona. 1984. **Catálogo de peixes comerciais do baixo Rio Tocantins**. 1ª edição. Eletronorte /CNPq/INPA. Manaus, AM. 80p.
- Sarmiento, J.; Bigorne, R.; Carvajal-Vallejos, F. M.; Maldonado, M.; Leciak, E. & T. Oberdorff (eds.) 2014. **Peces de Bolivia/Bolivian fishes**. IRD-Biofresh (EU). 211p.
- Saul, W. G. 1975. An ecological study of fishes at a site in Upper Amazonian Ecuador. **Proceedings of the Academy of Natural Sciences of Philadelphia, 127** (12): 93–134.
- Sayyari, E. & Mirarab, S. 2016. Fast coalescent-based computation of local branch support from quartet frequencies. **Molecular biology and evolution 33**(7): 1654–1668.
- Schlegel, A. 2017. Principal Component Analysis. (<https://www.r-bloggers.com/principal-component-analysis/>). Electronic version accessed 13 September 2017.
- Schomburgk, R.H. 1841. The Natural History of Fishes of Guiana.— Part I. *In*: Jardine, W. (Ed.), **The Naturalists' Library, Vol. 3**, W.H. Lizars, Edinburgh, 263 p., pls. 1–30.
- Schubart, O. 1964. Duas novas espécies de peixe da família Pimelodidae do Rio Mogi Guaçu (Pisces, Nematognathi). **Boletim do Museu Nacional do Rio de Janeiro, Zoologia, Nova Série 244**: 1–22.

- Schultz, L. P. 1944. The catfishes of Venezuela, with description of thirty-eight new forms. **Proceedings of the United States National Museum**, **94** (3172): 173–338.
- Shibatta, O. A. & C. C. Cheida. 2003. Composição em tamanho dos peixes (Actinopterygii, Teleostei) de ribeirões da bacia do rio Tibagi, Paraná, Brasil. **Revista Brasileira de Zoologia**, **20** (3): 469–473.
- Silfvergrip, A. M. C. 1996. **A systematic revision of the Neotropical catfish genus *Rhamdia* (Teleostei, Pimelodidae)**. Swedish Museum of Natural History, Stockholm. 156p., 8 pl.
- Silfvergrip, A. M. C. & H.-J. Paepke. 1997. Kritischer Katalog der Typen der Fischesammlung des Zoologischen Museums Berlin. Teil 7: Pimelodidae (Siluriformes). **Mitteilungen aus dem Zoologischen Museum in Berlin** **73** (1): 165–173.
- Sites, J. W., & Marshall, J. C. 2003. Delimiting species: a Renaissance issue insystematic biology. **Trends in Ecology & Evolution**, **18**(9), 462–470.
- Slobodian, V. 2013. **Taxonomia, Sistemática e Biogeografia de *Brachyrhamdia* Myers, 1927 (Siluriformes: Heptapteridae), com uma investigação sobre seu mimetismo com outros Siluriformes**. Unpublished Msc. dissertation, Universidade de São Paulo, Ribeirão Preto, Brazil. 316p.
- Slobodian, V, Akama, A. Dutra, G. M. 2017. A new species of *Pimelodella* (Siluriformes: Heptapteridae) from the Guiana Shield, Brazil. **Zootaxa** **4338** (1): 85–100.
- Slobodian, V. & Bockmann, F.A. 2013. A new *Brachyrhamdia* (Siluriformes: Heptapteridae) from Rio Japurá basin, Brazil, with comments on its phylogenetic affinities, biogeography and mimicry in the genus. **Zootaxa**, **3717**(1), 01–22.
- Smith, L. I. 2002. A tutorial on principal components analysis. **Cornell University, USA**, **51**(52), 65.
- Soares-Porto, L.M. 1994. Dieta e ciclo diurno de atividade alimentar de *Pimelodella lateristriga* (Müller e Troschel, 1849) (Siluroidei, Pimelodidae) no rio Ubatiba, Marica, Rio de Janeiro. **Brazilian Journal of Biology** **54** (3): 451–458.
- De Souza, L. S., Armbruster, J. W. & D. C. Werneke. 2012. The influence of the Rupununi portal on distribution of freshwater fish in the Rupununi district, Guyana. **Cybiurn**, **36**(1): 31–43.
- Souza-Shibatta, L.; Pezenti, L. F.; Ferreira, D. G.; Almeida, F. S.; Sofia, S. H. & O. A. Shibatta. 2013. Cryptic species of the genus *Pimelodella* (Siluriformes: Heptapteridae) from the Miranda River, Paraguay River basin, Pantanal of Mato Grosso do Sul, Central Brazil. **Neotropical Ichthyology**, **11**(1), 101-109.

- Spix, J. B. von & L. Agassiz. 1829. **Selecta genera et species piscium quos in itinere per Brasiliam annis MDCCCXVII-MDCCCXX jussu et auspiciis Maximiliani Josephi I... colleget et pingendo curavit Dr J. B. de Spix... Monachii**. Part 1: i–xvi + i–ii + 1–82, Pls. 1–48.
- Stamatakis, A. 2014. RAxML version 8: a tool for phylogenetic analysis and post-analysis of large phylogenies. **Bioinformatics** **30**(9): 1312–1313.
- Starks, E. C. 1906. On a collection of fishes made by P. O. Simons in Ecuador and Peru. **Proceedings of the United States National Museum** **30** (1468): 761–800, Pls. 65–66.
- Steindachner, F. 1864. Ichthyologische Notizen. **Sitzungsberichte der Mathematisch-Naturwissenschaftlichen Classe der Kaiserlichen Akademie der Wissenschaften** **49**: 200–214, Pls. 1–2.
- Steindachner, F. 1876a. Ichthyologische Beiträge (IV). **Sitzungsberichte der Kaiserlichen Akademie der Wissenschaften. Mathematisch-Naturwissenschaftliche Classe** **72** (1): 551–616, Pls. 1–13.
- Steindachner, F. 1876b. Die Süßwasserfische des südöstlichen Brasilien (III). **Anzeiger der Kaiserlichen Akademie der Wissenschaften, Mathematisch-Naturwissenschaftlichen Classe** **13** (4): 191.
- Steindachner, F. 1876c. Ichthyologische Beiträge (V). **Sitzungsberichte der Kaiserlichen Akademie der Wissenschaften. Mathematisch-Naturwissenschaftliche Classe** **74** (1): 49–240, Pls. 1–15
- Steindachner, F. 1877. Die Süßwasserfische des südöstlichen Brasilien (III). **Sitzungsberichte der Kaiserlichen Akademie der Wissenschaften. Mathematisch-Naturwissenschaftliche Classe** **74** (1): 559–694, Pls. 1–13.
- Steindachner, F. 1879. Über einige neue und seltene Fisch-Arten aus den k. k. zoologischen Museum zu Wien, Stuttgart, und Warschau. **Denkschriften der Kaiserlichen Akademie der Wissenschaften in Wien, Mathematisch-Naturwissenschaftliche Classe** **41**: 1–52, Pls. 1–9.
- Steindachner, F. 1882. Beiträge zur Kenntniss der Flussfische Südamerikas. IV. **Denkschriften der Kaiserlichen Akademie der Wissenschaften in Wien, Mathematisch-Naturwissenschaftliche Classe** **46** (1) (sometimes referred to 1883): 1–44, Pls. 1–7.
- Steindachner, F. 1902. Herpetologische und ichthyologische Ergebnisse einer Reise nach Südamerika, mit einer Einleitung von Therese Prinzessin von Bayern. **Denkschriften**

der Kaiserlichen Akademie der Wissenschaften in Wien, Mathematisch-Naturwissenschaftliche Classe 72: 89–148, Pls. 1-6.

- Steindachner, F. 1907. Über einige Fischarten aus dem Flusse Cubataõ im Staate Santa Catharina bei Theresopolis (Brasilien). **Sitzungsberichte der Kaiserlichen Akademie der Wissenschaften, Mathematisch-Naturwissenschaftlichen Klasse 116** (1): 475–492, Pls. 1–2.
- Streicher J.W., Schulte J.A. & J. J. Wiens. 2015. How should genes and taxa be sampled for phylogenomic analyses with missing data? An empirical study in Iguanian lizards. **Systematic Biology 65**(1): 128–145.
- Sullivan, J.P., Lavoue, S. & Hopkins, C.D. 2000. Molecular systematics of the African electric fishes (Mormyroidea: Teleostei) and a model for the evolution of their electric organs. **Journal of experimental Biology 203**(4):665–683.
- Sullivan, J. P., Muriel-Cunha, J. & J. G. Lundberg. 2013. Phylogenetic relationships and molecular dating of the major groups of catfishes of the Neotropical superfamily Pimelodoidea (Teleostei, Siluriformes). **Proceedings of the Academy of Natural Sciences of Philadelphia, 162** (1): 89–110.
- Swarbrick, B. 2012. **Multivariate Data Analysis for Dummies**. Wiley & Sons, England. 43p.
- Swofford, D. L. 1998. **PAUP*; phylogenetic analysis using parsimony (and other methods)**. Version 4.0. Sinauer, Sunderland, Massachusetts.
- Tamura, K., Peterson, D., Peterson, N., Stecher, G., Nei, M. & Kumar, S. 2011. MEGA5: molecular evolutionary genetics analysis using maximum likelihood, evolutionary distance, and maximum parsimony methods. **Molecular biology and evolution 28**(10): 2731–2739.
- Teresa, F. B. & L. Casatti. 2010. Importância da vegetação ripária em região intensamente desmatada no sudeste do Brasil: um estudo com peixes de riacho. **Pan-American Journal of Aquatic Sciences 5** (3): 444–453.
- Thompson, A.W., Betancur-R, R., López-Fernández, H. & Ortí, G. 2014. A time-calibrated, multi-locus phylogeny of piranhas and pacus (Characiformes: Serrasalminae) and a comparison of species tree methods. **Molecular phylogenetics and evolution 81**: 242–257.
- Trajano, E. 1987. **Biologia do bagre cavernícola *Pimelodella kronei* e de seu provável ancestral, *Pimelodella transitoria* (Siluriformes, Pimelodidae)**. São Paulo. São Paulo: Instituto de Biociências. Unpublished PhD. Thesis. 136p.

- Trajano, E. 1989. Estudo do comportamento espontâneo e alimentar e da dieta do bagre cavernícola, *Pimelodella kronei*, e seu provável ancestral epígeo, *Pimelodella transitoria* (Siluriformes, Pimelodidae). **Revista Brasileira de Biologia** **49**(3): 757–769.
- Trajano, E. 1991. Population ecology of *Pimelodella kronei*, troglobitic catfish from Southeastern Brazil (Siluriformes, Pimelodidae). **Environmental Biology of Fishes** **30**(4): 407–421.
- Trajano, E. 1994. Comparative study of the brain and olfactory organ of the troglobitic catfish, *Pimelodella kronei* (Ribeiro 1907), and its putative ancestor, *P. transitoria* (Ribeiro 1912) (Siluriformes Pimelodidae). **Tropical Zoology** **7**(1): 145–160.
- Trajano, E. 2006a. **Sistema Areias. 100 anos de estudos**. São Paulo: Redespeleo Brasil. 148p.
- Trajano, E. 2006b. Os estudos biológicos no Sistema Areias. *In*: Trajano, E. (org.) **Sistema Areias. 100 anos de estudos**. São Paulo: Redespeleo Brasil. 24–26 pp.
- Trajano, E. & H. A. Britski. 1992. *Pimelodella kronei* (Ribeiro, 1907) e seu sinônimo *Caecorhamdella brasiliensis* Borodin, 1927: Morfologia externa, taxonomia e evolução (Teleostomi, Siluriformes). **Boletim de Zoologia, São Paulo** **12**: 53-89.
- Trajano, E. & Bockmann, F.A. 1999. Evolution of ecology and behaviour in Brazilian heptapterine cave catfishes, based on cladistic analysis (Teleostei: Siluriformes). **Mémoires de Biospéologie** **26**: 123–129.
- Trajano, E., R. E. Reis & M. E. Bichuette. 2004. *Pimelodella spelaea*: a new cave catfish from central Brazil, with data on ecology and evolutionary considerations (Siluriformes: Heptapteridae). **Copeia** **2004** (2): 315–325.
- Trajano, E, Guil, A. L. F. & A. M. Silva. 2006. Os estudos biológicos no Sistema Areias. *In*: Trajano, E. (org.) **Sistema Areias. 100 anos de estudos**. São Paulo: Redespeleo Brasil. 24–26 pp.
- Valenciennes, A. 1835. Poissons [plates]. *In*: A. d'Orbigny. **Voyage dans l'Amérique méridionale**. Pls. 1–16.
- Valenciennes, A. 1847. Poissons. Catalogue des principales espèces de poissons, rapportées de l'Amérique méridionale. *In*: A. d'Orbigny. **Voyage dans l'Amérique méridionale**. P. Bertrand, Paris and V. Levrault, Strasbourg. 11p.
- Van der Stigchel, J. W. R. 1946. **The South American Nematognathi of the Museums at Leiden and Amsterdam**. Leiden. 204p

- Van der Stigchel, J. W. R. 1964. A new species of pimelodid catfish from eastern Brazil, *Pimelodella boschmai* nov. spec. **Zoologische Mededelingen (Leiden)** **39**: 327–330.
- Vanscoy, T., Lundberg, J. G. & Luckenbill, K. 2015 Bony ornamentation of the catfish pectoral-fin spine: comparative and developmental anatomy, with an example of fin-spine diversity using the Tribe Brachyplatystomini (Siluriformes, Pimelodidae). **Proceedings of the Academy of Natural Sciences of Philadelphia**, **164** (1), 177–212.
- Vari, R.P., Ferraris, C. J., Jr, Radosavljevic, A. & V. A. Funk. 2009. Checklist of the Freshwater Fishes of the Guiana Shield. **Bulletin of the Biological Society of Washington**, **17** (1):i–vii+1–95
- Volcan, M. V., Lanés, L. E. K., Gonçalves, Â. C., da Fonseca, A. P. & M. P. Cirne. 2012. The fish fauna of the Corrientes stream basin, Patos lagoon system, state of Rio Grande do Sul, southern Brazil. **Check List**, **8** (1), 77–82.
- Ward, R.D., T. S. Zemlak, B. H. Innes, P. R. Last & P. D. N. Hebert. DNA barcoding Australia's fish species. **Philosophical Transactions of the Royal Society B Biological Sciences** **360**(1462): 1847–1857.
- Wheeler, Q.D. 2004. Taxonomic triage and the poverty of phylogeny. **Philosophical Transactions of the Royal Society of London B: Biological Sciences** **359**(1444): 571–583.
- Wheeler, Q.D. & Meier, R. eds. 2000. **Species concepts and phylogenetic theory: a debate**. Columbia University Press. 256p.
- Whitworth, T. L., Dawson, R. D., Magalon, H., & Baudry, E. 2007. DNA barcoding cannot reliably identify species of the blowfly genus *Protocalliphora* (Diptera: Calliphoridae). **Proceedings of the Royal Society of London B: Biological Sciences** **274**(1619): 1731–1739.
- Wiemers M, Fiedler K. 2007. Does the DNA barcoding gap exist?—A case study in blue butterflies (Lepidoptera: Lycaenidae). **Frontiers in Zoology**, **4**: 8.
- Wilson, E.O. 2004. Taxonomy as a fundamental discipline. **Philosophical Transactions of the Royal Society of London B: Biological Sciences** **359**(1444): 739–739.
- Zarske, A. 2003. Wiederbeschreibung von *Rhamdia marthae* (Sands & Black, 1985) (Teleostei, Siluriformes, Pimelodidae). *Zoologische Abhandlungen; Staatliches Museum für Tierkunde in Dresden* **53**: 47–55.

Veronica Slobodian

Taxonomic revision of *Pimelodella* Eigenmann & Eigenmann, 1888 (Siluriformes: Heptapteridae): an integrative proposal to delimit species using a multidisciplinary strategy

Revisão taxonômica de *Pimelodella* Eigenmann & Eigenmann, 1888 (Siluriformes: Heptapteridae): uma proposta integrativa para a delimitação de espécies com estratégias multidisciplinares

v.2

Original version

Thesis Presented to the Post-Graduate Program of the Museu de Zoologia da Universidade de São Paulo to obtain the degree of Doctor of Science in Systematics, Animal Taxonomy and Biodiversity

Advisor: Mário César Cardoso de Pinna, PhD.

São Paulo
2017

“I do not authorize the reproduction and dissemination of this work in part or entirely by any electronic or conventional means.”

Serviço de Biblioteca e Documentação
Museu de Zoologia da Universidade de São Paulo

Cataloging in Publication

Slobodian, Veronica

Taxonomic revision of *Pimelodella* Eigenmann & Eigenmann, 1888 (Siluriformes: Heptapteridae) : an integrative proposal to delimit species using a multidisciplinary strategy / Veronica Slobodian ; orientador Mário César Cardoso de Pinna. São Paulo, 2017.

2 v. (811 f.)

Tese de Doutorado – Programa de Pós-Graduação em Sistemática, Taxonomia e Biodiversidade, Museu de Zoologia, Universidade de São Paulo, 2017.

Versão original

1. Peixes (classificação). 2. Siluriformes 3. Heptapteridae. I. Pinna, Mário César Cardoso de, orient. II. Título.

CDU 597.551.4

Summary

Volume 2

Tables, Figures and attachments.....318

Tables

Table 1: Nominal species available for <i>Pimelodella</i> genus.....	319
Table 2. Species analyzed in PCAs.....	323
Table 3. Species currently placed in <i>Pimelodella</i> and their status as proposed by this work.	
Table 4. Morphometric data of <i>Pimelodella australis</i> based on type and comparative materials.....	327
Table 5. Morphometric data of <i>Pimelodella avanhandavae</i> based on type and comparative materials.....	329
Table 6. Morphometric data of <i>Pimelodella boliviana</i> based on type and comparative materials.....	331
Table 7. Morphometric data of <i>Pimelodella insignis</i> , junior-synonym of <i>P. boschmai</i> , based on type material.....	333
Table 8. Morphometric data of <i>Pimelodella brasiliensis</i> and its junior-synonyms, <i>P. eigenmanni</i> and <i>P. rendahli</i> , based on type materials.....	335
Table 9. Morphometric data of <i>Pimelodella brasiliensis</i> and its junior-synonyms, <i>P. eigenmanni</i> and <i>P. rendahli</i> , based on type materials, discriminated by original species name.....	337
Table 10. Morphometric data of <i>Pimelodella buckleyi</i> based on type and comparative materials.....	340
Table 11. Morphometric data of <i>Pimelodella chagresi</i> based on type and comparative materials.....	342
Table 12. Morphometric data of <i>Pimelodella conquetaensis</i> based on type material.....	344
Table 13. Morphometric data of <i>Pimelodella cristata</i> and its junior-synonyms, <i>P. cristata</i> , <i>P. breviceps</i> , <i>P. dorseyi</i> , <i>P. hartwelli</i> , <i>P. ophthalmica</i> , <i>P. parnahybae</i> , <i>P. steindachneri</i> , <i>P. wessellii</i> , <i>P. witmeri</i> , based on type and comparative materials.....	346
Table 14: Morphometric data of <i>Pimelodella cristata</i> and its junior-synonyms, <i>P. cristata</i> , <i>P. breviceps</i> , <i>P. dorseyi</i> , <i>P. hartwelli</i> , <i>P. ophthalmica</i> , <i>P. parnahybae</i> , <i>P. steindachneri</i> , <i>P. wessellii</i> , <i>P. witmeri</i> , based on type and comparative materials, discriminated by original species name.....	348
Table 15: Meristic data of <i>P. cristata</i> and its junior-synonyms, <i>P. cristata</i> , <i>P. breviceps</i> , <i>P. cyanostygma</i> , <i>P. dorseyi</i> , <i>P. hartwelli</i> , <i>P. ophthalmica</i> , <i>P. parnahybae</i> , <i>P. steindachneri</i> , <i>P. wessellii</i> , <i>P. witmeri</i> , discriminated by the original species name and region.....	357
Table 16: Morphometric data of <i>Pimelodella cruxenti</i> based on type (as presented in original description) and comparative materials.....	368
Table 17: Morphometric data of <i>Pimelodella elongata</i> based on type and comparative material.....	370
Table 18: Morphometric data of <i>Pimelodella enochi</i> and <i>P. papariae</i> , its junior-synonym, based on type material and discriminated by original species name.....	372
Table 19: Morphometric data of <i>Pimelodella eutaenia</i> based on type and comparative material.....	374
Table 20: Morphometric data of <i>Pimelodella figueroai</i> based on type material.....	376
Table 21: Morphometric data of <i>Pimelodella geryi</i> and <i>P. procera</i> , its junior-synonym, based on type and comparative materials.....	378

Table 22: Morphometric data of <i>Pimelodella geryi</i> and <i>P. procera</i> , its junior-synonym, based on type and comparative materials, discriminated by original species name.....	380
Table 23: Morphometric data of <i>Pimelodella gracilis</i> and <i>P. taenioptera</i> , its junior-synonym, based on type and comparative materials.....	382
Table 24: Morphometric data of <i>Pimelodella gracilis</i> and <i>P. taenioptera</i> , its junior-synonym, based on type and comparative materials, discriminated by original species name.....	384
Table 25: Morphometric data of <i>Pimelodella griffini</i> based on type material.....	387
Table 26: Morphometric data of <i>Pimelodella grisea</i> based on type material.....	389
Table 27: Morphometric data of <i>Pimelodella harttii</i> based on type material.....	391
Table 28: Morphometric data of <i>Pimelodella hasemani</i> based on type and comparative materials.....	393
Table 29: Morphometric data of <i>Pimelodella howesi</i> based on type and comparative materials.....	395
Table 30: Morphometric data of <i>Pimelodella humeralis</i> based on type material.....	397
Table 31: Morphometric data of <i>Pimelodella ignobilis</i> and <i>P. pappenheimi</i> , its junior-synonym, based on type and comparative materials.....	399
Table 32: Morphometric data of <i>Pimelodella ignobilis</i> and <i>P. pappenheimi</i> , its junior-synonym, based on type and comparative materials, discriminated by original species name.....	401
Table 33: Morphometric data of <i>Pimelodella itapicuruensis</i> based on type material.....	404
Table 34: Morphometric data of <i>Pimelodella kronei</i> and <i>P. transitoria</i> , its junior-synonym, based on type and comparative materials.....	406
Table 35: Morphometric data of <i>Pimelodella kronei</i> and <i>P. transitoria</i> , its junior-synonym, based on type and comparative materials, discriminated by original species name.....	408
Table 36: Morphometric data of <i>Pimelodella lateristriga</i> and <i>P. bahiana</i> , its junior-synonym, based on type and comparative materials.....	411
Table 37: Morphometric data of <i>Pimelodella lateristriga</i> and <i>P. bahiana</i> , its junior-synonym, based on type and comparative materials, discriminated by original species name.....	413
Table 38: Morphometric data of <i>Pimelodella laticeps</i> based on type material.....	416
Table 39: Morphometric data of <i>Pimelodella laurenti</i> based on type and comparative materials.....	418
Table 40: Morphometric data of <i>Pimelodella leptosoma</i> based on type and comparative materials.....	420
Table 41: Morphometric data of <i>Pimelodella linami</i> based on type material.....	422
Table 42: Morphometric data of <i>Pimelodella longipinnis</i> based on type material.....	424
Table 43: Morphometric data of <i>Pimelodella macturki</i> based on type material.....	426
Table 44: Morphometric data of <i>Pimelodella meeki</i> and <i>P. rudolphi</i> , its junior-synonym, based on type and comparative materials.....	428
Table 45: Morphometric data of <i>Pimelodella meeki</i> and <i>P. rudolphi</i> , its junior-synonym, based on type and comparative materials, discriminated by original species name.....	430
Table 46: Morphometric data of <i>Pimelodella megalops</i> based on type and comparative materials.....	433
Table 47: Morphometric data of <i>Pimelodella megalura</i> based on type material.....	435
Table 49: Morphometric data of <i>Pimelodella modesta</i> based on type and comparative materials.....	439
Table 50: Morphometric data of <i>Pimelodella montana</i> based on type and comparative materials.....	441
Table 51: Morphometric data of <i>Pimelodella mucosa</i> based on type and comparative materials.....	443
Table 52: Morphometric data of <i>Pimelodella notomelas</i> based on type and comparative materials.....	445
Table 53: Morphometric data of <i>Pimelodella odynea</i> based on type material.....	447
Table 55: Morphometric data of <i>Pimelodella peruana</i> based on type and comparative materials.....	451

Table 56: Morphometric data of <i>Pimelodella reyesi</i> based on type and comparative materials.	453
Table 57: Morphometric data of <i>Pimelodella robinsoni</i> and <i>P. wolfi</i> , its junior-synonym, based on type material.....	455
Table 58: Morphometric data of <i>Pimelodella robinsoni</i> and <i>P. wolfi</i> , its junior-synonym, based on type material, discriminated by original species name.	457
Table 59: Morphometric data of <i>Pimelodella roccae</i> based on type and comparative materials.	460
Table 60: Morphometric data of <i>Pimelodella serrata</i> and <i>P. chaparae</i> , its junior-synonym, based on type and comparative materials.....	462
Table 61: Morphometric data of <i>Pimelodella serrata</i> and <i>P. chaparae</i> , its junior-synonym, based on type and comparative materials, discriminated by original species name.....	464
Table 62: Morphometric data of <i>Pimelodella spelaea</i> based on type material.	467
Table 63: Morphometric data of <i>Pimelodella straminea</i> based on type material.	469
Table 64: Morphometric data of <i>Pimelodella taeniophora</i> based on type and comparative materials.	471
Table 65: Morphometric data of <i>Pimelodella tapatapae</i> based on type material.....	473
Table 66: Morphometric data of <i>Pimelodella vittata</i> based on type and comparative materials.	475
Table 67: Morphometric data of <i>Pimelodella yuncensis</i> and <i>P. peruensis</i> , its junior-synonym, based on type and comparative materials.....	477
Table 68: Morphometric data of <i>Pimelodella yuncensis</i> and <i>P. peruensis</i> , its junior-synonym, based on type and comparative materials, discriminated by original species name.....	479
Table 69: Identification Key for the valid <i>Pimelodella</i> species diagnosable in this work. ..	482
Table 70: Complete material list analyzed for molecular taxonomy.....	497

Figures

Figure 1: Schematic for particular measurements taken point-to-point in a generalized <i>Pimelodella</i> specimen.	502
Figure 2: Schematic for head laterosensory canals, dorsal view, in a generalized <i>Pimelodella</i> specimen. Scale bar 2mm.....	503
Figure 3: Schematic for head laterosensory canals, lateral view, in a generalized <i>Pimelodella</i> specimen. Scale bar 2mm.....	504
Figure 4: Schematic for head laterosensory canals, ventral view, in a generalized <i>Pimelodella</i> specimen. Scale bar 2mm.	505
Figure 5: <i>Pimelodella australis</i> , holotype, FMNH 57962, 61.0 mm SL. Left lateral (A), and dorsal (B) views. Photo taken by M. W. Littmann.....	506
Figure 6: Ventral view of left pectoral-fin spine of <i>Pimelodella australis</i> , holotype, 61.0mm SL, total length of spine 12.6 mm.....	507
Figure 7: Schematic left lateral view of <i>Pimelodella australis</i>	508
Figure 8: <i>Pimelodella avandavae</i> , holotype, FMNH 57981, 69.0 mm SL. Left lateral (A), and dorsal (B) views. Photo taken by M. W. Littmann.....	509
Figure 9: Ventral view of left pectoral-fin spine of <i>Pimelodella avandavae</i> FMNH 57982, paratype, 78.8 mm SL, total length of spine 13.4 mm.....	510
Figure 10: Schematic left lateral view of <i>Pimelodella avandavae</i>	511
Figure 11: <i>Pimelodella boliviana</i> , holotype, FMNH 57976, 68.9 mm SL. Left lateral (A), and dorsal (B) views. Photo taken by M. W. Littmann.....	512
Figure 12: Ventral view of left pectoral-fin spine of <i>Pimelodella boliviana</i> A) FMNH 57977, paratype, 66.9 mm SL, total length of spine 11.5 mm; B) MZUSP 26015, 71.3 mm SL, total length of spine 11.7 mm.	513
Figure 13: Schematic left lateral view of <i>Pimelodella boliviana</i>	514

Figure 14: <i>Pimelodella boschmai</i> , holotype, RMNH 23248, 73.0 mm SL. Left lateral (A), and dorsal (B) views. Photo taken by Ronald de Ruiter	515
Figure 15: Ventral view of left pectoral-fin spine of A) <i>Pimelodella boschmai</i> , RMNH 23248, holotype, 73.0 mm SL; B) <i>Pimelodella insignis</i> , MZUSP 22317, syntype 66.4 mm SL, total length of spine 12.8 mm.	516
Figure 16: Schematic left lateral view of <i>Pimelodella boschmai</i>	517
Figure 17: <i>Pimelodella brasiliensis</i> , holotype, NMW 45612, 140.6 mm SL. Left lateral (A), and dorsal (B) views. Photos taken by Mark Sabaj. <i>Pimelodella eigenmanni</i> , junior-synonym of <i>P. brasiliensis</i> , paralectotype, MCZ 7438, 130.7 mm SL, left lateral (C), and dorsal (D) views. <i>Pimelodella rendahli</i> , junior-synonym of <i>P. brasiliensis</i> , holotype, ZMB 32031, 80.7 mm SL, left lateral (E), and dorsal (F) views, photo taken by ZMB staff.	518
Figure 18: Ventral view of left pectoral-fin spine of <i>Pimelodella brasiliensis</i> , NMW 45612, holotype, 140.6 mm SL, total length of spine 26.6 mm.....	519
Figure 19: Schematic left lateral view of <i>Pimelodella brasiliensis</i>	520
Figure 20: <i>Pimelodella buckleyi</i> , lectotype, BMNH 1880.12.8.98, 109.6 mm SL. Left lateral (A), and dorsal (B) views. Photo taken by Mark Allen.....	521
Figure 21: Ventral view of left pectoral-fin spine of <i>Pimelodella buckleyi</i> , BMNH 1880.12.8.98, lectotype, 109.6 mm SL, total length of spine 15.3 mm.....	522
Figure 22. Schematic left lateral view of <i>Pimelodella buckleyi</i>	523
Figure 23. <i>Pimelodella chagresi</i> , lectotype, MCZ 4947, 111.8 mm SL. Left lateral (A), and dorsal (B) views.	524
Figure 24. Ventral view of left pectoral-fin spine of <i>Pimelodella chagresi</i> , CAS 57903, 83.5 mm SL, total length of spine 15.1 mm.....	525
Figure 25. Schematic left lateral view of <i>Pimelodella chagresi</i>	526
Figure 26. <i>Pimelodella conquetaensis</i> , holotype, ZMB 32032, 93.2 mm SL. Left lateral (A), and dorsal (B) views. Photo taken by Mark Allen.....	527
Figure 27. Ventral view of left pectoral-fin spine of <i>Pimelodella conquetaensis</i> , ZMB 32032, holotype, 93.2 mm SL, total length of spine 16.5 mm.	528
Figure 28. Schematic left lateral view of <i>Pimelodella conquetaensis</i>	529
Figure 29. <i>Pimelodella cristata</i> , lectotype, ZMB 3053, 202.5 mm SL. Left lateral (A), and dorsal (B) views.	530
Figure 30. Ventral view of left pectoral-fin spine of <i>Pimelodella cristata</i> , ZMB 3052, paralectotype, 177.5 mm SL, total length of spine 27.8 mm.	531
Figure 31. Schematic left lateral view of <i>Pimelodella cristata</i>	532
Figure 32. Framed graphic of PC1 against PC2 of a Principal Component Analysis using all morphometric data scaled to SL or HL (except caudal-fin lobes, due to usual incompleteness of those in the material), based on type and comparative materials of <i>P. cristata</i> , <i>P. cruxenti</i> , <i>P. breviceps</i> , <i>P. dorseyi</i> , <i>P. gracilis</i> , <i>P. hartwelli</i> , <i>P. humeralis</i> , <i>P. ophthalmica</i> , <i>P. parnahybae</i> , <i>P. steindachneri</i> , <i>P. taenioptera</i> , <i>P. wessellii</i> , <i>P. witmeri</i> . Cumulative proportion of importance of components: 39.4%; proportion of Variance: PC1— 20.3%; PC2— 19.1%; standard deviation: PC1— 2.01; PC2— 2.0.	533
Figure 33. Framed graphic of PC1 against PC2 of a Principal Component Analysis using all morphometric data scaled to SL or HL (except caudal-fin lobes, due to usual incompleteness of those in the material), based on type and comparative materials, separated by drainages as follows: Amazon— Amazon rivers' specimens of <i>P. cristata</i> , <i>P. breviceps</i> , <i>P. hartwelli</i> , <i>P. ophthalmica</i> and Amazon rivers' specimens of <i>P. steindachneri</i> ; Guiana Shield— Guiana Shield rivers' specimens of <i>P. cristata</i> and <i>P. wessellii</i> ; Northeastern Brazil— <i>P. dorseyi</i> , <i>P. parnahybae</i> , Parnaíba drainage type-specimen of <i>P. steindachneri</i> and <i>P. witmeri</i> ; Paraná— <i>P. gracilis</i> and <i>P. taenioptera</i> ; <i>P. humeralis</i> . Cumulative proportion of importance of components: 37.8%; proportion of Variance: PC1— 21.5%; PC2— 16.3%; standard deviation: PC1— 2.07; PC2— 1.8.....	534
Figure 34. <i>Pimelodella breviceps</i> , holotype, NMW 45615, 326.2 mm SL. Left lateral (A), and dorsal (B) views.	535

Figure 35. <i>Pimelodella cyanostigma</i> , lectotype, ANSP 8382, 59.8 mm SL. Left lateral (A), and dorsal (B) views. Photo taken by Mark Sabaj.....	536
Figure 36. <i>Pimelodella dorseyi</i> , holotype, ANSP 69375, 95.8 mm SL. Left lateral (A), and dorsal (B) views. Photo taken by Murilo Pastana.....	537
Figure 37. <i>Pimelodella hartwelli</i> , holotype, ANSP 68644, 103.2 mm SL. Left lateral (A), and dorsal (B) views.....	538
Figure 38. <i>Pimelodella ophthalmica</i> , holotype, ANSP 21102, 109.9 mm SL. Left lateral (A), and dorsal (B) views.....	539
Figure 39. <i>Pimelodella parnahybae</i> , holotype, ANSP 69337, 84.0 mm SL. Left lateral (A), and dorsal (B) views. Photo taken by Kyle Luckenbill.....	540
Figure 40. <i>Pimelodella steindachneri</i> , lectotype, MCZ 7487, 150.4 mm SL. Left lateral (A), and dorsal (B) views. Photo taken by MCZ staff.....	541
Figure 41. <i>Pimelodella wesseli</i> , holotype, NMW 79188, 157.9 mm SL. Left lateral (A), and dorsal (B) views. Photo taken by Mark Sabaj and Kyle Luckenbill.....	542
Figure 42. <i>Pimelodella witmeri</i> , holotype, ANSP 69383, 137.5 mm SL. Left lateral (A), and dorsal (B) views. Photo taken by Kyle Luckenbill.....	543
Figure 43. <i>Pimelodella cruxenti</i> , lectotype, MHNLS 95.8 mm SL. Left lateral (A), and dorsal (B) views. Photo taken by Oscar Lasso-Alcalá.....	544
Figure 44. Ventral view of left pectoral-fin spine of <i>Pimelodella cruxenti</i> , ANSP 160647, 75.2 mm SL.....	545
Figure 46. Left lateral view (A) and dorsal view of head (B) of <i>Pimelodella cruxenti</i> , ANSP 160673, 127.7 mm SL. Photo taken by Mark Sabaj.....	547
Figure 47. <i>Pimelodella elongata</i> , lectotype, BMNH 1860.6.16.182, 136.8 mm SL. Left lateral (A), and dorsal (B) views. Photo taken by Mark Allen.....	548
Figure 48. Ventral view of left pectoral-fin spine of <i>Pimelodella elongata</i> , BMNH 1860.6.16.186, paralectotype, 96.1 mm SL, total length of spine 12.1 mm.....	549
Figure 49. Schematic left lateral view of <i>Pimelodella elongata</i>	550
Figure 50. <i>Pimelodella enochi</i> , holotype, ANSP 69378, 44.9 mm SL. Left lateral (A), and dorsal (B) views. Photo taken by Murilo Pastana.....	551
Figure 51. Ventral view of left pectoral-fin spine of <i>Pimelodella enochi</i> , ANSP 69378, 44.9 mm SL, total length of spine 6.8 mm.....	552
Figure 53. <i>Pimelodella papariae</i> , junior synonym of <i>P. enochi</i> , holotype, ANSP 69387, 109.6 mm SL. Left lateral (A), and dorsal (B) views. Photo taken by Murilo Pastana.....	554
Figure 54. Ventral view of left pectoral-fin spine of <i>Pimelodella papariae</i> , ANSP 69387, 109.6 mm SL, total length of spine (approximate) 18.5 mm (tip of spine was broken, and figure correspond to the complete aspect).....	555
Figure 55. <i>Pimelodella eutaenia</i> , lectotype, BMNH 1913.10.1.37, 126.3 mm SL. Left lateral (A), and dorsal (B) views. Photo taken by Mark Allen.....	556
Figure 56. Ventral view of left pectoral-fin spine of <i>Pimelodella eutaenia</i> , BMNH 1913.10.1.37, 126.3 mm SL, total length of spine 20.2 mm (A); BMNH 1913.10.1.38, 65.5 mm SL, total length of spine 12 mm (B).....	557
Figure 57. Schematic left lateral view of <i>Pimelodella eutaenia</i>	558
Figure 58. <i>Pimelodella floridablancaensis</i> , junior-synonym of <i>P. eutaenia</i> , paratype, CAR 695, 85.8 mm SL. Figure obtained from Ardila Rodriguez (2017).....	559
Figure 59. Ventral view of left pectoral-fin spine of <i>Pimelodella floridablancaensis</i> , CAR 07, obtained from Ardila Rodriguez (2017). Sizes of specimen or structure were not indicated, but paratype list cited c&s specimens between 74.9–93.2 mm SL.....	560
Figure 60. <i>Pimelodella figueroai</i> , ICN-MHN 2900, 71.8 mm SL. Left lateral view. Photo taken by Mauricio Leiva.....	561
Figure 61. <i>Pimelodella geryi</i> , holotype, ZMA 102235, 58 mm SL. Left lateral (A), and dorsal (B) views. Photo taken by Ronald De Ruiter.....	562
Figure 62. Ventral view of left pectoral-fin spine of <i>Pimelodella geryi</i> , holotype, ZMA 102235, 58 mm SL, total length of spine 10.0 mm (approximately).....	563
Figure 63. Schematic left lateral view of <i>Pimelodella geryi</i>	564

Figure 64. <i>Pimelodella procera</i> , junior-synonym of <i>P. geryi</i> , paratype, 61.5 mm SL. Left lateral view. Photo taken by Mário de Pinna.	565
Figure 65. <i>Pimelodella gracilis</i> , holotype, MHNH 9284-A, 170.1 mm SL. Left lateral (A), and dorsal (B) views. Photo taken by Mélyne Hautecoeur.....	566
Figure 66. Ventral view of left pectoral-fin spine of <i>Pimelodella gracilis</i> , holotype, MHNH 9284-A, 170.1 mm SL, total length of spine 28.5 mm.	567
Figure 67. Schematic left lateral view of <i>Pimelodella gracilis</i>	568
Figure 68. <i>Pimelodella taenioptera</i> , junior-synonym of <i>P. gracilis</i> , lectotype, MNRJ 691A, 157.8 mm SL. Left lateral (A), and dorsal (B) views.	569
Figure 69. Material identified as <i>Pimelodella taenioptera</i> from Souza-Shibatta <i>et al.</i> (2013), showing color pattern and dorsal-fin filament. MZUEL 6456, 124.6 mm SL, photo extracted from Souza-Shibatta <i>et al.</i> (2013).....	570
Figure 70. Framed graphic of PC1 against PC2 of a Principal Component Analysis using all morphometric data scaled to SL or HL (except caudal-fin lobes, due to usual incompleteness of those in the material), based on type and comparative materials of <i>Pimelodella</i> species with 46 or more total vertebrae (except <i>P. cruxenti</i>), discriminated by the names considered as valid in this work, being <i>P. cristata</i> , <i>P. gracilis</i> and <i>P. humeralis</i> . Cumulative proportion of importance of components: 37.8%; proportion of Variance: PC1— 21.4%; PC2— 16.5%; standard deviation: PC1— 2.07; PC2— 1.8.	571
Figure 71. <i>Pimelodella griffini</i> , holotype, FMNH 57974, 67.2 mm SL. Left lateral (A), and dorsal (B) views. Photo taken by M. W. Littmann.....	572
Figure 72. Ventral view of left pectoral-fin spine of <i>Pimelodella griffini</i> , holotype, FMNH 57974, 67.2 mm SL, total length of spine 11.3 mm.....	573
Figure 73. Schematic left lateral view of <i>Pimelodella griffini</i>	574
Figure 74. <i>Pimelodella grisea</i> , lectotype, BMNH 1902.5.27.36, 119.7 mm SL. Left lateral (A), and dorsal (B) views. Photo taken by Mark Allen.....	575
Figure 75. Ventral view of left pectoral-fin spine of <i>Pimelodella grisea</i> , lectotype, BMNH 1902.5.27.36, 119.7 mm SL, total length of spine 22.4 mm.....	576
Figure 76. Schematic left lateral view of <i>Pimelodella grisea</i>	577
Figure 77. <i>Pimelodella harttii</i> , holotype, NMW 45784, 150.2 mm SL. Left lateral (A), and dorsal (B) views.	578
Figure 78. Ventral view of left pectoral-fin spine of <i>Pimelodella harttii</i> , holotype, NMW 45784, 150.2 mm SL, total length of spine 25.6 mm.	579
Figure 79. Schematic left lateral view of <i>Pimelodella harttii</i>	580
Figure 80. <i>Pimelodella hasemani</i> , holotype, FMNH 57980, 60.6 mm SL. Left lateral (A), and dorsal (B) views. Photo taken by M. W. Littmann.....	581
Figure 81. Ventral view of left pectoral-fin spine of <i>Pimelodella hasemani</i> , FMNH 57980, 60.6 mm SL, total length of spine 10.6 mm.	582
Figure 82. Schematic left lateral view of <i>Pimelodella hasemani</i>	583
Figure 83. <i>Pimelodella hasemani</i> , UFRO-I 9741, 56.5 mm SL. Left lateral (A), and dorsal (B) views.....	584
Figure 84. <i>Pimelodella howesi</i> , ANSP 69036, 79.3 mm SL. Left lateral (A), and dorsal (B) views.....	585
Figure 85. Ventral view of left pectoral-fin spine of <i>Pimelodella howesi</i> , ANSP 69036, 79.3 mm SL, total length of spine 14.1 mm.....	586
Figure 86. Schematic left lateral view of <i>Pimelodella howesi</i>	587
Figure 87. <i>Pimelodella humeralis</i> , holotype, MPEG 34994, 77.4 mm SL. Left lateral (A) and dorsal (B) views.	588
Figure 88. Ventral view of left pectoral-fin spine of <i>Pimelodella humeralis</i> , holotype, MPEG 34994, 77.4 mm SL, total length of spine 12.0 mm.....	589
Figure 89. Schematic left lateral view of <i>Pimelodella humeralis</i>	590
Figure 90. <i>Pimelodella ignobilis</i> , lectotype, NMW 44479, 91.1 mm SL. Left lateral (A) and dorsal (B) views.	591

Figure 91. Ventral view of left pectoral-fin spine of <i>Pimelodella ignobilis</i> , paralectotype, NMW 44479, 98.9 mm SL, total length of spine 19.0 mm.	592
Figure 92. Schematic left lateral view of <i>Pimelodella ignobilis</i>	593
Figure 93. <i>Pimelodella pappenheimi</i> , junior-synonym of <i>P. ignobilis</i> , lectotype, ZMB 31951, 103.1 mm SL. Left lateral (A) and dorsal (B) views.	594
Figure 94. <i>Pimelodella itapicuruensis</i> , FMNH 57986, 60.2 mm SL. Left lateral (A) and dorsal (B) views.	595
Figure 95. Ventral view of left pectoral-fin spine of <i>Pimelodella itapicuruensis</i> , FMNH 57986, 60.2 mm SL, total length of spine 11.2 mm.	596
Figure 96. Schematic left lateral view of <i>Pimelodella itapicuruensis</i>	597
Figure 97. <i>Pimelodella kronei</i> , holotype, MNRJ 836, 120.1 mm SL. Left lateral (A) and dorsal (B) views.	598
Figure 98. Ventral view of left pectoral-fin spine of <i>Pimelodella kronei</i> , LESCO 170, 93.4 mm SL, total length of spine 12.5 mm.	599
Figure 99. Schematic left lateral view of <i>Pimelodella kronei</i>	600
Figure 100. Map of stream routs and flux of Areias system, obtained from Genthner <i>et al.</i> (2006: fig. 6). Arrows: Areias (1) and Bombas (2) ressurgences.	601
Figure 101. Right lateral view of head of <i>P. kronei</i> . Infraorbital series and nasal removed. (A) MZUSP 38725, Bombas resurgence, Iporanga; (B) MZUSP 27168, Areias system, Iporanga.	602
Figure 102. Right lateral view of head of <i>P. transitoria</i> . Infraorbital series and nasal removed. MZUSP 63365, Ribeirão Furnas, Areias system, Iporanga.	603
Figure 103. Right lateral view of <i>P. lateristriga</i> . Infraorbital series and nasal removed. USNM 301676, Rio Mucuri, Northeastern Mata Atlântica region.	604
Figure 104. (A) Dorsal view; (B) Ventral view; and (C) Left lateral view of head of a <i>Pimelodella</i> , showing the overall arrangement of cephalic laterosensorial system. Grey legends are for a simple pore for both <i>P. kronei</i> and <i>P. transitoria</i> . Purple legends are for different conditions (loss or duplication) of a pore in individuals of both species. Red legends are for loss or duplication of a pore exclusively for <i>P. kronei</i> specimens. Scale bar: 2mm.	605
Figure 105. Ventral view of left pectoral-fin spine of <i>Pimelodella kronei</i> , LESCO uncat. 113.2 mm SL, length of spine 12.5 mm, Areias system (A); LESCO 167 144.4 mm SL, length of spine 20.4 mm, Areias system (B); LESCO 169 110.7 mm SL, length of spine 13.4 mm, Bombas resurgence (C); and <i>P. transitoria</i> , LESCO uncat. 101.8 mm SL, length of spine 16.7 mm, Rio Betari, alojamento ouro grosso (D); LESCO 95 85.5 mm SL, length of spine 14.0 mm, Rio Betari (E); LESCO 168 98.1 mm SL, length of spine 15.9 mm, Gruta da Casa de Pedra (F).	606
Figure 106. Left lateral view of <i>Pimelodella transitoria</i> , LESCO 168, 98.1 mm SL.	607
Figure 107. Neotype of <i>Pimelodella transitoria</i> , a junior-synonym of <i>P. kronei</i> , MZUSP 403, 107.4 mm SL. Photo taken by Murilo Pastana.	608
Figure 108. <i>Pimelodella lateristriga</i> , holotype, ZMB 3038, 95,9 mm SL. Left lateral (A) and dorsal (B) views. Photo taken by Johanna Kapp.	609
Figure 109. Ventral view of left pectoral-fin spine of: (A) <i>Pimelodella lateristriga</i> , holotype, ZMB 3038, 95,9 mm SL, total length of spine 18.0 mm (approximated); (B) <i>Pimelodella lateristriga</i> , MZUSP 114867, 84 mm SL, total length of spine 14.5 mm; (C) <i>Pimelodella lateristriga</i> , MZUSP 93863, 99.5 mm SL, total length of spine 15.7 mm; (D) <i>Pimelodella bahiana</i> , lectotype, MNHN B612, 93.4 mm SL, total length of spine 16.1 mm.	610
Figure 110. Schematic left lateral view of <i>Pimelodella lateristriga</i>	611
Figure 111. <i>Pimelodella lateristriga</i> , MZUSP 121461, 112.7 mm SL. Left lateral (A) and dorsal (B) views. Photo taken by Murilo Pastana.	612
Figure 112. <i>Pimelodella bahiana</i> , lectotype, MNHN B612, 93.4 mm SL. Left lateral (A) and dorsal (B) views. Photo taken by MNHN staff.	613
Figure 113. <i>Pimelodella laticeps</i> , holotype, FMNH 57969, 49.0 mm SL. Left lateral (A) and dorsal (B) views. Photo taken by M. W. Littmann.	614

Figure 114. Ventral view of left pectoral-fin spine of <i>Pimelodella laticeps</i> , holotype, FMNH 57969, 49.0 mm SL, total length of spine 9.6 mm.....	615
Figure 115. Schematic left lateral view of <i>Pimelodella laticeps</i>	616
Figure 116. <i>Pimelodella laurenti</i> , holotype, ANSP 69380, 66.5 mm SL. Left lateral (A) and dorsal (B) views. Photo taken by Murilo Pastana.....	617
Figure 117. Ventral view of left pectoral-fin spine of <i>Pimelodella laurenti</i> , holotype, ANSP 69380, 66.5 mm SL, total length of spine 12.7 mm.....	618
Figure 118. Schematic left lateral view of <i>Pimelodella laurenti</i>	619
Figure 119. Left lateral view of <i>Pimelodella laurenti</i> , MZUSP 39441, 62.8 mm SL.....	620
Figure 120. <i>Pimelodella leptosoma</i> , holotype, ANSP 39340, 59.6 mm SL. Left lateral (A) and dorsal (B) views. Photo taken by Mark Sabaj.....	621
Figure 121. Ventral view of left pectoral-fin spine of <i>Pimelodella leptosoma</i> , holotype, ANSP 39340, 59.6 mm SL, total length of spine 8.5 mm.....	622
Figure 123. <i>Pimelodella leptosoma</i> , ANSP 179754. Left lateral (A) and dorsal (B) views. Photo taken by Mark Sabaj.....	624
Figure 124. <i>Pimelodella linami</i> , USNM 121132, holotype, 74.7 mm SL. Left lateral (A) and dorsal (B) views. Photo taken by Sandra Raredon.....	625
Figure 125. Ventral view of left pectoral-fin spine of <i>Pimelodella linami</i> , USNM 121132, holotype, 74.7 mm SL, total length of spine 10.7 mm.....	626
Figure 126. Schematic left lateral view of <i>Pimelodella linami</i>	627
Figure 127. <i>Pimelodella longipinnis</i> , AMNH 8642, holotype, 84.6 mm SL. Left lateral (A) and dorsal (B) views. Photo taken by Melanie Stiassny.....	628
Figure 128. Ventral view of left pectoral-fin spine of <i>Pimelodella longipinnis</i> , AMNH 8642, holotype, 84.6 mm SL, total length of spine 11.7 mm.....	629
Figure 129. Schematic left lateral view of <i>Pimelodella longipinnis</i>	630
Figure 130. Radiograph of <i>Pimelodella longipinnis</i> , AMNH 8642, holotype, 84.6 mm SL. Left lateral view.....	631
Figure 131. <i>Pimelodella macturki</i> , holotype, FMNH 53234, 53.5 mm SL. Left lateral (A) and dorsal (B) views. Photo taken by M. W. Littmann.....	632
Figure 132. Ventral view of left pectoral-fin spine of <i>Pimelodella macturki</i> , paratype, BMNH 1911.10.31.54, 52.9 mm SL, total length of spine 9.8 mm.....	633
Figure 133. Schematic left lateral view of <i>Pimelodella macturki</i>	634
Figure 134. <i>Pimelodella martinezi</i> , holotype, 68 mm SL, image from Fernández-Yépez (1970), unnum. page, pl. 35. Left lateral (A) and dorsal view of head (B).....	635
Figure 135. Schematic left lateral view of <i>Pimelodella martinezi</i>	636
Figure 137. Ventral view of left pectoral-fin spine of <i>Pimelodella meeki</i> , FMNH 57993, 97.1 mm SL, total length of spine 12 mm.....	638
Figure 138. Schematic left lateral view of <i>Pimelodella meeki</i>	639
Figure 139. <i>Pimelodella meeki</i> , MZUSP 51651, 112.2 mm SL. Left lateral (A) and dorsal (B) views. Photo taken by Murilo Pastana.....	640
Figure 140. <i>Pimelodella rudolphi</i> , lectotype, MNRJ 857A, 73.9 mm SL. . Left lateral (A) and dorsal (B) views.....	641
Figure 141. <i>Pimelodella megalops</i> , FMNH 53231, holotype, 74.7 mm SL. Left lateral (A) and dorsal (B) views. Photo taken by M. W. Littmann.....	642
Figure 142. Ventral view of left pectoral-fin spine of <i>Pimelodella megalops</i> , BMNH 1911.10.31.51, paratype, 67.5 mm SL, total length of spine 13.1 mm.....	643
Figure 143. Schematic left lateral view of <i>Pimelodella megalops</i>	644
Figure 144. <i>Pimelodella megalura</i> , MNRJ 865A, lectotype, 128.6 mm SL. Left lateral (A) and dorsal (B) views.....	645
Figure 145. Ventral view of left pectoral-fin spine of <i>Pimelodella megalura</i> , MNRJ 865A, lectotype, 128.6 mm SL, total length of spine 15.2 mm.....	646
Figure 146. Schematic left lateral view of <i>Pimelodella megalura</i>	647
Figure 147. <i>Pimelodella metae</i> , FMNH 58441, holotype, 58.0 mm SL. Left lateral (A) and dorsal (B) views. Photo taken by M. W. Littmann.....	648

Figure 148. Ventral view of left pectoral-fin spine of <i>Pimelodella metae</i> , FMNH 58441, holotype, 58.0 mm SL, total length of spine 9.1 mm.....	649
Figure 149. Schematic left lateral view of <i>Pimelodella metae</i>	650
Figure 150. <i>Pimelodella modesta</i> , BMNH 1860.6.16.190, lectotype, 100.4 mm SL. Left lateral (A) and dorsal (B) views. Photo taken by Mark Allen.....	651
Figure 151. Ventral view of left pectoral-fin spine of <i>Pimelodella modesta</i> , BMNH 1860.6.16.190, lectotype, 100.4 mm SL, total length of spine 14.8 mm.....	652
Figure 152. Schematic left lateral view of <i>Pimelodella modesta</i>	653
Figure 153. <i>Pimelodella montana</i> , CAS 63719, lectotype, 87.4 mm SL. Left lateral (A) and dorsal (B) views. Photo taken by CAS staff.....	654
Figure 154. Ventral view of left pectoral-fin spine of <i>Pimelodella montana</i> , CAS 63719, paralectotype, 85 mm SL, total length of spine 11 mm.	655
Figure 155. Schematic left lateral view of <i>Pimelodella montana</i>	656
Figure 156. <i>Pimelodella mucosa</i> , CAS 63720, holotype, 97.4 mm SL. Left lateral (A) and dorsal (B) views. Photo taken by CAS staff.....	657
Figure 157. Ventral view of left pectoral-fin spine of <i>Pimelodella mucosa</i> , CAS 63720, holotype, 97.4 mm SL, total length of spine 22.8 mm.	658
Figure 158. Schematic left lateral view of <i>Pimelodella mucosa</i>	659
Figure 159. <i>Pimelodella notomelas</i> , FMNH 57967, holotype, 38.9 mm SL. Left lateral (A) and dorsal (B) views. Photo taken by M. W. Littmann.....	660
Figure 160. Ventral view of left pectoral-fin spine of <i>Pimelodella notomelas</i> , FMNH 57967, holotype, 38.9 mm SL, total length of spine 7.4 mm.....	661
Figure 161. Schematic left lateral view of <i>Pimelodella notomelas</i>	662
Figure 162. <i>Pimelodella odynea</i> , USNM 121133, holotype, 88.3 mm SL. Left lateral (A) and dorsal (B) views. Photo taken by Sandra Raredon.....	663
Figure 163. Ventral view of left pectoral-fin spine of <i>Pimelodella odynea</i> , USNM 121133, holotype, 88.3 mm SL, total length of spine 12.9 mm.	664
Figure 164. Schematic left lateral view of <i>Pimelodella odynea</i>	665
Figure 165. <i>Pimelodella pectinifera</i> , holotype, MCZ 7508, 150.9 mm SL. Left lateral (A) and dorsal (B) views. Photo taken by MCZ staff.....	666
Figure 166. Ventral view of left pectoral-fin spine of <i>Pimelodella pectinifera</i> , holotype, MCZ 7508, 150.9 mm SL, total length of spine 31.4 mm.	667
Figure 167. Schematic left lateral view of <i>Pimelodella pectinifera</i>	668
Figure 168. <i>Pimelodella peruana</i> , holotype, CAS 63721, 40.3 mm SL. Left lateral (A) and dorsal (B) views. Photo taken by CAS staff.....	669
Figure 169. Ventral view of left pectoral-fin spine of <i>Pimelodella peruana</i> : (A) holotype, CAS 63721, 40.3 mm SL, total length of spine 6.3 mm; (B) FMNH 102541, 69.9 mm SL, total length of spine 11.2 mm.	670
Figure 170. Schematic left lateral view of <i>Pimelodella peruana</i>	671
Figure 171. <i>Pimelodella reyesi</i> , ICN-MHN 1331, 98.1 mm SL. Left lateral (A) and dorsal (B) views. Photo taken by Henry Zamora.....	672
Figure 172. Ventral view of left pectoral-fin spine of <i>Pimelodella reyesi</i> , ICN-MHN 1331, 98.1 mm SL, total length of spine 18.6 mm.....	673
Figure 173. Schematic left lateral view of <i>Pimelodella reyesi</i>	674
Figure 174. <i>Pimelodella robinsoni</i> , holotype, ANSP 69386, 73 mm SL. Left lateral (A) and dorsal (B) views. Photo taken by Murilo Pastana.....	675
Figure 175. Ventral view of left pectoral-fin spine of <i>Pimelodella wolffi</i> , junior-synonym of <i>P. robinsoni</i> , holotype, ANSP 69388, 88.9 mm SL, total length of spine 11.3 mm SL.....	676
Figure 176. Schematic left lateral view of <i>Pimelodella robinsoni</i>	677
Figure 177. <i>Pimelodella wolffi</i> , junior-synonym of <i>P. robinsoni</i> , holotype, ANSP 69388, 88.9 mm SL. Left lateral (A) and dorsal (B) views. Photo taken by Murilo Pastana.....	678
Figure 178. <i>Pimelodella roccae</i> , holotype, MCZ 30975, 139.8 mm SL. Left lateral (A) and dorsal (B) views. Photo taken by MCZ staff.....	679

Figure 179. Ventral view of left pectoral-fin spine of <i>Pimelodella roccae</i> , holotype, MCZ 30975, 139.8 mm SL, total length of spine 23.8 mm.	680
Figure 180. Schematic left lateral view of <i>Pimelodella roccae</i>	681
Figure 181. <i>Pimelodella serrata</i> , holotype, FMNH 57979, 55.7 mm SL. Left lateral (A) and dorsal (B) views. Photo taken by M. W. Littmann.	682
Figure 182. Left lateral detail of dorsal fin of <i>Pimelodella serrata</i> , UFRO-I 9739, 77.1 mm SL, to show dorsal-fin spine morphology.	683
Figure 183. Ventral view of left pectoral-fin spine of <i>Pimelodella serrata</i> , holotype, FMNH 57979, 55.7 mm SL, total length of spine 7.7 mm.	684
Figure 184. Schematic left lateral view of <i>Pimelodella serrata</i>	685
Figure 185. <i>Pimelodella serrata</i> , UFRO 9745, 83.4 mm SL. Left lateral (A) and dorsal (B) views. Photo extracted from Bockmann & Slobodian (2013).	686
Figure 186. <i>Pimelodella chaparae</i> , junior-synonym of <i>P. serrata</i> , holotype, ANSP 69021, 48.1 mm SL. Left lateral (A) and dorsal (B) views. Photo taken by Kyle Luckenbill.	687
Figure 187. <i>Pimelodella spelaea</i> , holotype, MZUSP 81726, 78.9 mm SL. Left lateral (A) and dorsal (B) views. Photo taken by Eduardo Baena.	688
Figure 188. Ventral view of left pectoral-fin spine of <i>Pimelodella spelaea</i> , holotype, MZUSP 81726, 78.9 mm SL, total length of spine 11.0 mm.	689
Figure 189. Schematic left lateral view of <i>Pimelodella spelaea</i>	690
Figure 190. <i>Pimelodella straminea</i> , lectotype, ANSP 21581, 41.2 mm SL. Left lateral (A) and dorsal (B) views. Photo taken by Kyle Luckenbill.	691
Figure 191. Ventral view of left pectoral-fin spine of <i>Pimelodella straminea</i> , lectotype, ANSP 21581, 41.2 mm SL, total length of spine 7.6 mm.	692
Figure 192. Schematic left lateral view of <i>Pimelodella straminea</i>	693
Figure 193. <i>Pimelodella taeniophora</i> , lectotype, BMNH 1895.5.17.27, 76.6 mm SL. Left lateral (A) and dorsal (B) views. Photo taken by Mark Allen.	694
Figure 194. Ventral view of left pectoral-fin spine of <i>Pimelodella taeniophora</i> , lectotype, BMNH 1895.5.17.27, 76.6 mm SL, total length of spine 13.6 mm.	695
Figure 195. Schematic left lateral view of <i>Pimelodella taeniophora</i>	696
Figure 196. <i>Pimelodella taeniophora</i> , MZUEL 6460, 93.2 mm SL, female, extracted from Souza-Shibatta <i>et al.</i> (2013).	697
Figure 197. <i>Pimelodella tapatapae</i> , holotype, CAS 57469, 121.6 mm SL. Left lateral (A) and dorsal (B) views.	698
Figure 198. Ventral view of left pectoral-fin spine of <i>Pimelodella tapatapae</i> , holotype, CAS 57469, 121.6 mm SL, total length of spine 18.1 mm.	699
Figure 199. Schematic left lateral view of <i>Pimelodella tapatapae</i>	700
Figure 200. <i>Pimelodella vittata</i> , lectotype, ZMB 9175, 61.8 mm SL. Left lateral (A) and dorsal (B) views. Photo taken by ZMB staff.	701
Figure 201. Ventral view of left pectoral-fin spine of <i>Pimelodella vittata</i> , paralectotype, ZMB 9175, 53.2 mm SL, total length of spine 9.0 mm.	702
Figure 202. Schematic left lateral view of <i>Pimelodella vittata</i>	703
Figure 203. <i>Pimelodella vittata</i> , paralectotype, NMW 44442, 57.5 mm SL. Left lateral (A) and dorsal (B) views. Photo taken by Mark Sabaj.	704
Figure 204. <i>Pimelodella yuncensis</i> , lectotype, ZMS 7870, 37.8 mm SL. Left lateral (A) and dorsal (B) views. Photo taken by Natasha Khardina.	705
Figure 205. Ventral view of left pectoral-fin spine of <i>Pimelodella yuncensis</i> , lectotype, ZMS 7870, 37.8 mm SL, total length of spine 5.3 mm.	706
Figure 206. Schematic left lateral view of <i>Pimelodella yuncensis</i>	707
Figure 207. Left lateral view of <i>Pimelodella yuncensis</i> , CAS 75890, 61.0 mm SL.	708
Figure 208. Holotype of <i>Rhamdia gilli</i> , USNM 53472, 138 mm SL.	709
Figure 209. <i>Pimelodella peruensis</i> , junior-synonym of <i>P. yuncensis</i> , holotype, ANSP 21932, 48.2 mm SL. Left lateral (A) and dorsal (B) views.	710
Figure 210. <i>Rhamdia altipinnis</i> , holotype, NMW 45601, 61.2 mm SL. Left lateral (A) and dorsal (B) views.	711

Figure 211. <i>Imparfinis macrocephalus</i> , paratype, MCZ 35879, 23.7 mm SL. Left lateral (A) and dorsal (B) views.	712
Figure 212. CT scan of <i>Imparfinis macrocephalus</i> , paratype, MCZ 35879, 23.7 mm SL. Left lateral (A) and dorsal (B) views. Scans obtained by Andrew Williston.....	713
Figure 213. <i>Pimelodus parvus</i> Güntert, 1942, holotype, NMBA 5302, 19.4 mm SL. Left lateral (A) and dorsal (B) views. Photo taken by Natasha Khardina.....	714
Figure 214. Simplified version of the species tree reconstructed through ASTRAL-III, based on COI, CytB, 36268e1 and 4174e20 genes, for a total of 90 specimens (80 <i>Pimelodella</i>). 715	
Figure 215. Clade A relative to Figure 214. Branch values correspond to bootstrap (%)..	716
Figure 216. Clade B relative to Figure 214. Branch values correspond to bootstrap (%)..	717
Figure 217. Clade C relative to Figure 214. Branch values correspond to bootstrap (%)..	718
Figure 218. Clade D relative to Figure 214. Branch values correspond to bootstrap (%)..	719
Figure 219. Clade E relative to Figure 214. Branch values correspond to bootstrap (%)..	720
Figure 220. Simplified version of the species tree reconstructed through ASTRAL-III, based on COI, CytB, 36268e1 and 4174e20 genes. Nodes with bootstrap value inferior to 50% were collapsed. Dotted boxes present the delimitation for taxa illustrated in Figures 221–226.....	721
Figure 221. Clade A relative to Figure 220. Branch values correspond to bootstrap (%)..	722
Figure 222. Clades B1, B2 and other taxa according to delimitation box in Figure 220. Branch values correspond to bootstrap (%).	723
Figure 223. Clade B3, according to delimitation box in Figure 220. Branch values correspond to bootstrap (%).	724
Figure 224. Clade C', according to delimitation box in Figure 220. Branch values correspond to bootstrap (%).	725
Figure 225. Clade D' and other taxa according to delimitation box in Figure 220. Branch values correspond to bootstrap (%).	726
Figure 226. Clade E', according to delimitation box in Figure 220. Branch values correspond to bootstrap (%).	727
Figure 227. Best tree obtained by a Maximum Likelihood analysis on concatenate matrix of COI, CytB, 36268e1 and 4174e20 genes. Node values correspond to bootstrap (%). Nodes with “-” were not recovered in bootstrap tree. Dotted boxes present the delimitation for taxa illustrated in Figures 228–233.....	728
Figure 228. Clade A, according to delimitation box in Figure 227. Branch values correspond to bootstrap (%).	729
Figure 229. Clade B2", according to delimitation box in Figure 227. Branch values correspond to bootstrap (%).	730
Figure 230. Clade B3", according to delimitation box in Figure 227. Branch values correspond to bootstrap (%), clades not recovered in bootstrap tree are indicate by -....	731
Figure 231. Specimens of orange delimitation box of Figure 227, corresponding to clade C" and other taxa. Branch values correspond to bootstrap (%), clades not recovered in bootstrap tree are indicate by -.....	732
Figure 232. Specimens of green delimitation box of Figure 227, corresponding to clade D" and other taxa. Branch values correspond to bootstrap (%).	733
Figure 233. Clade E", according to delimitation box in Figure 227. Branch values correspond to bootstrap (%), clades not recovered in bootstrap tree are indicate by -....	734
Figure 234. Distribution map of the following <i>Pimelodella</i> : <i>P. australis</i> .— red star: holotype and paratypes; <i>P. boschmai</i> .— purple star: holotype, purple circle: other material; <i>P. brasiliensis</i> .— yellow star: holotype, yellow circle: other material, yellow triangle: lectotype of <i>P. eigenmanni</i> , junior-synonym of <i>P. brasiliensis</i> ; <i>P. harttii</i> .— dark blue star: holotype, dark blue circle: other material; <i>P. ignobilis</i> .— green star: holotype; green circle: other material; <i>P. kronei</i> .— light blue star: holotype, light blue circle: other material; light blue triangle: neotype of <i>P. transitoria</i> , junior-synonym of <i>P. kronei</i> ; <i>P. lateristriga</i> .— pink star: holotype, pink circle: other material, pink triangle: lectotype of <i>P. bahiana</i> , junior-synonym of <i>P. lateristriga</i>	735

Figure 235. Distribution map of the following *Pimelodella*: *P. avanhandavae*.— red star: holotype, red circle: other material; *P. gracilis*.— purple star: lectotype, purple circle: other material, purple triangle: lectotype of *P. taenioptera*, junior-synonym of *P. gracilis*; *P. griffini*.— yellow star (same place as blue star): holotype, yellow circle: other material; *P. laticeps*.— dark blue star: holotype; dark blue circle: other material; *P. longipinnis*.— light green star: holotype; *P. meeki*.— dark green star: holotype, dark green circle: other material, dark green triangle: lectotype of *P. rudolphi*, junior-synonym of *P. meeki*; *P. pectinifera*.— light blue star: holotype; *P. straminea*.— pink star: holotype, pink circle: other material; *P. taeniophora*. — orange star: lectotype, orange circle: other material. 736

Figure 236. Distribution map of the following *Pimelodella*: *P. enochi*.— red star: holotype, red circle: other material, red triangle: holotype of *P. papariae*, junior-synonym of *P. enochi*; *P. itapicuruenensis*.— purple star: holotype, purple circle: other material; *P. laurenti*.— yellow star: holotype, yellow circle: other material; *P. mucosa*.— dark blue star: holotype; dark blue circle: other material; *P. notomelas*.— light green star: holotype, light green circle: other material; *P. robinsoni*.— dark green star: holotype, dark green circle: other material, dark green triangle: holotype of *P. wolffi*, junior-synonym of *P. robinsoni*; *P. spelaea*.— light blue star: holotype, light blue circle: other material; *P. vittata*.— pink star: holotype, pink circle: other material. 737

Figure 237. Distribution map of the following *Pimelodella*: *P. boliviana*.— red star: holotype, red circle: other material; *P. hasemani*.— purple star: holotype, purple circle: other material; *P. howesi*.— yellow star: holotype, yellow circle: other material; *P. megalura*.— dark blue star: holotype; dark blue circle: other material; *P. montana*.— light green star: holotype, light green circle: other material; *P. modesta*.— dark green star: holotype, dark green circle: other material; *P. peruana*.— pink star: holotype, pink circle: other material; *P. roccae*.— orange star: holotype, orange circle: other material. 738

Figure 238. Distribution map of the following *Pimelodella*: *P. buckleyi*.— red star: lectotype, red circle: other material, red triangle: paralectotype of *P. cyanostigma*, junior-synonym of *P. buckleyi*, red diamond: holotype of *P. copei*, junior-synonym of *P. buckleyi*; *P. conquetaensis*.— purple star: holotype; *P. cruxenti*.— yellow star: lectotype, yellow circle: other material; *P. elongata*.— dark blue star: lectotype; dark blue circle: other material; *P. eutaenia*.— light green star: lectotype, light green circle: other material; *P. figueroai*.— dark green star: paratype; *P. grisea*.— pink star: holotype, pink circle: other material. 739

Figure 239. Distribution map of the following *Pimelodella*: *P. chagresi*.— red star: lectotype, red circle: other material; *P. linami*.— purple star: holotype; *P. metae*.— yellow star: holotype, yellow circle: other material; *P. odynea*.— dark blue star: holotype; dark blue circle: other material; *P. reyesi*.— light green circle: other material; *P. serrata*.— dark green star: holotype, dark green circle: other material, dark green triangle: holotype of *P. chaparae*, junior-synonym of *P. serrata*; *P. yuncensis*.— pink star: lectotype, pink circle: other material. 740

Figure 240. Distribution map of the following *Pimelodella*: *P. cristata*.— red star: lectotype, red circle: other material, red triangle: holotype of *P. breviceps*, junior-synonym of *P. cristata*, red diamond: lectotype of *P. cyanostigma*, junior-synonym of *P. cristata*, red arrow: holotype of *P. dorseyi*, junior-synonym of *P. cristata*, red half diamond: holotype of *P. hartwelli*, junior-synonym of *P. cristata*, red pentagon: holotype of *P. parnahybae*, junior-synonym of *P. cristata*, red square: lectotype of *P. steindachneri*, junior-synonym of *P. cristata*, red elipse: holotype of *P. wessellii*, junior-synonym of *P. cristata*, red airplane: holotype of *P. witmeri*, junior-synonym of *P. cristata*; *P. geryi*.— purple star: holotype, purple circle: other material, purple triangle: holotype of *P. procera*, junior-synonym of *P. geryi*; *P. humeralis*.— yellow star: holotype, yellow circle: other material; *P. leptosoma*.— dark blue star: holotype; dark blue circle: other material; *P. macturki*.— light green star: holotype, light green circle: other material; *P. megalops*.— dark green star: holotype, dark green circle: other material. 741

Attachments

Attachment 1: Original description of <i>Pimelodella humeralis</i>, in the article “A new species of <i>Pimelodella</i> (Siluriformes: Heptapteridae) from the Guiana Shield, Brazil” of Slobodian <i>et al.</i> (2017).....	742
Attachment 2: Script to estimate gene trees in RStudio using RAxML.	743

Tables, figures and attachments

Table 1: Nominal species available for *Pimelodella* genus.

#	Described as	Authority	Transferred to current status by	Current status
1	<i>Pimelodus altipinnis</i>	Steindachner 1864	Van der Stigchel, 1946; Mees, 1974	<i>Pimelodella altipinnis</i> (Steindachner, 1864)
2	<i>Pimelodella laticeps australis</i>	Eigenmann 1917		<i>Pimelodella australis</i> Eigenmann, 1917
3	<i>Pimelodella avanhandavae</i>	Eigenmann 1917		<i>Pimelodella avanhandavae</i> Eigenmann, 1917
4	<i>Pimelodus bahianus</i>	Castelnau 1855	Eigenmann & Eigenmann, 1888	<i>Pimelodella bahiana</i> (Castelnau, 1855)
5	<i>Pimelodella boliviana</i>	Eigenmann 1917		<i>Pimelodella boliviana</i> Eigenmann, 1917
6	<i>Pimelodella boschmai</i>	Van der Stigchel, 1964		<i>Pimelodella boschmai</i> Van der Stigchel, 1964
7	<i>Pimelodus (Pseudorhamdia) brasiliensis</i>	Steindachner 1877	Eigenmann & Eigenmann, 1888	<i>Pimelodella brasiliensis</i> (Steindachner, 1877)
8	<i>Caecorhamdella brasiliensis</i>	Borodin, 1927a	Trajano & Britski, 1992	synonym of <i>Pimelodella kronei</i> Miranda Ribeiro, 1907a
9	<i>Pimelodus breviceps</i>	Kner 1858	Silfvergrip, 1996; Bockmann & Guazzelli, 2003	<i>Pimelodella breviceps</i> (Kner, 1858)
10	<i>Pimelodus buckleyi</i>	Boulenger 1887	Eigenmann & Eigenmann, 1888	<i>Pimelodella buckleyi</i> (Boulenger, 1887)
11	<i>Pimelodus chagresi</i>	Steindachner 1876	Eigenmann & Eigenmann, 1888	<i>Pimelodella chagresi</i> (Steindachner, 1876)
12	<i>Pimelodella chaparae</i>	Fowler 1940b		<i>Pimelodella chaparae</i> Fowler, 1940b
13	<i>Pimelodella cochabambae</i>	Fowler 1940b	Mees & Cala, 1989	<i>Imparfinis cochabambae</i> (Fowler, 1940b)
14	<i>Pimelodella conquetaensis</i>	Ahl 1925		<i>Pimelodella conquetaensis</i> Ahl, 1925
15	<i>Pimelodus cristatus</i>	Müller & Troschel 1849a	Eigenmann & Eigenmann, 1888	<i>Pimelodella cristata</i> (Müller & Troschel, 1849a)
16	<i>Pimelodella cruxenti</i>	Fernandez-Yépez 1950		<i>Pimelodella cruxenti</i> Fernandez-Yépez, 1950
17	<i>Rhamdia cyanostigma</i>	Cope 1870	Fowler, 1915	<i>Pimelodella cyanostigma</i> (Cope, 1870)
18	<i>Pimelodella dorseyi</i>	Fowler 1941a		<i>Pimelodella dorseyi</i> Fowler, 1941a
19	<i>Pimelodus (Pimelodella) eigenmanni</i>	Boulenger 1891	Eigenmann, 1910	<i>Pimelodella eigenmanni</i> Boulenger, 1891
20	<i>Pimelodella eigenmanni</i>	Meek 1905	Eigenmann, 1910	synonym of <i>Pimelodella meeki</i> Eigenmann, 1910
21	<i>Rhamdia eigenmanniorum</i>	Miranda-Ribeiro 1911	Bockmann & Guazzelli, 2003	<i>Pimelodella eigenmanniorum</i> (Miranda Ribeiro, 1911)
22	<i>Pimelodus elongatus</i>	Günther 1860	Eigenmann & Eigenmann, 1888	<i>Pimelodella elongata</i> Günther, 1860
23	<i>Pimelodella enochi</i>	Fowler 1941		<i>Pimelodella enochi</i> Fowler, 1941
24	<i>Pimelodella eutaenia</i>	Regan 1913		<i>Pimelodella eutaenia</i> Regan, 1913
25	<i>Pimelodella figueiroai</i>	Dahl 1961		<i>Pimelodella figueiroai</i> Dahl, 1961
26	<i>Pimelodella floridablancaensis</i>	Ardila Rodriguez 2017		<i>Pimelodella floridablancaensis</i> Ardila Rodriguez, 2017
27	<i>Pimelodella garbei</i>	Miranda Ribeiro 1918	Guazzelli, 1997; Bockmann & Guazzelli, 2003	synonym of <i>Pimelodella australis</i> Eigenmann, 1917
28	<i>Pimelodella geryi</i>	Hoedeman 1961		<i>Pimelodella geryi</i> Hoedeman, 1961

29	<i>Pimelodus gracilis</i>	Valenciennes 1835	Eigenmann & Eigenmann, 1888	<i>Pimelodella gracilis</i> (Valenciennes, 1835)
30	<i>Pimelodella griffini</i>	Eigenmann 1917		<i>Pimelodella griffini</i> Eigenmann, 1917
31	<i>Pimelodus</i> (<i>Pimelodella</i>) <i>griseus</i>	Regan 1903	Eigenmann, 1910	<i>Pimelodella grisea</i> Regan, 1903
32	<i>Pimelodus</i> (<i>Pseudorhamdia</i>) <i>hartii</i>	Steindachner 1877	Eigenmann & Eigenmann, 1888	<i>Pimelodella hartii</i> (Steindachner, 1877)
33	<i>Pimelodella hartwelli</i>	Fowler 1940a		<i>Pimelodella hartwelli</i> Fowler, 1940a
34	<i>Pimelodella hasemani</i>	Eigenmann 1917		<i>Pimelodella hasemani</i> Eigenmann, 1917
35	<i>Pimelodella howesi</i>	Fowler 1940b		<i>Pimelodella howesi</i> Fowler, 1940b
36	<i>Pimelodella humeralis</i>	Slobodian, Akama & Dutra 2017		<i>Pimelodella humeralis</i> Slobodian, Akama & Dutra, 2017
37	<i>Rhamdella ignobilis</i>	Steindachner 1907	Guazzelli, 1997; Bockmann & Miquelarena, 2008	<i>Pimelodella ignobilis</i> (Steindachner, 1907)
38	<i>Brachyrhamdia imitator</i>	Myers 1927	Bockmann & Guazzelli, 2003; Slobodian & Bockmann, 2013	<i>Brachyrhamdia imitator</i> Myers, 1927
39	<i>Pimelodella insignis</i>	Schubart 1964	Bockmann & Guazzelli, 2003	synonym of <i>Pimelodella boschmai</i> Van der Stigchel, 1964
40	<i>Pimelodella itapicuruensis</i>	Eigenmann 1917		<i>Pimelodella itapicuruensis</i> Eigenmann, 1917
41	<i>Typhlobagrus kronei</i>	Miranda Ribeiro 1907a	Pavan, 1946	<i>Pimelodella kronei</i> Miranda Ribeiro, 1907a
42	<i>Pimelodes lateristrigus</i>	Lichtenstein 1823	Eigenmann & Eigenmann, 1888	<i>Pimelodella lateristriga</i> (Lichtenstein, 1823)
43	<i>Pimelodus lateristrigus</i>	Müller & Troschel 1849b	Silfvergrip & Paepke, 1997; Bockmann & Guazzelli, 2003	synonym of <i>Pimelodella lateristriga</i> (Lichtenstein, 1823)
44	<i>Pimelodella laticeps</i>	Eigenmann 1917		<i>Pimelodella laticeps</i> Eigenmann, 1917
45	<i>Pimelodella laurenti</i>	Fowler 1941		<i>Pimelodella laurenti</i> Fowler, 1941
46	<i>Rhamdella leptosoma</i>	Fowler 1941	Bockmann & Miquelarena, 2008	<i>Pimelodella leptosoma</i> (Fowler, 1941)
47	<i>Pimelodella linami</i>	Schultz 1944		<i>Pimelodella linami</i> Schultz, 1944
48	<i>Rhamdella longipinnis</i>	Borodin 1927b	Bockmann & Miquelarena, 2008	<i>Pimelodella longipinnis</i> (Borodin, 1927b)
49	<i>Nannorhamdia macrocephala</i>	Miles 1943	Bockmann & Guazzelli, 2003; Bockmann & Miquelarena, 2008	<i>Pimelodella macrocephala</i> (Miles, 1943)
50	<i>Pimelodella macturki</i>	Eigenmann 1912		<i>Pimelodella macturki</i> Eigenmann, 1912
51	<i>Brachyrhamdia marthae</i>	Sands & Black 1985	Bockmann & Guazzelli, 2003; Slobodian & Bockmann, 2013	<i>Brachyrhamdia marthae</i> Sands & Black in Sands, 1985
52	<i>Pimelodella martinezi</i>	Fernandez-Yépez 1970		<i>Pimelodella martinezi</i> Fernández-Yépez, 1970
53	<i>Pimelodella meeki</i>	Eigenmann 1910		<i>Pimelodella meeki</i> Eigenmann, 1910
54	<i>Brachyrhamdia meesi</i>	Sands & Black 1985	Bockmann & Guazzelli, 2003; Slobodian & Bockmann, 2013	<i>Brachyrhamdia meesi</i> Sands & Black in Sands, 1985
55	<i>Pimelodella megalops</i>	Eigenmann 1912		<i>Pimelodella megalops</i> Eigenmann, 1912

56	<i>Pimelodella megalura</i>	Miranda-Ribeiro 1918		<i>Pimelodella megalura</i> Miranda Ribeiro, 1918
57	<i>Pimelodella metae</i>	Eigenmann 1917		<i>Pimelodella metae</i> Eigenmann, 1917
58	<i>Pimelodus modestus</i>	Günther 1860	Eigenmann & Eigenmann, 1888	<i>Pimelodella modestus</i> (Günther, 1860)
59	<i>Pimelodella montana</i>	Allen 1942		<i>Pimelodella montana</i> Allen in Eigenmann & Allen, 1942
60	<i>Pimelodella mucosa</i>	Eigenmann & Ward 1907		<i>Pimelodella mucosa</i> Eigenmann & Ward in Eigenmann, Ward & McAtee, 1907
61	<i>Pimelodus nigrofasciatus</i>	Perugia, 1897	Bockmann & Guazzelli, 2003	<i>Pimelodella nigrofasciata</i> (Perugia, 1897)
62	<i>Pimelodella notomelas</i>	Eigenmann 1917		<i>Pimelodella notomelas</i> Eigenmann, 1917
63	<i>Pimelodella chagresi odynea</i>	Schultz 1944	Bockmann & Guazzelli, 2003	<i>Pimelodella odynea</i> Schultz, 1944
64	<i>Pimelodus ophthalmicus</i>	Cope 1878	Bockmann & Guazzelli, 2003	<i>Pimelodella ophthalmica</i> (Cope, 1878)
65	<i>Pimelodella pallida</i>	Dahl 1961		<i>Pimelodella pallida</i> (Dahl, 1961)
66	<i>Rhamdella papariae</i>	Fowler 1941	Bockmann & Miquelarena, 2008	<i>Pimelodella papariae</i> (Fowler, 1941)
67	<i>Pimelodella pappenheimi</i>	Ahl 1925		<i>Pimelodella pappenheimi</i> Ahl, 1925
68	<i>Pimelodella parnahybae</i>	Fowler 1941		<i>Pimelodella parnahybae</i> Fowler, 1941
69	<i>Pimelodella parva</i>	Güntert 1942		<i>Pimelodella parva</i> Güntert, 1942
70	<i>Pimelodella pectinifer</i>	Eigenmann & Eigenmann 1888		<i>Pimelodella pectinifer</i> Eigenmann & Eigenmann, 1888
71	<i>Pimelodella peruana</i>	Eigenmann & Myers 1942		<i>Pimelodella peruana</i> Eigenmann & Myers in Eigenmann & Allen, 1942
72	<i>Pimelodella peruensis</i>	Fowler 1915		<i>Pimelodella peruensis</i> Fowler, 1915
73	<i>Pimelodella procera</i>	Mees 1983		<i>Pimelodella procera</i> Mees, 1983
74	<i>Pimelodella rambarrani</i>	Axelrod & Burgess 1987	Bockmann & Guazzelli, 2003; Slobodian & Bockmann, 2013	<i>Brachyrhamdia rambarrani</i> Axelrod & Burgess in Axelrod, 1987
75	<i>Pimelodella rendahli</i>	Ahl 1925		<i>Pimelodella rendahli</i> Ahl, 1925
76	<i>Pimelodella reyesi</i>	Dahl 1964		<i>Pimelodella reyesi</i> Dahl in Dahl & Medem, 1964
77	<i>Rhamdella robinsoni</i>	Fowler 1941	Bockmann & Miquelarena, 2008	<i>Pimelodella robinsoni</i> (Fowler, 1941)
78	<i>Pimelodella roccae</i>	Eigenmann 1917		<i>Pimelodella roccae</i> Eigenmann, 1917
79	<i>Pimelodella rudolphi</i>	Miranda-Ribeiro 1918		<i>Pimelodella rudolphi</i> Miranda Ribeiro, 1918
80	<i>Pimelodella serrata</i>	Eigenmann 1917		<i>Pimelodella serrata</i> Eigenmann, 1917
81	<i>Pimelodella spelaea</i>	Trajano, Reis & Bichuette 2004		<i>Pimelodella spelaea</i> Trajano, Reis & Bichuette, 2004
82	<i>Pimelodella steindachneri</i>	Eigenmann 1917		<i>Pimelodella steindachneri</i> Eigenmann, 1917
83	<i>Rhamdella straminea</i>	Cope 1894	Bockmann & Miquelarena, 2008	<i>Pimelodella</i> or <i>Rhamdia straminea</i> (Cope, 1894)
84	<i>Pimelodus (Pimelodella) taeniophorus</i>	Regan 1903	Eigenmann, 1910	<i>Pimelodella taeniophora</i> Regan, 1903
85	<i>Pimelodella taenioptera</i>	Miranda-Ribeiro 1914		<i>Pimelodella taenioptera</i> Miranda Ribeiro, 1914

86	<i>Pimelodella tapatapae</i>	Eigenmann 1920		<i>Pimelodella tapatapae</i> Eigenmann, 1920
87	<i>Pimelodella transitoria</i>	Miranda Ribeiro 1907b		<i>Pimelodella transitoria</i> Miranda Ribeiro, 1907b
88	<i>Pseudorhamdia vittatus</i>	Lütken 1874	Eigenmann & Eigenmann, 1888	<i>Pimelodella vittata</i> (Lütken, 1874)
89	<i>Pimelodus (Pseudorhamdia) wesseli</i>	Steindachner 1877	Eigenmann & Eigenmann, 1888	<i>Pimelodella wesseli</i> (Steindachner, 1877)
90	<i>Pimelodella witmeri</i>	Fowler 1941		<i>Pimelodella witmeri</i> Fowler, 1941
91	<i>Rhamdella wolfi</i>	Fowler 1941	Bockmann & Miquelarena, 2008	<i>Pimelodella wolfi</i> (Fowler, 1941)
92	<i>Pimelodella yuncensis</i>	Steindachner 1902		<i>Pimelodella yuncensis</i> Steindachner, 1902

Table 2. Species analyzed in PCAs.

<i>Pimelodella</i> species with data for PCA analyses
<i>Pimelodella australis</i> Eigenmann, 1917
<i>Pimelodella avanhandavae</i> Eigenmann, 1917
<i>Pimelodella bahiana</i> (Castelnau, 1855)
<i>Pimelodella boliviana</i> Eigenmann, 1917
<i>Pimelodella boschmai</i> Van der Stigchel, 1964
<i>Pimelodella brasiliensis</i> (Steindachner, 1877)
<i>Pimelodella breviceps</i> (Kner, 1858)
<i>Pimelodella buckleyi</i> (Boulenger, 1887)
<i>Pimelodella chagresi</i> (Steindachner, 1876)
<i>Pimelodella chaparae</i> Fowler, 1940b
<i>Pimelodella cristata</i> (Müller & Troschel, 1849a)
<i>Pimelodella cruxenti</i> Fernandez-Yépez, 1950
<i>Pimelodella cyanostigma</i> (Cope, 1870)
<i>Pimelodella dorseyi</i> Fowler, 1941a
<i>Pimelodella eigenmanni</i> Boulenger, 1891
<i>Pimelodella eigenmanniorum</i> (Miranda Ribeiro, 1911)
<i>Pimelodella elongata</i> Günther, 1860
<i>Pimelodella enochi</i> Fowler, 1941
<i>Pimelodella eutaenia</i> Regan, 1913
<i>Pimelodella geryi</i> Hoedeman, 1961
<i>Pimelodella gracilis</i> (Valenciennes, 1835)
<i>Pimelodella griffini</i> Eigenmann, 1917
<i>Pimelodella grisea</i> Regan, 1903
<i>Pimelodella harttii</i> (Steindachner, 1877)
<i>Pimelodella hartwelli</i> Fowler, 1940a
<i>Pimelodella hasemani</i> Eigenmann, 1917
<i>Pimelodella howesi</i> Fowler, 1940b
<i>Pimelodella humeralis</i> Slobodian, Akama & Dutra, 2017
<i>Pimelodella ignobilis</i> (Steindachner, 1907)
<i>Pimelodella itapicuruensis</i> Eigenmann, 1917
<i>Pimelodella kronei</i> Miranda Ribeiro, 1907a
<i>Pimelodella lateristriga</i> (Lichtenstein, 1823)
<i>Pimelodella laticeps</i> Eigenmann, 1917
<i>Pimelodella laurenti</i> Fowler, 1941
<i>Pimelodella leptosoma</i> (Fowler, 1941)
<i>Pimelodella linami</i> Schultz, 1944
<i>Pimelodella longipinnis</i> (Borodin, 1927b)
<i>Pimelodella macrocephala</i> (Miles, 1943)
<i>Pimelodella macturki</i> Eigenmann, 1912
<i>Pimelodella meeki</i> Eigenmann, 1910
<i>Pimelodella megalops</i> Eigenmann, 1912
<i>Pimelodella megalura</i> Miranda Ribeiro, 1918
<i>Pimelodella metae</i> Eigenmann, 1917

Pimelodella modesta (Günther, 1860)
Pimelodella montana Allen in Eigenmann & Allen, 1942
Pimelodella mucosa Eigenmann & Ward in Eigenmann, Ward & McAtee, 1907
Pimelodella notomelas Eigenmann, 1917
Pimelodella odynea Schultz, 1944
Pimelodella ophthalmica (Cope, 1878)
Pimelodella papariae (Fowler, 1941)
Pimelodella pappenheimi Ahl, 1925
Pimelodella parnahybae Fowler, 1941
Pimelodella parva Güntert, 1942
Pimelodella pectinifera Eigenmann & Eigenmann, 1888
Pimelodella peruana Eigenmann & Myers in Eigenmann & Allen, 1942
Pimelodella peruensis Fowler, 1915
Pimelodella procera Mees, 1983
Pimelodella rendahli Ahl, 1925
Pimelodella robinsoni (Fowler, 1941)
Pimelodella roccae Eigenmann, 1917
Pimelodella rudolphi Miranda Ribeiro, 1918
Pimelodella serrata Eigenmann, 1917
Pimelodella spelaea Trajano, Reis & Bichuette, 2004
Pimelodella steindachneri Eigenmann, 1917
Pimelodella taeniophora Regan, 1903
Pimelodella taenioptera Miranda Ribeiro, 1914
Pimelodella tapatapae Eigenmann, 1920
Pimelodella transitoria Miranda Ribeiro, 1907b
Pimelodella vittata (Lütken, 1874)
Pimelodella wesselii (Steindachner, 1877)
Pimelodella witmeri Fowler, 1941
Pimelodella wolfi (Fowler, 1941)
Pimelodella yuncensis Steindachner, 1902

Table 3. Species currently placed in *Pimelodella* and their status as proposed by this work.

#	Current species in <i>Pimelodella</i>	Status proposed by this work
	<i>Pimelodella altipinnis</i> (Steindachner, 1864)	<i>Rhamdia altipinnis</i>
1	<i>Pimelodella australis</i> Eigenmann, 1917	valid
2	<i>Pimelodella avanhandavae</i> Eigenmann, 1917	valid
	<i>Pimelodella bahiana</i> (Castelnau, 1855)	junior-synonym of <i>P. lateristriga</i>
3	<i>Pimelodella boliviana</i> Eigenmann, 1917	valid
4	<i>Pimelodella boschmai</i> Van der Stigchel, 1964	valid
5	<i>Pimelodella brasiliensis</i> (Steindachner, 1877)	valid
	<i>Pimelodella breviceps</i> (Kner, 1858)	junior-synonym of <i>P. cristata</i>
6	<i>Pimelodella buckleyi</i> (Boulenger, 1887)	valid
7	<i>Pimelodella chagresi</i> (Steindachner, 1876)	valid
	<i>Pimelodella chaparae</i> Fowler, 1940b	junior-synonym of <i>P. serrata</i>
8	<i>Pimelodella conquetaensis</i> Ahl, 1925	valid
9	<i>Pimelodella cristata</i> (Müller & Troschel, 1849a)	valid
10	<i>Pimelodella cruxenti</i> Fernandez-Yépez, 1950	valid
	<i>Pimelodella cyanostigma</i> (Cope, 1870)	junior-synonym of <i>P. cristata</i>
	<i>Pimelodella dorseyi</i> Fowler, 1941a	junior-synonym of <i>P. cristata</i>
	<i>Pimelodella eigenmanni</i> Boulenger, 1891	junior-synonym of <i>P. brasiliensis</i>
	<i>Pimelodella eigenmanniorum</i> (Miranda Ribeiro, 1911)	junior-synonym of <i>P. brasiliensis</i>
11	<i>Pimelodella elongata</i> Günther, 1860	valid
12	<i>Pimelodella enochi</i> Fowler, 1941	valid
13	<i>Pimelodella eutaenia</i> Regan, 1913	valid
14	<i>Pimelodella figueiroai</i> Dahl, 1961	valid
	<i>Pimelodella floridablancaensis</i> Ardila Rodriguez, 2017	junior-synonym of <i>P. eutaenia</i>
15	<i>Pimelodella geryi</i> Hoedeman, 1961	valid
16	<i>Pimelodella gracilis</i> (Valenciennes, 1835)	valid
17	<i>Pimelodella griffini</i> Eigenmann, 1917	valid
18	<i>Pimelodella grisea</i> Regan, 1903	valid
19	<i>Pimelodella harttii</i> (Steindachner, 1877)	valid
	<i>Pimelodella hartwelli</i> Fowler, 1940a	junior-synonym of <i>P. cristata</i>
20	<i>Pimelodella hasemani</i> Eigenmann, 1917	valid
21	<i>Pimelodella howesi</i> Fowler, 1940b	valid
22	<i>Pimelodella humeralis</i> Slobodian, Akama & Dutra, 2017	valid
23	<i>Pimelodella ignobilis</i> (Steindachner, 1907)	valid
24	<i>Pimelodella itapicuruensis</i> Eigenmann, 1917	valid
25	<i>Pimelodella kronei</i> Miranda Ribeiro, 1907a	valid
26	<i>Pimelodella lateristriga</i> (Lichtenstein, 1823)	valid
27	<i>Pimelodella laticeps</i> Eigenmann, 1917	valid
28	<i>Pimelodella laurenti</i> Fowler, 1941	valid
29	<i>Pimelodella leptosoma</i> (Fowler, 1941)	valid
30	<i>Pimelodella linami</i> Schultz, 1944	valid
31	<i>Pimelodella longipinnis</i> (Borodin, 1927b)	valid
	<i>Pimelodella macrocephala</i> (Miles, 1943)	<i>Imparfinis macrocephalus</i>
32	<i>Pimelodella macturki</i> Eigenmann, 1912	valid
33	<i>Pimelodella martinezi</i> Fernández-Yépez, 1970	valid
34	<i>Pimelodella meeki</i> Eigenmann, 1910	valid
35	<i>Pimelodella megalops</i> Eigenmann, 1912	valid
36	<i>Pimelodella megalura</i> Miranda Ribeiro, 1918	valid
37	<i>Pimelodella metae</i> Eigenmann, 1917	valid

38	<i>Pimelodella modesta</i> (Günther, 1860)	valid
39	<i>Pimelodella montana</i> Allen in Eigenmann & Allen, 1942	valid
40	<i>Pimelodella mucosa</i> Eigenmann & Ward in Eigenmann, Ward & McAtee, 1907	valid
41	<i>Pimelodella nigrofasciata</i> (Perugia, 1897)	valid
42	<i>Pimelodella notomelas</i> Eigenmann, 1917	valid
43	<i>Pimelodella odynea</i> Schultz, 1944	valid
	<i>Pimelodella ophthalmica</i> (Cope, 1878)	junior-synonym of <i>P. cristata</i>
	<i>Pimelodella pallida</i> (Dahl, 1961)	junior-synonym of <i>P. cristata</i>
	<i>Pimelodella papariae</i> (Fowler, 1941)	junior-synonym of <i>P. enochi</i>
	<i>Pimelodella pappenheimi</i> Ahl, 1925	junior-synonym of <i>P. ignobilis</i>
	<i>Pimelodella parnahybae</i> Fowler, 1941	junior-synonym of <i>P. cristata</i>
	<i>Pimelodella parva</i> Güntert, 1942	<i>Pimelodus parvus</i>
44	<i>Pimelodella pectinifera</i> Eigenmann & Eigenmann, 1888	valid
45	<i>Pimelodella peruana</i> Eigenmann & Myers in Eigenmann & Allen, 1942	valid
	<i>Pimelodella peruensis</i> Fowler, 1915	junior-synonym of <i>P. yuncensis</i>
	<i>Pimelodella procera</i> Mees, 1983	junior-synonym of <i>P. geryi</i>
	<i>Pimelodella rendahli</i> Ahl, 1925	junior-synonym of <i>P. brasiliensis</i>
46	<i>Pimelodella reyesi</i> Dahl in Dahl & Medem, 1964	valid
47	<i>Pimelodella robinsoni</i> (Fowler, 1941)	valid
48	<i>Pimelodella roccae</i> Eigenmann, 1917	valid
	<i>Pimelodella rudolphi</i> Miranda Ribeiro, 1918	junior-synonym of <i>P. meeki</i>
49	<i>Pimelodella serrata</i> Eigenmann, 1917	valid
50	<i>Pimelodella spelaea</i> Trajano, Reis & Bichuette, 2004	valid
	<i>Pimelodella steindachneri</i> Eigenmann, 1917	junior-synonym of <i>P. cristata</i>
51	<i>Pimelodella</i> or <i>Rhamdia straminea</i> (Cope, 1894)	<i>Pimelodella straminea</i>
52	<i>Pimelodella taeniophora</i> Regan, 1903	valid
	<i>Pimelodella taenioptera</i> Miranda Ribeiro, 1914	junior-synonym of <i>P. gracilis</i>
53	<i>Pimelodella tapatapae</i> Eigenmann, 1920	valid
	<i>Pimelodella transitoria</i> Miranda Ribeiro, 1907b	junior-synonym of <i>P. kronei</i>
54	<i>Pimelodella vittata</i> (Lütken, 1874)	valid
	<i>Pimelodella wesselii</i> (Steindachner, 1877)	junior-synonym of <i>P. cristata</i>
	<i>Pimelodella witmeri</i> Fowler, 1941	junior-synonym of <i>P. cristata</i>
	<i>Pimelodella wolfi</i> (Fowler, 1941)	junior-synonym of <i>P. robinsoni</i>
55	<i>Pimelodella yuncensis</i> Steindachner, 1902	valid

Table 4. Morphometric data of *Pimelodella australis* based on type and comparative materials.

	Holotype	Min.	Max.	n	x	SD
Total length (mm)	76,7	55,7	96,5	13	73,2	
Standard length (mm)	61,0	39,9	77,2	48	51,3	
	Percentages of SL					
Body depth (dorsal)	22,0	18,2	22,9	11	19,8	1,5
Body width (dorsal)	15,1	12,8	17,5	11	14,5	1,3
Cleithral width	19,8	18,4	21,2	11	19,3	0,8
Head length	32,3	30,9	33,9	11	32,4	1,0
Maxillary-barbel length (left side)	63,7	44,6	71,3	11	63,8	7,5
Outer mental-barbel length (left side)	26,6	17,2	29,1	11	24,4	3,4
Inner mental-barbel length (left side)	12,0	9,7	14,9	10	12,3	1,5
Predorsal length	37,1	35,4	37,9	11	36,5	1,0
Distance between snout tip and terminus of dorsal-fin base	51,1	48,4	51,1	11	49,7	0,7
Distance between snout tip and dorsal-fin distal end	62,5	56,1	62,5	11	60,1	1,9
Dorsal fin to adipose fin	11,5	10,0	16,4	11	12,2	1,7
Dorsal-fin base	14,1	13,3	15,5	11	14,6	0,6
Length of first dorsal-fin ray (unbranched)	19,3	17,2	22,4	8	20,0	1,6
Length of rigid part of first dorsal-fin ray	14,7	14,7	18,5	11	16,5	1,2
Length of second dorsal-fin ray (first branched)	21,5	19,2	21,9	11	20,3	1,0
Length of third dorsal-fin ray (second branched)	20,1	17,8	22,1	11	19,3	1,2
Prepectoral length	25,9	23,3	26,5	11	24,7	1,1
Distance between snout tip and terminus of pectoral-fin base	27,9	26,3	29,9	11	27,5	1,2
Distance between snout tip and pectoral-fin distal end	44,8	43,2	50,0	11	45,1	1,9
Length of first left pectoral-fin ray (unbranched)	22,8	19,8	25,4	11	22,1	1,4
Length of rigid part of first left pectoral-fin ray	20,6	17,4	22,2	11	20,0	1,4
Length of second left pectoral-fin ray (first branched)	21,3	18,5	21,6	10	20,4	1,0
Length of third left pectoral-fin ray (second branched)	19,5	17,4	21,0	7	18,8	1,3
Prepelvic length	49,6	43,6	49,6	11	47,3	1,8
Distance between snout tip and terminus of pelvic-fin base	51,0	48,3	52,7	11	50,2	1,2
Distance between snout tip and pelvic-fin distal end	65,8	61,6	67,1	10	64,4	1,7
Distance between pelvic fins	4,8	3,9	5,1	11	4,3	0,3
Length of first left pelvic-fin ray (unbranched)	13,0	11,6	15,5	10	13,7	1,3
Length of second left pelvic-fin ray (first branched)	15,0	13,5	16,8	9	15,2	1,3
Length of third left pelvic-fin ray (second branched)	15,6	13,5	16,2	8	15,2	0,9
Anal-fin base	15,0	12,1	18,0	11	14,8	1,5
Preanal length	70,3	66,5	71,3	11	69,0	1,5
Distance between snout tip and terminus of anal-fin base	83,9	80,4	84,8	11	82,6	1,2
Distance between snout tip and anal-fin distal end	91,3	88,3	92,5	11	90,2	1,4
Adipose-fin length	28,4	24,9	30,6	11	27,9	2,1
Preadipose length	62,2	57,7	63,3	11	61,5	1,7
Distance between snout tip and adipose-fin base end	89,6	86,3	89,6	11	88,2	0,9
Adipose-fin depth	4,3	3,7	5,0	11	4,3	0,4
Caudal-peduncle length posterior to adipose-fin	11,2	10,5	12,4	11	11,5	0,7
Caudal-peduncle depth at adipose-fin terminus	9,4	8,0	9,4	11	8,6	0,4
Snout-anus distance	55,8	54,2	56,2	11	55,2	0,6
Snout-urogenital papilla distance	59,9	57,8	62,9	11	60,1	1,7
Anus-urogenital papilla distance	4,8	3,8	10,1	11	5,5	1,9
Dorsal lobe of caudal fin length	26,1	23,3	29,0	10	25,5	1,7
Ventral lobe of caudal fin length	24,8	22,0	28,4	10	24,6	1,9

	Percentages of HL					
Head depth	54,2	48,5	54,3	11	51,5	2,5
Head width	57,4	54,1	62,8	11	58,2	2,8
Eye diameter (left)	18,7	16,9	24,4	11	20,6	2,3
Fleshy interorbital	26,0	24,0	29,2	11	26,4	1,7
Bony interorbital	21,3	18,0	22,7	11	20,8	1,3
Mouth gape	29,7	27,6	33,9	11	31,6	2,2
Snout length (left)	29,4	29,4	31,4	11	30,0	0,6
Distance between snout tip and posterior nare (left side)	19,2	18,9	21,5	11	19,9	0,9
Anterior internarial width	14,1	12,1	15,0	11	13,7	0,9
Posterior internarial width	16,6	14,9	17,0	11	16,2	0,6
Intranarial length (left side)	16,1	14,3	17,7	11	15,5	1,1

Table 5. Morphometric data of *Pimelodella avanhandavae* based on type and comparative materials.

	Holotype	Min.	Max.	n	x	SD
Total length (mm)	87,2	64,3	98,9	6	80,1	
Standard length (mm)	69,0	43,8	80,2	31	59,0	
Percentages of SL						
Body depth (dorsal)	19,1	17,8	20,5	7	19,0	1,0
Body width (dorsal)	16,5	12,8	17,9	7	14,7	1,9
Cleithral width	14,1	14,1	19,5	7	18,3	1,9
Head length	29,8	29,2	30,5	7	29,9	0,5
Maxillary-barbel length (left side)	68,9	62,6	74,7	7	68,4	4,1
Outer mental-barbel length (left side)	31,6	26,0	34,6	8	30,0	2,9
Inner mental-barbel length (left side)	18,7	14,4	21,6	8	18,4	2,4
Predorsal length	33,5	33,2	35,9	7	34,3	1,0
Distance between snout tip and terminus of dorsal-fin base	46,8	46,4	48,0	7	47,2	0,5
Distance between snout tip and dorsal-fin distal end	59,4	46,2	61,2	7	56,5	4,9
Dorsal fin to adipose fin	10,1	6,5	10,9	7	8,9	1,6
Dorsal-fin base	15,5	14,2	15,5	7	14,9	0,5
Length of first dorsal-fin ray (unbranched)	18,9	17,1	20,5	7	18,9	1,1
Length of rigid part of first dorsal-fin ray	13,9	12,8	15,7	7	14,1	1,0
Length of second dorsal-fin ray (first branched)	20,7	14,5	23,3	7	19,9	2,9
Length of third dorsal-fin ray (second branched)	21,4	18,0	22,6	7	20,4	1,7
Prepectoral length	22,8	21,5	24,5	7	22,9	1,0
Distance between snout tip and terminus of pectoral-fin base	25,9	24,0	27,9	7	25,9	1,3
Distance between snout tip and pectoral-fin distal end	40,8	40,0	45,5	7	42,1	2,0
Length of first left pectoral-fin ray (unbranched)	21,3	18,6	22,0	7	20,4	1,2
Length of rigid part of first left pectoral-fin ray	17,9	14,4	18,3	7	16,8	1,3
Length of second left pectoral-fin ray (first branched)	19,7	17,5	20,2	7	18,8	1,1
Length of third left pectoral-fin ray (second branched)	16,9	16,2	19,0	7	17,5	1,1
Prepelvic length	46,1	44,0	47,1	7	45,9	1,0
Distance between snout tip and terminus of pelvic-fin base	47,9	45,8	49,5	7	48,2	1,2
Distance between snout tip and pelvic-fin distal end	62,8	60,2	63,4	7	61,8	1,1
Distance between pelvic fins	4,7	3,4	5,3	6	4,4	0,8
Length of first left pelvic-fin ray (unbranched)	13,4	11,3	13,8	6	12,8	0,9
Length of second left pelvic-fin ray (first branched)	14,6	12,8	16,2	6	14,8	1,2
Length of third left pelvic-fin ray (second branched)	15,0	13,2	16,1	6	14,9	1,1
Anal-fin base	10,5	10,5	13,6	7	12,5	1,1
Preanal length	69,5	66,5	69,5	7	67,8	0,9
Distance between snout tip and terminus of anal-fin base	79,1	78,3	79,2	7	78,8	0,4
Distance between snout tip and anal-fin distal end	87,1	86,5	87,5	7	87,0	0,4
Adipose-fin length	37,7	33,5	38,7	7	36,1	2,2
Preadipose length	56,1	53,2	57,6	7	55,3	1,6
Distance between snout tip and adipose-fin base end	91,9	88,2	91,9	7	89,9	1,6
Adipose-fin depth	4,7	4,0	4,9	7	4,4	0,4
Caudal-peduncle length posterior to adipose-fin	8,1	7,9	11,6	7	9,1	1,5
Caudal-peduncle depth at adipose-fin terminus	8,1	7,8	9,0	7	8,6	0,5
Snout-anus distance	54,4	53,1	54,6	7	53,8	0,5

Snout-urogenital papilla distance	58,4	56,6	59,3	7	58,1	1,0
Anus-urogenital papilla distance	3,8	3,0	5,1	7	4,0	0,7
Dorsal lobe of caudal fin length	25,4	22,5	26,7	3	24,9	2,1
Ventral lobe of caudal fin length	24,5	22,0	25,8	4	24,1	1,6

Percentages of HL

Head depth	49,7	49,7	54,4	7	51,9	1,8
Head width	62,2	57,2	68,1	7	61,5	3,7
Eye diameter (left)	20,4	18,6	23,0	7	20,6	1,4
Fleshy interorbital	24,1	21,6	25,3	7	23,5	1,4
Bony interorbital	18,1	16,6	18,8	7	17,9	0,7
Mouth gape	32,9	23,6	42,3	7	33,4	5,7
Snout length (left)	31,3	29,5	33,0	7	31,3	1,3
Distance between snout tip and posterior nare (left side)	18,8	17,9	20,6	7	19,1	1,1
Anterior internarial width	12,4	11,3	17,1	7	13,6	1,9
Posterior internarial width	14,2	13,8	17,0	7	14,6	1,1
Intranarial length (left side)	15,6	11,8	17,4	7	14,8	1,8

Table 6. Morphometric data of *Pimelodella boliviana* based on type and comparative materials.

	Holotype	Min.	Max.	n	x	SD
Total length (mm)	-	-	92,0	1		
Standard length (mm)	68,9	60,0	71,3	4	66,8	
Percentages of SL						
Body depth (dorsal)	13,1	13,1	15,7	3	14,8	1,4
Body width (dorsal)	12,2	12,2	13,5	3	12,7	0,7
Cleithral width	16,1	16,1	16,8	3	16,5	0,4
Head length	29,5	29,3	30,0	3	29,6	0,3
Maxillary-barbel length (left side)	104,1	98,6	104,1	3	100,6	3,0
Outer mental-barbel length (left side)	31,9	28,7	31,9	3	30,2	1,6
Inner mental-barbel length (left side)	17,0	15,0	17,1	3	16,4	1,2
Predorsal length	32,5	32,2	33,0	3	32,6	0,4
Distance between snout tip and terminus of dorsal-fin base	47,4	46,1	48,0	3	47,2	1,0
Distance between snout tip and dorsal-fin distal end	58,8	57,0	59,7	3	58,5	1,4
Dorsal fin to adipose fin	11,9	6,1	11,9	3	9,7	3,1
Dorsal-fin base	15,5	15,5	15,9	3	15,7	0,2
Length of first dorsal-fin ray (unbranched)	21,0	19,1	21,0	2	20,1	1,3
Length of rigid part of first dorsal-fin ray	14,3	14,2	14,5	3	14,3	0,2
Length of second dorsal-fin ray (first branched)	21,4	19,9	21,4	2	20,6	1,1
Length of third dorsal-fin ray (second branched)	20,7	20,4	20,7	2	20,5	0,2
Prepectoral length	19,6	19,6	22,5	3	20,7	1,6
Distance between snout tip and terminus of pectoral-fin base	23,1	23,1	25,7	3	24,1	1,4
Distance between snout tip and pectoral-fin distal end	39,7	39,7	40,9	2	40,3	0,9
Length of first left pectoral-fin ray (unbranched)	-	18,7	-	1	-	-
Length of rigid part of first left pectoral-fin ray	16,3	16,3	17,1	3	16,6	0,4
Length of second left pectoral-fin ray (first branched)	18,4	17,6	18,4	3	17,9	0,4
Length of third left pectoral-fin ray (second branched)	17,2	14,8	17,2	3	16,0	1,2
Prepelvic length	43,4	41,9	44,2	3	43,2	1,2
Distance between snout tip and terminus of pelvic-fin base	46,0	44,0	46,0	3	45,2	1,1
Distance between snout tip and pelvic-fin distal end	58,9	56,2	59,7	3	58,3	1,9
Distance between pelvic fins	4,1	4,1	4,5	3	4,3	0,2
Length of first left pelvic-fin ray (unbranched)	13,1	12,6	13,1	3	12,8	0,3
Length of second left pelvic-fin ray (first branched)	14,5	13,6	14,7	3	14,3	0,6
Length of third left pelvic-fin ray (second branched)	14,9	13,2	14,9	3	14,3	1,0
Anal-fin base	13,3	13,3	14,7	3	14,2	0,7
Preanal length	67,9	66,4	67,9	3	66,9	0,9
Distance between snout tip and terminus of anal-fin base	81,1	80,1	81,1	3	80,5	0,6
Distance between snout tip and anal-fin distal end	89,4	86,9	89,4	2	88,2	1,8
Adipose-fin length	35,7	33,0	35,7	3	34,8	1,6
Preadipose length	56,9	52,8	57,8	3	55,8	2,6
Distance between snout tip and adipose-fin base end	90,4	88,7	90,4	3	89,8	0,9
Adipose-fin depth	5,5	4,6	5,5	3	5,0	0,5
Caudal-peduncle length posterior to adipose-fin	8,2	8,2	11,6	3	10,1	1,7
Caudal-peduncle depth at adipose-fin terminus	6,9	6,9	7,7	3	7,2	0,4
Snout-anus distance	48,5	46,3	48,5	3	47,3	1,1
Snout-urogenital papilla distance	52,5	50,4	52,5	3	51,4	1,1
Anus-urogenital papilla distance	3,9	3,7	4,0	3	3,9	0,2
Dorsal lobe of caudal fin length	-	29,9	-	1	-	-
Ventral lobe of caudal fin length	-	26,5	-	1	-	-
Percentages of HL						
Head depth	42,8	42,8	50,0	3	45,7	3,8
Head width	52,6	51,5	60,0	3	54,7	4,6
Eye diameter (left)	23,0	20,9	23,2	3	22,4	1,2

Fleshy interorbital	23,3	20,7	23,3	3	22,0	1,3
Bony interorbital	15,9	15,3	16,9	3	16,0	0,8
Mouth gape	29,0	29,0	32,2	3	30,7	1,6
Snout length (left)	29,1	28,9	32,7	3	30,2	2,1
Distance between snout tip and posterior nare (left side)	17,2	16,7	17,5	3	17,1	0,5
Anterior internarial width	12,1	11,9	15,5	3	13,2	2,0
Posterior internarial width	14,5	14,5	14,7	3	14,6	0,1
Intranarial length (left side)	15,1	15,1	15,9	3	15,4	0,4

Table 7. Morphometric data of *Pimelodella insignis*, junior-synonym of *P. boschmai*, based on type material.

	Lectotype	Min.	Max.	n	x	SD
Total length (mm)	95,5	86,1	103,3	3	95,0	
Standard length (mm)	77,6	66,4	78,3	3	74,1	
As percentages of SL						
Body depth (dorsal)	18,3	18,3	19,9	3	18,8	0,9
Body width (dorsal)	14,7	13,8	15,3	3	14,6	0,7
Cleithral width	17,0	17,0	17,1	3	17,0	0,0
Head length	29,6	29,0	30,7	3	29,8	0,8
Maxillary-barbel length (left side)	67,3	67,3	71,0	3	69,2	1,8
Outer mental-barbel length (left side)	29,5	29,5	33,2	3	31,4	1,9
Inner mental-barbel length (left side)	16,4	16,4	19,3	3	17,5	1,6
Predorsal length	32,3	32,3	33,0	3	32,7	0,4
Distance between snout tip and terminus of dorsal-fin base	46,7	46,7	48,2	3	47,2	0,8
Distance between snout tip and dorsal-fin distal end	-	-	-	-	-	-
Dorsal fin to adipose fin	10,4	6,5	11,1	3	9,3	2,5
Dorsal-fin base	14,9	14,0	14,9	3	14,5	0,5
Length of first dorsal-fin ray (unbranched)	35,0	30,3	47,7	3	37,7	9,0
Length of rigid part of first dorsal-fin ray	17,2	17,2	19,5	3	18,5	1,2
Length of second dorsal-fin ray (first branched)	20,8	20,8	22,3	3	21,7	0,8
Length of third dorsal-fin ray (second branched)	17,1	17,1	20,8	3	19,5	2,1
Prepectoral length	21,3	21,2	23,3	3	21,9	1,2
Distance between snout tip and terminus of pectoral-fin base	25,0	25,0	26,2	3	25,4	0,7
Distance between snout tip and pectoral-fin distal end	-	-	-	-	-	-
Length of first left pectoral-fin ray (unbranched)	20,7	20,7	22,3	3	21,7	0,9
Length of rigid part of first left pectoral-fin ray	16,9	16,9	19,3	3	18,3	1,3
Length of second left pectoral-fin ray (first branched)	18,8	18,8	20,5	3	19,8	0,9
Length of third left pectoral-fin ray (second branched)	16,9	16,9	17,9	3	17,4	0,5
Prepelvic length	45,4	45,4	45,9	3	45,6	0,2
Distance between snout tip and terminus of pelvic-fin base	47,4	47,4	48,0	3	47,8	0,4
Distance between snout tip and pelvic-fin distal end	60,5	60,5	62,0	3	61,3	0,8
Distance between pelvic fins	5,2	4,5	5,2	3	4,9	0,4
Length of first left pelvic-fin ray (unbranched)	12,4	12,4	14,2	3	13,2	0,9
Length of second left pelvic-fin ray (first branched)	14,0	14,0	16,2	3	15,2	1,2
Length of third left pelvic-fin ray (second branched)	14,1	14,1	16,7	3	15,0	1,5
Anal-fin base	12,3	11,7	13,1	3	12,3	0,7
Preanal length	68,0	65,8	68,0	3	66,9	1,1
Distance between snout tip and terminus of anal-fin base	78,9	76,9	78,9	3	77,8	1,0
Distance between snout tip and anal-fin distal end	85,2	82,9	85,2	3	84,3	1,3
Adipose-fin length	32,0	32,0	36,9	3	34,5	2,4
Preadipose length	56,9	54,1	56,9	3	55,2	1,5
Distance between snout tip and adipose-fin base end	88,8	84,0	88,8	3	86,7	2,4
Adipose-fin depth	4,5	4,5	5,0	3	4,7	0,3
Caudal-peduncle length posterior to adipose-fin	12,1	11,7	13,8	3	12,5	1,1
Caudal-peduncle depth at adipose-fin terminus	8,7	8,7	9,6	3	9,2	0,5
Snout-anus distance	52,7	49,6	53,4	3	51,9	2,0
Snout-urogenital papilla distance	64,2	61,9	64,2	3	63,0	1,2
Anus-urogenital papilla distance	11,7	10,4	11,7	3	11,1	0,6
Dorsal lobe of caudal fin length	27,9	27,9	31,5	3	29,4	1,9
Ventral lobe of caudal fin length	24,6	24,6	27,0	3	26,1	1,3
As percentages of HL						
Head depth	47,7	47,7	52,1	3	50,3	2,3
Head width	57,6	52,8	57,6	3	55,6	2,5
Eye diameter (left)	19,0	17,2	19,0	3	18,4	1,0

Fleshy interorbital	25,1	24,6	25,1	3	24,9	0,3
Bony interorbital	16,4	16,0	19,4	3	17,2	1,9
Mouth gape	34,6	29,4	35,3	3	33,1	3,3
Snout length (left)	34,2	32,3	34,2	2	33,2	1,4
Distance between snout tip and posterior nare (left side)	19,1	19,1	21,8	3	20,2	1,4
Anterior internarial width	13,4	12,5	13,4	3	12,8	0,5
Posterior internarial width	14,8	14,4	17,0	3	15,4	1,4
Intranarial length (left side)	15,2	14,8	15,4	3	15,1	0,3

Table 8. Morphometric data of *Pimelodella brasiliensis* and its junior-synonyms, *P. eigenmanni* and *P. rendahli*, based on type materials.

	Holotype	Min.	Max.	n	x	SD
Total length (mm)	189,9	99,8	189,9	6	138,2	
Standard length (mm)	140,6	80,7	140,6	9	112,9	
Percentages of SL						
Body depth (dorsal)	17,6	17,4	20,0	7	19,0	1,1
Body width (dorsal)	14,2	13,2	15,0	7	14,0	0,6
Cleithral width	18,2	16,7	18,9	7	17,8	0,7
Head length	28,1	28,1	30,1	7	29,1	0,8
Maxillary-barbel length (left side)	63,8	57,5	74,9	5	66,0	7,6
Outer mental-barbel length (left side)	21,3	18,8	28,2	6	23,7	3,2
Inner mental-barbel length (left side)	11,9	6,8	14,6	7	12,3	2,8
Predorsal length	29,4	29,4	34,9	7	33,1	1,8
Distance between snout tip and terminus of dorsal-fin base	45,9	45,7	49,1	7	46,7	1,2
Distance between snout tip and dorsal-fin distal end	59,8	55,5	59,8	7	58,0	1,4
Dorsal fin to adipose fin	15,7	11,9	18,6	7	15,4	2,7
Dorsal-fin base	13,1	10,9	16,1	7	14,0	1,6
Length of first dorsal-fin ray (unbranched)	22,7	19,9	22,7	5	21,3	1,2
Length of rigid part of first dorsal-fin ray	18,9	15,7	19,2	7	17,9	1,3
Length of second dorsal-fin ray (first branched)	23,6	17,7	23,6	7	20,9	2,2
Length of third dorsal-fin ray (second branched)	22,3	15,9	22,3	7	19,9	2,0
Prepectoral length	21,5	19,6	24,3	7	21,5	1,5
Distance between snout tip and terminus of pectoral-fin base	24,2	23,6	27,1	7	24,6	1,3
Distance between snout tip and pectoral-fin distal end	44,4	39,1	44,4	7	41,2	2,3
Length of first left pectoral-fin ray (unbranched)	22,5	20,3	22,5	4	21,2	0,9
Length of rigid part of first left pectoral-fin ray	20,9	18,5	20,9	6	19,3	0,9
Length of second left pectoral-fin ray (first branched)	22,7	17,2	22,7	7	19,2	1,7
Length of third left pectoral-fin ray (second branched)	21,2	16,0	21,2	7	17,5	1,8
Prepelvic length	44,6	44,6	49,2	7	46,9	1,6
Distance between snout tip and terminus of pelvic-fin base	47,5	47,5	51,4	7	49,1	1,4
Distance between snout tip and pelvic-fin distal end	64,2	59,3	65,0	7	62,4	2,1
Distance between pelvic fins	6,3	3,8	6,3	7	5,2	0,8
Length of first left pelvic-fin ray (unbranched)	14,4	11,2	14,4	7	12,3	1,1
Length of second left pelvic-fin ray (first branched)	17,9	12,1	17,9	7	14,1	1,8
Length of third left pelvic-fin ray (second branched)	18,7	12,9	18,7	7	14,5	2,0
Anal-fin base	13,7	12,9	14,7	7	13,7	0,6
Preanal length	66,2	64,4	70,3	7	67,2	2,2
Distance between snout tip and terminus of anal-fin base	87,0	78,1	87,0	7	80,8	3,1
Distance between snout tip and anal-fin distal end	89,1	84,1	89,2	7	87,2	1,9
Adipose-fin length	27,8	25,1	34,4	6	27,7	3,4
Preadipose length	62,3	55,4	64,8	6	60,5	3,5
Distance between snout tip and adipose-fin base end	88,0	84,1	88,6	6	87,1	1,7
Adipose-fin depth	4,2	3,5	4,8	6	4,1	0,6
Caudal-peduncle length posterior to adipose-fin	13,4	11,8	14,3	6	13,2	0,8
Caudal-peduncle depth at adipose-fin terminus	8,8	6,9	8,8	6	7,8	0,8
Snout-anus distance	52,6	49,1	54,6	6	52,2	2,0
Snout-urogenital papilla distance	59,4	53,3	59,4	6	56,3	2,3

Anus-urogenital papilla distance	8,1	3,2	8,1	6	4,7	1,8
Dorsal lobe of caudal fin length	34,9	23,3	34,9	4	26,4	5,7
Ventral lobe of caudal fin length	27,9	21,5	27,9	4	23,7	2,9

Percentages of HL

Head depth	52,0	46,3	53,3	7	49,8	2,5
Head width	59,3	54,0	65,7	7	58,6	3,8
Eye diameter (left)	23,8	19,0	25,5	7	22,1	2,1
Fleshy interorbital	19,9	17,8	25,9	7	20,3	2,7
Bony interorbital	15,2	11,8	22,9	7	15,6	3,5
Mouth gape	30,4	27,3	31,3	7	29,5	1,7
Snout length (left)	29,3	28,8	31,6	7	29,9	0,9
Distance between snout tip and posterior nare (left side)	18,0	18,0	19,5	7	18,8	0,6
Anterior internarial width	11,6	11,5	14,3	7	12,7	1,2
Posterior internarial width	14,3	12,8	15,2	7	13,9	0,8
Intranarial length (left side)	12,9	12,4	15,1	7	13,1	0,9

Table 9. Morphometric data of *Pimelodella brasiliensis* and its junior-synonyms, *P. eigenmanni* and *P. rendahli*, based on type materials, discriminated by original species name.

	<i>P. brasiliensis</i>	<i>P. eigenmanni</i>					<i>P. rendahli</i>	
	Holotype	Lectotype	Min.	Max.	n	x	SD	Holotype
Total length (mm)	189,9	130,0	128,7	166,0	3	141,6		99,8
Standard length (mm)	140,6	105,4	94,8	135,6	7	113,8		80,7
		Percentages of SL						
Body depth (dorsal)	17,6	20,0	17,4	20,0	4	19,0	1,3	19,0
Body width (dorsal)	14,2	13,2	13,2	15,0	4	14,0	0,8	14,3
Cleithral width	18,2	17,6	17,4	17,9	4	17,6	0,2	18,9
Head length	28,1	29,0	28,3	29,6	4	29,0	0,5	29,9
Maxillary-barbel length (left side)	63,8	-	72,7	74,9	2	73,8	1,6	60,8
Outer mental-barbel length (left side)	21,3	24,0	24,0	25,1	3	24,6	0,6	28,2
Inner mental-barbel length (left side)	11,9	13,1	11,1	14,6	4	13,2	1,5	14,4
Predorsal length	29,4	34,9	32,7	34,9	4	33,6	1,0	34,4
Distance between snout tip and terminus of dorsal-fin base	45,9	46,6	45,7	47,2	4	46,4	0,6	49,1
Distance between snout tip and dorsal-fin distal end	59,8	59,0	56,9	59,0	4	58,3	0,9	57,3
Dorsal fin to adipose fin	15,7	16,9	12,4	18,6	4	15,5	2,8	18,3
Dorsal-fin base	13,1	10,9	10,9	15,1	4	13,6	1,8	16,1
Length of first dorsal-fin ray (unbranched)	22,7	-	21,7	21,8	2	21,7	0,1	19,9
Length of rigid part of first dorsal-fin ray	18,9	15,7	15,7	19,2	4	18,1	1,6	17,7
Length of second dorsal-fin ray (first branched)	23,6	23,2	20,4	23,2	4	21,6	1,2	17,7
Length of third dorsal-fin ray (second branched)	22,3	20,6	19,7	21,1	4	20,4	0,6	19,5
Prepectoral length	21,5	19,6	19,6	22,4	4	21,0	1,2	24,3
Distance between snout tip and terminus of pectoral-fin base	24,2	23,8	23,8	25,6	4	24,3	0,9	27,1
Distance between snout tip and pectoral-fin distal end	44,4	39,1	39,1	40,8	4	40,1	0,7	44,4
Length of first left pectoral-fin ray (unbranched)	22,5	21,2	20,8	21,2	2	21,0	0,3	20,3
Length of rigid part of first left pectoral-fin ray	20,9	19,8	18,9	19,8	3	19,3	0,5	18,5
Length of second left pectoral-fin ray (first branched)	22,7	17,9	17,9	19,5	4	18,8	0,7	17,2
Length of third left pectoral-fin ray (second branched)	21,2	17,4	16,1	17,6	4	17,0	0,7	16,0

Prepelvic length	44,6	46,5	46,5	49,2	4	47,5	1,2	48,2
Distance between snout tip and terminus of pelvic-fin base	47,5	49,4	48,3	51,4	4	49,6	1,3	50,3
Distance between snout tip and pelvic-fin distal end	64,2	63,7	60,4	65,0	4	62,6	2,1	62,8
Distance between pelvic fins	6,3	5,0	5,0	5,7	4	5,3	0,3	5,1
Length of first left pelvic-fin ray (unbranched)	14,4	13,0	11,2	13,0	4	12,1	0,7	11,2
Length of second left pelvic-fin ray (first branched)	17,9	14,2	12,1	14,3	4	13,5	1,0	13,7
Length of third left pelvic-fin ray (second branched)	18,7	15,0	12,9	15,0	4	13,9	1,0	13,0
Anal-fin base	13,7	13,8	12,9	14,7	4	13,6	0,8	14,0
Preanal length	66,2	68,2	64,8	68,6	4	67,4	1,7	70,3
Distance between snout tip and terminus of anal-fin base	87,0	78,1	78,1	80,6	4	79,3	1,3	82,5
Distance between snout tip and anal-fin distal end	89,1	86,2	85,8	89,2	4	87,3	1,6	87,8
Adipose-fin length	27,8	25,1	25,1	27,1	4	26,1	1,1	23,3
Preadipose length	62,3	63,0	58,3	64,8	4	61,4	3,0	65,8
Distance between snout tip and adipose-fin base end	88,0	88,1	84,1	88,6	4	86,8	2,0	88,0
Adipose-fin depth	4,2	3,7	3,5	4,8	4	4,2	0,7	1,9
Caudal-peduncle length posterior to adipose-fin	13,4	13,4	11,8	14,3	4	13,2	1,0	11,7
Caudal-peduncle depth at adipose-fin terminus	8,8	6,9	6,9	8,8	4	7,8	0,8	7,5
Snout-anus distance	52,6	50,7	50,7	54,6	4	52,8	1,6	55,0
Snout-urogenital papilla distance	59,4	55,1	55,1	58,4	4	56,3	1,5	59,2
Anus-urogenital papilla distance	8,1	4,9	3,2	4,9	4	4,0	0,7	4,3
Dorsal lobe of caudal fin length	34,9	23,6	23,6	23,9	2	23,7	0,2	23,3
Ventral lobe of caudal fin length	27,9	22,3	22,3	23,1	2	22,7	0,6	-

Percentages of HL

Head depth	52,0	47,1	47,1	50,6	4	49,3	1,6	53,3
Head width	59,3	55,1	55,1	60,0	4	57,9	2,1	65,7
Eye diameter (left)	23,8	25,5	21,2	25,5	4	22,8	1,9	19,0
Fleshy interorbital	19,9	17,8	17,8	20,6	4	19,1	1,5	25,9
Bony interorbital	15,2	11,8	11,8	15,7	4	14,1	1,7	22,9
Mouth gape	30,4	30,5	27,3	31,3	4	29,2	2,0	31,0
Snout length (left)	29,3	28,8	28,8	31,6	4	30,0	1,2	30,1
Distance between snout tip and posterior nare (left side)	18,0	18,9	18,4	19,5	4	19,0	0,5	19,2

Anterior internarial width	11,6	12,5	12,5	14,3	4	13,5	0,8	11,5
Posterior internarial width	14,3	12,8	12,8	15,2	4	14,1	1,1	13,7
Intranarial length (left side)	12,9	12,6	12,4	15,1	4	13,2	1,3	13,5

Table 10. Morphometric data of *Pimelodella buckleyi* based on type and comparative materials.

	Lectotype	Min.	Max.	n	x	SD
Total length (mm)	133,2	111,5	158,5	4	73,2	
Standard length (mm)	109,6	89,7	120,6	4	51,3	
	Percentages of SL					
Body depth (dorsal)	14,6	14,6	20,6	4	17,3	3,0
Body width (dorsal)	12,9	12,9	16,8	4	14,2	1,7
Cleithral width	15,8	15,8	18,5	4	16,9	1,2
Head length	27,0	27,0	29,7	4	28,2	1,1
Maxillary-barbel length (left side)	62,6	62,6	74,9	4	66,0	6,0
Outer mental-barbel length (left side)	27,2	27,2	30,1	4	28,4	1,2
Inner mental-barbel length (left side)	15,2	14,8	17,4	4	15,8	1,1
Predorsal length	32,9	32,6	33,4	4	33,0	0,3
Distance between snout tip and terminus of dorsal-fin base	44,8	44,8	47,5	4	46,4	1,2
Distance between snout tip and dorsal-fin distal end	55,4	55,4	56,8	4	56,1	0,7
Dorsal fin to adipose fin	6,2	6,2	12,3	4	8,9	2,9
Dorsal-fin base	11,8	11,8	16,0	4	14,5	1,8
Length of first dorsal-fin ray (unbranched)	-	16,3	19,5	3	18,2	1,6
Length of rigid part of first dorsal-fin ray	11,5	11,5	14,5	4	12,9	1,4
Length of second dorsal-fin ray (first branched)	19,9	18,2	20,5	4	19,6	1,0
Length of third dorsal-fin ray (second branched)	17,9	17,9	22,5	4	19,5	2,1
Prepectoral length	18,2	18,2	21,5	4	20,2	1,5
Distance between snout tip and terminus of pectoral-fin base	20,4	20,4	24,5	4	23,0	1,8
Distance between snout tip and pectoral-fin distal end	35,2	35,2	39,3	4	37,6	1,9
Length of first left pectoral-fin ray (unbranched)	-	17,6	18,3	2	17,9	0,5
Length of rigid part of first left pectoral-fin ray	14,0	14,0	15,8	4	15,1	0,8
Length of second left pectoral-fin ray (first branched)	18,9	16,0	18,9	4	17,6	1,3
Length of third left pectoral-fin ray (second branched)	14,6	14,0	15,5	4	14,7	0,6
Prepelvic length	43,6	43,6	47,0	4	45,1	1,4
Distance between snout tip and terminus of pelvic-fin base	45,1	45,1	48,6	4	46,8	1,4
Distance between snout tip and pelvic-fin distal end	56,6	56,6	61,6	4	59,5	2,1
Distance between pelvic fins	4,6	4,2	4,7	4	4,5	0,3
Length of first left pelvic-fin ray (unbranched)	12,2	11,9	13,2	4	12,6	0,6
Length of second left pelvic-fin ray (first branched)	13,5	13,1	14,6	4	13,9	0,7
Length of third left pelvic-fin ray (second branched)	13,9	13,1	14,1	4	13,6	0,4
Anal-fin base	13,0	11,9	13,2	4	12,6	0,6
Preanal length	66,0	65,4	67,9	4	66,5	1,1
Distance between snout tip and terminus of anal-fin base	79,4	76,8	80,0	4	79,0	1,5
Distance between snout tip and anal-fin distal end	85,0	83,6	87,1	4	85,5	1,5
Adipose-fin length	37,6	32,6	37,6	4	35,0	2,8
Preadipose length	51,7	51,7	59,0	4	55,6	3,5
Distance between snout tip and adipose-fin base end	88,4	88,4	90,1	4	89,1	0,7
Adipose-fin depth	4,6	4,6	5,1	4	4,8	0,2
Caudal-peduncle length posterior to adipose-fin	10,2	9,1	12,2	4	10,4	1,3
Caudal-peduncle depth at adipose-fin terminus	10,0	8,8	10,4	4	9,6	0,7
Snout-anus distance	48,7	48,6	50,8	4	49,6	1,1
Snout-urogenital papilla distance	52,4	51,9	54,1	4	52,8	0,9
Anus-urogenital papilla distance	4,5	2,7	4,5	4	3,6	0,8
Dorsal lobe of caudal fin length	-	31,5	33,9	2	32,7	1,8
Ventral lobe of caudal fin length	25,2	21,7	25,2	3	23,7	1,8

	Percentages of HL					
Head depth	36,0	36,0	53,1	4	44,6	7,1
Head width	58,6	53,6	68,5	4	59,9	6,2
Eye diameter (left)	22,7	20,1	22,7	4	21,4	1,3
Fleshy interorbital	23,1	23,1	26,2	4	24,3	1,3
Bony interorbital	15,8	15,8	17,6	4	16,6	0,8
Mouth gape	33,5	31,6	38,0	4	34,8	2,8
Snout length (left)	30,0	29,3	31,4	4	30,2	0,9
Distance between snout tip and posterior nare (left side)	18,6	18,3	20,4	4	19,3	1,0
Anterior internarial width	12,3	12,3	14,8	4	14,0	1,2
Posterior internarial width	14,8	14,8	16,0	4	15,5	0,6
Intranarial length (left side)	13,2	13,2	14,5	4	13,8	0,6

Table 11. Morphometric data of *Pimelodella chagresi* based on type and comparative materials.

	Lectotype	Min.	Max.	n	x	SD
Total length (mm)	142,5	70,2	142,5	5	107,6	
Standard length (mm)	111,8	57,1	111,8	8	78,4	
	Percentages of SL					
Body depth (dorsal)	18,8	17,3	20,4	4	18,7	1,3
Body width (dorsal)	16,2	12,5	16,2	4	15,1	1,8
Cleithral width	18,0	17,0	19,3	4	18,0	1,0
Head length	29,3	29,2	32,5	4	30,2	1,5
Maxillary-barbel length (left side)	65,9	61,0	81,0	4	70,2	8,7
Outer mental-barbel length (left side)	22,1	22,1	26,7	4	24,7	2,0
Inner mental-barbel length (left side)	15,2	12,2	17,0	4	14,8	2,0
Predorsal length	32,9	32,9	34,2	4	33,6	0,5
Distance between snout tip and terminus of dorsal-fin base	47,6	47,6	51,1	4	48,7	1,6
Distance between snout tip and dorsal-fin distal end	57,9	57,9	62,2	4	59,7	1,8
Dorsal fin to adipose fin	16,7	11,5	16,7	4	14,3	2,3
Dorsal-fin base	15,6	14,5	15,7	4	15,3	0,5
Length of first dorsal-fin ray (unbranched)	20,9	20,9	22,6	4	22,0	0,8
Length of rigid part of first dorsal-fin ray	16,2	16,2	16,9	4	16,6	0,3
Length of second dorsal-fin ray (first branched)	21,8	20,9	21,9	4	21,5	0,5
Length of third dorsal-fin ray (second branched)	18,8	18,8	20,9	4	19,8	1,1
Prepectoral length	20,2	20,2	23,9	4	21,8	1,6
Distance between snout tip and terminus of pectoral-fin base	24,0	24,0	26,9	4	25,2	1,2
Distance between snout tip and pectoral-fin distal end	40,6	40,6	46,2	4	42,6	2,6
Length of first left pectoral-fin ray (unbranched)	20,8	19,9	23,0	4	21,0	1,4
Length of rigid part of first left pectoral-fin ray	16,4	16,4	19,7	4	18,0	1,3
Length of second left pectoral-fin ray (first branched)	18,1	17,1	19,8	4	18,5	1,2
Length of third left pectoral-fin ray (second branched)	16,9	16,4	17,6	4	17,1	0,6
Prepelvic length	46,7	44,9	48,3	4	46,8	1,4
Distance between snout tip and terminus of pelvic-fin base	48,7	48,7	50,6	4	49,7	0,8
Distance between snout tip and pelvic-fin distal end	65,1	64,1	65,1	4	64,5	0,4
Distance between pelvic fins	6,1	4,9	6,1	4	5,4	0,5
Length of first left pelvic-fin ray (unbranched)	14,7	13,3	14,7	4	14,1	0,7
Length of second left pelvic-fin ray (first branched)	16,7	14,5	16,7	4	15,3	1,0
Length of third left pelvic-fin ray (second branched)	15,7	14,4	15,7	4	15,0	0,6
Anal-fin base	13,8	13,0	16,1	4	14,0	1,4
Preanal length	65,6	65,6	70,7	4	67,7	2,2
Distance between snout tip and terminus of anal-fin base	79,0	79,0	80,6	4	79,8	0,7
Distance between snout tip and anal-fin distal end	86,2	86,2	87,7	4	86,8	0,7
Adipose-fin length	27,3	27,2	28,4	4	27,7	0,5
Preadipose length	62,0	60,7	62,4	4	61,5	0,8
Distance between snout tip and adipose-fin base end	88,5	87,3	88,5	4	88,1	0,5
Adipose-fin depth	3,5	3,5	5,4	4	4,2	0,8
Caudal-peduncle length posterior to adipose-fin	11,1	10,8	12,2	4	11,5	0,7
Caudal-peduncle depth at adipose-fin terminus	9,9	7,8	9,9	4	9,0	0,9
Snout-anus distance	54,8	53,2	55,7	4	54,7	1,1
Snout-urogenital papilla distance	58,9	57,0	60,3	4	58,5	1,5
Anus-urogenital papilla distance	4,3	3,0	5,8	4	4,3	1,2
Dorsal lobe of caudal fin length	28,4	19,8	28,4	4	24,8	3,8
Ventral lobe of caudal fin length	23,0	23,0	24,3	4	23,7	0,6
	Percentages of HL					
Head depth	51,7	47,7	51,8	4	50,1	2,0
Head width	60,1	52,5	60,1	4	56,2	3,4
Eye diameter (left)	22,3	19,3	22,3	4	20,8	1,3

Fleshy interorbital	24,6	20,6	24,6	4	23,2	1,8
Bony interorbital	17,1	14,4	18,3	4	16,3	1,7
Mouth gape	29,8	26,6	30,8	4	28,6	2,0
Snout length (left)	30,2	29,7	31,4	4	30,5	0,7
Distance between snout tip and posterior nare (left side)	18,6	17,0	19,0	4	18,4	0,9
Anterior internarial width	14,5	13,2	14,7	4	14,1	0,7
Posterior internarial width	16,3	13,7	17,1	4	15,6	1,5
Intranarial length (left side)	12,8	12,8	16,2	4	14,4	1,4

Table 12. Morphometric data of *Pimelodella conquetaensis* based on type material.

	Holotype
Total length (mm)	-
Standard length (mm)	93,2
Percentages of SL	
Body depth (dorsal)	16,8
Body width (dorsal)	15,0
Cleithral width	17,2
Head length	30,1
Maxillary-barbel length (left side)	-
Outer mental-barbel length (left side)	35,8
Inner mental-barbel length (left side)	-
Predorsal length	30,2
Distance between snout tip and terminus of dorsal-fin base	48,9
Distance between snout tip and dorsal-fin distal end	60,4
Dorsal fin to adipose fin	13,1
Dorsal-fin base	15,6
Length of first dorsal-fin ray (unbranched)	-
Length of rigid part of first dorsal-fin ray	-
Length of second dorsal-fin ray (first branched)	22,9
Length of third dorsal-fin ray (second branched)	20,6
Prepectoral length	22,4
Distance between snout tip and terminus of pectoral-fin base	25,7
Distance between snout tip and pectoral-fin distal end	41,5
Length of first left pectoral-fin ray (unbranched)	-
Length of rigid part of first left pectoral-fin ray	17,7
Length of second left pectoral-fin ray (first branched)	17,9
Length of third left pectoral-fin ray (second branched)	17,2
Prepelvic length	44,0
Distance between snout tip and terminus of pelvic-fin base	46,6
Distance between snout tip and pelvic-fin distal end	62,1
Distance between pelvic fins	5,5
Length of first left pelvic-fin ray (unbranched)	-
Length of second left pelvic-fin ray (first branched)	-
Length of third left pelvic-fin ray (second branched)	14,0
Anal-fin base	12,5
Preanal length	71,0
Distance between snout tip and terminus of anal-fin base	80,5
Distance between snout tip and anal-fin distal end	87,7
Adipose-fin length	28,8
Preadipose length	61,1
Distance between snout tip and adipose-fin base end	90,0
Adipose-fin depth	5,0
Caudal-peduncle length posterior to adipose-fin	9,4
Caudal-peduncle depth at adipose-fin terminus	7,9
Snout-anus distance	54,1
Snout-urogenital papilla distance	54,4

Anus-urogenital papilla distance	2,0
Dorsal lobe of caudal fin length	-
Ventral lobe of caudal fin length	-

Percentages of HL

Head depth	51,4
Head width	57,7
Eye diameter (left)	22,6
Fleshy interorbital	18,6
Bony interorbital	13,0
Mouth gape	27,0
Snout length (left)	28,2
Distance between snout tip and posterior nare (left side)	17,5
Anterior internarial width	11,5
Posterior internarial width	13,4
Intranarial length (left side)	12,3

Table 13. Morphometric data of *Pimelodella cristata* and its junior-synonyms, *P. cristata*, *P. breviceps*, *P. dorseyi*, *P. hartwelli*, *P. ophthalmica*, *P. parnahybae*, *P. steindachneri*, *P. wessellii*, *P. witmeri*, based on type and comparative materials.

	Lectotype	Min.	Max.	n	x	SD
Total length (mm)	242,5	94,4	419,0	26,0	160,9	
Standard length (mm)	202,5	82,6	326,2	32,0	128,8	
	Percentages of SL					
Body depth (dorsal)	18,2	13,3	22,2	32	17,8	2,2
Body width (dorsal)	11,2	8,8	16,5	32	12,9	2,0
Cleithral width	15,4	13,0	19,3	32	16,7	1,2
Head length	27,1	24,4	32,8	32	29,0	2,0
Maxillary-barbel length (left side)	81,6	63,4	104,2	29	83,4	10,2
Outer mental-barbel length (left side)	32,1	20,9	38,4	32	29,9	5,2
Inner mental-barbel length (left side)	17,1	10,7	22,4	32	16,6	3,3
Predorsal length	30,8	27,0	35,4	32	32,2	1,9
Distance between snout tip and terminus of dorsal-fin base	43,9	39,4	49,0	32	45,9	2,0
Distance between snout tip and dorsal-fin distal end	57,0	32,4	61,3	32	56,0	4,8
Dorsal fin to adipose fin	6,0	1,8	9,8	32	5,9	2,4
Dorsal-fin base	14,5	12,5	20,2	32	15,1	1,4
Length of first dorsal-fin ray (unbranched)	21,4	19,6	27,8	24	22,7	2,4
Length of rigid part of first dorsal-fin ray	18,0	14,3	22,2	27	18,3	2,1
Length of second dorsal-fin ray (first branched)	22,5	19,7	27,1	31	22,1	2,0
Length of third dorsal-fin ray (second branched)	21,5	17,4	25,8	31	20,7	1,9
Prepectoral length	18,9	17,2	26,6	32	21,4	2,1
Distance between snout tip and terminus of pectoral-fin base	23,1	19,6	29,9	32	24,5	2,0
Distance between snout tip and pectoral-fin distal end	37,9	34,0	48,9	32	39,5	3,3
Length of first left pectoral-fin ray (unbranched)	19,2	16,9	23,2	21	19,3	1,6
Length of rigid part of first left pectoral-fin ray	17,5	14,8	21,8	28	17,7	1,7
Length of second left pectoral-fin ray (first branched)	16,7	14,6	21,4	31	17,6	1,5
Length of third left pectoral-fin ray (second branched)	15,6	13,3	18,6	31	15,9	1,3
Prepelvic length	45,2	39,6	49,4	32	44,3	2,1
Distance between snout tip and terminus of pelvic-fin base	44,9	42,0	51,6	32	46,9	2,0
Distance between snout tip and pelvic-fin distal end	58,9	54,0	66,6	31	60,0	2,3
Distance between pelvic fins	4,5	4,0	6,5	32	5,2	0,7
Length of first left pelvic-fin ray (unbranched)	11,8	11,0	15,7	30	13,0	1,2
Length of second left pelvic-fin ray (first branched)	12,9	12,6	17,1	29	14,2	1,2
Length of third left pelvic-fin ray (second branched)	13,6	12,5	16,9	29	14,4	1,0
Anal-fin base	15,2	11,6	18,1	32	14,0	1,6
Preanal length	64,8	60,7	68,0	32	65,0	2,0
Distance between snout tip and terminus of anal-fin base	81,0	74,1	81,0	32	78,1	1,5
Distance between snout tip and anal-fin distal end	88,2	77,3	88,6	31	85,3	2,4
Adipose-fin length	43,0	36,7	45,4	32	41,9	2,2
Preadipose length	48,3	45,2	55,6	32	50,2	2,6
Distance between snout tip and adipose-fin base end	90,0	84,5	93,8	32	89,8	2,0

Adipose-fin depth	5,2	2,6	6,5	32	5,1	0,9
Caudal-peduncle length posterior to adipose-fin	11,5	7,2	11,5	32	9,5	1,0
Caudal-peduncle depth at adipose-fin terminus	8,3	6,0	9,2	32	8,2	0,7
Snout-anus distance	49,2	46,0	54,9	31	50,8	1,9
Snout-urogenital papilla distance	52,9	49,8	58,3	31	54,3	2,0
Anus-urogenital papilla distance	3,0	2,3	5,6	31	3,4	0,8
Dorsal lobe of caudal fin length	18,3	16,6	32,9	24	22,9	4,6
Ventral lobe of caudal fin length	21,7	18,5	29,7	25	23,5	2,6

Percentages of HL

Head depth	49,3	30,9	56,2	32	48,4	4,8
Head width	57,8	47,9	66,8	32	57,1	4,2
Eye diameter (left)	20,8	17,4	26,3	32	21,4	2,2
Fleshy interorbital	26,2	20,9	29,5	32	25,1	2,4
Bony interorbital	19,5	12,9	29,8	32	19,4	3,0
Mouth gape	32,6	25,6	36,1	32	30,4	2,8
Snout length (left)	35,4	32,6	39,0	32	35,2	1,4
Distance between snout tip and posterior nare (left side)	17,0	16,9	22,3	32	19,0	1,5
Anterior internarial width	14,4	12,0	16,4	32	13,9	1,1
Posterior internarial width	11,7	11,4	16,5	32	13,7	1,1
Intranarial length (left side)	11,4	11,4	17,3	32	14,4	1,3

Table 14: Morphometric data of *Pimelodella cristata* and its junior-synonyms, *P. cristata*, *P. breviceps*, *P. dorseyi*, *P. hartwelli*, *P. ophthalmica*, *P. parnahybae*, *P. steindachneri*, *P. wessellii*, *P. witmeri*, based on type and comparative materials, discriminated by original species name.

	<i>Pimelodella cristata</i>						<i>P. breviceps</i>	<i>P. dorseyi</i>		<i>P. hartwelli</i>
	Lectotype	Min.	Max.	n	x	SD	Holotype	Holotype	Paratype	Holotype
Total length (mm)	242,5	151,2	151,2	7,0	177,3		419,0	118,9	117,5	-
Standard length (mm)	202,5	82,6	82,6	9,0	135,9		326,2	95,8	95,8	103,2
	Percentages of SL									
Body depth (dorsal)	18,2	13,3	19,5	9	17,1	2,3	13,7	17,5	17,7	17,6
Body width (dorsal)	11,2	10,6	16,5	9	13,3	1,7	10,8	12,9	13,4	11,0
Cleithral width	15,4	14,8	17,7	9	16,4	1,0	13,0	16,9	16,6	15,7
Head length	27,1	26,1	31,1	9	27,7	1,6	24,4	29,7	29,8	29,7
Maxillary-barbel length (left side)	81,6	63,4	104,2	8	84,4	13,5	67,2	78,8	77,4	103,2
Outer mental-barbel length (left side)	32,1	23,2	37,2	9	30,5	4,8	22,0	22,4	23,1	36,1
Inner mental-barbel length (left side)	17,1	10,7	22,1	9	16,8	3,4	13,9	10,7	10,7	19,0
Predorsal length	30,8	29,4	34,1	9	31,1	1,3	27,0	31,4	33,1	33,1
Distance between snout tip and terminus of dorsal-fin base	43,9	41,7	47,5	9	44,8	1,6	39,4	46,4	46,1	47,2
Distance between snout tip and dorsal-fin distal end	57,0	52,5	57,1	9	54,8	1,9	56,0	55,1	55,7	58,8
Dorsal fin to adipose fin	6,0	3,0	9,8	9	6,7	1,9	6,3	4,3	4,1	6,6
Dorsal-fin base	14,5	12,9	15,7	9	14,7	0,9	12,5	14,6	15,6	14,8
Length of first dorsal-fin ray (unbranched)	21,4	19,6	24,7	9	21,9	1,4	27,8	21,3	20,6	20,8
Length of rigid part of first dorsal-fin ray	18,0	14,3	21,6	9	17,8	2,5	17,6	16,5	16,2	18,5
Length of second dorsal-fin ray (first branched)	22,5	19,7	23,6	9	21,4	1,3	25,5	20,3	19,7	22,8
Length of third dorsal-fin ray (second branched)	21,5	17,4	22,0	9	20,0	1,6	21,2	18,9	19,0	20,6
Prepectoral length	18,9	18,5	24,1	9	20,3	1,8	17,2	23,1	22,9	21,1
Distance between snout tip and terminus of pectoral-fin base	23,1	21,3	26,5	9	23,6	1,5	19,6	26,3	26,1	23,8
Distance between snout tip and pectoral-fin distal end	37,9	34,0	41,5	9	37,3	2,7	34,0	41,4	40,1	40,7
Length of first left pectoral-fin ray (unbranched)	19,2	16,9	23,2	6	18,9	2,3	17,0	18,3	18,4	19,9
Length of rigid part of first left pectoral-fin ray	17,5	14,8	19,7	9	16,9	1,5	15,6	16,9	17,9	18,2
Length of second left pectoral-fin ray (first branched)	16,7	15,8	21,4	9	17,3	1,7	14,6	16,1	17,3	17,8
Length of third left pectoral-fin ray (second branched)	15,6	13,3	18,6	9	15,5	1,5	13,6	14,5	15,7	16,2

Prepelvic length	45,2	41,9	47,3	9	44,0	1,8	39,6	44,1	42,6	42,9
Distance between snout tip and terminus of pelvic-fin base	44,9	43,9	49,1	9	46,4	1,7	42,0	46,8	46,7	46,5
Distance between snout tip and pelvic-fin distal end	58,9	57,1	61,2	9	59,5	1,5	54,0	61,1	59,7	59,6
Distance between pelvic fins	4,5	4,3	6,5	9	5,4	0,8	5,6	4,8	5,4	4,5
Length of first left pelvic-fin ray (unbranched)	11,8	11,2	14,6	8	12,4	1,0	11,2	13,3	13,0	12,6
Length of second left pelvic-fin ray (first branched)	12,9	12,6	15,3	8	13,9	1,1	12,8	14,4	13,3	13,3
Length of third left pelvic-fin ray (second branched)	13,6	12,5	16,4	8	14,1	1,2	13,4	14,5	14,5	14,2
Anal-fin base	15,2	12,5	18,1	9	15,3	2,2	14,2	13,5	15,3	13,6
Preanal length	64,8	60,7	68,0	9	64,2	2,7	64,0	63,2	64,9	65,6
Distance between snout tip and terminus of anal-fin base	81,0	78,1	81,0	9	79,2	1,0	77,0	78,0	76,9	78,3
Distance between snout tip and anal-fin distal end	88,2	81,9	88,2	9	85,6	2,3	83,7	84,6	85,7	85,5
Adipose-fin length	43,0	39,8	44,8	9	42,7	1,6	45,2	43,7	43,2	42,4
Preadipose length	48,3	46,6	52,6	9	50,0	2,2	45,2	48,2	48,9	52,2
Distance between snout tip and adipose-fin base end	90,0	84,5	93,8	9	90,2	3,0	90,4	89,4	87,8	90,9
Adipose-fin depth	5,2	4,0	6,2	9	5,0	0,8	4,4	5,8	5,4	3,8
Caudal-peduncle length posterior to adipose-fin	11,5	7,2	11,5	9	9,7	1,5	11,3	9,8	10,1	9,4
Caudal-peduncle depth at adipose-fin terminus	8,3	7,4	8,7	9	8,0	0,4	7,2	8,4	8,4	8,4
Snout-anus distance	49,2	48,8	53,4	9	50,5	1,6	46,0	51,2	50,3	49,8
Snout-urogenital papilla distance	52,9	51,9	56,9	9	54,1	2,0	49,8	54,3	53,2	53,0
Anus-urogenital papilla distance	3,0	3,0	5,6	9	3,7	0,7	3,1	2,7	2,7	2,5
Dorsal lobe of caudal fin length	18,3	18,3	32,9	8	23,6	5,9	27,8	26,5	24,7	-
Ventral lobe of caudal fin length	21,7	19,2	29,7	8	23,8	3,8	24,6	23,0	21,5	-

Percentages of HL

Head depth	49,3	30,9	56,2	9	46,7	7,1	50,8	50,3	50,1	53,2
Head width	57,8	53,9	66,8	9	59,1	4,6	52,7	60,2	57,3	53,2
Eye diameter (left)	20,8	19,5	26,3	9	21,6	2,1	17,4	19,7	22,1	22,5
Fleshy interorbital	26,2	21,0	26,6	9	24,3	2,0	26,9	26,0	26,1	23,9
Bony interorbital	19,5	12,9	20,7	9	17,3	2,5	20,7	20,6	18,7	18,5
Mouth gape	32,6	28,5	34,0	9	31,1	2,2	30,7	32,7	33,3	25,9
Snout length (left)	35,4	33,0	36,5	9	34,8	1,2	39,0	36,7	36,6	36,1
Distance between snout tip and posterior nare (left side)	17,0	17,0	21,7	9	19,1	1,3	18,8	22,3	20,9	19,0

Anterior internarial width	14,4	12,0	14,4	9	13,3	0,8	15,1	13,2	13,3	13,1
Posterior internarial width	11,7	11,7	14,5	9	13,0	0,8	13,8	15,1	14,6	13,2
Intranarial length (left side)	11,4	11,4	16,3	9	14,0	1,7	14,8	14,6	13,7	14,7

Table 14 (cont): Morphometric data of *Pimelodella cristata* and its junior-synonyms, *P. cristata*, *P. breviceps*, *P. dorseyi*, *P. hartwelli*, *P. ophthalmica*, *P. parnahybae*, *P. steindachneri*, *P. wessellii*, *P. witmeri*, based on type and comparative materials, discriminated by original species name.

	<i>P.</i>	<i>P. parnahybae</i>					
	<i>ophthalmica</i>	Holotype	Min.	Max.	<i>n</i>	<i>x</i>	SD
Total length (mm)	-	94,4	94,4	152,2	4,0	127,7	
Standard length (mm)	109,9	84,0	84,0	145,0	5,0	115,0	
Body depth (dorsal)	15,3	19,3	18,5	22,2	5	19,9	1,6
Body width (dorsal)	8,8	14,6	13,8	16,5	5	14,7	1,1
Cleithral width	17,4	17,3	16,9	18,5	5	17,5	0,6
Head length	30,8	30,3	28,6	31,1	5	29,9	1,0
Maxillary-barbel length (left side)	-	82,1	76,9	82,1	4	79,1	2,2
Outer mental-barbel length (left side)	31,2	32,0	24,4	32,0	5	30,0	3,2
Inner mental-barbel length (left side)	18,0	16,2	16,0	17,9	5	17,0	0,9
Predorsal length	34,8	34,1	32,8	34,9	5	33,6	0,9
Distance between snout and terminus of dorsal-fin base	47,5	47,4	45,7	47,4	5	46,9	0,8
Distance between snout tip and dorsal-fin distal end	56,2	58,2	32,4	59,1	5	52,5	11,3
Dorsal fin to adipose fin	3,2	9,7	5,2	9,7	5	8,1	1,8
Dorsal-fin base	15,3	17,2	14,4	17,2	5	15,8	1,1
Length of first dorsal-fin ray (unbranched)	-	21,1	19,8	23,6	4	21,9	1,8
Length of rigid part of first dorsal-fin ray	20,1	-	16,2	20,0	3	17,8	2,0
Length of second dorsal-fin ray (first branched)	-	20,7	20,1	25,9	5	22,0	2,4
Length of third dorsal-fin ray (second branched)	18,4	19,9	19,0	21,2	4	19,9	0,9
Prepectoral length	21,9	21,6	20,8	21,8	5	21,5	0,4
Distance between snout and terminus of pectoral-fin base	24,8	25,9	23,8	25,9	5	24,6	0,8
Distance between snout tip and pectoral-fin distal end	42,0	42,4	38,3	42,4	5	40,1	1,6
Length of first left pectoral-fin ray (unbranched)	20,0	19,5	18,2	19,9	4	19,1	0,8

Length of rigid part of first left pectoral-fin ray	19,5	18,4	16,2	18,4	4	17,2	0,9
Length of second left pectoral-fin ray (first branched)	17,3	19,3	16,8	19,3	5	18,1	0,9
Length of third left pectoral-fin ray (second branched)	15,8	18,0	14,8	18,0	5	16,4	1,2
Prepelvic length	46,3	42,9	42,9	46,7	5	45,3	1,4
Distance between snout and terminus of pelvic-fin base	47,9	45,2	45,2	49,4	5	47,2	1,6
Distance between snout tip and pelvic-fin distal end	59,1	58,1	58,1	61,2	4	59,9	1,4
Distance between pelvic fins	4,0	4,4	4,4	5,7	5	5,2	0,5
Length of first left pelvic-fin ray (unbranched)	11,0	14,2	11,6	14,2	4	13,1	1,1
Length of second left pelvic-fin ray (first branched)	-	14,6	13,5	14,9	4	14,1	0,7
Length of third left pelvic-fin ray (second branched)	-	14,2	13,9	14,4	4	14,1	0,3
Anal-fin base	12,1	13,5	11,6	13,7	5	12,9	0,9
Preanal length	66,8	65,2	65,2	67,6	5	66,5	0,9
Distance between snout tip and terminus of anal-fin base	76,3	79,4	78,8	79,9	5	79,3	0,4
Distance between snout tip and anal-fin distal end	82,0	87,0	87,0	88,5	4	87,5	0,7
Adipose-fin length	39,3	39,6	36,7	45,4	5	40,2	3,3
Preadipose length	50,2	52,5	51,2	54,5	5	53,1	1,3
Distance between snout tip and adipose-fin base end	85,8	90,6	89,8	91,2	5	90,4	0,5
Adipose-fin depth	2,6	4,6	4,6	6,0	5	5,3	0,6
Caudal-peduncle length posterior to adipose-fin	8,8	9,2	9,1	9,5	5	9,3	0,1
Caudal-peduncle depth at adipose-fin terminus	6,0	8,6	7,9	8,8	5	8,5	0,4
Snout-anus distance	-	49,9	49,9	54,8	5	51,9	1,8
Snout-urogenital papilla distance	-	52,6	52,6	56,6	5	54,3	1,6
Anus-urogenital papilla distance	-	2,3	2,3	3,5	5	2,9	0,4
Dorsal lobe of caudal fin length	-	-	18,0	23,1	3	20,1	2,7
Ventral lobe of caudal fin length	-	-	18,5	23,8	3	21,9	2,9
Head depth	43,1	50,9	48,1	50,9	5	49,6	1,2
Head width	53,3	57,3	52,2	62,5	5	57,5	4,4
Eye diameter (left)	23,8	24,7	21,6	25,4	5	23,1	1,8
Fleshy interorbital	23,3	29,5	21,1	29,5	5	24,3	3,3
Bony interorbital	18,3	21,1	18,3	29,8	5	21,7	4,7

Mouth gape	26,6	26,0	26,0	36,1	5	30,1	4,3
Snout length (left)	34,8	35,3	34,5	36,7	5	35,5	0,9
Distance between snout tip and posterior nare (left side)	17,7	22,3	17,5	22,3	5	19,1	1,9
Anterior internarial width	12,8	14,8	12,7	14,8	5	13,6	0,8
Posterior internarial width	11,4	16,5	12,8	16,5	5	13,8	1,5
Intranarial length (left side)	15,0	16,5	13,3	17,1	5	15,2	1,6

Table 14 (cont): Morphometric data of *Pimelodella cristata* and its junior-synonyms, *P. cristata*, *P. breviceps*, *P. dorseyi*, *P. hartwelli*, *P. ophthalmica*, *P. parnahybae*, *P. steindachneri*, *P. wessellii*, *P. witmeri*, based on type and comparative materials, discriminated by original species name.

	<i>P. steindachneri</i>						<i>P.</i>	<i>P. witmeri</i>					
	Lectotyp e	Min.	Max.	n	x	S D	<i>wessellii</i>	Holotyp e	Min.	Max.	n	x	S D
Total length (mm)	185,8	100,7	204,4	9,0	146,0		193,8	0,0	113,0	155,8	2,0	134,4	
Standard length (mm)	150,4	86,2	165,4	9,0	119,2		157,9	137,5	93,2	137,5	3,0	121,0	
Body depth (dorsal)	17,7	13,7	21,8	9	18,3	2,3	17,4	19,7	15,6	19,7	3	18,0	2,1
Body width (dorsal)	11,0	9,2	15,1	9	12,2	1,9	13,2	15,2	12,9	15,2	3	14,3	1,2
Cleithral width	16,8	15,5	19,3	9	17,2	1,4	15,7	17,3	16,5	17,3	3	17,0	0,4
Head length	26,5	26,5	32,8	9	29,6	2,5	28,6	29,6	29,6	30,0	3	29,8	0,2
Maxillary-barbel length (left side)	94,3	75,6	97,6	9	86,9	8,2	75,9	71,7	71,7	87,8	3	80,2	8,0
Outer mental-barbel length (left side)	32,9	24,5	38,4	9	33,2	5,0	30,1	20,9	20,9	25,5	3	23,7	2,4
Inner mental-barbel length (left side)	16,9	14,4	22,4	9	18,9	3,1	17,1	13,5	11,8	13,5	3	12,6	0,9
Predorsal length	29,8	29,8	35,4	9	32,7	2,3	31,7	32,2	32,2	32,9	3	32,5	0,4
Distance between snout and terminus of dorsal-fin base	44,6	44,4	49,0	9	46,5	2,1	46,0	46,6	46,6	48,4	3	47,3	1,0
Distance between snout tip and dorsal-fin distal end	61,3	54,9	61,3	9	59,2	1,5	58,0	54,8	54,8	57,5	3	56,2	1,3
Dorsal fin to adipose fin	2,8	1,8	9,7	9	4,5	3,2	5,8	5,7	4,2	6,1	3	5,3	1,0
Dorsal-fin base	16,1	13,2	20,2	9	15,2	2,3	15,6	16,0	15,5	16,0	3	15,7	0,2
Length of first dorsal-fin ray (unbranched)	26,9	20,0	27,4	6	24,3	3,0	22,8	-	-	-	0	-	-
Length of rigid part of first dorsal-fin ray	22,2	16,0	22,2	9	19,8	1,7	18,3	-	-	-	0	-	-
Length of second dorsal-fin ray (first branched)	27,1	21,2	27,1	9	23,7	2,1	23,3	20,9	20,0	20,9	3	20,5	0,5
Length of third dorsal-fin ray (second branched)	25,8	18,5	25,8	9	22,1	2,6	22,4	21,9	20,0	21,9	3	20,8	1,0
Prepectoral length	21,1	20,1	26,6	9	22,9	2,7	20,9	20,9	20,9	21,8	3	21,4	0,4
Distance between snout and terminus of pectoral-fin base	23,7	22,5	29,9	9	25,7	2,8	24,6	24,5	24,5	24,8	3	24,7	0,1
Distance between snout tip and pectoral-fin distal end	38,5	36,2	48,9	9	41,8	4,3	40,9	36,5	36,5	40,2	3	38,5	1,8

Length of first left pectoral-fin ray (unbranched)	20,7	19,1	23,0	5	20,7	1,7	19,4	-	-	-	0	-	-
Length of rigid part of first left pectoral-fin ray	18,4	15,7	21,8	9	18,9	2,2	18,1	-	-	-	0	-	-
Length of second left pectoral-fin ray (first branched)	18,4	15,3	20,9	9	18,4	1,7	17,3	17,2	17,2	18,6	2	17,9	1,0
Length of third left pectoral-fin ray (second branched)	17,0	14,3	18,6	9	16,8	1,3	15,0	-	15,6	16,5	2	16,1	0,7
Prepelvic length	43,6	41,4	49,4	9	44,6	2,8	44,5	45,6	44,6	46,7	3	45,7	1,1
Distance between snout and terminus of pelvic-fin base	45,7	44,6	51,6	9	47,6	2,7	45,9	48,7	47,7	48,7	3	48,3	0,5
Distance between snout tip and pelvic-fin distal end	60,5	57,2	66,6	9	61,5	3,1	60,1	62,3	59,9	62,3	3	60,9	1,2
Distance between pelvic fins	5,2	4,0	5,8	9	4,9	0,5	5,6	6,5	5,0	6,5	3	6,0	0,9
Length of first left pelvic-fin ray (unbranched)	15,2	12,7	15,7	9	14,1	1,1	12,7	13,0	11,9	13,0	3	12,6	0,6
Length of second left pelvic-fin ray (first branched)	16,4	12,7	17,1	9	15,3	1,5	13,7	14,5	13,7	14,5	3	14,0	0,4
Length of third left pelvic-fin ray (second branched)	16,9	13,4	16,9	9	15,2	1,2	13,9	15,0	14,0	15,0	3	14,6	0,5
Anal-fin base	15,3	12,5	15,5	9	13,8	1,2	13,6	13,0	13,0	13,3	3	13,2	0,2
Preanal length	61,1	61,1	66,1	9	64,3	1,9	66,0	67,2	65,3	67,2	3	66,6	1,1
Distance between snout tip and terminus of anal-fin base	75,5	74,1	78,6	9	76,4	1,4	78,4	78,0	77,0	79,8	3	78,3	1,5
Distance between snout tip and anal-fin distal end	83,7	77,3	86,4	9	83,7	2,8	87,0	85,6	85,6	88,6	3	86,7	1,7
Adipose-fin length	44,0	38,4	44,4	9	41,7	1,8	41,4	39,1	39,1	42,5	3	40,9	1,7
Preadipose length	46,9	45,3	55,6	9	49,7	3,1	48,7	50,6	50,4	52,6	3	51,2	1,2
Distance between snout tip and adipose-fin base end	90,0	87,2	92,2	9	89,7	1,5	90,0	87,5	87,5	90,8	3	89,1	1,7
Adipose-fin depth	5,5	4,2	6,3	9	5,3	0,7	4,1	6,1	4,7	6,5	3	5,7	0,9
Caudal-peduncle length posterior to adipose-fin	9,2	8,2	11,0	9	9,2	0,9	9,9	10,4	9,2	10,4	3	9,6	0,7
Caudal-peduncle depth at adipose-fin terminus	8,8	7,9	9,2	9	8,5	0,4	7,7	9,1	8,8	9,1	3	8,9	0,2
Snout-anus distance	48,6	48,6	54,9	9	51,0	2,1	51,3	52,7	51,4	52,7	3	52,2	0,7
Snout-urogenital papilla distance	53,6	51,0	58,3	9	55,4	2,0	54,0	55,2	55,2	56,1	3	55,6	0,4
Anus-urogenital papilla distance	5,2	2,6	5,2	9	4,1	0,8	3,2	3,3	2,6	3,3	3	2,9	0,4
Dorsal lobe of caudal fin length	20,0	16,6	30,2	8	22,6	4,6	23,5	-	18,2	-	1	18,2	-
Ventral lobe of caudal fin length	23,6	20,9	26,5	9	23,8	2,0	24,2	-	21,8	-	1	21,8	-
Head depth	53,7	41,1	55,7	9	50,2	4,5	48,2	48,5	2,6	48,5	3	45,7	2,4
Head width	62,0	47,9	62,0	9	56,1	4,8	57,3	60,3	2,6	60,3	3	56,0	4,1
Eye diameter (left)	22,7	17,6	24,4	9	20,5	2,1	22,0	18,0	2,6	21,8	3	19,7	1,9
Fleshy interorbital	29,0	20,9	29,2	9	26,2	2,5	25,5	22,9	2,6	25,8	3	23,8	1,8

Bony interorbital	24,2	17,2	24,2	9	21,0	2,4	18,9	18,4	2,6	20,1	3	18,6	1,4
Mouth gape	34,0	25,6	34,0	9	30,7	2,6	25,6	32,1	2,6	32,1	3	30,6	2,0
Snout length (left)	36,2	32,6	37,1	9	34,7	1,5	36,2	33,9	2,6	35,6	3	34,5	0,9
Distance between snout tip and posterior nare (left side)	16,9	16,9	21,6	9	18,5	1,7	19,2	19,1	2,6	19,8	3	19,0	0,9
Anterior internarial width	15,1	12,7	16,4	9	14,4	1,2	13,5	16,2	2,6	16,2	3	15,4	1,1
Posterior internarial width	13,9	13,9	15,0	9	14,6	0,4	11,7	13,8	2,6	14,5	3	13,9	0,6
Intranarial length (left side)	14,6	13,3	15,6	9	14,2	0,8	14,8	13,6	2,6	17,3	3	14,7	2,3

Table 15: Meristic data of *P. cristata* and its junior-synonyms, *P. cristata*, *P. breviceps*, *P. cyanostygma*, *P. dorseyi*, *P. hartwelli*, *P. ophthalmica*, *P. parnahybae*, *P. steindachneri*, *P. wessellii*, *P. witmeri*, discriminated by the original species name and region.

MERISTICS	GUIANA SHIELD																
	<i>P. CRISTATA</i> - GUIANA SHIELD																
	ZMB	ZMB	ZSM	FMNH	MZUS	MZUS	ANSP	ANSP	ANSP	ANSP	ANSP	ANSP	ANSP	ANSP	ANSP	ANSP	
	3052	3053	6070	105281	P	P	177229	198174	17579	16790	17578	ANSP 175790					
	paral	lecto					1	2	1	2	3	1	1	1	1	2	3
	ect.	type	1	1	1	1	1	2	1	2	3	1	1	1	1	2	3
Total Vertebrae	51	50	51				46		49	52	49	49	50	51	51	50	
Branchiostegal rays	6	6	7				6										
Ribs	10	9					10		9	9	10	10	10	10	9	10	
Branched dorsal-fin rays	6	6		6	6	6	6	6	6	6	6	6	6	6	6	6	
Branched pectoral-fin rays	9	9	9	9	8	8	9	9		10							
Branched pelvic-fin rays	5	5	5	5	5	5	5	5	5	5		5	5	5			
	ii-II-	ii-II-	iii-III-			ii-III-	ii-II-	ii-II-	ii-II-	ii-IV-	iii-III-		iii-II-	iii-III-	iii-III-	iii-III-	
Anal-fin rays	11	10	11	ii-II-11	ii-II-8	11	9	8	10	10	10	ii-III-8	11	11	10	10	
Procurrent rays on dorsal lobe of caudal fin	13	14					15										
Branched rays on dorsal lobe of caudal fin	7	7		7	7	7	7	7	7	7	7	7	7	7			
Branched rays on ventral lobe of caudal fin	8	8		8	8	8	8	8	8	8	9	8	8				
Procurrent rays on ventral lobe of caudal fin	17	20					16										
Rays directly associated to dorsal hypural plate	7	7					7		7	7	7	7	8				
Rays directly associated to ventral hypural plate	7	7					8		7	8	7	8	9				
1st pterigiophore of dorsal-fin inserted posterior to neural spine of vertebrae	4	4	4				4		4	4	4	4	4	4	4	4	4

Last pterigiophore of dorsal-fin inserted anterior to neural spine of vertebrae	11	11	11	11	11	11	11	11	11	11	11	11
1st pterigiophore of anal-fin inserted posterior to haemal spine of vertebrae	24	25	24	24	24	26	25	24	24	25	24	25
Last pterigiophore of anal-fin inserted posterior to haemal spine of vertebrae	35	35	34	30	33	35	34	33	35	36	34	35
Adipose-fin origin (vertical of vertebral centrum)	18	16		16		17	18	18	18	19	18	
Adipose-fin terminus (vertical of vertebral centrum)	45	43		43		46	44	44	43	45	45	
First caudal vertebrae	20	19	20				18	18	18	18	17	18

Table 15 (cont.): Meristic data of *P. cristata* and its junior-synonyms, *P. cristata*, *P. breviceps*, *P. cyanostygma*, *P. dorseyi*, *P. hartwelli*, *P. ophthalmica*, *P. parnahybae*, *P. steindachneri*, *P. wesselii*, *P. witmeri*, discriminated by the original species name and region.

MERISTICS	GUIANA SHIELD				
	<i>P. CRISTATA</i> - GUIANA SHIELD				<i>P. WESSELII</i>
	INPA 11149				NMW 79188
	1	2	3	4	holotype
Total Vertebrae	50	50	50	50	50
Branchiostegal rays					6
Ribs	10	9	10	10	10
Branched dorsal-fin rays	6	6	6	6	
Branched pectoral-fin rays					8
Branched pelvic-fin rays					5
Anal-fin rays	iii-II-10				iii-III-9
Procurrent rays on dorsal lobe of caudal fin					20
Branched rays on dorsal lobe of caudal fin	7		7	7	7
Branched rays on ventral lobe of caudal fin	8		8	8	8
Procurrent rays on ventral lobe of caudal fin					24
Rays directly associated to dorsal hypural plate	7		7	7	7
Rays directly associated to ventral hypural plate	9		10	9	9
1st pterigiophore of dorsal-fin inserted posterior to neural spine of vertebrae	4	4	4	4	4
Last pterigiophore of dorsal-fin inserted anterior to neural spine of vertebrae	11	11	11	11	12
1st pterigiophore of anal-fin inserted posterior to haemal spine of vertebrae	24	25	25	25	24
Last pterigiophore of anal-fin inserted posterior to haemal spine of vertebrae	35	36	36		33
Adipose-fin origin (vertical of vertebral centrum)	19	17	17	18	19
Adipose-fin terminus (vertical of vertebral centrum)	44	47	44	44	45
First caudal vertebrae	19	18	17	17	18

Table 15 (cont.): Meristic data of *P. cristata* and its junior-synonyms, *P. cristata*, *P. breviceps*, *P. cyanostygma*, *P. dorseyi*, *P. hartwelli*, *P. ophthalmica*, *P. parnahybae*, *P. steindachneri*, *P. wessellii*, *P. witmeri*, discriminated by the original species name and region.

MERISTICS	AMAZON				<i>P. BREVICEPS</i>
	<i>P. CRISTATA- AMAZONAS</i>				
	INPA 12522	INPA 14952	INPA 14955	INPA 14955	NMW 45615
	1	1	1	2	holotype
Total Vertebrae	50	50	50	50	51
Branchiostegal rays					
Ribs	10	10	10	10	8
Branched dorsal-fin rays	6	6	6	6	6
Branched pectoral-fin rays					8
Branched pelvic-fin rays					5
Anal-fin rays	ii-II-10	iii-III-10	iii-II-10		iv-II-10
Procurrent rays on dorsal lobe of caudal fin					20
Branched rays on dorsal lobe of caudal fin	7	7	7		7
Branched rays on ventral lobe of caudal fin	8	8	8		8
Procurrent rays on ventral lobe of caudal fin					24
Rays directly associated to dorsal hypural plate	7	7	7		7
Rays directly associated to ventral hypural plate	8	8	8		8
1st pterigiophore of dorsal-fin inserted posterior to neural spine of vertebrae	4	4	4	4	4
Last pterigiophore of dorsal-fin inserted anterior to neural spine of vertebrae	11	11	11	11	11
1st pterigiophore of anal-fin inserted posterior to haemal spine of vertebrae	25	24	25	25	25
Last pterigiophore of anal-fin inserted posterior to haemal spine of vertebrae	35	35	34	35	34
Adipose-fin origin (vertical of vertebral centrum)	21	18	19	19	19
Adipose-fin terminus (vertical of vertebral centrum)	45	44	44	45	45
First caudal vertebrae	18	17	17		

Table 15 (cont.): Meristic data of *P. cristata* and its junior-synonyms, *P. cristata*, *P. breviceps*, *P. cyanostygma*, *P. dorseyi*, *P. hartwelli*, *P. ophthalmica*, *P. parnahybae*, *P. steindachneri*, *P. wessellii*, *P. witmeri*, discriminated by the original species name and region.

MERISTICS	AMAZON			
	<i>P. CYANOSTIGMA</i>		<i>P. HARTWELLI</i>	<i>P. OPHTHALMICA</i>
	ANSP 8283	ANSP 8284	ANSP 68644	ANSP 21102
	lectotype	paralect.	holotype	holotype
Total Vertebrae	49	48	49	49
Branchiostegal rays			6	6
Ribs			9	9
Branched dorsal-fin rays			6	6
Branched pectoral-fin rays			8	8
Branched pelvic-fin rays			5	5
Anal-fin rays			ii-III-10	ii-III-8
Procurrent rays on dorsal lobe of caudal fin			16	9
Branched rays on dorsal lobe of caudal fin			7	7
Branched rays on ventral lobe of caudal fin			8	8
Procurrent rays on ventral lobe of caudal fin			20	17
Rays directly associated to dorsal hypural plate			7	7
Rays directly associated to ventral hypural plate			8	8
1st pterigiophore of dorsal-fin inserted posterior to neural spine of vertebrae	4	4	4	4
Last pterigiophore of dorsal-fin inserted anterior to neural spine of vertebrae			11	11
1st pterigiophore of anal-fin inserted posterior to haemal spine of vertebrae			23	25
Last pterigiophore of anal-fin inserted posterior to haemal spine of vertebrae			33	34
Adipose-fin origin (vertical of vertebral centrum)			18	21
Adipose-fin terminus (vertical of vertebral centrum)			44	44
First caudal vertebrae				

Table 15 (cont.): Meristic data of *P. cristata* and its junior-synonyms, *P. cristata*, *P. breviceps*, *P. cyanostygma*, *P. dorseyi*, *P. hartwelli*, *P. ophthalmica*, *P. parnahybae*, *P. steindachneri*, *P. wessellii*, *P. witmeri*, discriminated by the original species name and region.

MERISTICS	AMAZON							
	<i>P. STEINDACHNERI</i>							
	MCZ 7566	MCZ 7487	MCZ 7472	MCZ 7567	MCZ 7542	UFRO 9746	UFRO 9753	
	paralect.	paralect.	lectotype	paralect.	paralect.	paralect.	1	1
Total Vertebrae	49	50	47	49	48	48	47	47
Branchiostegal rays		6		6	6	6	6	6
Ribs	10	10	8	10	8	9	9	8
Branched dorsal-fin rays	6	6	6	6	6	6	6	6
Branched pectoral-fin rays	9		9	9	9	9	7	8
Branched pelvic-fin rays	5	5	5	5	5	5	5	5
Anal-fin rays	ii-III-11	ii-III-9	ii-III-8	ii-III-10	ii-III-10	ii-III-10	ii-III-9	iii-III-8
Procurrent rays on dorsal lobe of caudal fin			14	12		12	17	16
Branched rays on dorsal lobe of caudal fin	7	7	7	7	7	7	7	7
Branched rays on ventral lobe of caudal fin	8		8	8		8	8	9
Procurrent rays on ventral lobe of caudal fin			13	16		18	20	20
Rays directly associated to dorsal hypural plate	7	7	7	7	7	7	8	8
Rays directly associated to ventral hypural plate	7	8	8	8		8	10	10
1st pterigiophore of dorsal-fin inserted posterior to neural spine of vertebrae	4	4	4	4	4	4	4	4
Last pterigiophore of dorsal-fin inserted anterior to neural spine of vertebrae	11	11	12	12	11	12	11	11
1st pterigiophore of anal-fin inserted posterior to haemal spine of vertebrae	23	24	21	23	21	23	21	21
Last pterigiophore of anal-fin inserted posterior to haemal spine of vertebrae	34	34	31	32	31	33	29	28
Adipose-fin origin (vertical of vertebral centrum)	17	18	17	16	16	20	15	15

Adipose-fin terminus (vertical of vertebral centrum)	44	43	43	43	44	43	41	41
First caudal vertebrae	17	17						

Table 15 (cont.): Meristic data of *P. cristata* and its junior-synonyms, *P. cristata*, *P. breviceps*, *P. cyanostygma*, *P. dorseyi*, *P. hartwelli*, *P. ophthalmica*, *P. parnahybae*, *P. steindachneri*, *P. wessellii*, *P. witmeri*, discriminated by the original species name and region.

MERISTICS	NORTHEAST							
	<i>P. DORSEYI</i>		<i>P. PARNAHYBAE</i>					
	ANSP	ANSP	ANSP	MZUSP 104556			MZUSP	
	68375	69376	69337	1	2	3	43592	
	holotype	paratype	holotype					
Total Vertebrae	48	48	47					
Branchiostegal rays	6		6					
Ribs	9	10	9					
Branched dorsal-fin rays	6	6	6	6	6	6	6	
Branched pectoral-fin rays	8	8	9	8	8	9	9	
Branched pelvic-fin rays	5	5	5	5	5	5	5	
				ii-II-	ii-II-	ii-II-		
Anal-fin rays	ii-III-9	ii-III-10	ii-III-9	7	9	9	ii-II-9	
Procurrent rays on dorsal lobe of caudal fin	15		18					
Branched rays on dorsal lobe of caudal fin	7	7	7	7	7	7	7	
Branched rays on ventral lobe of caudal fin	8	8	8	8	8	8	8	
Procurrent rays on ventral lobe of caudal fin	19	18	19					
Rays directly associated to dorsal hypural plate	7	7	7					
Rays directly associated to ventral hypural plate	7	8	8					
1st pterigiophore of dorsal-fin inserted posterior to neural spine of vertebrae	4	4	4					
Last pterigiophore of dorsal-fin inserted anterior to neural spine of vertebrae	11	11	11					
1st pterigiophore of anal-fin inserted posterior to haemal spine of vertebrae	23	23	24					
Last pterigiophore of anal-fin inserted posterior to haemal spine of vertebrae	33	32	33					
Adipose-fin origin (vertical of vertebral centrum)	16	17	18					

Adipose-fin terminus (vertical of vertebral centrum)	42	42	43
First caudal vertebrae	16	17	

Table 15 (cont.): Meristic data of *P. cristata* and its junior-synonyms, *P. cristata*, *P. breviceps*, *P. cyanostygma*, *P. dorseyi*, *P. hartwelli*, *P. ophthalmica*, *P. parnahybae*, *P. steindachneri*, *P. wessellii*, *P. witmeri*, discriminated by the original species name and region.

MERISTICS	NORTHEAST			
	<i>P. STEINDACHNERI</i>	<i>P. WITMERI</i>		
	MCZ 7588	ANSP 69383	ANSP 69384	
	paralectotype	holotype	paratype	paratype
Total Vertebrae	46		1	3
Branchiostegal rays	6		46	
Ribs	9		6	
Branched dorsal-fin rays	6	6	9	
Branched pectoral-fin rays	8	6	6	6
Branched pelvic-fin rays	5	8	8	9
Anal-fin rays	ii-III-10	5	5	5
Procurrent rays on dorsal lobe of caudal fin		ii-II-9	iii-II-9	ii-II-9
Branched rays on dorsal lobe of caudal fin			15	
Branched rays on ventral lobe of caudal fin	8	7	7	7
Procurrent rays on ventral lobe of caudal fin		9	8	8
Rays directly associated to dorsal hypural plate			17	
Rays directly associated to ventral hypural plate	9		9	
1st pterigiophore of dorsal-fin inserted posterior to neural spine of vertebrae	4		8	
Last pterigiophore of dorsal-fin inserted anterior to neural spine of vertebrae	11		7	
1st pterigiophore of anal-fin inserted posterior to haemal spine of vertebrae	21		9	
Last pterigiophore of anal-fin inserted posterior to haemal spine of vertebrae	30		17	
Adipose-fin origin (vertical of vertebral centrum)	16		9	
Adipose-fin terminus (vertical of vertebral centrum)	41		8	
First caudal vertebrae	15		8	

Table 15 (cont.): Meristic data of *P. cristata* and its junior-synonyms, *P. cristata*, *P. breviceps*, *P. cyanostygma*, *P. dorseyi*, *P. hartwelli*, *P. ophthalmica*, *P. parnahybae*, *P. steindachneri*, *P. wessellii*, *P. witmeri*, discriminated by the original species name and region.

MERISTICS	MIN	COUNT	MIN	MAX	COUNT	MAX	MODE	COUNT	MODE
Total Vertebrae	46	3		52	1		50	13	
Branchiostegal rays	6	16		7	1		6	16	
Ribs	8	4		10	19		10	19	
Branched dorsal-fin rays	6	45		6	45		6	45	
Branched pectoral-fin rays	7	1		10	1		9	15	
Branched pelvic-fin rays	5	36		5	36		5	36	
Anal-fin rays									
Procurrent rays on dorsal lobe of caudal fin	9	1		20	2		15	3	
Branched rays on dorsal lobe of caudal fin	7	40		7	40		7	40	
Branched rays on ventral lobe of caudal fin	8	36		9	3		8	36	
Procurrent rays on ventral lobe of caudal fin	13	1		24	2		20	4	
Rays directly associated to dorsal hypural plate	7	26		9	1		7	26	
Rays directly associated to ventral hypural plate	7	6		10	3		8	16	
1st pterigiophore of dorsal-fin inserted posterior to neural spine of vertebrae	4	39		4	39		4	39	
Last pterigiophore of dorsal-fin inserted anterior to neural spine of vertebrae	11	33		12	4		11	33	
1st pterigiophore of anal-fin inserted posterior to haemal spine of vertebrae	21	5		26	1		24	12	
Last pterigiophore of anal-fin inserted posterior to haemal spine of vertebrae	28	1		36	3		35	9	
Adipose-fin origin (vertical of vertebral centrum)	15	2		21	2		18	11	
Adipose-fin terminus (vertical of vertebral centrum)	37	1		47	1		44	11	
First caudal vertebrae	15	1		20	2		18	8	

Table 16: Morphometric data of *Pimelodella cruxenti* based on type (as presented in original description) and comparative materials.

	Holotype	Min.	Max.	n	x	SD
Total length (mm)	-	163,2	163,2	1	163,2	
Standard length (mm)	110,6	85,8	127,7	6	102,0	
	Percentages of SL					
Body depth (dorsal)	21,0	17,6	21,0	5	19,5	1,6
Body width (dorsal)	-	13,4	13,4	1	13,4	-
Cleithral width	-	18,2	18,2	1	18,2	-
Head length	24,9	21,5	24,9	5	23,7	1,4
Maxillary-barbel length (left side)	113,2	86,4	113,2	5	103,8	10,6
Outer mental-barbel length (left side)	49,6	40,4	49,6	5	45,0	4,0
Inner mental-barbel length (left side)	33,4	27,2	33,4	5	30,0	2,7
Predorsal length	34,1	27,8	34,1	5	30,9	2,4
Distance between snout tip and terminus of dorsal-fin base	-	46,7	46,7	1	46,7	-
Distance between snout tip and dorsal-fin distal end	-	58,4	58,4	1	58,4	-
Dorsal fin to adipose fin	-	1,0	1,0	1	1,0	-
Dorsal-fin base	16,2	14,5	16,2	5	15,6	0,7
Length of first dorsal-fin ray (unbranched)	-	19,4	19,4	1	19,4	-
Length of rigid part of first dorsal-fin ray	13,0	11,2	13,3	5	12,3	1,0
Length of second dorsal-fin ray (first branched)	-	22,3	22,3	1	22,3	-
Length of third dorsal-fin ray (second branched)	-	24,0	24,0	1	24,0	-
Prepectoral length	-	20,7	20,7	1	20,7	-
Distance between snout tip and terminus of pectoral-fin base	-	23,4	23,4	1	23,4	-
Distance between snout tip and pectoral-fin distal end	-	34,0	34,0	1	34,0	-
Length of first left pectoral-fin ray (unbranched)	-	18,0	18,0	1	18,0	-
Length of rigid part of first left pectoral-fin ray	12,9	11,4	14,9	5	12,9	1,3
Length of second left pectoral-fin ray (first branched)	-	16,1	16,1	1	16,1	-
Length of third left pectoral-fin ray (second branched)	-	15,4	15,4	1	15,4	-
Prepelvic length	-	44,5	44,5	1	44,5	-
Distance between snout tip and terminus of pelvic-fin base	-	47,1	47,1	1	47,1	-
Distance between snout tip and pelvic-fin distal end	-	61,9	61,9	1	61,9	-
Distance between pelvic fins	-	5,3	5,3	1	5,3	-
Length of first left pelvic-fin ray (unbranched)	-	15,4	15,4	1	15,4	-
Length of second left pelvic-fin ray (first branched)	-	18,0	18,0	1	18,0	-
Length of third left pelvic-fin ray (second branched)	-	17,1	17,1	1	17,1	-
Anal-fin base	12,7	10,6	12,7	5	11,8	0,8
Preanal length	72,2	57,7	72,2	5	66,1	5,4
Distance between snout tip and terminus of anal-fin base	-	76,7	76,7	1	76,7	-
Distance between snout tip and anal-fin distal end	-	88,4	88,4	1	88,4	-
Adipose-fin length	56,5	47,1	56,5	5	51,6	3,7
Preadipose length	-	47,1	47,1	1	47,1	-
Distance between snout tip and adipose-fin base end	-	94,0	94,0	1	94,0	-
Adipose-fin depth	-	6,7	6,7	1	6,7	-

Caudal-peduncle length posterior to adipose-fin	24,7	18,9	24,7	5	23,2	2,4
Caudal-peduncle depth at adipose-fin terminus	10,9	9,0	10,9	5	9,8	0,8
Snout-anus distance	-	49,6	49,6	1	49,6	-
Snout-urogenital papilla distance	-	52,0	52,0	1	52,0	-
Anus-urogenital papilla distance	-	2,8	2,8	1	2,8	-
Dorsal lobe of caudal fin length	-	24,2	24,2	1	24,2	-
Ventral lobe of caudal fin length	-	29,0	29,0	1	29,0	-

Percentages of HL

Head depth	-	59,3	59,3	1	59,3	-
Head width	53,3	43,6	56,2	5	52,3	4,9
Eye diameter (left)	19,4	18,9	26,0	5	21,1	2,9
Fleshy interorbital	22,2	22,2	31,5	5	24,9	3,7
Bony interorbital	14,5	13,4	21,2	5	16,3	3,1
Mouth gape	-	49,5	49,5	1	49,5	-
Snout length (left)	-	36,7	36,7	1	36,7	-
Distance between snout tip and posterior nare (left side)	-	23,5	23,5	1	23,5	-
Anterior internarial width	-	20,1	20,1	1	20,1	-
Posterior internarial width	-	18,0	18,0	1	18,0	-
Intranarial length (left side)	-	19,4	19,4	1	19,4	-

Table 17: Morphometric data of *Pimelodella elongata* based on type and comparative material.

	Lectotype	Min.	Max.	n	x	SD
Total length (mm)	165,7	67,1	165,7	7	107,3	
Standard length (mm)	136,8	54,6	136,8	10	86,0	
Percentages of SL						
Body depth (dorsal)	14,6	13,3	16,6	9	15,5	1,2
Body width (dorsal)	11,2	11,1	13,5	9	11,9	0,9
Cleithral width	15,3	15,2	18,7	9	16,6	1,1
Head length	28,1	28,1	33,0	9	30,2	1,6
Maxillary-barbel length (left side)	32,2	28,9	80,7	9	41,8	16,4
Outer mental-barbel length (left side)	17,0	15,5	26,4	9	19,0	3,4
Inner mental-barbel length (left side)	11,0	9,7	15,9	9	12,1	2,0
Predorsal length	34,2	29,2	41,0	9	34,6	3,2
Distance between snout tip and terminus of dorsal-fin base	45,6	45,6	50,5	9	47,6	1,6
Distance between snout tip and dorsal-fin distal end	54,6	54,6	62,5	9	58,2	2,8
Dorsal fin to adipose fin	14,1	6,3	14,1	9	11,8	2,5
Dorsal-fin base	12,9	12,5	15,5	9	14,1	1,0
Length of first dorsal-fin ray (unbranched)	21,4	17,2	22,8	9	20,5	1,7
Length of rigid part of first dorsal-fin ray	13,2	12,2	16,4	9	14,1	1,4
Length of second dorsal-fin ray (first branched)	19,6	17,8	22,1	9	19,8	1,2
Length of third dorsal-fin ray (second branched)	18,3	17,7	21,2	9	19,3	1,3
Prepectoral length	20,2	13,5	23,0	9	20,1	2,7
Distance between snout tip and terminus of pectoral-fin base	23,6	22,7	25,5	9	24,0	1,0
Distance between snout tip and pectoral-fin distal end	37,6	36,5	42,0	9	39,0	1,9
Length of first left pectoral-fin ray (unbranched)	18,2	15,8	20,0	9	17,8	1,2
Length of rigid part of first left pectoral-fin ray	13,7	12,6	17,7	9	14,3	1,4
Length of second left pectoral-fin ray (first branched)	16,1	15,8	18,2	9	17,1	0,9
Length of third left pectoral-fin ray (second branched)	15,2	15,2	16,9	8	15,9	0,6
Prepelvic length	44,6	44,2	51,1	9	46,6	2,3
Distance between snout tip and terminus of pelvic-fin base	46,9	46,9	53,4	9	49,0	2,1
Distance between snout tip and pelvic-fin distal end	58,7	58,7	66,0	9	61,8	2,2
Distance between pelvic fins	5,0	3,0	5,1	9	4,3	0,7
Length of first left pelvic-fin ray (unbranched)	11,9	10,5	14,0	9	12,4	1,1
Length of second left pelvic-fin ray (first branched)	13,6	12,6	15,3	9	14,1	1,0
Length of third left pelvic-fin ray (second branched)	15,1	13,4	15,7	9	14,3	0,8
Anal-fin base	11,9	11,2	13,6	9	12,4	0,8
Preanal length	66,6	63,7	71,1	9	67,0	2,1
Distance between snout tip and terminus of anal-fin base	77,6	75,8	80,1	9	78,7	1,4
Distance between snout tip and anal-fin distal end	84,9	82,9	88,5	9	85,9	1,6
Adipose-fin length	29,8	27,3	36,5	9	31,8	2,7
Preadipose length	57,7	52,3	62,6	9	58,6	3,0
Distance between snout tip and adipose-fin base end	86,8	86,0	93,0	9	88,6	2,2
Adipose-fin depth	4,8	3,3	5,2	9	4,5	0,7
Caudal-peduncle length posterior to adipose-fin	12,0	5,3	13,9	9	10,4	2,5
Caudal-peduncle depth at adipose-fin terminus	7,6	6,4	9,1	9	8,1	0,9
Snout-anus distance	49,6	49,6	54,3	9	52,1	1,5

Snout-urogenital papilla distance	52,8	52,8	60,0	9	55,5	2,1
Anus-urogenital papilla distance	2,9	2,2	8,7	9	3,5	2,0
Dorsal lobe of caudal fin length	21,8	19,4	28,1	7	23,2	3,1
Ventral lobe of caudal fin length	20,6	19,3	22,9	7	20,9	1,3

Percentages of HL

Head depth	41,0	38,6	46,7	9	42,0	2,6
Head width	51,9	46,1	53,7	9	50,8	2,2
Eye diameter (left)	20,6	19,2	23,1	9	21,7	1,3
Fleshy interorbital	22,6	18,8	25,0	9	22,7	2,2
Bony interorbital	17,0	13,8	17,6	9	16,1	1,3
Mouth gape	28,9	26,7	30,4	9	28,8	1,5
Snout length (left)	32,5	30,4	33,2	9	32,0	1,0
Distance between snout tip and posterior nare (left side)	20,2	17,3	22,6	9	20,4	1,6
Anterior internarial width	13,7	11,0	14,9	9	12,7	1,3
Posterior internarial width	15,1	12,5	16,1	9	14,2	1,2
Intranarial length (left side)	12,1	11,5	16,1	9	13,6	1,6

Table 18: Morphometric data of *Pimelodella enochi* and *P. papariae*, its junior-synonym, based on type material and discriminated by original species name.

	<i>P. enochi</i>		<i>P. papariae</i>
	Holotype	Paratype	Holotype
Total length (mm)	53,6	54,0	130,6
Standard length (mm)	44,9	45,3	107,6
	Percentages of SL		
Body depth (dorsal)	15,2	16,1	13,7
Body width (dorsal)	13,6	14,0	16,2
Cleithral width	18,1	17,6	17,6
Head length	32,1	32,8	29,3
Maxillary-barbel length (left side)	79,4	80,9	75,7
Outer mental-barbel length (left side)	25,5	22,8	22,5
Inner mental-barbel length (left side)	14,8	11,9	11,2
Predorsal length	36,8	36,4	32,7
Distance between snout tip and terminus of dorsal-fin base	51,1	50,6	47,8
Distance between snout tip and dorsal-fin distal end	62,3	62,1	58,2
Dorsal fin to adipose fin	8,7	9,6	11,8
Dorsal-fin base	13,5	15,0	14,7
Length of first dorsal-fin ray (unbranched)	-	-	14,2
Length of rigid part of first dorsal-fin ray	15,0	13,1	11,4
Length of second dorsal-fin ray (first branched)	21,8	21,3	18,8
Length of third dorsal-fin ray (second branched)	18,8	21,8	16,6
Prepectoral length	22,9	23,3	20,9
Distance between snout tip and terminus of pectoral-fin base	26,2	25,2	22,3
Distance between snout tip and pectoral-fin distal end	44,6	44,1	36,5
Length of first left pectoral-fin ray (unbranched)	21,4	22,6	17,9
Length of rigid part of first left pectoral-fin ray	17,9	17,3	-
Length of second left pectoral-fin ray (first branched)	-	-	17,2
Length of third left pectoral-fin ray (second branched)	18,8	18,3	15,5
Prepelvic length	48,1	47,3	47,7
Distance between snout tip and terminus of pelvic-fin base	50,0	52,3	50,3
Distance between snout tip and pelvic-fin distal end	64,8	64,6	61,6
Distance between pelvic fins	3,7	4,5	4,8
Length of first left pelvic-fin ray (unbranched)	13,5	12,8	11,0
Length of second left pelvic-fin ray (first branched)	14,7	15,7	12,8
Length of third left pelvic-fin ray (second branched)	17,3	15,2	13,8
Anal-fin base	11,5	12,9	11,2
Preanal length	68,6	68,5	68,8
Distance between snout tip and terminus of anal-fin base	80,3	79,6	80,1
Distance between snout tip and anal-fin distal end	90,1	88,1	85,8
Adipose-fin length	31,9	31,0	30,2
Preadipose length	59,2	60,7	58,4
Distance between snout tip and adipose-fin base end	89,1	90,6	88,0
Adipose-fin depth	5,7	5,6	4,5
Caudal-peduncle length posterior to adipose-fin	10,2	11,3	11,1
Caudal-peduncle depth at adipose-fin terminus	8,1	8,4	8,9
Snout-anus distance	56,0	55,5	56,3

Snout-urogenital papilla distance	60,7	64,0	61,6
Anus-urogenital papilla distance	4,9	8,0	4,8
Dorsal lobe of caudal fin length	-	22,4	-
Ventral lobe of caudal fin length	-	24,1	22,8

Percentages of HL

Head depth	42,9	40,0	40,7
Head width	57,4	54,5	61,1
Eye diameter (left)	25,5	24,6	17,2
Fleshy interorbital	24,1	26,1	23,5
Bony interorbital	14,3	15,8	16,6
Mouth gape	30,5	29,8	30,8
Snout length (left)	30,3	30,6	33,1
Distance between snout tip and posterior nare (left side)	18,8	17,0	18,7
Anterior internarial width	13,8	14,3	13,1
Posterior internarial width	14,2	14,5	13,8
Intranarial length (left side)	12,5	15,7	13,3

Table 19: Morphometric data of *Pimelodella eutaenia* based on type and comparative material.

	Lectotype	Min.	Max.	n	x	SD
Total length (mm)	162,5	147,4	162,5	2	154,9	
Standard length (mm)	126,3	51,0	175,7	7	94,1	
	Percentages of SL					
Body depth (dorsal)	21,0	18,8	76,8	5	31,5	25,3
Body width (dorsal)	17,2	11,4	17,2	5	14,4	2,2
Cleithral width	17,3	12,2	17,4	5	16,2	2,2
Head length	30,2	21,6	34,0	5	29,2	4,6
Maxillary-barbel length (left side)	76,5	57,6	83,6	5	68,9	11,0
Outer mental-barbel length (left side)	25,9	22,0	33,2	5	25,3	4,7
Inner mental-barbel length (left side)	15,5	11,7	19,1	5	14,6	2,8
Predorsal length	36,0	24,8	36,0	5	32,9	4,7
Distance between snout tip and terminus of dorsal-fin base	48,2	35,1	50,0	5	45,8	6,0
Distance between snout tip and dorsal-fin distal end	56,8	42,8	62,9	5	55,6	7,6
Dorsal fin to adipose fin	14,9	10,5	15,5	5	13,6	2,3
Dorsal-fin base	15,1	11,5	15,8	5	14,4	1,7
Length of first dorsal-fin ray (unbranched)	20,9	14,9	23,0	5	19,4	3,0
Length of rigid part of first dorsal-fin ray	15,3	13,3	16,0	4	14,5	1,4
Length of second dorsal-fin ray (first branched)	20,3	15,3	23,0	4	19,7	3,2
Length of third dorsal-fin ray (second branched)	19,0	15,1	21,2	4	18,5	2,5
Prepectoral length	20,4	15,3	22,4	5	20,4	2,9
Distance between snout tip and terminus of pectoral-fin base	24,0	17,4	25,4	5	23,4	3,4
Distance between snout tip and pectoral-fin distal end	39,5	30,2	41,7	5	38,4	4,7
Length of first left pectoral-fin ray (unbranched)	20,4	16,2	21,3	5	19,5	2,0
Length of rigid part of first left pectoral-fin ray	16,0	12,7	18,3	5	15,6	2,0
Length of second left pectoral-fin ray (first branched)	17,9	14,3	21,1	5	18,2	2,5
Length of third left pectoral-fin ray (second branched)	16,2	12,2	19,7	5	16,6	2,7
Prepelvic length	48,1	34,6	48,1	5	44,7	5,7
Distance between snout tip and terminus of pelvic-fin base	49,2	36,9	50,1	5	46,8	5,5
Distance between snout tip and pelvic-fin distal end	62,5	46,8	64,1	5	59,7	7,3
Distance between pelvic fins	5,3	3,9	5,3	5	4,6	0,5
Length of first left pelvic-fin ray (unbranched)	12,5	10,0	13,1	5	12,0	1,2
Length of second left pelvic-fin ray (first branched)	13,4	11,1	16,0	5	14,0	1,8
Length of third left pelvic-fin ray (second branched)	14,3	11,5	16,1	5	14,3	1,7
Anal-fin base	13,2	10,7	68,3	5	23,7	25,0
Preanal length	67,5	51,4	81,7	5	67,0	10,7
Distance between snout tip and terminus of anal-fin base	80,4	62,0	81,6	5	77,0	8,4
Distance between snout tip and anal-fin distal end	87,0	67,1	89,5	5	84,1	9,6
Adipose-fin length	29,4	23,2	31,4	5	27,4	3,5
Preadipose length	61,4	44,6	63,2	5	58,4	7,8
Distance between snout tip and adipose-fin base end	89,1	68,7	92,1	5	86,0	9,7
Adipose-fin depth	4,9	3,8	5,6	5	4,9	0,7
Caudal-peduncle length posterior to adipose-fin	11,0	7,2	12,0	5	10,0	1,8
Caudal-peduncle depth at adipose-fin terminus	7,8	6,5	8,5	5	7,7	0,8
Snout-anus distance	52,2	40,5	53,2	5	49,7	5,3

Snout-urogenital papilla distance	56,1	43,2	56,3	5	53,0	5,5
Anus-urogenital papilla distance	3,1	2,6	4,0	5	3,3	0,5
Dorsal lobe of caudal fin length	26,7	20,3	26,7	3	23,6	3,2
Ventral lobe of caudal fin length	-	20,4	20,4	1	20,4	-

Percentages of HL

Head depth	44,8	42,7	49,0	5	46,3	2,6
Head width	54,0	48,5	60,3	5	55,8	4,7
Eye diameter (left)	20,8	18,4	22,5	5	20,5	1,6
Fleshy interorbital	21,2	21,2	24,7	5	22,3	1,4
Bony interorbital	13,9	12,6	17,1	5	15,2	2,0
Mouth gape	32,8	28,9	32,8	5	30,8	1,4
Snout length (left)	31,4	29,5	32,5	5	31,1	1,1
Distance between snout tip and posterior nare (left side)	20,2	17,3	20,9	5	19,5	1,4
Anterior internarial width	12,8	12,8	14,3	5	13,6	0,6
Posterior internarial width	13,4	13,4	15,1	5	13,9	0,7
Intranarial length (left side)	12,7	12,7	15,9	5	14,6	1,6

Table 20: Morphometric data of *Pimelodella figueroai* based on type material.

	Paratype
Total length (mm)	89,0
Standard length (mm)	71,8
Percentages of SL	
Body depth (dorsal)	15,4
Body width (dorsal)	12,5
Cleithral width	15,4
Head length	29,4
Maxillary-barbel length (left side)	68,2
Outer mental-barbel length (left side)	29,3
Inner mental-barbel length (left side)	13,0
Predorsal length	33,4
Distance between snout tip and terminus of dorsal-fin base	48,5
Distance between snout tip and dorsal-fin distal end	59,8
Dorsal fin to adipose fin	14,9
Dorsal-fin base	15,6
Length of first dorsal-fin ray (unbranched)	16,7
Length of rigid part of first dorsal-fin ray	16,0
Length of second dorsal-fin ray (first branched)	22,2
Length of third dorsal-fin ray (second branched)	22,3
Prepectoral length	23,9
Distance between snout tip and terminus of pectoral-fin base	26,5
Distance between snout tip and pectoral-fin distal end	40,7
Length of first left pectoral-fin ray (unbranched)	16,6
Length of rigid part of first left pectoral-fin ray	14,9
Length of second left pectoral-fin ray (first branched)	17,2
Length of third left pectoral-fin ray (second branched)	18,0
Prepelvic length	48,6
Distance between snout tip and terminus of pelvic-fin base	50,0
Distance between snout tip and pelvic-fin distal end	62,7
Distance between pelvic fins	5,9
Length of first left pelvic-fin ray (unbranched)	12,5
Length of second left pelvic-fin ray (first branched)	13,9
Length of third left pelvic-fin ray (second branched)	14,7
Anal-fin base	11,4
Preanal length	69,7
Distance between snout tip and terminus of anal-fin base	79,4
Distance between snout tip and anal-fin distal end	86,9
Adipose-fin length	28,5
Preadipose length	62,9
Distance between snout tip and adipose-fin base end	89,1
Adipose-fin depth	4,2
Caudal-peduncle length posterior to adipose-fin	-
Caudal-peduncle depth at adipose-fin terminus	8,4
Snout-anus distance	58,6
Snout-urogenital papilla distance	-

Anus-urogenital papilla distance	-
Dorsal lobe of caudal fin length	26,1
Ventral lobe of caudal fin length	27,2

Percentages of HL

Head depth	50,1
Head width	55,6
Eye diameter (left)	23,5
Fleshy interorbital	23,8
Bony interorbital	14,3
Mouth gape	32,1
Snout length (left)	33,1
Distance between snout tip and posterior nare (left side)	19,9
Anterior internarial width	14,2
Posterior internarial width	14,0
Intranarial length (left side)	14,7

Table 21: Morphometric data of *Pimelodella geryi* and *P. procera*, its junior-synonym, based on type and comparative materials.

	Holotype	Min.	Max.	n	x	SD
Total length (mm)	74,0	74,0	144,0	5	103,5	
Standard length (mm)	58,0	58,0	113,1	5	81,7	
Percentages of SL						
Body depth (dorsal)	19,0	12,5	19,0	5	16,2	2,6
Body width (dorsal)	-	11,3	14,3	4	12,4	1,4
Cleithral width	-	15,0	16,8	4	15,9	0,8
Head length	33,5	29,9	33,5	5	32,1	1,5
Maxillary-barbel length (left side)	-	82,2	99,1	4	90,8	8,0
Outer mental-barbel length (left side)	-	23,0	28,5	4	26,2	2,3
Inner mental-barbel length (left side)	-	12,0	14,7	4	12,9	1,2
Predorsal length	35,2	33,1	37,2	5	34,8	1,5
Distance between snout tip and terminus of dorsal-fin base	-	46,1	48,1	4	47,1	0,9
Distance between snout tip and dorsal-fin distal end	-	52,2	58,1	4	55,8	2,5
Dorsal fin to adipose fin	-	13,7	20,7	4	17,7	3,4
Dorsal-fin base	-	13,1	14,5	4	13,8	0,7
Length of first dorsal-fin ray (unbranched)	-	20,0	20,0	1	20,0	-
Length of rigid part of first dorsal-fin ray	-	16,0	17,7	3	16,7	0,9
Length of second dorsal-fin ray (first branched)	-	16,1	20,6	3	18,9	2,4
Length of third dorsal-fin ray (second branched)	-	13,5	19,6	3	16,6	3,0
Prepectoral length	-	22,1	23,4	4	22,7	0,5
Distance between snout tip and terminus of pectoral-fin base	-	24,9	27,0	4	25,8	1,0
Distance between snout tip and pectoral-fin distal end	-	40,8	42,0	4	41,2	0,6
Length of first left pectoral-fin ray (unbranched)	-	18,7	19,1	2	18,9	0,3
Length of rigid part of first left pectoral-fin ray	17,2	16,5	18,4	5	17,5	0,8
Length of second left pectoral-fin ray (first branched)	-	18,9	19,7	4	19,3	0,4
Length of third left pectoral-fin ray (second branched)	-	14,9	17,5	4	16,8	1,3
Prepelvic length	41,2	41,2	48,1	5	45,4	2,8
Distance between snout tip and terminus of pelvic-fin base	-	46,8	49,8	4	48,3	1,2
Distance between snout tip and pelvic-fin distal end	-	60,0	62,3	4	61,2	1,1
Distance between pelvic fins	-	4,3	6,4	4	5,5	1,0
Length of first left pelvic-fin ray (unbranched)	-	9,6	13,1	4	11,9	1,6
Length of second left pelvic-fin ray (first branched)	-	10,0	15,0	3	13,2	2,8
Length of third left pelvic-fin ray (second branched)	-	10,7	14,5	3	13,2	2,2
Anal-fin base	-	11,4	15,0	4	13,1	1,8
Preanal length	66,5	64,4	71,6	5	67,9	2,8
Distance between snout tip and terminus of anal-fin base	-	79,7	81,7	4	80,9	1,0
Distance between snout tip and anal-fin distal end	-	86,2	88,4	4	87,1	0,9
Adipose-fin length	30,5	23,8	30,5	5	27,5	2,9
Preadipose length	61,9	58,1	66,4	5	62,8	3,1
Distance between snout tip and adipose-fin base end	-	87,1	90,5	4	89,1	1,6
Adipose-fin depth	3,6	2,4	3,9	5	3,5	0,6
Caudal-peduncle length posterior to adipose-fin	-	11,2	12,0	4	11,5	0,4
Caudal-peduncle depth at adipose-fin terminus	7,6	6,4	7,6	5	6,9	0,5
Snout-anus distance	-	50,3	51,4	3	51,0	0,6

Snout-urogenital papilla distance	-	55,1	56,2	3	55,8	0,6
Anus-urogenital papilla distance	-	4,0	4,7	3	4,3	0,4
Dorsal lobe of caudal fin length	-	24,0	27,5	3	26,2	1,9
Ventral lobe of caudal fin length	27,6	22,7	27,6	3	24,4	2,7

Percentages of HL

Head depth	-	35,3	45,9	4	41,1	4,9
Head width	-	46,0	53,0	4	49,9	3,6
Eye diameter (left)	24,2	19,1	24,2	5	22,4	2,0
Fleshy interorbital	-	18,1	21,3	4	19,3	1,4
Bony interorbital	14,3	11,1	14,3	5	12,2	1,5
Mouth gape	-	26,0	28,9	4	27,9	1,3
Snout length (left)	23,6	23,6	33,8	5	30,7	4,2
Distance between snout tip and posterior nare (left side)	-	16,4	20,6	4	18,2	1,9
Anterior internarial width	-	6,3	12,3	4	9,9	2,9
Posterior internarial width	-	10,5	12,5	4	11,5	0,9
Intranarial length (left side)	-	9,7	16,0	4	13,0	3,0

Table 22: Morphometric data of *Pimelodella geryi* and *P. procera*, its junior-synonym, based on type and comparative materials, discriminated by original species name.

	<i>Pimelodella geryi</i>						<i>P. procera</i>		
	Hol.	Min.	Max.	n	x	SD	Par. 1	Par. 2	
Total length (mm)	74,0	74,0	144,0	3	108,5		110,3	82,0	
Standard length (mm)	58,0	58,0	113,1	3	85,2		91,2	61,5	
	Percentages of SL								
Body depth (dorsal)	19,0	16,9	19,0	3	17,9	1,0	14,6	12,5	
Body width (dorsal)	-	12,4	14,3	2	13,4	1,3	11,3	11,4	
Cleithral width	-	15,5	16,8	2	16,2	0,9	16,4	15,0	
Head length	33,5	29,9	33,5	3	31,6	1,8	33,5	32,1	
Maxillary-barbel length (left side)	-	95,8	99,1	2	97,5	2,3	86,0	82,2	
Outer mental-barbel length (left side)	-	23,0	28,5	2	25,7	3,8	26,5	26,8	
Inner mental-barbel length (left side)	-	12,0	14,7	2	13,4	1,9	12,5	12,6	
Predorsal length	35,2	33,1	35,2	3	34,3	1,1	37,2	34,1	
Distance between snout tip and terminus of dorsal-fin base	-	46,1	48,1	2	47,1	1,4	47,6	46,5	
Distance between snout tip and dorsal-fin distal end	-	56,8	58,1	2	57,4	1,0	56,2	52,2	
Dorsal fin to adipose fin	-	13,7	16,0	2	14,9	1,6	20,7	20,3	
Dorsal-fin base	-	14,3	14,5	2	14,4	0,1	13,4	13,1	
Length of first dorsal-fin ray (unbranched)	-	20,0	20,0	1	20,0	-	-	-	
Length of rigid part of first dorsal-fin ray	-	16,0	16,0	1	16,0	-	16,4	17,7	
Length of second dorsal-fin ray (first branched)	-	19,9	19,9	1	19,9	-	16,1	20,6	
Length of third dorsal-fin ray (second branched)	-	19,6	19,6	1	19,6	-	13,5	16,7	
Prepectoral length	-	22,7	23,4	2	23,0	0,5	22,7	22,1	
Distance between snout tip and terminus of pectoral-fin base	-	26,0	27,0	2	26,5	0,7	25,1	24,9	
Distance between snout tip and pectoral-fin distal end	-	40,9	42,0	2	41,4	0,8	40,8	41,1	
Length of first left pectoral-fin ray (unbranched)	-	18,7	19,1	2	18,9	0,3	-	-	
Length of rigid part of first left pectoral-fin ray	17,2	16,5	18,4	3	17,3	0,9	17,4	18,3	
Length of second left pectoral-fin ray (first branched)	-	18,9	19,6	2	19,2	0,5	19,7	19,1	
Length of third left pectoral-fin ray (second branched)	-	17,1	17,5	2	17,3	0,3	17,5	14,9	
Prepelvic length	41,2	41,2	47,6	3	44,3	3,2	48,1	46,1	
Distance between snout tip and terminus of pelvic-fin base	-	46,8	49,8	2	48,3	2,1	48,3	48,2	
Distance between snout tip and pelvic-fin distal end	-	60,0	62,0	2	61,0	1,4	62,3	60,5	
Distance between pelvic fins	-	4,3	5,1	2	4,7	0,6	6,4	6,2	
Length of first left pelvic-fin ray (unbranched)	-	11,8	13,0	2	12,4	0,8	9,6	13,1	
Length of second left pelvic-fin ray (first branched)	-	14,5	15,0	2	14,8	0,4	10,0	-	
Length of third left pelvic-fin ray (second branched)	-	14,4	14,5	2	14,4	0,0	10,7	-	
Anal-fin base	-	14,2	15,0	2	14,6	0,5	11,4	11,7	
Preanal length	66,5	64,4	67,4	3	66,1	1,5	71,6	69,4	
Distance between snout tip and terminus of anal-fin base	-	80,4	81,7	2	81,1	1,0	81,7	79,7	
Distance between snout tip and anal-fin distal end	-	86,2	87,1	2	86,6	0,6	88,4	86,9	
Adipose-fin length	30,5	28,2	30,5	3	29,5	1,2	23,8	25,1	
Preadipose length	61,9	58,1	64,2	3	61,4	3,1	66,4	63,3	
Distance between snout tip and adipose-fin base end	-	88,4	90,5	2	89,4	1,5	90,3	87,1	
Adipose-fin depth	3,6	3,6	3,9	3	3,7	0,2	2,4	3,8	
Caudal-peduncle length posterior to adipose-fin	-	11,2	11,2	2	11,2	0,0	11,7	12,0	

Caudal-peduncle depth at adipose-fin terminus	7,6	6,8	7,6	3	7,2	0,4	6,4	6,6
Snout-anus distance	-	50,3	51,4	2	50,8	0,7	51,4	-
Snout-urogenital papilla distance	-	55,1	56,0	2	55,5	0,7	56,2	-
Anus-urogenital papilla distance	-	4,0	4,2	2	4,1	0,1	4,7	-
Dorsal lobe of caudal fin length	-	24,0	27,5	2	25,8	2,4	-	27,0
Ventral lobe of caudal fin length	27,6	22,7	27,6	3	24,4	2,7	-	-

Percentages of HL

Head depth	-	44,3	45,9	2	45,1	1,1	35,3	38,8
Head width	-	52,7	53,0	2	52,9	0,2	47,8	46,0
Eye diameter (left)	24,2	23,1	24,2	3	23,6	0,5	19,1	21,9
Fleshy interorbital	-	18,7	19,0	2	18,8	0,3	21,3	18,1
Bony interorbital	14,3	11,1	14,3	3	12,3	1,8	11,1	13,3
Mouth gape	-	28,7	28,9	2	28,8	0,2	26,0	27,8
Snout length (left)	23,6	23,6	33,5	3	29,7	5,4	30,5	33,8
Distance between snout tip and posterior nare (left side)	-	18,8	20,6	2	19,7	1,3	16,9	16,4
Anterior internarial width	-	12,1	12,3	2	12,2	0,2	9,1	6,3
Posterior internarial width	-	11,9	12,5	2	12,2	0,4	10,5	11,1
Intranarial length (left side)	-	15,1	16,0	2	15,5	0,6	11,4	9,7

Table 23: Morphometric data of *Pimelodella gracilis* and *P. taenioptera*, its junior-synonym, based on type and comparative materials.

	Holotype	Min.	Max.	n	x	SD
Total length (mm)	210,6	93,7	210,6	10	144,9	
Standard length (mm)	170,1	75,1	170,1	13	114,7	
Percentages of SL						
Body depth (dorsal)	11,4	11,4	18,8	11	15,7	2,1
Body width (dorsal)	9,8	9,8	14,3	11	12,3	1,2
Cleithral width	15,2	15,2	17,7	11	16,8	0,8
Head length	26,1	26,1	30,5	11	27,8	1,3
Maxillary-barbel length (left side)	-	59,5	102,8	9	79,4	13,4
Outer mental-barbel length (left side)	28,7	26,0	42,1	10	31,3	4,6
Inner mental-barbel length (left side)	17,1	17,1	26,0	11	19,3	2,5
Predorsal length	28,8	26,4	34,7	11	30,9	2,3
Distance between snout tip and terminus of dorsal-fin base	43,5	43,1	48,9	11	44,6	1,7
Distance between snout tip and dorsal-fin distal end	55,1	53,4	64,0	11	57,2	3,6
Dorsal fin to adipose fin	3,2	3,2	11,0	11	6,4	1,9
Dorsal-fin base	13,0	12,1	16,8	11	13,8	1,3
Length of first dorsal-fin ray (unbranched)	-	19,4	33,3	10	25,0	4,4
Length of rigid part of first dorsal-fin ray	-	10,4	18,5	10	16,0	2,4
Length of second dorsal-fin ray (first branched)	20,8	19,9	28,9	11	22,1	2,6
Length of third dorsal-fin ray (second branched)	17,8	16,7	22,3	11	19,4	1,6
Prepectoral length	21,1	19,2	23,3	11	20,6	1,1
Distance between snout tip and terminus of pectoral-fin base	22,5	22,1	26,6	11	23,8	1,3
Distance between snout tip and pectoral-fin distal end	36,3	36,3	42,5	10	40,3	2,3
Length of first left pectoral-fin ray (unbranched)	16,7	16,7	22,6	10	20,7	2,1
Length of rigid part of first left pectoral-fin ray	16,7	16,7	19,4	11	17,9	0,8
Length of second left pectoral-fin ray (first branched)	18,8	16,2	20,9	10	18,5	1,3
Length of third left pectoral-fin ray (second branched)	15,0	14,9	18,2	10	16,2	1,0
Prepelvic length	45,0	39,1	46,1	10	43,3	2,1
Distance between snout tip and terminus of pelvic-fin base	46,8	41,4	48,0	11	45,8	1,9
Distance between snout tip and pelvic-fin distal end	59,0	54,1	61,7	11	58,4	2,4
Distance between pelvic fins	5,3	3,3	5,8	10	4,8	0,7
Length of first left pelvic-fin ray (unbranched)	11,2	11,2	14,5	11	13,2	1,1
Length of second left pelvic-fin ray (first branched)	13,7	13,7	16,9	11	15,2	0,9
Length of third left pelvic-fin ray (second branched)	13,8	13,8	16,1	10	15,0	0,7
Anal-fin base	10,4	9,6	15,8	11	11,4	1,6
Preanal length	68,9	60,7	68,9	11	66,2	2,4
Distance between snout tip and terminus of anal-fin base	78,3	75,5	82,6	11	77,5	2,0
Distance between snout tip and anal-fin distal end	84,3	83,1	89,9	11	85,0	2,1
Adipose-fin length	38,7	38,7	44,5	11	41,5	2,1
Preadipose length	59,6	47,9	59,6	11	51,4	3,4
Distance between snout tip and adipose-fin base end	89,0	85,3	93,1	11	90,4	2,3
Adipose-fin depth	4,8	2,3	4,8	11	3,9	0,8
Caudal-peduncle length posterior to adipose-fin	12,0	7,1	12,0	11	9,1	1,6
Caudal-peduncle depth at adipose-fin terminus	6,4	6,4	8,6	11	7,4	0,6
Snout-anus distance	52,8	48,6	52,8	10	50,4	1,7

Snout-urogenital papilla distance	56,6	52,6	59,7	10	56,2	1,9
Anus-urogenital papilla distance	2,7	2,7	10,6	10	5,4	2,6
Dorsal lobe of caudal fin length	24,4	17,0	34,0	9	23,1	5,0
Ventral lobe of caudal fin length	19,5	19,2	25,7	11	22,4	2,0

Percentages of HL

Head depth	42,5	42,5	52,1	11	47,0	3,1
Head width	53,1	53,1	64,1	11	59,2	3,4
Eye diameter (left)	18,8	16,5	23,8	11	20,0	1,9
Fleshy interorbital	23,6	21,6	26,8	11	23,3	1,6
Bony interorbital	19,6	15,8	22,6	11	18,1	2,1
Mouth gape	32,2	30,7	36,3	11	33,0	1,9
Snout length (left)	36,5	31,8	38,0	11	34,5	2,0
Distance between snout tip and posterior nare (left side)	13,4	13,4	20,6	11	18,1	2,0
Anterior internarial width	14,3	10,4	14,9	11	13,1	1,3
Posterior internarial width	12,2	10,9	15,0	11	13,3	1,3
Intranarial length (left side)	12,7	11,8	16,0	11	13,4	1,3

Table 24: Morphometric data of *Pimelodella gracilis* and *P. taenioptera*, its junior-synonym, based on type and comparative materials, discriminated by original species name.

	<i>P. gracilis</i>						<i>P. taenioptera</i>					
	Holotype	Min.	Max.	<i>n</i>	<i>x</i>	SD	Holotype	Min.	Max.	<i>n</i>	<i>x</i>	S D
Total length (mm)	210,6	93,7	210,6	4	154,0		157,8	116,7	163,9	6	138,8	
Standard length (mm)	170,1	75,1	170,1	6	116,2		123,4	97,3	125,0	7	113,4	
	Percentages of SL											
Body depth (dorsal)	11,4	11,4	18,4	4	15,6	3,1	14,2	14,2	18,8	7	15,8	1,5
Body width (dorsal)	9,8	9,8	12,9	4	12,0	1,5	12,1	11,4	14,3	7	12,5	1,2
Cleithral width	15,2	15,2	17,7	4	16,5	1,1	16,1	16,1	17,6	7	17,0	0,6
Head length	26,1	26,1	30,5	4	27,6	2,0	28,3	26,1	29,1	7	28,0	0,9
Maxillary-barbel length (left side)	-	59,5	102,8	4	84,7	19,6	59,5	59,5	80,1	6	72,3	8,0
Outer mental-barbel length (left side)	28,7	28,7	42,1	4	34,1	6,0	26,0	26,0	33,1	6	29,5	2,6
Inner mental-barbel length (left side)	17,1	17,1	26,0	4	20,6	3,8	18,0	17,2	20,9	7	18,6	1,2
Predorsal length	28,8	26,4	34,7	4	30,3	3,6	30,8	29,5	33,3	7	31,3	1,3
Distance between snout tip and terminus of dorsal-fin base	43,5	43,2	48,9	4	45,0	2,6	44,3	43,1	45,7	7	44,4	1,0
Distance between snout tip and dorsal-fin distal end	55,1	54,7	59,0	4	56,5	2,0	63,0	53,4	64,0	7	57,7	4,3
Dorsal fin to adipose fin	3,2	3,2	6,9	4	5,2	1,6	11,0	5,8	11,0	7	7,1	1,8
Dorsal-fin base	13,0	13,0	16,8	4	14,7	1,6	12,6	12,1	14,4	7	13,3	0,9
Length of first dorsal-fin ray (unbranched)	-	21,9	27,8	3	24,5	3,0	30,5	19,4	33,3	7	25,2	5,1
Length of rigid part of first dorsal-fin ray	-	17,8	17,9	3	17,9	0,0	10,4	10,4	18,5	7	15,2	2,4
Length of second dorsal-fin ray (first branched)	20,8	20,3	22,5	4	21,4	1,0	28,9	19,9	28,9	7	22,5	3,2
Length of third dorsal-fin ray (second branched)	17,8	17,8	22,3	4	19,7	1,9	16,7	16,7	21,2	7	19,2	1,6
Prepectoral length	21,1	20,2	23,3	4	21,2	1,4	20,3	19,2	21,1	7	20,3	0,7
Distance between snout tip and terminus of pectoral-fin base	22,5	22,5	26,6	4	23,8	1,9	23,8	22,1	24,7	7	23,7	1,0
Distance between snout tip and pectoral-fin distal end	36,3	36,3	41,3	3	38,1	2,8	38,8	38,8	42,5	7	41,3	1,3
Length of first left pectoral-fin ray (unbranched)	16,7	16,7	22,6	3	18,8	3,2	20,7	20,7	22,6	7	21,5	0,6
Length of rigid part of first left pectoral-fin ray	16,7	16,7	18,6	4	17,7	0,9	17,1	17,1	19,4	7	18,1	0,8

Length of second left pectoral-fin ray (first branched)	18,8	16,2	18,8	3	17,7	1,3	18,3	17,6	20,9	7	18,8	1,3
Length of third left pectoral-fin ray (second branched)	15,0	14,9	15,1	3	15,0	0,1	16,9	15,8	18,2	7	16,7	0,8
Prepelvic length	45,0	41,7	46,1	3	44,3	2,3	42,0	39,1	45,0	7	42,9	2,1
Distance between snout tip and terminus of pelvic-fin base	46,8	45,1	48,0	4	46,4	1,3	44,4	41,4	48,0	7	45,4	2,2
Distance between snout tip and pelvic-fin distal end	59,0	56,3	61,7	4	59,0	2,2	57,0	54,1	61,3	7	58,1	2,6
Distance between pelvic fins	5,3	4,6	5,8	3	5,2	0,6	4,7	3,3	5,4	7	4,6	0,7
Length of first left pelvic-fin ray (unbranched)	11,2	11,2	13,4	4	12,7	1,0	11,6	11,6	14,5	7	13,5	1,1
Length of second left pelvic-fin ray (first branched)	13,7	13,7	16,9	4	15,3	1,3	14,5	14,2	16,1	7	15,1	0,6
Length of third left pelvic-fin ray (second branched)	13,8	13,8	15,5	3	14,9	1,0	14,3	14,3	16,1	7	15,0	0,7
Anal-fin base	10,4	10,4	15,8	4	12,3	2,4	10,5	9,6	11,9	7	11,0	0,8
Preanal length	68,9	65,0	68,9	4	67,0	1,7	66,9	60,7	68,3	7	65,7	2,8
Distance between snout tip and terminus of anal-fin base	78,3	75,5	82,6	4	78,2	3,2	77,0	75,9	79,0	7	77,1	1,2
Distance between snout tip and anal-fin distal end	84,3	83,5	89,9	4	85,3	3,1	83,7	83,1	86,8	7	84,8	1,6
Adipose-fin length	38,7	38,7	41,6	4	39,7	1,3	39,9	39,9	44,5	7	42,6	1,7
Preadipose length	59,6	49,0	59,6	4	53,4	4,7	54,4	47,9	54,4	7	50,3	2,1
Distance between snout tip and adipose-fin base end	89,0	85,3	90,2	4	88,2	2,1	91,5	89,8	93,1	7	91,7	1,2
Adipose-fin depth	4,8	4,0	4,8	4	4,4	0,4	2,3	2,3	4,5	7	3,6	0,9
Caudal-peduncle length posterior to adipose-fin	12,0	7,3	12,0	4	10,2	2,1	9,0	7,1	9,5	7	8,5	0,8
Caudal-peduncle depth at adipose-fin terminus	6,4	6,4	8,6	4	7,6	0,9	6,9	6,9	8,0	7	7,3	0,4
Snout-anus distance	52,8	49,1	52,8	4	50,8	1,9	48,9	48,6	52,6	6	50,1	1,7
Snout-urogenital papilla distance	56,6	53,8	57,2	4	55,7	1,5	59,7	52,6	59,7	6	56,5	2,2
Anus-urogenital papilla distance	2,7	2,7	6,4	4	4,6	1,8	10,6	2,8	10,6	6	6,0	3,0
Dorsal lobe of caudal fin length	24,4	19,9	24,4	4	22,9	2,1	25,6	17,0	34,0	5	23,3	0,0
Ventral lobe of caudal fin length	19,5	19,5	25,7	4	22,9	2,8	19,2	19,2	23,5	7	22,1	1,5

Percentages of HL

Head depth	42,5	42,5	49,2	4	47,2	3,2	45,6	43,6	52,1	7	46,9	3,3
Head width	53,1	53,1	61,8	4	58,5	3,8	58,3	54,2	64,1	7	59,5	3,5
Eye diameter (left)	18,8	16,5	23,8	4	19,9	3,1	20,8	18,3	21,3	7	20,1	1,0
Fleshy interorbital	23,6	22,0	26,8	4	23,6	2,3	21,6	21,6	25,2	7	23,2	1,3
Bony interorbital	19,6	16,1	22,6	4	18,7	3,0	16,9	15,8	20,1	7	17,7	1,6
Mouth gape	32,2	30,7	32,7	4	31,6	1,0	32,4	31,6	36,3	7	33,7	1,9

Snout length (left)	36,5	31,8	36,5	4	33,9	2,4	34,0	32,7	38,0	7	34,8	1,8
Distance between snout tip and posterior nare (left side)	13,4	13,4	19,5	4	17,5	2,8	17,0	16,9	20,6	7	18,4	1,6
Anterior internarial width	14,3	11,6	14,3	4	13,1	1,3	13,9	10,4	14,9	7	13,1	1,5
Posterior internarial width	12,2	12,2	15,0	4	13,5	1,2	12,2	10,9	14,6	7	13,1	1,5
Intranarial length (left side)	12,7	12,7	14,8	4	13,6	1,1	11,9	11,8	16,0	7	13,3	1,5

Table 25: Morphometric data of *Pimelodella griffini* based on type material.

	Holotype	Min.	Max.	<i>n</i>	<i>x</i>	SD
Total length (mm)	-	-	-	-	-	-
Standard length (mm)	67,2	43,8	69,9	14	62,4	
	Percentages of SL					
Body depth (dorsal)	18,7	16,5	18,7	3	17,7	1,1
Body width (dorsal)	13,7	13,7	14,8	3	14,2	0,6
Cleithral width	17,8	16,7	17,8	3	17,4	0,6
Head length	30,7	30,3	31,1	3	30,7	0,4
Maxillary-barbel length (left side)	54,9	54,9	61,1	3	59,0	3,5
Outer mental-barbel length (left side)	18,0	18,0	21,4	3	19,7	1,7
Inner mental-barbel length (left side)	10,1	10,1	10,7	3	10,5	0,3
Predorsal length	35,1	34,2	36,4	3	35,2	1,1
Distance between snout tip and terminus of dorsal-fin base	50,4	47,5	50,4	3	49,0	1,4
Distance between snout tip and dorsal-fin distal end	75,0	58,6	75,0	3	65,0	8,8
Dorsal fin to adipose fin	16,9	12,7	16,9	3	15,0	2,2
Dorsal-fin base	13,5	13,5	14,1	3	13,8	0,3
Length of first dorsal-fin ray (unbranched)	39,1	20,1	39,1	3	30,2	9,6
Length of rigid part of first dorsal-fin ray	13,0	13,0	15,3	3	14,1	1,2
Length of second dorsal-fin ray (first branched)	21,5	19,8	21,5	3	21,0	1,0
Length of third dorsal-fin ray (second branched)	19,8	19,8	20,4	3	20,1	0,3
Prepectoral length	23,0	21,7	23,1	3	22,6	0,8
Distance between snout tip and terminus of pectoral-fin base	26,6	25,1	26,6	3	25,9	0,8
Distance between snout tip and pectoral-fin distal end	42,2	39,0	42,2	3	40,5	1,6
Length of first left pectoral-fin ray (unbranched)	0,0	19,0	19,6	2	19,3	0,4
Length of rigid part of first left pectoral-fin ray	16,8	16,8	17,2	3	16,9	0,2
Length of second left pectoral-fin ray (first branched)	19,5	19,2	19,5	3	19,4	0,1
Length of third left pectoral-fin ray (second branched)	15,8	15,8	18,4	3	17,5	1,5
Prepelvic length	48,8	47,5	49,0	3	48,4	0,9
Distance between snout tip and terminus of pelvic-fin base	51,4	50,9	51,6	3	51,3	0,3
Distance between snout tip and pelvic-fin distal end	64,4	62,6	64,4	3	63,6	0,9
Distance between pelvic fins	4,3	4,3	5,1	3	4,7	0,4
Length of first left pelvic-fin ray (unbranched)	13,0	11,3	13,0	3	12,5	1,0
Length of second left pelvic-fin ray (first branched)	13,0	13,0	14,1	3	13,7	0,6
Length of third left pelvic-fin ray (second branched)	14,2	14,2	15,7	3	14,8	0,8
Anal-fin base	14,9	12,5	14,9	3	13,8	1,2
Preanal length	68,6	67,9	68,7	3	68,4	0,5
Distance between snout tip and terminus of anal-fin base	80,0	80,0	80,4	3	80,2	0,2
Distance between snout tip and anal-fin distal end	87,9	86,7	87,9	3	87,3	0,6
Adipose-fin length	27,5	27,3	27,7	3	27,5	0,2
Preadipose length	62,9	58,6	65,1	3	62,2	3,3
Distance between snout tip and adipose-fin base end	89,3	83,5	89,5	3	87,4	3,4
Adipose-fin depth	3,8	3,8	5,0	3	4,5	0,6
Caudal-peduncle length posterior to adipose-fin	12,4	12,4	13,3	3	12,8	0,4
Caudal-peduncle depth at adipose-fin terminus	9,0	9,0	9,6	3	9,2	0,3
Snout-anus distance	54,5	54,0	54,5	3	54,3	0,2
Snout-urogenital papilla distance	63,4	58,1	63,4	3	60,8	2,6

Anus-urogenital papilla distance	9,8	4,2	9,8	3	6,9	2,8
Dorsal lobe of caudal fin length	-	-	-	-	-	-
Ventral lobe of caudal fin length	-	-	-	-	-	-

Percentages of HL

Head depth	47,9	43,3	47,9	3	46,3	2,6
Head width	56,8	54,5	56,8	3	56,0	1,3
Eye diameter (left)	16,6	16,6	19,5	3	18,5	1,6
Fleshy interorbital	27,0	23,7	27,0	3	25,6	1,7
Bony interorbital	16,0	15,8	16,5	3	16,1	0,3
Mouth gape	31,6	30,0	31,6	3	31,0	0,9
Snout length (left)	33,7	31,0	33,7	3	32,3	1,4
Distance between snout tip and posterior nare (left side)	22,5	19,8	22,5	3	20,7	1,5
Anterior internarial width	11,5	11,5	13,5	3	12,4	1,0
Posterior internarial width	14,3	13,5	14,7	3	14,2	0,6
Intranarial length (left side)	15,4	14,5	18,4	3	16,1	2,0

Table 26: Morphometric data of *Pimelodella grisea* based on type material.

	Lectotype	Min.	Max.	n	x	SD
Total length (mm)	150,8	124,5	150,8	3	140,2	
Standard length (mm)	119,7	99,7	119,7	3	112,1	
	Percentages of SL					
Body depth (dorsal)	20,2	19,7	20,2	3	19,9	0,3
Body width (dorsal)	17,2	15,0	21,4	3	17,9	3,3
Cleithral width	19,2	18,6	19,2	3	18,9	0,3
Head length	31,4	30,8	31,9	3	31,4	0,6
Maxillary-barbel length (left side)	67,1	57,4	67,1	2	62,2	6,9
Outer mental-barbel length (left side)	26,9	23,1	26,9	3	24,7	2,0
Inner mental-barbel length (left side)	14,8	12,4	14,8	3	13,9	1,3
Predorsal length	34,8	34,8	35,1	3	35,0	0,1
Distance between snout tip and terminus of dorsal-fin base	49,2	48,3	49,4	3	49,0	0,6
Distance between snout tip and dorsal-fin distal end	59,1	59,0	59,4	3	59,2	0,2
Dorsal fin to adipose fin	15,5	15,1	18,3	3	16,3	1,7
Dorsal-fin base	15,8	14,2	15,8	3	15,2	0,8
Length of first dorsal-fin ray (unbranched)	20,1	18,3	20,1	2	19,2	1,3
Length of rigid part of first dorsal-fin ray	16,6	13,9	16,6	3	15,2	1,3
Length of second dorsal-fin ray (first branched)	19,4	18,7	20,1	3	19,4	0,7
Length of third dorsal-fin ray (second branched)	17,5	16,4	19,7	3	17,9	1,7
Prepectoral length	21,2	19,5	21,2	3	20,6	1,0
Distance between snout tip and terminus of pectoral-fin base	25,2	22,6	25,2	3	24,3	1,5
Distance between snout tip and pectoral-fin distal end	41,2	39,4	41,2	3	40,3	0,9
Length of first left pectoral-fin ray (unbranched)	21,2	19,3	21,2	3	20,0	1,0
Length of rigid part of first left pectoral-fin ray	18,7	15,7	18,7	3	17,4	1,5
Length of second left pectoral-fin ray (first branched)	19,3	9,8	19,3	3	15,5	5,1
Length of third left pectoral-fin ray (second branched)	18,0	17,0	18,5	3	17,8	0,7
Prepelvic length	49,5	49,4	50,1	3	49,7	0,4
Distance between snout tip and terminus of pelvic-fin base	53,3	51,7	53,3	3	52,6	0,8
Distance between snout tip and pelvic-fin distal end	65,7	64,2	65,7	3	64,9	0,7
Distance between pelvic fins	5,1	4,9	5,1	3	5,0	0,1
Length of first left pelvic-fin ray (unbranched)	10,3	10,3	12,8	3	11,9	1,4
Length of second left pelvic-fin ray (first branched)	12,3	12,3	14,8	3	13,7	1,3
Length of third left pelvic-fin ray (second branched)	13,9	13,9	14,7	3	14,4	0,4
Anal-fin base	11,5	11,5	15,4	3	12,9	2,1
Preanal length	68,2	66,4	69,2	3	68,0	1,4
Distance between snout tip and terminus of anal-fin base	80,4	79,8	82,4	3	80,9	1,4
Distance between snout tip and anal-fin distal end	87,5	87,4	88,3	3	87,7	0,5
Adipose-fin length	25,6	23,2	27,0	3	25,2	1,9
Preadipose length	64,4	62,9	65,0	3	64,1	1,1
Distance between snout tip and adipose-fin base end	89,0	87,3	89,0	3	88,4	0,9
Adipose-fin depth	5,7	4,3	5,7	3	5,0	0,7
Caudal-peduncle length posterior to adipose-fin	12,6	11,6	12,9	3	12,4	0,7
Caudal-peduncle depth at adipose-fin terminus	9,9	8,5	9,9	3	9,1	0,7
Snout-anus distance	55,7	55,7	57,7	3	56,9	1,1
Snout-urogenital papilla distance	60,7	60,7	61,3	3	61,0	0,3

Anus-urogenital papilla distance	4,4	3,1	4,4	3	3,8	0,7
Dorsal lobe of caudal fin length	25,6	25,2	26,1	3	25,6	0,5
Ventral lobe of caudal fin length	21,0	20,5	23,9	3	21,8	1,8

Percentages of HL

Head depth	49,8	47,7	49,8	3	48,5	1,2
Head width	60,4	55,3	60,4	3	58,4	2,7
Eye diameter (left)	20,6	19,5	22,2	3	20,8	1,4
Fleshy interorbital	25,7	23,4	25,7	3	24,4	1,2
Bony interorbital	18,3	15,7	18,3	3	17,2	1,4
Mouth gape	33,0	30,7	33,6	3	32,5	1,6
Snout length (left)	30,5	28,8	30,5	3	29,9	0,9
Distance between snout tip and posterior nare (left side)	18,5	16,3	18,5	3	17,8	1,2
Anterior internarial width	10,8	10,8	14,0	3	12,1	1,6
Posterior internarial width	15,0	14,6	15,0	3	14,8	0,2
Intranarial length (left side)	12,4	11,8	12,4	3	12,0	0,3

Table 27: Morphometric data of *Pimelodella harttii* based on type material.

	Holotype
Total length (mm)	183,0
Standard length (mm)	150,2
Percentages of SL	
Body depth (dorsal)	20,0
Body width (dorsal)	17,6
Cleithral width	17,5
Head length	27,2
Maxillary-barbel length (left side)	-
Outer mental-barbel length (left side)	22,3
Inner mental-barbel length (left side)	12,0
Predorsal length	31,7
Distance between snout tip and terminus of dorsal-fin base	45,2
Distance between snout tip and dorsal-fin distal end	54,3
Dorsal fin to adipose fin	17,0
Dorsal-fin base	14,3
Length of first dorsal-fin ray (unbranched)	19,6
Length of rigid part of first dorsal-fin ray	-
Length of second dorsal-fin ray (first branched)	17,7
Length of third dorsal-fin ray (second branched)	17,2
Prepectoral length	20,2
Distance between snout tip and terminus of pectoral-fin base	23,3
Distance between snout tip and pectoral-fin distal end	38,3
Length of first left pectoral-fin ray (unbranched)	18,7
Length of rigid part of first left pectoral-fin ray	17,1
Length of second left pectoral-fin ray (first branched)	17,0
Length of third left pectoral-fin ray (second branched)	15,6
Prepelvic length	45,0
Distance between snout tip and terminus of pelvic-fin base	47,2
Distance between snout tip and pelvic-fin distal end	59,0
Distance between pelvic fins	5,2
Length of first left pelvic-fin ray (unbranched)	11,2
Length of second left pelvic-fin ray (first branched)	13,1
Length of third left pelvic-fin ray (second branched)	13,9
Anal-fin base	13,7
Preanal length	65,0
Distance between snout tip and terminus of anal-fin base	78,7
Distance between snout tip and anal-fin distal end	86,4
Adipose-fin length	28,0
Preadipose length	59,9
Distance between snout tip and adipose-fin base end	87,9
Adipose-fin depth	4,9
Caudal-peduncle length posterior to adipose-fin	12,1
Caudal-peduncle depth at adipose-fin terminus	9,5
Snout-anus distance	50,3
Snout-urogenital papilla distance	54,5

Anus-urogenital papilla distance	4,4
Dorsal lobe of caudal fin length	-
Ventral lobe of caudal fin length	21,5

Percentages of HL

Head depth	38,3
Head width	64,0
Eye diameter (left)	20,2
Fleshy interorbital	23,6
Bony interorbital	17,4
Mouth gape	33,8
Snout length (left)	30,5
Distance between snout tip and posterior nare (left side)	18,1
Anterior internarial width	12,5
Posterior internarial width	15,3
Intranarial length (left side)	12,8

Table 28: Morphometric data of *Pimelodella hasemani* based on type and comparative materials.

	Holotype	Min.	Max.	<i>n</i>	<i>x</i>	SD
Total length (mm)	-	50,7	71,3	6	62,8	
Standard length (mm)	60,6	34,4	60,6	66	43,0	
	Percentages of SL					
Body depth (dorsal)	16,7	15,6	18,0	7	17,0	0,8
Body width (dorsal)	14,0	11,0	14,7	7	13,0	1,4
Cleithral width	16,8	15,6	18,3	7	16,8	1,0
Head length	29,2	29,2	33,6	7	31,1	1,7
Maxillary-barbel length (left side)	71,4	68,5	78,9	5	73,4	4,6
Outer mental-barbel length (left side)	35,4	23,9	35,4	7	29,6	3,9
Inner mental-barbel length (left side)	16,5	13,0	17,1	7	15,2	1,7
Predorsal length	33,0	32,9	36,8	7	34,2	1,4
Distance between snout tip and terminus of dorsal-fin base	48,0	46,5	50,0	7	48,1	1,4
Distance between snout tip and dorsal-fin distal end	57,6	55,9	60,2	7	57,7	1,8
Dorsal fin to adipose fin	14,5	10,8	16,2	7	13,4	2,2
Dorsal-fin base	15,4	13,1	15,7	7	14,7	1,0
Length of first dorsal-fin ray (unbranched)	23,3	16,4	23,3	7	19,9	2,2
Length of rigid part of first dorsal-fin ray	17,0	16,0	17,9	7	16,9	0,7
Length of second dorsal-fin ray (first branched)	-	18,1	23,6	6	20,6	2,2
Length of third dorsal-fin ray (second branched)	20,9	17,0	20,9	6	18,8	1,8
Prepectoral length	22,6	20,2	23,7	7	21,8	1,2
Distance between snout tip and terminus of pectoral-fin base	25,4	23,5	27,4	7	24,9	1,3
Distance between snout tip and pectoral-fin distal end	39,8	38,1	42,9	6	40,4	2,0
Length of first left pectoral-fin ray (unbranched)	19,0	17,5	22,5	4	19,4	2,2
Length of rigid part of first left pectoral-fin ray	17,4	15,9	22,0	6	18,6	2,4
Length of second left pectoral-fin ray (first branched)	15,8	15,8	20,1	6	17,9	1,7
Length of third left pectoral-fin ray (second branched)	15,2	13,3	16,5	4	15,1	1,3
Prepelvic length	44,8	44,7	46,7	7	45,6	0,8
Distance between snout tip and terminus of pelvic-fin base	47,6	46,6	50,5	7	48,0	1,4
Distance between snout tip and pelvic-fin distal end	60,7	57,7	62,6	7	60,4	1,7
Distance between pelvic fins	4,3	2,9	4,4	7	3,7	0,5
Length of first left pelvic-fin ray (unbranched)	-	10,1	13,4	6	11,7	1,2
Length of second left pelvic-fin ray (first branched)	-	12,2	14,2	6	13,2	0,7
Length of third left pelvic-fin ray (second branched)	-	12,1	15,5	6	13,8	1,1
Anal-fin base	13,2	10,3	13,2	7	12,0	1,0
Preanal length	69,8	66,9	69,8	7	68,1	1,2
Distance between snout tip and terminus of anal-fin base	80,6	78,8	81,2	7	80,2	0,8
Distance between snout tip and anal-fin distal end	87,9	86,5	90,0	7	87,9	1,4
Adipose-fin length	27,8	24,1	32,2	7	27,8	3,4
Preadipose length	61,2	57,8	63,2	7	60,6	2,1
Distance between snout tip and adipose-fin base end	88,4	81,7	89,0	7	86,6	2,6
Adipose-fin depth	4,7	3,1	5,3	7	4,1	0,8
Caudal-peduncle length posterior to adipose-fin	14,0	12,2	15,1	7	13,4	1,0
Caudal-peduncle depth at adipose-fin terminus	7,4	6,4	8,1	7	7,2	0,6
Snout-anus distance	48,3	47,6	54,0	7	50,4	2,1

Snout-urogenital papilla distance	55,4	50,7	59,3	7	55,4	2,7
Anus-urogenital papilla distance	6,0	3,3	6,0	7	4,9	1,0
Dorsal lobe of caudal fin length	-	20,4	26,3	6	24,3	2,2
Ventral lobe of caudal fin length	-	25,0	31,0	6	28,4	2,2

Percentages of HL

Head depth	47,1	41,8	50,7	7	45,1	3,0
Head width	52,7	47,3	52,7	7	50,3	2,2
Eye diameter (left)	23,8	23,6	31,3	7	25,4	2,7
Fleshy interorbital	21,0	19,1	23,7	7	21,1	1,5
Bony interorbital	15,3	11,5	15,3	7	13,5	1,4
Mouth gape	29,4	25,3	31,5	7	28,5	2,3
Snout length (left)	30,0	26,6	52,5	7	31,5	9,3
Distance between snout tip and posterior nare (left side)	18,8	16,6	21,7	7	18,9	1,8
Anterior internarial width	13,1	11,3	14,5	7	12,8	1,1
Posterior internarial width	14,9	12,2	15,5	7	14,3	1,2
Intranarial length (left side)	17,9	12,6	17,9	7	14,6	1,7

Table 29: Morphometric data of *Pimelodella howesi* based on type and comparative materials.

	Holotype	Min.	Max.	n	x	SD
Total length (mm)	91,3	64,0	91,3	5	79,6	
Standard length (mm)	79,3	30,7	79,3	29	55,9	
	Percentages of SL					
Body depth (dorsal)	15,4	14,8	16,9	6	15,5	0,7
Body width (dorsal)	12,5	10,0	12,5	6	11,3	1,0
Cleithral width	16,0	16,0	17,4	6	16,7	0,6
Head length	29,1	28,9	31,3	6	29,9	0,9
Maxillary-barbel length (left side)	83,9	81,8	99,8	6	89,1	7,0
Outer mental-barbel length (left side)	40,4	32,0	43,3	6	37,9	4,8
Inner mental-barbel length (left side)	22,3	18,6	26,8	6	23,0	2,9
Predorsal length	29,3	29,3	35,0	6	32,2	2,3
Distance between snout tip and terminus of dorsal-fin base	45,9	44,0	48,3	6	46,1	1,5
Distance between snout tip and dorsal-fin distal end	60,4	54,6	62,7	6	59,1	2,7
Dorsal fin to adipose fin	7,2	6,1	10,0	6	8,5	1,5
Dorsal-fin base	16,0	13,6	19,5	6	15,5	2,1
Length of first dorsal-fin ray (unbranched)	28,2	21,7	28,2	5	25,8	2,5
Length of rigid part of first dorsal-fin ray	21,2	17,5	23,7	6	20,7	2,3
Length of second dorsal-fin ray (first branched)	21,9	16,8	23,2	5	21,3	2,6
Length of third dorsal-fin ray (second branched)	18,9	18,7	20,1	3	19,3	0,8
Prepectoral length	21,5	21,5	23,9	6	22,8	1,2
Distance between snout tip and terminus of pectoral-fin base	24,6	24,0	27,7	6	25,3	1,3
Distance between snout tip and pectoral-fin distal end	41,8	41,8	45,3	6	43,6	1,5
Length of first left pectoral-fin ray (unbranched)	20,2	20,2	23,4	6	21,6	1,5
Length of rigid part of first left pectoral-fin ray	17,8	17,8	20,2	6	18,9	0,9
Length of second left pectoral-fin ray (first branched)	17,8	17,8	20,2	4	18,8	1,0
Length of third left pectoral-fin ray (second branched)	16,7	15,7	18,0	3	16,8	1,1
Prepelvic length	46,6	44,5	48,4	6	46,2	1,5
Distance between snout tip and terminus of pelvic-fin base	48,3	46,7	50,2	6	48,2	1,2
Distance between snout tip and pelvic-fin distal end	62,6	59,9	65,9	6	63,2	2,1
Distance between pelvic fins	4,4	3,5	4,4	4	4,0	0,5
Length of first left pelvic-fin ray (unbranched)	-	15,5	15,9	2	15,7	0,3
Length of second left pelvic-fin ray (first branched)	-	16,7	17,0	2	16,8	0,3
Length of third left pelvic-fin ray (second branched)	-	15,2	17,5	2	16,4	1,7
Anal-fin base	12,0	11,3	12,2	6	11,7	0,4
Preanal length	68,9	64,3	68,9	6	67,2	1,7
Distance between snout tip and terminus of anal-fin base	80,7	75,1	80,7	6	78,8	1,9
Distance between snout tip and anal-fin distal end	88,0	82,4	88,0	6	86,5	2,0
Adipose-fin length	36,6	30,7	37,9	6	34,8	2,7
Preadipose length	53,6	49,4	60,3	6	54,1	3,6
Distance between snout tip and adipose-fin base end	88,8	83,9	88,8	6	87,0	1,8
Adipose-fin depth	2,8	2,8	3,3	5	3,1	0,2
Caudal-peduncle length posterior to adipose-fin	12,0	11,1	15,7	6	12,9	1,6
Caudal-peduncle depth at adipose-fin terminus	6,7	6,5	7,9	6	7,2	0,6
Snout-anus distance	52,7	50,0	53,5	4	51,9	1,6
Snout-urogenital papilla distance	55,6	55,4	58,7	4	56,7	1,5

Anus-urogenital papilla distance	2,5	2,5	6,2	4	4,9	1,6
Dorsal lobe of caudal fin length	-	31,5	33,8	2	32,7	1,6
Ventral lobe of caudal fin length	-	26,5	28,7	4	27,3	1,0

Percentages of HL

Head depth	48,6	44,6	49,1	6	47,5	1,8
Head width	57,4	53,1	57,4	6	55,2	1,5
Eye diameter (left)	16,5	16,5	20,6	6	19,1	1,5
Fleshy interorbital	24,6	24,1	27,5	6	25,1	1,2
Bony interorbital	19,4	16,8	20,8	6	19,0	1,4
Mouth gape	27,9	26,7	29,2	6	28,0	1,0
Snout length (left)	32,5	29,8	33,5	6	32,2	1,2
Distance between snout tip and posterior nare (left side)	18,4	18,4	21,0	6	19,4	1,0
Anterior internarial width	12,7	10,7	15,6	6	13,4	1,7
Posterior internarial width	13,7	13,7	14,9	6	14,2	0,4
Intranarial length (left side)	14,4	14,4	15,7	6	15,0	0,5

Table 30: Morphometric data of *Pimelodella humeralis* based on type material.

	Holotype	Min.	Max.	n	x	SD
Total length (mm)	93,5	60,3	95,8	17	87,1	
Standard length (mm)	77,4	50,3	77,7	17	71,4	
	Percentages of SL					
Body depth (dorsal)	17,9	17,2	21,7	17	18,6	1,1
Body width (dorsal)	11,4	11,4	14,4	17	12,6	0,7
Cleithral width	15,0	14,0	16,0	17	15,0	0,5
Head length	30,1	28,5	32,6	17	30,6	1,2
Maxillary-barbel length (left side)	97,4	93,4	122,1	17	108,8	8,1
Outer mental-barbel length (left side)	32,6	19,9	37,4	17	31,5	3,9
Inner mental-barbel length (left side)	17,3	16,0	33,5	17	18,7	4,0
Predorsal length	32,6	32,2	35,9	17	33,6	0,9
Distance between snout tip and terminus of dorsal-fin base	45,7	45,4	48,7	17	46,5	0,9
Distance between snout tip and dorsal-fin distal end	25,7	23,7	27,4	16	25,5	0,9
Dorsal fin to adipose fin	3,2	3,2	5,7	17	4,2	0,5
Dorsal-fin base	13,3	13,3	15,4	17	14,5	0,5
Length of first dorsal-fin ray (unbranched)	22,2	18,7	22,2	10	20,2	1,2
Length of rigid part of first dorsal-fin ray	16,7	14,5	18,8	17	16,3	1,2
Length of second dorsal-fin ray (first branched)	22,5	15,1	22,5	17	20,2	1,6
Length of third dorsal-fin ray (second branched)	18,6	13,8	21,5	17	19,4	1,9
Prepectoral length	21,9	21,2	25,7	17	23,0	1,3
Distance between snout tip and terminus of pectoral-fin base	25,2	23,9	29,8	17	25,8	1,6
Distance between snout tip and pectoral-fin distal end	15,5	13,5	18,9	17	16,7	1,1
Length of first left pectoral-fin ray (unbranched)	15,9	15,9	17,9	12	16,8	0,7
Length of rigid part of first left pectoral-fin ray	15,5	14,3	16,8	17	15,7	0,7
Length of second left pectoral-fin ray (first branched)	15,2	13,8	16,8	17	15,5	0,8
Length of third left pectoral-fin ray (second branched)	13,2	11,1	20,6	17	14,1	2,0
Prepelvic length	42,5	41,9	47,9	17	44,3	1,4
Distance between snout tip and terminus of pelvic-fin base	47,0	45,6	50,2	17	46,8	1,2
Distance between snout tip and pelvic-fin distal end	14,4	12,0	15,3	16	14,1	0,8
Distance between pelvic fins	4,0	3,1	4,4	17	4,0	0,4
Length of first left pelvic-fin ray (unbranched)	11,6	11,2	13,5	16	12,1	0,6
Length of second left pelvic-fin ray (first branched)	11,9	11,3	14,8	16	13,0	1,0
Length of third left pelvic-fin ray (second branched)	12,8	11,2	14,0	17	12,9	0,8
Anal-fin base	13,4	11,6	14,4	17	13,0	0,9
Preanal length	65,1	63,2	66,7	17	65,0	0,9
Distance between snout tip and terminus of anal-fin base	77,4	76,5	79,9	17	78,0	0,9
Distance between snout tip and anal-fin distal end	20,7	17,8	21,5	16	20,2	0,9
Adipose-fin length	42,4	41,8	45,3	17	43,2	0,9
Preadipose length	49,1	49,1	53,2	17	50,7	1,2
Distance between snout tip and adipose-fin base end	91,7	90,4	93,1	17	91,5	0,6
Adipose-fin depth	5,1	4,5	6,5	17	5,4	0,5
Caudal-peduncle length posterior to adipose-fin	22,5	19,4	23,8	17	22,4	0,9
Caudal-peduncle depth at adipose-fin terminus	7,3	6,7	7,7	17	7,3	0,3
Snout-anus distance	49,2	47,4	52,1	17	49,8	1,1
Snout-urogenital papilla distance	50,9	50,2	53,4	17	51,7	0,8

Anus-urogenital papilla distance	1,3	1,1	1,9	17	1,6	0,3
Dorsal lobe of caudal fin length	23,9	20,0	26,6	17	23,7	1,8
Ventral lobe of caudal fin length	24,9	21,9	26,3	17	24,5	1,2

Percentages of HL

Head depth	48,2	47,1	52,5	17	49,6	1,5
Head width	47,5	43,2	51,0	17	48,2	1,9
Eye diameter (left)	21,9	20,5	25,9	17	23,7	1,5
Fleshy interorbital	22,3	22,3	25,1	17	23,8	0,8
Bony interorbital	17,2	14,3	17,2	17	15,7	0,9
Mouth gape	24,8	24,7	29,9	17	26,4	1,4
Snout length (left)	35,9	32,2	37,4	17	35,1	1,4
Distance between snout tip and posterior nare (left side)	18,6	17,7	20,3	17	18,9	0,7
Anterior internarial width	12,5	12,5	15,2	17	14,0	0,8
Posterior internarial width	12,4	12,1	14,8	17	13,2	0,7
Intranarial length (left side)	14,3	11,9	15,7	17	13,7	1,1

Table 31: Morphometric data of *Pimelodella ignobilis* and *P. pappenheimi*, its junior-synonym, based on type and comparative materials.

	Lectotype	Min.	Max.	n	x	SD
Total length (mm)	109,9	105,1	151,7	14	122,5	
Standard length (mm)	91,1	84,2	119,9	14	99,4	
	Percentages of SL					
Body depth (dorsal)	18,8	15,0	20,5	14	18,1	1,7
Body width (dorsal)	14,4	11,7	16,3	14	14,1	1,3
Cleithral width	18,1	16,1	19,1	14	18,1	0,8
Head length	28,3	27,9	33,0	14	29,7	1,3
Maxillary-barbel length (left side)	41,1	41,1	67,4	14	54,2	7,5
Outer mental-barbel length (left side)	17,1	17,1	26,7	14	22,6	2,9
Inner mental-barbel length (left side)	8,7	8,6	13,4	14	11,3	1,6
Predorsal length	32,2	30,4	35,3	14	33,2	1,6
Distance between snout tip and terminus of dorsal-fin base	46,0	45,8	49,0	14	47,2	1,0
Distance between snout tip and dorsal-fin distal end	55,0	55,0	60,2	14	57,6	1,8
Dorsal fin to adipose fin	15,3	11,3	17,8	14	14,8	1,8
Dorsal-fin base	14,2	12,3	15,6	14	13,9	1,0
Length of first dorsal-fin ray (unbranched)	16,6	16,6	24,6	11	20,2	2,2
Length of rigid part of first dorsal-fin ray	15,1	15,1	20,7	13	17,1	1,5
Length of second dorsal-fin ray (first branched)	18,1	18,1	23,1	13	20,4	1,7
Length of third dorsal-fin ray (second branched)	18,3	18,3	22,9	14	20,3	1,6
Prepectoral length	23,0	21,5	26,3	14	22,9	1,2
Distance between snout tip and terminus of pectoral-fin base	25,9	23,5	28,1	14	25,3	1,3
Distance between snout tip and pectoral-fin distal end	41,4	38,6	46,8	14	42,4	2,0
Length of first left pectoral-fin ray (unbranched)	18,9	18,5	22,1	12	20,4	1,2
Length of rigid part of first left pectoral-fin ray	17,5	17,5	20,6	14	18,8	1,0
Length of second left pectoral-fin ray (first branched)	18,2	17,8	21,7	14	19,5	1,1
Length of third left pectoral-fin ray (second branched)	17,1	15,0	20,6	13	17,7	1,4
Prepelvic length	44,9	44,6	49,6	14	47,4	1,7
Distance between snout tip and terminus of pelvic-fin base	46,6	46,3	52,3	14	49,7	1,9
Distance between snout tip and pelvic-fin distal end	62,6	58,7	66,4	14	64,0	1,8
Distance between pelvic fins	5,9	4,5	6,2	14	5,2	0,5
Length of first left pelvic-fin ray (unbranched)	11,6	11,6	15,8	14	13,5	1,3
Length of second left pelvic-fin ray (first branched)	14,1	12,9	17,5	14	15,1	1,3
Length of third left pelvic-fin ray (second branched)	14,4	13,1	17,4	14	15,3	1,2
Anal-fin base	14,2	11,9	16,6	14	14,0	1,4
Preanal length	64,6	63,6	71,5	14	67,1	2,5
Distance between snout tip and terminus of anal-fin base	78,1	78,1	83,6	14	80,8	1,5
Distance between snout tip and anal-fin distal end	83,8	83,8	90,9	14	88,1	1,9
Adipose-fin length	26,4	24,4	29,6	14	27,0	1,4
Preadipose length	59,3	57,7	64,4	13	60,7	2,1
Distance between snout tip and adipose-fin base end	85,6	81,2	89,5	14	87,0	2,1
Adipose-fin depth	3,9	2,8	4,8	14	3,9	0,5
Caudal-peduncle length posterior to adipose-fin	14,3	11,4	15,0	14	12,8	1,0
Caudal-peduncle depth at adipose-fin terminus	8,9	6,9	8,9	14	8,0	0,6
Snout-anus distance	52,5	50,5	57,7	14	53,2	2,0

Snout-urogenital papilla distance	62,7	54,5	64,0	14	60,2	2,5
Anus-urogenital papilla distance	9,3	3,3	9,3	14	6,6	2,3
Dorsal lobe of caudal fin length	21,7	21,7	26,9	13	24,8	1,8
Ventral lobe of caudal fin length	20,5	20,5	24,3	14	22,7	1,2

	Percentages of HL					
Head depth	52,9	42,8	55,3	14	48,4	3,8
Head width	66,3	53,5	66,3	14	60,7	4,2
Eye diameter (left)	19,0	16,9	24,4	14	20,7	1,9
Fleshy interorbital	28,1	19,2	28,1	14	22,0	2,6
Bony interorbital	22,3	14,3	22,3	14	16,9	2,0
Mouth gape	34,9	26,1	35,4	14	31,6	3,1
Snout length (left)	34,9	28,1	35,2	14	31,6	2,2
Distance between snout tip and posterior nare (left side)	22,4	17,5	23,4	14	20,1	1,7
Anterior internarial width	14,0	9,7	14,4	14	12,6	1,3
Posterior internarial width	18,8	12,5	18,8	14	14,4	1,8
Intranarial length (left side)	15,2	11,9	15,3	14	14,0	1,1

Table 32: Morphometric data of *Pimelodella ignobilis* and *P. pappenheimi*, its junior-synonym, based on type and comparative materials, discriminated by original species name.

	<i>P. ignobilis</i>						<i>P. pappenheimi</i>					
	Lectotype	Min.	Max.	<i>n</i>	<i>x</i>	SD	Lectotype	Min.	Max.	<i>n</i>	<i>x</i>	SD
Total length (mm)	109,9	109,9	129,3	3	120,1		123,4	105,1	151,7	11	123,1	
Standard length (mm)	91,1	91,1	106,4	3	98,8		103,1	84,2	119,9	11	99,5	
	Percentages of SL											
Body depth (dorsal)	18,8	18,7	19,6	3	19,0	0,5	18,3	15,0	20,5	11	17,9	1,8
Body width (dorsal)	14,4	14,4	15,8	3	15,2	0,7	12,9	11,7	16,3	11	13,8	1,3
Cleithral width	18,1	18,1	19,1	3	18,5	0,6	17,8	16,1	18,9	11	18,0	0,8
Head length	28,3	28,3	30,4	3	29,7	1,2	29,7	27,9	33,0	11	29,7	1,4
Maxillary-barbel length (left side)	41,1	41,1	43,1	3	42,3	1,1	55,5	49,8	67,4	11	57,5	4,4
Outer mental-barbel length (left side)	17,1	17,1	18,8	3	18,2	0,9	24,8	20,6	26,7	11	23,8	1,8
Inner mental-barbel length (left side)	8,7	8,6	9,0	3	8,8	0,2	11,8	10,0	13,4	11	11,9	1,1
Predorsal length	32,2	32,2	34,4	3	33,2	1,1	32,2	30,4	35,3	11	33,2	1,8
Distance between snout tip and terminus of dorsal-fin base	46,0	45,8	47,7	3	46,5	1,0	46,9	46,1	49,0	11	47,5	0,9
Distance between snout tip and dorsal-fin distal end	55,0	55,0	57,3	3	55,9	1,3	56,7	55,1	60,2	11	58,0	1,7
Dorsal fin to adipose fin	15,3	11,3	15,3	3	13,3	2,0	16,7	13,1	17,8	11	15,2	1,6
Dorsal-fin base	14,2	12,3	14,3	3	13,6	1,1	15,6	12,4	15,6	11	13,9	1,1
Length of first dorsal-fin ray (unbranched)	16,6	16,6	18,2	2	17,4	1,2	21,4	18,7	24,6	9	20,8	1,9
Length of rigid part of first dorsal-fin ray	15,1	15,1	15,8	2	15,5	0,5	18,2	15,5	20,7	11	17,4	1,4
Length of second dorsal-fin ray (first branched)	18,1	18,1	19,1	3	18,6	0,5	21,1	18,5	23,1	10	20,9	1,6
Length of third dorsal-fin ray (second branched)	18,3	18,3	19,4	3	18,9	0,5	20,9	18,4	22,9	11	20,6	1,6
Prepectoral length	23,0	22,8	24,4	3	23,4	0,9	22,7	21,5	26,3	11	22,7	1,3
Distance between snout tip and terminus of pectoral-fin base	25,9	25,9	27,2	3	26,4	0,7	25,8	23,5	28,1	11	25,0	1,2
Distance between snout tip and pectoral-fin distal end	41,4	41,3	43,4	3	42,1	1,2	43,2	38,6	46,8	11	42,5	2,2
Length of first left pectoral-fin ray (unbranched)	18,9	18,5	20,7	3	19,4	1,2	19,0	19,0	22,1	9	20,7	1,1
Length of rigid part of first left pectoral-fin ray	17,5	17,5	19,2	3	18,1	1,0	17,9	17,9	20,6	11	19,0	0,9
Length of second left pectoral-fin ray (first branched)	18,2	17,8	19,5	3	18,5	0,9	18,2	18,2	21,7	11	19,8	1,0

Length of third left pectoral-fin ray (second branched)	17,1	15,0	17,1	3	16,4	1,2	18,2	15,9	20,6	10	18,1	1,2
Prepelvic length	44,9	44,9	49,6	3	47,4	2,4	44,6	44,6	49,0	11	47,4	1,6
Distance between snout tip and terminus of pelvic-fin base	46,6	46,6	52,3	3	50,1	3,1	48,0	46,3	51,5	11	49,5	1,6
Distance between snout tip and pelvic-fin distal end	62,6	62,6	64,9	3	64,0	1,2	62,5	58,7	66,4	11	63,9	2,0
Distance between pelvic fins	5,9	5,0	6,2	3	5,7	0,6	6,0	4,5	6,0	11	5,1	0,5
Length of first left pelvic-fin ray (unbranched)	11,6	11,6	11,8	3	11,7	0,1	12,9	12,6	15,8	11	13,9	1,0
Length of second left pelvic-fin ray (first branched)	14,1	12,9	14,3	3	13,8	0,7	13,3	13,3	17,5	11	15,5	1,2
Length of third left pelvic-fin ray (second branched)	14,4	13,1	14,9	3	14,1	1,0	15,0	13,6	17,4	11	15,6	1,0
Anal-fin base	14,2	11,9	14,2	3	13,0	1,2	14,9	12,5	16,6	11	14,3	1,3
Preanal length	64,6	64,6	70,9	3	68,5	3,4	66,2	63,6	71,5	11	66,7	2,2
Distance between snout tip and terminus of anal-fin base	78,1	78,1	82,4	3	80,8	2,3	79,8	79,0	83,6	11	80,8	1,4
Distance between snout tip and anal-fin distal end	83,8	83,8	89,4	3	87,0	2,8	87,0	86,0	90,9	11	88,4	1,6
Adipose-fin length	26,4	24,4	27,4	3	26,1	1,5	27,8	24,8	29,6	11	27,3	1,3
Preadipose length	59,3	57,7	59,3	3	58,4	0,8	61,8	58,9	64,4	10	61,4	1,8
Distance between snout tip and adipose-fin base end	85,6	81,2	87,2	3	84,7	3,1	87,9	85,2	89,5	11	87,6	1,3
Adipose-fin depth	3,9	3,9	4,5	3	4,2	0,3	4,3	2,8	4,8	11	3,8	0,5
Caudal-peduncle length posterior to adipose-fin	14,3	14,0	15,0	3	14,4	0,5	12,2	11,4	13,3	11	12,4	0,6
Caudal-peduncle depth at adipose-fin terminus	8,9	7,5	8,9	3	8,2	0,7	8,9	6,9	8,9	11	7,9	0,6
Snout-anus distance	52,5	52,5	57,7	3	55,4	2,7	50,5	50,5	54,2	11	52,6	1,3
Snout-urogenital papilla distance	62,7	62,0	63,2	3	62,7	0,6	59,9	54,5	64,0	11	59,5	2,3
Anus-urogenital papilla distance	9,3	5,8	9,3	3	7,3	1,8	8,9	3,3	9,2	11	6,4	2,4
Dorsal lobe of caudal fin length	21,7	21,7	23,2	3	22,3	0,8	26,7	23,8	26,9	10	25,6	1,1
Ventral lobe of caudal fin length	20,5	20,5	23,1	3	21,7	1,3	22,3	21,3	24,3	11	23,0	1,1

Percentages of HL

Head depth	52,9	50,3	52,9	3	51,3	1,4	48,3	42,8	55,3	11	47,6	3,9
Head width	66,3	64,2	66,3	3	65,4	1,1	62,5	53,5	65,0	11	59,4	3,8
Eye diameter (left)	19,0	16,9	20,4	3	18,8	1,8	18,5	18,5	24,4	11	21,2	1,6
Fleshy interorbital	28,1	25,7	28,1	3	26,5	1,4	21,2	19,2	22,1	11	20,8	0,9
Bony interorbital	22,3	17,7	22,3	3	19,8	2,3	17,4	14,3	17,4	11	16,2	1,0
Mouth gape	34,9	32,9	35,4	3	34,4	1,3	33,2	26,1	34,9	11	30,9	3,0
Snout length (left)	34,9	31,1	34,9	3	32,5	2,1	34,7	28,1	35,2	11	31,4	2,2

Distance between snout tip and posterior nare (left side)	22,4	20,0	22,4	3	20,8	1,4	23,4	17,5	23,4	11	19,9	1,7
Anterior internarial width	14,0	10,8	14,0	3	12,7	1,7	13,6	9,7	14,4	11	12,6	1,3
Posterior internarial width	18,8	15,1	18,8	3	16,8	1,9	16,0	12,5	16,0	11	13,8	1,2
Intranarial length (left side)	15,2	11,9	15,2	3	13,6	1,6	14,3	12,3	15,3	11	14,1	1,0

Table 33: Morphometric data of *Pimelodella itapicuruensis* based on type material.

	Holotype	Min.	Max.	n	x	SD
Total length (mm)	77,3	69,4	77,3	3	73,2	
Standard length (mm)	60,2	45,2	82,2	22	64,2	
	Percentages of SL					
Body depth (dorsal)	13,0	13,0	19,7	4	16,5	3,5
Body width (dorsal)	13,1	11,0	18,2	4	14,6	3,2
Cleithral width	13,2	13,2	17,3	4	15,6	2,0
Head length	28,7	27,4	28,9	4	28,2	0,7
Maxillary-barbel length (left side)	65,3	65,3	87,5	5	76,4	8,7
Outer mental-barbel length (left side)	23,6	21,0	24,4	5	22,6	1,4
Inner mental-barbel length (left side)	12,5	11,3	16,9	5	13,9	2,2
Predorsal length	32,8	31,3	34,9	4	33,1	1,5
Distance between snout tip and terminus of dorsal-fin base	46,5	44,9	47,3	4	46,2	1,0
Distance between snout tip and dorsal-fin distal end	61,7	56,4	61,7	4	58,9	2,2
Dorsal fin to adipose fin	11,1	11,1	11,9	4	11,5	0,4
Dorsal-fin base	14,9	14,1	16,4	4	15,3	1,0
Length of first dorsal-fin ray (unbranched)	21,8	18,1	27,4	4	21,4	4,4
Length of rigid part of first dorsal-fin ray	13,9	10,8	14,8	4	12,6	2,1
Length of second dorsal-fin ray (first branched)	26,2	20,9	26,2	4	23,1	2,5
Length of third dorsal-fin ray (second branched)	24,1	18,8	24,1	4	21,9	2,2
Prepectoral length	20,3	19,5	20,8	4	20,3	0,5
Distance between snout tip and terminus of pectoral-fin base	22,7	22,4	23,1	4	22,8	0,3
Distance between snout tip and pectoral-fin distal end	42,1	37,0	42,1	3	39,9	2,6
Length of first left pectoral-fin ray (unbranched)	22,1	15,9	22,1	4	19,1	2,6
Length of rigid part of first left pectoral-fin ray	18,6	14,3	18,6	4	16,3	1,9
Length of second left pectoral-fin ray (first branched)	20,8	17,8	20,8	3	19,0	1,6
Length of third left pectoral-fin ray (second branched)	18,6	16,1	18,6	2	17,4	1,8
Prepelvic length	45,2	41,3	45,2	4	43,9	1,7
Distance between snout tip and terminus of pelvic-fin base	48,5	44,4	48,5	4	46,5	1,7
Distance between snout tip and pelvic-fin distal end	62,1	57,2	62,1	4	60,0	2,0
Distance between pelvic fins	5,4	3,9	5,4	4	4,6	0,8
Length of first left pelvic-fin ray (unbranched)	16,1	12,3	16,1	4	13,7	1,7
Length of second left pelvic-fin ray (first branched)	17,7	13,1	17,7	4	15,3	1,9
Length of third left pelvic-fin ray (second branched)	18,0	14,2	18,0	4	15,8	1,6
Anal-fin base	12,4	12,4	14,0	4	12,9	0,7
Preanal length	62,4	62,4	66,6	4	64,6	1,7
Distance between snout tip and terminus of anal-fin base	76,7	76,5	79,4	4	77,4	1,4
Distance between snout tip and anal-fin distal end	85,2	84,6	87,4	4	85,7	1,2
Adipose-fin length	35,5	32,1	38,6	4	34,9	2,8
Preadipose length	56,5	56,0	57,1	4	56,5	0,4
Distance between snout tip and adipose-fin base end	88,8	87,8	90,8	4	88,8	1,4
Adipose-fin depth	5,0	2,6	5,0	4	3,7	1,0
Caudal-peduncle length posterior to adipose-fin	9,9	8,2	10,5	4	9,5	1,0
Caudal-peduncle depth at adipose-fin terminus	8,9	7,1	8,9	4	8,0	0,7
Snout-anus distance	51,1	47,4	51,1	4	49,6	1,6
Snout-urogenital papilla distance	60,9	52,4	60,9	4	57,5	4,0

Anus-urogenital papilla distance	10,5	5,0	10,5	4	7,7	2,7
Dorsal lobe of caudal fin length	26,6	26,6	30,7	3	29,0	2,1
Ventral lobe of caudal fin length	20,6	20,6	27,0	3	24,0	3,3

Percentages of HL

Head depth	43,2	43,2	54,6	4	49,4	6,0
Head width	52,8	52,8	61,5	4	57,2	4,2
Eye diameter (left)	26,3	21,3	26,3	4	24,6	2,4
Fleshy interorbital	23,1	22,4	25,7	4	23,7	1,4
Bony interorbital	16,2	15,7	18,7	4	17,2	1,5
Mouth gape	29,3	29,3	34,0	4	31,4	1,9
Snout length (left)	28,5	28,5	30,3	4	29,4	1,0
Distance between snout tip and posterior nare (left side)	17,4	17,4	20,9	4	18,9	1,5
Anterior internarial width	13,7	11,5	14,9	4	13,1	1,5
Posterior internarial width	13,6	13,5	18,5	4	14,8	2,5
Intranarial length (left side)	11,9	11,9	14,4	4	13,3	1,1

Table 34: Morphometric data of *Pimelodella kronei* and *P. transitoria*, its junior-synonym, based on type and comparative materials.

	Holotype	Min.	Max.	<i>n</i>	<i>x</i>	SD
Total length (mm)	144,7	93,8	192,7	19	125,7	
Standard length (mm)	120,1	72,9	164,7	28	105,5	
	Percentages of SL					
Body depth (dorsal)	21,9	16,3	21,9	13	18,5	1,7
Body width (dorsal)	15,9	11,5	17,7	13	14,4	1,6
Cleithral width	18,9	15,8	19,4	13	17,9	1,0
Head length	31,6	24,3	31,7	13	29,7	2,1
Maxillary-barbel length (left side)	38,0	30,0	69,1	19	44,5	11,1
Outer mental-barbel length (left side)	14,9	13,6	29,8	20	19,0	4,4
Inner mental-barbel length (left side)	9,1	6,0	16,4	20	9,7	2,2
Predorsal length	34,2	29,3	34,9	13	33,4	1,6
Distance between snout tip and terminus of dorsal-fin base	47,2	42,7	48,6	13	46,4	1,7
Distance between snout tip and dorsal-fin distal end	55,5	46,6	57,8	12	55,3	3,1
Dorsal fin to adipose fin	13,5	9,2	20,3	26	15,9	2,8
Dorsal-fin base	12,0	11,7	15,8	13	13,4	1,2
Length of first dorsal-fin ray (unbranched)	-	12,9	21,2	19	17,4	2,0
Length of rigid part of first dorsal-fin ray	-	10,3	17,5	23	13,7	1,9
Length of second dorsal-fin ray (first branched)	15,6	12,5	20,4	11	17,8	2,4
Length of third dorsal-fin ray (second branched)	16,3	12,0	20,6	11	17,4	2,4
Prepectoral length	24,6	20,5	25,6	13	22,9	1,5
Distance between snout tip and terminus of pectoral-fin base	27,6	23,4	30,0	13	25,9	1,8
Distance between snout tip and pectoral-fin distal end	41,8	35,0	43,1	13	39,9	2,5
Length of first left pectoral-fin ray (unbranched)	16,0	13,9	20,7	13	17,4	2,1
Length of rigid part of first left pectoral-fin ray	13,7	11,6	19,3	13	15,2	2,0
Length of second left pectoral-fin ray (first branched)	16,6	13,7	19,3	13	16,7	1,7
Length of third left pectoral-fin ray (second branched)	15,7	10,9	17,2	13	15,2	1,8
Prepelvic length	51,4	43,8	51,4	13	47,3	2,2
Distance between snout tip and terminus of pelvic-fin base	54,6	47,2	54,6	13	49,7	2,1
Distance between snout tip and pelvic-fin distal end	63,7	56,3	68,2	12	61,3	2,9
Distance between pelvic fins	5,2	3,9	5,6	13	4,6	0,5
Length of first left pelvic-fin ray (unbranched)	10,8	8,4	14,4	12	11,4	1,7
Length of second left pelvic-fin ray (first branched)	13,4	10,9	15,9	12	13,0	1,8
Length of third left pelvic-fin ray (second branched)	14,6	10,8	17,2	12	13,5	1,7
Anal-fin base	15,3	10,5	16,0	13	14,0	1,5
Preanal length	67,6	61,5	70,0	13	66,1	2,7
Distance between snout tip and terminus of anal-fin base	81,0	75,7	82,7	13	79,2	2,0
Distance between snout tip and anal-fin distal end	87,5	78,5	89,4	13	85,2	2,9
Adipose-fin length	27,4	22,4	32,5	26	26,9	2,3
Preadipose length	61,0	53,9	65,9	26	61,5	2,7
Distance between snout tip and adipose-fin base end	87,8	83,7	91,1	13	87,6	2,1
Adipose-fin depth	5,9	1,9	5,9	13	3,9	1,0
Caudal-peduncle length posterior to adipose-fin	11,4	11,2	14,8	13	12,8	1,1
Caudal-peduncle depth at adipose-fin terminus	8,4	7,0	9,0	13	7,9	0,6
Snout-anus distance	57,3	25,0	57,3	13	51,0	7,8

Snout-urogenital papilla distance	61,7	53,9	61,7	13	57,5	2,4
Anus-urogenital papilla distance	4,9	2,9	6,7	13	4,4	1,2
Dorsal lobe of caudal fin length	22,7	17,2	28,0	11	22,6	3,2
Ventral lobe of caudal fin length	19,3	15,9	25,0	11	19,9	2,6

Percentages of HL

Head depth	49,3	41,9	56,5	13	47,3	5,3
Head width	62,5	53,9	66,8	13	60,4	4,1
Eye diameter (left)	-	16,4	20,6	6	18,5	1,5
Fleshy interorbital	-	20,9	30,3	6	24,1	3,4
Bony interorbital	-	14,6	22,9	6	17,4	2,8
Mouth gape	36,7	31,2	36,7	13	33,5	1,5
Snout length (left)	-	29,5	39,6	6	32,6	3,4
Distance between snout tip and posterior nare (left side)	19,1	17,7	24,8	13	19,9	1,7
Anterior internarial width	12,5	12,0	16,2	13	13,8	1,2
Posterior internarial width	12,5	11,3	19,1	13	14,0	2,0
Intranarial length (left side)	11,6	11,6	18,9	13	15,3	1,6

Table 35: Morphometric data of *Pimelodella kronei* and *P. transitoria*, its junior-synonym, based on type and comparative materials, discriminated by original species name.

	<i>P. kronei</i>						<i>P. transitoria</i>					
	Holotype	Min.	Max.	n	x	SD	Neotype	Min.	Max.	n	x	SD
Total length (mm)	144,7	93,8	192,7	13	127,0		124,2	100,5	167,5	7	123,1	
Standard length (mm)	120,1	72,9	164,7	17	100,7		107,4	83,8	143,6	12	112,5	
		Percentages of SL						Percentages of SL				
Body depth (dorsal)	21,9	17,4	21,9	7	18,7	1,7	20,6	16,3	20,6	7	18,2	1,7
Body width (dorsal)	15,9	13,3	17,7	7	15,1	1,6	15,0	11,5	15,0	7	13,8	1,3
Cleithral width	18,9	15,8	18,9	7	17,6	1,2	17,8	17,2	19,4	7	18,2	0,8
Head length	31,6	27,0	31,7	7	30,1	2,1	24,3	24,3	31,1	7	29,2	2,3
Maxillary-barbel length (left side)	38,0	33,8	62,0	12	42,4	10,0	47,3	30,0	69,1	8	47,8	12,6
Outer mental-barbel length (left side)	14,9	13,6	25,5	12	17,4	3,8	21,7	16,3	29,8	9	21,2	4,4
Inner mental-barbel length (left side)	9,1	6,0	11,7	12	9,5	1,7	8,2	7,7	16,4	9	10,0	2,8
Predorsal length	34,2	29,3	34,9	7	32,8	2,1	34,6	33,2	34,6	7	34,0	0,5
Distance between snout tip and terminus of dorsal-fin base	47,2	42,7	47,2	7	45,5	1,9	47,7	45,5	48,6	7	47,3	1,0
Distance between snout tip and dorsal-fin distal end	55,5	46,6	56,8	6	53,6	3,9	56,6	53,8	57,8	7	56,7	1,3
Dorsal fin to adipose fin	13,5	9,2	20,3	15	15,2	3,1	18,5	12,5	19,4	12	16,8	2,1
Dorsal-fin base	12,0	11,7	14,2	7	12,6	0,9	13,6	13,2	15,8	7	14,2	0,8
Length of first dorsal-fin ray (unbranched)	-	12,9	18,9	11	16,5	1,6	18,7	16,2	21,2	7	19,0	1,7
Length of rigid part of first dorsal-fin ray	-	10,3	14,7	13	12,9	1,4	13,8	11,6	17,5	11	14,7	2,0
Length of second dorsal-fin ray (first branched)	15,6	12,5	19,8	6	16,9	2,7	0,0	16,6	20,1	4	18,6	1,5
Length of third dorsal-fin ray (second branched)	16,3	12,0	18,6	6	16,1	2,4	18,5	16,6	20,6	6	18,7	1,5
Prepectoral length	24,6	20,5	24,6	7	22,9	1,7	22,5	21,3	25,6	7	22,9	1,5
Distance between snout tip and terminus of pectoral-fin base	27,6	23,4	27,6	7	25,8	1,6	25,6	23,6	30,0	7	25,9	2,0
Distance between snout tip and pectoral-fin distal end	41,8	35,0	43,1	7	39,6	3,6	39,8	39,3	41,4	7	40,1	0,7
Length of first left pectoral-fin ray (unbranched)	16,0	13,9	19,6	7	16,5	2,2	15,9	15,9	20,7	7	18,4	1,6
Length of rigid part of first left pectoral-fin ray	13,7	11,6	16,1	7	13,7	1,5	16,9	14,7	19,3	7	16,6	1,3
Length of second left pectoral-fin ray (first branched)	16,6	13,7	18,8	7	16,1	1,9	14,9	14,9	19,3	7	17,2	1,3

Length of third left pectoral-fin ray (second branched)	15,7	10,9	17,1	7	14,6	2,4	14,9	14,9	17,2	7	15,9	0,8
Prepelvic length	51,4	43,8	51,4	7	46,6	2,4	47,2	46,7	51,0	7	48,0	1,7
Distance between snout tip and terminus of pelvic-fin base	54,6	47,2	54,6	7	49,1	2,6	50,1	48,6	52,4	7	50,3	1,5
Distance between snout tip and pelvic-fin distal end	63,7	56,3	63,7	6	60,4	2,9	61,7	58,6	68,2	7	62,1	3,0
Distance between pelvic fins	5,2	3,9	5,6	7	4,7	0,7	4,8	4,0	4,8	7	4,5	0,3
Length of first left pelvic-fin ray (unbranched)	10,8	8,4	13,1	6	11,0	1,9	11,8	10,0	14,4	7	11,6	1,6
Length of second left pelvic-fin ray (first branched)	13,4	10,9	15,5	6	13,1	1,9	12,4	11,1	15,9	7	12,9	1,8
Length of third left pelvic-fin ray (second branched)	14,6	10,8	14,7	6	13,4	1,6	12,6	12,0	17,2	7	13,6	1,9
Anal-fin base	15,3	12,0	16,0	7	14,3	1,4	10,5	10,5	15,3	7	13,6	1,6
Preanal length	67,6	61,5	67,6	7	64,5	2,4	70,0	65,4	70,0	7	67,8	1,8
Distance between snout tip and terminus of anal-fin base	81,0	75,7	81,0	7	78,2	1,6	79,1	77,2	82,7	7	80,1	1,8
Distance between snout tip and anal-fin distal end	87,5	78,5	87,5	7	83,5	2,7	86,5	83,8	89,4	7	86,9	1,9
Adipose-fin length	27,4	24,3	32,5	15	27,1	2,0	24,4	22,4	31,4	12	26,6	2,7
Preadipose length	61,0	53,9	62,9	15	60,0	2,3	64,5	60,1	65,9	11	63,3	2,0
Distance between snout tip and adipose-fin base end	87,8	83,7	87,8	7	86,2	1,4	87,6	86,8	91,1	7	89,1	1,6
Adipose-fin depth	5,9	1,9	5,9	7	4,1	1,2	2,5	2,5	5,0	7	3,7	0,9
Caudal-peduncle length posterior to adipose-fin	11,4	11,4	14,8	7	13,2	1,1	11,8	11,2	13,9	7	12,3	1,0
Caudal-peduncle depth at adipose-fin terminus	8,4	7,3	9,0	7	8,0	0,6	7,0	7,0	8,9	7	7,8	0,6
Snout-anus distance	57,3	50,5	57,3	7	52,5	2,3	54,7	25,0	56,2	7	49,4	10,9
Snout-urogenital papilla distance	61,7	53,9	61,7	7	57,0	2,6	56,5	54,4	60,6	7	58,0	2,2
Anus-urogenital papilla distance	4,9	2,9	6,7	7	4,9	1,3	3,2	3,0	5,3	7	4,0	0,9
Dorsal lobe of caudal fin length	22,7	18,2	26,3	6	22,0	2,7	17,2	17,2	28,0	5	23,6	4,0
Ventral lobe of caudal fin length	19,3	15,9	21,6	6	18,9	2,5	18,0	18,0	25,0	6	20,8	2,5

	Percentages of HL						Percentages of HL					
Head depth	49,3	42,1	55,4	7	47,4	5,1	56,5	41,9	56,5	7	47,2	6,0
Head width	62,5	53,9	64,4	7	61,0	3,4	66,8	55,8	66,8	7	59,9	4,8
Eye diameter (left)	-	-	-	-	-	-	20,3	16,4	20,6	7	18,5	1,5
Fleshy interorbital	-	-	-	-	-	-	30,3	20,9	30,3	7	24,1	3,4
Bony interorbital	-	-	-	-	-	-	22,9	14,6	22,9	7	17,4	2,8
Mouth gape	36,7	32,6	36,7	7	34,3	1,5	33,5	31,2	34,5	7	32,8	1,2
Snout length (left)	-	-	-	-	-	-	39,6	29,5	39,6	7	32,6	3,4

Distance between snout tip and posterior nare (left side)	19,1	17,7	20,0	7	19,2	0,7	24,8	17,9	24,8	7	20,5	2,2
Anterior internarial width	12,5	12,0	14,9	7	13,5	1,2	16,2	12,6	16,2	7	14,0	1,3
Posterior internarial width	12,5	11,3	14,9	7	13,3	1,3	19,1	12,3	19,1	7	14,8	2,3
Intranarial length (left side)	11,6	11,6	15,6	7	14,5	1,4	18,9	14,8	18,9	7	16,1	1,4

Table 36: Morphometric data of *Pimelodella lateristriga* and *P. bahiana*, its junior-synonym, based on type and comparative materials.

	Holotype	Min.	Max.	<i>n</i>	<i>x</i>	SD
Total length (mm)	118,0	71,1	140,1	15	112,9	
Standard length (mm)	95,9	39,9	112,7	21	77,8	
	Percentages of SL					
Body depth (dorsal)	13,6	13,6	20,2	15	17,3	1,8
Body width (dorsal)	11,2	11,2	14,4	15	13,0	1,0
Cleithral width	17,1	16,0	18,0	15	17,0	0,7
Head length	29,0	26,8	31,0	15	29,3	1,1
Maxillary-barbel length (left side)	64,8	51,2	76,3	13	63,3	7,1
Outer mental-barbel length (left side)	19,6	18,1	26,4	15	22,9	2,7
Inner mental-barbel length (left side)	12,0	7,6	15,0	15	11,9	2,1
Predorsal length	32,7	29,2	34,3	15	32,6	1,5
Distance between snout tip and terminus of dorsal-fin base	46,7	33,4	48,7	15	45,1	3,5
Distance between snout tip and dorsal-fin distal end	55,6	47,2	60,0	15	54,6	3,0
Dorsal fin to adipose fin	15,9	9,1	17,9	15	14,8	2,6
Dorsal-fin base	14,0	13,2	27,9	15	15,8	3,8
Length of first dorsal-fin ray (unbranched)	-	17,5	23,7	11	20,8	2,0
Length of rigid part of first dorsal-fin ray	-	14,3	19,8	14	16,4	1,9
Length of second dorsal-fin ray (first branched)	18,8	17,3	23,6	15	20,2	1,8
Length of third dorsal-fin ray (second branched)	15,7	11,6	21,6	15	18,1	2,5
Prepectoral length	20,1	18,8	27,4	15	21,4	2,1
Distance between snout tip and terminus of pectoral-fin base	22,5	22,5	29,8	15	24,7	1,9
Distance between snout tip and pectoral-fin distal end	38,2	37,0	47,3	15	41,1	2,7
Length of first left pectoral-fin ray (unbranched)	-	17,2	24,0	13	19,9	1,9
Length of rigid part of first left pectoral-fin ray	-	15,8	21,9	13	18,2	1,7
Length of second left pectoral-fin ray (first branched)	18,9	15,1	21,6	14	18,7	1,8
Length of third left pectoral-fin ray (second branched)	16,4	14,3	19,2	14	17,0	1,4
Prepelvic length	47,8	42,4	49,9	15	45,5	2,0
Distance between snout tip and terminus of pelvic-fin base	49,8	44,5	52,6	15	48,2	2,1
Distance between snout tip and pelvic-fin distal end	62,5	56,5	67,8	15	60,6	2,8
Distance between pelvic fins	3,9	3,9	5,1	15	4,5	0,5
Length of first left pelvic-fin ray (unbranched)	9,8	9,8	14,6	14	11,8	1,3
Length of second left pelvic-fin ray (first branched)	12,6	11,7	16,6	14	13,7	1,7
Length of third left pelvic-fin ray (second branched)	13,3	11,7	16,1	14	13,9	1,4
Anal-fin base	14,0	11,5	16,1	15	14,0	1,2
Preanal length	65,5	60,6	69,9	15	64,9	2,2
Distance between snout tip and terminus of anal-fin base	78,6	76,5	85,2	15	79,1	2,3
Distance between snout tip and anal-fin distal end	85,8	83,9	93,0	15	86,6	2,6
Adipose-fin length	27,4	25,7	33,5	15	28,2	2,4
Preadipose length	59,2	53,9	63,0	15	59,1	3,1
Distance between snout tip and adipose-fin base end	86,2	82,9	90,1	15	86,7	2,0
Adipose-fin depth	3,9	2,9	6,1	15	4,3	0,9
Caudal-peduncle length posterior to adipose-fin	13,7	10,2	16,0	15	13,3	1,3
Caudal-peduncle depth at adipose-fin terminus	7,8	6,4	9,0	15	7,8	0,6
Snout-anus distance	52,0	47,9	54,6	15	51,2	2,2

Snout-urogenital papilla distance	56,4	53,6	60,3	15	55,9	1,9
Anus-urogenital papilla distance	4,3	2,8	5,8	15	4,2	0,9
Dorsal lobe of caudal fin length	25,7	22,2	28,3	12	26,1	1,7
Ventral lobe of caudal fin length	22,0	18,4	26,3	14	23,0	2,4

Percentages of HL

Head depth	38,3	38,3	54,5	14	46,1	3,9
Head width	55,3	47,6	63,3	15	56,0	3,9
Eye diameter (left)	20,2	17,5	23,5	15	20,8	1,6
Fleshy interorbital	20,6	19,0	24,8	15	21,4	1,6
Bony interorbital	15,9	11,0	16,8	15	14,5	1,7
Mouth gape	30,4	27,0	34,9	15	31,3	2,3
Snout length (left)	29,5	28,3	33,0	15	30,7	1,3
Distance between snout tip and posterior nare (left side)	17,6	16,3	22,6	15	19,7	1,6
Anterior internarial width	12,2	10,8	14,9	15	13,0	1,2
Posterior internarial width	12,1	10,2	15,9	15	14,0	1,5
Intranarial length (left side)	14,7	11,2	16,2	15	14,6	1,4

Table 37: Morphometric data of *Pimelodella lateristriga* and *P. bahiana*, its junior-synonym, based on type and comparative materials, discriminated by original species name.

	<i>P. lateristriga</i>						<i>P. bahiana</i>					
	Holotype	Min.	Max.	<i>n</i>	<i>x</i>	SD	Lectotype	Min.	Max.	<i>n</i>	<i>x</i>	SD
Total length (mm)	118,0	71,1	140,1	11	111,1		115,7	103,4	133,7	3	117,6	
Standard length (mm)	95,9	39,9	112,7	17	74,6		93,4	81,0	101,0	3	91,7	
	Percentages of SL											
Body depth (dorsal)	13,6	13,6	20,2	11	17,2	1,8	16,2	15,1	19,8	3	17,4	2,2
Body width (dorsal)	11,2	11,2	13,8	11	12,6	0,9	14,3	13,6	14,4	3	14,1	0,4
Cleithral width	17,1	16,2	18,0	11	17,0	0,6	16,8	16,0	17,7	3	17,0	0,8
Head length	29,0	26,8	30,8	11	29,3	1,2	28,6	28,6	31,0	3	29,6	1,0
Maxillary-barbel length (left side)	64,8	51,2	76,3	10	64,4	7,7	57,4	57,4	62,2	3	59,7	2,4
Outer mental-barbel length (left side)	19,6	19,6	26,4	11	23,9	2,5	21,8	18,1	21,8	3	20,3	1,6
Inner mental-barbel length (left side)	12,0	10,2	15,0	11	12,6	1,6	9,3	7,6	12,4	3	10,0	2,1
Predorsal length	32,7	29,2	34,0	11	32,3	1,6	33,6	32,7	34,3	3	33,5	0,6
Distance between snout tip and terminus of dorsal-fin base	46,7	43,9	48,7	11	46,2	1,5	45,0	44,2	47,7	3	45,6	1,5
Distance between snout tip and dorsal-fin distal end	55,6	33,4	60,0	11	52,6	7,4	54,7	52,4	56,0	3	54,4	1,5
Dorsal fin to adipose fin	15,9	9,1	55,8	11	17,9	12,9	15,2	15,2	16,7	3	15,8	0,6
Dorsal-fin base	14,0	13,2	15,6	11	14,5	0,7	27,9	13,8	27,9	3	19,5	6,5
Length of first dorsal-fin ray (unbranched)	-	17,5	23,7	10	20,9	2,1	0,0	17,9	20,6	1	19,2	1,9
Length of rigid part of first dorsal-fin ray	-	14,6	19,8	10	17,0	1,9	15,3	14,3	16,0	3	15,0	0,9
Length of second dorsal-fin ray (first branched)	18,8	17,3	23,6	11	20,6	2,0	20,0	18,5	20,0	3	19,1	0,7
Length of third dorsal-fin ray (second branched)	15,7	11,6	21,6	11	18,1	2,9	19,8	16,6	19,8	3	18,0	1,3
Prepectoral length	20,1	18,8	27,4	11	21,1	2,3	24,2	21,2	24,2	3	22,4	1,3
Distance between snout tip and terminus of pectoral-fin base	22,5	22,5	40,4	11	25,9	5,2	26,6	24,2	26,6	3	25,5	1,1
Distance between snout tip and pectoral-fin distal end	38,2	24,1	47,3	11	39,7	6,0	41,1	39,6	42,1	3	41,2	1,2
Length of first left pectoral-fin ray (unbranched)	-	17,2	24,0	9	20,4	2,1	18,6	18,2	19,3	3	18,8	0,5
Length of rigid part of first left pectoral-fin ray	-	15,8	21,9	10	18,4	1,9	17,2	16,9	17,8	3	17,2	0,4
Length of second left pectoral-fin ray (first branched)	18,9	15,1	21,6	10	19,1	1,8	18,4	15,9	19,5	3	17,9	1,5

Length of third left pectoral-fin ray (second branched)	16,4	14,9	19,2	10	17,3	1,4	18,0	14,3	18,0	3	16,2	1,5
Prepelvic length	47,8	42,4	49,9	11	45,2	2,2	47,6	45,5	47,6	3	46,4	1,0
Distance between snout tip and terminus of pelvic-fin base	49,8	44,5	52,6	11	47,9	2,3	49,4	48,7	49,6	3	49,2	0,4
Distance between snout tip and pelvic-fin distal end	62,5	56,5	67,8	11	60,1	3,1	62,7	61,1	62,7	3	61,8	0,8
Distance between pelvic fins	3,9	3,9	5,0	11	4,5	0,4	5,1	4,0	5,1	3	4,5	0,6
Length of first left pelvic-fin ray (unbranched)	9,8	9,8	14,6	10	12,0	1,5	11,3	10,9	12,0	3	11,3	0,5
Length of second left pelvic-fin ray (first branched)	12,6	11,7	16,6	10	14,0	1,8	12,7	11,7	14,6	3	12,9	1,2
Length of third left pelvic-fin ray (second branched)	13,3	11,7	16,1	10	14,0	1,6	14,4	11,9	14,5	3	13,5	1,2
Anal-fin base	14,0	13,1	16,1	11	14,4	0,9	12,4	11,5	14,4	3	13,0	1,3
Preanal length	65,5	60,6	67,3	11	64,3	1,9	69,9	65,0	69,9	3	66,7	2,3
Distance between snout tip and terminus of anal-fin base	78,6	76,5	85,2	11	79,0	2,6	81,0	78,5	81,0	3	79,6	1,0
Distance between snout tip and anal-fin distal end	85,8	83,9	93,0	11	86,4	2,9	89,7	85,5	89,7	3	87,0	1,9
Adipose-fin length	27,4	25,7	33,5	11	28,9	2,5	26,7	25,9	26,9	3	26,5	0,4
Preadipose length	59,2	53,9	63,0	11	58,4	3,3	61,7	59,4	62,2	3	61,1	1,2
Distance between snout tip and adipose-fin base end	86,2	82,9	90,1	11	86,3	2,2	89,5	86,5	89,5	3	87,6	1,4
Adipose-fin depth	3,9	2,9	6,1	11	4,4	1,1	3,9	3,9	4,9	3	4,3	0,5
Caudal-peduncle length posterior to adipose-fin	13,7	12,0	16,0	11	13,7	1,0	10,2	10,2	13,7	3	12,2	1,5
Caudal-peduncle depth at adipose-fin terminus	7,8	6,4	8,6	11	7,7	0,6	9,0	7,1	9,0	3	7,8	0,8
Snout-anus distance	52,0	47,9	54,6	11	50,8	2,2	53,6	50,1	53,7	3	52,3	1,7
Snout-urogenital papilla distance	56,4	53,6	58,5	11	55,5	1,7	60,3	55,2	60,3	3	57,0	2,3
Anus-urogenital papilla distance	4,3	3,4	5,8	11	4,5	0,7	3,3	2,8	3,8	3	3,3	0,4
Dorsal lobe of caudal fin length	25,7	22,2	28,0	10	25,8	1,7	26,2	25,4	28,3	2	26,6	1,5
Ventral lobe of caudal fin length	22,0	19,7	26,3	10	23,3	1,9	23,6	18,4	26,3	3	22,2	3,5

Percentages of HL

Head depth	38,3	38,3	54,5	10	45,7	4,2	47,3	43,2	50,9	3	47,0	3,2
Head width	55,3	47,6	63,3	11	56,0	4,2	57,2	52,3	60,5	3	56,3	3,5
Eye diameter (left)	20,2	17,5	57,6	11	23,8	11,3	21,1	21,1	23,5	3	22,0	1,1
Fleshy interorbital	20,6	19,0	24,8	11	21,6	1,7	20,9	19,1	22,8	3	21,0	1,5
Bony interorbital	15,9	11,0	16,4	11	14,4	1,8	15,0	13,1	16,8	3	14,6	1,7
Mouth gape	30,4	27,0	34,9	11	30,8	2,4	32,7	31,1	34,5	3	32,8	1,4
Snout length (left)	29,5	29,1	33,0	11	30,9	1,3	31,1	28,3	31,1	3	30,0	1,2

Distance between snout tip and posterior nare (left side)	17,6	16,3	21,5	11	19,4	1,5	20,5	18,4	22,6	3	20,5	1,7
Anterior internarial width	12,2	12,1	14,9	11	13,2	1,1	10,8	10,8	14,1	3	12,5	1,5
Posterior internarial width	12,1	12,1	15,5	11	14,1	1,0	12,4	10,2	15,9	3	13,5	2,7
Intranarial length (left side)	14,7	13,3	16,2	11	14,9	0,9	12,5	11,2	16,1	3	13,8	2,4

Table 38: Morphometric data of *Pimelodella laticeps* based on type material.

	Holotype	Paratype
Total length (mm)	60,5	88,5
Standard length (mm)	49,0	72,7
Percentages of SL		
Body depth (dorsal)	19,8	18,9
Body width (dorsal)	14,3	16,0
Cleithral width	19,6	19,2
Head length	32,1	32,9
Maxillary-barbel length (left side)	54,3	50,6
Outer mental-barbel length (left side)	21,8	23,3
Inner mental-barbel length (left side)	12,3	13,7
Predorsal length	36,9	37,2
Distance between snout tip and terminus of dorsal-fin base	50,3	49,4
Distance between snout tip and dorsal-fin distal end	62,3	59,3
Dorsal fin to adipose fin	14,0	19,4
Dorsal-fin base	14,2	14,7
Length of first dorsal-fin ray (unbranched)	19,6	-
Length of rigid part of first dorsal-fin ray	16,5	13,5
Length of second dorsal-fin ray (first branched)	19,6	18,3
Length of third dorsal-fin ray (second branched)	20,8	17,5
Prepectoral length	25,0	22,9
Distance between snout tip and terminus of pectoral-fin base	27,4	25,5
Distance between snout tip and pectoral-fin distal end	45,5	41,0
Length of first left pectoral-fin ray (unbranched)	22,1	-
Length of rigid part of first left pectoral-fin ray	19,6	18,0
Length of second left pectoral-fin ray (first branched)	22,2	17,7
Length of third left pectoral-fin ray (second branched)	20,6	15,7
Prepelvic length	50,1	48,8
Distance between snout tip and terminus of pelvic-fin base	52,0	51,0
Distance between snout tip and pelvic-fin distal end	66,9	62,8
Distance between pelvic fins	6,0	4,5
Length of first left pelvic-fin ray (unbranched)	14,6	10,6
Length of second left pelvic-fin ray (first branched)	15,9	12,9
Length of third left pelvic-fin ray (second branched)	16,7	13,8
Anal-fin base	14,9	14,3
Preanal length	67,2	71,0
Distance between snout tip and terminus of anal-fin base	82,1	83,5
Distance between snout tip and anal-fin distal end	90,6	89,9
Adipose-fin length	25,7	24,5
Preadipose length	64,4	66,4
Distance between snout tip and adipose-fin base end	87,9	89,2
Adipose-fin depth	5,4	4,2
Caudal-peduncle length posterior to adipose-fin	11,1	10,4
Caudal-peduncle depth at adipose-fin terminus	9,7	8,6
Snout-anus distance	56,3	53,5
Snout-urogenital papilla distance	64,2	58,3

Anus-urogenital papilla distance	8,6	4,6
Dorsal lobe of caudal fin length	27,5	24,1
Ventral lobe of caudal fin length	25,8	23,9

Percentages of HL

Head depth	57,6	46,3
Head width	61,3	56,1
Eye diameter (left)	17,9	15,3
Fleshy interorbital	27,9	24,0
Bony interorbital	20,2	20,2
Mouth gape	33,7	24,7
Snout length (left)	30,7	28,0
Distance between snout tip and posterior nare (left side)	22,2	18,5
Anterior internarial width	14,6	10,8
Posterior internarial width	17,8	15,0
Intranarial length (left side)	14,8	14,1

Table 39: Morphometric data of *Pimelodella laurenti* based on type and comparative materials.

	Holotype	Min.	Max.	<i>n</i>	<i>x</i>	SD
Total length (mm)	77,6	76,4	115,2	4	87,6	
Standard length (mm)	66,5	59,5	92,7	5	69,7	
	Percentages of SL					
Body depth (dorsal)	20,8	18,7	22,1	5	20,0	1,4
Body width (dorsal)	15,2	12,6	18,9	5	15,8	2,4
Cleithral width	19,2	17,3	19,2	5	18,4	0,9
Head length	31,8	28,8	31,8	5	30,2	1,5
Maxillary-barbel length (left side)	90,6	79,6	102,1	5	87,7	9,2
Outer mental-barbel length (left side)	39,7	29,9	39,7	5	35,2	4,0
Inner mental-barbel length (left side)	20,2	14,4	23,3	5	18,9	3,4
Predorsal length	36,2	31,4	36,2	5	33,7	1,9
Distance between snout tip and terminus of dorsal-fin base	50,6	46,9	50,7	5	48,6	1,9
Distance between snout tip and dorsal-fin distal end	60,5	55,2	61,8	5	58,3	2,8
Dorsal fin to adipose fin	8,3	7,9	11,9	5	9,7	1,6
Dorsal-fin base	14,9	14,9	17,4	5	15,6	1,1
Length of first dorsal-fin ray (unbranched)	-	18,8	20,8	3	20,1	1,1
Length of rigid part of first dorsal-fin ray	21,2	15,0	21,2	4	17,2	2,8
Length of second dorsal-fin ray (first branched)	20,6	19,3	24,7	5	21,5	2,1
Length of third dorsal-fin ray (second branched)	19,3	18,2	22,2	5	20,6	1,7
Prepectoral length	25,0	20,9	26,9	5	23,6	2,4
Distance between snout tip and terminus of pectoral-fin base	29,0	25,0	30,3	5	27,8	2,0
Distance between snout tip and pectoral-fin distal end	43,6	28,5	46,0	5	40,7	7,3
Length of first left pectoral-fin ray (unbranched)	-	19,1	22,5	4	21,4	1,5
Length of rigid part of first left pectoral-fin ray	19,0	17,0	19,0	4	18,2	0,9
Length of second left pectoral-fin ray (first branched)	19,7	18,1	22,4	5	20,5	1,7
Length of third left pectoral-fin ray (second branched)	18,7	16,3	20,4	5	18,7	1,7
Prepelvic length	49,9	43,3	51,2	5	47,4	3,2
Distance between snout tip and terminus of pelvic-fin base	52,2	45,9	53,7	5	50,3	3,0
Distance between snout tip and pelvic-fin distal end	65,9	62,1	69,5	5	64,4	3,3
Distance between pelvic fins	5,0	3,9	5,1	5	4,8	0,5
Length of first left pelvic-fin ray (unbranched)	12,9	4,9	13,1	5	11,1	3,5
Length of second left pelvic-fin ray (first branched)	15,1	13,8	17,7	5	15,5	1,7
Length of third left pelvic-fin ray (second branched)	15,7	14,4	17,2	5	15,9	1,0
Anal-fin base	12,6	11,3	13,2	5	12,6	0,7
Preanal length	68,4	63,8	68,4	5	65,6	1,7
Distance between snout tip and terminus of anal-fin base	81,8	76,5	81,8	5	78,1	2,2
Distance between snout tip and anal-fin distal end	89,5	83,9	89,5	5	86,0	2,1
Adipose-fin length	37,8	32,4	49,9	5	37,1	7,5
Preadipose length	58,1	53,9	58,4	5	56,8	1,9
Distance between snout tip and adipose-fin base end	95,4	87,1	95,4	5	89,6	3,4
Adipose-fin depth	6,0	4,4	6,4	5	5,7	0,8
Caudal-peduncle length posterior to adipose-fin	8,9	8,9	11,9	5	10,7	1,1
Caudal-peduncle depth at adipose-fin terminus	8,2	7,9	9,7	5	8,4	0,7
Snout-anus distance	56,5	52,1	57,9	5	55,0	2,4

Snout-urogenital papilla distance	60,5	58,1	63,6	5	60,7	2,1
Anus-urogenital papilla distance	4,0	4,0	11,5	5	6,4	2,9
Dorsal lobe of caudal fin length	-	28,2	33,4	2	30,8	3,7
Ventral lobe of caudal fin length	-	20,9	28,6	4	24,9	3,7

Percentages of HL

Head depth	54,6	50,2	58,6	5	53,8	3,1
Head width	57,7	57,7	66,7	5	62,9	4,4
Eye diameter (left)	21,4	21,1	26,1	5	23,2	2,1
Fleshy interorbital	19,8	19,2	23,8	5	20,9	1,8
Bony interorbital	13,8	13,3	16,1	5	14,4	1,1
Mouth gape	25,8	25,8	35,5	5	31,9	4,0
Snout length (left)	29,2	29,2	32,9	5	31,4	1,4
Distance between snout tip and posterior nare (left side)	19,4	18,2	20,4	5	19,5	0,9
Anterior internarial width	12,9	12,9	15,0	5	13,6	0,8
Posterior internarial width	14,4	13,8	15,7	5	14,4	0,8
Intranarial length (left side)	14,6	14,6	16,4	5	15,9	0,7

Table 40: Morphometric data of *Pimelodella leptosoma* based on type and comparative materials.

	Holotype	Min.	Max.	<i>n</i>	<i>x</i>	SD
Total length (mm)	76,6	74,1	113,3	4	88,7	
Standard length (mm)	59,6	57,9	92,7	4	70,8	
	Percentages of SL					
Body depth (dorsal)	12,9	11,8	16,9	4	14,0	2,2
Body width (dorsal)	11,6	10,4	14,2	4	12,2	1,6
Cleithral width	14,7	14,7	16,7	4	15,6	0,9
Head length	27,1	27,0	28,7	4	27,6	0,8
Maxillary-barbel length (left side)	76,6	76,6	83,9	4	79,7	3,1
Outer mental-barbel length (left side)	21,2	21,2	35,1	4	27,0	6,4
Inner mental-barbel length (left side)	12,3	12,3	19,2	4	15,0	3,0
Predorsal length	31,0	27,9	33,0	4	30,9	2,2
Distance between snout tip and terminus of dorsal-fin base	45,9	44,4	47,0	4	45,5	1,2
Distance between snout tip and dorsal-fin distal end	0,0	55,3	58,1	3	56,8	1,4
Dorsal fin to adipose fin	8,1	7,2	11,5	4	8,6	2,0
Dorsal-fin base	15,0	13,9	15,4	4	14,7	0,7
Length of first dorsal-fin ray (unbranched)	0,0	16,6	19,2	2	17,9	1,8
Length of rigid part of first dorsal-fin ray	10,5	10,1	12,8	4	11,4	1,3
Length of second dorsal-fin ray (first branched)	0,0	17,4	19,9	3	18,8	1,2
Length of third dorsal-fin ray (second branched)	0,0	17,4	20,4	3	19,3	1,7
Prepectoral length	19,6	19,6	22,7	4	20,7	1,4
Distance between snout tip and terminus of pectoral-fin base	22,7	22,2	25,4	4	23,5	1,4
Distance between snout tip and pectoral-fin distal end	36,0	33,7	39,4	4	37,1	2,7
Length of first left pectoral-fin ray (unbranched)	17,0	17,0	20,0	3	19,0	1,7
Length of rigid part of first left pectoral-fin ray	14,2	14,2	16,1	3	15,3	1,0
Length of second left pectoral-fin ray (first branched)	16,6	16,6	19,1	3	18,0	1,3
Length of third left pectoral-fin ray (second branched)	15,4	15,4	17,1	3	16,4	0,9
Prepelvic length	41,8	41,8	45,5	4	43,7	1,6
Distance between snout tip and terminus of pelvic-fin base	44,3	43,5	48,2	4	45,7	2,3
Distance between snout tip and pelvic-fin distal end	55,5	55,5	61,3	4	58,4	2,5
Distance between pelvic fins	5,0	4,3	5,4	4	4,7	0,5
Length of first left pelvic-fin ray (unbranched)	8,7	8,7	12,7	4	11,2	1,9
Length of second left pelvic-fin ray (first branched)	12,5	12,5	14,2	4	13,4	0,8
Length of third left pelvic-fin ray (second branched)	13,1	13,1	13,9	4	13,5	0,4
Anal-fin base	15,6	12,4	15,6	4	14,0	1,5
Preanal length	67,0	66,4	67,1	4	66,9	0,3
Distance between snout tip and terminus of anal-fin base	79,5	78,6	79,5	4	79,0	0,4
Distance between snout tip and anal-fin distal end	88,0	86,3	88,0	4	87,0	0,7
Adipose-fin length	36,4	36,4	37,5	4	37,1	0,5
Preadipose length	54,4	53,5	54,7	4	54,1	0,5
Distance between snout tip and adipose-fin base end	90,7	89,4	91,3	4	90,6	0,8
Adipose-fin depth	4,0	3,5	4,6	4	4,1	0,4
Caudal-peduncle length posterior to adipose-fin	9,5	9,1	10,3	4	9,5	0,6
Caudal-peduncle depth at adipose-fin terminus	6,7	6,6	8,3	4	7,4	0,9
Snout-anus distance	46,9	46,9	50,7	4	48,8	1,7

Snout-urogenital papilla distance	51,0	51,0	55,5	4	53,3	1,8
Anus-urogenital papilla distance	4,4	3,9	4,9	4	4,4	0,4
Dorsal lobe of caudal fin length	32,0	24,1	32,0	2	28,1	5,6
Ventral lobe of caudal fin length	25,3	22,6	25,3	4	24,5	1,3

Percentages of HL

Head depth	44,0	44,0	49,3	4	46,1	2,4
Head width	57,9	57,7	58,9	4	58,2	0,5
Eye diameter (left)	24,0	22,8	29,7	4	25,6	3,0
Fleshy interorbital	22,4	20,8	24,0	4	22,8	1,5
Bony interorbital	15,7	10,9	17,1	4	14,0	2,9
Mouth gape	33,6	30,4	34,0	4	32,9	1,7
Snout length (left)	30,0	28,8	30,4	4	29,9	0,7
Distance between snout tip and posterior nare (left side)	17,9	17,8	20,7	4	18,9	1,4
Anterior internarial width	14,0	10,6	14,0	4	12,7	1,6
Posterior internarial width	14,6	14,1	15,3	4	14,6	0,5
Intranarial length (left side)	15,7	15,0	17,5	4	16,0	1,1

Table 41: Morphometric data of *Pimelodella linami* based on type material.

	Holotype
Total length (mm)	93,3
Standard length (mm)	74,7
Percentages of SL	
Body depth (dorsal)	17,2
Body width (dorsal)	13,3
Cleithral width	16,1
Head length	28,7
Maxillary-barbel length (left side)	63,3
Outer mental-barbel length (left side)	25,7
Inner mental-barbel length (left side)	14,3
Predorsal length	32,2
Distance between snout tip and terminus of dorsal-fin base	46,6
Distance between snout tip and dorsal-fin distal end	68,2
Dorsal fin to adipose fin	15,6
Dorsal-fin base	14,2
Length of first dorsal-fin ray (unbranched)	36,8
Length of rigid part of first dorsal-fin ray	13,5
Length of second dorsal-fin ray (first branched)	20,9
Length of third dorsal-fin ray (second branched)	18,4
Prepectoral length	22,9
Distance between snout tip and terminus of pectoral-fin base	26,1
Distance between snout tip and pectoral-fin distal end	39,1
Length of first left pectoral-fin ray (unbranched)	17,4
Length of rigid part of first left pectoral-fin ray	14,3
Length of second left pectoral-fin ray (first branched)	16,5
Length of third left pectoral-fin ray (second branched)	15,4
Prepelvic length	46,0
Distance between snout tip and terminus of pelvic-fin base	48,3
Distance between snout tip and pelvic-fin distal end	62,5
Distance between pelvic fins	4,2
Length of first left pelvic-fin ray (unbranched)	11,1
Length of second left pelvic-fin ray (first branched)	14,4
Length of third left pelvic-fin ray (second branched)	14,3
Anal-fin base	11,6
Preanal length	68,2
Distance between snout tip and terminus of anal-fin base	78,5
Distance between snout tip and anal-fin distal end	86,5
Adipose-fin length	28,2
Preadipose length	61,1
Distance between snout tip and adipose-fin base end	88,3
Adipose-fin depth	3,9
Caudal-peduncle length posterior to adipose-fin	10,1
Caudal-peduncle depth at adipose-fin terminus	9,8
Snout-anus distance	52,8
Snout-urogenital papilla distance	65,0

Anus-urogenital papilla distance	12,0
Dorsal lobe of caudal fin length	26,3
Ventral lobe of caudal fin length	23,4

Percentages of HL

Head depth	51,9
Head width	61,1
Eye diameter (left)	18,1
Fleshy interorbital	20,6
Bony interorbital	16,9
Mouth gape	30,4
Snout length (left)	32,1
Distance between snout tip and posterior nare (left side)	23,0
Anterior internarial width	12,3
Posterior internarial width	15,0
Intranarial length (left side)	17,0

Table 42: Morphometric data of *Pimelodella longipinnis* based on type material.

	Holotype
Total length (mm)	-
Standard length (mm)	84,6
Percentages of SL	
Body depth (dorsal)	13,9
Body width (dorsal)	10,2
Cleithral width	15,1
Head length	24,0
Maxillary-barbel length (left side)	76,4
Outer mental-barbel length (left side)	23,6
Inner mental-barbel length (left side)	16,7
Predorsal length	28,1
Distance between snout tip and terminus of dorsal-fin base	42,3
Distance between snout tip and dorsal-fin distal end	52,5
Dorsal fin to adipose fin	13,2
Dorsal-fin base	15,1
Length of first dorsal-fin ray (unbranched)	16,5
Length of rigid part of first dorsal-fin ray	9,2
Length of second dorsal-fin ray (first branched)	22,3
Length of third dorsal-fin ray (second branched)	-
Prepectoral length	16,9
Distance between snout tip and terminus of pectoral-fin base	20,3
Distance between snout tip and pectoral-fin distal end	33,4
Length of first left pectoral-fin ray (unbranched)	16,2
Length of rigid part of first left pectoral-fin ray	13,6
Length of second left pectoral-fin ray (first branched)	15,6
Length of third left pectoral-fin ray (second branched)	14,7
Prepelvic length	38,9
Distance between snout tip and terminus of pelvic-fin base	40,8
Distance between snout tip and pelvic-fin distal end	55,4
Distance between pelvic fins	3,8
Length of first left pelvic-fin ray (unbranched)	10,8
Length of second left pelvic-fin ray (first branched)	14,0
Length of third left pelvic-fin ray (second branched)	14,2
Anal-fin base	15,5
Preanal length	64,4
Distance between snout tip and terminus of anal-fin base	78,5
Distance between snout tip and anal-fin distal end	88,2
Adipose-fin length	35,4
Preadipose length	54,6
Distance between snout tip and adipose-fin base end	88,9
Adipose-fin depth	3,7
Caudal-peduncle length posterior to adipose-fin	10,7
Caudal-peduncle depth at adipose-fin terminus	7,1
Snout-anus distance	44,6
Snout-urogenital papilla distance	49,9

Anus-urogenital papilla distance	5,4
Dorsal lobe of caudal fin length	-
Ventral lobe of caudal fin length	-

Percentages of HL

Head depth	53,7
Head width	61,7
Eye diameter (left)	20,3
Fleshy interorbital	20,7
Bony interorbital	16,9
Mouth gape	30,6
Snout length (left)	30,7
Distance between snout tip and posterior nare (left side)	19,5
Anterior internarial width	14,2
Posterior internarial width	15,1
Intranarial length (left side)	13,2

Table 43: Morphometric data of *Pimelodella macturki* based on type material.

	Holotype	Min.	Max.	n	x	SD
Total length (mm)	66,3	48,6	74,1	7	62,3	
Standard length (mm)	53,5	36,4	60,4	18	48,2	
	Percentages of SL					
Body depth (dorsal)	19,5	17,6	21,9	9	19,4	1,5
Body width (dorsal)	14,5	11,5	15,5	9	13,4	1,2
Cleithral width	18,0	17,6	18,8	9	18,0	0,4
Head length	31,8	30,9	33,0	9	31,9	0,7
Maxillary-barbel length (left side)	71,7	62,7	78,9	9	71,1	6,2
Outer mental-barbel length (left side)	22,1	22,1	32,7	9	29,6	3,3
Inner mental-barbel length (left side)	16,6	14,1	18,7	9	16,9	1,5
Predorsal length	35,9	31,6	37,0	9	35,7	1,6
Distance between snout tip and terminus of dorsal-fin base	49,1	49,0	50,4	9	49,6	0,6
Distance between snout tip and dorsal-fin distal end	59,7	52,0	61,6	9	59,4	2,9
Dorsal fin to adipose fin	12,1	7,3	16,9	9	11,6	3,1
Dorsal-fin base	14,7	14,3	16,4	9	15,0	0,6
Length of first dorsal-fin ray (unbranched)	-	19,9	23,7	6	21,4	1,4
Length of rigid part of first dorsal-fin ray	16,4	15,1	18,7	9	16,9	1,1
Length of second dorsal-fin ray (first branched)	18,7	18,7	22,0	9	20,7	1,3
Length of third dorsal-fin ray (second branched)	18,3	15,3	20,9	8	19,0	1,7
Prepectoral length	21,6	21,6	24,4	9	23,1	0,9
Distance between snout tip and terminus of pectoral-fin base	24,8	24,8	27,6	9	26,3	0,9
Distance between snout tip and pectoral-fin distal end	39,5	39,5	46,9	9	43,6	2,0
Length of first left pectoral-fin ray (unbranched)	19,2	19,2	22,1	8	20,9	1,0
Length of rigid part of first left pectoral-fin ray	17,9	17,7	19,8	9	18,7	0,7
Length of second left pectoral-fin ray (first branched)	17,7	17,7	20,7	9	18,9	0,9
Length of third left pectoral-fin ray (second branched)	14,9	14,9	18,4	8	17,0	1,0
Prepelvic length	45,6	45,6	47,5	9	46,5	0,6
Distance between snout tip and terminus of pelvic-fin base	48,0	48,0	50,2	9	49,2	0,8
Distance between snout tip and pelvic-fin distal end	60,4	60,2	64,7	9	62,5	1,6
Distance between pelvic fins	4,3	3,7	5,3	9	4,2	0,6
Length of first left pelvic-fin ray (unbranched)	12,1	11,7	14,2	8	12,7	0,8
Length of second left pelvic-fin ray (first branched)	15,1	13,3	16,4	9	15,0	1,0
Length of third left pelvic-fin ray (second branched)	13,5	13,5	16,5	9	15,0	1,0
Anal-fin base	12,0	11,5	14,9	9	13,4	1,3
Preanal length	66,4	63,2	69,5	9	66,9	1,8
Distance between snout tip and terminus of anal-fin base	78,3	78,1	83,4	9	80,1	1,6
Distance between snout tip and anal-fin distal end	85,9	85,9	91,2	9	88,3	1,5
Adipose-fin length	26,0	23,7	30,7	9	27,4	2,3
Preadipose length	61,3	56,8	62,2	9	59,6	1,8
Distance between snout tip and adipose-fin base end	85,5	85,5	88,8	9	87,2	1,0
Adipose-fin depth	5,2	3,2	5,6	9	4,7	0,9
Caudal-peduncle length posterior to adipose-fin	13,5	12,0	14,6	9	13,0	0,9
Caudal-peduncle depth at adipose-fin terminus	8,8	7,1	9,0	9	8,3	0,6
Snout-anus distance	52,2	52,1	57,9	9	53,8	1,7
Snout-urogenital papilla distance	55,2	54,8	57,7	9	56,2	1,1

Anus-urogenital papilla distance	2,7	2,7	4,4	9	3,3	0,5
Dorsal lobe of caudal fin length	-	24,7	27,8	5	26,4	1,4
Ventral lobe of caudal fin length	25,1	22,6	32,0	5	26,1	3,7

Percentages of HL

Head depth	49,4	46,0	51,9	9	48,7	2,2
Head width	52,8	49,4	55,9	9	53,4	1,9
Eye diameter (left)	22,2	20,6	25,6	9	22,8	1,7
Fleshy interorbital	23,4	22,4	27,3	9	24,4	1,6
Bony interorbital	16,4	15,4	17,9	9	16,5	0,8
Mouth gape	30,0	25,7	31,5	9	28,4	1,9
Snout length (left)	27,9	26,9	30,5	9	28,6	1,2
Distance between snout tip and posterior nare (left side)	16,1	16,1	20,3	9	18,4	1,2
Anterior internarial width	12,0	11,9	14,6	9	13,0	0,8
Posterior internarial width	15,0	12,9	17,2	9	15,4	1,7
Intranarial length (left side)	13,9	12,6	17,4	9	14,5	1,6

Table 44: Morphometric data of *Pimelodella meeki* and *P. rudolphi*, its junior-synonym, based on type and comparative materials.

	Holotype	Min.	Max.	<i>n</i>	<i>x</i>	SD
Total length (mm)	123,1	48,9	134,7	15	93,4	
Standard length (mm)	100,2	30,2	112,2	39	52,9	
	Percentages of SL					
Body depth (dorsal)	23,7	15,9	23,7	15	19,6	2,3
Body width (dorsal)	17,4	12,4	18,8	15	16,1	1,7
Cleithral width	19,9	19,3	22,1	15	20,4	0,9
Head length	30,6	30,0	34,5	15	31,8	1,4
Maxillary-barbel length (left side)	56,9	42,7	70,3	13	56,6	8,3
Outer mental-barbel length (left side)	19,3	18,1	26,5	15	22,7	2,5
Inner mental-barbel length (left side)	11,4	8,6	15,5	15	13,3	1,8
Predorsal length	34,8	33,6	38,6	15	36,0	1,7
Distance between snout tip and terminus of dorsal-fin base	48,6	46,9	52,5	15	49,8	1,6
Distance between snout tip and dorsal-fin distal end	57,7	55,8	64,3	15	59,7	2,5
Dorsal fin to adipose fin	13,4	8,0	17,4	15	13,0	2,3
Dorsal-fin base	13,8	10,0	14,8	15	13,4	1,2
Length of first dorsal-fin ray (unbranched)	20,2	15,8	22,4	14	18,4	1,7
Length of rigid part of first dorsal-fin ray	11,4	11,4	17,1	15	13,8	1,6
Length of second dorsal-fin ray (first branched)	18,2	16,9	22,4	15	19,2	1,6
Length of third dorsal-fin ray (second branched)	18,8	15,7	20,4	14	18,4	1,3
Prepectoral length	22,0	20,8	30,0	15	24,3	2,6
Distance between snout tip and terminus of pectoral-fin base	25,2	24,4	32,1	15	27,3	2,4
Distance between snout tip and pectoral-fin distal end	38,4	38,1	48,5	15	42,0	3,4
Length of first left pectoral-fin ray (unbranched)	-	17,3	21,4	9	18,5	1,3
Length of rigid part of first left pectoral-fin ray	15,9	15,3	18,6	14	16,6	1,2
Length of second left pectoral-fin ray (first branched)	17,7	17,0	20,5	14	18,3	1,1
Length of third left pectoral-fin ray (second branched)	15,0	13,7	17,9	9	15,9	1,2
Prepelvic length	51,8	47,1	52,2	15	50,3	1,5
Distance between snout tip and terminus of pelvic-fin base	53,2	50,0	54,3	15	52,6	1,3
Distance between snout tip and pelvic-fin distal end	64,7	60,2	67,5	15	64,8	2,1
Distance between pelvic fins	5,9	3,1	5,9	15	4,6	0,7
Length of first left pelvic-fin ray (unbranched)	11,6	8,9	13,8	12	11,3	1,3
Length of second left pelvic-fin ray (first branched)	11,7	10,8	15,0	12	13,0	1,3
Length of third left pelvic-fin ray (second branched)	12,6	10,8	15,4	12	13,5	1,4
Anal-fin base	10,9	10,6	14,0	15	12,5	1,0
Preanal length	69,9	64,2	75,7	15	70,4	2,8
Distance between snout tip and terminus of anal-fin base	80,5	78,1	84,4	15	81,6	1,7
Distance between snout tip and anal-fin distal end	89,6	87,2	93,3	15	89,9	1,7
Adipose-fin length	27,9	25,8	34,3	15	29,1	2,8
Preadipose length	61,5	56,9	64,9	15	60,9	2,1
Distance between snout tip and adipose-fin base end	89,0	82,0	91,4	15	87,7	2,9
Adipose-fin depth	4,4	3,7	6,0	15	4,8	0,8
Caudal-peduncle length posterior to adipose-fin	10,7	8,7	12,2	15	10,7	1,0
Caudal-peduncle depth at adipose-fin terminus	10,7	8,0	11,6	15	9,6	1,1
Snout-anus distance	59,6	53,3	62,4	15	57,0	2,4

Snout-urogenital papilla distance	63,7	58,6	66,2	14	61,8	2,4
Anus-urogenital papilla distance	4,9	3,5	6,4	14	4,9	1,0
Dorsal lobe of caudal fin length	21,8	19,0	25,2	10	21,4	1,8
Ventral lobe of caudal fin length	20,3	17,6	25,1	13	20,5	2,0

Percentages of HL

Head depth	57,5	45,3	57,5	15	52,2	3,5
Head width	60,9	53,1	68,9	15	62,3	4,2
Eye diameter (left)	17,6	17,5	23,9	15	19,7	1,9
Fleshy interorbital	22,6	19,7	27,7	15	23,0	2,3
Bony interorbital	14,9	14,9	20,0	15	17,3	1,5
Mouth gape	32,3	29,1	34,9	15	32,1	1,7
Snout length (left)	30,8	29,0	33,8	15	31,6	1,3
Distance between snout tip and posterior nare (left side)	16,0	15,2	21,4	15	18,1	1,7
Anterior internarial width	10,2	10,2	14,5	15	12,7	1,2
Posterior internarial width	11,7	11,7	15,6	15	13,8	1,2
Intranarial length (left side)	11,5	10,8	15,1	15	13,1	1,6

Table 45: Morphometric data of *Pimelodella meeki* and *P. rudolphi*, its junior-synonym, based on type and comparative materials, discriminated by original species name.

	<i>P. meeki</i>						<i>P. rudolphi</i>					
	Holotype	Min.	Max.	<i>n</i>	<i>x</i>	SD	Lectotype	Min.	Max.	<i>n</i>	<i>x</i>	SD
Total length (mm)	123,1	51,8	134,7	5	105,6		88,1	48,9	119,7	10	87,2	
Standard length (mm)	100,2	30,2	112,2	29	45,8		73,9	41,4	101,2	10	73,3	
	Percentages of SL											
Body depth (dorsal)	23,7	17,6	23,7	5	20,3	2,4	21,2	15,9	22,9	10	19,2	2,3
Body width (dorsal)	17,4	13,8	18,8	5	16,6	2,0	17,0	12,4	18,8	10	15,9	1,6
Cleithral width	19,9	19,3	21,3	5	20,1	0,8	20,5	19,4	22,1	10	20,6	0,9
Head length	30,6	30,0	33,0	5	31,6	1,2	31,7	30,0	34,5	10	32,0	1,6
Maxillary-barbel length (left side)	56,9	42,7	65,6	5	53,2	8,7	43,5	43,5	70,3	8	58,8	7,8
Outer mental-barbel length (left side)	19,3	19,3	24,4	5	21,5	2,1	18,1	18,1	26,5	10	23,3	2,6
Inner mental-barbel length (left side)	11,4	11,4	15,5	5	13,6	1,6	8,6	8,6	15,2	10	13,2	1,9
Predorsal length	34,8	33,6	38,3	5	35,9	2,1	36,5	34,0	38,6	10	36,0	1,6
Distance between snout tip and terminus of dorsal-fin base	48,6	46,9	50,4	5	48,9	1,3	50,5	47,8	52,5	10	50,2	1,6
Distance between snout tip and dorsal-fin distal end	57,7	57,6	60,5	5	58,5	1,2	60,1	55,8	64,3	10	60,3	2,8
Dorsal fin to adipose fin	13,4	12,8	15,5	5	14,1	1,1	11,9	8,0	17,4	10	12,4	2,6
Dorsal-fin base	13,8	13,1	13,8	5	13,5	0,3	14,7	10,0	14,8	10	13,4	1,4
Length of first dorsal-fin ray (unbranched)	20,2	15,8	20,2	5	18,6	1,8	19,6	16,4	22,4	9	18,3	1,8
Length of rigid part of first dorsal-fin ray	11,4	11,4	15,7	5	13,4	2,2	17,1	12,5	17,1	10	14,1	1,3
Length of second dorsal-fin ray (first branched)	18,2	16,9	20,1	5	18,3	1,2	22,4	17,3	22,4	10	19,6	1,6
Length of third dorsal-fin ray (second branched)	18,8	17,2	19,3	4	18,2	1,1	20,4	15,7	20,4	10	18,5	1,5
Prepectoral length	22,0	20,8	24,8	5	22,9	1,6	24,5	21,2	30,0	10	25,0	2,8
Distance between snout tip and terminus of pectoral-fin base	25,2	24,4	27,6	5	26,0	1,3	26,8	25,3	32,1	10	27,9	2,7
Distance between snout tip and pectoral-fin distal end	38,4	38,1	43,7	5	40,5	2,4	40,7	38,3	48,5	10	42,7	3,7
Length of first left pectoral-fin ray (unbranched)	-	17,5	21,4	3	19,3	2,0	-	17,3	19,8	6	18,2	0,9
Length of rigid part of first left pectoral-fin ray	15,9	15,5	18,0	5	16,7	1,2	18,0	15,3	18,6	9	16,5	1,3
Length of second left pectoral-fin ray (first branched)	17,7	17,0	19,6	5	17,9	1,0	-	17,2	20,5	9	18,5	1,2

Length of third left pectoral-fin ray (second branched)	15,0	15,0	17,9	3	16,3	1,5	-	13,7	16,6	6	15,7	1,1
Prepelvic length	51,8	49,6	52,1	5	51,0	1,2	48,4	47,1	52,2	10	49,9	1,6
Distance between snout tip and terminus of pelvic-fin base	53,2	51,5	53,4	5	52,6	0,8	50,4	50,0	54,3	10	52,6	1,5
Distance between snout tip and pelvic-fin distal end	64,7	62,9	67,4	5	64,9	1,6	63,4	60,2	67,5	10	64,8	2,4
Distance between pelvic fins	5,9	3,1	5,9	5	4,5	1,1	5,1	4,1	5,5	10	4,6	0,5
Length of first left pelvic-fin ray (unbranched)	11,6	8,9	11,6	4	10,6	1,2	13,0	10,5	13,8	8	11,7	1,2
Length of second left pelvic-fin ray (first branched)	11,7	10,8	14,1	4	12,4	1,5	14,8	11,5	15,0	8	13,3	1,2
Length of third left pelvic-fin ray (second branched)	12,6	10,8	14,7	4	12,9	1,6	15,4	11,8	15,4	8	13,8	1,3
Anal-fin base	10,9	10,6	14,0	5	11,9	1,4	13,5	11,6	14,0	10	12,8	0,7
Preanal length	69,9	68,2	71,3	5	69,4	1,2	67,9	64,2	75,7	10	70,9	3,2
Distance between snout tip and terminus of anal-fin base	80,5	79,7	81,1	5	80,5	0,5	82,5	78,1	84,4	10	82,2	1,8
Distance between snout tip and anal-fin distal end	89,6	87,2	89,6	5	88,8	1,0	91,0	87,4	93,3	10	90,5	1,7
Adipose-fin length	27,9	25,8	28,2	5	26,9	1,1	27,0	26,9	34,3	10	30,2	2,7
Preadipose length	61,5	61,2	64,9	5	62,7	1,6	61,5	56,9	62,2	10	60,1	1,8
Distance between snout tip and adipose-fin base end	89,0	87,1	89,4	5	88,4	0,9	87,0	82,0	91,4	10	87,3	3,5
Adipose-fin depth	4,4	3,7	4,9	5	4,2	0,5	3,8	3,8	6,0	10	5,1	0,8
Caudal-peduncle length posterior to adipose-fin	10,7	8,7	12,2	5	10,6	1,3	10,8	9,4	11,7	10	10,7	0,8
Caudal-peduncle depth at adipose-fin terminus	10,7	8,0	10,7	5	9,6	1,3	9,4	8,1	11,6	10	9,5	1,0
Snout-anus distance	59,6	56,5	59,6	5	58,1	1,1	54,8	53,3	62,4	10	56,5	2,8
Snout-urogenital papilla distance	63,7	59,7	63,7	5	62,0	1,6	61,5	58,6	66,2	9	61,7	2,8
Anus-urogenital papilla distance	4,9	3,7	5,9	5	4,7	1,0	6,1	3,5	6,4	9	5,0	1,1
Dorsal lobe of caudal fin length	21,8	20,5	21,8	4	21,1	0,6	-	19,0	25,2	6	21,6	2,3
Ventral lobe of caudal fin length	20,3	17,6	20,3	5	19,4	1,2	-	18,2	25,1	8	21,2	2,2

Percentages of HL

Head depth	57,5	45,3	57,5	5	52,4	4,5	52,2	48,2	57,1	10	52,0	3,1
Head width	60,9	53,1	67,9	5	60,2	5,3	56,6	56,6	68,9	10	63,4	3,5
Eye diameter (left)	17,6	17,6	20,3	5	18,7	1,2	17,8	17,5	23,9	10	20,2	2,0
Fleshy interorbital	22,6	19,7	24,0	5	22,1	1,6	22,1	21,1	27,7	10	23,5	2,6
Bony interorbital	14,9	14,9	18,6	5	16,7	1,8	17,1	15,7	20,0	10	17,6	1,4
Mouth gape	32,3	29,1	32,3	5	30,6	1,4	32,1	31,2	34,9	10	32,8	1,4
Snout length (left)	30,8	29,0	32,5	5	30,6	1,3	32,7	30,6	33,8	10	32,1	1,0

Distance between snout tip and posterior nare (left side)	16,0	15,2	18,6	5	16,6	1,4	18,6	16,1	21,4	10	18,8	1,4
Anterior internarial width	10,2	10,2	13,7	5	11,8	1,4	12,2	11,8	14,5	10	13,1	0,9
Posterior internarial width	11,7	11,7	14,1	5	13,2	0,9	13,0	12,6	15,6	10	14,1	1,2
Intranarial length (left side)	11,5	10,8	15,0	5	13,2	1,9	12,5	10,8	15,1	10	13,1	1,5

Table 46: Morphometric data of *Pimelodella megalops* based on type and comparative materials.

	Holotype	Min.	Max.	<i>n</i>	<i>x</i>	SD
Total length (mm)	97,7	53,7	97,7	14	80,5	
Standard length (mm)	74,7	44,0	74,7	54	60,6	
	Percentages of SL					
Body depth (dorsal)	15,7	12,6	17,5	15	15,4	1,4
Body width (dorsal)	10,5	10,0	13,2	15	11,5	0,9
Cleithral width	14,9	10,1	16,2	15	14,9	1,4
Head length	27,5	27,5	31,1	15	29,4	0,9
Maxillary-barbel length (left side)	88,0	73,6	95,7	13	85,9	6,2
Outer mental-barbel length (left side)	38,5	29,2	38,7	15	35,7	2,7
Inner mental-barbel length (left side)	15,2	14,8	22,3	15	17,5	2,3
Predorsal length	30,5	29,1	35,6	15	32,1	1,6
Distance between snout tip and terminus of dorsal-fin base	44,9	44,9	50,4	15	46,5	1,5
Distance between snout tip and dorsal-fin distal end	55,9	55,9	59,3	15	57,6	1,0
Dorsal fin to adipose fin	12,3	8,9	16,8	15	12,9	1,7
Dorsal-fin base	14,7	14,1	16,4	15	15,2	0,8
Length of first dorsal-fin ray (unbranched)	20,6	15,9	22,4	14	19,7	1,9
Length of rigid part of first dorsal-fin ray	16,7	15,4	17,6	15	16,4	0,6
Length of second dorsal-fin ray (first branched)	21,6	18,8	22,9	15	20,9	1,2
Length of third dorsal-fin ray (second branched)	20,1	18,3	21,7	15	20,2	1,2
Prepectoral length	19,8	19,1	24,2	15	20,9	1,3
Distance between snout tip and terminus of pectoral-fin base	22,9	22,3	26,5	15	23,8	1,2
Distance between snout tip and pectoral-fin distal end	40,2	39,2	45,5	15	41,5	1,6
Length of first left pectoral-fin ray (unbranched)	21,0	18,5	22,4	14	20,6	1,3
Length of rigid part of first left pectoral-fin ray	17,5	17,4	20,2	15	18,8	0,9
Length of second left pectoral-fin ray (first branched)	19,4	17,2	20,9	15	19,3	1,1
Length of third left pectoral-fin ray (second branched)	17,7	15,9	18,9	13	17,6	0,8
Prepelvic length	41,0	41,0	46,2	15	43,1	1,4
Distance between snout tip and terminus of pelvic-fin base	43,5	43,4	48,4	15	45,6	1,6
Distance between snout tip and pelvic-fin distal end	57,6	56,0	63,2	15	59,3	1,8
Distance between pelvic fins	3,9	3,2	4,5	14	3,9	0,4
Length of first left pelvic-fin ray (unbranched)	12,7	11,7	15,5	15	12,7	0,9
Length of second left pelvic-fin ray (first branched)	14,6	13,1	16,5	15	14,7	0,8
Length of third left pelvic-fin ray (second branched)	15,3	13,7	16,2	15	14,8	0,7
Anal-fin base	14,1	11,9	15,1	14	13,8	0,9
Preanal length	64,9	60,7	67,4	14	65,0	1,7
Distance between snout tip and terminus of anal-fin base	78,6	73,1	81,0	14	78,6	1,9
Distance between snout tip and anal-fin distal end	86,8	81,7	89,8	14	87,1	1,9
Adipose-fin length	27,5	19,7	32,9	15	29,6	3,3
Preadipose length	57,4	53,5	63,4	15	58,3	2,5
Distance between snout tip and adipose-fin base end	84,1	84,1	89,1	14	87,4	1,3
Adipose-fin depth	4,3	2,1	5,3	15	4,2	0,8
Caudal-peduncle length posterior to adipose-fin	13,4	10,4	14,9	15	12,5	1,3
Caudal-peduncle depth at adipose-fin terminus	7,5	6,4	8,1	15	7,2	0,5
Snout-anus distance	48,8	46,8	50,8	15	49,0	1,2

Snout-urogenital papilla distance	56,7	51,9	59,6	15	55,3	2,1
Anus-urogenital papilla distance	8,2	4,4	9,0	15	6,4	1,7
Dorsal lobe of caudal fin length	20,0	20,0	32,2	12	26,3	3,2
Ventral lobe of caudal fin length	28,0	27,3	32,7	14	30,2	1,8

Percentages of HL

Head depth	47,2	41,1	50,1	15	45,0	2,4
Head width	52,8	45,2	54,6	15	50,0	2,2
Eye diameter (left)	31,7	24,5	33,6	15	29,9	2,8
Fleshy interorbital	17,1	16,3	22,6	15	19,5	1,7
Bony interorbital	10,4	9,5	13,8	15	11,4	1,2
Mouth gape	27,9	25,3	29,7	15	27,5	1,1
Snout length (left)	27,1	26,1	29,3	15	27,6	0,9
Distance between snout tip and posterior nare (left side)	18,1	16,5	22,1	15	18,8	1,7
Anterior internarial width	11,8	10,0	13,1	15	11,8	1,0
Posterior internarial width	14,1	11,9	16,4	15	13,6	1,4
Intranarial length (left side)	15,3	11,9	18,6	15	15,3	1,8

Table 47: Morphometric data of *Pimelodella megalura* based on type material.

	Lectotype	Min.	Max.	n	x	SD
Total length (mm)	197,9	111,3	197,9	7	159,9	
Standard length (mm)	128,6	70,0	143,6	17	112,8	
	Percentages of SL					
Body depth (dorsal)	16,8	11,9	17,6	6	15,5	2,0
Body width (dorsal)	13,4	12,0	14,1	6	13,0	0,8
Cleithral width	14,3	14,2	15,9	6	14,7	0,7
Head length	23,8	23,3	26,8	6	24,5	1,3
Maxillary-barbel length (left side)	57,2	54,3	72,5	6	62,7	7,4
Outer mental-barbel length (left side)	19,5	17,6	27,3	6	22,1	3,8
Inner mental-barbel length (left side)	9,9	9,9	17,9	6	12,7	3,1
Predorsal length	27,3	26,7	29,7	6	27,9	1,2
Distance between snout tip and terminus of dorsal-fin base	41,8	40,3	44,3	6	42,3	1,4
Distance between snout tip and dorsal-fin distal end	51,1	48,8	56,4	6	52,2	2,6
Dorsal fin to adipose fin	13,2	7,3	13,2	6	10,5	2,2
Dorsal-fin base	15,7	12,8	15,7	6	14,0	1,3
Length of first dorsal-fin ray (unbranched)	21,4	15,3	21,4	6	17,6	2,6
Length of rigid part of first dorsal-fin ray	10,3	8,3	13,4	6	9,8	1,9
Length of second dorsal-fin ray (first branched)	16,4	16,4	18,8	6	17,7	0,9
Length of third dorsal-fin ray (second branched)	18,2	17,7	19,7	6	18,9	0,8
Prepectoral length	17,2	16,0	18,6	6	17,3	1,1
Distance between snout tip and terminus of pectoral-fin base	20,1	18,7	22,6	6	20,7	1,5
Distance between snout tip and pectoral-fin distal end	30,9	29,4	35,7	6	32,4	2,3
Length of first left pectoral-fin ray (unbranched)	14,7	14,7	18,3	6	15,7	1,4
Length of rigid part of first left pectoral-fin ray	11,8	11,1	15,7	6	13,0	1,6
Length of second left pectoral-fin ray (first branched)	12,5	12,5	16,8	6	14,6	1,4
Length of third left pectoral-fin ray (second branched)	12,8	12,8	16,0	6	14,0	1,2
Prepelvic length	38,8	36,7	40,5	6	39,2	1,4
Distance between snout tip and terminus of pelvic-fin base	42,2	39,5	43,7	6	41,8	1,5
Distance between snout tip and pelvic-fin distal end	51,8	51,4	57,2	6	53,4	2,1
Distance between pelvic fins	4,3	3,7	4,9	6	4,4	0,5
Length of first left pelvic-fin ray (unbranched)	9,4	9,4	11,9	6	10,5	0,9
Length of second left pelvic-fin ray (first branched)	10,9	10,9	14,3	6	12,3	1,3
Length of third left pelvic-fin ray (second branched)	12,5	12,3	14,4	6	13,3	0,8
Anal-fin base	15,5	15,2	17,3	6	15,9	0,8
Preanal length	62,0	58,6	64,2	6	61,9	2,2
Distance between snout tip and terminus of anal-fin base	77,6	75,2	79,3	6	77,7	1,8
Distance between snout tip and anal-fin distal end	85,8	82,3	88,0	6	85,3	2,1
Adipose-fin length	38,8	37,6	40,8	6	39,4	1,4
Preadipose length	54,1	49,7	55,5	6	52,4	2,4
Distance between snout tip and adipose-fin base end	91,4	88,2	92,6	6	90,0	1,7
Adipose-fin depth	4,4	4,1	5,7	6	4,8	0,6
Caudal-peduncle length posterior to adipose-fin	9,3	8,8	10,7	6	9,9	0,7
Caudal-peduncle depth at adipose-fin terminus	7,6	6,9	8,1	6	7,6	0,4
Snout-anus distance	44,1	42,9	46,3	6	44,5	1,2
Snout-urogenital papilla distance	47,9	47,0	50,6	6	48,8	1,4

Anus-urogenital papilla distance	3,9	3,6	4,8	6	4,1	0,5
Dorsal lobe of caudal fin length	52,2	25,4	52,2	5	40,3	11,3
Ventral lobe of caudal fin length	26,9	24,4	26,9	5	25,3	0,9

Percentages of HL

Head depth	53,8	47,6	53,8	6	49,7	2,4
Head width	59,9	54,2	59,9	6	58,0	2,3
Eye diameter (left)	17,0	17,0	22,7	6	19,2	2,3
Fleshy interorbital	23,3	21,7	27,8	6	23,6	2,1
Bony interorbital	17,3	16,1	18,3	6	17,0	0,8
Mouth gape	37,0	30,4	37,0	6	33,4	2,7
Snout length (left)	30,5	29,3	32,8	6	31,6	1,4
Distance between snout tip and posterior nare (left side)	17,8	17,8	19,2	6	18,4	0,6
Anterior internarial width	13,7	11,6	15,5	6	14,0	1,3
Posterior internarial width	12,6	12,6	14,7	6	13,7	0,7
Intranarial length (left side)	14,7	12,3	14,7	6	13,6	1,0

Table 48: Morphometric data of *Pimelodella metae* based on type material.

	Holotype	Min.	Max.	n	x	SD
Total length (mm)	70,0	47,8	99,7	3	72,5	
Standard length (mm)	58,0	34,9	74,0	4	57,8	
	Percentages of SL					
Body depth (dorsal)	16,6	16,6	17,8	3	17,1	0,6
Body width (dorsal)	12,3	12,3	15,9	3	13,9	1,9
Cleithral width	16,6	16,6	18,2	3	17,4	0,8
Head length	29,1	29,1	32,2	3	30,2	1,7
Maxillary-barbel length (left side)	76,2	62,6	76,2	3	69,6	6,8
Outer mental-barbel length (left side)	25,1	25,1	26,1	3	25,4	0,6
Inner mental-barbel length (left side)	15,2	13,7	15,2	3	14,7	0,8
Predorsal length	32,4	32,4	36,1	3	34,6	2,0
Distance between snout tip and terminus of dorsal-fin base	47,4	47,4	52,6	3	49,8	2,6
Distance between snout tip and dorsal-fin distal end	58,1	58,1	66,1	3	60,9	4,5
Dorsal fin to adipose fin	11,2	11,1	13,9	3	12,1	1,6
Dorsal-fin base	15,2	14,6	17,2	3	15,7	1,4
Length of first dorsal-fin ray (unbranched)	18,1	18,0	19,8	3	18,6	1,0
Length of rigid part of first dorsal-fin ray	13,0	12,6	13,5	3	13,0	0,5
Length of second dorsal-fin ray (first branched)	22,3	18,1	22,3	3	20,8	2,3
Length of third dorsal-fin ray (second branched)	22,2	18,9	22,2	3	21,0	1,8
Prepectoral length	20,1	20,1	26,3	3	22,4	3,4
Distance between snout tip and terminus of pectoral-fin base	23,0	23,0	28,1	3	25,0	2,7
Distance between snout tip and pectoral-fin distal end	37,9	37,9	44,5	3	40,2	3,7
Length of first left pectoral-fin ray (unbranched)	20,2	20,2	20,6	3	20,4	0,2
Length of rigid part of first left pectoral-fin ray	15,8	15,8	17,2	3	16,5	0,7
Length of second left pectoral-fin ray (first branched)	18,0	18,0	19,6	3	19,0	0,8
Length of third left pectoral-fin ray (second branched)	15,6	15,6	18,8	3	17,3	1,6
Prepelvic length	41,7	41,7	49,8	3	46,0	4,1
Distance between snout tip and terminus of pelvic-fin base	43,3	43,3	51,4	3	47,4	4,0
Distance between snout tip and pelvic-fin distal end	56,2	56,2	66,6	3	61,4	5,2
Distance between pelvic fins	4,3	4,3	5,8	3	4,9	0,8
Length of first left pelvic-fin ray (unbranched)	12,6	11,9	13,0	3	12,5	0,6
Length of second left pelvic-fin ray (first branched)	14,1	14,1	15,6	3	14,8	0,8
Length of third left pelvic-fin ray (second branched)	14,1	14,1	16,4	3	15,4	1,2
Anal-fin base	12,9	11,8	12,9	3	12,4	0,6
Preanal length	64,1	64,1	73,2	3	68,6	4,5
Distance between snout tip and terminus of anal-fin base	77,6	77,6	87,0	3	81,5	4,9
Distance between snout tip and anal-fin distal end	86,1	86,1	95,9	3	90,5	5,0
Adipose-fin length	30,9	30,9	35,7	3	34,0	2,7
Preadipose length	57,2	57,2	60,5	3	59,1	1,7
Distance between snout tip and adipose-fin base end	88,2	88,2	95,1	3	91,3	3,5
Adipose-fin depth	4,4	4,4	5,8	3	5,0	0,7
Caudal-peduncle length posterior to adipose-fin	11,9	10,0	11,9	3	10,9	0,9
Caudal-peduncle depth at adipose-fin terminus	8,2	8,2	9,1	3	8,6	0,5
Snout-anus distance	47,6	47,6	57,8	3	52,2	5,2
Snout-urogenital papilla distance	52,1	52,1	62,3	3	56,4	5,3

Anus-urogenital papilla distance	4,5	4,2	4,6	3	4,4	0,2
Dorsal lobe of caudal fin length	-	30,5	33,2	2	31,9	2,0
Ventral lobe of caudal fin length	26,0	23,0	27,7	3	25,6	2,4

Percentages of HL

Head depth	45,9	45,9	50,9	3	48,0	2,6
Head width	55,3	54,1	60,4	3	56,6	3,3
Eye diameter (left)	19,1	19,1	20,3	3	19,5	0,6
Fleshy interorbital	23,4	21,0	25,9	3	23,4	2,4
Bony interorbital	16,8	16,4	18,6	3	17,3	1,2
Mouth gape	32,9	30,5	33,7	3	32,4	1,6
Snout length (left)	28,4	28,4	31,5	3	29,9	1,6
Distance between snout tip and posterior nare (left side)	15,9	15,9	20,8	3	18,2	2,5
Anterior internarial width	14,1	14,1	15,2	3	14,5	0,6
Posterior internarial width	16,5	15,2	16,8	3	16,1	0,9
Intranarial length (left side)	13,7	13,7	15,4	3	14,4	1,0

Table 49: Morphometric data of *Pimelodella modesta* based on type and comparative materials.

	Lectotype	Min.	Max.	n	x	SD
Total length (mm)	121,1	96,6	212,0	4	149,3	
Standard length (mm)	100,4	77,5	175,7	4	122,2	
	Percentages of SL					
Body depth (dorsal)	15,4	15,4	22,6	4	18,3	3,2
Body width (dorsal)	13,2	11,0	18,9	4	14,7	3,4
Cleithral width	16,8	16,0	18,1	4	17,2	1,0
Head length	28,2	28,0	28,6	4	28,3	0,3
Maxillary-barbel length (left side)	54,3	54,0	64,0	4	58,2	4,9
Outer mental-barbel length (left side)	20,7	20,7	30,0	4	25,2	4,0
Inner mental-barbel length (left side)	13,8	13,1	16,0	4	14,4	1,3
Predorsal length	32,4	31,6	32,7	4	32,3	0,5
Distance between snout tip and terminus of dorsal-fin base	46,6	45,1	46,8	4	46,3	0,8
Distance between snout tip and dorsal-fin distal end	55,6	54,9	57,8	4	56,0	1,2
Dorsal fin to adipose fin	11,3	10,1	12,7	4	11,6	1,1
Dorsal-fin base	14,9	14,3	16,3	4	15,0	0,9
Length of first dorsal-fin ray (unbranched)	18,4	18,4	20,9	4	19,2	1,2
Length of rigid part of first dorsal-fin ray	13,5	12,3	14,7	4	13,4	1,0
Length of second dorsal-fin ray (first branched)	18,2	17,6	21,9	4	19,3	1,9
Length of third dorsal-fin ray (second branched)	17,7	17,7	19,6	4	18,4	0,9
Prepectoral length	20,5	19,4	23,1	4	20,9	1,6
Distance between snout tip and terminus of pectoral-fin base	21,4	21,4	26,2	4	23,2	2,1
Distance between snout tip and pectoral-fin distal end	36,5	36,5	41,0	4	37,9	2,1
Length of first left pectoral-fin ray (unbranched)	17,7	17,7	18,8	4	18,2	0,5
Length of rigid part of first left pectoral-fin ray	14,7	14,5	16,7	4	15,5	1,1
Length of second left pectoral-fin ray (first branched)	16,5	16,4	17,3	4	16,7	0,4
Length of third left pectoral-fin ray (second branched)	15,8	14,1	15,8	4	15,0	0,7
Prepelvic length	43,5	43,0	48,6	4	45,6	2,8
Distance between snout tip and terminus of pelvic-fin base	45,7	44,2	50,2	4	47,2	2,8
Distance between snout tip and pelvic-fin distal end	57,0	57,0	63,4	4	60,6	3,2
Distance between pelvic fins	4,4	4,2	6,2	4	5,1	1,0
Length of first left pelvic-fin ray (unbranched)	12,1	11,4	12,1	4	11,9	0,3
Length of second left pelvic-fin ray (first branched)	13,0	13,0	15,7	4	14,1	1,2
Length of third left pelvic-fin ray (second branched)	13,6	13,6	15,4	4	14,6	0,8
Anal-fin base	14,3	12,9	14,3	4	13,3	0,7
Preanal length	64,0	64,0	68,6	4	66,5	2,0
Distance between snout tip and terminus of anal-fin base	78,1	78,1	80,5	4	79,2	1,0
Distance between snout tip and anal-fin distal end	85,8	85,5	87,0	4	86,2	0,7
Adipose-fin length	30,8	30,8	34,9	4	33,1	1,8
Preadipose length	58,5	56,3	58,9	4	58,0	1,1
Distance between snout tip and adipose-fin base end	87,0	86,6	90,2	4	88,1	1,7
Adipose-fin depth	4,9	4,2	5,6	4	4,8	0,6
Caudal-peduncle length posterior to adipose-fin	11,6	9,9	11,6	4	10,8	0,7
Caudal-peduncle depth at adipose-fin terminus	8,3	7,8	9,1	4	8,4	0,5
Snout-anus distance	48,3	48,3	52,0	4	50,0	1,6

Snout-urogenital papilla distance	54,0	54,0	58,3	4	55,8	2,0
Anus-urogenital papilla distance	5,0	3,8	5,4	4	4,9	0,7
Dorsal lobe of caudal fin length	23,2	22,2	25,0	4	23,7	1,3
Ventral lobe of caudal fin length	20,4	18,6	21,7	4	20,6	1,4

Percentages of HL

Head depth	45,4	45,4	60,1	4	52,6	7,1
Head width	50,9	50,2	66,8	4	58,2	8,9
Eye diameter (left)	20,0	17,3	20,9	4	19,2	1,6
Fleshy interorbital	23,4	22,6	28,6	4	25,6	3,1
Bony interorbital	17,7	17,0	21,8	4	19,0	2,2
Mouth gape	33,1	29,1	33,2	4	31,8	1,9
Snout length (left)	30,4	30,2	36,1	4	33,0	3,2
Distance between snout tip and posterior nare (left side)	17,6	16,8	20,8	4	18,9	2,0
Anterior internarial width	11,6	11,4	14,3	4	12,8	1,5
Posterior internarial width	14,7	13,8	17,7	4	15,8	1,8
Intranarial length (left side)	12,4	12,4	15,3	4	13,5	1,3

Table 50: Morphometric data of *Pimelodella montana* based on type and comparative materials.

	Lectotype	Min.	Max.	n	x	SD
Total length (mm)	-	125,0	192,0	3	152,7	
Standard length (mm)	87,4	87,4	155,6	5	122,2	
	Percentages of SL					
Body depth (dorsal)	18,0	17,3	23,2	5	20,0	2,4
Body width (dorsal)	14,2	14,2	19,6	5	17,2	2,2
Cleithral width	17,5	17,5	19,9	5	18,6	0,9
Head length	31,5	27,5	31,5	5	29,0	1,6
Maxillary-barbel length (left side)	75,8	56,2	83,2	4	71,2	11,4
Outer mental-barbel length (left side)	32,3	26,8	32,3	5	29,7	2,0
Inner mental-barbel length (left side)	18,9	18,9	21,5	5	19,7	1,1
Predorsal length	31,3	31,3	33,5	5	32,7	0,9
Distance between snout tip and terminus of dorsal-fin base	48,9	46,3	50,0	5	48,0	1,5
Distance between snout tip and dorsal-fin distal end	57,3	52,2	58,9	5	56,7	2,6
Dorsal fin to adipose fin	14,5	7,8	14,5	5	10,5	2,7
Dorsal-fin base	16,1	14,7	16,1	5	15,3	0,7
Length of first dorsal-fin ray (unbranched)	17,3	17,3	20,8	5	18,6	1,5
Length of rigid part of first dorsal-fin ray	14,1	12,3	15,1	5	13,9	1,0
Length of second dorsal-fin ray (first branched)	18,6	16,7	21,0	5	18,9	1,6
Length of third dorsal-fin ray (second branched)	17,8	15,3	20,2	5	17,9	1,7
Prepectoral length	25,6	20,1	25,6	5	22,4	2,1
Distance between snout tip and terminus of pectoral-fin base	27,8	23,3	27,8	5	25,1	1,8
Distance between snout tip and pectoral-fin distal end	32,9	32,9	43,5	5	38,9	3,9
Length of first left pectoral-fin ray (unbranched)	-	16,0	22,1	4	19,4	2,9
Length of rigid part of first left pectoral-fin ray	12,5	12,5	16,4	5	15,1	1,6
Length of second left pectoral-fin ray (first branched)	-	17,5	20,0	4	19,0	1,1
Length of third left pectoral-fin ray (second branched)	-	16,5	18,9	4	17,5	1,0
Prepelvic length	48,9	47,2	54,3	5	49,9	2,8
Distance between snout tip and terminus of pelvic-fin base	53,0	49,9	56,6	5	52,9	2,7
Distance between snout tip and pelvic-fin distal end	64,4	62,5	69,0	5	65,6	2,7
Distance between pelvic fins	4,7	4,7	6,7	5	5,8	0,8
Length of first left pelvic-fin ray (unbranched)	10,9	10,9	13,5	5	12,2	1,2
Length of second left pelvic-fin ray (first branched)	13,9	13,5	16,0	5	14,9	1,1
Length of third left pelvic-fin ray (second branched)	14,3	14,1	15,5	5	14,8	0,6
Anal-fin base	11,8	11,8	13,0	5	12,2	0,6
Preanal length	69,6	68,8	75,2	5	71,8	2,8
Distance between snout tip and terminus of anal-fin base	81,2	80,2	84,7	5	82,2	1,8
Distance between snout tip and anal-fin distal end	86,2	85,2	91,4	5	88,3	2,6
Adipose-fin length	30,0	30,0	37,1	5	33,9	2,9
Preadipose length	62,2	53,2	62,2	5	56,6	3,4
Distance between snout tip and adipose-fin base end	90,3	87,2	90,3	5	88,6	1,4
Adipose-fin depth	4,3	4,3	5,5	5	4,8	0,6
Caudal-peduncle length posterior to adipose-fin	11,7	10,2	12,5	5	11,3	0,9
Caudal-peduncle depth at adipose-fin terminus	9,5	9,5	12,8	5	11,2	1,3
Snout-anus distance	56,0	54,4	61,2	5	57,7	3,0

Snout-urogenital papilla distance	59,3	59,3	64,0	5	61,4	2,1
Anus-urogenital papilla distance	3,4	3,4	5,8	5	4,5	1,1
Dorsal lobe of caudal fin length	-	22,2	32,6	3	27,1	5,2
Ventral lobe of caudal fin length	23,0	22,4	25,7	4	23,8	1,5

Percentages of HL

Head depth	54,3	49,1	56,4	5	52,9	2,8
Head width	57,5	57,5	73,7	5	64,8	6,0
Eye diameter (left)	19,8	16,2	19,8	5	18,4	1,4
Fleshy interorbital	24,3	24,3	34,1	5	28,5	3,7
Bony interorbital	17,8	17,8	27,0	5	22,1	3,4
Mouth gape	34,4	34,4	41,6	5	37,4	3,3
Snout length (left)	30,0	30,0	35,0	5	33,2	2,1
Distance between snout tip and posterior nare (left side)	29,4	19,8	29,4	5	23,1	3,8
Anterior internarial width	13,0	13,0	17,6	5	15,3	1,6
Posterior internarial width	14,3	14,3	19,3	5	16,8	2,1
Intranarial length (left side)	13,5	13,3	16,9	5	15,1	1,6

Table 51: Morphometric data of *Pimelodella mucosa* based on type and comparative materials.

	Holotype	Comp.
Total length (mm)	123,2	117,1
Standard length (mm)	97,4	95,9
Percentages of SL		
Body depth (dorsal)	28,1	25,3
Body width (dorsal)	15,9	17,7
Cleithral width	21,2	26,1
Head length	35,9	35,0
Maxillary-barbel length (left side)	107,0	111,3
Outer mental-barbel length (left side)	23,7	31,2
Inner mental-barbel length (left side)	14,1	15,3
Predorsal length	35,0	17,7
Distance between snout tip and terminus of dorsal-fin base	54,9	20,2
Distance between snout tip and dorsal-fin distal end	65,2	61,4
Dorsal fin to adipose fin	10,8	11,3
Dorsal-fin base	17,9	16,2
Length of first dorsal-fin ray (unbranched)	18,8	19,9
Length of rigid part of first dorsal-fin ray	-	15,9
Length of second dorsal-fin ray (first branched)	21,9	19,7
Length of third dorsal-fin ray (second branched)	19,1	20,0
Prepectoral length	24,8	25,7
Distance between snout tip and terminus of pectoral-fin base	28,8	29,0
Distance between snout tip and pectoral-fin distal end	47,1	48,9
Length of first left pectoral-fin ray (unbranched)	-	23,3
Length of rigid part of first left pectoral-fin ray	23,4	21,3
Length of second left pectoral-fin ray (first branched)	21,3	21,9
Length of third left pectoral-fin ray (second branched)	19,6	19,7
Prepelvic length	50,1	49,5
Distance between snout tip and terminus of pelvic-fin base	51,6	52,0
Distance between snout tip and pelvic-fin distal end	67,7	66,0
Distance between pelvic fins	5,5	6,0
Length of first left pelvic-fin ray (unbranched)	14,5	12,9
Length of second left pelvic-fin ray (first branched)	15,6	15,5
Length of third left pelvic-fin ray (second branched)	16,9	15,6
Anal-fin base	14,0	13,0
Preanal length	69,9	70,3
Distance between snout tip and terminus of anal-fin base	82,3	83,1
Distance between snout tip and anal-fin distal end	92,2	91,6
Adipose-fin length	28,6	27,2
Preadipose length	65,2	64,3
Distance between snout tip and adipose-fin base end	89,9	88,8
Adipose-fin depth	6,7	5,8
Caudal-peduncle length posterior to adipose-fin	12,9	10,8
Caudal-peduncle depth at adipose-fin terminus	8,3	8,2
Snout-anus distance	55,5	56,7

Snout-urogenital papilla distance	60,2	59,6
Anus-urogenital papilla distance	5,0	4,4
Dorsal lobe of caudal fin length	26,6	27,8
Ventral lobe of caudal fin length	30,5	28,2

Percentages of HL

Head depth	49,7	54,2
Head width	57,4	61,9
Eye diameter (left)	19,7	19,0
Fleshy interorbital	24,4	26,7
Bony interorbital	23,4	22,7
Mouth gape	28,9	31,0
Snout length (left)	32,4	34,5
Distance between snout tip and posterior nare (left side)	16,2	16,8
Anterior internarial width	12,6	15,7
Posterior internarial width	14,2	13,6
Intranarial length (left side)	11,7	12,7

Table 52: Morphometric data of *Pimelodella notomelas* based on type and comparative materials.

	Holotype	Min.	Max.	<i>n</i>	<i>x</i>	SD
Total length (mm)	50,4	36,9	56,8	4	48,6	
Standard length (mm)	38,9	27,6	42,3	11	36,8	
	Percentages of SL					
Body depth (dorsal)	17,2	17,2	21,4	4	19,9	2,0
Body width (dorsal)	11,8	11,8	12,9	4	12,4	0,6
Cleithral width	17,5	17,5	21,9	4	18,9	2,1
Head length	31,5	31,5	36,3	4	32,8	2,3
Maxillary-barbel length (left side)	104,9	104,9	116,6	3	111,4	6,0
Outer mental-barbel length (left side)	36,9	30,6	36,9	3	34,0	3,2
Inner mental-barbel length (left side)	20,2	17,2	20,2	3	19,2	1,7
Predorsal length	35,8	34,0	40,0	4	36,2	2,7
Distance between snout tip and terminus of dorsal-fin base	50,0	49,8	52,4	4	50,5	1,2
Distance between snout tip and dorsal-fin distal end	62,2	61,4	65,7	4	63,2	1,9
Dorsal fin to adipose fin	9,8	9,2	17,0	4	11,6	3,7
Dorsal-fin base	15,6	15,0	16,7	4	15,6	0,8
Length of first dorsal-fin ray (unbranched)	18,8	14,7	20,2	4	18,3	2,5
Length of rigid part of first dorsal-fin ray	13,3	12,0	15,7	4	13,8	1,5
Length of second dorsal-fin ray (first branched)	23,5	17,5	24,1	4	21,6	3,0
Length of third dorsal-fin ray (second branched)	20,7	16,6	22,9	4	20,1	2,6
Prepectoral length	23,4	22,5	28,4	4	24,2	2,8
Distance between snout tip and terminus of pectoral-fin base	25,2	24,9	30,3	4	26,7	2,5
Distance between snout tip and pectoral-fin distal end	45,2	41,4	47,9	4	44,6	2,7
Length of first left pectoral-fin ray (unbranched)	-	20,8	22,1	2	21,4	0,9
Length of rigid part of first left pectoral-fin ray	19,0	16,3	19,8	4	17,9	1,8
Length of second left pectoral-fin ray (first branched)	19,8	19,2	21,1	4	20,1	0,8
Length of third left pectoral-fin ray (second branched)	17,3	17,3	19,6	4	18,3	0,9
Prepelvic length	44,6	44,5	48,9	4	46,1	2,1
Distance between snout tip and terminus of pelvic-fin base	47,0	46,5	52,1	4	48,5	2,5
Distance between snout tip and pelvic-fin distal end	60,4	60,4	69,9	4	63,2	4,5
Distance between pelvic fins	3,7	2,9	3,7	4	3,4	0,3
Length of first left pelvic-fin ray (unbranched)	14,8	13,8	15,8	4	14,8	0,8
Length of second left pelvic-fin ray (first branched)	16,3	15,8	16,5	4	16,3	0,3
Length of third left pelvic-fin ray (second branched)	15,9	14,7	15,9	3	15,4	0,6
Anal-fin base	14,8	12,6	14,8	4	13,6	1,1
Preanal length	71,8	68,4	71,8	4	69,7	1,5
Distance between snout tip and terminus of anal-fin base	81,6	80,1	82,6	4	81,7	1,1
Distance between snout tip and anal-fin distal end	91,1	89,8	91,7	4	90,9	0,8
Adipose-fin length	30,7	26,9	33,0	4	30,8	2,8
Preadipose length	56,2	56,2	60,6	4	58,4	1,8
Distance between snout tip and adipose-fin base end	90,5	87,7	90,6	4	89,4	1,4
Adipose-fin depth	4,8	4,6	4,9	4	4,8	0,1
Caudal-peduncle length posterior to adipose-fin	12,1	10,8	12,1	4	11,5	0,5
Caudal-peduncle depth at adipose-fin terminus	7,9	7,9	8,9	4	8,3	0,5
Snout-anus distance	47,5	47,5	55,7	4	51,1	3,4

Snout-urogenital papilla distance	54,5	53,9	59,9	4	55,8	2,8
Anus-urogenital papilla distance	5,9	4,4	5,9	4	5,1	0,6
Dorsal lobe of caudal fin length	31,7	24,2	31,7	3	28,5	3,9
Ventral lobe of caudal fin length	28,5	25,0	31,8	4	29,3	3,2

Percentages of HL

Head depth	49,8	49,8	50,4	4	50,2	0,3
Head width	49,3	49,3	62,1	4	54,5	5,9
Eye diameter (left)	24,6	19,0	25,5	4	22,7	2,9
Fleshy interorbital	23,0	23,0	26,1	4	24,3	1,3
Bony interorbital	18,2	18,2	20,2	4	19,0	0,9
Mouth gape	28,9	27,3	31,2	4	29,6	1,9
Snout length (left)	27,8	27,1	32,0	4	29,1	2,2
Distance between snout tip and posterior nare (left side)	19,0	17,2	19,7	4	18,6	1,1
Anterior internarial width	12,7	12,1	15,8	4	13,3	1,7
Posterior internarial width	14,7	14,6	17,5	4	15,7	1,4
Intranarial length (left side)	13,8	13,8	16,2	4	14,9	1,3

Table 53: Morphometric data of *Pimelodella odynea* based on type material.

	Holotype	Min.	Max.	<i>n</i>	<i>x</i>	SD
Total length (mm)	108,6	66,5	129,8	23	97,9	
Standard length (mm)	88,3	51,6	99,6	24	75,2	
	Percentages of SL					
Body depth (dorsal)	16,2	14,3	21,4	24	17,1	2,0
Body width (dorsal)	14,2	12,2	18,3	24	14,1	1,5
Cleithral width	16,6	15,7	18,7	24	17,3	0,7
Head length	29,5	26,7	31,2	24	29,3	1,2
Maxillary-barbel length (left side)	100,4	65,7	100,7	23	86,6	8,7
Outer mental-barbel length (left side)	35,0	23,3	37,8	24	30,2	3,9
Inner mental-barbel length (left side)	18,5	13,4	20,3	24	17,1	1,7
Predorsal length	32,3	29,6	34,5	24	32,4	1,0
Distance between snout tip and terminus of dorsal-fin base	46,3	45,4	49,1	24	47,1	0,9
Distance between snout tip and dorsal-fin distal end	58,3	56,3	61,3	24	58,6	1,4
Dorsal fin to adipose fin	15,6	11,0	16,7	24	13,6	1,6
Dorsal-fin base	15,1	14,5	16,8	24	15,6	0,7
Length of first dorsal-fin ray (unbranched)	23,0	20,0	26,2	21	22,1	1,5
Length of rigid part of first dorsal-fin ray	16,2	13,5	19,1	24	16,2	1,3
Length of second dorsal-fin ray (first branched)	21,6	19,1	24,7	24	21,5	1,4
Length of third dorsal-fin ray (second branched)	21,6	17,7	24,2	24	20,8	1,6
Prepectoral length	19,9	17,9	23,6	24	21,1	1,0
Distance between snout tip and terminus of pectoral-fin base	22,3	22,3	26,2	24	23,9	1,0
Distance between snout tip and pectoral-fin distal end	0,0	36,9	44,8	21	40,7	2,1
Length of first left pectoral-fin ray (unbranched)	0,0	16,1	22,9	21	20,0	1,7
Length of rigid part of first left pectoral-fin ray	14,6	12,8	19,3	24	16,8	1,7
Length of second left pectoral-fin ray (first branched)	18,0	14,4	22,9	23	18,5	1,5
Length of third left pectoral-fin ray (second branched)	0,0	14,9	19,4	22	17,1	1,2
Prepelvic length	45,1	42,2	50,0	24	45,8	1,7
Distance between snout tip and terminus of pelvic-fin base	46,9	44,5	53,4	24	48,0	1,9
Distance between snout tip and pelvic-fin distal end	60,3	59,2	66,5	24	62,1	2,0
Distance between pelvic fins	6,0	4,1	6,1	23	5,4	0,5
Length of first left pelvic-fin ray (unbranched)	12,5	9,9	14,7	24	12,1	1,1
Length of second left pelvic-fin ray (first branched)	14,3	11,5	16,2	24	14,4	1,2
Length of third left pelvic-fin ray (second branched)	14,8	13,8	17,1	24	15,1	0,8
Anal-fin base	12,0	11,4	15,8	24	13,3	1,2
Preanal length	67,7	65,1	71,6	24	67,5	1,6
Distance between snout tip and terminus of anal-fin base	78,4	70,5	82,4	24	79,5	2,3
Distance between snout tip and anal-fin distal end	86,5	81,5	90,6	24	87,5	1,8
Adipose-fin length	30,5	28,8	35,0	24	30,5	1,4
Preadipose length	60,2	57,0	62,4	24	59,5	1,3
Distance between snout tip and adipose-fin base end	87,9	87,0	91,2	24	88,9	1,1
Adipose-fin depth	3,8	3,4	5,4	24	4,4	0,6
Caudal-peduncle length posterior to adipose-fin	11,8	9,0	12,7	24	11,2	0,9
Caudal-peduncle depth at adipose-fin terminus	7,4	7,3	9,6	24	8,0	0,6
Snout-anus distance	51,7	49,6	55,5	23	52,1	1,6
Snout-urogenital papilla distance	55,9	54,6	63,7	23	57,8	2,3

Anus-urogenital papilla distance	4,6	3,1	10,0	23	5,9	1,9
Dorsal lobe of caudal fin length	26,6	21,8	41,9	23	32,6	4,5
Ventral lobe of caudal fin length	22,3	19,9	27,3	24	24,3	2,0

Percentages of HL

Head depth	43,0	41,7	54,3	24	46,0	3,2
Head width	54,0	51,5	64,2	24	58,2	3,7
Eye diameter (left)	16,1	15,3	21,7	24	19,2	1,5
Fleshy interorbital	22,2	19,0	25,6	24	22,2	1,8
Bony interorbital	15,5	12,2	19,9	24	15,3	1,9
Mouth gape	32,4	26,7	36,9	24	32,0	2,6
Snout length (left)	30,7	27,8	36,0	24	30,5	1,8
Distance between snout tip and posterior nare (left side)	18,2	16,8	21,8	24	19,3	1,4
Anterior internarial width	13,8	10,6	15,2	24	12,9	1,3
Posterior internarial width	14,9	11,4	18,5	24	14,2	1,8
Intranarial length (left side)	14,3	12,2	27,8	24	15,6	2,8

Table 54: Morphometric data of *Pimelodella pectinifera* based on type material.

	Holotype
Total length (mm)	187,6
Standard length (mm)	150,9
Percentages of SL	
Body depth (dorsal)	20,1
Body width (dorsal)	14,7
Cleithral width	18,9
Head length	29,3
Maxillary-barbel length (left side)	57,3
Outer mental-barbel length (left side)	25,5
Inner mental-barbel length (left side)	16,3
Predorsal length	33,0
Distance between snout tip and terminus of dorsal-fin base	47,3
Distance between snout tip and dorsal-fin distal end	57,8
Dorsal fin to adipose fin	14,2
Dorsal-fin base	15,9
Length of first dorsal-fin ray (unbranched)	-
Length of rigid part of first dorsal-fin ray	19,5
Length of second dorsal-fin ray (first branched)	21,6
Length of third dorsal-fin ray (second branched)	20,7
Prepectoral length	20,9
Distance between snout tip and terminus of pectoral-fin base	23,5
Distance between snout tip and pectoral-fin distal end	40,2
Length of first left pectoral-fin ray (unbranched)	-
Length of rigid part of first left pectoral-fin ray	20,8
Length of second left pectoral-fin ray (first branched)	19,2
Length of third left pectoral-fin ray (second branched)	17,7
Prepelvic length	48,5
Distance between snout tip and terminus of pelvic-fin base	50,5
Distance between snout tip and pelvic-fin distal end	63,9
Distance between pelvic fins	5,9
Length of first left pelvic-fin ray (unbranched)	12,0
Length of second left pelvic-fin ray (first branched)	13,6
Length of third left pelvic-fin ray (second branched)	13,9
Anal-fin base	13,2
Preanal length	67,2
Distance between snout tip and terminus of anal-fin base	80,3
Distance between snout tip and anal-fin distal end	88,6
Adipose-fin length	25,4
Preadipose length	60,5
Distance between snout tip and adipose-fin base end	85,8
Adipose-fin depth	4,7
Caudal-peduncle length posterior to adipose-fin	14,4
Caudal-peduncle depth at adipose-fin terminus	9,3
Snout-anus distance	52,1
Snout-urogenital papilla distance	56,4

Anus-urogenital papilla distance	4,7
Dorsal lobe of caudal fin length	-
Ventral lobe of caudal fin length	23,4

Percentages of HL

Head depth	50,8
Head width	58,5
Eye diameter (left)	18,7
Fleshy interorbital	21,5
Bony interorbital	14,6
Mouth gape	30,7
Snout length (left)	35,8
Distance between snout tip and posterior nare (left side)	22,2
Anterior internarial width	21,4
Posterior internarial width	11,8
Intranarial length (left side)	11,9

Table 55: Morphometric data of *Pimelodella peruana* based on type and comparative materials.

	Holotype	Min.	Max.	<i>n</i>	<i>x</i>	SD
Total length (mm)	45,8	45,8	88,7	4	74,5	
Standard length (mm)	40,3	40,3	69,9	4	59,9	
	Percentages of SL					
Body depth (dorsal)	13,4	13,4	16,1	4	15,3	1,3
Body width (dorsal)	10,7	10,7	15,7	4	13,4	2,1
Cleithral width	15,7	15,4	16,4	4	15,8	0,4
Head length	29,3	27,8	29,3	4	28,6	0,7
Maxillary-barbel length (left side)	62,5	62,5	87,1	4	78,0	10,9
Outer mental-barbel length (left side)	27,1	27,1	45,7	4	38,3	8,5
Inner mental-barbel length (left side)	15,1	15,1	21,7	4	19,3	2,9
Predorsal length	29,3	29,3	32,0	4	31,0	1,2
Distance between snout tip and terminus of dorsal-fin base	45,8	45,6	46,1	4	45,8	0,2
Distance between snout tip and dorsal-fin distal end	56,1	55,5	56,1	4	55,8	0,2
Dorsal fin to adipose fin	15,4	15,4	20,7	4	18,2	2,2
Dorsal-fin base	14,7	14,7	15,4	4	15,0	0,3
Length of first dorsal-fin ray (unbranched)	15,6	15,6	22,9	3	19,9	3,9
Length of rigid part of first dorsal-fin ray	15,6	15,6	17,3	4	16,4	0,9
Length of second dorsal-fin ray (first branched)	21,0	20,5	21,2	4	20,9	0,3
Length of third dorsal-fin ray (second branched)	17,0	17,0	19,4	4	18,3	1,0
Prepectoral length	23,8	20,0	23,8	4	21,2	1,8
Distance between snout tip and terminus of pectoral-fin base	25,3	23,8	25,3	4	24,4	0,6
Distance between snout tip and pectoral-fin distal end	41,0	32,8	41,0	2	36,9	5,8
Length of first left pectoral-fin ray (unbranched)	19,4	19,4	-	1	-	-
Length of rigid part of first left pectoral-fin ray	17,7	15,6	17,7	4	16,5	0,9
Length of second left pectoral-fin ray (first branched)	19,2	13,6	19,2	3	16,3	2,8
Length of third left pectoral-fin ray (second branched)	16,8	14,9	16,8	2	15,8	1,3
Prepelvic length	45,2	44,8	45,7	4	45,3	0,4
Distance between snout tip and terminus of pelvic-fin base	48,3	46,6	48,6	4	47,9	0,9
Distance between snout tip and pelvic-fin distal end	60,1	59,8	60,8	4	60,4	0,5
Distance between pelvic fins	3,0	3,0	4,3	4	3,7	0,6
Length of first left pelvic-fin ray (unbranched)	12,9	10,2	12,9	4	11,2	1,2
Length of second left pelvic-fin ray (first branched)	13,3	13,3	15,4	4	13,9	1,0
Length of third left pelvic-fin ray (second branched)	14,3	12,3	15,7	4	14,0	1,4
Anal-fin base	12,1	12,0	13,5	4	12,7	0,7
Preanal length	66,8	66,7	67,3	4	66,9	0,3
Distance between snout tip and terminus of anal-fin base	79,1	78,7	80,8	4	79,5	0,9
Distance between snout tip and anal-fin distal end	86,0	84,7	86,9	4	86,0	0,9
Adipose-fin length	23,1	23,1	25,9	4	24,3	1,4
Preadipose length	62,8	62,1	64,4	4	62,9	1,0
Distance between snout tip and adipose-fin base end	85,8	85,7	87,0	4	86,1	0,6
Adipose-fin depth	3,3	3,3	5,2	4	4,4	0,9
Caudal-peduncle length posterior to adipose-fin	13,5	13,5	15,0	4	14,2	0,6
Caudal-peduncle depth at adipose-fin terminus	7,0	6,5	7,0	4	6,9	0,2
Snout-anus distance	48,8	48,8	52,4	4	50,7	1,5

Snout-urogenital papilla distance	55,6	55,5	57,5	4	56,2	0,9
Anus-urogenital papilla distance	4,6	4,3	5,9	4	4,8	0,7
Dorsal lobe of caudal fin length	-	26,4	28,7	2	27,5	1,6
Ventral lobe of caudal fin length	-	29,2	-	1	-	-

Percentages of HL

Head depth	44,4	44,4	51,0	4	47,0	3,0
Head width	52,0	52,0	59,1	4	54,9	3,0
Eye diameter (left)	23,3	23,3	25,6	4	23,9	1,1
Fleshy interorbital	18,7	18,7	22,4	4	20,6	1,8
Bony interorbital	13,7	10,5	13,7	4	12,9	1,5
Mouth gape	28,4	28,4	31,9	4	30,0	1,4
Snout length (left)	24,7	24,7	28,3	4	26,5	2,0
Distance between snout tip and posterior nare (left side)	20,1	18,1	20,3	4	19,5	1,0
Anterior internarial width	14,1	12,4	14,1	4	13,4	0,8
Posterior internarial width	15,0	14,0	15,2	4	14,5	0,6
Intranarial length (left side)	13,2	13,2	16,1	4	14,8	1,3

Table 56: Morphometric data of *Pimelodella reyesi* based on type and comparative materials.

	Holotype	Comp.
Total length (mm)	-	130,2
Standard length (mm)	99,0	98,1
Percentages of SL		
Body depth (dorsal)	23,0	21,5
Body width (dorsal)	-	13,5
Cleithral width	17,8	16,4
Head length	30,0	30,7
Maxillary-barbel length (left side)	-	104,2
Outer mental-barbel length (left side)	-	40,4
Inner mental-barbel length (left side)	-	22,2
Predorsal length	32,1	35,7
Distance between snout tip and terminus of dorsal-fin base	-	49,9
Distance between snout tip and dorsal-fin distal end	-	62,4
Dorsal fin to adipose fin	-	12,3
Dorsal-fin base	-	16,5
Length of first dorsal-fin ray (unbranched)	-	20,4
Length of rigid part of first dorsal-fin ray	19,0	17,7
Length of second dorsal-fin ray (first branched)	-	23,5
Length of third dorsal-fin ray (second branched)	-	25,2
Prepectoral length	22,0	22,3
Distance between snout tip and terminus of pectoral-fin base	-	25,5
Distance between snout tip and pectoral-fin distal end	-	42,8
Length of first left pectoral-fin ray (unbranched)	-	20,4
Length of rigid part of first left pectoral-fin ray	16,9	18,9
Length of second left pectoral-fin ray (first branched)	-	21,4
Length of third left pectoral-fin ray (second branched)	-	21,0
Prepelvic length	48,1	46,8
Distance between snout tip and terminus of pelvic-fin base	-	48,9
Distance between snout tip and pelvic-fin distal end	-	65,3
Distance between pelvic fins	-	5,8
Length of first left pelvic-fin ray (unbranched)	-	14,5
Length of second left pelvic-fin ray (first branched)	-	16,5
Length of third left pelvic-fin ray (second branched)	-	17,3
Anal-fin base	-	12,2
Preanal length	66,0	69,5
Distance between snout tip and terminus of anal-fin base	-	81,5
Distance between snout tip and anal-fin distal end	-	89,1
Adipose-fin length	28,5	29,3
Preadipose length	-	61,1
Distance between snout tip and adipose-fin base end	-	89,2
Adipose-fin depth	-	5,1
Caudal-peduncle length posterior to adipose-fin	-	-
Caudal-peduncle depth at adipose-fin terminus	10,0	7,2
Snout-anus distance	58,2	54,3
Snout-urogenital papilla distance	-	54,0

Anus-urogenital papilla distance	-	-
Dorsal lobe of caudal fin length	25,2	33,1
Ventral lobe of caudal fin length	25,1	-

Percentages of HL

Head depth	-	43,2
Head width	-	47,2
Eye diameter (left)	16,7	18,7
Fleshy interorbital	-	21,0
Bony interorbital	25,7	18,8
Mouth gape	-	26,9
Snout length (left)	34,7	33,1
Distance between snout tip and posterior nare (left side)	-	20,5
Anterior internarial width	-	11,5
Posterior internarial width	-	13,6
Intranarial length (left side)	-	13,5

Table 57: Morphometric data of *Pimelodella robinsoni* and *P. wolffi*, its junior-synonym, based on type material.

	Holotype	Min.	Max.	<i>n</i>	<i>x</i>	SD
Total length (mm)	88,3	88,1	110,9	4	94,1	
Standard length (mm)	73,0	67,1	88,9	5	74,2	
	Percentages of SL					
Body depth (dorsal)	19,6	16,4	19,8	4	18,2	1,7
Body width (dorsal)	14,6	11,6	16,5	4	14,2	2,0
Cleithral width	16,6	16,6	19,1	4	17,5	1,1
Head length	26,0	26,0	32,3	5	29,1	2,4
Maxillary-barbel length (left side)	-	68,0	80,1	3	74,0	6,0
Outer mental-barbel length (left side)	22,0	19,4	22,0	4	20,6	1,1
Inner mental-barbel length (left side)	13,4	9,9	13,4	4	11,6	1,5
Predorsal length	29,0	29,0	35,5	4	32,5	2,7
Distance between snout tip and terminus of dorsal-fin base	46,8	46,5	49,9	4	48,0	1,6
Distance between snout tip and dorsal-fin distal end	55,2	55,2	60,9	4	58,2	2,5
Dorsal fin to adipose fin	7,9	7,8	10,9	4	8,7	1,5
Dorsal-fin base	13,9	13,9	15,8	4	15,1	0,8
Length of first dorsal-fin ray (unbranched)	-	-	-	-	-	-
Length of rigid part of first dorsal-fin ray	-	20,7	20,7	1	20,7	-
Length of second dorsal-fin ray (first branched)	17,1	17,1	21,6	4	20,2	2,1
Length of third dorsal-fin ray (second branched)	15,8	15,8	21,7	4	19,4	2,6
Prepectoral length	21,0	21,0	25,4	4	23,5	2,2
Distance between snout tip and terminus of pectoral-fin base	22,6	22,6	28,1	4	25,9	2,5
Distance between snout tip and pectoral-fin distal end	34,9	34,9	43,0	4	39,5	3,8
Length of first left pectoral-fin ray (unbranched)	-	17,1	20,1	3	18,4	1,5
Length of rigid part of first left pectoral-fin ray	-	13,4	15,9	3	14,7	1,3
Length of second left pectoral-fin ray (first branched)	14,4	14,4	18,2	4	16,7	1,7
Length of third left pectoral-fin ray (second branched)	12,9	12,9	17,0	2	15,0	2,9
Prepelvic length	45,5	45,5	51,5	4	47,4	2,7
Distance between snout tip and terminus of pelvic-fin base	47,0	47,0	54,4	4	50,0	3,1
Distance between snout tip and pelvic-fin distal end	59,1	59,1	68,5	4	63,5	3,9
Distance between pelvic fins	4,5	3,9	5,5	4	4,8	0,8
Length of first left pelvic-fin ray (unbranched)	10,2	10,2	13,7	4	12,6	1,6
Length of second left pelvic-fin ray (first branched)	12,5	12,5	16,0	4	15,0	1,7
Length of third left pelvic-fin ray (second branched)	13,6	13,6	16,7	4	15,5	1,4
Anal-fin base	13,5	13,5	14,8	4	13,9	0,6
Preanal length	66,3	63,5	69,0	4	65,8	2,4
Distance between snout tip and terminus of anal-fin base	79,6	78,5	80,6	4	79,4	0,9
Distance between snout tip and anal-fin distal end	87,3	86,9	88,9	4	87,5	1,0
Adipose-fin length	36,4	31,5	37,1	4	35,0	2,5
Preadipose length	52,9	52,9	58,7	4	55,7	2,9
Distance between snout tip and adipose-fin base end	88,9	88,5	89,7	4	89,2	0,6
Adipose-fin depth	5,2	4,7	5,8	4	5,3	0,5
Caudal-peduncle length posterior to adipose-fin	10,8	9,0	11,6	4	10,5	1,1
Caudal-peduncle depth at adipose-fin terminus	7,3	7,3	9,2	4	8,5	0,8
Snout-anus distance	48,3	48,3	59,5	4	53,2	4,6

Snout-urogenital papilla distance	52,4	52,4	63,2	4	60,3	5,3
Anus-urogenital papilla distance	3,8	3,8	9,7	4	6,7	3,1
Dorsal lobe of caudal fin length	-	24,8	25,4	2	25,1	0,5
Ventral lobe of caudal fin length	21,8	21,8	26,7	4	23,9	2,0

Percentages of HL

Head depth	56,0	50,2	58,7	4	54,2	3,9
Head width	64,0	62,9	66,9	4	65,0	1,9
Eye diameter (left)	17,6	17,6	23,9	5	20,7	2,9
Fleshy interorbital	24,3	22,4	26,6	4	24,1	1,9
Bony interorbital	18,5	14,6	18,5	4	15,8	1,8
Mouth gape	34,3	33,3	35,2	4	34,3	0,8
Snout length (left)	33,6	31,2	34,3	4	33,0	1,3
Distance between snout tip and posterior nare (left side)	21,9	18,8	21,9	4	19,8	1,4
Anterior internarial width	14,4	14,2	16,7	4	15,2	1,1
Posterior internarial width	17,3	13,6	17,3	4	15,2	1,5
Intranarial length (left side)	12,3	12,3	14,7	4	13,4	1,0

Table 58: Morphometric data of *Pimelodella robinsoni* and *P. wolfi*, its junior-synonym, based on type material, discriminated by original species name.

	<i>P. robinsoni</i>		<i>P. wolfi</i>					
	Holotype		Holotype	Min.	Max.	<i>n</i>	<i>x</i>	SD
Total length (mm)	88,3		110,9	88,1	110,9	3	96,0	
Standard length (mm)	73,0		88,9	67,1	88,9	4	74,5	
	Percentages of SL							
Body depth (dorsal)	19,6		16,4	16,4	19,8	3	17,8	1,8
Body width (dorsal)	14,6		11,6	11,6	16,5	3	14,0	2,4
Cleithral width	16,6		16,8	16,8	19,1	3	17,8	1,2
Head length	26,0		27,8	27,8	32,3	4	29,9	1,9
Maxillary-barbel length (left side)	-		74,0	68,0	80,1	3	74,0	6,0
Outer mental-barbel length (left side)	22,0		20,0	19,4	21,0	3	20,1	0,8
Inner mental-barbel length (left side)	13,4		11,1	9,9	12,0	3	11,0	1,1
Predorsal length	29,0		33,1	32,3	35,5	3	33,6	1,6
Distance between snout tip and terminus of dorsal-fin base	46,8		46,5	46,5	49,9	3	48,4	1,7
Distance between snout tip and dorsal-fin distal end	55,2		59,4	57,1	60,9	3	59,1	1,9
Dorsal fin to adipose fin	7,9		7,8	7,8	10,9	3	9,0	1,7
Dorsal-fin base	13,9		15,2	15,2	15,8	3	15,5	0,3
Length of first dorsal-fin ray (unbranched)	-		-	-	-	-	-	-
Length of rigid part of first dorsal-fin ray	-		20,7	20,7	20,7	1	20,7	-
Length of second dorsal-fin ray (first branched)	17,1		21,6	21,0	21,6	3	21,2	0,4
Length of third dorsal-fin ray (second branched)	15,8		21,7	19,2	21,7	3	20,6	1,3
Prepectoral length	21,0		25,3	22,3	25,4	3	24,3	1,7
Distance between snout tip and terminus of pectoral-fin base	22,6		27,6	25,2	28,1	3	27,0	1,6
Distance between snout tip and pectoral-fin distal end	34,9		42,4	37,9	43,0	3	41,1	2,8
Length of first left pectoral-fin ray (unbranched)	-		18,1	17,1	20,1	3	18,4	1,5
Length of rigid part of first left pectoral-fin ray	-		13,4	13,4	15,9	3	14,7	1,3
Length of second left pectoral-fin ray (first branched)	14,4		17,6	16,7	18,2	3	17,5	0,8
Length of third left pectoral-fin ray (second branched)	12,9		17,0	17,0	17,0	1	17,0	-

Prepelvic length	45,5	46,3	46,3	51,5	3	48,1	3,0
Distance between snout tip and terminus of pelvic-fin base	47,0	49,5	49,0	54,4	3	51,0	3,0
Distance between snout tip and pelvic-fin distal end	59,1	63,4	63,1	68,5	3	65,0	3,0
Distance between pelvic fins	4,5	3,9	3,9	5,5	3	4,9	0,9
Length of first left pelvic-fin ray (unbranched)	10,2	13,2	13,2	13,7	3	13,4	0,3
Length of second left pelvic-fin ray (first branched)	12,5	16,0	15,6	16,0	3	15,8	0,2
Length of third left pelvic-fin ray (second branched)	13,6	16,7	15,5	16,7	3	16,1	0,6
Anal-fin base	13,5	14,8	13,7	14,8	3	14,1	0,6
Preanal length	66,3	63,5	63,5	69,0	3	65,6	2,9
Distance between snout tip and terminus of anal-fin base	79,6	78,8	78,5	80,6	3	79,3	1,1
Distance between snout tip and anal-fin distal end	87,3	86,9	86,9	88,9	3	87,6	1,2
Adipose-fin length	36,4	35,0	31,5	37,1	3	34,6	2,8
Preadipose length	52,9	53,6	53,6	58,7	3	56,6	2,7
Distance between snout tip and adipose-fin base end	88,9	89,7	88,5	89,7	3	89,3	0,7
Adipose-fin depth	5,2	4,7	4,7	5,8	3	5,3	0,6
Caudal-peduncle length posterior to adipose-fin	10,8	11,6	9,0	11,6	3	10,4	1,3
Caudal-peduncle depth at adipose-fin terminus	7,3	8,8	8,8	9,2	3	8,9	0,2
Snout-anus distance	48,3	52,6	52,2	59,5	3	54,8	4,1
Snout-urogenital papilla distance	52,4	62,7	62,7	63,2	3	62,9	0,2
Anus-urogenital papilla distance	3,8	9,0	4,3	9,7	3	7,7	2,9
Dorsal lobe of caudal fin length	-	-	24,8	25,4	2	25,1	0,5
Ventral lobe of caudal fin length	21,8	26,7	23,5	26,7	3	24,6	1,8

Percentages of HL

Head depth	56,0	51,7	50,2	58,7	3	53,6	4,6
Head width	64,0	66,3	62,9	66,9	3	65,4	2,1
Eye diameter (left)	17,6	19,3	19,0	23,9	4	21,4	2,7
Fleshy interorbital	24,3	23,0	22,4	26,6	3	24,0	2,3
Bony interorbital	18,5	14,6	14,6	15,5	3	14,9	0,5
Mouth gape	34,3	33,3	33,3	35,2	3	34,3	0,9
Snout length (left)	33,6	34,3	31,2	34,3	3	32,9	1,6
Distance between snout tip and posterior nare (left side)	21,9	18,8	18,8	19,7	3	19,1	0,5

Anterior internarial width	14,4	16,7	14,2	16,7	3	15,5	1,3
Posterior internarial width	17,3	13,6	13,6	15,0	3	14,5	0,8
Intranarial length (left side)	12,3	12,9	12,9	14,7	3	13,8	0,9

Table 59: Morphometric data of *Pimelodella roccae* based on type and comparative materials.

	Holotype	Min.	Max.	n	x	SD
Total length (mm)	168,6	95,0	168,6	3	125,8	
Standard length (mm)	139,8	74,3	139,8	4	100,6	
	Percentages of SL					
Body depth (dorsal)	18,7	13,9	19,5	4	16,8	2,7
Body width (dorsal)	16,2	13,3	16,2	4	14,9	1,2
Cleithral width	18,9	15,9	18,9	4	17,3	1,2
Head length	28,4	27,4	31,4	4	28,9	1,7
Maxillary-barbel length (left side)	64,7	64,7	93,9	4	78,1	13,9
Outer mental-barbel length (left side)	28,7	28,7	40,5	4	33,1	5,2
Inner mental-barbel length (left side)	16,7	16,7	22,9	4	19,8	2,8
Predorsal length	32,1	29,1	34,3	4	31,8	2,1
Distance between snout tip and terminus of dorsal-fin base	46,6	46,4	49,6	4	47,5	1,5
Distance between snout tip and dorsal-fin distal end	55,9	54,8	59,7	4	56,7	2,1
Dorsal fin to adipose fin	12,5	6,5	12,5	4	8,6	2,6
Dorsal-fin base	14,0	14,0	17,5	4	15,8	1,5
Length of first dorsal-fin ray (unbranched)	-	18,8	22,9	3	20,6	2,1
Length of rigid part of first dorsal-fin ray	15,8	14,5	17,2	4	15,7	1,1
Length of second dorsal-fin ray (first branched)	19,4	19,0	21,8	4	20,1	1,2
Length of third dorsal-fin ray (second branched)	18,2	17,1	20,1	4	18,8	1,4
Prepectoral length	21,3	21,3	23,9	4	22,8	1,3
Distance between snout tip and terminus of pectoral-fin base	24,6	24,6	27,3	4	25,8	1,2
Distance between snout tip and pectoral-fin distal end	39,2	38,9	44,1	4	40,8	2,4
Length of first left pectoral-fin ray (unbranched)	20,9	18,3	22,2	4	20,3	1,7
Length of rigid part of first left pectoral-fin ray	17,0	14,9	17,8	4	16,6	1,3
Length of second left pectoral-fin ray (first branched)	18,3	15,9	18,3	3	17,5	1,4
Length of third left pectoral-fin ray (second branched)	17,2	14,3	17,2	4	15,7	1,4
Prepelvic length	45,0	42,9	48,1	4	46,0	2,5
Distance between snout tip and terminus of pelvic-fin base	47,9	45,5	50,4	4	48,3	2,2
Distance between snout tip and pelvic-fin distal end	59,5	57,6	64,8	4	60,9	3,1
Distance between pelvic fins	7,0	5,0	7,0	4	5,7	0,9
Length of first left pelvic-fin ray (unbranched)	12,7	12,7	14,5	4	13,2	0,9
Length of second left pelvic-fin ray (first branched)	15,7	13,1	15,7	4	14,5	1,2
Length of third left pelvic-fin ray (second branched)	15,9	14,0	15,9	4	15,0	0,9
Anal-fin base	15,2	15,2	16,5	4	15,7	0,7
Preanal length	63,5	63,1	67,3	4	64,7	1,9
Distance between snout tip and terminus of anal-fin base	78,2	78,2	80,6	4	79,5	1,2
Distance between snout tip and anal-fin distal end	86,6	86,3	87,4	4	86,9	0,5
Adipose-fin length	34,6	34,6	39,7	4	38,1	2,4
Preadipose length	58,2	51,7	58,2	4	55,2	2,7
Distance between snout tip and adipose-fin base end	88,4	87,3	92,1	4	89,5	2,1
Adipose-fin depth	4,4	4,1	5,2	4	4,5	0,5
Caudal-peduncle length posterior to adipose-fin	10,4	8,1	10,4	4	9,5	0,9
Caudal-peduncle depth at adipose-fin terminus	10,8	7,9	10,8	4	8,9	1,3
Snout-anus distance	53,4	50,0	55,5	4	53,2	2,4
Snout-urogenital papilla distance	57,0	54,1	59,5	4	57,1	2,3

Anus-urogenital papilla distance	3,9	3,5	4,8	4	3,9	0,6
Dorsal lobe of caudal fin length	-	29,0	29,0	1	29,0	-
Ventral lobe of caudal fin length	22,5	22,5	25,5	2	24,0	2,1

Percentages of HL

Head depth	50,4	38,4	55,9	4	47,4	7,5
Head width	64,0	60,8	66,9	4	63,2	2,8
Eye diameter (left)	15,1	15,1	19,3	4	16,6	1,9
Fleshy interorbital	26,3	25,2	28,0	4	26,2	1,3
Bony interorbital	19,4	19,4	21,4	4	20,4	0,9
Mouth gape	31,8	31,8	38,7	4	36,0	3,0
Snout length (left)	34,0	34,0	35,0	4	34,4	0,5
Distance between snout tip and posterior nare (left side)	19,4	19,0	21,8	4	20,4	1,3
Anterior internarial width	13,6	13,6	17,1	4	15,4	1,7
Posterior internarial width	15,8	15,1	17,1	4	16,1	0,8
Intranarial length (left side)	13,4	13,4	17,9	4	15,7	1,9

Table 60: Morphometric data of *Pimelodella serrata* and *P. chaparae*, its junior-synonym, based on type and comparative materials.

	Holotype	Min.	Max.	<i>n</i>	<i>x</i>	SD
Total length (mm)	-	58,3	124,0	7	89,6	
Standard length (mm)	55,7	34,7	99,5	10	63,9	
	Percentages of SL					
Body depth (dorsal)	15,6	13,7	20,1	8	17,3	2,3
Body width (dorsal)	9,3	9,3	15,3	8	12,7	2,0
Cleithral width	17,4	16,4	19,6	8	17,7	1,3
Head length	32,9	29,5	35,6	8	32,1	2,3
Maxillary-barbel length (left side)	100,3	77,1	102,9	6	89,3	10,9
Outer mental-barbel length (left side)	40,0	27,7	48,5	8	37,2	6,0
Inner mental-barbel length (left side)	18,0	14,8	26,1	8	17,7	3,6
Predorsal length	36,1	33,3	36,3	8	34,9	1,0
Distance between snout tip and terminus of dorsal-fin base	47,5	46,1	54,9	8	49,5	3,3
Distance between snout tip and dorsal-fin distal end	59,1	53,2	65,7	8	58,7	4,4
Dorsal fin to adipose fin	5,1	4,8	12,1	8	7,9	3,0
Dorsal-fin base	13,1	13,1	17,8	8	14,8	1,6
Length of first dorsal-fin ray (unbranched)	17,9	17,9	26,0	7	21,5	2,8
Length of rigid part of first dorsal-fin ray	13,9	13,9	22,9	8	19,3	3,0
Length of second dorsal-fin ray (first branched)	20,7	17,5	25,1	8	21,1	2,8
Length of third dorsal-fin ray (second branched)	-	16,6	21,4	5	18,8	1,9
Prepectoral length	23,5	21,3	27,0	8	23,3	1,7
Distance between snout tip and terminus of pectoral-fin base	26,1	24,9	30,5	8	26,9	1,7
Distance between snout tip and pectoral-fin distal end	42,0	37,2	49,3	8	43,9	4,1
Length of first left pectoral-fin ray (unbranched)	20,7	19,9	27,5	7	22,6	2,9
Length of rigid part of first left pectoral-fin ray	18,3	17,7	27,5	8	21,2	3,3
Length of second left pectoral-fin ray (first branched)	16,3	16,3	24,1	7	19,3	2,8
Length of third left pectoral-fin ray (second branched)	16,3	15,2	18,1	6	17,0	1,1
Prepelvic length	49,3	43,6	51,0	8	46,9	3,0
Distance between snout tip and terminus of pelvic-fin base	50,7	46,9	54,4	8	49,3	3,0
Distance between snout tip and pelvic-fin distal end	66,2	59,2	68,3	7	63,4	3,9
Distance between pelvic fins	3,3	2,9	14,7	8	5,2	3,9
Length of first left pelvic-fin ray (unbranched)	13,5	11,6	14,2	7	12,9	1,0
Length of second left pelvic-fin ray (first branched)	14,9	12,9	16,5	7	14,8	1,1
Length of third left pelvic-fin ray (second branched)	16,7	14,3	16,7	6	15,2	1,0
Anal-fin base	11,7	11,3	14,6	8	12,3	1,1
Preanal length	69,0	67,0	73,3	8	69,5	2,1
Distance between snout tip and terminus of anal-fin base	80,9	78,2	86,5	8	81,0	3,1
Distance between snout tip and anal-fin distal end	88,5	85,8	94,1	7	89,0	3,6
Adipose-fin length	38,4	28,9	38,4	8	34,2	3,6
Preadipose length	52,4	51,8	64,2	8	56,3	4,7
Distance between snout tip and adipose-fin base end	88,8	87,0	92,1	8	89,3	1,6
Adipose-fin depth	6,2	3,2	6,2	8	4,2	1,1
Caudal-peduncle length posterior to adipose-fin	10,6	9,6	12,9	8	11,5	1,1
Caudal-peduncle depth at adipose-fin terminus	7,3	5,8	8,7	8	7,1	1,0
Snout-anus distance	52,9	50,4	59,6	7	53,4	3,2

Snout-urogenital papilla distance	59,1	56,4	68,1	7	59,9	4,5
Anus-urogenital papilla distance	6,9	3,4	14,5	7	6,7	3,7
Dorsal lobe of caudal fin length	-	23,1	30,9	7	25,4	2,7
Ventral lobe of caudal fin length	-	23,9	33,5	7	27,5	3,4

Percentages of HL

Head depth	38,5	38,5	48,7	8	44,3	3,4
Head width	49,4	49,4	57,6	8	53,4	2,8
Eye diameter (left)	19,2	19,2	24,9	8	21,0	1,8
Fleshy interorbital	26,4	20,0	26,4	8	23,0	2,0
Bony interorbital	18,4	13,1	19,0	8	17,2	1,8
Mouth gape	29,3	25,2	31,4	8	28,1	1,8
Snout length (left)	33,9	29,0	33,9	8	31,9	1,7
Distance between snout tip and posterior nare (left side)	14,9	14,9	19,0	8	17,2	1,4
Anterior internarial width	14,1	11,9	14,6	8	13,5	0,9
Posterior internarial width	13,2	11,8	14,7	8	13,2	0,9
Intranarial length (left side)	12,7	12,6	16,9	8	14,1	1,6

Table 61: Morphometric data of *Pimelodella serrata* and *P. chaparae*, its junior-synonym, based on type and comparative materials, discriminated by original species name.

	<i>P. serrata</i>						<i>P. chaparae</i>	
	Holotype	Min.	Max.	n	x	SD	Holotype	Paratype
Total length (mm)	-	75,1	124,0	5	101,3		62,1	58,3
Standard length (mm)	55,7	34,7	99,5	8	67,9		48,1	47,5
	Percentages of SL							
Body depth (dorsal)	15,6	13,7	20,1	6	16,5	2,1	19,8	19,4
Body width (dorsal)	9,3	9,3	14,9	6	12,5	1,9	11,7	15,3
Cleithral width	17,4	16,4	18,8	6	17,1	0,9	19,6	19,3
Head length	32,9	29,5	32,9	6	31,0	1,3	35,1	35,6
Maxillary-barbel length (left side)	100,3	77,1	102,9	6	89,3	10,9	-	-
Outer mental-barbel length (left side)	40,0	35,4	48,5	6	39,5	4,8	33,2	27,7
Inner mental-barbel length (left side)	18,0	14,8	26,1	6	18,1	4,1	16,5	16,2
Predorsal length	36,1	33,3	36,3	6	34,9	1,2	34,6	35,3
Distance between snout tip and terminus of dorsal-fin base	47,5	46,1	50,8	6	47,8	1,6	54,9	53,7
Distance between snout tip and dorsal-fin distal end	59,1	53,2	59,1	6	56,5	2,0	65,7	65,1
Dorsal fin to adipose fin	5,1	4,8	12,1	6	6,9	2,8	10,2	11,4
Dorsal-fin base	13,1	13,1	15,0	6	14,0	0,6	17,8	16,5
Length of first dorsal-fin ray (unbranched)	17,9	17,9	23,6	5	20,4	2,3	26,0	22,5
Length of rigid part of first dorsal-fin ray	13,9	13,9	20,2	6	18,2	2,6	22,9	22,5
Length of second dorsal-fin ray (first branched)	20,7	17,5	23,8	6	20,1	2,4	25,1	23,1
Length of third dorsal-fin ray (second branched)	-	16,6	19,4	4	18,1	1,3	21,4	-
Prepectoral length	23,5	21,3	23,5	6	22,6	0,8	27,0	23,9
Distance between snout tip and terminus of pectoral-fin base	26,1	24,9	26,8	6	26,1	0,6	30,5	28,3
Distance between snout tip and pectoral-fin distal end	42,0	37,2	46,9	6	42,2	3,1	48,9	49,3
Length of first left pectoral-fin ray (unbranched)	20,7	19,9	21,6	5	21,0	0,7	25,9	27,5
Length of rigid part of first left pectoral-fin ray	18,3	17,7	21,2	6	19,5	1,4	24,6	27,5
Length of second left pectoral-fin ray (first branched)	16,3	16,3	19,4	5	17,8	1,3	21,7	24,1

Length of third left pectoral-fin ray (second branched)	16,3	15,2	17,4	4	16,5	1,0	18,0	18,1
Prepelvic length	49,3	43,6	49,3	6	45,6	2,0	50,7	51,0
Distance between snout tip and terminus of pelvic-fin base	50,7	46,9	50,7	6	47,9	1,4	54,4	53,1
Distance between snout tip and pelvic-fin distal end	66,2	59,2	66,2	5	61,6	2,8	68,3	67,7
Distance between pelvic fins	3,3	2,9	14,7	6	5,7	4,5	3,9	3,5
Length of first left pelvic-fin ray (unbranched)	13,5	11,6	13,6	5	12,6	0,9	13,1	14,2
Length of second left pelvic-fin ray (first branched)	14,9	12,9	15,1	5	14,3	0,9	15,6	16,5
Length of third left pelvic-fin ray (second branched)	16,7	14,3	16,7	4	15,0	1,1	15,9	14,9
Anal-fin base	11,7	11,3	12,7	6	11,9	0,6	12,8	14,6
Preanal length	69,0	67,0	69,6	6	68,4	1,0	71,7	73,3
Distance between snout tip and terminus of anal-fin base	80,9	78,2	80,9	6	79,5	1,2	84,9	86,5
Distance between snout tip and anal-fin distal end	88,5	85,8	88,5	5	87,0	1,3	94,1	93,9
Adipose-fin length	38,4	30,1	38,4	6	35,6	2,9	28,9	31,2
Preadipose length	52,4	51,8	58,1	6	54,1	2,3	64,2	62,1
Distance between snout tip and adipose-fin base end	88,8	87,0	92,1	6	88,9	1,7	90,3	90,6
Adipose-fin depth	6,2	3,2	6,2	6	4,0	1,1	4,1	5,5
Caudal-peduncle length posterior to adipose-fin	10,6	10,4	12,3	6	11,5	0,8	9,6	12,9
Caudal-peduncle depth at adipose-fin terminus	7,3	5,8	7,3	6	6,6	0,6	8,7	8,1
Snout-anus distance	52,9	50,4	55,5	5	52,4	2,0	59,6	52,0
Snout-urogenital papilla distance	59,1	56,4	68,1	5	59,5	4,9	64,3	57,6
Anus-urogenital papilla distance	6,9	5,9	14,5	5	8,0	3,6	3,7	3,4
Dorsal lobe of caudal fin length	-	23,1	25,4	5	24,0	0,9	30,9	26,7
Ventral lobe of caudal fin length	-	23,9	29,4	5	25,9	2,1	33,5	29,0

Percentages of HL

Head depth	38,5	38,5	48,1	6	43,3	3,2	48,7	45,9
Head width	49,4	49,4	57,6	6	53,2	3,1	55,6	52,2
Eye diameter (left)	19,2	19,2	24,9	6	21,2	2,1	20,0	20,6
Fleshy interorbital	26,4	20,0	26,4	6	22,8	2,2	22,5	24,4
Bony interorbital	18,4	13,1	18,4	6	16,8	1,9	19,0	18,0
Mouth gape	29,3	25,2	31,4	6	28,3	2,1	27,6	27,3
Snout length (left)	33,9	31,2	33,9	6	32,7	0,9	29,8	29,0

Distance between snout tip and posterior nare (left side)	14,9	14,9	19,0	6	17,0	1,5	18,3	17,3
Anterior internarial width	14,1	11,9	14,6	6	13,6	1,0	13,7	12,6
Posterior internarial width	13,2	11,8	14,1	6	13,0	0,8	14,7	13,3
Intranarial length (left side)	12,7	12,6	16,9	6	14,3	1,8	12,8	14,1

Table 62: Morphometric data of *Pimelodella spelaea* based on type material.

	Holotype	Min.	Max.	n	x	SD
Total length (mm)	98,2	53,2	98,2	6	83,9	
Standard length (mm)	78,9	42,4	78,9	7	65,7	
	Percentages of SL					
Body depth (dorsal)	16,7	14,7	17,9	7	16,1	1,4
Body width (dorsal)	13,7	10,2	13,7	7	12,3	1,3
Cleithral width	18,6	17,7	21,0	7	19,0	1,3
Head length	29,8	29,2	34,5	7	31,1	2,1
Maxillary-barbel length (left side)	63,2	47,5	72,5	6	59,8	10,1
Outer mental-barbel length (left side)	25,0	22,3	27,5	6	25,1	2,0
Inner mental-barbel length (left side)	13,5	13,5	16,7	6	14,9	1,2
Predorsal length	33,6	32,2	37,4	7	34,2	1,7
Distance between snout tip and terminus of dorsal-fin base	46,5	44,1	49,7	7	46,7	1,9
Distance between snout tip and dorsal-fin distal end	55,6	52,5	59,9	7	55,6	2,5
Dorsal fin to adipose fin	13,0	10,0	13,2	7	11,5	1,2
Dorsal-fin base	13,4	12,3	13,9	7	13,2	0,6
Length of first dorsal-fin ray (unbranched)	17,5	16,2	18,6	6	17,4	0,9
Length of rigid part of first dorsal-fin ray	13,9	13,0	15,9	7	14,7	1,0
Length of second dorsal-fin ray (first branched)	17,0	14,8	21,3	6	17,7	2,2
Length of third dorsal-fin ray (second branched)	15,9	15,3	20,2	7	17,1	1,6
Prepectoral length	21,9	21,9	25,9	7	23,8	1,6
Distance between snout tip and terminus of pectoral-fin base	24,5	24,5	28,7	7	26,0	1,7
Distance between snout tip and pectoral-fin distal end	40,0	36,9	46,5	7	40,8	3,4
Length of first left pectoral-fin ray (unbranched)	18,6	17,9	20,4	5	18,9	0,9
Length of rigid part of first left pectoral-fin ray	14,0	14,0	18,3	6	16,1	1,5
Length of second left pectoral-fin ray (first branched)	17,3	16,1	19,8	6	17,5	1,2
Length of third left pectoral-fin ray (second branched)	16,6	14,8	17,6	6	15,9	1,2
Prepelvic length	44,9	43,6	48,9	7	46,3	2,1
Distance between snout tip and terminus of pelvic-fin base	47,2	46,5	51,6	7	48,8	2,1
Distance between snout tip and pelvic-fin distal end	58,8	57,7	63,4	7	59,6	2,2
Distance between pelvic fins	4,8	3,1	4,8	7	3,9	0,6
Length of first left pelvic-fin ray (unbranched)	11,9	10,5	14,0	7	11,8	1,2
Length of second left pelvic-fin ray (first branched)	12,6	10,5	14,1	7	12,5	1,1
Length of third left pelvic-fin ray (second branched)	12,2	11,2	13,8	7	12,5	0,8
Anal-fin base	11,1	11,1	14,9	7	13,3	1,3
Preanal length	65,0	59,6	65,0	7	63,8	1,9
Distance between snout tip and terminus of anal-fin base	76,3	73,7	79,5	7	76,8	2,2
Distance between snout tip and anal-fin distal end	81,1	81,1	88,6	7	84,4	2,4
Adipose-fin length	30,5	27,2	30,7	7	29,1	1,4
Preadipose length	57,3	54,8	60,6	7	57,3	2,1
Distance between snout tip and adipose-fin base end	84,4	79,4	88,5	7	84,8	3,6
Adipose-fin depth	5,1	4,3	6,0	7	5,2	0,6
Caudal-peduncle length posterior to adipose-fin	14,5	12,9	15,5	7	14,3	0,8
Caudal-peduncle depth at adipose-fin terminus	7,3	5,0	7,9	7	6,6	0,9
Snout-anus distance	51,7	50,4	54,6	7	52,6	1,4
Snout-urogenital papilla distance	56,5	55,1	58,8	7	56,8	1,6

Anus-urogenital papilla distance	4,6	3,5	7,0	7	4,9	1,2
Dorsal lobe of caudal fin length	26,2	21,8	26,5	6	25,3	1,7
Ventral lobe of caudal fin length	22,4	20,5	27,3	6	22,2	2,6

Percentages of HL

Head depth	45,7	42,9	52,1	7	46,9	2,8
Head width	59,9	55,4	64,6	7	59,7	2,9
Eye diameter (left)	15,2	15,2	17,1	7	16,2	0,6
Fleshy interorbital	28,6	24,8	28,6	7	26,9	1,3
Bony interorbital	20,9	18,6	22,7	7	20,9	1,2
Mouth gape	34,0	32,0	35,3	7	33,4	1,2
Snout length (left)	33,3	31,5	33,3	7	32,1	0,6
Distance between snout tip and posterior nare (left side)	21,4	18,9	21,9	7	21,0	1,0
Anterior internarial width	13,7	12,5	16,5	7	14,3	1,6
Posterior internarial width	16,5	15,4	17,4	7	16,4	0,6
Intranarial length (left side)	13,1	11,8	16,1	7	13,9	1,4

Table 63: Morphometric data of *Pimelodella straminea* based on type material.

	Lectotype	Min.	Max.	n	x	SD
Total length (mm)	49,7	49,7	54,4	2	52,0	
Standard length (mm)	41,2	41,2	54,7	4	46,2	
	Percentages of SL					
Body depth (dorsal)	15,0	14,3	17,9	4	16,2	1,9
Body width (dorsal)	9,8	9,8	12,4	4	11,0	1,3
Cleithral width	16,6	16,6	18,7	3	17,9	1,1
Head length	31,3	31,2	31,9	4	31,6	0,3
Maxillary-barbel length (left side)	55,9	55,4	62,5	3	57,9	3,9
Outer mental-barbel length (left side)	20,6	17,4	20,6	3	19,3	1,7
Inner mental-barbel length (left side)	9,9	8,2	9,9	3	9,0	0,8
Predorsal length	34,9	34,9	35,8	3	35,3	0,4
Distance between snout tip and terminus of dorsal-fin base	45,8	45,8	48,9	3	47,8	1,7
Distance between snout tip and dorsal-fin distal end	54,3	54,3	58,1	3	56,3	1,9
Dorsal fin to adipose fin	11,8	11,8	17,8	3	15,0	3,0
Dorsal-fin base	28,0	15,0	28,0	3	19,6	7,3
Length of first dorsal-fin ray (unbranched)	20,5	18,8	22,6	3	20,6	1,9
Length of rigid part of first dorsal-fin ray	16,1	15,4	19,7	3	17,1	2,3
Length of second dorsal-fin ray (first branched)	17,5	17,5	21,4	3	19,8	2,1
Length of third dorsal-fin ray (second branched)	-	-	-	-	-	-
Prepectoral length	22,7	22,7	26,3	3	24,3	1,8
Distance between snout tip and terminus of pectoral-fin base	24,0	24,0	28,9	3	26,4	2,4
Distance between snout tip and pectoral-fin distal end	41,1	41,1	44,4	3	42,4	1,7
Length of first left pectoral-fin ray (unbranched)	20,5	20,5	22,5	4	21,4	0,9
Length of rigid part of first left pectoral-fin ray	18,5	18,5	20,9	4	19,5	1,1
Length of second left pectoral-fin ray (first branched)	-	-	-	-	-	-
Length of third left pectoral-fin ray (second branched)	-	-	-	-	-	-
Prepelvic length	45,9	45,9	47,4	3	46,5	0,8
Distance between snout tip and terminus of pelvic-fin base	49,8	49,8	50,5	2	50,2	0,6
Distance between snout tip and pelvic-fin distal end	59,7	59,7	63,0	3	61,8	1,9
Distance between pelvic fins	4,5	4,4	4,5	2	4,5	0,1
Length of first left pelvic-fin ray (unbranched)	10,9	10,9	14,5	2	12,7	2,6
Length of second left pelvic-fin ray (first branched)	-	15,4	15,4	1	15,4	-
Length of third left pelvic-fin ray (second branched)	13,8	13,8	13,8	1	13,8	-
Anal-fin base	13,1	13,1	15,4	3	14,0	1,2
Preanal length	68,8	66,1	70,2	3	68,4	2,1
Distance between snout tip and terminus of anal-fin base	81,4	79,9	81,4	2	80,6	1,0
Distance between snout tip and anal-fin distal end	87,9	83,4	90,3	3	87,2	3,5
Adipose-fin length	25,5	24,7	26,8	3	25,7	1,1
Preadipose length	62,8	58,7	65,6	3	62,4	3,5
Distance between snout tip and adipose-fin base end	81,3	81,3	89,1	3	85,4	3,9
Adipose-fin depth	3,2	2,4	3,2	2	2,8	0,5
Caudal-peduncle length posterior to adipose-fin	12,1	10,0	12,6	3	11,6	1,4
Caudal-peduncle depth at adipose-fin terminus	6,8	6,8	8,7	3	7,7	1,0
Snout-anus distance	-	-	-	-	-	-
Snout-urogenital papilla distance	-	-	-	-	-	-

Table 64: Morphometric data of *Pimelodella taeniophora* based on type and comparative materials.

	Lectotype	Min.	Max.	<i>n</i>	<i>x</i>	SD
Total length (mm)	96,5	73,5	114,0	9	92,7	
Standard length (mm)	76,6	59,1	92,7	9	74,5	
	Percentages of SL					
Body depth (dorsal)	17,9	14,9	19,6	9	17,6	1,5
Body width (dorsal)	12,1	11,7	15,0	9	12,7	1,1
Cleithral width	18,3	15,8	18,3	9	17,1	0,9
Head length	29,5	28,8	30,7	9	29,6	0,6
Maxillary-barbel length (left side)	102,6	73,9	115,6	9	94,6	12,5
Outer mental-barbel length (left side)	33,1	24,6	40,3	8	32,5	5,2
Inner mental-barbel length (left side)	21,6	18,1	26,9	8	21,6	3,2
Predorsal length	32,7	30,2	33,6	9	32,6	1,1
Distance between snout tip and terminus of dorsal-fin base	46,4	44,9	49,8	9	47,3	1,4
Distance between snout tip and dorsal-fin distal end	56,1	53,6	69,3	9	59,2	4,8
Dorsal fin to adipose fin	6,2	5,7	9,9	9	6,9	1,3
Dorsal-fin base	15,0	14,5	17,3	9	15,6	0,8
Length of first dorsal-fin ray (unbranched)	23,8	19,6	39,1	9	24,9	6,4
Length of rigid part of first dorsal-fin ray	17,5	15,9	21,4	9	17,4	1,8
Length of second dorsal-fin ray (first branched)	20,6	20,5	25,0	9	22,0	1,4
Length of third dorsal-fin ray (second branched)	21,0	18,6	23,4	9	20,7	1,4
Prepectoral length	21,4	21,0	24,0	9	21,9	1,1
Distance between snout tip and terminus of pectoral-fin base	24,2	23,6	27,2	9	24,9	1,1
Distance between snout tip and pectoral-fin distal end	40,6	37,4	44,8	9	41,1	2,4
Length of first left pectoral-fin ray (unbranched)	19,5	18,3	21,9	8	20,1	1,2
Length of rigid part of first left pectoral-fin ray	17,8	17,2	19,6	9	18,0	0,7
Length of second left pectoral-fin ray (first branched)	17,3	17,3	19,8	9	18,3	1,0
Length of third left pectoral-fin ray (second branched)	15,9	15,6	18,4	9	16,6	0,9
Prepelvic length	43,2	42,2	45,5	9	43,9	1,2
Distance between snout tip and terminus of pelvic-fin base	45,4	45,1	49,8	9	46,8	1,6
Distance between snout tip and pelvic-fin distal end	59,0	58,4	63,7	9	61,1	1,9
Distance between pelvic fins	4,7	3,0	4,8	8	4,1	0,7
Length of first left pelvic-fin ray (unbranched)	13,6	12,5	15,9	9	13,8	1,0
Length of second left pelvic-fin ray (first branched)	14,6	14,6	17,5	9	15,5	0,9
Length of third left pelvic-fin ray (second branched)	14,5	14,5	17,1	9	15,7	1,0
Anal-fin base	12,6	11,1	14,2	9	12,3	1,1
Preanal length	64,4	64,4	70,3	9	66,7	1,9
Distance between snout tip and terminus of anal-fin base	77,8	77,7	80,1	9	78,5	0,9
Distance between snout tip and anal-fin distal end	85,5	84,0	89,9	9	86,6	1,8
Adipose-fin length	36,2	34,4	40,8	9	36,6	2,0
Preadipose length	51,9	51,9	56,0	9	53,8	1,1
Distance between snout tip and adipose-fin base end	86,9	86,9	91,4	9	88,8	1,3
Adipose-fin depth	3,4	3,4	6,1	9	4,5	0,9
Caudal-peduncle length posterior to adipose-fin	12,4	9,8	12,4	9	11,1	1,0
Caudal-peduncle depth at adipose-fin terminus	8,6	7,8	9,3	9	8,6	0,5
Snout-anus distance	49,6	49,6	54,3	8	51,8	1,8

Snout-urogenital papilla distance	55,2	55,2	64,6	8	58,5	3,4
Anus-urogenital papilla distance	6,0	3,4	10,7	8	6,1	2,5
Dorsal lobe of caudal fin length	27,7	22,0	29,7	9	25,5	2,4
Ventral lobe of caudal fin length	24,0	22,7	28,2	9	25,2	2,2

	Percentages of HL					
Head depth	52,5	45,2	53,8	9	49,0	2,7
Head width	56,6	53,8	62,1	9	57,0	2,7
Eye diameter (left)	25,1	19,7	25,1	9	22,7	1,8
Fleshy interorbital	23,9	20,3	23,9	9	22,5	1,3
Bony interorbital	17,4	13,9	18,1	9	16,5	1,7
Mouth gape	32,4	27,6	36,1	9	31,9	2,2
Snout length (left)	30,9	29,1	33,4	9	31,5	1,4
Distance between snout tip and posterior nare (left side)	16,9	16,5	19,4	9	17,7	1,0
Anterior internarial width	12,7	9,6	13,9	9	12,3	1,2
Posterior internarial width	13,3	12,0	14,5	9	13,5	0,9
Intranarial length (left side)	10,3	10,3	16,2	9	13,2	2,0

Table 65: Morphometric data of *Pimelodella tapatapae* based on type material.

	Holotype
Total length (mm)	156,2
Standard length (mm)	121,6
Percentages of SL	
Body depth (dorsal)	21,2
Body width (dorsal)	15,4
Cleithral width	17,6
Head length	30,1
Maxillary-barbel length (left side)	90,4
Outer mental-barbel length (left side)	33,3
Inner mental-barbel length (left side)	17,0
Predorsal length	34,4
Distance between snout tip and terminus of dorsal-fin base	50,6
Distance between snout tip and dorsal-fin distal end	59,1
Dorsal fin to adipose fin	5,3
Dorsal-fin base	15,5
Length of first dorsal-fin ray (unbranched)	16,5
Length of rigid part of first dorsal-fin ray	-
Length of second dorsal-fin ray (first branched)	19,6
Length of third dorsal-fin ray (second branched)	18,8
Prepectoral length	21,4
Distance between snout tip and terminus of pectoral-fin base	25,0
Distance between snout tip and pectoral-fin distal end	41,6
Length of first left pectoral-fin ray (unbranched)	18,3
Length of rigid part of first left pectoral-fin ray	14,9
Length of second left pectoral-fin ray (first branched)	18,2
Length of third left pectoral-fin ray (second branched)	17,0
Prepelvic length	45,0
Distance between snout tip and terminus of pelvic-fin base	47,1
Distance between snout tip and pelvic-fin distal end	62,1
Distance between pelvic fins	6,8
Length of first left pelvic-fin ray (unbranched)	14,1
Length of second left pelvic-fin ray (first branched)	16,0
Length of third left pelvic-fin ray (second branched)	15,9
Anal-fin base	13,1
Preanal length	66,8
Distance between snout tip and terminus of anal-fin base	79,0
Distance between snout tip and anal-fin distal end	87,4
Adipose-fin length	31,5
Preadipose length	57,1
Distance between snout tip and adipose-fin base end	87,6
Adipose-fin depth	4,6
Caudal-peduncle length posterior to adipose-fin	10,6
Caudal-peduncle depth at adipose-fin terminus	10,7
Snout-anus distance	48,1
Snout-urogenital papilla distance	52,9

Anus-urogenital papilla distance	5,0
Dorsal lobe of caudal fin length	27,8
Ventral lobe of caudal fin length	29,5

Percentages of HL

Head depth	46,8
Head width	56,5
Eye diameter (left)	18,9
Fleshy interorbital	26,9
Bony interorbital	22,2
Mouth gape	29,5
Snout length (left)	31,0
Distance between snout tip and posterior nare (left side)	18,3
Anterior internarial width	19,1
Posterior internarial width	16,3
Intranarial length (left side)	13,0

Table 66: Morphometric data of *Pimelodella vittata* based on type and comparative materials.

	Lectotype	Min.	Max.	n	x	SD
Total length (mm)	76,1	76,1	136,7	11	111,4	
Standard length (mm)	61,8	33,1	111,9	22	73,6	
	Percentages of SL					
Body depth (dorsal)	17,5	17,4	19,8	12	18,7	0,8
Body width (dorsal)	15,0	13,6	15,7	12	14,6	0,7
Cleithral width	18,2	17,2	18,9	12	18,2	0,6
Head length	30,2	28,7	34,2	21	30,6	1,5
Maxillary-barbel length (left side)	-	44,2	78,3	11	68,3	10,0
Outer mental-barbel length (left side)	26,3	21,9	30,0	12	26,0	2,7
Inner mental-barbel length (left side)	14,8	9,3	17,9	12	14,3	1,9
Predorsal length	33,6	32,1	37,6	12	34,0	1,4
Distance between snout tip and terminus of dorsal-fin base	47,9	45,5	49,9	12	48,1	1,2
Distance between snout tip and dorsal-fin distal end	57,7	54,6	61,2	12	58,6	1,7
Dorsal fin to adipose fin	10,7	6,2	17,2	12	9,7	2,9
Dorsal-fin base	14,5	12,5	17,2	12	14,5	1,5
Length of first dorsal-fin ray (unbranched)	-	14,8	23,0	10	19,7	2,7
Length of rigid part of first dorsal-fin ray	13,8	12,0	17,5	12	14,8	1,8
Length of second dorsal-fin ray (first branched)	18,0	17,3	23,8	12	20,6	1,9
Length of third dorsal-fin ray (second branched)	18,5	17,7	23,2	12	20,2	1,7
Prepectoral length	21,1	21,1	26,2	11	23,2	1,8
Distance between snout tip and terminus of pectoral-fin base	23,8	23,8	30,0	11	26,0	1,9
Distance between snout tip and pectoral-fin distal end	40,0	39,9	47,2	10	42,5	2,7
Length of first left pectoral-fin ray (unbranched)	19,5	15,7	22,9	11	19,1	2,1
Length of rigid part of first left pectoral-fin ray	15,7	13,0	18,8	11	16,1	1,6
Length of second left pectoral-fin ray (first branched)	17,9	14,9	20,8	11	18,1	1,7
Length of third left pectoral-fin ray (second branched)	16,2	13,9	18,7	11	16,7	1,4
Prepelvic length	45,8	44,8	50,3	11	47,1	1,8
Distance between snout tip and terminus of pelvic-fin base	49,4	47,9	53,6	11	50,1	1,9
Distance between snout tip and pelvic-fin distal end	61,4	58,8	67,6	11	62,7	2,8
Distance between pelvic fins	3,7	2,8	6,0	9	4,6	1,0
Length of first left pelvic-fin ray (unbranched)	10,6	9,9	15,6	11	12,1	1,6
Length of second left pelvic-fin ray (first branched)	12,7	12,2	17,4	11	14,1	1,6
Length of third left pelvic-fin ray (second branched)	13,4	12,8	16,3	11	14,3	1,1
Anal-fin base	14,8	10,0	19,7	11	14,3	2,3
Preanal length	65,1	64,0	70,0	11	67,5	2,1
Distance between snout tip and terminus of anal-fin base	79,4	77,9	82,1	11	80,4	1,4
Distance between snout tip and anal-fin distal end	86,3	84,9	91,6	11	88,5	2,1
Adipose-fin length	32,1	30,0	38,1	11	33,6	2,6
Preadipose length	57,7	54,2	61,6	11	56,2	2,4
Distance between snout tip and adipose-fin base end	89,5	85,5	90,7	11	88,6	1,8
Adipose-fin depth	3,4	2,9	6,0	11	4,7	1,1
Caudal-peduncle length posterior to adipose-fin	11,1	9,7	11,8	11	10,5	0,6
Caudal-peduncle depth at adipose-fin terminus	7,7	6,8	10,7	11	9,4	1,3
Snout-anus distance	52,2	52,2	59,4	11	55,0	2,3
Snout-urogenital papilla distance	57,2	56,7	65,8	11	61,0	3,2

Anus-urogenital papilla distance	4,1	3,3	11,0	11	6,8	2,6
Dorsal lobe of caudal fin length	-	23,1	30,0	8	26,2	2,2
Ventral lobe of caudal fin length	-	21,9	26,4	9	23,7	1,4

Percentages of HL

Head depth	49,2	44,0	59,0	12	50,3	3,7
Head width	57,5	57,1	66,2	12	60,9	3,4
Eye diameter (left)	20,8	15,4	22,2	12	20,4	1,9
Fleshy interorbital	27,6	21,2	27,6	12	23,8	2,1
Bony interorbital	17,7	13,6	20,2	12	16,7	1,9
Mouth gape	32,2	29,8	39,3	12	34,8	2,5
Snout length (left)	29,8	29,6	33,4	12	31,4	1,4
Distance between snout tip and posterior nare (left side)	18,4	17,3	22,7	12	19,0	1,5
Anterior internarial width	14,3	12,2	15,7	12	13,6	1,0
Posterior internarial width	14,9	12,5	15,9	12	14,4	1,0
Intranarial length (left side)	10,7	10,7	17,2	12	13,4	2,0

Table 67: Morphometric data of *Pimelodella yuncensis* and *P. peruensis*, its junior-synonym, based on type and comparative materials.

	Lectotype	Min.	Max.	n	x	SD
Total length (mm)	44,5	44,5	84,6	9	69,1	
Standard length (mm)	37,8	37,8	69,9	10	58,5	
	Percentages of SL					
Body depth (dorsal)	17,0	17,0	22,9	9	19,9	1,8
Body width (dorsal)	9,7	9,7	15,9	9	14,2	1,8
Cleithral width	18,0	17,2	20,7	9	18,3	1,0
Head length	30,8	30,0	33,3	9	31,0	1,0
Maxillary-barbel length (left side)	27,5	27,5	61,5	9	47,2	9,4
Outer mental-barbel length (left side)	13,3	13,3	20,4	9	18,4	2,1
Inner mental-barbel length (left side)	7,6	7,6	13,1	9	11,1	1,6
Predorsal length	38,0	31,4	38,0	9	35,1	2,1
Distance between snout tip and terminus of dorsal-fin base	43,5	43,5	49,7	9	48,1	1,9
Distance between snout tip and dorsal-fin distal end	54,0	54,0	60,3	9	58,8	1,9
Dorsal fin to adipose fin	15,4	7,5	15,4	9	10,3	2,7
Dorsal-fin base	12,7	12,7	16,5	9	14,3	1,1
Length of first dorsal-fin ray (unbranched)	12,4	12,4	23,9	9	17,7	3,3
Length of rigid part of first dorsal-fin ray	9,4	9,4	19,0	8	13,2	2,8
Length of second dorsal-fin ray (first branched)	17,5	16,6	22,8	9	19,1	1,9
Length of third dorsal-fin ray (second branched)	17,1	16,0	20,8	9	18,8	1,6
Prepectoral length	22,0	22,0	24,7	9	22,9	1,0
Distance between snout tip and terminus of pectoral-fin base	24,3	24,3	27,0	9	25,4	0,9
Distance between snout tip and pectoral-fin distal end	38,0	38,0	44,1	9	40,9	1,7
Length of first left pectoral-fin ray (unbranched)	16,0	15,3	20,2	9	17,5	1,5
Length of rigid part of first left pectoral-fin ray	14,1	13,8	17,3	9	14,9	1,1
Length of second left pectoral-fin ray (first branched)	15,7	15,7	19,8	9	17,5	1,4
Length of third left pectoral-fin ray (second branched)	16,4	15,6	19,4	8	16,7	1,2
Prepelvic length	45,1	45,1	48,4	9	47,2	1,1
Distance between snout tip and terminus of pelvic-fin base	46,2	46,2	51,5	9	49,8	1,5
Distance between snout tip and pelvic-fin distal end	57,6	57,6	64,5	9	62,9	2,0
Distance between pelvic fins	-	3,7	5,1	8	4,4	0,5
Length of first left pelvic-fin ray (unbranched)	9,5	9,5	13,6	8	12,1	1,3
Length of second left pelvic-fin ray (first branched)	12,3	12,3	15,4	8	14,1	1,2
Length of third left pelvic-fin ray (second branched)	13,7	12,7	15,2	8	14,0	0,9
Anal-fin base	10,7	7,6	15,7	9	13,3	2,7
Preanal length	66,4	66,0	70,3	9	67,6	1,4
Distance between snout tip and terminus of anal-fin base	76,3	76,3	84,6	9	80,8	2,4
Distance between snout tip and anal-fin distal end	83,2	83,2	91,7	8	88,1	2,6
Adipose-fin length	25,4	25,4	37,8	9	34,9	3,7
Preadipose length	60,2	51,2	60,7	9	56,9	3,1
Distance between snout tip and adipose-fin base end	82,6	82,6	93,2	9	90,0	3,2
Adipose-fin depth	2,9	2,8	5,8	9	4,2	1,2
Caudal-peduncle length posterior to adipose-fin	10,2	7,4	10,7	9	9,1	1,2
Caudal-peduncle depth at adipose-fin terminus	7,3	7,3	11,7	9	10,3	1,4
Snout-anus distance	-	53,2	56,5	8	54,9	1,2

Snout-urogenital papilla distance	-	57,5	65,7	8	60,8	3,3
Anus-urogenital papilla distance	-	3,7	9,9	8	6,0	2,5
Dorsal lobe of caudal fin length	20,6	20,6	24,8	8	23,5	1,5
Ventral lobe of caudal fin length	21,9	19,6	23,5	8	21,7	1,4

Percentages of HL

Head depth	43,8	43,8	57,4	9	51,1	4,1
Head width	57,5	54,4	66,8	9	59,7	3,5
Eye diameter (left)	21,3	18,2	22,7	8	20,7	1,6
Fleshy interorbital	24,4	23,7	29,4	9	26,3	2,0
Bony interorbital	19,1	16,6	23,5	9	19,4	2,0
Mouth gape	25,6	25,6	37,0	9	31,9	3,4
Snout length (left)	27,5	27,5	31,6	9	29,7	1,4
Distance between snout tip and posterior nare (left side)	11,8	11,8	22,4	9	19,5	3,2
Anterior internarial width	12,6	12,5	15,3	9	13,7	1,0
Posterior internarial width	15,3	15,2	18,9	9	17,2	1,4
Intranarial length (left side)	13,7	10,1	17,7	9	14,8	2,4

Table 68: Morphometric data of *Pimelodella yuncensis* and *P. peruensis*, its junior-synonym, based on type and comparative materials, discriminated by original species name.

	<i>P. yuncensis</i>						<i>P. peruensis</i>	
	Lectotype	Min.	Max.	<i>n</i>	<i>x</i>	SD	Holotype	
Total length (mm)	44,5	44,5	84,6	8	71,3		50,8	
Standard length (mm)	37,8	37,8	69,9	9	59,6		48,2	
			Percentages of SL					
Body depth (dorsal)	17,0	17,0	22,9	8	19,9	1,9	19,8	
Body width (dorsal)	9,7	9,7	15,9	8	14,1	1,9	14,7	
Cleithral width	18,0	17,2	18,5	8	18,0	0,4	20,7	
Head length	30,8	30,0	33,3	8	31,1	1,0	30,5	
Maxillary-barbel length (left side)	27,5	27,5	61,5	8	47,8	9,9	42,4	
Outer mental-barbel length (left side)	13,3	13,3	20,4	8	18,4	2,3	18,0	
Inner mental-barbel length (left side)	7,6	7,6	13,1	8	11,0	1,7	11,8	
Predorsal length	38,0	32,2	38,0	8	35,6	1,7	31,4	
Distance between snout tip and terminus of dorsal-fin base	43,5	43,5	49,7	8	48,0	2,0	48,9	
Distance between snout tip and dorsal-fin distal end	54,0	54,0	60,3	8	58,7	2,0	59,7	
Dorsal fin to adipose fin	15,4	7,5	15,4	8	10,6	2,7	7,6	
Dorsal-fin base	12,7	12,7	16,5	8	14,2	1,1	15,0	
Length of first dorsal-fin ray (unbranched)	12,4	12,4	23,9	8	18,0	3,5	15,6	
Length of rigid part of first dorsal-fin ray	9,4	9,4	19,0	7	13,3	3,0	12,8	
Length of second dorsal-fin ray (first branched)	17,5	17,4	22,8	8	19,4	1,8	16,6	
Length of third dorsal-fin ray (second branched)	17,1	17,1	20,8	8	19,1	1,2	16,0	
Prepectoral length	22,0	22,0	23,8	8	22,7	0,7	24,7	
Distance between snout tip and terminus of pectoral-fin base	24,3	24,3	26,5	8	25,2	0,7	27,0	
Distance between snout tip and pectoral-fin distal end	38,0	38,0	44,1	8	40,9	1,8	41,0	
Length of first left pectoral-fin ray (unbranched)	16,0	15,3	20,2	8	17,6	1,6	16,5	
Length of rigid part of first left pectoral-fin ray	14,1	14,1	17,3	8	15,1	1,1	13,8	

Length of second left pectoral-fin ray (first branched)	15,7	15,7	19,8	8	17,7	1,4	16,1
Length of third left pectoral-fin ray (second branched)	16,4	15,6	19,4	7	16,8	1,3	16,1
Prepelvic length	45,1	45,1	48,4	8	47,4	1,0	46,1
Distance between snout tip and terminus of pelvic-fin base	46,2	46,2	51,5	8	49,9	1,6	49,1
Distance between snout tip and pelvic-fin distal end	57,6	57,6	64,5	8	62,8	2,2	63,1
Distance between pelvic fins	-	3,7	5,1	7	4,3	0,5	5,1
Length of first left pelvic-fin ray (unbranched)	9,5	9,5	13,6	8	12,1	1,3	-
Length of second left pelvic-fin ray (first branched)	12,3	12,3	15,4	8	14,1	1,2	-
Length of third left pelvic-fin ray (second branched)	13,7	12,7	15,2	8	14,0	0,9	-
Anal-fin base	10,7	7,6	15,5	8	13,0	2,7	15,7
Preanal length	66,4	66,3	70,3	8	67,8	1,4	66,0
Distance between snout tip and terminus of anal-fin base	76,3	76,3	82,9	8	80,4	2,0	84,6
Distance between snout tip and anal-fin distal end	83,2	83,2	91,7	8	88,1	2,6	-
Adipose-fin length	25,4	25,4	37,8	8	34,8	3,9	35,8
Preadipose length	60,2	51,2	60,7	8	56,5	3,1	60,0
Distance between snout tip and adipose-fin base end	82,6	82,6	93,2	8	89,9	3,4	91,1
Adipose-fin depth	2,9	2,8	5,8	8	4,4	1,2	2,8
Caudal-peduncle length posterior to adipose-fin	10,2	7,4	10,7	8	9,1	1,2	9,5
Caudal-peduncle depth at adipose-fin terminus	7,3	7,3	11,7	8	10,3	1,5	10,2
Snout-anus distance	-	53,2	56,5	7	54,8	1,2	55,9
Snout-urogenital papilla distance	-	57,5	65,7	7	60,2	3,2	64,4
Anus-urogenital papilla distance	-	3,7	9,9	7	5,6	2,3	9,3
Dorsal lobe of caudal fin length	20,6	20,6	24,8	8	23,5	1,5	-
Ventral lobe of caudal fin length	21,9	19,6	23,5	8	21,7	1,4	-

Percentages of HL

Head depth	43,8	43,8	54,8	8	50,3	3,6	57,4
Head width	57,5	54,4	62,3	8	58,9	2,5	66,8
Eye diameter (left)	21,3	18,2	22,0	7	20,4	1,4	22,7
Fleshy interorbital	24,4	23,7	29,4	8	26,0	1,9	28,6

Bony interorbital	19,1	16,6	20,5	8	18,9	1,3	23,5
Mouth gape	25,6	25,6	37,0	8	32,0	3,6	30,9
Snout length (left)	27,5	27,5	31,2	8	29,4	1,3	31,6
Distance between snout tip and posterior nare (left side)	11,8	11,8	22,3	8	19,2	3,3	22,4
Anterior internarial width	12,6	12,5	15,3	8	13,8	1,1	13,2
Posterior internarial width	15,3	15,2	18,9	8	17,0	1,4	18,5
Intranarial length (left side)	13,7	10,1	17,7	8	15,1	2,5	12,7

Table 69: Identification Key for the valid *Pimelodella* species diagnosable in this work.

Species	Maxillary barbel reaching at/between	Supraoccipital process width	Supraoccipital process shape	Supraoccipital process constriction near base
<i>Pimelodella australis</i>	between adpressed pelvic terminus and anal fin origin	narrow	triangular	absent
<i>Pimelodella avanhandavae</i>	origin and last fifth of adpressed anal fin	narrow	rectangular	absent
<i>Pimelodella boliviana</i>	at least origin of caudal-fin	narrow	rectangular	absent
<i>Pimelodella boschmai</i>	first third of anal fin base	moderate large	rectangular	absent
<i>Pimelodella brasiliensis</i>	half and terminus of anal fin	moderate large	rectangular	present
<i>Pimelodella buckleyi</i>	origin and half of anal fin base	narrow	rectangular	absent
<i>Pimelodella chagresi</i>	pelvic-fin terminus and last fifth of adpressed anal-fin	wide	rectangular	absent
<i>Pimelodella coquetanesis</i>	half anal-fin base	narrow	rectangular	absent
<i>Pimelodella cristata</i>	half adpressed anal and caudal origin	wide	rectangular	present
<i>Pimelodella cruxenti</i>	surpassing caudal origin	narrow	triangular	absent
<i>Pimelodella elongata</i>	half adpressed pectoral to first fourth of adpressed pelvic	moderate large	rectangular	present
<i>Pimelodella enochi</i>	half and terminus of anal fin	moderate large	rectangular	absent
<i>Pimelodella eutaenia</i>	half and terminus of anal fin	narrow	triangular	absent
<i>Pimelodella figueroai</i>	half adipose			
<i>Pimelodella geryi</i>	half adipose to caudal origin	narrow	rectangular	absent
<i>Pimelodella gracilis</i>	half anal adpressed and caudal-fin origin	wide	rectangular	present
<i>Pimelodella griffini</i>	half and terminus of pelvic fin	narrow	rectangular	absent
<i>Pimelodella grisea</i>	half adpressed pelvic and terminus of anal fin	moderate large	triangular	absent
<i>Pimelodella harttii</i>	half and terminus of pelvic fin	moderate large	triangular	absent
<i>Pimelodella hasemani</i>	first fourth and anal fin terminus	moderate large	triangular	absent
<i>Pimelodella howesi</i>	last fifth of adipose and surpassing caudal-fin origin	wide	rectangular	absent
<i>Pimelodella humeralis</i>	surpassing caudal origin	wide	rectangular	present
<i>Pimelodella ignobilis</i>	adpressed pelvic and anal-fin origin	moderate large	triangular	absent
<i>Pimelodella itapicuruensis</i>	anal-fin origin and terminus	narrow	triangular	absent
<i>Pimelodella kronei</i>	dorsal fin spine and anal fin origin	narrow	triangular	absent
<i>Pimelodella</i>	anal-fin origin and terminus	narrow	rectangular	absent

<i>lateristriga</i>				
<i>Pimelodella laticeps</i>	pelvic fin origin to its first third adressed	narrow	triangular	absent
<i>Pimelodella laurenti</i>	adressed anal and caudal-fin origin	narrow	rectangular	absent
<i>Pimelodella leptosoma</i>	half and terminus of anal fin	narrow	rectangular	absent
<i>Pimelodella linami</i>	adressed pelvic terminus	narrow	triangular	absent
<i>Pimelodella longipinnis</i>	anal fin terminus	narrow	rectangular	absent
<i>Pimelodella macturki</i>	anal-fin origin and its last third	moderate large	rectangular	absent
<i>Pimelodella martinezi</i>	anal fin terminus	narrow	rectangular	absent
<i>Pimelodella meeki</i>	pelvic fin origin and anal fin origin	narrow	rectangular	absent
<i>Pimelodella megalops</i>	anal-fin terminus and caudal-fin origin	narrow	rectangular	absent
<i>Pimelodella megalura</i>	anal-fin origin and terminus	narrow	rectangular	absent
<i>Pimelodella metae</i>	anal-fin origin and terminus	narrow	triangular	absent
<i>Pimelodella modesta</i>	pelvic fin terminus and anal fin origin	moderate large	rectangular	absent
<i>Pimelodella montana</i>	anal-fin origin and terminus	moderate large	triangular	absent
<i>Pimelodella mucosa</i>	surpassing caudal origin	wide	rectangular	present
<i>Pimelodella notomelas</i>	surpassing caudal origin	narrow	triangular	absent
<i>Pimelodella odynea</i>	anal-fin terminus and caudal-fin origin	moderate large	rectangular	absent
<i>Pimelodella pectinifera</i>	second third of adressed pelvic fin	narrow	rectangular	absent
<i>Pimelodella peruana</i>	adipose origin and adressed anal fin	narrow	rectangular	absent
<i>Pimelodella reyesi</i>	anal-fin origin			
<i>Pimelodella robinsoni</i>	first third and anal fin terminus	narrow	triangular	absent
<i>Pimelodella roccae</i>	first fourth of adressed anal to caudal-fin origin	moderate large	triangular	absent
<i>Pimelodella serrata</i>	anal-fin terminus and caudal-fin origin	wide	both	absent
<i>Pimelodella spelaea</i>	half pelvic and half adressed anal	narrow	rectangular	absent
<i>Pimelodella straminea</i>	second third to terminus of adressed pelvic fin	narrow	triangular	absent
<i>Pimelodella taeniphora</i>	anal-fin terminus and caudal-fin origin	moderate large	rectangular	absent
<i>Pimelodella tapatapae</i>	caudal-fin origin	narrow	triangular	absent
<i>Pimelodella vittata</i>	anal fin origin and its first third	narrow	triangular	absent
<i>Pimelodella yuncensis</i>	half pectoral and terminus of adressed pelvic fin	narrow	triangular	absent

Table 69 (cont.): Identification Key for the valid *Pimelodella* species diagnosable in this work.

Species	SOC process reaches anterior prenuchal plate	Dorsal lamina of Weberian complex vertebrae	Dorsal-fin spine length
<i>Pimelodella australis</i>	yes	just anteriormost part	three fourths of first dorsal fin total length
<i>Pimelodella avanhandavae</i>	yes	anteriormost to half	three fourths of first dorsal fin total length
<i>Pimelodella boliviana</i>	yes	along all extension	two thirds of first dorsal fin total length
<i>Pimelodella boschmai</i>	yes		
<i>Pimelodella brasiliensis</i>	yes	just anteriormost part	three fourths of first dorsal fin total length
<i>Pimelodella buckleyi</i>	yes	anteriormost to half	two thirds of first dorsal fin total length
<i>Pimelodella chagresi</i>	yes	along all extension	three fourths of first dorsal fin total length
<i>Pimelodella coquetanesis</i>	yes	just anteriormost part	
<i>Pimelodella cristata</i>	yes	anteriormost to all	three fourths of first dorsal fin total length
<i>Pimelodella cruxenti</i>	yes	just anteriormost part	two thirds of first dorsal fin total length
<i>Pimelodella elongata</i>	yes	just anteriormost part	two thirds of first dorsal fin total length
<i>Pimelodella enochi</i>	yes	anteriormost to half	two thirds of first dorsal fin total length
<i>Pimelodella eutaenia</i>	yes	along all extension	three fourths of first dorsal fin total length
<i>Pimelodella figueroai</i>	yes		
<i>Pimelodella geryi</i>	yes		three fourths of first dorsal fin total length
<i>Pimelodella gracilis</i>	yes	along all extension	two thirds of first dorsal fin total length
<i>Pimelodella griffini</i>	yes	just anteriormost part	two thirds of first dorsal fin total length
<i>Pimelodella grisea</i>	yes	along all extension	three fourths of first dorsal fin total length
<i>Pimelodella harttii</i>	yes	just anteriormost part	three fourths of first dorsal fin total length
<i>Pimelodella hasemani</i>	yes	along all extension	three fourths of first dorsal fin total length
<i>Pimelodella howesi</i>	yes	along all extension	three fourths of first dorsal fin total length
<i>Pimelodella humeralis</i>	yes	anteriormost to half	three fourths of first dorsal fin total length

<i>Pimelodella ignobilis</i>	yes	just anteriormost part	three fourths of first dorsal fin total length
<i>Pimelodella itapicuruensis</i>	no	just anteriormost part	half first dorsal fin total length
<i>Pimelodella kronei</i>	yes	just anteriormost part	three fourths of first dorsal fin total length
<i>Pimelodella lateristriga</i>	yes	just anteriormost part	three fourths of first dorsal fin total length
<i>Pimelodella laticeps</i>	yes	just anteriormost part	three fourths of first dorsal fin total length
<i>Pimelodella laurenti</i>	yes	along all extension	two thirds of first dorsal fin total length
<i>Pimelodella leptosoma</i>	no	just anteriormost part	two thirds of first dorsal fin total length
<i>Pimelodella linami</i>	yes	just anteriormost part	half first dorsal fin total length
<i>Pimelodella longipinnis</i>	no	just anteriormost part	two thirds of first dorsal fin total length
<i>Pimelodella macturki</i>	yes	along all extension	two thirds of first dorsal fin total length
<i>Pimelodella martinezi</i>	yes		
<i>Pimelodella meeki</i>	yes	just anteriormost part	three fourths of first dorsal fin total length
<i>Pimelodella megalops</i>	yes	along all extension	three fourths of first dorsal fin total length
<i>Pimelodella megalura</i>	no	just anteriormost part	half first dorsal fin total length
<i>Pimelodella metae</i>	no	just anteriormost part	two thirds of first dorsal fin total length
<i>Pimelodella modesta</i>	yes	just anteriormost part	two thirds of first dorsal fin total length
<i>Pimelodella montana</i>	no	just anteriormost part	two thirds of first dorsal fin total length
<i>Pimelodella mucosa</i>	yes	along all extension	three fourths of first dorsal fin total length
<i>Pimelodella notomelas</i>	yes	just anteriormost part	three fourths of first dorsal fin total length
<i>Pimelodella odynea</i>	yes	midlength to all	two thirds of first dorsal fin total length
<i>Pimelodella pectinifera</i>	yes	just anteriormost part	two thirds of first dorsal fin total length
<i>Pimelodella peruana</i>	yes	anteriormost to all	three fourths of first dorsal fin total length
<i>Pimelodella reyesi</i>			three fourths of first dorsal fin total length
<i>Pimelodella robinsoni</i>	no	just anteriormost part	
<i>Pimelodella roccae</i>	yes	just anteriormost part	two thirds of first dorsal fin total length
<i>Pimelodella serrata</i>	yes	along all extension	three fourths of first dorsal fin total length
<i>Pimelodella spelaea</i>	yes	just anteriormost part	three fourths of first dorsal fin total length

<i>Pimelodella straminea</i>	yes	along all extension	length three fourths of first dorsal fin total length
<i>Pimelodella taeniophora</i>	yes	anteriormost to all	three fourths of first dorsal fin total length
<i>Pimelodella tapatapae</i>	no	just anteriormost part	half first dorsal fin total length three fourths of first dorsal fin total length
<i>Pimelodella vittata</i>	yes	just anteriormost part	length
<i>Pimelodella yuncensis</i>	no	just anteriormost part	two thirds of first dorsal fin total length

Table 69 (cont.): Identification Key for the valid *Pimelodella* species diagnosable in this work.

Species	Pectoral-fin spine format	Dentations on posterior margin of pectoral-fin spine	Dentations morphology
<i>Pimelodella australis</i>	curved	basal two thirds	medium, distalmost straighter; basal more retrorse
<i>Pimelodella avanhandavae</i>	curved	basal two thirds	large
<i>Pimelodella boliviana</i>	roughly straight	basal two thirds	small triangular, broad based, straighter towards apex and base
<i>Pimelodella boschmai</i>	curved	basal two thirds	small
<i>Pimelodella brasiliensis</i>	curved	basal three fourths	small to none
<i>Pimelodella buckleyi</i>	roughly straight	almost entire margin	long, acute, inclined
<i>Pimelodella chagresi</i>	curved	almost entire margin	triangular, inclined
<i>Pimelodella coquetanensis</i>	curved	basal two thirds	triangular, inclined
<i>Pimelodella cristata</i>	curved	almost entire margin	small
<i>Pimelodella cruxenti</i>	roughly straight	basal three fourths	long, curved
<i>Pimelodella elongata</i>	roughly straight	basal two thirds	small
<i>Pimelodella enochi</i>	roughly straight	basal two thirds	average, triangular, not so retrorse
<i>Pimelodella eutaenia</i>	roughly straight	basal two thirds	moderate
<i>Pimelodella figueroai</i>		basal three fourths	small
<i>Pimelodella geryi</i>	roughly straight	basal half	triangular, large, inclined
<i>Pimelodella gracilis</i>	curved	basal three fourths	small
<i>Pimelodella griffini</i>	curved	basal two thirds	large, hook-like
<i>Pimelodella grisea</i>	curved	basal three fourths	triangular, broad base, hook-like
<i>Pimelodella harttii</i>	curved	basal two thirds	large, hook-like
<i>Pimelodella hasemani</i>	curved	almost entire margin	large, curved apex
<i>Pimelodella howesi</i>	curved	basal two thirds	triangular, broad based, inclined
<i>Pimelodella humeralis</i>	curved	basal three fourths	triangular, inclined
<i>Pimelodella ignobilis</i>	curved	basal two thirds	triangular, broad based, inclined
<i>Pimelodella itapicuruiensis</i>	roughly straight	basal half	straight to retrorse
<i>Pimelodella kronei</i>	curved	basal half	large, hook-like
<i>Pimelodella lateristriga</i>	curved	basal three fourths	straight to retrorse
<i>Pimelodella laticeps</i>	roughly straight	basal two thirds	large, curved apex
<i>Pimelodella laurenti</i>	roughly straight	basal two thirds	triangular, broad based, inclined
<i>Pimelodella leptosoma</i>	roughly straight	basal two thirds	triangular, inclined
<i>Pimelodella linami</i>	roughly straight	basal two thirds	triangular, broad based, inclined
<i>Pimelodella longipinnis</i>	roughly straight	basal two thirds	

<i>Pimelodella macturki</i>	curved	basal two thirds	large, hook-like
<i>Pimelodella martinezi</i>	curved		
<i>Pimelodella meeki</i>	curved	basal two thirds	straight to retrorse
<i>Pimelodella megalops</i>	curved	basal three fourths	large, curved apex
<i>Pimelodella megalura</i>	curved	basal two thirds	small
<i>Pimelodella metae</i>	roughly straight	basal half	small
<i>Pimelodella modesta</i>	curved	basal two thirds	moderate
<i>Pimelodella montana</i>	roughly straight	basal half	small
<i>Pimelodella mucosa</i>	curved	basal two thirds	small
<i>Pimelodella notomelas</i>	roughly straight	basal two thirds	small
<i>Pimelodella odynea</i>	roughly straight	basal two thirds	moderate to large
<i>Pimelodella pectinifera</i>	curved	almost entire margin	moderate, numerous, curved
<i>Pimelodella peruana</i>	curved	basal three fourths	triangular, broad based, inclined
<i>Pimelodella reyesi</i>	roughly straight	basal two thirds	large, curved apex
<i>Pimelodella robinsoni</i>	roughly straight	basal two thirds	triangular, broad based, inclined
<i>Pimelodella roccae</i>	curved	basal three fourths	small
<i>Pimelodella serrata</i>	curved	almost entire margin	large, hook-like
<i>Pimelodella spelaea</i>	curved	basal two thirds	triangular, broad based, inclined
<i>Pimelodella straminea</i>	curved	basal two thirds	moderate to large
<i>Pimelodella taeniophora</i>	curved	basal two thirds	triangular, large, inclined
<i>Pimelodella tapatapae</i>	roughly straight	basal three fourths	small
<i>Pimelodella vittata</i>	roughly straight	basal two thirds	small
<i>Pimelodella yuncensis</i>	curved	basal two thirds	triangular, small

Table 69 (cont.): Identification Key for the valid *Pimelodella* species diagnosable in this work.

Species	Adipose fin	Caudal fin lobes	Hypural 5	Total vertebrae	S6 pores
<i>Pimelodella australis</i>	four times or more in SL	dorsal slightly longer	free	39-41	2 pores far apart
<i>Pimelodella avanhandavae</i>	less than three times in SL	dorsal slightly longer	free	41-45	2 pores near or 1 pore right after canal connection
<i>Pimelodella boliviana</i>	three times in SL	dorsal slightly longer	free	40-42	2 pores far apart
<i>Pimelodella boschmai</i>	three times in SL	dorsal slightly longer	free		1 pore with canal
<i>Pimelodella brasiliensis</i>	four times in SL	dorsal slightly longer	free	42-43	2 pores near or 1 pore right after canal connection
<i>Pimelodella buckleyi</i>	two and half to three	subequal	free	43-44	1 pore with canal
<i>Pimelodella chagresi</i>	three and half times in SL	dorsal slightly longer	free	39-41	2 pores near or 1 pore right after canal connection
<i>Pimelodella coquetanensis</i>	three and half times in SL		free	46-52	40
<i>Pimelodella cristata</i>	two to less than three times in SL	all	free		1 pore with canal
<i>Pimelodella cruxenti</i>	two or less in SL	ventral longer	free	41-43	47
<i>Pimelodella elongata</i>	three to three and half times in SL	dorsal slightly longer	free		1 pore with canal
<i>Pimelodella enochi</i>	three times in SL	subequal	free	40-41	2 pores near
<i>Pimelodella eutaenia</i>	three to four times in SL		free	42-44	2 pores near or 1 pore right after canal connection
<i>Pimelodella figueroai</i>	three and half times in SL	subequal			
<i>Pimelodella geryi</i>	three to four times in SL	dorsal slightly longer	free	42-43	1 pore without canal
<i>Pimelodella gracilis</i>	two to two and half times in SL	all	free	41-42	46
<i>Pimelodella griffini</i>	more than three and half times in SL		free		1 pore with canal
<i>Pimelodella grisea</i>	three to four times in SL	subequal	free	39-41	2 pores near or 1 pore right after canal connection
<i>Pimelodella hartii</i>	more than three and half times in SL	dorsal slightly longer	free	42-43	42
<i>Pimelodella hasemani</i>	three to four times in SL	ventral longer	free		1 pore without canal
<i>Pimelodella howesi</i>	two and half to three	dorsal slightly longer	free	43-44	2 pores far apart
<i>Pimelodella humeralis</i>	two times in SL	subequal	free	47-49	1 pore with canal
<i>Pimelodella ignobilis</i>	three and half to four times in SL	dorsal slightly longer	free	40-43	1 pore with canal
<i>Pimelodella itapicuruensis</i>	two and half to three	dorsal slightly longer	free	41-44	2 pores near
<i>Pimelodella kronnei</i>	three to four and half times in SL	dorsal slightly longer	free	42	2 pores near or 1 pore right after canal connection
<i>Pimelodella lateristriga</i>	three to three and half times in SL	dorsal slightly longer	free		2 pores near

<i>Pimelodella laticeps</i>	four times in SL	subequal dorsal lobe notably longer	free	39-40	2 pores far apart
<i>Pimelodella laurenti</i>	two to three times in SL	longer	free	39-41	1 pore without canal
<i>Pimelodella leptosoma</i>	two and half to three	dorsal slightly longer	free	41-44	2 pores near
<i>Pimelodella linami</i>	three and half times in SL	dorsal slightly longer	free		41 1 pore with canal
<i>Pimelodella longipinnis</i>	almost three times in SL		fused		42 2 pores near
<i>Pimelodella macturki</i>	three to four times in SL	all	free	39-41	2 pores near
<i>Pimelodella martinezi</i>	more than three times in SL	dorsal slightly longer			2 pores near or 1 pore right after canal connection
<i>Pimelodella meeki</i>	three to four times in SL	dorsal slightly longer	free	40-41	connection
<i>Pimelodella megalops</i>	three to five times in SL	ventral longer	free	39-42	2 pores far apart
<i>Pimelodella megalura</i>	two and half times in SL	dorsal lobe notably longer	both		
<i>Pimelodella metae</i>	two and half to three	longer	states	43-46	2 pores near
<i>Pimelodella modesta</i>	three times in SL	dorsal slightly longer	free	41-42	2 pores near
<i>Pimelodella montana</i>	two and half to three	dorsal slightly longer	free		41 1 pore without canal
<i>Pimelodella mucosa</i>	three and half times in SL	subequal	free		41 1 pore with canal
<i>Pimelodella notomelas</i>	three to three and half times in SL	ventral longer	free		41 2 pores near
		subequal	free		40 2 pores far apart
		dorsal lobe notably longer			
<i>Pimelodella odynea</i>	three to three and half times in SL	longer	free	41-43	1 pore with canal
		dorsal lobe notably longer			
<i>Pimelodella pectinifera</i>	four times in SL	longer	free		42 1 pore without canal
<i>Pimelodella peruana</i>	four times or more in SL	subequal	free	42-43	1 pore with canal
<i>Pimelodella reyesi</i>	three and half times in SL	subequal		41-42	
					2 pores near or 1 pore right after canal connection
<i>Pimelodella robinsoni</i>	two and half to three	subequal	free	41-43	connection
<i>Pimelodella roccae</i>	two and half to three	dorsal slightly longer	free	41-42	1 pore with canal
					2 pores near or 1 pore right after canal connection
<i>Pimelodella serrata</i>	two and half to three	subequal	free	41-44	connection
<i>Pimelodella spelaea</i>	three to three and half times in SL	dorsal slightly longer	free	40-41	1 pore without canal
<i>Pimelodella straminea</i>	three and half to four times in SL	ventral longer	free	40-41	2 pores far apart
<i>Pimelodella taeniophora</i>	two and half to three	subequal	free	40-42	1 pore with canal
<i>Pimelodella tapatapae</i>	three times in SL	ventral longer	free		41
<i>Pimelodella vittata</i>	two and half to three	dorsal slightly longer	free		42 1 pore with canal
<i>Pimelodella yuncensis</i>	two and half to four times in SL	subequal	free	37-41	1 pore without canal

Table 69 (cont.): Identification Key for the valid *Pimelodella* species diagnosable in this work.

Species	Midlateral stripe width	Midlateral stripe definition	Dorsal fin coloration
<i>Pimelodella australis</i>	wide	not well delimited	basal dark, followed by hyaline, distal dark
<i>Pimelodella avanhandavae</i>	wide	well delimited	basal dark, followed by hyaline, distal dark
<i>Pimelodella boliviana</i>	moderate	not well delimited	basal hyaline, distal half brown
<i>Pimelodella boschmai</i>	narrow to moderate	not well delimited	basal hyaline, distal half brown
<i>Pimelodella brasiliensis</i>	moderate	not well delimited	basal hyaline, distal half brown
<i>Pimelodella buckleyi</i>	wide	not well delimited	basal dark, followed by hyaline, distal dark
<i>Pimelodella chagresi</i>	wide	well delimited	completely dark
<i>Pimelodella coquetanesis</i>	wide	not well delimited	basal hyaline, distal half brown
<i>Pimelodella cristata</i>	narrow	not well delimited	hyaline, brown, hyaline, brown
<i>Pimelodella cruxenti</i>	narrow	not well delimited	basal dark, followed by hyaline, distal dark
<i>Pimelodella elongata</i>	wide	not well delimited	basal hyaline, distal half brown
<i>Pimelodella enochi</i>	moderate	not well delimited	basal hyaline, distal half brown
<i>Pimelodella eutaenia</i>	moderate to wide	moderate delimited	basal hyaline, distal half brown
<i>Pimelodella figueroai</i>	narrow	not well delimited	hyaline
<i>Pimelodella geryi</i>	wide	well delimited	basal hyaline, distal half brown
<i>Pimelodella gracilis</i>	wide	not well delimited	basal dark, followed by hyaline, distal dark
<i>Pimelodella griffini</i>	wide	not well delimited	basal dark, followed by hyaline, distal dark
<i>Pimelodella grisea</i>	moderate		basal hyaline, distal half brown
<i>Pimelodella harttii</i>	moderate	well delimited	basal dark, followed by hyaline, distal dark
<i>Pimelodella hasemani</i>	narrow to moderate	not well delimited	basal hyaline, distal half brown
<i>Pimelodella howesi</i>	moderate to wide	not well delimited	basal hyaline, distal half brown
<i>Pimelodella humeralis</i>	narrow	well delimited	hyaline, brown, hyaline, brown
<i>Pimelodella ignobilis</i>	wide	not well delimited	basal dark, followed by hyaline, distal dark
<i>Pimelodella itapicuruensis</i>	narrow to moderate	not well delimited	basal dark, followed by hyaline, distal dark
<i>Pimelodella kronei</i>	moderate	not well delimited	basal dark, followed by hyaline, distal dark

<i>Pimelodella lateristriga</i>	wide	well delimited	basal dark, followed by hyaline, distal dark
<i>Pimelodella laticeps</i>	wide	not well delimited	basal dark, followed by hyaline, distal dark
<i>Pimelodella laurenti</i>	moderate to wide	not well delimited	basal dark, followed by hyaline, distal dark
<i>Pimelodella leptosoma</i>	moderate	not well delimited	basal dark, followed by hyaline, distal dark
<i>Pimelodella linami</i>	wide	not well delimited	basal dark, followed by hyaline, distal dark
<i>Pimelodella longipinnis</i>	narrow	not well delimited	hyaline
<i>Pimelodella macturki</i>	moderate	well delimited	basal dark, followed by hyaline, distal dark
<i>Pimelodella martinezi</i>	narrow	not well delimited	
<i>Pimelodella meeki</i>	moderate to wide	not well delimited	basal dark, followed by hyaline, distal dark
<i>Pimelodella megalops</i>	narrow	well delimited	basal hyaline, distal half brown
<i>Pimelodella megalura</i>	wide	not well delimited	basal dark, followed by hyaline, distal dark dorsal fin medium brown near base, followed by a hyaline stripe, then a dark brown to black stripe, and distal portion of rays clear
<i>Pimelodella metae</i>	moderate	not well delimited	
<i>Pimelodella modesta</i>	narrow	well delimited	basal hyaline, distal half brown
<i>Pimelodella montana</i>	wide	well delimited	basal dark, followed by hyaline, distal dark
<i>Pimelodella mucosa</i>	wide	not well delimited	basal dark, followed by hyaline, distal dark
<i>Pimelodella notomelas</i>	narrow	not well delimited	basal dark, followed by hyaline, distal dark
<i>Pimelodella odynea</i>	wide	well delimited	completely dark
<i>Pimelodella pectinifera</i>	absent		hyaline
<i>Pimelodella peruana</i>	narrow	well delimited	hyaline
<i>Pimelodella reyesi</i>	wide	well delimited	hyaline
<i>Pimelodella robinsoni</i>	moderate	not well delimited	basal hyaline, distal half brown
<i>Pimelodella roccae</i>	moderate	not well delimited	basal dark, followed by hyaline, distal dark
	narrow to		
<i>Pimelodella serrata</i>	moderate	not well delimited	completely dark
<i>Pimelodella spelaea</i>	narrow	not well delimited	hyaline
<i>Pimelodella</i>	wide	not well delimited	basal dark, followed by hyaline, distal dark

<i>straminea</i>			
<i>Pimelodella</i>			
<i>taeniophora</i>	wide	not well delimited	basal dark, followed by hyaline, distal dark
<i>Pimelodella</i>			
<i>tapatapae</i>	moderate	not well delimited	basal hyaline, distal half brown
<i>Pimelodella vittata</i>	wide	not well delimited	basal dark, followed by hyaline, distal dark
<i>Pimelodella</i>			
<i>yuncensis</i>	narrow	not well delimited	completely dark

Table 69 (cont.): Identification Key for the valid *Pimelodella* species diagnosable in this work.

Species	Paired dorsolateral stripe	extension of paired dorsolateral stripe	other coloration marks
<i>Pimelodella australis</i>	present	supraoccipital process	hyaline stripe on dorsal fin does not encompass unbranched fin ray; dark brown mark between dorsal and adipose fins; paired stripe at dorsal-fin base; paired stripe along anterior half of adipose fin
<i>Pimelodella avanhandavae</i>	present	half of adipose fin	
<i>Pimelodella boliviana</i>	present	supraoccipital process	
<i>Pimelodella boschmai</i>	absent		brown stripe from snout to orbit
<i>Pimelodella brasiliensis</i>	absent		head overall darker
<i>Pimelodella buckleyi</i>	absent		distal third of dorsal fin extremely dark; might present a dark brown oval mark at anterior limit of lateral line
<i>Pimelodella chagresi</i>	present	two thirds of adipose fin	
<i>Pimelodella coquetanesis</i>	absent		
<i>Pimelodella cristata</i>	absent		
<i>Pimelodella cruxenti</i>	absent		body overall dark brown; dorsal-fin hyaline stripe does not encompass unbranched ray
<i>Pimelodella elongata</i>	absent		
<i>Pimelodella enochi</i>	absent		
<i>Pimelodella eutaenia</i>	present	first third of adipose	
<i>Pimelodella figueroai</i>			
<i>Pimelodella geryi</i>	absent		distal half of dorsal fin notably dark, black
<i>Pimelodella gracilis</i>	present	first third of adipose	
<i>Pimelodella</i>	present	terminus of adipose fin	

<i>griffini</i>			
<i>Pimelodella</i>			
<i>grisea</i>			
<i>Pimelodella</i>			
<i>hartii</i>	present	supraoccipital process	
<i>Pimelodella</i>			
<i>hasemani</i>	absent		dorsal region of body darker, especially between dorsal and adipose fins
<i>Pimelodella</i>			
<i>howesi</i>	absent		ventral lobe of caudal fin might be slightly darker
<i>Pimelodella</i>			
<i>humeralis</i>	absent		humeral mark
<i>Pimelodella</i>			
<i>ignobilis</i>	absent		hyaline stripe on dorsal fin does not encompass unbranched ray; dorsal region of head and body slightly darker
<i>Pimelodella</i>			
<i>itapicuruensis</i>	present	dorsal-fin terminus	
<i>Pimelodella</i>			
<i>kronoi</i>	present	supraoccipital process	might be completely unpigmented; dorsal region of head might be darker
<i>Pimelodella</i>			
<i>lateristriga</i>	absent		dorsal region of head darker
<i>Pimelodella</i>			
<i>laticeps</i>	absent		dark brown region between dorsal and adipose fins
<i>Pimelodella</i>			
<i>laurenti</i>	present	supraoccipital process	dark region at dorsal-fin base
<i>Pimelodella</i>			
<i>leptosoma</i>	absent		distal third of dorsal fin extremely dark
<i>Pimelodella</i>			
<i>linami</i>	absent		
<i>Pimelodella</i>			
<i>longipinnis</i>	absent		dark region at dorsal-fin base
<i>Pimelodella</i>			
<i>macturki</i>	absent		distal third of dorsal fin with dark brown or black pigment; anterodorsal region of pseudotympanum with scattered melanophores
<i>Pimelodella</i>			
<i>martinezi</i>			
<i>Pimelodella</i>			
<i>meekei</i>	present	supraoccipital process	hyaline stripe on dorsal fin does not encompass unbranched fin ray
<i>Pimelodella</i>			
<i>megalops</i>			
<i>Pimelodella</i>	see other		
<i>megalura</i>	coloration		dorsal region of body from supraoccipital process to adipose darker

	marks		
<i>Pimelodella metae</i>	absent		
<i>Pimelodella modesta</i>	absent		dorsal region of body overall darker; ventral caudal lobe darker
<i>Pimelodella montana</i>	present	first third of adipose	
<i>Pimelodella mucosa</i>	present	half dorsal-fin base	
<i>Pimelodella notomelas</i>	present	supraoccipital process	head dorsally darker
<i>Pimelodella odynea</i>	present	adipose terminus	
<i>Pimelodella pectinifera</i>			uniformely brownish
<i>Pimelodella peruana</i>	present	adipose origin	lower caudal-fin lobe heavily pigmented; pseudotympanum with scattered melanophores
<i>Pimelodella reyesi</i>	present	adipose terminus	
<i>Pimelodella robinsoni</i>	absent		
<i>Pimelodella roccae</i>	present	adipose terminus	
<i>Pimelodella serrata</i>	absent		
<i>Pimelodella spelaea</i>	present	dorsal-fin terminus	light brown region between dorsal and adipose fins
<i>Pimelodella straminea</i>	absent		dorsal fin hyaline stripe does not encompass unbranched ray
<i>Pimelodella taeniophora</i>	present	supraoccipital process	
<i>Pimelodella tapatapae</i>	absent		
<i>Pimelodella vittata</i>	present	dorsal-fin terminus	hyaline stripe does not encompass unbranched dorsal fin ray, neither other rays
<i>Pimelodella yuncensis</i>	absent		region adjacent to midlateral stripe lighter

Table 70: Complete material list analyzed for molecular taxonomy.

Institution	Lot	specimen	#	Identification
LBP	9	3599	1	<i>Pimelodella gracilis</i>
LBP	9	3598	2	<i>Pimelodella gracilis</i>
LBP	9	3549	3	<i>Pimelodella gracilis</i>
LBP	9	3548	4	<i>Pimelodella gracilis</i>
LBP	9	3588	5	<i>Pimelodella gracilis</i>
LBP	9	3587	6	<i>Pimelodella mucosa</i>
LBP	9	3589	7	<i>Pimelodella gracilis</i>
LBP	821	8621	8	<i>Pimelodella meeki</i>
LBP	821	8610	9	<i>Pimelodella meeki</i>
LBP	821	8645	10	<i>Pimelodella meeki</i>
LBP	821	8623	11	<i>Pimelodella meeki</i>
LBP	826	8720	12	<i>Tauayia bifasciata</i>
LBP	1737	12883	13	<i>Brachyglanis</i> sp. <i>Pimelodella</i> sp. cristata
LBP	2189	15549	14	group
LBP	2468	16321	15	<i>Phenacorhamdia</i> sp.
LBP	3332	20457	16	<i>Pimelodella australis</i>
LBP	3628	21649	17	<i>Rhamdia</i> sp.
LBP	3628	21648	18	<i>Pimelodella ignobilis</i>
LBP	3667	21750	19	<i>Pimelodella meeki</i>
LBP	3667	21748	20	<i>Pimelodella meeki</i>
LBP	3667	21749	21	<i>Imparfinis</i> sp.
LBP	4082	23503	22	<i>Pimelodella boliviana</i>
LBP	4082	23504	23	<i>Pimelodella serrata</i>
LBP	4092	23530	24	<i>Pimelodella cristata</i>
LBP	4782	25614	25	<i>Pimelodella australis</i>
LBP	5027	25969	26	<i>Imparfinis</i> sp.
LBP	5286	26772	27	<i>Pimelodella cristata</i>
LBP	5286	26773	28	<i>Pimelodella cristata</i>
LBP	5286	26771	29	<i>Pimelodella</i> aff. <i>leptosoma</i>
LBP	6835	33104	30	<i>Pimelodella lateristriga</i>
LBP	6634	31970	31	<i>Pimelodella avanhandavae</i>
LBP	6634	31967	32	<i>Pimelodella avanhandavae</i>
LBP	6835	33100	33	<i>Pimelodella lateristriga</i>
LBP	7488	35557	34	<i>Pimelodella kronei</i>
LBP	7488	35590	35	<i>Pimelodella kronei</i>
LBP	7395	35395	36	<i>Rhamdia quelen</i>
LBP	7395	35394	37	<i>Rhamdia quelen</i>
LBP	7889	37053	38	<i>Pimelodella kronei</i>
LBP	7899	37071	39	<i>Pimelodella lateristriga</i>
LBP	8075	37213	40	<i>Pimelodella gracilis</i>
LBP	8176	38152	41	<i>Rhamdioglanis frenatus</i>
LBP	8302	40014	42	<i>Pimelodella brasiliensis</i>
LBP	8302	40012	43	<i>Pimelodella brasiliensis</i>
LBP	9134	42728	44	<i>Pimelodella leptosoma</i>
LBP	8476	42467	45	<i>Pimelodella taeniophora</i>
LBP	8476	42468	46	<i>Pimelodella taeniophora</i>
LBP	9134	43043	47	<i>Pimelodella leptosoma</i>
LBP	9134	43042	48	<i>Pimelodella leptosoma</i>
LBP	9942	46681	49	<i>Imparfinis stictonotus</i>
LBP	9240	44456	50	<i>Pimelodella gracilis</i>
LBP	9240	44455	51	<i>Pimelodella gracilis</i>
LBP	9362	43950	52	<i>Pimelodella modesta</i>
LBP	9362	43951	53	<i>Pimelodella modesta</i>
LBP	9345	43902	54	<i>Pimelodella modesta</i>

LBP	9496	44622	55	<i>Rhamdia sp.</i>
LBP	9496	44621	56	<i>Pimelodella sp.</i>
LBP	9496	44624	57	<i>Pimelodella sp.</i>
LBP	9496	44623	58	<i>Pimelodella sp.</i>
LBP	10477	49157	59	<i>Pimelodella vittata</i>
LBP	11002	50527	60	<i>Pimelodella boliviana</i>
LBP	11002	50528	61	<i>Pimelodella boliviana</i>
LBP	11002	50529	62	<i>Pimelodella boliviana</i>
LBP	12044	51805	63	<i>Pimelodella aff. boliviana</i>
LBP	12044	51806	64	<i>Pimelodella aff. boliviana</i>
LBP	18896	54987	65	<i>Pimelodella australis</i>
LBP	12874	53498	66	<i>Pimelodella cristata</i>
LBP	13766	57080	67	<i>Pimelodella cristata</i>
LBP	13766	57083	68	<i>Pimelodella cristata</i>
LBP	13766	57081	69	<i>Pimelodella cristata</i>
LBP	13766	57082	70	<i>Pimelodella cristata</i>
LBP	14600	61044	71	<i>Pimelodella meeki</i>
LBP	14600	61045	72	<i>Pimelodella meeki</i>
LBP	15863	64153	73	<i>Pimelodella aff. gracilis</i>
UFRO	14298	2304	74	<i>Pimelodella serrata</i>
UFRO	23913	7304	75	<i>Pimelodella howesi</i>
UFRO	13484	6674	76	<i>Pimelodella howesi</i>
UFRO	7502	5920	77	<i>Pimelodella cristata</i>
UFRO	14300	2303	78	<i>Pimelodella gracilis</i>
UFRO	17668	8030	79	<i>Pimelodella cristata</i>
UFRO	17108	7982	80	<i>Pimelodus sp.</i>
LESCI	uncat		81	<i>Pimelodella kronei</i>
LESCI	uncat		82	<i>Pimelodella kronei</i>
LESCI	uncat		83	<i>Pimelodella kronei</i>
ANSP	179752	2089	84	<i>Pimelodella sp.</i>
				<i>Pimelodella sp. cristata</i>
ANSP	189109	6922	85	group
				<i>Pimelodella sp. cristata</i>
ANSP	189109	6923	86	group
				<i>Pimelodella sp. cristata</i>
ANSP	189109	6950	87	group
ANSP	189112	6998	88	<i>Pimelodella megalops</i>
ANSP	189112	7001	89	<i>Pimelodella megalops</i>
ANSP	182412	A5063	90	<i>Pimelodella taeniophora</i>
ANSP	182412	A5066	91	<i>Pimelodella taeniophora</i>
ANSP	182415	A5209	92	<i>Pimelodella avanhandavae</i>
ANSP	182415	A5205	93	<i>Pimelodella avanhandavae</i>
ANSP	185051	P4042	94	<i>Pimelodella aff. megalops</i>

Table 71: Successfully sequenced specimens per gene.

#	Identification	COI	CytB	36298e1	4174e20
1	<i>Pimelodella gracilis</i>	X	X	X	X
2	<i>Pimelodella gracilis</i>	X	X	X	X
3	<i>Pimelodella gracilis</i>	X	X	X	
4	<i>Pimelodella gracilis</i>			X	
5	<i>Pimelodella gracilis</i>	X	X	X	
6	<i>Pimelodella mucosa</i>	X	X		
7	<i>Pimelodella gracilis</i>	X	X	X	
8	<i>Pimelodella meeki</i>				
9	<i>Pimelodella meeki</i>	X	X	X	X
10	<i>Pimelodella meeki</i>	X	X	X	X
11	<i>Pimelodella meeki</i>	X	X		
12	<i>Tauayia bifasciata</i>	X	X		
13	<i>Brachyglanis sp.</i>	X	X	X	X
14	<i>Pimelodella sp. cristata</i> group	X	X	X	X
15	<i>Phenacorhamdia sp.</i>	X	X		X
16	<i>Pimelodella australis</i>	X	X	X	X
17	<i>Rhamdia sp.</i>	X	X	X	
18	<i>Pimelodella ignobilis</i>	X	X		X
19	<i>Pimelodella meeki</i>	X	X		X
20	<i>Pimelodella meeki</i>	X	X	X	X
21	<i>Imparfinis sp.</i>				X
22	<i>Pimelodella boliviana</i>	X	X	X	
23	<i>Pimelodella serrata</i>	X	X	X	X
24	<i>Pimelodella cristata</i>	X	X	X	X
25	<i>Pimelodella australis</i>	X	X	X	X
26	<i>Imparfinis sp.</i>	X	X		X
27	<i>Pimelodella cristata</i>	X	X	X	
28	<i>Pimelodella cristata</i>	X	X	X	X
29	<i>Pimelodella aff. leptosoma</i>	X	X		
30	<i>Pimelodella lateristriga</i>	X	X		X
31	<i>Pimelodella avanhandavae</i>	X	X	X	
32	<i>Pimelodella avanhandavae</i>	X	X	X	
33	<i>Pimelodella lateristriga</i>	X	X		
34	<i>Pimelodella kronei</i>	X	X		
35	<i>Pimelodella kronei</i>	X	X	X	
36	<i>Rhamdia quelen</i>	X	X	X	
37	<i>Rhamdia quelen</i>	X	X	X	
38	<i>Pimelodella kronei</i>			X	X
39	<i>Pimelodella lateristriga</i>	X	X	X	
40	<i>Pimelodella gracilis</i>	X	X	X	
41	<i>Rhamdioglanis frenatus</i>	X	X		
42	<i>Pimelodella brasiliensis</i>	X	X	X	
43	<i>Pimelodella brasiliensis</i>	X	X		
44	<i>Pimelodella leptosoma</i>	X	X	X	
45	<i>Pimelodella taeniophora</i>	X	X	X	
46	<i>Pimelodella taeniophora</i>	X	X	X	
47	<i>Pimelodella leptosoma</i>	X	X	X	
48	<i>Pimelodella leptosoma</i>	X	X		
49	<i>Imparfinis stictonotus</i>	X	X		X
50	<i>Pimelodella gracilis</i>	X	X		
51	<i>Pimelodella gracilis</i>	X	X	X	X
52	<i>Pimelodella modesta</i>	X	X	X	X
53	<i>Pimelodella modesta</i>			X	X
54	<i>Pimelodella modesta</i>	X	X	X	

55	<i>Rhamdia</i> sp.	X	X	X	
56	<i>Pimelodella</i> sp.	X	X	X	
57	<i>Pimelodella</i> sp.	X	X	X	X
58	<i>Pimelodella</i> sp.	X	X	X	X
59	<i>Pimelodella vittata</i>	X	X	X	X
60	<i>Pimelodella boliviana</i>	X	X		X
61	<i>Pimelodella boliviana</i>	X	X	X	X
62	<i>Pimelodella boliviana</i>	X	X	X	X
63	<i>Pimelodella</i> aff. <i>boliviana</i>	X	X	X	X
64	<i>Pimelodella</i> aff. <i>boliviana</i>	X	X	X	
65	<i>Pimelodella australis</i>	X	X		X
66	<i>Pimelodella cristata</i>			X	
67	<i>Pimelodella cristata</i>	X	X	X	
68	<i>Pimelodella cristata</i>	X	X	X	X
69	<i>Pimelodella cristata</i>	X	X	X	X
70	<i>Pimelodella cristata</i>	X	X	X	X
71	<i>Pimelodella meeki</i>		X		
72	<i>Pimelodella meeki</i>	X	X		
73	<i>Pimelodella</i> aff. <i>gracilis</i>	X	X		
74	<i>Pimelodella serrata</i>	X	X	X	X
75	<i>Pimelodella howesi</i>	X	X	X	
76	<i>Pimelodella howesi</i>	X	X	X	X
77	<i>Pimelodella cristata</i>	X	X	X	X
78	<i>Pimelodella gracilis</i>	X	X	X	X
79	<i>Pimelodella cristata</i>	X	X	X	
80	<i>Pimelodus</i> sp.	X	X	X	
81	<i>Pimelodella kronei</i>				
82	<i>Pimelodella kronei</i>				
83	<i>Pimelodella kronei</i>				
84	<i>Pimelodella</i> sp.		X	X	X
	<i>Pimelodella</i> sp. <i>cristata</i>				
85	group		X	X	
	<i>Pimelodella</i> sp. <i>cristata</i>				
86	group		X	X	
	<i>Pimelodella</i> sp. <i>cristata</i>				
87	group		X	X	
88	<i>Pimelodella megalops</i>		X	X	
89	<i>Pimelodella megalops</i>		X	X	
90	<i>Pimelodella taeniophora</i>		X	X	
91	<i>Pimelodella taeniophora</i>			X	
92	<i>Pimelodella avanhandavae</i>		X		
93	<i>Pimelodella avanhandavae</i>		X	X	
94	<i>Pimelodella</i> aff. <i>megalops</i>			X	

Table 72: Fragment length, number of parsimony informative sites, GC content and mean bootstrap values per gene.

	Fragment length	Parsimony informative sites	GC content	Mean bootstrap value
COI	581	21	0.46	72.35
CytB	743	23.82	0.44	76.78
36298e1	790	21.14	0.42	80.92
4174e20	866	28.87	0.37	80.24

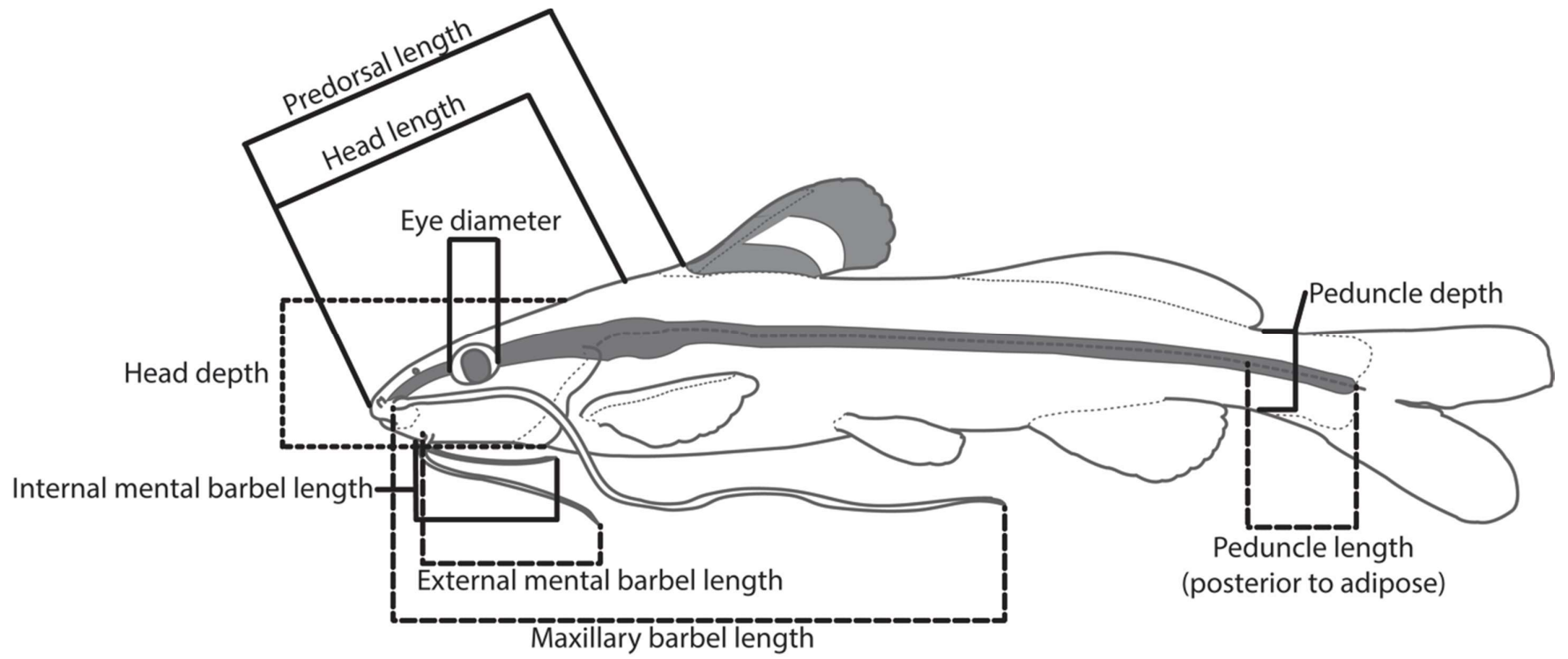


Figure 1: Schematic for particular measurements taken point-to-point in a generalized *Pimelodella* specimen.

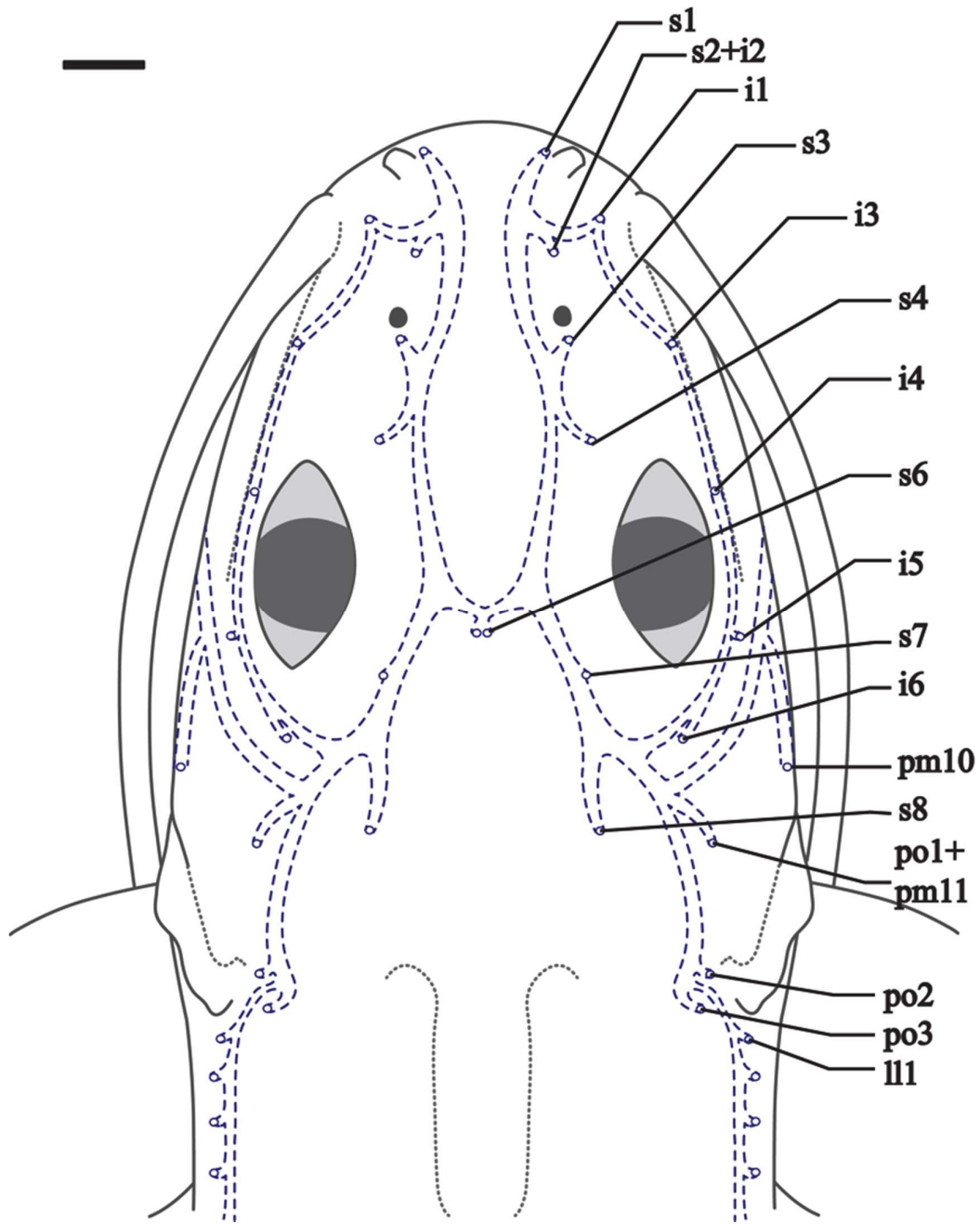


Figure 2: Schematic for head laterosensory canals, dorsal view, in a generalized *Pimelodella* specimen. Scale bar 2mm.

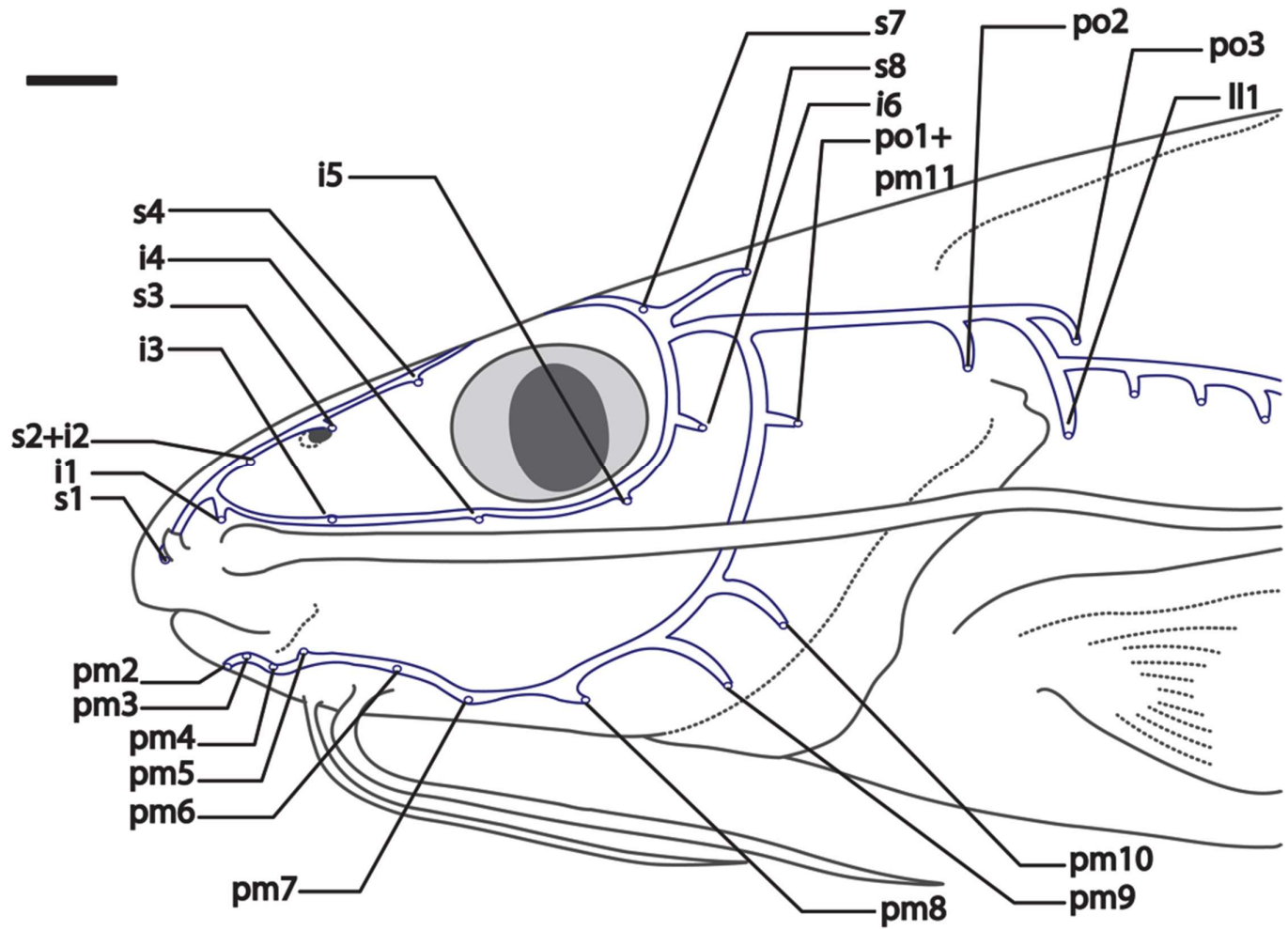


Figure 3: Schematic for head laterosensory canals, lateral view, in a generalized *Pimelodella* specimen. Scale bar 2mm.

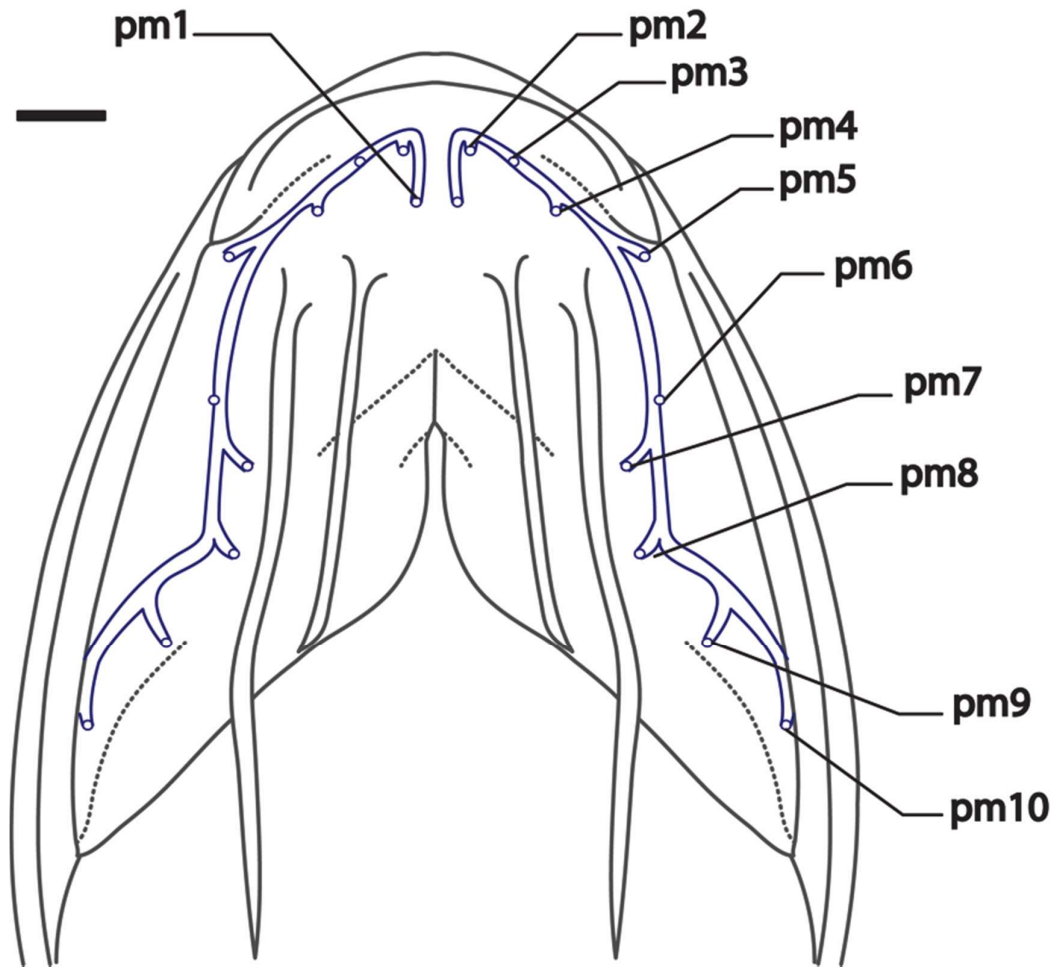


Figure 4: Schematic for head laterosensory canals, ventral view, in a generalized *Pimelodella* specimen. Scale bar 2mm.



Figure 5: *Pimelodella australis*, holotype, FMNH 57962, 61.0 mm SL. Left lateral (A), and dorsal (B) views. Photo taken by M. W. Littmann.

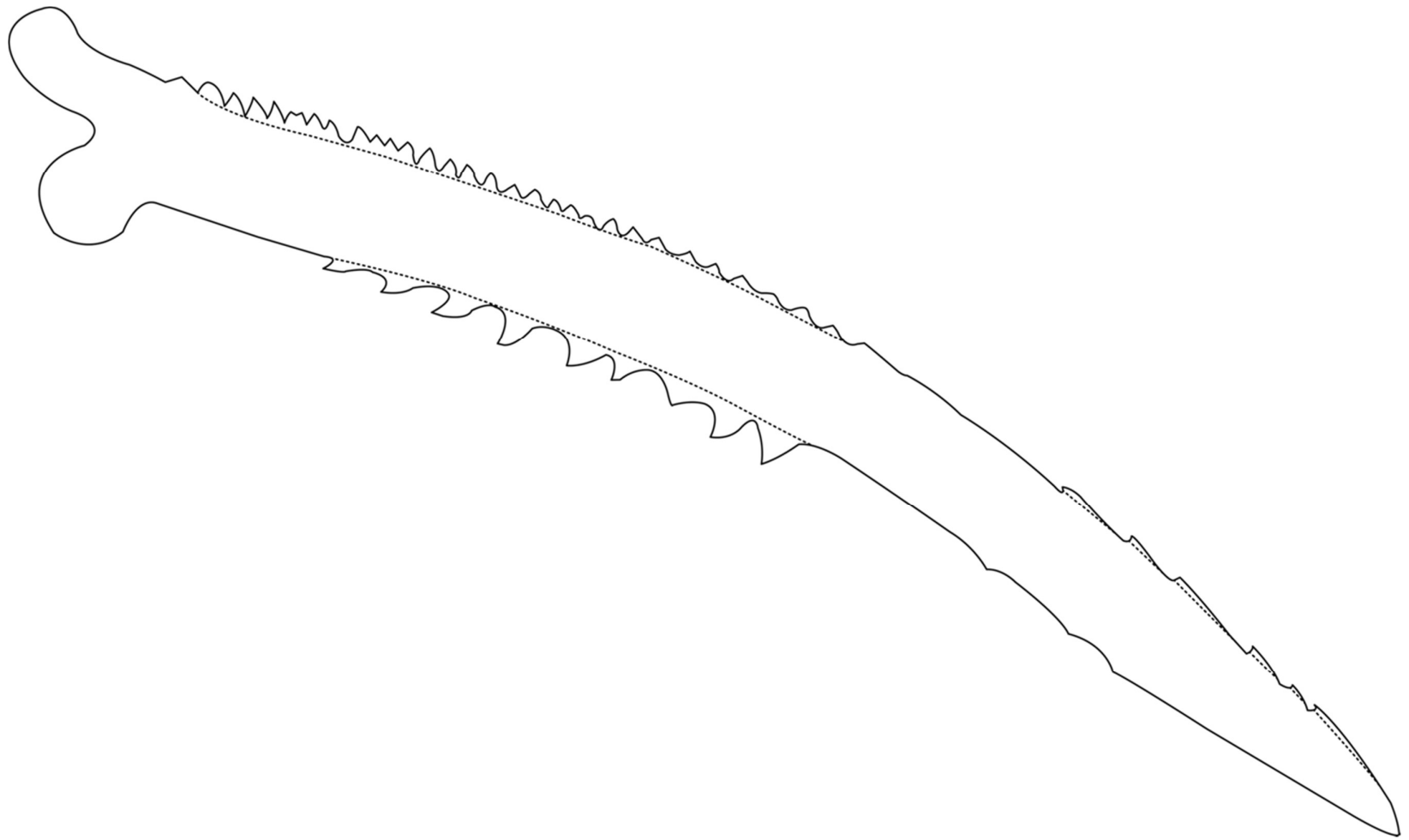


Figure 6: Ventral view of left pectoral-fin spine of *Pimelodella australis*, holotype, 61.0mm SL, total length of spine 12.6 mm.

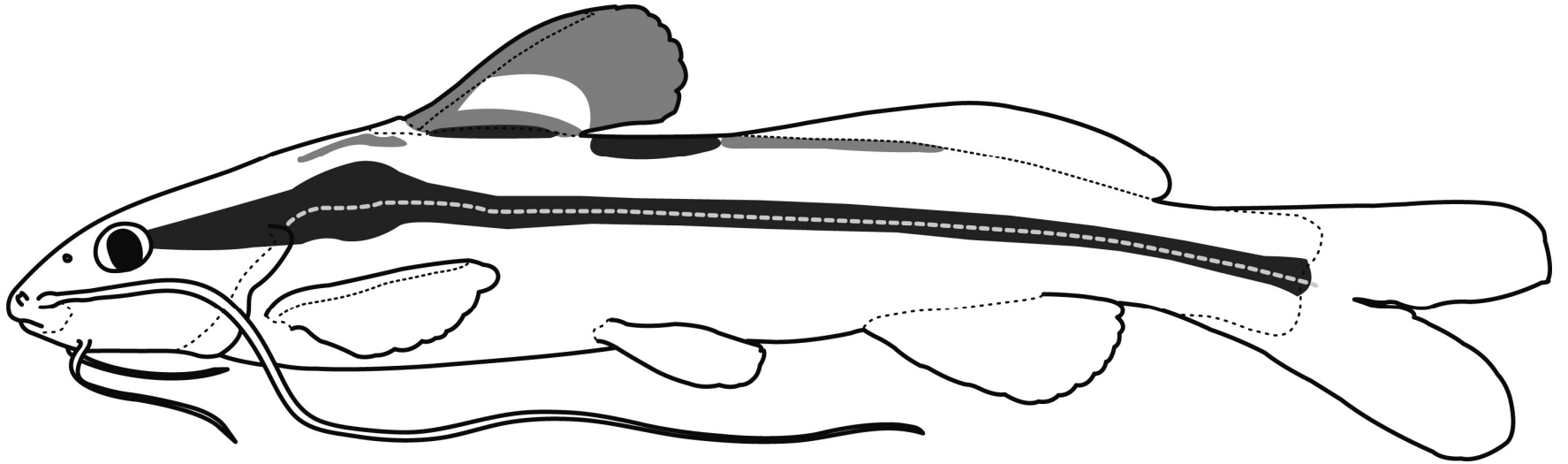


Figure 7: Schematic left lateral view of *Pimelodella australis*.



Figure 8: *Pimelodella avanhandavae*, holotype, FMNH 57981, 69.0 mm SL. Left lateral (A), and dorsal (B) views. Photo taken by M. W. Littmann.

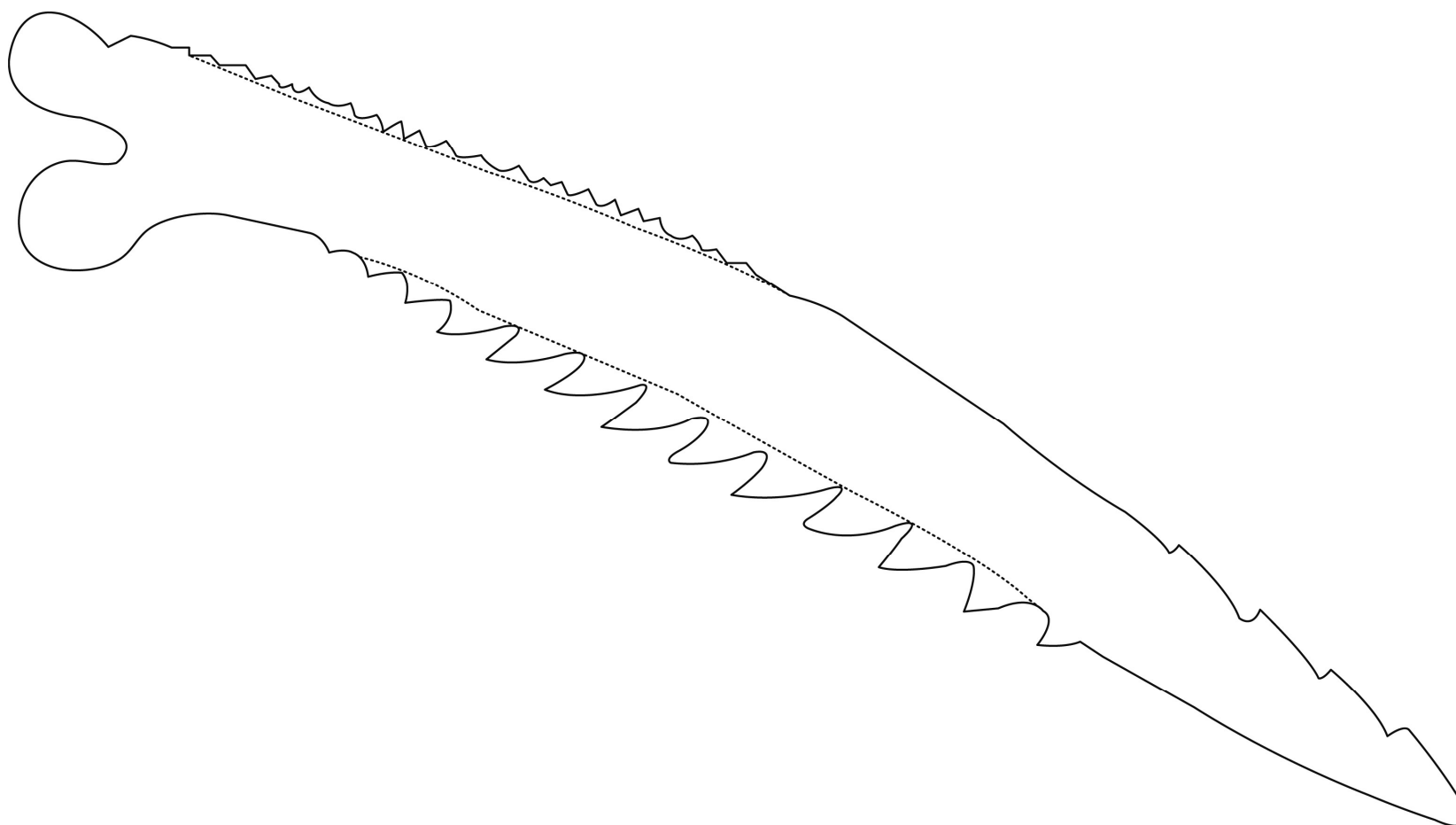


Figure 9: Ventral view of left pectoral-fin spine of *Pimelodella avanhandavae* FMNH 57982, paratype, 78.8 mm SL, total length of spine 13.4 mm.

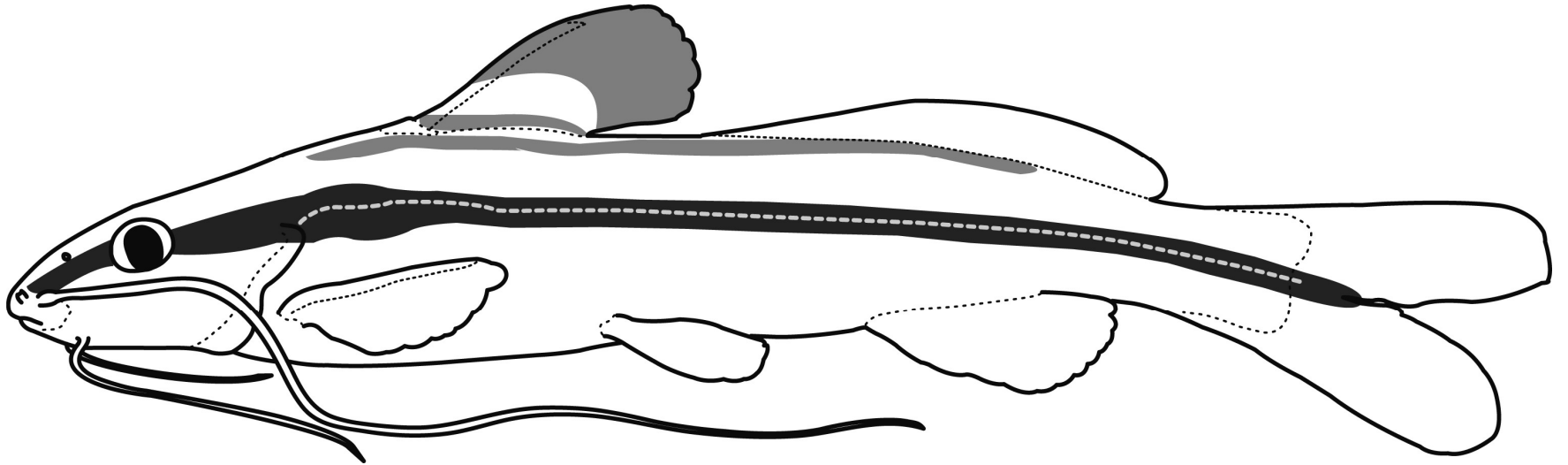


Figure 10: Schematic left lateral view of *Pimelodella avanhandavae*.



Figure 11: *Pimelodella boliviana*, holotype, FMNH 57976, 68.9 mm SL. Left lateral (A), and dorsal (B) views. Photo taken by M. W. Littmann.

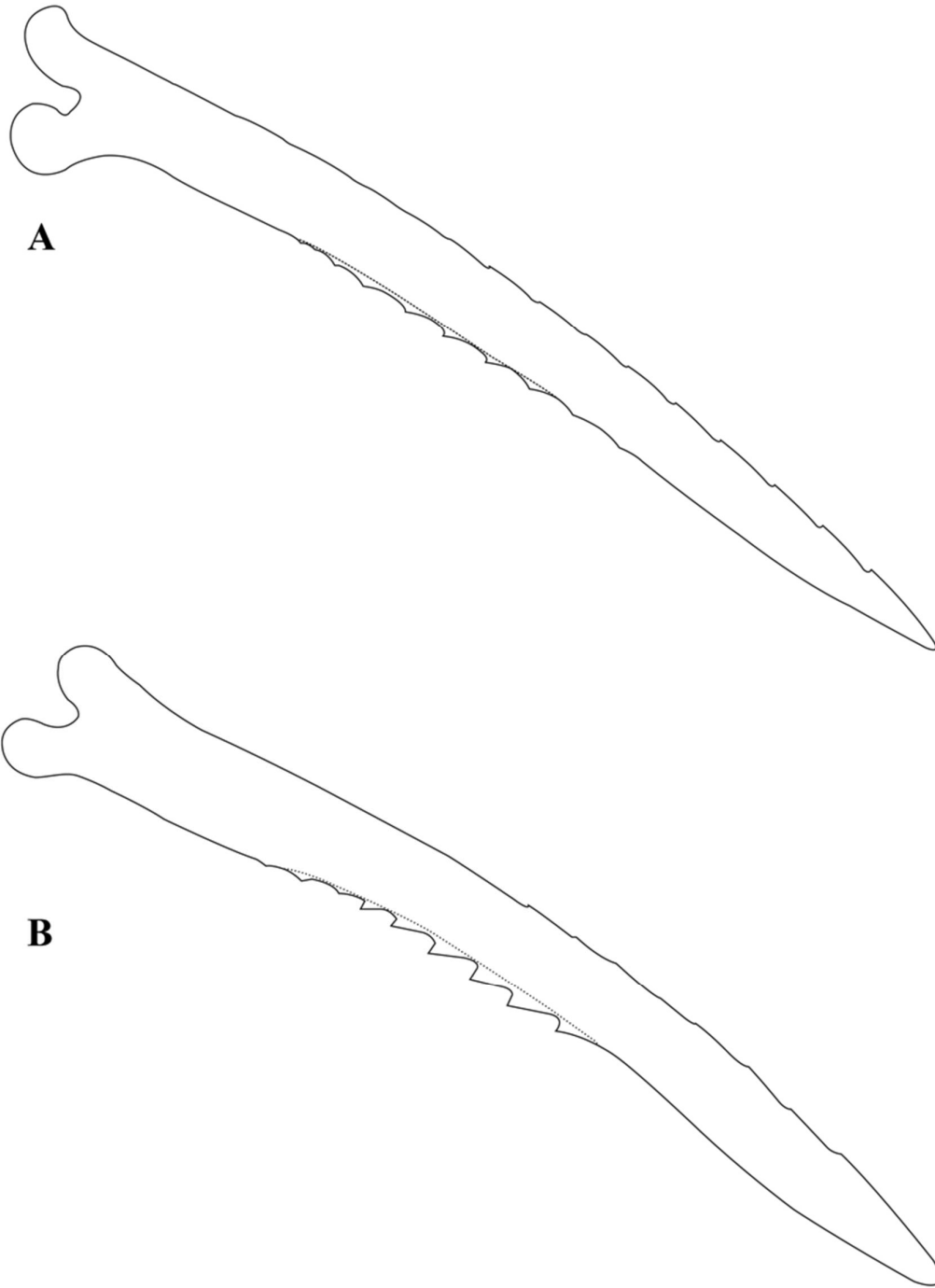


Figure 12: Ventral view of left pectoral-fin spine of *Pimelodella boliviana* A) FMNH 57977, paratype, 66.9 mm SL, total length of spine 11.5 mm; B) MZUSP 26015, 71.3 mm SL, total length of spine 11.7 mm.

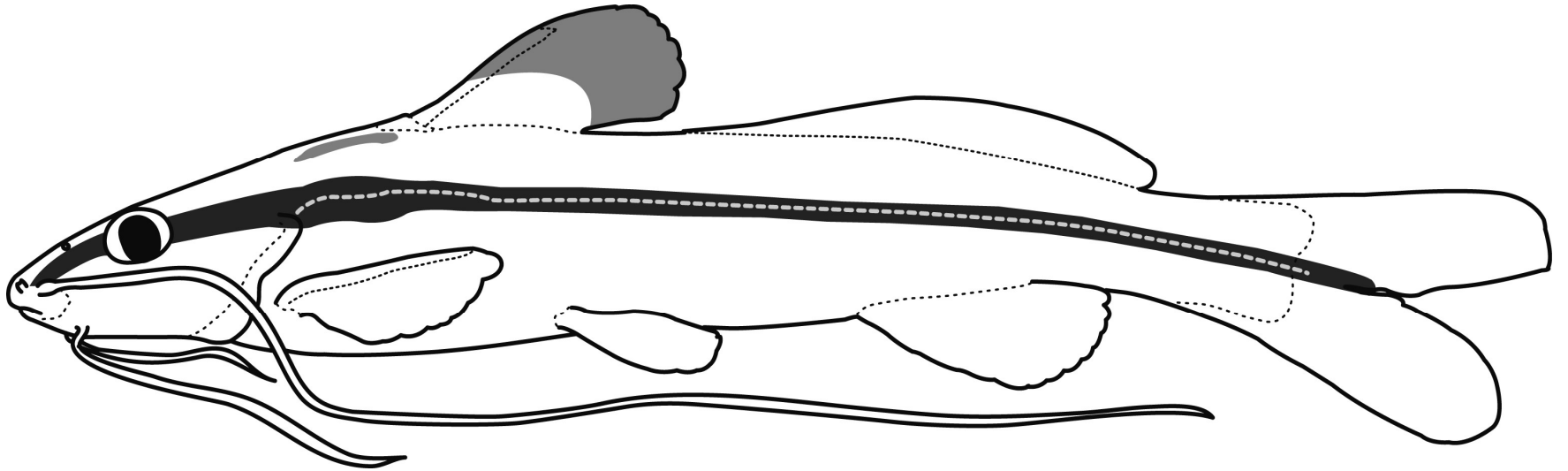


Figure 13: Schematic left lateral view of *Pimelodella boliviana*.



Figure 14: *Pimelodella boschmai*, holotype, RMNH 23248, 73.0 mm SL. Left lateral (A), and dorsal (B) views. Photo taken by Ronald de Ruiter.

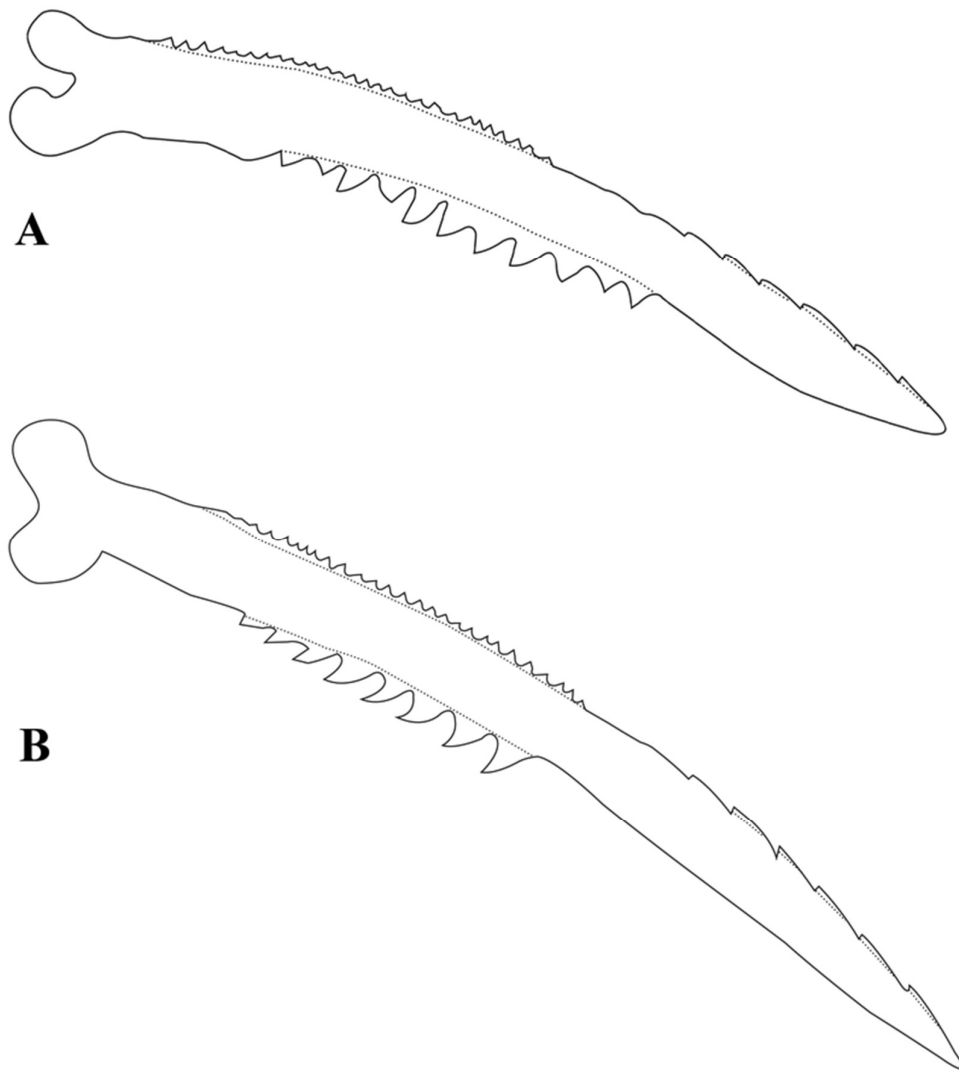


Figure 15: Ventral view of left pectoral-fin spine of A) *Pimelodella boschmai*, RMNH 23248, holotype, 73.0 mm SL; B) *Pimelodella insignis*, MZUSP 22317, syntype 66.4 mm SL, total length of spine 12.8 mm.

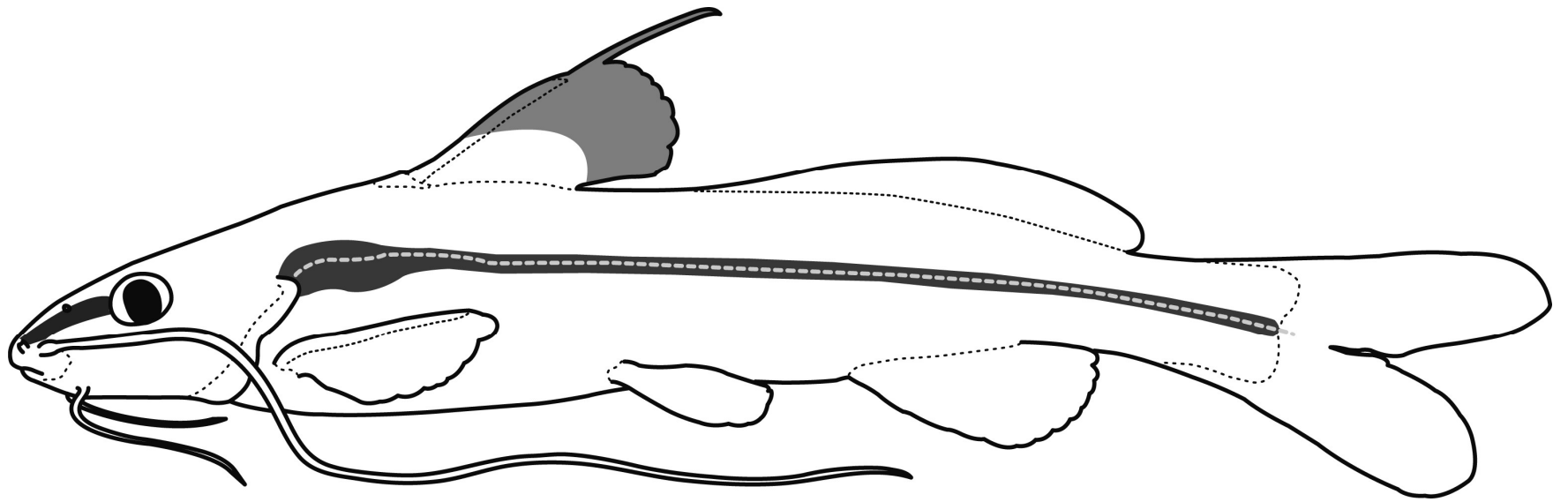


Figure 16: Schematic left lateral view of *Pimelodella boschmai*



Figure 17: *Pimelodella brasiliensis*, holotype, NMW 45612, 140.6 mm SL. Left lateral (A), and dorsal (B) views. Photos taken by Mark Sabaj. *Pimelodella eigenmanni*, junior-synonym of *P. brasiliensis*, paralectotype, MCZ 7438, 130.7 mm SL, left lateral (C), and dorsal (D) views. *Pimelodella rendahli*, junior-synonym of *P. brasiliensis*, holotype, ZMB 32031, 80.7 mm SL, left lateral (E), and dorsal (F) views, photo taken by ZMB staff.

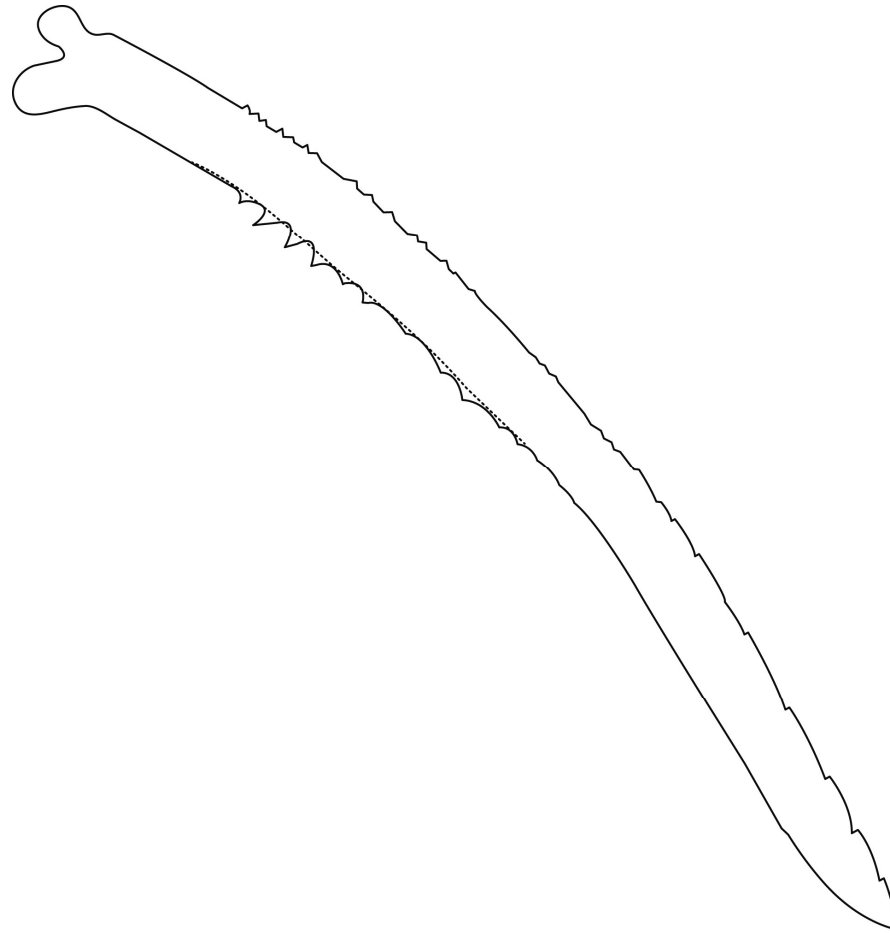


Figure 18: Ventral view of left pectoral-fin spine of *Pimelodella brasiliensis*, NMW 45612, holotype, 140.6 mm SL, total length of spine 26.6 mm.

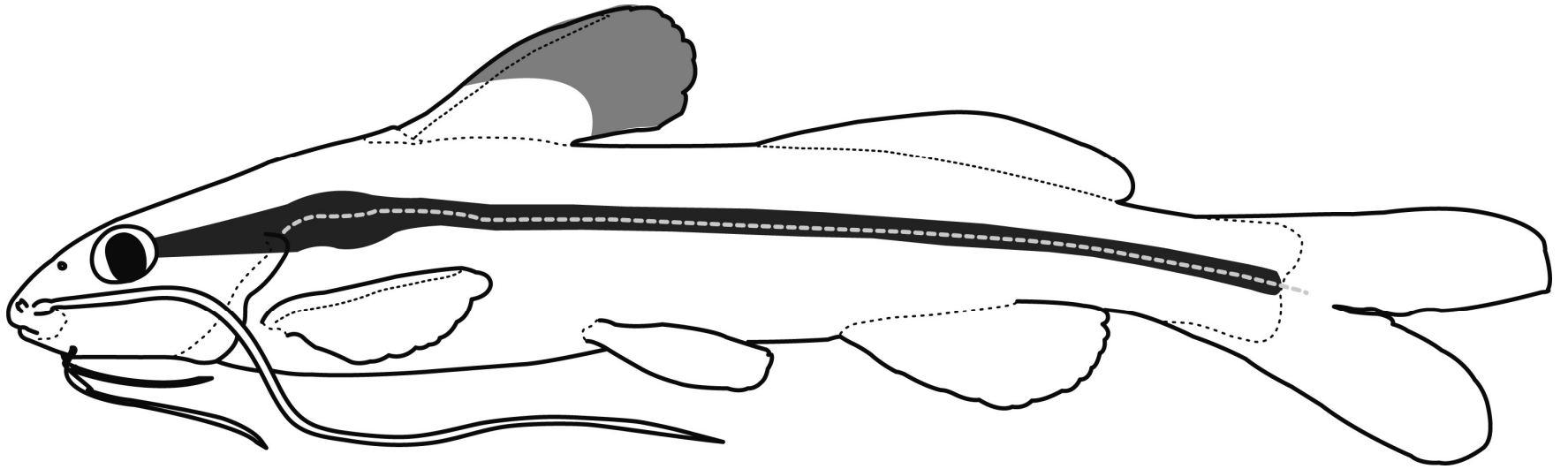


Figure 19: Schematic left lateral view of *Pimelodella brasiliensis*



Figure 20: *Pimelodella buckleyi*, lectotype, BMNH 1880.12.8.98, 109.6 mm SL. Left lateral (A), and dorsal (B) views. Photo taken by Mark Allen.

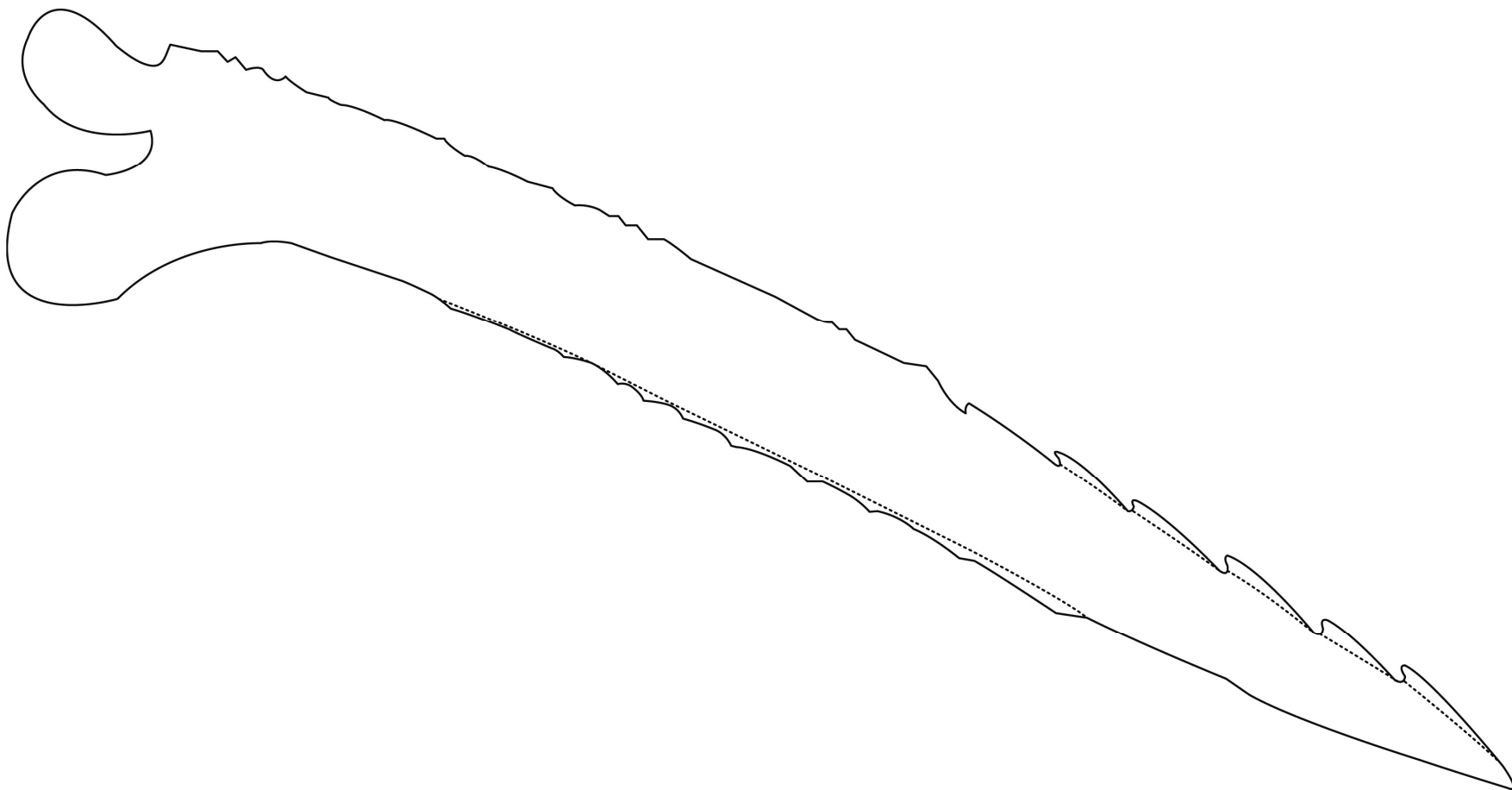


Figure 21: Ventral view of left pectoral-fin spine of *Pimelodella buckleyi*, BMNH 1880.12.8.98, lectotype, 109.6 mm SL, total length of spine 15.3 mm.

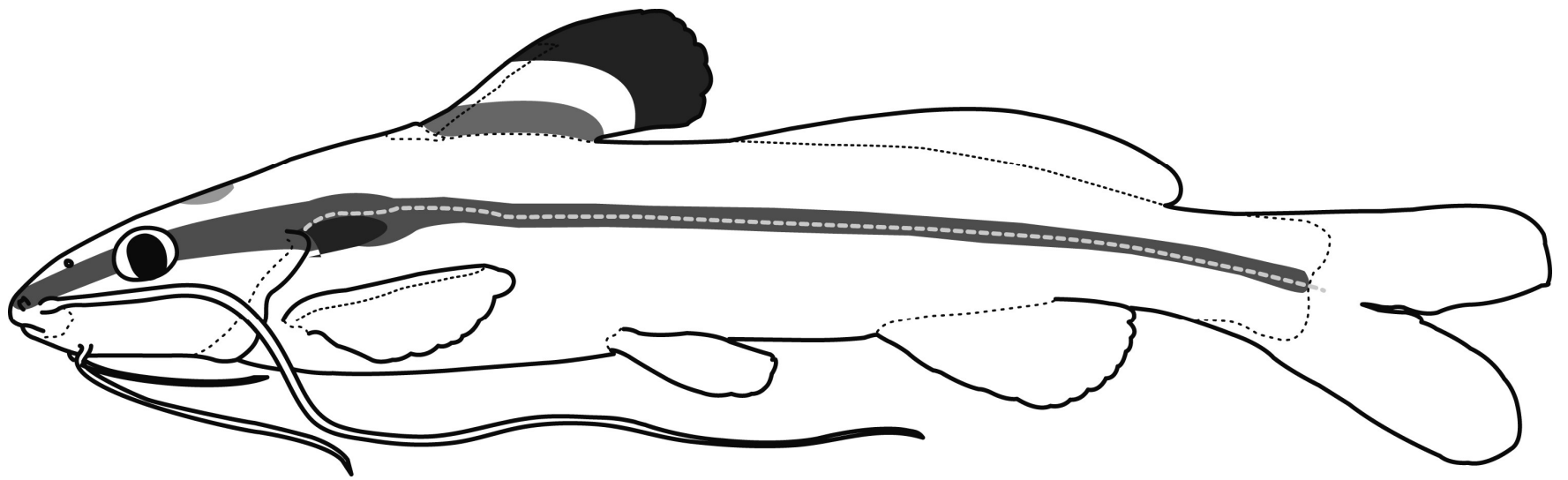


Figure 22. Schematic left lateral view of *Pimelodella buckleyi*



Figure 23. *Pimelodella chagresi*, lectotype, MCZ 4947, 111.8 mm SL. Left lateral (A), and dorsal (B) views.

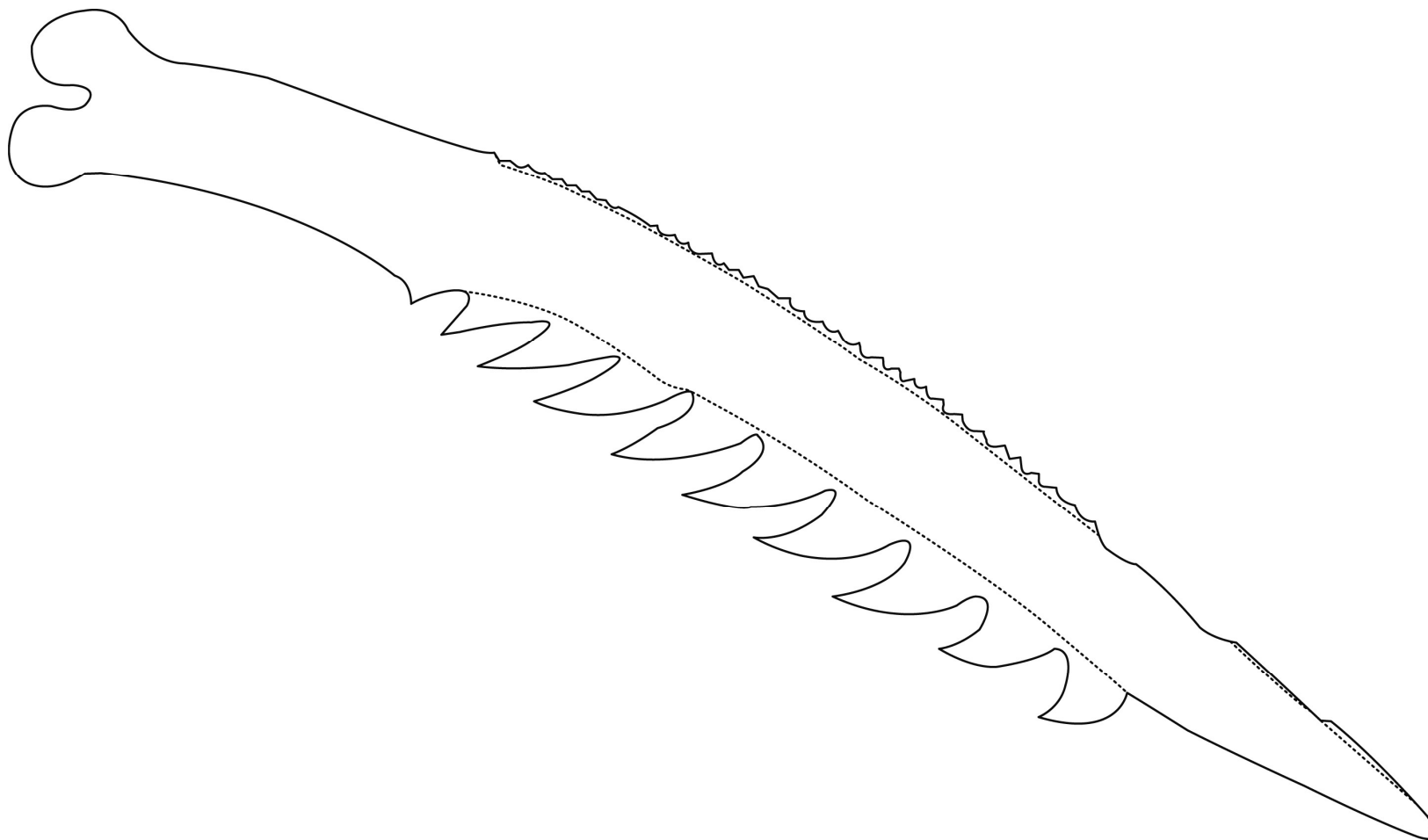


Figure 24. Ventral view of left pectoral-fin spine of *Pimelodella chagresi*, CAS 57903, 83.5 mm SL, total length of spine 15.1 mm.

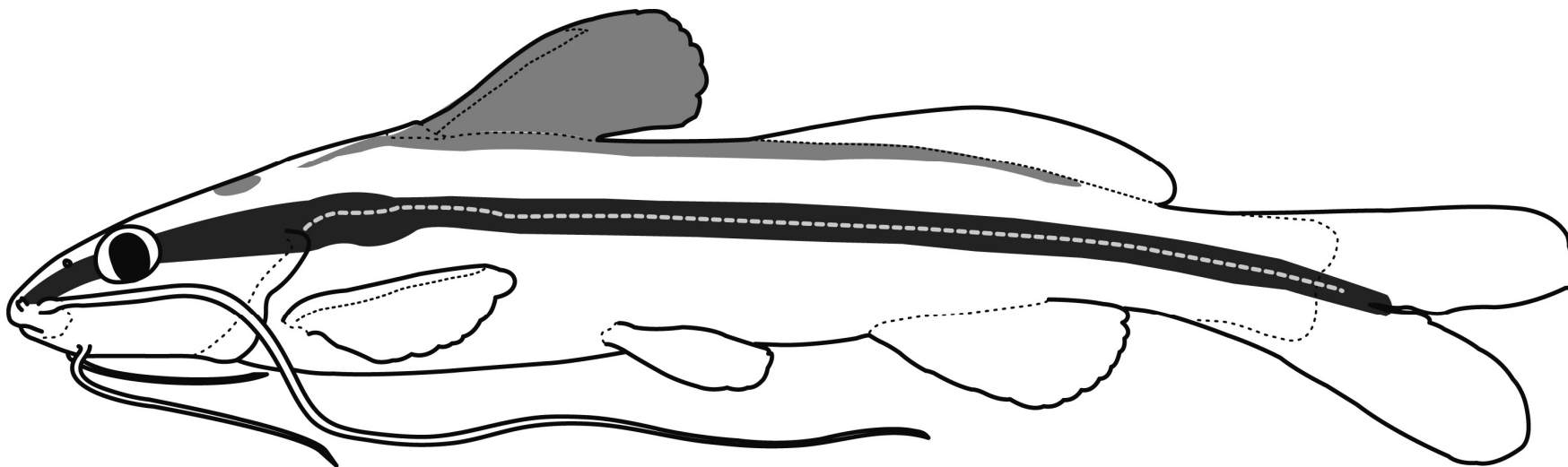


Figure 25. Schematic left lateral view of *Pimelodella chagresi*



Figure 26. *Pimelodella conquetaensis*, holotype, ZMB 32032, 93.2 mm SL. Left lateral (A), and dorsal (B) views. Photo taken by Mark Allen.

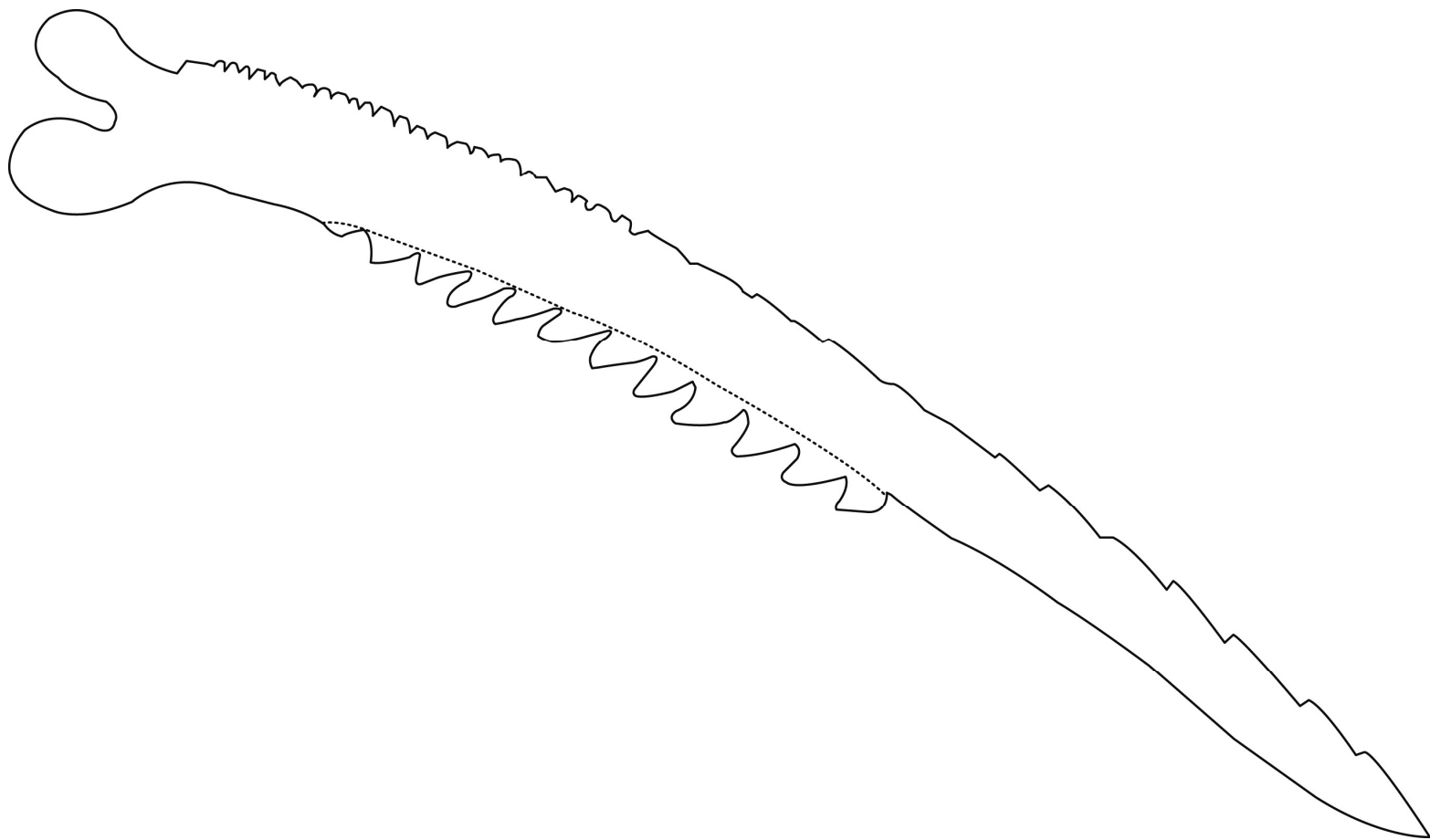


Figure 27. Ventral view of left pectoral-fin spine of *Pimelodella conquetaensis*, ZMB 32032, holotype, 93.2 mm SL, total length of spine 16.5 mm.

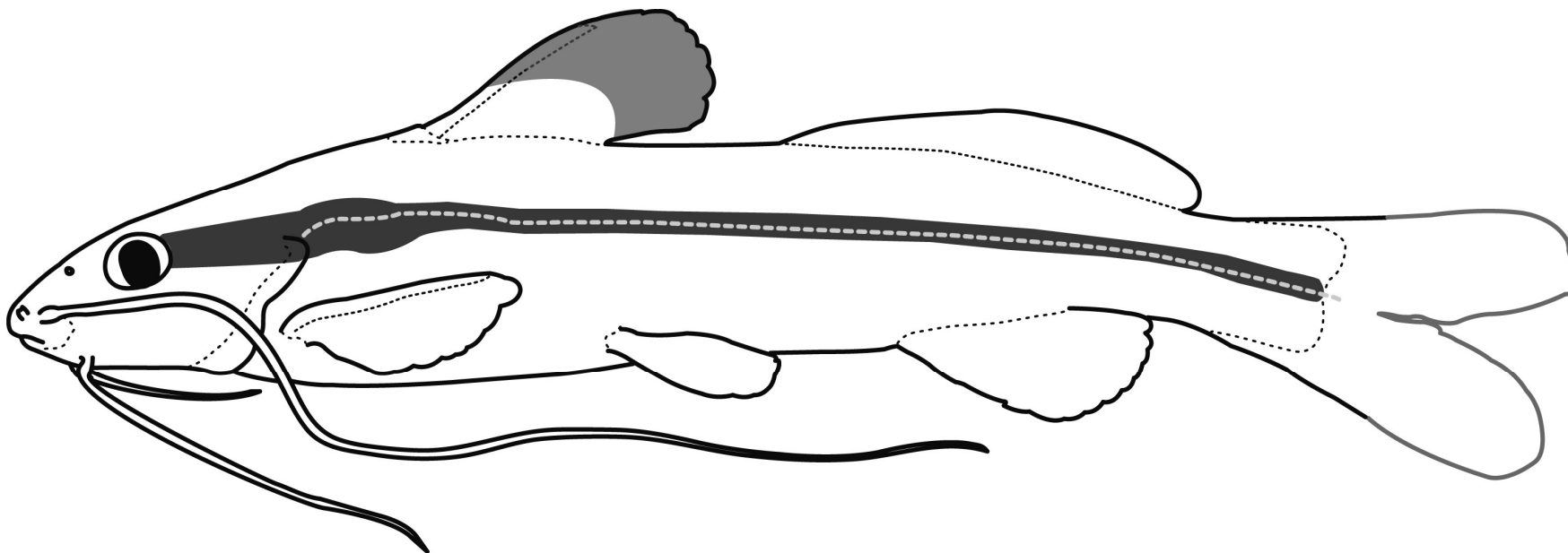


Figure 28. Schematic left lateral view of *Pimelodella conquetaensis*.



Figure 29. *Pimelodella cristata*, lectotype, ZMB 3053, 202.5 mm SL. Left lateral (A), and dorsal (B) views.

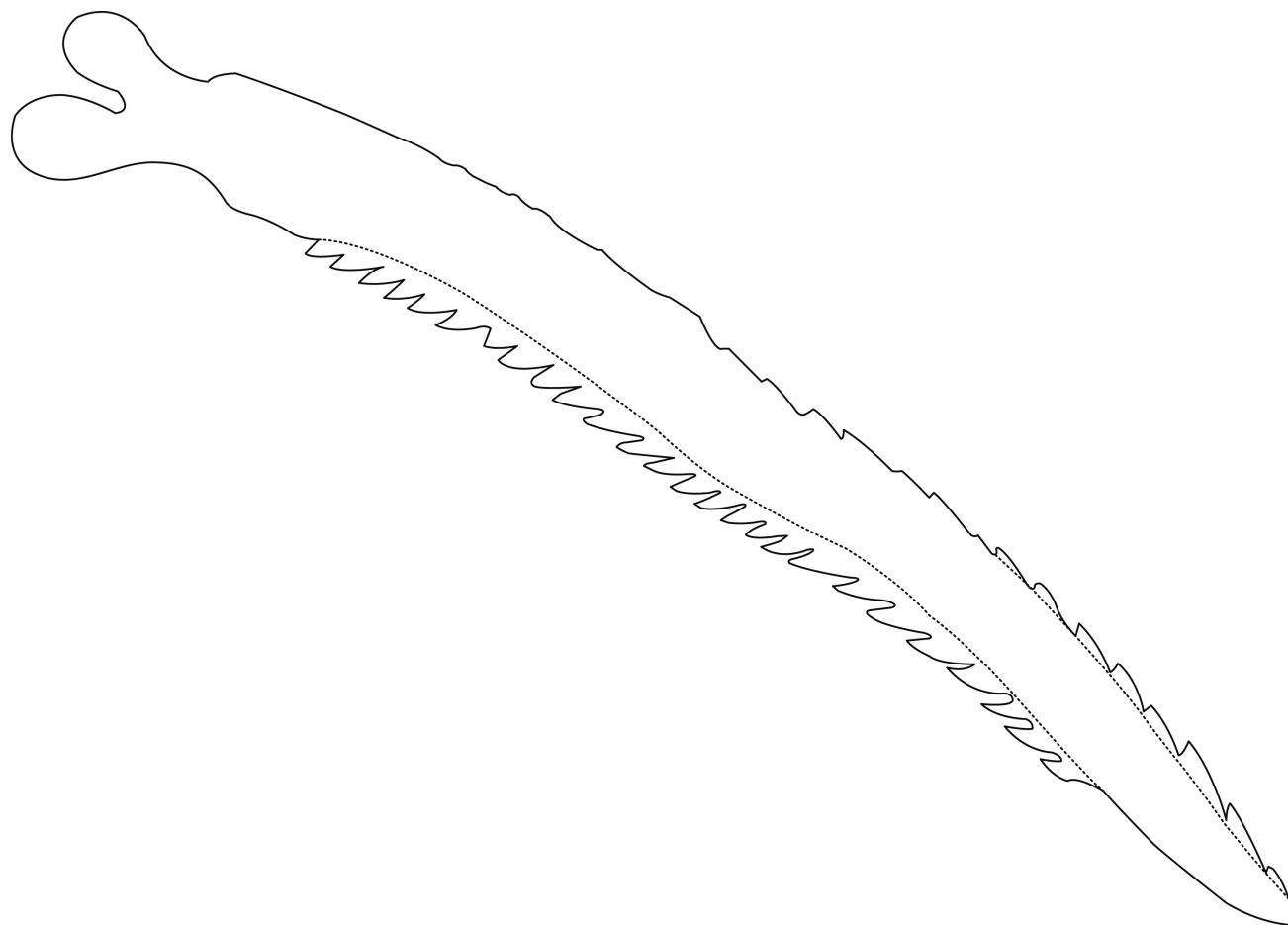


Figure 30. Ventral view of left pectoral-fin spine of *Pimelodella cristata*, ZMB 3052, paralectotype, 177.5 mm SL, total length of spine 27.8 mm.

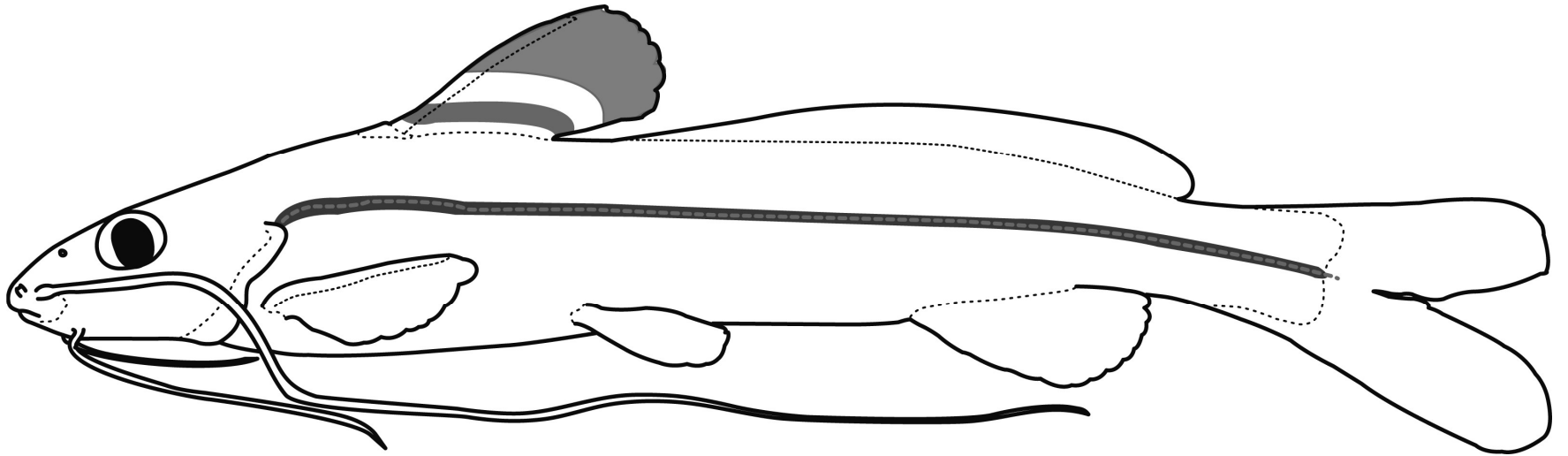


Figure 31. Schematic left lateral view of *Pimelodella cristata*.

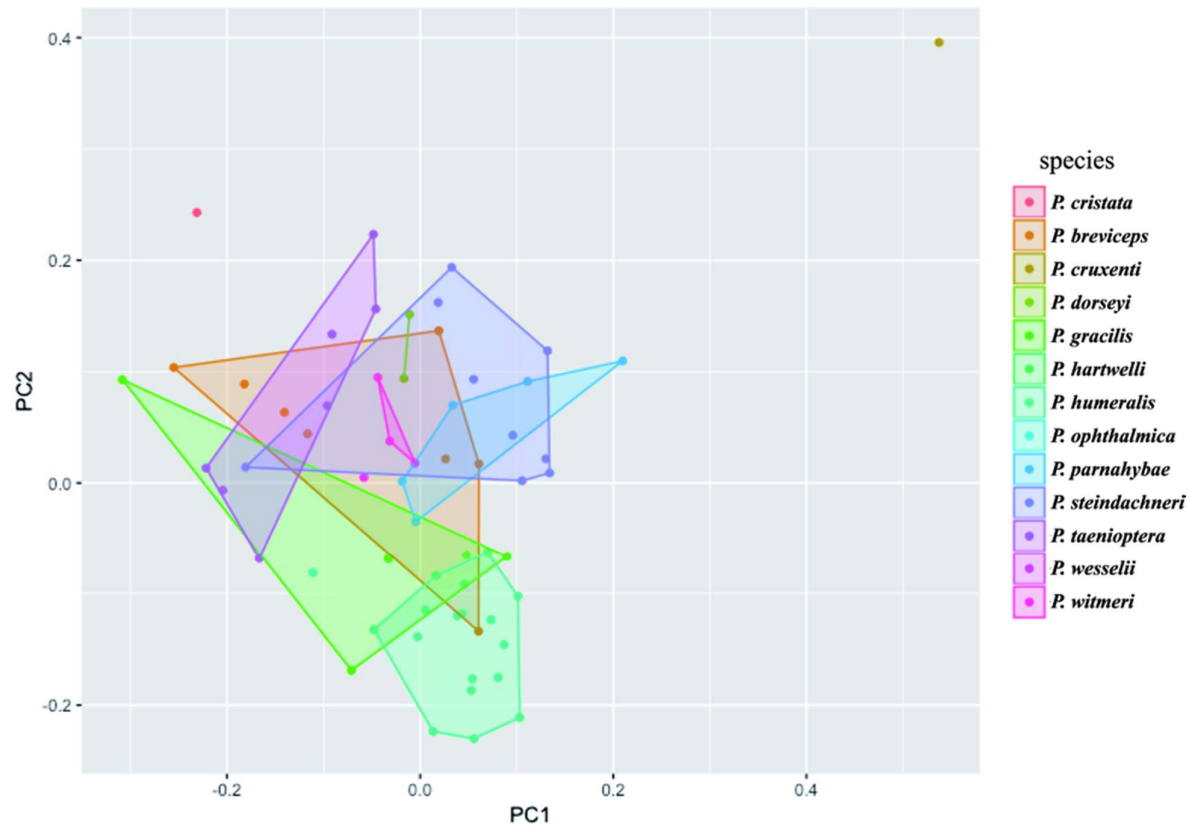


Figure 32. Framed graphic of PC1 against PC2 of a Principal Component Analysis using all morphometric data scaled to SL or HL (except caudal-fin lobes, due to usual incompleteness of those in the material), based on type and comparative materials of *P. cristata*, *P. cruxenti*, *P. breviceps*, *P. dorseyi*, *P. gracilis*, *P. hartwelli*, *P. humeralis*, *P. ophthalmica*, *P. parnahybae*, *P. steindachneri*, *P. taenioptera*, *P. wessellii*, *P. witmeri*. Cumulative proportion of importance of components: 39.4%; proportion of Variance: PC1— 20.3%; PC2— 19.1%; standard deviation: PC1— 2.01; PC2— 2.0.

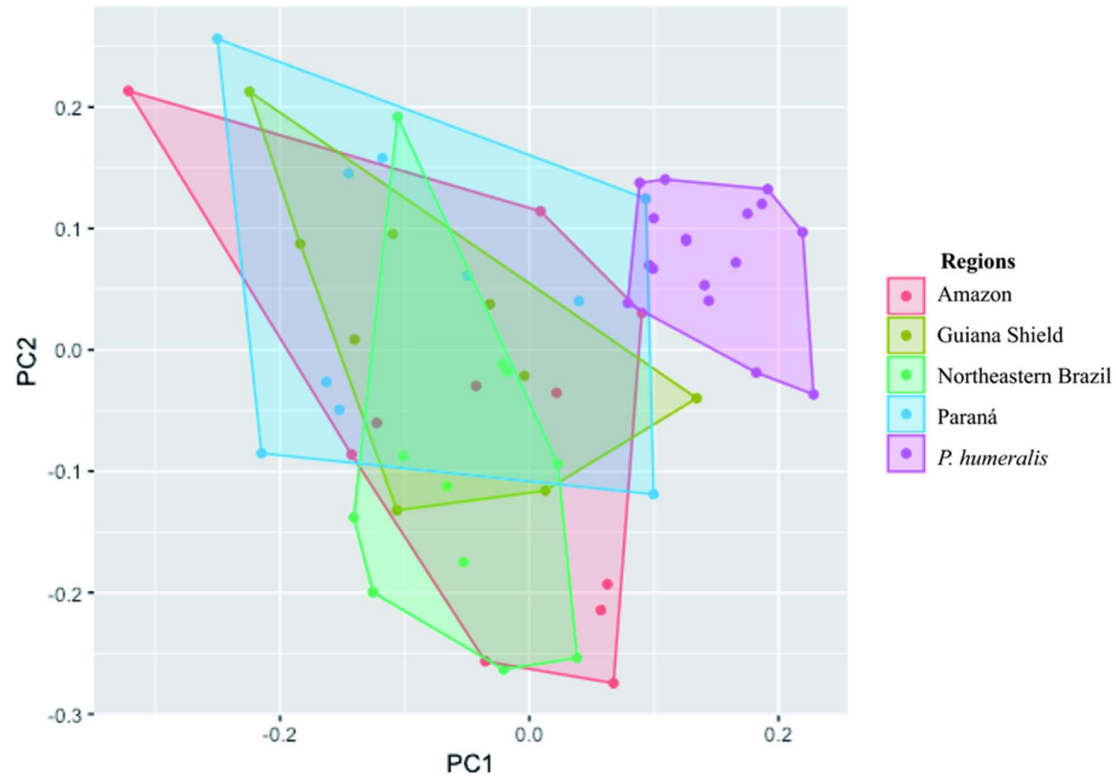


Figure 33. Framed graphic of PC1 against PC2 of a Principal Component Analysis using all morphometric data scaled to SL or HL (except caudal-fin lobes, due to usual incompleteness of those in the material), based on type and comparative materials, separated by drainages as follows: Amazon— Amazon rivers' specimens of *P. cristata*, *P. breviceps*, *P. hartwelli*, *P. ophthalmica* and Amazon rivers' specimens of *P. steindachneri*; Guiana Shield— Guiana Shield rivers' specimens of *P. cristata* and *P. wesseli*; Northeastern Brazil— *P. dorseyi*, *P. parnahybae*, Parnaíba drainage type-specimen of *P. steindachneri* and *P. witmeri*; Paraná— *P. gracilis* and *P. taenioptera*; *P. humeralis*. Cumulative proportion of importance of components: 37.8%; proportion of Variance: PC1— 21.5%; PC2— 16.3%; standard deviation: PC1— 2.07; PC2— 1.8.



Figure 34. *Pimelodella breviceps*, holotype, NMW 45615, 326.2 mm SL. Left lateral (A), and dorsal (B) views.



Figure 35. *Pimelodella cyanostigma*, lectotype, ANSP 8382, 59.8 mm SL. Left lateral (A), and dorsal (B) views. Photo taken by Mark Sabaj.



Figure 36. *Pimelodella dorseyi*, holotype, ANSP 69375, 95.8 mm SL. Left lateral (A), and dorsal (B) views. Photo taken by Murilo Pastana.



Figure 37. *Pimelodella hartwelli*, holotype, ANSP 68644, 103.2 mm SL. Left lateral (A), and dorsal (B) views.

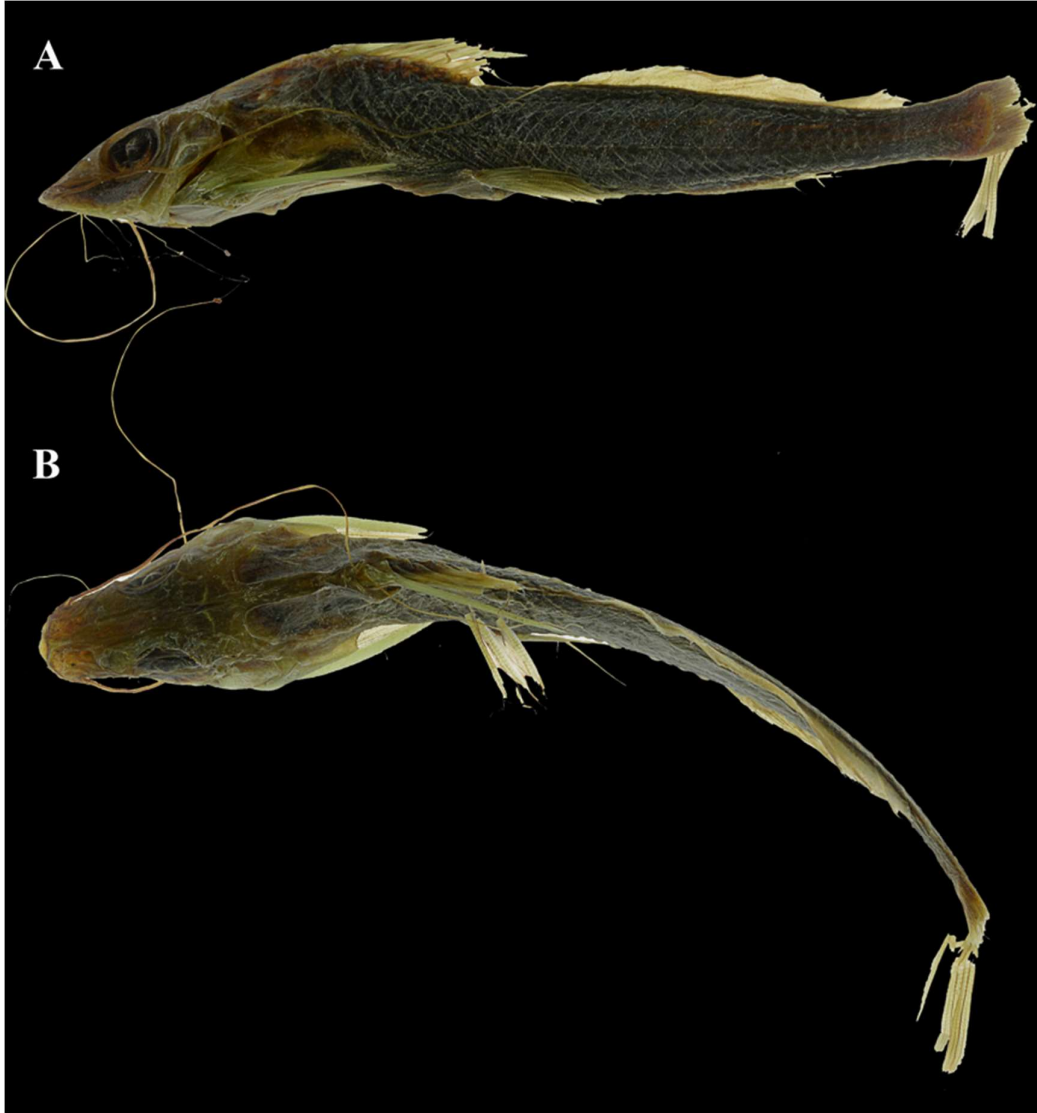


Figure 38. *Pimelodella ophthalmica*, holotype, ANSP 21102, 109.9 mm SL. Left lateral (A), and dorsal (B) views.

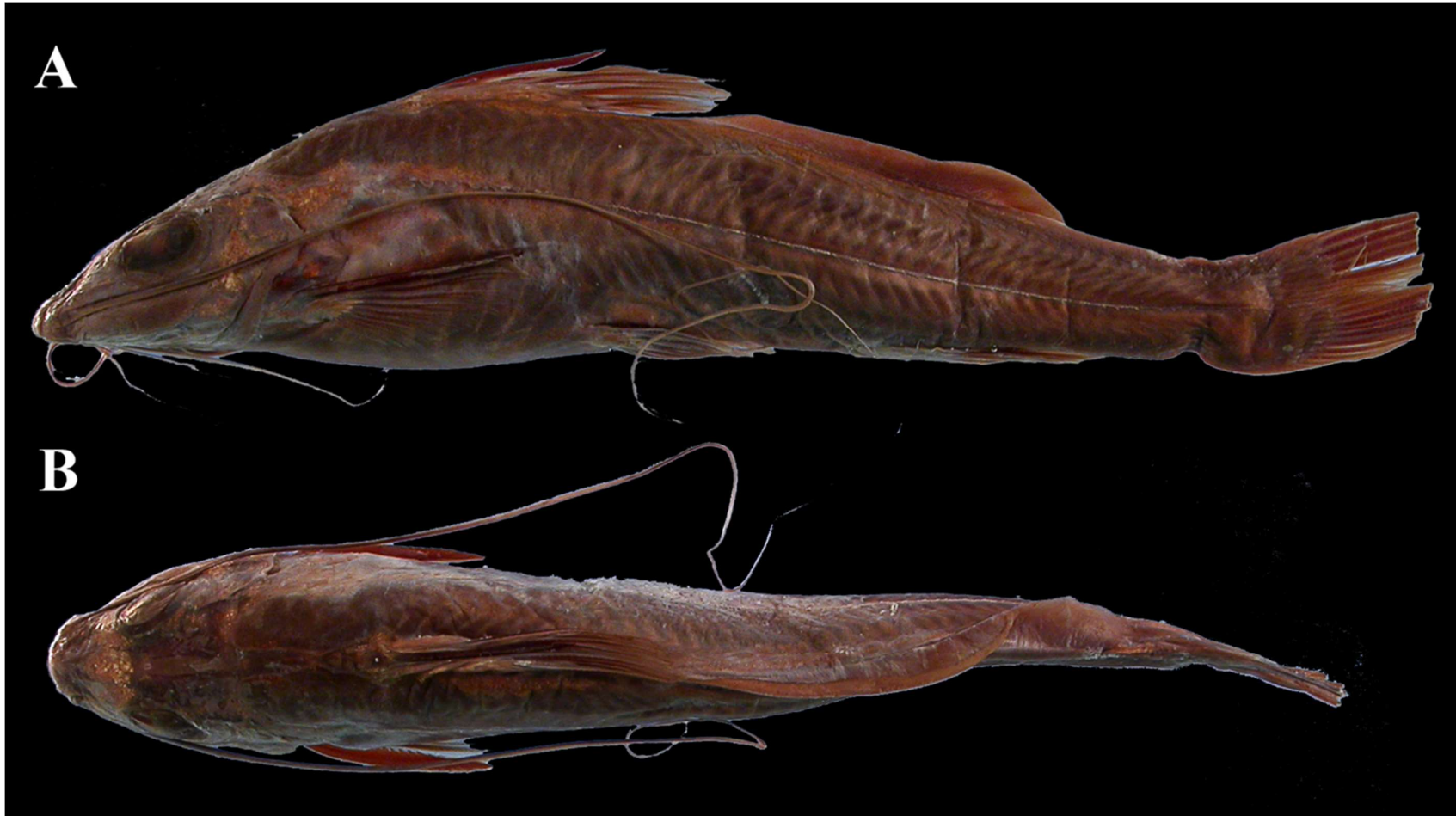


Figure 39. *Pimelodella parnahybae*, holotype, ANSP 69337, 84.0 mm SL. Left lateral (A), and dorsal (B) views. Photo taken by Kyle Luckenbill.



Figure 40. *Pimelodella steindachneri*, lectotype, MCZ 7487, 150.4 mm SL. Left lateral (A), and dorsal (B) views. Photo taken by MCZ staff.



Figure 41. *Pimelodella wesseli*, holotype, NMW 79188, 157.9 mm SL. Left lateral (A), and dorsal (B) views. Photo taken by Mark Sabaj and Kyle Luckenbill.



Figure 42. *Pimelodella witmeri*, holotype, ANSP 69383, 137.5 mm SL. Left lateral (A), and dorsal (B) views. Photo taken by Kyle Luckenbill.



Figure 43. *Pimelodella cruxenti*, lectotype, MHNLS 95.8 mm SL. Left lateral (A), and dorsal (B) views. Photo taken by Oscar Lasso-Alcalá.

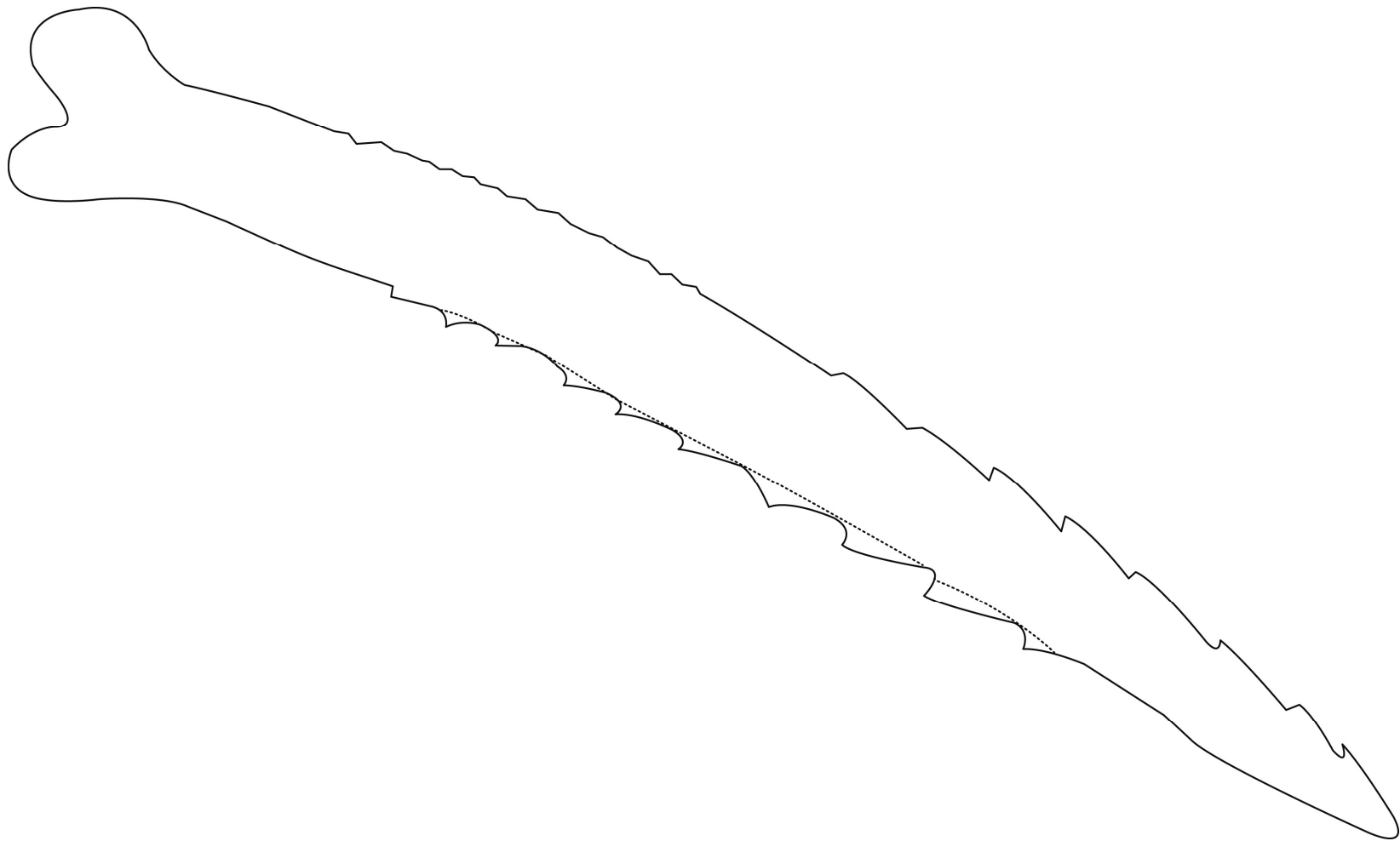


Figure 44. Ventral view of left pectoral-fin spine of *Pimelodella cruxenti*, ANSP 160647, 75.2 mm SL.

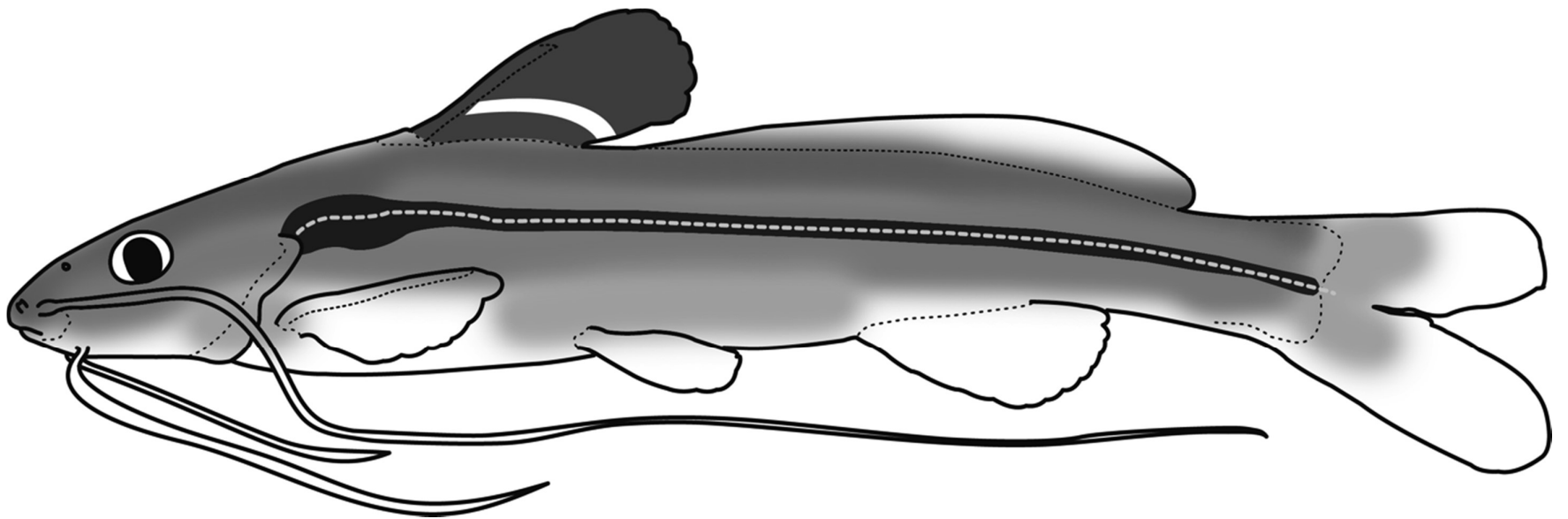


Figure 45. Schematic left lateral view of *Pimelodella cruxenti*.

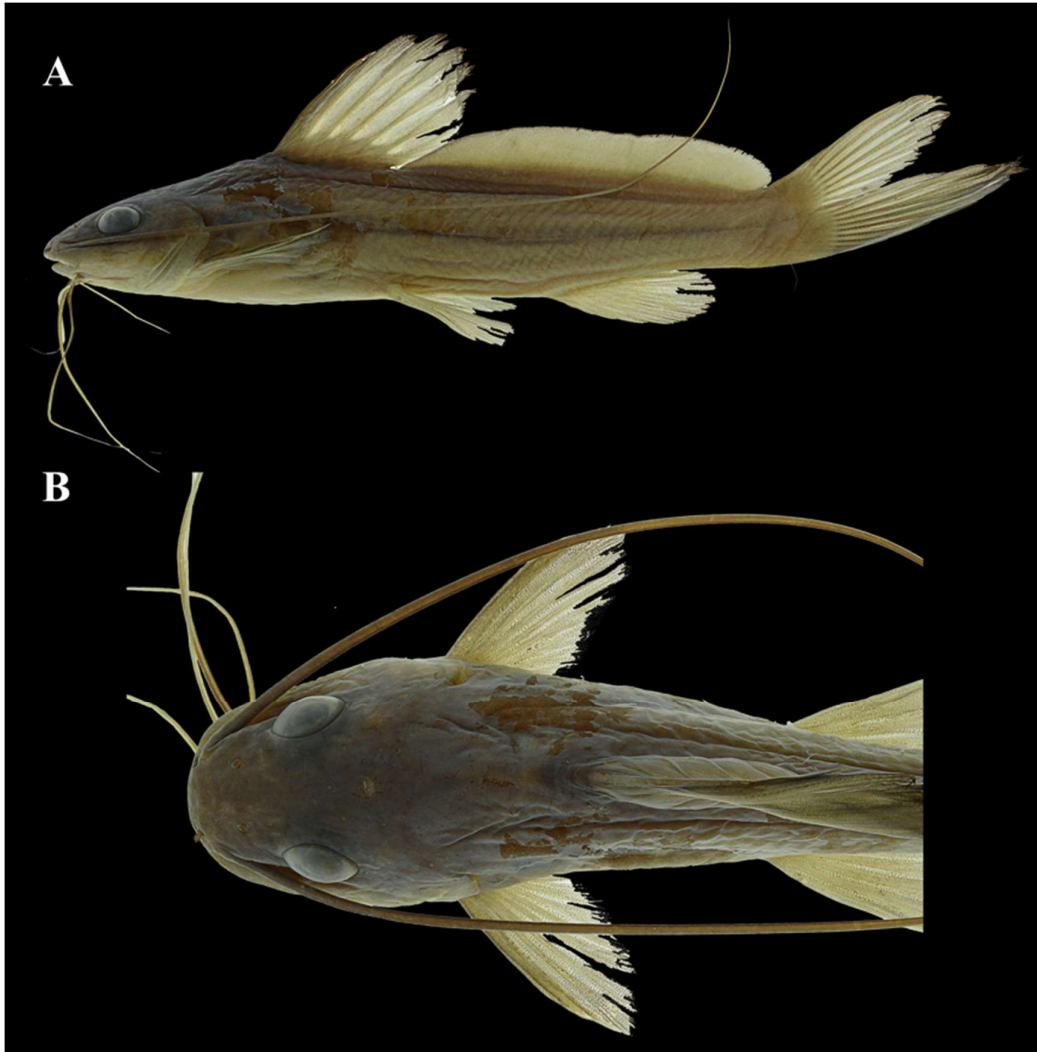


Figure 46. Left lateral view (A) and dorsal view of head (B) of *Pimelodella cruxenti*, ANSP 160673, 127.7 mm SL. Photo taken by Mark Sabaj.



Figure 47. *Pimelodella elongata*, lectotype, BMNH 1860.6.16.182, 136.8 mm SL. Left lateral (A), and dorsal (B) views. Photo taken by Mark Allen.

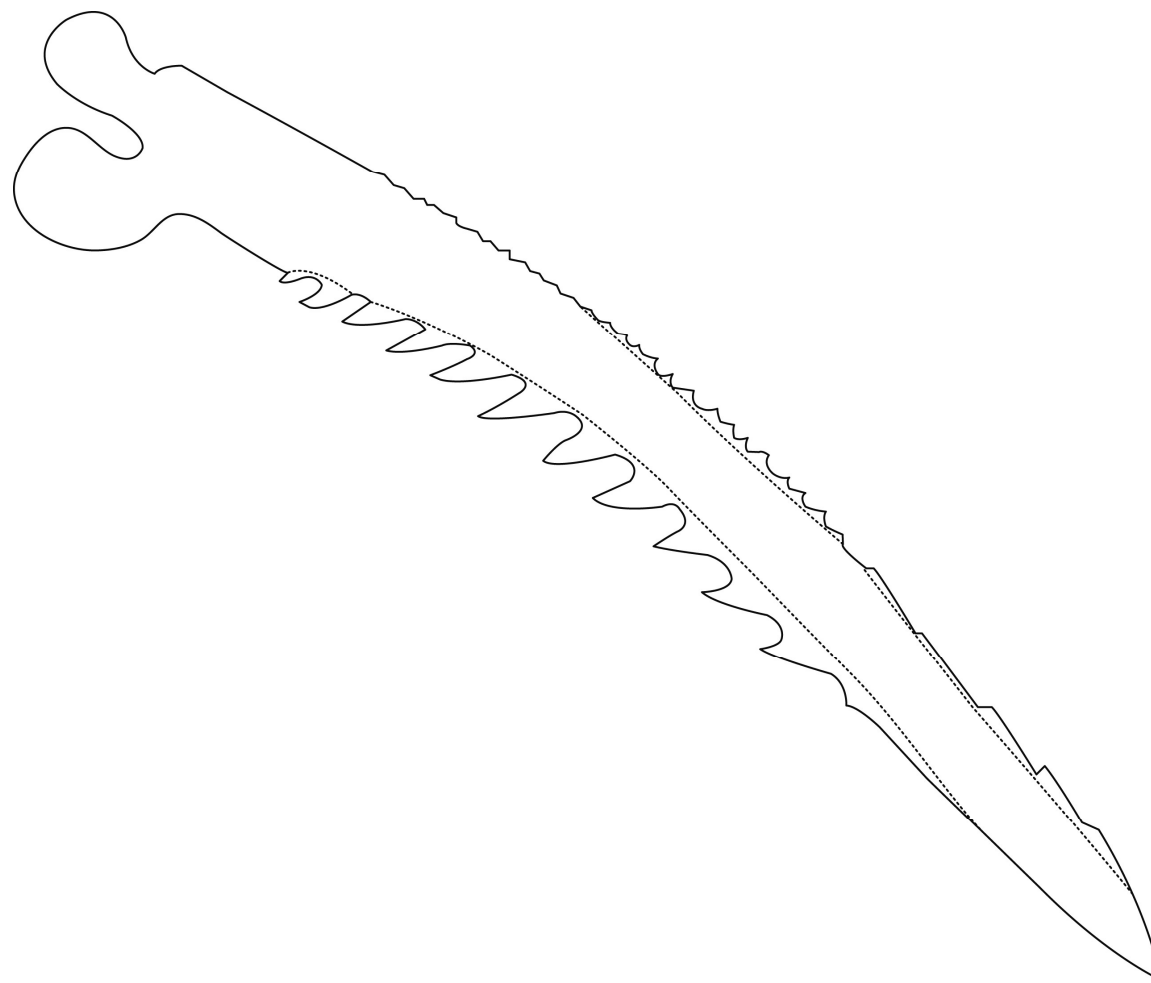


Figure 48. Ventral view of left pectoral-fin spine of *Pimelodella elongata*, BMNH 1860.6.16.186, paralectotype, 96.1 mm SL, total length of spine 12.1 mm.

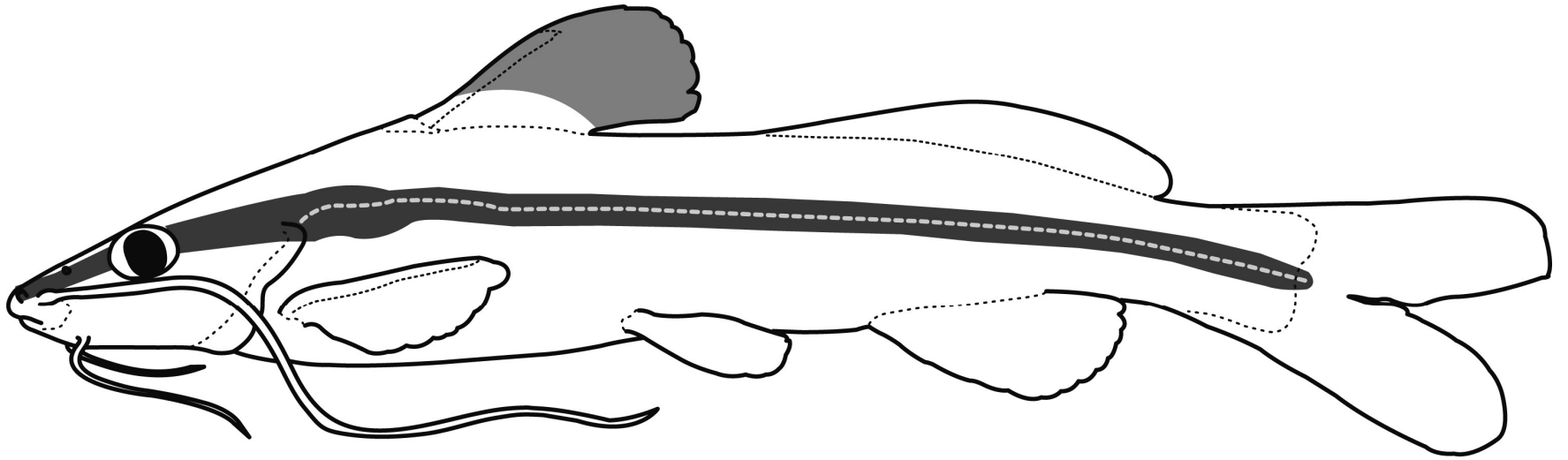


Figure 49. Schematic left lateral view of *Pimelodella elongata*.



Figure 50. *Pimelodella enochi*, holotype, ANSP 69378, 44.9 mm SL. Left lateral (A), and dorsal (B) views. Photo taken by Murilo Pastana.

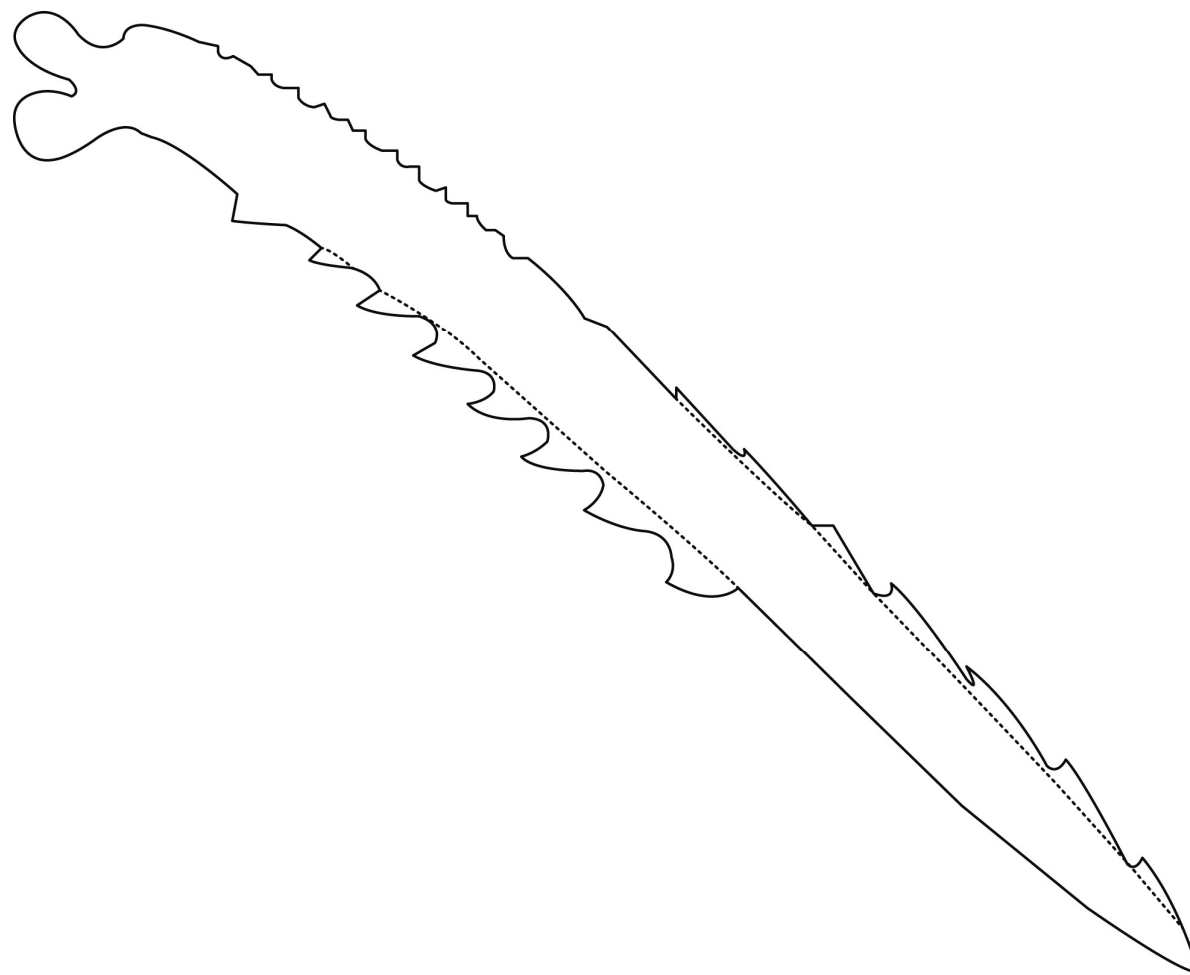


Figure 51. Ventral view of left pectoral-fin spine of *Pimelodella enochi*, ANSP 69378, 44.9 mm SL, total length of spine 6.8 mm.

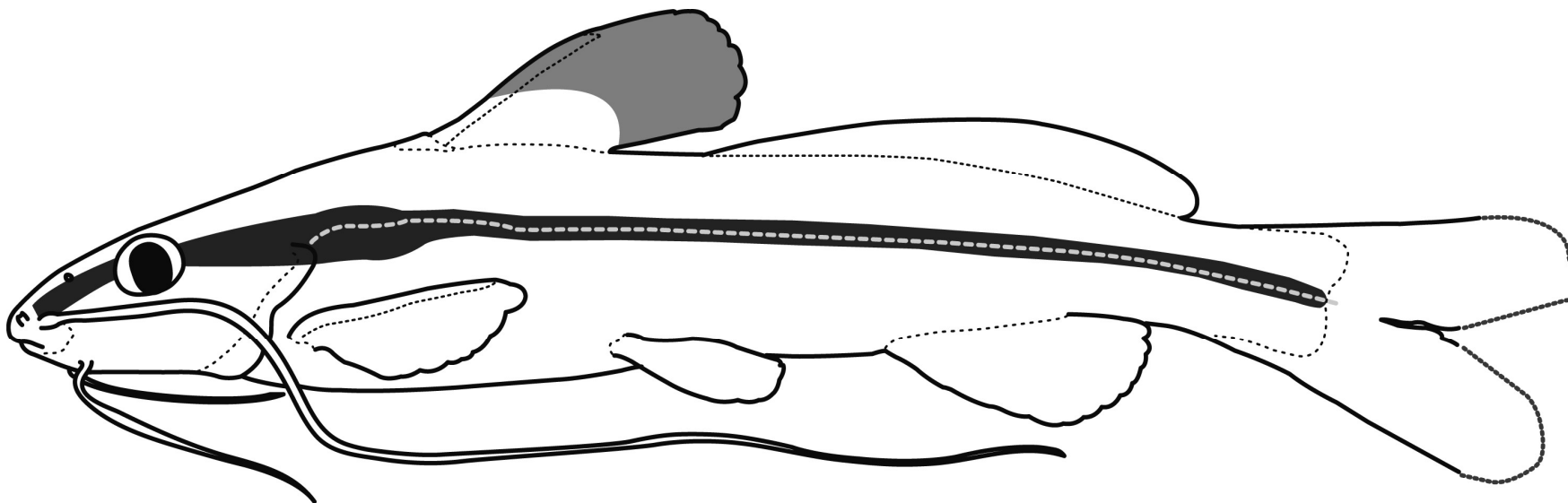


Figure 52. Schematic left lateral view of *Pimelodella enochi*.



Figure 53. *Pimelodella papariae*, junior synonym of *P. enochi*, holotype, ANSP 69387, 109.6 mm SL. Left lateral (A), and dorsal (B) views. Photo taken by Murilo Pastana.

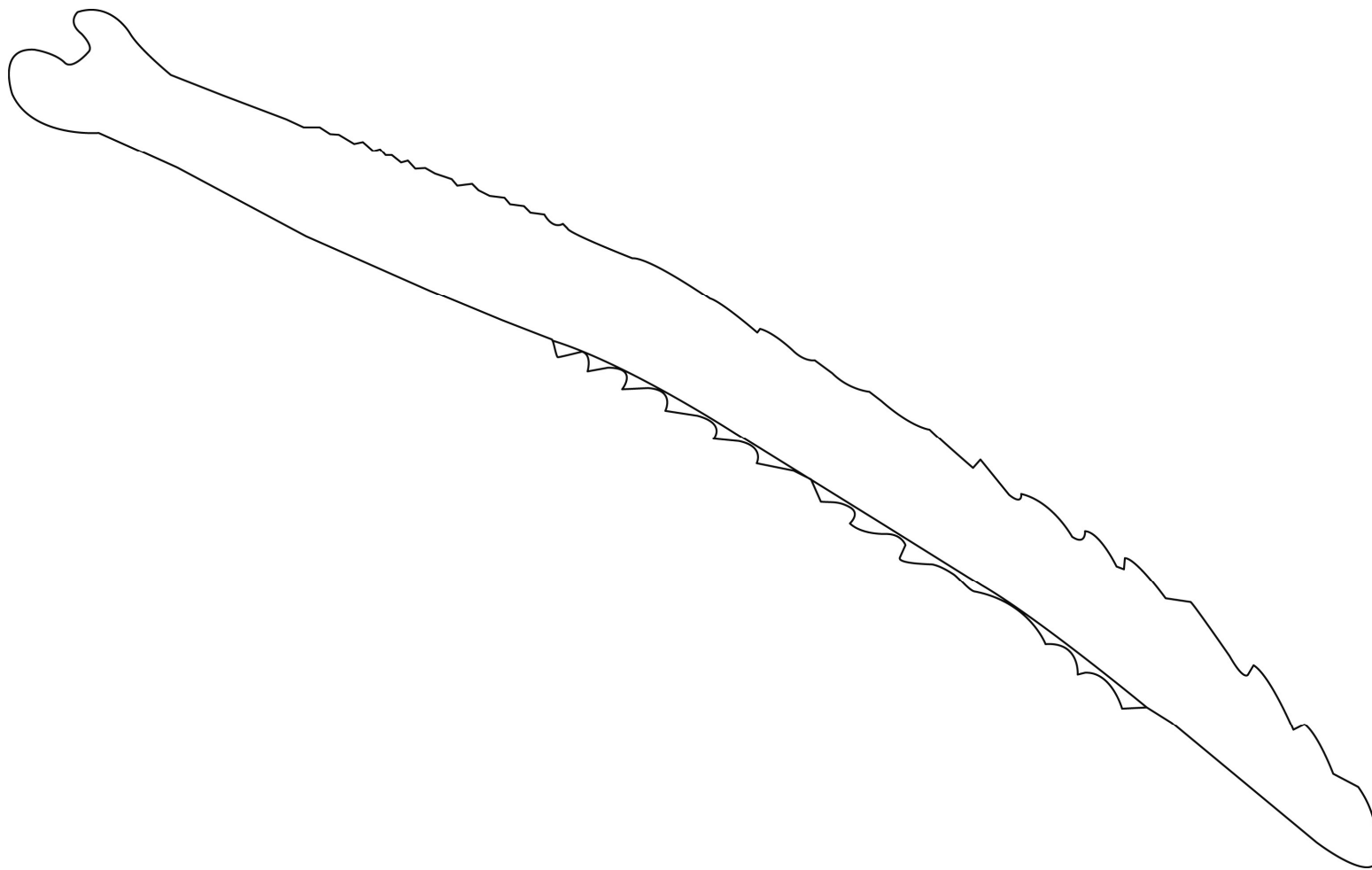
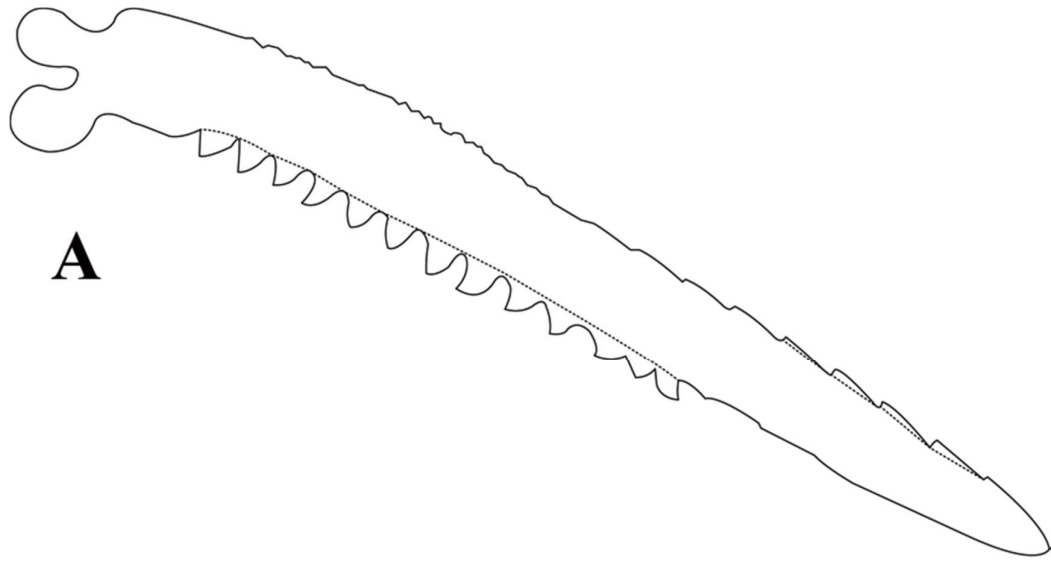


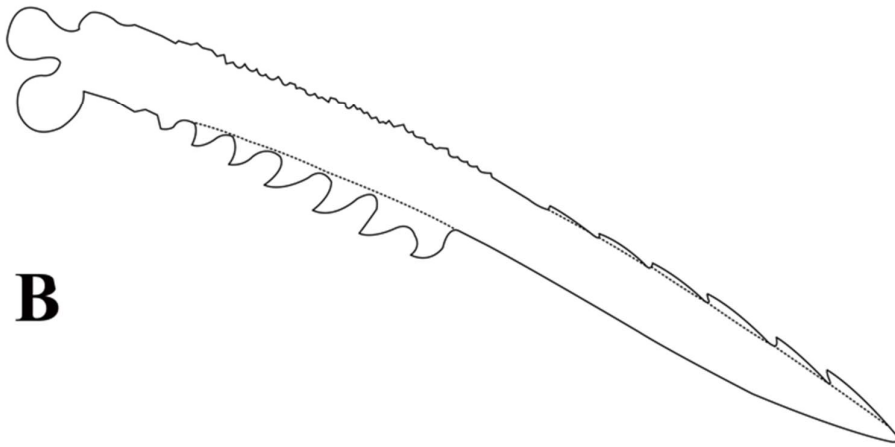
Figure 54. Ventral view of left pectoral-fin spine of *Pimelodella papariae*, ANSP 69387, 109.6 mm SL, total length of spine (approximate) 18.5 mm (tip of spine was broken, and figure correspond to the complete aspect).



Figure 55. *Pimelodella eutaenia*, lectotype, BMNH 1913.10.1.37, 126.3 mm SL. Left lateral (A), and dorsal (B) views. Photo taken by Mark Allen.



A



B

Figure 56. Ventral view of left pectoral-fin spine of *Pimelodella eutaenia*, BMNH 1913.10.1.37, 126.3 mm SL, total length of spine 20.2 mm (A); BMNH 1913.10.1.38, 65.5 mm SL, total length of spine 12 mm (B).

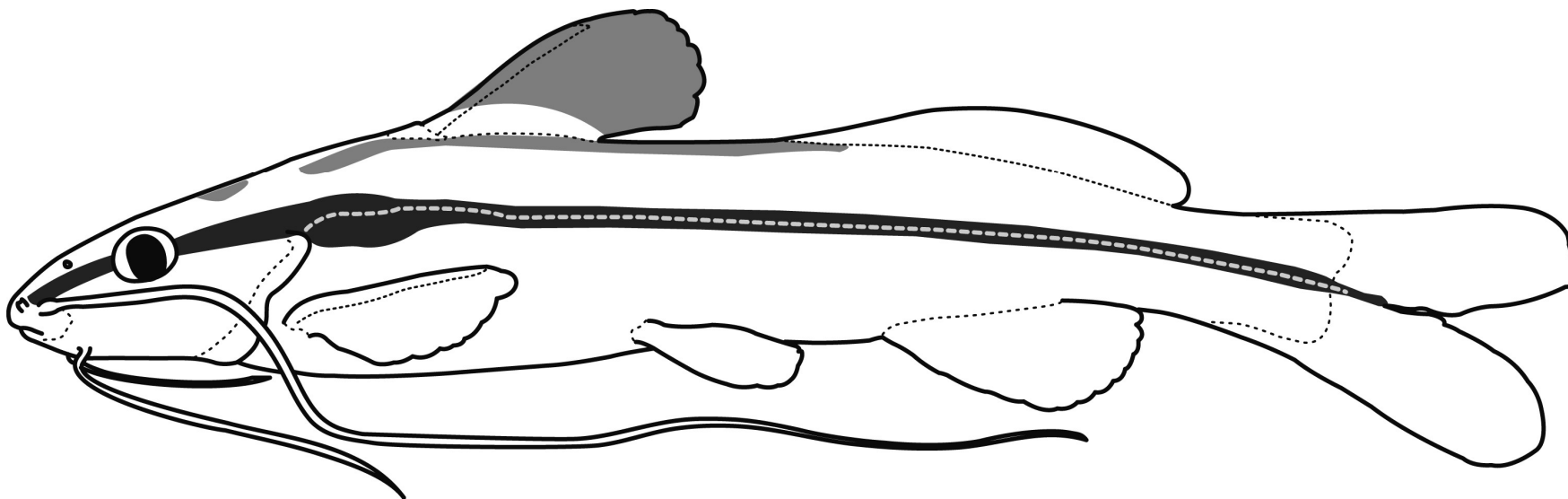


Figure 57. Schematic left lateral view of *Pimelodella eutaenia*.



Figure 58. *Pimelodella flridablancaensis*, junior-synonym of *P. eutaenia*, paratype, CAR 695, 85.8 mm SL. Figure obtained from Ardila Rodriguez (2017).

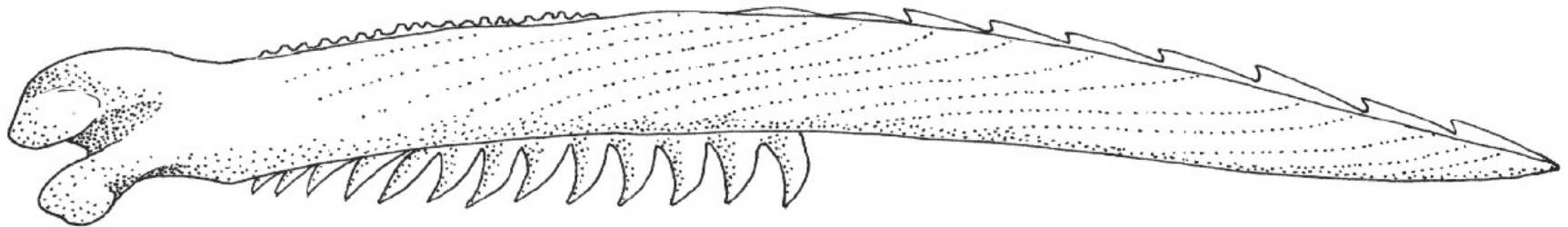


Figure 59. Ventral view of left pectoral-fin spine of *Pimelodella floridablancaensis*, CAR 07, obtained from Ardila Rodriguez (2017). Sizes of specimen or structure were not indicated, but paratype list cited c&s specimens between 74.9–93.2 mm SL.



Figure 60. *Pimelodella figueroai*, ICN-MHN 2900, 71.8 mm SL. Left lateral view. Photo taken by Mauricio Leiva.



Figure 61. *Pimelodella geryi*, holotype, ZMA 102235, 58 mm SL. Left lateral (A), and dorsal (B) views. Photo taken by Ronald De Ruiter.

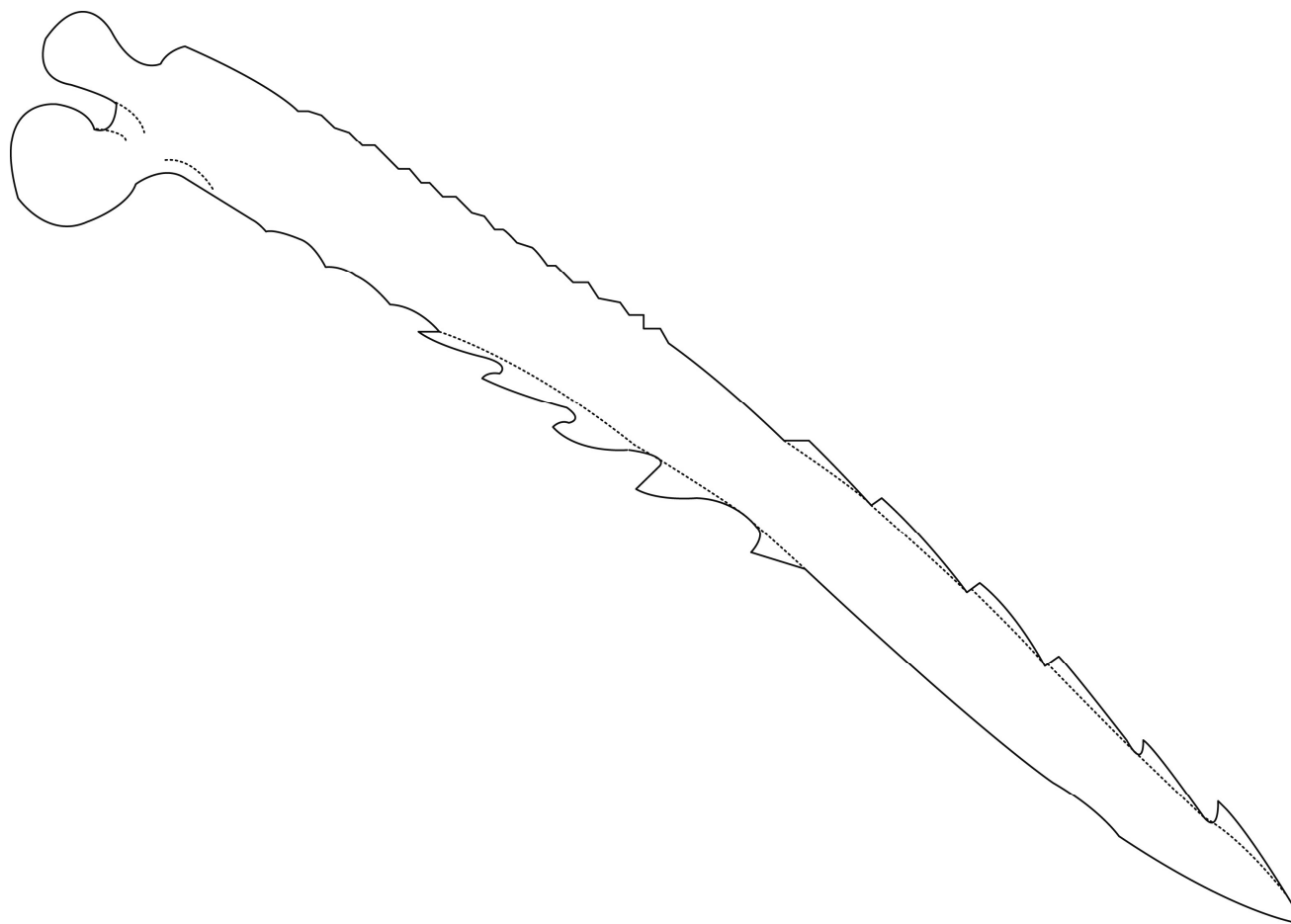


Figure 62. Ventral view of left pectoral-fin spine of *Pimelodella geryi*, holotype, ZMA 102235, 58 mm SL, total length of spine 10.0 mm (approximately).

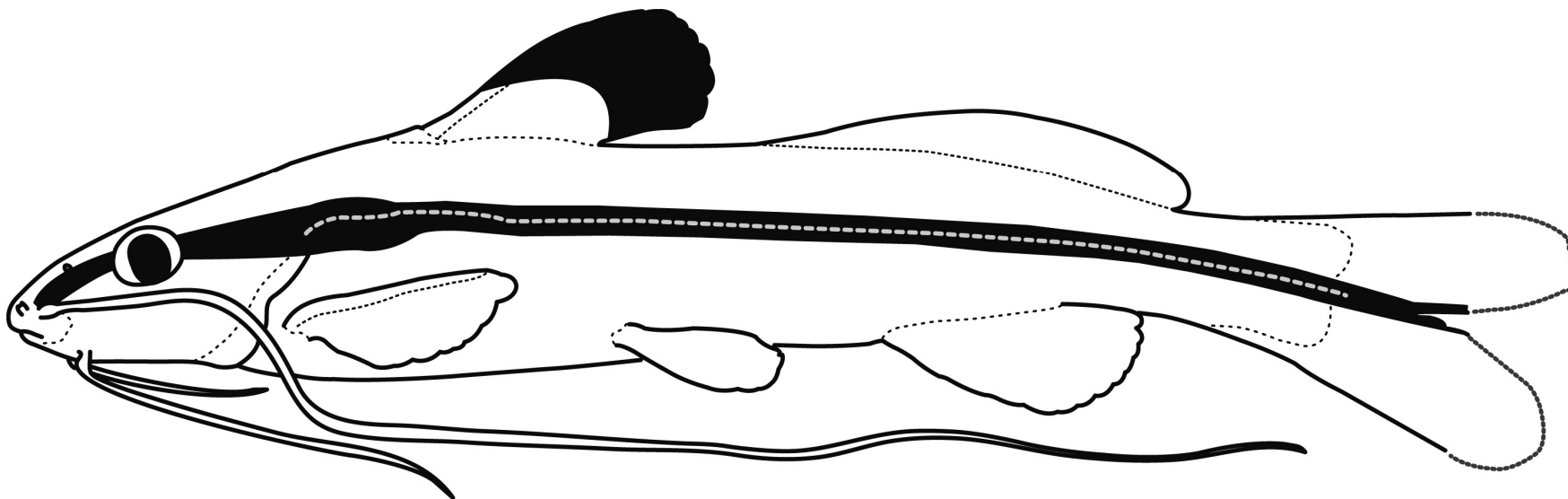


Figure 63. Schematic left lateral view of *Pimelodella geryi*.

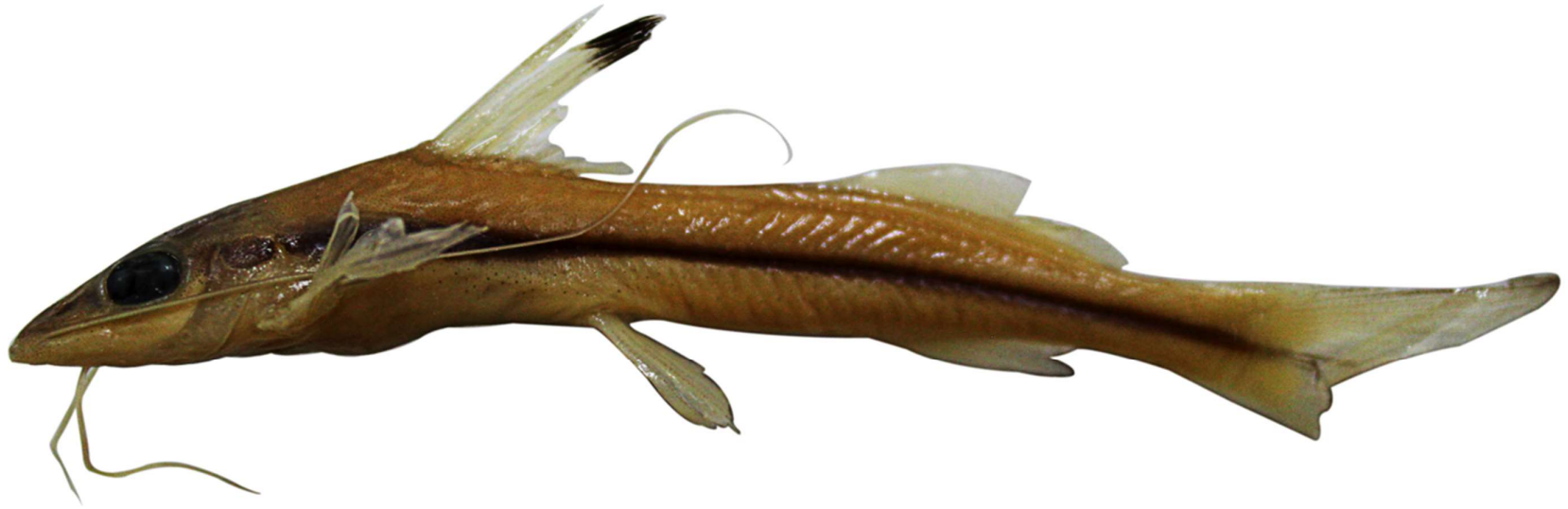


Figure 64. *Pimelodella procera*, junior-synonym of *P. geryi*, paratype, 61.5 mm SL. Left lateral view. Photo taken by Mário de Pinna.



Figure 65. *Pimelodella gracilis*, holotype, MHNH 9284-A, 170.1 mm SL. Left lateral (A), and dorsal (B) views. Photo taken by Mélyne Hautecoeur.

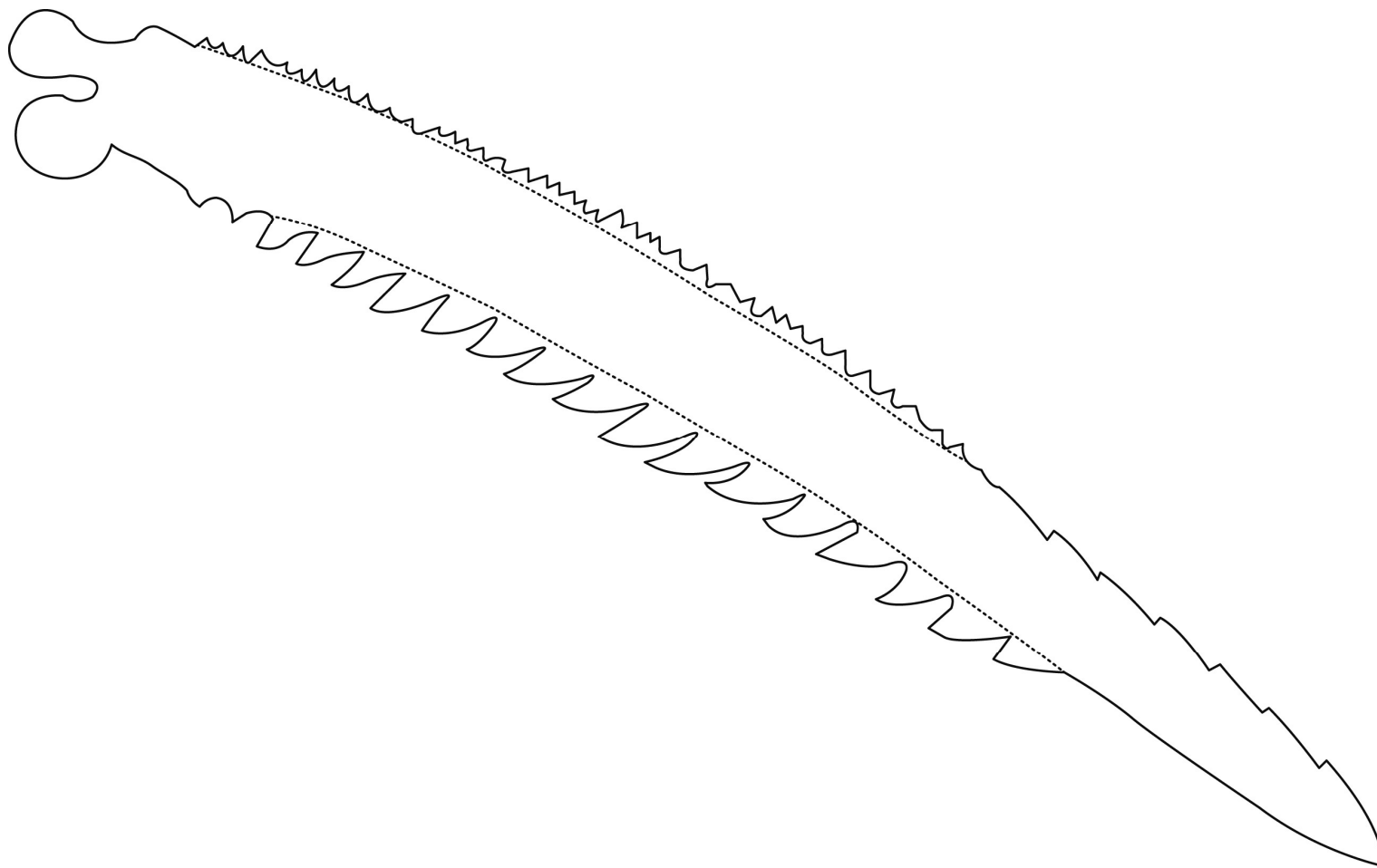


Figure 66. Ventral view of left pectoral-fin spine of *Pimelodella gracilis*, holotype, MHNH 9284-A, 170.1 mm SL, total length of spine 28.5 mm.

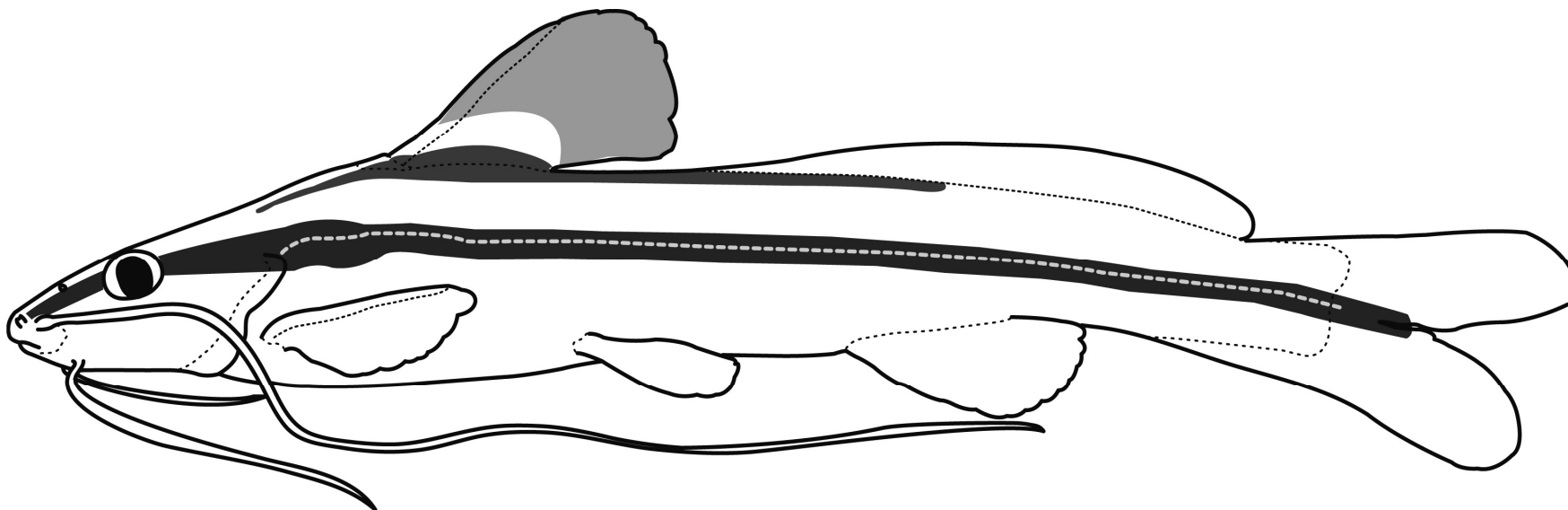


Figure 67. Schematic left lateral view of *Pimelodella gracilis*.

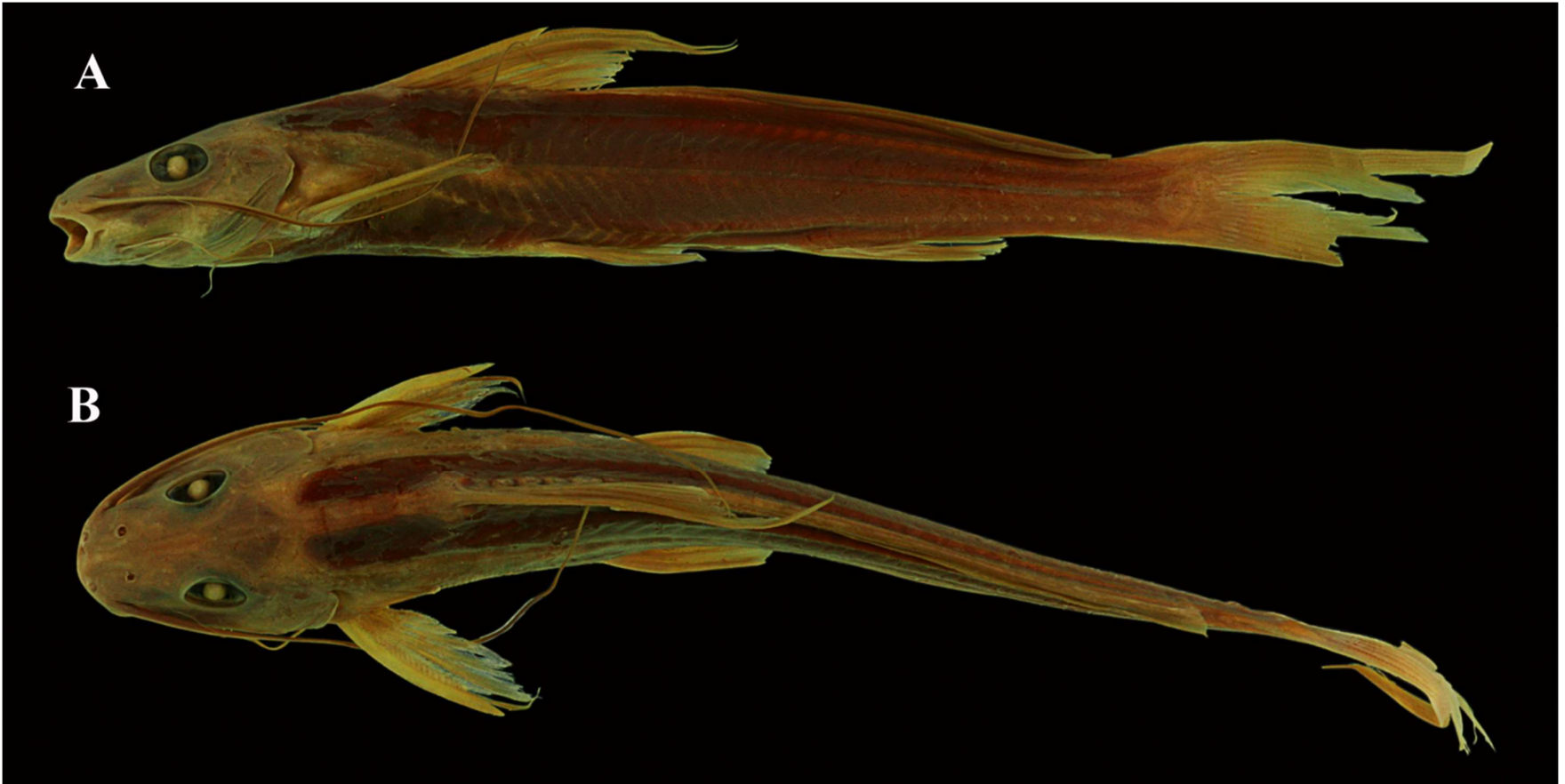


Figure 68. *Pimelodella taenioptera*, junior-synonym of *P. gracilis*, lectotype, MNRJ 691A, 157.8 mm SL. Left lateral (A), and dorsal (B) views.

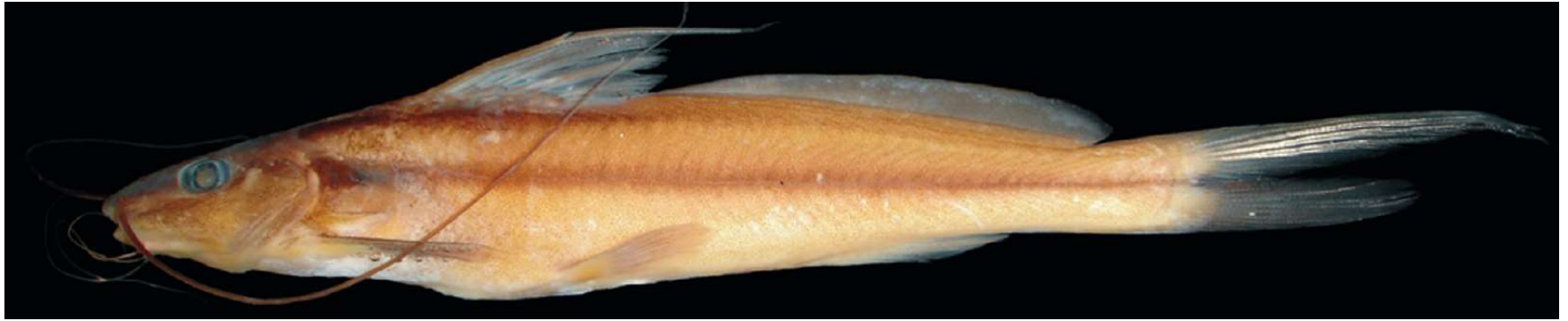


Figure 69. Material identified as *Pimelodella taenioptera* from Souza-Shibatta *et al.* (2013), showing color pattern and dorsal-fin filament. MZUEL 6456, 124.6 mm SL, photo extracted from Souza-Shibatta *et al.* (2013).

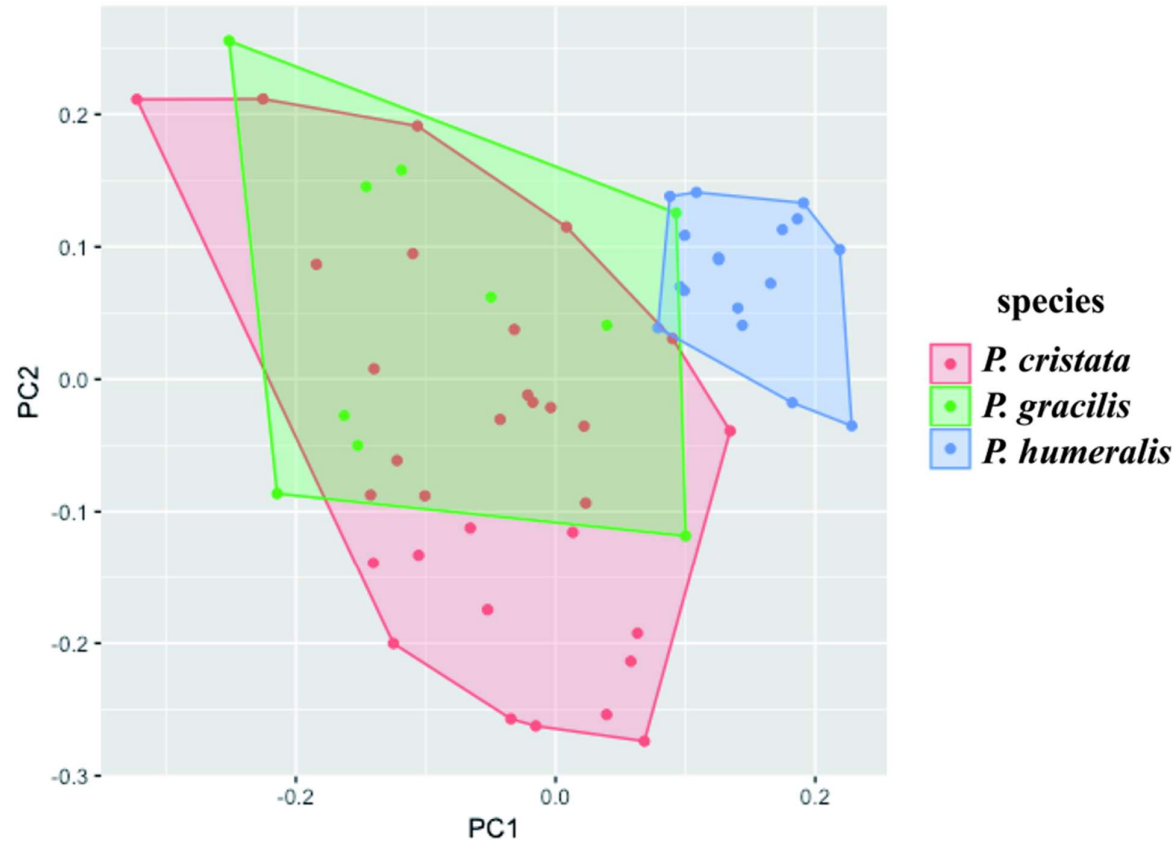


Figure 70. Framed graphic of PC1 against PC2 of a Principal Component Analysis using all morphometric data scaled to SL or HL (except caudal-fin lobes, due to usual incompleteness of those in the material), based on type and comparative materials of *Pimelodella* species with 46 or more total vertebrae (except *P. cruxenti*), discriminated by the names considered as valid in this work, being *P. cristata*, *P. gracilis* and *P. humeralis*. Cumulative proportion of importance of components: 37.8%; proportion of Variance: PC1— 21.4%; PC2— 16.5%; standard deviation: PC1— 2.07; PC2— 1.8.



Figure 71. *Pimelodella griffini*, holotype, FMNH 57974, 67.2 mm SL. Left lateral (A), and dorsal (B) views. Photo taken by M. W. Littmann.

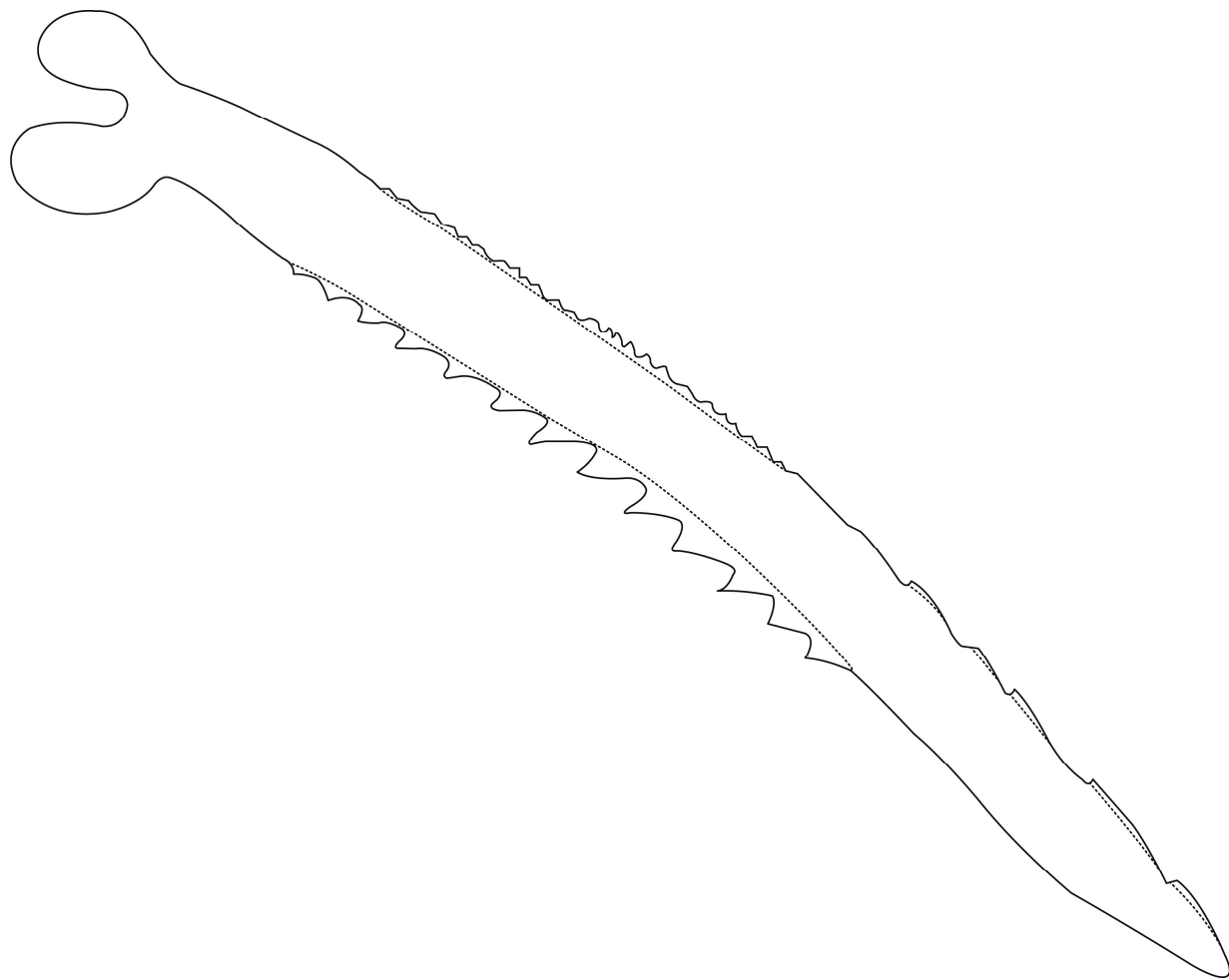


Figure 72. Ventral view of left pectoral-fin spine of *Pimelodella griffini*, holotype, FMNH 57974, 67.2 mm SL, total length of spine 11.3 mm.

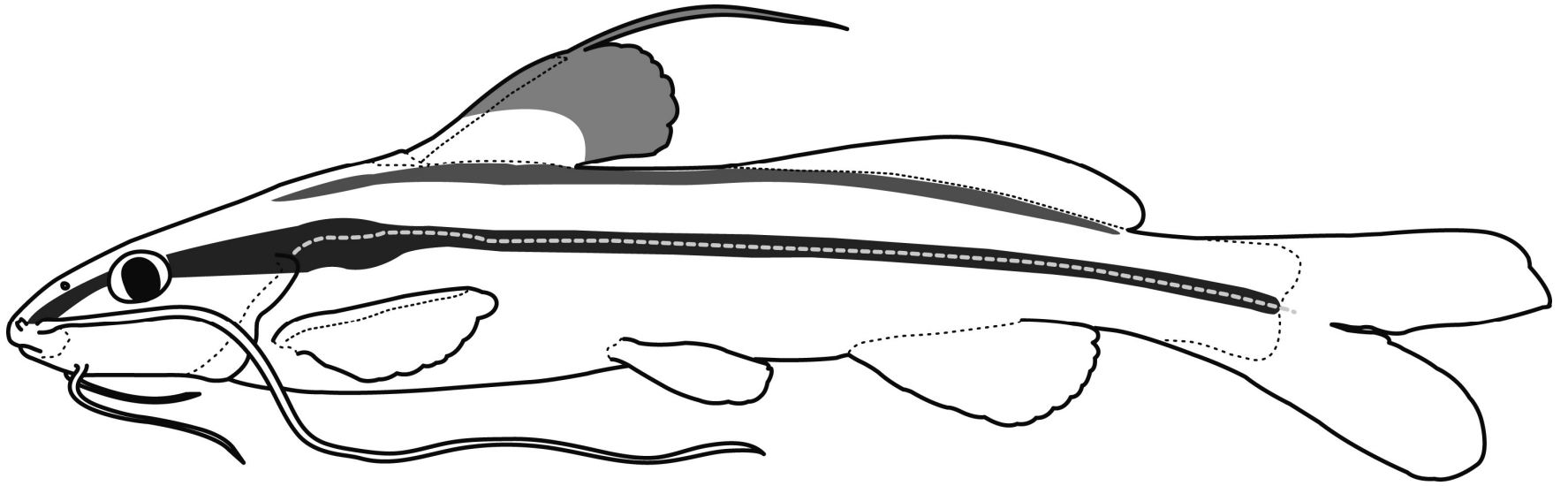


Figure 73. Schematic left lateral view of *Pimelodella griffini*.



Figure 74. *Pimelodella grisea*, lectotype, BMNH 1902.5.27.36, 119.7 mm SL. Left lateral (A), and dorsal (B) views. Photo taken by Mark Allen.

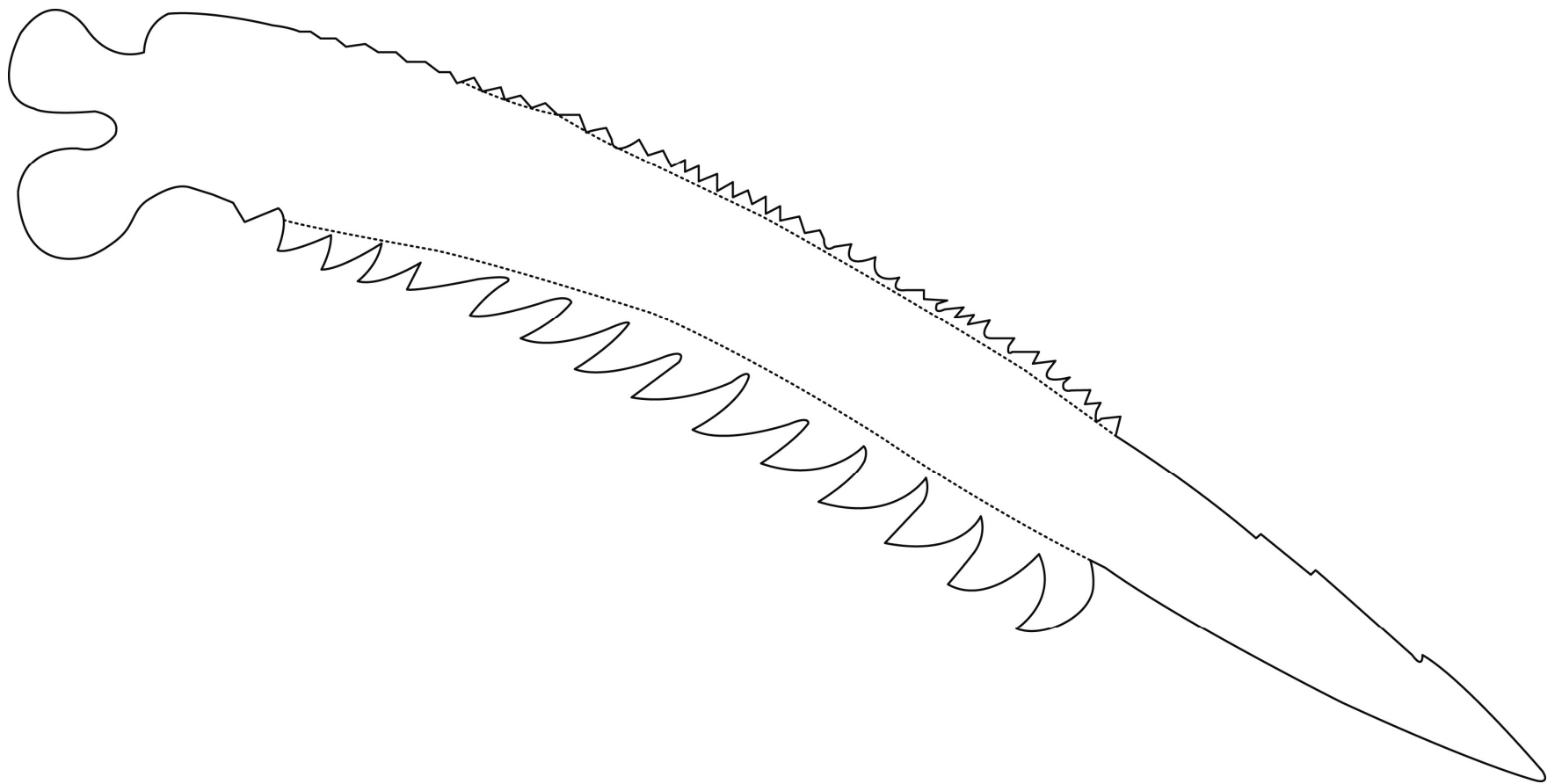


Figure 75. Ventral view of left pectoral-fin spine of *Pimelodella grisea*, lectotype, BMNH 1902.5.27.36, 119.7 mm SL, total length of spine 22.4 mm.

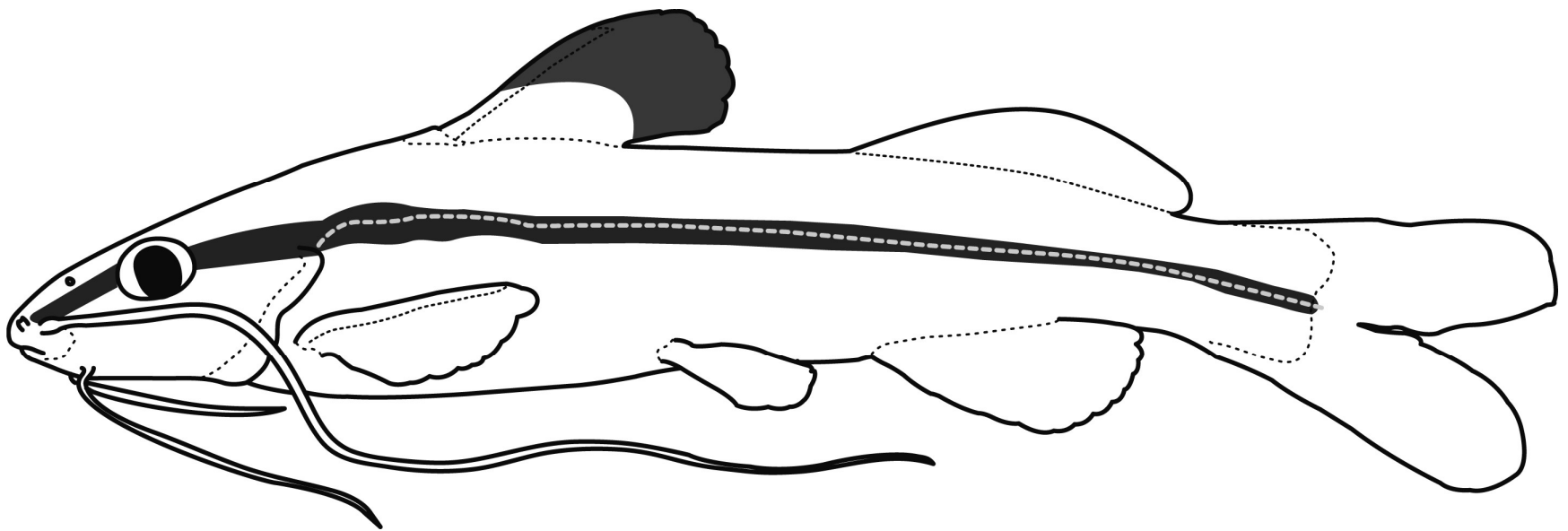


Figure 76. Schematic left lateral view of *Pimelodella grisea*.



Figure 77. *Pimelodella harttii*, holotype, NMW 45784, 150.2 mm SL. Left lateral (A), and dorsal (B) views.

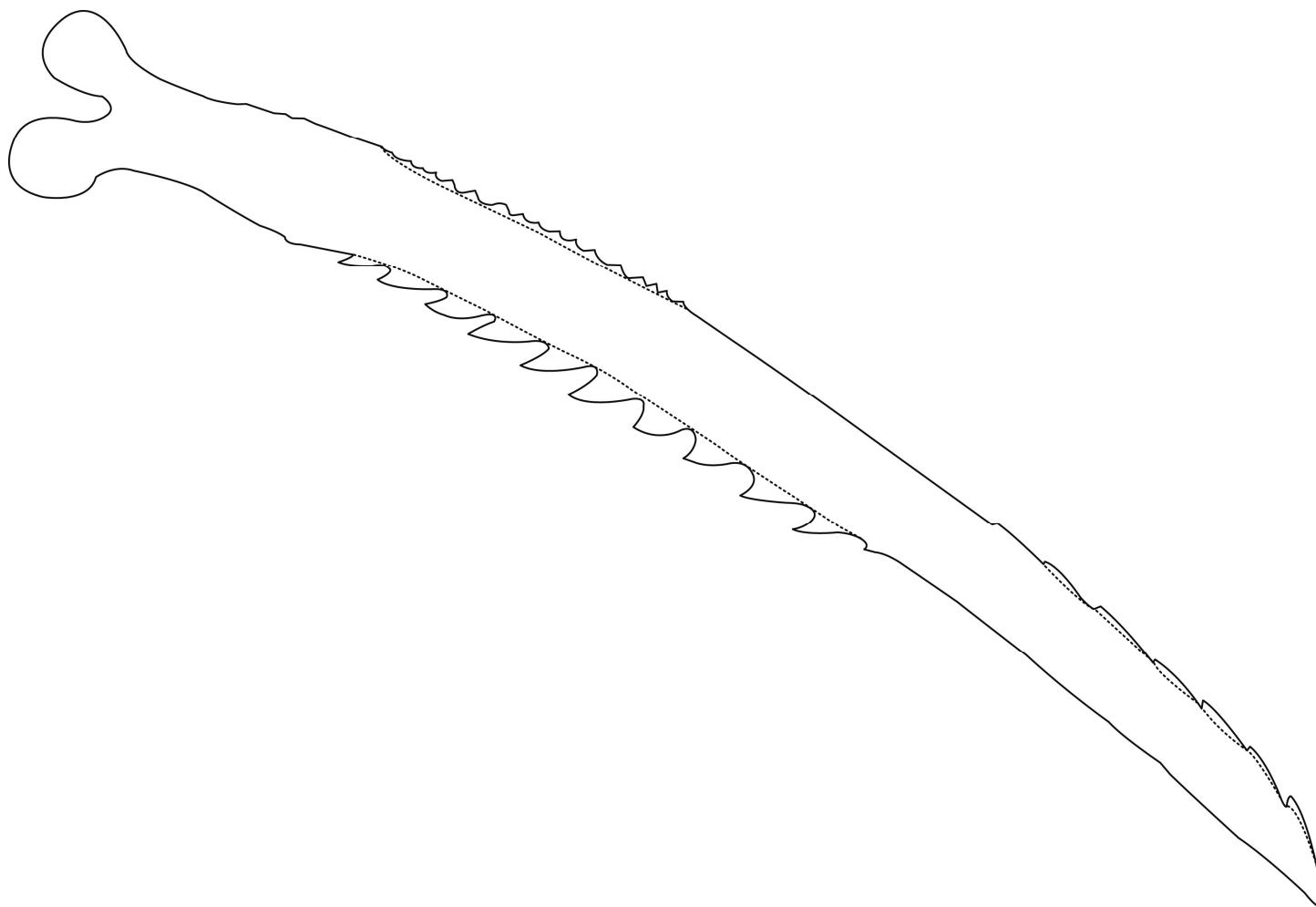


Figure 78. Ventral view of left pectoral-fin spine of *Pimelodella harttii*, holotype, NMW 45784, 150.2 mm SL, total length of spine 25.6 mm.

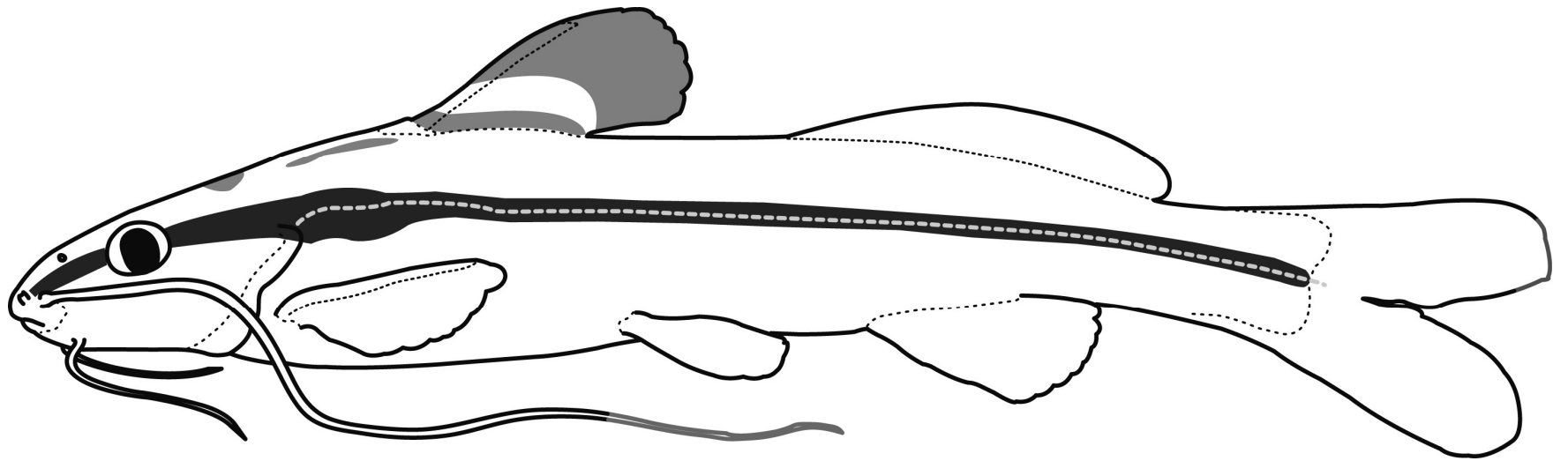


Figure 79. Schematic left lateral view of *Pimelodella harttii*.



Figure 80. *Pimelodella hasemani*, holotype, FMNH 57980, 60.6 mm SL. Left lateral (A), and dorsal (B) views. Photo taken by M. W. Littmann.

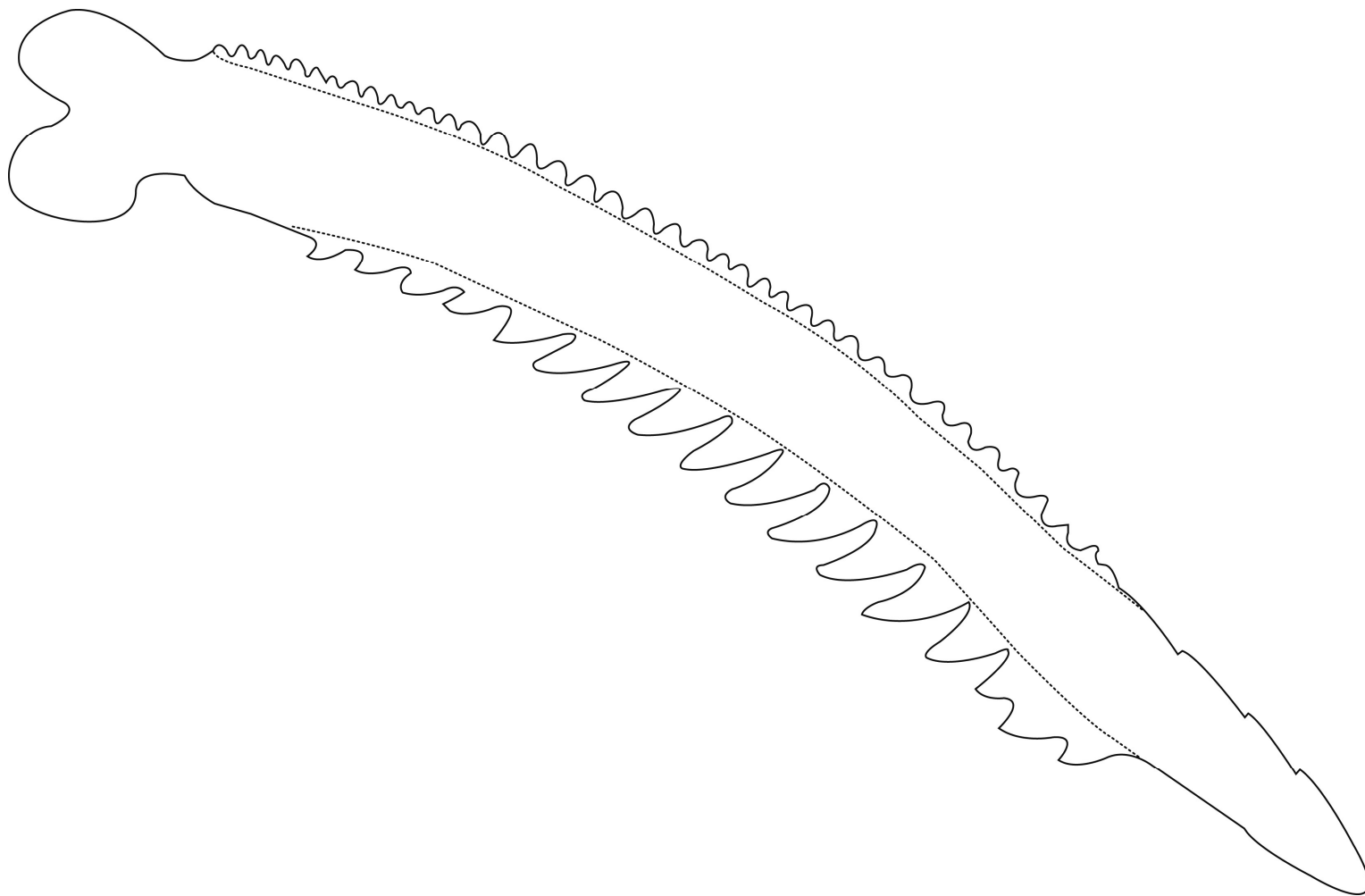


Figure 81. Ventral view of left pectoral-fin spine of *Pimelodella hasemani*, FMNH 57980, 60.6 mm SL, total length of spine 10.6 mm.

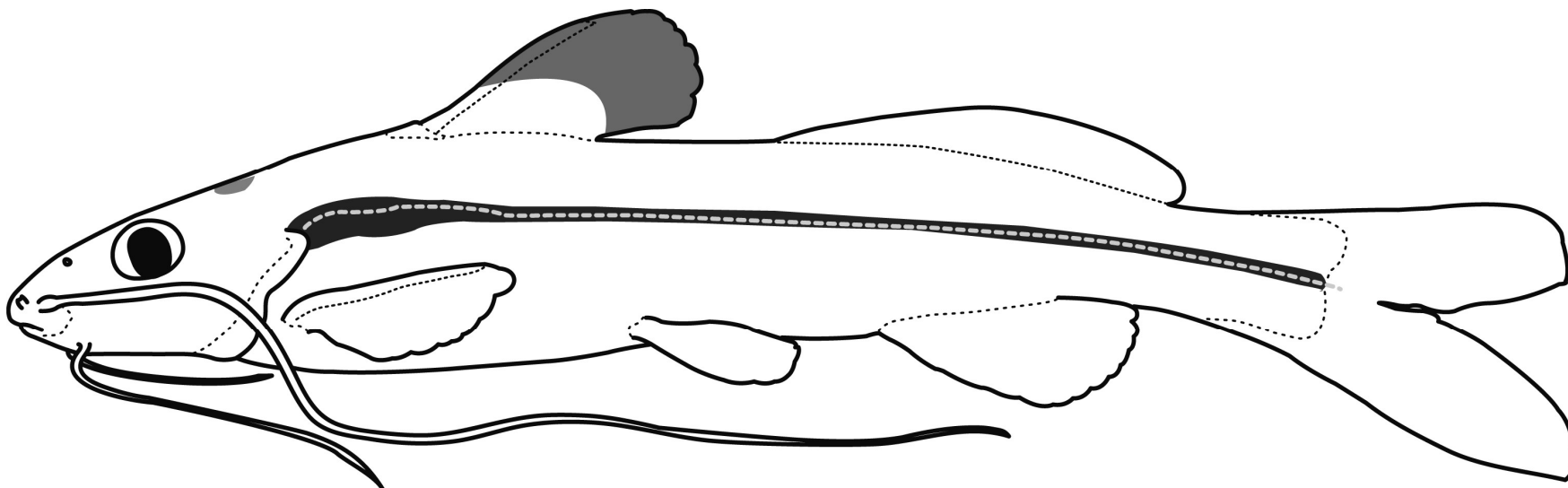


Figure 82. Schematic left lateral view of *Pimelodella hasemani*.

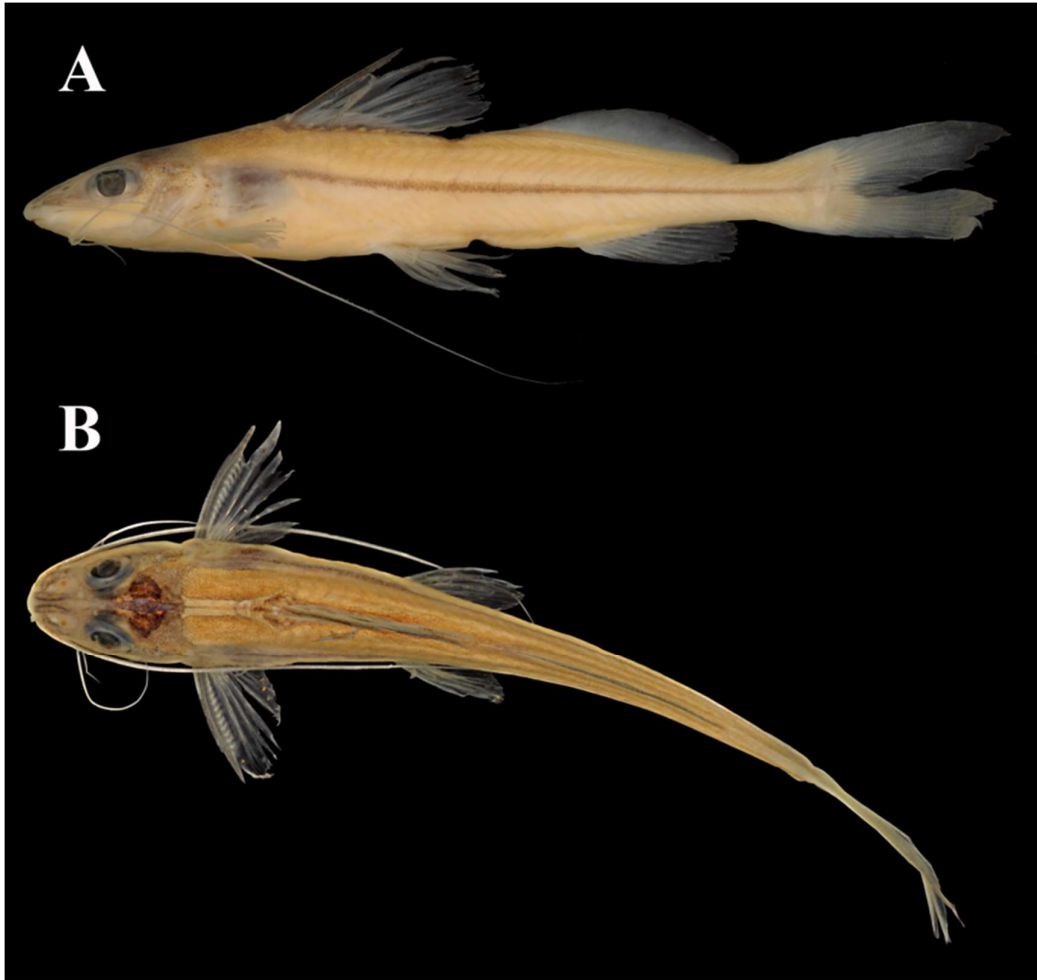


Figure 83. *Pimelodella hasemani*, UFRO-I 9741, 56.5 mm SL. Left lateral (A), and dorsal (B) views.



Figure 84. *Pimelodella howesi*, ANSP 69036, 79.3 mm SL. Left lateral (A), and dorsal (B) views.

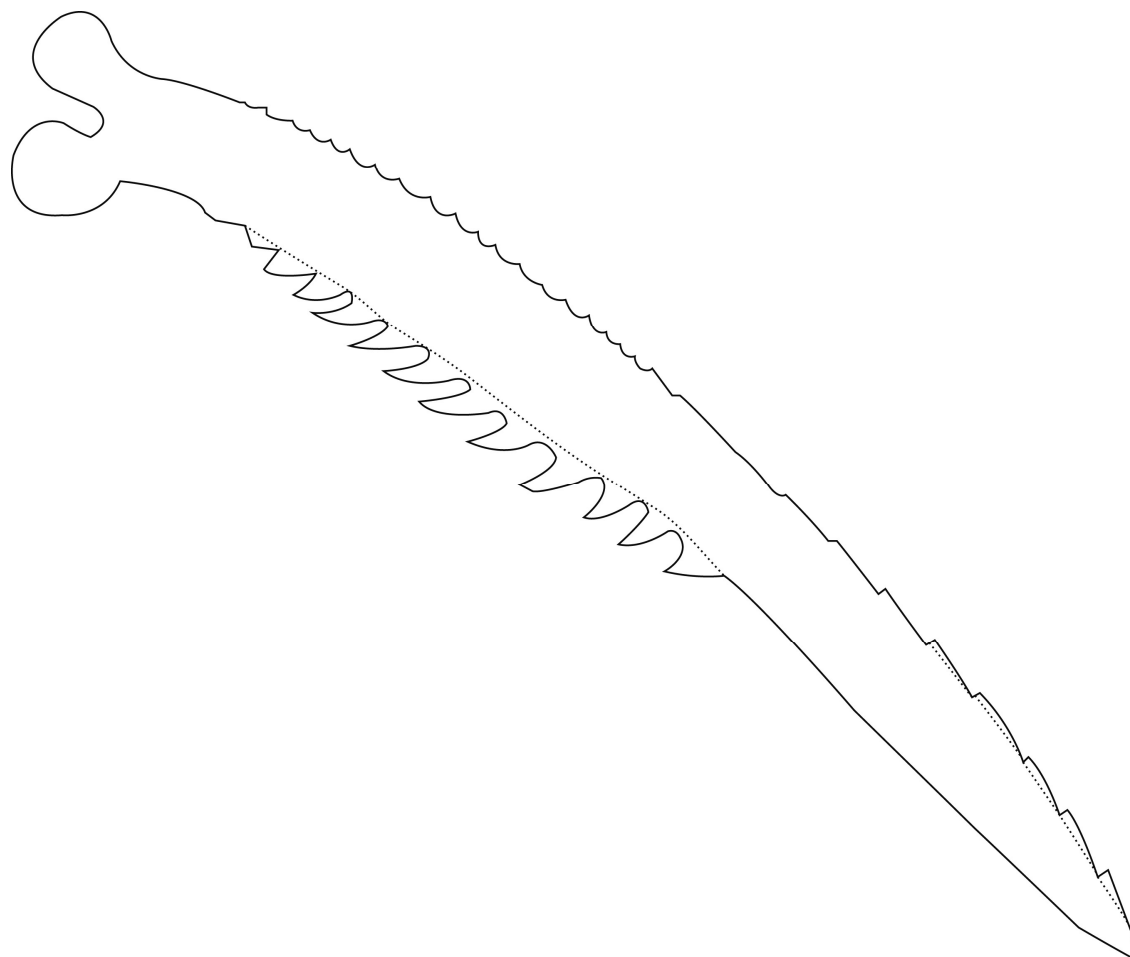


Figure 85. Ventral view of left pectoral-fin spine of *Pimelodella howesi*, ANSP 69036, 79.3 mm SL, total length of spine 14.1 mm.

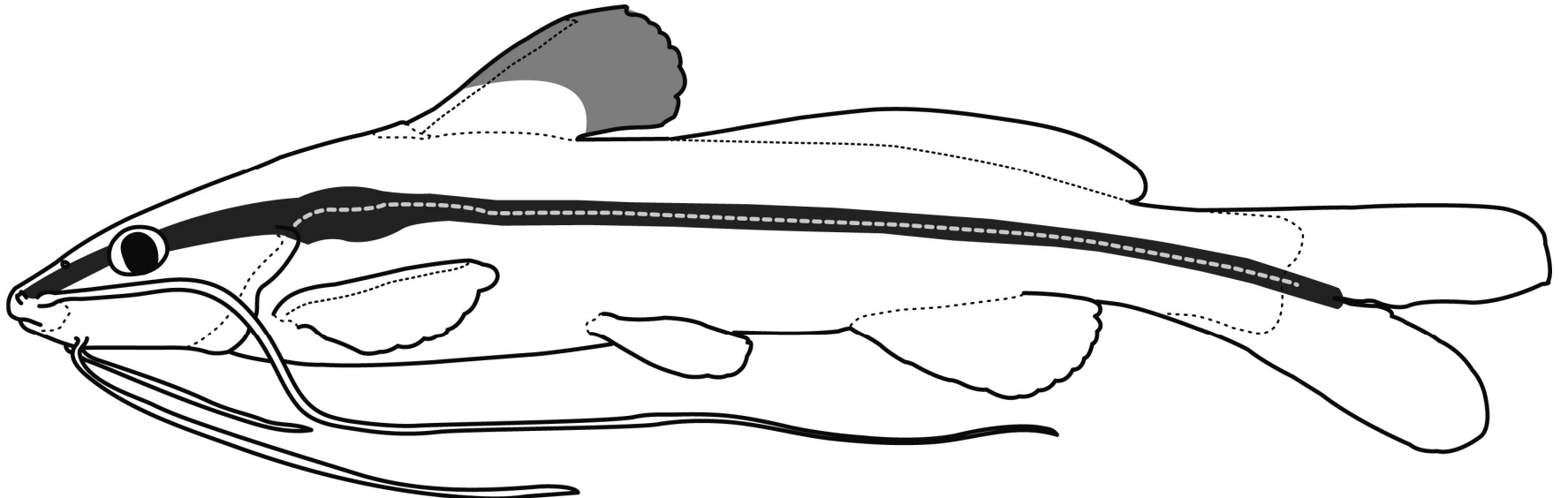


Figure 86. Schematic left lateral view of *Pimelodella howesi*.



Figure 87. *Pimelodella humeralis*, holotype, MPEG 34994, 77.4 mm SL. Left lateral (A) and dorsal (B) views.

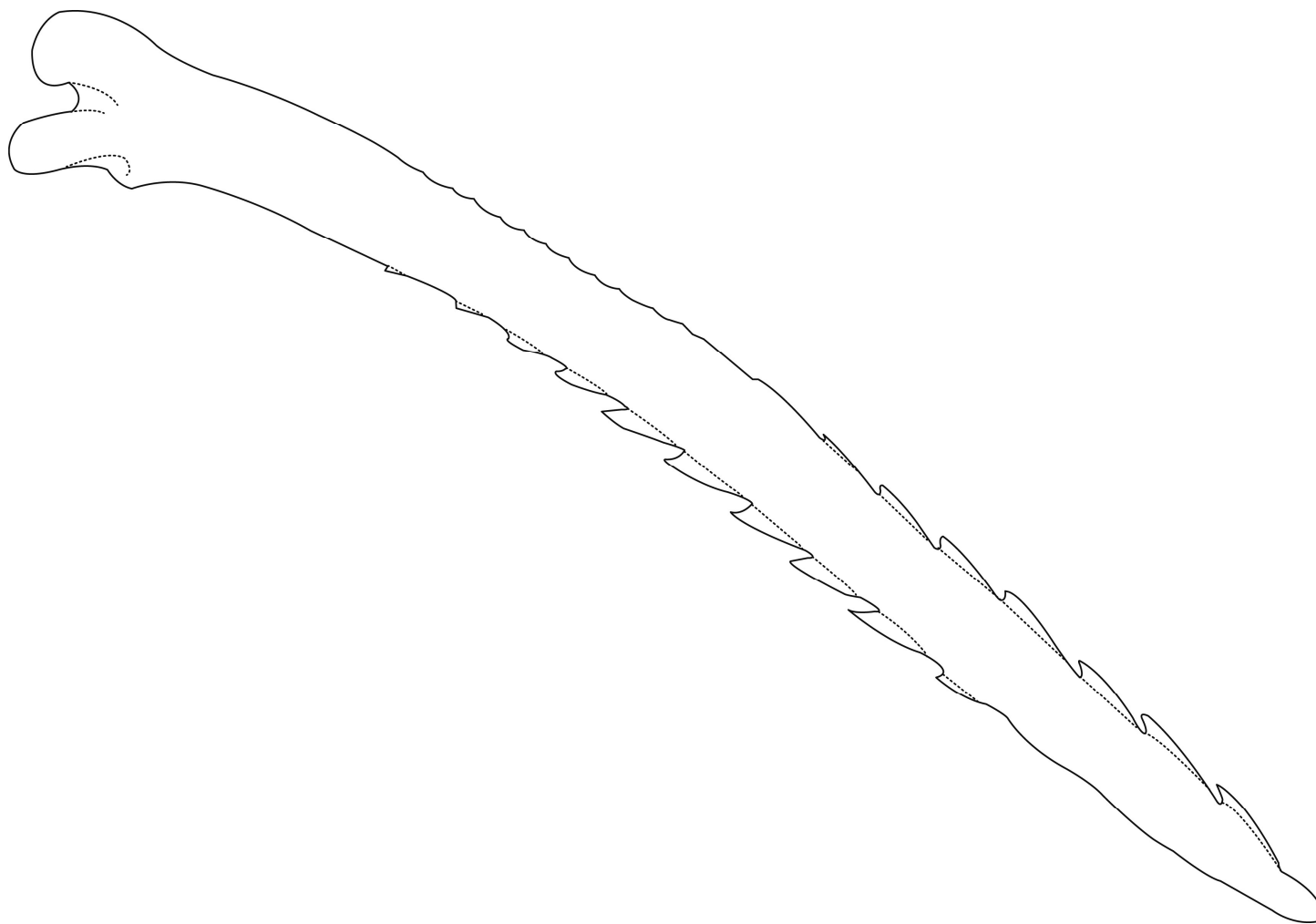


Figure 88. Ventral view of left pectoral-fin spine of *Pimelodella humeralis*, holotype, MPEG 34994, 77.4 mm SL, total length of spine 12.0 mm.

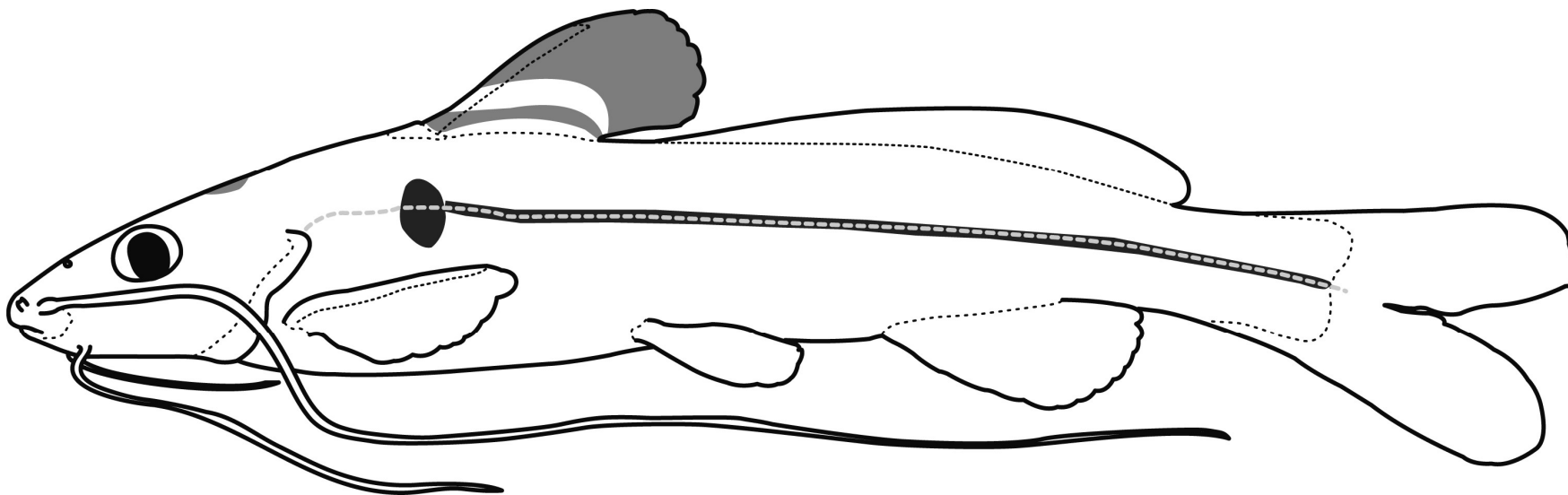


Figure 89. Schematic left lateral view of *Pimelodella humeralis*.



Figure 90. *Pimelodella ignobilis*, lectotype, NMW 44479, 91.1 mm SL. Left lateral (A) and dorsal (B) views.

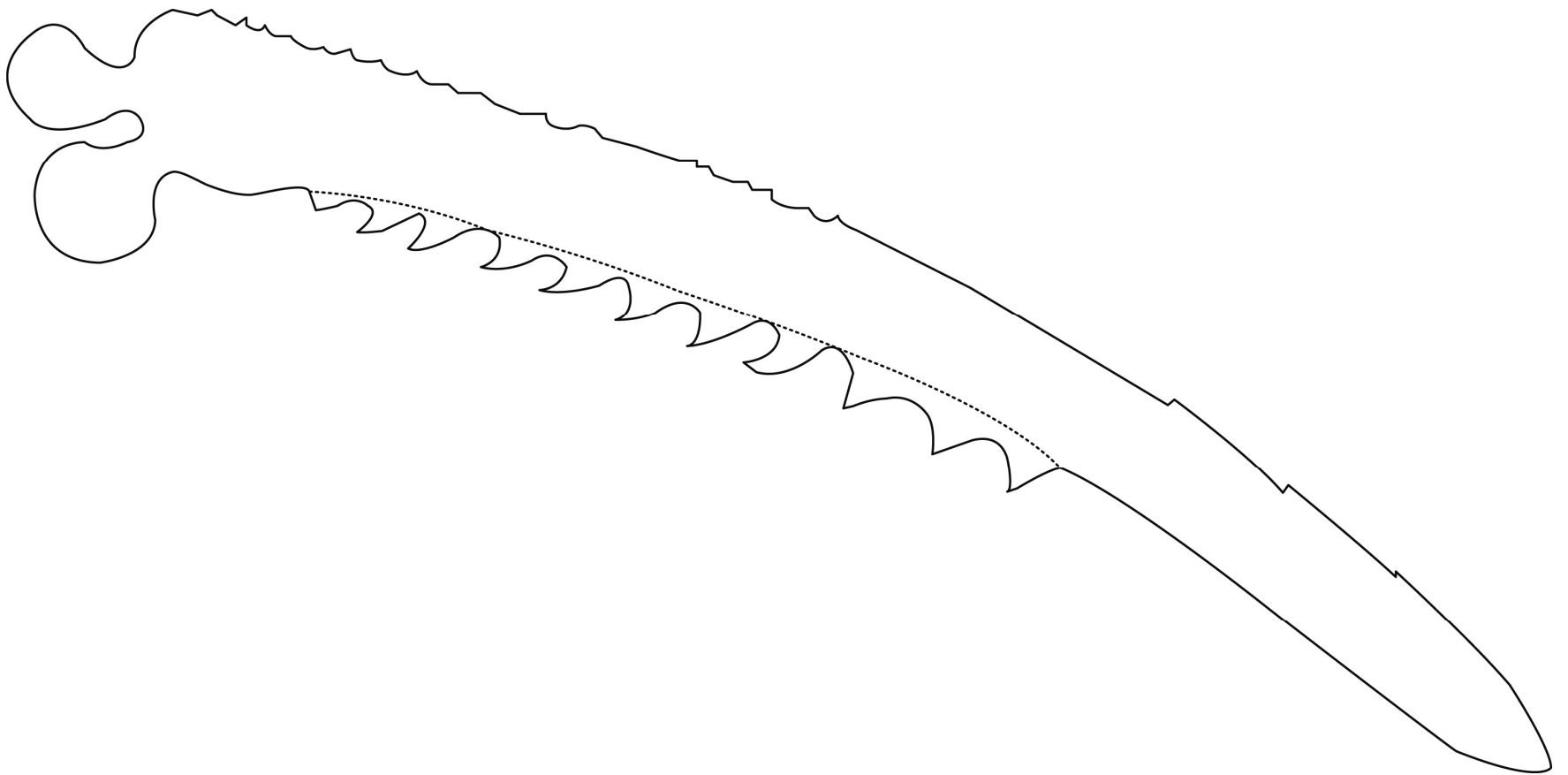


Figure 91. Ventral view of left pectoral-fin spine of *Pimelodella ignobilis*, paralectotype, NMW 44479, 98.9 mm SL, total length of spine 19.0 mm.

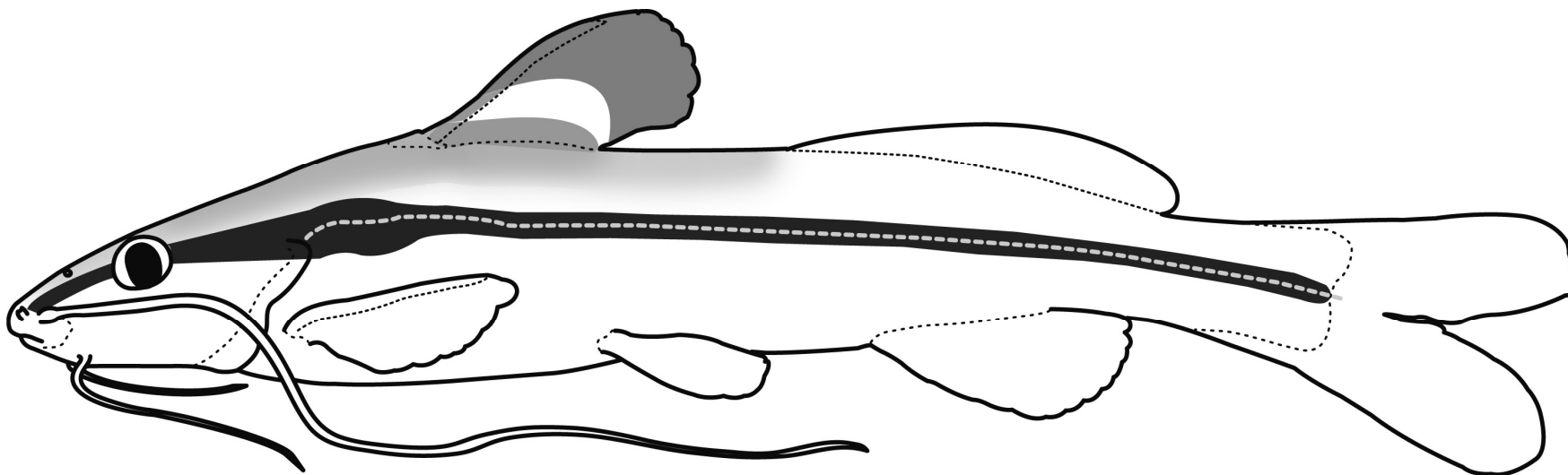


Figure 92. Schematic left lateral view of *Pimelodella ignobilis*.



Figure 93. *Pimelodella pappenheimi*, junior-synonym of *P. ignobilis*, lectotype, ZMB 31951, 103.1 mm SL. Left lateral (A) and dorsal (B) views.



Figure 94. *Pimelodella itapicuruensis*, FMNH 57986, 60.2 mm SL. Left lateral (A) and dorsal (B) views.

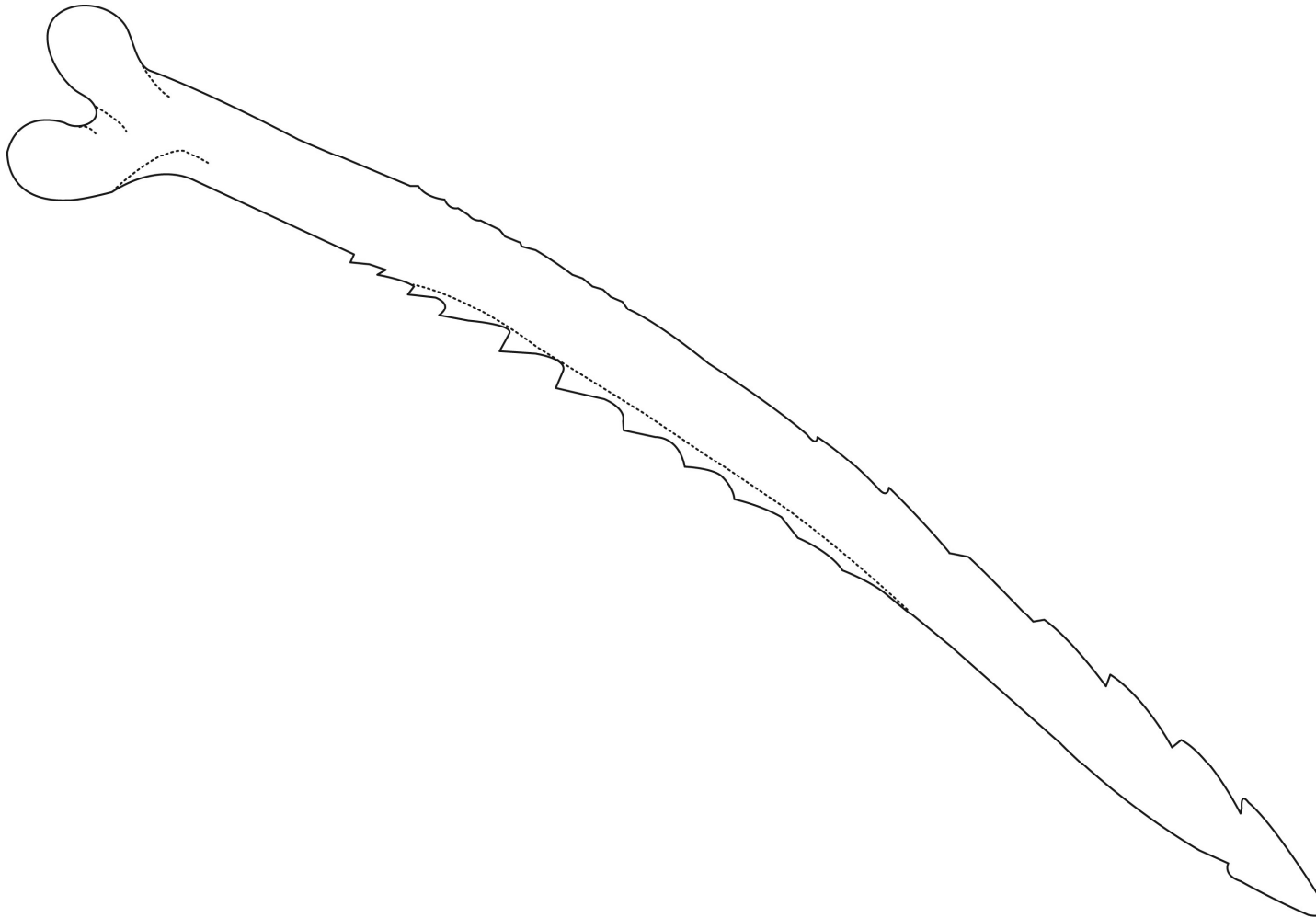


Figure 95. Ventral view of left pectoral-fin spine of *Pimelodella itapicuruensis*, FMNH 57986, 60.2 mm SL, total length of spine 11.2 mm.

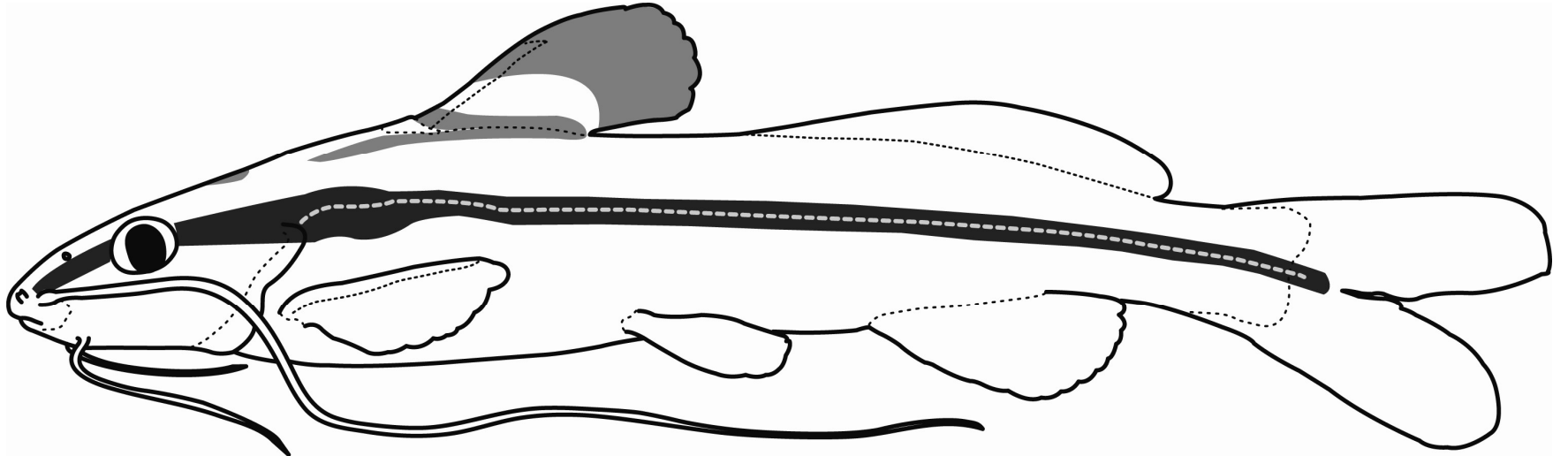


Figure 96. Schematic left lateral view of *Pimelodella itapicuruensis*.



Figure 97. *Pimelodella krontei*, holotype, MNRJ 836, 120.1 mm SL. Left lateral (A) and dorsal (B) views.

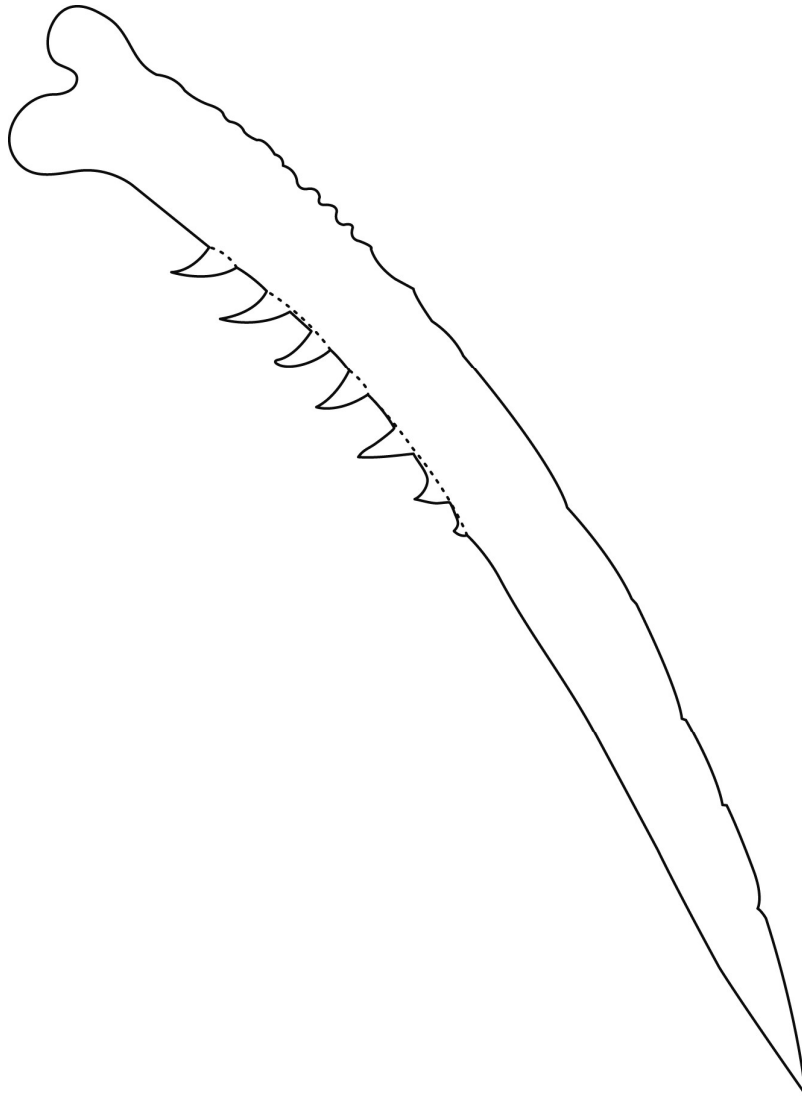


Figure 98. Ventral view of left pectoral-fin spine of *Pimelodella kronei*, LESC I 170, 93.4 mm SL, total length of spine 12.5 mm.

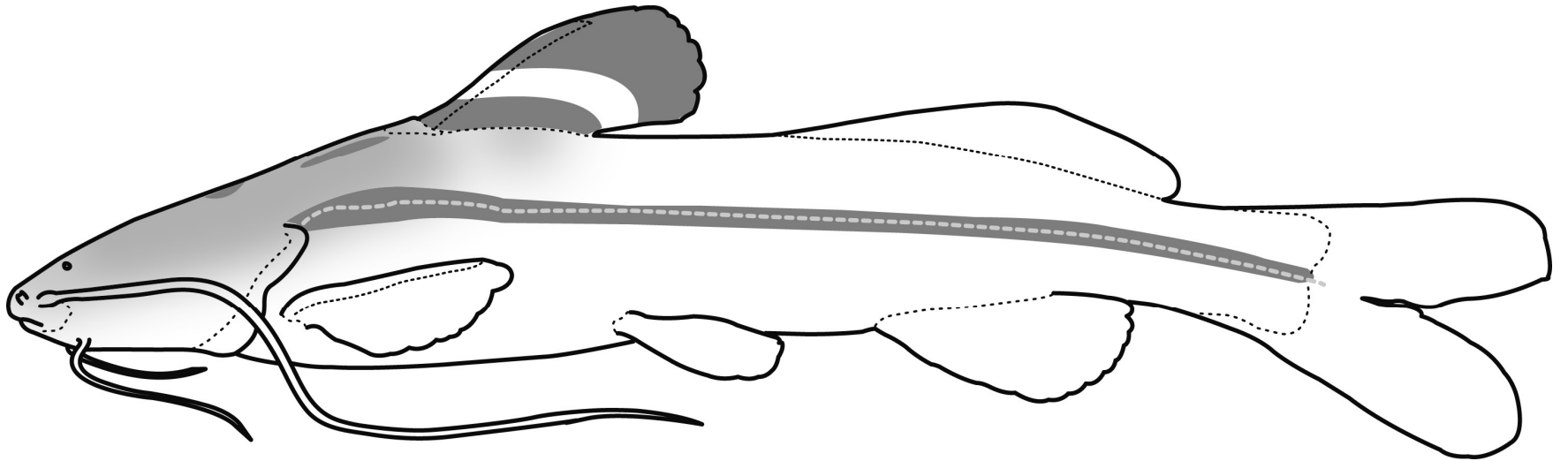


Figure 99. Schematic left lateral view of *Pimelodella kronei*.

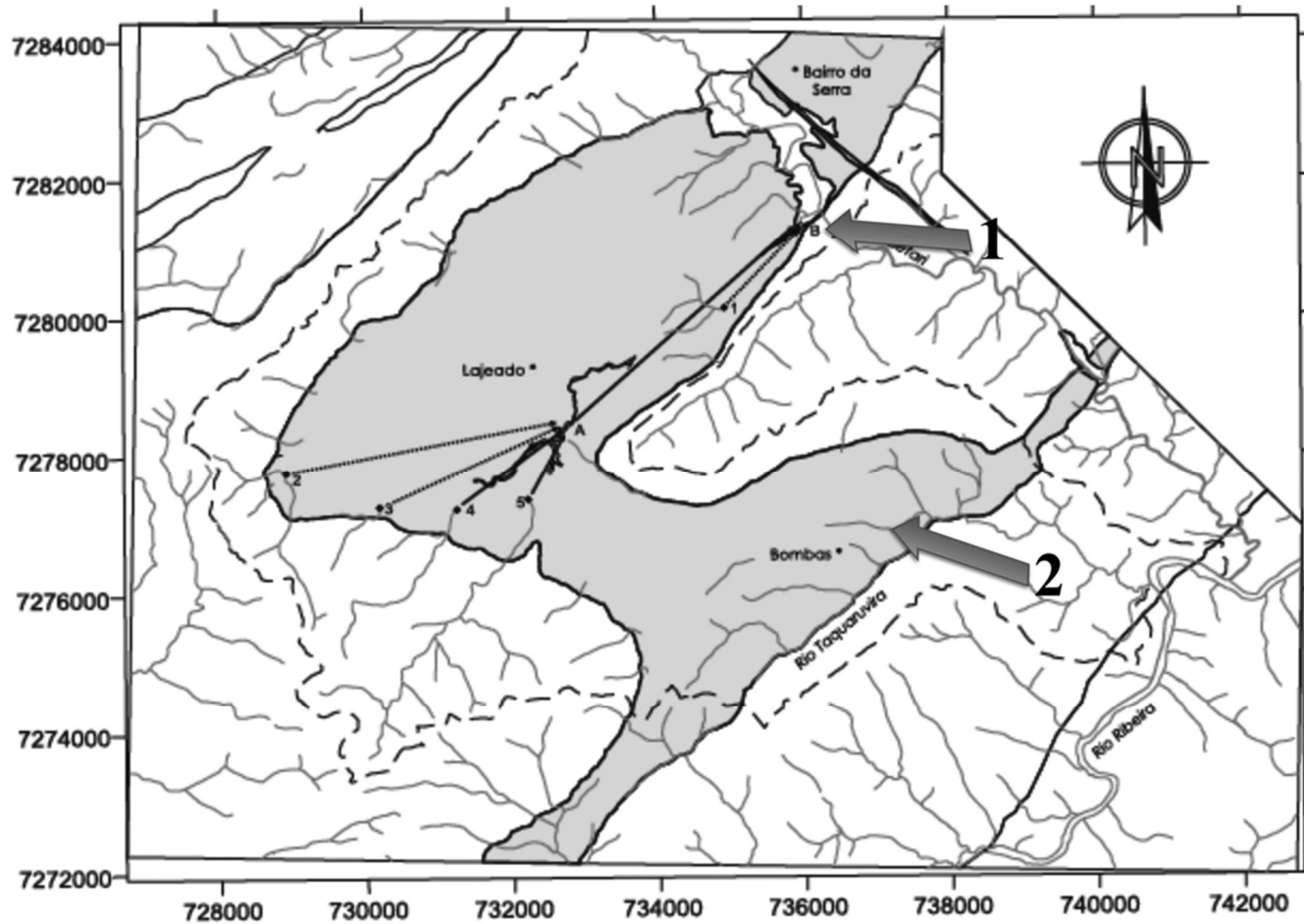


Figure 100. Map of stream routes and flux of Areias system, obtained from Genthner *et al.* (2006: fig. 6). Arrows: Areias (1) and Bombas (2) ressurgences.

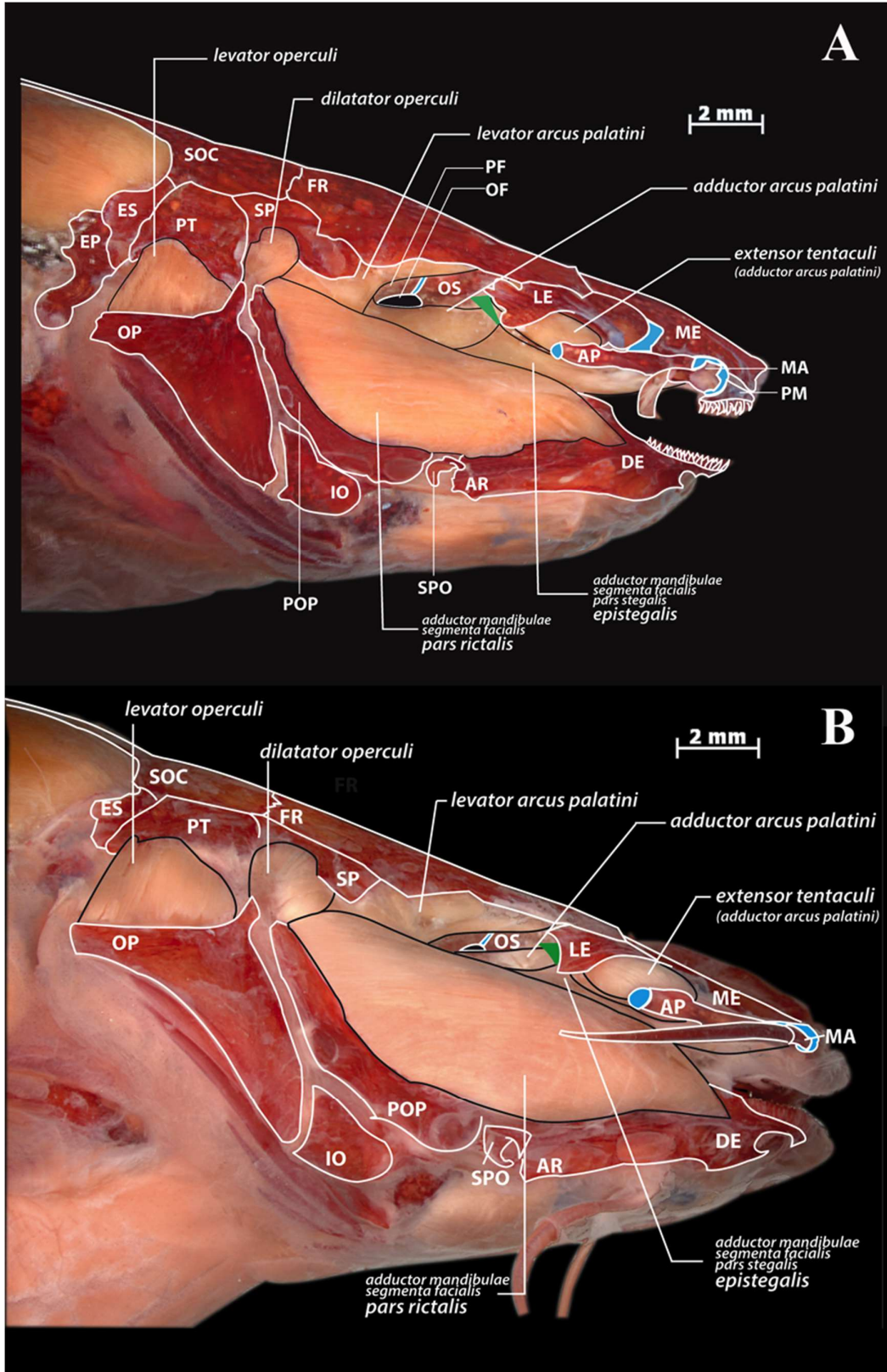


Figure 101. Right lateral view of head of *P. kronei*. Infraorbital series and nasal removed. (A) MZUSP 38725, Bombas resurgence, Iporanga; (B) MZUSP 27168, Areias system, Iporanga.

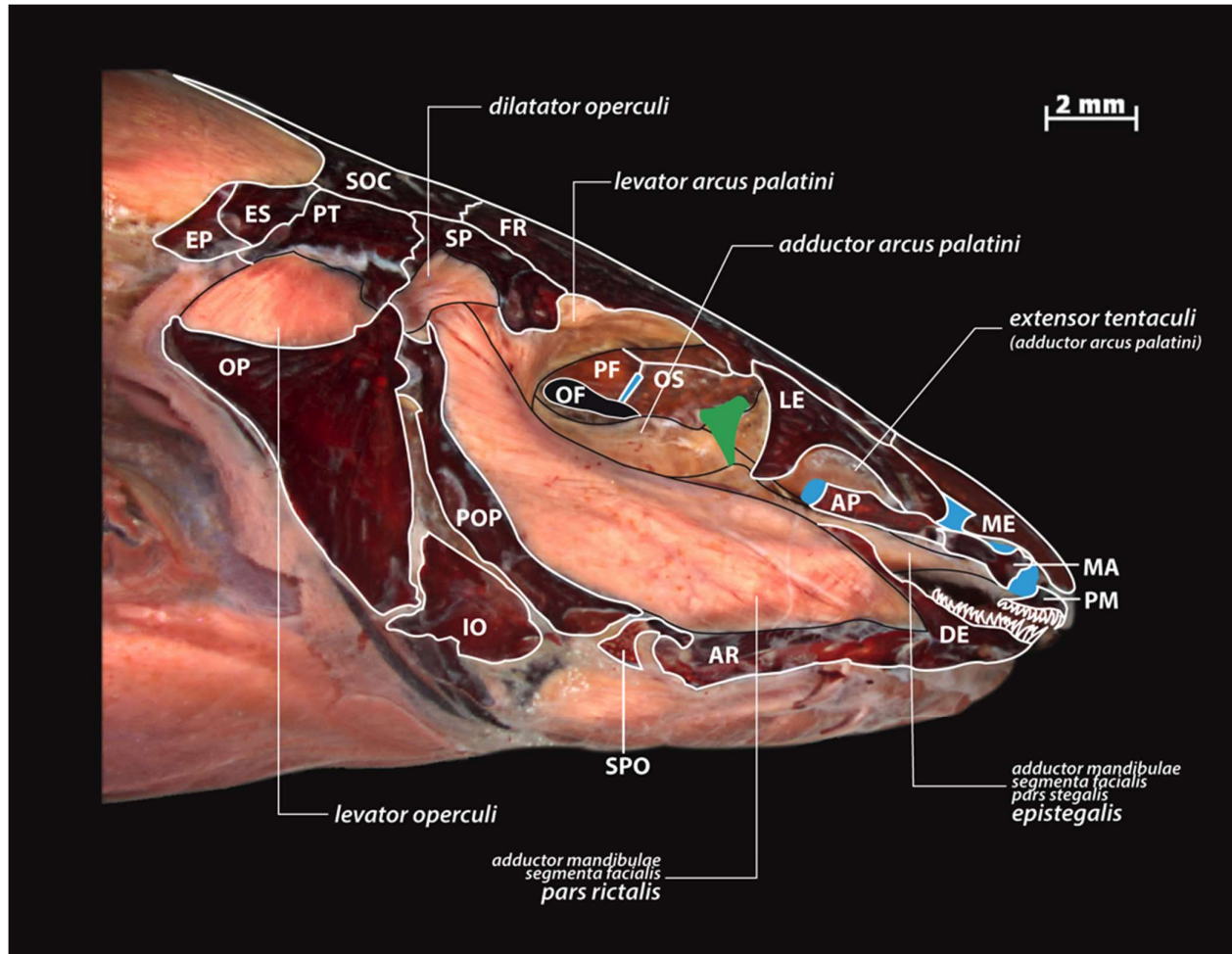


Figure 102. Right lateral view of head of *P. transitoria*. Infraorbital series and nasal removed. MZUSP 63365, Ribeirão Furnas, Areias system, Iporanga.

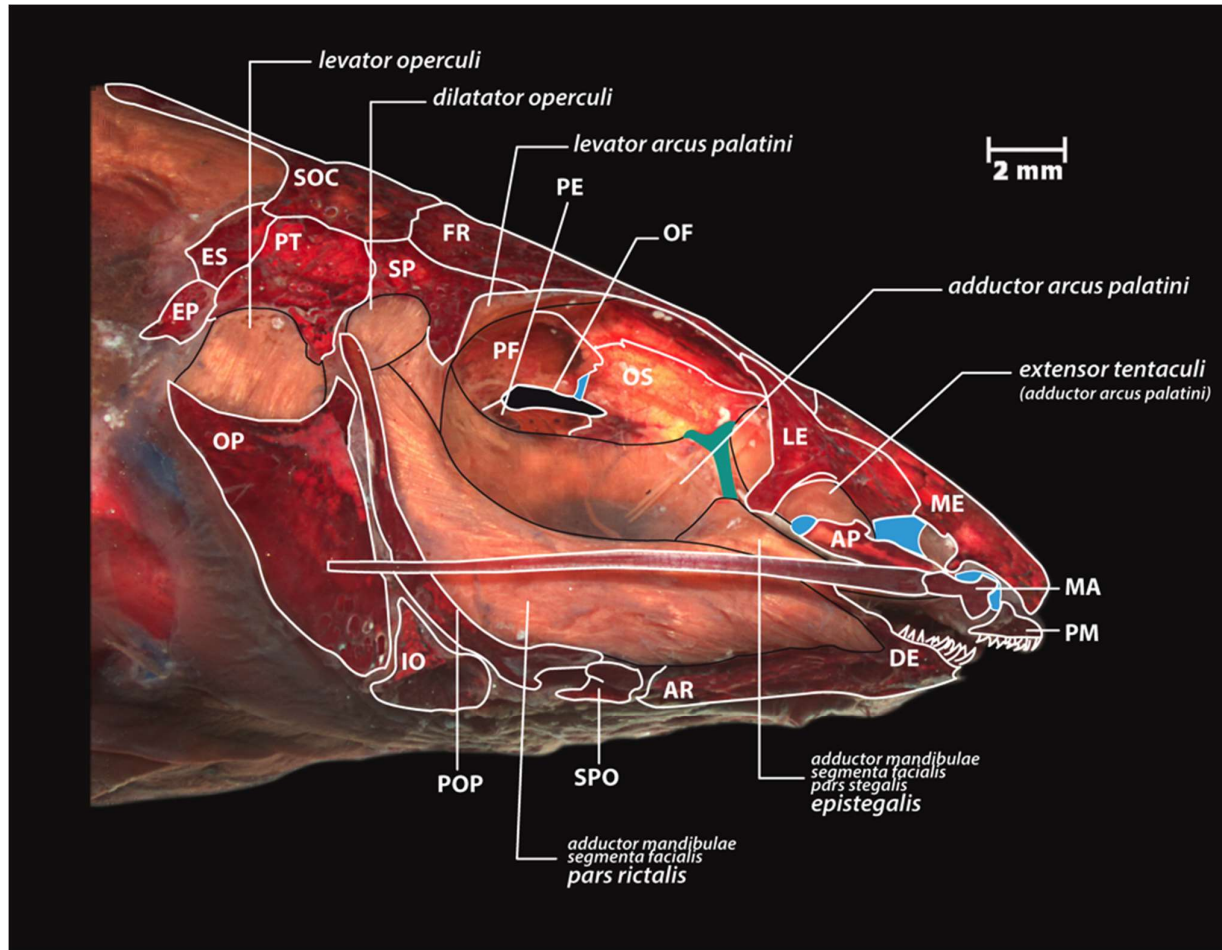


Figure 103. Right lateral view of *P. lateristriga*. Infraorbital series and nasal removed. USNM 301676, Rio Mucuri, Northeastern Mata Atlântica region.

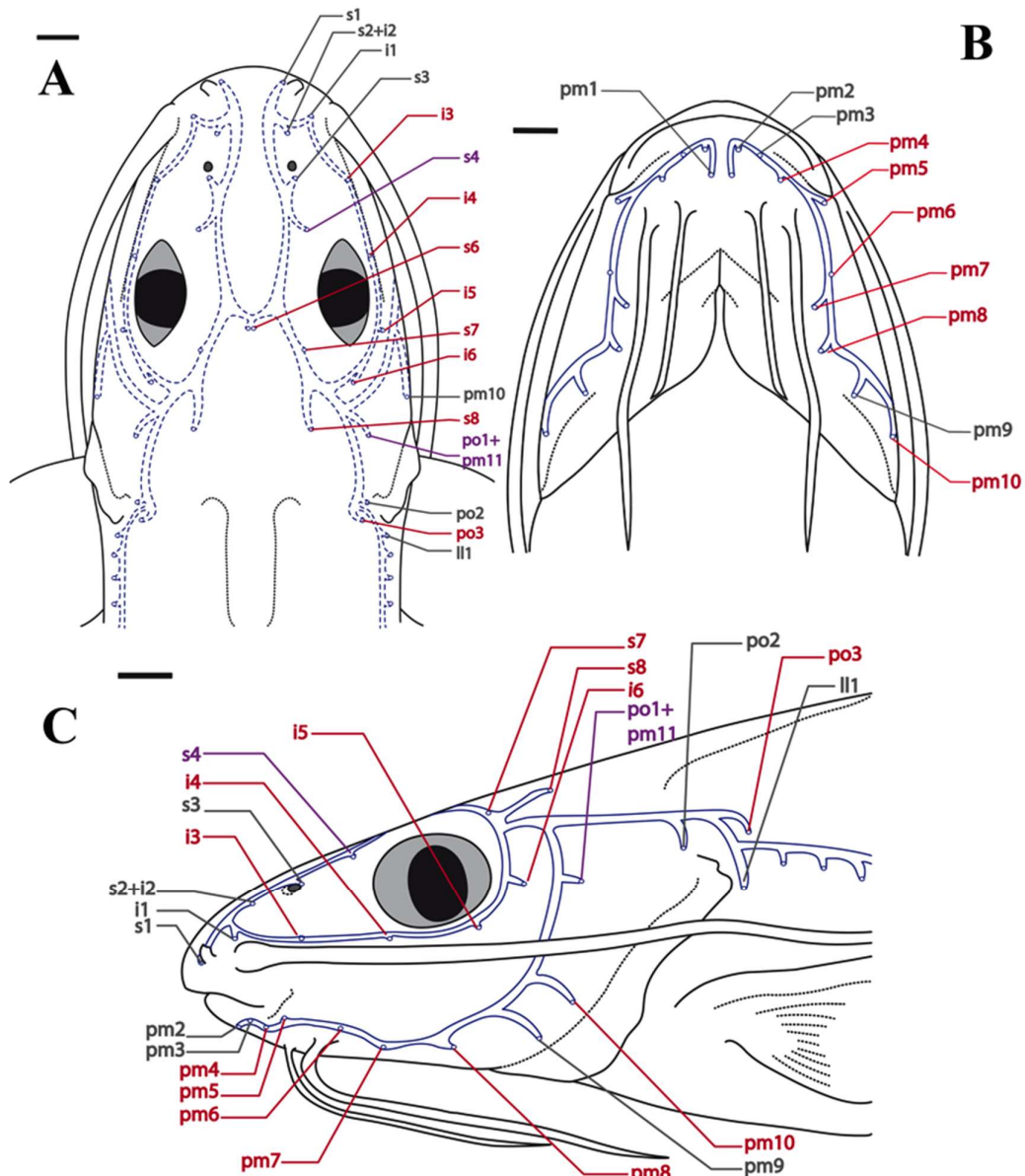


Figure 104. (A) Dorsal view; (B) Ventral view; and (C) Left lateral view of head of a *Pimelodella*, showing the overall arrangement of cephalic laterosensory system. Grey legends are for a simple pore for both *P. kronei* and *P. transitoria*. Purple legends are for different conditions (loss or duplication) of a pore in individuals of both species. Red legends are for loss or duplication of a pore exclusively for *P. kronei* specimens. Scale bar: 2mm.

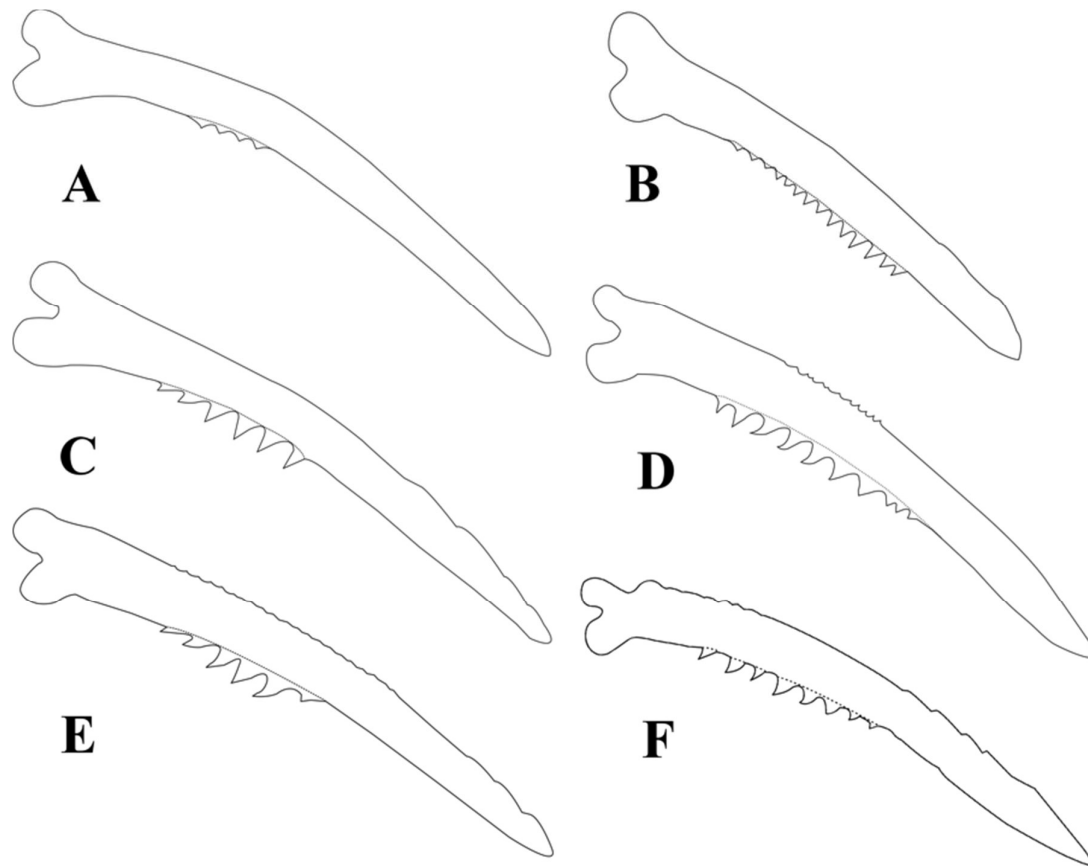


Figure 105. Ventral view of left pectoral-fin spine of *Pimelodella kronei*, LESCI uncat. 113.2 mm SL, length of spine 12.5 mm, Areias system (A); LESCI 167 144.4 mm SL, length of spine 20.4 mm, Areias system (B); LESCI 169 110.7 mm SL, length of spine 13.4 mm, Bombas resurgence (C); and *P. transitoria*, LESCI uncat. 101.8 mm SL, length of spine 16.7 mm, Rio Betari, alojamento ouro grosso (D); LESCI 95 85.5 mm SL, length of spine 14.0 mm, Rio Betari (E); LESCI 168 98.1 mm SL, length of spine 15.9 mm, Gruta da Casa de Pedra (F).



Figure 106. Left lateral view of *Pimelodella transitoria*, LESCI 168, 98.1 mm SL.



Figure 107. Neotype of *Pimelodella transitoria*, a junior-synonym of *P. kronei*, MZUSP 403, 107.4 mm SL. Photo taken by Murilo Pastana.



Figure 108. *Pimelodella lateristriga*, holotype, ZMB 3038, 95,9 mm SL. Left lateral (A) and dorsal (B) views. Photo taken by Johanna Kapp.

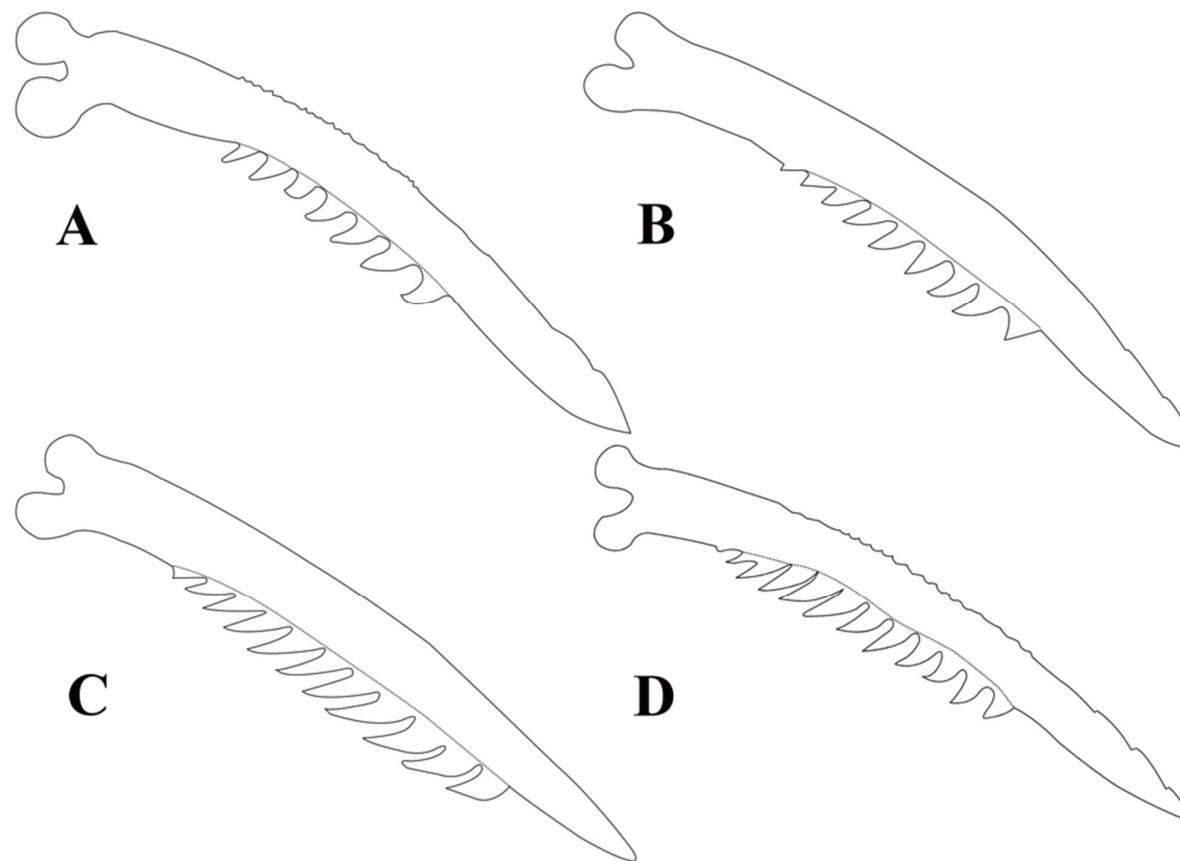


Figure 109. Ventral view of left pectoral-fin spine of: (A) *Pimelodella lateristriga*, holotype, ZMB 3038, 95,9 mm SL, total length of spine 18.0 mm (approximated); (B) *Pimelodella lateristriga*, MZUSP 114867, 84 mm SL, total length of spine 14.5 mm; (C) *Pimelodella lateristriga*, MZUSP 93863, 99.5 mm SL, total length of spine 15.7 mm; (D) *Pimelodella bahiana*, lectotype, MNHN B612, 93.4 mm SL, total length of spine 16.1 mm.

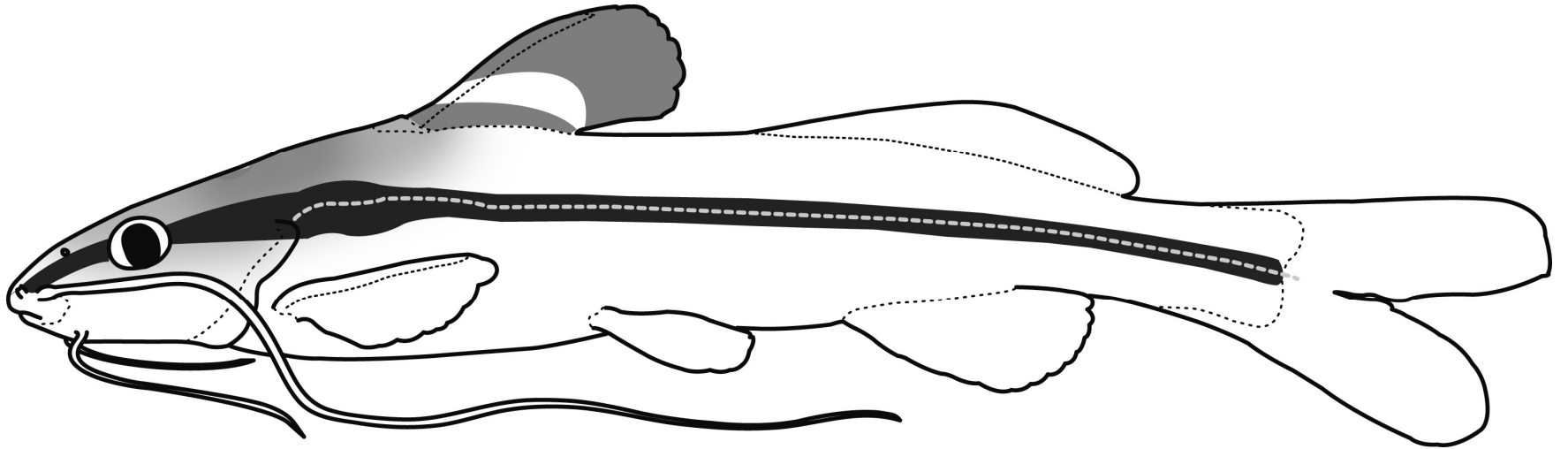


Figure 110. Schematic left lateral view of *Pimelodella lateristriga*.



Figure 111. *Pimelodella lateristriga*, MZUSP 121461, 112.7 mm SL. Left lateral (A) and dorsal (B) views. Photo taken by Murilo Pastana.



Figure 112. *Pimelodella bahiana*, lectotype, MNHN B612, 93.4 mm SL. Left lateral (A) and dorsal (B) views. Photo taken by MNHN staff.



Figure 113. *Pimelodella laticeps*, holotype, FMNH 57969, 49.0 mm SL. Left lateral (A) and dorsal (B) views. Photo taken by M. W. Littmann.

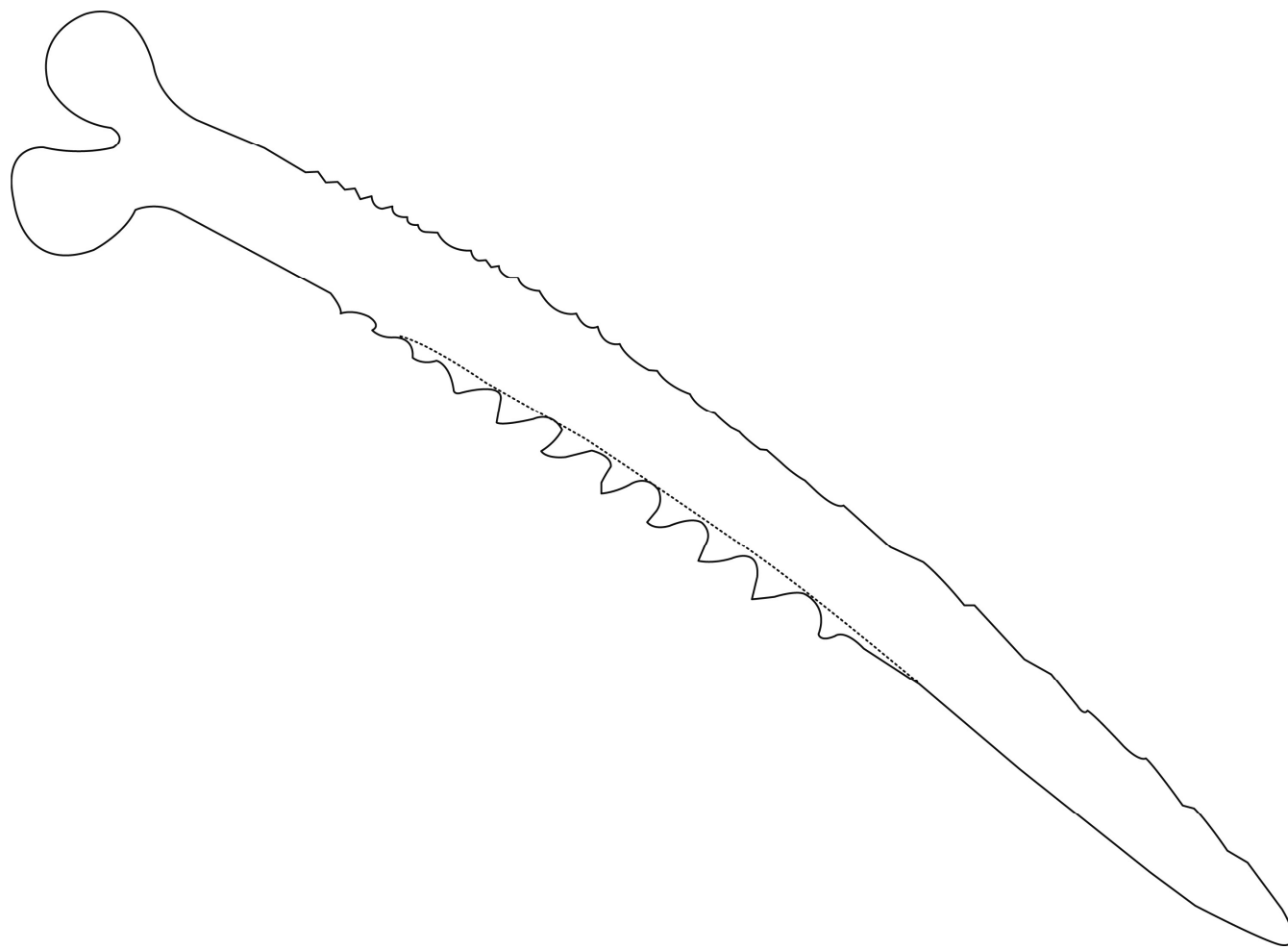


Figure 114. Ventral view of left pectoral-fin spine of *Pimelodella laticeps*, holotype, FMNH 57969, 49.0 mm SL, total length of spine 9.6 mm.

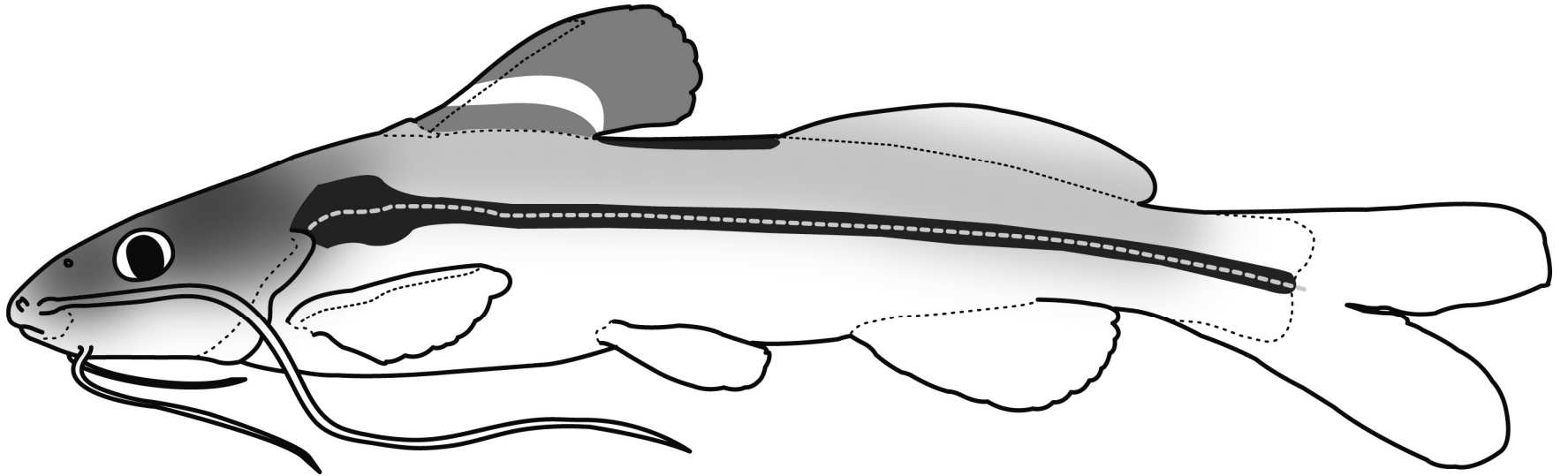


Figure 115. Schematic left lateral view of *Pimelodella laticeps*.



Figure 116. *Pimelodella laurenti*, holotype, ANSP 69380, 66.5 mm SL. Left lateral (A) and dorsal (B) views. Photo taken by Murilo Pastana.

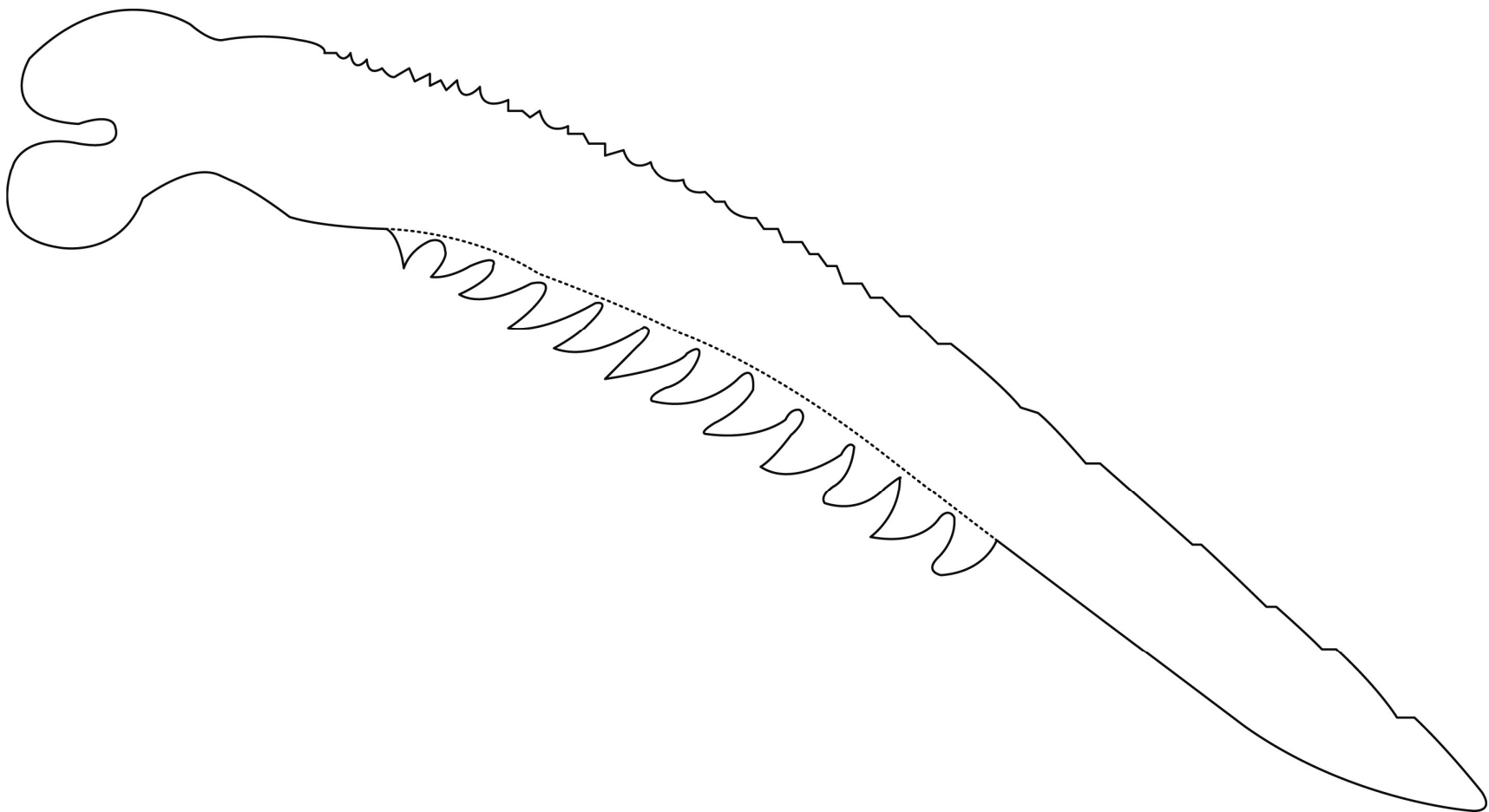


Figure 117. Ventral view of left pectoral-fin spine of *Pimelodella laurenti*, holotype, ANSP 69380, 66.5 mm SL, total length of spine 12.7 mm.

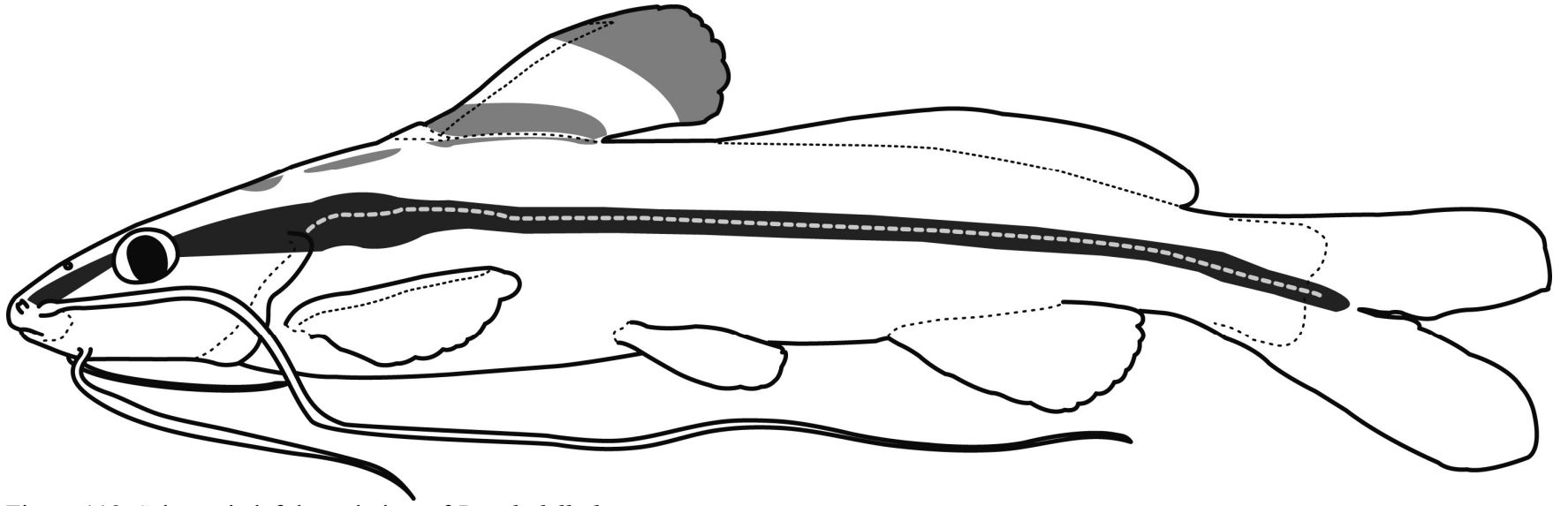


Figure 118. Schematic left lateral view of *Pimelodella laurenti*.



Figure 119. Left lateral view of *Pimelodella laurenti*, MZUSP 39441, 62.8 mm SL.



Figure 120. *Pimelodella leptosoma*, holotype, ANSP 39340, 59.6 mm SL. Left lateral (A) and dorsal (B) views. Photo taken by Mark Sabaj.

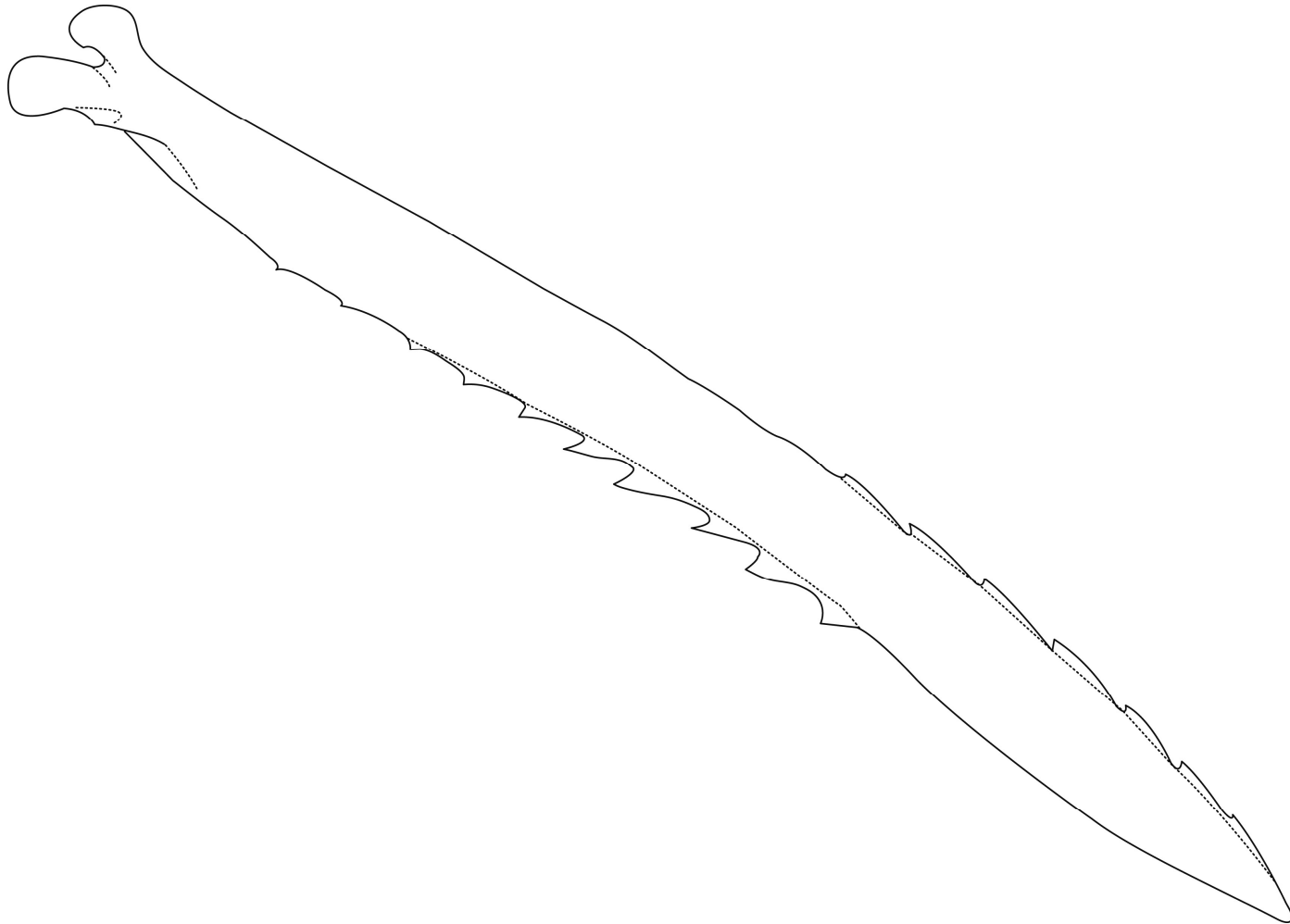


Figure 121. Ventral view of left pectoral-fin spine of *Pimelodella leptosoma*, holotype, ANSP 39340, 59.6 mm SL, total length of spine 8.5 mm.

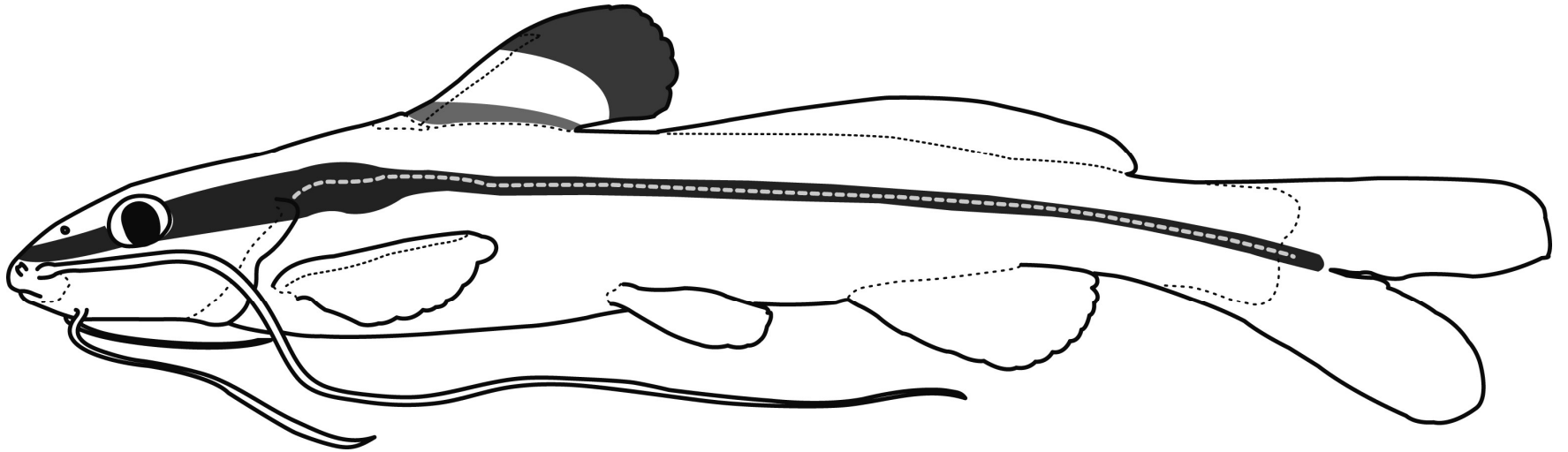


Figure 122. Schematic left lateral view of *Pimelodella leptosoma*.

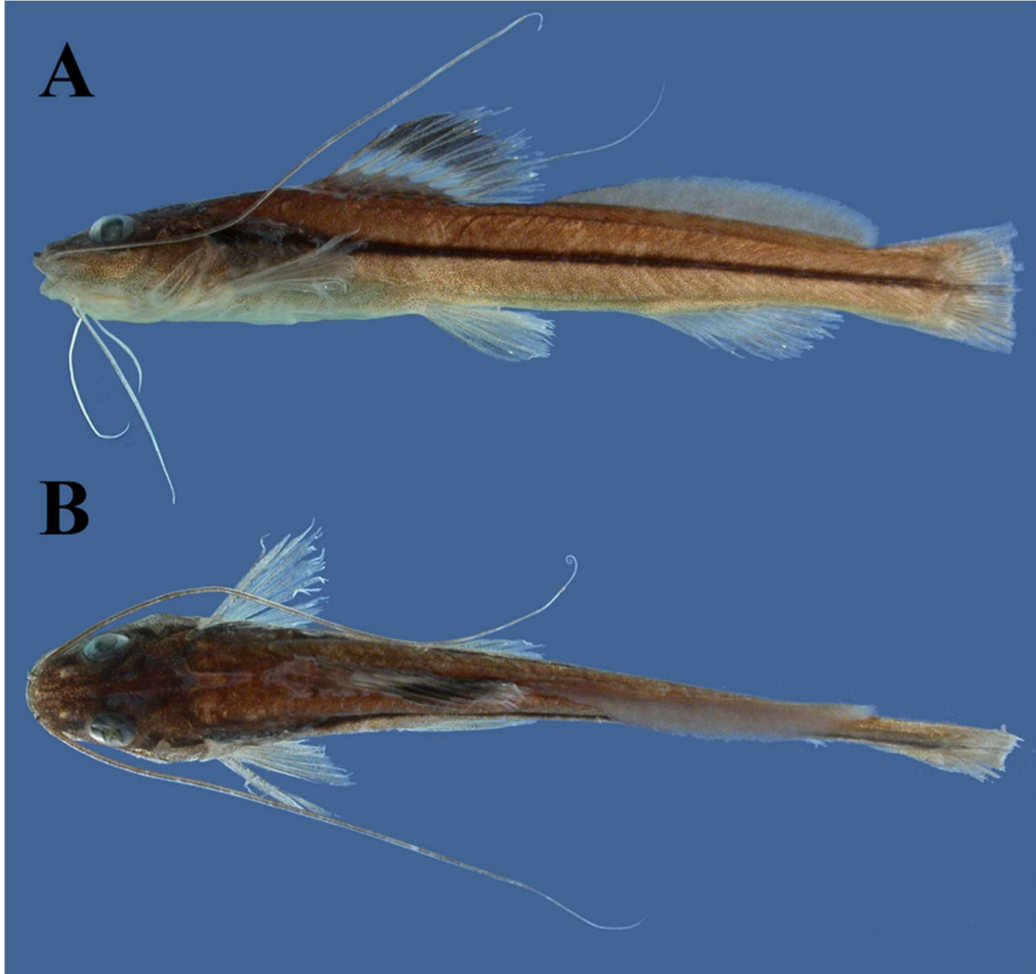


Figure 123. *Pimelodella leptosoma*, ANSP 179754. Left lateral (A) and dorsal (B) views. Photo taken by Mark Sabaj.



Figure 124. *Pimelodella linami*, USNM 121132, holotype, 74.7 mm SL. Left lateral (A) and dorsal (B) views. Photo taken by Sandra Raredon.

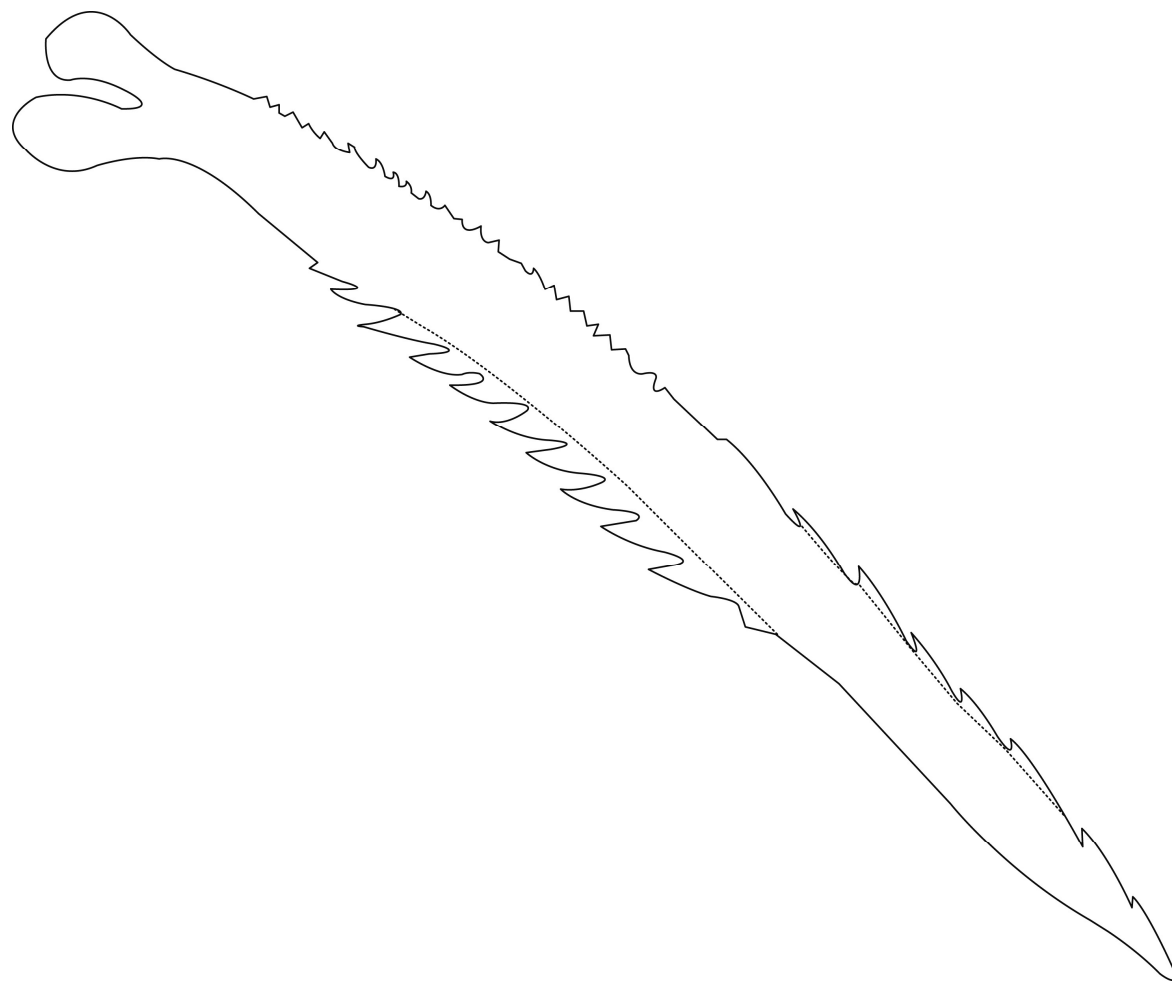


Figure 125. Ventral view of left pectoral-fin spine of *Pimelodella linami*, USNM 121132, holotype, 74.7 mm SL, total length of spine 10.7 mm.

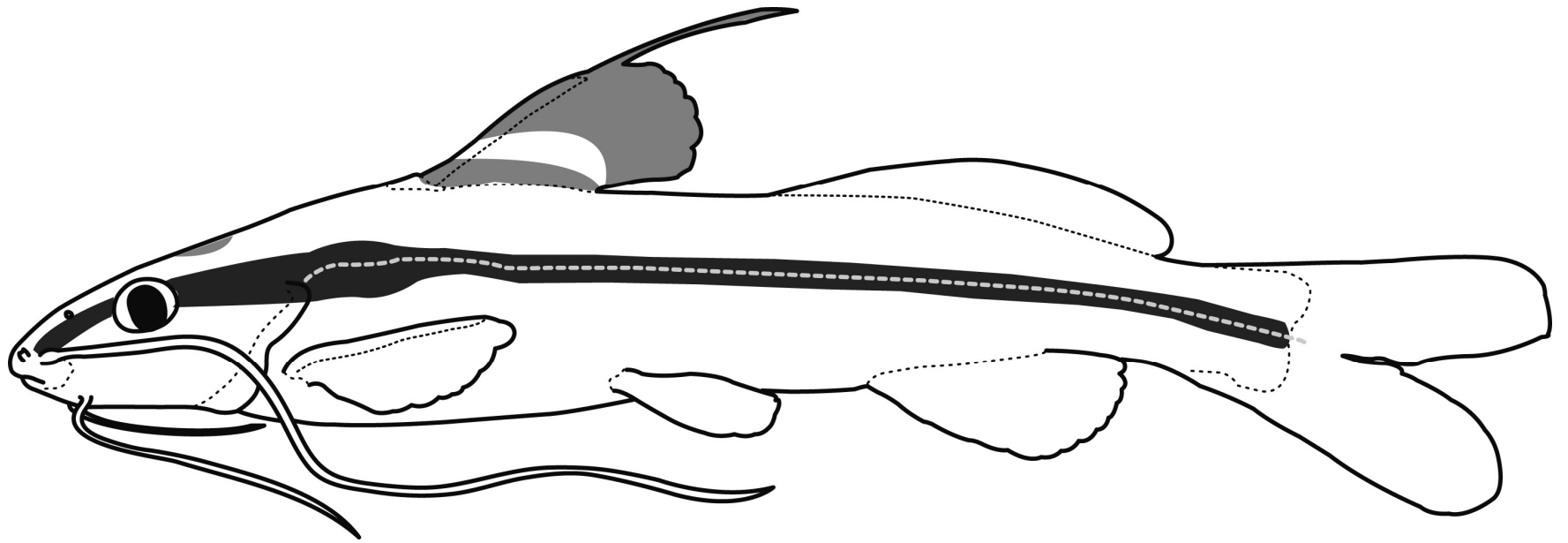


Figure 126. Schematic left lateral view of *Pimelodella linami*.



Figure 127. *Pimelodella longipinnis*, AMNH 8642, holotype, 84.6 mm SL. Left lateral (A) and dorsal (B) views. Photo taken by Melanie Stiassny.

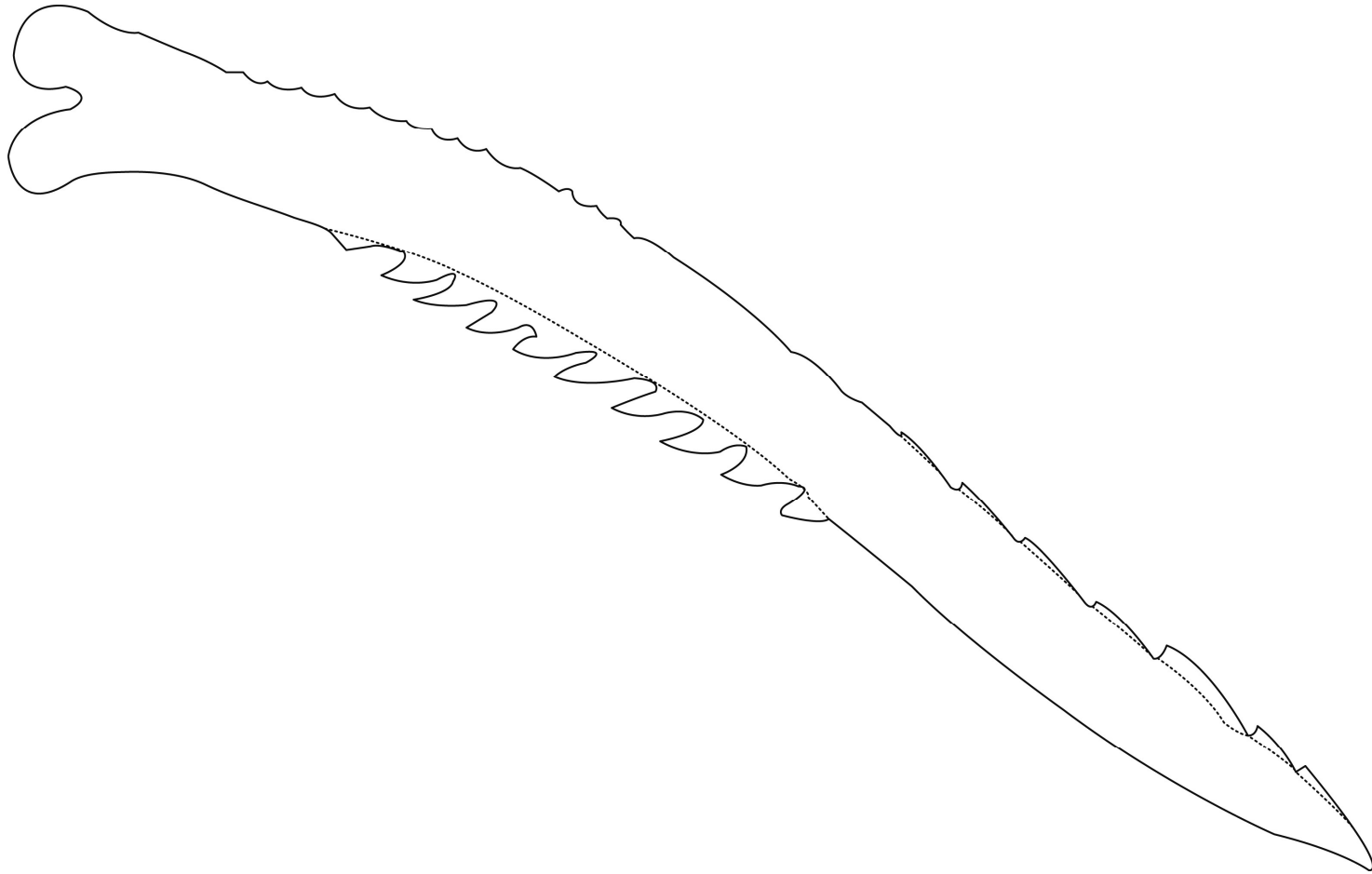


Figure 128. Ventral view of left pectoral-fin spine of *Pimelodella longipinnis*, AMNH 8642, holotype, 84.6 mm SL, total length of spine 11.7 mm.

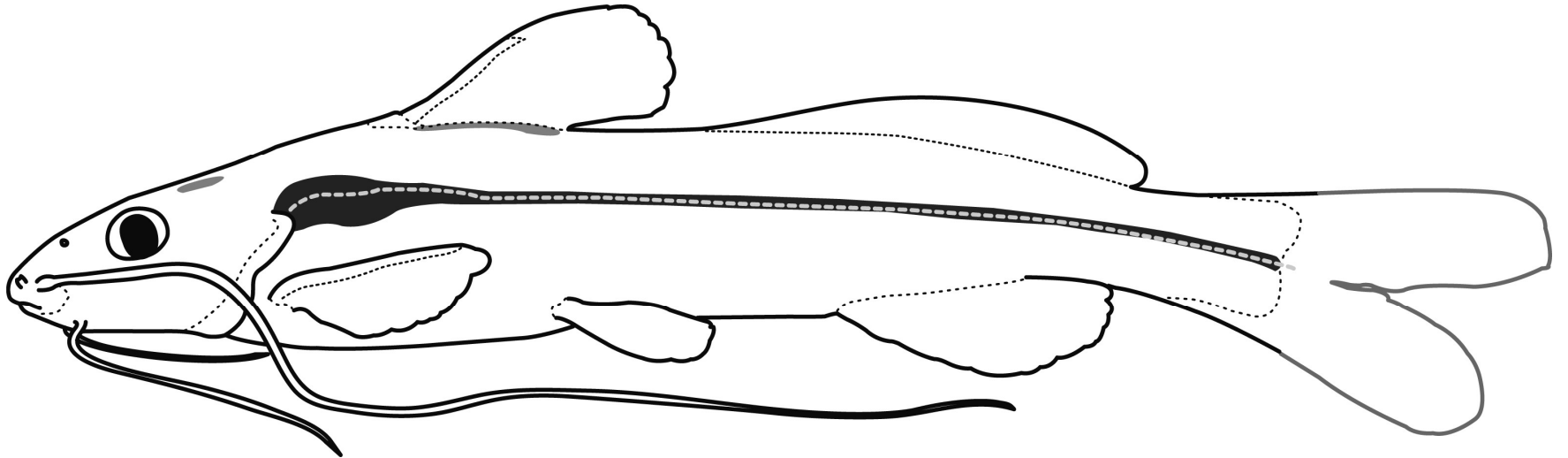


Figure 129. Schematic left lateral view of *Pimelodella longipinnis*.

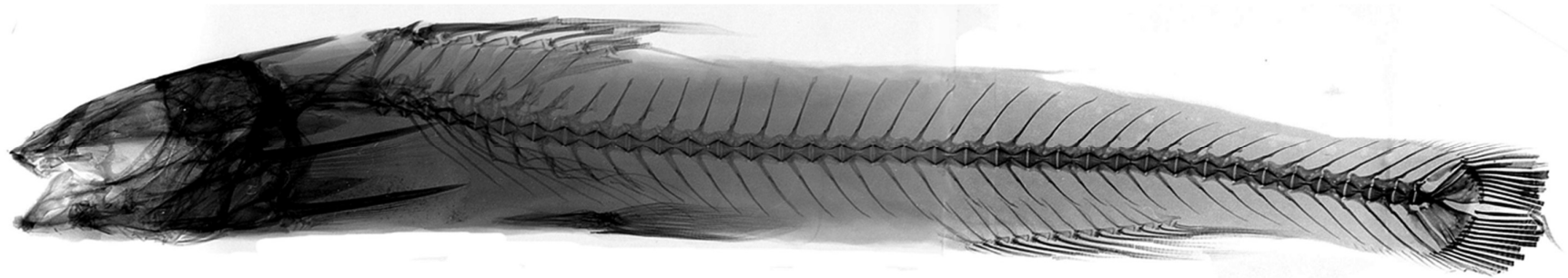


Figure 130. Radiograph of *Pimelodella longipinnis*, AMNH 8642, holotype, 84.6 mm SL. Left lateral view.



Figure 131. *Pimelodella macturki*, holotype, FMNH 53234, 53.5 mm SL. Left lateral (A) and dorsal (B) views. Photo taken by M. W. Littmann.

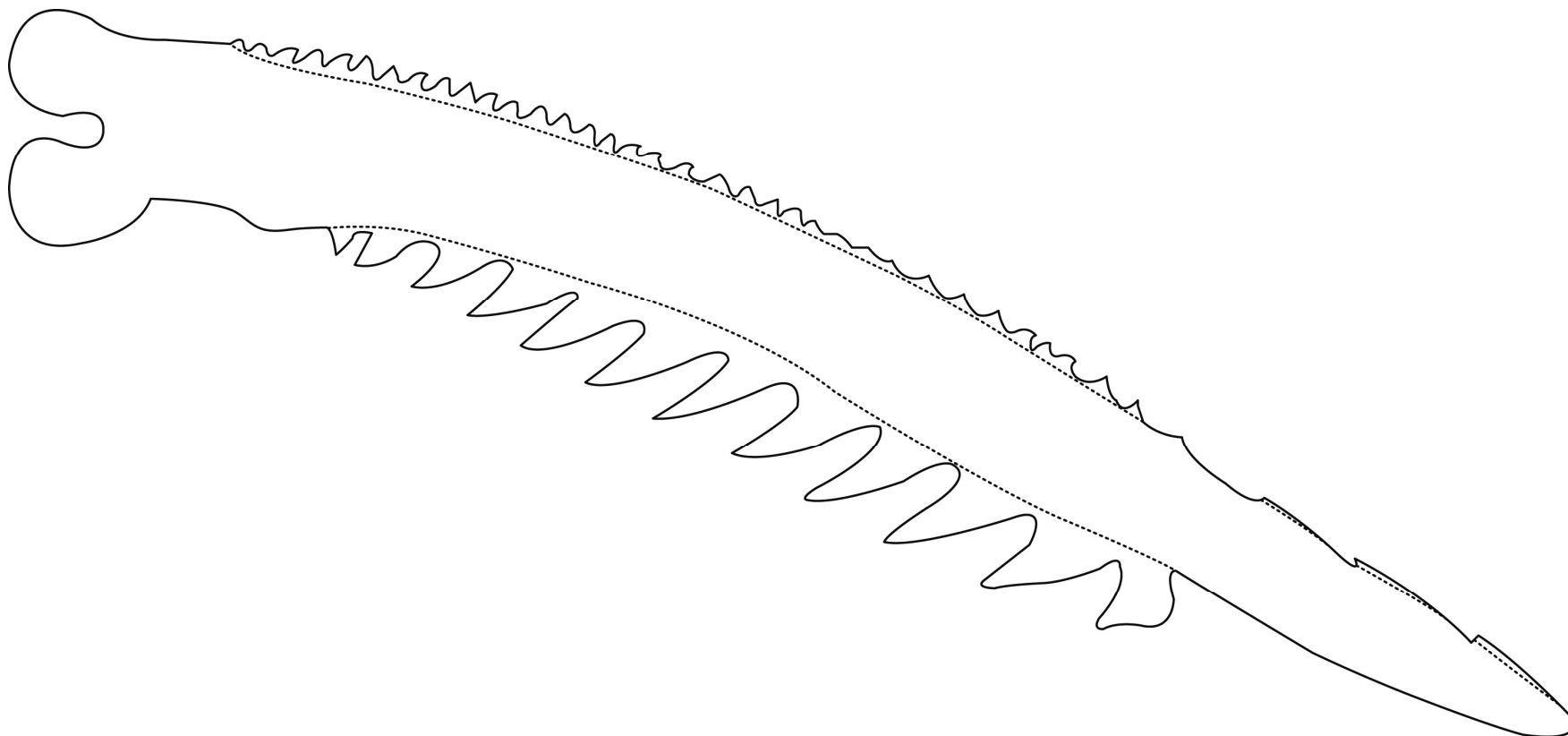


Figure 132. Ventral view of left pectoral-fin spine of *Pimelodella macturki*, paratype, BMNH 1911.10.31.54, 52.9 mm SL, total length of spine 9.8 mm.

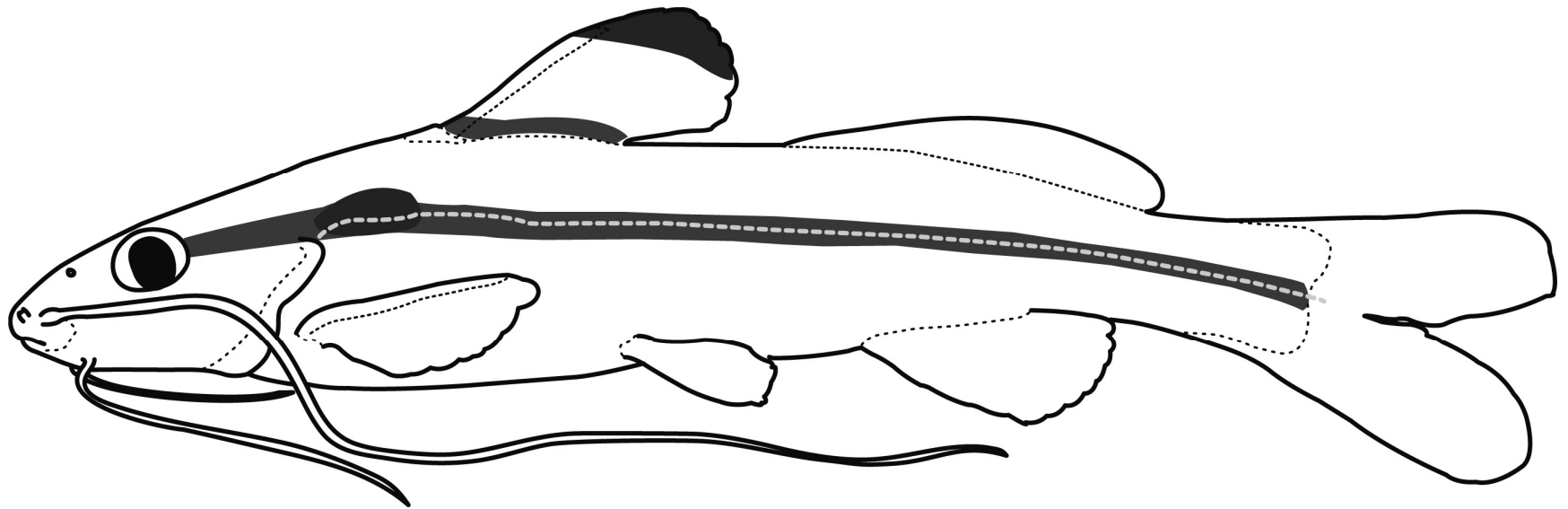


Figure 133. Schematic left lateral view of *Pimelodella macturki*.



Figure 134. *Pimelodella martinezi*, holotype, 68 mm SL, image from Fernández-Yépez (1970), unnum. page, pl. 35. Left lateral (A) and dorsal view of head (B).

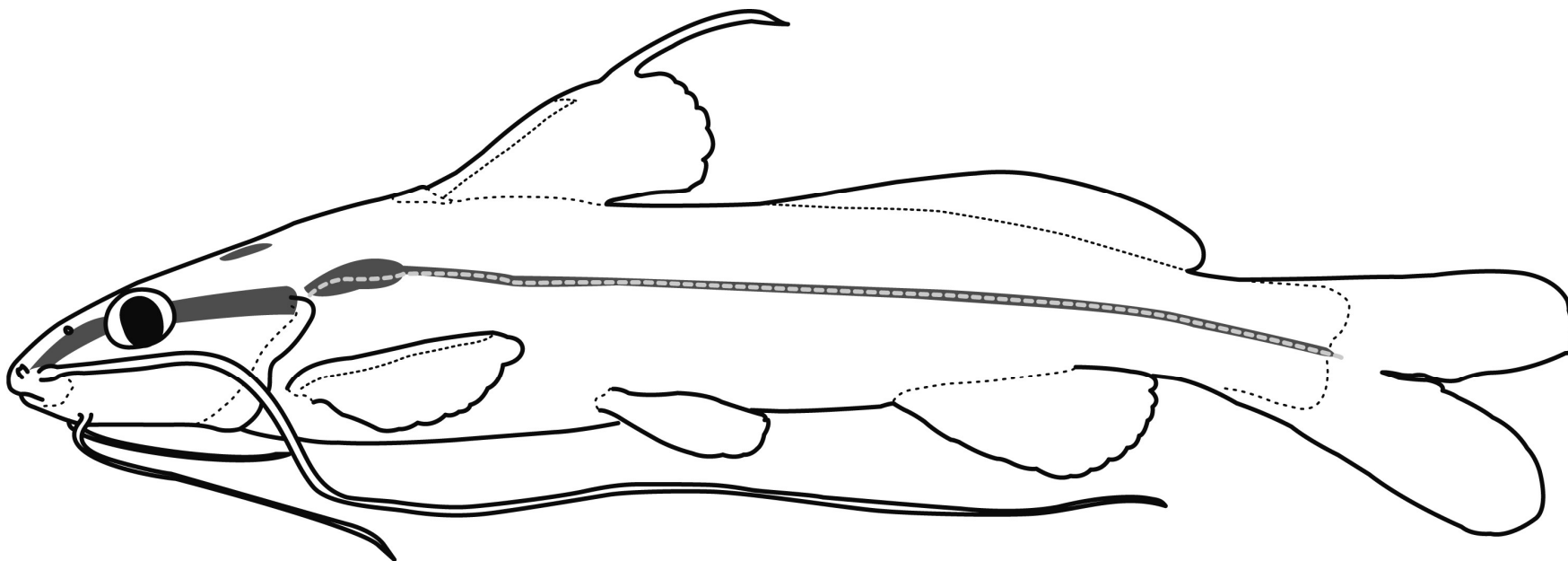


Figure 135. Schematic left lateral view of *Pimelodella martinezi*.

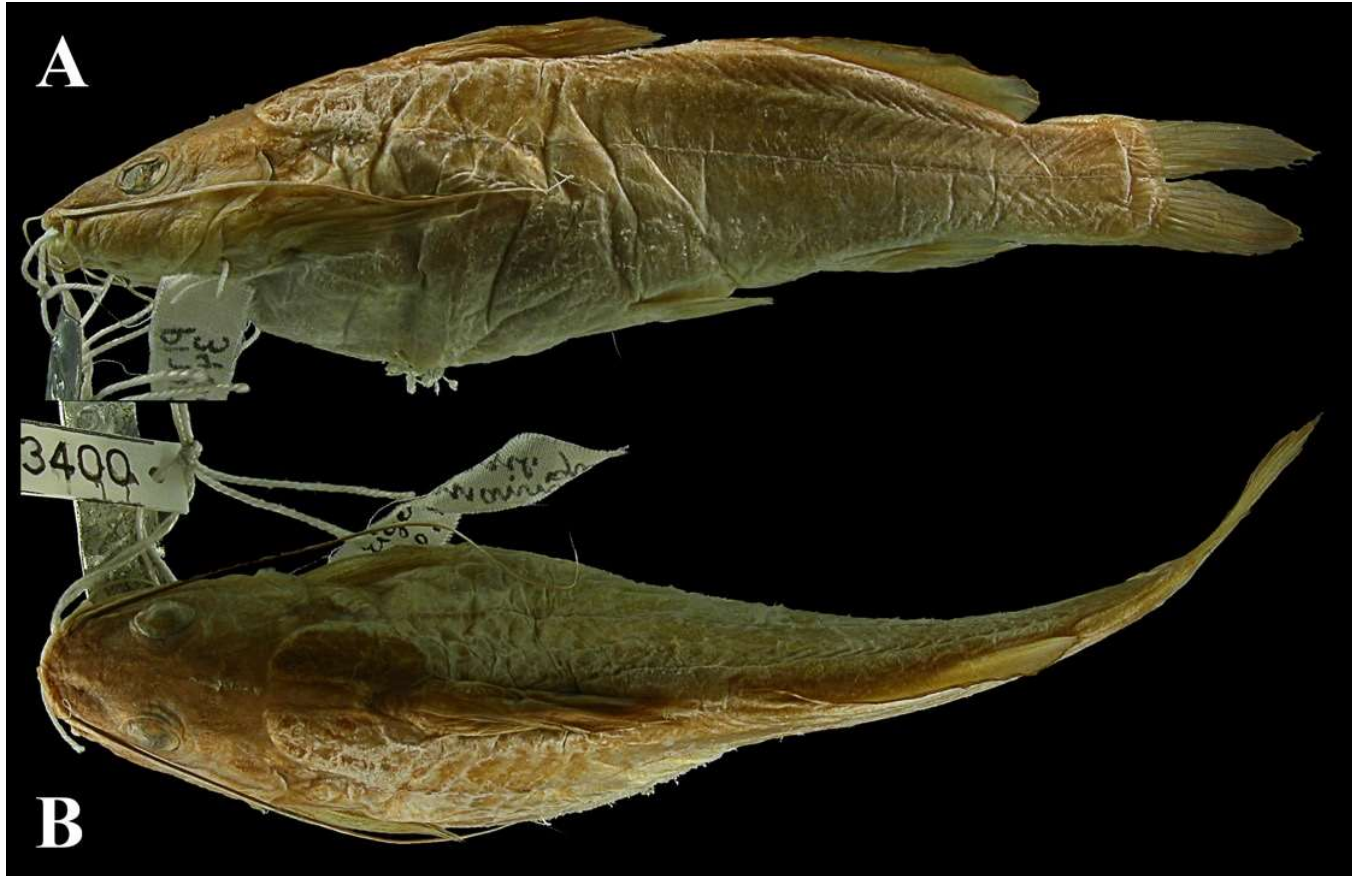


Figure 136. *Pimelodella meeki*, holotype, FMNH 3400, 100.2 mm SL. Left lateral (A) and dorsal (B) views. Photo taken by M. W. Littmann.

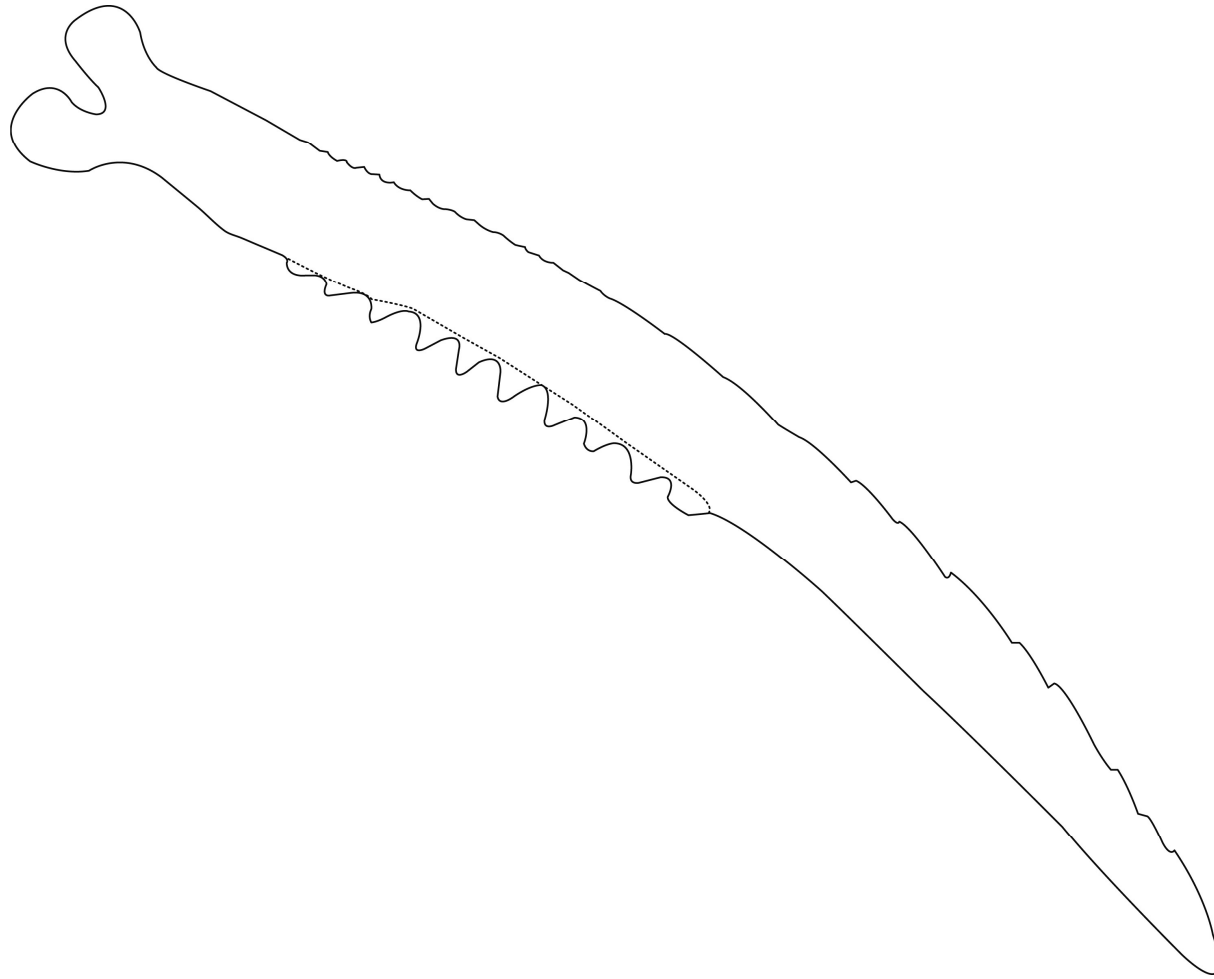


Figure 137. Ventral view of left pectoral-fin spine of *Pimelodella meeki*, FMNH 57993, 97.1 mm SL, total length of spine 12 mm.

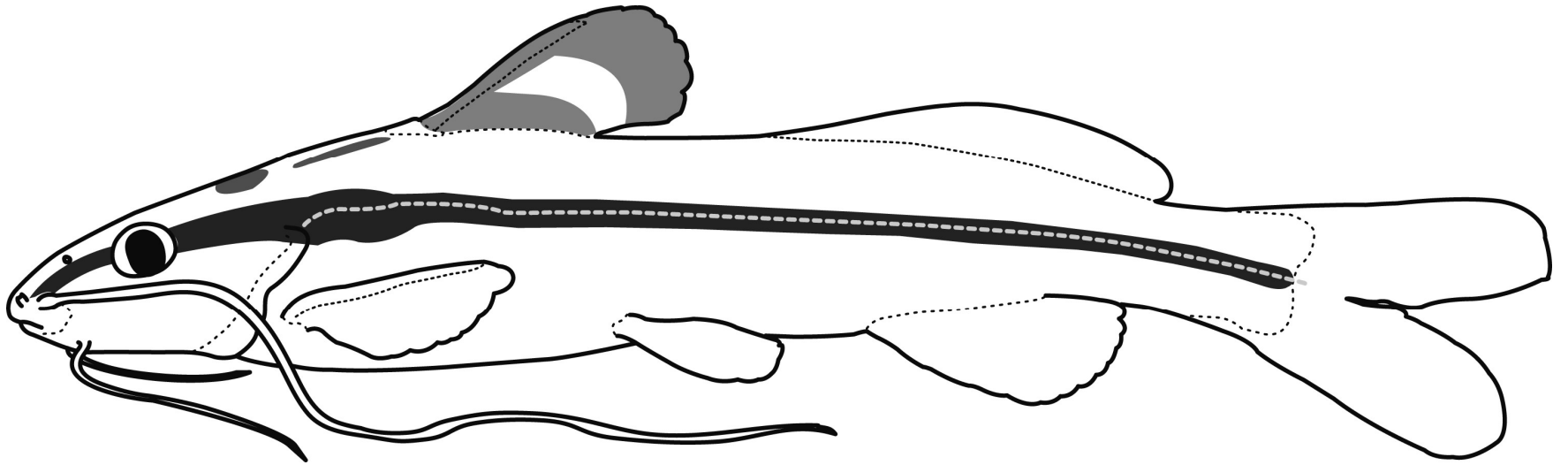


Figure 138. Schematic left lateral view of *Pimelodella meeki*.



Figure 139. *Pimelodella meeki*, MZUSP 51651, 112.2 mm SL. Left lateral (A) and dorsal (B) views. Photo taken by Murilo Pastana.



Figure 140. *Pimelodella rudolphi*, lectotype, MNRJ 857A, 73.9 mm SL. . Left lateral (A) and dorsal (B) views.



Figure 141. *Pimelodella megalops*, FMNH 53231, holotype, 74.7 mm SL. Left lateral (A) and dorsal (B) views. Photo taken by M. W. Littmann.

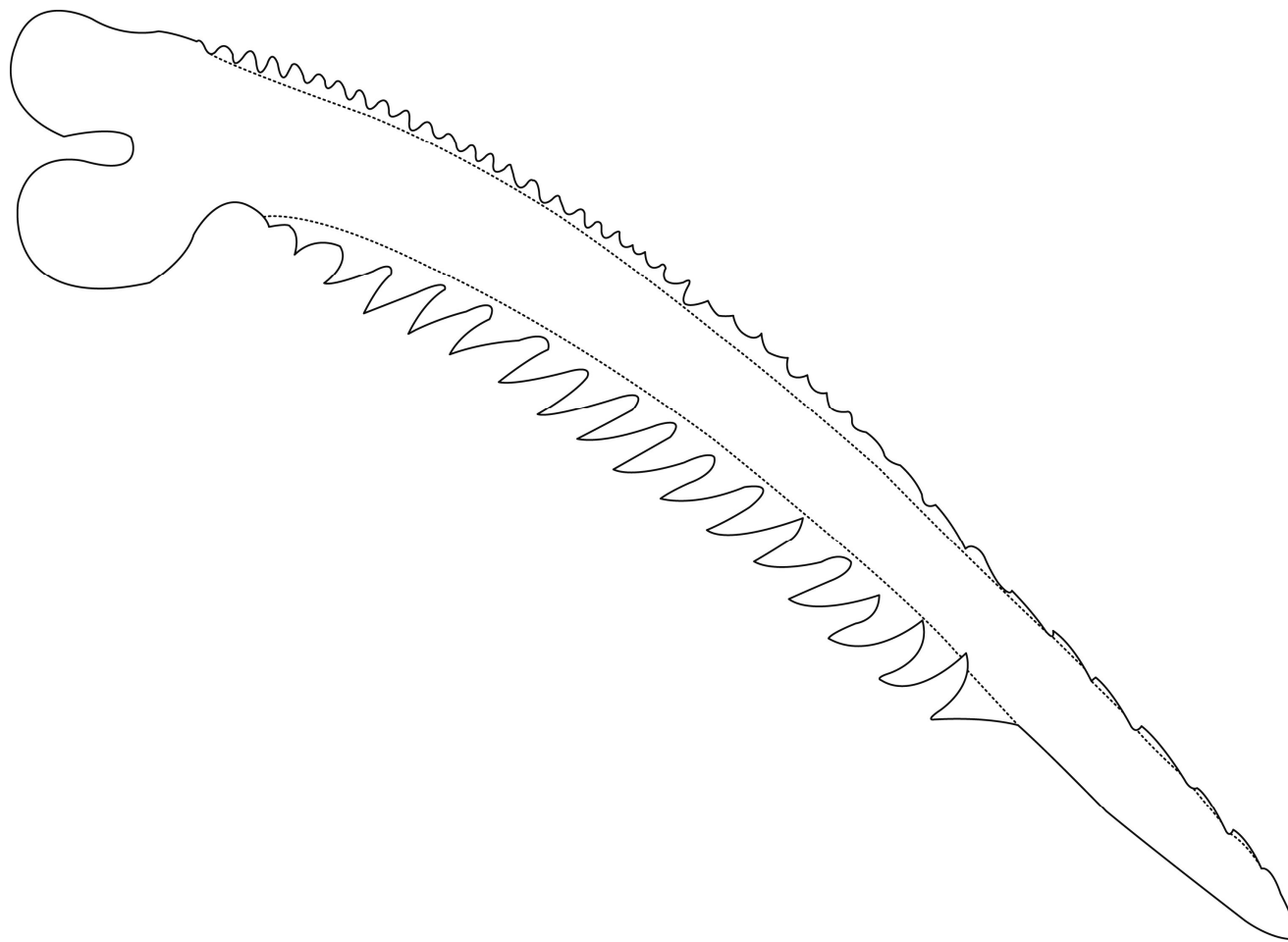


Figure 142. Ventral view of left pectoral-fin spine of *Pimelodella megalops*, BMNH 1911.10.31.51, paratype, 67.5 mm SL, total length of spine 13.1 mm.

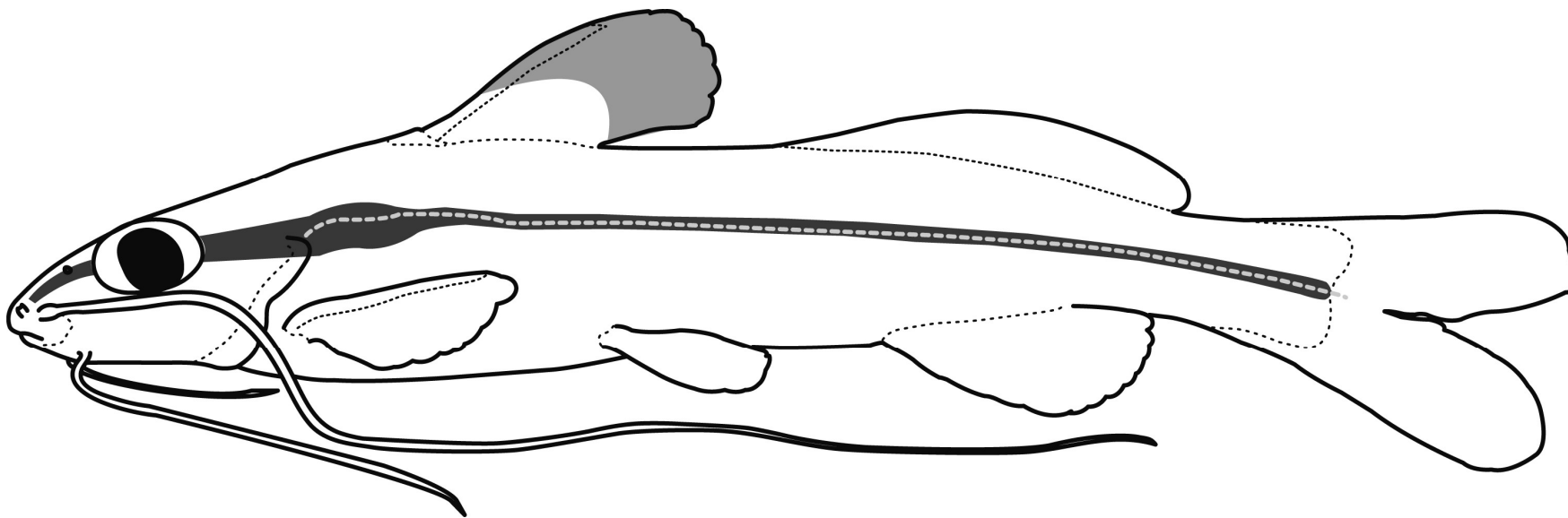


Figure 143. Schematic left lateral view of *Pimelodella megalops*.

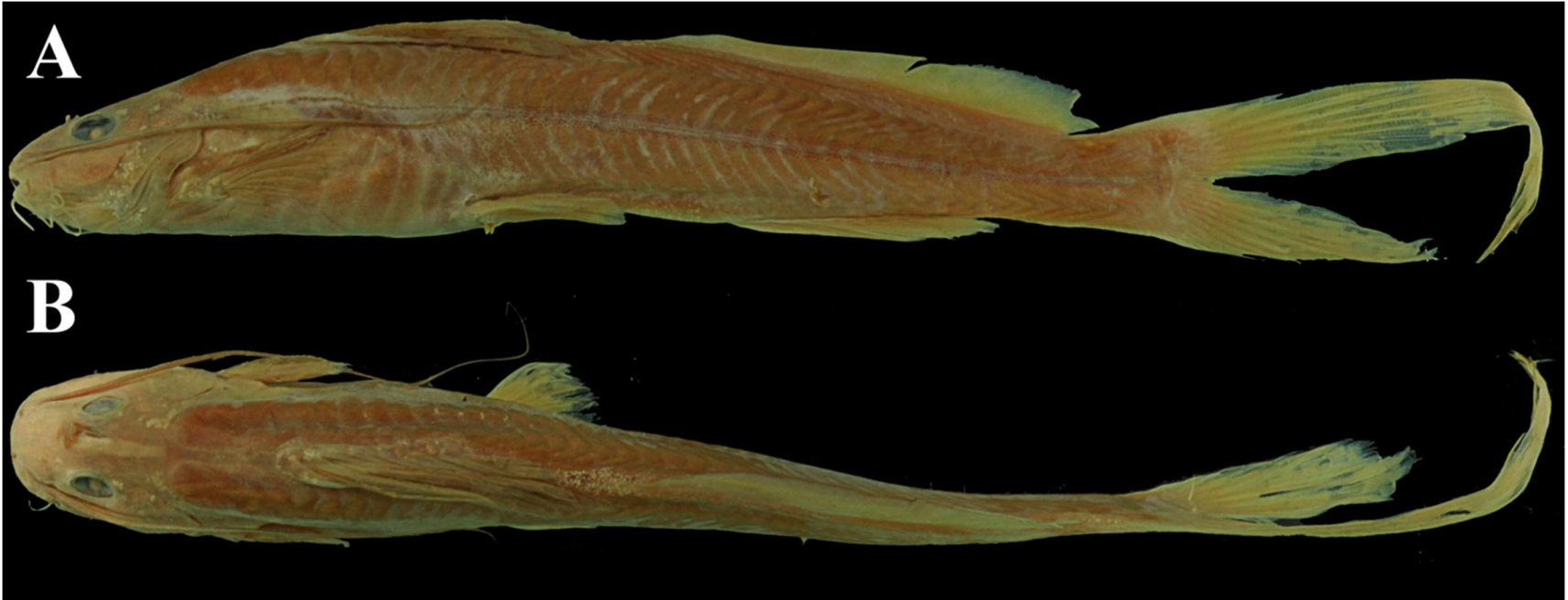


Figure 144. *Pimelodella megalura*, MNRJ 865A, lectotype, 128.6 mm SL. Left lateral (A) and dorsal (B) views.

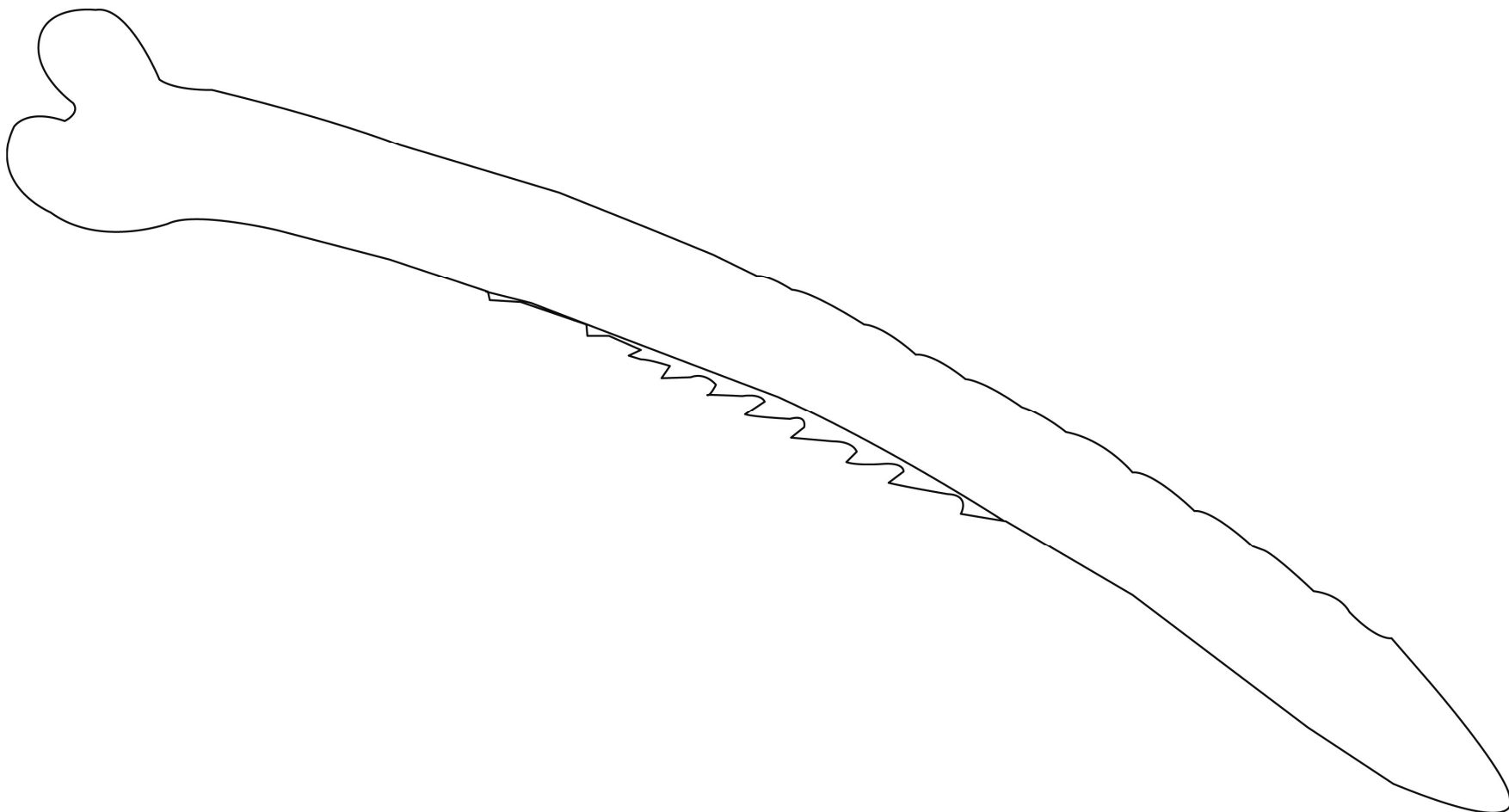


Figure 145. Ventral view of left pectoral-fin spine of *Pimelodella megahura*, MNRJ 865A, lectotype, 128.6 mm SL, total length of spine 15.2 mm.

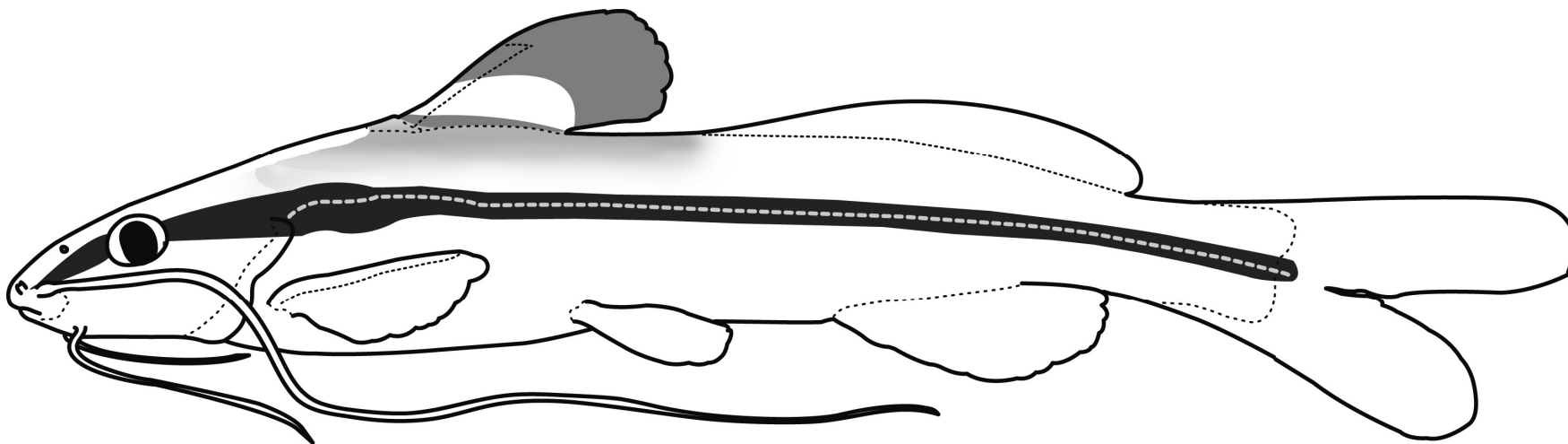


Figure 146. Schematic left lateral view of *Pimelodella megalura*.



Figure 147. *Pimelodella metae*, FMNH 58441, holotype, 58.0 mm SL. Left lateral (A) and dorsal (B) views. Photo taken by M. W. Littmann.

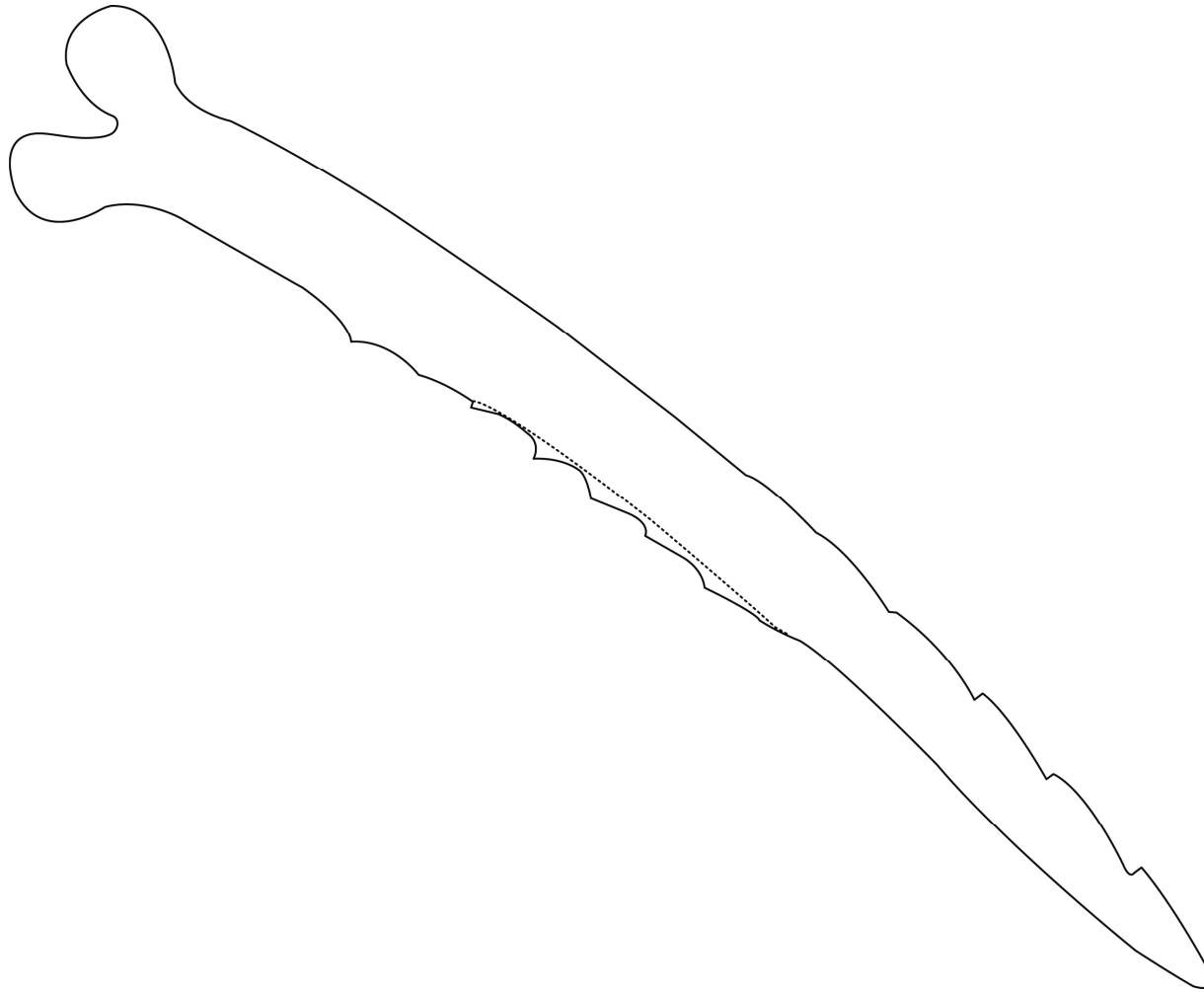


Figure 148. Ventral view of left pectoral-fin spine of *Pimelodella metae*, FMNH 58441, holotype, 58.0 mm SL, total length of spine 9.1 mm.

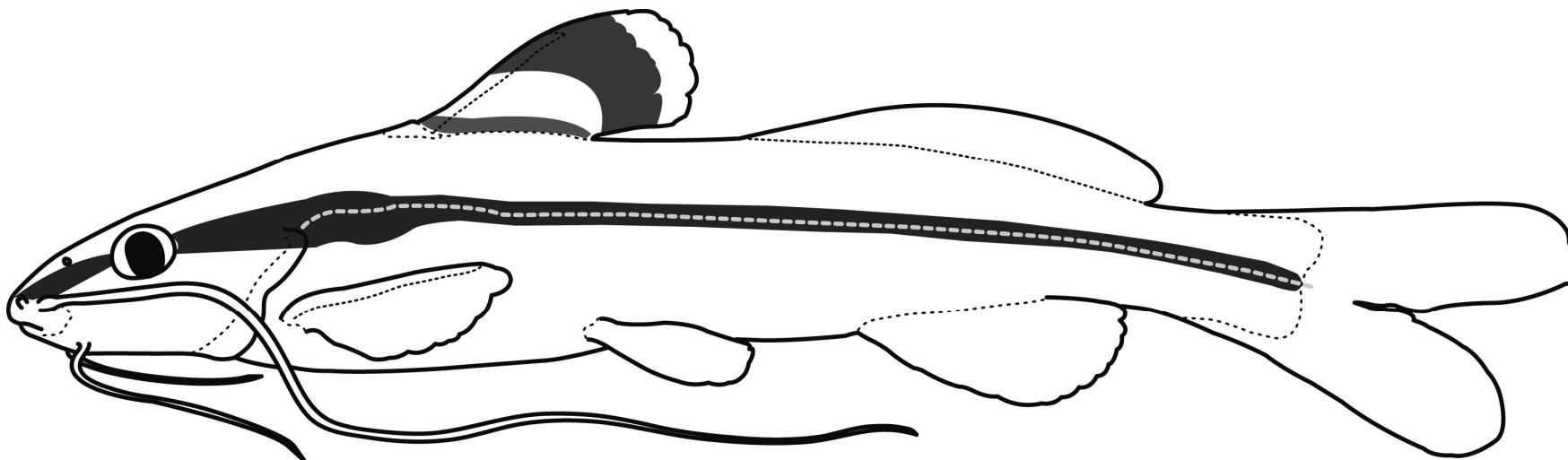


Figure 149. Schematic left lateral view of *Pimelodella metae*.



Figure 150. *Pimelodella modesta*, BMNH 1860.6.16.190, lectotype, 100.4 mm SL. Left lateral (A) and dorsal (B) views. Photo taken by Mark Allen.

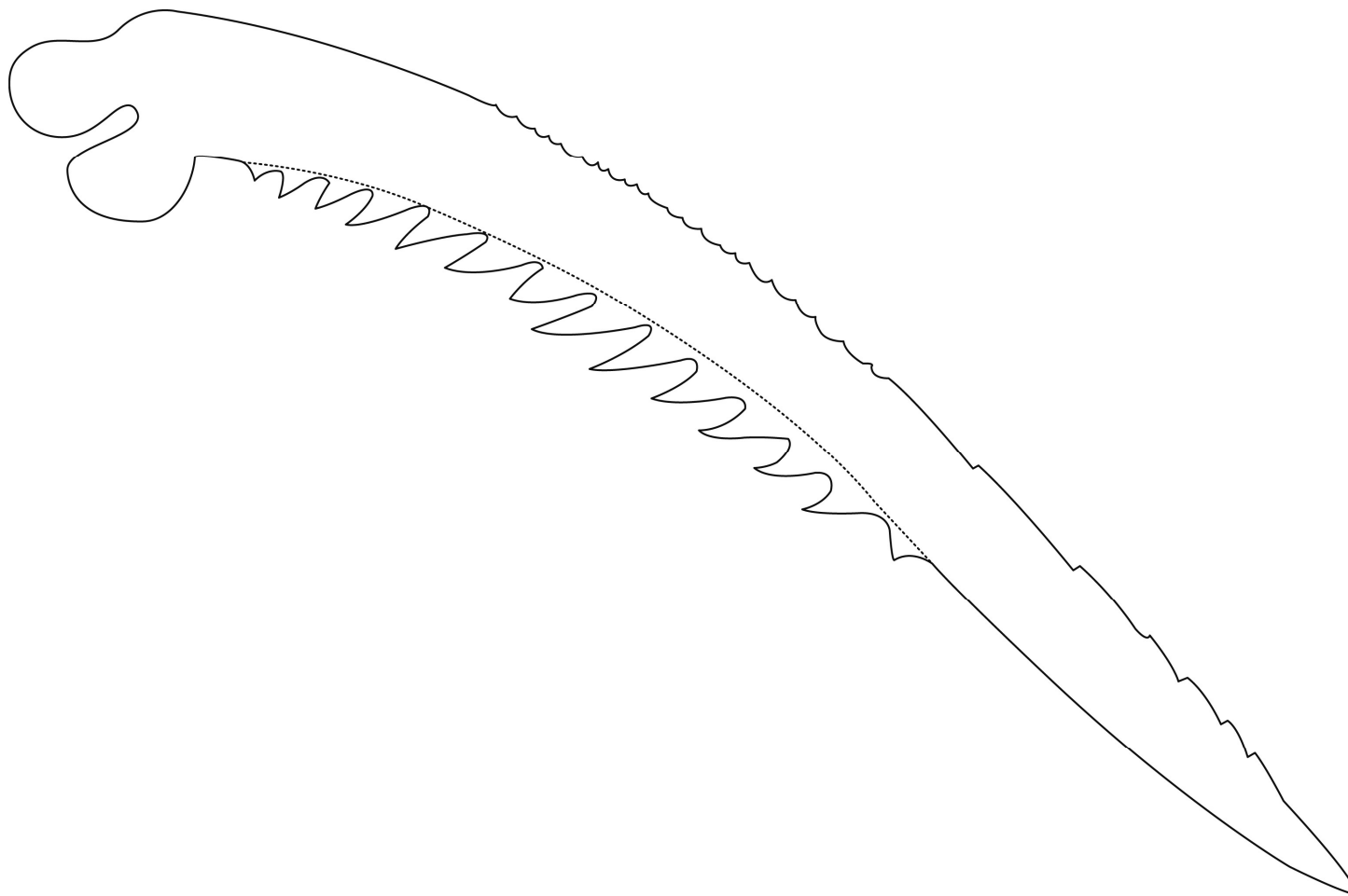


Figure 151. Ventral view of left pectoral-fin spine of *Pimelodella modesta*, BMNH 1860.6.16.190, lectotype, 100.4 mm SL, total length of spine 14.8 mm.

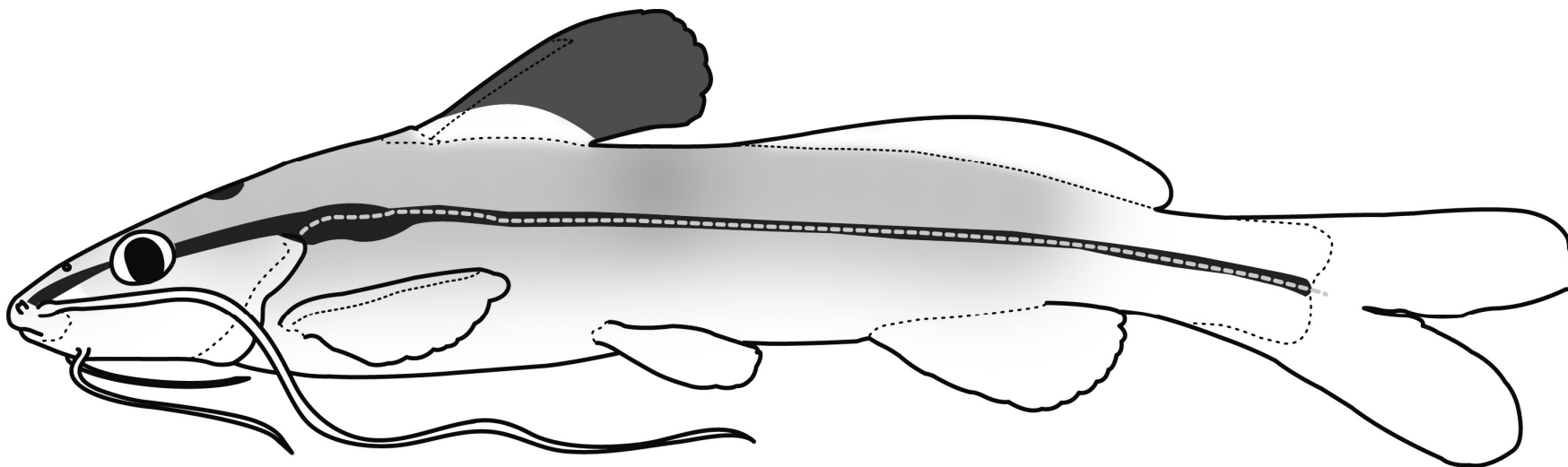


Figure 152. Schematic left lateral view of *Pimelodella modesta*.



Figure 153. *Pimelodella montana*, CAS 63719, lectotype, 87.4 mm SL. Left lateral (A) and dorsal (B) views. Photo taken by CAS staff.

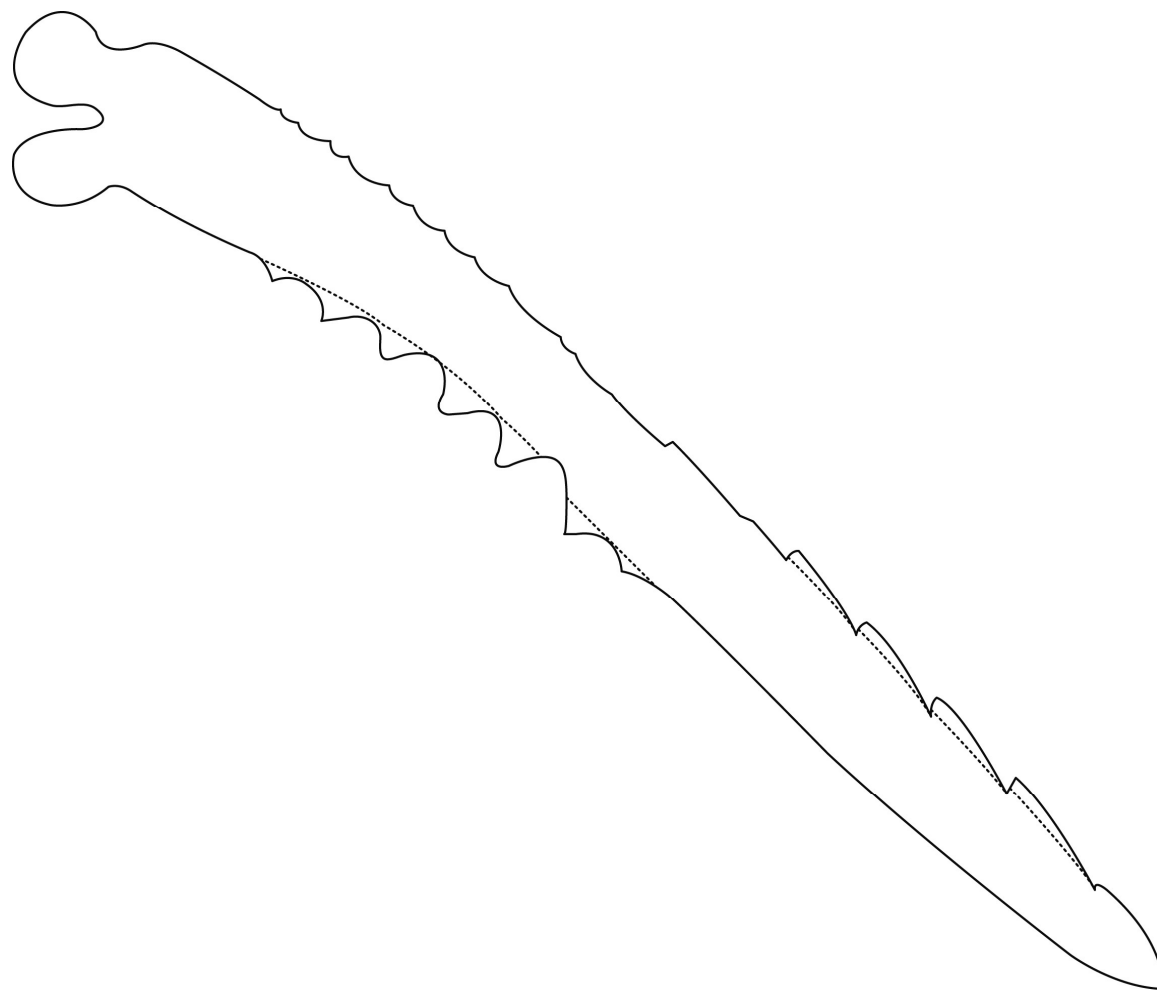


Figure 154. Ventral view of left pectoral-fin spine of *Pimelodella montana*, CAS 63719, paralectotype, 85 mm SL, total length of spine 11 mm.

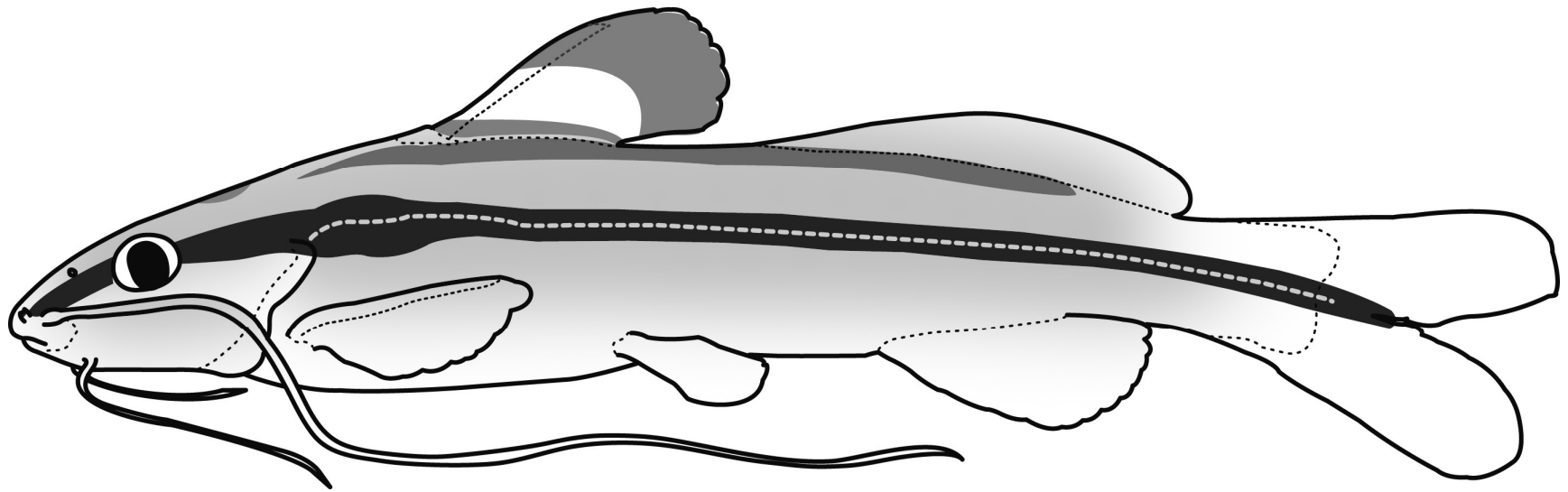


Figure 155. Schematic left lateral view of *Pimelodella montana*.



Figure 156. *Pimelodella mucosa*, CAS 63720, holotype, 97.4 mm SL. Left lateral (A) and dorsal (B) views. Photo taken by CAS staff.

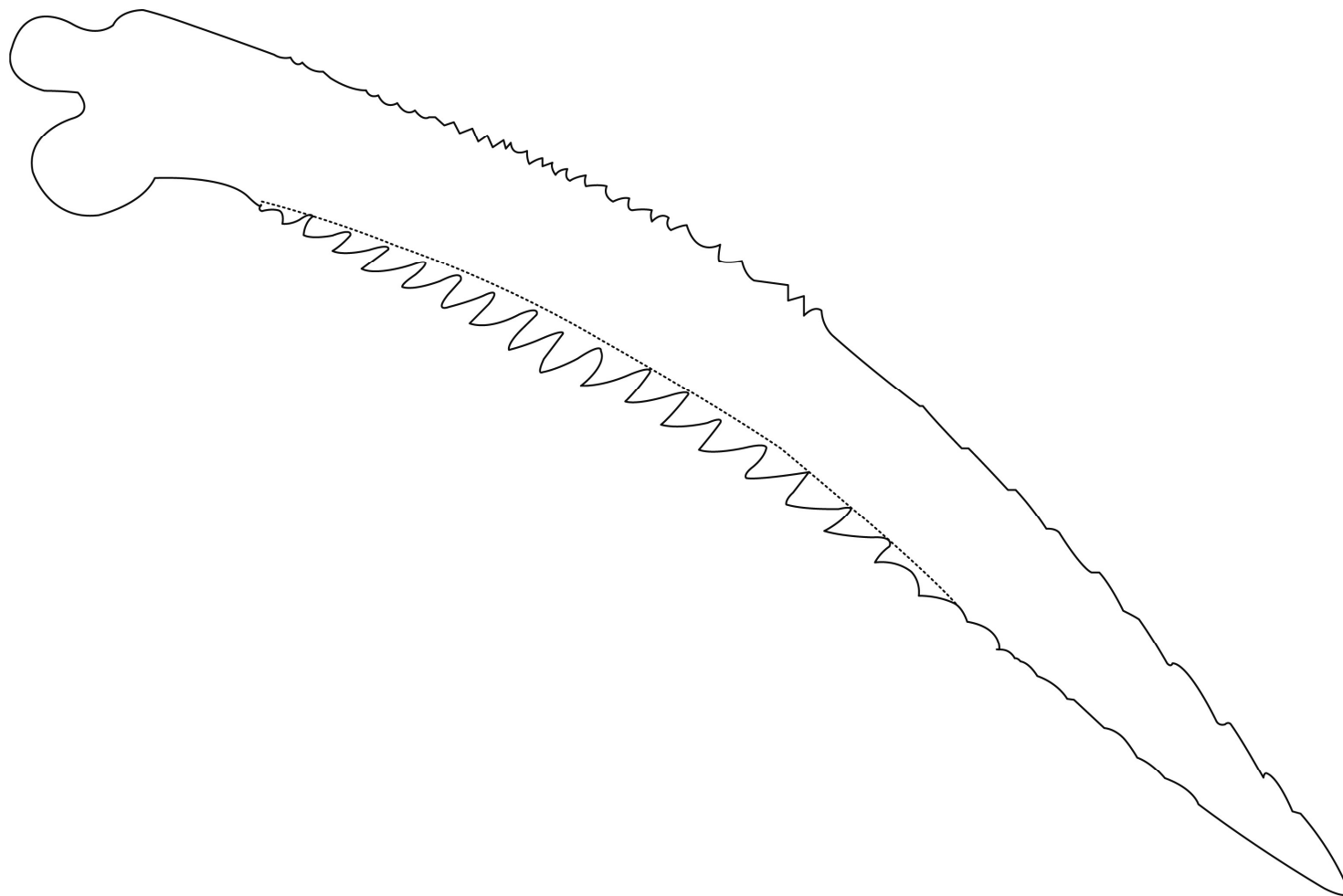


Figure 157. Ventral view of left pectoral-fin spine of *Pimelodella mucosa*, CAS 63720, holotype, 97.4 mm SL, total length of spine 22.8 mm.

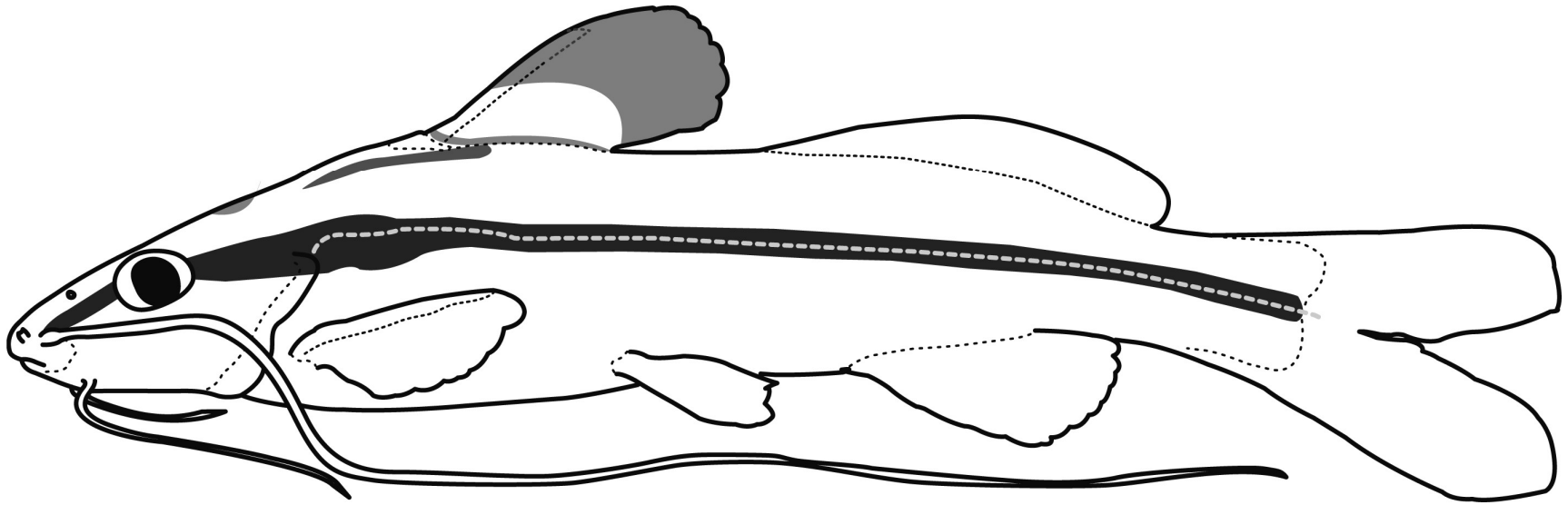


Figure 158. Schematic left lateral view of *Pimelodella mucosa*.



Figure 159. *Pimelodella notomelas*, FMNH 57967, holotype, 38.9 mm SL. Left lateral (A) and dorsal (B) views. Photo taken by M. W. Littmann.

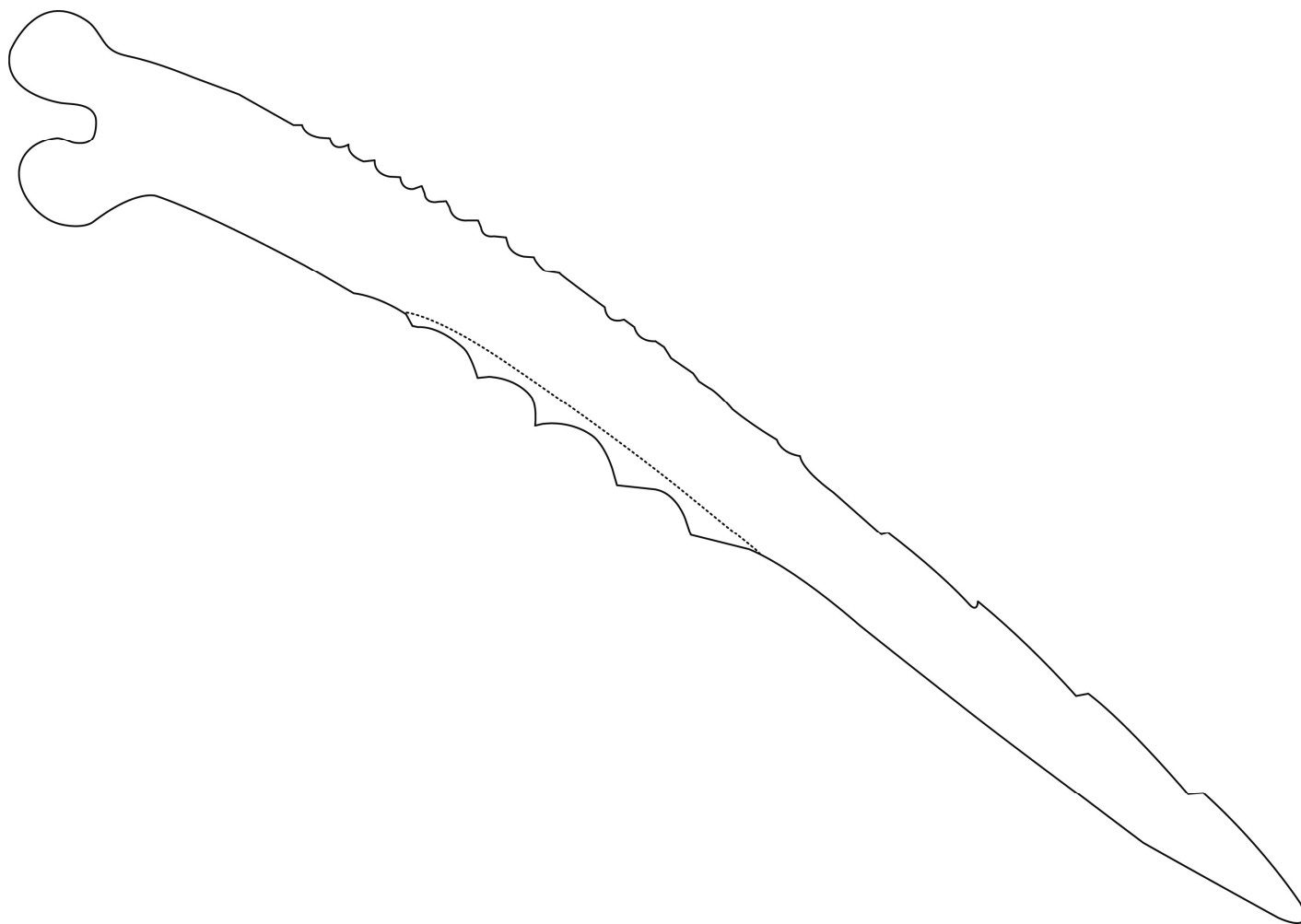


Figure 160. Ventral view of left pectoral-fin spine of *Pimelodella notomelas*, FMNH 57967, holotype, 38.9 mm SL, total length of spine 7.4 mm.

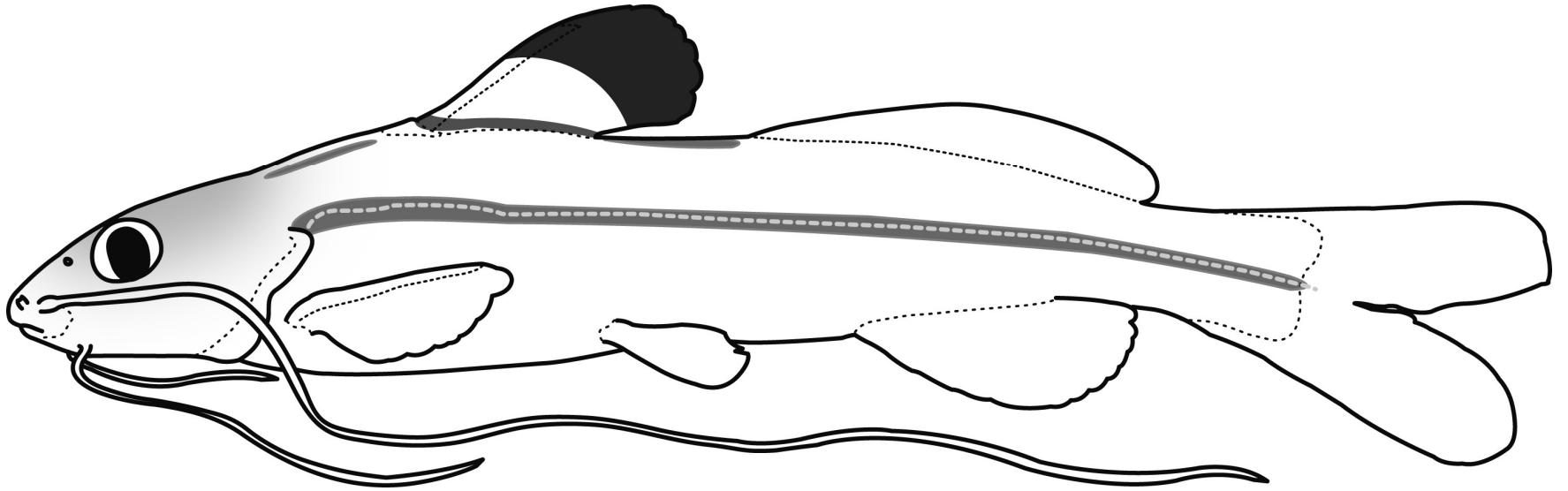


Figure 161. Schematic left lateral view of *Pimelodella notomelas*.



Figure 162. *Pimelodella odynea*, USNM 121133, holotype, 88.3 mm SL. Left lateral (A) and dorsal (B) views. Photo taken by Sandra Raredon.

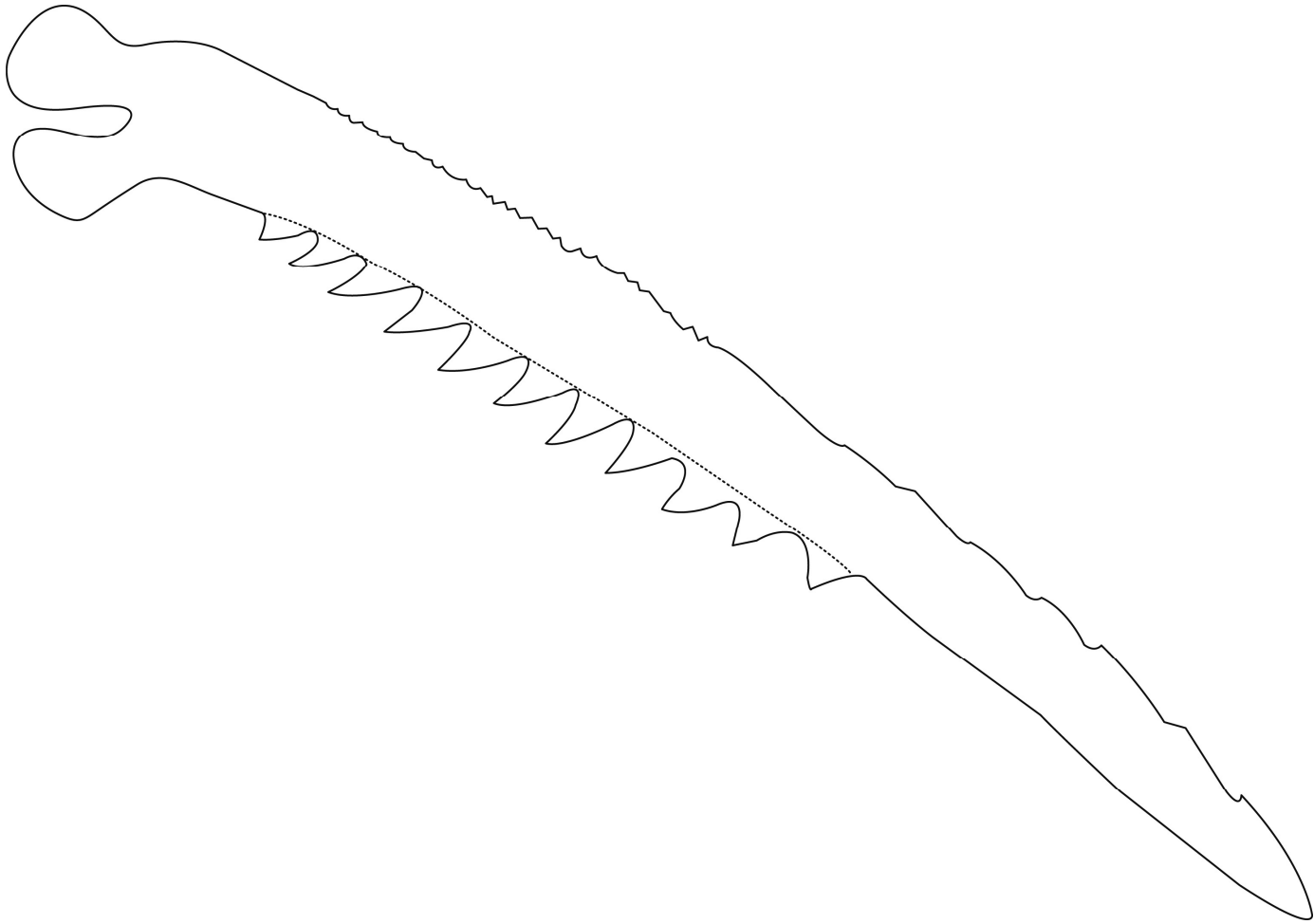


Figure 163. Ventral view of left pectoral-fin spine of *Pimelodella odynea*, USNM 121133, holotype, 88.3 mm SL, total length of spine 12.9 mm.

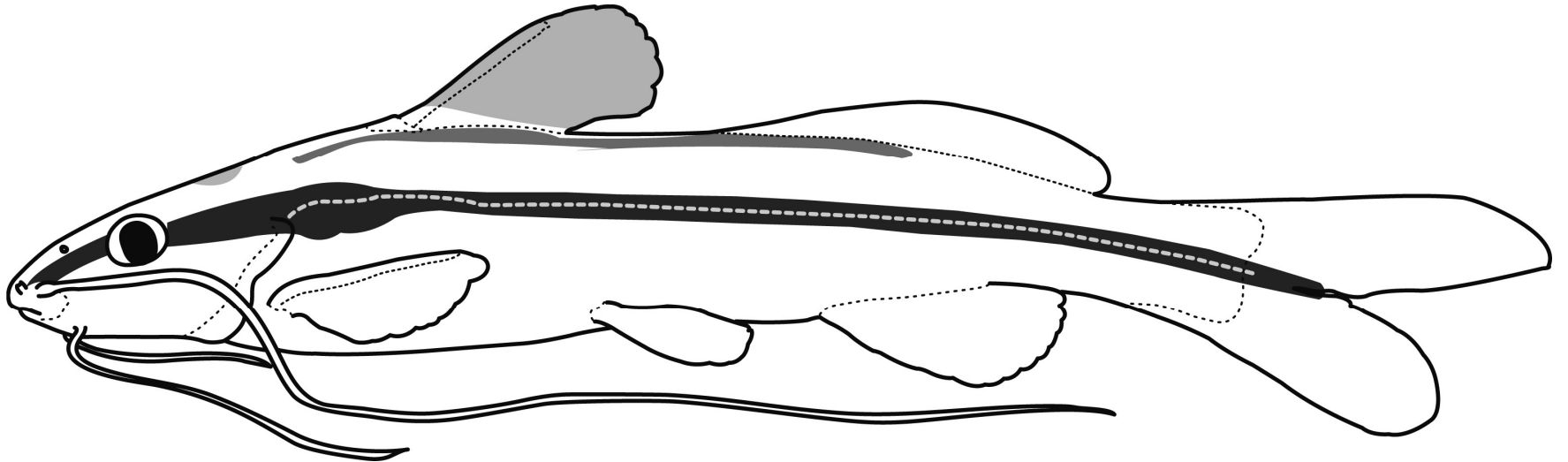


Figure 164. Schematic left lateral view of *Pimelodella odynea*.



Figure 165. *Pimelodella pectinifera*, holotype, MCZ 7508, 150.9 mm SL. Left lateral (A) and dorsal (B) views. Photo taken by MCZ staff.

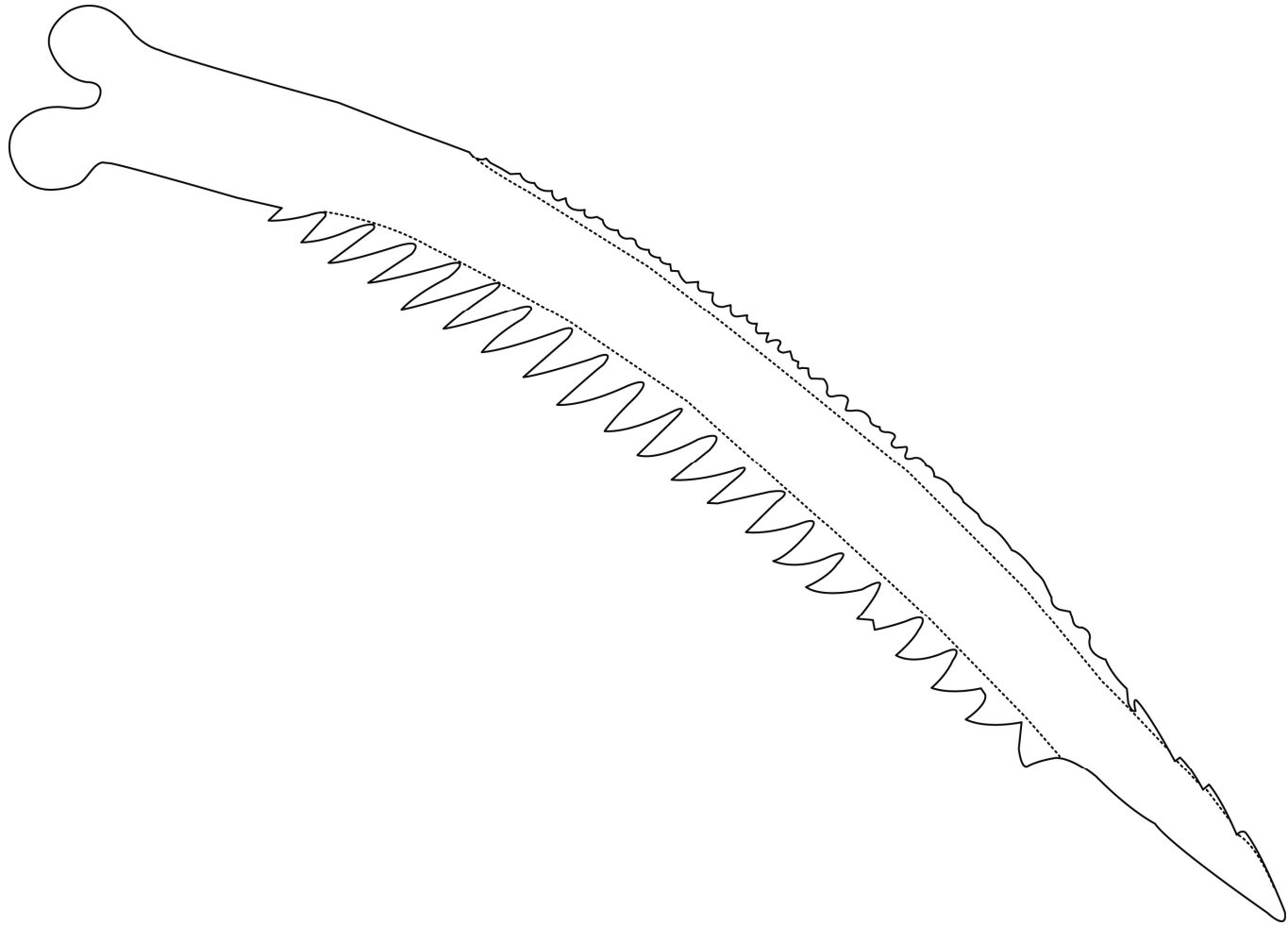


Figure 166. Ventral view of left pectoral-fin spine of *Pimelodella pectinifera*, holotype, MCZ 7508, 150.9 mm SL, total length of spine 31.4 mm.

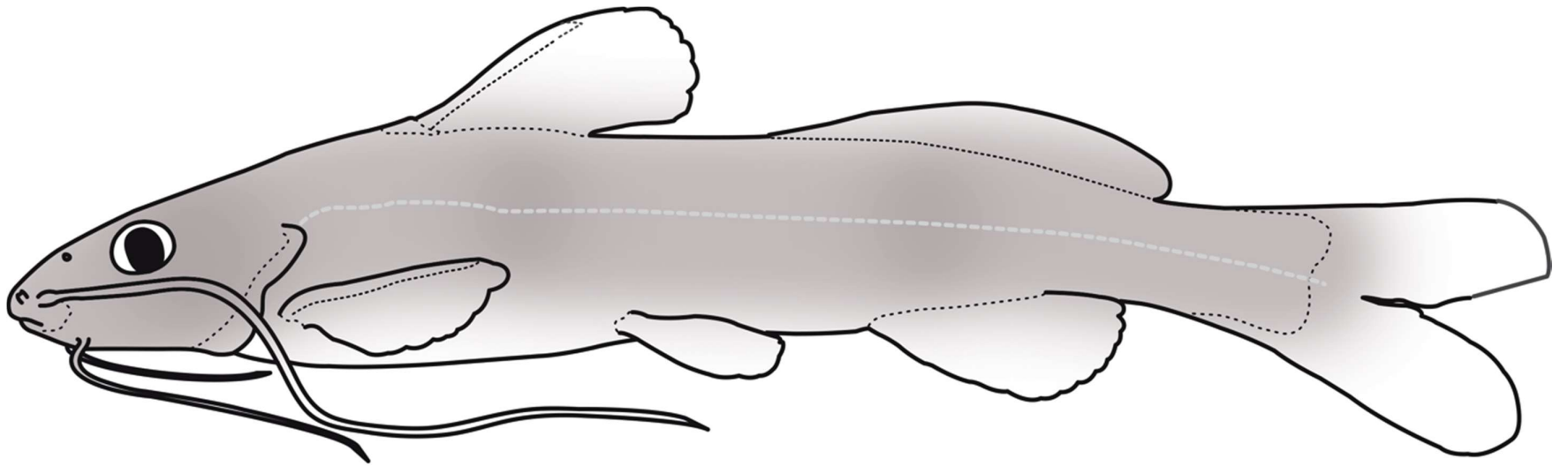


Figure 167. Schematic left lateral view of *Pimelodella pectinifera*.



Figure 168. *Pimelodella peruana*, holotype, CAS 63721, 40.3 mm SL. Left lateral (A) and dorsal (B) views. Photo taken by CAS staff.

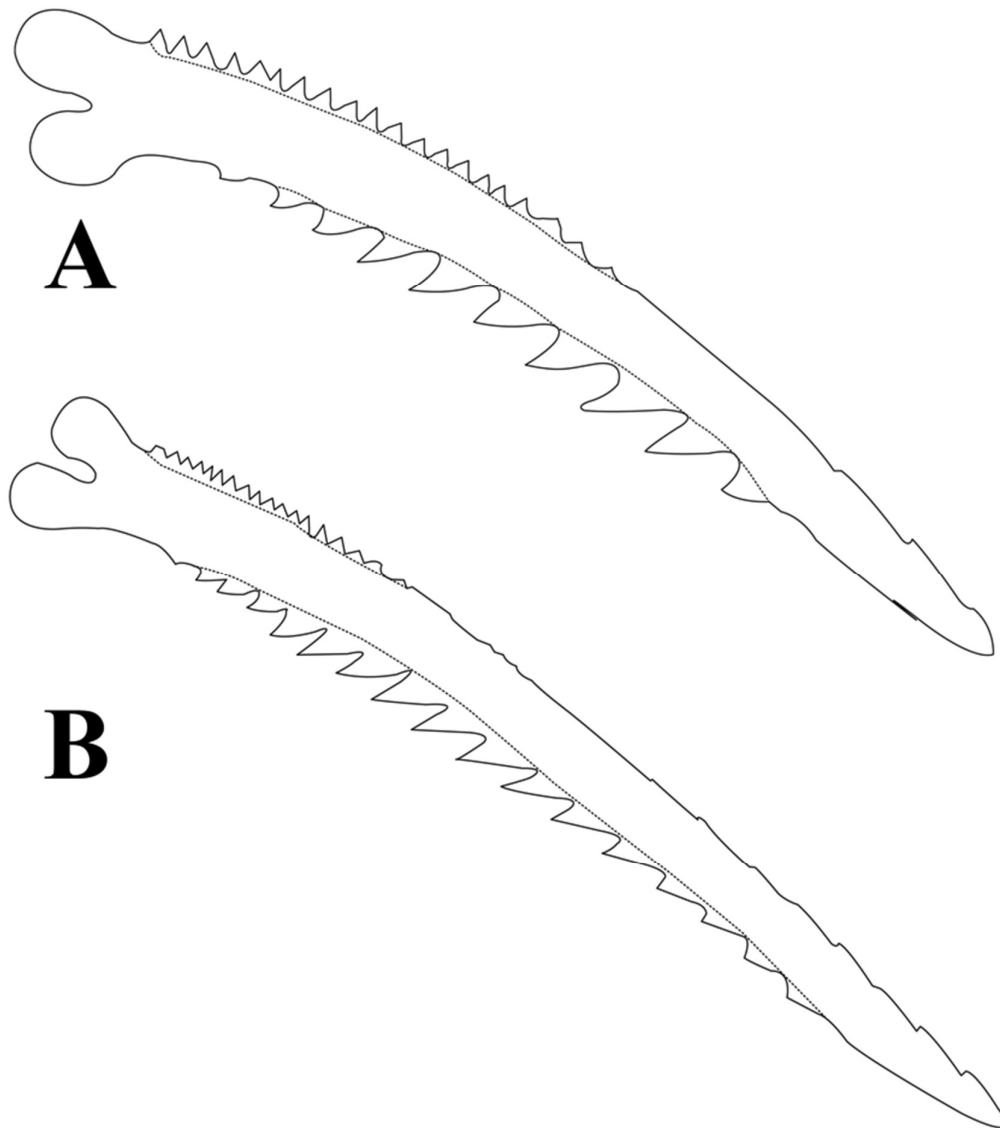


Figure 169. Ventral view of left pectoral-fin spine of *Pimelodella peruana*: (A) holotype, CAS 63721, 40.3 mm SL, total length of spine 6.3 mm; (B) FMNH 102541, 69.9 mm SL, total length of spine 11.2 mm.

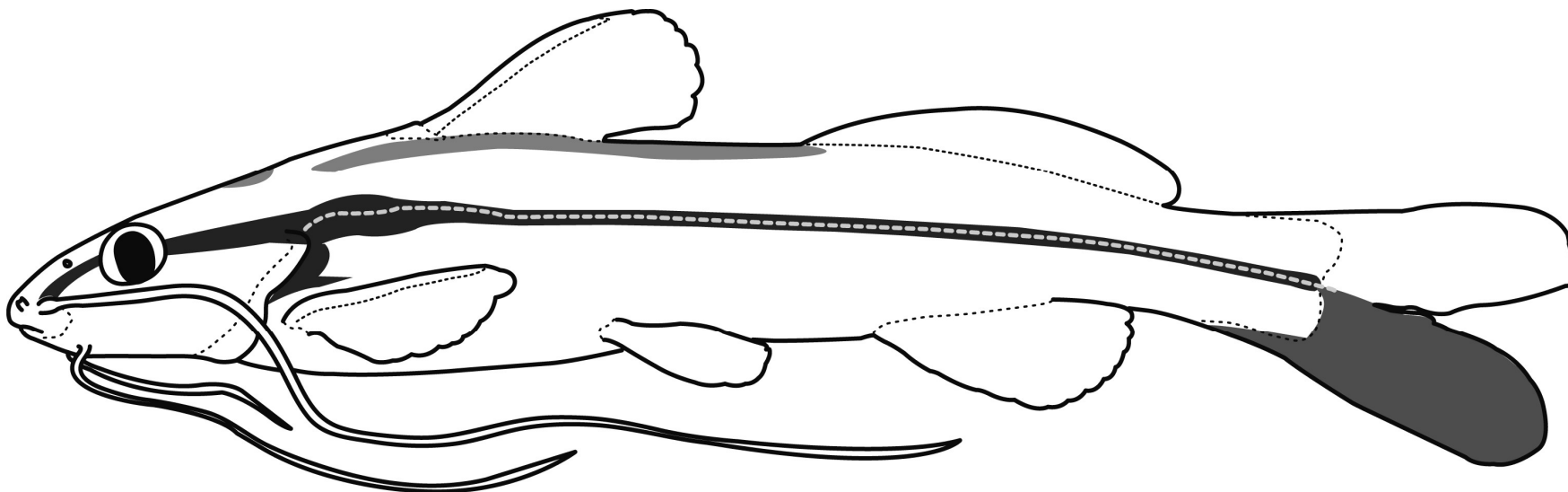


Figure 170. Schematic left lateral view of *Pimelodella peruana*.



Figure 171. *Pimelodella reyesi*, ICN-MHN 1331, 98.1 mm SL. Left lateral (A) and dorsal (B) views. Photo taken by Henry Zamora.

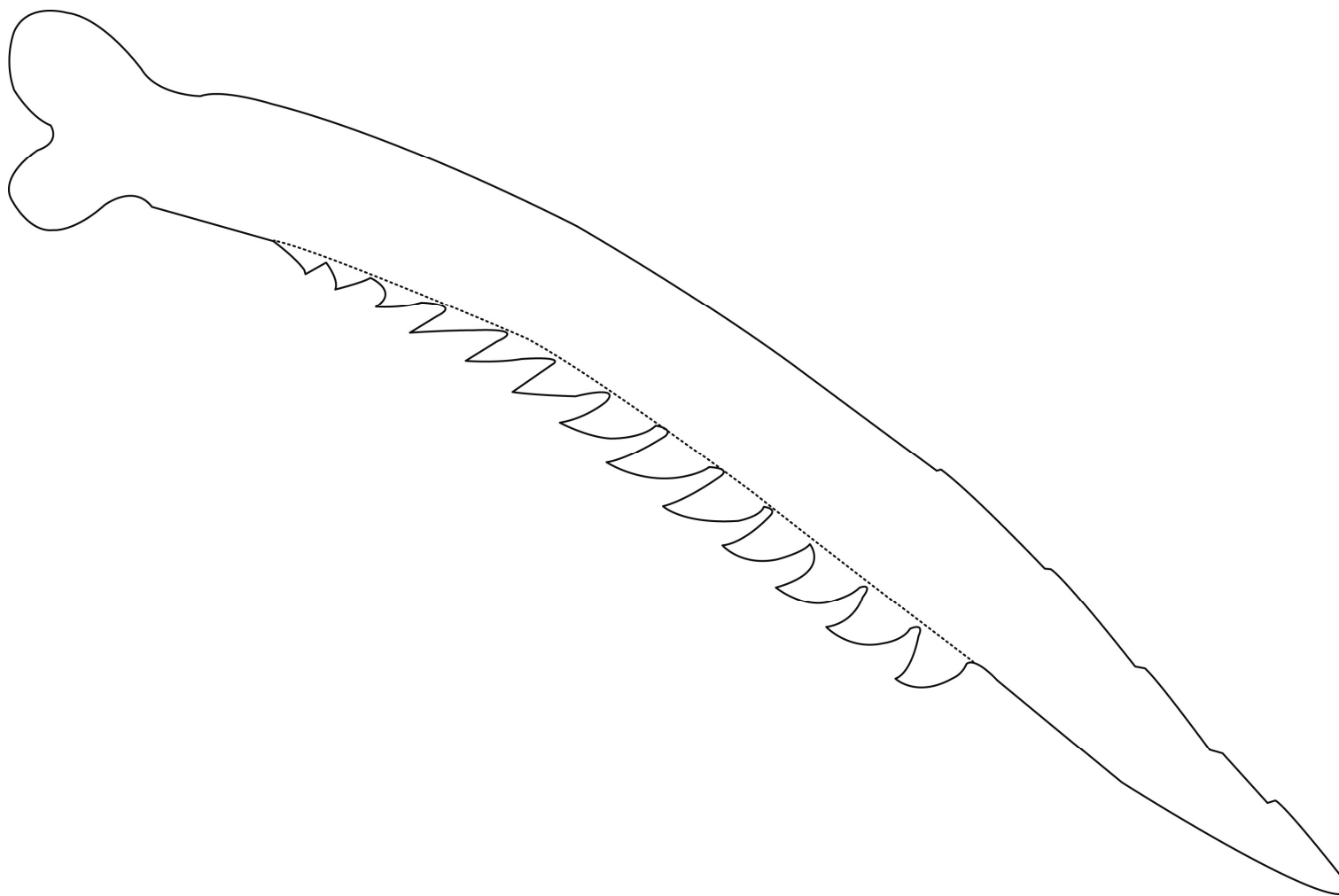


Figure 172. Ventral view of left pectoral-fin spine of *Pimelodella reyesi*, ICN-MHN 1331, 98.1 mm SL, total length of spine 18.6 mm.

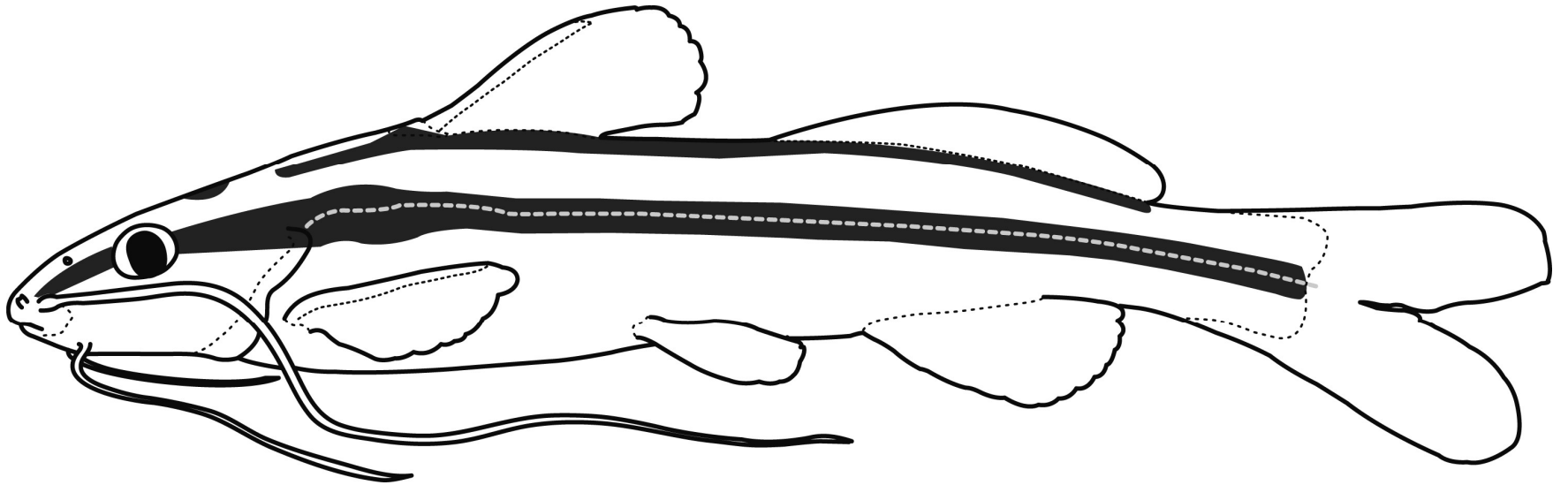


Figure 173. Schematic left lateral view of *Pimelodella reyesi*.



Figure 174. *Pimelodella robinsoni*, holotype, ANSP 69386, 73 mm SL. Left lateral (A) and dorsal (B) views. Photo taken by Murilo Pastana.

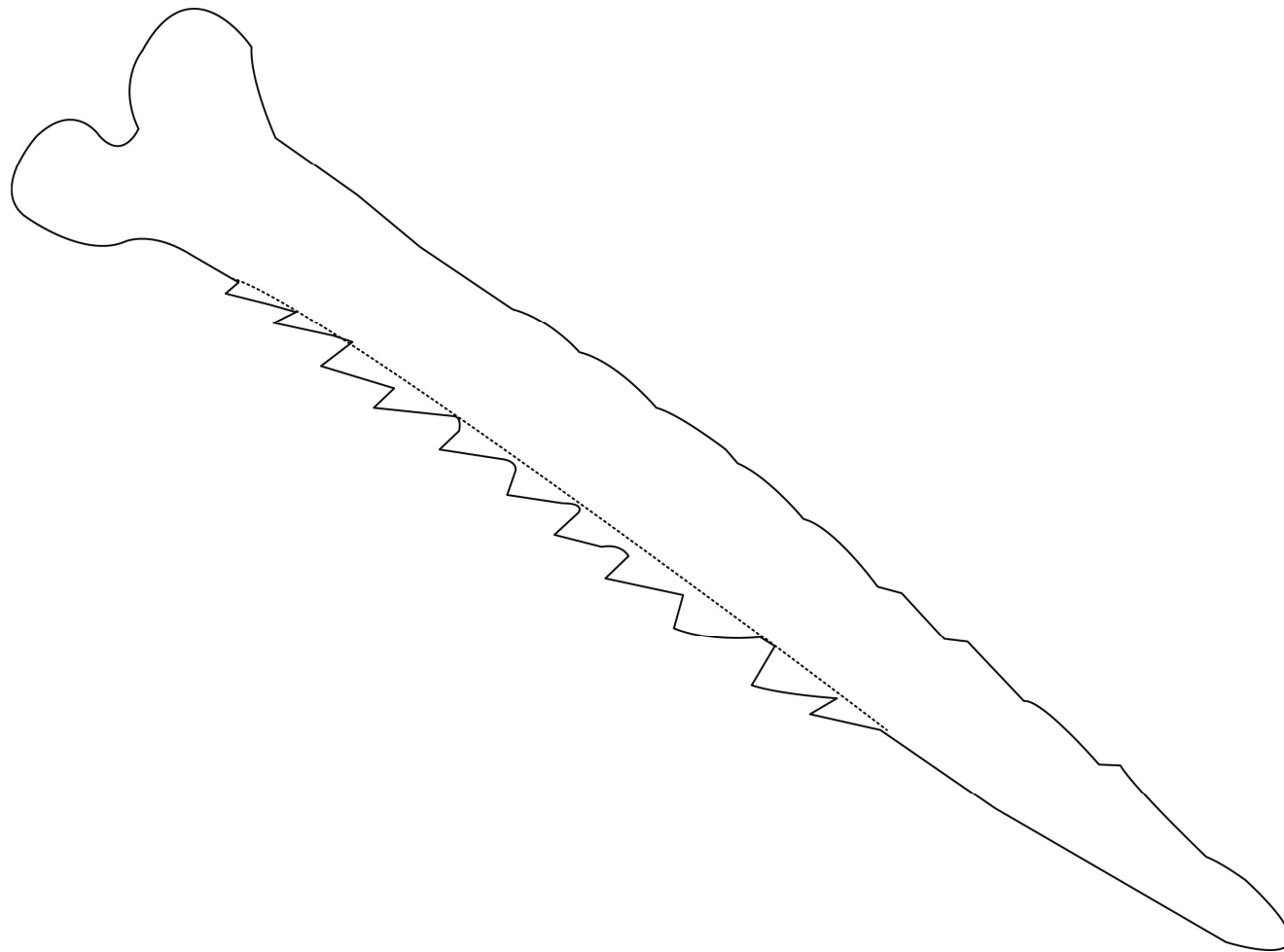


Figure 175. Ventral view of left pectoral-fin spine of *Pimelodella wolfi*, junior-synonym of *P. robinsoni*, holotype, ANSP 69388, 88.9 mm SL, total length of spine 11.3 mm SL.

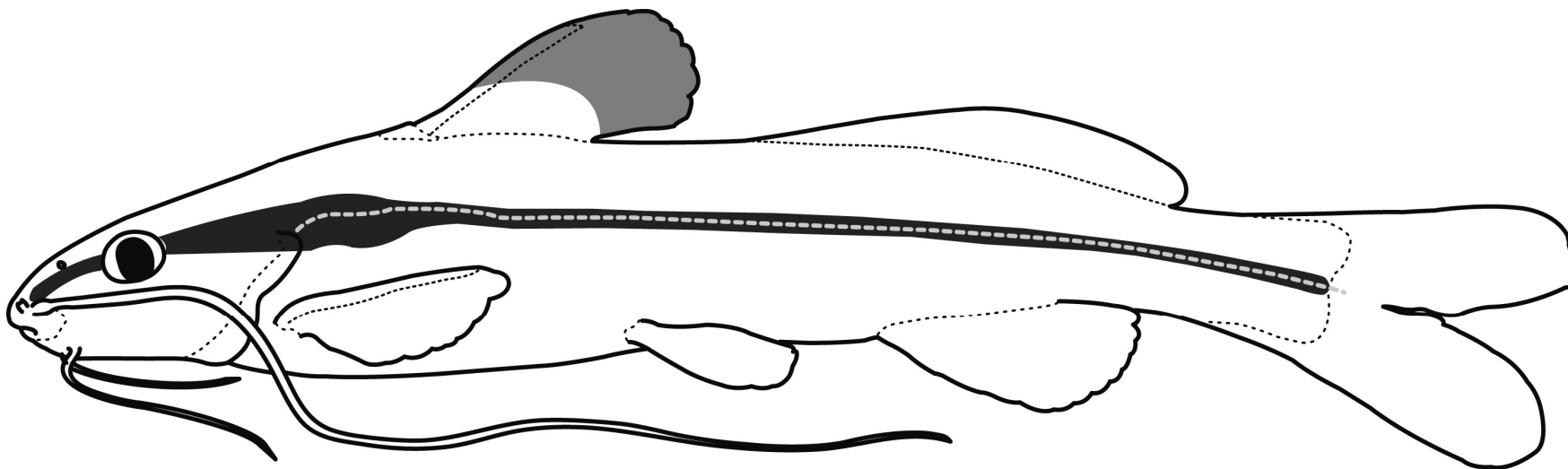


Figure 176. Schematic left lateral view of *Pimelodella robinsoni*.



Figure 177. *Pimelodella wolffi*, junior-synonym of *P. robinsoni*, holotype, ANSP 69388, 88.9 mm SL. Left lateral (A) and dorsal (B) views. Photo taken by Murilo Pastana.



Figure 178. *Pimelodella roccae*, holotype, MCZ 30975, 139.8 mm SL. Left lateral (A) and dorsal (B) views. Photo taken by MCZ staff.

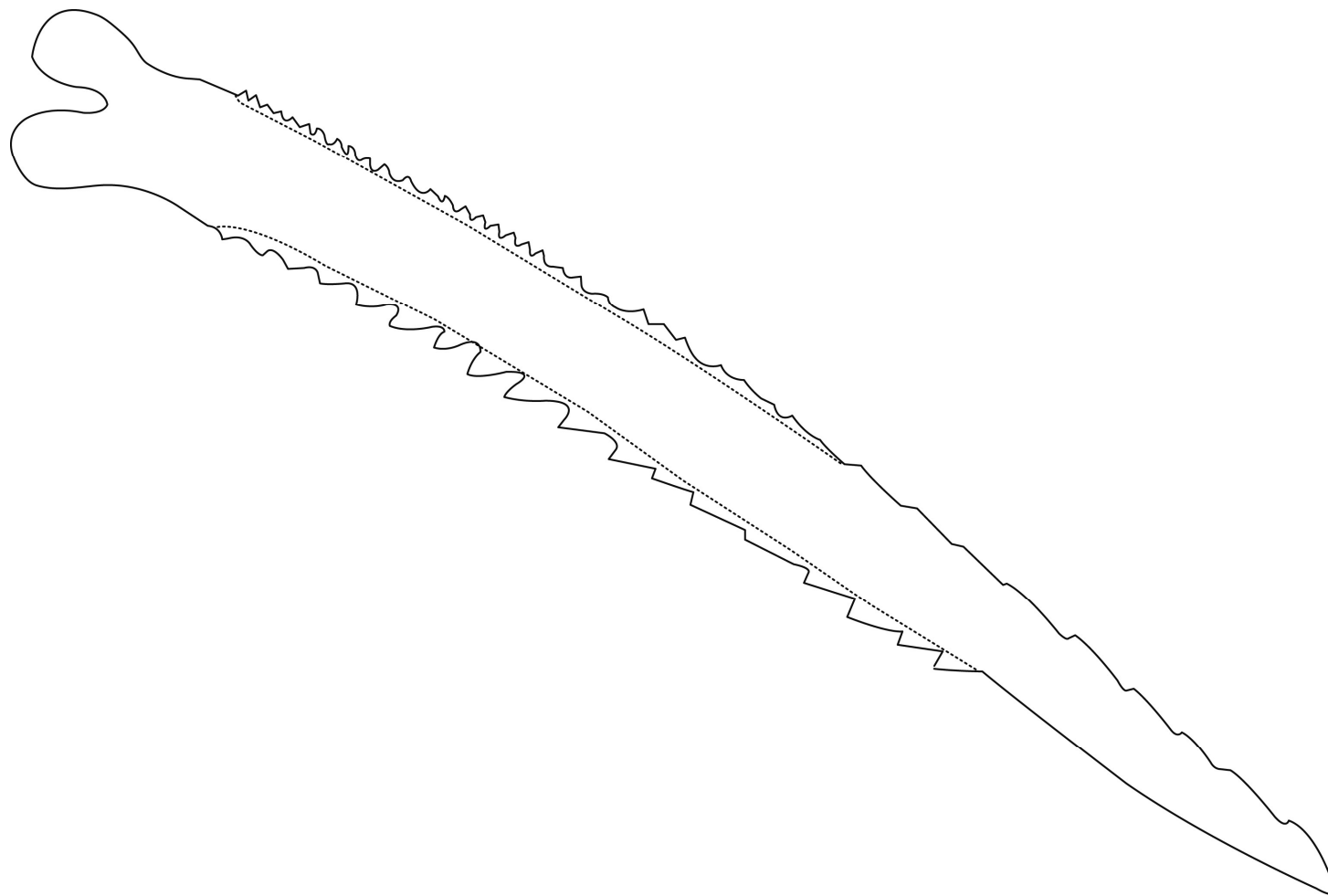


Figure 179. Ventral view of left pectoral-fin spine of *Pimelodella roccae*, holotype, MCZ 30975, 139.8 mm SL, total length of spine 23.8 mm.

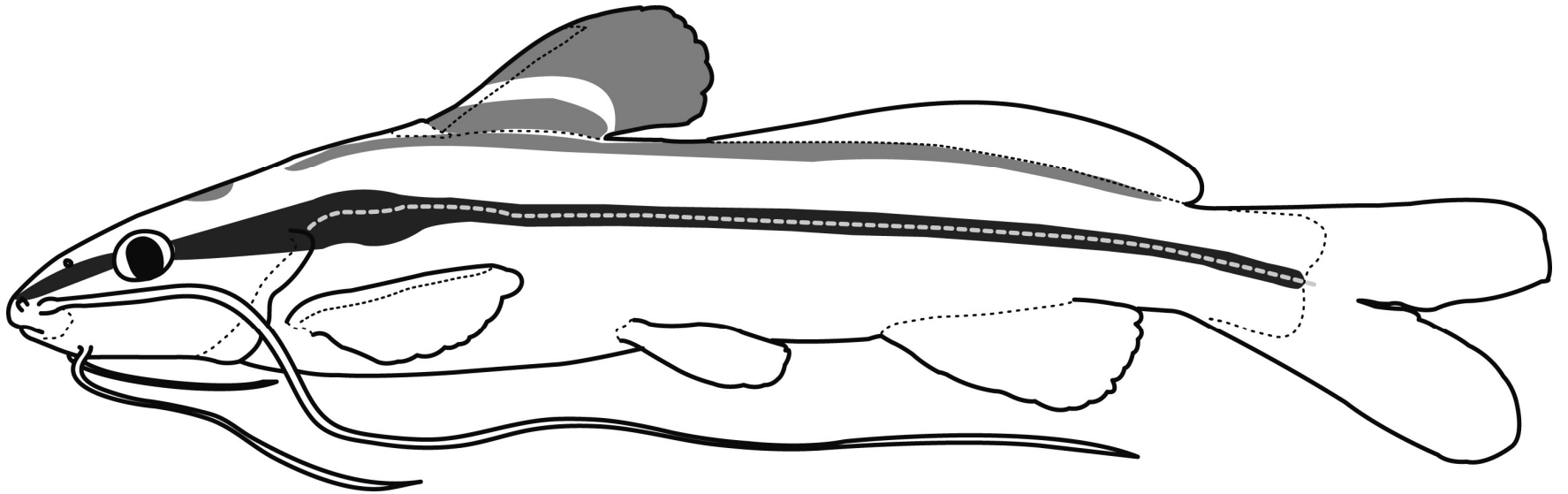


Figure 180. Schematic left lateral view of *Pimelodella rocae*.



Figure 181. *Pimelodella serrata*, holotype, FMNH 57979, 55.7 mm SL. Left lateral (A) and dorsal (B) views. Photo taken by M. W. Littmann.

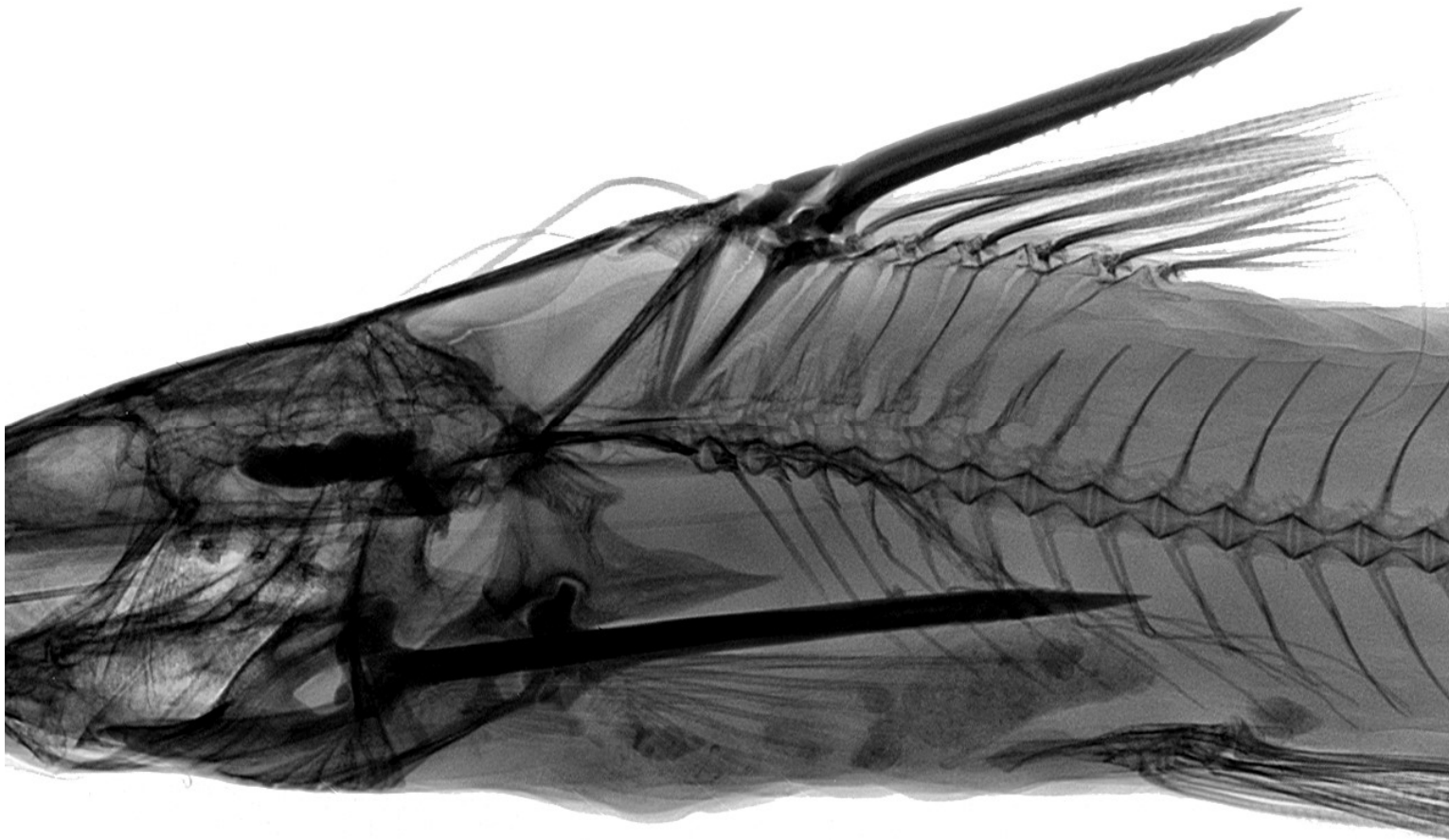


Figure 182. Left lateral detail of dorsal fin of *Pimelodella serrata*, UFRO-I 9739, 77.1 mm SL, to show dorsal-fin spine morphology.

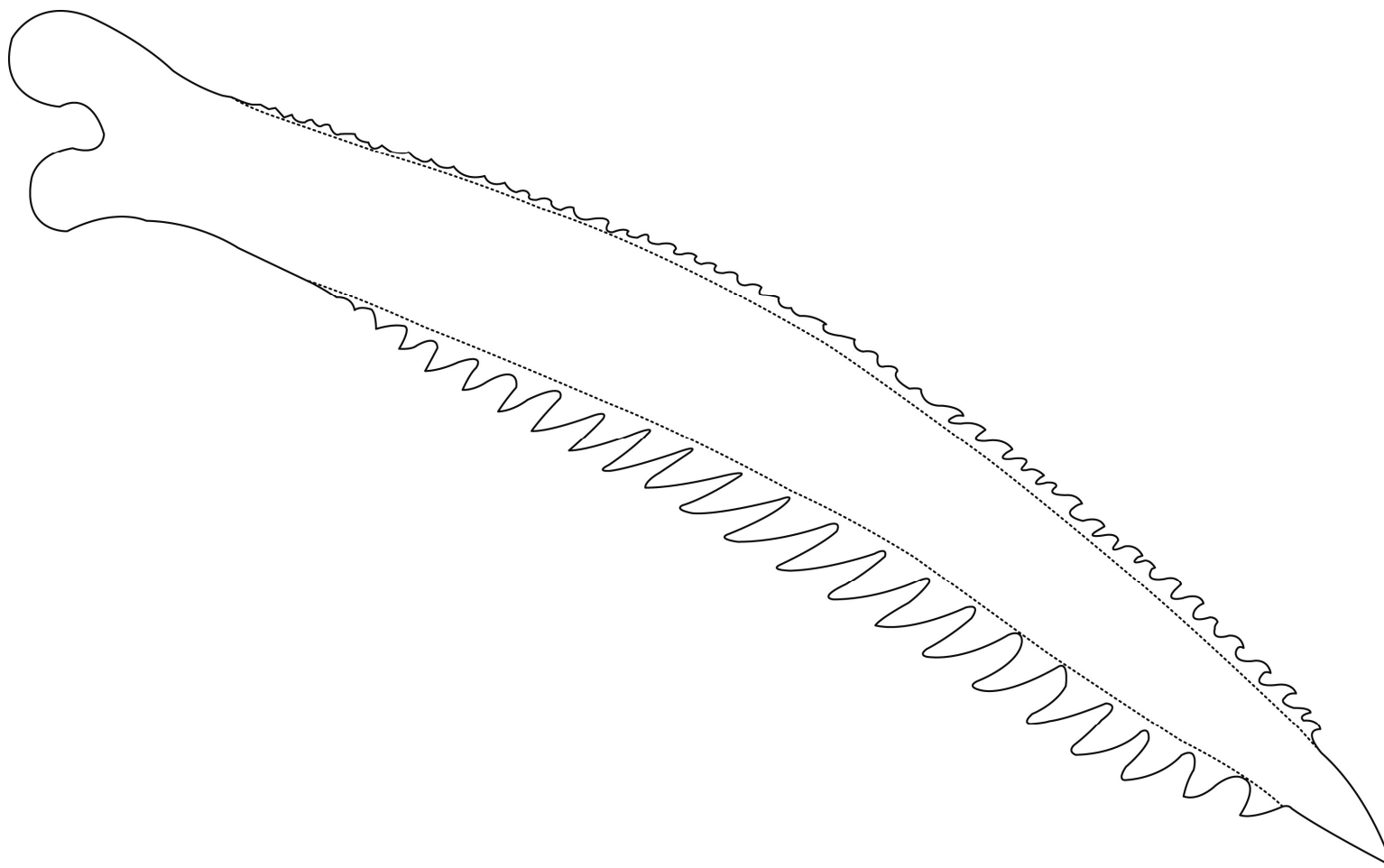


Figure 183. Ventral view of left pectoral-fin spine of *Pimelodella serrata*, holotype, FMNH 57979, 55.7 mm SL, total length of spine 7.7 mm.

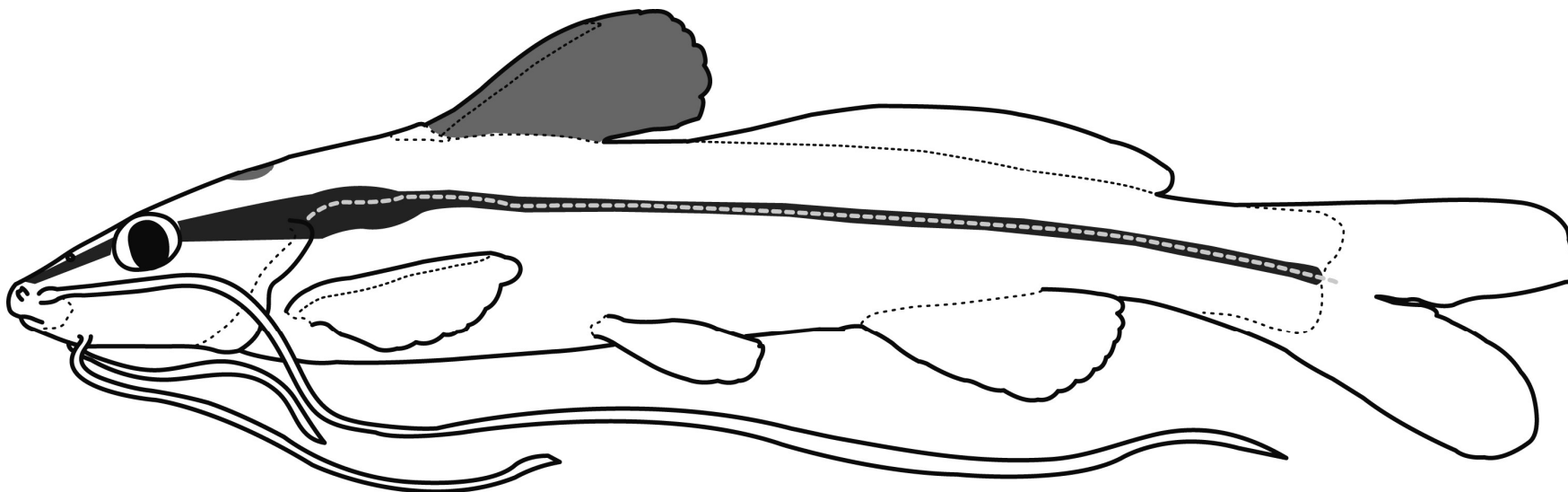


Figure 184. Schematic left lateral view of *Pimelodella serrata*.



Figure 185. *Pimelodella serrata*, UFRO 9745, 83.4 mm SL. Left lateral (A) and dorsal (B) views. Photo extracted from Bockmann & Slobodian (2013).



Figure 186. *Pimelodella chaparae*, junior-synonym of *P. serrata*, holotype, ANSP 69021, 48.1 mm SL. Left lateral (A) and dorsal (B) views. Photo taken by Kyle Luckenbill.



Figure 187. *Pimelodella spelaea*, holotype, MZUSP 81726, 78.9 mm SL. Left lateral (A) and dorsal (B) views. Photo taken by Eduardo Baena.

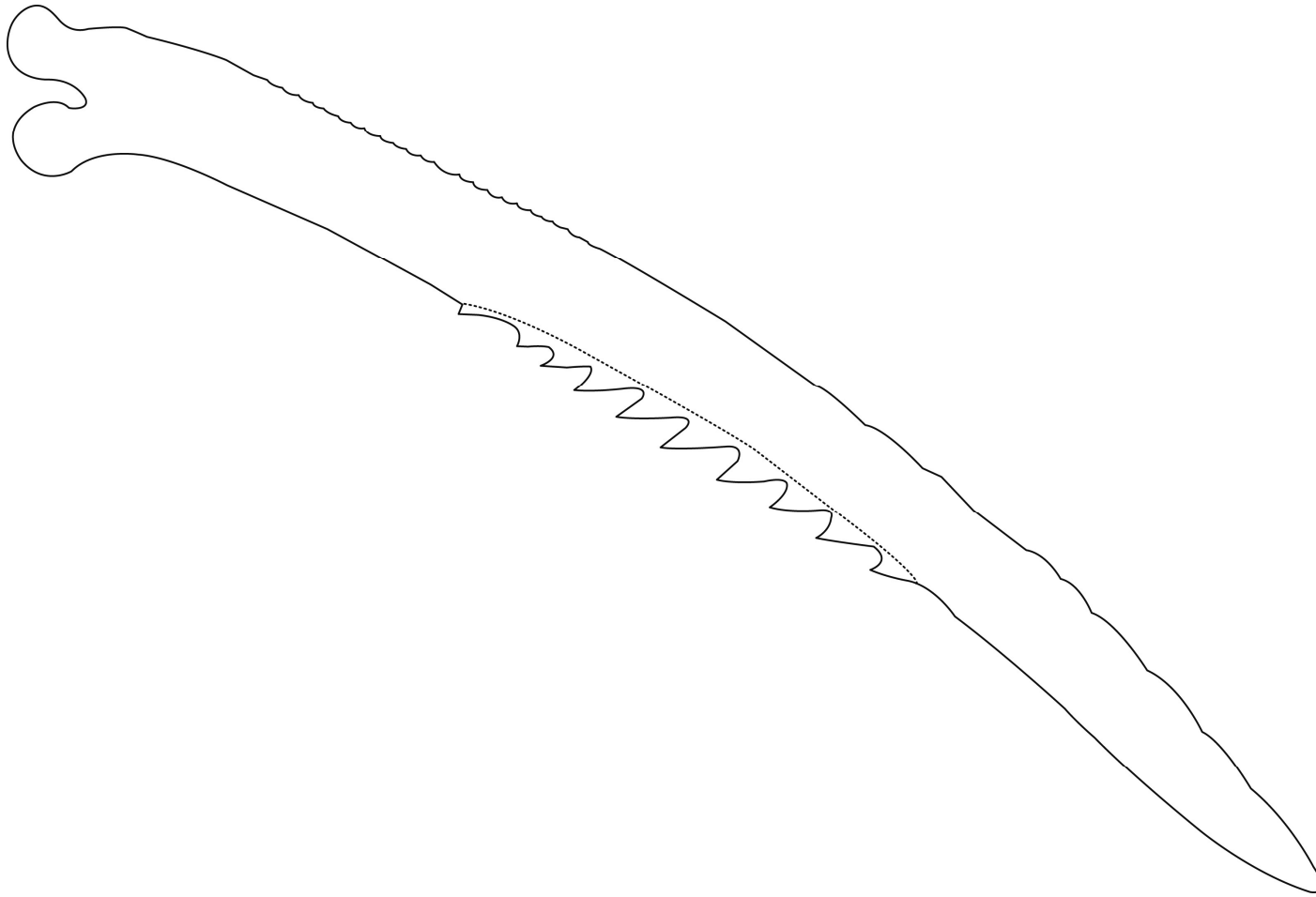


Figure 188. Ventral view of left pectoral-fin spine of *Pimelodella spelaea*, holotype, MZUSP 81726, 78.9 mm SL, total length of spine 11.0 mm.

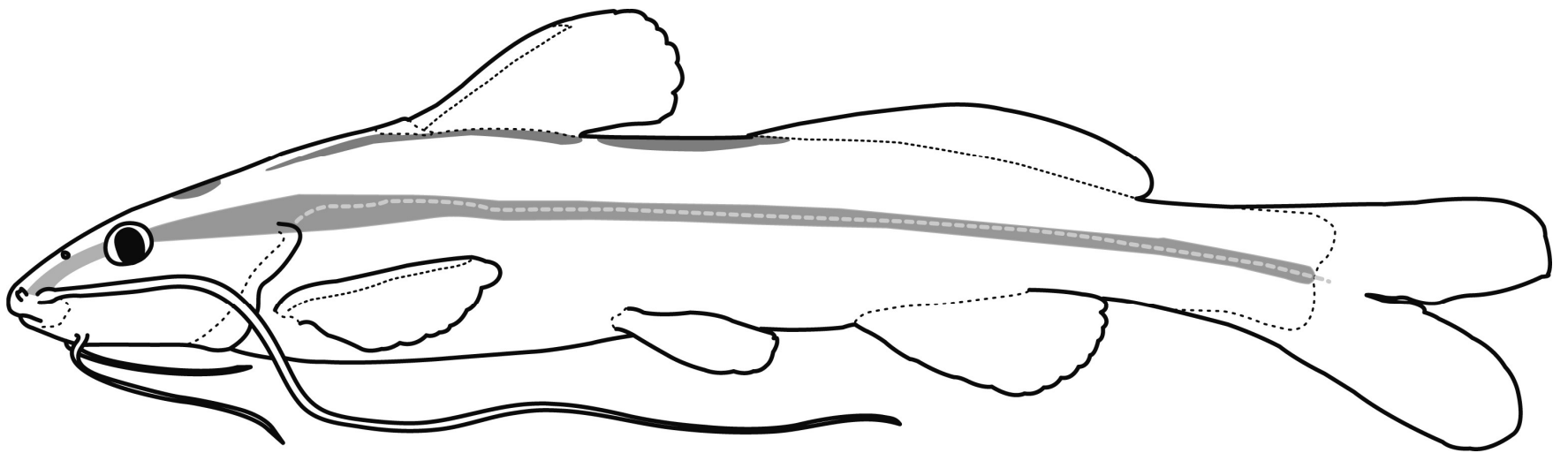


Figure 189. Schematic left lateral view of *Pimelodella spelaea*.



Figure 190. *Pimelodella straminea*, lectotype, ANSP 21581, 41.2 mm SL. Left lateral (A) and dorsal (B) views. Photo taken by Kyle Luckenbill.

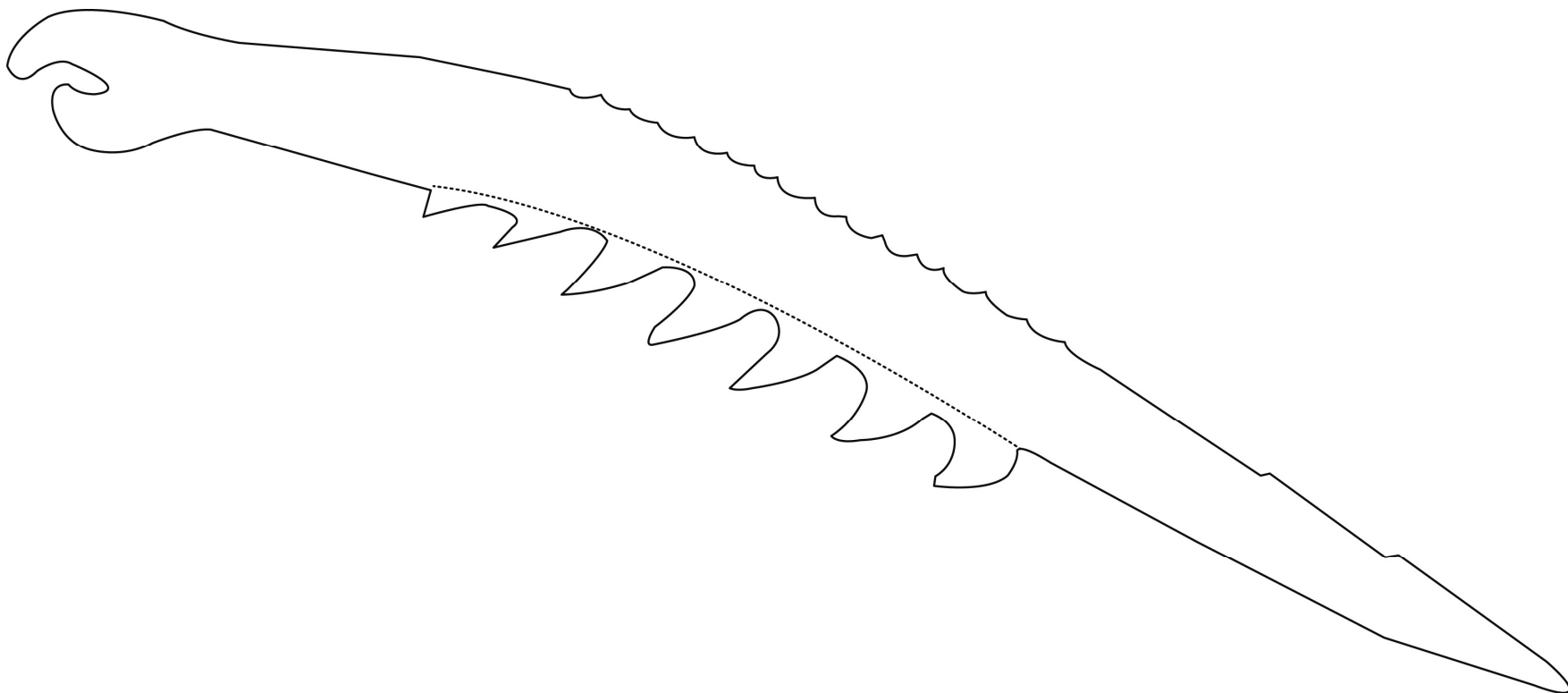


Figure 191. Ventral view of left pectoral-fin spine of *Pimelodella straminea*, lectotype, ANSP 21581, 41.2 mm SL, total length of spine 7.6 mm.

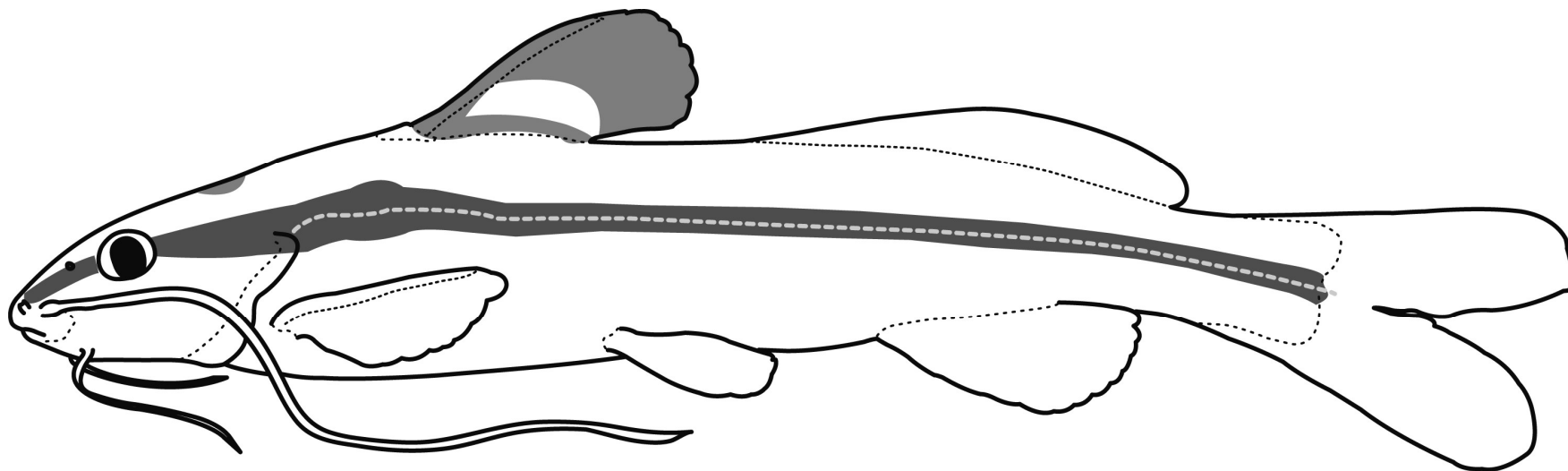


Figure 192. Schematic left lateral view of *Pimelodella straminea*.



Figure 193. *Pimelodella taeniophora*, lectotype, BMNH 1895.5.17.27, 76.6 mm SL. Left lateral (A) and dorsal (B) views. Photo taken by Mark Allen.

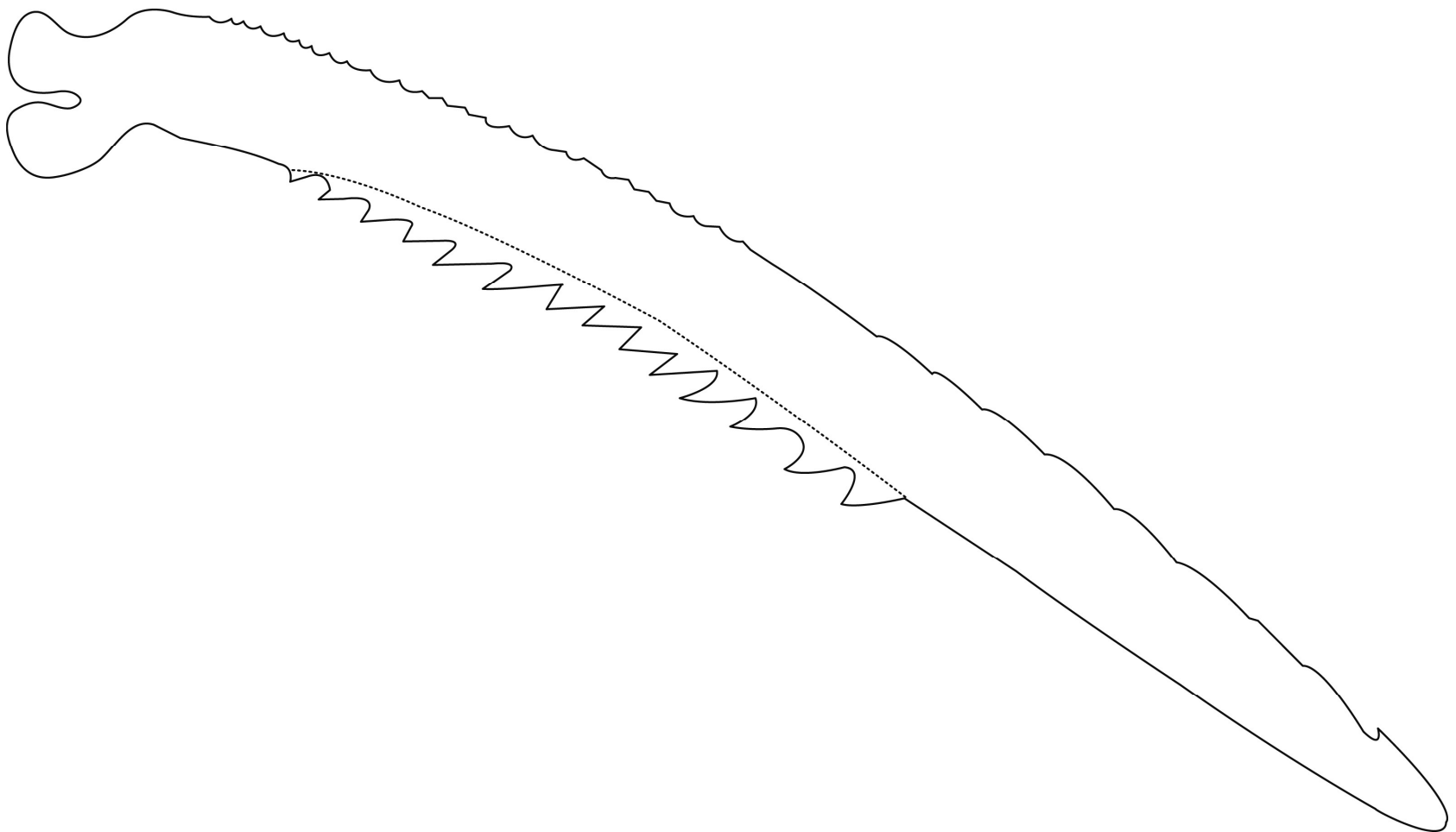


Figure 194. Ventral view of left pectoral-fin spine of *Pimelodella taeniophora*, lectotype, BMNH 1895.5.17.27, 76.6 mm SL, total length of spine 13.6 mm.

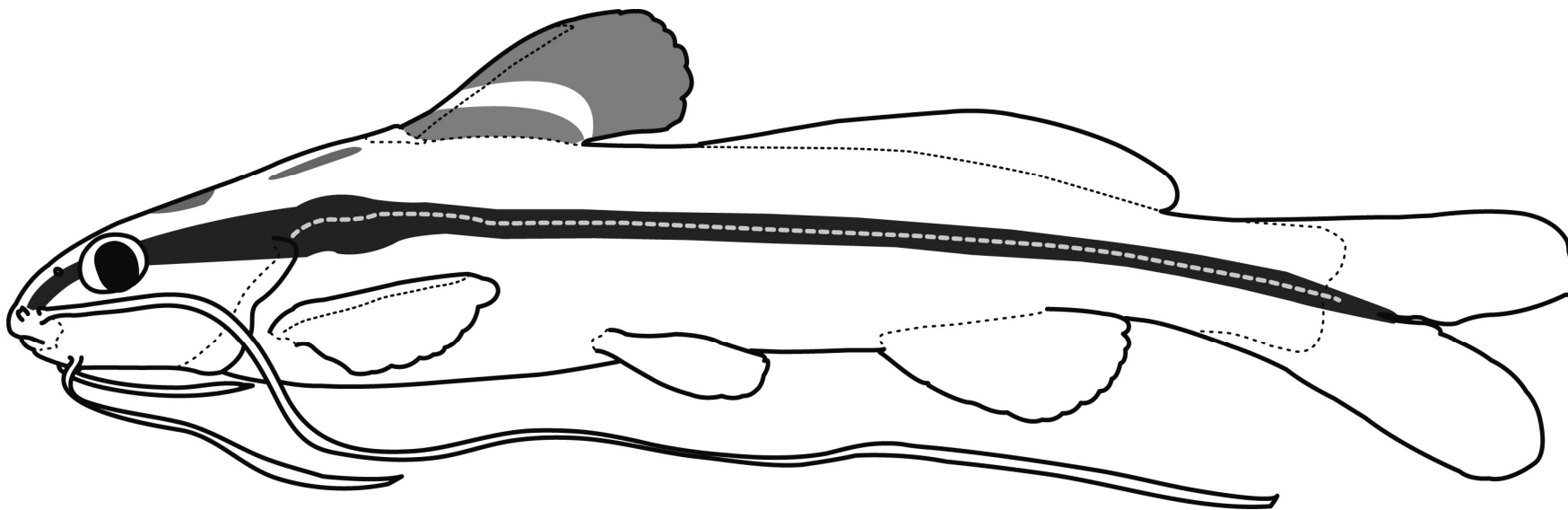


Figure 195. Schematic left lateral view of *Pimelodella taeniophora*.



Figure 196. *Pimelodella taeniophora*, MZUEL 6460, 93.2 mm SL, female, extracted from Souza-Shibatta *et al.* (2013).



Figure 197. *Pimelodella tapatapae*, holotype, CAS 57469, 121.6 mm SL. Left lateral (A) and dorsal (B) views.

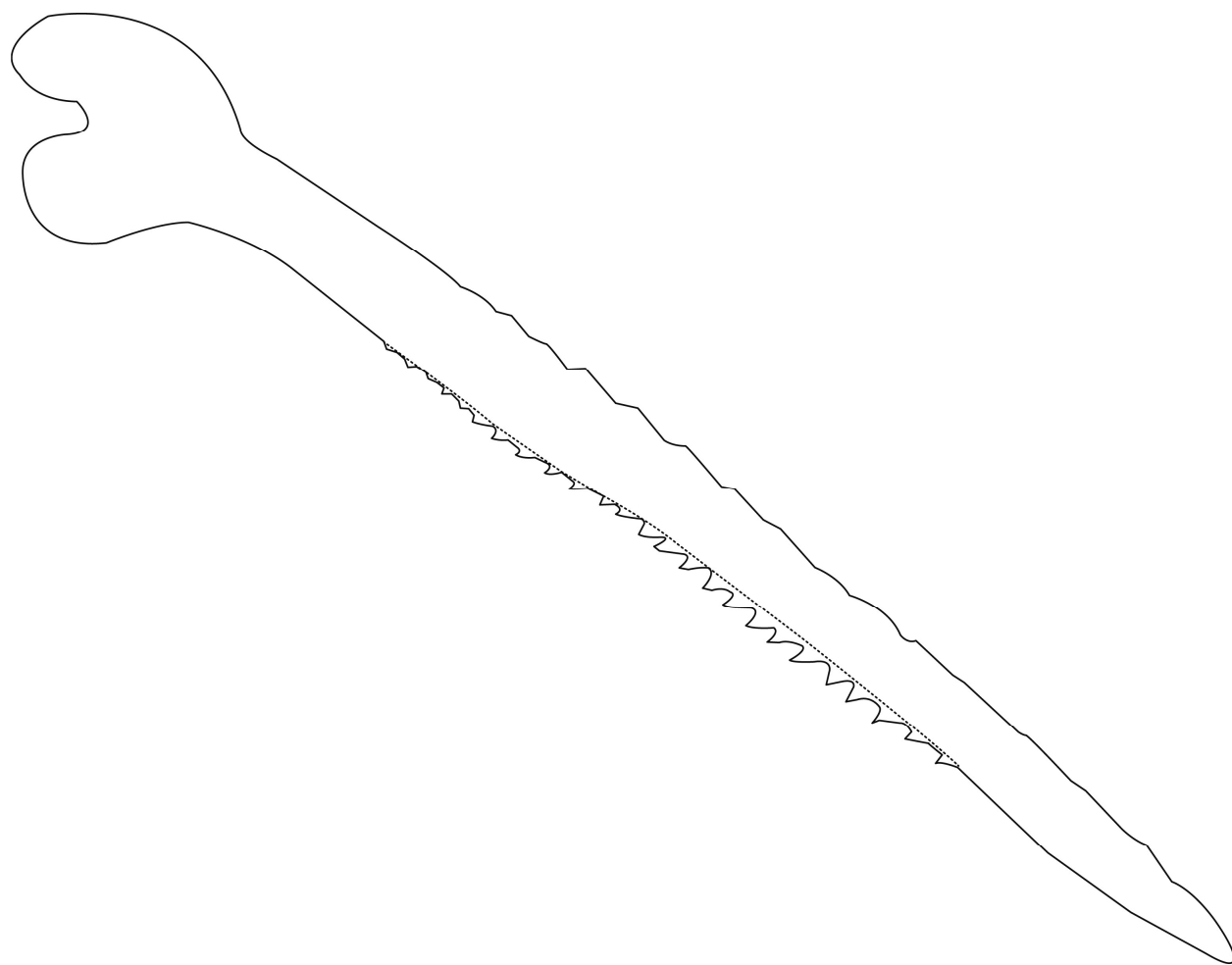


Figure 198. Ventral view of left pectoral-fin spine of *Pimelodella tapatapae*, holotype, CAS 57469, 121.6 mm SL, total length of spine 18.1 mm.

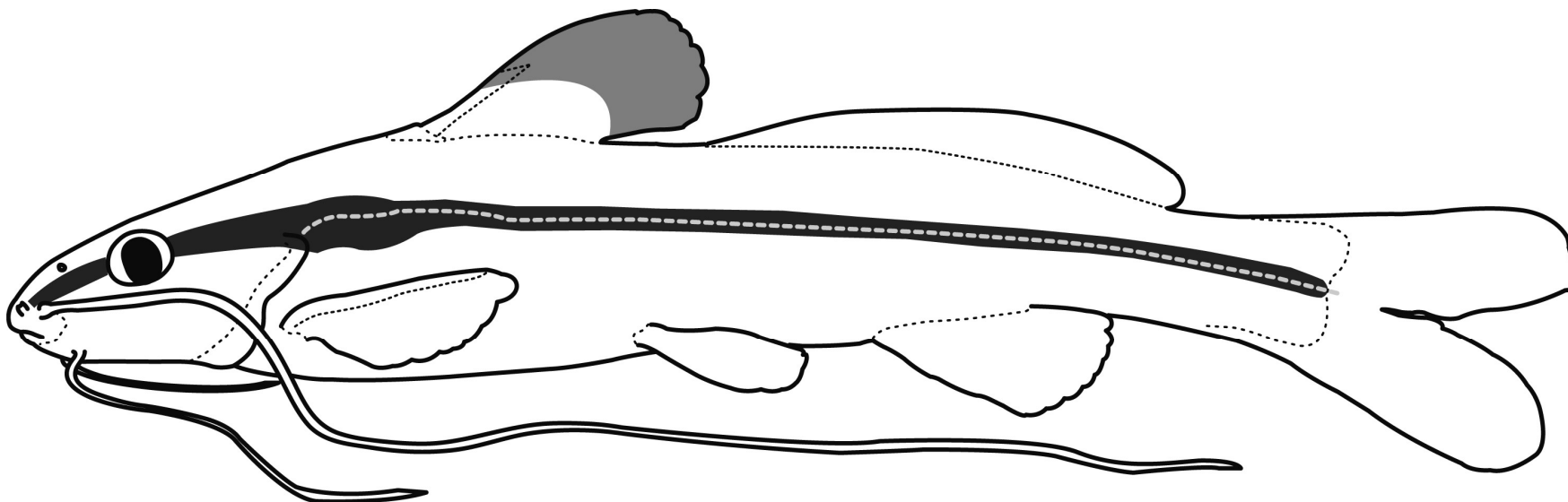


Figure 199. Schematic left lateral view of *Pimelodella tapatapae*.



Figure 200. *Pimelodella vittata*, lectotype, ZMB 9175, 61.8 mm SL. Left lateral (A) and dorsal (B) views. Photo taken by ZMB staff.

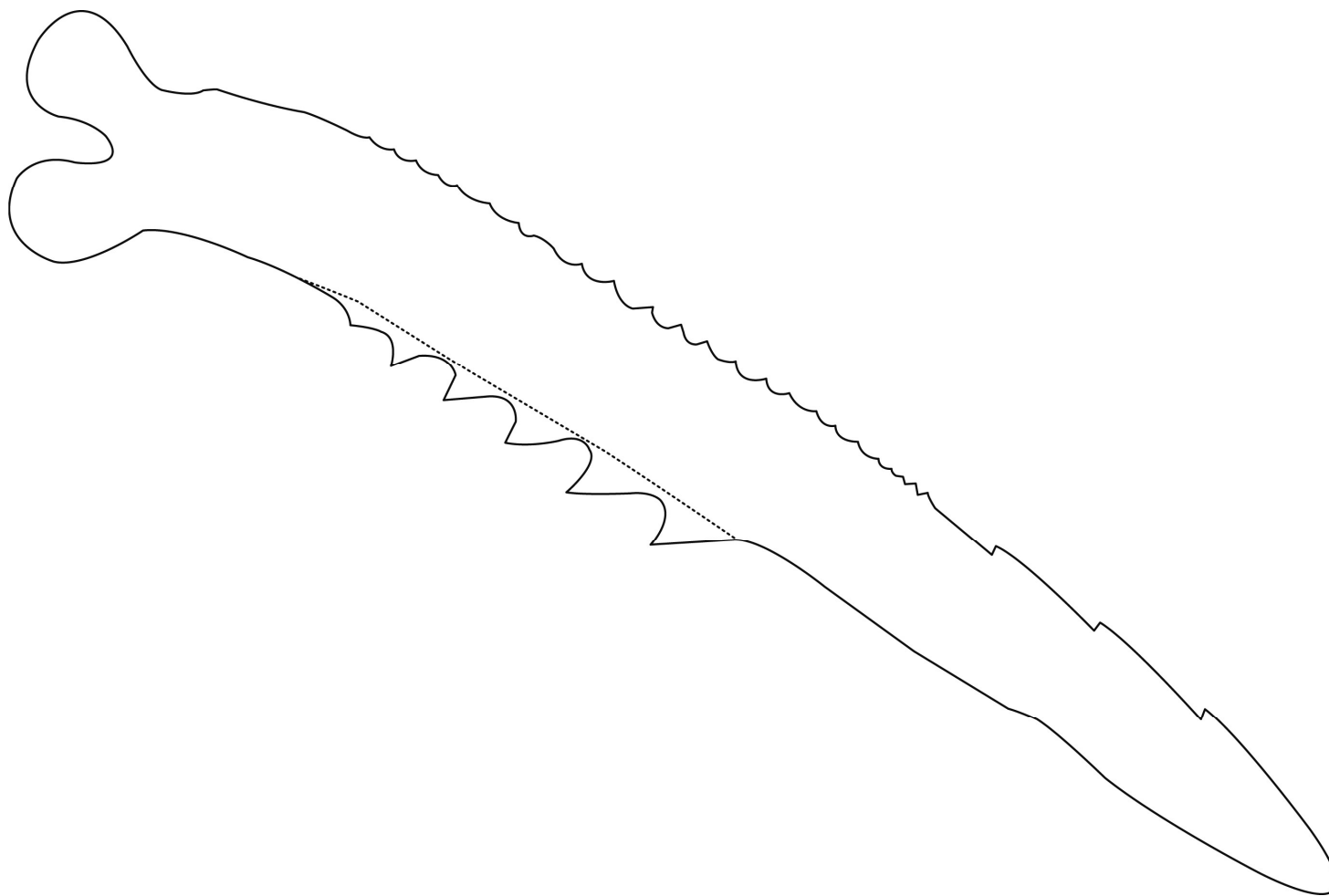


Figure 201. Ventral view of left pectoral-fin spine of *Pimelodella vittata*, paralectotype, ZMB 9175, 53.2 mm SL, total length of spine 9.0 mm.

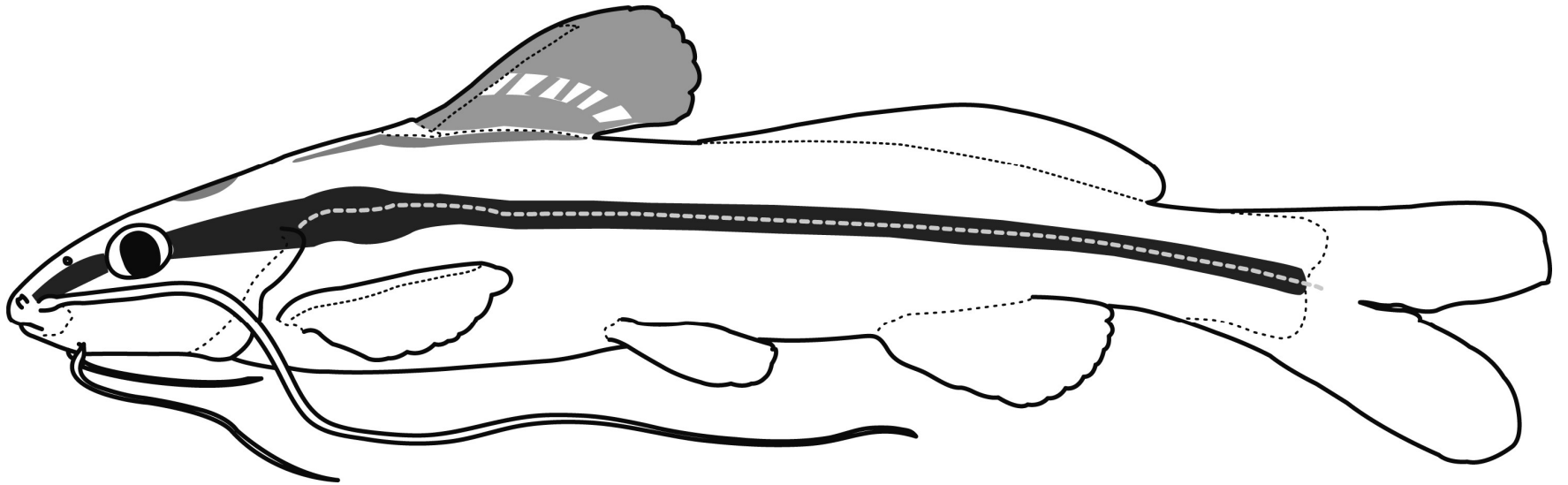


Figure 202. Schematic left lateral view of *Pimelodella vittata*.

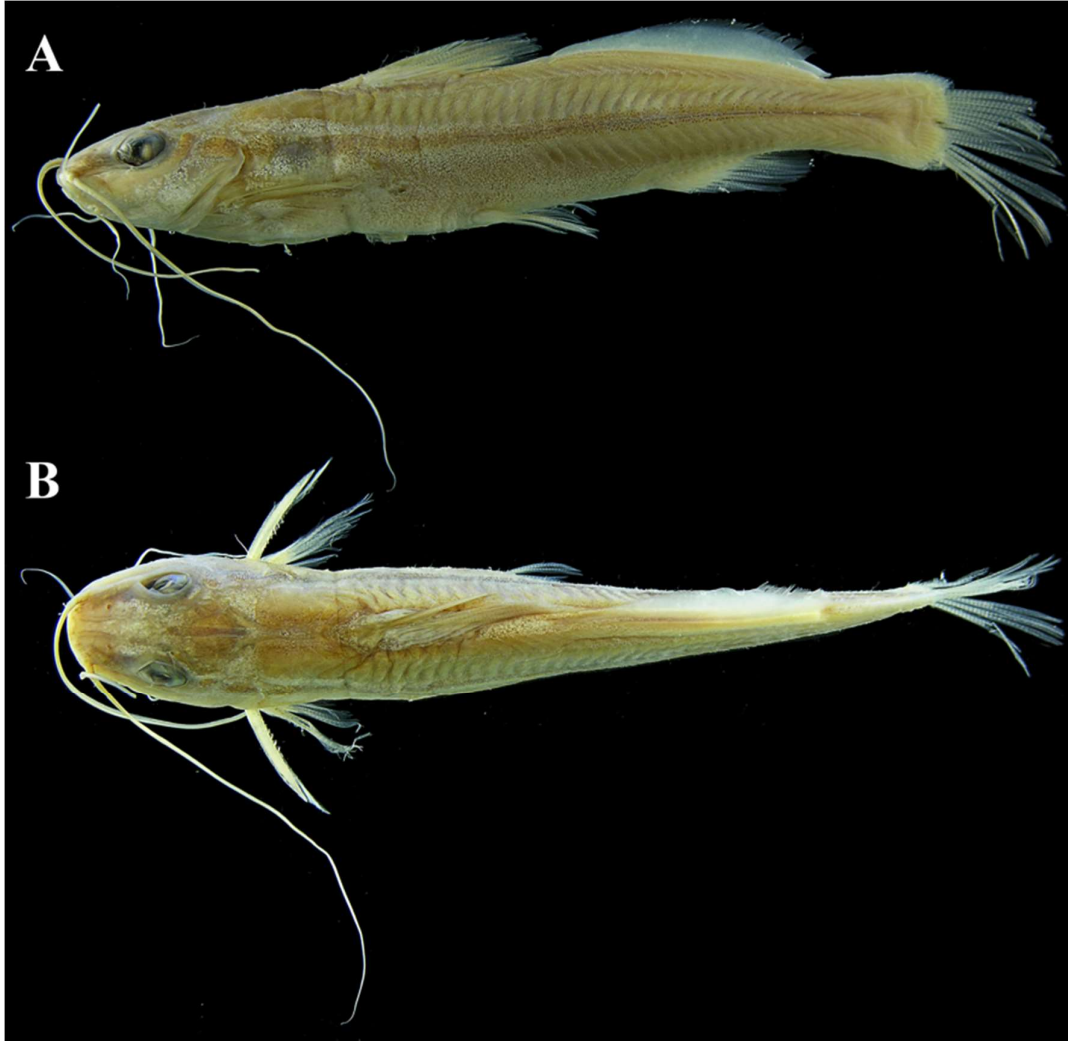


Figure 203. *Pimelodella vittata*, paralectotype, NMW 44442, 57.5 mm SL. Left lateral (A) and dorsal (B) views. Photo taken by Mark Sabaj.



Figure 204. *Pimelodella yuncensis*, lectotype, ZMS 7870, 37.8 mm SL. Left lateral (A) and dorsal (B) views. Photo taken by Natasha Khardina.

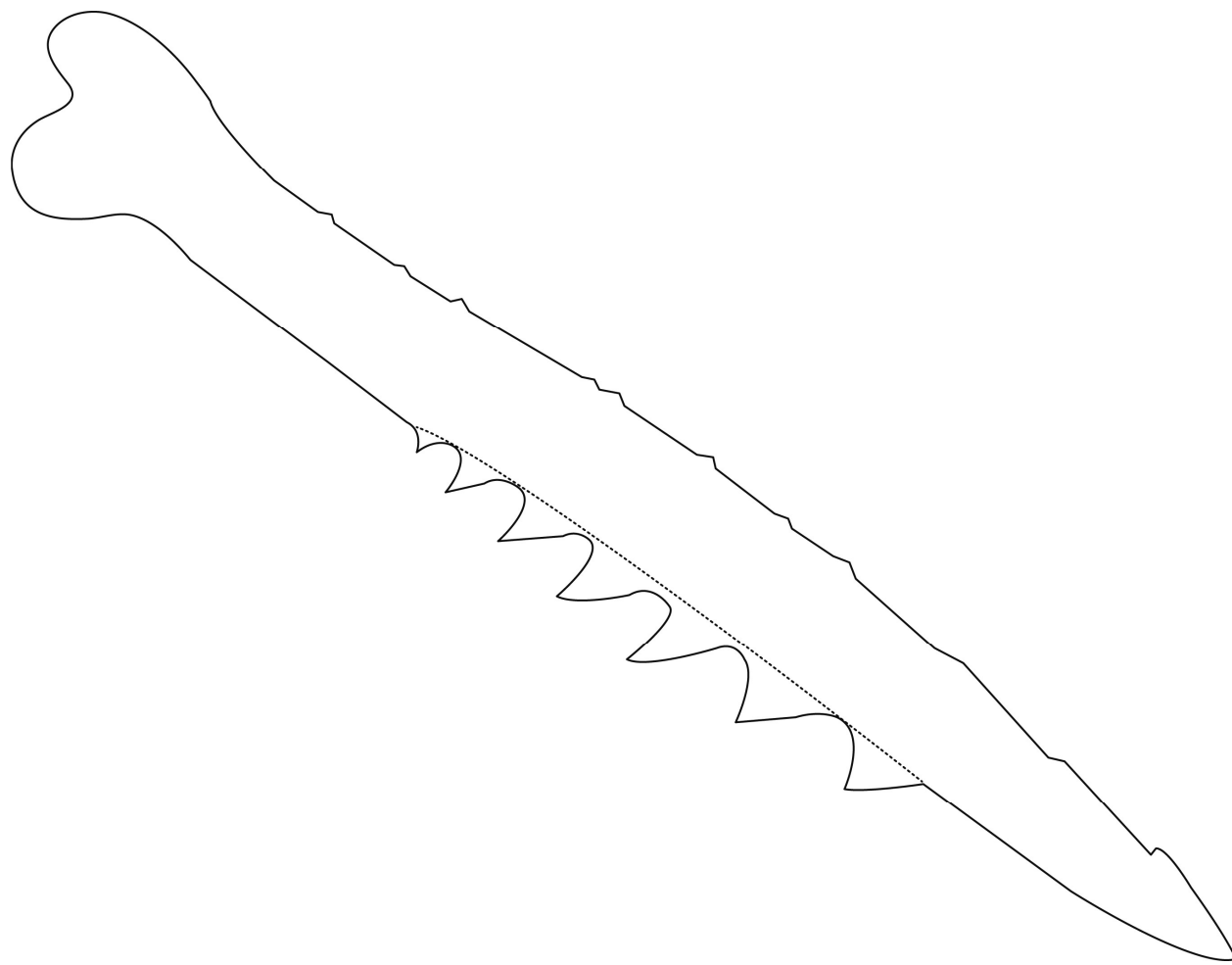


Figure 205. Ventral view of left pectoral-fin spine of *Pimelodella yuncensis*, lectotype, ZMS 7870, 37.8 mm SL, total length of spine 5.3 mm.

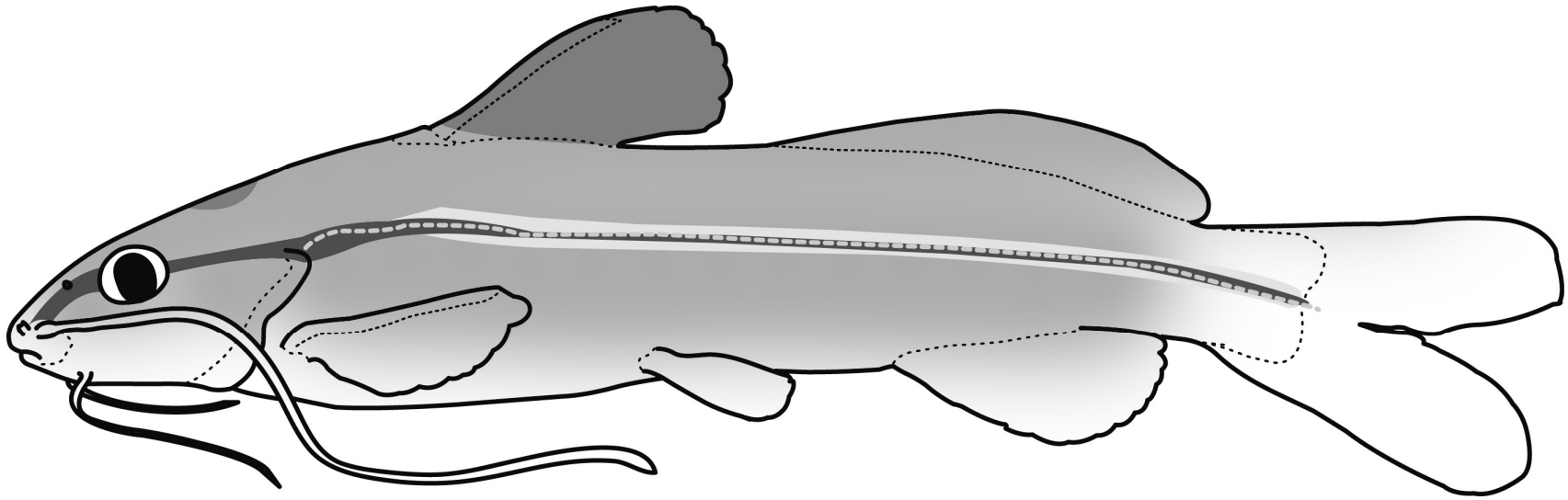


Figure 206. Schematic left lateral view of *Pimelodella yuncensis*.



Figure 207. Left lateral view of *Pimelodella yuncensis*, CAS 75890, 61.0 mm SL.



Figure 208. Holotype of *Rhamdia gilli*, USNM 53472, 138 mm SL.



Figure 209. *Pimelodella peruensis*, junior-synonym of *P. yuncensis*, holotype, ANSP 21932, 48.2 mm SL. Left lateral (A) and dorsal (B) views.



Figure 210. *Rhamdia altipinnis*, holotype, NMW 45601, 61.2 mm SL. Left lateral (A) and dorsal (B) views.



Figure 211. *Imparfinis macrocephalus*, paratype, MCZ 35879, 23.7 mm SL. Left lateral (A) and dorsal (B) views.

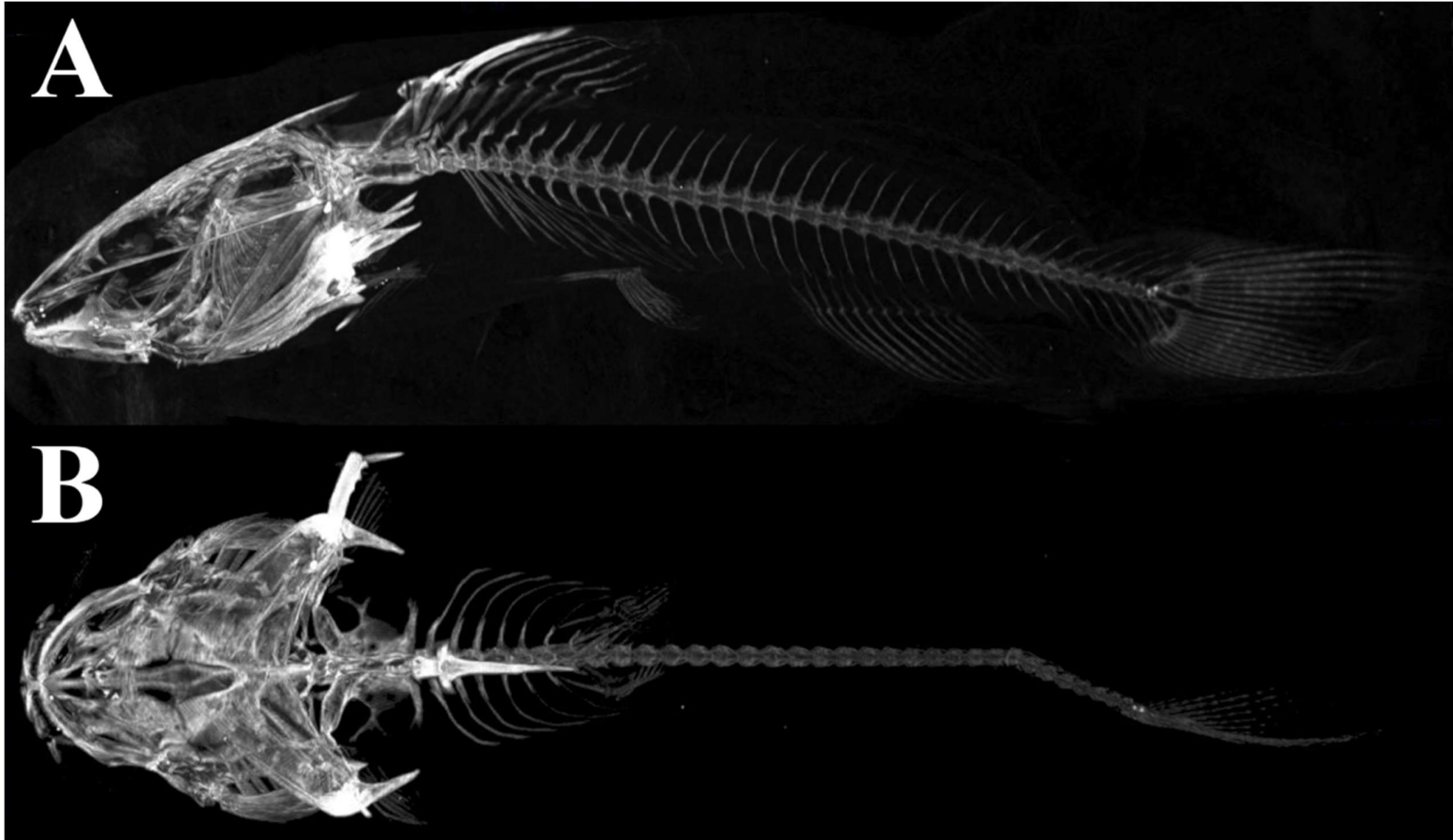


Figure 212. CT scan of *Imparfinis macrocephalus*, paratype, MCZ 35879, 23.7 mm SL. Left lateral (A) and dorsal (B) views. Scans obtained by Andrew Williston.



Figure 213. *Pimelodus parvus* Güntert, 1942, holotype, NMBA 5302, 19.4 mm SL. Left lateral (A) and dorsal (B) views. Photo taken by Natasha Khardina.

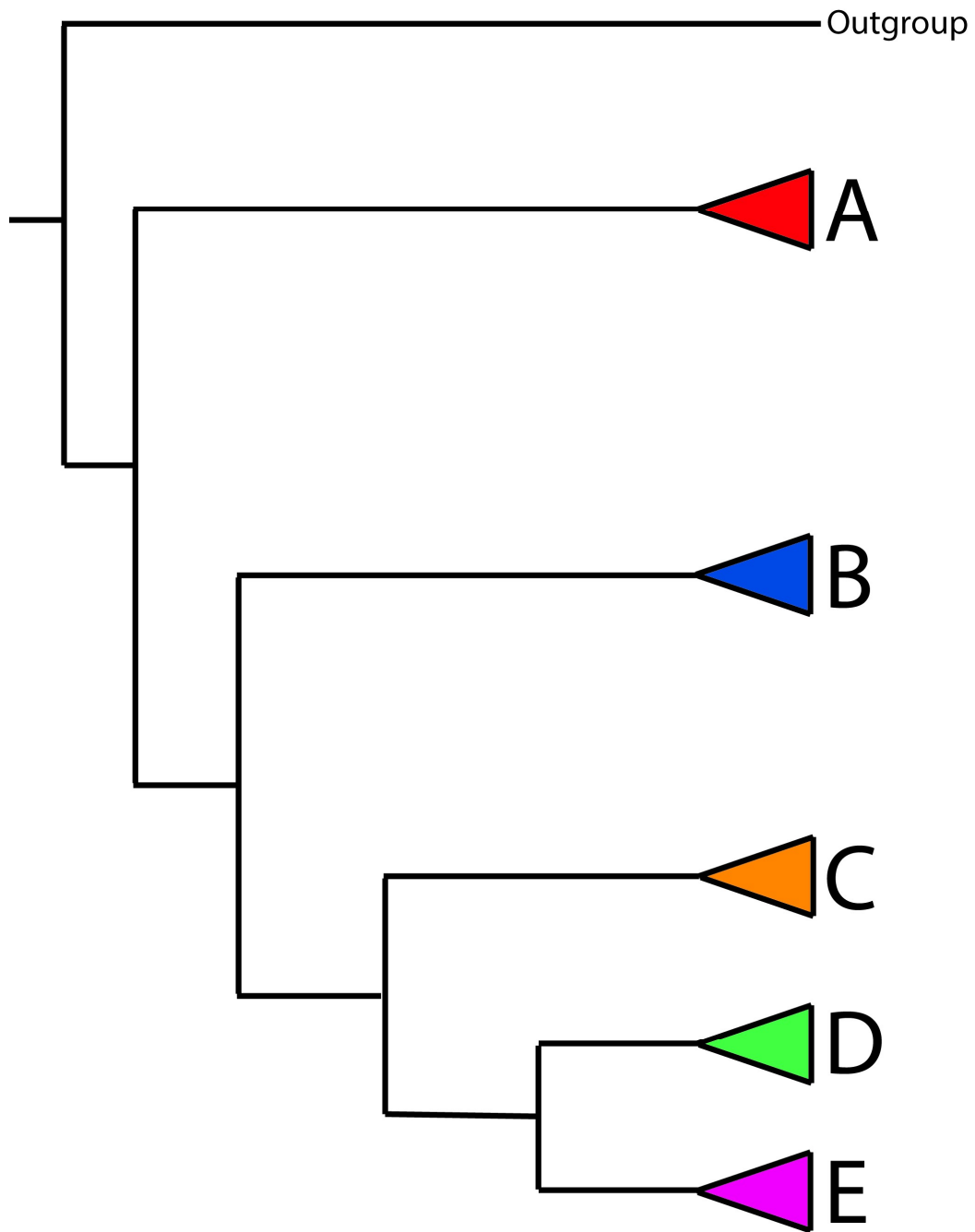


Figure 214. Simplified version of the species tree reconstructed through ASTRAL-III, based on COI, CytB, 36268e1 and 4174e20 genes, for a total of 90 specimens (80 *Pimelodella*).

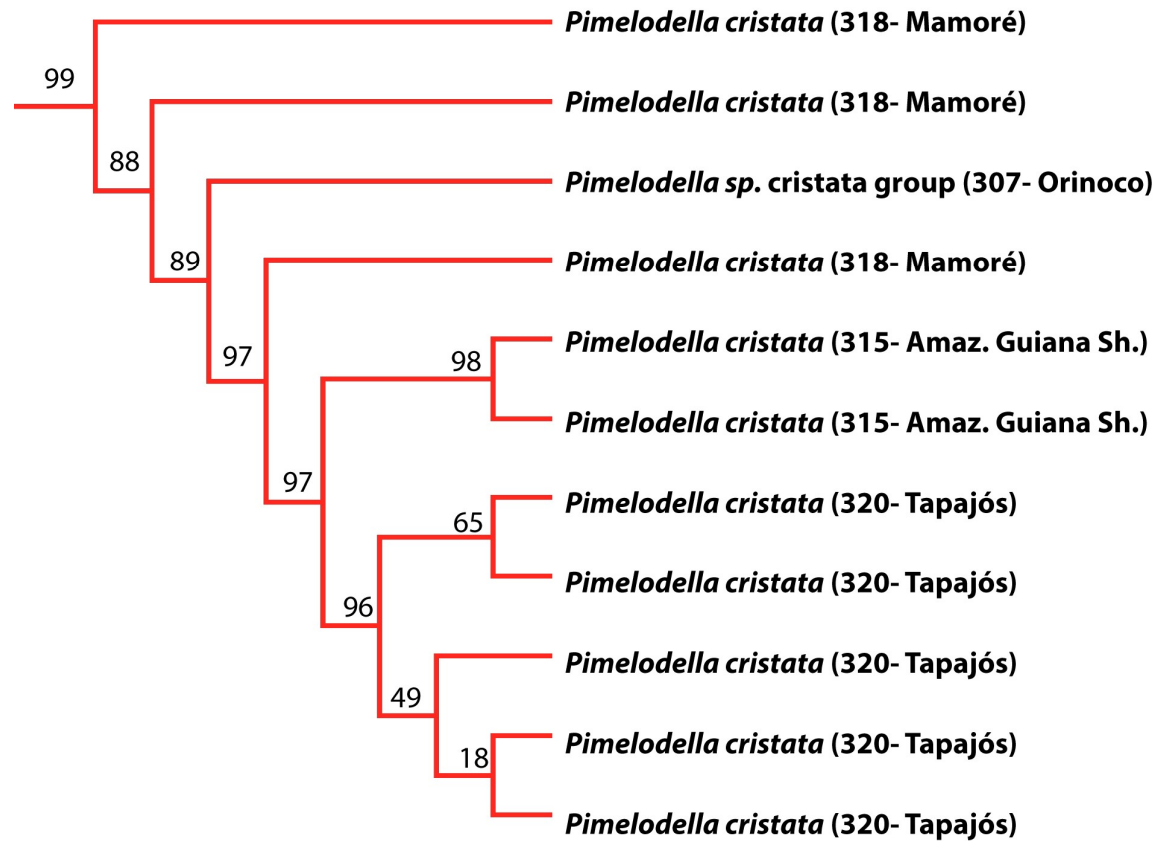


Figure 215. Clade A relative to Figure 214. Branch values correspond to bootstrap (%).

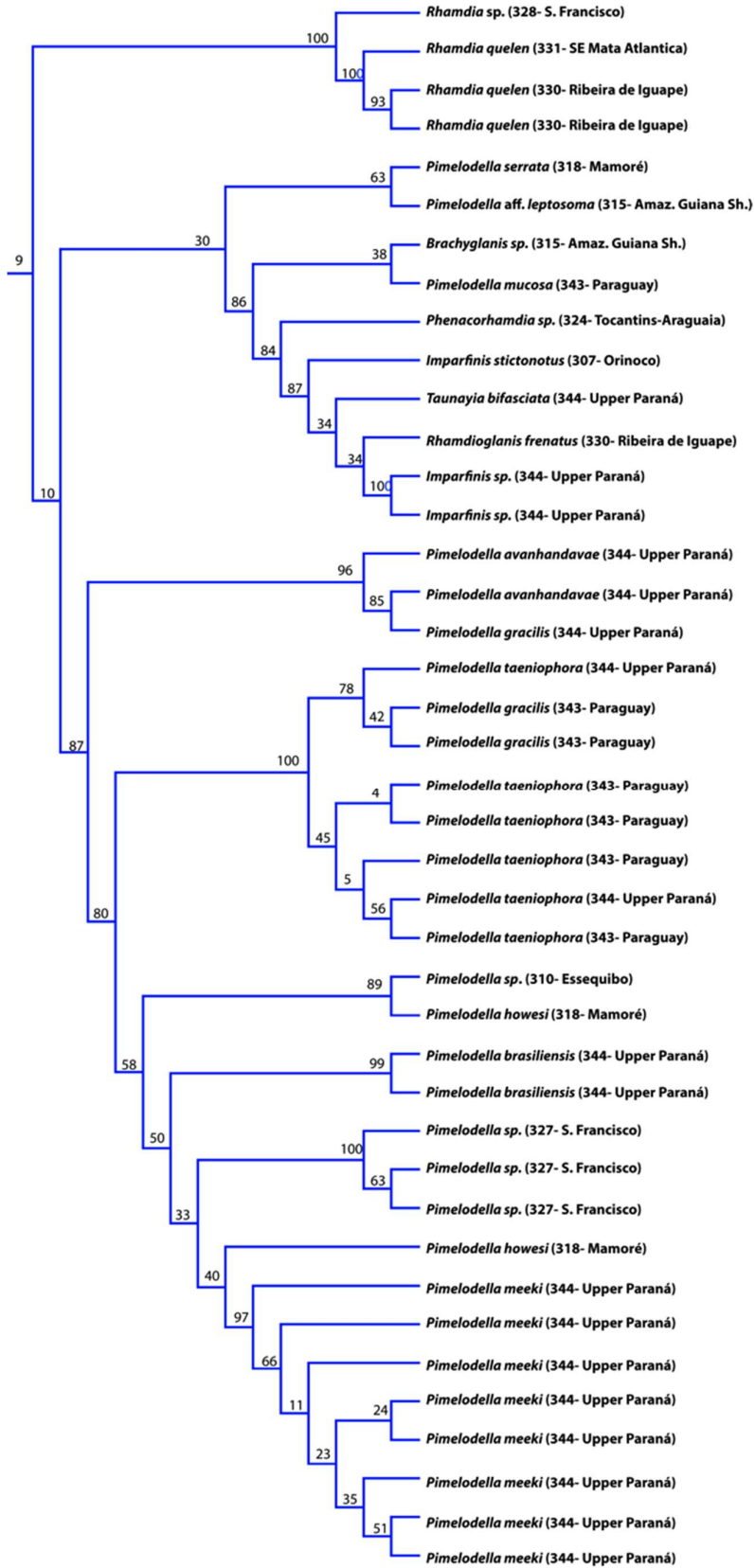


Figure 216. Clade B relative to Figure 214. Branch values correspond to bootstrap (%).

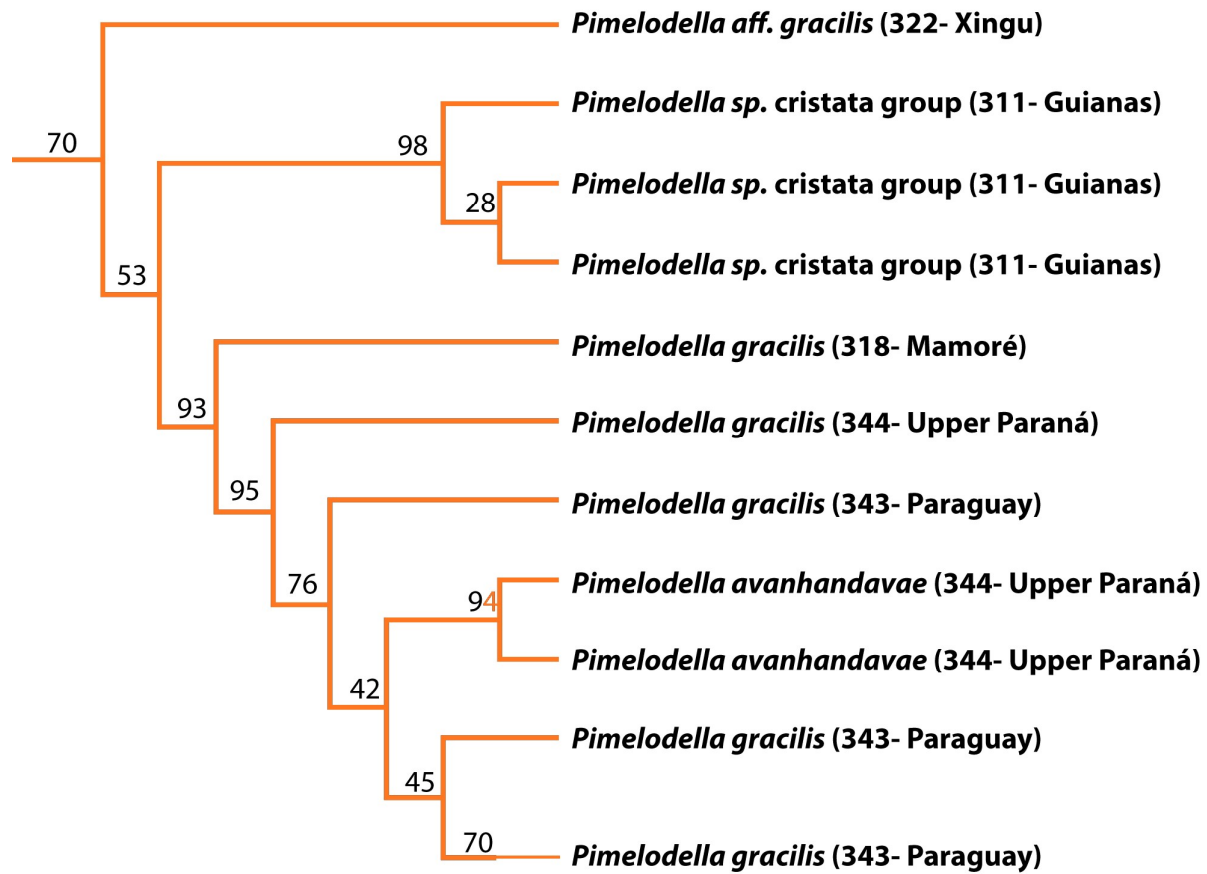


Figure 217. Clade C relative to Figure 214. Branch values correspond to bootstrap (%).

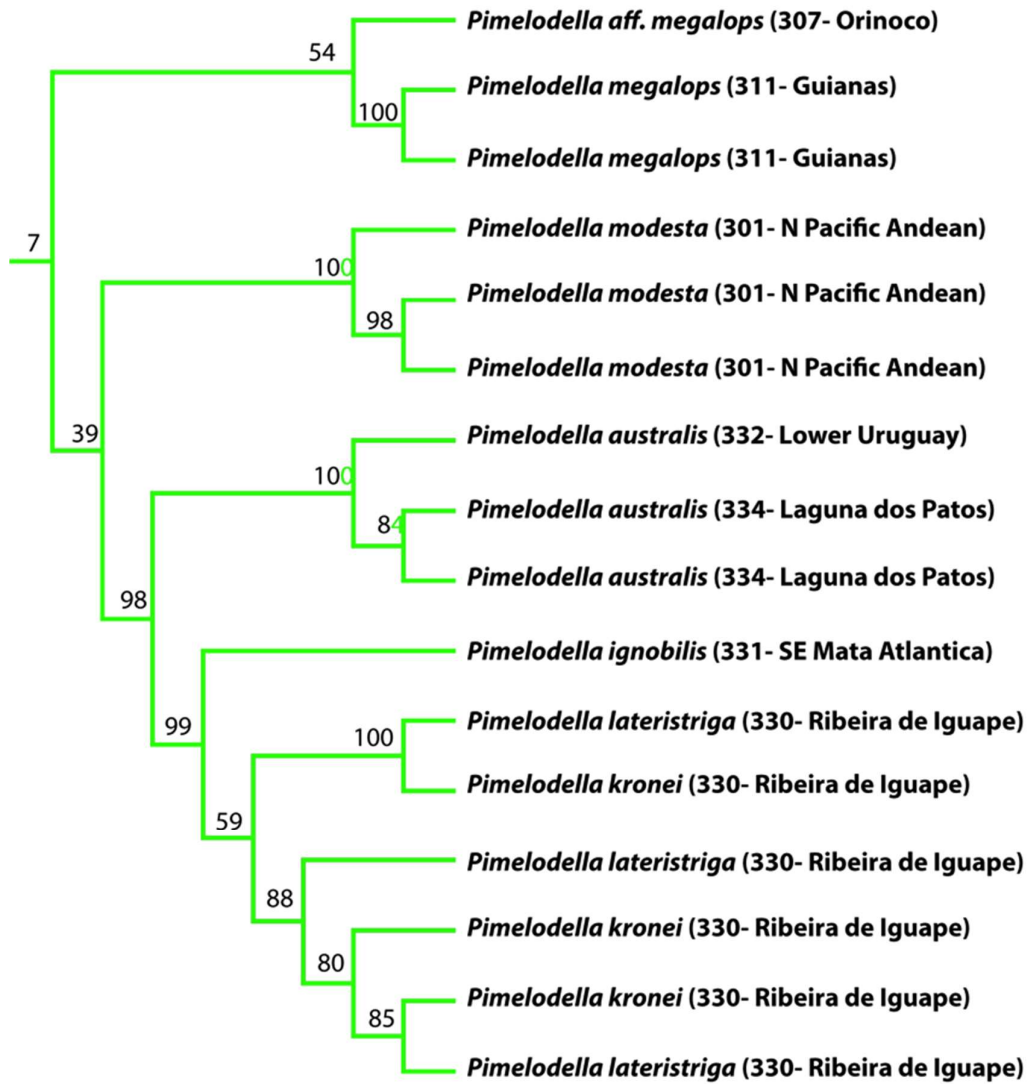


Figure 218. Clade D relative to Figure 214. Branch values correspond to bootstrap (%).

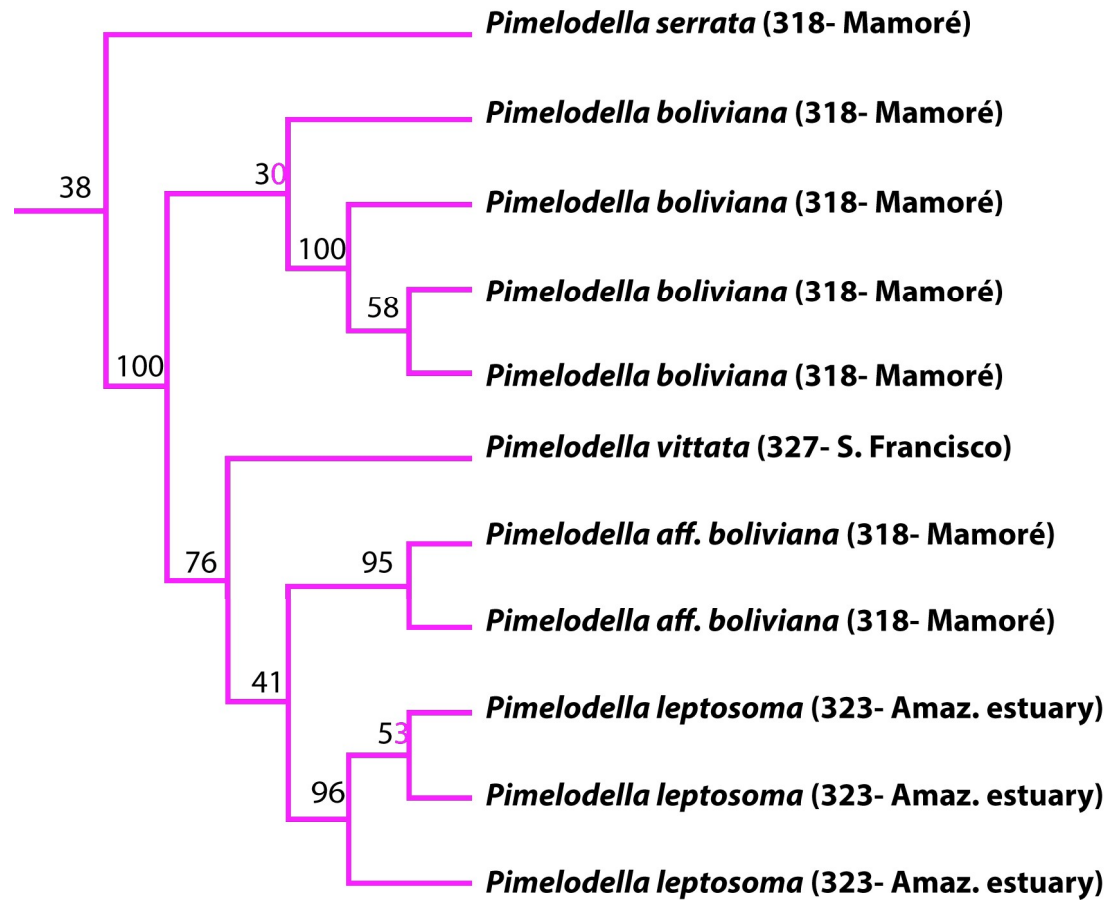


Figure 219. Clade E relative to Figure 214. Branch values correspond to bootstrap (%).

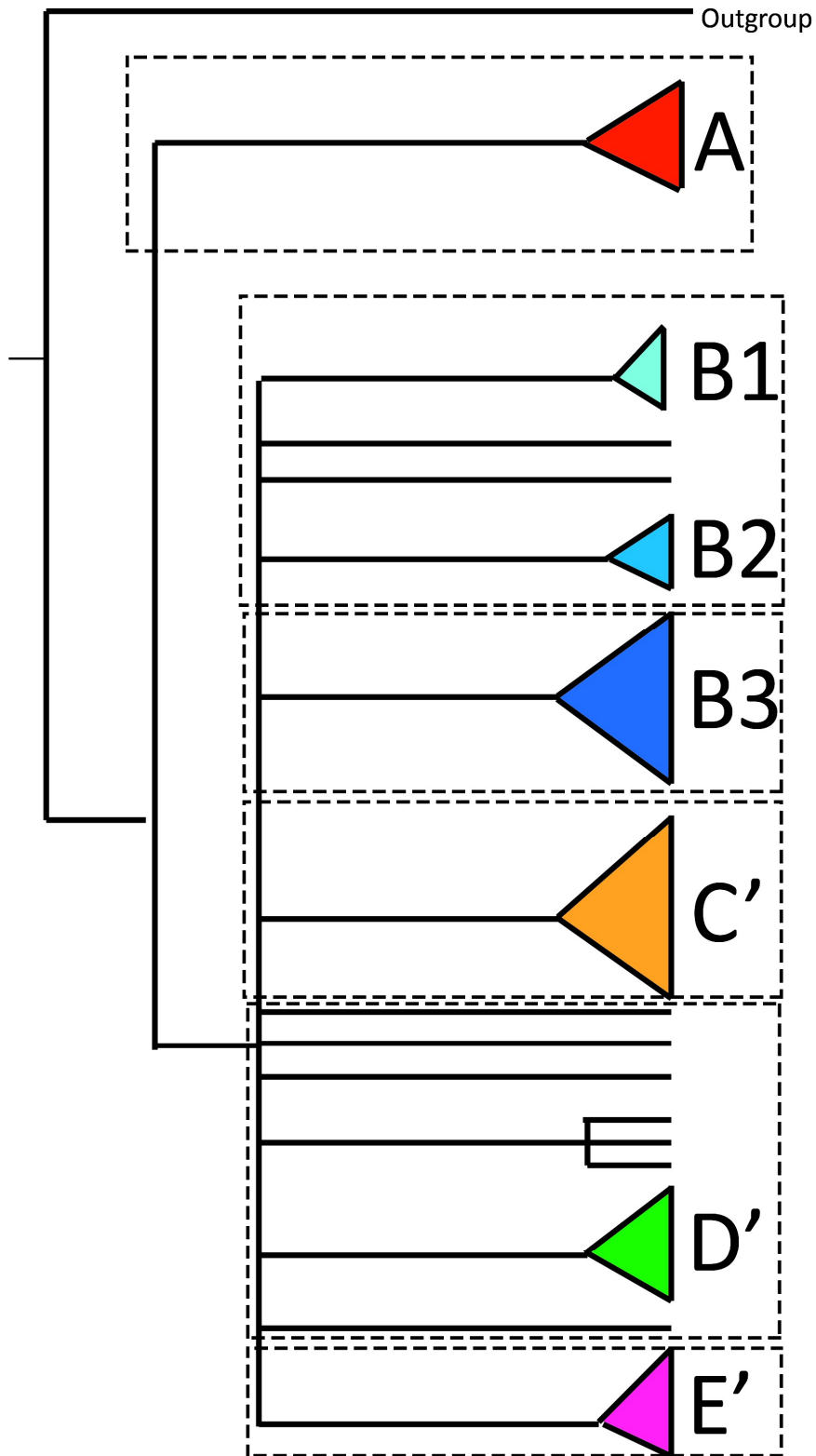


Figure 220. Simplified version of the species tree reconstructed through ASTRAL-III, based on COI, CytB, 36268e1 and 4174e20 genes. Nodes with bootstrap value inferior to 50% were collapsed. Dotted boxes present the delimitation for taxa illustrated in Figures 221–226.

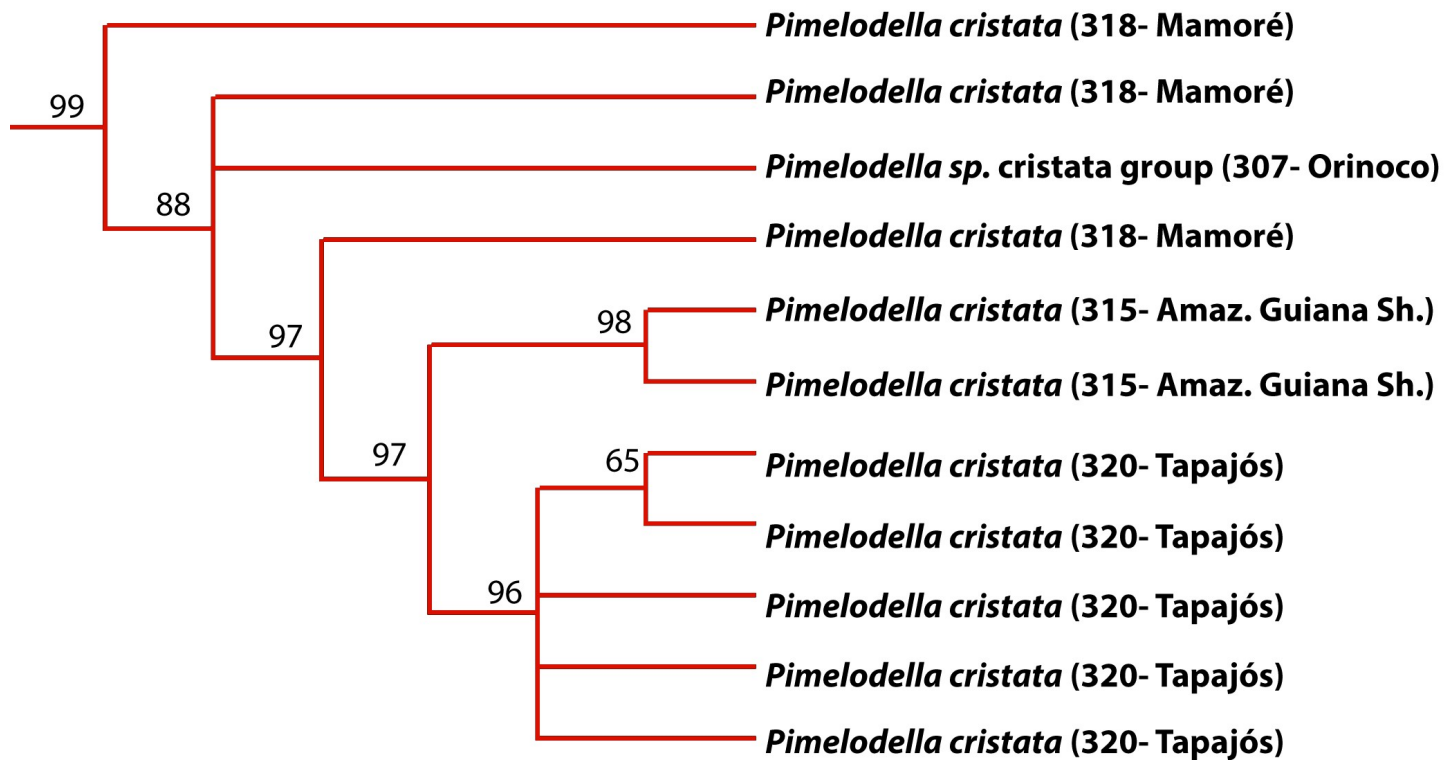


Figure 221. Clade A relative to Figure 220. Branch values correspond to bootstrap (%).

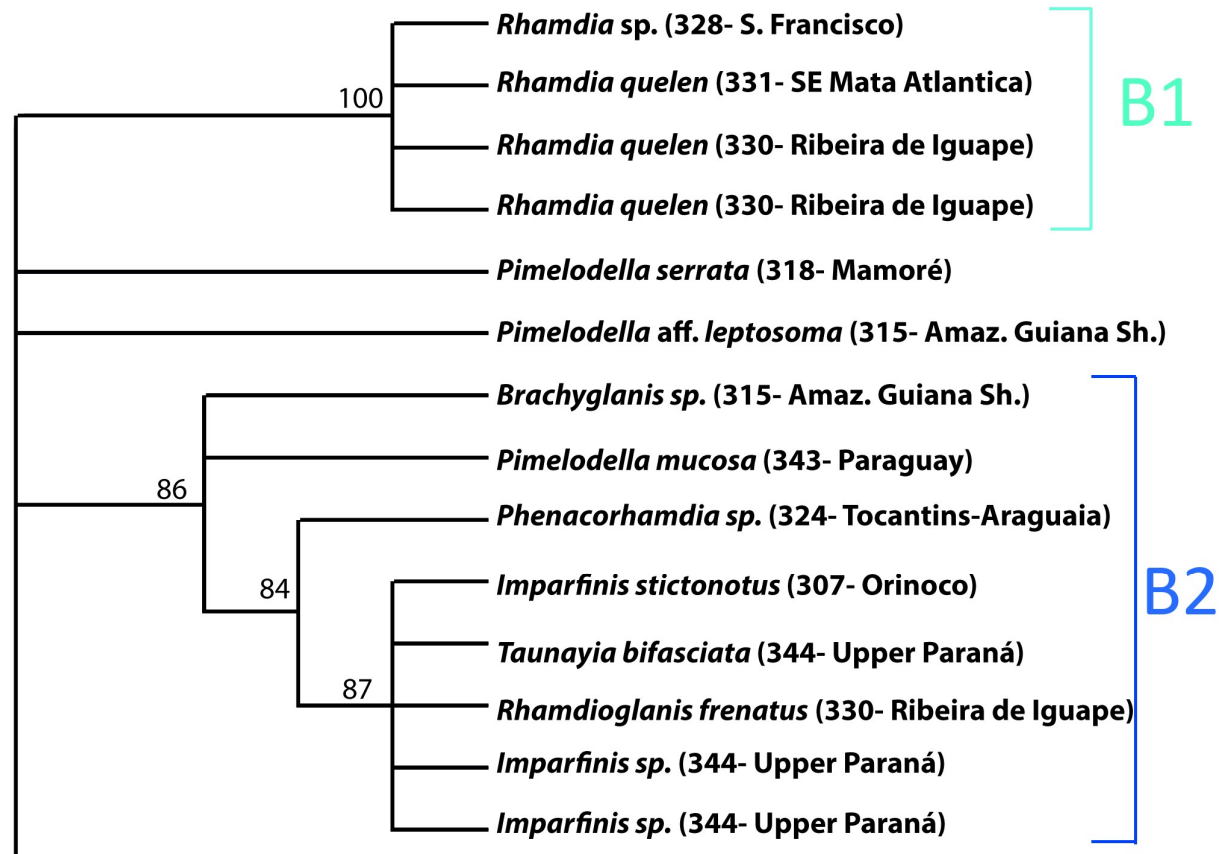


Figure 222. Clades B1, B2 and other taxa according to delimitation box in Figure 220. Branch values correspond to bootstrap (%).

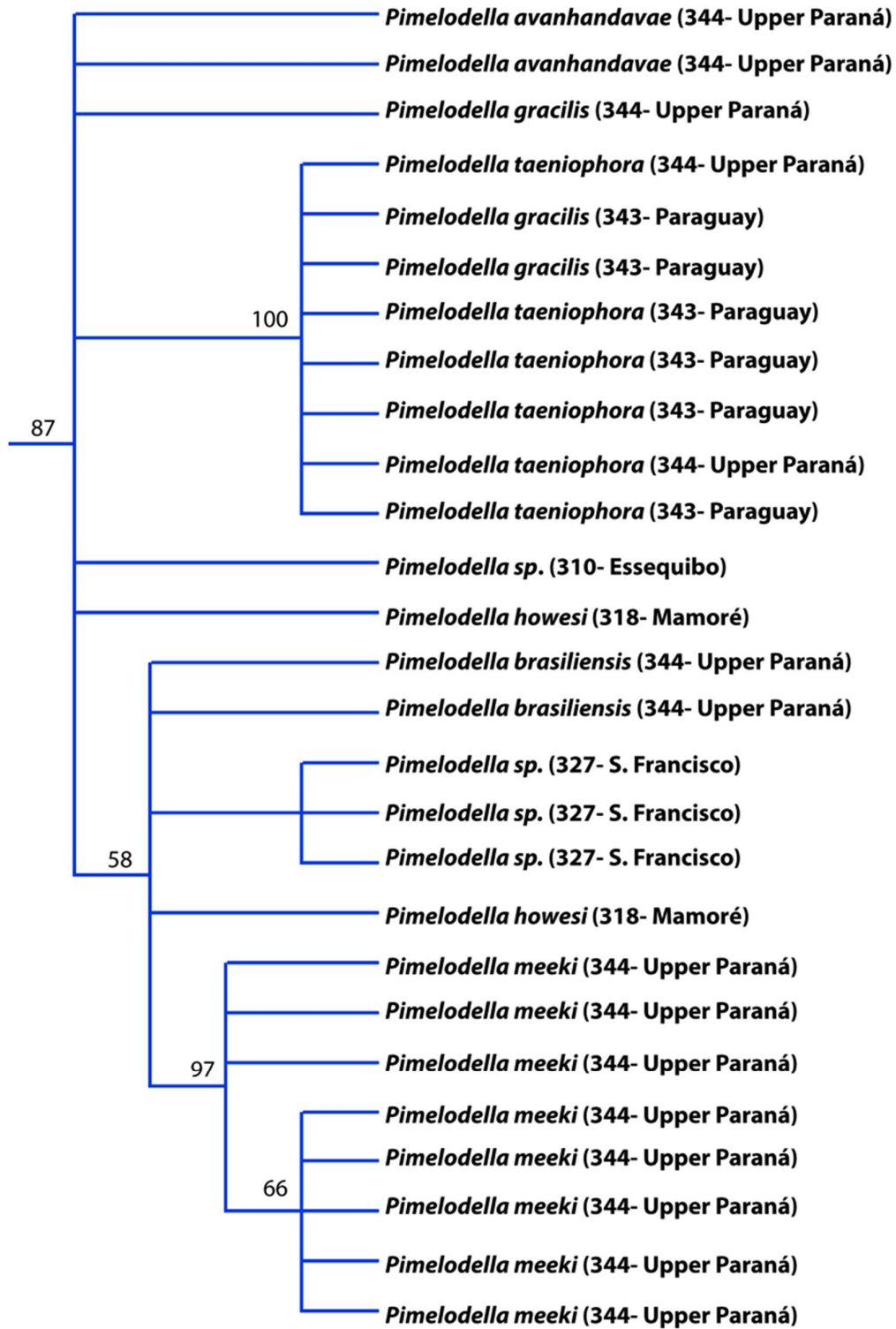


Figure 223. Clade B3, according to delimitation box in Figure 220. Branch values correspond to bootstrap (%).

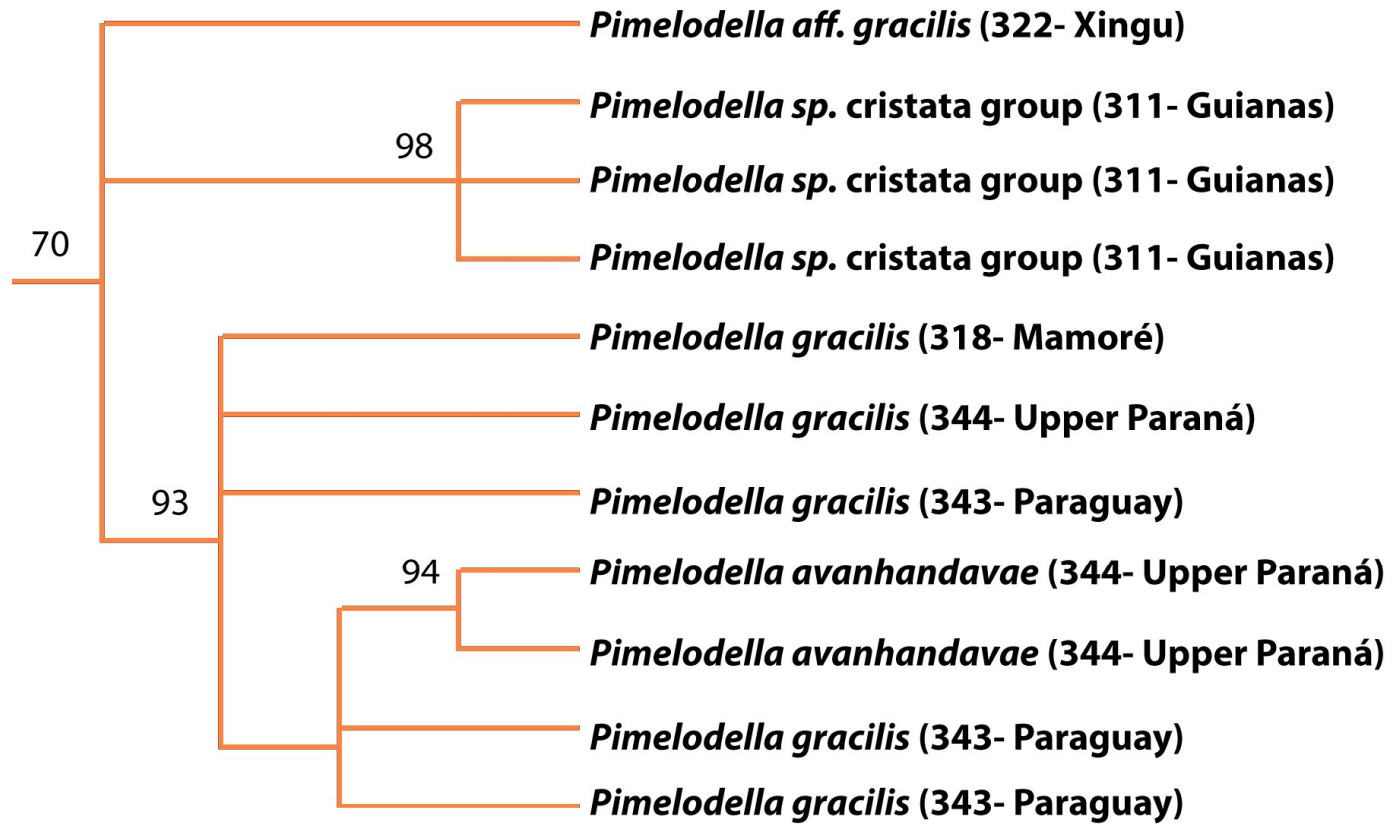


Figure 224. Clade C', according to delimitation box in Figure 220. Branch values correspond to bootstrap (%).

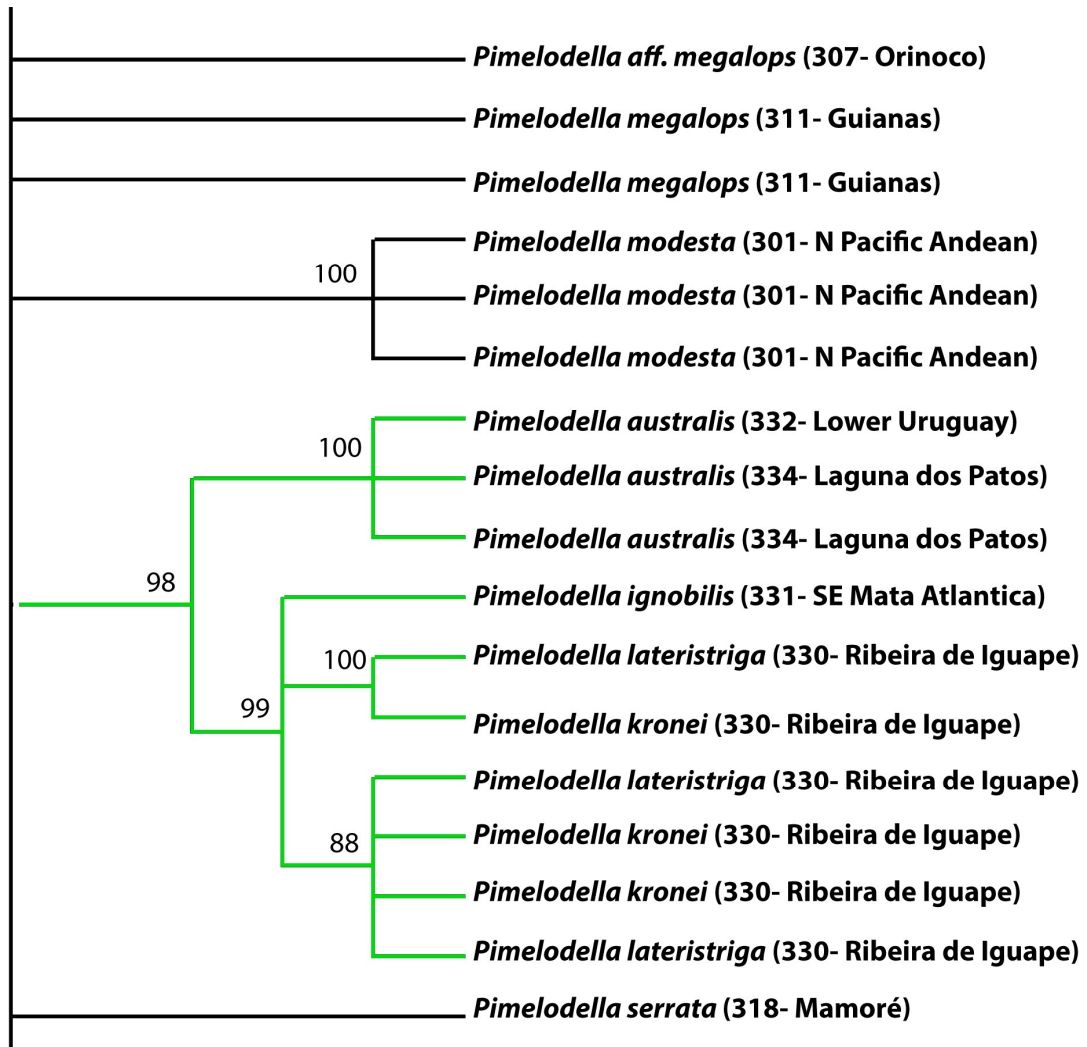


Figure 225. Clade D' and other taxa according to delimitation box in Figure 220. Branch values correspond to bootstrap (%).

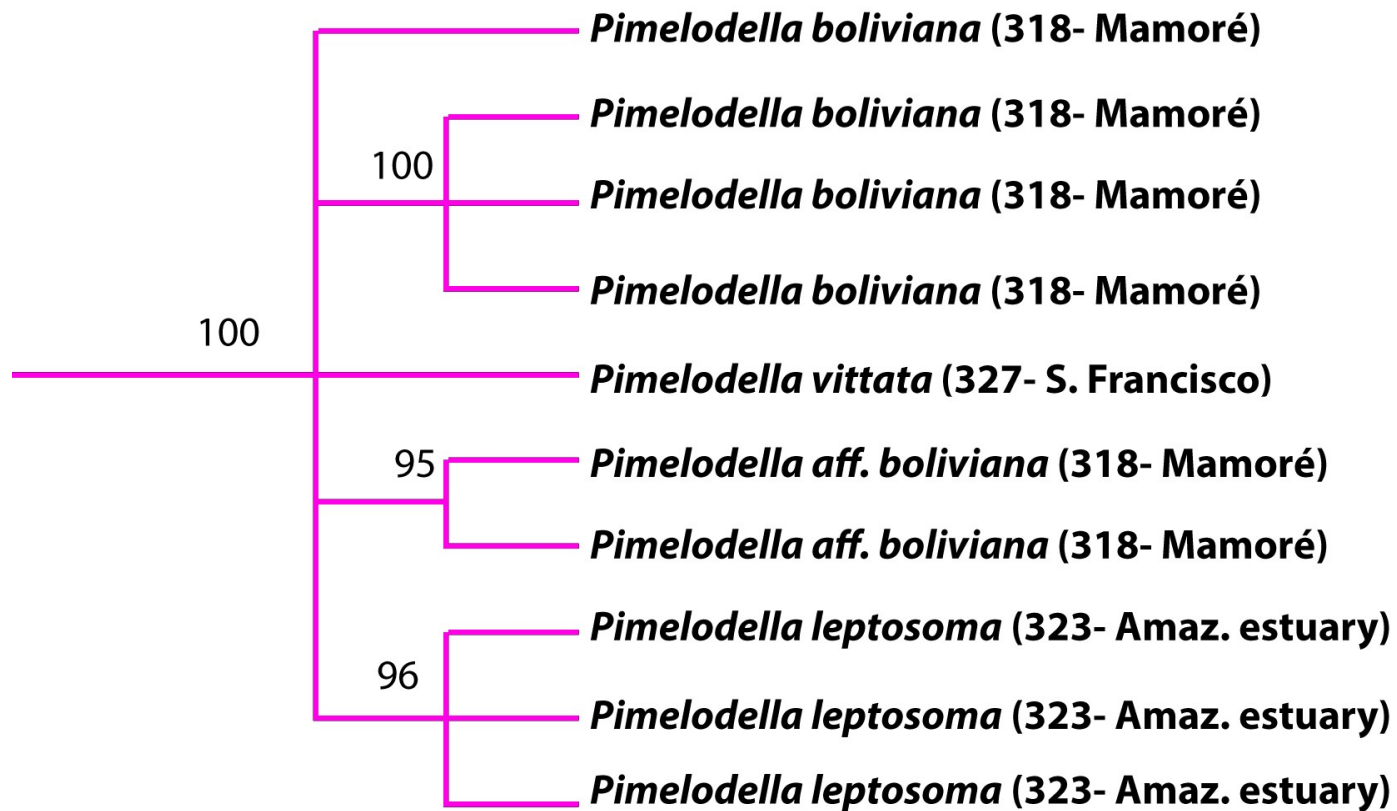


Figure 226. Clade E', according to delimitation box in Figure 220. Branch values correspond to bootstrap (%).

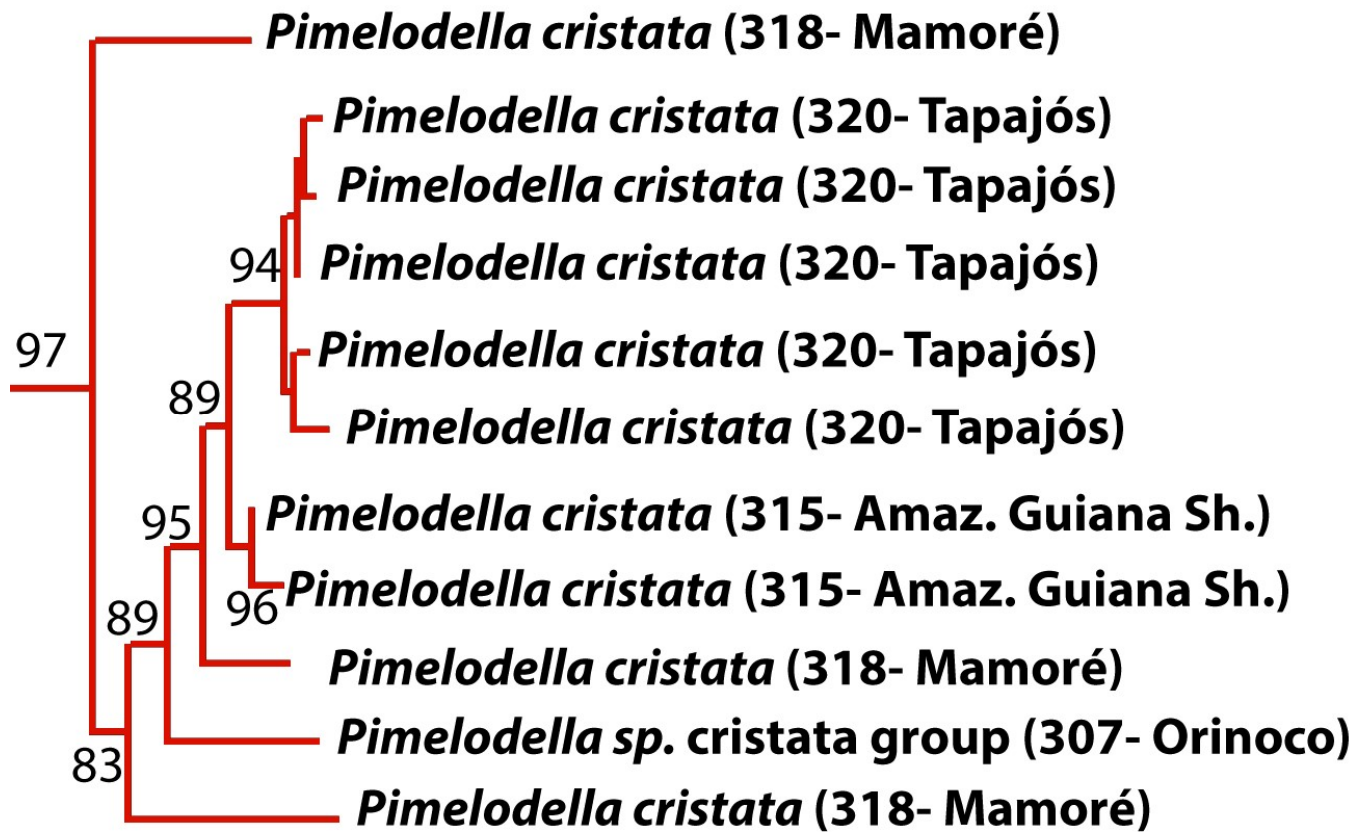


Figure 228. Clade A, according to delimitation box in Figure 227. Branch values correspond to bootstrap (%).

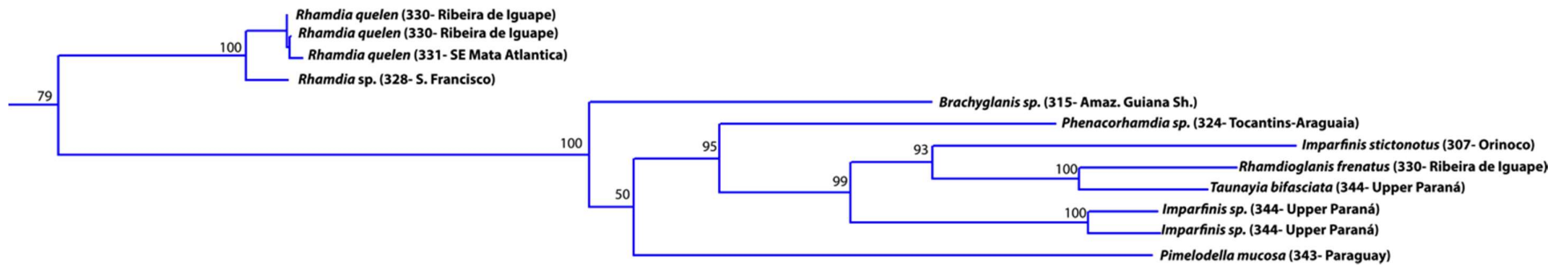


Figure 229. Clade B2”, according to delimitation box in Figure 227. Branch values correspond to bootstrap (%).

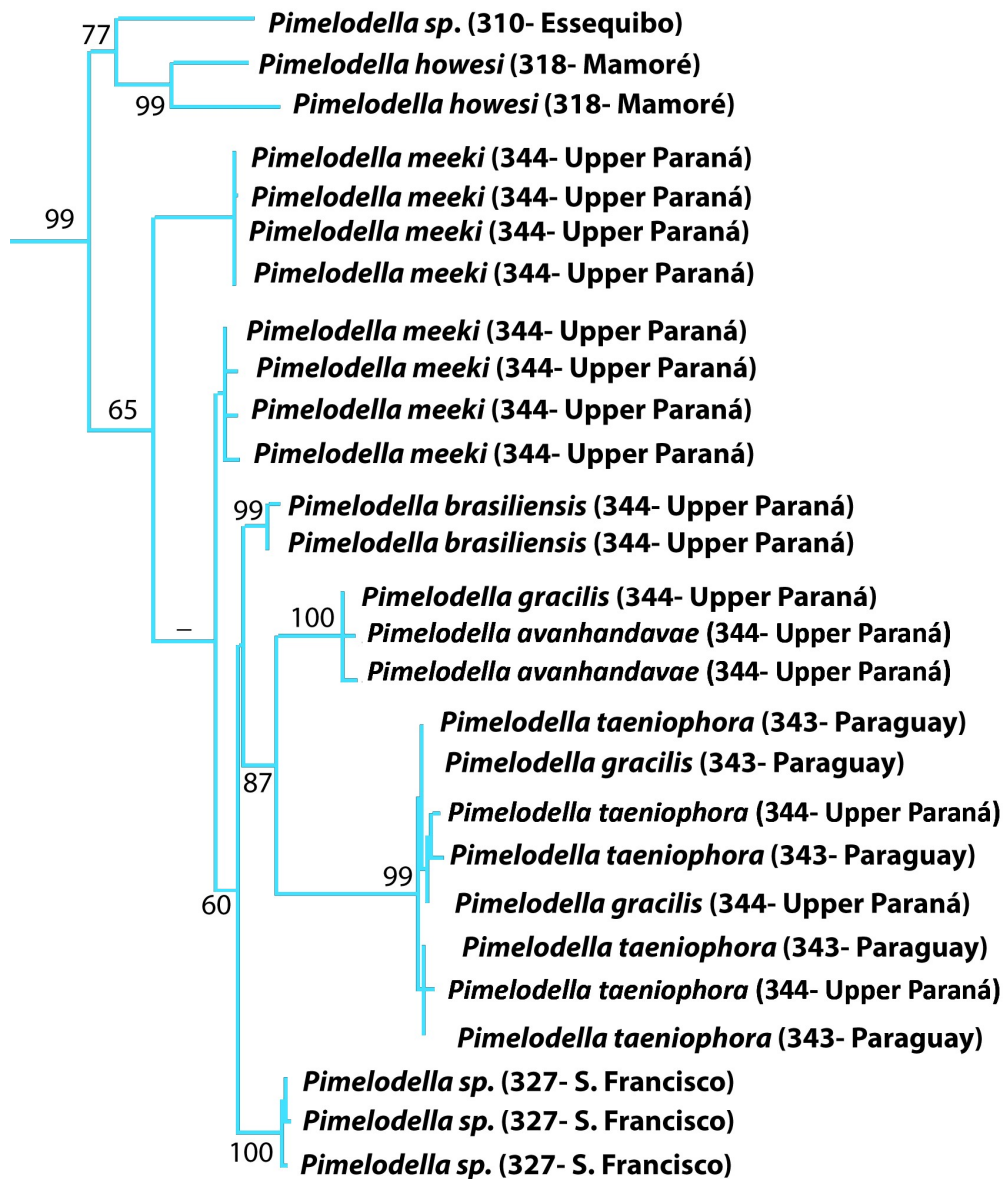


Figure 230. Clade B3'', according to delimitation box in Figure 227. Branch values correspond to bootstrap (%), clades not recovered in bootstrap tree are indicate by -.

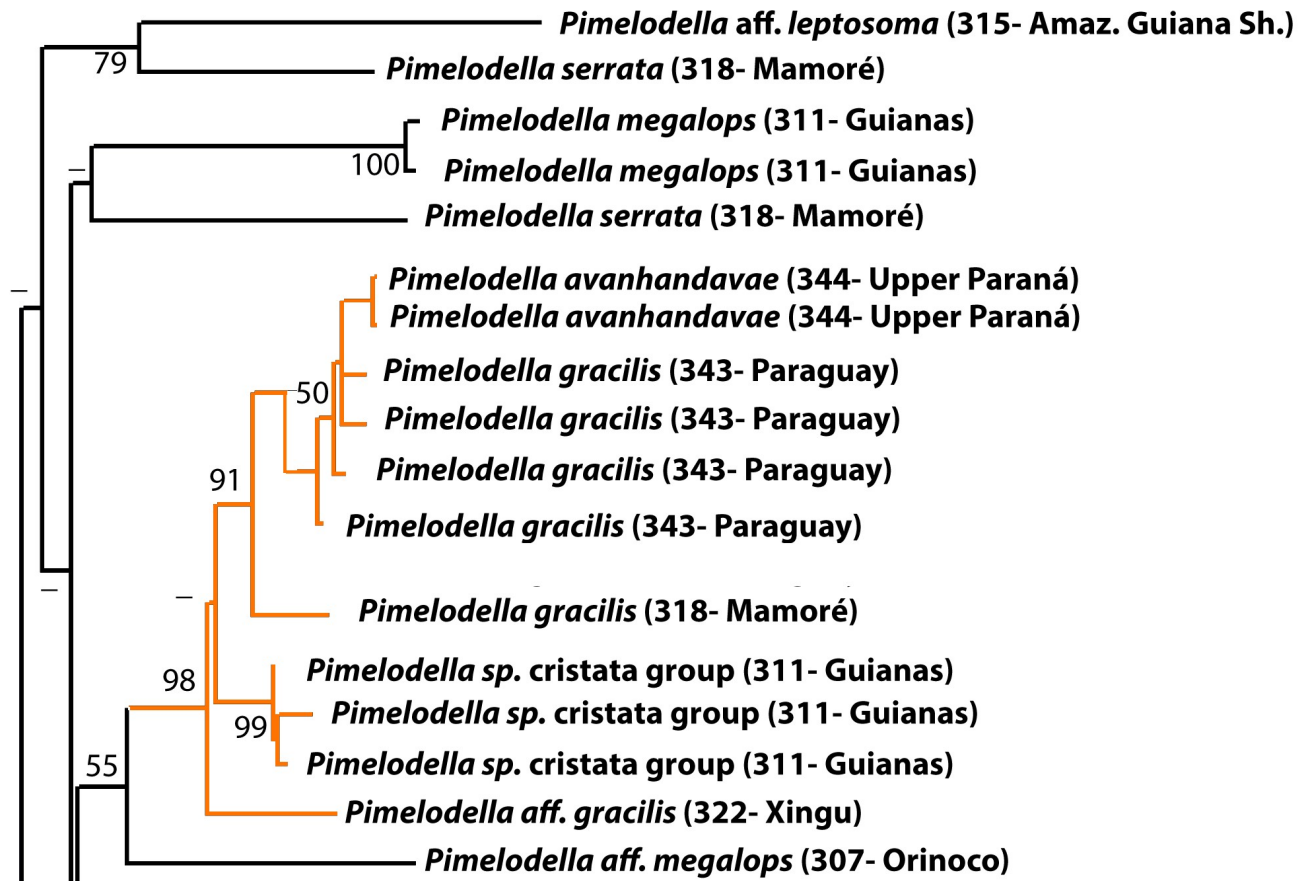


Figure 231. Specimens of orange delimitation box of Figure 227, corresponding to clade C” and other taxa. Branch values correspond to bootstrap (%), clades not recovered in bootstrap tree are indicate by –.

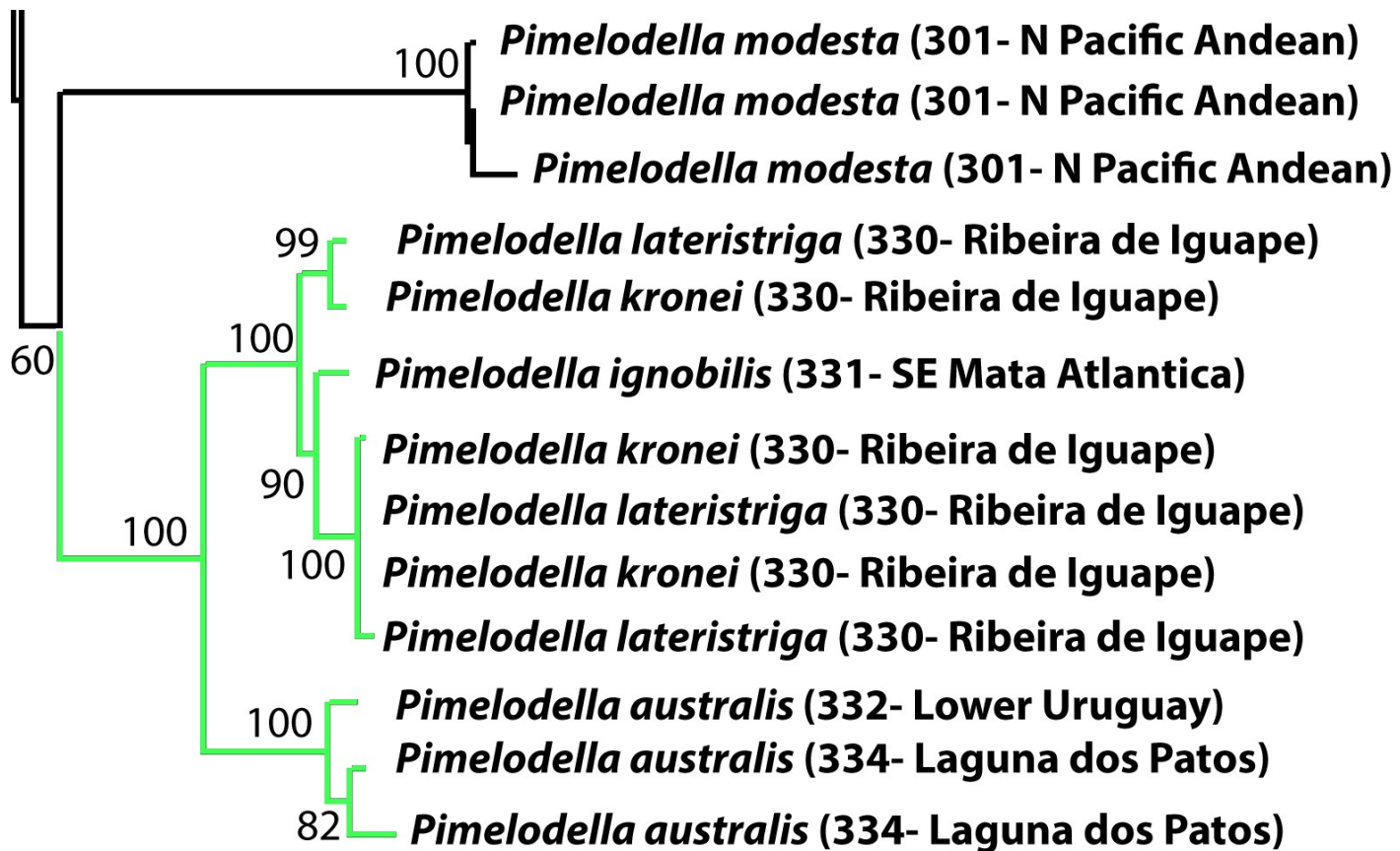


Figure 232. Specimens of green delimitation box of Figure 227, corresponding to clade D” and other taxa. Branch values correspond to bootstrap (%).

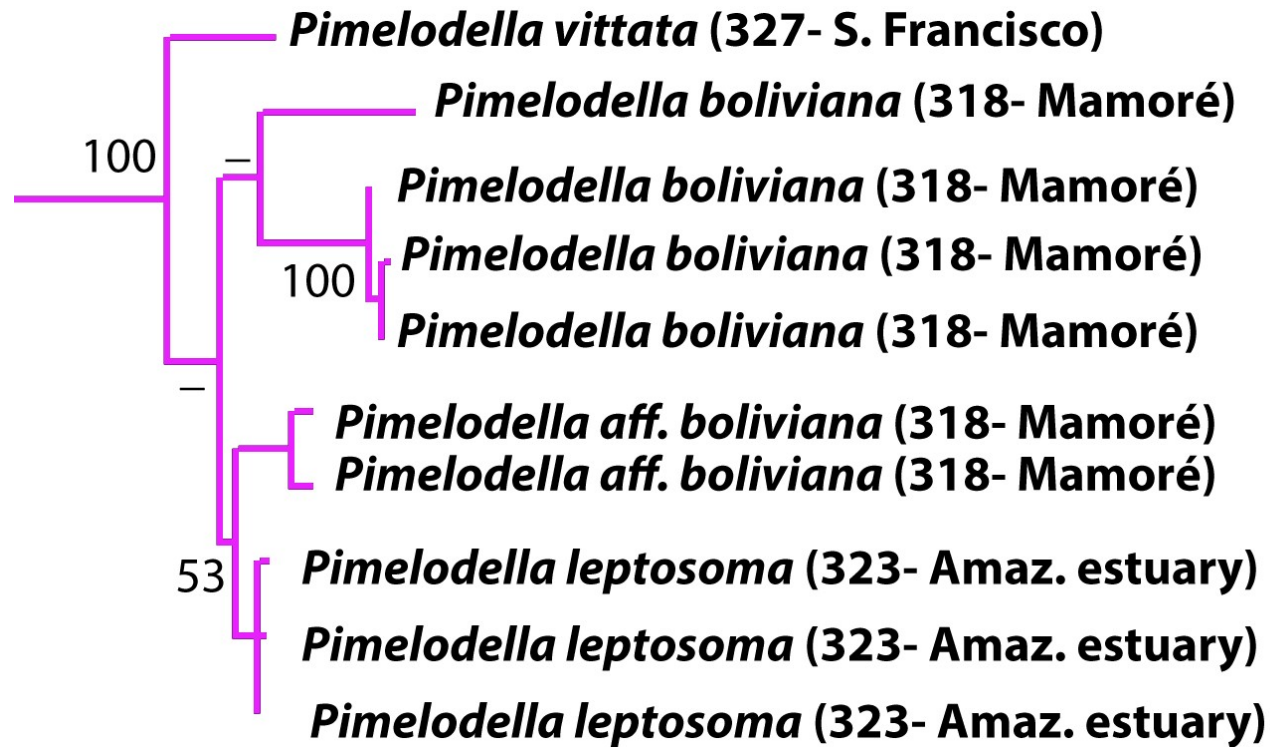


Figure 233. Clade E', according to delimitation box in Figure 227. Branch values correspond to bootstrap (%), clades not recovered in bootstrap tree are indicate by -.

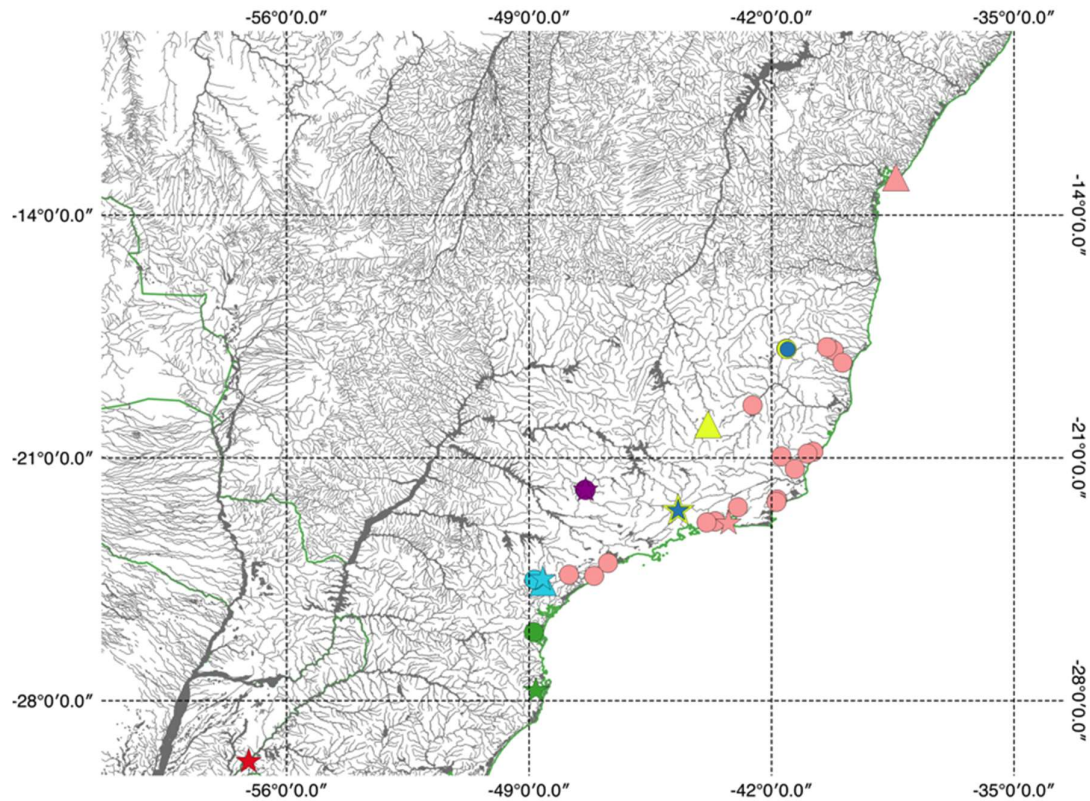


Figure 234. Distribution map of the following *Pimelodella*: *P. australis*.— red star: holotype and paratypes; *P. boschmai*.— purple star: holotype, purple circle: other material; *P. brasiliensis*.— yellow star: holotype, yellow circle: other material, yellow triangle: lectotype of *P. eigenmanni*, junior-synonym of *P. brasiliensis*; *P. harttii*.— dark blue star: holotype, dark blue circle: other material; *P. ignobilis*.— green star: holotype; green circle: other material; *P. kronei*.— light blue star: holotype, light blue circle: other material; light blue triangle: neotype of *P. transitoria*, junior-synonym of *P. kronei*; *P. lateristriga*.— pink star: holotype, pink circle: other material, pink triangle: lectotype of *P. bahiana*, junior-synonym of *P. lateristriga*.

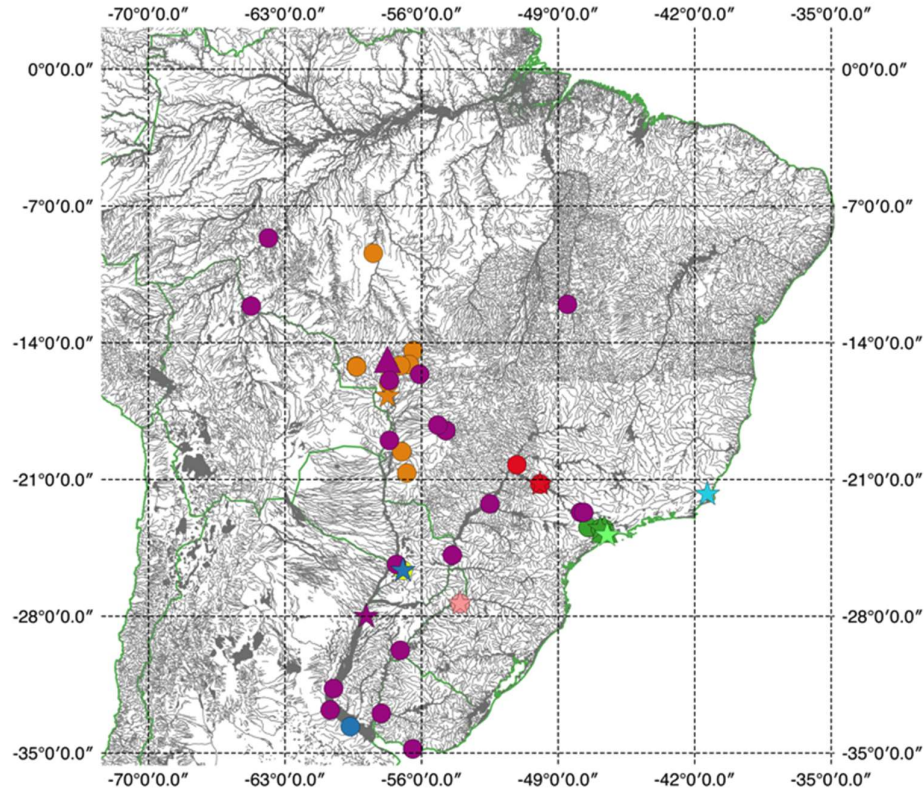


Figure 235. Distribution map of the following *Pimelodella*: *P. avanhandavae*.— red star: holotype, red circle: other material; *P. gracilis*.— purple star: lectotype, purple circle: other material, purple triangle: lectotype of *P. taenioptera*, junior-synonym of *P. gracilis*; *P. griffini*.— yellow star (same place as blue star): holotype, yellow circle: other material; *P. laticeps*.— dark blue star: holotype; dark blue circle: other material; *P. longipinnis*.— light green star: holotype; *P. meeki*.— dark green star: holotype, dark green circle: other material, dark green triangle: lectotype of *P. rudolphi*, junior-synonym of *P. meeki*; *P. pectinifera*.— light blue star: holotype; *P. straminea*.— pink star: holotype, pink circle: other material; *P. taenioptera*. — orange star: lectotype, orange circle: other material.

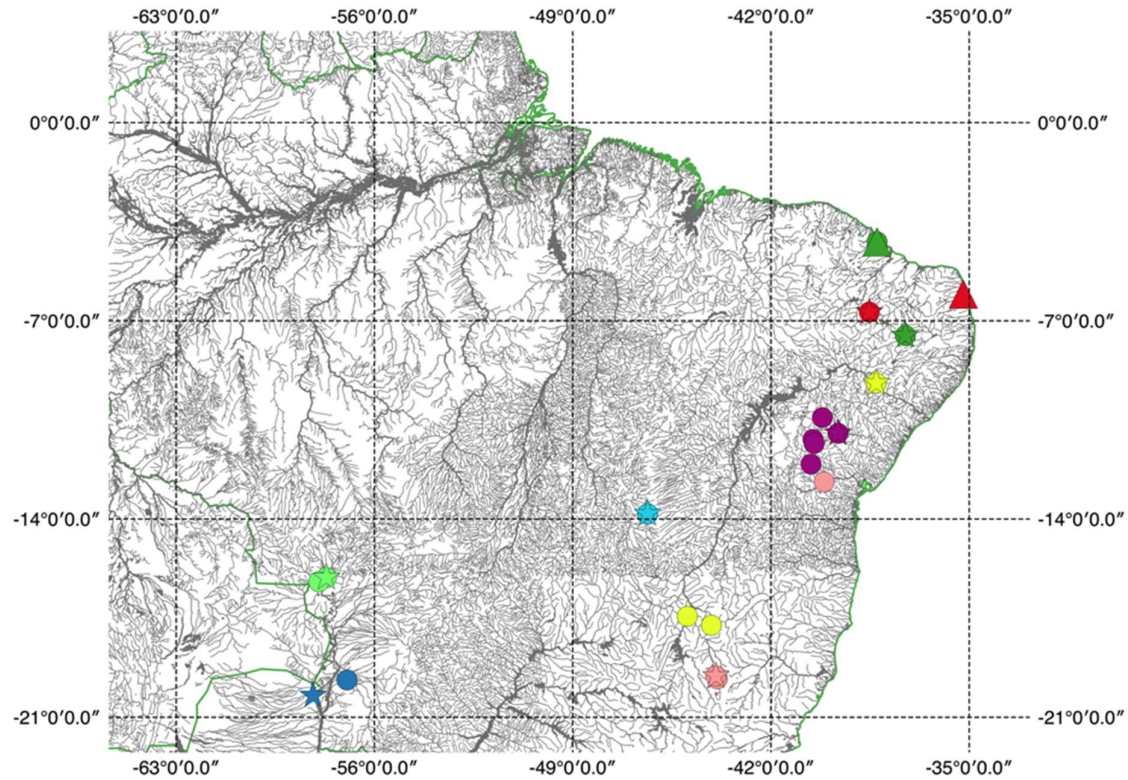


Figure 236. Distribution map of the following *Pimelodella*: *P. enochi*.— red star: holotype, red circle: other material, red triangle: holotype of *P. papariae*, junior-synonym of *P. enochi*; *P. itapicuruensis*.— purple star: holotype, purple circle: other material; *P. laurenti*.— yellow star: holotype, yellow circle: other material; *P. mucosa*.— dark blue star: holotype; dark blue circle: other material; *P. notomelas*.— light green star: holotype, light green circle: other material; *P. robinsoni*.— dark green star: holotype, dark green circle: other material, dark green triangle: holotype of *P. wolffi*, junior-synonym of *P. robinsoni*; *P. spelaea*.— light blue star: holotype, light blue circle: other material; *P. vittata*.— pink star: holotype, pink circle: other material.

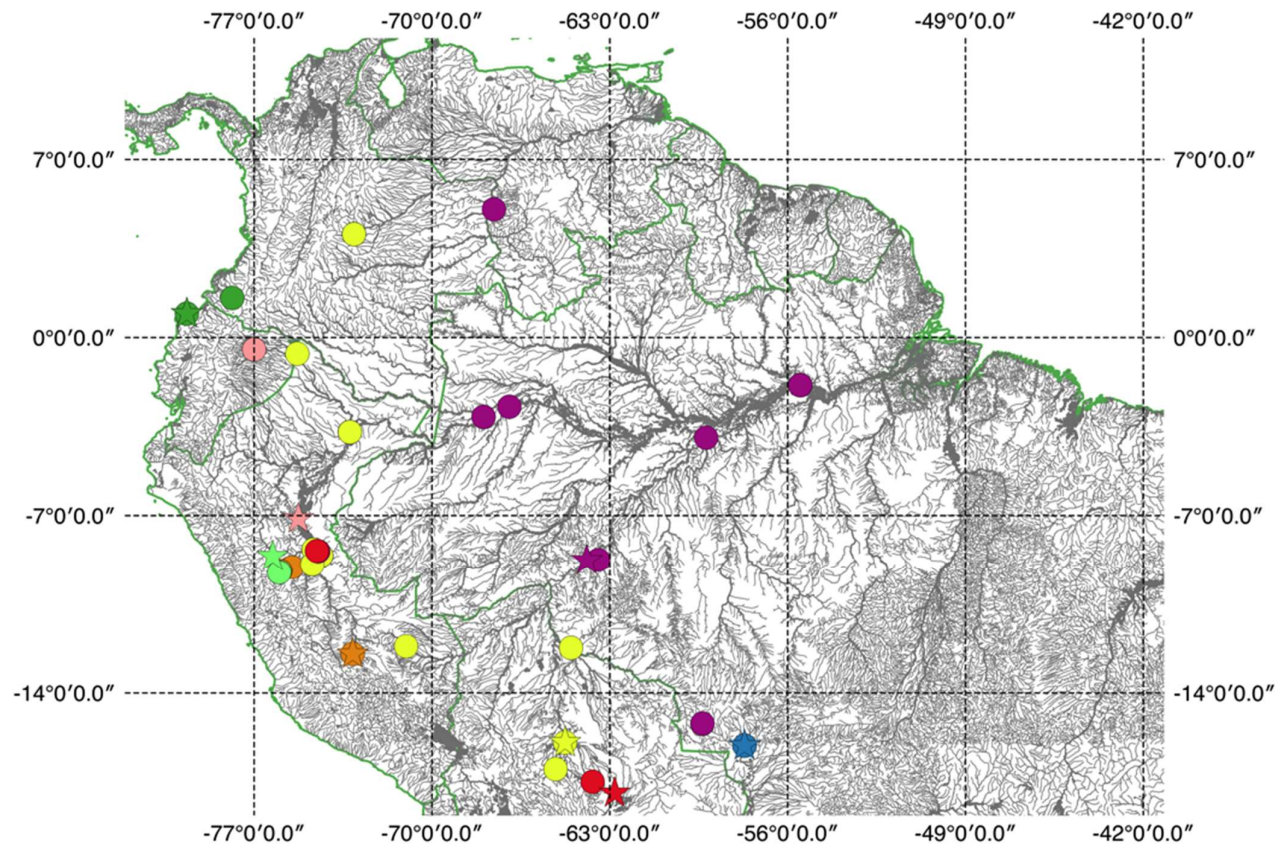


Figure 237. Distribution map of the following *Pimelodella*: *P. boliviana*.— red star: holotype, red circle: other material; *P. hasemani*.— purple star: holotype, purple circle: other material; *P. howesi*.— yellow star: holotype, yellow circle: other material; *P. megalura*.— dark blue star: holotype; dark blue circle: other material; *P. montana*.— light green star: holotype, light green circle: other material; *P. modesta*.— dark green star: holotype, dark green circle: other material; *P. peruana*.— pink star: holotype, pink circle: other material; *P. rocae*.— orange star: holotype, orange circle: other material.

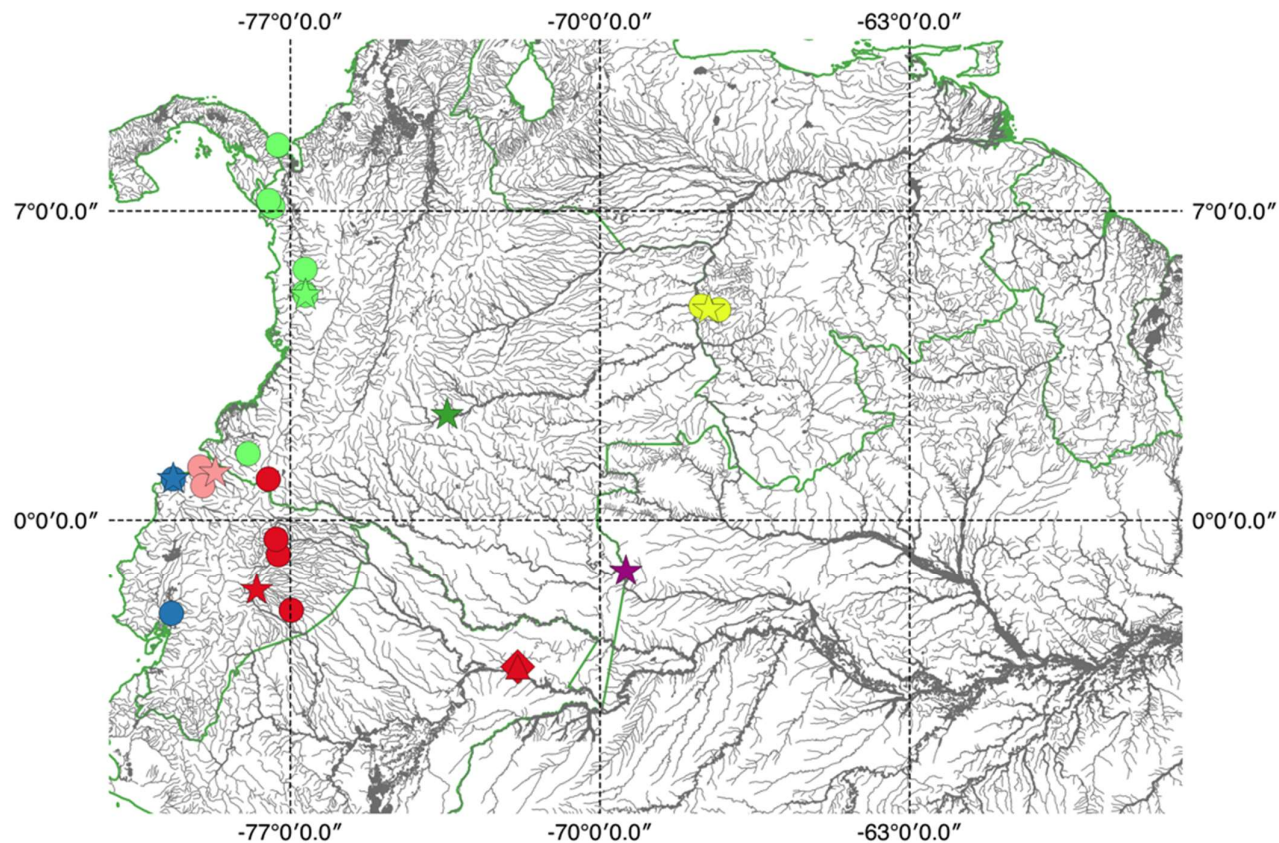


Figure 238. Distribution map of the following *Pimelodella*: *P. buckleyi*.— red star: lectotype, red circle: other material, red triangle: paralectotype of *P. cyanostigma*, junior-synonym of *P. buckleyi*, red diamond: holotype of *P. copei*, junior-synonym of *P. buckleyi*; *P. conquetaensis*.— purple star: holotype; *P. cruxenti*.— yellow star: lectotype, yellow circle: other material; *P. elongata*.— dark blue star: lectotype; dark blue circle: other material; *P. eutaenia*.— light green star: lectotype, light green circle: other material; *P. figueroai*.— dark green star: paratype; *P. grisea*.— pink star: holotype, pink circle: other material.

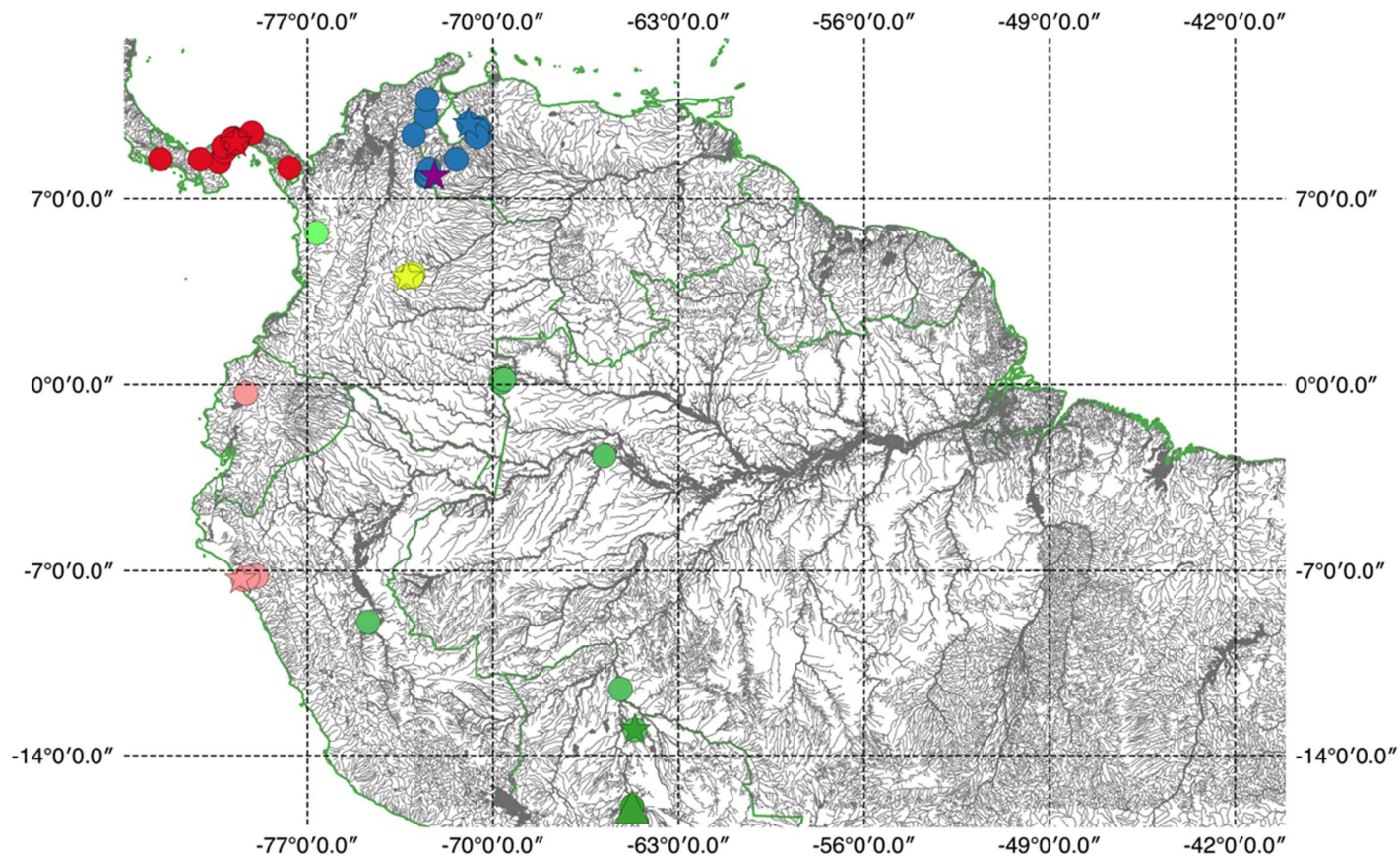


Figure 239. Distribution map of the following *Pimelodella*: *P. chagresi*.— red star: lectotype, red circle: other material; *P. linami*.— purple star: holotype; *P. metae*.— yellow star: holotype, yellow circle: other material; *P. odynea*.— dark blue star: holotype; dark blue circle: other material; *P. reyesi*.— light green circle: other material; *P. serrata*.— dark green star: holotype, dark green circle: other material, dark green triangle: holotype of *P. chaparae*, junior-synonym of *P. serrata*; *P. yuncensis*.— pink star: lectotype, pink circle: other material.

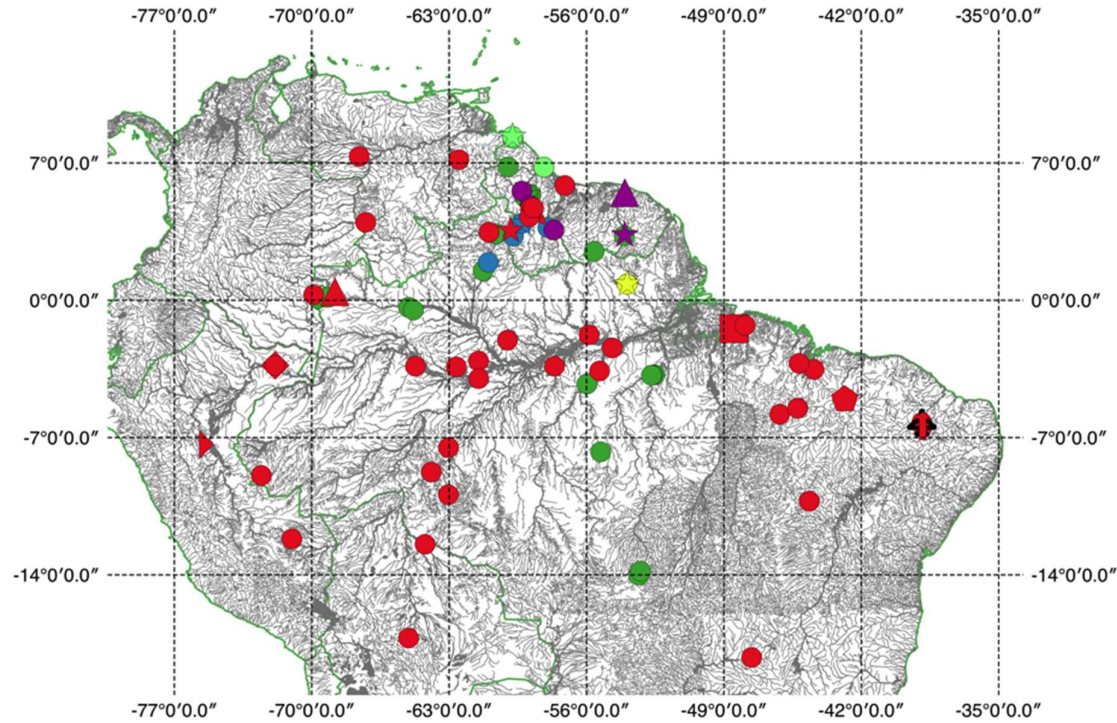


Figure 240. Distribution map of the following *Pimelodella*: *P. cristata*.— red star: lectotype, red circle: other material, red triangle: holotype of *P. breviceps*, junior-synonym of *P. cristata*, red diamond: lectotype of *P. cyanostygma*, junior-synonym of *P. cristata*, red arrow: holotype of *P. dorseyi*, junior-synonym of *P. cristata*, red half diamond: holotype of *P. hartwelli*, junior-synonym of *P. cristata*, red pentagon: holotype of *P. parnahybae*, junior-synonym of *P. cristata*, red square: lectotype of *P. steindachneri*, junior-synonym of *P. cristata*, red ellipse: holotype of *P. wessellii*, junior-synonym of *P. cristata*, red airplane: holotype of *P. witmeri*, junior-synonym of *P. cristata*; *P. geryi*.— purple star: holotype, purple circle: other material, purple triangle: holotype of *P. procera*, junior-synonym of *P. geryi*; *P. humeralis*.— yellow star: holotype, yellow circle: other material; *P. leptosoma*.— dark blue star: holotype; dark blue circle: other material; *P. macturki*.— light green star: holotype, light green circle: other material; *P. megalops*.— dark green star: holotype, dark green circle: other material.

Attachment 1: Original description of *Pimelodella humeralis*, in the article “A new species of *Pimelodella* (Siluriformes: Heptapteridae) from the Guiana Shield, Brazil” of Slobodian *et al.* (2017).



A new species of *Pimelodella* (Siluriformes: Heptapteridae) from the Guiana Shield, Brazil

VERONICA SLOBODIAN^{1,4}, ALBERTO AKAMA² & GUILHERME MOREIRA DUTRA³

¹Museu de Zoologia da Universidade de São Paulo, Seção de peixes, Av. Nazaré, 481, 04263-000, São Paulo, SP, Brazil.

²Museu Paraense Emílio Goeldi, Setor de Ictiologia, Avenida Magalhães Barata, 376, 66040-170 Belém, PA, Brazil

³Programa de Capacitação Institucional, Museu Paraense Emílio Goeldi, Coordenação de Zoologia, Avenida Magalhães Barata, 376, 66040-170, Belém, PA, Brazil.

⁴Corresponding author. E-mail: verorp@gmail.com

Abstract

A new species of *Pimelodella* is described from the Rio Ipitanga, Rio Jari basin, a left bank tributary of the Rio Amazonas in Brazil. The new species is diagnosed from all congeners by having a dark oval mark on the humeral region. It also differs from all congeners by a unique set of characters, including the presence of 47 to 49 total vertebrae, unpigmented areas dorsally and ventrally adjacent to the dark midlateral stripe, and maxillary barbels reaching at least to vertical through caudal fin insertion. Faunal similarities between the southern part of the eastern Guiana Shield and coastal drainages in the Guianas and Suriname are discussed.

Resumo

Uma espécie nova de *Pimelodella* é descrita do rio Ipiranga, bacia do rio Jari, tributário da margem esquerda do rio Amazonas, Brasil. A espécie nova é diagnosticada de todas as congêneres com base em uma marca escura oval na região humeral. Também se difere de suas congêneres por uma combinação exclusiva de caracteres, incluindo 47 a 49 vértebras totais, uma região não-pigmentada adjacente à faixa escura lateral, dorsal e ventralmente, e barbilhões maxilares alcançando pelo menos a inserção da nadadeira caudal. Similaridades entre a fauna da porção sul do Escudo das Guianas e das drenagens das Guianas e Suriname são discutidas.

Key words: Biodiversity; Freshwater ichthyofauna; humeral mark; taxonomy

Introduction

Pimelodella Eigenmann & Eigenmann 1888 is an important component of the freshwater fish fauna of the Neotropics. With 79 valid species, *Pimelodella* is the most species-rich genus of Heptapteridae, a family composed of 211 total species in 24 genera (Eschmeyer and Fong 2017). *Pimelodella* is distributed throughout cis- and trans-andean Neotropical drainages from Panamá to Argentina (Eschmeyer, Fricke & van der Laan, 2017). Due to unsettled taxonomic and systematic problems, the genus represents one of the most difficult bottlenecks for understanding the diversity of Neotropical freshwater fishes. The taxonomic problems result from a highly conservative morphology, species with putatively wide distributions, and lack of comprehensive studies on the numerous specimens vouchered in natural history collections. Many species of *Pimelodella* lack rigorous taxonomic study and, to some degree, those considered valid merely correspond to a list of available names.

Carl Eigenmann (1917) revised *Pimelodella* and *Typhlobagrus*, the latter a monotypic genus proposed by Miranda Ribeiro (1907) for his new species *T. kronei*. Eigenmann (1917) recognized 35 taxa in *Pimelodella* (34 species plus one subspecies) including 12 taxa (11 species plus one subspecies) he described as new. Eigenmann (1917) also provided a diagnosis of the genus based on several non-unique features. Since Eigenmann's (1917)

revision, *Typhlobagrus* has been synonymized with *Pimelodella*, and several species have been described, removed from or transferred to *Pimelodella* (Ferraris, 2007). As diagnosis for other related genera were redefined (Bockmann & Miquelarena, 2008, Slobodian, 2013, and Slobodian & Bockmann, 2013), *Pimelodella* remains distinguished from other heptapterids by the following unique character combination: body moderately elongated, usually between 12–30 cm standard length; supraoccipital process long, reaching the anterior nuchal plate; anterior and posterior fontanels open, long, separated by epiphyseal bar; limits of eye well defined by free orbital rim, especially pronounced anteriorly and dorsally; pectoral fin with single unbranched ray (spine) strong and pungent, bearing both anterior and posterior dentations, and 7–9 (usually 8) branched rays; branchiostegal rays usually 6; caudal fin deeply forked; median caudal-fin rays not articulated to hypural plate; hypural 5 as a single structure and not fused to hypural plate; body generally with dark midlateral stripe extending from the snout or posterior to the head until the insertion of or onto the median caudal-fin rays.

Herein, we describe a distinct new species from the Rio Ipitinga (Rio Jari basin) that is consistent with the aforementioned diagnosis of *Pimelodella*.

Material and methods

Measurements were taken as point-to-point distances with digital calipers under a dissecting scope, following Slobodian & Bockmann (2013). Measurements of head parts are presented as proportions of head length (HL), except for measurements of barbels which were converted to proportions of standard length (SL); head length and measurements of body parts are given as proportions of standard length. Meristics and fin position follow Bockmann & Castro (2010). Vertebral counts include the anteriormost elements modified into the complex vertebra counted as five, all free vertebrae, and the compound caudal centrum (PU1+U1) counted as one (Lundberg & Baskin, 1969). Number of specimens counted for meristics are presented in parenthesis, and holotype counts are indicated by an asterisk. The cleared and staining protocol (c&s) followed Taylor and Van Dyke (1985); osteological data on remaining specimens was obtained with aid of X-ray (xr) images. Osteological terminology and laterosensory-canal nomenclature follow Bockmann & Miquelarena (2008). Nomenclature on pectoral-fin and dorsal-fin spines ornamentations follow Vanscoy *et al.* (2015), and dentations are considered retrorse if pointed towards base of the spine. Distal tip of pectoral-fin spine may bear 1–2 incipient dentations not completely ossified, derived from spine segments in formation; incipient dentations not included in count of pectoral-fin spine dentations. Institutional codes followed Sabaj (2016).

Results

Pimelodella humeralis Slobodian, Akama & Dutra new species

Figures 1–3, Table 1

Pimelodella sp.—Aleixo *et al.*, 2011:20 [*in list of species*].

Holotype. MPEG 34994, 77.4 mm SL, xr, Brazil, Pará, Almeirim, Rio Ipitinga, Rio Jari basin, left bank tributary of the Rio Amazonas, 0°49'38.3"N 53°55'29.6"W, 28 Oct 2008, T. M. S. Freitas.

Paratypes. MPEG 15712, 3, 67.3–70.4 mm SL, xr (1, 77.4 mm SL); MZUSP 119908, 1, 73.0 mm SL, xr; USNM 432550, 1, 50.3 mm SL, xr, same data as the holotype. ANSP 203219, 2, 71.8–72.5 mm SL, xr; MPEG 15744, 5, 71.7–77.5 mm SL, xr (1, 77.5 mm SL), 1 c&s (71.0 mm SL); MZUSP 121686, 1, 68.3 mm SL, 1 c&s (76.1 mm SL); USNM 432551, 1, 77.7 mm SL, Brazil, Pará, Almeirim, Rio Ipitinga, Rio Jari basin, left bank tributary of the Rio Amazonas, 0°49'0.4"N 53°55'43.6"W, 29 Oct 2008, T. M. S. Freitas.

Diagnosis. *Pimelodella humeralis* differs from all congeners by having a dark anteriorly oblique blotch in the humeral region (Fig. 1), its anterior limit slightly ahead of vertical through the spinelet, and its posterior limit at vertical through the base of second branched dorsal-fin ray. Moreover, *P. humeralis* differs from most congeners (except *P. breviceps*, *P. cristata*, *P. dorseyi*, *P. gracilis*, *P. ophthalmica*, *P. parnahybae*, *P. steindachneri*, *P. taenioptera*, *P. wessellii* and *P. witmeri*) by having 47 to 49 total vertebrae (vs. 37 to 44 total vertebrae). *Pimelodella humeralis* differs from *P. breviceps*, *P. cristata*, *P. dorseyi*, *P. gracilis*, *P. ophthalmica*, *P. parnahybae*, *P.*

steindachneri, *P. taenioptera* and *P. wessellii* by having 8–11 retrorse triangular, broad-based and strongly inclined dentations confined to basal three-fourths of pectoral-fin spine posterior margin (vs. 11–25 retrorse, narrow-base dentations along almost entire pectoral-fin spine posterior margin in *P. breviceps*, *P. cristata*, *P. dorseyi*, *P. gracilis*, *P. ophthalmica*, *P. parhanybae*, *P. steindachneri*, *P. taenioptera* and *P. wessellii*; condition unknown in *P. witmeri*), and also by the presence (vs. absence) of unpigmented region dorsally and ventrally adjacent to the dark midlateral stripe. The new species is further distinguished from *P. breviceps* by maxillary barbels reaching at least the caudal-fin insertion (vs. maxillary barbels not surpassing vertical through middle rays of anal fin); from *P. steindachneri*, *P. taenioptera* and *P. wessellii* by longest ray of dorsal-fin 18.7–22.5% SL (vs. 23.1–28.0% SL); from *P. dorseyi* and *P. gracilis* by the relatively longer dorsal-fin spine (spine 13.6–24.7% vs. 25.0–50.0% shorter than first dorsal-fin ray total length); from *P. breviceps* and *P. taenioptera* by having caudal-fin lobes subequal (vs. dorsal lobe distinctly longer); from *P. gracilis* by having dark midlateral stripe from pseudotympanum to the caudal-fin insertion narrow (vs. wide), and dorsal region of body lacking dark stripes (vs. paired diffuse dark stripes evident from posterior region of head to at least adipose-fin insertion); from *P. ophthalmica*, *P. parhanybae*, *P. steindachneri*, *P. wessellii* and *P. witmeri* by the having dorsal fin pigmentation composed of hyaline stripe near base, followed distally by a dark stripe, another hyaline stripe and distalmost two-fifths dark (vs. dorsal fin dark near base, followed distally by a hyaline stripe and rest of fin darker; condition uncertain in *P. breviceps*, *P. cristata*, *P. gracilis* and *P. taenioptera*).



FIGURE 1. *Pimelodella humeralis*, holotype, MPEG 34994, 77.4 mm SL. Brazil, Pará, Rio Jari basin, Rio Ipitinga. Left lateral (A) and dorsal (B) views.

Description. Measurements in Table 1. Body of moderate height, depth at dorsal-fin origin five times or more in standard length, and compressed, body width at dorsal-fin origin not exceeding half of head length (Fig. 1). Greatest body depth at dorsal-fin origin. Dorsal profile straight from snout to dorsal-fin origin; slightly concave from that point to adipose-fin origin. Profile slightly convex along adipose fin base, and concave along caudal peduncle. Ventral profile of body slightly convex from snout to posterior limit of branchiostegal membrane, convex

between branchiostegal membrane and pelvic-fin origin, slightly concave from the latter to anal-fin origin, and broadly concave from that point to caudal insertion.

Pseudotympanum large, oval, dorsal to posterior process of cleithrum and reaching 6th vertebrae (6). Posterior process of cleithrum triangular, its dorsal border straight to slightly concave. Axillary pore present at pectoral-fin base. Anus and urogenital papilla adjacent. Urogenital papilla short, triangular and tubular.

Head deep, depth at supraoccipital-process base half of head length. Mouth subterminal. Eye slightly elliptical, its greatest diameter along horizontal axis, placed dorsolaterally. Limits of eye well defined by a free orbital rim; margin distinctly invaginated, especially along anterior and dorsal portions. Bony interorbital distance smaller than eye diameter. Anterior naris tubular; posterior naris enclosed anteromedially by shallow flap. Premaxilla and dentary each with five or six rows of small villiform teeth. Barbels thin, and slightly depressed, elliptical in cross-section. Maxillary barbel finishing between verticals through anterior and posterior limits of caudal-fin, respectively. Outer mental barbel, when stretched parallel to main body axis, finishing between verticals through almost posterior limit of adpressed pectoral-fin and pelvic fins origin. Inner mental barbels, when lying stretched parallel to main body axis, finishing between verticals through pectoral-fin origin and posterior limit of pectoral-fin base, respectively. Branchiostegal membranes almost entirely free, united to isthmus only at medial apex and not joined to each other anteriorly. Branchiostegal rays 6 (8). Supraoccipital process relatively large, reaching anterior nuchal plate; shape subrectangular, distal third slightly tapered, sometimes with a discrete constriction near base. Dorsal lamina of Weberian complex vertebrae reaching supraoccipital process near its anteriormost part, or anterior half extension, but never along its entire length.

Dorsal fin triangular, distal margin convex, depressed tip finishing between verticals through second-fifth and last fourth of adpressed pelvic-fin, respectively. Dorsal-fin rays I,6 (17) plus anteriormost spinelet. Distance between terminus of dorsal-fin base and adipose-fin origin about a third of dorsal-fin base. Anteriormost dorsal-fin pterygiophore inserted posterior to neural spine of vertebra 4 (8); posteriormost dorsal-fin pterygiophore located ahead of neural (or pseudoneural) spine of vertebrae 11* (5) or 12 (1). Spinelet large with wide base and rounded distal tip. Unbranched dorsal-fin ray (Fig. 2) mostly ossified as a spine; rigid part usually relatively long (approximately a fourth or less shorter than the first dorsal-fin ray total length); distal half of anterior margin with serrae. Posterior margin of dorsal-fin spine with serrae along distal third, and small, straight to retrorse, dentations along second-third of its length.

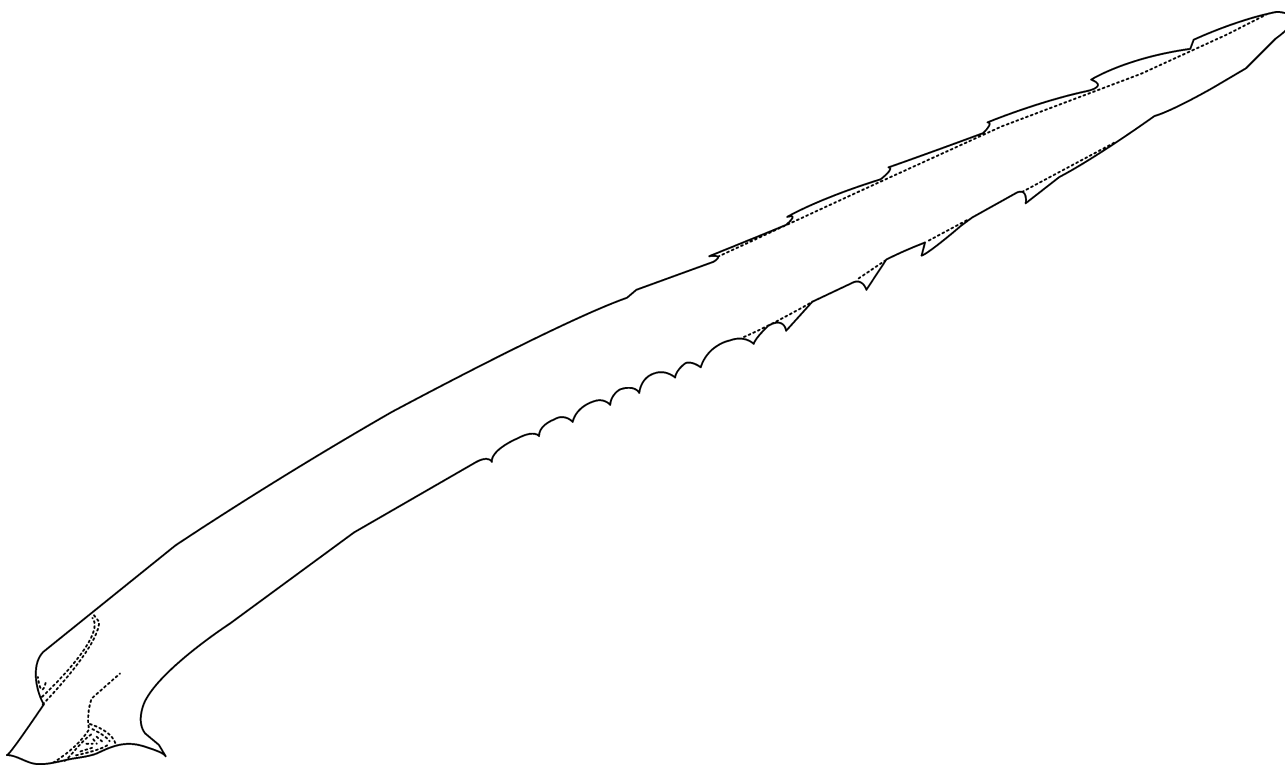


FIGURE 2. Left lateral view of dorsal-fin spine in *Pimelodella humeralis*, paratype, MZUSP 121686, 76.1 mm SL, total length of spine 11.3 mm.

Pectoral-fin rays I,8 (6)– I,9* (11), pectoral fin triangular with concave distal border. First pectoral-fin ray curved with proximal portion rigid, forming a spine (Fig. 3), and short distal tip flexible and distinctly segmented. Anterior margin of pectoral-fin spine with minute, smooth-sided, straight dentations along its basal half (except for a smooth anterior ridge near the spine base), and serrae along its distal half; posterior margin with 8–11 retrorse dentations along its basal three-quarters (10 dentations in holotype).

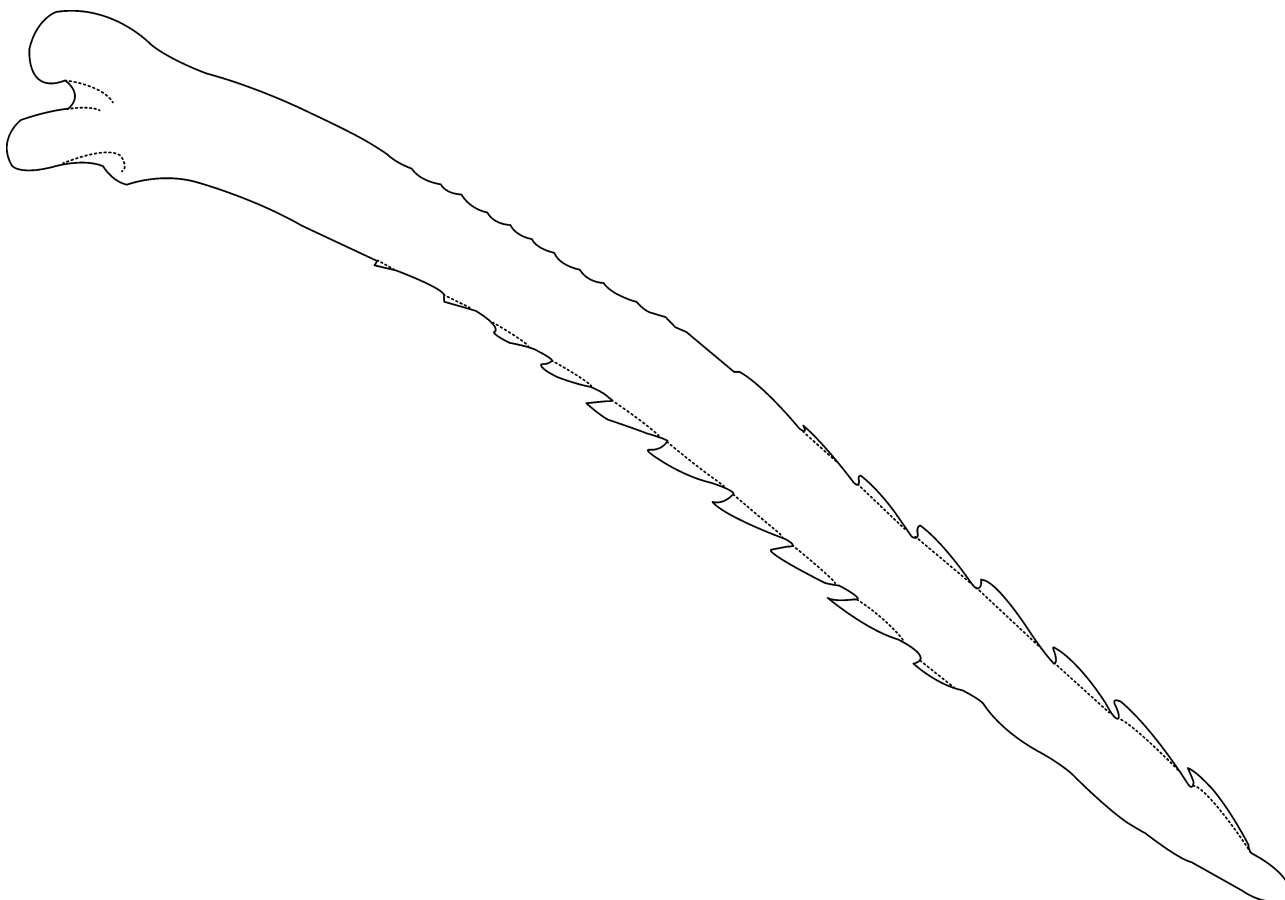


FIGURE 3. Ventral view of left pectoral-fin spine in *Pimelodella humeralis*, holotype, MPEG 34994, 77.4 mm SL, total length of spine 12.0 mm.

Pelvic-fin rays i,5 (17), extended pelvic fin triangular with straight distal border. Pelvic-fin origin at or slightly posterior to vertical through terminus of dorsal-fin base. Tip of adpressed pelvic fin surpassing adipose-fin origin, but never exceeding the first quarter of its base. First unbranched ray distinctly shorter than first and second branched rays, the latter two roughly the same size; remaining rays progressively shorter.

Anal-fin rays iv,10 (1), v,10* (9), vi,10 (5), v,11 (1) or vi,11 (11); distal border of extended anal fin convex. Two or three anteriormost anal-fin rays vestigial, unsegmented, embedded in thick skin fold. Anal-fin origin surpassing first quarter of adipose-fin base, but never exceeding its half; anal-fin adpressed terminus between verticals through 85 and 90% of adipose-fin base, respectively. Tip of anteriormost anal-fin pterygiophore inserted posterior to hemal spine of vertebra 22 (1), 23 (4) or 24* (3). Tip of posteriormost anal-fin pterygiophore inserted ahead of hemal spine of vertebra 31 (1), 32* (2) or 33 (5).

Adipose fin very long, twice in SL, forming ascending elevated curve in lateral profile with deepest point approximately at midlength. Adipose fin emerging gradually, its posterior limit as a rounded, free lobe. Adipose-fin origin at vertical through vertebral centra 14 (1), 16* (4) or 17 (3); adipose-fin terminus at vertical through vertebral centra 43 (8).

Caudal fin deeply forked, lobes subequal. Caudal peduncle length usually more than three times its depth or slightly longer. Dorsal lobe with 7* (16), rarely 8 (1) branched, 1 (17) unbranched principal, and 15 (1) to 20 (1) (holotype 17) procurrent fin-rays. Ventral lobe with 8* (16), rarely 9 (1) branched, 1 (17) unbranched principal, and 13 (1) to 25 (1) (holotype 20) procurrent fin-rays. Parahypural not fused to Hypural 1. Hypurals 1 and 2 completely

co-ossified into single ventral caudal plate. Hypurals 3 and 4 completely fused to each other. Hypural 5 not fused to hypural 3+4. Single rod-like autogenous epural. Hypurapophysis and secondary hypurapophysis fused, forming a horizontal shelf (hypurapophysis type C of Lundberg & Baskin, 1969). Median caudal-fin rays not articulated directly to caudal plate. Seven (8) rays articulated to dorsal caudal-fin plate (5 on hypurals 3+4 and 2 on hypural 5) and 7 (4) or 8* (4) rays articulated to ventral caudal-fin plate (5 or 6 on hypurals 1+2 and 2 on parahypural). Total vertebrae 47 (1) to 49 (2), usually 48* (5). Ribs 9 (9).

Head laterosensory canals with simple (unbranched) tubes usually ending in single pore. Supraorbital canal continuous and connected to infraorbital branch anteriorly (forming complex s2+i2 pore), and posteriorly to the otic branch. Supraorbital laterosensory canal with at least five branches: s1, s2, s3, s6 (epiphyseal branch), and s8 (parietal branch). Contralateral epiphyseal branches fused to each other medially, with single opening; a small canal towards posterior midline of head (13).

TABLE 1. Morphometric data for *Pimelodella humeralis* based on holotype and 16 paratypes. Abbreviations: Min—minimum; Max—maximum; n—number of specimens; x—average; SD—standard deviation.

	Holotype	Min.	Max.	n	x	SD
Total length (mm)	93.5	60.3	95.8	17	87.1	
Standard length (mm)	77.4	50.3	77.7	17	71.4	
Percentages of SL						
Body depth (dorsal)	17.9	17.2	21.7	17	18.6	1.1
Body width (dorsal)	11.4	11.4	14.4	17	12.6	0.7
Cleithral width	15.0	14.0	16.0	17	15.0	0.5
Head length	30.1	28.5	32.6	17	30.6	1.2
Maxillary-barbel length (left side)	97.4	93.4	122.1	17	108.8	8.1
Outer mental-barbel length (left side)	32.6	19.9	37.4	17	31.5	3.9
Inner mental-barbel length (left side)	17.3	16.0	33.5	17	18.7	4.0
Predorsal length	32.6	32.2	35.9	17	33.6	0.9
Distance between snout tip and terminus of dorsal-fin base	45.7	45.4	48.7	17	46.5	0.9
Distance between snout tip and dorsal-fin distal end	25.7	23.7	27.4	16	25.5	0.9
Dorsal fin to adipose fin	3.2	3.2	5.7	17	4.2	0.5
Dorsal-fin base	13.3	13.3	15.4	17	14.5	0.5
Length of first dorsal-fin ray (unbranched)	22.2	18.7	22.2	6	20.2	1.2
Length of rigid part of first dorsal-fin ray	16.7	14.5	18.8	17	16.3	1.2
Length of second dorsal-fin ray (first branched)	22.5	15.1	22.5	17	20.2	1.6
Length of third dorsal-fin ray (second branched)	18.6	13.8	21.5	17	19.4	1.9
Prepectoral length	21.9	21.2	25.7	17	23.0	1.3
Distance between snout tip and terminus of pectoral-fin base	25.2	23.9	29.8	17	25.8	1.6
Distance between snout tip and pectoral-fin distal end	15.5	13.5	18.9	17	16.7	1.1
Length of first left pectoral-fin ray (unbranched)	15.9	15.9	17.9	11	16.8	0.7
Length of rigid part of first left pectoral-fin ray	15.5	14.3	16.8	17	15.7	0.7
Length of second left pectoral-fin ray (first branched)	15.2	13.8	16.8	17	15.5	0.8
Length of third left pectoral-fin ray (second branched)	13.2	11.1	20.6	17	14.1	2.0
Prepelvic length	42.5	41.9	47.9	17	44.3	1.4
Distance between snout tip and terminus of pelvic-fin base	47.0	45.6	50.2	17	46.8	1.2
Distance between snout tip and pelvic-fin distal end	14.4	12.0	15.3	16	14.1	0.8
Distance between pelvic fins	4.0	3.1	4.4	17	4.0	0.4
Length of first left pelvic-fin ray (unbranched)	11.6	11.2	13.5	16	12.1	0.6

.....continued on the next page

TABLE 1. (Continued)

	Holotype	Min.	Max.	n	x	SD
Length of second left pelvic-fin ray (first branched)	11.9	11.3	14.8	16	13.0	1.0
Length of third left pelvic-fin ray (second branched)	12.8	11.2	14.0	17	12.9	0.8
Anal-fin base	13.4	11.6	14.4	17	13.0	0.9
Preanal length	65.1	63.2	66.7	17	65.0	0.9
Distance between snout tip and terminus of anal-fin base	77.4	76.5	79.9	17	78.0	0.9
Distance between snout tip and anal-fin distal end	20.7	17.8	21.5	16	20.2	0.9
Adipose-fin length	42.4	41.8	45.3	17	43.2	0.9
Preadipose length	49.1	49.1	53.2	17	50.7	1.2
Distance between snout tip and terminus of adipose-fin base	91.7	90.4	93.1	17	91.5	0.6
Adipose-fin depth	5.1	4.5	6.5	17	5.4	0.5
Caudal-peduncle length	22.5	19.4	23.8	17	22.4	0.9
Caudal-peduncle depth	7.3	6.7	7.7	17	7.3	0.3
Snout-anus distance	49.2	47.4	52.1	17	49.8	1.1
Snout-urogenital papilla distance	50.9	50.2	53.4	17	51.7	0.8
Anus-urogenital papilla distance	1.3	1.1	1.9	17	1.6	0.3
Dorsal lobe of caudal fin length	23.9	20.0	26.6	17	23.7	1.8
Ventral lobe of caudal fin length	24.9	21.9	26.3	17	24.5	1.2
	Percentages of HL					
Head depth	48.2	47.1	52.5	17	49.6	1.5
Head width	47.5	43.2	51.0	17	48.2	1.9
Eye diameter (left)	21.9	20.5	25.9	17	23.7	1.5
Fleshy interorbital	22.3	22.3	25.1	17	23.8	0.8
Bony interorbital	17.2	14.3	17.2	17	15.7	0.9
Mouth gape	24.8	24.7	29.9	17	26.4	1.4
Snout length (left)	35.9	32.2	37.4	17	35.1	1.4
Distance between snout tip and posterior nare (left side)	18.6	17.7	20.3	17	18.9	0.7
Anterior internarial width	12.5	12.5	15.2	17	14.0	0.8
Posterior internarial width	12.4	12.1	14.8	17	13.2	0.7
Intranarial length (left side)	14.3	11.9	15.7	17	13.7	1.1

Coloration in alcohol. Background body coloration yellowish (Fig. 1). Ventral region of head and body lighter. Conspicuously dark humeral blotch, anterior limit slightly ahead of vertical through the spinelet and posterior limit at vertical through base of second branched dorsal-fin ray. Dark midlateral stripe well delimited, narrow, extending from region posterior to humeral blotch to caudal-fin insertion. Regions dorsally and ventrally adjacent to midlateral stripe unpigmented. Dorsal-fin base, especially near distal radials region, heavily pigmented. Dorsal fin darkly pigmented except for two hyaline stripes: one near its base and the other almost at its half. Dorsal surface of maxillary barbel darker than ventral surface.

Distribution and habitat. *Pimelodella humeralis* is only known from the Rio Ipitinga, a major right bank tributary of the Rio Jari which drains the eastern Guiana Shield into the lower Amazon (Fig. 4). The Ipitinga headwaters are located in the Colinas do Amapá geomorphological formation (approx. 300 m elevation), where it has many rapids along the main channel. The specimens were collected along a sandy beach in the middle stretch of the river (Fig. 5). Water parameters measured during the collection event were: 26.1–26.7°C; pH 4.25–4.46; conductivity 76–77 mS.

Etymology. The specific epithet *humeralis* refers to the conspicuous dark blotch in the humeral area, a feature not observed in any other nominal species of *Pimelodella*. An adjective.

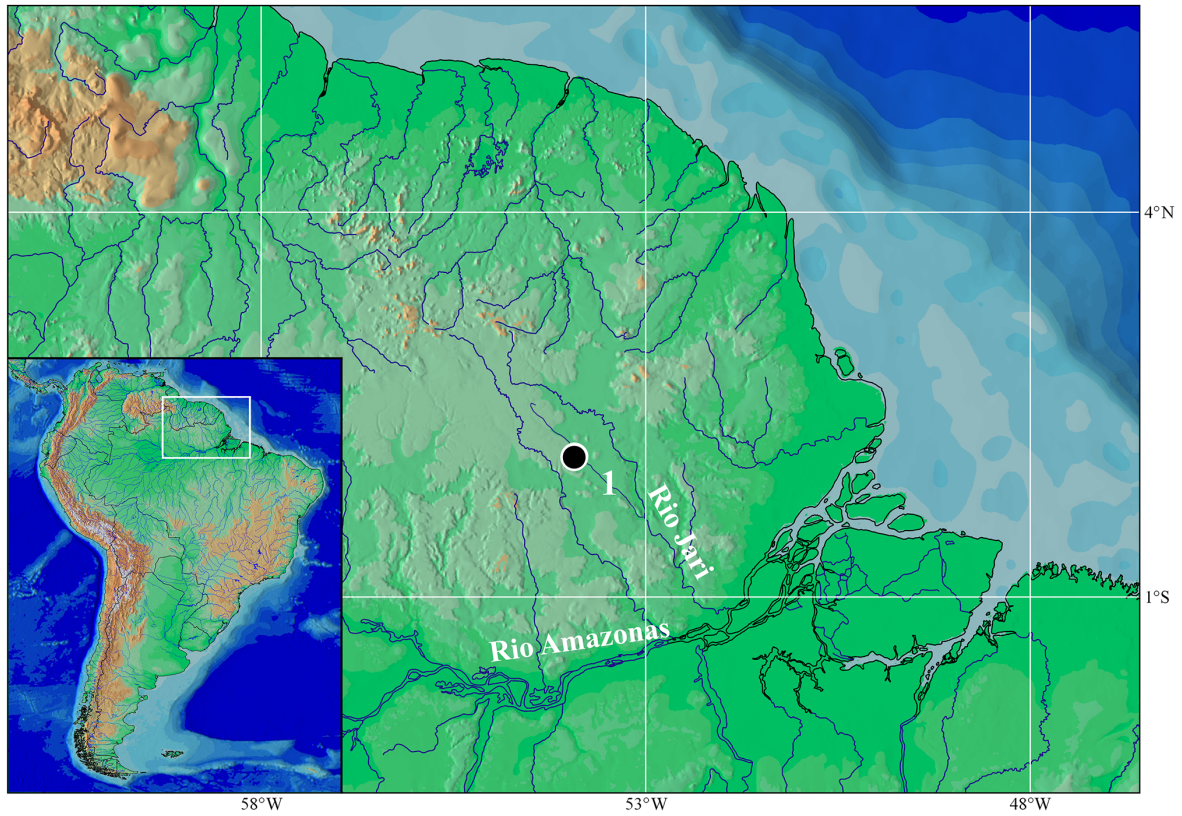


FIGURE 4. Distribution of *Pimelodella humeralis* in Rio Ipitinga (1), northern South America; black circle represents more than one lot and locality.



FIGURE 5. Sand beach in Rio Ipitinga where *Pimelodella humeralis* was collected.

Discussion

The overall taxonomic diversity of *Pimelodella* remains unclear despite the revision by Eigenmann (1917) and subsequent efforts (e.g., Mees, 1983; Guazzelli, 1997; Bockmann & Slobodian, 2013; Souza-Shibatta *et al.*, 2013). Only a few species of *Pimelodella* have been rigorously investigated with a modern, comparative perspective. The current list of 79 valid species (Eschmeyer, Fricke & van der Laan, 2017) largely corresponds to a list of available names assigned to the genus by Bockmann & Guazzelli (2003) and Ferraris (2007). A complete taxonomic revision of *Pimelodella* is in preparation (VS). Meanwhile, the delimitation of subgroups within *Pimelodella* allows one to localize problematic species.

Although overall morphology is similar among species of *Pimelodella*, some characters are useful for taxonomic delimitations such as vertebral counts, pectoral-fin spine morphology and color patterns. Such characters, however, are not immune to overlapping conditions between species especially when geographic and ontogenetic variation are taken into account (Mees, 1983; Bockmann & Slobodian, 2013). As in other Neotropical catfishes (e.g., Sabaj & Arce, 2017), single characters, no matter how consistent for a particular population, may become fragile in broader comparisons. Therefore, diagnoses of species in *Pimelodella* should not rely on one or a few autapomorphies, but on an exclusive combination of characters to survive future tests of taxonomic validity.

The number of total vertebrae is an important character for delimiting species groups in *Pimelodella*. Although most species of *Pimelodella* have between 37 and 44 total vertebrae (and the range can be as high as 3 vertebrae within a particular species), some species have consistently 46 or more vertebrae, such as *P. breviceps* (Kner, 1858), *P. cristata* (Müller & Troschel, 1849), *P. dorseyi* Fowler, 1941, *P. gracilis* (Valenciennes, 1835), *P. ophthalmica* (Cope, 1878), *P. parnahybae* Fowler, 1941, *P. steindachneri* Eigenmann, 1917, *P. taenioptera* Miranda-Ribeiro, 1914, *P. wessellii* (Steindachner, 1877), *P. witmeri* Fowler, 1941, and the species described here, *P. humeralis*.

Among the *Pimelodella* species with 46 or more vertebrae, only in the description of *P. dorseyi* is there any reference to a darkened humeral region, specifically a “greyish suffusion above pectoral and behind gill opening” (Fowler, 1941: 129, fig. 5). Based on this description and our observation of the type specimens, Fowler’s greyish suffusion corresponds to part of the pseudotympanum and is in fact due to the thin layer of skin overlying the gas bladder in that area, which extends from a region posterior to opercle anteriorly, until the vertical through spinelet to second dorsal branched ray, depending on the species. Regarding *Pimelodella* species with relatively low vertebral counts, three were described as also having a dark humeral mark: *P. buckleyi* (Boulenger, 1887), from rivers in Ecuador and Peru; *P. laurenti* Fowler, 1941, from the lower Rio São Francisco basin; and *P. rendahli* Ahl, 1925, from an unknown locality in Brazil. The mark of *P. buckleyi* is described as “a dark brown spot on the shoulder, at the origin of the lateral line” (Boulenger, 1887: 275) and is also shown in an illustration as a small blotch just posterior to the opercle, at anterior limit of the pseudotympanum, and continuous with the dark midlateral stripe (Boulenger, 1887, pl. XX, fig. 1). *Pimelodella laurenti* was described as having a “grayish suffusion above humeral extension” (Fowler, 1941: 133), which also corresponds to the darker appearance of the pseudotympanum (Fowler, 1941: fig. 17). The humeral mark in *P. rendahli* is described as a big dark mark posterior to the branchial opening (Ahl, 1925: 127) and is similar to the one described for *P. buckleyi*. None of those dark humeral marks present any resemblance to the condition in *Pimelodella humeralis* in which the humeral blotch is mostly posterior to the pseudotympanum and only slightly overlaps it dorsally and posteriorly. The slightly darkened nature of the pseudotympanum in *P. dorseyi*, *P. buckleyi*, *P. laurenti* and *P. rendahli* is fairly common among *Pimelodella* species and results of the absence of light-colored subjacent musculature (VS, pers. obs.). Other species (e.g., *P. megalops* Eigenmann, 1912) may have scattered, superficial melanophores near this pseudotympanum region. In sum, the darkened pseudotympanum is not suitably diagnostic for the previously mentioned species.

The morphology of the pectoral-fin spine is currently used to diagnose species of *Pimelodella*. The pectoral-fin spine in *P. humeralis* is distinguished by having the combination of serrae along distal half of anterior margin, and posterior margin with 8–11 broad-based, triangular, strongly inclined, blade-like retrorse dentations. That morphology shares a slightly resemblance with the following: *P. geryi* Hoedeman, 1961, from the Marowjine River basin, Suriname (Fig. 6A); *P. itapicuruensis* Eigenmann, 1917, from the Rio Itapicuru, Brazil (Fig. 6B); and *P. leptosoma* (Fowler, 1914), from the Essequibo River basin, Guyana (Fig. 6C). In those three species, the pectoral-fin spine also bears serrae along the distal half of anterior margin; but, in *P. geryi* and *P. itapicuruensis* the spine

also has small straight dentations regularly spaced along the basal half of its anterior margin. Also, the dentations along the posterior margin of the pectoral-fin spine in those three species are not as broad-based as in *P. humeralis*, despite being similarly inclined and blade-like. The conditions described here are for specimens of similar standard lengths, since the number and morphology of the pectoral-fin spine ornamentations may vary ontogenetically (Bockmann & Slobodian, 2013; Vanscoy *et al.*, 2015).

Pectoral-fin spine morphology aside, *Pimelodella humeralis* is easily distinguishable from *P. geryi*, *P. itapicuruensis* and *P. leptosoma* by the presence (*vs.* absence) of the dark humeral blotch, by having 46–49 (*vs.* 41–44) total vertebrae, the longer adipose fin, 41.8–45.3% SL (*vs.* 33.3–37.5% SL in *P. itapicuruensis* and *P. leptosoma* and 23.8–25.1% SL in *P. geryi*) and by the narrow midlateral stripe well delimited from the humeral mark to caudal-fin insertion (*vs.* midlateral stripe of moderate width and well delimited from snout to median caudal-fin rays in *P. geryi*; moderate width and poorly delimited from snout to median caudal-fin rays in *P. itapicuruensis* and from snout to caudal-fin insertion in *P. leptosoma*). Such differences are particularly important since *P. geryi* and *P. leptosoma* were collected with *P. humeralis* in the Rio Ipitinga.

The ichthyofauna of the southern slope of the eastern Guiana Shield was poorly known until recent explorations yielded a variety of newly described species: *Stenolicmus ix* Wosiacki, Coutinho & Montag, 2011; *Cyphocharax aninha* Wosiacki & Miranda, 2013; *Hypomasticus lineomaculatus* Birindelli, Peixoto, Wosiacki & Britski, 2013; and *Parotocinclus halbothi* Lehmann, Lazzarotto & Reis, 2014. This region shows a certain faunistic similarity to rivers draining the eastern Guiana Shield to the north, as listed by Vari *et al.* (2009). For example, *Parotocinclus halbothi* is also known from the upper Maroni on the north side of the Guiana Shield (Lehmann *et al.*, 2014). Another example is *Hypomasticus lineomaculatus*, which occurs on the southern face of the shield and is probably related to *H. despaxi* from French Guiana and Suriname to the north (Birindelli *et al.*, 2013). The other two species of *Pimelodella* collected with *P. humeralis* in the south-flowing Rio Ipitinga are previously known from north-flowing drainages in Guyana (*P. leptosoma*) and Suriname (*P. geryi*). Thus, the distributions of all three species of *Pimelodella* reinforce the eastern Guiana Shield as a large area of endemism.

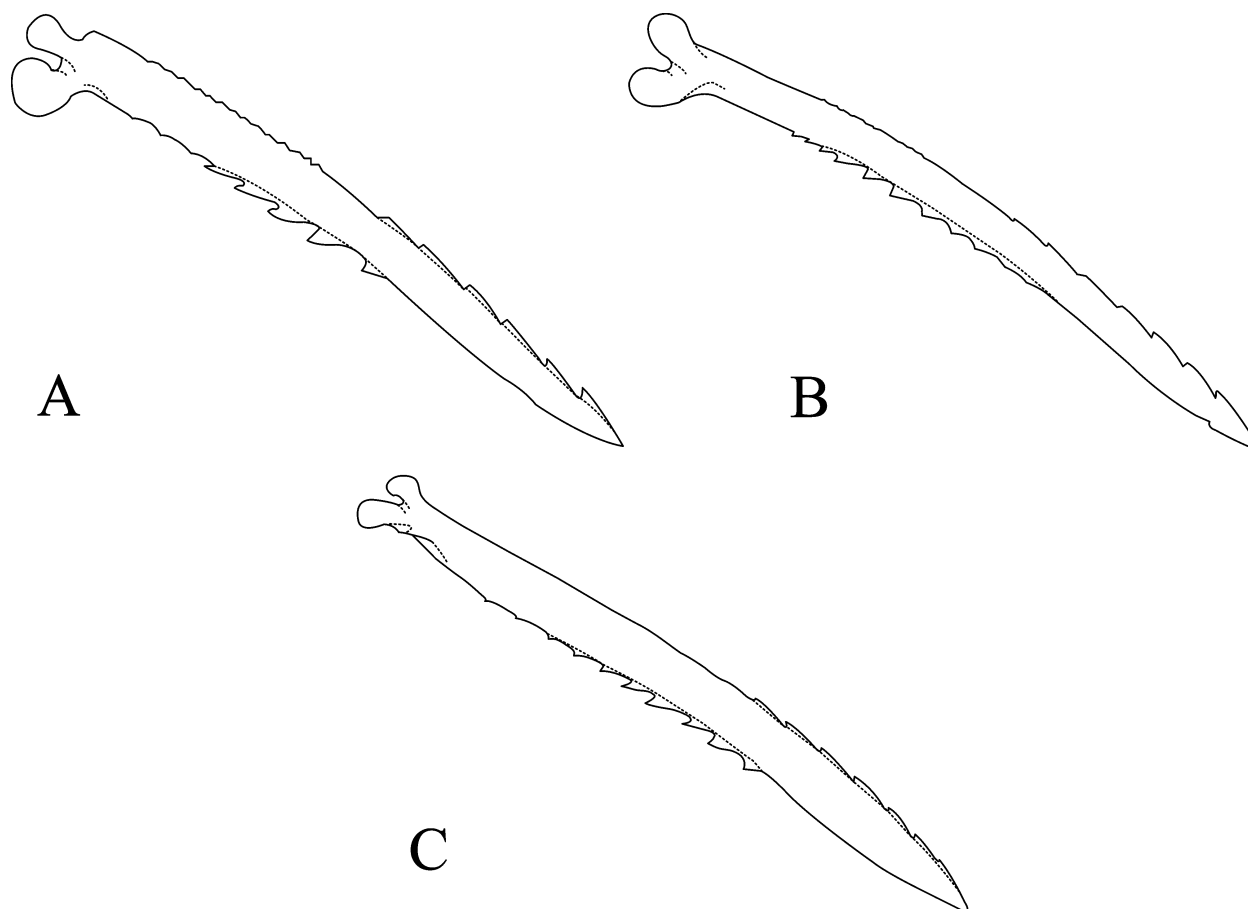


FIGURE 6. Ventral view of left pectoral-fin spine in: A. *Pimelodella geryi*, holotype, ZMA 102235, 58.0 mm SL; spine length 10.0 mm; *P. itapicuruensis*, holotype, FMNH 57986, 60.2 mm SL; spine length 11.2 mm; *P. leptosoma*, holotype, ANSP 39340, 59.6 mm SL; spine length 8.5 mm.

Comparative material

- Pimelodella altipinnis*: NMW 45601, 1, xr, 61.2 mm SL, holotype, Guyana, Demerara.
- Pimelodella australis*: FMNH 57962, 1, xr, 61.0 mm SL, holotype, Brazil, Rio Uruguay; FMNH 57963, 21, xr, 40.5–70.8 mm SL, paratypes, Brazil, Rio Uruguay; FMNH 57964, 16, xr, 39.9–63.1 mm SL, paratypes, Brazil, Rio Ibicuhy; FMNH 57965, 2, xr, 43.6–44.5 mm SL, paratype, Brazil, Rio Jacuhy; FMNH 57966, 4, xr, 43.2–48.9 mm SL, paratypes, Brazil, Rio Guahyba.
- Pimelodella avanhandavae*: FMNH 57981, 1, xr, 69.0 mm SL, holotype, Brazil, Rio Tietê; FMNH 58982, 23, xr, 46.5–80.2 mm SL, paratypes, Brazil, Tietê; FMNH 58068, 7, xr, 43.8–60.2 mm SL, paratypes, Brazil, Rio Tietê.
- Pimelodella bahiana*: MNHN B 612, 2, xr, 93.4–100.1, syntypes, Brazil, Bahia, Freshwaters of Bahia.
- Pimelodella boliviana*: FMNH 57976, 1, xr, 68.9 mm SL, holotype, Bolivia, Santa Cruz de La Sierra; FMNH 57977, 1, xr, 66.9 mm SL, paratype, Bolivia, Prov. del Sara Buenavista.
- Pimelodella boschmai*: RMNH 23248, 1, xr, holotype, Brazil, São Paulo, Rio Mogi-guaçu, observed photos and x-rays.
- Pimelodella brasiliensis*: NMW 45612, 1, xr, 140.6 mm SL, holotype, Brazil, "Rio Parahyba" (probably Paraíba do Sul).
- Pimelodella breviceps*: NMW 45615, 1, xr, 326.2 mm SL, holotype, Brazil, Amazonas, "Marabitanos" (probably Marabitanas).
- Pimelodella buckleyi*: BMNH 1880.12.8.98-99, 2, xr, 89.7–109.5 mm SL, syntypes, Ecuador, Canelos.
- Pimelodella chagresi*: MCZ 4947, 2, xr, 91.4–111.8 mm SL, paratypes, Panamá, Río Obispo.
- Pimelodella chaparae*: ANSP 69021, 1, xr, 48.1 mm SL, holotype, Bolivia, Boca Chaparae, Cochabamba; ANSP 69022-69035, 14, xr, 32.6–51.2 mm SL, paratypes, Bolivia, Boca Chaparae, Cochabamba.
- Pimelodella conquetaensis*: ZMB 32030, 1, xr, 93.2 mm SL, holotype, Colombia, "vom Rio Coqueta, S. O. Columbien" (probably Rio Caquetá, Colombia).
- Pimelodella copei*: ANSP 8362, 1, xr, 115.1 mm SL, holotype, Ecuador, Río Ambyiacu; ANSP 8363, 1, xr, 115.6 mm SL, paratype, Ecuador, Río Ambyiacu.
- Pimelodella cristata*: ZMB 3052, 1, xr, 177.4 mm SL, syntype, Guyana, "Takutu und Mahu" (probably Tacutu and Mahu rivers); ZMB 3053, 1, xr, 202.5 mm SL, syntypes, Guyana, "Takutu und Mahu" (probably Tacutu and Mahu rivers).
- Pimelodella cyanostigma*: ANSP 8381, 1, xr, 71.1 mm SL, syntype, Ecuador, Pebas; ANSP 8382, 1, xr, 59.9 mm SL, syntype, Ecuador, Pebas; ANSP 8383, 1, xr, 50.6 mm SL, syntype, Ecuador, Pebas.
- Pimelodella dorseyi*: ANSP 69375, 1, xr, 95.8 mm SL holotype, Brazil, Rio Salgado, Icó; ANSP 69376, 1, xr, 95.8 mm SL, paratype, Brazil, Rio Salgado, Icó.
- Pimelodella eigenmanni*: BMNH 1889.11.14.6, 1, xr, 105.4 mm SL, lectotype, Brazil, Minas Gerais, "Macacos" (probably Ribeirão dos Macacos, trib. of Rio das Velhas); MCZ 7438, 5, xr, 94.8–130.7 mm SL, paralectotypes, Brazil, Minas Gerais, "Macacos" (probably Ribeirão dos Macacos, trib. of Rio das Velhas); MCZ 7510, 1, xr, 135.6 mm SL, paralectotype, Brazil, Rio de Janeiro, "Rio Parahyba" (Rio Paraíba do Sul).
- Pimelodella elongata*: BMNH 1860.6.16.182-185, 4, xr, 54.6–136.8 mm SL, syntypes, Ecuador, Esmeraldas, "Freshwaters of Esmeraldas"; BMNH 1860.6.16.186-189, 4, xr, 71.3–96.1 mm SL, syntypes, Ecuador, Esmeraldas, "Freshwaters of Esmeraldas"; BMNH 1860.6.16.191 and 194, 2, xr, 84.5–93.8 mm SL, syntypes, Ecuador, Esmeraldas, "Freshwaters of Esmeraldas".
- Pimelodella enochi*: ANSP 69378, 1, xr, 44.9 mm SL, holotype, Brazil, Paraíba, Açude Pilões; ANSP 69379, 1, xr, 45.3 mm SL, paratype, Brazil, Paraíba, Açude Pilões.
- Pimelodella eutaenia*: BMNH 1913.10.1.37-40, 4, xr, 51.0–126.3 mm SL, syntypes, Colombia, "Rio Condoto (Spurrell) and the Rio Sipi (Palmer).
- Pimelodella geryi*: ZMA 102235, 1, xr, 58.0 mm SL, holotype, French Guyana, mainland, Litany River. MPEG 15690, 21, Brazil, Rio Ipitinga; MPEG 15691, 15, Brazil, Rio Ipitinga.
- Pimelodella gracilis*: MNHN A-9284, 1, xr, 170.1 mm SL, syntype, Argentina, "Corrientes dans le Parana et les autres rivières au-dessus de 28° de latitud sud".
- Pimelodella griffini*: FMNH 57974, 1, xr, 67.2 mm SL, holotype, Paraguay, Sapucaí, (Mountain rills near Sapucay); FMNH 57975, 7, xr, 43.8–69.9 mm SL, paratypes, Paraguay, Sapucaí, (Mountain rills near Sapucay).

- Pimelodella grisea*: BMNH 1902.5.27.36, 1, xr, 119.7 mm SL, syntype, Ecuador, Rio Durango; BMNH 1902.7.29.47, 1, xr, 116.8 mm SL, syntype, Ecuador, Rio Vaqueria; BMNH 1902.7.29.58, 1, xr, 99.7 mm SL, syntype, Ecuador, Rio Sapayo.
- Pimelodella hartii*: NMW 45784, 1, xr, 150.2 mm SL, holotype, Brazil, "Rio Parahyba" (probably Paraíba do Sul).
- Pimelodella hartwelli*: ANSP 68644, 1, xr, 103.2 mm SL, holotype, Peru, Contamana; Ucayali River.
- Pimelodella hasemani*: FMNH 57980, 1, xr, 60.6 mm SL, holotype, Brazil, Porto Velho, "San Antonio de Rio Madeira"; CAS 75823, 3, paratypes, Brazil, Rio Ica; Rio Putomajo, Rio Içá (tributary of Rio Solimoes near the Brazilian-Colombian border. In Colombian territory, Rio Içá is called Rio Putomayo). MCZ 7502, 3, 35.6–40.2 mm SL, paratypes, Brazil, Rio Amazonas at Obidos; MCZ 7572, 1, xr, 50.9 mm SL, paratype, Brazil, Rio Hyutahy (Rio Jutai); MCZ 7577, 49, 35.1–50.1 mm SL, paratypes, Brazil, Amazonas, Rio Ica; Rio Putomajo, Rio Içá (tributary of Rio Solimoes near the Brazilian-Colombian border. In Colombian territory, Rio Içá is called Rio Putomayo); MCZ 7579, 2, 50.1–55.5 mm SL, Brazil, Rio Amazonas at Obidos, 1°52'S, 55°30'W; MCZ 7580, 9, xr, 37.0–54.2 mm SL, paratypes, Brazil, Rio Amazonas at Obidos; MCZ 7581, 1, xr, 39.1 mm SL, paratype, Brazil, Rio Amazonas at Obidos.
- Pimelodella howesi*: ANSP 69036, 1, xr, 79.3 mm SL; holotype, Bolivia, Rio Chimore; ANSP 69037-69056, 25, xr, 30.7–73.8 mm SL, paratypes, Bolivia, Rio Chimore; ANSP 69057-69064, 8, xr, 51.2–60.6 mm SL, paratypes, Bolivia, Rio Chapare.
- Pimelodellas ignobilis*: NMW 44479, 3, xr, 109.9–129.25 mm SL, syntypes, Brazil, Santa Catarina, Águas Mornas.
- Pimelodella itapicuruiensis*: FMNH 57986, 1, xr, 60.2 mm SL, holotype, Brazil, Rio Itapicurú; FMNH 57987, 13, xr, 56.1–79.3 mm SL, paratypes, Brazil, Rio Itapicurú; FMNH 57951, 1, xr, 57.5 mm SL, paratype, Brazil, Bahia, Rio de Jacobina; FMNH 57953, 5, xr, 45.2–56.0 mm SL, paratypes, Brazil, Bom Fim, Rio Itapicurú; FMNH 57988, 2, 62.4–67.6 mm SL, paratypes, Brazil, Rio Agua Branca.
- Pimelodella kroniei*: MNRJ 836, 1, xr, 120.1 mm SL, holotype, Brazil, São Paulo, Iporanga, "Iguape, em aguas das cavernas do Iporanga".
- Pimelodella lateristriga*: ZMB 3038, 1, xr, 95.9 mm SL, holotype, Brazil, Rio de Janeiro.
- Pimelodella laticeps*: FMNH 57969, 1, xr, 49.0 mm SL, holotype, Paraguay, Sapucaí; FMNH 57970, 3, xr, 61.5–72.7 mm SL, paratypes, Paraguay, Sapucaí.
- Pimelodella laurenti*: ANSP 69380, 1, xr, 66.5 mm SL, holotype, Brazil, Jatoba, Rio São Francisco; ANSP 69381, 2, xr, paratypes, Brazil, Jatoba, Rio São Francisco.
- Pimelodella leptosoma*: ANSP 39340, 1, xr, 59.6 mm SL, holotype, Guyana, Rupununi river; ANSP 39341, 1, xr, 57.9 mm SL, paratype, Guyana, Rupununi river; MPEG 15743, 9, Brazil, Rio Ipitinga.
- Pimelodella linami*: USNM 121132, 1, xr, 74.7 mm SL, holotype, Venezuela, Rio Torbes.
- Pimelodella longipinnis*: AMNH 8642, 1, xr, 84.6 mm SL, holotype, Brazil, São Paulo (Alto Paraná or Coastal basins in São Paulo).
- Pimelodella macturki*: FMNH 53234, 1, xr, 53.5 mm SL, holotype, Guyana, Creek into Mora Passage; BMNH 1911.10.31.54, 1, xr, 51.4, paratype, Guyana, Creek into Mora Passage; BMNH 1911.10.31.55, 1, xr, 39.7 mm SL, paratype, Guyana, Trenches at Morawhanna; CAS 63691, 3, xr, paratype, Guyana, Georgetown trenches; CAS 63692, 1, xr, 51.4 mm SL, paratype, Guyana, Georgetown trenches; CAS 63693, 4, xr, paratypes, Guyana, Choca trenches at Morowhanna; FMNH 7388, 1, 36.4 mm SL, paratype, Guyana, Mora Passage; FMNH 53235, 4, 43.5–55.0 mm SL, paratypes, Guyana, Trenches at Morawhanna; FMNH 53573, 44.3–60.4 mm SL, paratypes, Guyana, Trenches at Morawhanna; FMNH 53574, 1, xr, 52.0 mm SL, paratype, Guyana, Georgetown trenches; MCZ 30073, 1, xr, 48.1 mm SL, paratype, Guyana, Creek into Mora Passage; MCZ 30074, 1, 43.8 mm SL, paratype, Guyana, Trenches at Morawhanna; USNM 66263, 1, xr, 37.6 mm SL, paratype, Guyana, Trenches at Morawhanna.
- Pimelodella meeki*: FMNH 3400, 1, xr, 100.2 mm SL, holotype, Brazil, São Paulo.
- Pimelodella megalops*: FMNH 53231, 1, xr, 74.7 mm SL, holotype, Guyana, Tumatumari; BMNH 1911.10.31.52, 4, xr, 61.3–69.4 mm SL, paratypes, Guyana, Tumatumari; CAS 63717, 5, xr, 58.4–70.4 mm SL, paratypes, Guyana, Potaro river at Tumatumari; MCZ 30075, 2, xr, 52.8–61.2 mm SL, paratype, Guyana, Lower Potaro River at Tumatumari; FMNH 7387, 2, 59.6–65.1 mm SL, paratypes, Guyana, Lower Potaro River at Tumatumari; FMNH 53232, 32, 42.1–72.5 mm SL, paratypes, Guyana, Lower Potaro River at Tumatumari; FMNH 53233, 1, xr, 44.0 mm SL, paratype, Guyana, Crab Falls.

- Pimelodella megalura*: MNRJ 865, 4, xr, 85.1–128.6 mm SL, lectotypes, Brazil, Mato Grosso, São Luiz de Cáceres; MZUSP 1986, 1, paralectotype, Brazil, Mato Grosso, São Luiz de Cáceres; MZUSP 5265–5279, 12, xr, 70.0–143.6 mm SL, paralectotypes, Brazil, Mato Grosso, São Luiz de Cáceres.
- Pimelodella metae*: FMNH 58441, 1, xr, 58.0 mm SL, holotype, Colombia, Río Negro; CAS 75835, 1, xr, 34.9 mm SL, paratype, Colombia, Quebrada Cramalote at Villavicencio; FMNH 58442, 2, xr, 64.3–74.0 mm SL, paratypes, Colombia, Río Meta.
- Pimelodella modesta*: BMNH 1860.6.190-191, 2, xr, 77.5–121.1 mm SL, syntypes, Ecuador, "Fresh waters of Esmeralda".
- Pimelodella montana*: CAS 63719, 1, xr, 87.4 mm SL, syntype, Peru, Rio Huallaga at Huanuco.
- Pimelodella mucosa*: CAS 63720, 1, xr, 97.4 mm SL, holotype, Paraguay, Rio Paraguay; Bahia Negra on west bank.
- Pimelodella notomelas*: FMNH 57967, 1, xr, 38.9 mm SL, holotype, Brazil, Mato Grosso, Cáceres; FMNH 57968, 5, 27.6–39.5 mm SL, paratypes Brazil, Mato Grosso, Cáceres; FMNH 57983, 2, xr, 42.0–42.3 mm SL, paratypes, Brazil, Mato Grosso, Rio Jauru.
- Pimelodella odynea*: USNM 121133, 1, xr, 88.3 mm SL, holotype, Venezuela, Río San Juan Above Bridge South of Mene Grande; USNM 82618, 1, xr, paratype, Venezuela, Sierra de Perija; USNM 101610, 1, xr, paratype, Colombia, Río Pamplonita; USNM 121134, 47, xr, 44.7–81.5, paratypes, Venezuela, Río Motatan; USNM 121135, 2, xr, 52.2–60.8 mm SL, paratypes, Venezuela, Río Apon; USNM 121136, 103, xr, 23.4–78.8 mm SL, paratypes, Venezuela, Río Motatan; USNM 121137, 3, xr, 68.7–75.5 mm SL, paratypes, Venezuela, Río San Pedro; USNM 121138, 3, xr, 49.3–80.1 mm SL, paratypes, Venezuela, Río Machango; USNM 121139, 1, xr, 74.0 mm SL, paratype, Venezuela, Río Tachira; USNM 121140, 86, xr, 25.4–85.67 mm SL, paratypes, Venezuela, Río Motatan; USNM 121141, 24, xr, 53.1–82.3 mm SL, paratypes, Venezuela, Río San Juan; USNM 121142, 18, xr, 31.4–89.4 mm SL, paratypes, Venezuela, Río Socuy; USNM 121143, 8, xr, paratypes, Venezuela, Río Jimelles; USNM 121144, 2, xr, 66.4–77.1 mm SL, paratypes, Venezuela, Río Machango; USNM 121213, 17, xr, 39.4–68.1 mm SL, paratypes, Venezuela, Río Negro; USNM 121252, 1, xr, 99.6 mm SL, paratype, Colombia, Cucuto.
- Pimelodella ophthalmica*: ANSP 21102, 1, xr, 109.4 mm SL, holotype, Peru, Peruvian Amazon.
- Pimelodella papariae*: ANSP 69387, 1, xr, 107.6 mm SL, holotype, Brazil, Rio Grande do Norte, Lago Papary.
- Pimelodella pappenheimi*: ZMB 31951, 2, xr, 103.1–111.2 mm SL, syntypes, Brazil, Santa Catarina, Corupá.
- Pimelodella parnahybae*: ANSP 69377, 1, xr, 84.0 mm SL, holotype, Brazil, Rio Parnaíba
- Pimelodella pectinifera*: MCZ 7508, 1, xr, 150.9 mm SL, holotype, Brazil, Rio Muriaé.
- Pimelodella peruana*: CAS 63721, 1, xr, 40.3 mm SL, holotype, Peru, Río Ucayali at Inahuaya.
- Pimelodella peruensis*: ANSP 21932, 1, xr, 48.2 mm SL, holotype, Peru, Peruvian Amazon.
- Pimelodella procera*: RMNH 28588, 1, xr, holotype, French Guyana, "Crique Balaté", Maroni-Marowine basin; MBNH 1983-5, 3, xr, 61.5–91.2 mm SL, paratypes, French Guyana, "Crique Balaté", Maroni-Marowine basin.
- Pimelodella rendahli*: ZMB 32031, 1, xr, 80.7 mm SL, holotype, No locality
- Pimelodella robinsoni*: ANSP 69386, 1, xr, 73.0 mm SL, holotype, Brazil, Pernambuco, São Jose do Egito.
- Pimelodella roccae*: MCZ 30975, 1, xr, 139.9 mm SL, holotype, Peru, Río Comerciato; CAS 63722, 1, xr, 91.4 mm SL, paratype, Bolivia, Río Comerciato.
- Pimelodella rudolphi*: MNRJ 857, 1, xr, 73.9 mm SL, lectotype, Brazil, Mercado de São Paulo; MZUSP 1061, 1, xr, 66.2 mm SL, paralectotype, Brazil, Rio Tamanduateí; MZUSP 2259, 1, xr, 41.4 mm SL, paralectotype, Brazil, Sorocaba; MZUSP 2260, 1, xr, 87.3 mm SL, paralectotype, Brazil, Rio Tietê; MZUSP 2261, 1, xr, 101.2 mm SL, paralectotype, Brazil, Rio Tietê; MZUSP 5260, 1, xr, paralectotype, Brazil, Sorocaba; MZUSP 5261, 1, xr, 42.6 mm SL, Brazil, São Paulo, Sorocaba; MZUSP 5262, 1, xr, 90.5 mm SL, paralectotype, Brazil, Rio Tietê; MZUSP 5263, 1, xr, 99.5 mm SL paralectotype, Brazil, Rio Tietê; MZUSP 5264, 1, xr, 86.4 mm SL, paralectotype, Brazil, Rio Tietê.
- Pimelodella serrata*: FMNH 57978, 1, xr, 55.7 mm SL, holotype, Bolivia, Río Machupo; FMNH 57979, 1, xr, 86.0 mm SL, paratype, Bolivia, Río Machupo.
- Pimelodella spelaea*: MZUSP 81726, 1, xr, 78.9 mm SL, holotype, Brazil, Goiás, São Bernardo cave; MZUSP 81727, 1, xr, 42.4 mm SL, paratype, Brazil, Goiás, São Bernardo cave; MZUSP 81728, 1, xr, 47.1 mm SL, paratype, Brazil, Goiás, São Bernardo cave; MZUSP 81729, 4, xr, 69.0–76.6 mm SL, paratypes, Brazil, Goiás, São Bernardo cave.

- Pimelodella steindachneri*: MCZ 7472, 1, xr, 135.5 mm SL, syntype, Brazil, Lago Cudajas (Lago Badajos); MCZ 7487, 1, xr, 150.4 mm SL, syntype, Brazil, Pará, Baía do Marajó; MCZ 7542, 1, xr, 165.4 mm SL, syntype, Brazil, Lago Manacapuru; MCZ 7566, 2, xr, 96.8–123.6 mm SL, syntype, Brazil, Maués; MCZ 7567, 1, xr, 106.4 mm SL, syntype, Brazil, Rio Amazonas at Santarém; MCZ 7588, 1, xr, 120.2 mm SL, syntype, Brazil, Rio Poti.
- Pimelodella straminea*: ANSP 21581, 1, xr, 41.2 mm SL, syntype, Brazil, Rio Grande do Sul, countryside near the mountains; ANSP 21583, 1, xr, 44.0 mm SL, syntype, Brazil, Rio Grande do Sul, countryside near the mountains; ANSP 21584, 1, xr, 44.9 mm SL, syntype, Brazil, Rio Grande do Sul, countryside near the mountains; ANSP 21604, 1, xr, 54.7 mm SL, syntype, Brazil, Rio Grande do Sul, countryside near the mountains.
- Pimelodella taeniophora*: BMNH 1895.5.27-28, 2, xr, 59.6–76.6 mm SL, syntypes, Brazil, Descalvados.
- Pimelodella taenioptera*: MNRJ 691, 3, xr, 119.7–125.0 mm SL, lectotypes, Brazil, Rio Sepotuba.
- Pimelodella tapatapae*: CAS 57469, 1, xr, 121.6 mm SL, holotype, Venezuela, Mouth of Río Tapatapa.
- Pimelodella vittata*: ZMB 9175, 2, xr, 53.2–61.8 mm SL, syntypes, Brazil, small lakes and streams into Rio das Velhas.
- Pimelodella wessellii*: NMW 79188, 1, xr, 157.9 mm SL, holotype, Guyana, Essequibo river.
- Pimelodella witmeri*: ANSP 69383, 1, xr, 137.5 mm SL, holotype, Brazil, Rio Jaguaribe; ANSP 69384, 3, xr, 75.8–132.3 mm SL, paratype, Brazil, Rio Jaguaribe.
- Pimelodella wolffi*: ANSP 69388, 1, xr, 88.9 mm SL, holotype, Brazil, Rio Choro; ANSP 69389–91, 3, xr, 67.1–71.0 mm SL, paratype, Brazil, Rio Choro.
- Pimelodella yuncensis*: ZSM 7870, 1, xr, syntype, Peru, Pecosmayo, Río Jequetepeque basin.

Acknowledgements

Authors are especially thankful to F. Bockmann for all the information provided; J. Lundberg for the insights regarding the genus and suggestions; A. Netto-Ferreira and M. Sabaj for suggestions and corrections; M. Arce, R. Arrindell, M. Britto, H. Britski, P. Buckup, R. Castro, D. Catania, W. Crampton, K. Hartel, J. Kapp, D. Johnson, C. Lucena, Z. Lucena, J. Lundberg, J. Maclaine, C. McMahan, S. Mochel, O. Oyakawa, A. Palandacic, L. Parenti, M. de Pinna, L. Rapp Py-Daniel, S. Raredon, R. Reis, R. de Ruiter, S. Schaefer, K. Swagel, R. Vari, and W. Wosiacki for providing assistance during visits at their institutions, loaning and providing information on type material. M. Pastana prepared Figure 1. Research funding for VS was provided by Fundação de Amparo à Pesquisa do Estado de São Paulo (FAPESP, projects # 2013/18623-4, 2015/26804-4 and 2017/01073-0). GMD was supported by Conselho Nacional de Desenvolvimento Científico e Tecnológico (CNPq) through the Programa de Capacitação Institucional (MPEG/MCTI) (300066/2016-3).

Literature cited

- Ahl, E. (1925) Neue südamerikanische Fische aus dem Zool. Museum Berlin. *Sitzungsberichte der Gesellschaft Naturforschender Freunde zu Berlin*, 1923, 106–109. [in German]
- Aleixo, A., Montag, L.F.A., Wosiacki, W.B., Silva, F.R., Freitas, T.M.S., Peixoto, L.A.W., Araújo, A.B., Avila-Pires, T.C., Hoogmoed, M.S., Rocha, W.A., Poletto, F., Lima, M.F.C., Silva, M.C., Rossi, R.V., Miranda, C.L., Fonseca, R.T.D., Silva, M.R.P., Souza, M.G.C., Coelho, R.F.R. & Carmo, A. (2011) Diagnóstico da Biodiversidade das Unidades de Conservação Estaduais do Mosaico Calha Norte, estado do Pará – Reserva Biológica Maicuru. *In: Secretaria de Estado de Meio Ambiente, Plano de manejo da Reserva Biológica Maicuru: Anexos*, Secretaria de Estado de Meio Ambiente, Belém, pp. 5–71.
- Birindelli, J.L.O., Peixoto, L.A.W., Wosiacki, W.B. & Britski, H.A. (2013) New Species of *Hypomasticus* Borodin, 1929 (Characiformes: Anostomidae) from Tributaries of the Lower Rio Amazonas, Brazil. *Copeia*, 2013, 464–469. <https://doi.org/10.1643/CI-12-148>
- Bockmann, F.A. & Castro, R.M.C. (2010) The blind catfish from the caves of Chapada Diamantina, Bahia, Brazil (Siluriformes: Heptapteridae): description, anatomy, phylogenetic relationships, natural history, and biogeography. *Neotropical Ichthyology*, 8 (4), 673–706. <https://doi.org/10.1590/S1679-62252010000400001>
- Bockmann, F.A. & Guazzelli, G.M. (2003) Family Heptapteridae (Heptapterids). *In: Reis, R.E., Kullander, S.O. & Ferraris Jr.,*

- C.J. (Eds.), *Check List of the Freshwater Fishes of South and Central America*. Edipucrs, Porto Alegre, pp. 406–431.
- Bockmann, F.A. & Miquelarena, A.M. (2008) Anatomy and phylogenetic relationships of a new catfish species from northeastern Argentina with comments on the phylogenetic relationships of the genus *Rhamdella* Eigenmann and Eigenmann 1888 (Siluriformes, Heptapteridae). *Zootaxa*, 1780, 1–54.
- Bockmann, F.A. & Slobodian, V. (2013) Heptapteridae. In: Queiroz, L.J., Torrente-Vilara, G., Ohara, W.M., Silva, T.H.P., Zuanon, J. & Doria, C.R.C. (Eds.), *Peixes do Rio Madeira. Vol. 3. Dialetto*, São Paulo, pp. 12–71. [in Portuguese]
- Boulenger, G.A. (1887) An account of the fishes collected by Mr. C. Buckley in eastern Ecuador. *Proceedings of the Zoological Society of London*, 1887 (2), 274–283.
<https://doi.org/10.1111/j.1096-3642.1887.tb02962.x>
- Cope, E.D. (1878) Synopsis of the fishes of the Peruvian Amazon, obtained by Professor Orton during his expeditions of 1873 and 1877. *Proceedings of the American Philosophical Society*, 17 (101), 673–701.
- Eigenmann, C.H. (1912) The freshwater fishes of British Guiana, including a study of the ecological grouping of species, and the relation of the fauna of the plateau to that of the lowlands. *Memoirs of the Carnegie Museum*, 5 (1), 1–578.
<https://doi.org/10.5962/bhl.part.14515>
- Eigenmann, C.H. (1917) *Pimelodella* and *Typhlobagrus*. *Memoirs of the Carnegie Museum*, 7, 229–258.
- Eschmeyer, W.N. & Fong, J.D. (2017) Species by Family/Subfamily. Available from: <http://researcharchive.calacademy.org/research/ichthyology/catalog/SpeciesByFamily.asp> (accessed 3 May 2017)
- Eschmeyer, W.N., Fricke, R. & van der Laan, R. (Eds.) (2017) Catalog of Fishes: Genera, Species, References. Available from: <http://researcharchive.calacademy.org/research/ichthyology/catalog/fishcatmain.asp> (accessed 3 May 2017)
- Ferraris Jr., C.J. (2007) Checklist of catfishes, recent and fossil (Osteichthyes: Siluriformes), and catalogue of siluriform primary types. *Zootaxa*, 1418 (1), 1–628.
<https://doi.org/10.11646/zootaxa.1418.1.1>
- Fowler, H.W. (1914) Fishes from the Rupununi River, British Guiana. *Proceedings of the Academy of Natural Sciences of Philadelphia*, 66, 229–284.
- Fowler, H.W. (1941) A collection of fresh-water fishes obtained in eastern Brazil by Dr. Rodolpho von Ihering. *Proceedings of the Academy of Natural Sciences of Philadelphia*, 93, 123–336.
- Guazzelli, G.M. (1997) *Revisão das Espécies de Pimelodella Eigenmann & Eigenmann, 1888 (Teleostei: Siluriformes: Pimelodidae) dos Sistemas Costeiros do Sul e Sudeste Brasileiro*. Unpublished Master Dissertation, Pontifícia Universidade Católica do Rio Grande do Sul, Porto Alegre, 150 pp. [in Portuguese]
- Hoedeman, J.J. (1961) Notes on the ichthyology of Surinam and other Guianas, 8, Additional records of siluriform fishes, 2. *Bulletin of Aquatic Biology*, 2 (23), 129–139.
- Kner, R. (1858) Ichthyologische Beiträge. II, Abtheilung, *Sitzungsberichte der Kaiserlichen Akademie der Wissenschaften, Mathematisch-Naturwissenschaftliche Classe*, 26 (373), 373–448. [in German]
- Lehmann, P., Lazzarotto, H. & Reis, R.E. (2014) *Parotocinclus halbothi*, a new species of small armored catfish (Loricariidae: Hypoptopomatinae), from the Trombetas and Marowijne River basins, in Brazil and Suriname. *Neotropical Ichthyology*, 12, 27–33.
<https://doi.org/10.1590/S1679-62252014000100002>
- Lundberg, J.G. & Baskin, J.N. (1969) The caudal skeleton of the catfishes, order Siluriformes. *American Museum Novitates*, 2398, 1–49.
- Mees, G.F. (1983) Naked catfishes from French Guiana (Pisces, Nematognathi). *Zoologische Mededelingen (Leiden)*, 57, 43–58.
- Miranda Ribeiro, A. (1907) Uma novidade ichthyologica. *Kosmos*, 4 (1), 3 unnumbered pages. [in Portuguese]
- Miranda Ribeiro, A. (1914) Pimelodidae, Trachycorystidae, Cetopsidae, Bunocephalidae, Auchenipteridae, e Hypophthalmidae. In: *Comissão de Linhas Telegraficas Estrategicas de Matto-Grosso ao Amazonas*, Anexo No. 5 (História Natural: Zoologia, pp. 1–13. [in Portuguese]
- Müller, J. & Troschel, F.H. (1849) Fische. In: *Reisen in Britisch-Guiana in den Jahren 1840-44, Im Auftrag Sr. Majestat des Königs von Preussen ausgeführt von Richard Schomburgk*, 3, pp. 618–644. [in German]
- Sabaj, M.H. (2016) Standard symbolic codes for institutional resource collections in herpetology and ichthyology: an online reference, Version 6.5, American Society of Ichthyologists and Herpetologists. Available from: <http://www.asih.org/> (accessed 3 May 2017)
- Sabaj, M.H. & Arce, M. (2017) Taxonomic assessment of the Hard-Nosed Thornycats (Siluriformes: Doradidae: *Trachydoras* Eigenmann 1925) with description of *Trachydoras gepharti*, n. sp. *Proceedings of the Academy of Natural Sciences of Philadelphia*, 166 (1), 1–53.
<https://doi.org/10.1635/053.166.0102>
- Slobodian, V. (2013) *Taxonomia, Sistemática e Biogeografia de Brachyrhamdia Myers, 1927 (Siluriformes: Heptapteridae), com uma investigação sobre seu mimetismo com outros Siluriformes*. Unpublished Master Dissertation, Universidade de São Paulo, Ribeirão Preto, 316 pp. [in Portuguese]
- Slobodian, V. & Bockmann, F.A. (2013) A new *Brachyrhamdia* (Siluriformes: Heptapteridae) from Rio Japurá basin, Brazil, with comments on its phylogenetic affinities, biogeography and mimicry in the genus. *Zootaxa*, 3717 (1), 1–22.
<https://doi.org/10.11646/zootaxa.3717.1.1>
- Souza-Shibatta, L., Pezenti, L.F., Ferreira, D.G., Almeida, F.S.D., Sofia, S.H. & Shibatta, O.A. (2013) Cryptic species of the

- genus *Pimelodella* (Siluriformes: Heptapteridae) from the Miranda River, Paraguay River basin, Pantanal of Mato Grosso do Sul, Central Brazil. *Neotropical Ichthyology*, 11 (1), 101–109.
<https://doi.org/10.1590/S1679-62252013000100012>
- Steindachner, F. (1877) Die Süßwasserfische des südöstlichen Brasilien, III. *Sitzungsberichte der Kaiserlichen Akademie der Wissenschaften, Mathematisch-Naturwissenschaftliche Classe, Wien, Abt. I Botanik, Zoologie, Anatomie, Geologie und Paläontologie*, 74, 559–694, pls. 1–13. [in German]
- Taylor, W.R. & Van Dyke, G.C. (1985) Revised procedures for staining and clearing small fishes and other vertebrates for bone and cartilage study. *Cybium*, 9, 107–119.
- Valenciennes, A. (1835) Poissons [plates]. In: d'Orbigny, A. (Ed.), *Voyage dans l'Amérique méridionale (le Brésil, la République Orientale de l'Uruguay, la République Argentine, la Patagonie, la République du Chili, la République de Bolivie, la République du Pérou), Exécuté Pendant les Années 1826, 1827, 1828, 1829, 1830, 1832 et 1833. Vol. 5. Part 2.* Bertrand et Levraut, Paris, pls. 1–3.
- Vanscoy, T., Lundberg, J.G. & Luckenbill, K. (2015) Bony ornamentation of the catfish pectoral-fin spine: comparative and developmental anatomy, with an example of fin-spine diversity using the Tribe Brachyplatystomini (Siluriformes, Pimelodidae). *Proceedings of the Academy of Natural Sciences of Philadelphia*, 164 (1), 177–212.
<https://doi.org/10.1635/053.164.0107>
- Vari, R.P., Ferraris Jr., C.J., Radosavljevic, A. & Funk, V.A. (2009) Checklist of the freshwater fishes of the Guiana Shield. *Bulletin of the Biological Society of Washington*, 17, 1–93.
<https://doi.org/10.2988/0097-0298-17.1.i>
- Wosiacki, W.B. & Miranda, D.P.S. (2013) Description of a new small species of the genus *Cyphocharax* (Characiformes: Curimatidae) from the Lower Amazon Basin. *Copeia*, 13, 627–633.
<https://doi.org/10.1643/CI-12-127>
- Wosiacki, W.B., Coutinho, D.P. & Montag, L.F.A. (2011) Description of a new species of sand-dwelling catfish of the genus *Stenolicmus* (Siluriformes; Trichomycteridae). *Zootaxa*, 2752, 62–68.

Attachment 2: Script to estimate gene trees in RStudio using RAxML.

```
library(ips)
library(ape)
library(phangorn)
rm(list=ls())
#Aqui vc troca a localizacao abaixo pela localizacao da sua pasta no seu computador.
setwd("~/Desktop/PimelodellaGT")

#Generating necessary objects that will be used later.
loci <-dir("data")
tr <-list()
n <-length(loci)
stats<-data.frame(num.parsimony.informative.sites=0,gc.content=0,fragment.length=0,
mean.bs=0)

#Now I'll read each locus in turn, run a bootstrap analysis using a GTRGAMMA model and
100 reps
#per locus.
for (i in 1:n){
  dat<-read.dna(paste("data/",loci[i], sep=""), format="fasta")
  #running rapid Bootstrap analysis and searching for the best-scoring ML tree
simultaneously
  # m = "GTRGAMMA" - model of evolution
  # f = "a" - activate rapid bootstrap analysis and searching for the best ML tree
  # N - number of bootstrap reps
  # p - random seed for starting parsimony tree
  # x - random seed for rapid bootstrapping

  #Aqui vc troca a localizacao do RAxML pela localizacao no seu computador
tr [[i]]<- raxml(dat, m = "GTRGAMMAI", f = "a", N = 200, p = 492874, x = 19495,
exec = "/Applications/standard-RAxML-master/raxmlHPC-AVX",file =
"pimelo")

  xx<-data.frame(num.parsimony.informative.sites=pi(dat),
gc.content=base.freq(dat)[3]+base.freq(dat)[2],
fragment.length=dim(dat)[2],
mean.bs=mean(as.numeric(tr[[i]]$bipartitions$node.label),
na.rm=TRUE))
  rownames(xx)<-loci[i]
  stats<-rbind(stats,xx)
  write.csv(stats, "res/loci.stats.csv")
}

for (i in 1:n) write.tree(tr[[i]]$bestTree, file="trees/trees.tre", append=TRUE)

for (i in 1:n) write.tree(tr[[i]]$bootstrap, file="boots/bootstrap.tre", append=TRUE)
```